AUBE '04

13th International Conference on Automatic Fire Detection

14. - 16. September 2004

Universität Duisburg-Essen, Duisburg, Germany

S.L. Rose-Pehrsson, J.C. Owrutsky, S.C. Wales, J.P. Farley, F.W. Williams
Naval Research Laboratory, Washington, DC, USA
D.A. Steinhurst, C.P. Minor
Nova Research, Inc., Alexandria, VA, USA
D.T. Gottuk, J.A. Lynch
Hughes Associates, Inc., Baltimore, MD, USA

Volume Sensor for Damage Assessment and Situational Awareness

Abstract

A multi-sensory approach is being used to develop a new detection capability for improved damage assessment and situational awareness. As part of the Advanced Damage Countermeasures (ADC) program, the U.S. Navy seeks to develop and demonstrate improved damage control capabilities that will be incorporated into new ship designs. This work represents the progress to date of a multi-year program to identify, evaluate, and adapt video image detection technologies for shipboard damage control. Various spectral and acoustic signatures, new video imaging techniques, and image recognition methods are being investigated to enhance and expand detection capabilities to provide a broad range of situational awareness for a space. The goal is to develop a sensor system that is able to detect event signatures within the volume of a space (i.e., a "volume sensor") rather than relying on spot-type fire detectors. A number of real-scale test series were conducted both to obtain a database for each of the technologies and to evaluate potential detection algorithms. Tests included a range of fire and nuisance sources, flooding and water breach scenarios, and actual shipboard background environmental conditions. This work provides an assessment of the utility of the various signatures studied as components for the volume sensor. New alarm algorithms have been developed using different spectral and acoustic signatures combined with video input data. The coupling of acoustic signals with video image detection systems not only provides enhanced discrimination between fire and nuisance events, but also expands the system to include the detection of other damage control events such as flooding.

Introduction

The U.S. Naval Research Laboratory (NRL) is developing a real-time, remote detection system for shipboard situational awareness. The Advanced Volume Sensor Task is an important element of the U.S. Office of Naval Research, Future Naval Capabilities program, Advanced Damage Countermeasures (ADC). The ADC program seeks to develop and demonstrate improved damage control capabilities for reduced manning aboard future naval vessels. The objective of the Advanced Volume Sensor Task is to develop an affordable detection system that will identify shipboard damage control conditions and provide an alarm for events such as fire, explosions, pipe ruptures, and flooding level. The project uses an inexpensive, multi-sensory approach that takes advantage of existing and emerging technology in the rapidly growing fields of optics, acoustics, image analysis and computer processing. In addition, this technology utilizes conventional surveillance cameras, which are currently being incorporated into new ship designs, and therefore will provide multiple system functions with the same hardware. The goal is to develop a robust, low cost system with no false alarms.

The Advanced Volume Sensor Task is in the fourth year of a five-year, five-phase program. The first phase consisted of a literature review and an industry review of current and emerging technologies [1]. Based on the study, several technologies were identified as having potential for meeting some of the objectives of the volume sensor development effort. Work preformed during the second year provided a basis for moving forward with the use of video image detection (VID) for shipboard applications [2]. A full-scale laboratory evaluation of two VID systems using a variety of fire and nuisance sources indicated that these systems using smoke alarm algorithms could provide equivalent fire detection capabilities when compared to spot-type smoke detectors for most of the conditions evaluated. The third phase assessed potential technologies that will be used in developing a volume sensor system. The tasks included the evaluation of video image detection [3,4,5], spectral [6,7] and acoustic sensors [8], and the development of advanced algorithms [9,10] and long wavelength imaging [11]. All of these methods were evaluated using damage control events including fire, flooding and pipe ruptures. Each technology provides unique information for use in the Volume Sensor Prototype.

The successful components are now being integrated into a prototype system. Optimization of the detection methods and development of multivariate data analysis and fusion methods are the primary focus of the current work. The volume sensor system will be further enhanced and demonstrated next year. The goal for the demonstration is to integrate the Volume Sensor into a supervisory control system (SCS) and to demonstrate the system with a newly developed hybrid gaseous/water mist suppression system.

Volume Sensor Concept

Several technologies have been evaluated for the development of the volume sensor. Video image detection is the main detection method with the other technologies being used to enhance and expand the capabilities. Full-scale laboratory and shipboard tests were conducted to develop a database of events. Figure 1 illustrates the basic concept.

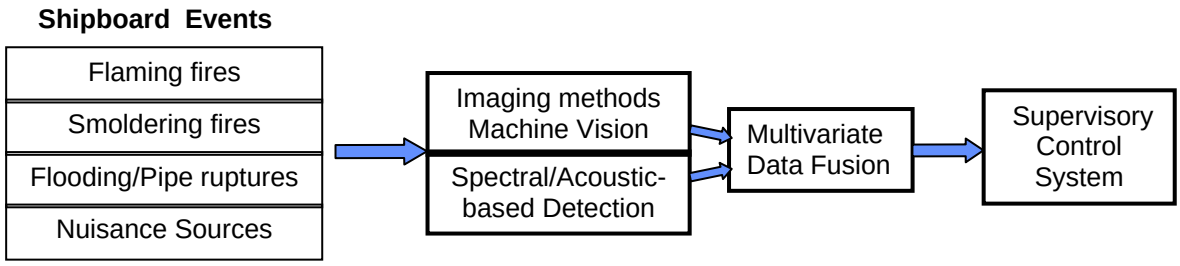

Fig 1. Main components for Volume Sensor Development

Three commercial video-based fire detection systems were evaluated in the shipboard environment. Two systems performed well with approximately 80% correct detection of small incipient fires and nuisance events, and a 20% false detection rate [12]. The alarm times for the VID systems are comparable to ionization detection systems for flaming fires and much faster than either ionization or photoelectric smoke detection systems for smoldering fires. Two of the manufacturers have been working with NRL to improve their detection systems for Navy applications. Recent versions of these VID systems include detection algorithms for both fire and smoke. While there has been considerable progress in improving the detection sensitivity, the false alarm rate needs to be reduced. This objective is being pursued by combining the VID systems with other types of sensors, such as other optical and acoustic detection methods.

Two distinct approaches to optical detection outside the visible are being pursued [6,7, 13]. These are long wavelength video detection (LWVD), which provide some degree of both spatial and spectral resolution or discrimination, and single or multiple element narrow spectral band detectors, which are spectrally but not spatially resolved and operate with a wide field of view at specific wavelengths ranging from the mid infrared to the ultraviolet. The primary advantages of long wavelength imaging are the higher contrast for hot objects and more effective detection of reflected flame emission compared to images obtained from cameras operating in the visible region. This allows for improved detection of flaming fires that are not in the field of view of the camera. The approach is a compromise between expensive, spectrally discriminating cameras operating in the mid IR and inexpensive, thermally insensitive visible cameras. Our approach exploits the long wavelength response of standard CCD arrays used in many cameras (e.g., camcorders and surveillance cameras). This region is slightly to the red (700-1000 nm) of the ocular response (400-650 nm). A long pass filter transmits light with wavelengths longer than a cutoff, typically in the range 700-900 nm. This increases the contrast for fire, flame, and hot objects and suppresses the normal video images of the space, thereby effectively providing some degree of thermal imaging. There is more emission from hot objects in this spectral region than in the visible (<600 nm). Testing has demonstrated detection of objects heated to 400ºC or higher. A simple luminosity-based algorithm has been developed and used to evaluate camera/filter combinations for fire, smoke and nuisance event detection [11].

The other optical detection method is a collection of narrowband, single element spectral sensors. These include commercial off the shelf (COTS) UV/IR flame detectors modified so that the individual outputs can be monitored independently. Other sensors operating in narrowbands (10 nm) at visible (589 nm) and near infrared wavelengths (766 and 1060 nm) were also investigated; the spectral bands were chosen to match flame emission features identified in spectra measured for fires with different fuels. In a stand-alone configuration, combinations of the single channels were found to yield comparable results as the COTS flame detectors for identifying fires, both in and out of the field of view, and better performance for detecting some smoke events and several nuisance sources. It is expected that one or more of the single element sensors

will significantly reduce the false alarms without degrading the sensitivity in a combined system that includes VID and LWVD elements.

Another key aspect of the Volume Sensor Task is the evaluation of acoustic signatures for enhanced discrimination of damage control events, particularly flooding and pipe ruptures. A representative set of fire and water acoustic event signatures and common shipboard background noises have been measured. Measurements were made aboard the ex-USS *Shadwell* and in a full-scale laboratory test for fire, in a wet trainer for flooding/ruptures, and on two vessels, naval and research, for shipboard ambient noise. The event signatures and noise signals are being compared in the time and time-frequency domains. Results have indicated that clear differences in the signatures are present and algorithms are being developed to distinguish the various events. Flooding and pipe ruptures are loud events, and a simple broadband energy detector, in the high frequency band 7-17 kHz with an exponential average has been effective even in a noisy environment like an engine room. The algorithm being developed for the Volume Sensor Prototype uses the variance of the level with time for discrimination of events. Some nuisance events, grinding, cutting torches and arc welding, are also loud, but have level variations with time that distinguish them from flooding and pipe rupture events. Fire events are the quietest, however, some distinctive characters are observed.

Pattern recognition and data fusion algorithms have being developed to intelligently combine the individual technologies with the goal to expand detection capabilities (flame, smoke, flood, pipe ruptures, hot objects) and to reduce the false alarm rate. Enhanced sensitivity, improved event discrimination, and shorter response times will be the milestones for success. The algorithms being developed capture the strengths of specific sensor types and systems while minimizing their weaknesses. The successful components are currently being integrated into a prototype system. Visual images and machine vision are used for motion and shape recognition to detect flaming and smoldering fires, pipe and hull ruptures, and flooding. Spectral and acoustic signatures are being used to detect selected events and to enhance event discrimination. Long wavelength image analysis provides early detection of hot surfaces, high sensitivity for ignition sources, and the capability of detecting reflected fire emission, thereby

reducing the reliance on LOS in VID systems (i.e., it provides better coverage of a space or fewer cameras). The various detection methods are being combined in a modular architectural design that allows this system to be expanded with the latest sensor technology to new and different missions. Optimization of the detection methods and development of the machine vision and multivariate data analysis methods are a major emphasis of the work.

Results

Figure 2 shows a schematic diagram of the system being developed. The Volume Sensor uses an innovative architecture that has been designed to collect and combine video with other input from a heterogeneous network of distributed sensors and systems. The system will monitor events, provide pre-alarm and alarm conditions for unusual events, plus store, archive and index alarms for easy recall. Two fusion machines are being developed. One uses the VID input from one commercial company and the other uses the input from the other system. Both VID manufacturers were contracted to provide middleware to allow their systems to communicate over a network to the Volume Sensor Fusion Machine. The communication protocol has been designed to transfer sensor data and algorithm output from sensor subsystems to a central machine for processing by a fusion algorithm. There, sensor output is analyzed in a decision tree parallel to pattern recognition on the combined raw sensor data for event pre-alarm conditions. A pre-alarm triggers a second tier of more sophisticated algorithms incorporating decision rules, pattern recognition, and Bayesian evaluation specific to the event condition. Techniques being investigated include feature selection, data clustering, Bayesian classification, Fisher discriminant analysis, and neural networks.

Figure 3 shows the graphical user interface (GUI). The GUI displays all the information being combined in the Volume Sensor Prototype and gives the alarm condition based on analysis by the Volume Sensor Fusion Machine. Three camera images are shown, two visible and one near infrared (NIR). Each sensor technology is displayed, as is the overall Volume Sensor result and alarm. In the example shown below, the system indicates an alarm for a flaming fire based on the input from all the

available sensors. Preliminary results using a limited set of data have indicated a large improvement in the sensitivity and a significant reduction in the false alarm rate. More work is necessary to achieve no false alarms. The Volume Sensor Prototype design can incorporate new sensors and detection technologies as they are developed or needed.

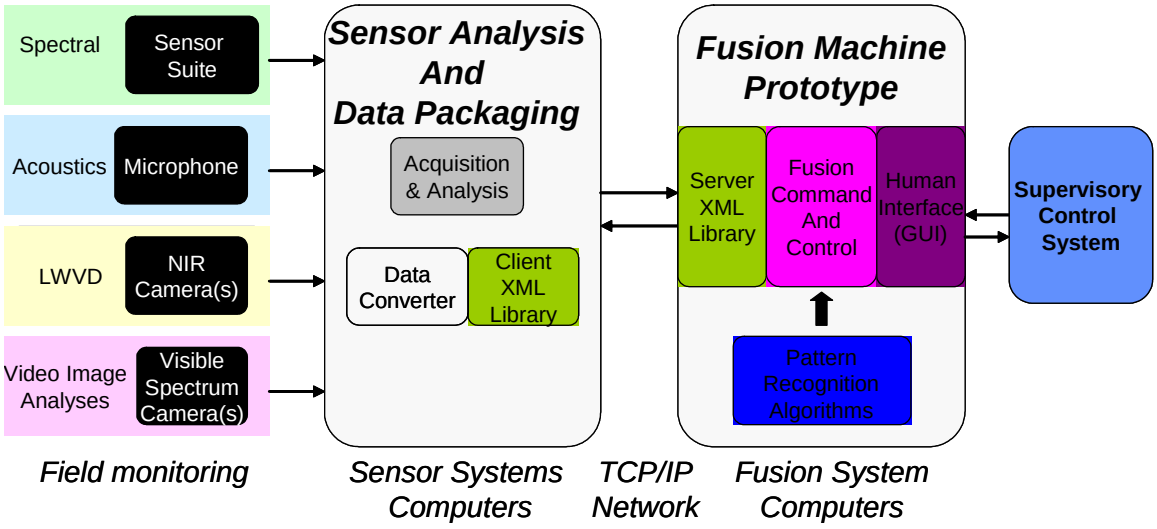

Fig 2. Volume Sensor Prototype Schematic

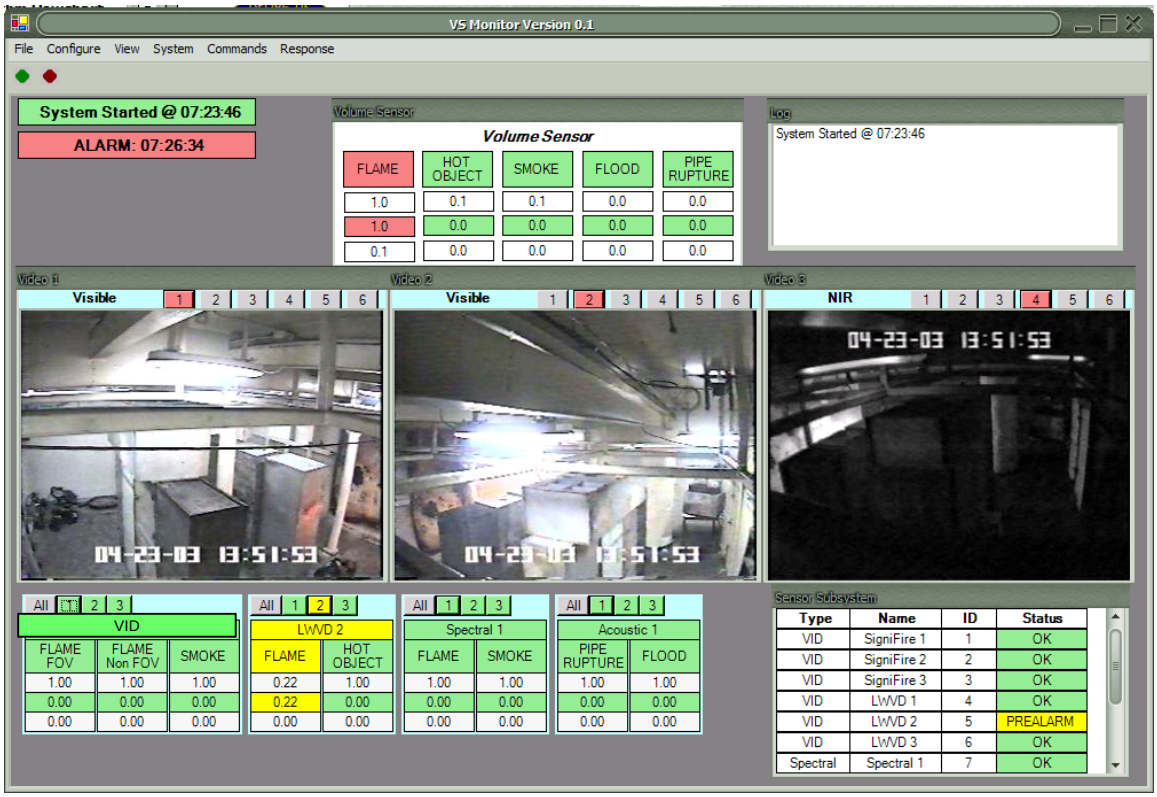

Fig 3. Volume Sensor Prototype graphical user interface

References

1. Rose-Pehrsson, S.L., Owrutsky, J.C., Gottuk, D.T., Geiman, J.A., Williams, F.W., and Farley, J.P., "Phase I: FY01 Investigative Study for the Advanced Volume Sensor," NRL/MR/6110—03-8688, June 30, 2003.

2. Gottuk, D.T., Harrison, M.A., Scheffey, J.L., Rose-Pehrsson, S.L., Williams, F.W. and Farley, J.P., "An Initial Evaluation of Video-Based Fire Detection Technologies," NRL/MR/6180—04-8737, January 9, 2004.

3. Harrison, M.A., Gottuk, D.T., Rose-Pehrsson, S.L., Owrutsky, J.C., Williams, F.W. and Farley, J. P. "Video Image Detection (VID) Systems and Fire Detection Technologies: Preliminary Results from the Magazine Detection System Response Tests," NRL Letter Report 6180/0262, Naval Research Laboratory, Washington, DC, July 21, 2003.

4. Gottuk, D.T., Harrison, M.A., Rose-Pehrsson, S.L., Owrutsky, J.C., Farley J. P., and Williams, F.W., "Shipboard Evaluation of Fire Detection Technologies for Volume Sensor Development: Preliminary Results," NRL Letter Report 6180/0282, Naval Research Laboratory, Washington, DC, August 28, 2003.

5. Lynch, J.A., Gottuk, D.T., Rose-Pehrsson, S.L., Owrutsky, J.C., Steinhurst, D.A., Minor, C.P., Wales, S.C., Williams, F.W. and Farley, J. P., "Volume Sensor Development Test Series 2 – Lighting Conditions, Camera Settings, and Spectral and Acoustic Signatures," NRL/MR/6180--04-XXXX, June 2004 (in review).

6. Owrutsky, J.C., Steinhurst, D.A., Nelson, H.H., and Williams, F.W., "Spectral Based Volume Sensor Component," NRL/MR/6110--03-8694, July 30, 2003.

7. Steinhurst, D.A., Owrutsky, J.C., Rose-Pehrsson, S.L., Gottuk, D.T., Williams, F.W., and Farley, J.P., "Spectral-Based Volume Sensor Testbed VS1 Test Series Results ex-USS SHADWELL, April 20-25, 2003," NRL Letter Report 6110/075, Naval Research Laboratory, Washington, DC, June 27, 2003.

8. Wales, S.C., McCord, M.T., Lynch, J.A., Rose-Pehrsson, S.L., and Williams, F.W., "Acoustic Event Signatures for Damage Control: Water Events and Shipboard Ambient Noise," NRL/MR/7120—04-XXXX, June 2004 (in review).

9. Rose-Pehrsson, S.L., Owrutsky, J.C., Williams, F.W., Steinhurst, D.A., and Minor, C.P., "Volume Sensor Algorithm Development: Feasibility Study for the Improvement of Video-Based Smoke and Fire Detection Using Near Infrared Cameras," NRL Ltr Rpt 6110/051, Naval Research Laboratory, Washington, DC, April 14, 2004.

10. Rose-Pehrsson, S.L., and Williams, F.W., "Volume Sensor Algorithm Development: Application of a Machine Learning Approach to On-Board Fire Detection Using Video Cameras," NRL Ltr Rpt 6110/052, Naval Research Laboratory, Washington, DC, April 14, 2004.

11. Steinhurst, D.A., Minor, C.P., Owrutsky, J.C., Rose-Pehrsson, S.L., Gottuk, D.T., Williams, F.W., and Farley, J.P., "Long Wavelength Video-Based Event Detection, Preliminary Results from the CVNX and VS1 Test Series, ex-USS SHADWELL, April 7-25, 2003," NRL/MR/6110-03-8733, December 31, 2003.

12. Gottuk, D.T., Lynch, J.A., Rose-Pehrsson, S.L., Owrutsky, J.C., and Williams, F.W., "Video Image Fire Detection for Shipboard Use," *AUBE'04 – Proceedings of the 13th International Conference on Automatic Fire Detection*, Duisburg, Germany, September 14-16, 2004.

13. Owrutsky, J.C., Steinhurst, D.A., Minor, C.P., Rose-Pehrsson, S.L., Gottuk, D.T., and Williams, F.W., "Long Wavelength Video Detection of Fire in Ship Compartments," *AUBE'04 – Proceedings of the 13th International Conference on Automatic Fire Detection*, Duisburg, Germany, September 14-16, 2004.

Peter Schildhauer

Allianz Zentrum für Technik GmbH
Ismaning, Deutschland

Methoden der Bandursachenermittlung

Abstract

Fire investigation is a complex problem, which in Germany has to be solved by experts of criminal police and private investigators of insurance companies under different respects. Since there are a lot of different influences on the evidence available, such as the fire itself, the work of the fire services, the owner of not burned items, etc. a fire investigator needs every little information about the place and the time, the fire started.
This means, that the data available from a fire detection system after a fire are a very precious source of information.
Place, time and sequence of responding detectors give an precise view on the fire spread. Based on these data it can for example be said, whether there are hints of a possibly unnatural fire cause (arson) or not.
Examples out of the real life give an idea what a fire detection system and its data are good for in fire investigation procedures.

Einführung

Auf den ersten Blick hat automatische Branderkennung nicht viel mit Brandursachenermittlung zu tun. Die Branderkennung soll durch frühzeitige Entdeckung von Brandanzeichen und entsprechende Alarmierungsmittel Menschenleben retten, die Brandbekämpfung erleichtern und Sachwerte vor Schäden schützen. Die Brandermittlung beginnt erst da, wo selbst die Feuerwehr die Brandstelle bereits verlassen hat. So scheint es wenigstens...
Ziel der Brandursachenermittlung ist es zunächst, festzustellen, auf welche Weise, also durch welche äußeren Umstände, Stoffeigenschaften, menschlichen Handlungen oder Unterlassungen ein Brand entstehen konnte. Dabei gibt es jedoch unterschiedliche

Blickwinkel, je nach dem, wer die Ermittlung durchführt. Zunächst hat die Kriminalpolizei (mit oder ohne Unterstützung des Landeskriminalamtes oder des Bundeskriminalamtes) im Auftrag der zuständigen Staatsanwaltschaft zu ermitteln, ob der Brand durch eine nach § 306, StGB strafbare Handlung oder Unterlassung verursacht wurde oder nicht. Ist dies nicht der Fall oder aber nicht beweisbar, wird die Akte entweder ohne Eröffnung eines Strafverfahrens geschlossen oder ein Gericht entscheidet, dass eine solche Handlung nicht vorliegt.

Nach den Kollegen der Kriminalpolizei haben privatwirtschaftliche Ermittler die Möglichkeit, die Brandstelle zu untersuchen. Dabei kann es um die Verteidigung eines Beschuldigten gehen, um Unterstützung der Nebenklage in einem Strafverfahren oder um zivilrechtliche Ansprüche. Bei der Ermittlung durch oder für einen Versicherer spielen Aspekte wie Obliegenheitsverletzung, Übereinstimmung der verbrannten Gegenstände mit den versicherten nach Wert und Menge, Haftung, Regressmöglichkeiten, aber auch Erkenntnis zur Schadenvermeidung an ähnlichen Anlagen, Gebäuden oder sonstigen Werten eine Rolle. Oftmals ist bei einem sich anbahnenden Rechtsstreit Stellung zu Gutachten der Gegenseite zu nehmen, ob die dargestellten Sachverhalte in sich schlüssig sind und mit den Befunden auf der Brandstelle übereinstimmen.

Grundzüge der Arbeitsweise

Grundsätzlich ist zu unterscheiden zwischen Zündquelle und Brandursache. Unter Zündquelle versteht man eine Energiequelle (Funken, Flammen, heiße Gase, heiße Oberflächen, etc.), welche der Größe nach hinsichtlich Geometrie und Eigenschaften des zu entzündenden Stoffes diesen zu entzünden vermag.

Die Brandursache hingegen ist die Summe aller Umstände, einschließlich menschlicher Handlungen und Unterlassungen, die einer hinreichend großen Zündquelle ermöglichten, an einer geeigneten Stelle eines brennbaren Stoffes unter Luftatmosphäre oder einem anderen Oxidationsmittel wirksam zu werden.

Das hört sich kompliziert an und ist es in den meisten Fällen auch.

Man wird auf der Brandstelle versuchen, anhand der Brand- und Rauchspuren und dem zunehmenden Abbrand zuerst den Brandausbruchsbereich einzugrenzen. Hier gilt es den zuerst in Brand gesetzten Stoff zu identifizieren. Aus dessen Geometrie, Lage im

Raum, Kombinationen mit anderen Stoffen und den daraus folgenden Zündeigenschaften lässt sich meist Lage und Größe einer geeigneten Zündquelle rekonstruieren. Nach dieser Zündquelle, bzw. nach Objekten und deren Relikten, aus denen die Zündenergie hervorgegangen sein kann, wird im Brandausbruchsbereich gesucht.
Umgekehrt besteht die Möglichkeit, dass eine potentielle Zündquelle (Ofen, elektrisches Gerät o.ä.) erhalten geblieben ist. Dann ist nach einem Stoff zu suchen, der gezündet worden sein kann. Hier ist auch zu klären, ob der betreffende Stoff betriebsmäßig in der Nähe der Zündquelle auftaucht oder durch welche Umstände er im Brandfall in die Nähe der Zündquelle gelangen konnte.
Oft muss sich die Untersuchung mit der Suche nach einem brennbaren Stoff und einer Zündquelle befassen. Dies insbesondere dann, wenn es keine Zeugen gibt, diese sich an nichts zweckdienliches erinnern können oder verstorben sind.
Finden sich im Brandschutt asservierungsfähige Stoffe, können Proben genommen werden, um die Feststellung der Stoffeigenschaften und die Stoffidentifikation im Labor vorzunehmen und eventuell das Brandgeschehen in einem Brandraum in Originalgröße nachzustellen.

Der Brandursachenermittler steht immer vor dem mitunter großen Problem, dass er nie der erste auf der Brandstelle ist. Zunächst verändert das Feuer selbst die brennende Umgebung, so dass sie selbst für mit ihr vertraute Personen bis zur Unkenntlichkeit verändert werden kann. Vor dem Brandermittler ist als nächstes immer die Feuerwehr tätig, wodurch sich im Rahmen der Gefahrenabwehr (bisweilen auch außerhalb derselben) unvermeidbare Veränderungen des Brandortes ergeben. Nach dem Abrücken der Feuerwehr können des Weiteren umfangreiche Verkehrssicherungsmaßnahmen wie Abstützen, Abdecken, Absperren oder auch Niederreißen von Wandteilen, Dachstühlen oder Decken notwendig werden, welche vom zuständigen Bauamt veranlasst werden. Bevor die Standfestigkeit nicht festgestellt wurde, dürfen strenggenommen nicht einmal die Kollegen von der Kriminalpolizei die Brandstelle betreten. Die privatwirtschaftlichen Ermittler haben auf die Freigabe durch die Kriminalpolizei zu warten. Auf diesem Wege vergehen manchmal Tage, oft auch Wochen, bevor eine Brandstelle begehbar ist. Auch der Eigentümer hat ein berechtigtes Interesse, noch

erhaltene Gegenstände vor der weiteren Schädigung durch Löschwasser oder Wettereinflüsse zu bewahren und entfernt sie aus dem Brandbereich. Schließlich sind Brandstellen oft nicht genügend vor „Katastrophentouristen“ zu sichern.

Oft sind dann die Unterschiede zwischen der ursprünglichen Lage und der aufgefundenen Lage nicht mehr zu rekonstruieren, zumal es nur selten Fotodokumente vom Zustand unmittelbar vor dem Brand gibt, mit denen man die Brandstelle abgleichen könnte. Da helfen nur aufwändige Ermittlungen bei allen auf der Brandstelle tätigen Personengruppen. Meist können diese sich aber auch nicht mehr genau erinnern, ob ein bestimmter Gegenstand lag oder stand, sich über oder unter einem anderen befand, oder in diesem Raum oder jenem.

Da Brandermittler oft mit Pathologen verglichen werden, die ja die Ermittlung von Todesursachen betreiben, sei die Bemerkung erlaubt, dass diese im Hinblick auf die verfügbare Spurenlage verglichen mit Brandermittlern die bessere Ausgangsposition haben. Allerdings möchte ich trotzdem nicht mit ihnen tauschen.

Es ist also insgesamt ein zwar interessantes, aber mühseliges Geschäft, dem oft genug der Erfolg versagt bleibt, die Ursache mit allen einflussnehmenden Details beweisen oder auch „nur“ anhand von Indizien aufklären zu können. Fehlen objektive Sachbeweise, müssen mögliche Ursachen der Reihe nach eliminiert werden (sogenanntes Ausschlussverfahren). Bleibt unter Berücksichtigung aller bekannten Fakten nur eine mögliche Ursache übrig, muss dies die Brandursache sein. Meist bleiben jedoch mehrere Möglichkeiten, die anhand von Wahrscheinlichkeits-betrachtungen weiter eingegrenzt werden können; ein gerichtsverwertbarer „Beweis“ ist das aber nicht.

Kurz gesagt gleicht die Brandursachenermittlung einem bisweilen kriminalistischen Puzzlespiel, von dem aber weder die Anzahl der Teile bekannt ist, noch, welches Bild das Puzzle später eigentlich darstellen wird.

Um im Bild zu bleiben ist der Ermittler umso erfolgreicher, je mehr Puzzlesteine erhalten geblieben sind und für die Untersuchung zur Verfügung stehen. Die Wahrscheinlichkeit, dass die Ursache eines Brandes aufgeklärt werden kann, steigt also in dem Maße an, wie nach einer erfolgreichen Brandbekämpfung eine durch die Feuerwehr und das Feuer selbst möglichst wenig veränderte Szenerie übrigbleibt oder

Zeugen mit sehr präzisen Angaben verfügbar sind. An dieser Stelle erweist sich die Bedeutung der Brandentdeckung im allgemeinen und der automatischen Branderkennung im Besonderen für die erfolgreiche Arbeit des Brandermittlers.

Unterstützung der Brandursachenermittlung durch die Brandentdeckung

Aus dem hinlänglich bekannten Diagramm, das den Zusammenhang von Branddauer und Schadenhöhe wiedergibt, geht nicht nur die Bedeutung einer frühen Brandentdeckung für die Einleitung und den Erfolg von Brandbekämpfungsmaßnahmen hervor (von Personenrettung ganz zu schweigen), sondern es zeigt implizit auch, dass eine frühe Brandentdeckung auch mehr erhalten hilft, was anschließend für eine erfolgreiche Untersuchung benötigt wird.

Das heißt, die Brandentdeckung hilft grob gesagt auf dreierlei Art bei der Ursachenermittlung:

- Brandentdeckung in jeder Form und Bekämpfung vor Eintritt des Vollbrandes erhält objektive Spuren
- Automatische Brandentdeckung (z.B. durch Heimrauchmelder, aber auch in jeder anderen frühzeitigen Form) rettet Menschen, die möglicherweise als Zeugen befragt werden können
- Automatische Brandmeldeanlagen liefern Aufzeichnungen über Anzahl und Reihenfolge von ansprechenden Detektoren mit Zeit- und Ortsangaben, so dass auch später noch der Brandverlauf objektiv dokumentiert ist.

Naturgemäß kommt in Brandfällen den Daten der automatischen Brandmeldeanlage eine besondere Schlüsselstellung zu, da sie sowohl räumlich als auch zeitlich die Brandentstehung eingrenzen helfen, sofern die Daten nach dem Brand noch verfügbar sind. An Fällen aus der Praxis soll gezeigt werden, welche Bedeutung die Daten der Brandmeldeanlage auch für die Rekonstruktion unklarer Brandverläufe haben kann.

Im Einzelfall können u.a. folgende Gesichtspunkte von großer Bedeutung sein:

- Wurden alle vom Brand betroffenen Räume mit Brandmeldern überwacht?
- Wenn nicht, aus welchem Grund?

- Waren die vorhandenen Melder in Stückzahl und Bauart für die vorhandene Brandlast geeignet?
- Wurden sie regelmäßig auf Funktion überprüft?
- Wo lief der Alarm auf?
- War die Anlage ganz oder gruppenweise abgeschaltet?
- Wer hat ggfs. die Abschaltung aus welchem Grund und zu welchem Zeitpunkt veranlasst?
- Warum wurde nicht wieder eingeschaltet?
- Welcher Melder hat an welcher Stelle zu welchem Zeitpunkt reagiert?
- In welchen Zeitabständen und welcher Reihenfolge folgten weitere Melder?
- An welchen stellen befanden sich diese?
- Ergibt sich daraus eine logische Reihenfolge bzgl. der Brandausbreitung?
- Wie lange dauerte es vom Notruf (automatisch oder manuell) bis zum Eintreffen der Löschkräfte?

<u>Fall 1: keine Brandmeldeanlage, Brandentdeckung durch Passanten</u>

In der Nacht vom 27.12. auf den 28.12. wurde gegen 03:00 Uhr früh ein Passant auf die erleuchteten Fenster einer Kirche in einer deutschen Kleinstadt aufmerksam. Die Kirche liegt auf einem kleinen Hügel inmitten von Bäumen etwas abseits der Straße. Sie wurde im 13. JH aus Feldsteinen erbaut, Dachstuhl und Einrichtung bestanden aus Holz. Der kleine Glockenturm war als Dachreiter in der Mitte des Langschiffes aufgesetzt. Das Dach war mit Reet gedeckt. Anzeichen für gewaltsames Eindringen an Fenstern und Türen wurden nicht gefunden. Zuletzt war die Kirche am 26.12. mittags genutzt worden. Anschließend wurden alle elektrischen Verbraucher ausgeschaltet und die Kirche verschlossen. Wachskerzen seien aus Sicherheitsgründen nicht verwendet worden. Da das Innere zumeist aus Holz bestand, hätte mit einer BMA das Gebäude mit hoher Wahrscheinlichkeit gerettet werden können. Auch wäre eine präzisere Antwort bezüglich der Brandursache möglich gewesen, so dass man Maßnahmen hätte ergreifen können, um ähnliche Vorfälle künftig zu vermeiden. Wegen der späten Brandentdeckung war der Feuerwehr ein Innenangriff nicht mehr möglich. Die Kirche brannte außer einigen Anbauten vollständig aus. Die Glocke wurde im verkohlten Holz nach dem Brand nicht mehr wiedergefunden. Wegen der starken Zerstörung konnte

zwar ein Brandausbruchsbereich eingegrenzt werden. Als Brandursache blieb per Ausschlussverfahren nur ein technischer Defekt am Hausanschlusskasten übrig, wobei das versagende Bauteil jedoch nicht mehr ermittelt werden konnte. Für Brandstiftung gab es keinerlei Anhaltspunkte. Gänzlich ausgeschlossen werden (im Sinne von bewiesenermaßen) kann auch sie nicht.

Fall 2: keine BMA; Brandentdeckung durch Bewohner desselben Dorfes

In diesem Fall war eine Kindertagesstätte betroffen. Der Brand ereignete sich an einem Gründonnerstag, an dem die KiTa gegen 13.00 Uhr verlassen wurde. Das Fenster des Büros blieb gekippt und wurde üblicherweise von der Putzfrau später geschlossen. Der Hausmeister war bis ca. 15:15 Uhr mit Reinigungsarbeiten an der Dachrinne beschäftigt. Entdeckt wurde der Brand von einem Dorfbewohner durch die in einer Entfernung von ca. 500 m sichtbaren, aufsteigenden Rauchwolken gegen 15:45 Uhr. Da brennende Kerzen, Tabakglut, Sonneneinstrahlung, Selbstentzündung, Heißarbeiten etc. ausgeschlossen werden konnten (z.T. nur anhand von Aussagen), blieben auch hier die möglichen Ursachen technischer Defekt von elektrischen Geräten oder Anschlüssen oder aber Brandstiftung übrig.

Hier hätte der Schaden am Gebäude, das wegen der Holzbauweise und der starken Verrauchung wahrscheinlich neugebaut wird, mit einer frühzeitigen Branderkennung stark verringert werden können. Auch die Brandursache wäre sicherlich aufzuklären gewesen, wenn früher hätte eingegriffen werden können.

Fall 3: Branderkennung vorhanden, Weiterleitung an BF außer Funktion

Ein größeres, in zwei Abschnitten errichtetes Betonfertigteilgebäude von rechteckigem Grundriss war der Länge nach auf zwei Firmen aufgeteilt. In einer Firma wurde auf teuren Maschinen produziert, in der anderen befand sich hauptsächlich ein Lager. Als das Feuer im Lager am frühen Morgen von einem Mitarbeiter entdeckt wurde, drückte er den Druckknopfmelder, etwa zeitgleich mit einem Kollegen an einer anderen Stelle, worauf beide das Gebäude verließen. Was beide nicht erkennen konnten, war, dass der Druckknopfalarm anscheinend von der Brandmeldezentrale nicht an die Leitstelle der Feuerwehr weitergeleitet wurde. Der Brand wurde schließlich von der BMA des Nachbarbetriebes erkannt und erfolgreich gemeldet. Bei der Untersuchung stellte sich

heraus, dass die Übertragungseinheit der Feuerwehr als Schnittstelle zwischen BMA und Feuerwehrfernmeldenetz nicht ausgelöst worden war. Beim Eintreffen der Feuerwehr war der Raum mit der BMZ noch nicht vom Brand betroffen. Da sich der Brand jedoch sehr schnell ausdehnte, war der brandtechnisch nicht vom Lager abgetrennte BMZ-Raum nicht zu retten. Glücklicherweise konnte jedoch der zweite Betrieb fast vollständig gehalten werden. Zu Beginn der Brandbekämpfung wären also noch Daten verfügbar gewesen, die Aufschluss über den Betriebszustand der BMZ hätten liefern können, nach dem Übergriff der Flammen wurde die BMZ jedoch so stark beschädigt, dass diese Rückschlüsse nicht mehr möglich waren.

Fall 4: BMA vorhanden, Aufschaltung auf Wachdienstzentrale

In einer fernüberwachten verfahrenstechnischen Anlage war nach Feierabend noch eine Kontrolle eines Messgerätes im Verwaltungsgebäude durchgeführt worden. Kurz darauf wurde von Passanten der Brand entdeckt und die örtliche Feuerwehr alarmiert. Die einzige zum Zeitpunkt der Brandentstehung im Gebäude anwesende Person verstarb, so dass genaue Aussagen eines direkten Zeugen zum Schadenablauf nicht verfügbar waren. Möglicherweise hätte dieser Brand früher bekämpft werden können, denn die Alarme der BMA liefen bereits 8 min vor der Alarmierung der Feuerwehr in der Zentrale des Wachdienstes (ständig besetzte Stelle, ca. 600 km entfernt) auf, wo anscheinend jedoch nicht bekannt war, wer bei einem Brandalarm zu benachrichtigen ist. Da der Brandort ein überaus komplexes Spurenbild zeigte, war die Ermittlung äußerst schwierig. Da es keinen Anlass gab, an den Daten der Alarmierungsreihenfolge zu zweifeln, bevor die Kabel zerstört wurden, konnte aus der Reihenfolge der ansprechenden Rauchmelder auf die Brandausbreitungsrichtung gefolgert werden, was letztlich dabei half, zusammen mit den Erklärungen für die einzelnen Brandspuren eine klarere Vorstellung vom Brandverlauf zu bekommen und begründete Rückschlüsse auf die Brandursache ziehen zu können. Es sei aber darauf hingewiesen, dass das Ergebnis eine plausible Erklärung war, jedoch kein Beweis im strengen Sinn. Da derzeit noch ein Zivilverfahren anhängig ist, mögen diese Hinweise genügen. Über den Fall wird zu einem geeigneten Zeitpunkt noch zu berichten sein.

Fall 5: BMA vorhanden, Alarmierung erfolgreich

Der Brand fand auf einem Transportschiff auf hoher See statt. Nach erfolgreicher Bekämpfung mit Bordmitteln ergaben sich zwei unterschiedliche Versionen über den Brandentstehungsort auf zwei unterschiedlichen Ladedecks. Eine Version steht in Übereinstimmung mit der Überzahl an Zeugenaussagen, Beobachtungen und dem Ausdruck der Brandmeldeanlage. Die andere Version stützt sich alleine auf die Aussage zweier Offiziere, wonach wegen Fehlalarmen auf dem bewussten Deck diese Melderlinie abgeschaltet worden sei und man auch mehr als eine Woche später nach der Beladung des zunächst leeren Decks noch vergessen habe, sie wieder einzuschalten. Da der tatsächliche Brandentstehungsort massive finanzielle Auswirkungen hätte, wurde dieser Frage intensiv nachgegangen. Das Verständnis der BMA führte zusammen mit anderen speziellen Umständen dieses Falles zu erheblichen Zweifeln an der Richtigkeit dieser zweiten Version. Da auch dieser Fall aufgrund seiner Komplexität noch nicht endgültig geklärt ist, kann hier im Detail nicht weiter darauf eingegangen werden.

Fazit

Es sollte verdeutlicht werden, welche Ziele die Ermittlung der Ursache in einem Brandfall hat und welche Hindernisse der Klärung im Wege stehen. Da „Brand“ an sich bereits ein hochkomplexes Geschehen darstellt, das durch den Einfluss menschlicher Handlungen (Brandbekämpfung, Verkehrssicherung, Bergung, etc.) oftmals nicht eben erleichtert wird, muss jede Information genutzt werden, die verfügbar ist. Eine wesentliche Quelle objektiver Informationen stellen BMA und evtl. vorhandene oder erzeugbare Ausdrucke über Zeitpunkte und -abfolgen von aufgelaufenen Alarmen dar. Mitunter sind sie sogar maßgeblich an der Aufklärung von Brandfällen beteiligt. Diese Möglichkeit setzt jedoch voraus, dass ein in Brand geratenes Objekt mit einer BMA ausgestattet war. Daher sollten auch Objekte, für die keine Pflicht besteht, eine BMA einzubauen, wenn sie hohe Werte (auch historische z.B. Kirchen) enthalten und anders nicht geschützt werden können, mit einer solchen Anlage ausgerüstet werden.

B. Bansemer, F.-W. Wittbecker
Universität Wuppertal, Deutschland

Rauchgasanalyse mit FTIR-Spektroskopie zur Ermittlung toxischer Materialpotenziale

Abstract

The use of FTIR spectroscopy for fire effluent analysis continues to gain in importance. In contrast to conventional selective methods, the FTIR technique is capable of measuring all toxicologically relevant fire gases such as CO, CO_2, HCN etc. simultaneously. This paper outlines the operating principle of FTIR and its applicability in terms of fire gas analysis. Emphasis is placed on the method-specific main problems: the calibration and the analysis of fire gas spectra.

Einleitung

Traditionell werden in der Rauchgasanalytik verschiedene selektive Verfahren für die einzelnen Rauchgaskomponenten verwendet, die zum Teil sehr zeitaufwendig sind. Die FTIR-Spektroskopie stellt in der Rauchgasanalytik eine relativ neue Methode dar, die sich zurzeit für brandtechnologische Untersuchungen noch in der Exploration befindet, in anderen Bereichen jedoch erprobt seit langem eingesetzt wird. Diese Analysemethode bietet den essentiellen Vorteil, dass alle toxikologisch relevanten Rauchgaskomponenten simultan und zeitaufgelöst bestimmbar sind.

In dem vorliegenden Beitrag wird erläutert, wie die FTIR-Methode speziell in rauchgastoxikologischen Untersuchungen eingesetzt wird. Dabei wird gezielt auf die in diesem Anwendungsbereich auftretenden Hauptschwierigkeiten eingegangen: die Kalibrierung des Spektrometers und die Auswertung von Rauchgasspektren. Die nachfolgenden Ausführungen sind Ergebnisse einer Forschungsarbeit[1], in der ein Modell zur szenarioabhängigen Beurteilung des toxischen Potenzials von Materialien und Produkten im Brandfall entwickelt wurde. Die dem Modell zu Grunde liegenden experimentellen Untersuchungen erfolgten mit einer neu entwickelten Versuchsapparatur im Labormaßstab, mit der materialspezifische Rauchgase unter systematischer Variation der Zersetzungsbedingungen erzeugt wurden. Die Konzentrationen der

toxischen Hauptkomponenten (CO, CO_2, HCN etc.) wurden FTIR-spektroskopisch bestimmt und auf dieser Basis toxische Materialpotenziale prognostiziert und szenarioabhängig dargestellt.

Funktionsprinzip der FTIR-Spektroskopie

Die Analyse von Gasen mit spektralanalytischen Verfahren basiert auf der Eigenschaft von Gasmolekülen, elektromagnetische Strahlung zu absorbieren. Üblicherweise erfolgt die Analyse im mittleren infraroten Spektralbereich (MIR, von ca. 400 bis 4000 cm^{-1}), in dem fast alle gasförmigen Substanzen intensive Absorptionsbanden besitzen. Gasmoleküle, die mit elektromagnetischer Strahlung in Wechselwirkung treten, nehmen Energie auf und werden zu Schwingungen und Rotationen angeregt. Die physikalischen Eigenschaften eines Moleküls, wie Atommassen und -abstände sowie Bindungskräfte und -winkel, bestimmen dessen individuelle Absorptionscharakteristik. Nur in bestimmten, molekülspezifischen Spektralbereichen wird Strahlung absorbiert, wodurch im Spektrum charakteristische Banden erzeugt werden. In Abbildung 1 ist ein Rauchgasspektrum von Polyamid 6 dargestellt, in dem die Absorptionsbanden diverser Brandgase zu erkennen sind. Anhand der Lage und der Form ihrer Absorptionsbande(n) lässt sich eine Substanz identifizieren, die Intensität der Bande(n) gibt Auskunft über die Konzentration des Stoffes. Ein Molekül kann aber nur dann durch IR-Strahlung zu Schwingungen und Rotationen angeregt werden, wenn es ein elektrisches Dipolmoment (eine ungleichmäßige Ladungsverteilung) besitzt oder dieses durch die Schwingungsanregung erzeugt wird. Dies ist bei allen mehratomigen und heteronuklearen zweiatomigen Molekülen (z. B. CO) der Fall. Elemente (z. B. Rn) und homonukleare zweiatomige Moleküle (z. B. N_2 und O_2) erfüllen diese Voraussetzung nicht und sind daher IR-spektralanalytisch nicht detektierbar.

Abbildung 2 zeigt schematisch den Aufbau eines FTIR-Spektrometers. Das besondere Merkmal der FTIR-Spektroskopie ist, dass die IR-Strahlung zunächst zur Interferenz gebracht wird, bevor sie die (Gas-)Probe passiert. Dazu wird ein Michelson-Interferometer eingesetzt, das aus einem halbdurchlässigen Spiegel (dem Strahlteiler) sowie einem festen und einem beweglichen totalreflektierenden Spiegel besteht. Trifft die von einer IR-Quelle emittierte Strahlung auf den Strahlteiler, wird die Hälfte der Strahlung in Richtung des beweglichen Spiegels transmittiert und die andere Hälfte in

Richtung des festen Spiegels reflektiert. Beide Teilstrahlen werden von den Spiegeln zurückgeworfen und treffen wieder auf den Strahlteiler, wo wiederum die Hälfte der Strahlung (Teilstrahlen A und B) in Richtung des Detektors reflektiert wird, während die andere Hälfte (Teilstrahlen C und D) durchgelassen wird und für die Messung verloren geht. Da beide auf den Strahlteiler treffende Strahlhälften kohärent sind, interferieren sie bei der Rekombination in Abhängigkeit von der Auslenkung x des beweglichen Spiegels konstruktiv oder destruktiv. Die Bewegung des Spiegels erzeugt also einen optischen Gangunterschied beider Teilstrahlen, wodurch jede einzelne Wellenlänge der Ausgangsstrahlung durch ihr spezifisches Interferenzmuster „markiert" wird.

Der Detektor registriert die Intensität der empfangenen Strahlung I_D in Abhängigkeit von der Spiegelauslenkung x und wandelt dieses Signal in ein elektrisches Signal, das als Interferogramm bezeichnet wird, um. Das Interferogramm $I(x)$ ist eine *orts*abhängige Darstellung der Strahlungsintensität, die zu jeder Spiegelposition x die Summe der Intensitäten I aller emittierten Wellenzahlen $\tilde{\nu}$ angibt. Durch Fouriertransformation wird das Interferogramm $I(x)$ in ein Spektrum $S(\tilde{\nu})$, also eine *wellenzahl*abhängige Darstellung der Strahlungsintensität, umgewandelt. Die Struktur dieser Spektren, die als *Intensitäts*- oder *Einstrahlspektren* bezeichnet werden, wird neben der Absorptionscharakteristik der Gasprobe zusätzlich durch die Intensitätsverteilung der Strahlungsquelle, die Transmissionsfunktion des Spektrometers sowie die Empfindlichkeit des Detektors bestimmt. Diese Parameter sind bei jedem Spektrometer individuell verschieden und unterliegen darüber hinaus diversen Umgebungseinflüssen (z. B. Temperaturdifferenzen). Wegen ihrer variablen Struktur sind Intensitätsspektren zur Auswertung nicht geeignet, denn die quantitative Spektralanalyse beruht auf dem Vergleich mit Kalibrierspektren. Die Störeinflüsse lassen sich eliminieren, indem zunächst ein *Hintergrund*spektrum (i. d. R. von der Umgebungsluft oder von einem nicht IR-aktiven Gas wie z. B. Stickstoff) und anschließend ein *Proben*spektrum der zu analysierenden Gasprobe aufgenommen werden. Der Quotient aus beiden Intensitätsspektren ergibt ein *Transmissions*spektrum, welches nicht die spektrale Gesamtintensitätsverteilung zeigt, sondern nur den Anteil der durchgelassenen Strahlungsintensität in Abhängigkeit von der Wellenzahl. Üblicherweise wird das Transmissionsspektrum in ein *Extinktions*spektrum (vgl. Abb. 1) umgerechnet. Dies erfolgt auf der

Basis des *Lambert-Beerschen Gesetzes*, welches (in diesem Kontext) die Schwächung der Strahlungsintensität beim Durchlaufen einer absorbierenden Gasprobe beschreibt:

$$E(\tilde{\nu}) = \varepsilon(\tilde{\nu}) \cdot c \cdot d = -\ln T(\tilde{\nu}) = -\ln \frac{I(\tilde{\nu})}{I_0(\tilde{\nu})} \qquad (1)$$

Das Produkt aus dem (wellenzahlabhängigen) Extinktionskoeffizienten ε, der Konzentration der absorbierenden Substanz c und der Schichtdicke der Gasprobe (bzw. der Absorptionsstrecke) d wird als Extinktion E bezeichnet. Die Transmission T ist das Verhältnis der Strahlungsintensität nach dem Durchlaufen der Gasprobe I zur ursprünglichen Strahlungsintensität I_0. Demnach ist die Extinktion der negative natürliche Logarithmus der Transmission (Anmerkung: Das Lambert-Beersche Gesetz lässt sich statt zur Basis *e* äquivalent z. B. zur Basis 10 darstellen).

Der Extinktionskoeffizient, der das spezifische Absorptionsverhalten der Analysesubstanz beschreibt, ist für eine bestimmte Wellenzahl konstant und die Schichtdicke der Gasprobe ändert sich bei Verwendung derselben Gaszelle ebenfalls nicht. Theoretisch ergibt sich daraus ein linearer Zusammenhang zwischen Extinktion und Konzentration, während zwischen Transmission und Konzentration ein exponentieller Zusammenhang besteht. Daher ist die Extinktion für die quantitative Gasanalyse die günstigere Größe. In der Praxis treten jedoch Abweichungen vom Lambert-Beerschen Gesetz auf, worauf nachfolgend noch näher eingegangen wird. Weiterhin ist zu berücksichtigen, dass Gleichung (1) nur für konstante Versuchsbedingungen gültig ist, da $E(\tilde{\nu})$ zusätzlich von der Gastemperatur und dem Gasdruck abhängt.

Verwendetes Spektrometer

Die im Kontext dieses Beitrages durchgeführten Toxizitätsuntersuchungen erfolgten mit einem FTIR-Spektrometer des Typs IFS 85 der Firma *Bruker Optik GmbH*, das standardmäßig mit einem *Globar* als IR-Quelle und einem DTGS-Detektor ausgestattet ist. Die Spektrenaufnahme umfasste den Spektralbereich von 550 bis 4000 cm^{-1} bei einer spektralen Auflösung von 2 cm^{-1} und 32 Scans pro Messung. Eine Gaszelle mit einer optischen Pfadlänge von 10 cm und KBr-Fenstern kam zum Einsatz. Die gesamte Gasprobenentnahmestrecke der neu entwickelten Versuchsapparatur – einschließlich der Gaszelle – wurde mit 160 °C beheizt, um die Kondensation von Wasserdampf und anderen Zersetzungsprodukten zu verhindern. Hydrophile Substanzen, wie z. B. Chlor-

wasserstoff, würden sich andernfalls im Kondensat lösen und für die Analyse verloren gehen. Für die Spektrenauswertung ist es erforderlich, dass die Temperatur und der Druck der Gasprobe bekannt sind, da die Extinktion von diesen Parametern abhängt. Wegen der konstanten Temperierung der Gaszelle traten keine zu berücksichtigen Temperaturdifferenzen auf. Da der Umgebungsdruck aber variabel ist, wurde bei der Spektrenaufnahme der Druck in der Gaszelle gemessen und die Extinktion im resultierenden Spektrum mit dem idealen Gasgesetz korrigiert.

Kalibrierung und Spektrenauswertung

Die FTIR-spektroskopische Analyse von Rauchgasen unbekannter Zusammensetzung basiert auf dem Vergleich mit Kalibrierspektren der zu analysierenden Rauchgaskomponenten. In Abbildung 3 sind die Rauchgaskomponenten aufgeführt, mit denen das verwendete Spektrometer kalibriert wurde. Zur Aufnahme der Kalibrierspektren kamen Prüfgase mit 3 bis 9 verschiedenen Konzentrationen pro Substanz zum Einsatz. Die Anzahl der Konzentrationen richtete sich nach dem Verlauf der Extinktion-Konzentration-Beziehung der betreffenden Substanz bzw. nach dem Ausmaß der Abweichung vom Lambert-Beerschen Gesetz. Abbildung 3 zeigt außerdem die spektralen Absorptionsbereiche und die Extinktionsmaxima der kalibrierten Komponenten. Hieraus wird deutlich, dass die Auswertung der Spektren bei der Rauchgasanalyse durch FTIR-Spektroskopie ein zentrales Problem darstellt. Da die meisten Brandgase IR-aktiv sind, enthalten Rauchgasspektren oft zahlreiche Absorptionsbanden. Viele dieser Banden überlagern sich partiell oder vollständig, wodurch die qualitative und quantitative Analyse der interessierenden Substanzen erschwert wird. Insbesondere besitzt Wasserdampf, der bei Verbrennungsprozessen immer freigesetzt wird, intensive Absorptionsbanden in weiten Bereichen des MIR. Diese Problematik betrifft vor allem die Analyse von Substanzen mit geringen Extinktionskoeffizienten. Beispielsweise tritt die (einzige) NO-Bande (1750 bis 2000 cm^{-1}) selbst bei höheren Konzentrationen kaum aus dem spektralen Rauschen hervor und sie wird zudem generell von einer Wasserdampfbande überlagert, so dass die erreichbare Messgenauigkeit dieser Substanz vergleichsweise gering ist. Dagegen bereitet die Analyse von CO keine größeren Schwierigkeiten, denn die relativ intensive CO-Bande (2000 bis 2250 cm^{-1}) interferiert nur an ihren Grenzen mit einer CO_2- bzw. Wasserdampfbande (vgl. Abb. 1).

Wie nachfolgend erläutert wird, existieren multivariate Kalibriermethoden, die bei der Spektrenauswertung Überlagerungen berücksichtigen. Allerdings müssen dazu alle Störkomponenten, die die Analysesubstanz in dem für die Kalibrierung gewählten Spektralbereich überlagern, in die Kalibrierung einbezogen werden. Wegen der komplexen und nur begrenzt prognostizierbaren Zusammensetzung von Rauchgasen besteht bei der Analyse generell die Gefahr, dass nicht kalibrierte Rauchgaskomponenten die interessierende Substanz überlagern. In diesem Fall ist das zuvor erstellte Kalibriermodell zu modifizieren oder sogar neu zu entwickeln.

Ein weiteres Problem bei der Auswertung von Rauchgasspektren ist die begrenzte Gültigkeit des Lambert-Beerschen Gesetzes (Gleichung (1)). In Abbildung 4 ist exemplarisch für CO der theoretische Verlauf der Extinktion-Konzentration-Beziehung nach dem Lambert-Beerschen Gesetz tatsächlich gemessenen Werten gegenübergestellt. Es wird deutlich, dass sich in der Praxis mit steigender Konzentration ein zunehmend nichtlinearer Verlauf einstellt. Die primäre Ursache hierfür ist die spektrale Auflösung der aufgenommenen Spektren[2]. Bei hohen Auflösungen werden die Abweichungen geringer, weil die realen (feinen) Strukturen der Absorptionsbanden besser erfasst werden. Das nichtlineare Verhalten tritt substanzspezifisch unterschiedlich deutlich in Erscheinung. Bei den in dieser Arbeit durchgeführten Messungen mit einer Auflösung von 2 cm^{-1} zeigte sich, dass bei einigen Rauchgaskomponenten, deren maximal zu erwartenden Konzentrationen hinreichend klein waren, die Annahme einer linearen Beziehung zwischen Extinktion und Konzentration zu ausreichend genauen Ergebnissen führte.

Im Hinblick auf die erläuterten Probleme ist die Wahl einer geeigneten Kalibriermethode von besonderer Bedeutung. Das einfachste Verfahren beschränkt sich auf die Betrachtung singulärer Extinktionswerte. Dabei werden die Kalibrierspektren der Analysesubstanz nur bei einer diskreten Wellenzahl ausgewertet. Mit den Extinktion-Konzentration-Wertepaaren lässt sich dann eine Kalibrierfunktion formulieren, mit der unbekannte Spektren quantitativ analysiert werden können. Die ausschließliche Berücksichtigung eines einzigen Punktes des Spektrums führt allerdings zu unsicheren Ergebnissen, da z. B. statistische Schwankungen unmittelbar in die Analyse eingehen. Eine zuverlässigere Methode ist es, die Bandenfläche über einem begrenzten Spektralbereich mit der Konzentration zu korrelieren. Beide Verfahren werden als *univariat*

bezeichnet, da nur eine einzige spektrale Information (ein Extinktionswert bzw. eine Fläche) in die Kalibrierung einbezogen wird. Zwar können Abweichungen vom Lambert-Beerschen Gesetz durch Kalibrierfunktionen höherer Ordnung ohne weiteres berücksichtigt werden, doch im Falle interferierender Substanzen im betrachteten Spektralbereich führen univariate Auswertemethoden meist zu unbrauchbaren Ergebnissen.

Die Analyse von Rauchgasspektren setzt deswegen die Verwendung von *multivariaten* Kalibriermethoden voraus. Im Gegensatz zu univariaten Methoden werden bei diesen Verfahren spektrale Strukturen berücksichtigt, d. h. einem Konzentrationswert werden mehrere Extinktionswerte zugeordnet. So gelingt es, Substanzen auch bei vollständiger Überlagerung durch Störkomponenten quantitativ zu analysieren. Verbreitet eingesetzt wird das auf Faktorenanalyse basierende *Partial Least Squares* (*PLS*)-Verfahren[3,4]. Der PLS-Algorithmus ist in der Lage, geringe Abweichungen vom Lambert-Beerschen Gesetz zu berücksichtigen. C_3H_4O, HCN, NH_3, NO, NO_2 und SO_2 zeigten bei der gewählten Auflösung ein annähernd lineares Verhalten. Für diese Substanzen wurden jeweils ein PLS-Modell erstellt. Die Kalibrierung der übrigen Substanzen erfolgte durch *Implicit Non-Linear Latent Variable Regression* (*INLR*)[5]. PLS und INLR sind prinzipiell sehr ähnlich. Als wesentlicher Unterschied wird beim INLR-Algorithmus die Extinktionsmatrix um quadratische beziehungsweise kubische Variablen erweitert, wodurch Nichtlinearitäten erfasst werden können. Beide Kalibriermethoden sind als kommerzielle Software erhältlich.

Kalibriermodellbildung und Validierung

Bei der Erstellung der Kalibriermodelle für die einzelnen Analysesubstanzen ist die Wahl des Spektralbereiches von besonderer Bedeutung. Optimal geeignet sind Bereiche, in denen die Absorptionsbande der Analysesubstanz selbst bei geringen Konzentrationen deutlich aus dem spektralen Rauschen hervortritt und zudem nicht von Störkomponenten überlagert wird. Da diese Situation bei Rauchgasspektren normalerweise nicht gegeben ist, ist i. d. R. mindestens eine interferierende Komponente in das Modell aufzunehmen. Beispielsweise basiert das im Rahmen dieser Arbeit erstellte SO_2-Modell auf insgesamt 22 Kalibrierspektren (4 SO_2, 3 C_3H_4O-, 4 HCN- und 11 H_2O-Spektren mit jeweils unterschiedlichen Konzentrationen).

Nach erfolgter Eingabe der Kalibrierspektren und Festlegung des Spektralbereichs wird das Modell berechnet. Dabei werden die Spektraldaten mit den Konzentrationsdaten durch Regression korreliert. Die Anpassung der Kalibrierspektraldaten durch das Modell lässt sich durch verschiedene statistische Größen, u. a. den Bestimmungskoeffizienten R^2, beurteilen. Auf diese Weise kann festgestellt werden, ob der gewählte Algorithmus (PLS oder INLR) die Extinktion-Konzentration-Beziehung der Kalibriersubstanz adäquat erfasst. Um die tatsächliche Vorhersagequalität des Modells zu bewerten, ist aber eine Validierung mit unabhängigen, d. h. dem Modell nicht bekannten Proben erforderlich. In dieser Arbeit wurde für jedes Kalibriermodell eine Validierung mit zusätzlich erzeugten Testspektren durchgeführt. Dazu wurden die vorhandenen Prüfgase durch Zumischung von Stickstoff verdünnt. Die Validierprobenkonzentrationen lagen tendenziell in der Mitte der Kalibrierkonzentrationswerte, um die Analysequalität abseits der Modellstützpunkte zu prüfen. Zur Beurteilung der Modellqualität bezüglich der Analyse realer Rauchgasspektren wurden neben Einzelkomponentenspektren auch Gemischspektren verwendet, die zusätzlich Absorptionsbanden interferierender Komponenten enthielten. Die Gemischspektren wurden mit der Spektroskopiesoftware durch Spektrenaddition erzeugt. Durch die Bestimmung der Testspektrenkonzentrationen mit den einzelnen Kalibriermodellen und die anschließende statistische Auswertung konnte dann beurteilt werden, welche substanzspezifischen Messgenauigkeiten bei der Analyse der realen (mit der neu entwickelten Versuchsapparatur erzeugten) Rauchgase zu erwarten waren.

Die CO- und CO_2-Modelle wurden zusätzlich durch vergleichende Messungen mittels NDIR-Spektroskopie validiert. Es zeigte sich eine gute Übereinstimmung beider Analyseverfahren. Die mittleren relativen Abweichungen betrugen $\overline{\delta}_{CO}$ = 4,40 % und $\overline{\delta}_{CO_2}$ = 6,73 %.

Zusammenfassung

Die Kalibrierung eines FTIR-Spektrometers zur Analyse von Rauchgasen stellt einen komplexen Prozess dar. Die Aufnahme der Kalibrier- und Validierspektren, die Herstellung der Validierproben, die Bildung der Kalibriermodelle sowie deren Optimierung erfordern viel Zeit. Beim Einsatz der FTIR-Spektroskopie in der Rauchgasanalytik wird die Leistungsfähigkeit dieser Methode vor allem von der

Absorptionsbandenlage und dem Extinktionskoeffizienten der zu analysierenden Substanz bestimmt. Die Verwendung geeigneter Kalibriermethoden vorausgesetzt, lässt sich beispielsweise CO relativ einfach erfassen, während die Bestimmung von NO größere Schwierigkeiten bereitet. Darüber hinaus ist bei der Untersuchung von toxischen Materialpotenzialen damit zu rechnen, dass nicht kalibrierte Substanzen erzeugt werden, die zu falschen Messergebnissen führen. Der signifikante Vorteil der FTIR-Spektroskopie im Vergleich zu anderen Rauchgasanalyseverfahren besteht in der Ökonomie dieser Methode, weil sämtliche relevanten Komponenten simultan erfasst werden können.

Literatur

[1] B. Bansemer: *Ein Modell zur szenarioabhängigen Beurteilung der Rauchgastoxizität*, Dissertation, Universität Wuppertal (2003),
© 2004 ProBusiness GmbH, Berlin, ISBN 3-937343-54-7

[2] P.L. Hanst, S.T. Hanst: *Gas Analysis Manual for Analytical Chemists in Two Volumes*, Infrared Analysis Inc., Anaheim (1993)

[3] D.M. Haaland, E.V. Thomas: *Partial least squares methods for spectral analysis, Part 1: Relation to other quantitative calibration methods and the extraction of qualitative information*, Analytical Chemistry, Vol. 60, Nr.11, S. 1193-1202 (1988)

[4] P. Geladi, B.R. Kowalski: *Partial least squares regression: a tutorial*, Analytica Chimica Acta 185, S. 1-17 (1986)

[5] A. Berglund, S. Wold: *INLR, Implicit Non-Linear Latent Variable Regression*, Journal of Chemometrics, Vol. 11, S. 141-156 (1997)

Abbildungen

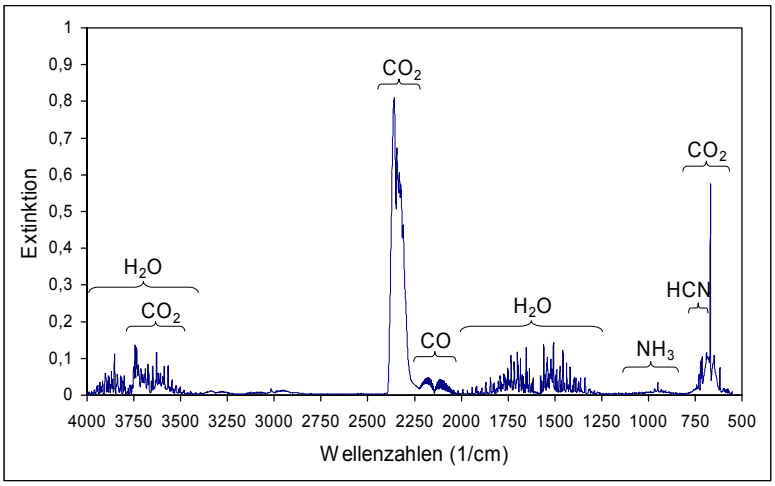

Abb. 1: Rauchgasspektrum von Polyamid

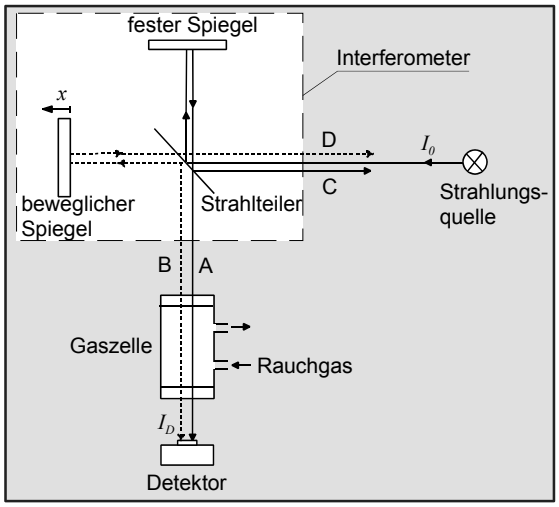

Abb. 2: Funktionsprinzip der FTIR-Spektroskopie

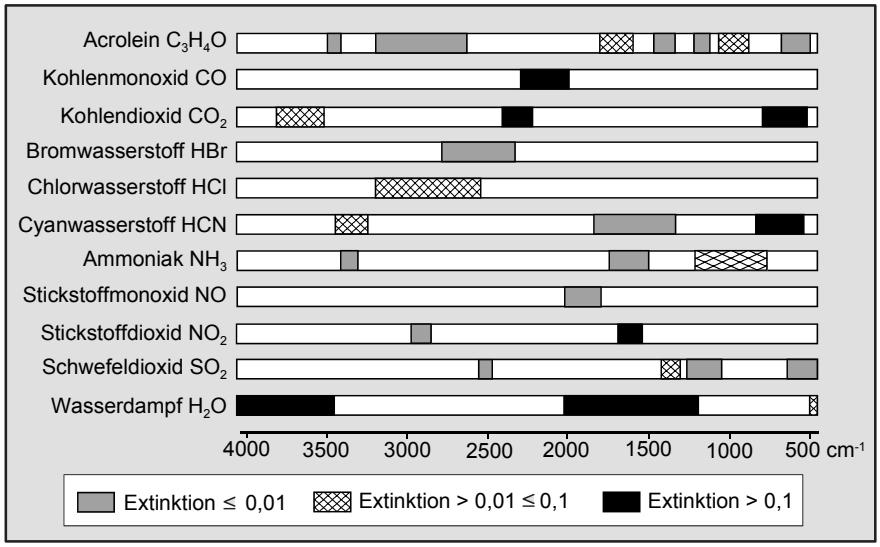

Abb. 3: Absorptionsbereiche und maximale Extinktion der kalibrierten Brandgase

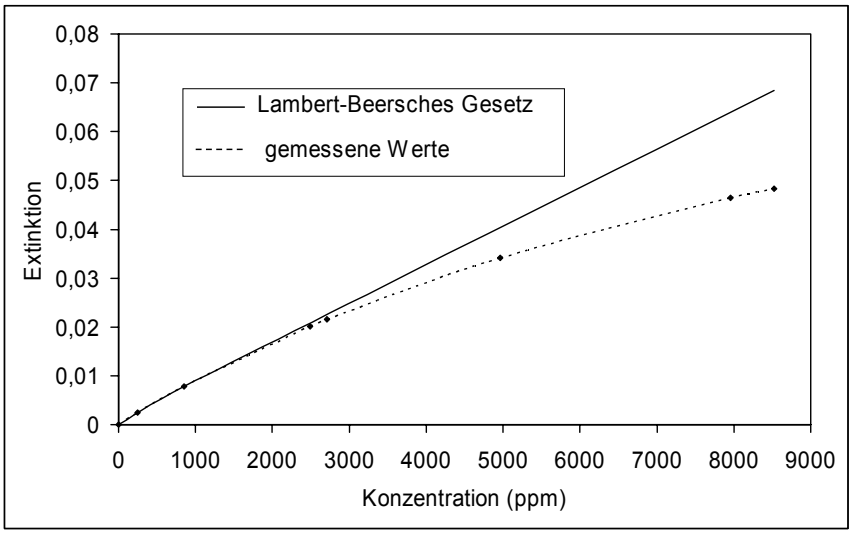

Abb. 4: Beziehung zwischen Extinktion und Konzentration für die CO-Absorptionslinie bei 2172,418 cm^{-1} bei einer spektralen Auflösung von 2 cm^{-1}

Wolfgang J. Friedl
Ingenieurbüro für Sicherheitstechnik, Munich, Germany

Falschmeldungen von Brandmeldeanlagen/How to reduce false alarms

Abstract

Messages or signals from automatic fire detection systems are in need to be taken very serious. Regularly occurring false fire alarms are leading to high direct and indirect costs as well as to a situation that fire alarms will be ignored. This will unnecessarily endanger human life and real assets. Because automatic fire detection systems just advise but don't extinguish a fire, they must send the signals to the earliest possible time to the highest possible extend of reliability. The fire brigade must be called without any delay to reduce the fire damage and fire consequential loss or fire loss of profits.

The initiative to avoid false alarms must come from the operating companies, because the manufacturer or installing companies may earn more money with systems producing false fire alarms compare to systems working properly for years. There are different starting points to reduce the amount of false alarms to a minimum. In case one topic would be either forgotten or disregarded the probability of problems caused by the system would increase. Of course the operating company of an automatic fire detection system has direct and indirect influence on these topics. The speaker will present the professional planning scheme to be followed in order to establish a well functioning automatic fire detection system for various company divisions and applications:

- Develop/design/manufacture (Quality)
- Plan/select (Internal processes, types of signals)
- Correct choice of the detector principle
- Install (Installation)
- Operate (Utilization changes)
- Maintenance (Service, repair, retrofitting)

Korrekte Anzahl von Rauchmeldern in Räumen

Es gibt für Unternehmen, die Brandmeldeanlagen installiert haben möchten, vier Möglichkeiten, diese nach zugelassenen Vorgaben zu errichten:

1. Meist nach dem VdS (Verband der Schadenversicherer e. V.)
2. TÜV-Richtlinien für Brandmeldeanlagen
3. DIN-Normen für Brandmeldeanlagen
4. FM-Richtlinien (USA-Versicherer: Factory Mutual International)

Für die Dichte von Rauchmeldern ist die VdS-Richtlinie Nr. 2095 „Planung für automatische Brandmeldeanlagen – Planung und Einbau“ maßgebend. Demzufolge gilt:

- Wenn man im Brandfall primär mit der Rauchbildung und nicht mit Wärme oder Wärmestrahlen rechnet, sind Rauchmelder die einzig sinnvollen Brandmelder (Punkt 4.7.1 in der VdS 2095)
- Man wählt heute optische Rauchmelder (abgekürzt: O-Melder), die zwar noch erlaubten Ionisations-Rauchmelder (abgekürzt: I-Melder) sind aus Gründen des Strahlenschutzes und vor allem aus Gründen der Problematik der Entsorgung nach einem Brand nicht mehr zu wählen
- Tipp: Noch vorhandene I-Melder sollen bei der nächsten Wartung oder Inspektion gegen O-Melder ausgetauscht werden
- Rauchmelder (egal, ob I- oder O-Melder) sind bis Raumhöhen von 12 m bedenkenlos zugelassen für Räume
- Rauchmelder dürfen entsprechend der Herstellerangaben im allgemeinen bis Luftgeschwindigkeiten von 20 m/s (ca. 70 km/h) betrieben werden; ansonsten benötigt man Rauchgas-Ansaugsysteme für Bereiche, in denen höhere Luft-Durchsatzgeschwindigkeiten auftreten können, ohne die Meßergebnisse negativ zu beeinflussen

- Rauchmelder können bis zu einer Feuchtigkeit von 95 % relativer Luftfeuchtigkeit eingesetzt werden
- Allgemein gilt für die Melderdichte: Anzahl und Anordnung der Rauchmelder ist so zu wählen, dass Brände in der Entstehungsphase zuverlässig erkannt werden können (z. B. auf Luftströmungen durch Klimaanlagen, Produktionsanlagen sowie Fenster, Oberlichte und Türen achten)
- In Jedem Raum des Überwachungsbereichs, auch in kleinen Räumen, muss es nach der VdS 2095 mindestens einen Melder geben (Anmerkung des Referenten: Das macht auch Sinn, ansonsten wird der grosse Vorteil von automatischen Brandmeldern, die Brandfrüherkennung, ad absurdum geführt)
- Allgemein gilt für Rauchmelder:
  - Bei Räumen bis 80 m² Grundfläche: 80 m² je Melder
  - Bei Räumen über 80 m² Grundfläche: 60 m² bei einer Raumhöhe bis 6 m und 80 m² bei einer Raumhöhe über 6 m (gemessen von der Oberkante des Doppelbodens, nicht vom Rohboden aus) je Melder
  - Dabei gilt noch zusätzlich, dass von irgend einem Punkt an der Decke der horizontale Abstand zum nächsten Melder nicht mehr als 6,7 m (bei Räumen bis 80 m² Grundfläche und bis 12 m Raumhöhe oder bei Räumen über 80 m² und mit einer Raumhöhe von über 6 m) bzw. 5,8 m (bei Räumen über 80 m² Grundfläche und bis 6 m Raumhöhe) betragen darf
- Speziell für EDV-Bereiche gilt lt. VdS 2095 (wenn die EDV-Bereiche mindestens feuerhemmend oder höherwertiger von den angrenzenden Bereichen abgetrennt sind):
  - Für abgehängte Decken (so vorhanden):
    - Maximal 40 m² je Rauchmelder
    - Maximaler Abstand eines Punktes der Decke zum nächsten Melder: 4,73 cm
  - Für den Raum:
    - Maximal 25 m² je Rauchmelder
    - Maximaler Abstand eines Punktes der Decke zum nächsten Melder: 3,75 cm
  - Für den Doppelboden (so vorhanden):
    - Maximal 40 m² je Rauchmelder

- Maximal zulässiger horizontaler Abstand irgend eines Punktes der Decke zum nächsten Melder: 4,73 cm

- Die Höhe eines Doppelbodens ist nicht von Bedeutung, d. h. die Höhe hat keinen Einfluß auf die Art und den Umfang der Überwachung

- Speziell für die an die EDV-Bereiche angrenzenden Räumlichkeiten wie Arbeitsvorbereitung, Peripheriegeräte, Elektrogeräte usw. gilt lt. VdS 2095 (wenn die EDV-Bereiche mindestens feuerhemmend oder höherwertiger von den angrenzenden Bereichen abgetrennt sind):
  - Für abgehängte Decken (so vorhanden):
    - Maximal 60 m² je Rauchmelder
    - Maximal zulässiger horizontaler Abstand irgend eines Punktes der Decke zum nächsten Melder: 5,81 cm
  - Für den Raum:
    - Maximal 40 m² je Rauchmelder
    - Maximal zulässiger horizontaler Abstand irgend eines Punktes der Decke zum nächsten Melder: 4,73 cm
  - Für den Doppelboden (so vorhanden):
    - Maximal 60 m² je Rauchmelder
    - Maximaler Abstand eines Punktes der Decke zum nächsten Melder: 5,81 cm
  - Für weitere an diese Räumlichkeiten angrenzenden Räume, die nicht dem EDV-Bereich zugehörig sind, gilt lt. VdS 2095 (wenn die EDV-Bereiche mindestens feuerhemmend oder höherwertiger von den angrenzenden Bereichen abgetrennt sind): Pauschal ist keine Überwachung erforderlich, diese wäre aber äusserst sinnvoll; evtl. kann es jedoch sein, dass die Baugenehmigung oder die Betreibergenehmigung oder der Versicherungsvertrag es vorsehen, dass auch diese Bereiche überwacht werden müssen

- Bei Anordnung der Rauchmelder in Zweimelderabhängigkeit sind die eben genannten Überwachungsbereich je Melder um mindestens 30 % zu reduzieren

- Ist die Zweimelderabhängigkeit für die Ansteuerung von einer Brandlöschanlage gedacht (meist: vorgesteuerte Sprinkleranlage), so sind die genannten Überwachungsbereiche je Melder um 50 % zu reduzieren

Alternativen zur sofortigen Alarmmeldung

Auch wenn man durch Verzögerungen den großen Vorteil von automatischen Brandmeldeanlagen zum Teil kompensiert, so mag es doch Bereiche, Anlagen oder Situationen geben, wo man darüber nachdenken muss und wo die Alarmverzögerung eine tragbare Alternative zur direkten Alarmierung ist. Dies zum einen, um Kosten zu sparen, aber natürlich auch, um die Zeit der Feuerwehrler nicht unnütz zu vergeuden. Vor allem, wenn Menschenleben nicht gefährdet sind, kann man über solche Alternativen nachdenken. Möglich ist z. B.:

- Alarmweiterleitung nur ausserhalb der Anwesenheit von Mitarbeitern
- Einteilung in Voralarm und Hauptalarm; der Voralarm wird intern gemeldet, der Hauptalarm geht dann direkt und verzögerungsfrei zur Feuerwehr
- Alte (bewährte, aber teure) Technik: Brandmeldeanlagen mit erhöhter Zuverlässigkeit (sog. Duo-Technik); d. h. dass es eine 2-Melder-Abhängigkeit gibt (nur wenn 2 Melder aus einem Überwachungsbereich Alarm melden, gibt es Alarm); lt. VdS die Melderdichte um 30 – 50 % erhöhen
- Rauchgas-Ansaugsysteme haben 3 Alarmstufen und individuell eingestellte Werte: Infoalarm, Voralarm und Hauptalarm; nur der Hauptalarm wird direkt durch geschaltet
- Eingebaute Alarmverzögerung z. B. 30 s, damit kann man kurzfristig auftretende Störgrößen ausblenden
- Zentrale mit Meldereinzelidentifizierung anschaffen (d. h. man kann „problematische“ Melder gezielt angehen, Ursachen analysieren, ...)
- Schutz- bzw. Prallblech am/vor dem Melder anbringen
- Andere Melderart für einzelne Melder wählen
- Man misst zwei physikalisch unterschiedliche Prinzipien (Rauch und Wärme) und schaltet diese miteinander nicht ODER, sondern UND
- u. a. m.

Heute mögliche Arten von automatischen Brandmeldern

- Rauchmelder
  - Optische Melder (O-Melder)
    - Vorwärts streuende Melder
    - Rückwärts streuende Melder
    - Durchlicht-Rauchmelder
  - Ionisationsmelder (I-Melder, radioaktiv)
  - Lichtschranken (günstiger Anschaffungspreis und geringe Unterhaltskosten bei guter Detektionswahrscheinlichkeit)
- Wärmemelder
  - Maximalmelder
  - Differenzialmelder
  - Differenzmelder
- Flammenmelder
  - UV-Melder
  - IR-Melder
- Sondermelder
  - Wärmemess-Kupferrohr (Druckveränderung)
  - Wärmemessleitungen (Widerstandsveränderung durch Temperatur)
  - Explosionsgeschützte Melder
  - Akustische Melder (Waldbrandmelder)
  - Überwachungssatelliten für Großbrände, meist nur sinnvoll für Einsätze im Freien
- Automatische Brandlöschanlagen (durchgeschaltet zur Feuerwehr)
  - Wasserlöschanlagen/Sprinkleranlagen (naß, trocken, Kombi, vorgesteuert)
  - Gaslöschanlagen (CO_2, Argon, Inergen, Stickstoff)
  - Pulverlöschanlagen
  - Schaumlöschanlagen

Mögliche Ursachen für Fehlalarme

- Fehler in der Planung, Installation, Wartung und/oder Betreiben
- Verfahrenstechnische Veränderungen im Betrieb
- Analysen für Fehlalarme selber machen, evtl. ist die Firma wenig daran interessiert, ausführliche Analysen durchzuführen und Fehler zu finden; je Fehlalarm mindestens festhalten:
  - Uhrzeit und Tag
  - Betriebliche Besonderheiten
  - Feststellen, ob es Reinigungsarbeiten kurz vor dem Fehlalarm gab
  - Vorsatz ausschließen
  - Linie bzw. Melder notieren
  - Klimatische Gegebenheiten (Temperatur, Feuchte, Sonnenstrahlung)
  - Sonstige Auffälligkeiten notieren
  - Mögliche Ursachen, Vermutungen, notieren
- Raummelder können bzw. müssen direkt durchgeschaltet werden, Anlagen zur Objektüberwachung müssen dies nicht
- Bauliche Veränderungen der Räumlichkeiten
- Eigene Handwerker und Fremdfirmen darauf hinweisen, dass Rauch (Schweißen) und Staub (Bohren) zu Fehlalarmen führen kann, d. h. diese Arbeiten sind vorab zu melden und die Melder dieser Bereiche sind abzutrennen (evtl. ist es nötig, dies mit der Behörde und/oder dem Versicherer vorab pauschal oder jedesmal wieder zu klären und genehmigt zu bekommen)
- Veraltete Anlage; man beachte, dass Brandmeldeanlagen in etwa halb so schnell altern wie ein PC, d. h. Anlagen, die vor 5 und mehr Jahren installiert wurden – und die Probleme bereiten (bei den anderen ist eine Veränderung nicht nötig, die kann man noch weiter betreiben) – sollten gegen moderne Anlagen (Brandmeldezentrale – Brandmeldecomputer) ausgetauscht werden
- Pauschal sollen Brandmeldeanlagen nach max. 12 Jahren ausgetauscht werden

- Der Name eines großen Errichter-Unternehmens muss nicht bedeuten, dass die Qualität seiner Planung, Beratung, Installation und Wartung auch „groß“ ist
- Wenige, unsolide Anbieter bieten günstige Anschaffungspreise, um dann an der Wartung und den Fehlalarmen zu verdienen
- Man hat nicht das günstigste, sondern das billigste Angebot genommen (Achtung: Hier wird oft erst mit der Wartung Geld verdient ...)
- Veraltete Technik; moderne Anlagen können:
  - Melder einzeln erkennen
  - Verschmutzungen als solche und nicht als Alarm melden
  - Ausfälle erkennen und als solche melden
  - Kabelunterbrechungen erkennen und als solche melden
  - Evtl. vorzeitig nötige Wartungs- bzw. Austauscharbeiten anzeigen
  - Praktisch alle Teile der Anlage periodisch und selbständig überprüfen
- Bei Leasingverträgen auf die Vertragsgestaltung achten, z. B.:
  - Laufzeit (evtl. verlängert sich die Laufzeit stillschweigend mit jeder Nachrüstung bzw. Veränderung an der Anlage)
  - Gesamtkosten beachten; Leasing mag nur auf den 1. Blick günstiger sein
  - In der Vertragsgestaltung die Problematik der Fehlalarme fixieren
- Ebenfalls beachten: Nicht nur die Anschaffungskosten, sondern auch die Unterhaltskosten
- Andere Techniken (lineare Melder, Wärmemesskabel) sind oft in Anschaffung und Unterhalt (besonders bei hohen Hallen > 7 m) wesentlich preiswerter
- Klimatische Veränderungen über 12 Monate bei der Planung berücksichtigen:
  - Wanderung der Sonne über das Jahr (erhöhte Wärmestrahlung nur zu bestimmten Tageszeiten bzw. in bestimmten Wochen/Monaten)
  - Tau
  - Hitze, Dämpfe durch Produktionsmaschinen (z. B. Gummi- bzw. Kunststoffpressmaschinen)
  - Betriebliche Veränderungen
  - Direkte Sonnenstrahlung, also Hitze (aber auch Kälte) beachten

Vermeiden von Fehlalarmen

Nur das mehrgleisige Vorgehen kann Fehlalarme (unerwünschte Alarme) minimieren und dazu gehören die folgenden 6 Punkte:

1. Sorgfältige Entwicklung
   Nur die grundsätzlich solide entwickelten Produkte eines ebenso soliden Herstellers bilden die Grundlage, dass dessen Anlagen und ihre Bestandteile über Jahre ordnungsgemäß funktionieren. Beispielsweise dürfen Probleme wie EMV (elektromagnetische Verträglichkeit) nicht zu Fehlalarmen führen

2. Exakte Fertigung
   Ausschließlich korrekt, ordentlich hergestellte Bauteile garantieren, dass die zugesagte Qualität auch eingehalten wird; dies kann, muss aber nicht ein Kriterium für den Herstellungsort sein

3. Richtige Auswahl
   Falsche Melder führen immer zu Problemen. Nutzungen, Nutzungsänderungen, Veränderungen über das Jahr, Umbauten, Produktionsverlagerungen und vieles mehr ist zu berücksichtigen bei der Erstinstallation, aber auch bei Änderungen

4. Korrektes Errichten
   Nur gut geschulte, fähige Monteure – die über die Funktionsweisen der Melder bescheid wissen, können die hoch sensiblen Anlagen auch korrekt installieren

5. Richtiges Betreiben
   Nutzungsänderungen sind vorab mit dem Errichter zu erörtern, um Probleme konstruktiv zu vermeiden

6. Regelmäßiges Instandhalten
   Die Anlagen müssen gewartet werden, sonst bringen sie entweder auch im Brandfall keine Alarmmeldung, oder verstärkt Fehlalarme.

Schlussworte

Fehlalarme bringen unsoliden Firmen ebenso Umsatz wie ständig kranke Patienten unsoliden Ärzten. Insofern kann es sein, dass die Triebfeder zum Abstellen der Fehlalarme vom Unternehmen selber ausgehen muss und nicht von der Fachfirma. Man muss grundlegend bei der Planung bereits die Weichen in die richtige Richtung stellen: Moderne Techniken (Brandmeldecomputer), die wesentlich sicherere und in allen Punkten bessere Loop-Technik, die jeweils richtigen Melder sowie ggf. individuelle Maßnahmen an einzelnen Meldern werden dazu führen, dass es eine vertretbar geringe Anzahl von Fehlalarmen gibt. „Vertretbar“ bedeutet z. B. bei einem Unternehmen, die Feuerwehr nicht öfters als einmal pro Jahr ohne Gefahr zu rufen.

Man muss auch berücksichtigen, dass erstens Fehlalarme grundsätzlich berechnet werden (z. B. 650,- €) und dass zweitens weit über 90 % der Feuerwehrmänner hauptberuflich einem anderen Beruf nachgehen. Diese Personen werden also aus der Freizeit geholt, aus den Betten geklingelt, wenn es (mal wieder) einen Fehlalarm gegeben hat. Insofern hat man auch eine soziale Verpflichtung diesen Menschen und ihren Familien gegenüber, Fehlalarme abzustellen. Übrigens haben die Berufsfeuerwehren auch ohne vergebens gefahrene Einsätze genügend Arbeit, d. h. auch diese Personen werden durch unnötig gefahrene Einsätze gestört und verärgert.

Als elementares Problem ist noch zu nennen, dass Alarme von Gefahrenmeldeanlagen von den Mitarbeitern oft nicht mehr ernst genommen werden, wenn es zu viele Fehlalarme gibt – brennt es dann wirklich, wird nicht oder verspätet reagiert!

Es ist heute möglich, Brandmeldeanlagen (und auch Brandlöschanlagen sowie Einbruchschutzanlagen) zu installieren, die auf der einen Seite zuverlässig detektieren, auf der anderen Seite keine oder kaum Fehlalarme liefern – und dies gilt auch für besonders schwierige Einsatzbereiche. Wenn „anständige“ Errichterfirmen (und das ist die überwiegende Mehrheit) solide Planen und mit dem Betreiber von Anfang an offen und konstruktiv zusammen arbeiten, dann kann man von vorne herein davon ausgehen, dass es keine größeren Probleme mit der Anlage gibt.

Jörg Bärenfänger
Novar GmbH
R&D ACS Novar GmbH
Germany

Holger Hirsch
Universität Duisburg Essen
Energietransport und Speicherung
Germany

EMV von Brandmeldeanlagen

Anforderungen durch eine sich ändernde elektromagnetische Umwelt

1 Abstract

The electromagnetic environment, in which fire alarm systems have to operate, is at present subject to major changes.
The increasing use of wireless communication systems in the frequency range above 1 GHz requires on the one hand an adequate interference immunity of equipment, which is operated in the vicinity, and on the other hand a sufficient limitation of the rf-emission. Systems working on a broadband base need special attention because in the past these systems have only insufficiently been taken into account, especially in the context of the test specifications. Recently the standardization covers this steadily changing electromagnetic landscape in drafts of standards.
For manufacturers of electrical products with long product cycle times a timely examination of the respective requirements and a corresponding interpretation for product revisions and new developments is important for the success of the product at the market.
The current and also the future standardization and law plays an important role especially for the development of safety relevant products, like fire alarm systems. The specifications to be used are obviously a union set of all the approval requirements existing in the relevant sale regions.

Here the current requirements and especially these requirements are shown, which will become relevant for the technical product qualification of fire alarm systems in the future. Current standards and draft standards according to rf-immunity and rf-emission of the products, including their application areas and transition time periods are explained.
Measuring results for typical fire alarm applications (panels and field devices) show, where product group specific challenges have to be solved. Exemplarily performed measurements in accordance with the new draft of EN 61000-4-6 and with the new EN 55022 are compared with the currently valid EMC requirements. Additional results of measurements using broadband interfering signals are shown which aren't covered by standards and drafts yet.

2 Aktuelle und zukünftige technische Vorgaben zur Produktqualifizierung von Brandmeldeanlagen

Neben den für Europa bindenden Normen der EN 54 Reihe, gibt es eine Vielfalt an nationalen und internationale Richtlinien und Normen, die bei der Entwicklung, Zulassung und Betrieb einer Brandmeldeanlage berücksichtigt werden müssen. Diese Normen beschreiben sowohl einzelne Produkte, als auch ihr Zusammenspiel in einem Brandmeldesystem.
Im Laufe der nächsten Jahre erfolgt in der EU die Harmonisierung der einzelnen Normen der o.g. EN 54 Reihe unter der Bauproduktenrichtlinie. Für einige Normen ist die Übergangszeit bereits Mitte 2005 abgelaufen. Ab diesem Zeitpunkt dürfen nur gemäß Bauproduktenrichtlinie zertifizierte Produkte CE gekennzeichnet und in den europäischen Markt gebracht werden. Damit ist, nach Ablauf einer Übergangszeit von etwa 3 Jahren zur Harmonisierung aller relevanten EN 54 Normen, in Europa nur noch die „third-party" Zertifizierung von Brandmeldeprodukten möglich. Herstellererklärungen über die Richtlinienkonformität wird es dann nur noch für Produkte geben, die keinen harmonisierten EN-Normen zuzuordnen sind. Weiterhin müssen noch diverse nationale Anforderungen berücksichtigt werden, die in einer schätzungsweise 10 Jahre dauernden Übergangszeit weiter Anwendung finden werden. Erst nach Ablauf dieser Zeitspanne ist zu erwarten, dass ein CE gekennzeichnetes Produkt ohne Berücksichtigung der nationalen Normen am Markt durchsetzbar ist.

Eine EG-Konformitätserklärung zur CE Kennzeichnung von Brandmeldetechnik-produkten sollte die folgenden Richtlinien umfassen:
- Bauproduktenrichtlinie 89/106/EEC,
- EMV-Richtlinie 89/336/EEC und
- Niederspannungsrichtlinie 73/23/EEC.

Zusätzlich können, je nach Produkt und Anwendung, folgende Richtlinien angewandt werden:
- R&TTE-Richtlinie 1999/5/EC (Radio Equipment and Telecommunications Terminal Equipment) und
- ATEX Richtlinie 94/9/EC.

Die Bedeutung der Normen, die unter der EMV-Richtlinie harmonisiert sind, wird durch direkte Verweise aus den Normen der EN-54-Reihe unterstrichen. Damit spielen die einschlägigen EMV-Normen, wie die EN 50130-4 für die Störfestigkeit und die EN 55022 für die Störaussendung eine bedeutende Rolle bei der Produktqualifizierung. Neben der EN 55022 können für die Störaussendung auch die Fachgrundnormen EN 61000-6-3 oder –4 genutzt werden. Allerdings verweisen diese für den Einsatzbereich „Wohnbereich, Geschäfts- und Gewerberbereiche sowie Kleinbetriebe" wieder auf die Grundnorm EN 55022.

Im Rahmen des „Maintenance Programmes“ für Normen der Organisationen IEC und ISO ändern sich zwangsläufig auch die europäischen Normen EN 55022 „Einrichtungen der Informationstechnik, Funkstöreigenschaften“ und die EN 61000-4-6 „Prüf- und Messverfahren; Störfestigkeit gegen leitungsgeführte Störgrößen, induziert durch hochfrequente Felder“ in einigen gravierenden Punkten.
So erweitert sich der Anwendungsbereich der EN 55022 um eine Messung der leitungsgeführten, asymmetrischen Störgrößen auf Signalleitungen. Diese Erweiterung des Anwendungsbereiches trifft neben Herstellern von Brand- und Einbruchmeldetechnik, die Gebäudeleittechnik und z.B. auch Hersteller der Industrieautomation. Infolge dieser Erweiterung müssen in Gebäuden installierte Netze, zu denen auch Ringleitungen der Brandmeldeanlagen gehören, wie Telekommunikationsnetze betrachtet werden deren Störaussendungen definierten Grenzwerten unterliegen. In den zurzeit zur Abstimmung publizierten Normentwürfen (CDV stage) soll der Frequenzbereich nach oben auf 18 GHz erweitert werden. Anwendbar soll diese Frequenzerweiterung nur auf solche Produkte sein, bei denen relevante Frequenzanteile aufgrund der inneren Oszillatoren erwartet werden dürfen.

Eine frequenzmäßige Erweiterung ist auch für Störfestigkeitsprüfungen vorgesehen. Die neuesten Entwürfe der Fachgrundnormen (CDV stage) sehen mittlerweile für die Störfestigkeit gegen elektromagnetische Felder eine obere Frequenzgrenze von 2,7 GHz vor. Die zur Prüfung anzuwendende Grundnorm IEC 61000-4-3 wird demnächst als CDV erscheinen, in dem die obere Frequenzgrenze zwar offen ist, Prüfschärfegrade aber bis zu 6 GHz definiert sind.
Hält das Produkt diese Normen (nach deren Harmonisierung innerhalb der EU) ein, so darf der Hersteller vermuten, dass das Produkt die in der EMV-Richtlinie nur verbal formulierten EMV-Schutzanforderungen einhält und er kann das Produkt in Verkehr bringen. Im Zuge der Diskussion um leitungsgeführte Breitbandkommunikation erlangt das aus einzelnen Geräten und Leitungen bestehende Netzwerk allerdings eine besondere Bedeutung. Aufgrund sich anbahnender Streitigkeiten zwischen Herstellern und Betreibern von Breitbandtelekommunikationsprodukten und Funkvertretern sah sich die europäische Kommission veranlasst, ein Normungsmandat an CENELEC und ETSI zu erteilen, bei dem eine Norm für Anforderungen an den Betrieb von Netzwerken festgelegt werden soll („Netzwerk“-Norm). Aufgrund der stark unterschiedlichen Interessenlagen der Industrievertreter und der Funk-Vertreter konnte eine Einigung bislang aber nicht erzielt werden. Seitens des deutschen Gesetzgebers ist daher kürzlich, quasi im europäischen Alleingang, im Zuge des Frequenzmanagements eine „Frequenzbereichszuweisungsplanverordnung“ mit einer speziellen Nutzungs-bestimmung (NB30) verabschiedet worden, die erheblich schärfere Grenzwerte für die Störaussendung von Telekommunikationsnetzen festlegt. Um diese Verschärfung in Einklang mit den europäisch harmonisierten Produktnormen zu bringen, wird argumentiert, dass die Störaussendungen, die nicht mit den zur Kommunikation

notwendigen Signalen zusammenhängen (Schmal- oder breitbandige Aussendungen von Schaltnetzteilen, Prozessortakten, etc.), nach wie vor durch den Produktstandard abgedeckt werden. Die Aussendungen aber, die im Zusammenhang zu den Kommunikationssignalen stehen jedoch mit den neuen, schärferen Grenzwerten bewertet werden sollen. Ob aus Sicht eines gestörten Rundfunkhörers diese Unterscheidung sinnvoll ist, ist mehr als zweifelhaft. Für nationale Regelungen, die den europäischen Warenverkehr erschweren können, sehen die europäischen Verträge einen Notifizierungsprozess vor. Die Bundesregierung hat daher derzeit die von ihr vorgesehenen Einschränkungen bei der Europäischen Kommission eingereicht. Eine Reaktion steht indes noch aus.
Auch wenn diese Regelungen formal nur auf klassische Telekommunikationsnetze anzuwenden sind, zeigen die Diskussionen in den Standardisierungsgremien, dass die in NB30 definierten Grenzwerte früher oder später Richtwerte für die Störfallbewertung durch die Regulierungsbehörden werden. Diese Grenzwerte müssen folglich von allen Herstellern von Produkten ernstgenommen werden, die in irgendeiner Form leitungsgeführte Kommunikation nutzen wie z.B. im Fall der Brandmeldesysteme.

3 Änderungen der elektromagnetischen Umgebung in der Praxis

Soll die Produktentwicklung mit einer gewissen Weitsicht erfolgen, so ist es ratsam, nicht nur die Normenlage zu reflektieren, sondern die elektromagnetische Umgebung zu analysieren, in dem das Produkt eingesetzt werden soll. Die Normung folgt üblicherweise mit einem Zeitversatz von rund 5 Jahren. Speziell bei sicherheitsrelevanten Produkten darf sich der Hersteller aus Produkthaftungsgründen nicht mit dem allein in Normen dokumentierten Stand der Technik orientieren, sondern muss alle darüber hinaus gehende Erkenntnisse berücksichtigen. Insofern sind aktuell verwendete Geräte und Systeme sowie Zukunftstrends in die elektromagnetische Umgebung einzubeziehen.
Im Bereich der mobilen Sendefunkgeräte sind derzeit Mobiltelefone nach dem GSM-Standard im Gebrauch. Die nächste Generation (UMTS) befindet sich in der Markteinführung. Zudem sind eine Vielzahl von anderen Systemen (RFID, Wireless LAN, Short Range Devices) im Einsatz. Diese neueren Systeme nutzen vielfach Frequenzen, die über die in der aktuellen Normung abgelegten Frequenzgrenze von 1 GHz hinausgehen. Daneben werden ausgefeiltere Modulations- und Codierungsverfahren verwendet, so dass das Sendespektrum teilweise stark von dem des aus Zeiten des AM-Rundfunks stammenden Prüfsignals abweicht. Breitbandige Kommunikationssysteme sind aufgrund ihrer Fehlertoleranz und Adaptivität kaum durch schmalbandige Störsignale zu beeinflussen. Das breitbandige Spektrum eines modernen Sendefunkgerätes mit hinreichender Signalamplitude könnte aber kritischere Störphänomene bedingen.
Bezüglich der EMV-Koordination sind derzeit ungünstige Entwicklungen zu beobachten, welche die Festlegung adäquater Grenzwerte und damit die

Standardisierung behindern. Einerseits werden immer mehr Geräte und Systeme auch im häuslichen Umfeld eingesetzt, die intern hochfrequente Signale verarbeiten (Takt eines Mikrocontrollers), eine breitbandigere leitungsgeführte Komunikation nutzen (Bussysteme) und/oder auf niedrige Verluste ausgelegte leistungselektronische Einheiten nutzen (Schaltnetzteile, Lichtsteuerungen). Somit hat sich das gesamte elektromagnetische Rauschen über die letzten Jahre/Jahrzehnte angehoben. Andererseits besteht aus verschiedenen Gründen seitens der Funkbetreiber das Interesse, die Sendeleistung und damit Kosten zu verringern, was durch bessere Technologie in den Empfängern ermöglicht wird. Eine weitere Verschärfung ergibt sich dadurch, dass aus Komfortgründen keine externe Antenne sondern eine in einen Empfänger integrierte Antenne genutzt werden soll. Dieses Komfortbedürfnis ist von ITU in der Form berücksichtigt worden, dass der Referenzempfänger nicht mehr eine externe sondern eine interne Antenne nutzt. Dieser bei ITU definierte Referenzempfänger wird als Basis für die Störmodelle herangezogen. Waren sich die Vertreter der beiden kontroversen Interessensgruppen in der Vergangenheit einig über die Grenzwerte für die unbeabsichtigte Emission der Geräte, so klafft heute in den Forderungen eine Lücke von nahezu 40 dB. Es darf daher nicht verwundern, dass in der Arbeitsgruppe, die sich mit der Erstellung der „Netzwerk“-Norm beschäftigt und auch nachher bei der Abstimmung in den einzelnen nationalen Normungsgremien keine Einigung erzielt werden konnte.

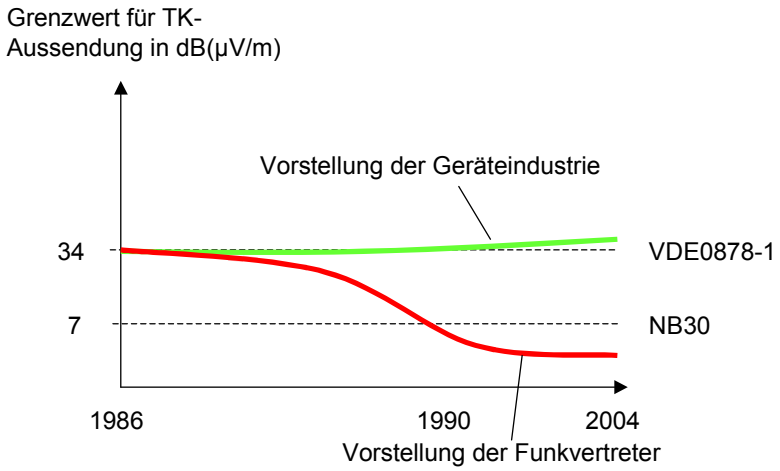

Abb.1 Vorstellung der Interessensgruppen zur Lage des Störaussendungs-Grenzwerts am Beispiel der Frequenz 30 MHz bei einem Abstand von Quelle und Messantenne von 30 m (NB30 mit 20 dB/Dekade auf 30 m umgerechnet)

4 Störspannungs- und Störstrommessung am TK-Port nach DIN EN 55022

4.1 Messobjekt

Ein Ring mit 68 automatischen Brandmeldern wird an einer Zentrale 8000C betrieben. Als Verbindungsleitung zwischen den Meldern und der Zentrale ist ein ca. 20 m langes Kabel des Typs IY(ST)Y 4x0.8 eingesetzt. Die Schirmung der Ringleitung ist zunächst an der Zentrale einseitig aufgelegt (worst case Installationspraxis). Die Rauchmelder

werden im Normalfall ca. alle 50 s abgefragt. Einen Brandfall melden sie initiativ an die Zentrale. Eine zweite Zentrale 8000M, ohne angeschlossene Brandmelder, ist über eine Backbone Verbindung mit einer Länge von ca. 20 m mit der ersten Zentrale verbunden. Dabei werden wahlweise folgende Backbonetypen verwendet:

- 62 kBaud mit IY(ST)Y 4x0.8-Kabel (geschirmt) und
- 500 kBaud mit Cat-3-Kabel (geschirmt).

4.2 Messaufbau zur Messung der Funkstörspannung und des Funkstörstromes

Die Störspannungs- bzw. Störstrommessungen werden entsprechend der Methode aus Kapitel 9.5.3.3 und 9.5.3.4 (DIN EN 55022) resp. Anhang C.1.2 durchgeführt.
Die Spannungsmessung erfolgt direkt am Schirm der Ring- und Backbonekabel im Abstand von etwa 30 cm von der Zentrale. Auf die in der Norm beschriebene, jedoch in den Normungsgremien umstrittene kapazitive Koppelzange wird aus Gründen einer besseren Reproduzierbarkeit verzichtet.. Die HF-Entkopplung zur angeschlossenen Brandmelder oder zweiten Zentrale erfolgt über die Ferritzange (siehe Abb. 2).
Zur Strommessung wird an gleicher Stelle ein 150 Ohm-Widerstand zwischen Schirm und Bezugsmasse des Kabels angeschlossen. Mit einer Stromzange wird der asymmetrische Strom auf der Kabelstrecke gemessen (siehe Abb. 3).

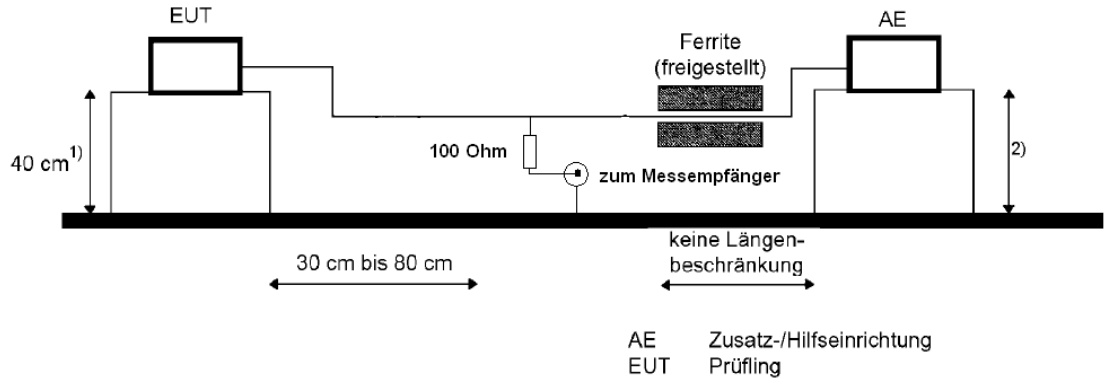

Abb. 2 Messanordnung für Störspannungsmessung (Quelle: EN 55022, mod.)

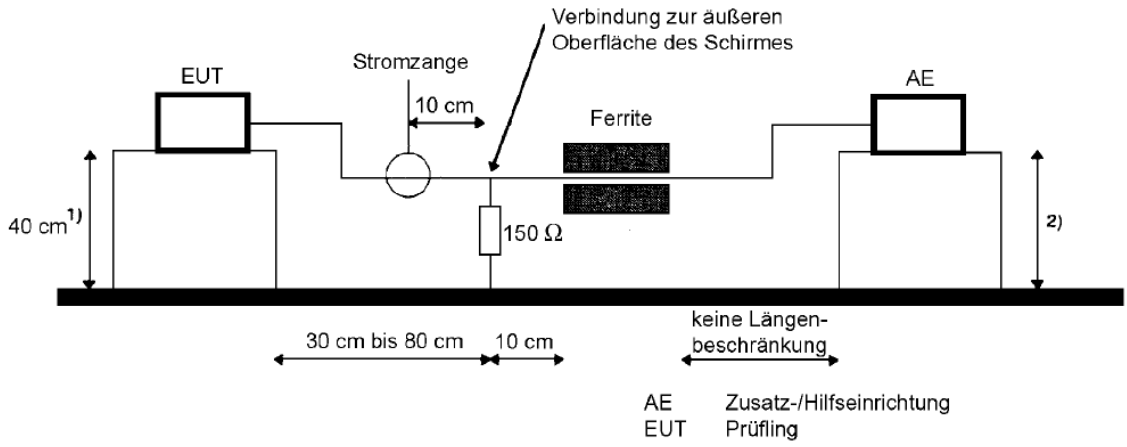

Abb. 3 Messanordnung für Störstrommessung (Quelle: EN 55022)

Die Messung der Störspannung und des Störstroms erfolgt in Anlehnung an die nachstehend dargestellten Prüfanordnungen. Anstelle der in der Norm nicht näher spezifizierten kapazitiven Koppeleinrichtung zur Störspannungsmessung wird hier direkt die Störspannung auf dem Schirm des Kabels erfasst.

4.3 Messungen

Im Folgenden werden nur die Ergebnisse der Störspannungs- und Störstrommessungen der 500 kBaud Backboneverbindung dargestellt. Die Ergebnisse der 62,5 kBaud Backboneverbindung und der Melderringleitung zeigen in etwa die gleichen Störpegel wie die breitbandigere 500 kBaud Strecke, so dass hier nicht gesondert darauf eingegangen werden soll.

4.3.1 Störspannungs- und Störstrommessung 500 kBaud Backbone

Wie die Ergebnisse der Störspannungs (Abb. 4) und Störstrommessung (Abb. 5) zeigen, werden die Grenzwerte durch das vermessene Brandmeldesystem sicher eingehalten.

Anhand der Abbildungen 4 und 5 ist zu erkennen, dass die gemessenen „worst case“ Werte immer um mehr als 10 dB unterhalb der Grenzwerte liegen. Grund hierfür ist sicherlich die Optimierung von Sensoren und Aktoren einer Brandmeldeanlage auf geringsten Energieverbrauch. Dies ist zum einen bedingt durch den Betrieb großer Leitungslängen, zum anderen durch eine Begrenzung der zu verwendenden Akkukapazitäten für die Notstromversorgung. Eine Vergrösserung des Messabstandes zwischen Prüfling und dem Strom/Spannungsabgriff um 20 cm ergab bei den Messungen der 500 kBaud Backboneverbindung zwar eine Verringerung des Störstromes um 5 dB im Frequenzbereich um 5 MHz, jedoch vergrösserte sich der Wert im Bereich um 12 MHz um den gleichen Betrag. Grund hierfür sind frequenz- und ortsabhängige Stehwellen auf dem Leitungsschirm.

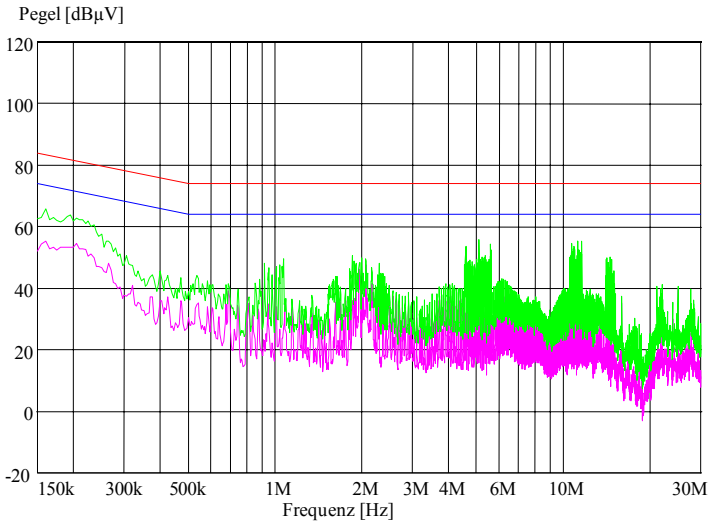

Abb. 4 Störspannung, „worst case“ Kommunikation

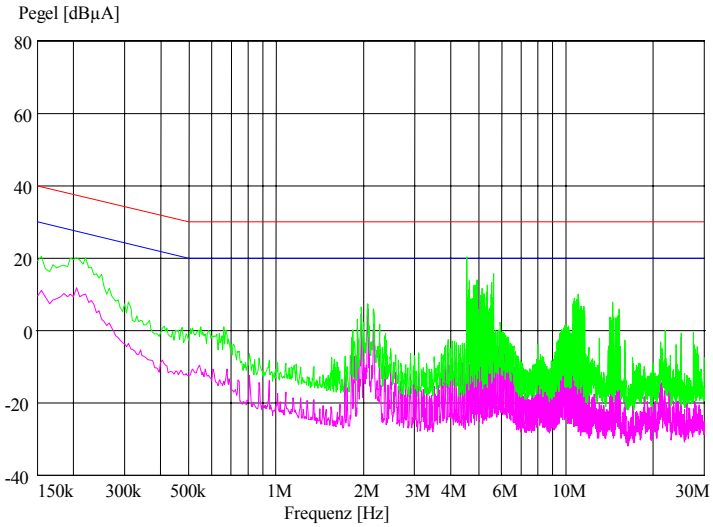

Abb. 5 Störstrom, „worst case“ Kommunikation

Die derzeitigen Anforderung werden sicher eingehalten. Bei zukünftigen Produkten mit höheren Übertragungsraten aufgrund integrierter Zusatzdienste muss allerdings einer möglicherweise anstehenden Verschärfung der Grenzwerte Rechnung getragen werden.

5 Gestrahlten Störemission einer typischen Brandmeldezentrale gemäß EN 55022

5.1 Messobjekt

Ein Ring mit 20 automatischen Brandmeldern 9200 wird an einer Zentrale 8000C betrieben. Als Verbindungsleitung zwischen den Meldern und der Zentrale wird ein ca. 30 m langes Kabel des Typs IY(ST)Y 4x0.8 eingesetzt. Die Schirmung der Ringleitung ist an der Zentrale einseitig aufgelegt. Die Rauchmelder werden im Normalfall ca. alle 50s abgefragt. Einen Brandfall melden sie initiativ an die Zentrale. Die Zentrale 8000C befindet sich als Messobjekt in einer Absorberhalle, die automatischen Brandmelder werden durch Filter entkoppelt außerhalb der Halle plaziert.

5.2 Messaufbau zur Messung der Funkstörsstrahlung

Die Störaussendungsmessungen werden entsprechend der Methode aus Kapitel 10 der DIN EN 55022 in der derzeit gültigen Version (obere Grenzfrequenz 1 GHz) durchgeführt.

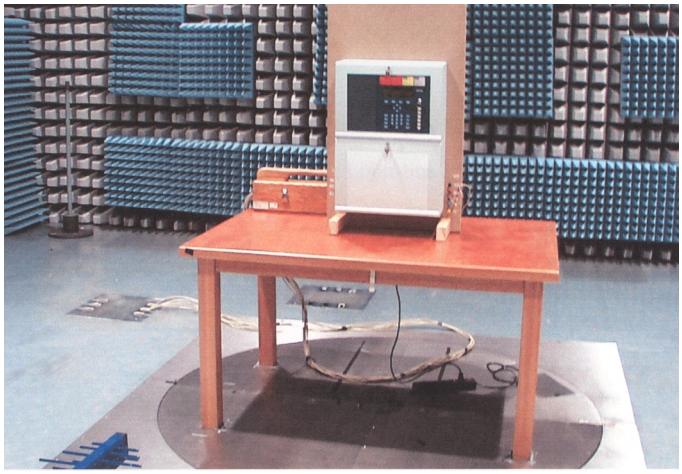

Abb. 6 Störfeldstärke, Normalbetrieb

5.3 Messergebnisse

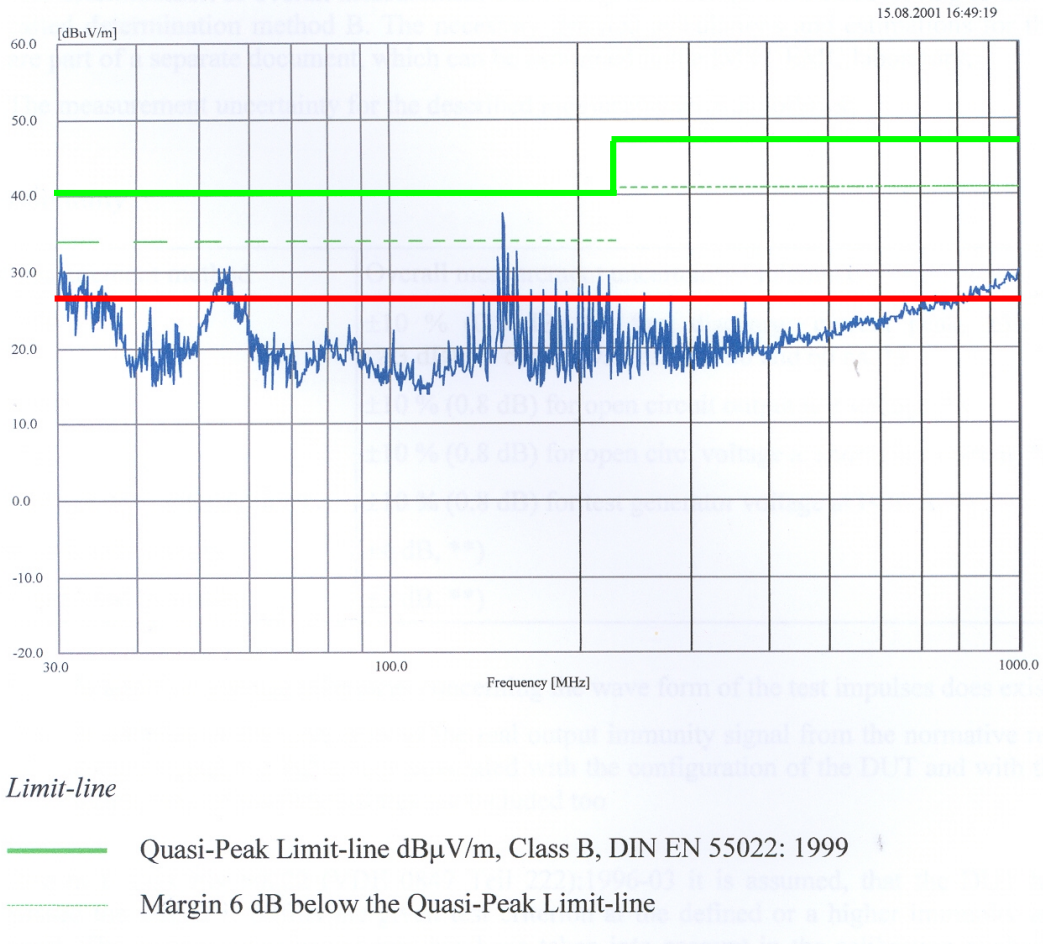

Abb. 7 Ergebnis der Störfeldstärkemessung in der Absorberhalle. Neben dem derzeit gültigen Grenzwert aus der Produktnorm (obere Grenzwertlinie) ist der von der Regulierungsbehörde für Telekommunikationsnetze definierte NB30-Grenzwert (untere Grenzwertlinie) eingetragen.

Die Zentrale hält die Grenzwerte für Einrichtungen der Klasse B gemäß der EN 55022 ein. Wie zu erkennen ist werden die Grenzwerte um durchschnittlich mehr als 10 dBµV/m unterschritten. Der maximale Peak-Wert liegt um etwa 4 dBµV/m unterhalb des Grenzwertes. Nachmessung im Frequenzbereich bis zu 18 GHz zeigen, dass hier keine signifikanten Emissionen mehr auftreten.

Eine Ausdehnung des Anwendungsbereichs des von der Regulierungsbehörde definierten NB30-Grenzwerts auf ein breiteres Produktspektrum, was im Störungsfall sehr wahrscheinlich wird, hätte jedoch Auswirkungen auf den Betrieb einer Brandmeldeanlage. Bei einer positiven Notifizierung der entsprechenden Verordnung könnte die merkwürdige Situation entstehen, dass die Vermarktung der Brandmeldeprodukte zwar bei nachgewiesener Übereinstimmung mit den harmonisierten Normen nicht behindert werden darf, der Betrieb könnte aber aufgrund einer Überschreitung der schärferen Grenzwerte durch die Regulierungsbehörde untersagt werden, was sich natürlich auf Fälle einer nachgewiesenen Funkstörung begrenzen würde. Somit hätte die Verordnung Richtschnurcharakter, auch wenn sie formal nur auf Telekommunikationsnetze anwendbar ist.

Aus Gründen der Marktakzeptanz bliebe einem Hersteller angesichts der drohenden Betriebsbeschränkung nichts anderes übrig, als die Produkte entsprechend der neuen Grenzwertsituation zu modifizieren. Dies ist mit erheblichen Kosten verbunden, die einseitig von der Industrie getragen werden müssten. Da der Anwendungsbereich der NB30 sich explizit nicht auf Brandmeldeanlagen erstreckt, würden zum jetzigen Zeitpunkt Lobbying und juristische Schritte ins Leere laufen. Es ist aber ratsam die technisch/politischen Entwicklungen genau zu beobachten, um im geeigneten Moment gegensteuern zu können.

Es muss speziell bei Geräten der Sicherheitstechnik, die die heute gültigen Störaussendungsnormen einhalten offen die Frage gestellt werden:

„Ist der Gesellschaft der Schutz des Rundfunkempfangs
oder die Sicherheit des Menschens wichtiger ?“

Zusätzlich muss beachtet werden, dass Hersteller, die ihre Produkte weltweit vertreiben sich in allen - auch europäischen - Märkten nie einer aktiven Marktüberwachung gegenüber sehen. Nur in Deutschland und Österreich findet eine derartige Überwachung bezüglich der EMV-Eigenschaften statt. Damit sind Produkte, die diesen hohen Anforderungen genügen zwar technologisch an der Spitze, kostenmäßig sind sie dafür in allen anderen Märkten, ausser Deutschland und Österreich, nicht mehr konkurrenzfähig.

6 Störfestigkeit gegen eingeströmte HF nach DIN EN 61000-4-6: 2001 und der neuen Version der IEC 61000-4-6: 2003

Im Rahmen des Maintenance Prozesses ist die in IEC 61000-4-6 beschriebene Methode geändert worden. Über die Norm ist Ende letzten Jahres parallel von IEC-Mitgliedern (als IEC 61000-4-6) und CENELEC-Mitgliedern (als EN 61000-4-6) abgestimmt worden. Das Abstimmungsergebnis ergab ein positives Ergebnis für die internationale Norm IEC 61000-4-6 und ein negatives Ergebnis für die europäische Norm EN 61000-4-6, was sich trotz gleicher Stimmabgabe der europäischen Vertreter durch die in Europa übliche Stimmengewichtung ergab. Somit ergibt sich für einen im internationalen Markt tätigen Produkthersteller das Problem, das für den europäischen Markt nach der nun nach wie vor gültigen „alten Version“ der Norm geprüft, für den außereuropäischen Raum jedoch die internationale Version heranzuziehen ist. Um Doppelprüfaufwand einzusparen, wird untersucht, welche der beiden Normversionen kritischer für das Produkt Brandmeldesystem ist.

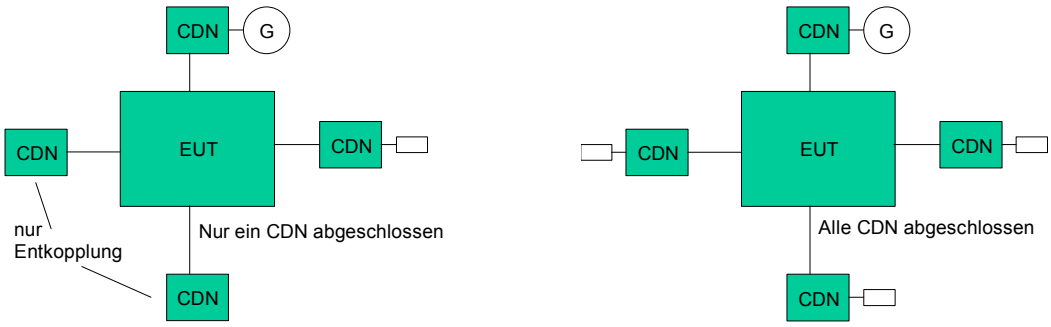

Abb. 8 Prüfphilosophien der neuen IEC 61000-4-6 (links) und der „alten“ EN 61000-4-6 (rechts)

Für die Störfestigkeitsprüfungen werden Netzleitung, Busleitung und beide Brandmelderleitungen über entsprechende CDN (CDN-M3 für die Netzleitung, CDN-S9 für die Busleitung zwischen den Zentralen, 2 CDN-S4 für die Leitungen zum Brandmelderring). Der Schirm der Brandmelderleitungen ist bei dieser Untersuchung einseitig aufgelegt. Für die Prüfung nach der in Europa gültigen Norm EN 61000-4-6 werden sämtliche angeschlossene CDN mit 50 Ohm abgeschlossen.

Die Zentrale erweist sich in der vorliegenden Form als außerordentlich störfest. Nach beiden Verfahren lässt sich eine Funktionsbeeinflussung bis zu einem Pegel bis 25 V (EMK) bei amplitudenmodulierten Signal (bis zu 99 %, 1 kHz Sinus) nicht erkennen. Daher wird ein breitbandigeres Prüfsignal mit Hilfe eines Rauschgenerators, der an den Modulationseingang des Prüfsignalgenerators angeschlossen wird, verwendet, so dass sich ein etwa 500 kHz-breites, glockenförmiges Spektrum ergibt (Abb. 9). Bei Einkopplung über die CDN-S9 in die Essernet-Leitung (Schirme nicht aufgelegt) ergibt sich nach der alten Methode der EN 61000-4-6 eine Störungsmeldung nach etwa 1 Minute bei der Frequenz 10,7 MHz bei einem Störfestigkeitspegel von 16 V (EMK).

Der Störfestigkeitspegel erhöht sich auf 20 V (EMK), wenn die neue Methode der IEC 61000-4-6 angewandt wird (Abschluss der beiden CDN-S4 entfernt).

Die aus Sicht der Hersteller von Brandmeldeanlagen wichtigen Ergebnisse sind:

1) Die „alte“ EN 61000-4-6-Methode stellt für die Brandmeldezentralen die kritischere Prüfung dar. Dies lässt sich physikalisch dadurch begründen, dass der HF-Strom, der in den Einspeisepunkt eingekoppelt wird, aufgrund des Abschlusses sämtlicher Leitungen höher wird. Es dürfte also ausreichend für den europäischen und außereuropäischen Markt sein, wenn nach der alten EN 61000-4-6 geprüft wird.
2) Die in der Norm abgelegte Modulation stellt nicht die worst-case-Situation dar. Ein breitbandigeres Signal ist in der Lage, eine Reaktion in der Brandmeldeanlage auszulösen, die bei einem normgerechten Signal nicht auftritt. Aus Produkthaftungsgründen ist die Auswertung der Signale von Funkdiensten, die in der Umgebung der Brandmeldesysteme betrieben werden angeraten. Neben der normgerechten Prüfung ist es zum weiteren Sammeln von Erfahrung sinnvoll, Prüfungen zumindest exemplarisch auch mit nicht normgerechten, dafür aber praxisrelevanteren Prüfsignalen durchzuführen.

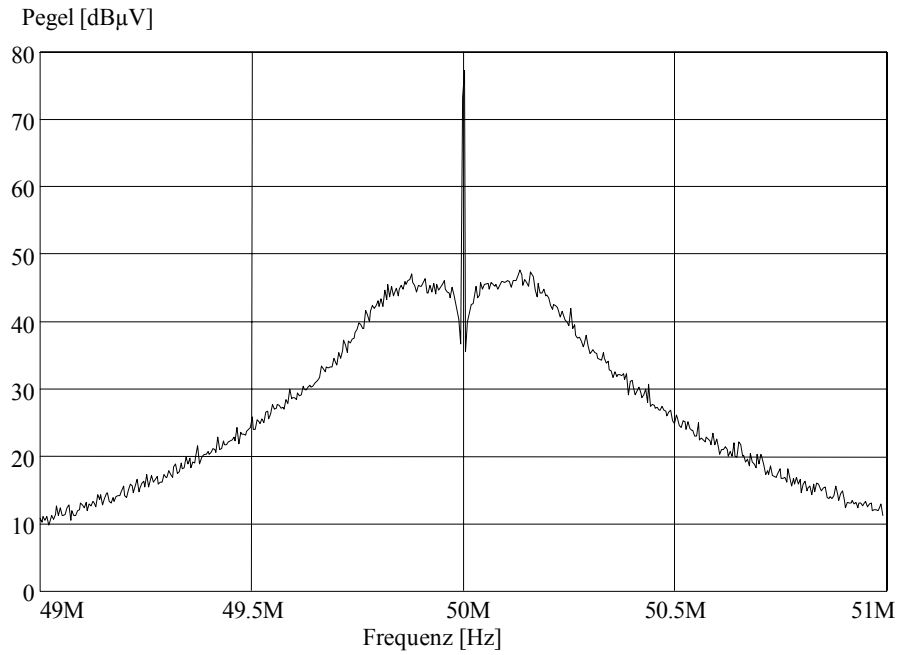

Abb. 9 Spektrums des Breitbandprüfsignales

Im Gegensatz zur vorangegangenen Diskussion über die Störaussendung, ist die Lösung dieser Aufgaben als hochrangiges Ziel zu werten, in dem Bestreben eine Brandmeldeanlage immer störfester und somit sicherer zu machen. Gleichsam werden so auch Fehlalarme verringert und somit das Vertrauen in die Brandmeldetechnik weiter gestärkt.

7 Zusammenfassung

Als wichtigstes Ergebniss der Störausswendungsmessungen kann festgehalten werden, dass die derzeitigen Anforderungen bezüglich leitungsgebundener Störaussendung von „Nicht-Netz-Leitungen“ von handelsüblichen Brandmeldeanlagen erfüllt werden. Gleichsam sind auch die bisher anzuwendenden Grenzwerte für die feldgebundene Störabstrahlung sicher eingehalten. Sollte allerdings, wie dargestellt, die NB30 als defacto-Standard in Kraft treten, ist es zu erwarten, dass erhebliche Anstrengungen seitens der Industrie erforderlich sind um diese Grenzwerte einzuhalten.

Zusammenfassend ist zu sagen, dass sich hinsichtlich der EMV-Koordination die Industrie nicht die Vorgaben von Funkern resp. Regulierungsbehörden aufdiktieren lassen darf. Die in der europäische Normung festgelegten Grenzwerte müssen als Kompromiss zwischen wirtschaftlichem Aufwand und Nutzen sowie Frequenzschützern und –nutzern gefunden werden. Darüberhinaus muss klar sein, dass für den Fall keiner Einigung die schon seit langem bekannten Grenzwerte weiterhin gültig bleiben müssen. Hinsichtlich der Störfestigkeit sind global operierende Hersteller von Brandmeldeanlagen gut beraten, weiterhin die „alte“ DIN EN 61000-4-6 von 2001 anzuwenden. Damit können sowohl die Anforderungen der europäischen, als auch die der aussereuropäischen Zertifizierungsinstitute erfüllt werden.

Allerdings sollte beachtet werden, dass die in den Normen geforderte Modulation nicht die worst-case-Situation darstellt. Auf die sich immer weiter verbreitenden breitbandigen Störsignale reagiert eine Brandmeldeanlage unter Umständen störanfälliger. Aus Gründen der Produkthaftung und nicht zuletzt der Produktqualität ist eine Auswertung der Signale von Funkdiensten, die in der Umgebung der Brandmeldesysteme betrieben werden angeraten. Mit Hilfe dieser Ergebnisse können dann praxisrelevante Prüfungen, insbesondere bei Neuentwicklungen durchgeführt werden.

Produkte von Herstellern, die dieses berücksichtigen sind damit sehr wahrscheinlich in der Lage auch zukünftigen normativen EMV-Anforderungen gerecht zu werden, ohne aufwändige Redesigns durchführen zu müssen.

Ulrich Oppelt, Bernd Siber
Bosch Sicherheitssysteme GmbH, Ottobrunn, Germany

in Rauchmelder f r sthetische mgebung

Abstract
In buildings with representative character an emphasis is given in a consistent appearance with harmonized design of all room elements. Common fire detectors inevitably interrupt the consistent appearance in environments like foyers, museums or historical buildings. To solve such inconsistencies, a smoke detector will be presented, which can be flush mount in the ceiling and which will unobtrusively fit into nearly every environment through neutral elegance.

1. Allgemeines

Systeme für die Meldung von Bränden im Entstehungszustand ben tigen empfindliche Messmittel für die Erfassung der charakteristischen Kenngr en einer Brandsituation. Da ein Brand überall im Gebäude entstehen kann und die physikalischen Brandkenngr en im Frühstadium eines Brandes lokal begrenzt sind, muss für eine umfassende berwachung ein Gebäude flächendeckend mit Branddetektoren ausgerüstet werden. Eine solche umfassende berwachung schlie t zwangsläufig auch Räume mit repräsentativem Charakter oder architektonischen Anspruch ein.

Die am häufigsten eingesetzten Branddetektoren sind Rauchmelder, die nach dem Ionisationsprinzip oder nach dem Streulichtprinzip arbeiten. Beide Arten von Rauchmeldern ben tigen eine Messkammer zur Detektion von Rauch, in die der Rauch über vorhandene ffnungen aufgrund einer natürlichen oder von dem Entstehungsbrand erzeugten Luftstr mung eindringt. Aus diesem Grund muss die Messkammer einige entimeter unter der Raumdecke angebracht werden, um den Rauch frühzeitig und sicher detektieren zu k nnen. Würde die Messkammer innerhalb der Decke angebracht, so würde der Rauch erst sehr spät oder gar nicht im Verlauf eines Entstehungsbrandes in die Messkammer eindringen. Um in diesem Fall ein frühzeitiges Ansprechen des Rauchmelders

zu erreichen, müsste – wie bei Rauchansaugsystemen – die Raumluft unter der Decke aktiv angesaugt werden, was zu einem erheblichen konstruktiven Mehraufwand führen würde. Aufgrund der ben tigten Messkammer ragen daher alle „punktf rmige“ Rauchmelder um ihre Bauh he sichtbar in den überwachten Raum hinein.

Eine Brandmeldeanlage und damit auch alle Melder, die im gesamten Gebäude verteilt sind, erfüllen für den Nutzer einen vorbeugenden weck. Die eigentliche Funktion der Anlage kommt erst im Falle eines Brandes zum Tragen. Da ein Brand ein seltenes und auch kein gewünschtes Ereignis ist, hat für den Nutzer eine solche Anlage zunächst einmal keinen direkt sichtbaren Nutzen. usätzlich entstehen Kosten und Aufwand für die Aufrechterhaltung der Betriebsbereitschaft. Darüber hinaus sind seine Räumlichkeiten mit –zig, hunderten oder sogar tausenden von Meldern bestückt, die sichtbar aus der Decke ragen. Ferner fällt bei Decken, die nicht wei gehalten oder gar farblich strukturiert sind, ein gängiger wei er Brandmelder allein schon durch seine Farbe auf. Die Anpassung der Farbe eines Brandmelders an die Deckenfarbe ist bisher aufgrund des logistischen Aufwandes bei der Melderfertigung mit erheblichen Mehrkosten verbunden.

Viele Räumlichkeiten in Gebäuden werden für eine spezieller Nutzung ausgelegt. In Industriebauten k nnen das z.B. Fabrikhallen sein, die speziell für effiziente Produktion oder logistische Abläufe geplant und gebaut sind. In Gebäuden wie Hotels, Theatern und Museen wiederum gibt es Räumlichkeiten, bei deren Nutzung ein ffentlicher und repräsentativer Charakter eine wesentliche Rolle spielt. Das Erscheinungsbild solcher Räumlichkeiten soll insbesondere Kunden und Publikumsverkehr ansprechen und wird oftmals von Architekten auf Wunsch des Bauherrn aufwendig gestaltet. Hier nun beginnt der Konflikt zwischen der Forderung nach einem Brandfrüherkennungssystem, das funktionsbedingt sichtbar in Form lauter kleiner runder „Joghurtdosen“ an der Decke hängt und der gewünschten einheitlichen st rungsfreien Gestaltung des repräsentativen Umfelds. Betrachtet man sich die Historie von Brandmeldern, so ist in der Gestaltung der Melder über die Jahrzehnte hinweg ein Trend zur optischen Versch nerung durch entsprechendes Design zu erkennen. Trotzdem bleibt auf Grund des verwendeten Prinzips einer Rauchme kammer eine Geräteform, welche die einheitliche glatte Fläche

einer Decke optisch deutlich unterbricht. Die einzigste M glichkeit diesen Konflikt zu l sen bestand bisher darin, ein Rauchansaugsystem mit entsprechend hohen Installationskosten in diesen Bereichen einzusetzen.

Um den eigentlich gegensätzlichen Forderungen nach architektonischem Anspruch und Schutzfunktion gegen Brände bei vertretbaren Kosten entgegenzukommen, würde es ausreichen ein Brandmeldeprinzip zu finden, das sich unauffällig in die Gestaltung der meisten Räumlichkeiten einfügt. Wie oben dargelegt spielt eine wesentliche Rolle für die Unauffälligkeit, dass nichts aus der Decke herausragt und die gleichmä ige Ebene der Decke unterbricht. Ein weiteres Kriterium ist sicher, dass auch eine m gliche Farbgestaltung nicht durch die Farbe des Melders unterbrochen wird. Trotzdem muss das Arbeitsprinzip des Melders den hohen Ansprüchen an seine Schutzfunktion entsprechen. Im Folgenden soll am Beispiel der neuen deckenbündigen Melderserie FAP 500 gezeigt werden, wie diese Problematik gel st werden kann.

2. Anforderungen an das Me system

Bei einem Streulichtbrandmelder wird die Rauchdichtemessung üblicherweise in einer labyrinthartig gestalteten Messkammer durchgeführt. Aufgabe der Kammer ist es, Umgebungslicht vom lichtempfindlichen Empfänger fernzuhalten, worauf die kompliziert gestalteten Raucheintritts ffnungen zurückzuführen sind.

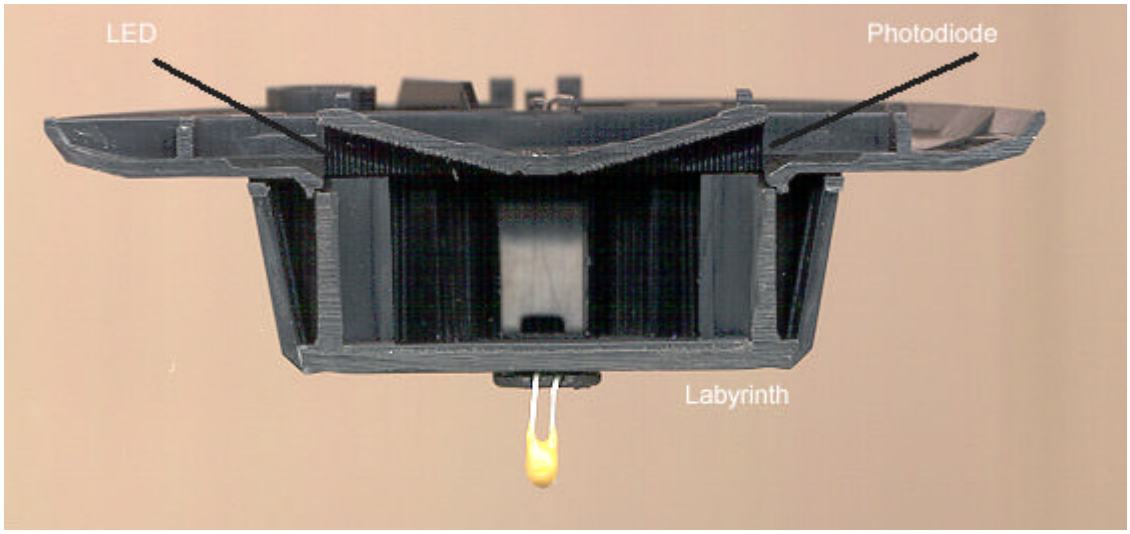

Abb.1: Schnitt durch Melder mit Labyrinth

Weiterhin soll die Kammer das Eindringen von Insekten und Staubpartikeln verhindern, die ein von Rauch nicht unterscheidbares Messsignal und damit u.U. einen Falschalarm erzeugen würden. Ferner wird von der Messkammer verhindert, dass Gegenstände in den Streupunkt gelangen k nnen. Um die Messkammer nicht unn tig gro zu gestalten, müssen ferner Ma nahmen zur Unterdrückung von unerwünschten Reflektionen des von der Lichtquelle ausgesandten Lichtes an den eigentlichen Kammerwänden getroffen werden.

Entfernt man die Kappe der Messkammer und gestaltet die Anordnung von Lichtquelle und Lichtempfänger geschickt, so erhält man ein flaches Me system mit im Grundsatz gleichen Rauchmesseigenschaften wie mit einer umgebenden Kammerwand.

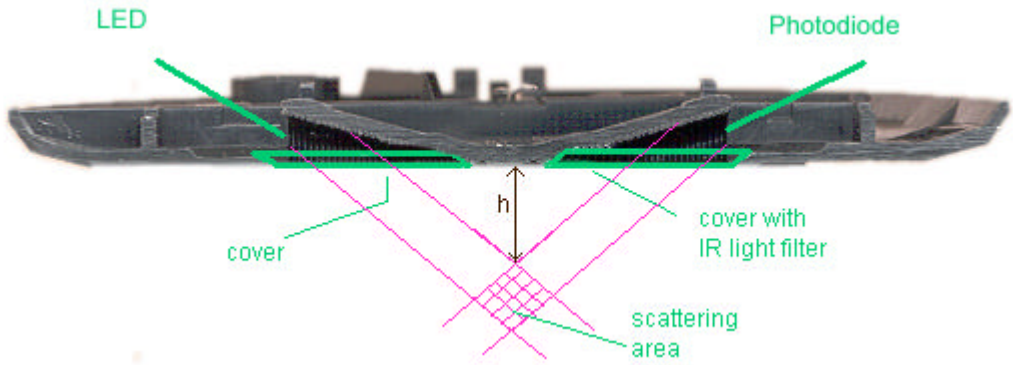

Abb. 2: Schnitt durch Melder ohne Labyrinth

Nebenbei fällt der Raucheindringwiderstand bedingt durch den Str mungswiderstand der Kammerwände weg. Wird ein solcher flacher Melder bündig in eine Decke eingebaut, so ist die wesentliche Forderung an die sthetik in Räumen erfüllt. Der Streupunkt für die Rauchmessung liegt au erhalb des eigentlichen Gehäuses einige entimeter unterhalb der Decke, wo Rauch gut gemessen werden kann. Erkauft wird die sthetik damit, dass Methoden zur Unterdrückung der Einflussgr en „Umgebungslicht“ und „Insekten/Gegenstände“ gefunden werden müssen.

3. Einfluss von Umgebungslicht

Als Umgebungslicht müssen unterschiedliche Lichtquellen berücksichtigt werden, die sich in Intensität, Farbspektrum und Modulation unterscheiden.

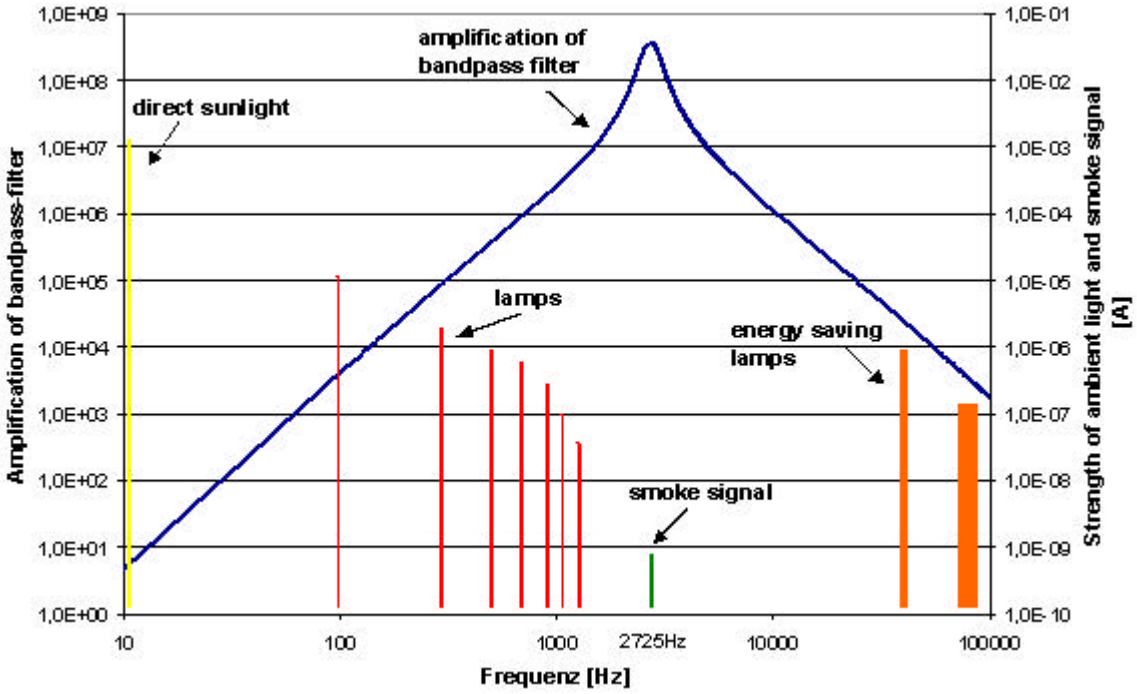

Abb. 3: Frequenzdiagramm und Filterkurve

Da für die Beeinflussung des Melders die Lichtintensität am Lichtempfänger eine Rolle spielt, muss dabei auch der Abstand zur Lichtquelle und der Einfallswinkel berücksichtigt werden. Sonnenlicht ist nicht moduliert und tritt in Intensitäten bis 100000 lux auf. Der Gleichanteil des von Glühlampen ausgehenden Lichtes ist in der Regel weniger intensiv, jedoch gibt es auch Frequenzanteile, die mit 100Hz und entsprechenden Oberwellen moduliert sind. Am wenigsten überschaubar sind Leuchtstofflampen und so genannte Energiesparlampen, bei denen die Startelektronik das Licht bis in Bereiche von mehreren 100 kHz moduliert. Ferner ist das Frequenzspektrum dieser Lampen von Hersteller zu Hersteller unterschiedlich. Um eine sichere Funktion eines Streulichtbrandmelders zu gewährleisten, muss das von Rauch gestreute Licht eindeutig vom einfallenden Licht der verschiedenen Lichtquellen unterschieden werden.

Dies wird durch folgende Ma nahmen erreicht:

a) Für die Streulichtmessung wird als Lichtquelle eine LED mit einem Emissionsmaximum bei 880nm verwendet. Um sichtbares Fremdlicht zu unterdrücken wird ein optisches Kantenfilter an der Empfangsdiode verwendet, welches sichtbares Licht mit einer Wellenlänge kleiner als 800nm steilflankig unterdrückt.

b) Messungen haben ergeben, dass auch bei Verwendung eines optischen Kantenfilters eine Dämpfung von mehr als 120dB erforderlich ist, um bei dem direkten Einfall von Licht einer sehr hellen Fremdlichtquelle und einem geringen Abstand dieser Lichtquelle zum Brandmelder (z.B. beim Blendtest der DIN EN54-7) das Fremdlicht ausreichend zu dämpfen. Dies wird durch einen analogen aktiven Bandpass fünfter Ordnung erreicht, mit dem das Streulichtsignal gefiltert und verstärkt wird.
c) Dem analogen Bandpassfilter nachgeschaltet wird ein phasenempfindliches synchrones Filter, welches synchron zur Sendefrequenz der LED arbeitet. Die Mittenfrequenz des Filters ist in einen Frequenzbereich gelegt, in dem keine St rfrequenzen durch Energiesparlampen erwartet werden. Da die Frequenzbereiche der Energiesparlampen nicht durch die Hersteller offengelegt sind, wurden sie durch Versuche mit m glichst vielen Lampen verschiedenster Hersteller auch aus anderen Bereichen der Welt ermittelt.

Mit dieser dreistufigen Filterma nahme kommt der Melder mit Beleuchtungssituationen zurecht, die in der Praxis auf Grund des deckenbündigen Einbaus (im Normalfall kein direkter Einfall des Lichtes auf den Melder, da das Licht von der Decke in Richtung Boden abgestrahlt wird) in dieser Form kaum anzutreffen sein dürften.

4. Einfluss von Insekten und Gegenständen

Insekten, die sich auf der Oberfläche des Melders befinden, k nnen sofern sie sich im Streupunkt (d.h. dem geometrischen Schnittpunkt der optischen Achsen des Lichtempfängers und Lichtsenders) befinden, das von der Lichtquelle des Streulichtbrandmelders ausgehendes Licht zum Lichtempfänger reflektieren und so wie Rauch ein Signal am Lichtempfänger erzeugen. Hat der Streupunkt einen ausreichenden Abstand von der Melderoberfläche (gr er als die Gr e eines Insektes), dann kann dieser Fall nicht mehr eintreten. Eine solche Anordnung bedeutet jedoch, wenn man die maximale Gr e von 5-6cm von Insekten betrachtet, geometriebedingt eine rückwärts streuenden Anordnung mit zudem relativ langen Strahlengängen. Dies führt aufgrund des kleiner werdenden ffnungswinkels zu einer starken Abnahme des Streulichtsignals am Lichtempfänger und damit auch zu einem schlechter werdenden Verhältnis von vom Rauch verursachten Streulichtsignal zum vom Fremdlicht erzeugten St rsignal.

Um trotzdem eine ausreichende Unempfindlichkeit gegenüber Insekten zu erreichen, ist bei der Brandmelderserie FAP 500 eine Anordnung mit zwei voneinander unabhängigen Streupunkten gewählt worden. Beide Streupunkte liegen in einem so gro en Abstand voneinander, dass ein einzelnes Insekt nicht beide Streupunkte gleichzeitig beeinflussen kann.

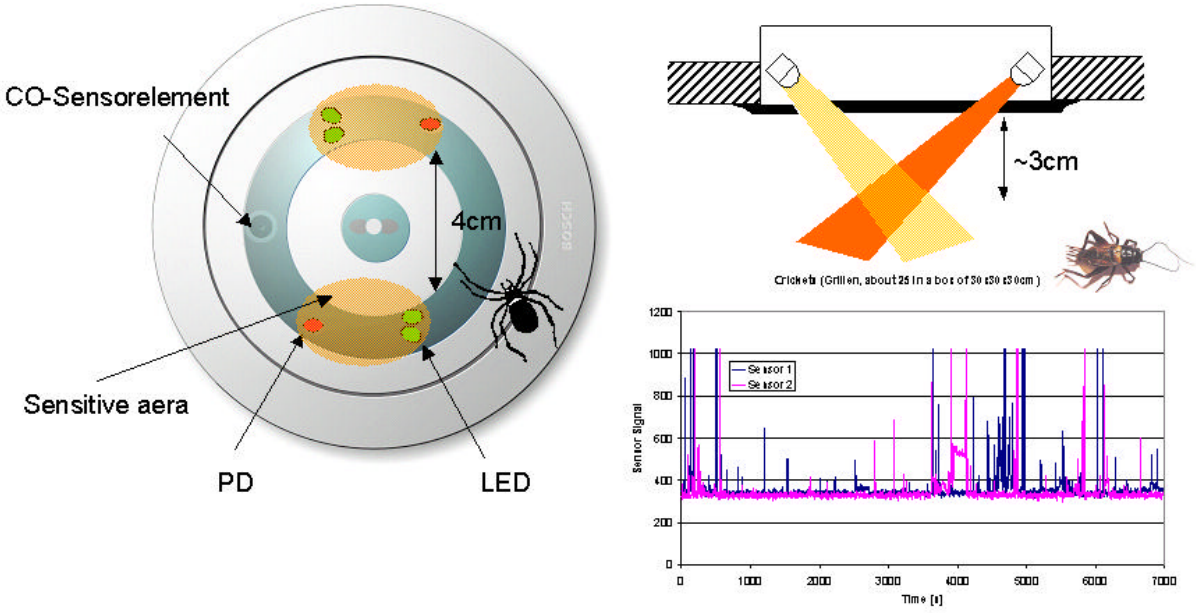

Abb. 4: Sensorflächen

Die beiden Signale erlauben eine differenzierte Beurteilung über das optische Umfeld im Nahbereich des Melders. In der Signalverarbeitung kann dadurch das in etwa symmetrische Ansteigen der Signale beider Streupunkte bei Vorliegen von Brandrauch von einer unsymmetrischen Signalverteilung, wenn ein Insekt sich in einem Streupunkt aufhält, unterschieden werden. Ferner k nnen durch eine zeitliche Analyse beider Streulichtsignale weitere Hinweise gefunden werden, um zwischen Rauch (langsames stetiges Ansteigen des Streulichtsignals) und Gegenständen (schnell und unstetig ansteigendes Streulichtsignal) zu unterscheiden.

5. Farbliche Anpassung

Eine Unauffälligkeit des Melders an der Decke ist nur gegeben, wenn auch die Farbe des Melders an die Farbe der Decke angepasst ist. blicherweise würde das bedeuten, dass für jede gewünschte Farbe das Gehäuse in entsprechender Farbe produziert werden

muss, was zu einem sehr hohen logistischen Aufwand führt. Ferner geht bei einer Umgestaltung des Raumes m glicherweise die Farbanpassung wieder verloren.
Bei der Brandmelderserie FAP 500 wird eine elegante Farbanpassung dadurch erm glicht, dass die Melder eine transparente Abdeckscheibe mit einer Aussparung besitzen, in die Farbringe eingelegt werden k nnen. Diese Farbringe werden als Satz dem Melder mitgeliefert.

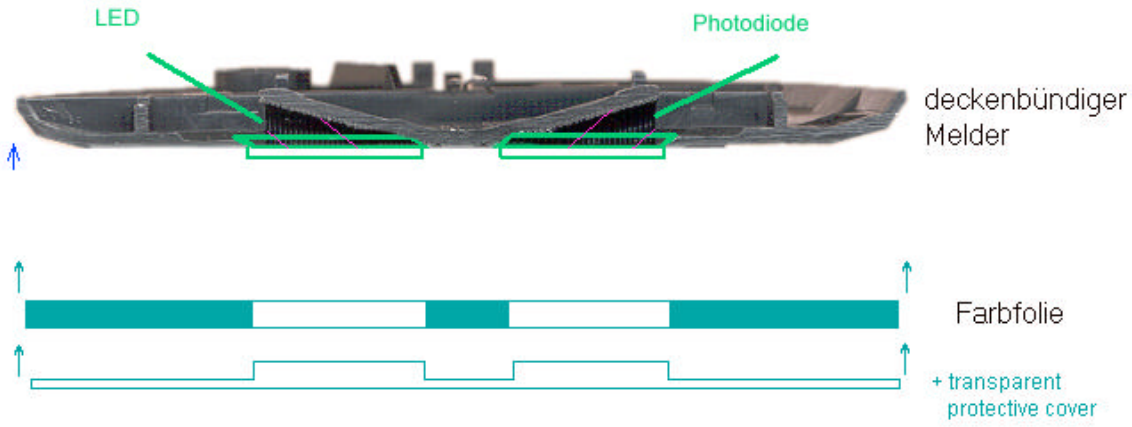

Abb. 5: Farbringwechsel

Der Farbsatz ist so ausgerichtet, dass er das gesamte Farbspektrum mit jeweils zwei unterschiedlichen Farbt nen abdeckt. Die Abdeckscheibe selbst ist leicht matt gestaltet, so dass sich bei Betrachtung ein scheinbarer Farbverlauf ergibt, was erlaubt, mit einem eingeschränkten Satz an Farben sich an alle Decken anzupassen. Das Einlegen bzw. das Austauschen der Farbringe wird vor Ort durch den Facherrichter durchgeführt. Damit ist zum einen eine optimale Adaption an die Deckenfarbe gewährleistet, zum anderen kann bei einer Umgestaltung die Farbe erneut angepasst werden.

6. Verschmutzungserkennung

Die glatte Oberfläche eines deckenbündigen Melders erscheint auch geeignet für den Einsatz in Anwendungen mit starkem Staub- und Flusenanfall. Gerade gr ere Flusen und Staubpartikel, die die ffnungen der Messkammer eines Brandmelders blockieren k nnen (siehe Abb. 6), finden an der glatten Oberfläche des Melders keinen Haltepunkt.

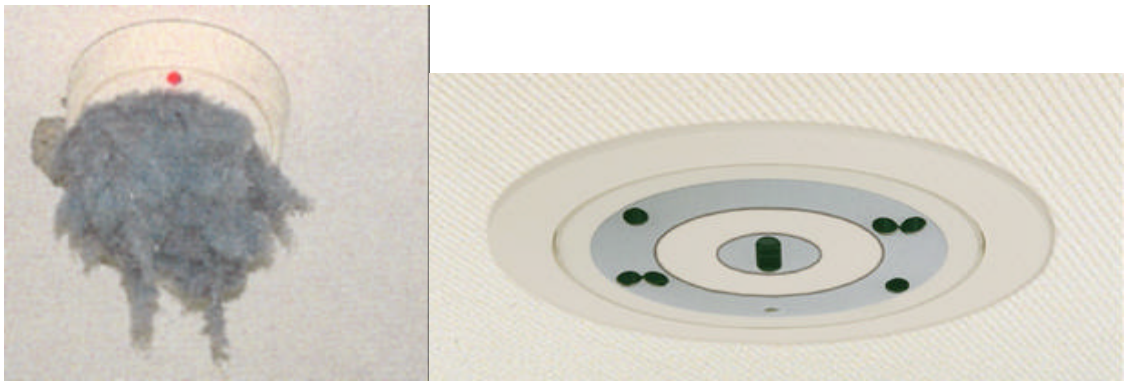

Abb. 6: Verschmutzungseigenschaften

Die glatte Oberfläche erlaubt zudem ein einfaches Entfernen von ggf. trotzdem vorhandener Ablagerungen. Damit eventueller Staubbelag die Funktion des Melders nicht beeinträchtigt prüft der Melder mit einem weiteren Sensor den Verschmutzungsgrad der Oberfläche.

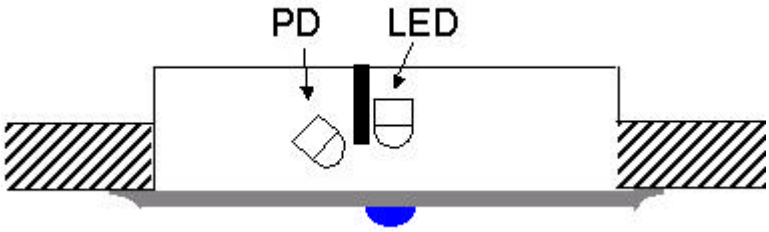

Abb. 7: Verschmutzungssensor

Das Arbeitsprinzip ähnelt dem Streulichtsensor für die Rauchmessung, nur dass LED und Photoempfänger direkt nebeneinander angeordnet sind und ein Streulichtsignal durch die Staubpartikel direkt auf der Oberfläche generiert wird. Mit dem Verschmutzungssensor kann auch erkannt werden, falls der Melder fälschlicherweise mit Farbe angestrichen wird.

7. Mehrkriterienmelder

Die Verbesserung gegenüber physikalischen St reinflüssen durch die Kombination von Sensoren für unterschiedliche Brandkenngr en ist an anderer Stelle ausführlich diskutiert worden 1 . Mit dem Einsatz eines zusätzlichen CO-Sensors ist es m glich, ohne Verlust von Detektionsempfindlichkeit, die Schwelle der optischen Sensoren im Ruhe-

zustand zu deutlich unempfindlicheren Werten zu verschieben und damit die uverlässigkeit des Melders in Bereichen mit hohen Wertkonzentrationen zu erh hen.

Abb. 8: Multisensordetektor mit CO-Sensor

Ein CO-Sensor liefert gerade bei einem deckenbündigen Brandmelder ohne optisches Labyrinth ein wichtiges Signal zur Unterscheidung von Rauch von Insekten/Gegenständen.

8. usammenfassung

In vielen Bereichen moderner Gebäude besteht der Konflikt zwischen der Notwendigkeit von Geräten für die Brandfrüherkennung und der Unterbrechung der sthetik durch genau diese Gerätschaften. Mit der Entwicklung eines Melders der sich flach an die Decke schmiegt und sich dabei auch farblich an die bestehende Umgebung anpasst ist ein wesentlicher Schritt zur L sung des gestalterischen Dilemmas gelungen. Durch die besonderen Ma nahmen zur Filterung von Umgebungslicht und die spezielle Auslegung der Sensorik zur Eliminierung von St rungen durch Insekten und sonstigen St rgr en ist es gelungen, ohne Verlust an Detektionsempfindlichkeit und Melderzuverlässigkeit, einen Melder zur Verfügung zu stellen, der überall da seine Einsatzberechtigung hat, wo Brandschutz und Raumgestalten gemeinsam eine Rolle spielen.

Lit.:

1 : U. Oppelt, Measuring results of a combined optical, thermal and CO detector in real sites and classifying the signals, AUBE 2001

Thomas G. Cleary
Building and Fire Research Laboratory
National Institute of Standards and Technology
Gaithersburg, MD 20899 U.S.A.

A Test Methodology for Multiple Sensor Multiple Criteria Alarms

Abstract

Multiple sensor-multiple criteria fire alarms hold promise for improving fire detection by both increasing sensitivity to fire while decreasing nuisance alarms. Eventually, to provide a fair assessment of performance, some type of uniform testing protocol needs to be advanced in order to demonstrate to stakeholders (standards organizations, testing laboratories, manufacturers, governmental organizations, fire departments and affiliated national organizations, and consumers) the value of various alarm designs. Standard fire sensitivity tests provide one way to assess fire detection performance, but there are no consensus standards related to nuisance sources. NIST is working on a test methodology based on reproducing fire and nuisance conditions in the fire emulator/detector evaluator (FE/DE). Full-scale fire and nuisance tests conducted as part of the Home Smoke Alarm Project supplied the data for comparisons to scenarios emulated in the FE/DE. Comparisons of two of these tests, a smoldering chair and cooking oil fire, to their emulated scenarios in the FE/DE are described and shortcomings identified. Based on these results and previously reported emulated fire and nuisance tests, the proposed methodology shows promise in relating full-scale smoke alarm tests to reproducible laboratory tests at a level sufficient to assess alarm performance where sensors respond to convected heat, smoke and combustion gases, or nuisance products. However, more test development is needed in order to more closely match real-scale test conditions to emulations and to demonstrate repeatability.

Introduction

Available test methods are sufficient to assess the performance of current smoke alarm designs. However, new fire alarm designs may not be sufficiently challenged by current test methods. One of the main driving forces for new fire alarm designs is the desire to reduce nuisance alarms. Several designs have been proposed using

combinations of particulate, gas sensing, thermal and other sensors, with alarm criteria requiring anything from simple to more complex sensor signal processing and computations. Room-scale fire sensitivity tests found in EN 54 1 and UL 268 2 standards produce common potential fire environments, and present to an alarm all the stimuli it would experience during fire including: smoke, gas and heat exposures, and flow velocities produced by the fire plumes. No such testing protocols exist for nuisance alarm sources. While room-scale protocols for nuisance sources could be developed as a compliment to the fire sensitivity tests, another alternative is to reproduce both fire and nuisance test results in a laboratory-scale instrument to improve repeatability and reproducibility with less effort than room-scale experiments. This idea is not new. Denny 3 describes a small-scale test tunnel used to transport fire and non-fire stimuli to sensors to provide realistic data used to train a discriminating fire detector. Grosshandler 4 introduced the concept of a universal fire emulator/detector evaluator, who s objective is to produce well-controlled environments and to eliminate run-to-run variations observed in full-scale tests. The embodiment of Grosshandler s concept is the fire emulator/detector evaluator (FE/DE) tunnel 5 , and this device is the crux of the test methodology introduced here. Full-scale fire and nuisance tests conducted as part of the Home Smoke Alarm Project NIST TN 1455; 6 supplied the data for comparisons to scenarios emulated in the FE/DE.

The Home Smoke Alarm Project was a multi-year effort designed primarily to evaluate the current state of residential smoke alarms by examining how different types of smoke alarm technologies respond, and how their number, and locations in residential applications impact on life safety. The project included several aspects in the design of experiments to produce data needed to assess new technologies, and to more fully characterize the experimental conditions in order to reproduce those test environments in the FE/DE. Special attention was paid to the selection of realistic fire scenarios that emphasized the main types of fires that cause injury and death as indicated by U.S. residential fire statistics. These include upholstered furniture fires, and cooking fires. Fire tests were performed in both a single-story, and a two-story home. Nuisance source tests were also conducted in the single-story home; selected results from those tests are detailed in another paper in this conference 7 .

Full scale fire scenarios included: flaming and smoldering upholstered chairs, flaming and smoldering mattresses, and cooking oil fires. The bulk of the nuisance scenarios were related to cooking activities including: frying, deep-frying, baking, broiling, boiling, and toasting, in addition to cigarette smoke and burning candle exposures. Additionally, smoldering cotton and wood block sources similar to the EN-54 fire sensitivity test fires TF2 and TF3 1 , and smoldering polyurethane foam block tests were performed to provide comparative results to the nuisance test series. The product of the number of tests (70), and smoke alarm locations (4 to 8) yielded over 400 separate alarm environments.

The desire is to identify a small subset of these (fire and nuisance) environments that captured characteristic alarm producing conditions for residential applications, and that can be successfully reproduced in the FE/DE. A suitable subset of emulated tests forms the basis of a test methodology for residential alarms where performance assessments are made based on realistic fire and nuisance scenarios. NIST TN 1455 has complete descriptions of nuisance tests and several emulated nuisance scenario tests performed in the FE/DE that demonstrated similar environments and would lead to nuisance alarms 6 . A previously emulated flaming fire scenario based on an EN54 TF4 polyurethane foam mat fire in a multi-room configuration demonstrated similar characteristics to the flaming chair and mattress tests 8 . Specifically, the FE/DE was programmed to reproduce rapid increases in flow velocity, smoke and CO concentration, and air temperature observed in the model calculations for two discrete detector locations. The rate of rise in smoke and CO concentration, air temperature, and flow speed were similar to the flaming chair and mattress tests, and within the range of the FE/DE. The exact details of a flaming chair or mattress fire scenario are yet to be programmed into the FE/DE.

The focus here is on the single-story home results of a smoldering chair test, and a cooking oil fire test. These two tests produced characteristically different environments in their pre-flaming stages compared to flaming fire tests, and they presented a challenge to emulate in the FE/DE.

ome Smoke Alarm ro ect Tests

The test structure was a complete manufactured home, constructed off-site and transported to NIST. Its nominal dimensions were 20.1 m long and 4.2 m wide, with an interior ceiling that was pitched from the centerline at a height of 2.4 m to a height of 2.1 m at the exterior walls. The home was placed inside the Large Fire Test Facility building for all tests conducted. A schematic of the single-story home is shown in figure 1. The approximate locations of selected smoke meters, thermocouples, detectors, gas sampling, and velocity probes are shown. The notation for these

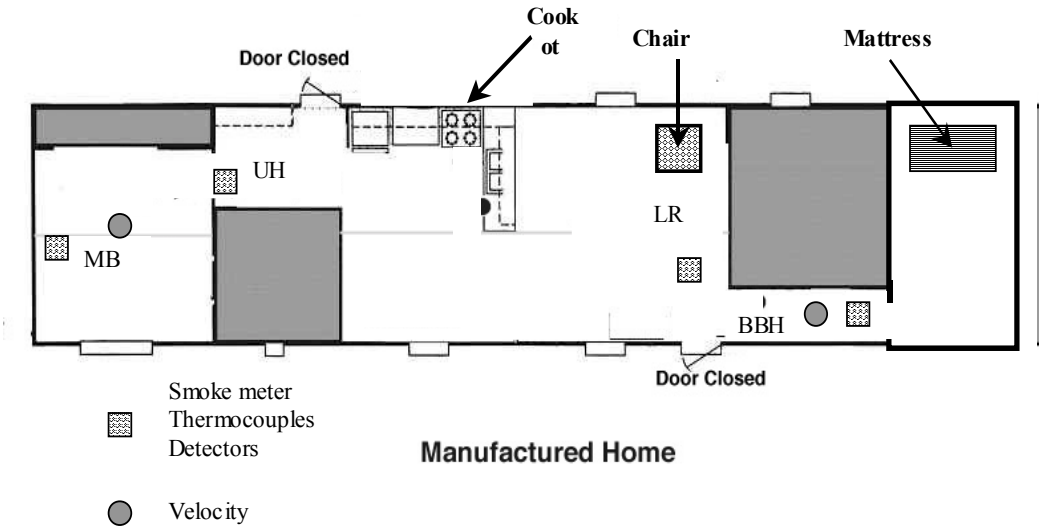

Figure 1 Schematic of Manufactured ome

locations are: MB – master bedroom, UH – utility hallway, LR – living room, and BBH – back bedroom hallway. Dark shaded areas are closed off. Full details on the configuration, exact location of measurements points, and alarms, materials burned, and the scenarios are given in the final report (NIST TN 1455 6 .) Only a brief description of the two selected fire tests is presented here, along with selected data.

A smoldering chair test was examined (SDC 34 in 6). The chair was remotely ignited by an electrically heated nichrome wire inserted into a slit made in the fabric and foam on the front face of the seat cushion. The heated wire initiated a smoldering process

that progressed until substantial portions of the chair foam were smoldering. The chair transitioned from smoldering to flaming after over an hour. At time = 0 s, the ignition sequence started.

A cooking oil fire was examined (SDC41 in 6). 500 ml of cooking oil was placed in a 0.3 m diameter saut pan, which was put on a propane gas range burner. The heat output from the burner was nominally 1.5 kW. At time t = 0 s, the propane burner was ignited. The oil continued to heat until it ignited about 1200 s later. Suppression followed soon after ignition.

Test series data from selected smoke meters, thermocouples, CO and CO_2 gas analyzers, and monitored smoke alarms are presented below. These graphs were constructed from the test data files 9 . Velocity measurements were made with 2-D sonic anemometers located 2 cm from the ceiling. According to the manufacturer, uncertainty in the velocity measurements is stated as 1 cm/s. The two velocity components were combined to give a scalar speed of the ceiling jet at the measurement location. The interconnect signal of residential smoke alarms were monitored and the transition from low to high voltage was used as the indication of alarm. Because of the built in delay between a local alarm and the interconnect signal, the uncertainty in the alarm time was estimated as 5 s. All data presented here was from devices and sampling locations nearest to one another, but in neither case were all measurements taken from the same location. This introduces uncertainty in the comparisons to the FE/DE tests where all measurements are taken at the same location.

F D Tests

The FE/DE was used to emulate a smoldering upholstered furniture fire, and a cooking oil fire. The objective here was to demonstrate that important features of the selected scenarios could be reproduced in the FE/DE. The FE/DE has been described elsewhere 5,6 . It is a single-pass “wind tunnel” that allows for the control of flow velocity, air temperature, gas species, and aerosol concentrations at a test section where sensors and alarms are exposed to these environmental conditions.

A foam block sample 10 cm x 10 cm x 8 cm in size, taken from an un-burned chair seat cushion of the same type smoldered in the fire test series, was used to produce the smolder smoke in the FE/DE emulation of the smoldering scenario. A nichrome wire loop, similar to the igniting wire in the full-scale tests, was inserted into a 3 cm long, 2 cm deep slit made in the foam block. The foam block was placed at the bottom of the vertical riser in the FE/DE, approximately 4 m from the test section. The wire was energized with an alternating current set at a level to initiate sustained smoldering in the block. The fan speed was set to provide mean flow velocity of 0.15 m/s in the duct.

Approximately 5.0 ml of corn oil placed in a 10 cm diameter glass dish which was put on a 750 Watt electric hot plate produced the smoke for the overheated cooking oil scenario. The hot plate was located at the bottom of the vertical riser in the FE/DE. The fan speed was set to provide a mean flow velocity of 0.1 m/s in the duct. Measurement uncertainty in smoke optical density, CO and CO_2 concentration, flow velocities and air temperatures recorded in the FE/DE have been previously estimated as $3x10^{-4}$ m^{-1}, $2.5x10^{-4}$ % volume fraction, $2x10^{-3}$ % volume fraction, 1 cm/s, and 1 ^{o}C respectively [5].

Results and Analysis

Results from the smoldering chair test are shown in figure 2. Figure 2A shows the optical density and air temperature 2 cm below the ceiling in the living room, and the time to reach alarm for the photoelectric and ionization alarms. Figure 2B shows the gas concentration results for CO and CO_2 at a sampling location 90 cm below the ceiling in the living room. The mean ceiling jet flow speed in back bedroom hallway, the closest measurement location to the living room area, was about 0.12 m/s for the time period prior to flaming.

The emulated smolder test is shown in figure 3 along with the smoldering chair test graphs re-scaled for comparison in figure 4. During this test, the power was turned on at 60 s and the foam block transitioned to flaming at about 940 s. The fan speed setting that produced a mean flow speed of 0.15 m/s at the test section was consistent with the

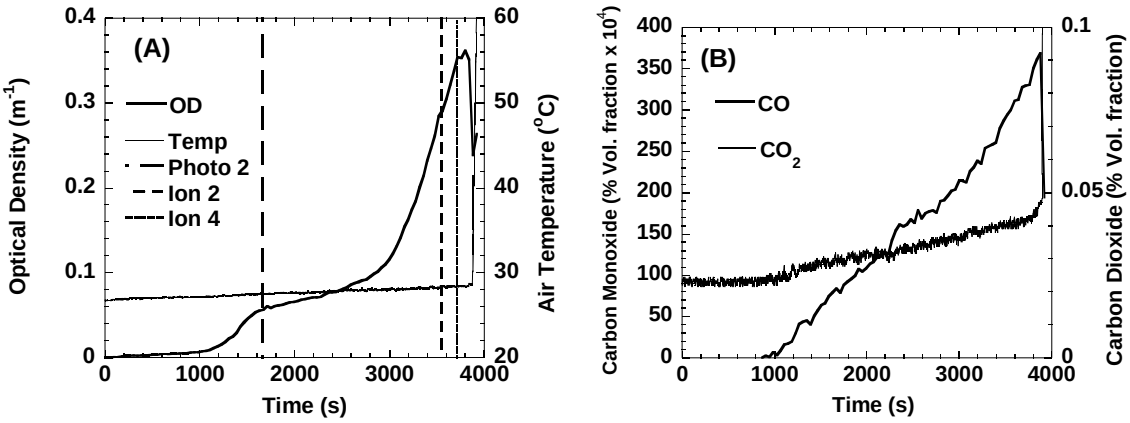

Figure Results for the smoldering chair test

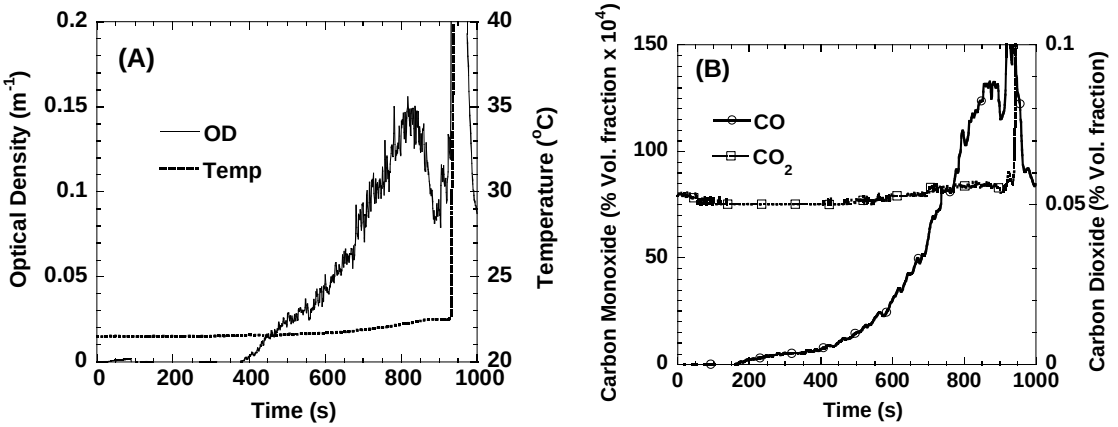

Figure Results from the F D smoldering foam block

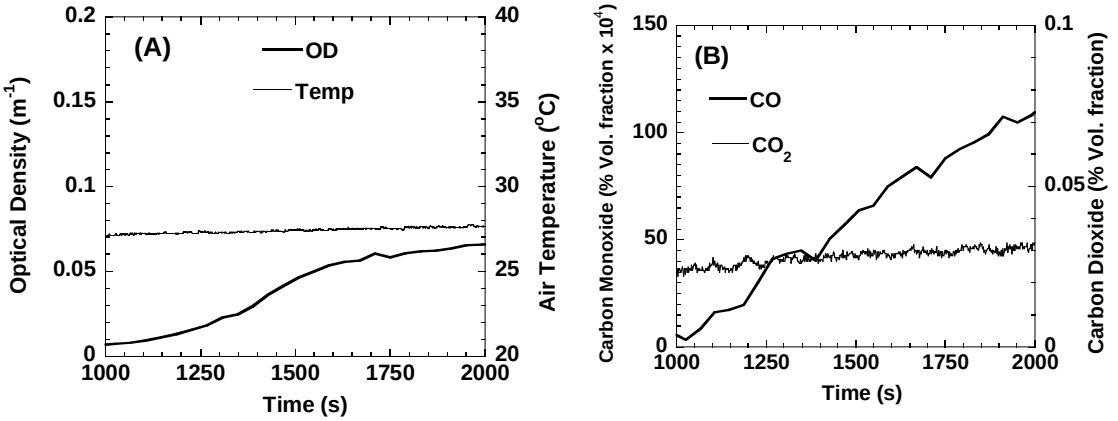

Figure Results from the smoldering chair test re-scaled graphs

chair test results. Prior to flaming ignition, air temperature and carbon dioxide concentration increased slightly, which was the same trend observed in the smoldering fire test. Carbon monoxide started to increase around 200 s, while the smoke optical density started to increase 200 s later. The initial rates of smoke and carbon monoxide increase were greater in the FE/DE test than the smoldering chair test. The FE/DE smoke optical density reached a value twice as high as the fire test, while the CO values were comparable at the end of the time comparison.

Results from the cooking oil fire test are shown in figure 5. Figure 5A shows the optical density and air temperature 2 cm below the ceiling in the living room, and alarm times for the living room location. Figure 5B shows the gas concentration results for CO and CO_2 at a sampling location 90 cm below the ceiling in the living room location. No velocity data was gathered during this test however, comparable velocity data from a nuisance cooking source test (hot oil deep frying with a LP gas cook top 6) gathered from a living room location yielded a mean ceiling jet speed of 0.15 m/s. The initial carbon dioxide and temperature increase prior to oil ignition was attributed to the propane burner. Optical density started to increase around 100 s, gradually at first, then more rapidly after 400 s. Carbon monoxide concentration started to increase around 400 s.

The emulated cooking oil test is shown in figure 6 along with cooking oil fire graphs re-scaled for comparison in figure 7. Power to the electric hot plate was turned on at 60 s and turned off at 1980 s; the oil never ignited. The air temperature started to increase around 500 s, indicative of the time it took to heat up the hot plate. Optical density started to increase around 1000 s while CO concentration started to increase 500 s later. The CO_2 was essentially constant throughout the test. The FE/DE cooking oil test lacks the CO_2 from the propane combustion and early smoke (perhaps from the burner) that activated an ionization alarm. The rate of increase observed for smoke, CO and temperature were similar for the FE/DE emulation and the cooking oil test, however, the CO concentration lagged the smoke optical density during the FE/DE test.

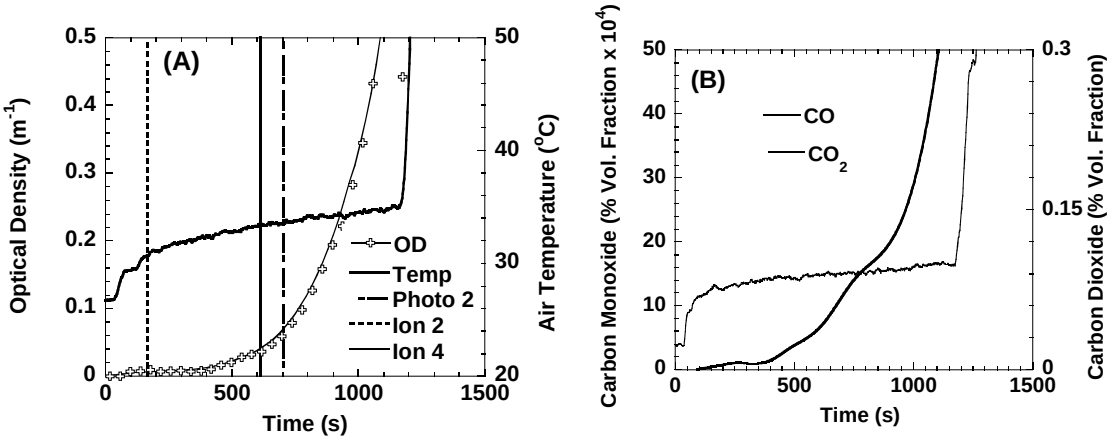

Figure Results for the cooking oil test

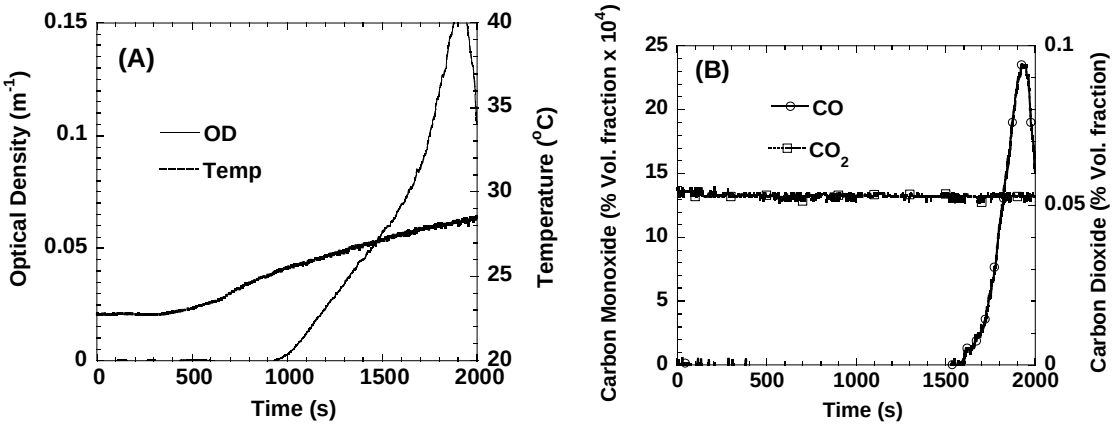

Figure Results from the F D heated oil test

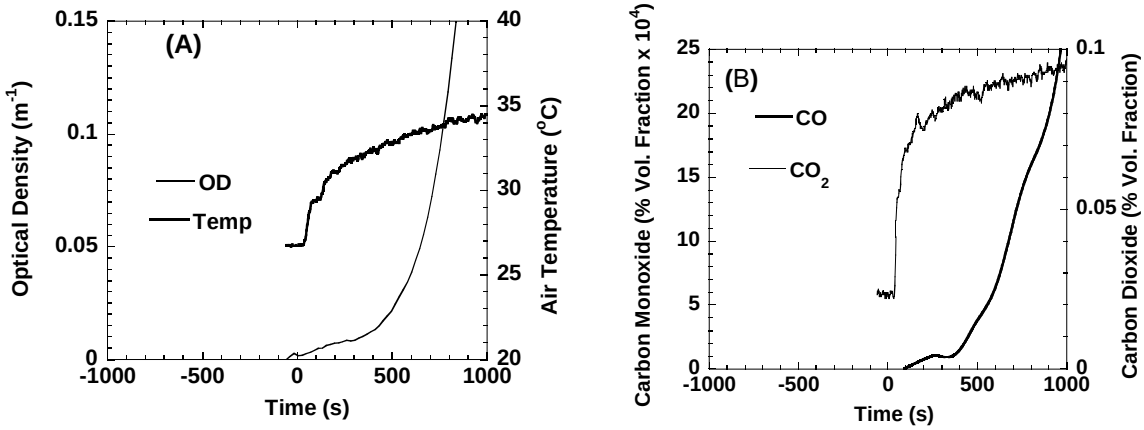

Figure Results from the cooking oil fire test re-scaled graphs

Conclusions

The levels of smoke, combustion gases, and temperatures developed during the selected fire tests showed that they are within the operational range of the FE/DE. The FE/DE smoldering foam block test displayed early fire signatures of smoke CO and CO_2 production, temperature and flow velocities comparable to the smoldering chair test. The FE/DE heated cooking oil test lacked early smoke production observed in the cooking oil fire test. For the most part, temperature, CO, optical density observations were similar to the cooking oil fire test. More testing needs to be performed to demonstrate a level of repeatability for these emulated test conditions. Successful emulation of these and other fire conditions in the FE/DE will allow for continued smoke alarm evaluation against the fire environments produced in the comprehensive Home Smoke Alarm Project test series for years to come. Furthermore, in addition to these tests, emulation of residential nuisance sources and standard fire sensitivity test conditions in the FE/DE would provide a more complete assessment of the performance of advanced multi-sensor, multi-criteria alarms.

References

1 EN 54: Components of Automatic Fire Detection Systems, Part 9, Fire Sensitivity Test, European Committee for Standardization, Brussels, 1982.

2 UL 268: Standard for Smoke Detectors for Fire Protective Signaling Systems, 4th ed., Underwriters Laboratories, Inc., Northbrook Il., 1996.

3 Denny, S., "Development of a Discriminating Fire Detector for Use in Residential Occupancies;" Report FP 93-07, M.S. Thesis, University of Maryland, 1993.

4 Grosshandler W. L., "Toward the Development of a Universal Fire Emulator/Detector Evaluator," Fire Safety Journal 29, 113-128, 1997.

5 Cleary, T., Donnelly, M., and Grosshandler, W., "The Fire Emulator/Detector Evaluator: Design, Operation, and Performance," 12th International Conf. on Automatic Fire Detection AUBE 99, Gaithesburg, MD, USA , pp. 312-323, 2001.

6 Bukowski, R., Peacock, R., Averill, J., Cleary, T., Bryner, N., Walton, W., Reneke, P., and Kuligowski, E., "Performance of Home Smoke Alarms," NIST Tech. Note 1455, 2003.

7 Cleary, T., "Residential Nuisance Source Characteristics for Smoke Alarm Testing,", 13th International Conf. on Automatic Fire Detection AUBE 04, Duisburg, Germany, 2004.

8 Cleary, T., Donnelly, M., Mulholland, G., and Farouk, B., "Fire Detection Performance Predictions in a Simulated Multi-room Configuration," 12th Int. Conf. on Automatic Fire Detection AUBE 99, Gaithesburg, MD, USA , pp. 455-469, 2001.

9 Peacock, R., Averill, J., Bukowski, R., and Reneke, P., "Home Smoke Alarm Project, Manufactured Home Tests," NIST Report of Test FR 4016, 2003.

Armin Riemer, Heiner Politze, Tido Krippendorf
Novar GmbH, Dieselstrasse 2, 41469 Neuss, Germany

Realisation of a ide-range optical detector using different a elengths and se eral scattering angles

1 Introduction

Today, optical smoke detectors that are based on the light scattering principle are dominant on the market with over 90% market share worldwide 1 despite increasing relevance of new technologies. Until now, the technical potential of optical detectors using the light scattering principle is not fully used. Already in 1999 tests proved, that the type and quality of an aerosol can be identified by using several scattering angles simultaneously 2 . By using also several light sources with different wavelengths the detection range relating to the size of aerosol particles can be increased considerably. The combination of both of these principles increases the detection bandwidth considerably within a consistent sensitivity range. Additionally false alarms sources can successfully be identified and suppressed by recognising their typical signal characteristics. Variable parameter adjustments in the detector allow a wide application adjustment.

Theoretical background

Normally, optical smoke detectors are based on the scattering principle. In this measurement principle the light of an emission source is scattered by aerosol particles of smoke. The scattered light will than be detected by a photo diode. When light as an electromagnetic wave is scattered, several physical effects influences the intensity of the scattered light depending on the type of aerosol (e.g. particle size) and depending on the wavelength of the used light:

- Refraction
- Diffraction
- Reflection
- Rayleigh scattering
- Mie scattering

The major influence on these physical effects has got the ratio between the size d of an aerosol particle and the wavelength λ of the incident light. The physical effects refraction, diffraction and reflection are so-called macroscopic effects or optical effects. These optical effects appear, if the size of the aerosol particle is much more higher than the wavelength (ca. $d \quad 3\ \lambda$). In this range, the intensity of the optical effects is nearly independent to the wavelength. If aerosol particles are much smaller than the wavelength ($d \quad 0.1\ \lambda$), the Rayleigh scattering is the major effect. The intensity of Rayleigh scattering depends on the wavelength in fourth order (see fig. 1) and depends on the viewing angle (fig. 2). In the transient area between Rayleigh scattering and optical effects ($0.1\ \lambda \quad d \quad 3\ \lambda$) the theory of Mie scattering describes the scattering behaviour. The Mie scattering predominant based on resonance effects between the aerosol particle and the electromagnetic wave and depends also very strong on the wavelength (see fig. 2). The full range over all scattering effects and their intensity is shown in fig. 2.

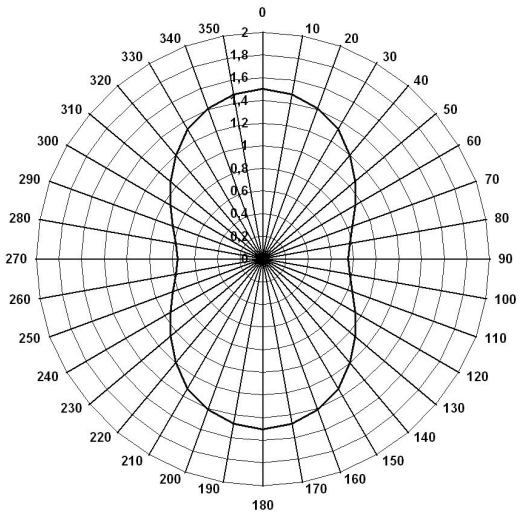

Fig 1: Angle dependency of Rayleigh scattering

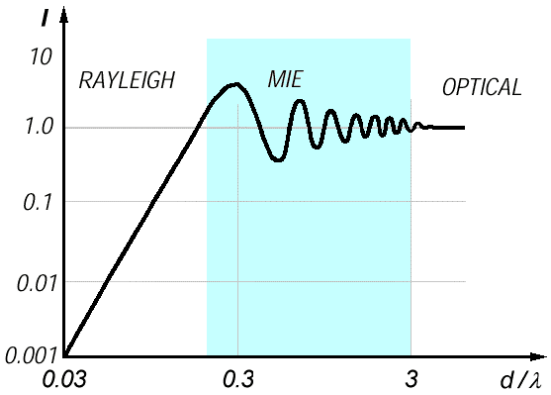

Fig. 2: Relative scattering ratio

While measuring smoke, one important property is, that the aerosol particles don t have the same size. Rather the particle size is a complex distribution function, which depends on a couple of effects. One major effect is the temperature of the fire, which emits the aerosol. As rule of thumb it can be said: Increasing fire temperature leads to smaller aerosol particles. This is also one reason, why optical smoke detectors normally are very insensitive to smaller aerosols e.g. test fire 1 (TF1, open wood fire) of the EN54 3 and are very sensitive to bigger aerosols e.g. test fire 2 (TF2, smouldering wood fire).

Measurement setup and results

Due to the many influencing factors on the particle size distribution of smoke, a calculation or a simulation of a scattering systems appears hopeless. Because of this, a special measurement setup (see fig. 3) has been created, which can be put into the EN54 smoke tunnel. The aim of this setup is to determine the dependency of the scattering angle by using two wavelengths while applying several types of smoke one by one. The tests have been performed inside the EN54 smoke tunnel for realizing a nearly static aerosol environment while measuring the angle dependency. The small inevitable drift of the aerosol concentration while one angle circulation has been compensated by using the optical and ionization reference systems (SICK and MIC) of the smoke tunnel. Using this setup the relative intensity of scattering signal has been measured using 470nm and 880nm wavelength for a couple of smoke types in correspondence to the EN54 test fires.

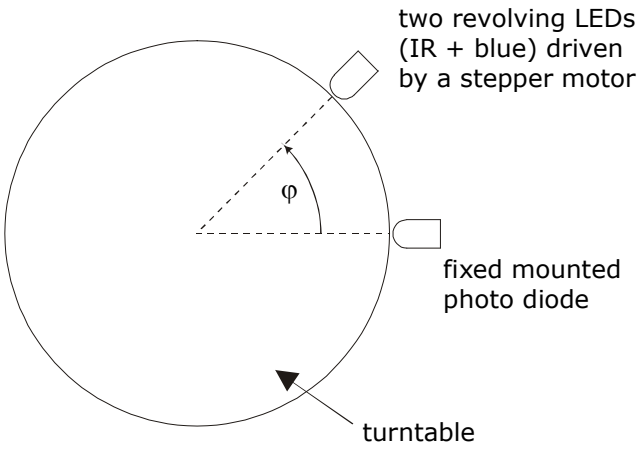

Fig 3: Measurement setup

By evaluating the measurement results in a logarithmic scale, 1999 already could be demonstrated 2 , that a characteristic ratio between the measurement values of two fixed angles depending on the type of smoke can be observed using one wavelength (880nm). In this case the values of the angle are not important but need to be fixed.

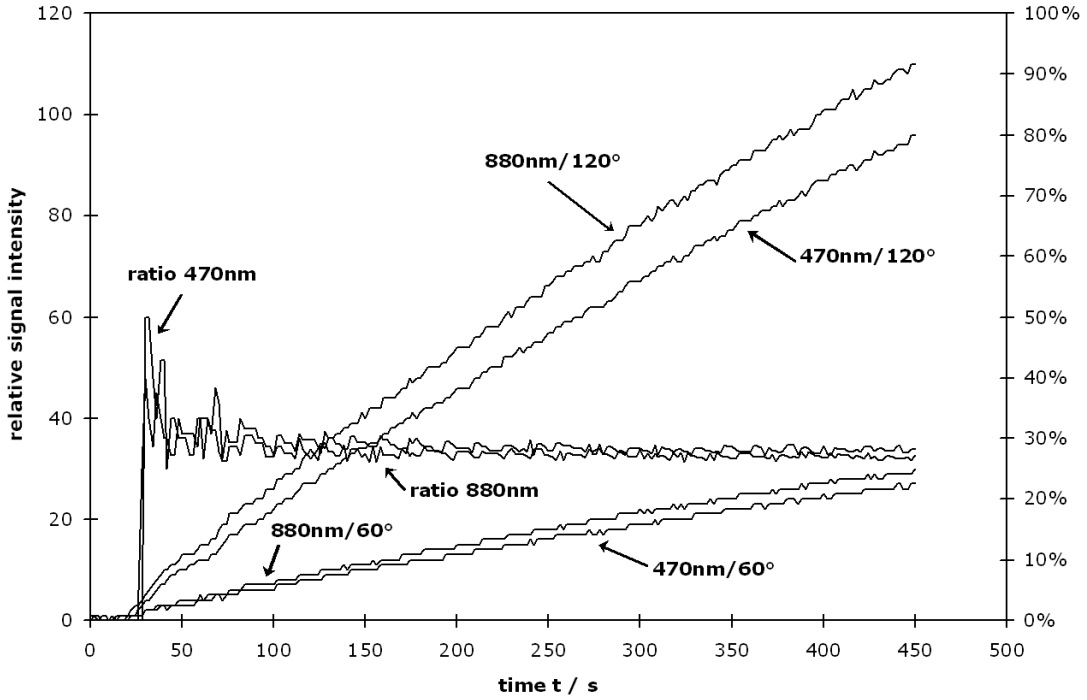

Fig. 4: Scattering results of paraffin with two several scattering angles

Using now an additional wavelength of 470nm the ratio of the measurement values at the same two angles also gives a characteristic value depending on the type of smoke (see fig. 4). But the most interesting point is, that the signal intensity is much higher for smoke with small particles, which can be explained by Rayleigh scattering. This effect also depends on the type of aerosol respectively smoke, which is a result of the whole scattering theory. The consequence of these results is, that on one hand the signal intensity can be increased a lot for smokes, which can normally be detected very difficult by an optical detector. On the other hand the type of smoke can be determined redundant by crosschecking the characteristic ratios e.g. for parametric adjustment of the detector s sensitivity to special environment like steam or fog.

Setup of a T detector ith t o a elengths

On the basis of these results Novar GmbH has built up a special fire detector, which can measure the scattering signals for two wavelengths and also two scattering angles quasi simultaneously. Fig. 5 shows the mechanical setup of this new detector with its smoke chamber. The scattering angles have been selected to 60 and 120 degree. Only in this combination it s possible to measure nearly the same smoke volume with both, the two wavelengths as well as the two angles. This is very important to get comparable results of both wavelengths and for reducing fluctuations and artefacts.

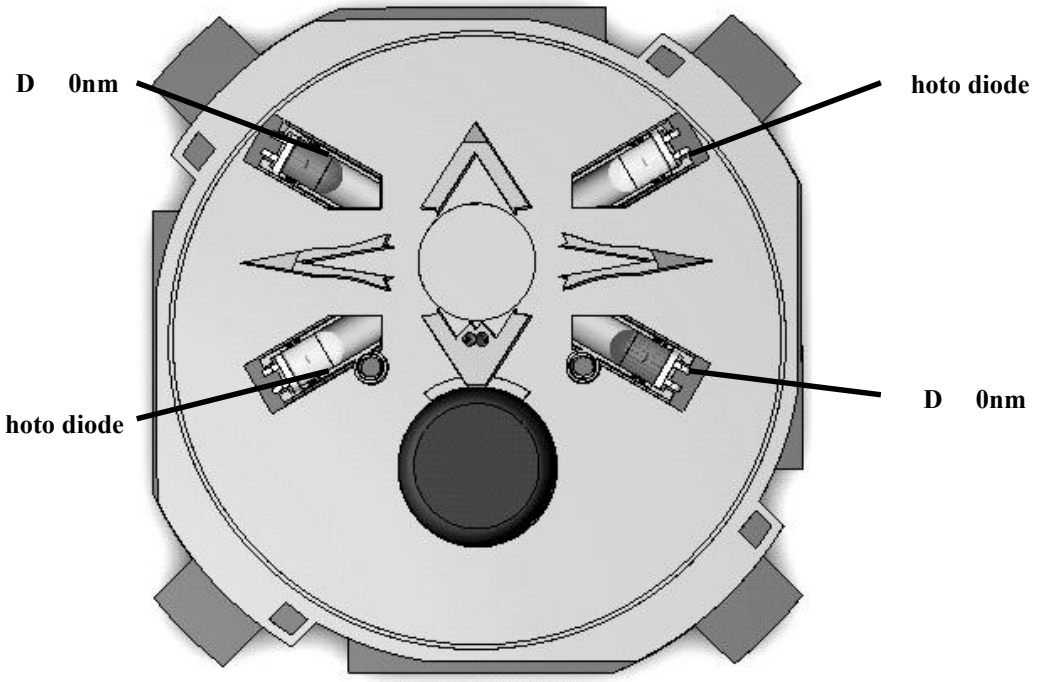

Fig 5: Setup of the new X T detector

Conclusions

It could be demonstrated, that an optical smoke detector with two scattering angles and two wavelengths is achievable. The exceptional advantage of this solution is that the typical negative characteristics of optical smoke detectors can be fully compensated by using the new measurement principles, like poor detection of hot fires (e.g. TF1) with small aerosol particles or fires with dark smoke (e.g. TF4, TF5) 3 as well as the high sensitivity e.g. to steam or fog. At the same time the typical positive characteristics of the optical scattering principle, in comparison to other detection principles (e.g. ionisation, gas or extinction detectors), like long-term stability, consistency against corrosive environments, low power consumption as well as low production and calibration costs are not influenced.

References

1 Novar GmbH, internal market analysis, Neuss, Germany (2003).

2 T. Krippendorf: „Streulichtmelder mit mehreren Streuwinkeln“, AUBE 99 Duisburg/ Germany, Proceedings (1999) 219 – 225.

3 EN54 part 7 (2000).

Jun-ichi Watanabe, Takayuki Nishikawa, Shoichi Oka, Masayuki Amano, Shigeki Shimomura

Matsushita Electric Works Ltd., Kadoma, Osaka, JAPAN

erformance e aluation of ne concept smoke and heat combined detection algorithm

Abstract

The market demands for fire detectors are always early detection and less false alarms. To meet these demands, the new concept of fire detection algorithm has been developed. This new concept is based on the three new features: new smoke and heat combined sensing, flexible delay time function, and adaptive learning. And the detector which integrated these three functions into one unit has been developed. The detector with this new concept can turn a conventional fire alarm system into a highly functional alarm system that has less non-fire alarms and detect all the Test Fires specified in EN54, and also reduce the operators and installers tasks to adjust detectors to meet the environment where they are installed.

1 Introduction

An automatic fire detection system needs to detect fires and give alarms under various conditions as quickly as possible. On the other hand, false alarms have to be reduced in order to keep reliability of the detection system. Coexistence of those somewhat contradictory performances is demanded to fire detection systems by the market.

Although fire detector can be divided roughly into smoke detector and heat detector,

due to the difference in detectable amount of smoke and heat, it can not always detect an early stage of fire, which occurs in various environments. In recent years, to overcome these weaknesses, fire detectors which combine smoke detection and heat detection are becoming increasingly popular. However, the frequency of non-fire alarms is also increased if both detection algorithms are simply combined.

In this paper, in order to aim an early detection of fire and reduction of non-fire alarms, the new concept of fire detection algorithm, which makes a judgment based on the amount of both smoke and heat and also incorporates adaptive learning, is proposed.

The algorithm proposed here is a new concept, and the evaluation method is not defined on the existing technical standards. So that, the performance evaluation was requested to Duisburg University in order to obtain an objective evaluation of this new algorithm.

In this report, this new algorithm is explained in full detail, and the method and the results of the performance evaluation are also reported.

Fire udgment Algorithm

The new algorithm consists of three new features, smoke and heat combined judgment, flexible delay time function, and adaptive learning. Each feature is described below.

1 Smoke and eat Combined udgment Algorithm

Characteristics of the smoke and heat generation in case of a fire are roughly classified into three types as following.

A: Generation of smoke is dominant and heat is barely generated; smoldering fire.

B: Simultaneous generation of both heat and smoke; flaming fire.

C: Generation of heat is dominant and smoke is barely generated; alcohol fire.

Figure 1 shows relationship between above three fire types and the judgment levels of (a) optical smoke detector (using scattered light), (b) smoke and heat combined detector (simple combination of smoke and heat detectors. Indicated as simple combined detector in following texts), and (c) new smoke and heat combined detector (new proposed detector indicated as new combined detector). Smoke density (%/m) is shown in the horizontal axis, and the temperature rise (deg.C / unit time) is shown in the vertical axis. If either of smoke density or a temperature rise rate goes into the fire judgment domain in the figure, it will be judged as a fire.

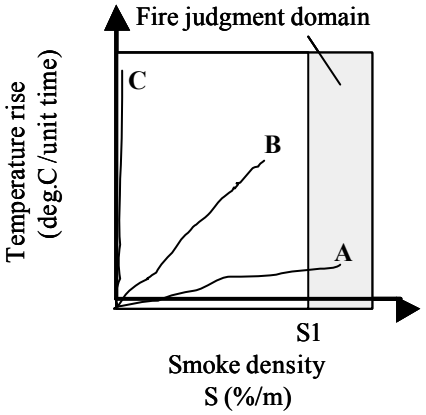

(a) The fire judgment domain of an optical smoke detector

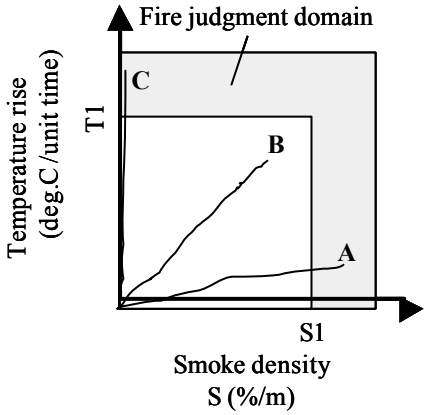

(b) The fire judgment domain of a simple combined detector

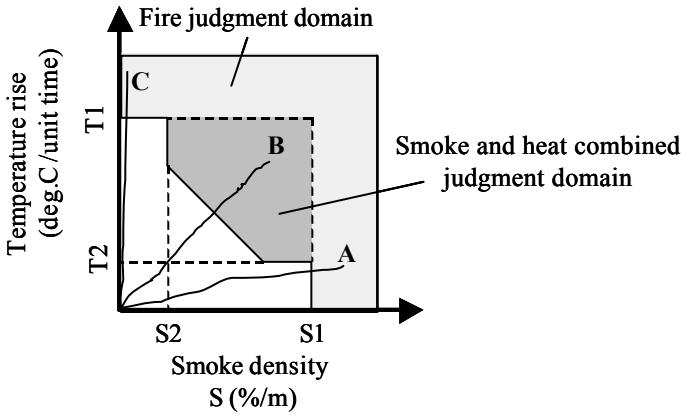

(c) The fire judgment domain of a new combined detector

Figure 1. Comparison of fire judgment domains

In the case of smoke detector of Figure 1 (a), the smoke level of A-type-fire is in the fire judgment domain of an optical smoke detector, and is detected earlier than other fire types. Meanwhile, B-type-fire at an early stage is not detected yet and the smoke level needs to go up further in order to be detected. In the case of C-type-fire, since smoke is barely generated, the alarm does not go off at all.

Figure 1(b) shows the detection range of the detector which simply combines optical smoke detector and rate of rise heat detector on an OR basis. This detector, although A-type-fire and C-type-fire tend to go into a fire judgment domain, it is still hard to detect the fire such as B-type-fire at an early stage.

Then, in order to realize early detection of all types of fires, a smoke and heat combined judgment domain is newly prepared in Figure 1(c), and this algorithm can successfully detect even an early stage of complex fires such as B-type-fire. The fire judgment threshold is expressed by the following formulas.

1 (% / m) (2 (deg.C)) (1)

1 (deg.C) (2 (% / m)) (2)

, Const. (2 (deg.C), 2 (% / m)) (3)

, is the threshold of a smoke and heat combined domain, and expresses a constant value. Thus, by adding a smoke and heat combined judgment domain, the early detection of a complex fire can be achieved.

Fle ible Delay Time Function

In order to reduce false alarms, there are some conventional fire detection systems which utilize the accumulative function to monitor the smoke density level, and if the

level exceeds a certain amount for a fixed accumulation period, the alarm goes off. Our company has developed a flexible system to vary the delay time (accumulation time) using fuzzy technology[1]. This system monitors past smoke density profiles and compares them with the waveform of the detector output. The probability of a fire is judged to be low, then the delay time is extended. On the other hand, if the probability of a fire is judged to be high, then the delay time is decreased in order to achieve early detection.

Utilizing this function, false alarms from transient non-fire factors, such as cigarette smoke and steam, can be prevented, and alarms can be promptly activated in case of a real fire. As a result, coexistence of both early detection of a real fire and reduction of false alarm has been achieved.

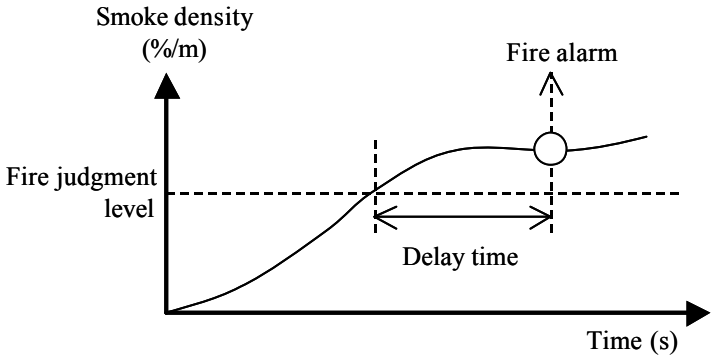

Figure 2. Outline of delay time

Adapti e earning

Detectors are installed in various environments so that fire hazard factors are different depending on the installed locations. For this reason, it is difficult to set a single judgment rule for all installed locations so that the judgment rule has to be modified for each places to suit the fire hazard factors of that particular location. Due to this difficulty of deciding a single judgment rule, "adaptive learning", in which the detector automatically adjust the judgment rule to suit the installed environment, is proposed.

Conformity to the installed environment is achieved by using more sensitive

threshold level, learning threshold, to monitor the frequency of each of smoke density, temperature rise, and smoke and temperature combined level being exceeded. Also, fire judgment rules of formula (1) - (3) vary in relation to this monitored frequency.

Changes of the fire judgment rule by this adaptive learning are shown in Figure 3. For example, if the variation in the smoke density is large, and as a result the monitored frequency of the smoke density exceeding the learning threshold is also high, then the delay time to alarm is set to be longer. By using this method, false alarms due to transient smoke, such as cigarette smoke, can be reduced. In an environment where the variation in temperature is large, the threshold of the temperature rise rate is increased or may be changed to a fixed temperature alarm mode. Using this method, false alarms caused by rapid temperature rises due to building heating systems in winter are reduced.

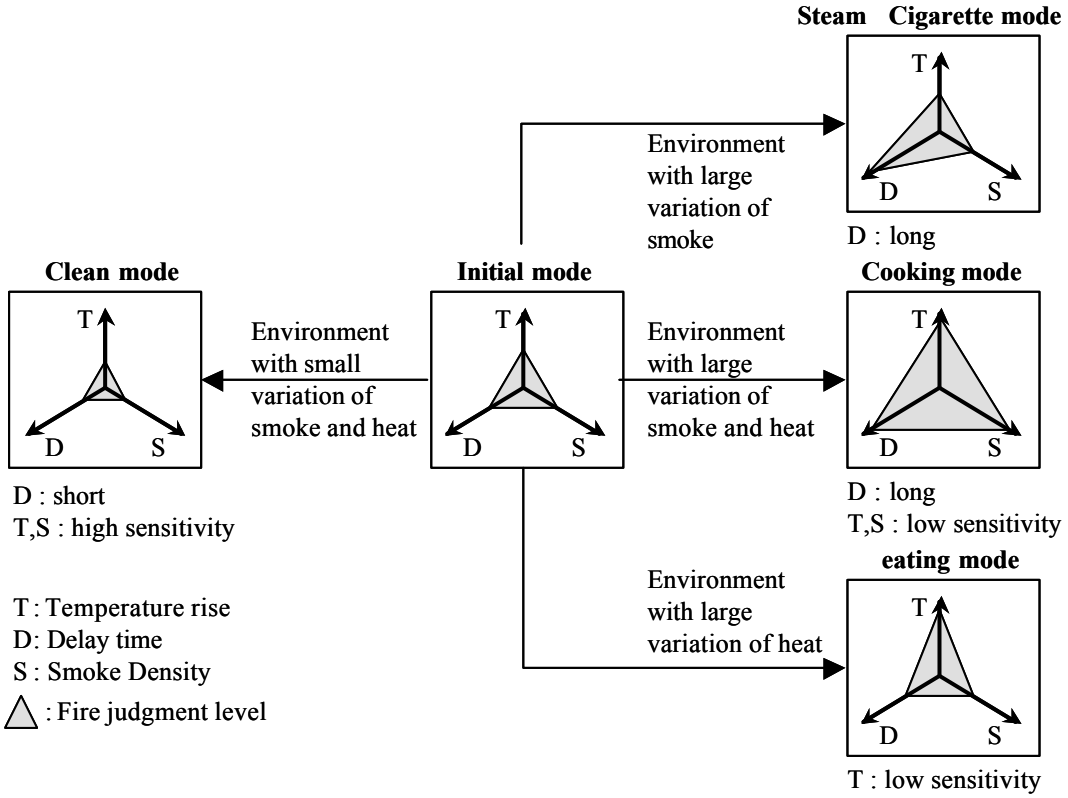

Figure 3. Changes of the fire judgment rule by adaptive learning

On the other hand, if the frequency which exceeds the learning threshold is small, the delay time is set shorter, and the fire judgment level of smoke and a temperature rise will also be lowered, and as a result, the detector is set to higher sensitivity. In an environment with little change in smoke density, such as a non-smoking office or a clean room, the detector automatically adjusts itself to be more sensitive to smoke level.

Thus, an early detection of real fires and reduction of false alarms can be achieved without any need to select different types of detector for the environment of each location at the time of installation. Fire detectors automatically find the best judgment rule by themselves.

Moreover, these three functions are processed by built-in CPU of the detector, and do not need special processing by a control panel. Therefore new combined detector reduces the operators and installers tasks to adjust the detector to meet the installed environment.

alidity erification of the Algorithm

1 erformance of Fire Detection

1 1 Classification of a Fire

Condition of Test Fire (TF) for evaluating the detection performance of a fire detector is specified to EN standard (European Standard) in detail. Fire detection performance evaluation of this new concept detector was performed under following conditions based on EN54 [2)].

The fire test room size is 10 m depth, 7 m width, 4 m height, with the fire source on the floor at the center of the room. The detector was installed on the ceiling, 3 m offset from the center of the room. The fire was classified into 6 different fires as shown in Table 1. The quantity of fuel and the examination method etc. are as EN54 specified.

1 Measured alues

The measured values are the analog output (temperature, smoke density) of a detector, and the temperature rise (dT) and smoke density (m-value, y-value) near a detector. The m-value is an optical smoke density, and y-value is an ionization smoke density. The details of each value are specified by EN54.

1 erformance Standards

Using the measured value of the above parameters at the detector alarms, performance standard of the detector is classified based on EN54, as shown in Table 2.

1 aluation Result

The performance results of the new combined detector, the optical smoke detector, and the simple combined detector are shown in Table 3. Figure 4 shows the detector s output at TF1. The arrows in Figure 4 show the time when each detector started to alarm.

Table 1. Test Fire classification

Name	Classification	Characteristic
TF1	Flaming wood fire	Flaming with gray smoke
TF2	Smoldering wood fire	Smoldering with white
TF3	Smoldering cotton fire	Smoldering with white
TF4	Flaming polyurethane	Flaming with gray smoke
TF5	Flaming n-heptane fire	Flaming with gray smoke
TF6	Alcohol Fire	Flaming but no smoke

Table 2. Fire detector performance standards

Class	Performance standard		
	m-value (dB/m)	y-value(-)	dT (deg.C)
A	0.5 or less	1.5 or less	15 or less
B	1.0 or less	3.0 or less	30 or less
C	2.0 or less	6.0 or less	60 or less
N	Alarmed during test , but value out with test range		
-	No alarm during test		

Table 3. Fire detection performance results

Type of detector	TF1	TF2	TF3	TF4	TF5	TF6
a	N	C	B	C	C	-
b	N	C	B	C	C	B
c	C	C	B	B	B	B

a : optical smoke detector, b : simple combined detector, c : new combined detector

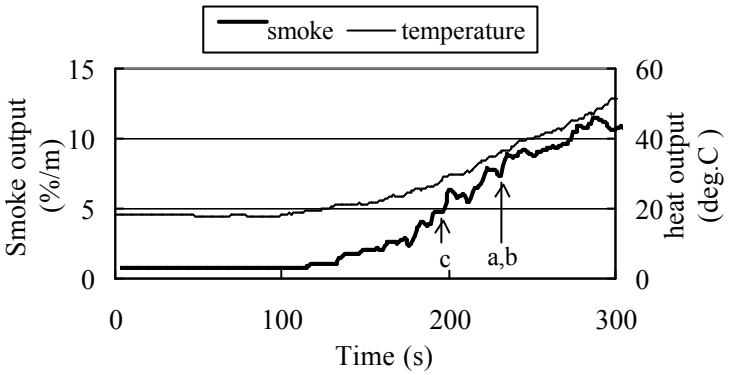

Figure 4. The output of a detector (TF1)

Following can be assured from Table 3.

- The new combined detector has outstanding performance which can detect all test fires at an early stage compared to the other detectors.
- The new combined detector s performance is superior to simple combined detector when the fire is flaming fire which generates heat and smoke simultaneously.
- The new combined detector outperforms optical smoke detector at detection of flaming fire.

alidity of Adapti e earning

The adaptive learning algorithm is a new concept, and the evaluation methods are not defined on the existing technical standards, so that performance evaluation was

requested to Duisburg University in order to obtain objective evaluation of this new algorithm. This chapter describes this evaluation method and the results of it. The evaluation is focused on both sides of fire detection performance and performance under non-fire environment.

1 Fire Detection erformance in ach earning Mode

Evaluation of fire detection performance is done as explained in previous chapter. The performance results were compared by the average detection time in each mode for each Test Fires.

The results are shown in Table 4. The detector which is in the clean mode, sensitive mode, detects the fire earlier than the detector in other modes. The detectors in the other 3 modes tend to delay a little to alarm, but the detection performance remains good.

Table 4. Comparison between fire detection performances in each learning mode

Average detection time (difference from the detection time in initial mode in sec.)

Learning mode	TF1	TF2	TF3	TF4	TF5	TF6
Clean	-10	-12	-17	-11	6	
Initial						
Steam / Cigarette		17	16	4		
Cooking	13			3	9	
Heating					3	116

- : earlier than initial mode, : later than initial mode, : same as initial mode

erformance at on-Fire n ironments in ach earning Mode

Performance at non-fire environment was evaluated based on the market data which uniquely collected by Duisburg University. The market data was collected by analog detectors installed in six different locations at five different institutions, which include

an iron mill and a hospital. Using the data sampled from these various locations, a computer simulation was done to evaluate the effectiveness of the algorithm.

Analog detectors used to sample the real life environment data may have different properties (smoke inflow, smoke dispersion characteristics, etc.) from new combined detectors, but for this evaluation, these properties are assumed to be the same.

Almost all of the installation locations are not environment where a new combined detector would give alarm, however, at one location, the simulation showed that the detector falsely alarmed frequently. The location is a kitchen of a hospital with huge pots giving off a large amo unt of steam.

Table 5. Number of false alarms in hospital kitchen simulation

The case of mode fixation

Learning mode	Times
Clean	45
Initial	40
Steam / Cigarette	25
Cooking	37
Heating	38

The case of of adaptive learning is operated

Initial mode	Times
Clean	23
Initial	23
Steam / Cigarette	23
Cooking	23
Heating	23

The following describes the evaluation result of adaptive learning algorithm based on the hospital kitchen data. The number of false alarms of the detector in this hospital kitchen simulation is shown in Table 5. Compared to the detector set to fixed mode (Table 5. left), the detector in varied modes with learning algorithm (Table 5. right) had less false alarms, so that the effectiveness of learning algorithm is proven.

Real ife aluation of the earning Algorithm

Since the above-mentioned evaluation was a computer simulation using sampled data,

an actual evaluation in a real life environment during six months was taken. Detectors were installed in a 6-story building with 9060m^2 total floor areas and 223 detectors with proposed new combined fire judgment algorithm were installed. Among these 223 detectors, 20 detectors installed in the office areas and hallways, were used to evaluate mode changes. All of these 20 detectors were in clean mode at the time of analysis. However, in spite of being in the clean (sensitive) mode, no false alarm occurred during six months of evaluation. Therefore the effectiveness of adaptive learning has been confirmed. All detectors were in sensitive mode and could therefore detect fire at an early stage.

Conclusion

It is clear from the evaluation results that detectors with the proposed new combined fire judgment algorithm can detect all Test Fires at an early stage. In particular, the detection capability of the flaming fire, which was a weak point of an optical smoke detector using scattered light, was improved.

Reduction of false alarms is also achieved by the automatic adjustment of the fire judgment algorithm in response to the installation environment.

R F R C S

1) S. Nakanishi, et al., ,
Proceeding of the 10th Conference on Automatic Fire Detection (AUBE 95), 1995

2) EN54 / 9, Components of automatic fire detection systems – Part 9 : Fire sensitivity test (1982)

David K. Churches
Saudi Arabian Aramco, Saudi Arabia

Multi-Criteria Polarized Optical Smoke Sensor

Abstract

The paper discusses a discriminating multi-criteria optical smoke detection device that can differentiate between the presence of transitory post combustion products and nuisance aerosols such as water vapor and solid particulate dusts in air suspension.

The device uses a low-power monochromatic laser emitting a narrow cone shaped beam with a single sensing chamber. The monochromatic light beam is directed through an input polarizer into the sensing chamber and then subsequently exits via a coaxially mounted output polarizer-analyzer oriented optically perpendicular to the input polarizer.

When air enters the chamber of the detection device under no-fire quiescent condition, an electronic optical sensor mounted oblique to the light beam in the sensing chamber and a second electronic optical sensor mounted after the output polarizer-analyzer perpendicular to the light beam, measures zero magnitude since both sensors are optically obscured from the light beam.

Under real-fire smoke conditions or in the presence of nuisance aerosols, the oblique-mounted electronic optical sensor in the sensing chamber measures the de-polarization angular-reflectance of the monochromatic light beam proportional to the nature and density of the detected phenomena. At the same time the second sensor mounted after the output polarizer-analyzer, measures the rotational de-polarization due to optical refraction and phase-shift proportional to the nature and density of the detected phenomena.

The research results indicated that the combination of the measured phenomena from both sensors appeared to be uniquely different for unlike aerosols, since post-combustion products such as smoke recorded dissimilar values for rotational refractance and angular reflectance, compared to nuisance aerosols such as water vapor and solid particulate dusts in air suspension. It was concluded that detector configuration was suitable for further development as a multi-criteria optical smoke detection device that has the capability of discriminating between real-fire and non-fire aerosol phenomena.

Thorsten Schultze, Thorsten Kempka, Ingolf Willms
University Duisburg-Essen, Campus Duisburg, Germany

Audio-Video Fire-Detection of Open Fires

Abstract

In the scope of the development of a video-based fire detection system, investigations on the dynamic behaviour of open flames have been made. Standardised fires were recorded with different audio and video systems and their flow and flickering analysed. This paper sketches the analyses performed and shows some achieved cognitions.

Introduction

The video based fire detection is getting more attractive as the number of installed video systems is increasing and their implementation still getting cheaper. Many video systems are also combined audio-video systems, providing a second channel for detection, the acoustic one. But before thinking of the realisation of such an audio-video detection system it is necessary to investigate how fires can be recognised in a video-sequence or the acoustic data.

Within this study, analyses of the dynamic characteristics of predefined EN 54 part 9 test-fires (ISO 7240) were done. Audio as well as video recordings have been made, using different recording systems. A low-noise microphone was used for the acoustic recordings. Video data have been recorded with a common digital-video camera and a high-speed CMOS camera.

Two major dynamic properties of flames are of special interest: the flickering and the flow movement. It is known from literature that the flickering of open fires is among others related to the size of the burning surface. Within this study the evolution of the flickering frequency of flames has been traced for different types of fires. Furthermore the acoustic data has been compared with the video recordings, in order to analyse the influence of the flame flickering on the acoustics. To study the flow movements of flames, image processing methods like the motion estimation were tested and adapted.

Due to the big amount of data, this contribution will only describe briefly the three main analyses performed, reporting some interesting results.

Flame flickering

The flickering of open fires arises from turbulences of flames. It is known from literature, that the frequency range of the flame flickering is among others a function of the pool size, being inverse proportional to the size of the burning surface.

Various analyses of the acoustic emissions of flames were performed in the range of ultrasound. However, in this investigation we concentrated on the range of the flickering frequency of flames (under 10 Hz). Therefore a special sensitive microphone has been chosen for the recordings. In order to evaluate the evolution of the spectral characteristics of the acoustic emissions of flames, the recorded signal was first divided into short segments of a few seconds. For each segment, the power density spectrum (PDS) has been build. Finally all calculated PDS were placed side by side, building a spectrogram. In the spectrogram shown beneath, the power density is coded by colors and plotted against the frequency and time. In acoustics a spectrogram is usually called a sonagram.

The video data for this type of analysis was recorded with a usual digital video camera. To allow a comparison between the acoustic and optical emissions, the recorded video signal, usually a function of the three variables width, height and time, had to be reduced to a function of the time only. The reduction was done in such a way that the number of image points (pixels) constituting the flame was determined in each frame. Afterwards the same spectral analysis as for the acoustic data has been done.

In the spectrogram in figure 1 the power density spectrum of the video recordings of an ethanol pool fire is shown. The PDS is normalised on the highest value; the x-axis shows the time in seconds and the y-axis the frequency in hertz. The power is coded by grey tones: dark points are regions with great power, light points have less power. The corresponding values for each tone are shown in the grey scale.

The pool had a size of 43.5 cm per 43.5 cm, filled with 2.3 kg ethanol. The fire was

ignited at the time $t = 0$ s and extinguished completely 720 s after ignition.

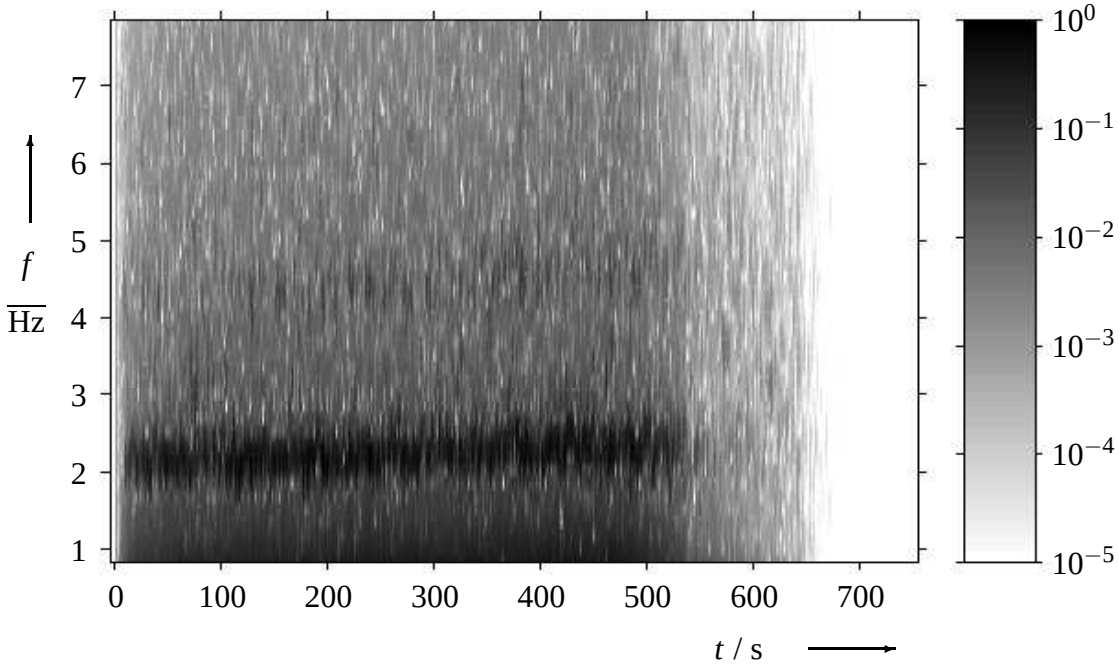

Figure 1: Spectrogram of an ethanol pool fire.

Immediately after ignition the power rises up in the whole spectrum. About 520 s after ignition the average power begins to decrease, reaching the smallest value 720 s after ignition. Unfortunately, due to the typography technique used, these slight differences in colour in the last 70 s are not visible. But it is striking that the greatest power is measured in the range of about 2 Hz. Comparing the values of the fire size and the measured frequency range to literature, this region at about 2 Hz can be assigned to the flickering frequency of the flame. This line does not persist up to the extinction of the fire, but only up to 530 s after ignition. The explanation for this behaviour is the lack of fuel on the pool surface at the end of the fire. In this period the fuel does no longer cover the whole pool surface and the fire breaks down into many independent flames, burning separately on fuel puddles. As a consequence the spectral characteristics of the flame are changed.

Comparing the video data to the acoustic analysis, interesting similarities can be seen. In the next diagram (figure 2) a sonagram is shown, where the acoustic signal of the

same ethanol pool fire has been analysed. As in the previous diagram, the power density is plotted against frequency f and time t. The power is coded by grey tones. The ignition is at $t = 0$ s and the total extinction at $t = 720$ s.

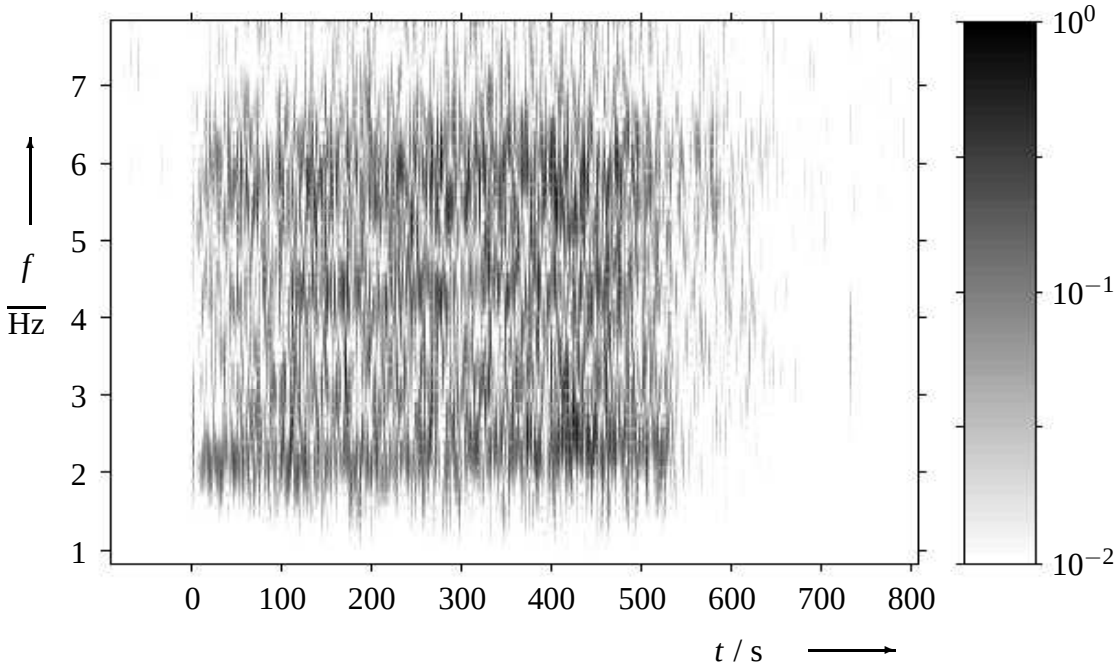

Figure 2: Sonagram of an ethanol pool fire.

After ignition the power density increases, mainly at 2 Hz and 6 Hz. Especially the higher values around 2 Hz are interesting, as the flickering frequency of the flame ranges in the same frequency band. This line at 2 Hz rises immediately after ignition and disappears 190 s before the fire completely extinguishes, as in the video analysis. Both analyses show the same characteristics. Therefore it can be concluded that the flickering frequency can be seen in both recordings, the acoustic and the video data. The explanation for this effect lies in the rising flame rolls, which are mainly responsible for the flame flickering. They arise in an explosive manner, increasing not only the luminous area, but also emitting acoustic waves.

The analysis of the ethanol pool fire shows an almost constant flickering frequency. This is an expected result, as the burning surface (the pool size) is constant during the whole fire. The relation of the flickering frequency to the burning surface can be seen in the evaluation of the wood crib fire. This fire is ignited in the middle of the crib and

spreads out with increasing time. The result is a decaying flickering frequency over the time, up to the point when the whole crib is burning. But other tests show that the influences of the type of fuel are not negligible. A n-heptan fire, for example, shows strong changes in the flickering frequency over the time, although it is also a pool fire with constant pool size. The change of flickering frequency of a flame implies therefore not necessarily a change of the size of the burning surface.

Motion estimation

By capturing the flame with a video system it is possible to get a description of the fire in three dimensions: the height, the width and the time. In image processing so called motion estimation algorithms are used to follow and predict movements in video sequences. These techniques are implemented among others in the video format conversion or in e.g. high-end television sets, being available as a hardware solution.

The most common techniques are based on the so called 'block based algorithms'. There the original video frame is divided into blocks, which are searched for in the next video frame. However, the motion estimation of flames is not trivial, due to the fast movements of flames and fast change of structure, respectively brightness. As a consequence, simple block based algorithms detect false motions. To prevent this problem, a new motion estimator has been designed, reinforcing physical coherences like inertia. The underlying structure of the new algorithm is based on a known block based motion estimation technique.

In figure 3 the reader sees the stream lines of the flame movements superimposed on a screenshot of the flame image. This flame of the ethanol pool fire with a pool size of 43.5 cm per 43.5 cm has been recorded with 250 frames per second. The motion was traced over 4 s and the mean motion plotted as white stream lines.

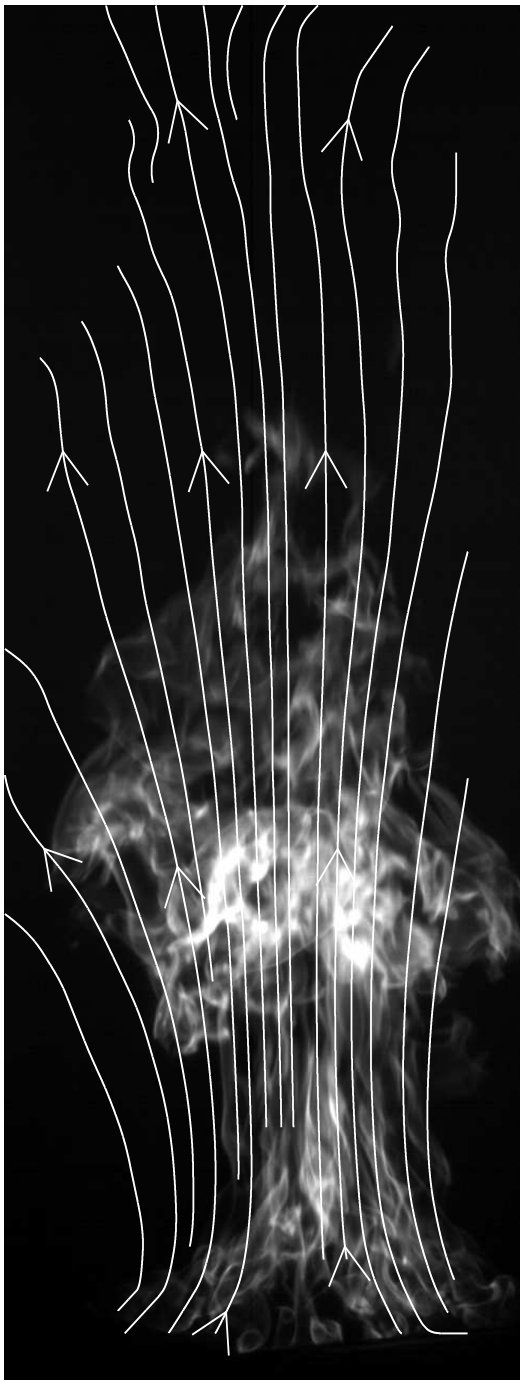

Figure 3: Stream lines of an ethanol pool fire.

The stream lines shown in figure 3 rise up, spreading out at the flame top. The bundling region at the bottom corresponds to the flame neck. Tracing with good results is only possible in images recorded with high-speed video cameras (at least twenty times faster

than usual cameras).

The detected motion corresponds to patterns expected from literature.

Simplified flow analysis

From the last two sections it can be concluded that the full description of the flow of flames in video sequences is only possible with a complex analysis. However, the flame flickering can be easily extracted from the video sequence by reducing the three variable video function $s(w,h,n)$, with height (line number) h, width w and frame number n, to a function of the time only. Therefore a third analysis is of interest, where the degree of freedom of the describing video signal, i.e. the number of variables, is reduced only by one.

This analysis is done in such a way that for each video frame, the mean value of the brightness is calculated for each line in that frame as follows:

$$g(h,n) = \frac{1}{\mathrm{W}} \sum_{i=1}^{\mathrm{W}} s(i,h,n)$$

with W corresponding to the total number of pixels in each line, h the line index and n the frame number. In a video sequence with N frames and H lines in each frame, the calculation leads to the matrix $\overline{\mathrm{G}}$ with

$$\overline{\mathrm{G}} = \begin{pmatrix} g(1,1) & g(1,2) & \cdots & g(1,\mathrm{N}) \\ g(2,1) & \ddots & & \vdots \\ \vdots & & \ddots & \vdots \\ g(\mathrm{H},1) & g(\mathrm{H},2) & \cdots & g(\mathrm{H},\mathrm{N}) \end{pmatrix}$$

For the analysis the resulting matrix is plotted as a grey scale image: each value corresponds to a grey tone.

In figure 4 such an analysis of the same ethanol pool fire as described above is shown. The raw data for this analysis has been recorded with a usual digital video camera. The x-axis is the time ($t = n/(\text{frame rate})$) axis (proportional to the frame number) and the y-axis the height or line number (h). The mean brightness (between 0 and 255) is coded by grey tones, as shown in the scale aside. It is possible to see a periodic pattern, where

large mean values of the brightness rise up during the time to even higher positions, until reaching a certain height. Further on it is eye-catching that these resulting curves have the shape of a parabola.

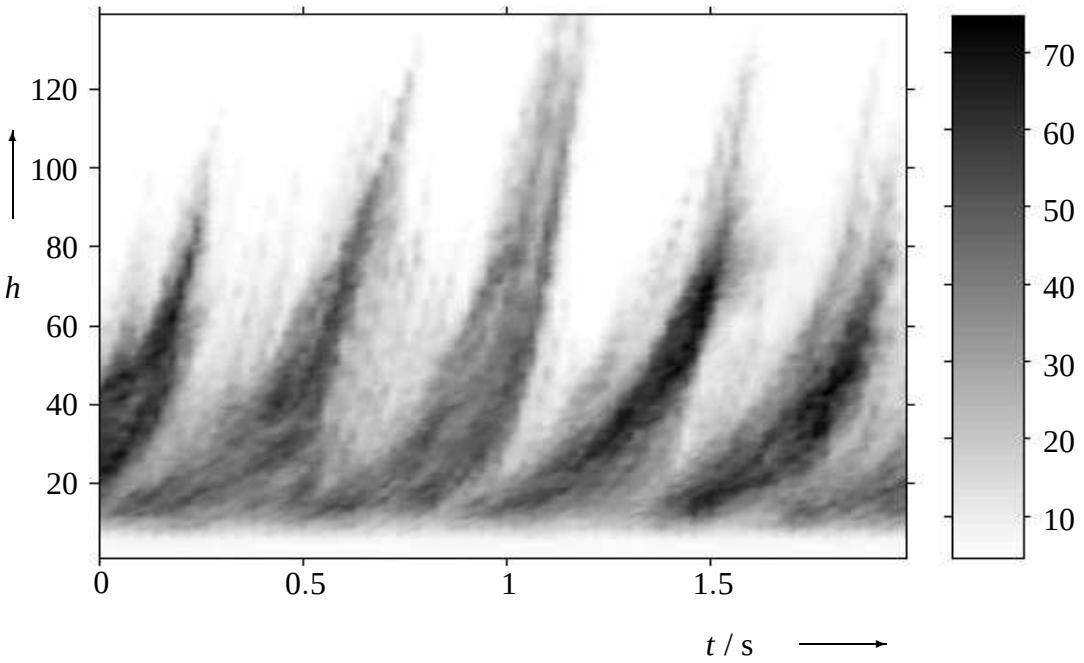

Figure 4: Evaluation of an ethanol pool fire.

The results can be interpreted in the following way: The flame flickering is caused mainly by arising fire rolls. These rolls are bright and wide, resulting in a high mean brightness. As their path in the time-height diagram corresponds to a parabola, it can be concluded that the rolls rise upward in an accelerated movement. At a certain height the fire roll extinguishes and a new one is built at the bottom of the flame. Further analyses have shown that this behavior is common for all analysed flame types, giving a possible criterion for detection.

Conclusion

In this paper the analysis of the dynamic characteristics of flames has been briefly described. The evaluation shows that the flickering of flames is not only optically, but also acoustically measurable. The dependence of the flickering frequency of flames on their size has been displayed. However, it is not possible to estimate the fire size on the basis of its flickering frequency, as fuel characteristics are not negligible. The flow analysis using motion estimation has been shown. Finally a simplified flow analysis has been presented, based on the computation of the mean value of brightness in each video frame line. The method shows interesting results, as the patterns of different flames have similar characteristics. The fact that there is no need of a special video system makes the method interesting for the automatic video based fire detection.

Literature

[1] de Haan, G. *Video Processing for multimedia systems, 3rd Edition* Eindhoven: University Press Eindhoven, 2003

[2] Hölemann, H. *Vorlesung zum Brand- und Explosionsshutz* Manuscript from lecture at University GH Wuppertal, 2000

[3] Portscht, Rainer *Forschungsbericht des Landes Nordrhein-Westfalen: Messung und Analyse des Zeitverhaltens der von offenen Bränden emittierten Temperaturstrahlung* Opladen: Westdeutscher Verlag GmbH, 1971

[4] Schultze, Thorsten *Untersuchungen zur Audio-Video-Detektion von offenen Bränden* Diploma Thesis, Duisburg, 2003

Hongyong YUAN, Tao CHEN, Guofeng SU, Xueming SHU, Weicheng FAN
State Key Laboratory of Fire Science, University of Science and Technology of China, Hefei 230027, Anhui, P. R. China

hotoacoustic Multi-sensor Fire Detection

Abstract

A photoacoustic fire detection method that can detect both CO and smoke particles on-line was developed. It was realized based on gas filter technique and particle scattering theory. A CO gas cell and a reference gas cell were used in the system to meter the CO absorption and smoke particles' extinction of the IR light in the measuring path. By processing the signal attenuation of the two cells, CO concentration and smoke particles' density in the measuring path can be obtained simultaneously.

ey ords photoacoustic, fire detection, gas detection, smoke particles

1 Introduction

Early and reliable fire detection has been so far demanded not only for residential use but also for industrial use. However, the sensitivity and reliability of conventional detectors can hardly meet current fire protection requirements 1 . Now the fire detection using gaseous signatures is becoming a remarkable and promising technology that shows better sensitivity and reliability 2,3 . Among the gaseous combustion products such as CO, CO_2, NO_x, CH_4 and H_2O, CO is the most common combustion product and naturally becomes the main fire signature. Among the current commercial gas sensors, Taguchi sensors are most commonly used for they are simple in construction for gas sensing. However, their selectivity is still not very satisfying because of cross-sensitivity. Usually, gas sensors are used together with other fire detectors to realize multi-sensor multi-criteria fire detection 4,5,6 .

Recently, researchers have recurred to photoacoustic technology in gas detection, which has better sensitivity and selectivity. Nebiker and Pleisch 7 presented a possible design of a photoacoustic gas sensing system and stated the possibility of introducing this technology into fire detection area. However, the membrane used in their design may cause response delay in application, especially when the system needs to be reset. Guofeng Su 8 presented another on-line photoacoustic system design using gas filter

omenclatures

	gas concentration in CO photoacoustic cell
	CO concentration in the measuring path
	smoke concentration in the measuring path
d	average diameter of the smoke particles
	initial intension of the modulated light
	extinction coefficient of smoke particles
	length of the photoacoustic cell
	length of the measuring path
	refractive index of smoke particle
	number of smoke particles in the light transmission path
	sensitivity of the microphone
	absorption efficiency factor
	extinction efficiency factor
	scattering efficiency factor
	initial photoacoustic signal
	photoacoustic signal in tests
	volume of the photoacoustic cell
	scale factor in scattering theory defined as $\pi d\ \lambda$
α	absorption coefficient of CO gas
γ	the thermodynamic properties of the gas
τ	the thermal relaxation time of the cell
ω	modulation frequency of the light

techniques like some gas analyzers. In this model, a photoacoustic cell filled with pure CO gas was used as a gas filter (shown in Figure 1). This technical design realized the on-line detection of the gaseous fire products by metering the signal attenuation after CO enters the measuring path, but it also has its limitation. As fire smoke is a mixture of CO gas and smoke particles, the light extinction of the smoke particles in the measuring path was not amended in the model.

Here another detection model was developed. The technical design was improved from Su's work however a reference gas cell was added to compensate and meter the smoke

particles' extinction. CO concentration and smoke density in the measuring path can be obtained simultaneously. Photoacoustic CO smoke multi-sensor detection is possibly to be realized.

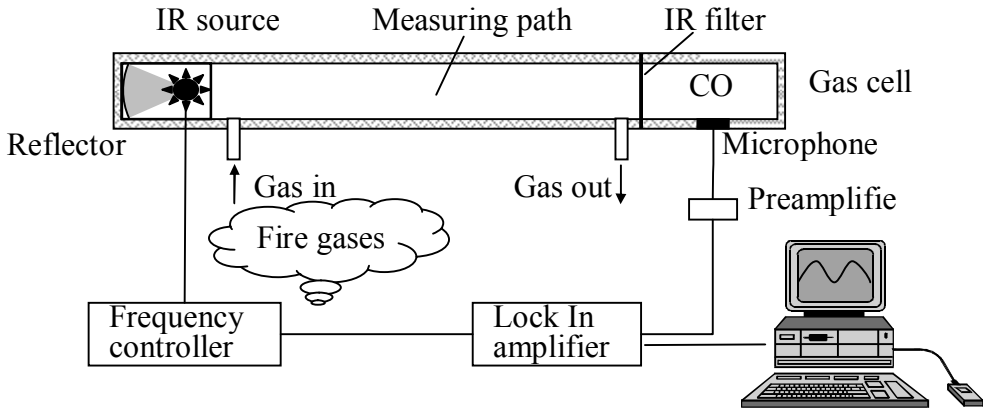

Figure1. Gas filter photoacoustic gas detection system

rinciple

d

Photoacoustic gas analysis technology is based on infrared absorption technology. During a photoacoustic measurement the sample is enclosed in a photoacoustic (PA) cell. When the modulated infrared light hits the sample, some of the energy is absorbed by the molecules in the sample resulting in a temperature rise. This rise will generate an expansion and pressure wave. Then the periodic pressure wave can be recorded using a microphone in the cell and the signal further gives the gas concentration.

According to Lambert-Beer law and photoacoustic theory, for a nonresonant PA cell, the PA signal can be derived as a simplified expression [9]

$$\frac{1}{}(\quad 1)\frac{_0 1 \quad \exp(\qquad)}{\sqrt{1/\ ^2 \quad ^2}}. \qquad (1)$$

Fire detection systems are required of the capability to be used on-line and possess rapid temporal response. Yet photoacoustic gas detection was often limited for its "sample and measure" type operating procedure. Gas filter technology is commonly used on online gas analysis devices based on infrared absorption spectrometry [10]. Its basic method all involve the absorption spectrum of the reference gas sample, relative to the gas to be measured [11]. Selectivity is realized by the gas cell instead of optical filters.

The measuring part of the system 12 is shown in Figure 2. Compared to the design in Figure 1, a reference cell was added and arranged tandem to the CO cell. The first PA cell was filled with the gas identical to what we wish to detect (here is CO) and work as a gas filter. The reference cell was filled with some pure gas that would commonly not be a fire product, such as propane (C_3H_8), to meter the smoke extinction in the path. The broadband IR source can cover the absorption lines of CO and C_3H_8 at 4.66μ and 3.36μ respectively. The band pass optical filters have good transparency in 3μ to 5μ for the selectivity is realized by the cells. The PA cells are nonresonant cells working in infrasound band to avoid the noise in audible band.

Initially, the photoacoustic signals were recorded as and . When the fire products enter the measuring path, the signals would fall down because of the light extinction. The attenuation of represents the absorption of CO and the extinction of smoke particles at 4.66μ . However, the attenuation of represents the extinction of smoke particles at 3.36μ since there was no propane in the fire products

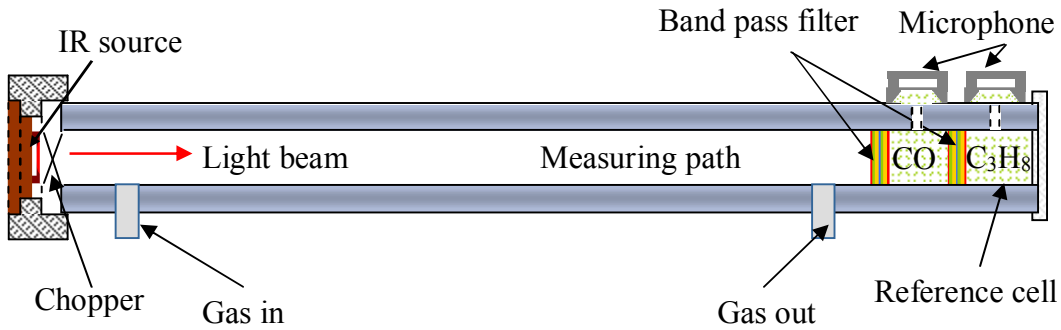

Figure 2. Scheme of the measuring part of CO smoke detection system

The light extinction of CO cell can be expressed as

$$_0 \exp\ (\ _1 \qquad)\ , \tag{2}$$

where represents at 4.66μ . When light extinction occurs, considering α 1 and 1, we have

$$\frac{1}{}(\quad 1)\frac{_0\ 1\quad _1\qquad\qquad 1\quad \exp(\qquad)}{\sqrt{1/\ ^2\quad ^2}}. \tag{3}$$

For both CO cell and C_3H_8 cell

$$\frac{_1}{_2} = \frac{\_\_\_\_\_}{\_\_\_\_\_}. \quad (4)$$

The superscript means the corresponding parameter of C_3H_8 cell. represents at 3.36μ . If the relationship between and is known, and can be obtained. Supposing independent scattering and single scattering in smoke particles 13 ,

$$\frac{}{4}d^2 \quad (\ ,d), \quad (5)$$

where according to the particle scattering theory 14 . Thus we have

$$\frac{_2}{_1} \quad \frac{\_\_\_\_,_2}{\_\_\_\_,_1}. \quad (6)$$

and represent at 3.36μ and 4.66μ respectively has different expression in Rayleigh scattering (0.1) and Mie scattering (0.1). The expression of in Rayleigh theory is much simpler than that in Mie theory. Actually, Rayleigh scattering is a special form of the Mie scattering when 1 and 1. The truncation error is magnitude. For normal precision, Rayleigh theory is applicable when 0.3 15 . For the wavelengths of 3.6μ and 4.66μ , the maximum scale factor is 0.224 using the data (shown in Table 1) obtained by Shenyang Fire Research Institute of China (SFRI). Thus here is expressed using Rayleigh theory

$$\frac{8}{3} \ ^4 \mathrm{Re}\left(\frac{^2 \ 1}{^2 \ 2}\right)^2 \quad 4 \ \mathrm{Im}\left(\frac{^2 \ 1}{^2 \ 2}\right). \quad (7)$$

Table 1. Diameters of smoke particles of test fires

Fire type	Particle count	Average diameter	Ceiling height
Flaming wood	2.24 e 6	186nm	4m
Wood pyrolysis	9.11 5	159nm	4m
Smoldering cotton	2.28e 6	177nm	4m
Flaming polyurethane	3.25 e 6	217nm	4m
Flaming decahydronaphthalene	1.69e 6	240nm	4m
Flaming ethanol	4.93 e 4	85nm	4m

Based on references 16,17,18,19 , the refractive index of smoke particles is independent of fuel type and Im( ) is not a very small number. Using the wavelength dependence equation in reference 16 , it can be concluded from equation 7 and 8 that

$$\frac{-2}{1} \quad {}_1\mathrm{Im}\ \frac{{}^{2}_{1}\ 1}{{}^{2}_{1}\ 2} \quad / \quad {}_2\mathrm{Im}\ \frac{{}^{2}_{2}\ 1}{{}^{2}_{2}\ 2} \quad \frac{\lambda_1}{\lambda_2}. \tag{8}$$

Finally, the smoke density and CO concentration can be expressed as

$$\frac{1}{\frac{1}{2}} \quad \frac{\qquad}{\qquad} \quad \frac{\qquad}{\qquad} \quad . \tag{9}$$

periments and Simple Detection Algorithm

After building the experimental system, the CO measuring was calibrated with CO gas of standard concentration. Then the experiments of Chinese standard test fires (SH1 wood pyrolysis, SH2 smoldering cotton, SH3 flaming polyurethane, SH4 flaming heptane and SH5 flaming ethanol) were performed. Each test fire was put in a 0.5m(L) 0.5m(W) 1.2m(H) box with only a little fuel. Fire products were sampled from the top position of the box to the measuring path by a fan through a PVC pipe about 3m long. The unit of CO concentration is ppm and smoke density dB/m expressed using smoke extinction.

The test results are shown in Table 2. Figure 3 shows the test results of SH1. Figure 4 shows the growth rate of CO concentration within 100 second calculated by a special linear regression of the signals described in reference 12 .

Table 2. Test results of Chinese standard test fires

Test Fires	Max.	Time for	10ppm	Max.	Time for	0.2dB/m
SH1	40ppm	77s		1.52dB/m	100s	
SH2	50ppm	25s		1.22dB/m	14s	
SH3	34ppm	40s		0.78dB/m	45s	
SH4	23ppm	44s		0.78dB/m	13s	
SH5	10ppm	--		0.14dB/m	--	

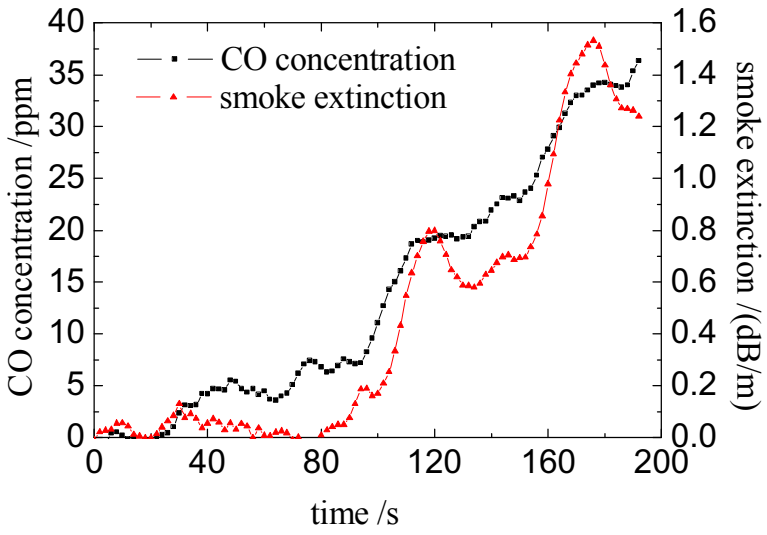

Figure 3. Test results of SH1 Wood Pyrolysis

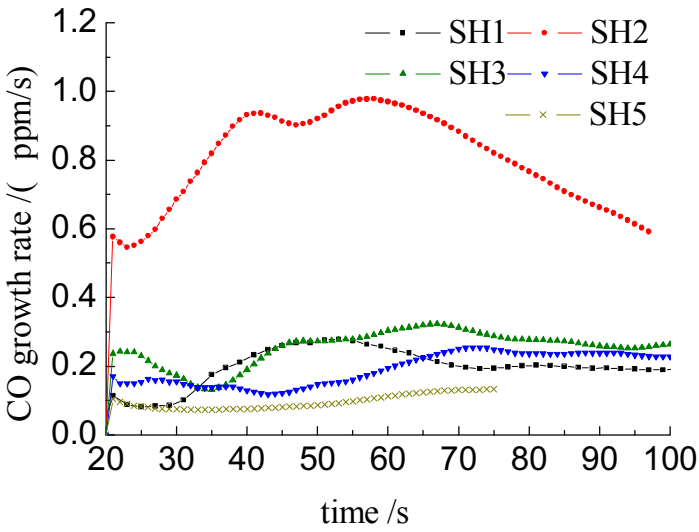

Figure 4. Growth rate of the CO concentration of the test fires

A simple rule-based fuzzy logical fire detection algorithm 20 was used to distinguish the test fires from signal variations caused by circumstance noise. CO concentration ( ), smoke extinction ( ) calculated above were regarded as input signals from two sensors. The growth rate of CO concentration ( ) in Figure 4 was also an input. The signal level

of and was classified into classes low, medium and high according to their values. The signal level of was classified into classes low and high. The detection rule base was defined as

d *d* *d* *d*

The base consists of 18 rules, which is quite complex. To simplify the processing of the rules in the algorithm, the classes low, medium and high were assigned to integer "0", "1" and "2" respectively. Finally the rules in the algorithm were integrated into

( ) (3) (2 3) .

The sensor signals and alarm algorithm computation output of SH1 were shown in Figure 5.

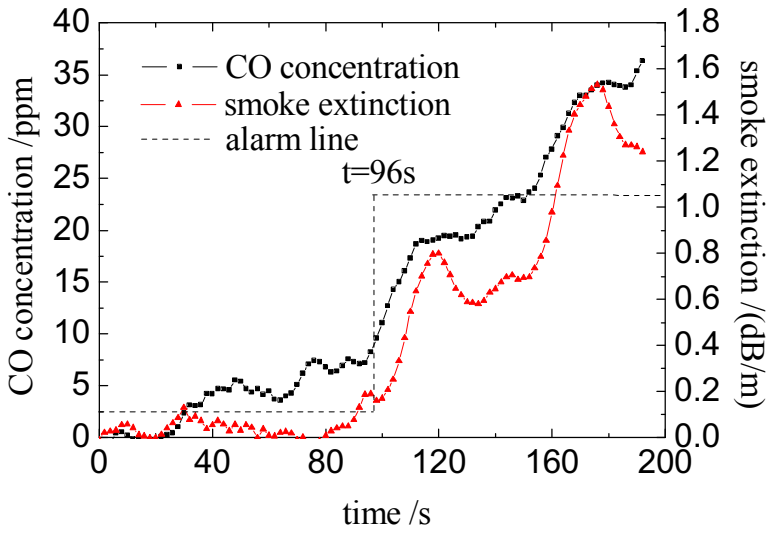

Figure 5. Alarm output for SH1 Wood Pyrolysis

Conclusion

Photoacoustic gas detection provides precise and high-performance monitoring for a variety of gases. It is an interesting attempt to use it in fire detection area. By the use of gas filter technique in photoacoustic systems, online detection of low-level carbon monoxide and other gaseous fire products can be achieved. Moreover, based on particle scattering theory, smoke particles in the measuring path were detected with a reference PA cell. CO concentration and smoke extinction were obtained simultaneously and used

as signal inputs for alarm algorithms to realize multi-sensor multi-criteria fire detection. Future work may be improving the anti-noise capability of the system and having more tests. Sensitive and reliable fire detection system is expected based on this model. Photoacoustic detectors may have great possibility in practical use in the future. Though its structure and power consumption may not permit it to be a spot-type detector, one possible solution is to embed it into an air-sample fire detection system.

Ackno ledgement

This work gained supports from Innovation Program of CAS and 973 Chinese Fundamental Research Program. Thanks to SFRI and Mr. Shao uan for their help.

References

1 Hall JR, Cote AE. American s fire problem and fire protection. Fire Protection Handbook, 17th ed.. uincy, MA: NFPA, 1991.

2 Bjarne CHR. Hagen, James A. Milke. The use of gaseous fire signatures as a mean to detect fires, Fire Safety J. 2000; 34:55-67.

3 Jackson MA, Robins I. Gas sensing for fire detection: measurements of CO, CO_2, H_2, O_2 and smoke density in European standard fire tests. Fire Safety J. 1994; 22:181-205.

4 Susan L. Rose-Pehrsson. Multi-criteria fire detection systems using a probabilistic neural network. Sensors and Actuators B. 2000;69:325-335.

5 Daniel T. Gottuk et al. Advanced fire detection using multi-signature alarm algorithms. Fire Safety J. 2002;37:381-394.

6 James A. Milke. Using multiple sensors for discriminating fire detection. Fire Suppression and Detection Research Application Symposium. Research and Practice: Bridging the Gap. Proceedings. National Fire Protection Research Foundation. February 24-26, 1999, Orlando, FL, 150-164.

7 P.W. Nebiker, R.E. Pleisch. Photoacoustic gas detection for fire warning. Fire Safety J. 2001;36:173-180.

8 Guofeng Su. Photoacoustic Gas Monitor Based Fire Detector. Ph.D. Dissertation. University of Science and Technology of China. July, 2003. in Chinese

9 Yin R, Wang T, ian ML. Photoacoustic and photothermic technologies and their applications. Beijing, China: Science Press, 1999. in Chinese

10 u J , Wu H, et al. The portable CO/CO_2 NDIR analyzer. Control and Instruments in Chemical Industry. 2000; 27:54-55. in Chinese

11 J. P. Dakin, H. O. Edwards, B. H. Weigl. Progress with optical gas sensors using correlation spectroscopy. Sensors and Actuators B. 1995; 29:87-93.

12 Tao Chen. Photoacoustic multi-sensor fire detection for gas and smoke particles. Ph.D. dissertation. University of Science and Technology of China. April, 2004. in Chinese

13 Wang NN. The technology and application of particle size measuring using optical methods. Atomic Energy Press, Beijing, 2000. in Chinese

14 H. C. van de Hulst. Light scattering by small particles. John Wiley Sons, New York , 1984.

15 S. Twomey. Developments in Atmospheric Science, 7 - Atmospheric Aerosols. Elsevier Scientific Publishing Company Amsterdam-Oxford-New York, 1977.

16 H. Chang and T. T. Charalampopoulos. Determination of the wavelength dependence of refractive indices of flame soot. Proceedings: Mathematical and Physical Sciences, Volume 430, Issue 1880 (Sep. 8, 1990), 577-591.

17 Smyth K. C., Shaddix C. R.. The elusive history of m=1.57-0.56i for the refractive index of soot. Combustion and Flame. 1996, 107: 314-320.

18 Lee, S.C., and Tien, C.L.. Eighteenth Symposium (International) on Combustion, The Combustion Institute, Pittsburg, 1159-1166, 1981.

19 Koylu, U.O. and Faeth G. M.. Spectral extinction coefficients of soot aggregates from turbulent diffusion flames. Combustion Institute/Eastern States Section. Chemical and Physical Processes in Combustion. Proceedings. Fall Technical Meeting, 1995. October 16-18, 1995, Worcester, MA, 211-214.

20 Thomas Cleary and Takashi Ono. Enhanced residential fire detection by combining smoke and CO sensors. Proceedings, AUBE'01, Maryland, USA. 2001.

P. Fischer
University of Applied Sciences, Dortmund, Germany
P. Palensky
Vienna University of Technology, Vienna, Austria

Safety and Security in Communication Standards for Building Automation and Control Systems

Abstract

This paper gives an overview about the aspects of safety and security in the current international and European communication standards for building automation and control systems (BACS). Safety and security, in this context, covers critical applications like intrusion detection, fire alarm or access control. The requirements needed for these special applications and the status of the realization of it in the three communication standards BACnet, KNX and LonWorks is described.

Introduction

At the end of the 1980ies, the first communication standards for building automation and control systems were under development. Some of these standards were part of industrial communication systems like PROFIBUS [DIN 91c, DIN 91d], others are for building automation purposes, only, like FND [AMEV 88] or BACnet [ANSI 95]. In that time the first DDC (direct digital control) controllers were available on the market and a building automation and control system had an hierarchical architecture with one main central, one or more sub-centrals, some controllers and a lot of sensors and actuators. All sensors and actuators were connected directly to the controllers via a 20mA interface or a 0V to 10V interface. Because of this system structure the devices were located in the different levels of the “pyramid”, the centrals on the Management level, the controllers and automation stations on the Automation Level and the application specific controllers, the sensors, and the actuators on the Field Level (Fig 1).

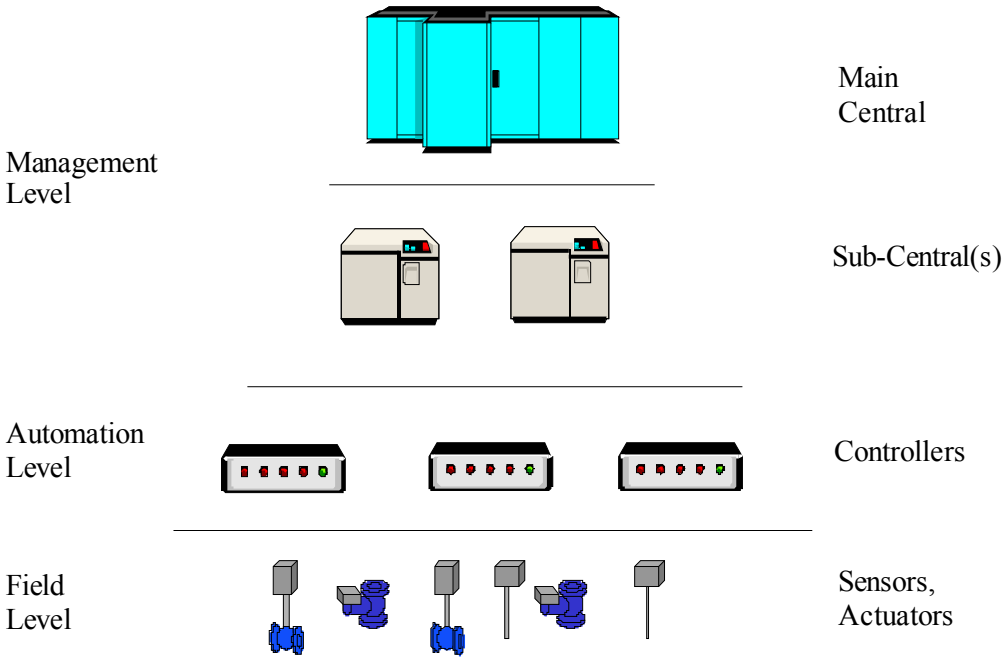

Fig. 1: Old Structure of a Building Automation and Control System

When the CEN Technical Committee TC 247 “Controls for Mechanical Building Services” started to work on building automation and control standards its working group WG4 “System-neutral Data Transmission” got the scope:

Standardization of system-neutral data transmission methods between products and systems in HVAC applications. The work is intended to develop HVAC specific applications of existing communication methods, one for each level.

Therefore, the architecture was based on the respective hardware and communication systems were related to the corresponding hardware “levels”. “Interoperation” of different industries in a building was a fiction which should come true in future. With the progress of the DDC technology the controllers became more powerful. The architecture became a more flat one, the functionality of the devices was increasing and the hierarchical structure began to change into distributed systems. So today the title of TC247 has changed to “Building Automation, Controls and Building Management” and WG4 is now called “Open Data Communication”. In large buildings the interoperation of different systems from different manufacturers using standardized communications is finally state of the art – including safety and security applications.

Requirements for the Communication Systems

For safety and security applications the requirements have to be divided into two parts, related to the ISO/OSI Basic Reference Model, called "7-Layers-Model" (Fig 2). One part describes the requirements for a "secure" data transmission, the other one the requirements for "secure and safe" applications.

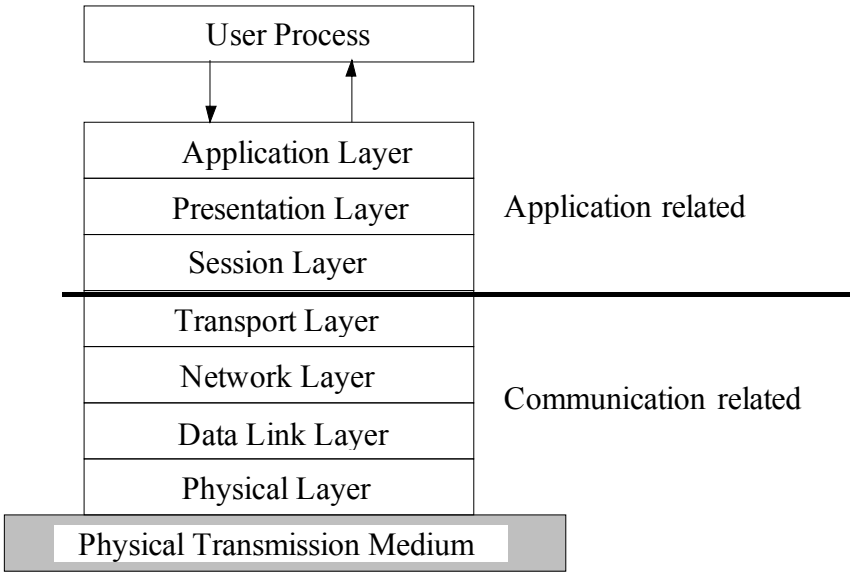

Fig. 2: ISO/OSI Basic Reference Model divided into two parts

Communication Related Requirements

First, there are the parameters required by every communication system like

- Throughput: how many data packets can be transmitted in a given time frame, especially if an "alarm flood" occurs like in case of fire (this is not only depending on the data transmission rate)?
- (Bit) error rate: how high is the probability of an error during transmission? What happens in case of an transmission error (nothing, detection and notification, detection and automatic repetition, or detection and automatic error correction)? How many errors can be detected?
- Response time: how long does it take after receiving a request to send out the required response (e.g. fire alarm)?
- Maximum PDU (protocol data unit) size: how much information can be transmitted during one atomic communication?
- Time out: what is the maximum waiting time for a response?
- Number of repetition: how many repetitions are allowed if an error has occurred?

- Deterministic or non-deterministic medium access: What is needed, a guaranteed response time with a well known maximum or a response time not predictable, but in most cases very fast?
- Connection-less or connection-oriented services: What is needed, a communication in a “letter-style” (writing a letter, putting it into a mail box and hoping that it will arrive) or in a “telephone-style” (dialing a number, getting a free tone, hearing the communication partner and starting the communication)?

Unlike ordinary BACS applications, critical applications very much rely on the parameters mentioned above . Additionally, there are special requirements like fire resistant cables, intrinsic safety, and others. The next group in the communication related requirements are the attacks to communication networks, especially in an IP-based environment. Potential attackers try to get access to network resources via a sophisticated mixture of password attacks, address spoofing, telephone line scanning, port scanning, eavesdropping, snooping, local exploits, etc. commonly known as “hacking”. Depending on the used technology, the attacker tries to exploit a number of weaknesses to get access. There are three aspects of communication systems that are subject to attacks:

- Data confidentiality (e.g. by eavesdropping)
- Data integrity (e.g. by manipulating the data)
- Data availability (e.g. by denial of service DoS attacks)

Data confidentiality and integrity are typically ensured by means of cryptographic algorithms, while availability is not that easy to protect. All these threats, however, have to be recognized and filtered in the communication related layers of the used protocol stack.

Therefore, if you want a secure communication system (related to the lower four layers of the ISO/OSI Basic Reference Model) you should either not allow any communication links outside of your automation system or you have to be prepared for all these above mentioned threats.

Functional Related Requirements

From a communication point of point of view the objects and services of the application layer of the protocol stack have to serve the “safety application”, e.g. fire detection and alarming. There have to be objects and services available for theses special applications.

But there is another question that comes up: What kind of building is it where the building automation and control system is installed? Is it a hospital, an airport, or a bank? Are there HVAC (Heating, Ventilation and Air-Conditioning) applications? As an example let us assume a Swiss bank which does most of the European money exchange within Europe and North-America in their computer center. In this center there is - as a part of the BACS - an HVAC system installed. The communication lines from and to the computers are protected by a firewall, so a direct attack to the IT infrastructure is unpromising. But nevertheless if someone has access to the building automation system and changes the setpoint of the room temperature controller in the computer center to 50°C the business will collapse within 15 minutes [FISC 00].
That means that the application itself has to be checked. Is it possible with a normal function used in an irregular way to damage the whole system, the building, or in the worst case to hurt people. Secure, robust and reliable data transport is the basis for security relevant automation systems, but the top-level application itself is as important as the data transport.

Standardized Communication Systems

The above mentioned standardization committee CEN/TC247 has published the three communication systems BACnet (EN/ISO 16484-5), Control Network Protocol based on the LonWorks technology (prEN14908) and KNX as part of the European standard series “Home and Building Electronic System” (EN50090).

BACnet

BACnet, initiated by the American Society of Heating, Refrigerating & Air Conditioning Engineers ASHRAE [ASH 95], is now an ISO standard [ISO 03]. Within this BACnet standard there is a clear separation between communication and functional relationship to safety and security requirements. The section “Network Security” of the standard defines a limited security architecture for BACnet which is optional. The intent of this architecture is to provide peer entity, data origin, and operator authentication, as well as data confidentiality and integrity. Other types of communications security, such as access control and non-repudiation, are not provided in the BACnet standard. Systems that require these services may add them to BACnet in a proprietary manner.
The Life Safety Point object type is one of two safety related BACnet object types whose properties represent the externally visible characteristics associated with

initiating and indicating devices in fire, life safety and security applications. The condition of a Life Safety Point object is represented by a mode and a state. Typical applications of the Life Safety Point object include automatic fire detectors, pull stations, sirens, supervised printers, etc. Similar objects can be identified in security control panels.

The other one is the Life Safety Zone object type defining an object whose properties represent the externally visible characteristics associated with an arbitrary group of BACnet Life Safety Point and Life Safety Zone objects in fire, life safety and security applications. The condition of a Life Safety Zone object is represented by a mode and a state. Typical applications of the Life Safety Zone object include fire zones, panel zones, detector lines, extinguishing controllers, remote transmission controllers, etc. Similar objects can be identified in security control panels.

The BACnet Life Safety Working Group is still working on more object type definitions needed by the different devices.

KNX

KNX is the successor of the European Installation Bus EIB, European Home System EHS and Batibus [SAUT 00]. Volume 4 "Hardware Specifications and Tests" of the KNX Handbook provides the constructional requirements for KNX devices, dealing mainly with Electrical, Functional, Environmental Conditions and Quality features needed to comply with the KNX certified design quality level [KNX 04]. Part 4/1 "Safety and Environmental Requirements for Application Products" lays down hardware requirements to be met for KNX certification by application products. The requirements are based on European standardization and fix the obligatory use for hardware certification of the European family standard for Home and Building Electronic Systems EN 50090-2-2 in conjunction with an appropriate product standard. Part 4/2 "Safety and Environmental Requirements for Basic and System Components" lays down hardware requirements to be met for KNX certification by basic and system components and devices. 50090-2-3 and 50090-2-4 define Functional Safety for KNX [HBES 04].

Control Network Protocol based on LonWorks Technology

CNP (Control Network Protocol) is the European Standard for LonWorks networks (also known as LON) [CEN 04], a universal control network technology, very popular for automating large office buildings.

The LonTalk protocol offers the standard means of securing its transport, cyclic redundancy checks for packets, repeat/retry transmission, acknowledged services, etc. [LOY 01].

On top of this protocol the so-called LonMark Objects implement the function-related part of the BACS. There are profiles for devices and functions ranging from light switches to network management. The LonMark profiles 5035 (Identifier Sensor) and 11001 – 11011 (various Smoke/Fire Initiators and Detectors) are examples for safety- and security- relevant functional profiles [LONM 02].

A new project called "LonSafety" [LONS 04] extends the existing safety features of LonWorks even more and intends to achieve SIL 3 (IEC 61508) and to increase the availability of LonWorks networks. First products are expected 2005.

Conclusion

All three "main players" in the open and standardized BACS business offer some security/safety related features and are partially even extending them. Proprietary and specialized networks very often beat these open systems in terms of price or special features, since they do not need to be universal. We, however, believe that the open and standardized way is the only way with future for BACS.

Safety and security was not an issue, when these technologies were "invented" [PAL 04]. Therefore, BACS applications that deal with personal safety are often implemented by using safety-able and certified technologies like PROFIBUS or ASI Safety although they are not suitable at all for BACS. This is why for instance LonWorks is now extended with LonSafety.

One has to be careful if theses networks are compared. [SNO 03] for instance sees BACnet more suitable for safety relevant functions since it uses priorities while LonWorks is an "idempotent" network. This and other differences between the three networks do not really count, they are functionally equivalent and every network can somehow implement any behavior of the others [KAS 04].

Sure, universal BACS networks like the three subjects of this study can not yet fully compete with highly specialized and proprietary safety networks. Considering the total costs and the future of standards, however, open systems are unbeatable. It is a wise guess to count on standardized technologies for building automation.

References

[AMEV 88] AMEV (Hrsg.): Planung und Ausführung von firmenneutralen Datenübertragungssystemen in öffentlichen Gebäuden und Liegenschaften (FND) Teil 1, FND-Spezifikation - Vertrieb: Druckerei Bernhard GmbH, Weyersbusch 8, 5632 Wermelskirchen, 1988

[ANSI 95] ANSI/ASHRAE Standard 135-1995, A Data Communication Protocol for Building Automation and Control Networks - Atlanta: ASHRAE, December 1995

[ASH 95] ANSI/ASHRAE Standard 135-1995 - BACnet - A Data Communication Protocol for Building Automation and Control Networks. American Society of Heating, Refrigerating and Air- Conditioning Engineers, Inc., 1995.

[CEN 04] prEN 14908-1 Open Data Communication in Building Automation, Controls and Building Management - Building Network Protocol - Part 1: Protocol Stack, European Committee for Standardisation (CEN)

[DIN 91c] DIN 19 245, Teil 1, Process Field Bus Datenübertragung, Medium Zugriffs Methoden und Übertragungsprotokolle, Dienst-Schnittstelle zur Anwendungschicht, Management - Berlin: Beuth, April 1991

[DIN 91d] DIN 19 245, Teil 2, Process Field Bus Kommunikationsmodell, Dienste für Nutzer-Anwendungen, Protokoll-Spezifikation, Codierung, Schnittstelle zur Sicherungsschicht, Management - Berlin: Beuth, April 1991

[FISC 00] Fischer, P.: Kommunikationsprobleme in der Regeltechnik. In: VDI-TGA: Gebäudetechnik - Aus Schäden lernen - VDI-Berichte 1517, Düsseldorf: VDI, 2000

[HBES 04] EN 50090: Home and building electronic systems (HBES).

[ISO 03] Building automation and control systems Part 5: Data communication protocol. ISO 16484-5:2003, International Standards Organisation, 2003.

[ISO 03] ISO 16484 - Building Automation and Control Systems – Part 5: Data Communication Protocol. ISO/CEN, 2003

[KAS 04] Kastner, W., Palensky, P., Rausch, T., Roesener Ch.: “A Closer Look on

Today s Home and Building Networks", in Proceedings of the 2004 IEEE AFRICON Conference, Gabarone, Botswana, 2004

[KNX 04] Konnex Association. KNX Specifications, Version 1.1, 2004

[LONM 02] LonMark Application Layer Interoperability Guidelines V3.3, LonMark Interoperability Association, USA, 2002

[LONS 04] LonSafety Project Homepage http://www.lonsafety.com/

[LOY 01] Loy, D., Dietrich, D. and. Schweinzer, H.-J (Eds.), Open Control Networks, LonWorks/EIA 709 Technology, Kluwer Academic Publishers, 2001

[PAL 04] Palensky, P.: "Requirements for the Next Generation of Building Networks", in Proceedings of the 10th International Conference on Information Systems Analysis and Synthesis ISAS, Orlando, Florida, 2004

[SAUT 00] Sauter T., Dietrich D., Kastner W. (Eds.), EIB Installation Bus System, Publicis, 2000.

[SNO 03] Snoonian, D.: "Smart Buildings" in IEEE Spectrum August 2003

A. Trevisi, G. Sica

Siemens Building Technologies Italy
EUSAS

The new challenges in the world of Building Automation in respect of market needs

Abstract

An overview on today's trend in Building Automation is presented. The expectations for comfort, safety, security and service are growing and market competitive pressure demand facilities matching business needs more closely, high level of efficiency and profitability as well as reduction of operating costs. The analysis of the most important requirements inside the concept of an integrated management system is built on the platform where the interchangeableness, interoperability, connectivity, compatibility and conformity define an open and interoperable system. In this context proper space has been assigned to open system architecture based on standards and on integration of all technical application in a building, taking in account in all the cases the market needs, like the integration in office environment, data exchange related to the users activity, remote management and use of wireless technologies, decentralisation of operability, scalability of the system and so on. The relevant requirements are qualified for the various system levels of *Management, Automation* and *Field*. Then the major expected benefits are listed, stressing the importance to lower cost for devices, software, engineering and for operator training; to rise in value of integrated functionality; to implement higher quality solutions as well as better long maintainability; to reach more transparency of the technical installations; to avoid vendor dependency and to obtain more efficiency operability. Then the influence of IT technology is evaluated in respect of the benefit to have the building management within reach of the users from any place at any time, simply operating for a global connectivity. Finally an outlook is given on the near future in the world of Building Automation.

Introduction - the architectonic and functional quality of the building

A new approach has been established for designing the building under the pressure of the relevant financial investment and the variety as well as the tendency to change the activities and functions inside the buildings. In fact beside the formal and physical

uniqueness of the building, the use destination never can be assumed as definitive but it must be considered only temporary and intended to be modified in a more or less period of time. In other words the functional and behavioural lay out of *the system building – user* becomes the priority to be defined. As a consequence the most important roles in the designing activity are played by:

- architect designer,
- facilities and plants designer,
- management activities and services designer.

Then the quality of the building rises by their integration and interaction as well as by their ability to establish an hierarchy on the main elements of the design, to avoid conflicts and to reach significant economic synergies. This new approach gives the solution to the past conceptual antagonism between the architectonic and functional quality of the building. The building automation, combined with other disciplines, is relevant part in resolving the rigidity of the architectonic quality versus the flexibility of the functional quality.

The Building Automation and the relevant disciplines combined

The value of the combination of the building automation with other disciplines depends mainly by the additional expected benefits through the technical connection of different system parts allowing an useful change of information data at level of the different subsystems and a better functionality. For instance, upon a fire incident the combination of different disciplines play a very important role: the building control system pressurizes the fire area, brings back to the ground floor the elevators, switchs on the emergency light, plugs in the smoke venting devices; closes fire doors; the access control system opens the doors according to a programmed procedure; the evacuation systems manages the exit of the people along the escape routes. The most important expected benefits are an improved overall system performance in terms of higher efficiency, better functionality, better reliability, increased user friendliness and operational safety. In addition it is expected a lower cost of installation, engineering, commissioning, operation and service. It is worthwhile to mention that in Europe greater importance has been assigned to this integration, defined as technical integration. The integration of multiple control and monitoring tasks into one building solution has been considered to be a global trend of increasing importance. Mainly

building automation has been combined with fire systems and then with security systems and finally with both fire and security systems. The related activities are specified as *Building Management* and *Danger Management*. A market analysis, presented in Rome the last year during an EUSAS workshop, gave the below listed results:

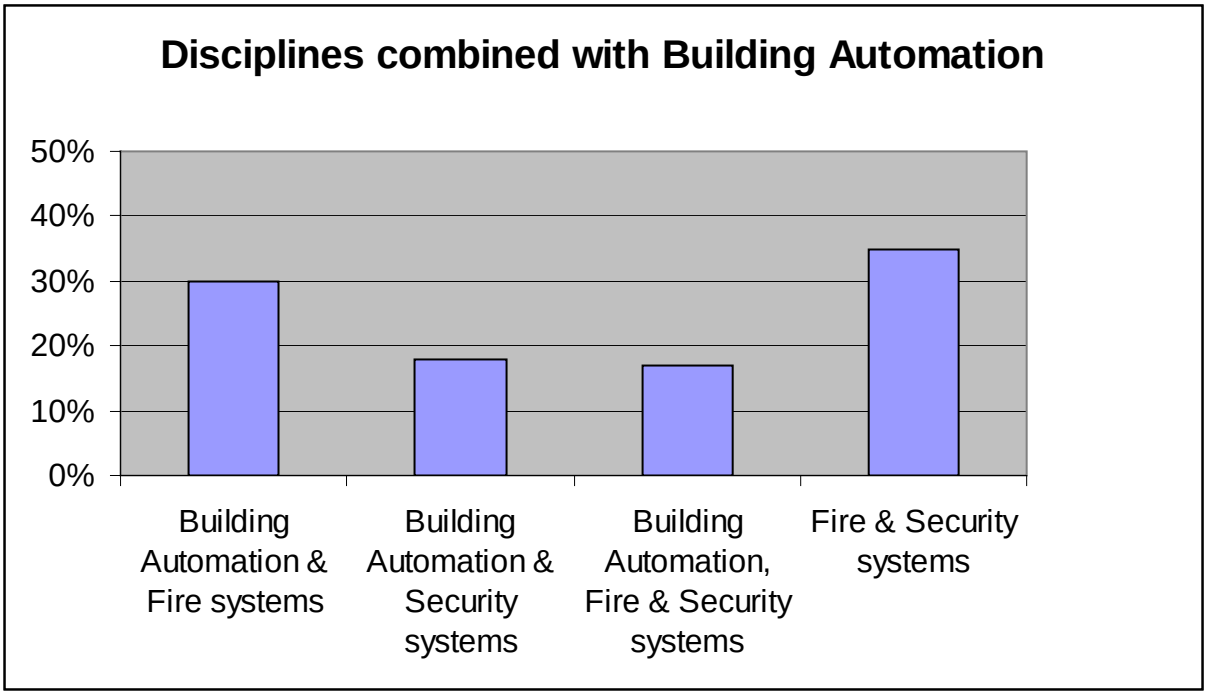

The same market analysis gave the following results regarding the different type of organisation:

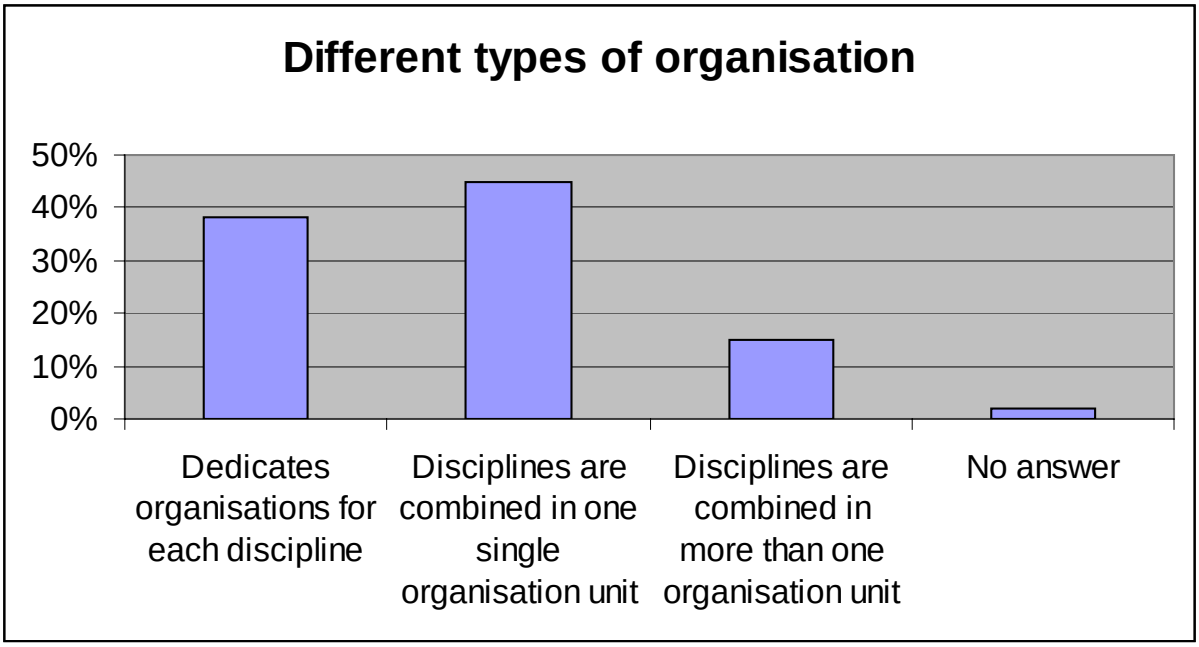

The presence of different type of organisations for the management building and the danger management has been justified by specific reasons.

The Building Management involves supervision and tuning of processes related to heating, air conditioning, air quality, comfort and energy. The operators must have the capability to manage rather complex activities like system performance and performance analysis. They need very good technical knowledge. In addition the user interface of the system has to provide a broad range of options.

On the other hand the Danger Management needs the efficient management of critical events mainly fire and intrusion alarms. Then the operators must possess the capability to manage emergency procedure under both time and psychological pressure.

Building and danger management can be both at different levels of complexity related to the specific application.

The expectations from market point of view

The generally perceived trend and the expectations of the market privilege the integration and the combination of different disciplines. Nevertheless the progress seems to be lower than foreseen. Mainly this situation is depending by local different codes of practice, different standard, different point of views of authorities like the Fire Brigades, who have the mandatory competence on fire systems and privilege the autonomy of the fire safety systems.

In addition the general attitude of the manufacturers focused on developping proprietary non standard communication solutions, with the scope to create a barrier to integration of third parties systems. Whereas the way forward consists on the implementation of open system standards for the communication.

This concept must be applied in all structure levels, namely in

- Field devices level with related Field bus,
- Automation device level with related Automation network,
- Management level with related Management network.

The following table presents the different types of integration related to hierarchical level, devices and communication:

Hierarchical level	**Devices**	**Main facilities and processes.** **Communications**
Management level	Management stations	Large data quantities and complex data structure. Complex network architectures. Standard IT networks are widely used between Management stations. Most frequently the problem of connecting different application in an integrated system is solved at this level.
Automation level	Automation level devices like control panels, complex I / O modules (e.g. PLC's), complex operator terminals	The automation bus networks Automation level to Management level devices. Peer – to – Peer functional interactions. Interoperability. Local Norms and mandatory rules can represent relevant constraints (like Fire Brigades regulations)
Field level	Field level devices like detectors, manual call point, I/O modules, simple operator terminals	Small data quantities, simpler data structure. Frequent data transmission, partially peer – to – peer for processing data. Simple installation. Cost reductions in networking and maintenance. Possible improved performances by combined criteria. The field bus connects the field devices among them and with to the devices of the Automation level. Local Norms and mandatory rules can represent relevant constraints (like Fire Brigades regulations)

To realise an “open” and “interoperable” system it is necessary to implement for each of the above mentioned hierarchical levels the conditions of

- *interchangeability,*
- *interoperability,*
- *connectivity,*
- *compatibility,*
- *conformity.*

The *interchangeability* allows to exchange devices with the same function by different manufacturers. The *interoperability* represents the capability of an equipment or system by different manufacturers to share information, implementing daily operations and performing a variety of functions on a peer – to peer basis, leaving them as much as possible autonomous. The relevant functions include monitoring, controlling, reporting, scheduling, alarms and monitored events handling with acknowledgement and reset according the situations, viewing and editing trend as well as history archive and reporting and so on. The *connectivity* allows devices to share the same physical network, using same services and options of the protocol, ensuring total compatibility in the transmission. *Compatibility* allows the use of the same protocol, avoiding any type of interference along the communication channel. *Conformity* defines the compliance to the applicable norms and technical specification. In this respect it is worthwhile to mention that Cenelec Technical Specifications CLC/TS 50398 – Alarm systems – Combined and integrated alarm systems – General requirements - require specifically that *the relevant standards to each application shall apply, that common facilities shall comply with all application standards for which they are standard required, that the most severe integrity requirement of each of the standards shall apply, that dedicated facilities have to comply with the relevant application standards (unless they are additional facilities*).

Conclusions

The generally perceived trend and market expectations as well as the reasons can be listed in the following way:

- Open system architecture based on recognised standards and standard communication solutions.

The penetration of systems integration may be gradually improved as manufacturers begin to implement open system standard for communication and stop to develop proprietary non – standard communication solutions.

- Solutions tailored to the user's specific needs;

The system applications, the types of tasks to be integrated, the disciplines to be combined must meet the user's specific needs.

- Compatibility among the various systems.

The benefits expected are made fruitless if a proper compatibility does exist among the systems. The market expectations are matched using the same protocol and avoiding any type of interference on the communication channel.

- Wireless technology and Web technology, where applicable, in order to operate at anytime from everywhere.

The use of innovative technologies take the benefit for the users to have building management in their fingertips from any place and at any time; having independent access, via mobile or any Internet device; using compliance to IT world for a global connectivity.

- Scalability.

The easy extension of the system, avoiding or bringing down the interference on daily activities in the building, becomes a strength point for convincing the user to adopt such type of solution.

- Lowering cost of technical infrastructures and software; lowering cost and time for engineering, commissioning and service.

It is worthwhile to remind that the cost reduction is a priority for all.

In conclusion the implementation of the above performances represents a major factor for a comprehensive, efficiency enhancing building automation and its establishment will not more lag behind the expectations. The users finally can take the relevant benefit in terms of productivity, functionality, reliability, efficiency as well as of cost reduction.

References

- CLC/TS 50398 – Alarm systems – Combined and integrated alarm systems – General requirements

Tributes

- EUSAS workshop on Integrated Systems in Rome 16-17 June 2003
- Polytechnic of Milan – BEST Building Environment Science and Technology Master 2003 – 2004 in “Building Automation, Fire Safety, Security and related services”

Bernhard Isler
Siemens Building Technologies AG, Fire & Security Products, Männedorf, Switzerland

BACnet™ integrated danger detection and building control systems

Abstract

BACnet™ (**B**uilding **A**utomation and **C**ontrol **net**work) [1], a building automation and control network protocol standard, developed by ASHRAE (American Society of Heating, Refrigerating and Air-Conditioning Engineers, Inc.) allows to build integrated systems covering heating, cooling, ventilation, air conditioning, lighting, fire detection, security, energy consumption management and other building control functionality.

Introduction

In today buildings, complex and distributed electronic systems are installed to control and operate heating, cooling, ventilation, air conditioning, lighting, fire detection, security, energy consumption control etc. The trend goes towards fully integrated systems, allowing interactions among all these systems, both for automatic control and human operation.

To achieve this, the systems need to be networked and data communication between (and mostly also inside) the systems takes place. For interoperability, data communication requires definitions for data transport, syntax of data and semantic interpretation, so called protocols. BACnet™ provides a comprehensive set of definitions for both interactions among systems and for data communication inside systems.

History

In the past, the building automation and control industry developed and deployed a tremendous number of proprietary data communication protocols for their respective systems. This led to extremely high integration costs, and locked customers to their system vendors.

ASHRAE, the American Society of Heating, Refrigerating and Air-Conditioning Engineers, initiated, in 1987, a project for an open data communication protocol standard. The goal was to allow simple integration of the different systems of a building, and even systems composed of devices from multiple vendors.

In 1995, the first version of this standard ANSI/ASHRAE 135-1995, named BACnet, was published and got ANSI (American National Standards Institute) approval.
The BACnet™ standard is today available in version 2001, and four approved addenda (A to D). Aside the ANSI approval, the standard is also approved by ISO as ISO 16484-5, the network protocol standard on management and automation level in the ISO BACS (Building Automation and Control System) standard suite 16484. It is the only ISO approved BACS standard available for automation and management level.

BACnet™ Overview

BACnet™ uses a simplified OSI model with 4 protocol layers, and a comprehensive data model and services definition on top of these layers. The definitions are completely free from software, hardware or other implementation constraints, therefore not bound to any computing platform technology.

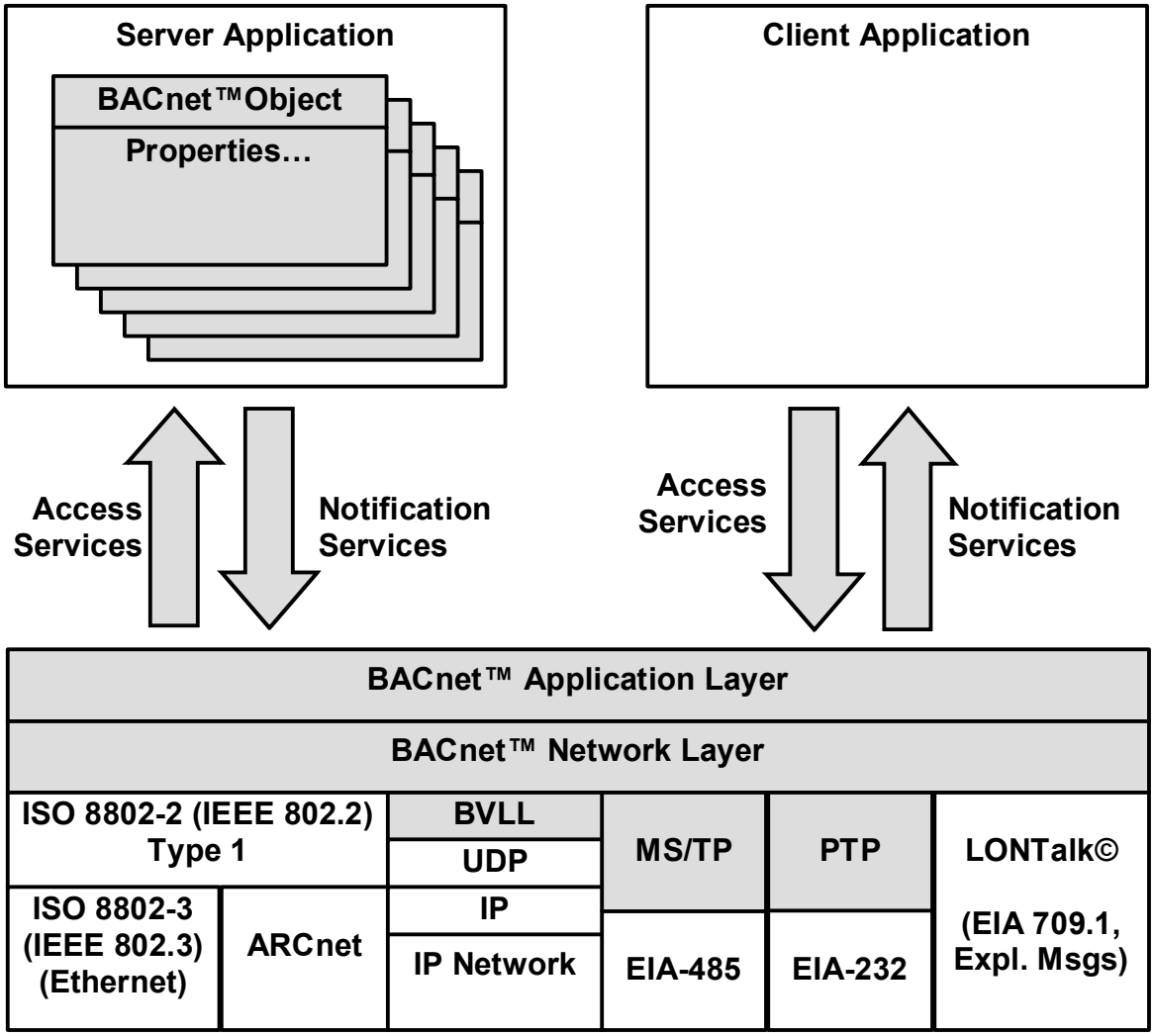

Figure 1: BACnet Architecture

Datalink and Physical Layers

According figure 1, various standard technology options are available for physical and datalink layer. ARCnet and Ethernet may be used directly, on datalink level without IP network layer. MS/TP (Master-Slave/Token Passing) is a low cost multidrop link based on EIA 485. PTP (Point-To-Point) serves as half-router link, based on RS-232, allowing dial-up and modem connections in wide area applications. LONTalk© is used in explicit message mode.

A vendor may use a proprietary datalink. Such a datalink needs to provide a minimal set of features, but may cover additional requirements such as redundancy.

The BVLL (BACnet™ Virtual Link Layer) allows using IP networks as a datalink layer in the BACnet™ protocol stack. This datalink layer option gains growing importance,

since it allows to run BACnet™ on IT infrastructure and in IP based WANs (Wide Area Networks).

For addressing devices on a datalink, the respective datalink or MAC-Addressing scheme is used. On IP, for example, the IPv4 32-bit address plus 16-bit UDP port number is used.

Any physical layer option supported by the respective datalink technology may be used. This includes Coax Cables, Twisted Pair, Power Lines, POTS lines, RF, Wireless LANs etc.

Network Layer

The BACnet™ network layer enables inter-networks, built of different datalink technologies. It supports, through use of PTP links and half-routers, temporary connections, wide area applications and dial-in/dial-up setups.

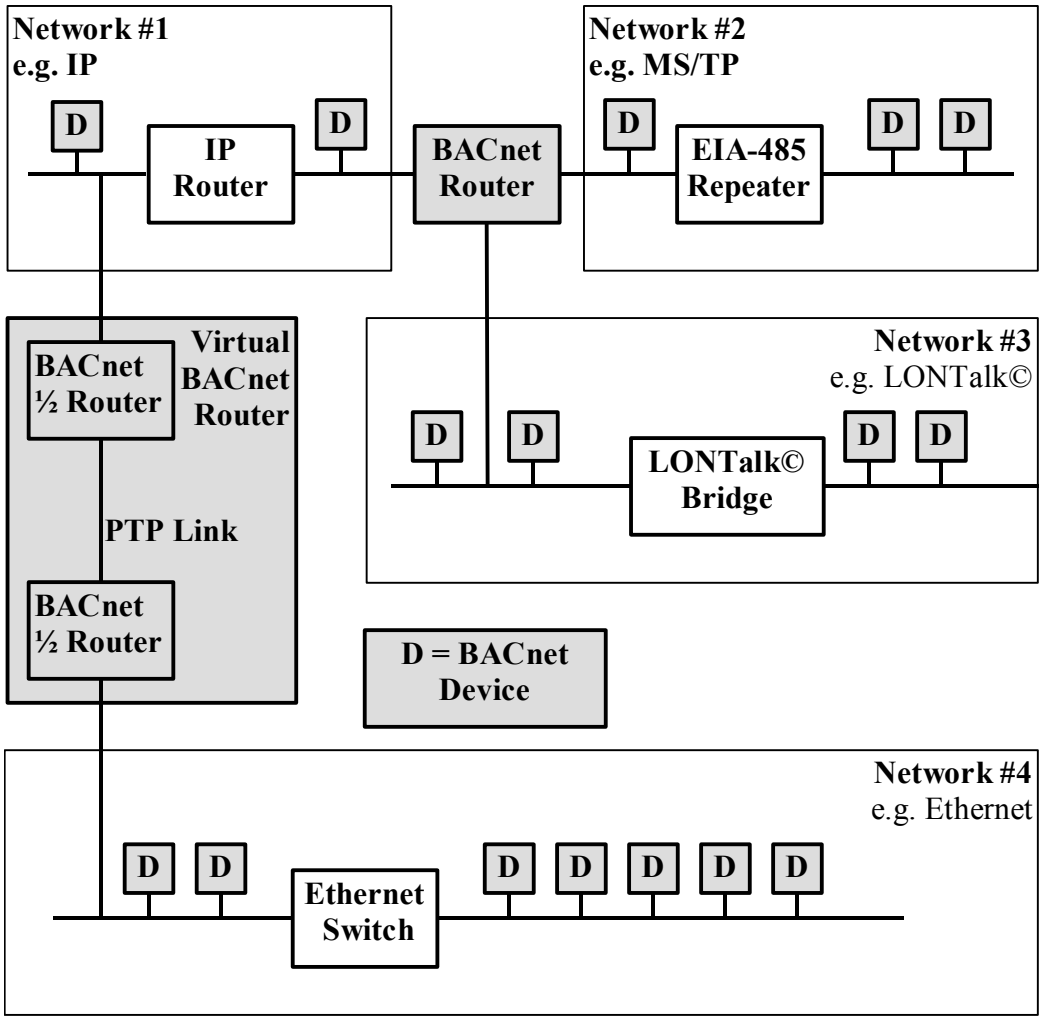

Figure 2: BACnet™ Network Topology

The routing of messages is based on 16-bit network numbers. Every network connected to the BACnet™ inter-network gets such a 16-bit network number assigned.

BACnet defines its own network layer due to different reasons: At the time of early BACnet definitions, IP networking was not commonly available. Very small BACnet™ devices did/do not have the capability to run an IP stack. Lack of very low cost standard datalink technology below IP (e.g. EIA-485).

Application Layer

The BACnet™ application layer provides generic unconfirmed and confirmed services.

Unconfirmed services are used typically for broadcasting of notifications and lookup queries. No receipt acknowledgment is expected. The message size is restricted to the message size supported by the underlying datalink technology. Unconfirmed services can be addressed to a single node (Unicast), all nodes within a specified network (Multicast), or to all nodes inter-network-wide (Global Broadcast).

Confirmed services are used for requests requiring a response. Both the request and the response message can be larger than the message size of the transport network. In this case the application layer applies segmentation. This way any size of message can be transferred. Confirmed services can be addressed to a single node only (Unicast).

Network Security

Up to now, BACnet defines a DES (Data Encryption Standard) based security scheme for ciphering and authentication. The current approach is no longer satisfying, since small keys (56 bits) are used, and authorization is not covered. There are also some problems detected which are related to the block ciphering scheme of DES.

There are activities in the BACnet™ project to overcome these problems. A first set of definitions is expected to get approved within a time frame of one year.

Today available work-around is either to use dedicated network installations, or to use IP based network security technologies in the IP datalink option. Of course any proprietary approach could be implemented, but this might break interoperability.

Application Protocol

On top of the communication protocol stack, one of the most important features of BACnet™ can be found. This is the data model and services definition, or application protocol. It covers data modeling and addressing, service syntax and semantic definitions. The functionality covered is data sharing, alarm and event management, scheduling, trending, logging, device management and network management. This enables true interoperability among different systems and devices, even multi-vendor setups. Interactions between devices and single seat workstation operation are possible with a single protocol.

Data Model

The data model defines a set of object types. These object types represent the features of a device. Each object type is defined as a set of well-defined properties. A vendor may introduce proprietary object types if required.

Every BACnet™ device consists of a set of object instances of any defined type. A 32-bit Object Identifier identifies object instances. This identifier must be unique within the device. Alternatively, an object can be identified or searched for by its object name.

The properties within an object are a subset of the overall property set defined by BACnet™. A unique number identifies properties. Vendors may add proprietary properties if required.

There are basic object types for representation of Binary Inputs/Values/Outputs, Analog Inputs/Values/Outputs and Multistate Inputs/Values/Outputs. More complex object types represent Files, Control Programs, Command Macros, Feedback Loops, Schedules, Calendars, Averaged Values, Data Collections (Groups), Trend Logs and Event Logs. For event handling, there are Event Enrollment and Notification Class object types available.

Fire and intrusion detection application related object types represent Life Safety Points and Life Safety Zones. For energy management applications, Puls Counter and Accumulator Objects are defined.

A device itself is represented by the Device Object. This is a single object among all others present in a device. Its object identifier and object name is restricted to be unique inter-network-wide. This device object identifier may be used as a logical address of the

device. Look-up services allow resolving from this logical address to the network number and the MAC address of the device.

Look-up Services

Services are defined to find devices and objects in an inter-network.

To resolve a logical address of a device (the device object's identifier!) to the network number of the network the device is connected to, and to get the datalink address of the device, a query request ("Who-Is") is broadcast. The device searched for responds by a presence message ("I-Am"), which allows the requesting device to retrieve its network number and datalink address.

To find an object by its name, i.e. to resolve the object name to the object identifier and device address, a query request ("Who-Has") is defined. The device containing the object searched for responds with a message containing the device's logical address and the object's identifier. This allows the requesting device to formulate further service requests to access the device.

Data Sharing Services

Data sharing services include reading and writing of properties, aggregations or selections of. To avoid polling of values in interactions, change-of-value reporting services for subscription and value change notifications are defined.

Alarm and Event Services

BACnet™ defines two ways to get notifications of events or alarms happening in objects: Intrinsic reporting and algorithmic reporting. Event or alarm notifications are intended for human indication and treatment.

Every object that supports intrinsic reporting has a number of properties, which define the reporting behavior of the object. Well-defined algorithms are used to determine when events happen and how they are notified.

In algorithmic reporting, Event Enrollment objects are configured to define the source data and algorithm applied on to generate events or alarms.

Events are routed through device-local Notification Class objects, at which client applications can subscribe for event and alarm notifications.

A human operator, depending on the configuration within the source object or Notification Class object, may be required to acknowledge events or alarms.
For Life Safety Zones and Points, silencing and resetting is done through the dedicated Life Safety Operation service.

File Services

A BACnet™ device may represent files through file objects. Files may hold configuration data, log data, sample data etc. Files are accessed through dedicated file access services.

Device and Network Management Services

There is a set of services defined to control device operation and to configure and manage the inter-network.

System Specification

Customers are able to specify their desired system from a functional standpoint. BACnet™ offers means for doing this, the so-called BIBBs (BACnet™ Interoperability Building Blocks) and device profiles. The functionality is not necessarily to be provided by a single vendor, it can be realized by an optimum combination of devices from different vendors. Since the standard is not bound to computer technologies, the customer has also a clear and open migration scenario over the lifetime of the system (10 to 30+ years). The system can be extended, changed or renewed without being required to have a single supplier, which supports the system over extremely long life cycles.

Fire and Intrusion Detection System Modeling

Since the BACnet™ version 1995 addendum C, approved since 2001, now incorporated into the standard's version 2001; there are data models and services available, which allow to model fire or intrusion detection systems. Based on this, fire or intrusion detection systems can interoperate inherently with other vendor's fire or security systems, other building control systems and with standard operator workstations.

Fire and intrusion detection systems are modeled as a collection of objects within devices. These devices are most typically control panels.

The Life Safety Point object represents peripherals like detectors, actuators, indicators and other physical devices. Among the basic state and operation mode properties, there are a number of other properties, which represent direct sensor reading, maintenance, sensitivity etc.

The Life Safety Zone object represents logical entities like fire zones or intrusion sections.

The objects can be related to each other in a hierarchical, tree-like structure with possibly multiple levels. The relations may span device boundaries even. Life Safety Points are always arranged as leafs, while the Life Safety Zones act as tree nodes.

The primary value, or Present Value in BACnet™ terms, is the Life Safety state. This state may latch until a Life Safety operation "reset" is applied. The actual, non-latched state is available as a property too.

The Life Safety objects can be switched in their operation mode, such as armed, disarmed, on, off, manned, unmanned etc.

All Life Safety objects contain properties, which represent the audible and visual alarm indicators associated to the entity the object represents. The Life Safety operation allows controlling these indicators.

Standard event handling services are used for alarming and alarm acknowledging. For silencing visual and audible alarm indications as well as to reset latched states to their actual value, the Life Safety operation service is used.

Testing and Certification

There is a companion standard for testing and certification of BACnet™ devices. This standard is ANSI/ASHRAE 135.1-2003. It is intended to get ISO approval and to incorporate this testing standard into ISO 16484 as part 6.

The BMA (BACnet Manufacturers Association) has established the BTL (BACnet Testing Laboratory) in USA, which is entitled to run certification tests according the standard. Devices passing these tests are allowed to carry the BTL mark.

In Europe, the BIG-EU (BACnet Interest Group Europe) is on the way to establish a testing laboratory in Europe, which will be enabled to certify devices to carry the BTL mark.

Next Steps

There is the version 2004 of the BACnet™ standard on the way to publication by ASHRAE. It will include all addenda of the 2001 version, and therefore does not contain new material.

Two new addenda A and B to the 2004 version are currently under public review and define new extensions to the standard.

At this time, there are activities in the BACnet™ standard project to define data models and services for Access Control and CCTV (Closed Circuit Television). Once done, interactions can be implemented inherently to/from such systems even.

Further application areas under development are lighting and load control modeling.

Network security is under improvement. The solution intended should provide authentication, ciphering and authorization. It will provide network security not just only on IP networks, but on any datalink option available.

To get integration of the building automation and control system towards IT systems such as office applications or enterprise resource management systems, Web Services definitions are under development.

To support engineering data exchange and device definitions, XML based modeling languages are under development.

References and further information

[1] ANIS/ASHRAE 135-2001, ASHRAE, ISSN 1041-2336
Available as paper copy, electronic copy (PDF) or on a CD-ROM at ASHRAE Bookstore at www.ashrae.org. Addenda A to D to 2001 version are available for free download on this web site too.

[2] BACnet Web Site: www.bacnet.org

[3] BMA Web Site: www.bacnetassociation.org

[4] BTL Web Site: www.bacnetassociation.org/bacnet_testing.htm

[5] BIG-EU Web Site: www.big-eu.org

R. Conrads
VdS Schadenverhütung, Köln, Germany

Wireless detection and alarm systems

Abstract

History

Until beginning of the 90ies wireless alarm systems (AS) where signals were transmitted via radio links, had no good reputation in Germany because of lack of quality and reliability. Several systems were on the market, but more or less all on a low level of technology. Very often normal AS equipment was connected to transmitters and receivers from remote control equipment e. g. model aircrafts or CB radio equipment; a technique which could not result in reliable systems.

Improvements with new technologies

Then the technology improved – besides others in connection with the boom of the mobile phone technology. Systems were designed as a complexity taking into consideration the special factors of alarm systems and radio technology. VdS set up rules for alarm systems, first for class A used in residential risks.

The technology used in those days were typically 433 MHz solutions with on frequency. Because of the easy possibility of tampering the use of such systems in commercial risks was not permitted.

The problem of single channel alarm systems was on one hand that almost all systems worked with one frequency (433,920 MHz). This fact in agglomerations lead to reciprocate interference of systems.

Furthermore wireless head-sets were offered in the market which also worked with the same frequency range, units which were operating often 24 h and blocked the transmission channel for the alarm systems. The solution were wireless alarm systems with multi-channel technology, automatic band-scanning and channel-hopying technology. These systems picked out those channels which were “free”. But the vicinity to strong amateur radio stations in the 433 MHz-band (sometimes which several 1000 W radiated power) and the possibility of tampering with free purchasable transmitters still caused specific problems.

To solve this problem multi-band and multi-channel alarm systems were developed using 433 MHz-technology plus the new 868 MHz-band for SRD-use (SRD = short range devices). The 868 MHz-band has the advantage that power is limited as well as transmission time and the fact that no complete transmitters are available. This technology admits a faulty free operation on base of multiple transmission channels as well as high level of resistance against tamper attacks. Regarding the resistance against tamper attacks it is to be taken into consideration that a pure detection and signaling of the blocked transmission path cannot be the solution (this is a false alarm!); the performance shall be that other users of radio frequencies as well as deliberate influences (tamper) should not negatively affect any function of the alarm system.

Forecast

With the increasing technology of wireless communication also wireless alarm systems will get more reliable. Self-learning systems without any need of adjustment will be the future, also alarm systems using radio and wired transmission paths – so-called hybrid systems.

Dierk Nahrstedt
Siemens Building Technologies Fire and Security Products GmbH & Co. oHG, München, Germany

Radio Transmission Procedure for Private Fire & Intrusion Alarm Systems with Maximum Availability

Abstract

Radio technology has been established for decades now in the sphere of private alarm technology, particularly for intrusion alarm systems and social alarms with and without fire alarms. The advantages that radio offers in terms of communication (clean installation and mobile emergency buttons) were so great that there was a willingness to accept the disadvantage of the relatively poor availability of these simple systems. However, to date this technology has not been able to disassociate itself from this reputation of offering inadequate availability. Professional security providers still recommend a wired system in preference to their customers, or simply do not offer radio alarm systems at all.

Better-protected frequency bands and technological advances are opening up completely new possibilities. Of key interest in this context are transmission procedures that offer automatic routing. They abolish the coverage restriction, solve the problem of fading, automatically balance out higher attenuations as a result of obstructions and are easy and fast to install.

The ad-hoc routing procedures familiar from literature, i.e. distance vector routing and link state routing, are very suitable for detector networks and will be presented briefly. The latter is more economical in terms of the radio channel and is hence the preferred choice. The presentation illustrates the procedure derived on this basis and the main features of the system handling. Information is provided on incorporating unidirectional telegrams and the resulting problems.

The live receiver in the routers normally offers power supply from batteries. Thanks to the enhanced development of the procedures and protocols, the power consumption of routing detectors has been improved such that a lifetime of some two to four years is now possible with three AA batteries.

The presentation concludes with a demonstration of the routing mechanism of the first ad-hoc network for radio intrusion and fire alarm system for private applications to come on the market.

Einleitung

Die Funktechnik ist aufgrund ihrer vielen Vorteile seit Jahrzehnten in der privaten Meldertechnik etabliert. Die einfache und saubere Montage ohne aufwendige Verkabelung ist sicherlich der Hauptgrund für den Einsatz von Funk. Die Installationsorte sind flexibel und können jederzeit neuen Anforderungen angepasst werden. Durch Funk können mobile Notrufknöpfe in Alarmsysteme integriert werden. Eine hohe Verfügbarkeit war bei einfachen unidirektionalen Funksystemen nicht immer gegeben. Besser geschützte Frequenzbänder und der technologische Fortschritt eröffnen hier völlig neue Möglichkeiten.

Anforderungen

Um eine möglichst hohe Verfügbarkeit eines Funksystems erreichen zu können, ergeben sich folgende Anforderungen:
Vorzugsweise ist ein Frequenzband zu wählen, dass möglichst frei ist von konkurrierenden Anwendungen. Als günstig erweisen sich Frequenzbänder, die für Anwendungen im Short Range Device Bereich freigegeben sind, dies ist zum Beispiel das SRD Frequenzband bei 868 MHz. Dieses Frequenzband bietet günstige Voraussetzungen, da hier die Sendeleistung begrenzt und der Duty Cycle klar definiert ist.
Möchte man Nachrichten mit höchster Zuverlässigkeit, wie es die kommerzielle Brandmeldetechnik fordert, übertragen, so ist nur ein bidirektionales

Übertragungsverfahren geeignet. Damit ist sichergestellt, dass die Nachrichten auch beim Empfänger ankommen.

Die Reichweite eines Funksystems wird vorrangig bestimmt durch die Sendeleistung, die Empfindlichkeit des Empfängers und die gewählte Frequenz. Bei hochwertigen Systemen im Bereich 868 MHz hat man Reichweiten von ca. 500m im Freifeld, in Gebäuden jedoch geht die Reichweite auf Werte zwischen 10m und 50m zurück, stark abhängig von der Anzahl und Beschaffenheit der zu durchdringenden Wände. Innerhalb von Gebäuden wird die Funkübertragung durch Mehrwegeausbreitung bestimmt. Reflexionen, Absorption der Energie und Überlagerung der Funkwellen, aber auch geringe Nutzungsänderungen führen zu Fadingeffekten. Dadurch können die Feldstärken am Empfangsort stark schwanken und es kann zur zeitweisen völligen Auslöschung aufgrund der Überlagerung der Funkwellen kommen. Diese Auslöschungen sind zeitlich begrenzt und können sich durch minimale Änderung der Umgebung wieder aufheben (siehe auch Vortrag K. H. Schreyer: The Radio Wave as a Transmission Medium in Modern Fire Alarm Systems).

Setzt man in Gebäuden ein sternförmiges Übertragungsverfahren nach dem Master-Slave Prinzip ein, so ist die Reichweite unter Umständen nicht groß genug, um alle Orte eines Hauses von einer Basisstation auf direktem Wege sicher erreichen zu können. Somit wären dann doch wieder Kabel nötig, um diverse Funkgateways an mehreren Orten installieren zu können.

Lösungsansatz

Um das Reichweitenproblem lösen zu können, benötigt man mindestens Repeater, die Nachrichten einfach weiterleiten können. Repeater sind kostspielig, da sie in der Regel keine eigene Melderfunktion besitzen, und haben zusätzlich eine hohen Energieverbrauch, da sie ständig aktiv sein müssen. Ein starres Repeatersystem hat auch den Nachteil, dass die Fadingeffekte im Repeaternetz ebenfalls nicht vermieden werden können.

Besser geeignet sind deshalb Meldernetzwerke mit routenden Übertragungsprozeduren. Meldernetzwerke haben den Vorteil, dass jeder Melder mehrere Möglichkeiten bzw. Wege kennt, um seine Nachrichten an einen Empfänger abzusetzen. Selbsttätige Routingverfahren führen zu einer sehr einfachen Installation. Ist das Meldernetz

hinreichend eng, was bei Brandmeldeanlagen unterstellt werden kann, so ist das System selbständig in der Lage, die günstigsten Kommunikationsnetze zu ermitteln. Ein selbstroutendes System kann auf sich im Betrieb verändernde Umgebungsbedingungen reagieren und immer wieder die Übertragungswege den neuen Gegebenheiten anpassen.

Routingverfahren

Routingverfahren werden in einer Vielzahl in der Literatur beschrieben.

Für Meldernetze gelten Ad-hoc Routingverfahren wie das “Distance Vector Routing” und das “Link State Routing” als sehr geeignet.

Alle Routingverfahren haben gemeinsam, dass die routenden Teilnehmer Routingtabellen ermitteln, in denen die Wege zu anderen Teilnehmern hinterlegt sind.

Die Verfahren “Distance Vector Routing” und “Link State Routing” sind zunächst dadurch gekennzeichnet, dass jeder Teilnehmer alle Partner ermittelt, die er von seinem Ort aus direkt erreichen kann. Beim “Distance Vector Routing” trägt der Teilnehmer diese gewonnenen Informationen in seine Tabellen ein. Allen Nachbarn schickt der Teilnehmer nun die ihm bekannten günstigsten Routen und somit alle Informationen, die er über das Netzwerk besitzt. Die Partner empfangen die Nachricht, aktualisieren ihre eigenen Routinglisten und schicken die aktualisierten Tabellen an ihre direkten Nachbarn weiter. Somit wird Schritt für Schritt jedem Teilnehmer die gesamte Netzstruktur bekannt gemacht. Nach mehreren Runden Nachrichtenaustausch konvergieren diese Distanz Vektoren. Man kann sich vorstellen, dass hierzu bei größeren Systemen eine Unmenge an Nachrichten benötigt wird, bis das System erst einmal in einen eingeschwungenen Zustand kommt. Hinzu kommt der nicht unerhebliche Stromverbrauch aufgrund der hohen Anzahl von Nachrichten, die schon allein mit der Zellenkonfiguration zusammenhängen.

Ist das System jedoch eingeschwungen, so kann ein Teilnehmer, der eine Nachricht schicken will, den kürzesten Pfad zum Partner ermitteln und die Nachricht auf schnellstem Wege übertragen.

Das Verfahren ist nur für kleinere Zellengrößen geeignet, da mit steigender Teilnehmerzahl der administrative Datenverkehr rapide ansteigt und die Funkzelle vorrangig mit Konfigurationsaufgaben beschäftigt wäre.

Beim „Link State Routing“ ermittelt jeder Teilnehmer seine direkten Nachbarn und schickt nur diese Erreichbarkeitsliste an die anderen Teilnehmer des Netzwerks. Jeder Partner, der die Nachricht empfängt, kann anhand dieser Information seine Routingtabellen anpassen und somit Schritt für Schritt die komplette Netzwerkstruktur ermitteln. Beim Link State Routing konvergieren die Routingtabellen schneller. Somit ist der Funkkanal während der Konfigurationsphase weniger belastet. Ein weiterer Vorteil des Link State Routing ist die schnellere Reaktion auf Veränderungen in der Zellenstruktur. Fällt ein Teilnehmer aus, dann genügen wenige Telegramm, um die Veränderungen in der Funkzelle bekannt zu machen. Somit ist dieses Verfahren gerade bezüglich der Funktechnik besser geeignet.

Beide Verfahren erfordern einen hohen Aufwand sowohl in der Rechen- und Speicherkapazität jedes Teilnehmers, da mit der Größe der Netze der Aufwand für die Routingtabellen ansteigt.

Routingverfahren für die private Funkmeldetechnik

Bei Verwendung von Routingverfahren in der Meldetechnik steht die Frage des Stromverbrauchs mit im Vordergrund.

Generelles Problem ist der bei Routern ständig mitlaufende Empfänger. Moderne Funkempfänger liegen beim Stromverbrauch im Bereich von 20mA. So wäre bei einem Batteriewechselintervall von 3 Jahren eine Kapazität von 500Ah erforderlich. Alkali Mangan Batterien vom Typ AA (Mignon) liegen in der Kapazität bei 2Ah!

Die Aufgabe bestand also darin, ausgehend von den bekannten Routingverfahren die Prozeduren so weiterzuentwickeln und auf die Funktechnik anzupassen, dass eine Speisung aus Batterien möglich ist und gleichzeitig alle Vorteile des Routings genutzt werden können.

In der privaten Meldetechnik geht die Hauptrichtung der Nachrichtenübermittlung zu einer Meldezentrale hin. Dieser Pfad hat oberste Priorität, um Alarme sicher übertragen zu können. Des weiteren benötigt man eine stabile Nachrichtenübermittlung von der Zentrale weg, um Alarmierungsmittel, Aktoren und Steuerungen schalten zu können. Punk zu Punkt Verbindungen zwischen einzelnen Meldern haben eine niedrigere Priorität.

Es wurde eine Prozedur entwickelt, die mit verhältnismäßig wenig Speicheraufwand im Mikroprozessor auskommt, damit die Funkmodule auch von der Kostenseite her für den privaten Einsatz in Frage kommen.

Ähnlich wie beim Link State Routing ermittelt jeder Funkteilnehmer zunächst alle erreichbaren Nachbarteilnehmer. Diese Erreichbarkeitsliste sendet er jedoch nur in Richtung Zentrale. Um die Richtung eindeutig bestimmen und eine Pfadoptimierung durchführen zu können, wurden Kommunikationsebenen eingeführt. Dabei liegen Teilnehmer mit direktem Kontakt zur Zentrale auf dem Kommunikationslevel 0. Für jeden Router von der Zentrale weg erhöht sich der Kommunikationslevel um 1.

Die Meldung der Erreichbarkeitsliste wird von den anderen Teilnehmern auf dem Weg zur Zentrale mitgehört, die diese Informationen auswerten und ihre eigenen Routinglisten anpassen.

Es ergibt sich eine Struktur laut Bild 1:

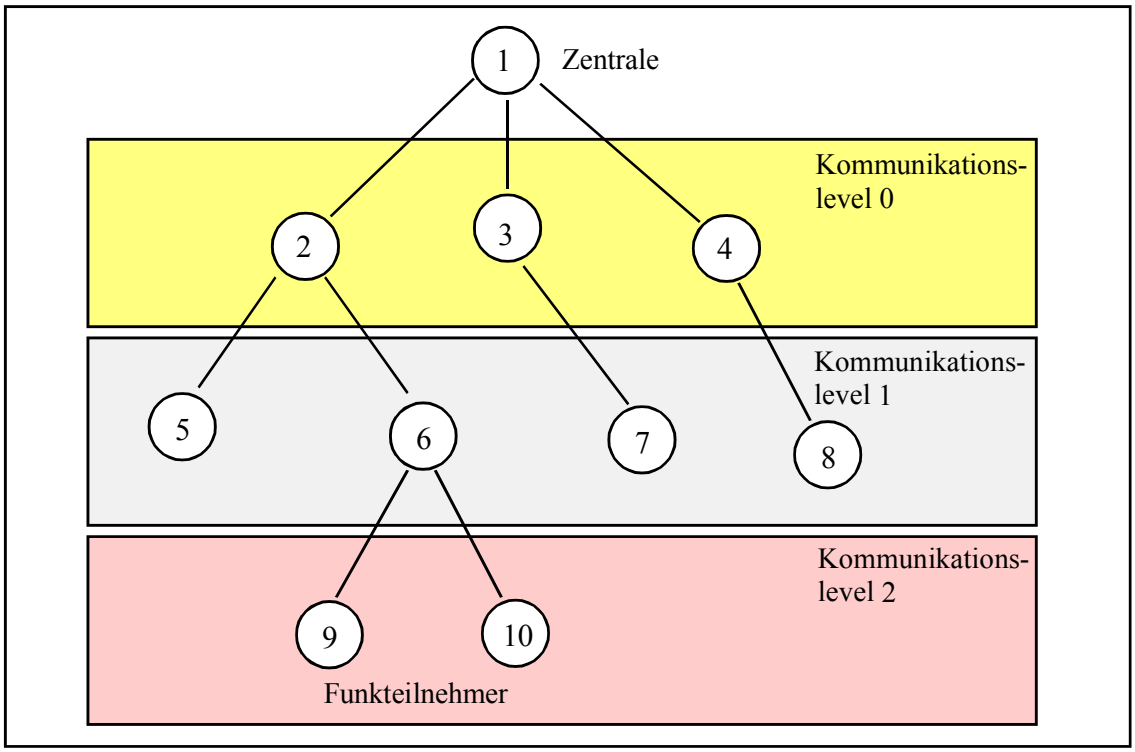

Bild 1: Struktur einer SiRoute Funkzelle

Im Vergleich zum Link State Routing speichert jeder Teilnehmer nicht die komplette Netzwerkstruktur ab. Vielmehr besteht die Routingliste eines Teilnehmers aus

Einträgen, über welchen Nachbarn ein anderer Teilnehmer erreicht werden kann. Jeder Funkmelder kennt also nur den nächsten Hop auf dem Weg zum gewünschten Empfänger. Dies spart einerseits Speicherplatz und zweitens reduziert es die Anzahl von Nachrichten, die zur Konfiguration des Netzwerks notwendig sind. Die Routingliste eines Teilnehmers ist in Bild 2 beispielhaft dargestellt.

Teilnehmer	1	2	3	4	5	6	7	8	9	10
nächster Hop zum Teilnehmer	1	x	3	-	5	6	-	-	6	6

Bild 2: Routingtabelle von Teilnehmer 2

Die routenden Funkteilnehmer arbeiten bidirektional, alle Nachrichten werden vom Empfänger quittiert. Dies gewährleistet eine sichere Übertragung der Alarme und Störungsmeldungen in Richtung Zentrale.

Um das Problem des Stromverbrauchs zu lösen, wird der Empfänger jedes Teilnehmers in periodischen Abständen kurz eingeschaltet. Beim Senden von Nachrichten wird zunächst durch Senden eines Announcements angekündigt, dass eine Nachricht gesendet wird. Das Announcement enthält außerdem den Zeitpunkt für das Senden der Nutznachricht. Die Länge des Announcements ist so bemessen, dass alle benachbarten Teilnehmer das Sendeanliegen registrieren können und nur dann länger auf Empfang schalten, wenn die Nachricht gesendet wird. Durch dieses Verfahren konnte der Stromverbrauch soweit gesenkt werden, dass bei Versorgung aus Batterien eine Lebensdauer von bis zu 4 Jahren erreicht werden kann.

Meldungen in Richtung Zentrale werden in die Richtung mit absteigendem Kommunikationslevel gesendet. Somit erzielt man eine hohe Sicherheit, dass die Nachricht den optimalen Weg nimmt.

Fällt eine Teilstrecke auf dem Weg zur Zentrale aus, dann kommen die Vorzüge des Routings zum Einsatz. Der Teilnehmer, der die aktuell zu übertragende Nachricht gerade hat, schickt einen Rundruf, ob andere benachbarte Teilnehmer noch einen Weg zur Zentrale kennen. Von allen antwortenden Teilnehmern erhält der mit dem niedrigstem Kommunikationslevel die Nachricht, um sie dann entsprechend seiner Routingtabelle weiter zur Zentrale zu schicken. Somit kann das System optimal auf äußere Einflüsse reagieren und eine sichere Übertragung gewährleisten.

Werden Nachrichten (Befehle) von der Zentrale an einen Signalgeber geschickt, so wird ebenfalls anhand der Routingtabellen der aktuelle Weg ausgelesen und die Nachricht zuverlässig übertragen.

Die Einbindung unidirektionaler Teilnehmer ist für mobile Alarmmeldungen (z.B. Überfall) und Steuerungen über Funkfernbedienungen interessant, die Implementierung in das bidirektionale System ist eine besondere Herausforderung.

Möchte man das Routing auch für die unidirektionalen Telegramme nutzen, so kann man die unidirektionalen Telegramme durch den bidirektionalen Teilnehmer adaptieren und dann als quasi-bidirektionale Nachricht in Richtung Zentrale weiterschicken. In der Praxis wird es jedoch häufig vorkommen, dass die unidirektionale Nachricht von mehreren Funkmeldern gehört wird. Um zu vermeiden, dass die Nachricht mehrfach adaptiert wird und damit den Funkverkehr unnötig erhöht, ist ein Verfahren sinnvoll, damit sich nur ein Melder zuständig fühlt.

Gelöst wurde das Problem durch eine Broadcast Meldung mit Antwortzeitschlitzen, in dem der Melder mit niedrigster Teilnehmernummer die Nachricht adaptiert und den anderen Meldern mitteilt, dass diese die Nachricht ignorieren sollen.

Da sich jedoch nicht alle Melder gegenseitig hören, kann es trotzdem vorkommen, dass eine unidirektionale Nachricht mehrfach auf verschiedenen Wegen in Richtung Zentrale übertragen wird. Somit muss durch intelligente Auswertung der eintreffenden Telegramme bei der Zentrale sichergestellt werden, dass eintreffende unidirektionale Kommandos nicht mehrfach ausgeführt werden.

Routing in der Praxis

Anhand eines Beispiels soll nun gezeigt werden, wie das Routing in der Praxis aussieht und wie auf Störungen reagiert wird.

Bild 3 zeigt eine Funkzelle mit wenigen Teilnehmern, wobei drei Melder direkten Kontakt zur Zentrale haben und ein Melder über zwei Hops verbunden ist. Melder 4 ist aktuell über Melder 2 mit der Zentrale verbunden und möchte einen Alarm senden. In der Routingtabelle des Melders 4 steht Melder 2 als nächster Hop in Richtung Zentrale. Melder 4 versucht deshalb als erstes, die Meldung zu Melder 2 zu schicken.

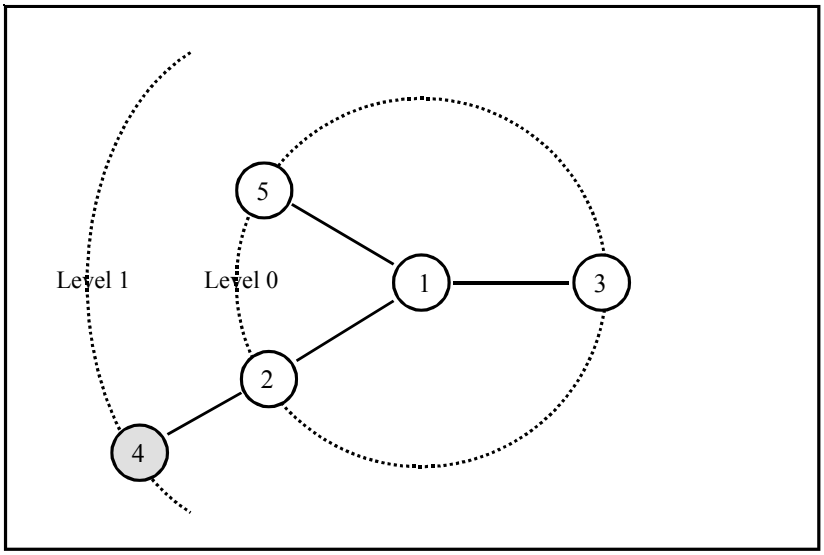

Bild 3: Beispiel für Routing

Im Beispiel ist der Weg zu Melder 2 aufgrund einer zeitweiligen Störung (verursacht durch Fadingeffekte) nicht verfügbar, dies bemerkt Melder 4 aufgrund der fehlenden Quittierung. Diese Störung des Übertragungsweges kann durch die Routingmechanismen ausgeglichen werden und führt dadurch nicht zu einer Systemstörung.

In Bild 4 wird das Verfahren deutlich. Der Melder 4 schickt einen Rundruf, ob andere Teilnehmer einspringen können. Es antwortet der ebenfalls in Reichweite von Melder 4 befindliche Teilnehmer 5.

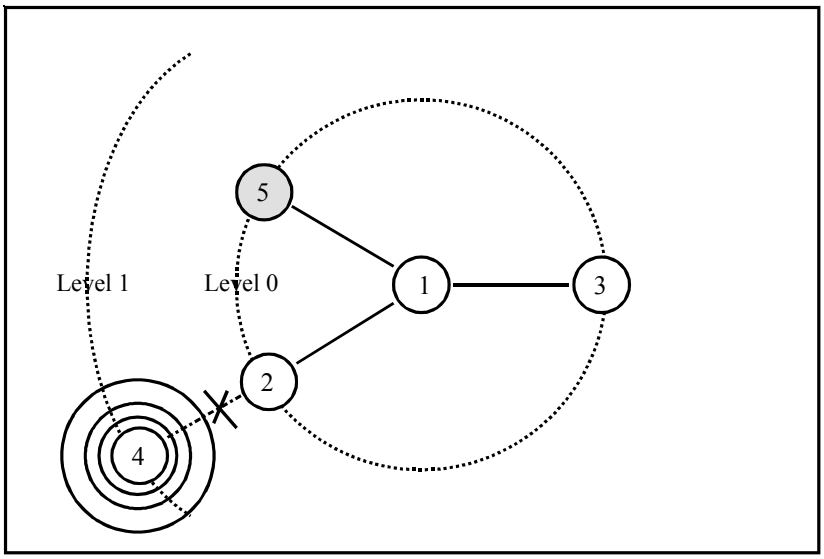

Bild 4: Reaktion auf Störung

Bild 5 zeigt, dass Melder 4 nun seine Nachricht über den neuen Weg erfolgreich absetzen kann. Durch die Quittierung der Nachricht ist sichergestellt, dass die Nachricht über den neuen Weg erfolgreich beim Empfänger angekommen ist. Melder 5 schickt die Alarmmeldung weiter in Richtung Zentrale, die den Empfang ebenfalls quittiert.

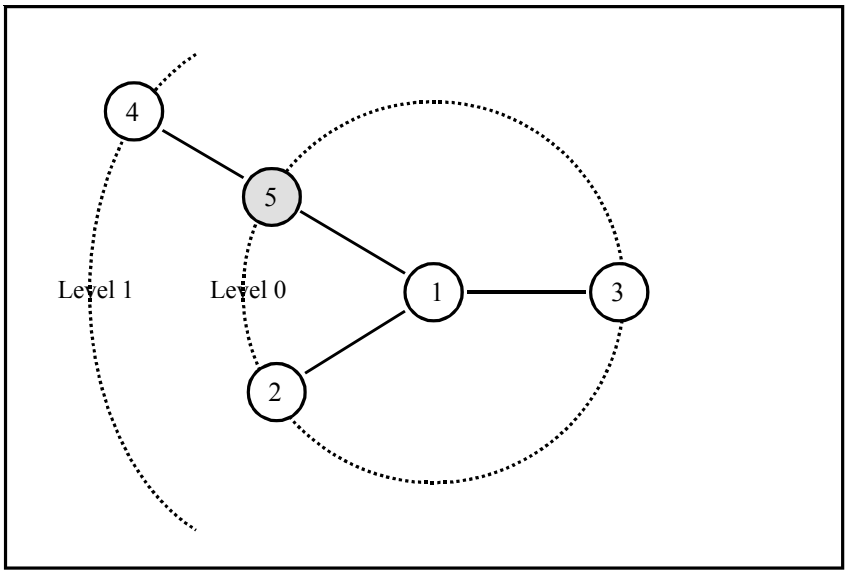

Bild 5: Nachricht wird über neuen Weg gesendet

Bei diesem Beispiel zeigt sich, wie wichtig ein bidirektionales Verfahren ist. Störungen können sofort erkannt werden, das Routing erlaubt eine sofortige Reaktion auf Störungen des Übertragungsweges, so dass keine Systemstörung entsteht. Dadurch erreicht man höchste Verfügbarkeit im Funksystem.

Zusammenfasssung

Durch bidirektionalen Funkbetrieb und intelligente Routingverfahren kann höchste Verfügbarkeit für die Funkmeldetechnik erreicht werden. Optimierte Algorithmen haben den Strombedarf soweit gesenkt, dass eine Batterielebensdauer über viele Jahre erreicht wird.

Durch den selbstroutenden Mechanismus ist eine einfachste Installation des Funksystems gegeben. Das bidirektionale Verfahren mit den Meldungsquittierungen und die Vorzüge des Routings gewährleisten höchste Sicherheit und gleichzeitig schnellste Übertragung der Daten im Funksystem.

Karlheinz Schreyer
Siemens Building Technologies Fire and Security Products GmbH & Co. oHG

The Radio Wave as a Transmission Medium in Modern Fire Alarm Systems

Abstract:
Radio waves can be used as a transmission medium in fire alarm systems in order to increase security. However, there are a number of factors that must be considered when designing the system. Because of their mutual dependency and repercussions, even the security experts involved find it difficult to gain perspective of the problem.

A detailed problem in relation to radio wave propagation is dealt with in the second part on the basis of empirical data, i.e. wave propagation in buildings. Despite a number of daring simplifications in evaluating fatigue tests, it appears that the attenuation of a radio wave during use can be controlled using suitable devices and procedures. This applies in particular for systems in the top technology class. On the other hand, however, the evidence suggests that a stable connection cannot be achieved if the attenuation reserve is inadequate. Responsible use of the technology is called for if fire alarm systems based on radio wave transmission are to operate reliably. Receivers with a sensitivity rate of less than –110 dBm should be used with care and should only be accepted if the overlying procedure has prominent features.

1. Einleitung

Maßnahmen sichern Übertragung

Sicherheit gab es auf der Welt noch nie zum Nulltarif. Die von allen angestrebte Geborgenheit bedeutet letztendlich Aufwand und kostet damit Geld. Aktuelle Beispiele sind die lebenserhaltenden Ausgaben im Gesundheitswesen, der Airbag im Auto, die Kosten der Feuerwehr usw. Auch die Sicherheit, die wir für unsere Brandmeldeanlagen reklamieren, muss und musste schon immer (vom Kunden) bezahlt werden.

Unsicherheiten bei Draht – Sicherheiten bei Funk

Trotz aller Aufwendungen bleibt bei jeder Technik ein Restrisiko. Das gilt für herkömmliche Übertragungswege genauso wie für drahtlose. Relative Stärken und Schwächen sind in Summe zwischen Draht und Funk gleichmäßig verteilt, bei Leibe aber nicht deckungsgleich. Es scheint, als habe bei den herkömmlichen Anlagen der Gewöhnungseffekt blind gemacht gegen seine Probleme. Ein Draht ist auf seiner ganzen Verlegungslänge durch energiereiche, parallel in kleinen Abständen geführte Leitungen zu beeinflussen. Eine in der Wand verlegte Leitung kann durch Unachtsamkeit durch eine simple Bohrmaschine unterbrochen werden. Schlampige Installation in den vielen Verteilern kann zu Wackelkontakten führen und Wassereinbruch in die Verteiler zu schleichenden Erdschlüssen und Oxidationen. Eine nachlässige Projektierung mag im Brandfall zuerst zu einem Leitungsausfall (mit einer undramatischen Störungsanzeige) führen, der in Folge eine Alarmierung verhindert.

Eine Funkverbindung kennt solche über lange Strecken verteilte Störungsquellen nicht. Sie sind höchstens punktförmig bei den Sendern und Empfängern zu beeinflussen. Dafür wird Funk von anderen Phänomenen tangiert. Einen Ansatz, wie die Sicherheit von Funkübertragung bewertet werden kann, wird im folgenden gegeben.

2. Einflussgrößen einer sicheren Übertragung über Funk

Rechtliche Vorschriften

Behörden regeln, wer einen bestimmten Teil des Spektrums benutzen darf und unter welchen Bedingungen.

Es ist nicht unüblich, ein und den selben Bereich des Spektrums mehrfach zu vergeben und unterschiedliche Grenzwerte (Bandbreite, Sendeleistung, Duty Cycle usw.) zu erlauben. Im Bereich um 433 MHz sind z.B. die Funkamateure mit bestimmten Nutzungsbedingungen aktiv. Während in einem Teilbereich des „Funkamateurbandes“ jeder beliebige Nutzer arbeiten darf, aber mit deutlich weniger Leistung und in Teilbereichen mit einer Duty Cycle Restriktion.

Andere Nutzer

Die Eignung eines Funkbandes für die Gefahrenmeldetechnik hängt ohne Zweifel von den zugelassenen Nutzern und den auf sie bezogenen Bedingungen ab. Bei ungleichen Bedingungen wird es schwierig. Ein schwächeres Gerät kann sich nicht gegen das stärkere durchsetzen. Selbst wenn der Starke wollte, kann er den weiter entfernten Schwachen nicht empfangen und wir ihn einfach überfahren.

Es gilt auch den Verkehr auf dem Funkkanal abzuschätzen um vorherzusagen ob es zu behindernden Kollisionen kommen wird. Reservierte Frequenzen helfen die eigene Übertragung sicherer zu machen.

Funkgeräte

Das Funkgerät und die im Folgenden beschriebene Prozedur ist die Antwort des Herstellers auf alle negativen Einflüsse. Dabei spielen die Empfindlichkeit, die Bandbreite und die Dynamik, das ist das Verhältnis eines starken Fremdträgers zum kleinsten in seiner Anwesenheit gerade noch empfangbaren Nutzpegels. Hilfreich ist darüber hinaus die Möglichkeit fremden Nutzern auszuweichen also Frequenzen zu wechseln.

Funkprozeduren

Sinnvolle Prozeduren und die Möglichkeiten auftretende Fehler im Telegramm zu korrigieren sind ebenfalls Mittel des Herstellers um negative Einflüsse zu minimieren.

Bewertung

Die Liste der Einflussgrößen auf eine Funkübertragung wird an dieser Stelle nicht weiter verfeinert. Es soll viel mehr gezeigt werden, dass sie ausreichen, die Eignung von Funkgeräten und Bändern für den Einsatz in Brandmeldeanlagen prinzipiell zu untersuchen. Dazu wurden sie in die Tabelle 1 eingetragen und mit Bewertungsgrenzen versehen. Die Einhaltung oder Überschreitung der Grenzen wird über ein Bonus-Malus-Verfahren bewertet. Das Ergebnis darf dann einen bestimmten Wert nicht überschreiten. Die Bonus- und Malus-Werte wurden bewusst nicht in die Tabelle aufgenommen, da sie

mit anderen Fachleuten noch nicht abgestimmt wurden. Ebenso sind die Bewertungsgrenzen bis zu einem gewissen Grade willkürlich.

Sogar mit Draht ausgeführte Übertragungswege können mit dieser Tabelle bewertet werden. Es sind dazu lediglich die Begriffe allgemeiner zu formulieren. Aus dem Übertragungskanal würde ein Adernpaar werden und dem Frequenzband entspräche das Kabel. Es wurden sogar sinnvolle Ergebnisse erzielt.

Auswahlkriterium	Grenzen	**Bonus/Malus**
Gibt es erlaubte Anwender mit größerer Reichweite im Band? -> Größte im Band zugelassenen Leistung / eigene Ausgangsleistung	P_{fremd} /P_{eigen}	t.b.d.
Gibt es erlaubte Nahstörer im Band? Wie viele eigene Kanäle darf ein fremder Nutzer gleichzeitig blockieren?	> 50 % 10 % bis 50 % < 10 %	t.b.d. t.b.d. t.b.d.
Ist ein Duty Cycle für alle Nutzer vorgeschrieben?	<= 1 <= 0,1 <= 0,01 <= 0,001	t.b.d. t.b.d. t.b.d. t.b.d.
Gibt es reservierte Alarmkanäle	Alarm allgemein Life safety	t.b.d. t.b.d.
Robustheit des Gerätes gegen andere Nutzer im gleichen Band (inband dynamic)	< 30 dB < 70 dB > 70 dB	t.b.d. t.b.d. t.b.d.
Robustheit gegen Nutzer außerhalb der eigenen Bänder (outband dynamic)	< 60 dB > 60 dB	t.b.d. t.b.d.
Kann das eigene Funkgerät Störern ausweichen und wie viele Kanäle stehen zur Verfügung?	1 < 6 > 6	t.b.d. t.b.d. t.b.d.
Kann das eigene Funkgerät auf andere Bänder oder Subbänder ausweichen?	Ja nein	t.b.d. t.b.d.

Tabelle 1

3. Der Wellencharakter und ihr Einfluss auf die Sicherheit der Übertragung

Der Wellencharakter der Funkausbreitung unterscheidet die drahtlose Übertragung von dem bisher Gewohnten. Deshalb wird im Folgenden untersucht, ob diese physikalische Basis geeignet ist, eine verlässliche Übertragung zu gewährleisten.

Ausbreitung über Wellen (anders als Licht)

Die Ausbreitung der Funkwellen wird gerne mit den beim Licht bekannten Phänomenen verglichen. Da es sich beim Licht ebenfalls um elektromagnetische Wellen handelt, liegt das nahe. Dabei ist aber das normale Umgebungslicht als nicht kohärente Strahlung als Beispiel nicht so gut geeignet, wie die kohärente Strahlung von Lasern. Überlagerungen und Auslöschungen sind nur hierbei zu erkennen.

Reflexionen und Überlagerungen

Ein Bild von den realen Verhältnissen in Gebäuden entwirft am besten die Vorstellung, dass alle Wände und Gegenstände halbdurchlässige Spiegel sind und die Strahlungsquelle kohärent ist. Zusätzlich sind Beugungseffekte an allen Gegenständen sowie Kanten zu berücksichtigen, da bei Frequenzen von über 100 MHz die Wellenlängen und Gegenstände in etwa in die gleiche Größenordung kommen.

Ergebnis der Überlagerungen an Beispielen aus der Literatur

Viele wissenschaftliche Veröffentlichungen und Untersuchungen beschäftigen sich mit Methoden zur Vorhersage der Wellenverteilung in Gebäuden. Bild 1 zeigt eine Simulation, wie sich eine Wellenfront ablöst und in einem Raum ausbreitet.

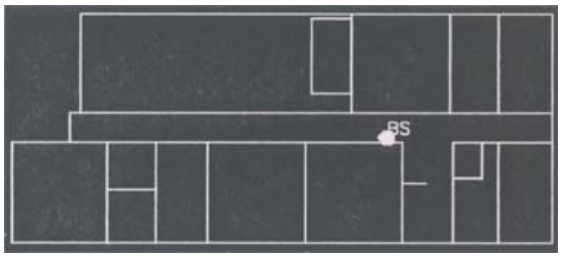

1 ns

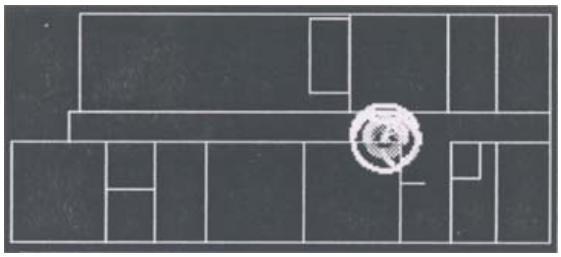

7 ns

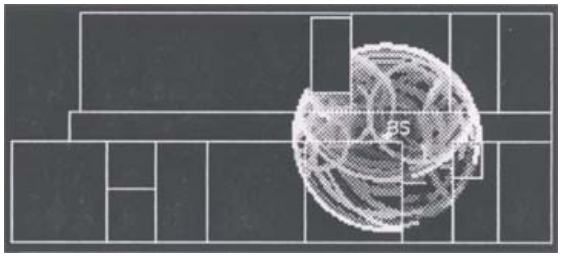

20 ns

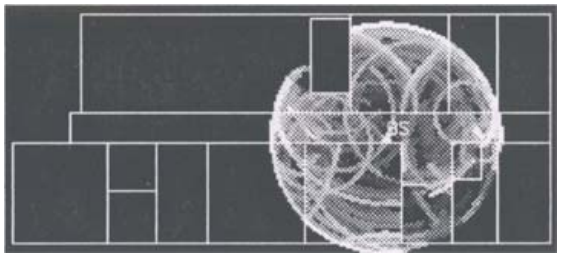

25 ns

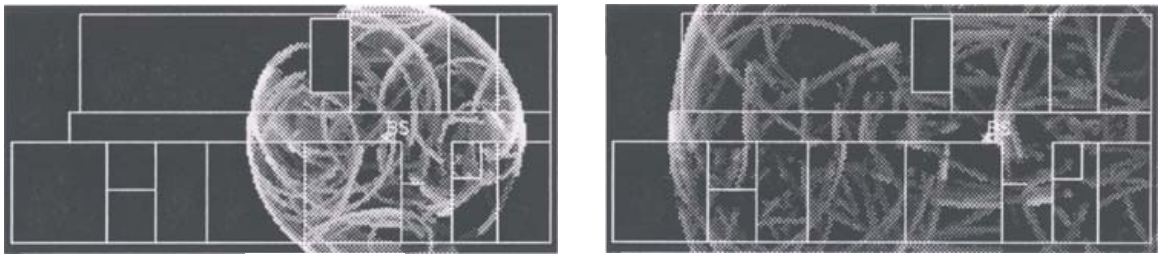

30 ns 70 ns

Bild 1 Wellenausbreitung, Quelle: RTH Aachen

Aufgrund zigfacher Überlagerungen bilden sich stehende Wellen mit unvorhersehbarer Amplituden- und Phasenverteilung.

Allerdings scheitern Simulationen jedes Mal beim Umsetzen in die Praxis, weil die für die Simulationen notwendigen Eingangsdaten fehlen. Bei realen Gebäuden kennt letztendlich niemand das Material der Wände, den genauen Verlauf von Leitungen in den Wänden oder den Ort von Schränken, Tischen und Blumentöpfen.

Im Folgenden werden deshalb die in Versuchen gewonnenen Messergebnisse diskutiert um die Phänomene zu studieren und Schlüsse für die Anwendung zu ziehen.

Für ETSI, dem europäischen Institut zur Normung auf dem Gebiet der Telekommunikation, untersuchte die Firma Bosch die Amplitudenverteilung in einem Flur in einem Abstand von 10 m zum Sender. Bild 2 wurde dem System reference document of protocols for short messages exchange (ETSI ERM-RP08(00)47 V0.0.3 (2000-03)) entnommen.

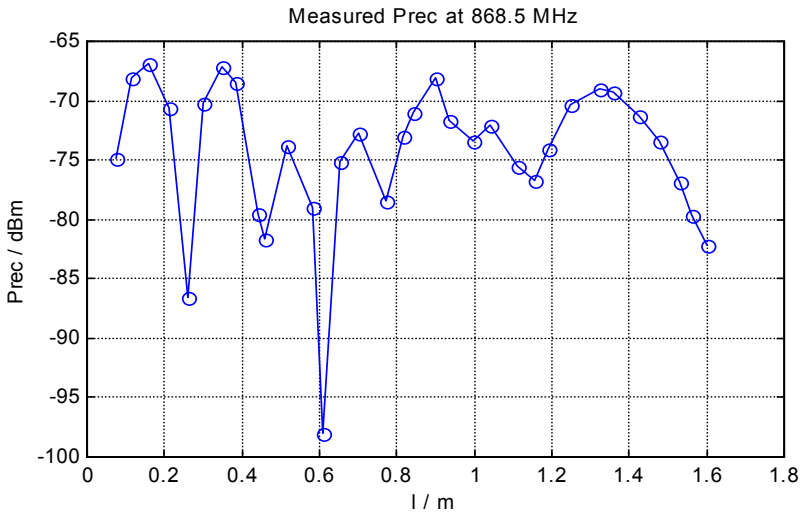

Bild 2

Die Größe der Amplitudenschwankung überrascht zuerst einmal den Betrachter. Die Streuung überstreicht einen Wertebereich von 30 dB. Das ist immerhin eine Variation der Energiedichte im Feld um Faktor 1000!

Solche Schwankungen sind beileibe kein Zufall. Aus der Technischen Kurzinformation Nr. 2/99 des Instituts für Rundfunktechnik ist das in Bild 3 gezeigte Spektrogramm entnommen.

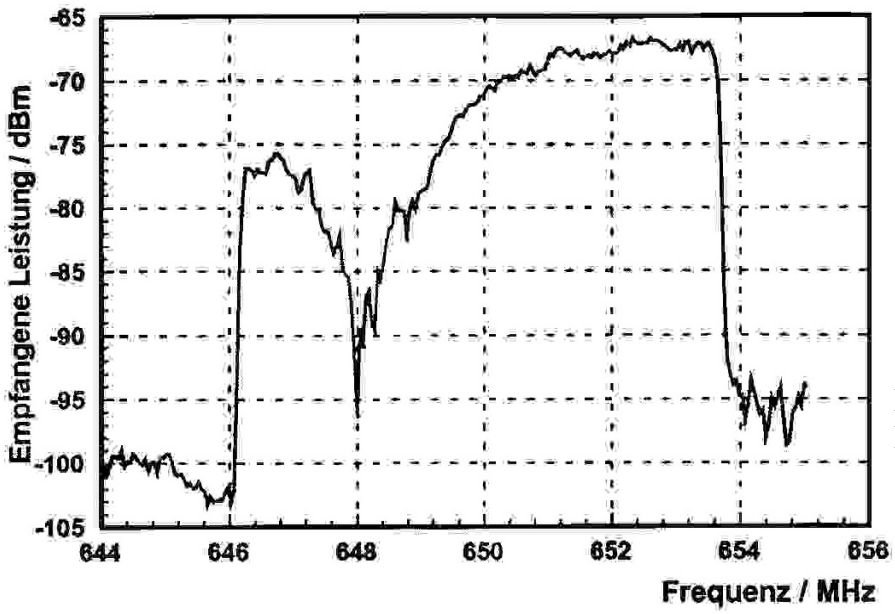

Raum
B 217

Bild 3

Untersucht wurden die spektralen Ausbreitungsbedingungen in einem normalen Gebäude. Der Einbruch der Feldstärke liegt ebenfalls bei 30 dB.

Testanlage

Bild 4

Um weiteres statistisches Material aus der Praxis zu sammeln, entschlossen wir uns vor Jahren zu einen Dauerversuch. Wir setzten dazu in 2 Funkzellen 30 Funkrauchmelder aus dem Brandmeldesystem SIGMASPACE ein. Sie wurden realitätsnah in dem in Bild 4 gezeigten Bürogebäude installiert.

Bild 5 zeigt die während ungefähr einer Woche gemessenen Pegel. Auch hier schwankt die Energie am Empfangsort um fast 30 dB.

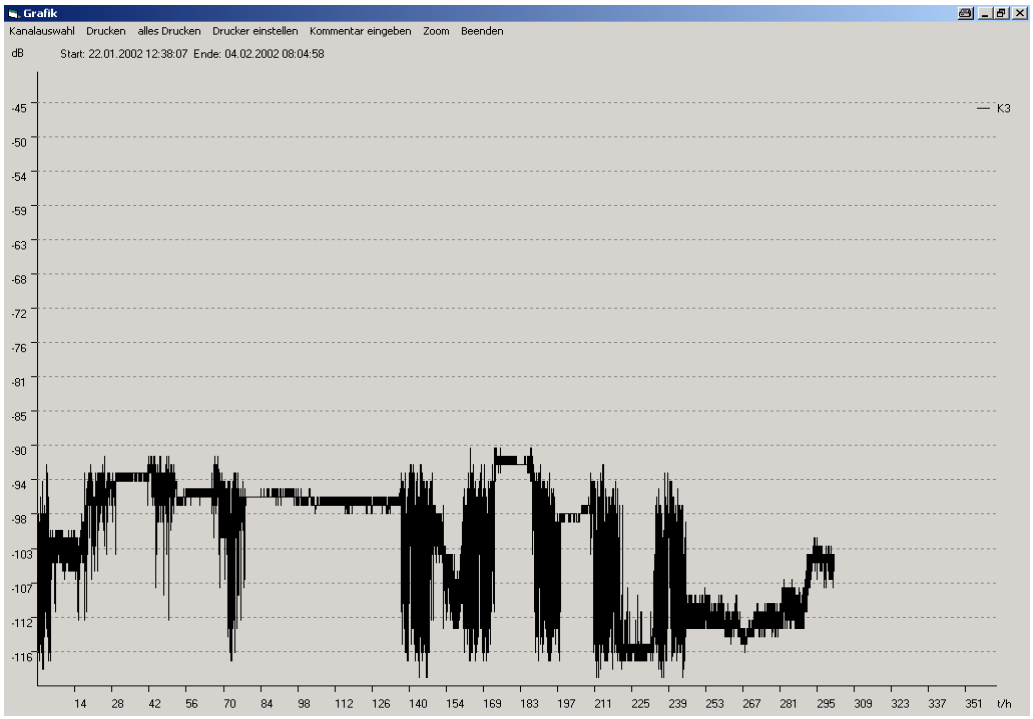

Bild 5

Klar erkenntlich auf dem Bild sind die Arbeitstage mit ihrem starken Auf und Ab, die Ruhe in den Nächten und an den Wochenenden (lange ruhige Phasen).

Die statistische Verteilung der Feldstärke über einen Zeitraum vom 21.11.01 bis 2.6.02 gibt Bild 6 wieder. Ihm liegt eine Datenbasis von mehr als 664 000 Messungen zugrunde. Die Auswertungen der anderen Melder des Dauerversuches liefern in etwa das gleiche Bild.

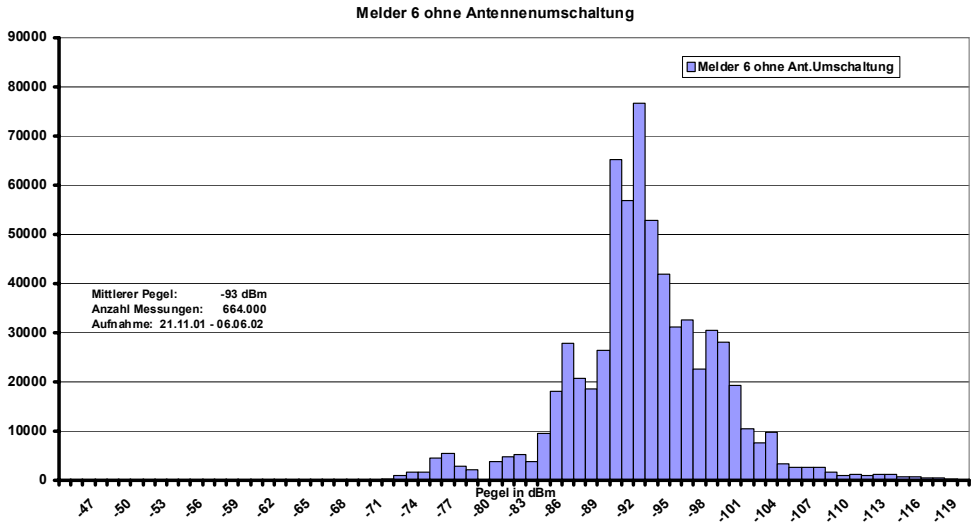

Bild 6

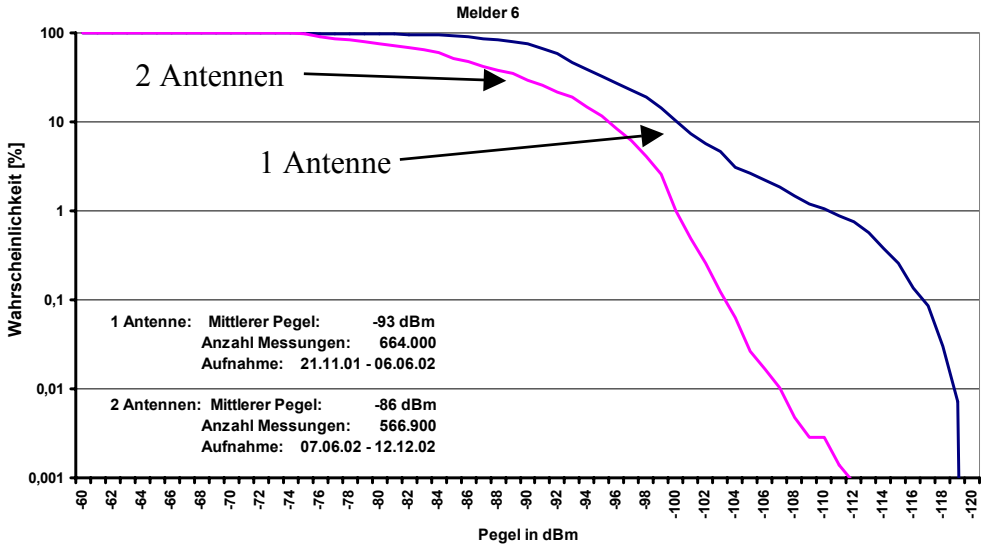

Bild 7

Die interessante Frage ist nun, ob bei diesen Pegelverhältnissen Störungen zu erwarten sind. Dazu betrachten wir das aus dem Datensatz des Melders 6 abgeleitete Bild 7 näher. Es gibt Auskunft darüber, wie die Wahrscheinlichkeit vergeblicher Übertragungsversuche steigt, wenn die Empfindlichkeit des Empfängers sinkt.

Die rechte Kurve zeigt die Verhältnisse eines Funkgerätes mit nur einer Antenne. Der „lineare“ Bereich lässt die Vereinfachung zu, dass eine Steigerung der Empfangsleistung um 11 dB, also von –100 dBm auf –111 dBm die Wahrscheinlichkeit eines Fehlversuchs von 10 % auf 1 % reduziert.

Die linke Kurve gibt Auskunft über die verlorenen Übertragungsversuche, wenn eine alternative Antenne zur Verfügung steht. Es fällt auf, dass sie steiler verläuft und

grundsätzlich tiefer liegt. Bei obigen Pegelwerten sinkt die Fehlerwahrscheinlichkeit von ungefähr 10^{-2} auf etwas weniger als 10^{-5}.

Man ist gut beraten erst nach mindestens drei erfolglosen Übertragungsversuchen am Bedienfeld eine Störung anzuzeigen. Am Beispiel von SIGMASPACE sind bis dahin knapp 100 Sekunden vergangen. Aus der Tabelle 2 ist die Restfehlerwahrscheinlichkeit zu entnehmen.

Melder 6			
Ohne Diversity Antenne, Mittelwert –93 dBm		Mit Diversity Antenne, Mittelwert –86 dBm	
Bei –100 dBm Empfindlichkeit	Bei –111 dBm Empfindlichkeit	Bei –100 dBm Empfindlichkeit	Bei –111 dBm Empfindlichkeit
Wahrscheinlichkeit einer Einzelstörung: 10^{-1}	Wahrscheinlichkeit einer Einzelstörung: 10^{-2}	Fehlerwahrscheinlich einer Einzelstörung: 10^{-2}	Fehlerwahrscheinlich einer Einzelstörung: 10^{-4} (extrapoliert)
Fehlerwahrscheinlich nach 3 Versuchen: **1 Störung alle 8,3 h**	Fehlerwahrscheinlich nach 3 Versuchen: **1 Störung alle 347 d**	Fehlerwahrscheinlich nach 3 Versuchen: **1 Störung alle 347 d**	Fehlerwahrscheinlich nach 3 Versuchen: **1 Störung alle 950 000 a**

Tabelle 2

4. Zusammenfassung

Trotz einiger gewagter Vereinfachungen bei der Auswertung der Dauerversuche zeigt sich, dass die betriebsmäßige Dämpfung einer Funkwelle durch geeignete Geräte und Prozeduren beherrscht werden kann. Das gilt besonders für Systeme der technologischen Spitzenklasse. Andererseits erkennt man aber auch, dass bei nicht ausreichender Dämpfungsreserve keine stabile Verbindung zu erreichen ist. Nur der verantwortungsvolle Umgang mit der Technologie ermöglicht einen verlässlichen Betrieb einer Funk-Brandmeldeanlage. Empfänger mit weniger als –110 dBm Empfindlichkeit sind mit Vorsicht zu betrachten und sollten nur akzeptiert werden, wenn die überlagerte Prozedur hervorstechende Eigenschaften aufweist.

Abschließend sei noch einmal betont, dass die Empfindlichkeit nicht die alleinige Grundlage einer sicheren Funkübertragung darstellt (siehe Tabelle 1).

Faouzi Derbel
Siemens Building Technologies Fire and Security Products GmbH Co. oHG
D-81679 Munich, Germany

ireless Communication for alarm systems ith Short Range Radio

Abstract

The integration of Wireless communication in alarm systems leads to the possibility to extend beyond buildings without external wiring on existing surfaces and to save enormous networking costs as well as to reduce business lost due to installation issues. Additionally wireless communication enables the easy adaptation up on changes of utilization. The wireless communication in security and safety applications needs to satisfy various different requirements in terms of reaction times with regard to alarm or disturbance recognition and transmission duration as well as in terms of physical issues such as interference handling, interruption handling, collision detection and handling.

This paper presents two types of wireless communications for alarm systems with short range radio for the industrial (SIGMASPACE) and the residential (SiRoute) markets depending on the posed requirements, especially regarding reaction times in case of alarms and disturbances.

The SIGMASPACE is designed as a hybrid system including many gateways on the wired communication bus and master slave communication fulfilling the EN54 Standards. The SiRoute system is based on a multi-hop mesh network that allows low battery power consumption, high ranges in buildings independently of structures and reaction times according to EN 50131-1. The wireless communication is performed in an exclusive frequency band for short range devices by 868 MHz with regulated effective radiated powers and transmission duration (Duty cycle).

1 Important Factors influencing the design of ireless alarm system design

The wireless alarm systems consist generally of wireless sensors and a base station or control panel and are characterized with many nodes or participants and with the air as transmission channel. This transmission channel is shared with other wireless systems. Therefore we have to take into account the wireless sensor and the transmission channel characteristics by investigating wireless alarm systems.

Wireless Sensors consists generally of the sensor element that is in contact with environment in order to detect events, a processor unit and a wireless device for the control and the transmission of the messages, and a power supply unit.

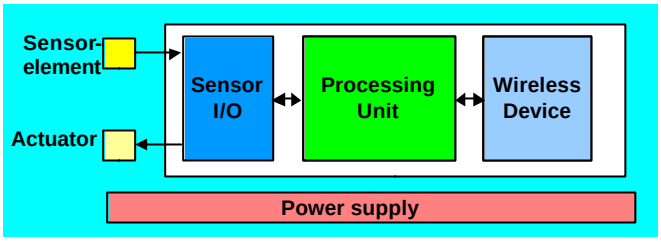

Fig. 1: Structure of a wireless sensor [1]

1.1 Energy consumption

The wireless sensor element is normally battery powered. Battery life times of about 3–5 years are generally required; therefore it is very important to investigate the power consumption issue. Power consumption can be divided in three domains: sensing, data processing and communication. Of the three domains, a sensor node expends maximum energy in data communication [2]. Because of the power consumption of the transceiver in active mode is much greater than in standby, the wireless sensor must operate its transceiver in a low duty cycle mode. Simultaneously and especially in case of alarms in security and safety applications, the wireless system has to forward alarm messages in a very short time of about 10s. Additionally the system has to transmit periodically alive messages in order to recognize disturbances in the transmission paths as well as in the sensor itself. This contradiction makes the development of wireless sensors in security and safety applications a challenge.

In order to show the importance of taking care about energy consumption of the communication part in wireless sensor networks, assuming we have a peer to peer connection, and the communication links are symmetrical (equal time is spent for transmitting and receiving), to meet a 1-year battery life time with a battery with 750-mAh, the average current drain of

$$\frac{750\,\text{mAh}}{8760\,\text{h}} \quad 86 \quad \text{A}$$

is required for the communication [3].

The average current drain can be calculated as follows:

(1)

with

= Fraction of time either receiver or transmitter is on,

= Current of transmitting or receiving,

= Current where the transmitter or receiver are of, but sensor works.

Under the assumption that the 19,5 , 30 and 86 the

0,0029 or 0,29%.

That means during 3600s, the transceiver has only a total time of 10,44 s to transmit messages to other wireless sensors or control panels.

1 a e propagation in Buildings

Effects of multiple path scattering due to reflection, diffraction and attenuation dominate the propagation of radio waves between the transmitter and the receiver inside buildings. The field strength by the receiver is the sum of the superimposed waves. Therefore, the materials and the construction of a building (walls, ceilings etc.) are decisive for the achievable range. Table I shows the attenuation of some possible obstacles.

Table 1: Relation of attenuation and materials 4

Room divider	Very low	1 dB
Dry tiles	Concrete low	6 dB
Chalky sandstone	Moderate	8 dB
Chalky sandstone planar Elements	Moderate	8 dB
Wooden board wall	Moderate	8 dB
Wet tiles moderate	A few dB	10 dB
Coated plasterboard (double wall)	High	15 dB
Reinforced	Concrete high	30 dB
Thick, wet tiled wall	Very high	40 dB

Fig. 2 shows the multi-path scattering effects of the wave propagation in buildings. Waves propagate to the destination; they will be reflected on walls and conducted to the destination. The flatter the falling angle the better the reflection factor is. Depend-

ing on the features of the walls or obstacles, a part of the wave is attenuated and the other part accesses to other rooms in the building.

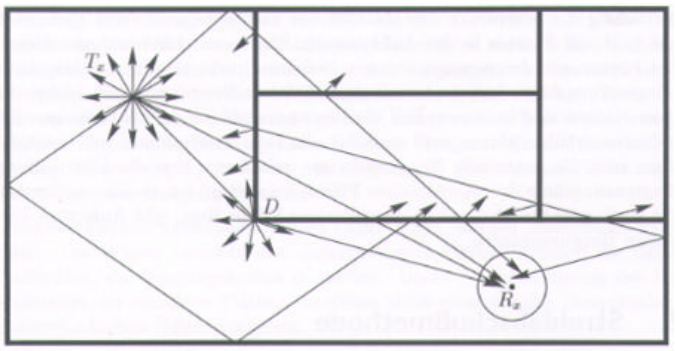

Fig. 2: Multi-path scattering [5]

The wave parts will be superimposed at the receiver location and depending on the phase states this lead to amplification or to fading of the signal. The more the transmitter is far from the receiver the more multi-path scattering takes place and the more fading problems occur.

The observation of the field strength of a wireless detector over many days shows that the field strength can vary up to 30 dB, that is up to factor 1000. This variation has been confirmed in the literature [6]. This can be explained by moving persons and vehicles, or just by opening or closing doors.

1 Interferences

Frequency bands belong to rare resources, therefore different wireless systems have to share these frequency bands, this leads to collisions and interferences. Therefore the wireless systems designer has to consider these troubles and reach good filtering features of the wanted signal as well as good values in terms of adjacent channel selectivity (ACS). The ACS is defined as the ability to demodulate a received signal at the sensitivity limit, with the presence of a sine component in the adjacent channel [7]. Typical requirements for ACS are 50 to 70 dB.

Re uirements on ireless systems

Due to the mentioned and expected effects that influence the transmission quality of the messages, the radio modules have to posses a high sensitivity in the range of -110 dBm. Additionally the installation of wireless devices should be done under the consideration of a fading margin of about 30 dB. Therefore it is advantageous to have a

high link budget to allow that. Fig. 3 shows some possibilities to fulfil the requirements on wireless systems.

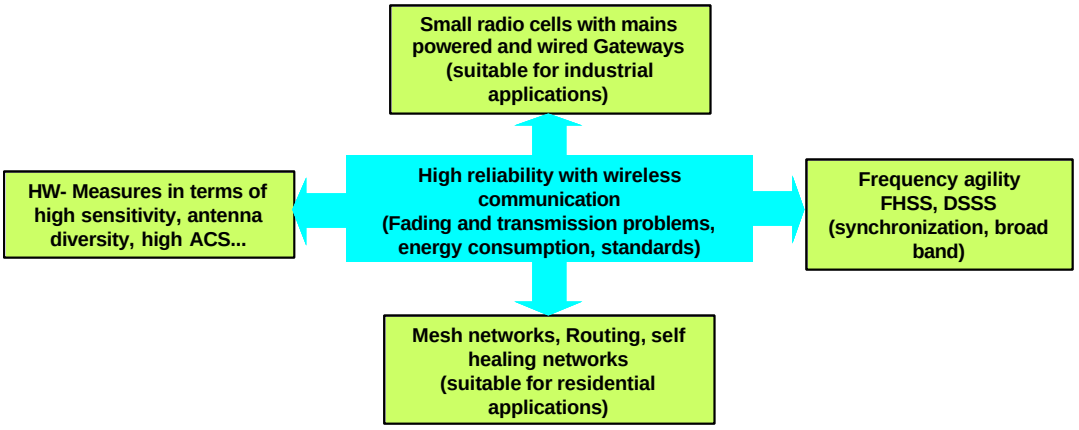

Fig. 3: Possibilities to fulfil the requirements on wireless systems

On the basis of studies in our laboratories an improvement of sensitivity of around 3 dB can lead to reducing the BER (bit error rate) by factor 10. In order to avoid Fading problems, it is recommended to change polarization by introducing antenna diversity for the arriving electromagnetic waves, According to our own experiences the antenna diversity leads to an improvement of the BER by approximately factor 100, which is very important for the reliability of the radio system.

Another way to deal with effects that influence the transmission reliability of wireless systems is the deployment of the spread spectrum technology. This technology is characterized with much higher bandwidth occupancy of the transmitted signal than in systems using conventional modulation. We distinguish between FHSS (Frequency Hopping Spread Spectrum) and DSSS (Direct Sequence Spread Spectrum). By FHSS the carrier frequently hops on predetermined sequence to avoid interfering signals and new frequencies are generated with pseudo random pattern. The advantages of FHSS are that Fading and disturbances are only available for short time period and can be arranged to avoid portions of spectrum, which is strong occupied by other systems. The disadvantages are related to the synchronization and the susceptibility to narrow band interference, collisions for short periods are also possible.

By DSSS the data signal is spread onto a much larger range of frequencies using a specific coding scheme, DSSS signal has a high redundancy factor and suitable for avoiding fading problems, is more difficult to intercept since the signal is hard to distinguish

from background noise and can be used in combination with existing narrowband. The disadvantages are related to the long acquisition time due to long chip sequences.

The third measure to avoid transmission problems is to introduce a network with routing possibilities. If transmission troubles occur with one route the network should be able to find out a new alternative route with respect to the requirements in terms of reaction times. This approach allows the possibility to realize a pure wireless system.

1 Re uirements of the residential market

The residential market requires autonomous alarm systems that are low priced and offer an all around protection of buildings and persons. In terms of HW-requirements the transceiver should be low cost and therefore do not offer a high sensitivity or high dynamic range etc., lifetime of about 2 years is acceptable. The reaction time of the control panel in case of disturbances due to message miss transmission or sensor problems can be also defined as 4 h (similar to EN 50131-1), The alarm transmission to the control panel has to be in the range of 10 s.

The network architecture in residential applications should be mesh. A hybrid architecture 4 with wired gateways is not acceptable due to costs related to wiring the system. Additionally the use of repeaters 8 is not advantageous, the repeaters are generally mains powered and have to be planned in the right way and mostly independent of the placement of mains access points. Therefore each device must be able to operate as a router in order to forward the messages of its neighbour.

Reali ation

1 Residential Market

Low priced devices can be reached by introducing standards like Bluetooth, WLAN, KonnexRF, igBee, etc. It is therefore advantageous to examine the suitability of these standards for the considered application. The required batteries life times leads to the deplo yment of wireless technologies with minimal power consumption. The desired wireless alarm system consists generally of sensors and actuators; the bit rate is therefore generally low. Bluetooth or WLAN are therefore not suitable for the desired application. The KonnexRF standard is only suitable for small home installations deploying

repeaters, which are mains powered. igBee is a new wireless standard for low data rate radio devices in different target markets, for instance monitoring, automation, personal healthcare, HVAC, and lighting. The standardization of igBee is in process and is advantageous for interoperability between radio devices of different manufacturers.

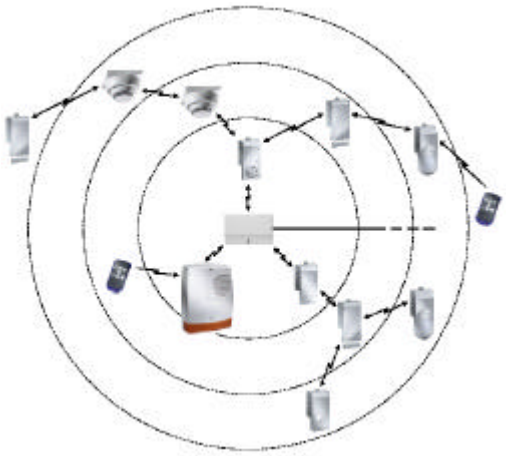

Fig. 4: SiRoute System

For residential applications we suggest the SiRoute system, s. Fig. 4. The SiRoute system is a pure wireless system with a radio cell, that can handle 50 battery-powered devices as a multi hop mesh wireless sensor network with a smart routing procedure. The SiRoute system communicates in the frequency bands by 868 MHz and 915 MHz for the US-Market. The receiver bandwidth is 150 KHz in order to minimize the interference with other low cost wireless systems with bandwidths of about 600 KHz. The sensitivity of the wireless device is in the range of –95 dBm and the ERP (Effective radiated power) is 10 mW. Alarms can be transmitted within 10s and disturbances can be detected within 4h in relation to the EN 50131-1. The battery lifetime is estimated to be 3 years.

1 1 Smart Routing protocol in SiRoute

Protocols in the area of wireless sensor networks represent an active area for many research and development organizations. Protocols in this category includes for instance the destination-sequenced distance vector DSDV protocol, the temporally ordered routing algorithm TORA, which is suitable for big networks with mobility issues, and the global state routing GSR. These protocols have been developed under the assumption that the wireless nodes are mobile 3 .

The DSDV protocol tries to produce an image of the current whole net topology and stores this in one or more tables. Each node stores the distance from all and for all known destinations in a table. DSDV data processing procedure is based on the shortest way. The DSDV protocol is only suitable for small networks. As an improvement the AODV (Ad-Hoc On-Demand Distance Vector Routing protocol) has been introduced. In this protocol only information about neighbours are maintained (local state information). Only the way to the destination is calculated or determined. The number of hops or transmissions to the destination is optimized.

Another important routing protocol is the GRad protocol 9 . This protocol belongs to the category of on-demand routing protocols, in which routes are established only when nodes wish to communicate with one another; no attempt is made to maintain state when there is no data to send. A node desiring to send a message, simply broadcasts the message, along the nodes, which allow a minimization of cost value to the destination. Of all neighbouring nodes receiving the broadcast, only those that can deliver the message at lower cost than the stated cost value will forward the message. All other nodes will simply ignore the message. The message slides down a cost gradient to the destination. GRaD requires a cost value for every potential destination in the network, for large networks this can be a significant storage problem.

The described routing mechanisms are not suitable for the required features for alarm systems in the residential market. A group of them store the routes in big routing tables and are not suitable for low priced wireless devices with small storage capacities. The others are not suitable for battery-powered devices; they are designed for mains powered devices or network coordinators

A new routing mechanism has been developed for the alarm systems in residential applications. The routing protocol in SiRoute is proactive and table driven. Every participant disposes a Routing table in which the communication partners to reach the master are listed. The hop number gives the number of the communication level, which is required to reach the master. At the setup process, a participant determines which other participants are attainable and which can route the messages to the master. The optimization process to choose the suitable partner takes into account the communication level as well as the quality of the radio reception. The system can manage uni- as well as bidirectional messages. By receiving a message, the radio partner compares the

number of the communication levels of the transmitter to its own and tries to forward the message to the radio partner with lower communication level.
The communication between radio partners or nodes is regulated with an announcement message, which is broadcasted. The radio partners hear periodically in order to detect messages. The radio partner confirms the transmission with an acknowledgement.
With this mechanism it is possible to save energy from batteries by taking into account only the partners that can optimize the routing process and therefore a small routing table is required.

Reali ation for the industrial Market

For the industrial market the SIGMASPACE product range has been developed as a wireless system that enjoys the VdS-Approval in Germany fulfilling the EN54 standards 5 . The SIGMASPACE is a hybrid system, the control panel communicates with the wireless detectors via gateways. Each gateway can handle up to 30 devices. The radio module in SIGMASPACE possesses two antennas, which are orthogonal to each other and a transceiver with –115 dBm sensitivity. The ERP is 5 mW. Each alarm will be transmitted within 10 s to the control panel and disturbances will be signalized within 100 s. The detector power supply is realized with two batteries in order to reach a lifetime of about 6-7 years. A High reliability and resistance to interference has been realized with a 25 kHz narrow-band receiver. With this receiver the exclusive alarm channels in the frequency band by 868 MHz can be used. SW-mechanisms such as channel allocation checking by commissioning and telegram routing over neighbours are also implemented in order to reach a reliable transmission. The wireless system is based on a bi-directional radio transmission. The system integrity is tested every 30 s to quickly recognize transmission disturbances.

Summary

Wireless communication for alarm systems in building needs to satisfy many requirements with regard to network topology, reaction times in case of alarms or disturbances transmission and especially to the reliability of the wireless transmission by considering the physical effects that can occur, for instance the fading of the electromagnetic waves and interferences with other systems in the same frequency band.

For the residential market a new wireless technology named SiRoute has been developed allowing the installation of autonomous wireless systems with transmission procedures that leads to high communications range in buildings independently of the structure and the propagation characteristics. The SiRoute wireless system is based on multi hop networks with wireless sensors that can reach 3 years battery lifetime.

For the industrial market, the SIGMASPACE wireless system has been developed with strict requirements with regard to reaction times and battery lifetime. Alarms can be transmitted within 10s and disturbances can be recognized within 100s. SIGMASPACE offers HW- and SW mechanisms in order to enhance the communication reliability and fulfil the EN54 standards..

References

1 F. Golatowski: lecture Hardwarenahe Programmierung; Institut für angewandte Mikroelektronik, Universität Rostock.

2 I. F. Akyildiz, W. Su, Y. Sankarasubramaniam, E. Cayirci: Wireless Sensor networks, a survey; Computer Networks 38 (2002) 393-422 ; Elsevier

3 Edgar H., Callaway, Jr.: Wireless Sensor Networks; Auerbach Publications, ISBN 0-8493-1823-8

4 SIGMASPACE Radio Smoke Detector, Product publication

5 T. Schüberl: Polarimetrische Modellierung der elektromagnetischen Wellenausbreitung in pikozellularen Funknetzen; Shaker Verlag 1997; ISBN 3-8265-3098-5

6 LPRA Radio Design Course, Radio Solutions 2002, London 2002

7 Frank Karlsen: Guidelines to low cost wireless system design; Wireless 2001, Munich Germany

8 Penczynski, P.: Home Automation in Europe; Intelligent Living Conference Nov. 97, Hannover, Germany

9 Robert D. Poor: Gradient Routing in Ad Hoc Networks; Media Laboratory, Massachusetts Institute of Technology Cambridge

Thomas Kaiser
Universität Duisburg-Essen, Duisburg, Germany
Jianliang Shi
Fraunhofer Institute for Microelectronic Circuits and Systems, Duisburg, Germany
Nima Tavangaran, Ingolf Willms
Universität Duisburg-Essen, Duisburg, Germany

A Comparison of ZigBee/802.15.4 vs. Ultra-Wideband Transmission Techniques for Wireless Fire and Intrusion Detectors

Abstract

Recently, wireless sensor networking has been becoming a disruptive technology in such fields as industrial control and monitoring, building automation and security, automotive sensing. The motivation for use of wireless technology includes the reduction of installation cost, the avoidance of the "last meter connectivity problem" and intelligent maintenance. Many types of wireless sensors, for example fire and intrusion detectors, are based on proprietary solutions, which are uncomfortable for the customer because of lack of product interoperability and vendor dependence. On the other hand, the lack of standardized technologies that can address the requirements both at the application level and from the communication point of view has become the hurdle of the widespread of wireless sensor systems.

The above constraints suggest the necessity of an open global standard to enable the cost-effective, reliable wireless monitoring and control products. The recently finished IEEE 802.15.4 standard and the corresponding undergoing Zigbee standard represent the achievements of the efforts addressing these kinds of requirements. Zigbee/802.15.4 operates at 868/915MHz, or 2.4GHz and belongs to classical *narrowband* transmission systems. An entire opposite transmission approach is based on extremely low power signals with ultra-wide bandwidth (UWB). UWB belongs to the few wireless key emerging technologies and is under intense discussion for various areas of applications, e.g. highest data rates in the order of several hundred MBit/s for indoor communications, ranging and positioning with accuracy in the sub-centimeter range, and recently also for low power and low data rate applications.

Aim of this contribution is to compare narrowband vs. ultrawideband transmission with special emphasis on wireless fire and intrusion detector networks.

Introduction

The Zigbee/802.15.4 standards, with such features as ultra low complexity, ultra low power and low bit rate, are ideally suited for wireless fire and intrusion detectors. Numerous wireless fire and intrusion detectors are based on proprietary solutions, which are uncomfortable for the customer because of lack of product interoperability and vendor dependence. From this point of view ZigBee seems to be the right choice in order to serve future market demands. On the other hand, in early 2004 the Institute of Electrical and Electronics Engineers (IEEE) 802.15 Working Group voted to form a new study group to investigate amendment to 802.15.4 for an alternative physical layer with additional features like precision ranging/location capability, high aggregate throughput, scalable data rates, and extremely low power consumption. All the features can be principally achieved with Ultra-Wideband Technology.

The aim of this contribution is to shed some light on the pros and cons of Zigbee vs. UWB with emphasis on their application for wireless fire and intrusion detectors. For example, because ZigBee is a conventional narrowband technique operating with a carrier frequency of either 2.4 GHz (Global), 915 MHz (North American) or 868 MHz (Europe) it suffers from other narrowband interferences as well as the known fading phenomenon. In contrast, UWB may not only mitigate narrowband interferers simply by notch filtering or other advanced signal processing techniques, but also mitigates fading by non-destructive impulsive transmission. For both approaches, the very low duty cycle guarantees low power consumption and co-existence, but the lack of severe fading in UWB transmission may result in a reduced path loss and consequently in a larger coverage. However, according to current American regularization, UWB systems are allowed to operate mainly in the frequency range between 3.1 GHz and 10.6 GHz with a maximum power spectral density of -41.25 dBm/MHz, resulting in a maximum transmit power of less than 0dBm. Compared to Zigbee, this higher frequency range causes additional attenuation by walls and other obstacles and therefore limits the coverage gain. In turn, due to long spreading sequences, UWB devices can principally be designed to work below the noise floor so that jamming becomes extremely difficult.

Such a property is beneficial especially for intrusion detectors. Note also the pulse duration in the sub-nanosecond range providing a fine time resolution and enabling precise ranging with centimeter resolution. All these facts open the question whether UWB represents a valuable alternative to standardized narrowband transmission systems. The following section summarizes the properties of UWB whereas the next section deals about Zigbee/802.15.4. Then, the individual link budgets are calculated and compared for different carrier frequencies, typical data rates in wireless fire and intrusion detectors, and bandwidths in order to allow a quantitative comparison. A conclusion and an outlook finalize this contribution.

The Ultra-Wideband Approach

Ultra-wideband systems are considered as systems that are operating with a large absolute bandwidth of more than 500 MHz. Using a large bandwidth in UWB systems provide us with several possibilities and advantages compared to other narrowband systems. First, the spectral density of the transmit signal can be made rather small and consequently the probability of interference to narrowband systems is greatly reduced. Immunity to narrowband interference, mitigating fading, high data rate and a better propagation in different environments are among other advantages of UWB systems [1]. In February 2002, the American Federal Communication Commissions (FCC) issued its first report and order on UWB technology, thereby providing regulations to support deployment of UWB radio systems. After that, a great deal of efforts and money has been invested in finding solutions for implementation of this technology in practice.

Modulation

The most popular current modulation schemes are Pulse-Position Modulation (PPM), Pulse-Amplitude Modulation (PAM) and Orthogonal Frequency Division Multiplex (OFDM), whereas the extensions Direct Sequence (DS) and Time Hopping (TH) enable multiple accesses to the common transmission medium.

PPM encodes the data through different positions in time and PAM encodes the data through signal amplitudes. TH assigns to multiple different codes, where the codes in turn represent a particular pattern in a series of pulses per transmitted bit, i.e. the transmitted signal in time hopping is represented by

$$s_{tr}(t) = \sum_{i=-\infty}^{\infty} a_{\lfloor i/N_f \rfloor} x_{tr}(t - iT_f - c_i T_c),$$

where $x_{tr}(t)$ is the transmitted pulse, T_f the frame duration, T_c pulse duration or chip interval, N_f the number of pulses representing a single bit, c_i the periodical code word for each user and finally $a_{\lfloor i/N_f \rfloor} = \pm 1$ represents the binary information hidden in the pulse train and $\lfloor \ \rfloor$ is the floor operator giving the largest integer smaller than or equal to its argument. The transmitted pulse is often simplified as a Gaussian mono-pulse

$$x_{tr}(t) = k\left[(t - T_c)/\tau\right] e^{-\left[(t-T_c)/\tau\right]^2},$$

where k is a normalizing factor and τ is the monocycle's duration. One way to satisfy the FCC-mask requirements is taking derivatives of $x_{tr}(t)$ and adequately adjusting the center frequency. In UWB-OFDM, the regulated frequency band is divided into several sub-bands with individual bandwidth of 500 MHz and sub-dividing each sub-band into 128 tones, each with a bandwidth of approx. 4 MHz. UWB-OFDM permits adaptive selection of sub-bands in order to fulfill regional regulations requirements or for reasons of co-existence.

The Zigbee/802.15.4 Standard

The purpose of *IEEE 802.15.4* is to provide a standard for ultra low complexity, ultra low cost, ultra low power consumption and low data rate wireless connectivity devices. It defines a standard for a Low Rate Wireless Personal Area Network (LR_WPAN) working in the industrial, scientific, and medical (ISM) bands. The scope of the standard is to define the physical layer (PHY) and medium access control (MAC) sublayer specifications for low data rate wireless connectivity with fixed, portable, and moving devices with no battery or very limited battery consumption requirements typically operating in the personal operating space (POS) of 10m [2].*ZigBee* is an alliance of semiconductor manufacturers, technology providers, and OEM's dedicated to providing the upper layers of the protocol stack (from network to application, including application profiles) atop the IEEE 802.15.4 PHY and MAC layers [4]. The ZigBee protocol together with IEEE 802.15.4 standard provides an open standard for low-power wireless networking of monitoring and control devices.

Highlights of IEEE 802.15.4 standard

As noted before, the goal of IEEE 802.15.4 standard is to provide '4- (ultra) low' reliable wireless connectivity. This section presents some unique features of the standard that enable the performance vision to be met. First of all, IEEE 802.15.4 standard works in ISM band and its service involves little or no infrastructure. This feature allows power-efficient, inexpensive solutions to be implemented for a wide range of devices. Other notable features of the standard will be described as follows.

Modulation and related features

IEEE 802.15.4 provides two PHY options: one for 868/915 MHz bands, and the other for 2.4 GHz band. The 868 MHz band is available in most European countries; the 915 MHz band is available in North America, and the 2.4GHz band is available in most countries worldwide. Table 1 summarizes the modulation formats of different frequencies. As is shown in Table 1, both PHYs use direct sequence spread spectrum (DSSS) methods, which results in low-cost IC implementation via largely digital circuits. Data modulation schemes are simple raised-cosine-shaped BPSK for 868/915 MHz PHY, and half-sine-shaped O-QPSK in the 2.4GHz PHY. Each of these modulation schemes maintains a peak-to-average carrier power ratio of one, which minimizes both power consumption and implementation complexity [3].

PHY (MHz)	Freq. band (MHz)	Spreading parameters		Data parameters			Amount of channel
		Chip rate (kchip/s)	Modulation	Bit rate (kb/s)	Symbol rate (symbols /s)	Symbols	
868/ 915	868-868.6	300	BPSK	20	20	Binary	1
	902-928	600	BPSK	40	40	Binary	10
2450	2400-2483.5	2000	O-QPSK	250	62.5	16-ary ortho-gonal	16

Table 1 Frequency bands and data rates

Further, the 868 and 915MHz bands are considered close enough in frequency that similar, if not identical, hardware can be used for both, lowing the implementation costs

[5]; the 2.4GHz PHY supports 16 channels in an 83.5MHz bandwidth, which means a channel spacing of 5MHz, and this greatly eases the transmit and receiver filter requirements.

Coexistence features

IEEE 802.15.4 standard provides several mechanisms that enhance coexistence with other wireless devices operating in the same frequency band, among them, channel selection/ access and its supporting functions, low transmit power, low duty cycle, modulation and channel alignment are notable mechanisms. The ability to detect channel occupancy and perform dynamic channel selection is an important mechanism for coexistence. The IEEE 802.15.4 MAC layer includes a scan function, which, when performing dynamic channel selection, either at network initialization or in response to an outage, will scan a set of predefined channels. PHY layers, on the other hand, contain several lower-level functions, such as receiver energy detection (ED), link quality indication (LQI), and channel switching, which make the channel relocation possible. The mechanisms provided by both PHY layer and MAC layer are intended for use as part of a channel selection algorithm at the network layer.

IEEE 802.15.4 PHYs provide the capability to perform clear channel assessment (CCA) in its CSMA-CA mechanism. The CCA is based on: ED over a threshold, detection of IEEE 802.15.4 packet, or both. Use of the ED option improves coexistence by allowing transmission backoff if the channel is occupied by any device using any protocol. Among other coexistence features, low duty cycle (under 1%) obviously will make the devices less likely to cause interference to other standards; the operating power of IEEE 802.15.4 devices are expected to be between –3 and 10dBm, with 0 dBm being typical. This is much less than other kind of devices and therefore will cause less interference. The use of DSSS not only improves the performance of the receiver by reducing the impact of interference from other kind of devices, but also causes less interference to others.

Low power consumption features

In many applications that use IEEE802.15.4 standard, the devices will be battery powered where their replacement or recharging in relatively short intervals is

impractical; therefore the power consumption is of significant concern. This standard was developed with the limited power supply availability in mind. The protocol has been developed to favor battery-powered devices. The PHY layer of the IEEE 802.15.4 standard provides numerous features which enable the low active power consumption, for example, DSSS, constant envelope modulation, no duplex operation, etc [6].

Although the specification has been designed to minimize the active power consumption of compliant devices, it is impossible to reach the goal of at least a few months' of operation with a single battery by reducing the active power alone. Most first-generation IEEE 802.15.4 chips will consume 20–30 mA from a 2 V supply (40–60 mW) while active, which indicates that low power consumption is achieved largely by low-duty-cycle operation. To support low duty cycles, the IEEE 802.15.4 MAC layer enables beacon packet being as short as 544us in 2.4GHz band, while the superframe period may be extended from 15.36ms to over four minutes. This results in a duty cycle that may be set from 2.3% to 2.16 ppm[3]. Furthermore, non-beacon mode enables a device to remain in a standby mode indefinitely unless otherwise to satisfy the regulatory requirements. Another MAC layer power saving feature includes 'battery life extension (BLE)' mode, in which the CSMA-CA backoff exponent is limited to range 0-2. This greatly reduces receiver duty cycle in low offered traffic applications.

A Link Budget Based Quantitative Comparison

A quantitative comparison between UWB and ZigBee link budgets gives us a better insight on the applicability of each system for wireless low power and low data rate systems. First of all we consider the UWB frequency range 3.1 GHz - 10.6 GHz and compare the link-budgets for both systems. Then, we alternatively investigate the UWB frequency range 0.5 GHz - 1 GHz while being aware of potential interferers like GSM or TV signals.

Table 2 shows a quantitative comparison of UWB and ZigBee link budgets with a tentative throughput of 2400bps where the whole bandwidth between 3.1 GHZ and 10.6 GHz for UWB is taken into account. Note that the pathloss coefficient is more or less dependent on the bandwidth. Here, we assume an average pathloss coefficient of 2.5 for

UWB and 3.5 for a narrowband signal, which is in well agreement with published measurement results [7]. The total pathloss can be modelled by:

$$PL = 20\log_{10}\frac{4\pi d_0}{\lambda} + 10\alpha\log_{10}\frac{d}{d_0},$$

where $d_0 = 1\text{m}$, λ is the wavelength, α is the pathloss coefficient and d is the distance between transmitter and receiver which is fixed to 10m in Table 2. The received power $Pr = Pt + Gt + Gr - PL$ depends on the transmitted power Pt, the transmit Gt and receive Gr antenna gains and the path loss. Thermal noise is mainly determined by the low noise amplifier at the receiver $N = -174dBm + 10\log_{10} Rb$, where Rb represents the throughput. The total average noise power per bit is given by $Pn = N + Nf$, where Nf is the receiver's noise figure. The processing gain (PG) is defined as $PG = 10\log(\text{spreading factor})$, where the spreading factor is the number of pulses used to decode a single bit. Finally, the targeted link margin is calculated by $M = Pr - Pn - S - I + PG$, where S and I are minimum E_b/N_0 [i] and implementation loss, respectively. E_b/N_0 is the measure of signal to noise ratio for a digital communication system. It is simply defined as the ratio of Energy per Bit (E_b) to the Spectral Noise Density (N_0). Exploiting the full UWB bandwidth with a high center frequency of 6.85 GHz causes a significant pathloss compared to ZigBee. According to Table 2, the total pathloss for UWB at 10m is around 74.2 dB, while for ZigBee with 868 MHz center frequency is only 66.2 dB.

Consequently, decreasing the center frequency and keeping the bandwidth at its minimum of 500 MHz, i.e. considering the range 3.1GHz-3.6 GHz, might present an alternative approach. The corresponding link budget is shown in Table 3 and the pathloss (PL) as well as its distance to the processing gain (PG) in Figure 1. Only 6.3 dB improvement in total pathloss can be gained which is still far away from ZigBee's counterpart in terms of pathloss. Note that the quantity *PG-PL* is a good measure for the signal power available at the detector for data reconstruction and takes into account possible signal processing at the receiver and is therefore rather meaningful because of direct proportionality to the bit error rate.

Hence, if no signal processing is present at the receiver (e.g. due to cost constraints), Zigbee/IEEE802.15.4 outperforms UWB up to a distance of approximately 10m. Otherwise, if the receiver does include signal processing, UWB shows better performance for distances greater than 3m.

	UWB	**ZigBee**	
Geometric center frequency (Fc)	**6850**	**868**	**MHz**
Throughput (Rb)	2400	2400	bps
3-dB bandwidth	7500	0.3	MHz
Alpha (Pathloss exponent)	2.5	3.5	---
Average transmit power (Pt)	-2.6	-3	dBm
Transmitted power for 1 MHz	-41.3	2.2	dBm
Path loss at 1m	49.2	31.2	dB
Total Path loss at 10 m	74.2	66.2	dB
Rx power at 10m (Pr)	-76.8	-69.2	dBm
Average noise power per bit (N)	-140.2	-140.2	dBm
Rx noise figure (Nf)	7.0 [9]	7.0	dB
Total Ave. noise power per bit (Pn)	-147.2	-147.2	dBm
Minimum E_b/N_o (S)	3.6 [9]	8.7	dB
Implementation loss (I)	3.0 [9]	3.0	dB
Processing Gain (PG)	19.2	11.8	dB
Link Margin at 10m	**83**	**78.1**	**dB**

Table 2 UWB (3.1GHz-10.6 GHz) and ZigBee link budget comparison

This preliminary conclusion motivates us to consider an even lower frequency-band like 0.5 GHz-1 GHz. Before doing any calculation we first take a closer look at the radio spectrum to see which services are being offered in this frequency range. The main interfering services are TV broadcasting signals which occupy in the United States a huge bandwidth from 470-806 MHz. Cellular phones, biomedical telemetry devices and navy radars are other examples of interfering services [8].

Coming back to our comparison, Table 4 shows the link-budget for both systems where UWB is now limited to the 0.5GHz-1 GHz range. The total pathloss for UWB is 54.9dB and for ZigBee 66.2dB which finally shows a distinct improvement for UWB. Figure 2 gives a better feeling how fast the pathloss for ZigBee grows comparing to UWB and finally results in a difference of 11.3dB at a distance of 10m. Most interestingly, we can

see this result in the received power, where for both UWB and ZigBee, the received power is exactly the same (-69.2 dBm) while ZigBee suffers from a much larger transmit power (-14.3 dBm for UWB and -3 dBm for ZigBee).

	UWB	**ZigBee**	
Geometric center frequency (Fc)	**3350**	**868**	**MHz**
Throughput (Rb)	2400	2400	bps
3-dB bandwidth	500	0.3	MHz
Alpha (Pathloss exponent)	2.5	3.5	---
Average transmit power (Pt)	-14.3	-3	dBm
Transmitted power for 1 MHz	-41.3	2.2	dBm
Path loss at 1m	42.9	31.2	dB
Total Path loss at 10m	67.9	66.2	dB
Rx power at 10m (Pr)	-82.2	-69.2	dBm
Average noise power per bit (N)	-140.2	-140.2	dBm
Rx noise figure (Nf)	7.0	7.0	dB
Total Ave. noise power per bit (Pn)	-147.2	-147.2	dBm
Minimum E_b/N_o (S)	3.6	8.7	dB
Implementation loss (I)	3.0	3.0	dB
Processing Gain (PG)	19.2	11.8	dB
Link Margin at 10m	**77.6**	**78.1**	**dB**

Table 3 UWB (3.1GHz-3.6 GHz) and ZigBee link budget comparison

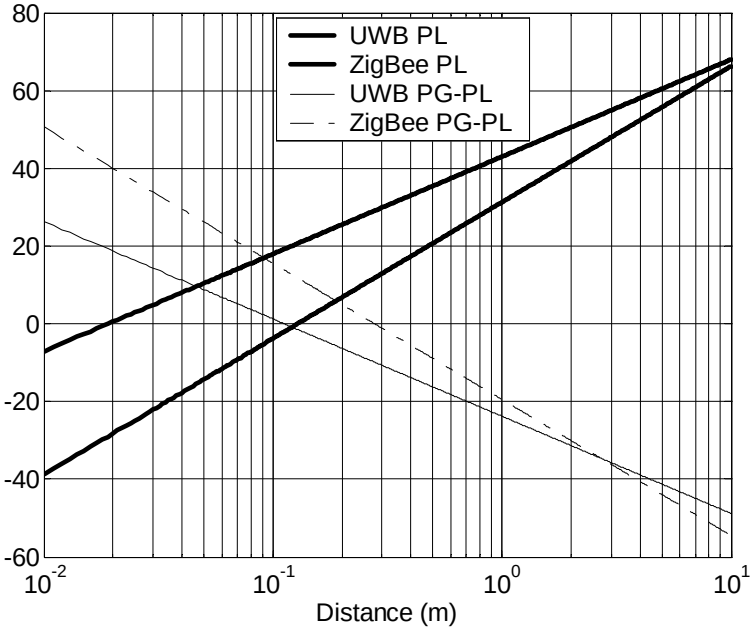

Fig. 1 Pathloss and its difference to processing gain for UWB and Zigbee/ IEEE 802.15.4 as a function of distance and frequency range 3.1GHz-3.6 GHz

	UWB	**ZigBee**	
Geometric center frequency (Fc)	**750**	**868**	**MHz**
Throughput (Rb)	2400	2400	bps
3-dB bandwidth	500	0.3	MHz
Alpha (Pathloss exponent)	2.5	3.5	---
Average transmit power (Pt)	-14.3	-3	dBm
Transmitted power for 1 MHz	-41.3	2.2	dBm
Path loss at 1m	29.9	31.2	dB
Total Path loss at 10m	54.9	66.2	dB
Rx power at 10m (Pr)	-69.2	-69.2	dBm
Average noise power per bit (N)	-140.2	-140.2	dBm
Rx noise figure (Nf)	7.0	7.0	dB
Total Ave. noise power per bit (Pn)	-147.2	-147.2	dBm
Minimum E_b/N_o (S)	3.6	8.7	dB
Implementation loss (I)	3.0	3.0	dB
Processing Gain (PG)	19.2	11.8	dB
Link Margin at 10m	**90.6**	**78.1**	**dB**

Table 4 UWB (0.5-1 GHz) and ZigBee link budget comparison

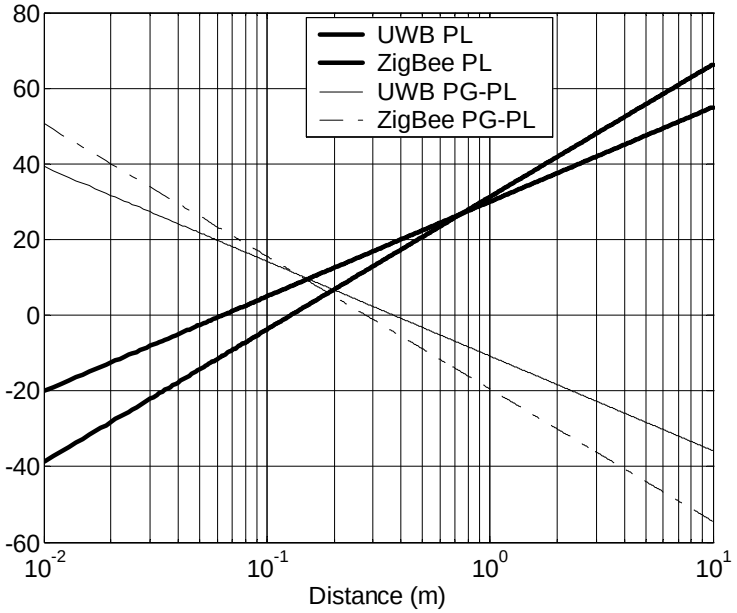

Fig. 2 Pathloss and its difference to processing gain for UWB and Zigbee/ IEEE802.15.4 as a function of distance and the frequency range 0.5-1.0 GHz

Observe that now UWB outperforms Zigbee/IEEE802.15.4 for distances larger than 10cm (1m) if signal processing at the receiver is (not) carried out, respectively.

Conclusions and Outlook

In this paper, we conduct a comparison study of Zigbee/IEEE 802.15.4 technology vs. ultra-wideband technology with application to wireless sensor networking, particularly wireless fire and intrusion detection. The details of both technologies are introduced and their general characteristics extracted and compared. In particular, a quantitative comparison is carried out by studying the individual link budget of Zigbee/IEEE 802.15.4 and that of UWB at different carrier frequencies and bandwidth's. Our results show that decreasing the frequency range down to 0.5GHz-1.0GHz while keeping the bandwidth at 500MHz, pathloss of UWB and Zigbee/IEEE 802.15.4 are in the same order. However, the more relevant measure *PG-PL* favors UWB for distances larger than a few centimeters. In turn, for the conventional frequency region 3.1GHz-3.6GHz, Zigbee/IEEE 802.15.4 outperforms UWB for distances smaller than 3m (10m), if signal processing at the receiver is (not) taken into account, respectively.

Both Zigbee/802.15.4 and UWB technologies share some attractive features such as ultra low power consumption, low cost and coexistence. The UWB technology holds some further features like multi-path mitigation, precision location and immunity to interception. From this point of view, we believe that both technologies will be the wave of the future of wireless sensor networking, where UWB is advantageous for wireless fire and intrusion detection if the location of the detector becomes relevant or if the receiver can be equipped with signal processing. For example, jamming in UWB is already rather difficult because of the low spectral density, but the UWB inherent ranging facility further complicates jamming. This might be beneficial in particular for intrusion detectors.

Otherwise, for extremely low cost fixed sensor networks with insignificant sensor positions and small sensor spacings, Zigbee/IEEE802.15.4 seems to be the favorite technique. However, note that UWB allows rather cheap transmitters because mixer and oscillator are not required. Moreover, a remarkably battery saving can be expected from UWB based sensor networks, provided that the mentioned interferers can be

significantly suppressed. Other related criteria, like antenna size restrictions, need to be investigated further. In conclusion, if striving for a product, all hardware related criteria and not only the link budget have to be taken into account for selection of the most adequate technological approach.

References

[1] A. F. Molisch, Y. G. Li, Y. Nakache, P. Orlik, M. Miyake, Y. Wu, S. Gezici, H. Sheng, S. Y. Kung, H. Kobayashi, H. Vincent Poor, A. Haimovich, and J. Zhang, "A low-cost time-hopping impulse radio system for high data rate transmission", to appear in EURASIP Special Issue "UWB – State of the Art", October 2004

[2] IEEE Std 802.15.4-2003, IEEE Standard for Information technology — Telecommunications and information exchange between systems — Local and metropolitan area networks — Specific requirements — Part 15.4: Wireless Medium Access Control (MAC) and Physical Layer (PHY), Specifications for Low-Rate Wireless Personal Area Networks (LR-WPANs).

[3] J. A. Gutierrez, E. H. Callaway, R. L. Barrett, Low-rate Wireless Personal Area Networks: Enabling Wireless Sensors with IEEE 802.15.4. Standards Informaiton Network, IEEE Press, 2003.

[4] Homepage of ZigBee™ Alliance, http://www.zigbee.com/

[5] E. Callaway, P. Gorday, L. Hester, J.A. Gutierrez, M. Neave, B. Heile, V. Bahl, "Home networking with IEEE 802.15.4: A developing standard for low-rate wireless personal area networks," *IEEE Communication Magazine*, vol. 40, no. 8, pp. 70-77, August 2002.

[6] E. Callaway, "Low power consumption features of the IEEE 802.15.4/Zigbee LR-WPAN standard," Mini-tutorial, ACM Sensys'03, Los Angeles, CA, USA, November 5-7, 2003.

[7] S. Ghassemzadeh, V. Tarokh, "The Ultra-Wideband Indoor Pathloss Model", IEEE P802.15 Working Group for Wireless Personal Area Networks (WPANs), July, 8, 2002

[8] The Federal Communications Commission's table of frequency allocations, 47 C.F.R. 2.106, Revised on April 13, 2004

[9] G. R. Aiello, G. D. Rogerson, "Ultra-Wideband Wireless Systems", IEEE microwave magazine, June 2003

Walter W. Jones
National Institute of Standards and Technology, Gaithersburg, MD, US

Development of a multi-criteria algorithm for fast and reliable fire detection

Abstract

The purpose of detecting fires early is to provide an alarm when there is an environment which is deemed to be a threat to people or a building. High reliability detection is based on the supposition that it is possible to utilize a sufficient number of sensors to ascertain unequivocally that there is a growing threat either to people or to a building and provide an estimation of the seriousness of the threat. It has been shown to be possible to detect fires early and reliably using the analog signal of the current generation of fire detectors. The best combination for early detection has been shown to be the complement of ionization, photoelectric, carbon monoxide and temperature. This is "best" in the sense that it is possible, using current day sensors, to see characteristic signatures very early, as well as to deduce quantitative information beyond the normal tenability limits. This paper will demonstrate this with an example using a neural network trained with a model of fire growth and smoke spread.

Introduction

The purpose of detecting fires early is to provide an alarm consistent with an environment which is deemed to be a threat to people or a building. High reliability detection is based on the supposition that it is possible to utilize a sufficient number of sensors to ascertain unequivocally that there is a growing threat either to people or to a building and provide an estimation of the seriousness of the threat.

The current generation of fire detection systems[1] is designed to respond to smoke, heat, gaseous emission or electromagnetic radiation generated during smoldering and flaming combustion. Smoke is sensed either by light scattering or changes in conductive properties of the air, heat by thermistors, the electromagnetic spectrum by photodiodes and photovoltaic cells, and gas concentrations by chemical cells[2]. An important facet of the present work is utilization of sensors which are currently in use in fire detection

systems, as well as those available from other systems, such as energy management and security. The information from the sensors themselves is analog data, measuring temperature, obscuration, species density, heat flux and other characteristics of the environment. What is needed is a means to provide earlier warning, and more useful information before and after alarm using these sensor suites.

Curve Matching Algorithms

Curve matching covers a wide range of mathematical techniques, from functional analysis to neural networks. Functional analysis is most useful when the signal to noise ratio is high[3] and one can match the signal to a specific curve of interest, for example, relating a t^2 signal to a heat release rate. Neural network analysis is useful when only the general shape of the curve is known and detail is not justified by the available signal. The regions 1, 2 and 3 in figure (1) show conceptually such a delineation. For all three regions, a pattern can be discerned. However, pattern matching is most usefully applied to the early, noisy signals in region 1 which does not lend themselves to definite statements of functional form, that is, when the signal-to-noise ratio is not high enough to provide a measure of the environment, typically S/N~2 to 4. Region 2 is the current range of available detection when point measurements provide sufficient signal to alarm, typically S/N~3 to 5. Region 3 is appropriate for signal extraction for fire following when the signal to noise ratio is typically greater than 10. We want to push detection capability into region 1, yet classify it correctly in terms of advice to the fire service or occupants.

Classification of fire types into low, medium and high likelihood consequences has implications for both fire service as first responders, and building maintenance personnel who might be able to fix problems before they rise to emergency status.

Figure (2) shows a typical sensor reading from a fire, carbon monoxide in this case. Detecting the presence of a fire traditionally has been to measure such signals, and provide an alarm when some condition is reached, for example, when the opacity is high or the carbon monoxide too high. Shown in the figure are alarm points for several detection strategies, an ionization detector, a photoelectric detector, and the CO*Ion

algorithm discussed previously. The example is a surrogate for the range of signals which might be used for detection of fires[4]. Currently, temperature (T), opacity (OD), ionization (Ion) and carbon monoxide (CO) are the core signals we will focus on. In addition to these, carbon dioxide (CO_2), volatile organic hydrocarbons (VOC), nitrogen-oxygen compounds (NO), oxygen(O_2) and water concentration (RH) are possible future signals to incorporate.

An example of using pattern matching is discussed in the paper by Rose-Phersson et al.[5] The focus of the paper was the use a probabilistic neural network to combine signals from several transducers to reduce the likelihood of both false positives and false negative responses from detector systems. While this is similar to what we will use to reduce the time delay, the focus was on more reliable detection. The goal behind their work was to automate response to fires (e.g. sprinkler activation), so very high reliability is even more important than early detection. They demonstrated the optimal sensor set to be ionization, photoelectric, carbon monoxide and carbon dioxide, with temperature providing the best confirmation signal. In our case, we will work from the premise that the patterns we see will result in an alarm condition from the installed alarm base, so we want to respond as early as possible to these signals or patterns, in order to reduce the response time of the firefighters.

An Example of Implementation of a Neural Net Algorithm

An artificial neural networks (ANN) is a collection of mathematical models that emulate some of the observed properties of biological nervous systems and draw on the analogies of adaptive biological learning. The key element of the ANN paradigm is the structure of the information processing system. It is composed of a large number of highly interconnected processing elements that are analogous to neurons and are tied together with weighted connections that are analogous to synapses.

Learning in biological systems involves adjustments to the synaptic connections that exist between the neurons. This is true of ANNs as well. Learning typically occurs by example through training, or exposure to a “truthed” set of input/output data where the training algorithm iteratively adjusts the connection weights (synapses). These

connection weights store the knowledge necessary to solve specific problems.

ANNs are good pattern recognition engines and robust classifiers, with the ability to generalize in making decisions about imprecise input data. They offer ideal solutions to a variety of classification problems such as speech, character and signal recognition where the physical processes are not understood or are highly complex. They are often good at solving problems that are too complex for conventional technologies (e.g., problems that do not have an algorithmic solution or for which an algorithmic solution is too complex to be found) and are often well suited to problems that people are good at solving, but for which traditional methods are not (you know a fire when you see it!).

The study of fire occupies a unique niche in the world of science and engineering because an unwanted fire is considered a failure in the sense that it is not a desirable outcome and is to be avoided. Detection and suppression are thus posed as means to avoid failure, which can be well characterized. For detection in particular, we have well defined failures which can be tested fairly reproducibly. In this highly regulated environment, in order for detectors to be approved for use they must detect fires as defined in UL 268 and EN 54 tests. In addition, there are nuisance criteria when the detectors should not alarm. While these latter are well recognized (dust, for example), there are no formal tests, though a simple negative (no fire) should in no case produce an alarm (a false positive). For the UL tests, there is a time prior to when the alarms should not activate.

The biggest difficulty in training neural networks is the extent of the training scenarios available. In fire research, the work has been limited to experimental data sets. Typically the training set consists of tens to hundreds of scenarios, while ANNs need tens of thousands to produce highly reliable classification. Using the fire model, CFAST, we can generate a very large set of training and testing scenarios.

For this example, we consider the use of single head (multisensor) detector in a single compartment. The sensor suite consisted of four sensors: oxygen, carbon monoxide, opacity and temperature. A more complete characterization would consider each sensor

separately, as well as all combinations. This would provide a sense of the effect of losing a sensor (fault detection).

We have a model for fires which has been extensively tested, CFAST[6]. We used this model to generate training and testing scenarios which cover a very fine delineation of the event to be detected. Using such a model allows us to generate the tens of thousands to hundreds of thousands of examples necessary to provide sufficient training for a network.

The base case used: Standard atmosphere of 101,300 Pa, A single compartment of 13x13x2.4 m, Two cracks (one vertical, one horizontal) to account for leakage, One door of (0.9 x 2.3) m and One window of (0.9 x 1) m.

Starting with this base case, variations of the base case scenario were generated based on

(3) Ambient conditions: outside to inside temperature the same or ±15 ˚C
(3) Wind: none, into door (away from window if present) or away from door
(3) Fire size: (1, 10, 100) kw - note: no fire at all is a special case
(3) Position of fire: floor, and 0.5 m, 1.0 m above the floor in the center of the room
(4) Door width: open, ½, 1/4, 1/8 width
(2) Window: open or closed (0.9 m x 2.3 m)
(4) CO: (0.0, 0.001, 0.01 and 0.05) kg/kg or (0%, 0.1%, 1% and 5%) by fraction
(3) Smoke yield (optical depth): (0, 0.01, 0.05) kg/kg or (0%, 1% and 5%) by fraction
(2) Hydrogen carbon ratio in the fuel: (0, 0.2) kg/kg

This is 20,768 variations, which were then used to train the neural network. The scenarios were 300 second calculations with a time slice every 30 seconds. While this suite is sufficient to demonstrate the feasibility of training multisensor networks, a somewhat more comprehensive set of scenarios might include variable room size, non-rectilinear compartments and a range of radiative fraction, which would increase the number of scenarios, calculation and training time about an order of magnitude.

Three training exercises were performed: 1) a subset of the parameter space comprising 5000 scenarios, and 5000 for testing; 2) a complete set of scenarios (20726), and a small subset for testing (42) (total of 20768); and 3) preconditioning to supplement training for those cases when a fire is known to exist.

In order to be considered fast, the detection scheme must be at least fast as current detection algorithms. For high reliability, we are looking for means of seeing all real fire (no false negatives), and not responding to those deemed to be nuisances (no false positives). A metric for the former will be discussed as part of the analysis of results. The metric for false positives (nuisance alarms in the present context) and false negatives (missing a real fire), the scenarios are either fires or nuisance signals. Except for the base case of no heat release, which by definition is not a fire, the remainder are classified as real or nuisance by whether they pose a threat at any point in the curve to people or property. The classification is based on the ISO Toxicity Specification[7]. For exercises 2 and 3, of the total scenario space, 15 916 cases were fires and 4 852 non-fires. These latter (23%) are nuisance signals in the present context. A more complete classification scheme would further classify these according to Tables 1 through 3.

Mathematically, a neural network is a set of weight matrices which multiply sensor signals, and use a function (in our case a linear ramp) to combine the results. This provides a classification of data. Schematically, it is shown in figure (3), where **p** represents the measurement points, a vector of length R (in our case, this is the number of sensors), **b** a bias vector for the algorithm (always set to zero in our training), **w** the weight matrix (the answer so to speak). In the following training cases, we used R=4, but typically, it can range from 1 (a single sensor) to 9 (see ref.) which would be a very general multi-criterion sensor head.

The end point of such a system is a weight matrix which when multiplied by the sensor suite (**p**) produces a classification number; we used a simple classification of true or false (fire or non-fire). We trained a network with a single hidden layer of 10 neurons, and a single output layer using a linear transfer function. Thus we have only one matrix which needs to be adjusted. The training method used was Levenberg-Marquardt[8]. We have a set of four sensors, with 31 points (30 intervals). The data were presented to the learning algorithm, which modified the weight matrix (**w**) until a (defined) error level was reached.

We applied this technique using the Matlab[9] simulation tool, with the Neural Network Toolbox. Each data set was presented to network, and it adjusted the weight matrix. After completing the training, the network was presented test data, and classified the new sensor readings as a fire or non-fire event. Since we are concerned with a binary decision, the results were descritized to 0 or 1. In actuality, the data was a spectrum and additional training could be provided to further refine the classification scheme to non-fire, nuisance or significant event.

For the first case, there were no false positives or false negatives. That is, all fires were detected and no alarms when a fire did not exist. The time to alarm was generally the same for conventional detection and the trained network. The time to do the CFAST calculations was approximately 45 minutes, and the training time approximately 1 hour.

The time/temperature curve shown in figure (4) has the alarm points overlaid. The solid lines are example 1 and the dashed lines example 2. The vertical ticks are the corresponding detection time for conventional detection (green) and the neural net with training (red).

For the second example, all 20768 scenarios were used. In order to test the network, 42 of the 20768 scenarios were used for testing and not used for training. This then constituted a sampling of data which the network should be able to recognize. Of the forty two tested, there were no false positives (nuisance alarms), that is no fire detected when a fire did not exist; however, there was one false negative, not showing an alarm when a fire was present. This is about a 2% failure rate. The scenario which failed is marginal for the network, and to improve performance, the scenario suite needs to be extended to provide a finer resolution. In actual commercial detection systems, false negatives occur (3 to 20)% of the time[10] and false positives (30 to 50)% of the time, so we have improved on the detection capability as well as reduced the time to detection.

This training was done with a 10 neuron system. A systems with 20 neurons and two hidden layers was tried as well, without improvement. The time to detection for this second training example was always as early as conventional detection, as shown in

figure (5). The time to do the CFAST calculations was approximately 2 hours, and the training time approximately 3 hours. The two cases shown, 007051 and 017658, are randomly picked from the 42 test cases.

For the third training example, the truth vector (when the fire exists) was preconditioned for those cases we know a fire will exist. For example, for the 100 kW source, it will at some time be considered a fire. For these cases we can set the training vector to "true" at after the first interval. Once again, there were no false positives and a single false negative (same case as before). The time labeled "preconditioned" in figure (5) was the response for the two cases shown in the figure for the example 2 testing regimen, 007051 and 017658, thus showing the value of using additional information in the training regimen.

This third training example takes advantage of the fire problem. We start with the scenarios. These produce curves of time, temperature, co, and so on. At some point we decide there is a fire. At the simplest level, used in 1 and 2, it is done the based on commercial detection schemes or the toxicity assessment discussed earlier. However, we can add to that information base, by noting that certain scenarios are going to be classified as fires, and tell the system from the beginning. For example, a 100 kW fire will must be detected, as must a 5 % CO condition. So for certain scenarios, one tell the system that it is a fire after the first interval. That gets factored into the weight matrix so that curves of similar shapes trigger an alarm very early. And even ones that are close do so. It is because we are matching curves (high precision) and not trying to get detailed information (high accuracy) that this technique is so appealing in this application.

Observations

There is additional work which needs to be done before this can be used in actual sensor suites: final testing for this case needs to include an example experiment such as the Smoke Detector Tests[11]. In addition, the standard qualification tests and a set of nuisance signals must be included. This latter will require an instrument transfer function, which can be measured using the FE/DE test apparatus[12]. Finally, the training

suite ought to be extended to include the wide range of geometries which exist in practice rather than just those used for qualification testing. The training of a neural network should allow this extension and would improve the robustness of detection systems. This then allows one to include cases which currently cause alarms, such as steam, but are clearly not fires.

A further extension would be to go beyond the simple alarm/no-alarm classification we have done here and report on nuisance alarms as distinct from fires. Interestingly, a cursory inspection of the testing scenarios shows that the network is doing a reasonable characterization of the scenarios in terms of the type of fires. It is likely that this work could be extended to classification according to Tables 1 through 3. This is important in that a nuisance signal is often a precursor to more serious conditions. The prime example is the case of an oven (and even more commonly a toaster oven) which can develop the right conditions (and measurable effluent) but has a low level fire until a door is opened.

Conclusions

The full gamut of fire detection is possible utilizing currently available sensor technology. It has been shown that it is possible to detect fires early and reliably using the analog signal of the current generation of fire detectors. The best combination for early detection has been shown to be the complement of ionization, photoelectric, carbon monoxide and temperature. This is “best” in the sense that it is possible, using current day sensors, to see signatures very early, as well as to deduce quantitative information beyond the normal tenability limits.

The most useful of the algorithms studied is the curve matching concept embodied in neural network methods. In training such algorithms, it is important to use a sufficiently large set of training and testing samples so that that the algorithm is robust. We would expect a single experiment to provide very early detection for that single response curve. However, as the number of training sets is increased, incorporating variations in geometry and insult, the time to reliable detection increases. As the number of sensors used increases, we expect the detection time to decrease. The trade-off is in the

necessity for using large (more than 10,000) sample sets. With a judicious use of modeling and experimental testing, this should not be a burdensome exercise. We have demonstrated the training of a neural network to shown that it is possible, including very early detection. Although we find a 2 % error rate with the present training regimen, this is still considerably better than current detection (3 to 30)% as well as methods proposed to date (2 to 10)%.

Table 1. Nuisance signals (low likelihood)

Hairspray, Nail polish remover , bleach, furniture cleaning agents, disinfectants
Toaster effluents - except as can be classified as incipient fires
Ovens, Boiling water, coffee, showers and other steam sources
Dust and sawdust, concrete dust, overcooked popcorn and other microwave products
Propane and kerosine heaters and stoves, candles, cigarettes and matches
Heating systems (furnace)

Table 2. Incipient (long time to disaster) fires

Toaster oven effluents, Welding and arc welding, Cook-top effluents, frying bacon
Smoldering mattress, chair or other cushion furniture: cotton, down

Table 3. Fires (prompt)

Open cellulose fires (crumpled newspaper)
Flaming mattress, chair or other cushion furniture: cotton and foam
Liquid pool fire (heptane, gasoline, alcohol, paint thinner, acetone, vegetable oil)
Wood (wood based) furniture such as bookcases
Smoldering mattress, chair or other cushion furniture: foam
Power and signaling cables, Interior wall coverings such as wallpaper

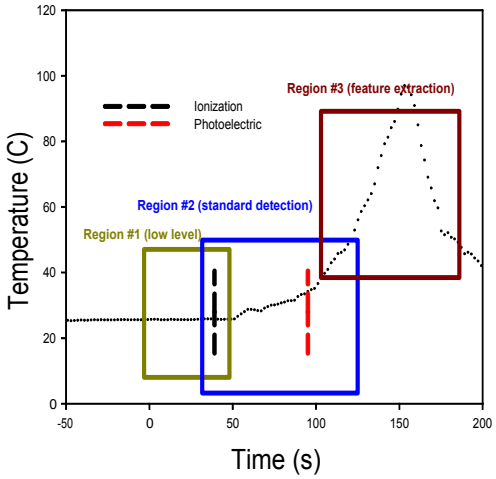

Figure 1. Delineation of detection regions for a flaming fire.

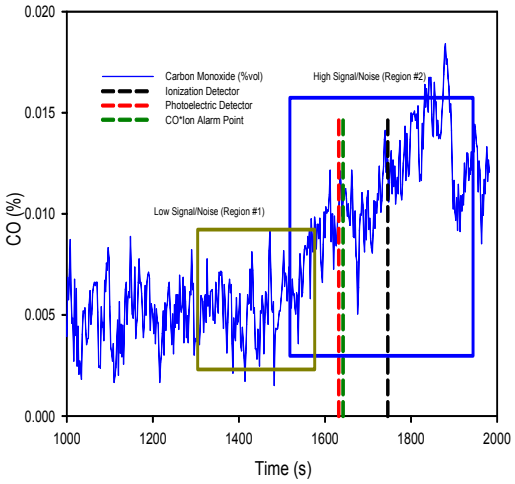

Figure 2. Carbon monoxide signal in SD 37, showing regions for curve matching algorithms.

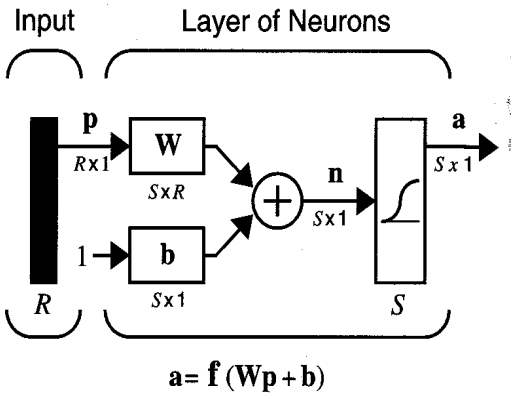

Figure 3. Schematic of a network layer.

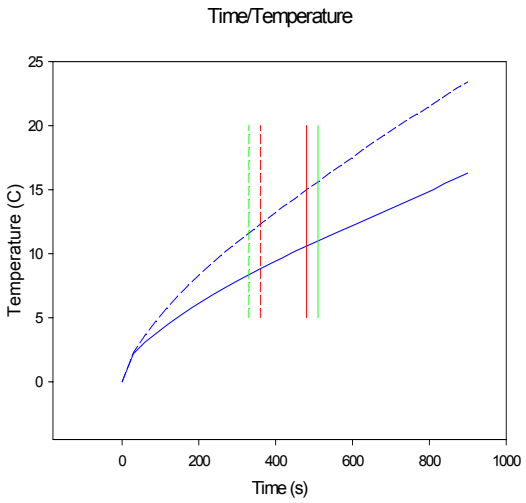

Figure 4. Time/temperature curve for two of the 5000 test cases in example one.

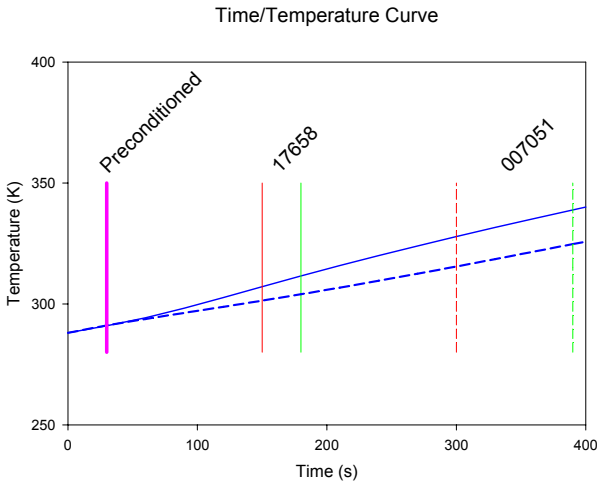

Figure 5. Time/temperature curves for two of the test cases for the second example. Green markers are for standard detection strategies and red for detection with the network. The marker labeled "preconditioned" is the result of these same test cases when the training vector is preconditioned for known fires.

References

1. A Review of Measurements and Candidate Signatures for Early Fire Detection, W.L. Grosshandler, NIST Internal Report 5555 (1995).

2. The Use of Surface and Thin Film Science in the Development of Advanced Gas Sensors, S. Semancik and R. Cavicchi, Applied Surface Science *70/71*, 337 (1993).

3. *Functional Data Analysis*, J.O. Ramsay and B.W. Silverman, Springer-Verlag, New York (1997).

4. Identification of Fire Signatures for Shipboard Multi-criteria Fire Detection Systems, D.T. Gottuk, S.A. Hill, C.F. Schemel, B.D. Strehlen, R.E. Shaffer, S.L. Rose-Pehrsson, P.A. Tatem, and F.W. Williams, NRL Memorandum Report, NRL/MR/6180-99-8386 (1999).

5. Multi-Criteria Fire Detection Systems using a Probabilistic Neural Network, S.L. Rose-Pehrsson, R.E. Shaffer, F.W. Williams, D.T. Gottuk, S.A. Hill and B.D. Strehlen, Sensors and Actuators, *B 69*, 325 (2000).

6. Technical Reference for CFAST: An Engineering Tool for Estimating Fire and Smoke Transport, W. Jones, G. Forney, R. Peacock and P. Reneke, NIST TN 1431 (2000).

7. ISO/TS 13571:2003, Life Threatening Components of fire - Guidelines for the estimate of time available for escape using fire data, International Organization for Standardization 1, rue de Varembé, Case postale 56, CH-1211 Geneva 20, Switzerland.

8. D. Marquardt, An algorithm for least squares estimation of non-linear parameters, SIAM J., 11:431 – 441, 1963; K. Levenberg. A Method for the solution of certain nonlinear problems in least squares. Quart. Appl. Math, 2:164 – 168, 1944.

9. The Matlab Development Environment, The MathWorks, Inc., Apple Hill Drive, Natick, MA 01760.

10. Analysis of Fire Signature Data Toward the Development of an Advanced Fire Detector, Progress Report on NIST Grant 1D0076 by J. Milke (September, 2001).

11. Performance of Home Smoke Alarms, Analysis of the Response of Several Available Technologies in Residential Fire Settings, R. Bukowsi, J Averill, R. Peacock, T. Cleary, N. Bryner, W. Walton, P. Reneke and E. Kuligowski, NIST TN 1455 (2003).

12. Fire Emulator/Detector Evaluator: Design, Operation, and Performance, T. Cleary, M. Donnelly, and W. Grosshandler, NIST SP 965, Proceedings of the 12 International Conference on Automatic Fire Detection, AUBE ‘01, Gaithersburg (2001); Towards the Development of a Universal Fire Emulator-Detector Evaluator, W. Grosshandler, Fire Safety Journal *29*, 113 (1997).

Werner Straumann, (werner.straumann@securiton.ch)
Securiton AG / CH-3052 Zollikofen / Switzerland
Stefan Fischer, (fischer@fastcom-technology.com)
Fastcom Technology S.A. / CH-1006 Lausanne / Switzerland

Algorithms for Smoke and Fire Detection and their Integration into Existing Systems and Installations

Abstract

Video-based event detection systems are becoming increasingly important for the early detection of smoke and fire. But do universally applicable image processing algorithms for such an application really exist, and, if yes, can they be implemented without going through a lengthy calibration process, specific to different environmental conditions? This paper will discuss such new algorithms and methods, and demonstrate how these methods can be integrated into existing security and surveillance installations. The benefits and the reliability of such systems will also be addressed, as well as the influence of the site conditions on the image acquisition.

The above statements will be justified using examples, and the requirements for the choice of such algorithms, for the integration in existing security installations and for the systematic testing of such systems, will be discussed.

1 Introduction

Conventional fire alarm systems have been available for a long time. They are type-approved, and have the benefit of a low false alarm rate. Video-based early fire and smoke detection systems can be used in parallel to conventional systems in order to significantly reduce the detection time. A higher security standard can thus be achieved by combining an approved fire alarm system with a video based early fire detection system. The key advantage of a video based system is the reduced time for an intervention, as well as the detection of the spread of smoke which would not be detected by temperature-based fire detection systems often used in tunnels.

Video-based early fire detection systems are particularly well suited for aircraft hangars, railway stations, large halls, road tunnels, where CCTV-cameras are today already installed. Such configurations lend themselves quite well to the principle of human verification of the detected incident, ensuring suitable and timely decisions before human intervention.

2 Known Algorithms for Smoke and Fire Detection

2.1 Publications about Video-Based Smoke and Fire Detection

Publications on video-based smoke and fire detection are rare in the scientific literature. Because of the commercial interest of video-based smoke and fire detection, a number of patents have been published representing the state of the art in this domain.

2.2 Algorithms for Smoke Detection

Generally, smoke in a video image is characterized by the fact that images become darker with time, detail and contours are lost and image contrast decreases. However in some cases, smoke clouds may be illuminated by light sources, which results in a brightness increase and gain in contrast and detail. White smoke also provokes a gain in brightness.

The simplest approach for smoke detection uses the pixel intensity or brightness and some kind of clustering method, as well as a procedure for determining the evolution of intensity over time. The evolution of the intensity feature may either be determined as a change in a number of frames or by using a reference image. The acquisition of reference images is straightforward: when little or no changes are expected in a scene, the image can be taken as the reference image. Practical experimentation shows however that the acquisition of reference images is sometimes difficult in particular in scenes where background information varies a lot. An example is that of road tunnels, where dense traffic makes it nearly impossible to capture an image where no vehicle is present.

Reference [5] describes a system using pixel intensity of groups of pixels and their evolution with time. In reference [6], reference images are used in order to determine the evolution of image intensity.

2.3 Algorithms for Flame Detection

Fire and flames are characterized by a bright center and a flickering border. The criteria that can be used to detect fire include the shape of the bright region, its growth over time and the flicker frequency of the border of the flames.

Reference [1] describes a flame detection algorithm that uses clusters of pixels and frequency measurements on these pixels. A certain range of frequencies is used to determine which pixels correspond to flames. In reference [7], the intensity values and cluster of average values are examined in order to determine the probability of the presence of flames. Reference [8] also describes a flame detection system that measures the flickering frequency of flames. Finally, reference [9] claims another method using multiple frames from a video sequence for flame detection.

2.4 Fusion and Decision Analysis

The system described in [10] uses other image features to identify smoke and fire in addition to brightness. Examples are among others, hue, saturation, contrast, and edge content. Using fast algorithms and computations on rectangular image regions, efficient detection of smoke or fire in an image can be achieved. Significant changes of these features over a certain period of time are characteristic for smoke and fire events.

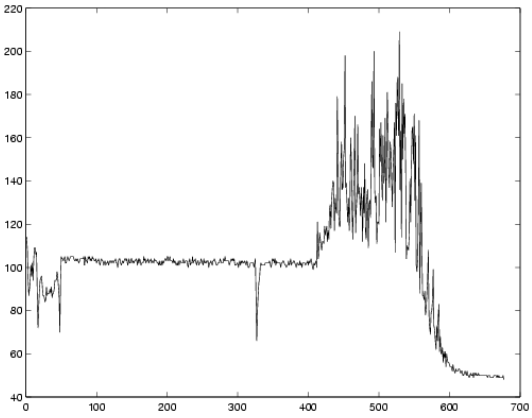

Figure-1

Figure-1 shows the brightness feature sampled 2.5 times per second in a region of pixels on the flickering border of a flame. The loss of brightness after frames 500 is caused by the auto-iris of the camera triggered by the bright flame.

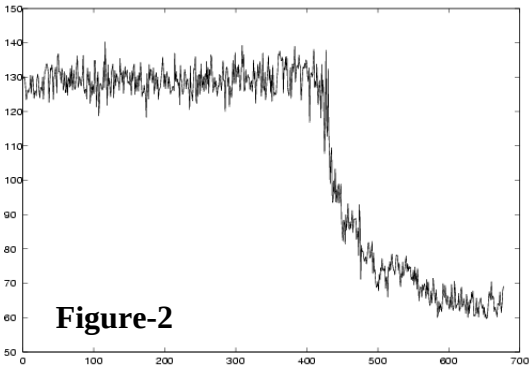

Figure-2 demonstrates the loss of brightness in a block of pixels under influence of smoke arriving after frame 400. This camera was mounted near the fire.

Figure-3 shows the same event (fire) viewed from a distant camera. The smoke is detected later and the loss of brightness is different, because of the long distant between camera and fire. The smoke covers the scene slowly in the observed region, because of the slower dissipation.

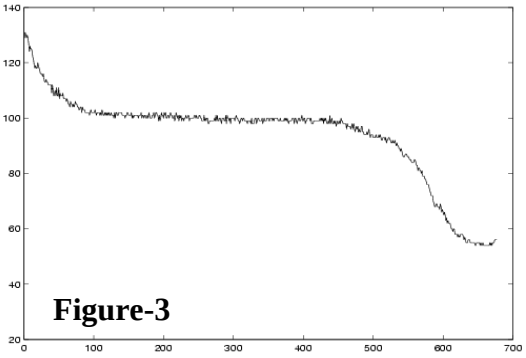

The system must take into consideration the history of the features and can detect significant changes using statistical tests. For smoke events it can be expected that regions become darker, unless white smoke is expected. Flames always provoke brighter pixels. Using statistical tests allows for the system to adapt to different environments.

The brightness and other feature results can now be combined and a decision can be taken with a rule-based approach or using a statistical decision fusion. The statistical decision fusion is similar to a 1st degree neural network.

Filtering out blocks that are unconnected and only taking into consideration clusters of blocks with specific shapes can be used to eliminate unwanted alarms.

2.5 Choice of Algorithms

As in all security systems, finding the optimal balance between detection time and resilience to false alarms is a complex objective. Beyond a certain threshold, high false alarm rates can render smoke and fire detections system unusable and are the determining factor for client acceptance of such a system.

3 Requirements for a Software Solution

The algorithms are only one aspect of a system for smoke and fire detection. In order to achieve a good detection rate and a low rate of unwanted alarms, the detection results from a number of algorithms must be combined. The algorithms providing the decision bases are published in the scientific literature and are therefore easily accessible; the real value of a software solution however lies in the decision engine combining the different detection results.

Other requirements for software solutions are facilities for the detection of additional events such as "video loss", "dark image", "video noise", interfaces with other alarm management systems and a graphical user interface providing the possibility to view alarm images, act upon alarms and events and the possibility to save log files with alarm images.

4 Environmental Conditions

The environmental conditions, and the type of application, have a strong influence on the detection quality of a video based system. Therefore, in a good product, standard configuration profiles should be used for different applications or environment types to minimize the need of individual calibration of each installation.

The most important influences are:

Lighting conditions: Type of illumination, day night changes, dust, fog, soiled walls (slow changes), reflections (sun, car headlights, ...), blooming, …

Moving Objects: vehicles, car, train, cranes, conveyer belt, persons, animals, ...

Miscellaneous: Wind, air flows, shadows, sprayed water from wet streets, snow, clouds, sun, ...

Cameras: A good camera and lens, as well as a good camera position, are as important as the environmental conditions. The shutter and auto-iris response and the mounting angles of cameras will also have a strong influence on the detection quality of a video based system.

4.1 Road Tunnels

In general road tunnels are not sufficiently illuminated to ensure good video images for video based detection, and at night time the illumination is often reduced even more. Brighter illumination reveals more detail in the video images, and car headlights and reflections have less impact on the overall video image. Also with a good illumination the security for the car drivers increases as it can prevent them for falling asleep.

Remark: If the headlights of a vehicle are directly aligned with the optical axis of the camera, anti blooming or auto-iris control tend to overreact, resulting in dark or flickering images. Vehicles moving away from the camera generally cause less of these problems because the rear lighting is significantly less bright than headlights.

4.2 Industrial Installations

Most modern production sites are well illuminated, therefore different problems are encountered than those of road tunnels (low illumination, headlights).

The challenge in industrial installations can be the presence of large moving objects in the field of view of cameras, such as cranes, stored equipment and vehicles. In this environment it is important to find out the best camera position and angle to prevent situations where, for example, a crane transporting large objects covers the complete field of view of the camera, making image analysis impossible during certain time intervals.

Other difficulties in industrial installation include: the influence of doors or windows to the outside which allow direct sunlight, to enter the facility; and other scheduled or unscheduled light changes.

4.3 Outdoor installations

Outdoor environments are a challenge for computer-based scene recognition due to the constantly and drastically changing weather and light conditions (day/night, sun, clouds, wind, snow, fog, storm…). However, smoke and fire events that are sufficiently large

can be detected reliably in outdoor settings. Examples are detection of smoke of forest fires [2,4] or fire detection in waste storage facilities.

5 Detection security (quality)

In a video based early fire detection system, it is important to have a fast detection of fire and smoke, even if you have to accept and handle more unwanted alarms as in a conventional fire alarm system. For dedicated test fires (as described in paragraph 7) the detection rate should be near to 100%, with an alarm triggered in less than 1 minute. In practical applications, you are never be sure to detect all the events because of unpredictable environmental influences. E.g. the headlights of a car in an accident could cause blooming in CCTV-cameras, or the accident may block parts of the field of view of the camera, etc. In these cases it is important to have an additional approved fire alarm system, even if it is a slower one. In the other 95% of cases, you have the advantage of a faster fire alarm using the video based “early fire and smoke detection system”. Even if the system doesn’t detect 100% of the events, the over all security will increase in the same way as if a security guard is hired; He won’t see everything but he will see a lot and the overall security will increase through his presence

6 Unwanted Alarms

Unwanted alarms are defined as conditions that trigger an alarm, when no actual smoke or fire event can be observed. Unwanted alarms are related to each different type of environment. Unwanted alarms are normally not caused by a malfunction of the system, but rather a reaction due to an image condition that is very similar to fire or smoke events. Through visual verification, a human observer will eliminate such false alarms in a few seconds.

Examples for false alarms in road tunnels include vehicle headlights and subsequent camera brightness compensation (auto iris) resulting in loss of brightness. In some cases indicator lights are erroneously detected as flames. Different types of tunnel wall surfaces reflect light in different ways, dense traffic with vehicle headlights facing the camera may sometimes cause light reflections having the appearance of flames.

Tunnel exits in the field of view of the camera, represent a challenge similar to that of outdoor image analysis (see paragraph 4.3).

7 Test Methods

Today there are no recognized, generally accepted standards for testing of video-based smoke and fire detection systems. The currently used practices consist of live fire tests and long-term false alarm tests, in order to determine the detection rate and the false alarm rate in the intended surroundings.

Live test for detection security: Test fires should be representative for the type of event expected, and of its surroundings. Since it is not possible, for example, in a road tunnel, to burn a new car for each test (with a heat release of about 5 MW or more), burning several liters fuel (e.g. n-heptane or a mixture of gas and diesel) on a small surface area (e.g. 0.5 square meters), can be used to test the quality and the detection speed of the system. (This type of test represents a heating power of about 1 MW.)

Live test for false alarm rate: The system needs to be configured for the installation under test; also the detection sensitivity should be configured. Under normal operating conditions, a period of one week to one month is needed to find the true number of false alarms for each camera. With the help of alarm log files and the alarm images it is possible to classify the unwanted alarms in groups to optimise the system.

Automatic testing with sets of digitised image sequences, test chambers or video mixing of events and environments are methods that can be used for algorithm development and optimisation, parameter tuning, as well as for benchmark tests. But these tests do not replace the live tests.

8 Combination with other Installations

As discussed above, the video based early fire detection systems are mostly faster than conventional fire alarm systems. Certified fire alarm systems are not as fast, but the false alarm rate is much lower and the detection security is approved. The best of both worlds is achieved by combining the two systems to achieve a higher security level.

An interesting concept for road tunnels would be the combination of a video based early fire detection system with a thermal based fire alarm system, e.g. by temperature sensitive cables, laser-systems or barometric systems. The result is a higher reliability, faster reaction time in most cases and more information (the fire alarm system detects the fire source, while the video system detects the spread of the smoke).

9 Examples and Installations

The following two examples were recorded in the “Faesenberg” highway tunnel that joins Switzerland and Germany on 18th March 2004. The tunnel illumination is about 60 lux (representing daytime illumination) and about 5 lux (representing nighttime illumination).

This picture shows the fire alarm snapshot of a live test fire in March 2004. Two liters N-Heptan on a surface of 0.5 square meters with a thermal power of about 1 MW.

Figure-4

Detection times:

Fire pre-alarm after 19s / alarm 23s.

Smoke pre-alarm after 23s / alarm 30s.

Reflections of the fire on the road and on the wall were also detected.

In this example the smoke was detected by a camera far away from the fire source. Smoke was transported by the ventilation through the tunnel.

Figure 5

Figure 6

A typical false fire alarm caused by the combination of white smoke and the illumination in the road tunnel: smoke is detected as fire.

References

The date in patent references is the publication date when not stated otherwise.

[1] Flame detection method and apparatus, European Patent EP058313 (also published as GB2269454 and US5510772), 1994-02-16.

[2] Method for automatic detection of fires, particularly of forest fires, European Patent EP0818766, 1998-01-14.

[3] Fire detection system, European Patent EP0822526 (also published as JP10049771 and US5926280), 1998-02-04.

[4] Method and system for automatic forest fire recognition, European Patent EP0984413, 2000-03-08.

[5] Video smoke detection system, European Patent EP1220178, 2002-07-03.

[6] Method and apparatus for the detection of smoke and / or fire in spaces, European Patent EP1239433, 2002-09-11.

[7] Flame detection method and apparatus, US Patent US5510772, 1996-04-23.

[8] Early fire detection method and apparatus, US Patent US6184792, 2001-02-06.

[9] Method and apparatus of detecting fire by flame imaging, WO02093525, 2002-11-21.

[10] Werner Straumann, "Combined Surveillance Through Video Image Analysis", in Videodetection, Sensor technology for intrusion prevention and fire detection, 27th - 28th May 2002, Cologne, Germany.

Daniele Casagrande
Università degli Studi di Trieste

Farbod Kayhan
Institute for Scientific Interchange

Viktoryia Viktorovna Semeshenko
Institut National Polytechnique de Grenoble
and

Cristiano Zambon
System Sensor R & D

A smooth neural approximator for multi-criteria fire detection

Introduction

Multi-criteria fire detectors base their decisions, of whether to alarm or not, on signals read by different types of transducers. So far, many different algorithms have been designed for merging all of the input data in order to obtain a decision as close as possible to the intended one (see, for instance, [2]).

However, these kinds of algorithms can only approximate the real alarm region in a segmented way, i.e. dividing the original region in many parts and using some tricks to interpolate the surface. At the end, the appoximation region will have a lot of non-linearity corners, and will be hard to take under control when input signals move across these corners.

A different approach in algorithm design is the neural approximation (see [3]). Neural networks are usually designed by using learning algorithms, such as back propagation or self-organisation. Unfortunately, this kind of approach has an intrinsic over-training possibility that formally reduces the practical realization (see [4]). In reality, there is no way to guarantee that the error surface has no peak outside the set of points used for the validation test. Of course, when the neural network is used as an alarm estimator, this unpredictable behaviour is absolutely unacceptable.

On the other hand, there is a widely known particular kind of neural network, the perceptrons, that does not require a learning process. The aim of the research presented herein is to understand if it is possible, under some conditions, to use perceptrons to characterize a volume in $\mathbb{R}^n$ approximating the alarm region. If this

could be done, the stability of the detector would be assured since each perceptron is intrinsically stable.
The conclusion of the research is that if the alarm region is convex than it can be approximated with a given accuracy provided that a sufficient number of neurons are used. On the other hand, if the alarm region is not convex an algorithm has been designed to divide it into convex volumes and to merge the outputs of all perceptrons.

Notation and definitions

The proof of the *separation property* of a perceptron, i.e. the property of separating the space $\mathbb{R}^n$ into two half spaces, is widely explained in [1]. Here we report only the decision function of a neuron; as a function $f : \mathbb{R}^n \longrightarrow \{0, 1\}$ such that:

$$f(x_1, \ldots, x_n) = \begin{cases} 0 & \text{if } \sum_i w_i x_i \leqslant \theta \\ \\ 1 & \text{if } \sum_i w_i x_i > \theta \end{cases} \tag{1}$$

where the w_i is the weight associated to each input and θ is the threshold of the neuron.
In practical cases, one prefers to use the sigmoid:

$$f(x_1, \ldots, x_n) = \frac{1}{1 + e^{-\tau(\sum_i w_i x_i - \theta)}} \quad . \tag{2}$$

A sigmoid is more difficult to realize than a step function but gives a better approximation of how a decision should be made (see [5]). In fact, in this case, the separation property becomes the property of determining a "degree of belonging", in the sense that the value corresponding to a point on $x \in \mathbb{R}^n$ is a number as close to one as x is deep inside the given half-space.
We define the *alarm region* to be the set of the points of the input space in which the device should give an alarm. The set of the remaining points will be called the *safe region.*

Characterization of the alarm region

Unfortunately, the alarm region is not assigned by any international standard's agreement and cannot be found with mathematical reasoning. It must be deducted from experimental data and on personal experience. Nevertheless, an important property will be pointed out which will help in defining the alarm region regardless of its convexity.
Let us consider, for the sake of simplicity, only the (T, S) plan, where T denotes

temperature and S smoke density; each input of the neural network is then a point on this plane. The following basic property is then reasonable: if a point is in the alarm region $\mathcal{A}$, by increasing the smoke, while maintaining the temperature constant, another alarm point can be found; the same happens if one increases the temperature keeping the smoke constant or, even more evidently, increasing both quantities. In other words (see Figure 1(a)):

$$\text{Axiom 1: } P = (T_P, S_P) \in \mathcal{A} \Rightarrow (T_P + h, S_P + k) \in \mathcal{A}, \forall h, k \in [0, \infty) \quad . \tag{3}$$

A similar property holds for a safe point (see Figure 1(b)):

$$\text{Axiom 2: } Q = (T_Q, S_Q) \notin \mathcal{A} \Rightarrow (T_Q - h, S_Q - k) \notin \mathcal{A}, \forall h, k \in [0, \infty) \quad . \tag{4}$$

Now, the boundary of the fire region is not known but can be guessed with the

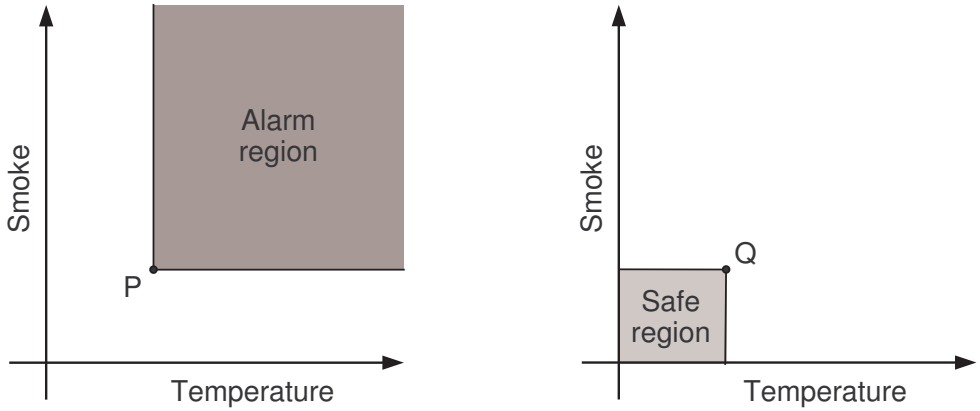

(a) (b)

Figure 1: Graphical explanation of Axiom 1 (a) and Axiom 2 (b)

following reasoning. For a point on the boundary both (3) and (4) are verified and the situation is as shown in Figure 2(a). Actually, one of the two properties must be slightly modified ruling out the case $(h, k) = (0, 0)$ in order to prevent the point from belonging both to the fire and to the non-fire regions. Let's assume, now, that the points A and B are known to belong to the boundary; what can be guessed about the curve $\gamma(T, S)$ describing the boundary between A and B? The properties (3) and (4) imply that γ is inside the white rectangle in Figure 2(b) and that locally it can always be expressed as a monotonic function $S = S(T)$ or $T = T(S)$. If one chooses to express it as $S = f(T)$ in the whole interval $[T_A, T_B]$. If f is unknown, what would be the best estimation for it?

Without loss of generality, one can set $A = (T_A, 0)$ and $B = (0, S_B)$. As an

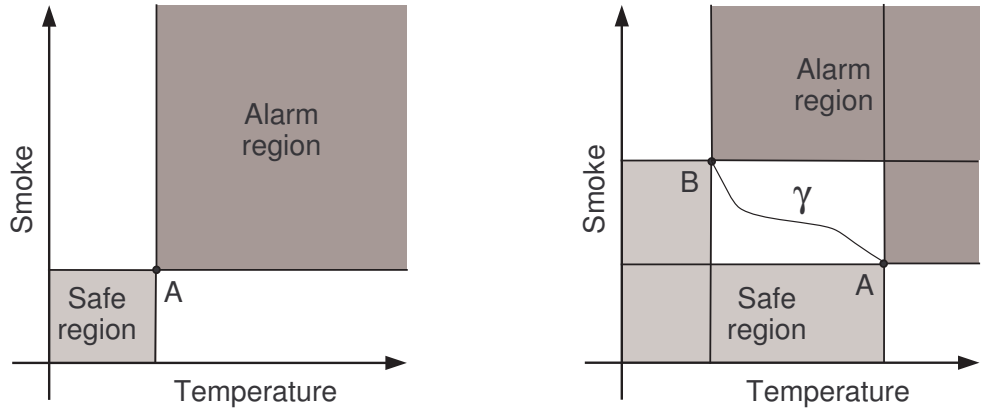

(a) (b)

Figure 2: Explanation of the reasoning used to biuld the boundary region

estimation of the error that is made by considering a wrong boundary an error function has been defined to be the distance between the real boundary and the estimated one. That is, given an estimator function g:

$$\epsilon(f,g) = \int_0^{T_A} |f(T) - g(T)| dT \quad , \tag{5}$$

which, in practice, is the area between the two functions[1], an optimal estimator for f is a function $\hat{g}$ that minimizes the error for all possible f's:

$$\hat{g} \text{ s.t. } \epsilon(f,\hat{g}) = \min_g \left(\max_f (\epsilon(f,g)) \right) \quad . \tag{6}$$

It is easy to see that such a g must have the following property:

$$\int_0^{T_A} g(T) dT = \frac{T_A S_B}{2} \quad . \tag{7}$$

In fact, if property (7) is not fulfilled, there are two possible cases:

- $\int_0^{T_A} g(T) dT < \frac{T_A S_B}{2}$

  In this case if the actual boundary is (for $0 < \delta < T_A$)

$$f(T) = \begin{cases} S_B & \text{for} \quad T \leqslant T_A - \delta \\ -\frac{S_B}{\delta} T + \frac{S_B T_A}{\delta} & \text{for} \quad T_A - \delta \leqslant T \leqslant T_A \end{cases} \quad , \tag{8}$$

[1] this function can be modified if false alarm and a missed alarm have different weights in the calculation of the decision error.

the integral (5) becomes

$$\int_0^{T_A-\delta} [S_B - g(T)]\, dT + \int_{T_A-\delta}^{T_A} |f(T) - g(T)| dT \quad . \tag{9}$$

For a sufficiently small δ, the second term of (9) is negligible and the first one is greater than $\frac{S_B T_A}{2}$.

- $\int_0^{T_A} g(T)dT > \frac{T_A S_B}{2}$

  In this case if the actual boundary is (for $0 < \delta < T_A$)

$$f(T) = \begin{cases} -\frac{S_B}{\delta}T + S_B & \text{for} \quad 0 < T \leqslant \delta \\ 0 & \text{for} \quad \delta \leqslant T \leqslant T_A \end{cases} \quad , \tag{10}$$

  an analogous reasoning can be made.

So far, just by assuming *Axiom 1* and *Axiom 2* we have found the property (7) for the boundary between the alarm and the safe regions. The simplest function fulfilling it is the straight line connecting A and B:

$$\hat{g}(T) = \frac{S_B}{T_A}T + S_B \quad , \tag{11}$$

and is the function that will be used to characterize the alarm region.

Improving the algorithm for non-convex regions

If a perceptron is used in order to take advantage of its separation property to characterize the alarm region, one has to be sure that at least one of the two regions is convex. On the other hand, what is the reasoning upon which the characterization of the separation surface is based? Does it always provide a convex region?

Let us take into account, for the sake of simplicity, a two-dimensional detector, for example a photo/thermal detector. The performance of this device must be at least as good as the performance of one of the detectors it uses, therefore if the photo/thermal plane is considered, a naive approximation of the alarm region can be found by considering only the thresholds (see Figure 3 (a)).

Nevertheless, in this case there is no data fusion between the two transducers and the device is just working as two separate detectors. A first idea to improve the performance could be to connect the two thresholds; in this way the photo-sensitivity is increased or decreased but the approximation is still too rough. (see Figure 3 (b)).

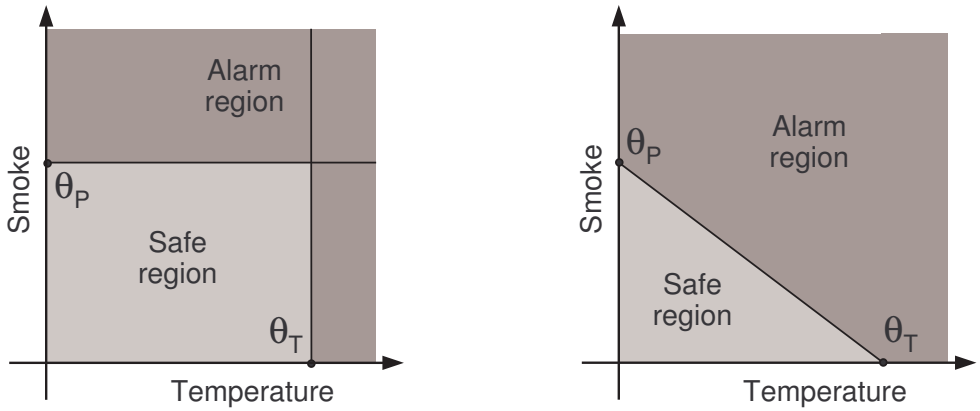

(a) (b)

Figure 3: Two simple approximations of the separation surface. In (a) no data fusion is used; in (b) a simple straight line is used in order to provide convex regions.

To have a separation line closer to the real one[2] two different photo thresholds and two different thermal thresholds can be set, as shown in Figure 4 (a). In this case,

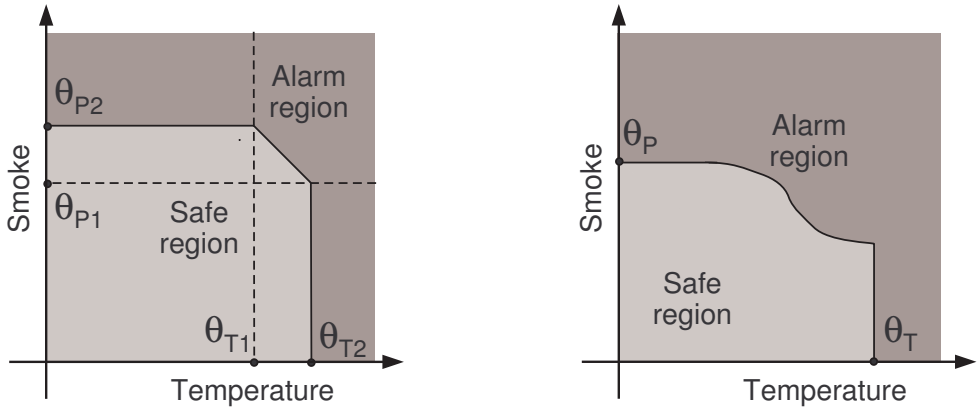

(a) (b)

Figure 4: Two improvements of the separation surface. In (a) the safe region is still convex; in (b) neither of the regions is convex but the approximation is much closer to the reality.

the device can work better than the previous one especially regarding the sensitivity to smoke; if the temperature is sufficiently high the smoke sensitivity is increased. In this case, the normal region is still convex and the conclusion of the previous section is still valid.

[2]always according to EN-54

Unfortunately, this kind of solution is applicable only in these simple cases. If one analyses more deeply the real situation, a better estimation of the separation surface turns out to be similar to the one in Figure 4 (b) (this surface is based upon System Sensor's experimental data). In this case, both regions are non-convex, and neither the alarm region nor the safe one can be described with a single perceptron.
The most simple solution is to approximate the alarm region with the nearest existing convex surface, as shown in Figure 5 (a). In this situation, the achieved accuracy

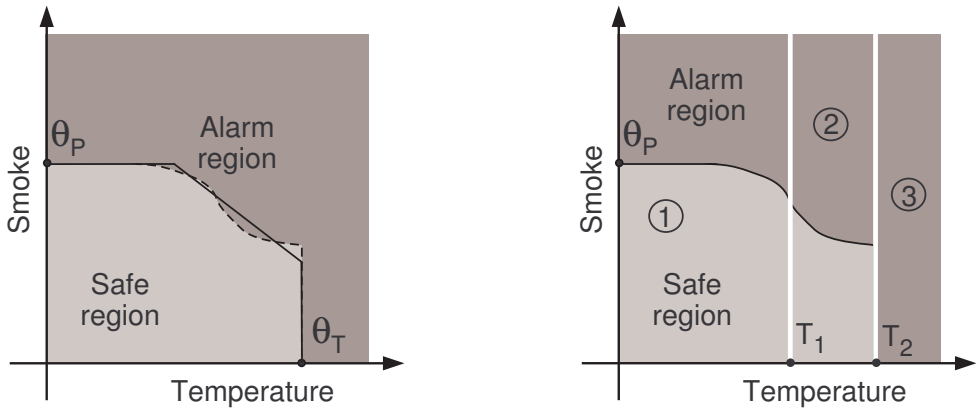

(a) (b)

Figure 5: Two applications of the perceptron to separate the alarm and the safe region. In (a) a simple perceptron gives a rough approximation; in (b) using three perceptrons a better approximation is achieved

could be good enough; nevertheless, it is easy to understand that as the number of transducers increases, the non-convexity of the alarm region becomes more and more defined. When the convex approximation is no longer acceptable, the normal neural structure based on the multilayer perceptron is no longer useful.
An obvious solution is then to divide the original region into a set of convex regions; actually, it has been proven that, given a maximum error ϵ it is always possible to approximate a given non convex n-dimensional region $\mathcal{A}$ into m convex regions such that the error is less than ϵ. In practice, the whole space is devided into a number of regions, for each of which, either the alarm or the safe region is convex. Then for each of them a perceptron can be designed and the final decision of the device, will be a logical combination of the multiple outputs, each given from a different perceptron-based neural network.
For example, the alarm region of Figure 4 (b) can be characterized by dividing the whole space into three vertical stripes as in Figure 5 (b). It is easy to see that the

regions 1, 2 and 3 are convex. The final alarm region can be obtained using a simple logic function synthesising the following behaviour: the output produces "alarm" when:

$$t < T_1 \text{ AND } (T, P) \text{ is outside region 1}$$
$$\text{OR}$$
$$T_1 \leqslant t < T_2 \text{ AND } (T, P) \text{ is inside region 2}$$
$$\text{OR}$$
$$T_2 \leqslant t \text{ AND } (T, P) \text{ is inside region 3.}$$

In this way, by combining a digital selector and three different neural networks, one can obtain, with the simple perceptron layer, a good non-linear approximation in the desired alarm region.

However, in order to realize this in practice, the solution can be improved if one uses a sigmoidal non-linearity instead of a step function; in this way the digital selector is no longer needed, and the non-convexity is neglected by the smoothing property of the sigmoid. In fact, let us refer to the same example (see Figure 6 where the white lines represent the boundary regions) and assume to have two more perceptrons approximately characterizing the two non-convex regions 4 and 5, respectively. Moreover, let the answer of the sigmoid be equal to the corresponding

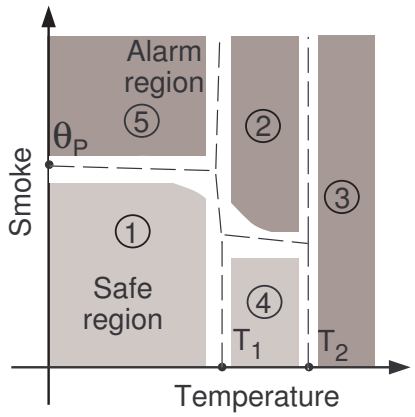

Figure 6: figura

step function when the (T, P) is far from the threshold θ of the neuron and assume it is equal to a value δ - such that $0 < \delta < 1$ - when the (T, P) is around θ. Finally, let $\mathcal{P}_i$ the output of the i-th perceptron, $\mathcal{R}_i$ the i-th region and $\mathcal{B}_{ij}$ the boundary between regions i and j. The answer of the three perceptrons will then be:

$$\mathcal{P}_1 = \begin{cases} 1 & \text{if} \quad (T,P) \in \mathcal{R}_1 \\ 0 & \text{if} \quad (T,P) \in \mathcal{R}_2 \bigcup \mathcal{R}_3 \bigcup \mathcal{R}_4 \bigcup \mathcal{R}_5 \bigcup \mathcal{B}_{23} \bigcup \mathcal{B}_{24} \bigcup \mathcal{B}_{25} \bigcup \mathcal{B}_{34} \\ \delta & \text{if} \quad (T,P) \in \mathcal{B}_{12} \bigcup \mathcal{B}_{14} \bigcup \mathcal{B}_{15} \end{cases}$$

$$\mathcal{P}_2 = \begin{cases} 1 & \text{if} \quad (T,P) \in \mathcal{R}_2 \\ 0 & \text{if} \quad (T,P) \in \mathcal{R}_1 \bigcup \mathcal{R}_3 \bigcup \mathcal{R}_4 \bigcup \mathcal{R}_5 \bigcup \mathcal{B}_{14} \bigcup \mathcal{B}_{15} \bigcup \mathcal{B}_{34} \\ \delta & \text{if} \quad (T,P) \in \mathcal{B}_{12} \bigcup \mathcal{B}_{23} \bigcup \mathcal{B}_{24} \bigcup \mathcal{B}_{25} \end{cases}$$

$$\mathcal{P}_3 = \begin{cases} 1 & \text{if} \quad (T,P) \in \mathcal{R}_3 \\ 0 & \text{if} \quad (T,P) \in \mathcal{R}_1 \bigcup \mathcal{R}_2 \bigcup \mathcal{R}_4 \bigcup \mathcal{R}_5 \bigcup \mathcal{B}_{12} \bigcup \mathcal{B}_{14} \bigcup \mathcal{B}_{15} \bigcup \mathcal{B}_{24} \bigcup \mathcal{B}_{25} \\ \delta & \text{if} \quad (T,P) \in \mathcal{B}_{23} \bigcup \mathcal{B}_{34} \end{cases}$$

$$\mathcal{P}_4 = \begin{cases} 1 & \text{if} \quad (T,P) \in \mathcal{R}_4 \\ 0 & \text{if} \quad (T,P) \in \mathcal{R}_1 \bigcup \mathcal{R}_2 \bigcup \mathcal{R}_3 \bigcup \mathcal{R}_5 \bigcup \mathcal{B}_{12} \bigcup \mathcal{B}_{15} \bigcup \mathcal{B}_{23} \bigcup \mathcal{B}_{25} \\ \delta & \text{if} \quad (T,P) \in \mathcal{B}_{14} \bigcup \mathcal{B}_{24} \bigcup \mathcal{B}_{34} \end{cases}$$

$$\mathcal{P}_5 = \begin{cases} 1 & \text{if} \quad (T,P) \in \mathcal{R}_5 \\ 0 & \text{if} \quad (T,P) \in \mathcal{R}_1 \bigcup \mathcal{R}_2 \bigcup \mathcal{R}_3 \bigcup \mathcal{R}_4 \bigcup \mathcal{B}_{12} \bigcup \mathcal{B}_{14} \bigcup \mathcal{B}_{23} \bigcup \mathcal{B}_{24} \bigcup \mathcal{B}_{34} \\ \delta & \text{if} \quad (T,P) \in \mathcal{B}_{15} \bigcup \mathcal{B}_{25} \end{cases}$$

Now, by using only $\mathcal{P}_1$ and $\mathcal{P}_4$ the sum $1 - \mathcal{P}_1 - \mathcal{P}_4$ can be calculated for each region and each boundary. It will be:

$$\begin{array}{ccc} \mathcal{R}_1 : 1-1-0=0 & \mathcal{R}_2 : 1-0-0=1 & \mathcal{R}_3 : 1-0-0=1 \\ \mathcal{R}_4 : 1-0-1=0 & \mathcal{R}_5 : 1-0-0=1 & \mathcal{B}_{12} : 1-\delta-0 \simeq 0.5 \\ \mathcal{B}_{14} : 1-\delta-\delta \simeq 0 & \mathcal{B}_{15} : 1-\delta-0 \simeq 0.5 & \mathcal{B}_{23} : 1-0-0=1 \\ \mathcal{B}_{24} : 1-0-\delta \simeq 0.5 & \mathcal{B}_{25} : 1-0-0=1 & \mathcal{B}_{34} : 1-0-\delta \simeq 0.5 \end{array}$$

As the results of this simple operation show, within the original alarm region ($\mathcal{R}_2 \bigcup \mathcal{R}_3 \bigcup \mathcal{R}_5 \bigcup \mathcal{B}_{23} \bigcup \mathcal{B}_{25}$) the answer is one; within the original safe region ($\mathcal{R}_1 \bigcup \mathcal{R}_4 \bigcup \mathcal{B}_{14}$) the answer is zero and only within the original boundaries ($\mathcal{B}_{12} \bigcup \mathcal{B}_{15} \bigcup \mathcal{B}_{24} \bigcup \mathcal{B}_{34}$) the answer is a number near 0.5.

A similar result can be obtained considering only $\mathcal{P}_2$, $\mathcal{P}_3$ and $\mathcal{P}_5$ and calculating $\mathcal{P}_2 + \mathcal{P}_3 + \mathcal{P}_5$.

In conclusion, for this simple case a good estimation of the alarm region can be given by a simple analogue adder or subtracter circuit, combining the networks outputs in one of the following ways:

$$\text{Alarm} = (2) + (3) + (5)$$
$$\text{Alarm} = \text{Not}(\ (1) + (4)\ )$$

Conclusions

We have used a novel approach, based on perceptron neural networks, which in some particular conditions behave as a non linear ideal approximator of the alarm region. It has been proved that in reality, even though the base hypothesis of convexity is not satisfied, it is always possible to split the alarm region into a number of convex regions, and use a digital selector to take the right network output. Moreover, using the smooth non linearity, instead of the step one, the digital selector becomes useless and a fully analog system can be obtained, with the use of only one linear combiner at the output of various neural networks.

References

1. M. Minsky and S. Papert, "Perceptrons: An Introduction to Computational Geometry", MIT Press, Cambridge, 1969.

2. T. Moriizumi, T. Nakamoto and Y. Sakuraba, "Pattern recognition in electronic noses by artificial neural network models", in *Sensors and Sensory Systems for an Electronic Nose*, J.W. Gardner and P.N. Bartlett eds., Kluweer Academic Publishers, Amsterdam, 1992.

3. B. Kosko, "Neural Networks for signal processing", Prentice Hall, 1992.

4. R. Hecht-Nielsen, "Neurocomputing", Addison-Wesley Longman, 1989.

5. J.M. Cruz and L.O. Chua, "Design of high-speed, high-density CNNS in CMOS technology", *Int. J. Circ. Theory Appl.*, **20**, 1992, pp. 555–572.

S. Penney

Tyco Safety Products, Sunbury - on - Thames, England

Use of Coincidence Detection to Improve Spurious Alarm Immunity

Abstract

Of all the new techniques proposed for early fire detection only carbon monoxide gas detection has realised any market potential, and that has been limited, with the point optical detector remaining as the main means of fire detection. This paper describes the development of a combined gas, heat, and optical detector, and investigates how each sensor signal can be most effectively combined.

The work faced challenges from 2 directions; the detector hardware had to be a practical proposition in terms of reliability, and production; and the signal processing needed to have a high degree of discrimination for 'genuine' fires. Before this could be achieved a number of investigations were needed to define the operational parameters both in terms of fire and potential 'false' alarm sources. The resultant detector embodies a solution to both these challenges.

Introduction

Ideally, we want to detect all unwanted fires in very early stages. As engineers in fire protection, this is obviously one of the major goals for each new fire detection system that we develop. This of course would be easy, were it not for the 'false positives' of very sensitive systems. So, within the fire detection community, the 'Holy Grail' we are seeking, is to be able to distinguish between genuine early fire indicators, and spurious alarm sources. Unlike the knights of old, what we are hunting for is not a magical relic that can be found by extracting information from the dust of the past.

Certainly past techniques have come a long way, and many sophisticated algorithms have been designed to try to extract more detail from the data presented to us by optical, and optical heat combinations. Indeed, our hosts here at Duisburg have built a considerable reputation, for their fuzzy logic analysis approach.[Ref. 1] The difficulty that

we have, is that there simply isn't sufficient raw information available for effective processing, and our Holy Grail remains hidden from the relic hunters.

Approach

A further degree of freedom can be provided to fire algorithms, by adding a carbon monoxide detection element, whose development was presented here in 1999,[Ref. 2] Since this time, thousands of carbon monoxide detectors have been fitted in a variety of applications, and it is now field proven as a detection means in its own right.

With this additional degree of freedom, the potential algorithm set increases enormously. In many ways, this would lend itself to the fuzzy approach using the carbon monoxide input to provide 2 additional linguistic variables. However, there are some practical difficulties; with the increase in complexity.

One of the constraints is that both measurements and algorithms need to be applied in real time using existing fire control equipment, without compromising system specifications. [Ref. 3] Another is that the probabilistic nature of fuzzy algorithms, has led to difficulties with field testing and fire types that customers perceive to be significant. For this reason an approach based on more conventional logic rules was pursued.

Preparing the ground

Before algorithm development could be undertaken, there were three major hurdles to be overcome. Firstly, there was the difficulty of combining all three technologies in a single device. There was a practical need for this device to fit the same overall mechanical envelope as the optical/heat detector, in order to use existing production equipment. It was also necessary to ensure that circuitry for each detection element does not compromise the operation of another one. Thirdly, even without adopting the fuzzy approach, it is still necessary to acquire the 'expert' knowledge (sensor response data) for all three sensors in both fire and spurious alarm scenarios.

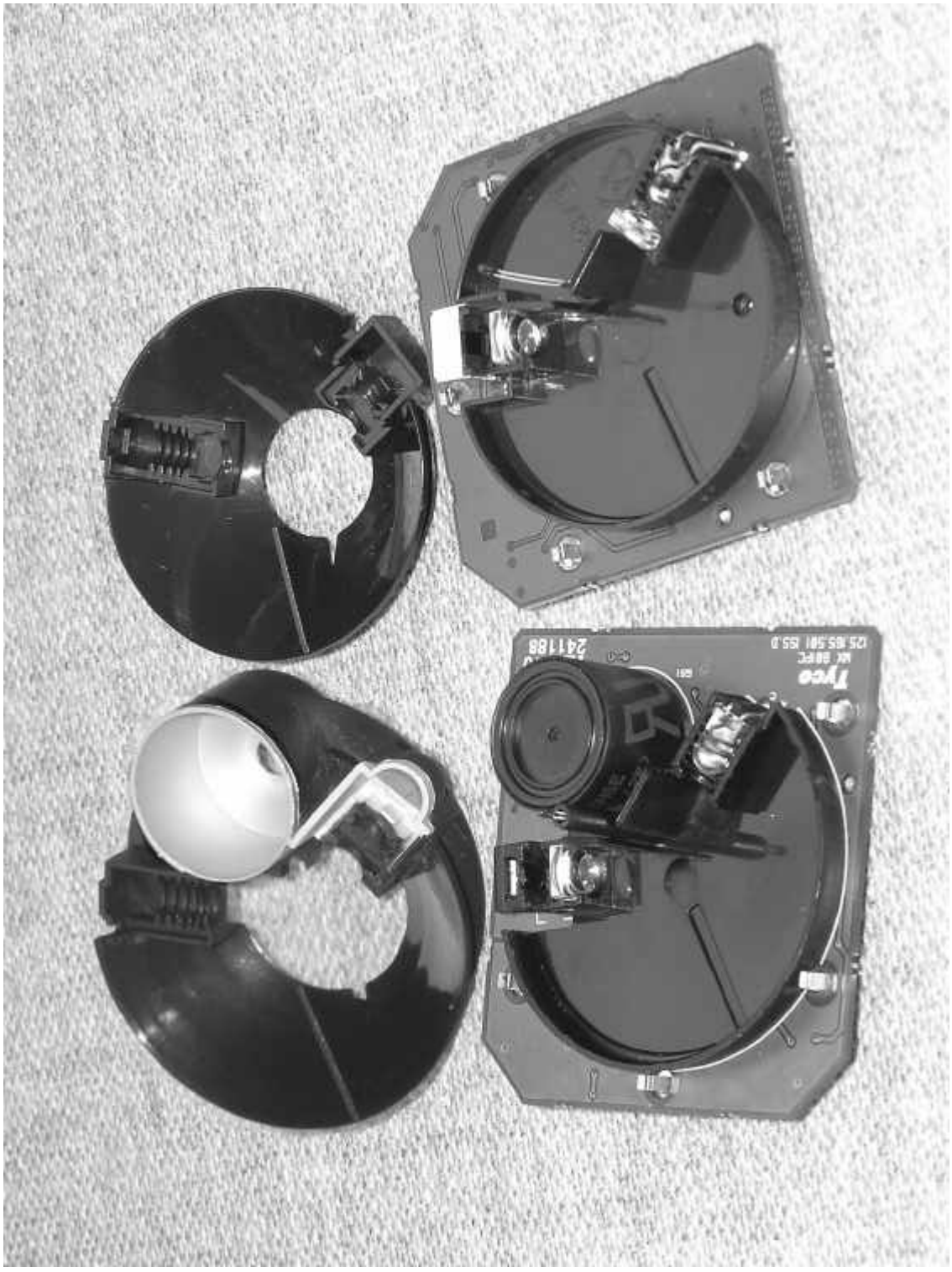

Figure 1: Existing heat optical detector PCB with chamber (top picture), compared with triple sensor arrangement (lower picture).

Feasibility

A hardware feasibility study using stereolithographic models demonstrated that including a carbon monoxide sensor within a ‘dead’ area of the existing labyrinth could be done, without too many adjustments to optical design. (See Figure 1).

The PCB was a slightly different problem, as the existing optical layout was already tight. In order to fit the carbon monoxide sensing circuit on as well some features would have to be removed. The optical and carbon monoxide self-test circuits were replaced by a means for continuously monitoring all three-sensor elements. This both reduces component count; and enables any sensor failure to be identified immediately.

Defining operational requirements

Traditionally fire detectors are approved against a series of standard test fires, [Ref. 4] and often not much else. Certainly, EN54 test fires (and fire tests defined by other national standards and proposed standards), provide a rich source of data, as they are well characterised, and any new algorithm will need to satisfy their criteria.

To maintain customer focus, a review was made of fire scenarios that presented a high perceived cause for concern. From this a series of ‘critical’ fire tests were established and from these tests a fire information base for each sensor element was built.

The justification of the three-sensor approach is to reduce false alarms. So potential spurious alarm data is as important as fire test data. This required a more inventive approach, as there is no definition of what a spurious alarm source is. For this, the market was used to get a customer view of what constitutes a spurious alarm.

For an industrial process with an inherently high fire risk, in a difficult environment, spurious alarms may well be tolerated, or even expected, causing only minor local disturbance. On the other hand, a cruise ship, or hospital evacuation is costly. By collecting field reports of ‘nuisance’ alarms, customer perception was used to guide in the design of a number of false alarm scenarios, to provide suitable spurious alarm data.

Building the database

During the research phase for the original carbon monoxide fire detector, a considerable body of fire test data, from carbon monoxide, optical, and heat detectors run in parallel had been gathered along with some data on potential false alarm sources. [Ref. 2,5]

However, some fundamental research into sensor responses was still required for the mathematical model to determine what the detector characteristics needed to be. The fires of most concern were those that start in electrical and electronic equipment. With the increase in the number of electrical appliances, this was perceived as high risk. The potential false alarm that raised greatest concern, was steam from a shower in a relatively confined area such as a passenger cabin, or a hotel bedroom. As smoking is increasingly regarded as an antisocial activity, with smokers relegated to designated areas, the perceived potential for false alarm from this source is greatly reduced.

Accordingly, the fire database was built up from results from the test fires, from electrical PCB fires in enclosures, and for false alarm data there was a typical ‘smokers’ room, and 2 types of shower test, (door either open continuously, or intermittently).

Establishing limiting factors

In each of these data sets, there were the 3 main variables, temperature, optical reading, and carbon monoxide reading. Associated with these is an averaged rate of change of each of the parameters. From observation of results, it was easy to see that not all scenarios would present limiting conditions for algorithm development. For example, TF3 (smouldering cotton wick) is high in carbon monoxide and visible particulates, so detection is certain whatever approach is taken. In this way, we could reduce the number of data sets used in the analysis.

It was observed that all fires gave either a clear optical signal, or high carbon monoxide levels, or both were present. The approach taken was to choose the optical sensor as a ‘key’ sensing input, with heat and carbon monoxide sensors mathematically modifying

the optical signal. A high carbon monoxide threshold was chosen as a fail-safe for smouldering fires, removing the need for those data sets in the algorithm definition.

Building a model

With the optical channel to provide the base signal, the next question faced is how should this be modified by the other inputs to produce a result that improves fire detection and minimises false alarms. The optical element requires a very insensitive setting for false alarm rejection, making the overall measurement range considerably larger than current optical detectors, it can then be enhanced to get the fire sensitivity.

Work had been carried out on a previous detector, to investigate the optimal way to enhance an optical detector to meet hot test fires, whilst keeping the baseline sensitivity adequate for the cooler fire requirements. This formed the basis for temperature enhancement of optical signal in the model. This is a sliding scale of enhancement based on the positive temperature difference from a 2-minute moving average.

The question remained as to how best to use the carbon monoxide input. Although this could also be an enhancement applied to the optical signal, it was decided that it would be easier to both visualise, and implement if the carbon monoxide input was used to modify the threshold point at which alarm, rather than modifying the optical signal.

The initial mathematical model was constructed within an Excel workbook, with each worksheet containing a set of results and derived data sets for a fire or false alarm scenario. The derived data was made as generic as possible, with a basic temperature enhanced optical output, a carbon monoxide derivative output, and two potential threshold variation equations. A control spreadsheet was generated that could simultaneously change the variables used in all the spreadsheets simultaneously.

Each sheet had a corresponding graph displaying the data sets in relation to the two potential threshold lines. This construction whilst appearing empirical enabled visualisation of ‘What if’ conditions on every critical condition simultaneously:

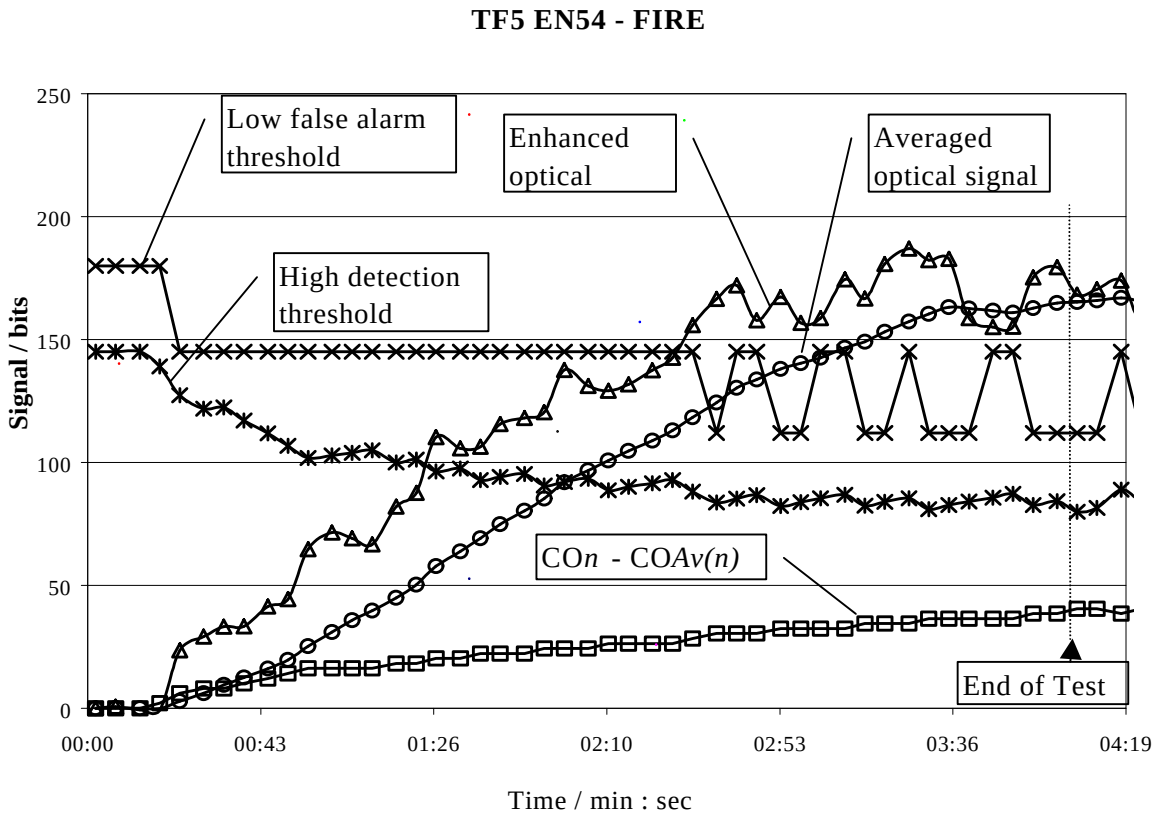

Figure 2. Typical representation of fire test results in a spreadsheet.

Initial analysis

One of the first benefits of this model was that it became apparent that false alarm conditions were considerably noisier than fire conditions. Applying a moving average to the optical signal removes the probability of a few peaks leading to alarm generation.

Because of the way the model was constructed, the number of samples used for performing the moving average could be varied to see the overall effect as the peaks were smoothed out. Although not appearing mathematically rigorous; this clear simple method enables an 'at a glance' determination of the best averaging sample size.

The second thing that was also apparent was that the carbon monoxide level was not going to provide a reliable consistent method of reducing optical threshold. This was most noticeable in the Decalin fire,[Ref. 6] and electrical fires where the absolute carbon monoxide levels are very low. Although the optical alarm threshold could be lowered

on this basis, any above average carbon monoxide background levels would remove the false alarm discrimination.

The derived data that seemed most appropriate as a threshold modifier was to use a difference value between the carbon monoxide level and a long term moving average. This has the effect of the resultant appearing as a combination of the carbon monoxide level and the rate at which that level was reached.

Redefining the problem

Following this initial work, we derived 3 equations, with a single unknown variable in each of them:

Averaged CO output, CO_{Av}

$$CO_{Av(n)} = \frac{(k-1)\ CO_{Av(n-1)} + CO_n}{k}$$

Where:

CO_n	CO at time $t=n$
$CO_{Av(n-1)}$	Average CO at time $t=n-1$
k	Samples for average

Alarm Threshold, A_{th}

$$A_{th} = 145 - [j * CO(RoR)]$$

Where:

CO(RoR)	CO*n* minus $CO_{Av(n)}$ (Positive results only)
j	Threshold modifier

Averaged Enhanced Optical output, EOAv

$$EOAv(n) = \frac{(p-1)\ EOAv(n-1) + EOn}{p}$$

Where:

EOn	EO at time t=n
$EO_{Av(n-1)}$	Averaged EO at time $t=n-1$
p	Samples for average

The question now is how to determine the optimum values for the 3 unknown variables k, j, and p. With all the data available, this could present a significant problem if

tackled mathematically. With the spreadsheet based visual model it becomes considerably simpler.

The best way of doing this is using an iterative process. A value of k needs to be sufficient to give an output significant enough to give a clear level of enhancement on the Decalin and Electrical fires, yet not cause significant enhancement on the Cigarette test. This then provides a good starting point for determining the other values.

Once the initial k value has been chosen, p for the optical moving average can be selected. This has to be chosen such that TF2 (pyrolysis), TF4 (polyurethane) and TF5 (n-heptane) are able to track relatively well; but the spurious noise signals from the shower data are minimised.

Having determined the k, and p values, establishing j is a question of varying the value until all fire types just reach alarm, with all non-fires failing to reach alarm. By displaying the critical graphs on the same sheet, with the 3 variables in 3 cells on that sheet, this can be done in a very straightforward way. It also enables 'what if' investigations on what happens when extreme values of the variables are used.

Selection of algorithm for practical use

A critical factor in the work so far is that it is based on simulations on a restricted data set. This will almost certainly have a corresponding spread in real life situations, and there may be an overlap between combinations of parameters seen in real fires and those seen in false alarm situations.

While the aim is to have one detector that serves both to provide detection of all fires and rejection of all spurious alarms, this is unlikely to be achievable using a single algorithm. However, the situation improves if we allow the user to bias the detector to either maximise false alarm rejection, or fire sensitivity. The person fitting the detector in their premises is usually best placed to evaluate which places the greatest risk to their business - false alarms or real fires.

So two algorithms were developed, one should be robust enough to miss every possible false alarm, the other should be sensitive enough to detect every possible fire at the earliest point, but retain a good resistance to false alarm.

Despite the complexity of what has gone into the development, the end user is left with a simple decision in the way they want to use the detector. Do they want enhanced resistance to false alarms, with a similar level of detection as they have currently; or do they want to have an enhanced assurance of detecting every possible fire, with a similar level of false alarm immunity.

Final choice

For the high detection alarm, the base sensitivity threshold of the optical sensor was lowered, and a low (optical averaging) p value was chosen to ensure no signals would be missed and the threshold would be lowered sufficiently. For the high false alarm resistance a slightly different approach was adopted.

As well as having a higher p value to give a higher smoothing of the optical signal from noise, there were 3 discrete thresholds chosen, depending on the carbon monoxide CO_n - $CO_{Av(n)}$ value. This removes any effects from minor fluctuations in this parameter, and gives an overall better resistance to spurious signals.

Conclusion

The results of this work has been the development of a fire detector that shows considerable promise as a means of reducing unwanted spurious alarm signals. The large experimental database has provided a solid base for the development of the coincidence detection algorithms.

At present these detectors are going through an extended approval programme, and field trials are underway to prove the theoretical model is able to deliver an improvement in real live situations.

References

(1) MÜLLER H-Ch. SIEBEL R.: "New Designed Dual-Sensor-Multi-logic-Detection Algorithm", Project Report from Gerhard Mercator Universität-GH Duisburg to Tyco, (April 4, 2000).

(2) PENNEY, S. J.: "Development of a New Fire Detection Technology", Proceedings 11, Internationale Konferenz über Automatische Brandentdeckung, P458-467, (Duisburg 1999).

(3) SIEBEL R.: "Strategies for the Development of Detection Algorithms", Proceedings, 12th International Conference on Automatic Fire Detection P163-175, (Gaithersburg 2001).

(4) EN54-7: 2000 "Fire detection and fire alarm systems – Part 7: Smoke detectors – Point detectors using scattered light, transmitted light or ionization. "

(5) DODGSON, J.R., SIMPSON, R.I. , LOWE, M., AUSTEN,M., BENTLEY,S., and WOOD, S.: "HPO2 Technical Closure Report", Internal Report XX. 2064/8, (September1994).

(6) CEA 4021: "Requirements and tests methods for multisensor detectors, which respond to smoke and heat, and smoke detectors with more than one smoke sensor. " (July 2003)

Martin Berentsen[1], Thomas Kaiser[1], Shu Wang[2]

1: Fachgebiet Nachrichtentechnische Systeme, Institut für Nachrichten- u. Kommunikationstechnik, Fakultät für Ingenieurwissenschaften, Universität Duisburg-Essen, Bismarckstrasse 81, 47048 Duisburg, e-mail: berentsen@sent5.uni-duisburg.de, thomas.kaiser@uni-duisburg.de

2: Department of Electronics and Information Engineering, Huazhong University of Science and Technology, Wuhan 430074, P.R. China,
e-mail: shuwang@mail.hust.edu.cn

Advanced Signal Processing on Temperature Sensor Arrays for Fire Location Estimation

ABSTRACT

This paper first reconsiders briefly the basics of fire source location estimation in a closed room. In this approach, temperature sensors arrays are used to extract relevant parameters out of the propagation of hot gases, caused by a fire, in order to perform location estimation. In addition to earlier publications [7],[8],[9] two ideas to increase robustness will be presented, and a faster calculation method for the required time delay estimation will be proposed. The algorithms satisfying the real-time requirements for prototype implementation.

1. Introduction

To give an answer to the question: "Where is a fire located ?", this paper is structured into three parts. The first will give an overview about the location principle with temperature sensor arrays. These algorithms are verified by numerous fire experiments. A prototype system was also presented [9]. The second part discusses an optimization method related to the robustness of the implementation. The third part presents an idea for a numerically efficient time fast delay estimation method. This estimation is required for the location estimation of the fire source, which seems to be useful for the proposed location method. When we are talking about fire location estimation, we have to take a look at a fire in an

early stage. The hot gases are rising up from the fire place near the floor to the ceiling. Then the hot gases will propagate along the ceiling to the walls. Such a behavior is shown in figure 1. Due to more or less strong turbulences the shape of the temperature wavefronts

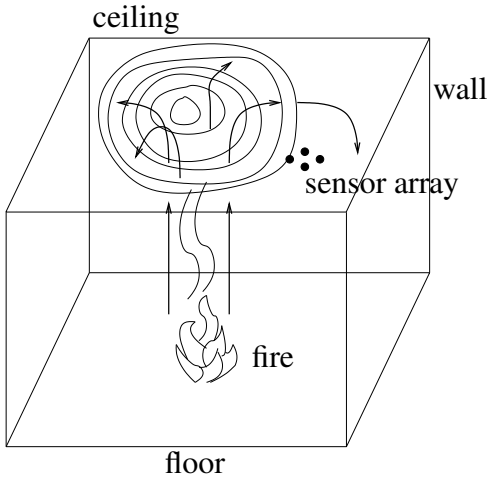

Figure 1: fire in a closed room shown with shematic flow directions

will not be perfectly circular. However, if we average in time, an almost circular shape can be expected. This observation is fundamental for the so called ”far field” algorithm, which will be explained in the following. However, this circular behavior seems to be of limited duration. When a fire grows up, the hot gases become more turbulent, and the propagation becomes more and more of non-circular shape.
Some boundary conditions must be fulfilled for the following considerations:

- The ceiling should be flat with a low heat conductivity.
- The flow current velocity $\vec{v}$ of the hot gases should be nearly constant under the ceiling in the early state of fire.
- The fire is near the floor level.
- The walls are at the same temperature.
- The fire is not located directly next to a wall.
- Other air currents, e.g. caused by a heating system, should be neglected.

2. Far Field Algorithm

In the so-called "far field" scenario the propagation of the hot gases under the ceiling can be modeled as a stochastic temperature $T(x,y,t)$ wave front of circular shape. Suppose a flat ceiling, a radius r can be introduced as

$$r = (x-x_0)^2 + (y-y_0)^2,$$

where (x_0, y_0) represents the coordinates of the projection from the fire to the ceiling. With the given assumptions the waveform is of circular shape, its expectation $\mathrm{E}\{X\}$ becomes only a function of time on a fixed radius

$$\mathrm{E}\{T(x,y,t)\}\big|_{(x-x_0)^2+(y-y_0)^2=r} = f(t), \qquad r \in \mathbb{R}_+.$$

Note that $T(x,y,t) = T(r,t)$ is only a function of radius and time. Hence, we use the notation $T(r,t)$ instead of $T(x,y,t)$ in the following. Note also that a fixed point (x_n, y_n), e.g. the location of the n-th sensor, the temperature function $T(t)|_{r_n}$ is only a function of time.

Since the meaningful frequencies in the case of fire are limited up to approx. 10Hz [1], a sampling frequency of $f_A \leq 100\mathrm{Hz}$ seems to be more than sufficient. Assuming a rather simple model, the temperature samples from N sensors at the location (x_n, y_n) can be modeled as

$$T_n(k) = S_n(k) + N_n(k), \quad n = 1(1)N, \tag{1}$$

where $S_n(k)$ might be interpreted as a deterministic signal caused by the fire, and the noise $N_n(k)$ represents thermal noise and potential turbulences. If the range r between the fire place projection under the ceiling (x_0, y_0) and the location of the sensor array $(x_n, y_n)$is quite large compared to the array dimensions $(d \times d \ll r)$, the temperature wave under the ceiling can be seen as a *quasi* planar wavefront. In figure 2 such an array of sensors S_1, S_2, S_3, S_4, is shown in the distance r from the fire place projection under the ceiling. The wavefront is shown as *quasi* planar with velocity $\vec{v}$.

With knowledge of the geometric order of the sensors inside the array and the assumption of a quasi planar wavefront with the velocity $\vec{v}$, this illustrated wave reaches sensor S1

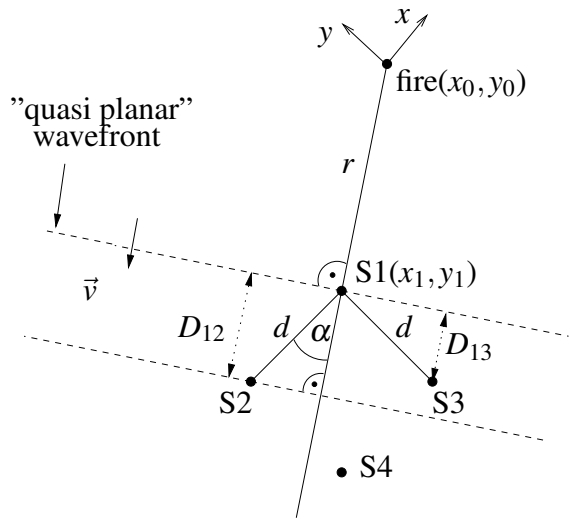

Figure 2: geometrical arrangement of the sensor array in the far field behaviour

first, then S3, then S2 and finally S4. In the following the time delay between S_n and S_m is denoted as D_{nm}.

Based on this signal model the location estimation problem can be reduced to a *time delay estimation problem*

$$T_1(k) = S(k) + N_1(k)$$

$$T_n(k) = \alpha_n S(k - k_{1n}) + N_n(k), \quad n \neq 1$$

with unknown delays k_{1n} and scaling factor α_n. Observe that the deterministic signal $S(k) \stackrel{\text{def}}{=} S_1(k)$ arrives as a delayed replica $S(k-k_{1n})$ at sensor S_n.

Several signal processing algorithms for time delay estimation have been investigated [2],[6]. In order to understand the principles, we will focus on the so-called SCC-algorithm (Simple Cross Correlation) only. The cross-correlation between the first and the n-th sensor output is defined as

$$R_{1n}(\kappa) = E\{T_1(k)T_n(k+\kappa)\}, \quad n = 2(1)4.$$

Assuming uncorrelated noise $N_n(k)$ yields

$$R_{1n}(\kappa) = E\{S(k)S(k-k_{1n}+\kappa)\}, \quad n = 2(1)4.$$

Obviously, the maximum of $R_{1n}(\kappa)$ occurs for $\kappa = k_{1n}$, since the argument becomes for arbitrary $S(k)$ always positive. Hence, in order to estimate k_{1n}, only maximum of the cross

correlation has to be searched. Usually $R_{1n}(\kappa)$ is estimated by averaging the temperature sample vectors from $T_1(k)$ and $T_n(k)$. However, because of the non stationarity of a fire, a moving average

$$\hat{R}_{1n}(\kappa,k) = \frac{1}{L}\sum_{l=m}^{L+m-a} T_1(l)Tn(l+\kappa), \quad n = 2(1)4, \quad k = \frac{m}{M},$$

$$m = 0(M)K-L, \quad \kappa = -\kappa_{max}(1)\kappa_{max}.$$

is more meaningful. Such a time-variant correlation can either be exploited to track propagation of fires, or, if the fire is becoming more and more turbulent, to stop the location estimation in case of highly dynamical and therefore unreliable results. Note that the hat indicates an estimation. The non-stationarity of the signals is taken into account by the time dependence $k = \frac{m}{M}$ of $\hat{R}_{1n}(\kappa,k)$. The measured signals are composed of non-overlapping blocks with length L. In order to save processing power, the estimation is only calculated each M-th time instant, where $M > 1$ and integer. κ_{max} should be chosen small in order to limit the required processing power .

After estimating the time delays, the mathematical relations between these delays and the parameters r, α and $\vec{v}$ are necessary. For $r \gg d$, i.e. quasi planar wavefronts, it follows

$$|\vec{v}|\frac{k_{12}}{f_A} = d\cos\alpha, \qquad |\vec{v}|\frac{k_{13}}{f_A} = d\sin\alpha.$$

So the parameters α and $\vec{v}$ can be written as

$$\alpha = \arctan(\frac{k_{13}}{k_{12}}), \qquad |\vec{v}| = f_A\frac{d\cos\alpha}{k_{12}},$$

where d and f_A are known a-priori. Actually, the fourth sensor S_4 seems to be redundant, but it can be exploited to further improve the estimation by averaging.

$$\hat{\alpha} = \frac{1}{3}\left(\arctan(\frac{\hat{k}_{13}}{\hat{k}_{12}}) + \arctan(\frac{\hat{k}_{23}}{\hat{k}_{14}}) + \arctan(\frac{\hat{k}_{24}}{\hat{k}_{34}}) + \frac{\pi}{4}\right), \tag{2}$$

$$|\hat{\vec{v}}| = f_A\, d\ \text{median}\left(\frac{\sin\hat{\alpha}}{\hat{k}_{13}}; \frac{\cos\hat{\alpha}}{\hat{k}_{12}}; \frac{\sin\hat{\alpha}}{\hat{k}_{24}}; \frac{\cos\hat{\alpha}}{\hat{k}_{34}}; \frac{\sqrt{2}\sin(\hat{\alpha}-\frac{\pi}{4})}{\hat{k}_{23}}; \frac{\sqrt{2}\cos(\hat{\alpha}-\frac{\pi}{4})}{\hat{k}_{14}}\right). \tag{3}$$

Note that the "median" operation increases robustness against outliers. Beside $\hat{\alpha}$ a second angle is required for triangulation the location. In our case we place another sensor array in the same observation room, so that two angles $\hat{\alpha}_1$ and $\hat{\alpha}_2$ can be determined to

perform location estimation. In order to evaluate the quality of the estimation an *error measurement* is required

$$\Delta r(k) = \sqrt{(x_0 - \hat{x}_0(k))^2 + (y_0 - \hat{y}_0(k))^2}. \tag{4}$$

The error distance $\Delta r(k)$ allows to investigate the proposed algorithm by real experiments.

3. Near Field Algorithm

The "far field" algorithm fails, if the temperature wavefront is not quasi planar as assumed. Exploiting the spatial signature as an *additional* information is the aim of the following approach. First, we take a closer look into the the array environment, illustrated in figure 3. Observe that three triangles can be defined between the single sensors S2, S3 and S4, the sensor S1 and the fire source coordinates (x_0, y_0). Writing down the relations for these

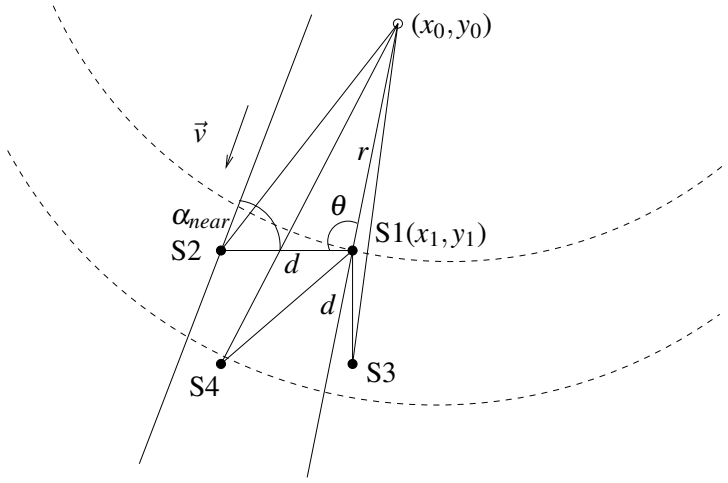

Figure 3: Sensor array geometric inside the circular wavefront behaviour

triangles, we obtain

$$(|\vec{v}|\frac{k_{12}}{f_a} + r)^2 = r^2 + d^2 - 2rd\cos(\theta) \tag{5}$$

$$(|\vec{v}|\frac{k_{13}}{f_a} + r)^2 = r^2 + d^2 - 2rd\cos(\frac{3\pi}{2} - \theta) = r^2 + d^2 + 2rd\sin(\theta) \tag{6}$$

$$(|\vec{v}|\frac{k_{14}}{f_a} + r)^2 = r^2 + \sqrt{2}d^2 - 2\sqrt{2}rd\cos(\frac{\pi}{4} + \theta) = 2d^2 + r^2 - 2rd\cos(\theta) + 2rd\sin(\theta). \tag{7}$$

Rewriting these three equations leads to

$$(|\vec{v}|\frac{k_{12}}{f_a})^2 - d^2 = r(-2(|\vec{v}|\frac{k_{12}}{f_a}) - 2d\cos(\theta)) \tag{8}$$

$$(|\vec{v}|\frac{k_{13}}{f_a})^2 - d^2 = r(-2(|\vec{v}|\frac{k_{13}}{f_a}) - 2d\sin(\theta)) \tag{9}$$

$$(|\vec{v}|\frac{k_{14}}{f_a})^2 - 2d^2 = r(2d\sin(\theta) - 2(|\vec{v}|\frac{k_{14}}{f_a}) - 2d\cos(\theta)). \tag{10}$$

Equation (8), (9) and (10) yield immediately

$$r = \frac{(|\vec{v}|\frac{k_{14}}{f_a})^2 - (|\vec{v}|\frac{k_{12}}{f_a})^2 - (|\vec{v}|\frac{k_{13}}{f_a})^2}{2\left((|\vec{v}|\frac{k_{12}}{f_a})^2 + (|\vec{v}|\frac{k_{13}}{f_a})^2 - (|\vec{v}|\frac{k_{14}}{f_a})\right)}. \tag{11}$$

For the angle α_{near} it is possible to calculate three delays; for example

$$\alpha_{near} = \pi - \theta, \;\; \tan\theta = \frac{(|\vec{v}|\frac{k_{13}}{f_a})^2 + 2r(|\vec{v}|\frac{k_{12}}{f_a}) - d^2}{d^2 - (|\vec{v}|\frac{k_{12}}{f_a})^2 - 2r(|\vec{v}|\frac{k_{12}}{f_a})}. \tag{12}$$

However, the velocity $|\vec{v}|$ of the hot gases inside the array are yet unknown. For reasons of simplifying and implementability $\left|\hat{\vec{v}}\right|$ is taken from equation (3), meaning some mixture between near- and far field approach. We further define an angle δ, which represents the maximum difference between the single estimations inside equation (2). With the definition of a threshold, for example $\delta \leq 10°$, we have found a criteria for the algorithm choice. The estimator output value $\hat{\alpha}$ will be chosen over this criteria between equation (2) and (12). With this method we do not only detect bad values from the "far" algorithm. We also try to increase the accuracy of the complete estimator.

4. 1-bit Time Delay Estimation

Although complexity has been reduced, the proposed time delay estimation with correlation methods still requires significant processing power. In order to further reduce complexity, a so called "1-bit" algorithm is applied. It depends on to the signal shape, the array geometry and size, and the velocity $\vec{v}$ inside the array. The basic principle is illustrated in the following four figures for signals $S_1(k)$ and $S_2(k)$ taken from two sensors. The low complexity algorithm works as follows.

1. Step: The two signals $S_1(k)$ and $S_2(k)$ for time delay estimation has to be offset free, this can be easily achieved by high pass filtering.

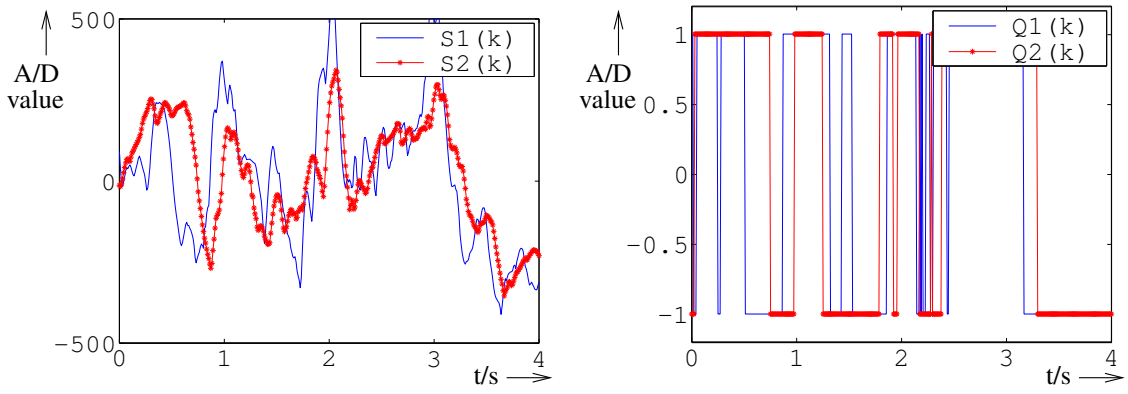

Figure 4: a) $S_1(k)$ and $S_2(k)$ as output of step 1 b) $Q_1(k)$ and $Q_2(k)$ as output of step 2

2. Step: The signals are "1-bit" quantizied.

$$Q_n(k) = \begin{cases} 1 & : \text{ if } S_n(k) \geq 0 \text{ (positive)} \\ -1 & : \text{ if } S_n(k) < 0 \text{ (negative)} \end{cases}$$

After this step the sign of the delay time can be extracted by memorizing the signal changing steps.

3. Step: Now these rectangular signals $Q_1(k)$ and $Q_2(k)$ are multiplied sample by sample by each other

$$P_{12}(k) = Q_1(k) \cdot Q_2(k).$$

The output function $P_{12}(k)$ includes the delay times. They have to be counted based on this function and be averaged for a fixed time window.

4. Step: Now the discrete time steps between the signal steps from +1 to -1 and -1 to +1 has to be counted. The results are shown in figure 5b.

Note that this approach only requires 1-bit processing leading to efficient implementations with low power requirements.

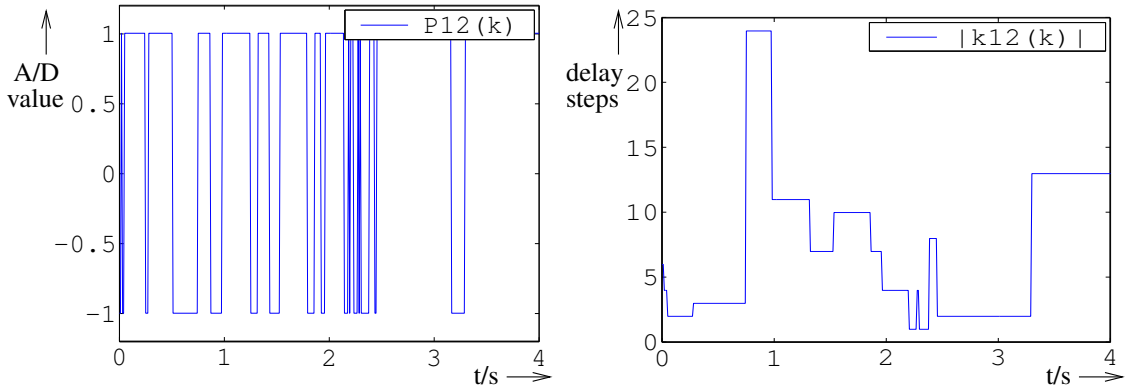

Figure 5: a) $P_{12}(k)$ out of step 3 b) $|k_{12}(k)|$ as delay step value

5. Conclusion

With respect to a practical implementation, a ”low calculation power” method for optimization seems to be found. The idea of using the worse estimation values from the ”far” algorithm and recalculate them with the ”near” algorithm seems to be practicable. Also the ”1-bit” time delay estimation algorithm seems to be feasible enough for an implementation. So, first these algorithms have to be verified by practical experiments. Then, for a suceeding evaluation of the prototype system these two optimizations will be taken into account.

References

[1] G. Cox, R. Chitty, ”Some Stochastic Properties of fire Plumes”, Fire and Materials, vol. 6, no. 3+4, 1982

[2] G. C. Carter, ”Coherence and Time delay Estimation”, Proceedings of the IEEE, vol. 75, no. 2, pp. 236-255, February 1987

[3] L. Eikermann, ”Ortsbestimmung von Bränden unter der Verwendung eines Temperatursensorfeldes”, Studienarbeit,Gerhard-Mercator-Universität Duisburg, 1997

[4] L. Eikermann, ”Weitere Untersuchungen zur Ortsbestimmung von Bränden”, Diplomarbeit, Gerhard-Mercator-Universität Duisburg, 1997

[5] A. Telljohann ”Vorarbeiten zum Aufbau eines Prototypen zur Ortsbestimmung von Bränden”, Studienarbeit, Gerhard-Mercator-Universität Duisburg, 1999

[6] R. Sprenger ”Ein erster Ansatz zur signalprozessorbasierten Brandortbestimmung”, Diplomarbeit, Gerhard-Mercator-Universität Duisburg, 1999

[7] T. Kaiser, ”Ortsbestimmung von Bränden mit Temperatursensorgruppen”, AUBE 99 proceedings, pp.52-66, 1999

[8] T. Kaiser ”Fire Detection with Temperature Sensor arrays”, IEEE Carnahan Conference proceedings, 2000

[9] M.Berentsen, T.Kaiser: ”Fire location estimation using temperature sensor arrays”, AUBE 01 proceedings, pp. 432-443, 2001

Rainer Siebel

Universität, Duisburg-Essen, Germany

Test of fire detection algorithms using artificially generated events

Abstract

The paper proposes a test method which is particularly suitable for the test of the false alarm rejection features of detection algorithms. It describes how to generate signal events artificially, which are similar to those occurring in practice and thus may or may not cause false or unwanted alarms. The generated events are of random nature, i.e. the signal shape, amplitude and duration of the events is randomly varied and the points in time, where these events occur, are randomly selected according to a well defined signal model. A set of parameters controls the event density, the probability for the duration of events, the fluctuation and the full dynamic range.

The whole signal model uses only one pseudo random generator and generates a modified "random walk process". Thus, it is either possible to reproduce with the same set of parameters for the signal model the same random sequence of events or, alternatively, to generate different random signal sequences using a different seed for the pseudo random generator. The test procedure is carried out in form of a computer simulation in time lapse mode and thus requires the detection algorithm to be available as a C-program.

1. Introduction

Modern fire detectors show good detection capabilities in the case of test fires as well as in genuine fires, but the rate of false or unwanted alarms is quite high (about 10..20 false or unwanted alarms per true alarm). The more automatic fire detectors are installed, the more serious becomes the false alarm problem.

There are various possible means available for reducing the false alarm rate:

- A professional design of the hardware for fire sensors and detectors.
- The use of multi-sensor fire detectors.

- The implementation of advanced detection algorithms with pre-selectable operating modes for different installation environments.
- The automatic adaptation of detection algorithms to varying environmental conditions.

However, the test of the false alarm resistance of fire detectors is in any case a difficult problem and, probably for this reason, test laboratories do not test the false alarm behaviour at all. It may be possible to define and standardize a limited number of false alarm tests, but the application of such tests is time-consuming and expensive.
A cheap alternative exists at least for the test of detection algorithms. Modern fire detectors use more sophisticated methods than a simple comparison of the fire-sensor signal with an alarm threshold. Such detection algorithms are usually implemented on microprocessors; hence there exist detection programs usually written in C, C++ or assembler. If we could generate artificial but somehow typical fire sensor signals for false alarm-relevant events and define for different environments the density of such events in time, this might help to optimise the overall performance of detection algorithms and/or to compare the quality of different detection algorithms using time lapse computer simulation methods.
The shortcoming of this method is that we do not test the features of the sensors and their hardware with respect to false alarm-relevant environmental events. But we definitely know, that the corresponding sensor signals of such events are of a random nature in genuine fire situations as well as in No-fire environments. Even if the statistical features of generated artificial events do not perfectly match what occurs in practice, the application of such a method is better than no false alarm test at all, and for adaptive detection algorithms it is the only reasonable method.

2. Design targets for the test generator.

Almost everywhere in our industrialized world controlled combustion processes occur, for example, in the combustion motors of cars and machines, in the heating of buildings, combustion processes in production plants, lighted cigarettes, cooking etc. Consequently, combustion products like smoke, gas, heat are found almost everywhere. Moreover,

sensors used for fire detection purposes show cross-sensitivities for other environmental components, e.g. dust, vapours etc. for smoke sensors, some gas sensors respond to various chemical components. Moreover, the ambient temperature varies significantly during the day and over the year in normal environments.

From field measurements in different No-fire environments it is known, that fire sensors generate signals of a more or less long duration and of more or less high amplitudes, which may or may not cause false or unwanted alarms. Such events occur at random in time with different event densities, depending on the installation environment.

Hence, a generator for such events should generate events at random points in time with random shapes, amplitudes and durations. Moreover it should enable the adjustment of

1. the dynamic range and quantization of the output signals,
2. the event density, i.e. the average number of events per time period with the aim of simulating more or less “dirty” environments,
3. the probability for the occurrence of high amplitudes, i.e. the probability for the event amplitude to exceed a given percentage of the adjusted dynamic range,
4. and/or the probability for the occurrence of long event durations, which usually cannot be adjusted independently of the event amplitude.
5. the sample rate,
6. and the test period in years.

3. Realization of the test generator.

The heart of the event generator is a pseudo random number generator, which produces statistically independent uniformly distributed random numbers and is initialized with a so called “seed value”. With the same seed value it always produces the same sequence of random numbers. Hence, all signals derived from this source can be reproduced. This is advantageous, because it is possible to test two different detection algorithms with identical event sequences. Alternatively, it is possible to test the same detection algorithm with different event sequences if a different initial seed value is used.

First it is necessary to generate those random points in time where the signal events occur with a predetermined event density λ.

$$\lambda = \frac{\text{number of events}}{\text{time period}} = \frac{n}{T} \quad (1)$$

Since the time is quantized by the predetermined sample rate Δt, there are $\frac{T}{\Delta t}$ samples in the whole time interval T. Thus, it is necessary to generate n numbers - independent of each other - using a random generator which produces uniformly distributed numbers in the range $\frac{T}{\Delta t}$. These numbers represent the time-instances, in which events occur. The gaps between all of these time-instances are filled with nominal No-fire values.
The test time period T may be some years. Thus, $\frac{T}{\Delta t}$ is usually a very large number. For a sample rate Δt =1/s and a test period T=1 year, $\frac{T}{\Delta t} \approx 31 \cdot 10^6$.

The method for generating events, which show typical characteristics of smoke sensor responses is a so-called “modified random walk process”. The underlying theory is discussed in the appendix together with the theoretical background for the calculation of the probability for the duration and height of such events. This method provides two independently adjustable parameters p and Δx. p controls the probability for the duration of events, which is not independent of the maximum amplitude of such events, because long events usually show higher amplitudes than short events. The positive real parameter Δx is used to adjust the fluctuation of generated events, but does not change the probability for the duration of events. An additional vertical scale factor v provides the adjustment for the full dynamic range of the signals. A few generated typical events of comparatively long duration, which resemble the output signals of smoke sensors in the earliest phase of a fire, are shown in **Fig. 1**.
The probability of the length of events is calculated in the Appendix. The results are shown in **Fig. 2**. Obviously, most of the generated events are of a quite short duration n. The lower p, the lower the probability to obtain long events. Example: with the parameter $p = 0.45$ the probability of generating an event of length $n = 150$ is $\approx 10^{-4}$, in other words, on the average, one of $\approx 10^{+4}$ generated events shows a length of 150 samples, whereas with $p = 0.35$ one of $\approx 10^{+6}$ generated events shows a length of 150 samples.

Moreover, it is necessary to find the probability for the amplitudes of long events to exceed a given threshold. The event generator is designed in such a way, that all samples

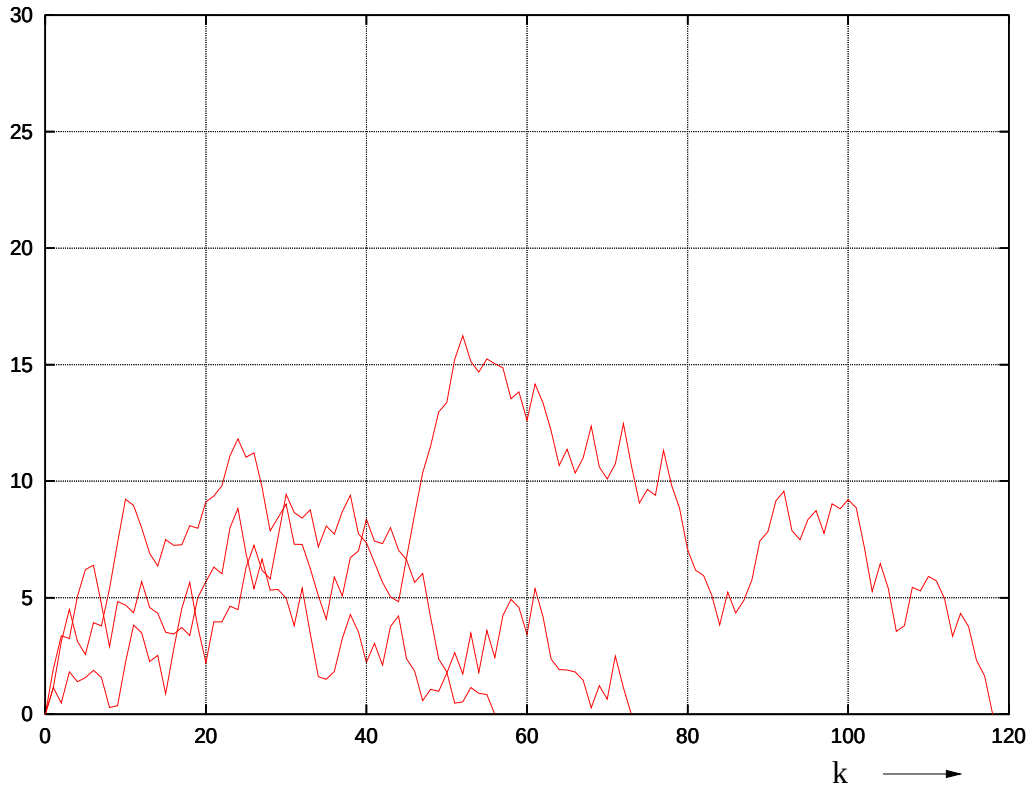

Fig. 1: Three examples of events with comparatively long duration

of an event must be positive and that the highest possible amplitude is $y(n)_{\max} = 2n \cdot \Delta x$, although $y(n)_{\max}$ is extremely unlikely to occur. Thus, the most frequently occurring events of short duration show comparatively low amplitudes. Since the parameter Δx does not change the probability for the length of events, it is normalized to $\Delta x = 1$ for the calculations. Two contour diagrams in **Fig. 3** show these probabilities for long events as functions of n and the parameter p. The negative numbers on the contour lines indicate the $\log_{10}$ of these probabilities. Clearly, an event which exceeds a threshold value $y_s >> 0$ at the n-th sample has a total length, which must be much longer than n. This happens quite seldom, according to **Fig. 2** for large n. Moreover, the probability for the amplitude to exceed $y_s = 10$ or $y_s = 20$ is low (for example 10^{-4} for $n = 100$, $p = 0.35$ and $y_s = 10$). Hence, for $\Delta x = 1$ and $p < 0.45$ it is very unlikely to obtain events of a higher amplitude than 20. It is not impossible, however, because the event generator represents a pure stochastic model.

With the same generator it is also possible to generate events, which resemble a typical

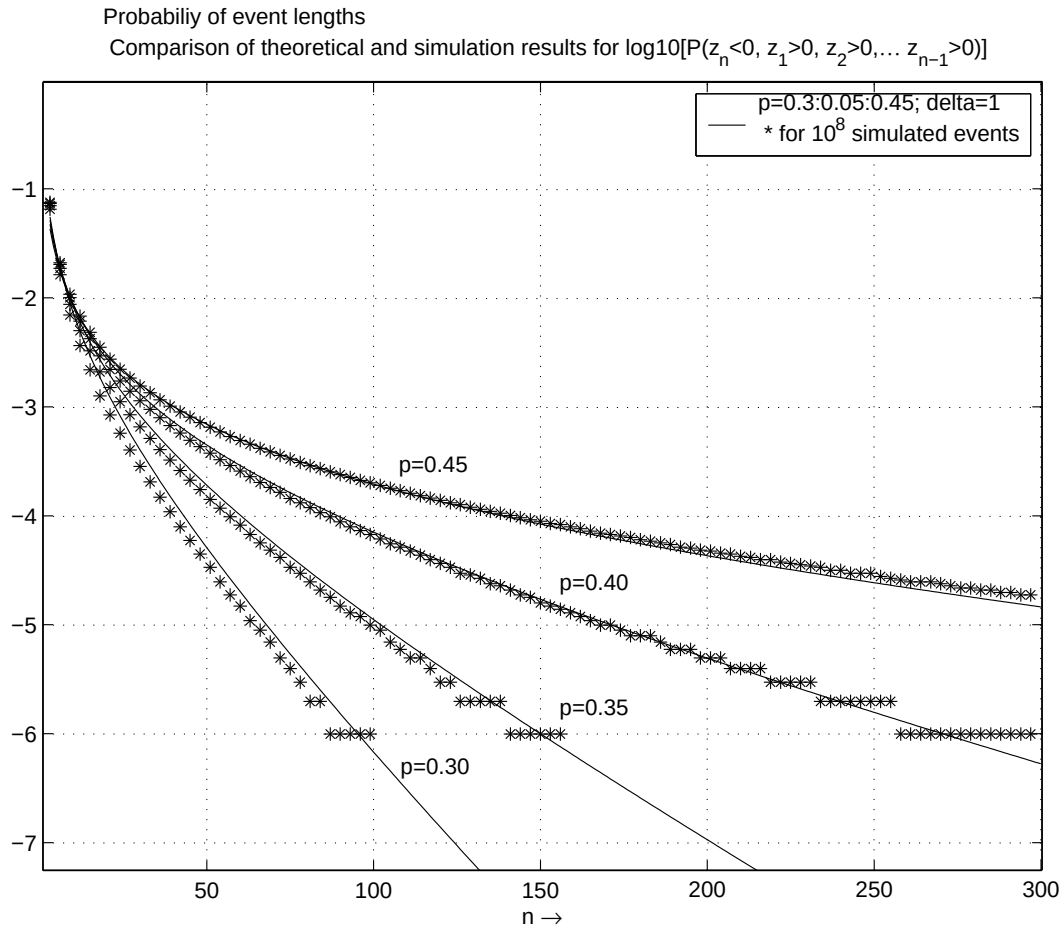

Fig. 2: Comparison of simulation results (*) and theoretical calculations —— for the probability of the length of events. The vertical scale is logarithmic.

fire situation. With parameter $p > 0.5$ it is more likely that the generated event exceeds a certain saturation value rather than to return to zero beforehand. The parameter Δx, in this case, allows to adjust the amplitude fluctuation. A few examples of such events are shown in **Fig. 4**.

Events as shown in **Fig. 1** and **Fig. 4** are similar to smoke sensor events in No-fire and fire situations, respectively. Heat or gas sensor signals are usually smoother. The same event generator can be used, however, to generate heat and/or gas sensor events. This requires passing generated signals through adequately chosen low-pass filters. The corresponding theoretical considerations for this technique would exceed the scope and the number of permitted pages for this publication. It is possible however, to generate simultaneously smoke, heat, and gas events either mutually independent or jointly dependent.

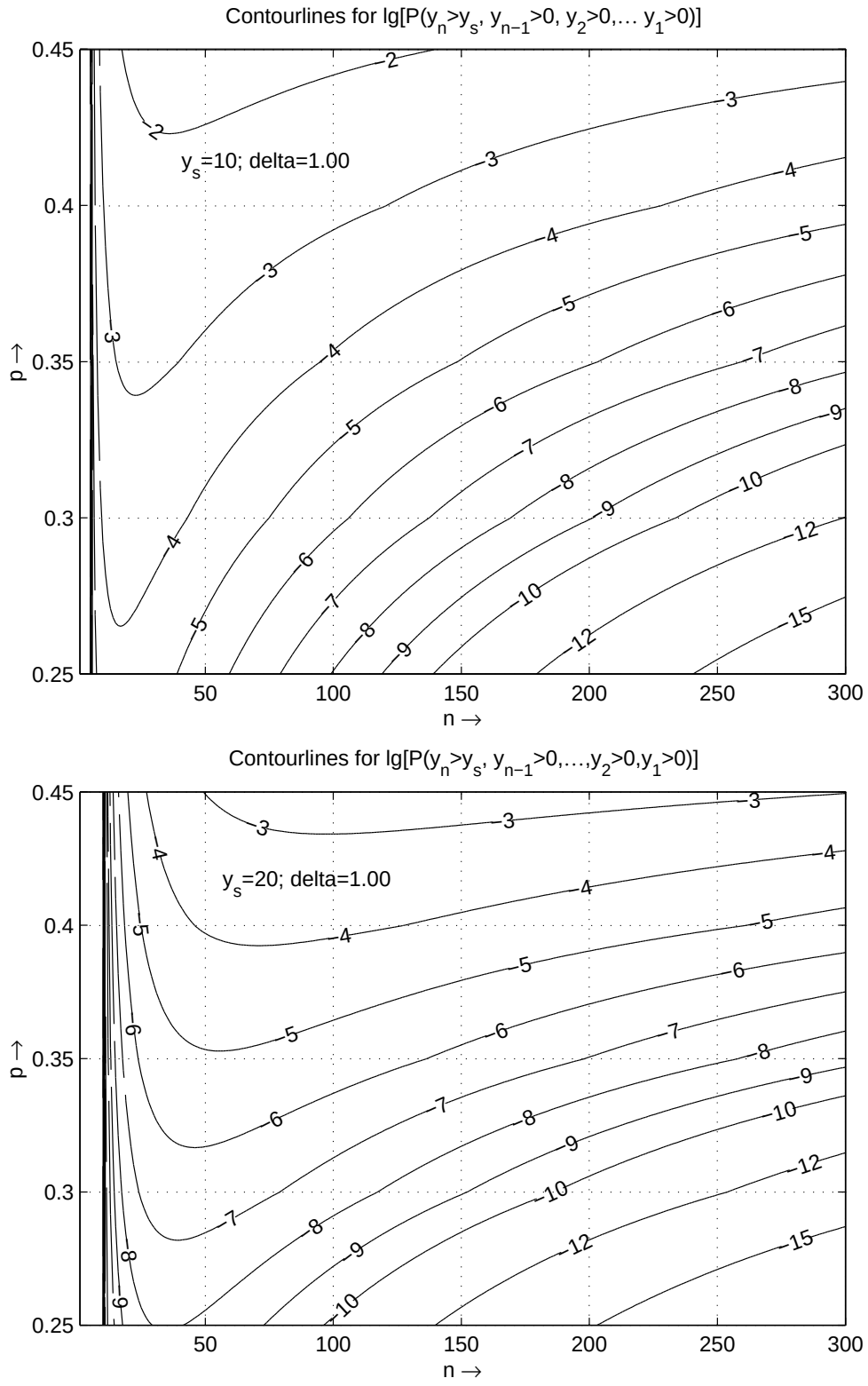

Fig. 3: Contour lines as a function of p and n for the log10-Probability of events to exceed the value $y_s = 10 \cdot \Delta x$ (upper diagr.) or the value $y_s = 20 \cdot \Delta x$ (lower diagr.) at the n-th sample and all previous values of the event are > 0. Here: $\Delta x = 1$.

Example: the probability for an event to exceed the value $10 \cdot \Delta x = 10$ after 149 previous positive samples equals 10^{-5} if $p = 0.35$.

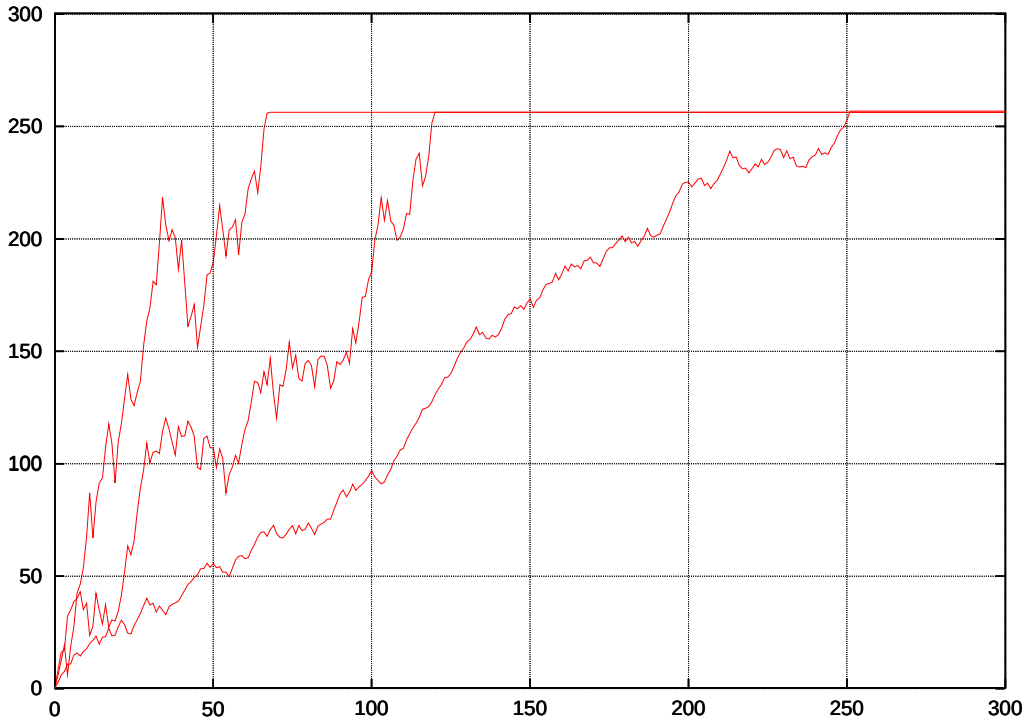

Fig. 4: Three examples of artificially generated smoke sensor fire signals

Summary

One method has been discussed how to generate signals artificially, which resemble smoke sensor signals in fire and No-fire situations. This method is useful particularly for the test of the false/unwanted alarm behaviour of detection algorithms using computer simulations in time-lapse mode if the detection algorithm is available as a program code. The underlying well-defined random model can be extended to generate the smoother heat or gas-sensor signals as well. Thus, it may be used to test multi-sensor/multi-criteria detection algorithms. Although this pure stochastic model generates signal sequences of random nature for the length, height and shape of events, the complete chain of events may be reproduced, which is advantageous for comparison tests of the behaviour of different detection algorithms.

Appendix - Theoretical considerations concerning the event generator

A brief representation of the theoretical background for the model of the event generator is given in the following for those readers who might be interested in it.

The aim is to generate discrete-time functions (events) $\boldsymbol{y}(k)$ with $k \in \{0,(1),n\}$ of random shape, length and amplitude. Only one pseudo-random generator is used for this purpose which generates uniformly distributed random numbers $\boldsymbol{x}$ in the range $0 \ldots 2\Delta x$.
The generation procedure is as follows:

1. The first generated number forms the first sample of the event $\boldsymbol{y}(1) = \boldsymbol{x}^{(1)}$, where $\boldsymbol{x}^{(j)}$ denotes the j-th realization of the random generator.

2. The next generated number $\boldsymbol{x}_h^{(2)}$ is compared with a variable threshold $p_{\text{thr}} = p \cdot 2\Delta x$ with p in the range $0 \ldots 1$. If $\boldsymbol{x}_h^{(2)} \leq p_{\text{thr}}$ the subsequent generated number $\boldsymbol{x}^{(2)}$ is added (otherwise subtracted) from $\boldsymbol{y}(1)$ and forms the second sample of the event $\boldsymbol{y}(2) = \boldsymbol{y}(1) + \boldsymbol{x}^{(2)}$.

The second step above is repeated with always new random numbers $\boldsymbol{x}_h^{(k)}$ and $\boldsymbol{x}^{(k)}$ as long as $\boldsymbol{y}(k) > 0 \quad \forall k \in 1 \ldots n-1$. Hence, the event terminates at $\boldsymbol{y}(n)$ if $\boldsymbol{y}(n) < 0$. The last sample $\boldsymbol{y}(n)$ is subsequently set to zero.
This process generates the required events. A few realizations of events with comparatively long duration are shown in **Fig. 1**.

Such events are sections of "modified random walk" sequences and are so-called "first order Markov sequences" if the pseudo-random generator produces independent numbers $\boldsymbol{x}$. Though the Markov features are easy to prove, the proof is omitted here.
The event generation process can alternatively be described as follows:

$$\boldsymbol{y}(1) \;=\; |\boldsymbol{x}_1|, \quad \boldsymbol{y}(2) = \boldsymbol{y}(1) + \boldsymbol{x}_2, \quad \boldsymbol{y}(3) = \boldsymbol{y}(2) + \boldsymbol{x}_3, \ \ldots\ , \boldsymbol{y}(n) = |\boldsymbol{x}_1| + \sum_{k=2}^{n} \boldsymbol{x}_k \quad (2)$$

with probability densities (pdf's) for the random variables $f_{|\boldsymbol{x}_1|}(x) = f_{|\boldsymbol{x}|}(x)$ and $f_{\boldsymbol{x}}(x) = f_{\boldsymbol{x}_k}(x)$ as shown in **Fig. 5**, i.e. all random variables $\boldsymbol{x}_k \; \forall k \geq 2$ have the same pdf.
Clearly, $\boldsymbol{y}(n)$ as shown in **Eq. 2** can take positive or negative values for each $n \geq 2$ but, as an additional condition, each event is terminated on the first occurrence of a negative value.

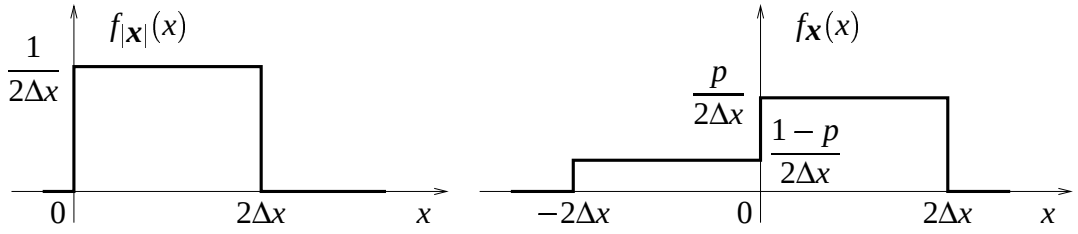

Fig. 5: Probability densities for the first $|\boldsymbol{x}_1|$ (left) and subsequent $\boldsymbol{x}_k$ samples

The joint pdf for n samples $\boldsymbol{y}(1)$, $\boldsymbol{y}(2)$, ... ,$\boldsymbol{y}(n)$ of such a first order Markov process is given by:

$$f_{\boldsymbol{y}(n),\boldsymbol{y}(n-1),\,\ldots\,,\boldsymbol{y}(2),\boldsymbol{y}(1)}(y_n,y_{n-1},\ldots,y_2,y_1) = f_{\boldsymbol{x}}(y_n-y_{n-1})\cdot f_{\boldsymbol{x}}(y_{n-1}-y_{n-2})\cdot\ldots \\ \ldots\cdot f_{\boldsymbol{x}}(y_2-y_1)\cdot f_{|\boldsymbol{x}|}(y_1) \qquad (3)$$

Calculation of the probability for the length of events.

A zero-crossing occurs between the $n-1$st and n-th sample if $\boldsymbol{z}_n = \boldsymbol{y}(n)/\boldsymbol{y}(n-1) < 0$. The calculation of this probability $P(\boldsymbol{z}_n) < 0)$ is comparatively simple, but not sufficient, because it includes all events which show previous zero-crossings. Since the event generation process terminates automatically each event with the first zero-crossing, it is necessary to calculate instead the following probability

$$P([\boldsymbol{z}_n<0]\cap[\boldsymbol{y}(n-1)>0]\cap[\boldsymbol{y}(n-2)>0]\cap\ \ldots\ \cap[\boldsymbol{y}(2)>0]\cap[\boldsymbol{y}(1)>0]) = \\ = \int_{-\infty}^{0}\int_{0}^{\infty}\overset{n-1}{\cdots}\int_{0}^{\infty} f_{\boldsymbol{z}_n(n),\boldsymbol{y}(n-1),\,\ldots\,,\boldsymbol{y}(2),\boldsymbol{y}(1)}(z_n,y_{n-1},\ldots,y_2,y_1)\,\mathrm{d}z_n\,\mathrm{d}y_{n-1}\ldots\mathrm{d}y_1 \qquad (4)$$

which seems to be hopelessly complicated because this is an n-fold integral, to be calculated for all lengths n in the range $2 < n \leq 300$ or even higher values. Nevertheless, it is possible to calculate this n-fold integral recursively.

At first it is necessary to calculate $f_{\boldsymbol{z}_n(n),\boldsymbol{y}(n-1),\,\ldots\,,\boldsymbol{y}(2),\boldsymbol{y}(1)}(z_n,y_{n-1},\ldots,y_2,y_1)$ from $f_{\boldsymbol{y}(n),\boldsymbol{y}(n-1),\,\ldots\,,\boldsymbol{y}(2),\boldsymbol{y}(1)}(y_n,y_{n-1},\ldots,y_2,y_1)$ which is shown for n=3 only; the extension to higher n is straight forward. Consider the following equation system of random variables: $\boldsymbol{z}_3 = \boldsymbol{y}_3/\boldsymbol{y}_2$, $\boldsymbol{z}_2 = \boldsymbol{y}_2$, $\boldsymbol{z}_1 = \boldsymbol{y}_1$, where the abbreviation $\boldsymbol{y}(i) = \boldsymbol{y}_i\ \forall i$ is used.

$$f_{\boldsymbol{z}_3,\boldsymbol{z}_2,\boldsymbol{z}_1}(z_3,z_2,z_1) = \sum_{\ell}\frac{f_{\boldsymbol{y}_3,\boldsymbol{y}_2,\boldsymbol{y}_1}(y_3(z_{3_\ell}),y_2(z_{2_\ell}),y_1(z_{1_\ell}))}{|J(z_j,y_i)|} \qquad (5)$$

$|J(z_j,y_i)|$ is the Jacobian determinant, which is calculated for the given simple equation

system as follows:

$$|J(z_j,y_i)| = \begin{vmatrix} \frac{\partial z_3(y_3,y_2),}{\partial y_3} & \frac{\partial z_3(y_3,y_2)}{\partial y_2} & \frac{\partial z_3(y_3,y_2)}{\partial y_1} \\ \frac{\partial z_2(y_2)}{\partial y_3} & \frac{\partial z_2(y_2)}{\partial y_2} & \frac{\partial z_2(y_2)}{\partial y_1} \\ \frac{\partial z_1(y_1)}{\partial y_3} & \frac{\partial z_1(y_1)}{\partial y_2} & \frac{\partial z_1(y_1)}{\partial y_1} \end{vmatrix} = \begin{vmatrix} \frac{1}{y_2} & -\frac{y_3}{(y_2)^2} & 0 \\ 0 & 1 & 0 \\ 0 & 0 & 1 \end{vmatrix} = \frac{1}{|y_2|} \tag{6}$$

With the given equation system and **Eq.'s 5 and 3** follows:

$$\begin{aligned} f_{\mathbf{z}_3,\mathbf{z}_2,\mathbf{z}_1}(z_3,z_2,z_1) &= |z_2| \cdot f_{\mathbf{y}_3,\mathbf{y}_2,\mathbf{y}_1}(z_3 \cdot z_2, z_2, z_1) \\ &= |z_2| \cdot f_{\boldsymbol{X}}(z_3 \cdot z_2 - z_2) \cdot f_{\boldsymbol{X}}(z_2 - z_1) \cdot f_{|\boldsymbol{X}|}(z_1) \\ &= |z_2| \cdot f_{\boldsymbol{X}}(z_2 \cdot (z_3 - 1)) \cdot f_{\boldsymbol{X}}(z_2 - z_1) \cdot f_{|\boldsymbol{X}|}(z_1) \\ &\quad \text{and the extension to higher } n \text{ results in:} \\ f_{\mathbf{z}_n,\ldots\mathbf{z}_2,\mathbf{z}_1}(z_n,\ldots z_2,z_1) &= |z_{n-1}| \cdot f_{\boldsymbol{X}}(z_{n-1} \cdot (z_n - 1)) \cdot f_{\boldsymbol{X}}(z_{n-1} - z_{n-2}) \cdot \ldots \\ &\qquad \ldots \cdot f_{\boldsymbol{X}}(z_2 - z_1) \cdot f_{|\boldsymbol{X}|}(z_1) \end{aligned} \tag{7}$$

Hence, **Eq. 4** can be rewritten using **Eq. 7**:

$$\begin{aligned} &P([\mathbf{z}_n < 0] \cap [\mathbf{z}_{n-1} > 0] \cap [\mathbf{z}_{n-2} > 0] \cap \ldots \cap [\mathbf{z}_2 > 0] \cap [\mathbf{z}_1 > 0]) = \\ &= \int_{-\infty}^{0} \int_{0}^{\infty} \overset{n-1}{\cdots} \int_{0}^{\infty} |z_{n-1}| \cdot f_{\boldsymbol{X}}(z_{n-1} \cdot (z_n - 1)) \cdot f_{\boldsymbol{X}}(z_{n-1} - z_{n-2}) \cdot \ldots \\ &\qquad \ldots \cdot f_{\boldsymbol{X}}(z_2 - z_1) \cdot f_{|\boldsymbol{X}|}(z_1) \, \mathrm{d}z_n \, \mathrm{d}z_{n-1} \ldots \mathrm{d}z_1 \\ &= \int_{0}^{\infty} \overbrace{\int_{-\infty}^{0} f_{\boldsymbol{X}}(z_{n-1} \cdot (z_n - 1)) \, \mathrm{d}z_n}^{g(z_{n-1})} \cdot |z_{n-1}| \cdot f_{\boldsymbol{X}}(z_{n-1} - z_{n-2}) \cdot \ldots \\ &\qquad \ldots \cdot \int_{0}^{\infty} f_{\boldsymbol{X}}(z_3 - z_2) \int_{0}^{\infty} f_{\boldsymbol{X}}(z_2 - z_1) \cdot f_{|\boldsymbol{X}|}(z_1) \, \mathrm{d}z_1 \, \mathrm{d}z_2 \ \ldots \ \mathrm{d}z_{n-1} \\ &= \int_{0}^{\infty} g(z_{n-1}) \cdot |z_{n-1}| \cdot f_{\boldsymbol{X}}(z_{n-1} - z_{n-2}) \cdot \ldots \\ &\qquad \underbrace{\ldots \cdot \int_{0}^{\infty} f_{\boldsymbol{X}}(z_3 - z_2) \underbrace{\int_{0}^{\infty} f_{\boldsymbol{X}}(z_2 - z_1) \cdot f_{|\boldsymbol{X}|}(z_1) \, \mathrm{d}z_1}_{g_1(z_2)} \, \mathrm{d}z_2 \ \ldots \ \mathrm{d}z_{n-1}}_{g_2(z_3)} \end{aligned} \tag{8}$$

This arrangement of the equation looks slightly more friendly and shows how this n-fold integration can be carried out recursively. Unfortunately, the lower limits of the integrals which determine $g_i(z_{i+1}) \, \forall i \in \{1,(1),n-2\}$ are not $-\infty$. If they were $-\infty$, these integrals

would denote the $n-3$-fold convolution $f_{\boldsymbol{X}} * \ldots * f_{\boldsymbol{X}}$ of the same densities convoluted with $f_{|\boldsymbol{X}|}$ and at least for sufficiently large n all integrals of the second line of **Eq. 8** could easily be approximated by a Gaussian density. Nevertheless, since the functions $f_{\boldsymbol{X}}$ and $f_{|\boldsymbol{X}|}$ are known (see **Fig. 5**) it is even possible to calculate a closed form solution of **Eq. 8** although this would be a laborious and time consuming task for large n.

Fortunately, for the given $f_{\boldsymbol{X}}$ and $f_{|\boldsymbol{X}|}$ all functions $g_i(z_{i+1})$ are zero outside the range $-2\Delta x \leq z_{i+1} \leq (i+1)2\Delta x$ thus, a numerical solution is possible. Moreover, a modified successive convolution procedure is applicable, as shown in the following, using the unit step function $s(z)$:

$$\begin{aligned}
\text{1. step:} \quad & g_1(z_2) &&= f_{\boldsymbol{X}}(z_2) * f_{|\boldsymbol{X}|}(z_2) \\
\text{2. step:} \quad & g_2(z_3) &&= f_{\boldsymbol{X}}(z_3) * [s(z_3) \cdot g_1(z_3)] \\
\text{3. step:} \quad & g_3(z_4) &&= f_{\boldsymbol{X}}(z_4) * [s(z_4) \cdot g_2(z_4)] \\
\vdots \quad & \vdots && \vdots \\
\text{n-2. step:} \quad & g_{n-2}(z_{n-1}) &&= f_{\boldsymbol{X}}(z_{n-1}) * [s(z_{n-1}) \cdot g_{n-3}(z_{n-1})] \\
\text{last step:} \quad & \text{calculate} && \int_0^\infty |z_{n-1}| \cdot g(z_{n-1}) \cdot g_{n-2}(z_{n-1})\, \mathrm{d}z_{n-1}
\end{aligned} \tag{9}$$

The function $g(z_{n-1}) = \int_{-\infty}^{0} f_{\boldsymbol{X}}(z_{n-1} \cdot (z_n - 1))\, \mathrm{d}z_n$ in the last step of the recursive scheme above can be determined separately by visualizing $f_{\boldsymbol{X}}(z_{n-1} \cdot (z_n - 1))$ (see **Fig. 6 and 5**).

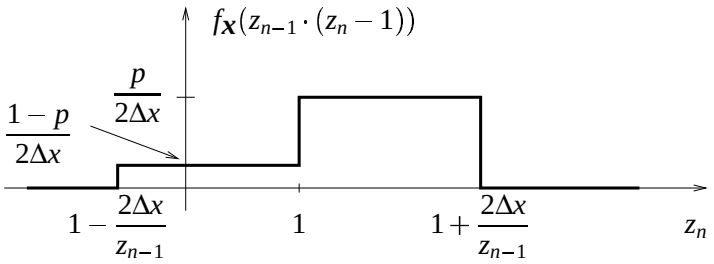

Fig. 6: Scaled pdf $f_{\boldsymbol{X}}(z_{n-1} \cdot (z_n - 1))$

$$\begin{aligned}
g(z_{n-1}) &= \int_{-\infty}^{0} f_{\boldsymbol{X}}(z_{n-1} \cdot (z_n - 1))\, \mathrm{d}z_n \\
&= \begin{cases}
\dfrac{1-p}{2\Delta x} \cdot \left(\dfrac{2\Delta x}{z_{n-1}} - 1 \right) & \text{for} \quad \dfrac{2\Delta x}{z_{n-1}} > 1, \quad \text{and} \quad z_{n-1} > 0 \\
0 & \text{for} \quad \dfrac{2\Delta x}{z_{n-1}} < 1, \quad \text{and} \quad z_{n-1} > 0 \\
\dfrac{p}{2\Delta x} \cdot \left(\dfrac{2\Delta x}{z_{n-1}} - 1 \right) & \text{for} \quad \dfrac{2\Delta x}{z_{n-1}} > 1, \quad \text{and} \quad z_{n-1} < 0
\end{cases}
\end{aligned} \tag{10}$$

Since the integration in the last step of **Eq. 9** is carried out only for positive z_{n-1} the absolute signs for $|z_{n-1}|$ can be omitted and only the first two results of **Eq. 10** are used. Thus, integral for the last step in **Eq. 9** can be re-written as follows:

$$\begin{aligned}&\int_0^{\infty} |z_{n-1}| \cdot g(z_{n-1}) \cdot g_{n-2}(z_{n-1})\, \mathrm{d}z_{n-1} \;= \\ &= (1-p) \int_0^{2\Delta x} \left(1 - \frac{z_{n-1}}{2\Delta x}\right) \cdot g_{n-2}(z_{n-1})\, \mathrm{d}z_{n-1} \end{aligned} \tag{11}$$

Although a closed form solution for these calculations is possible, it would be far too time-consuming. For this reason, the whole scheme has been programmed in MATLAB and carried out recursively. A comparison between the results achieved with a C-programmed computer simulation of the event generator and the theoretical justification, as elaborated above, is shown in **Fig. 2**. Obviously, there are only marginal differences, which increase for low probabilities and small values of p. This is certainly due to the shortcomings of numerical calculations. However, the results show, that for long event lengths n the probability of occurrence decreases rapidly with p and n. For example, with $p = 0.35$ and $n = 150$ this probability is $\approx 10^{-6}$. Note that the vertical scale is logarithmic.

Calculation of the probability for events to exceed a certain amplitude.

In order to get a feeling for the amplitudes of events of considerably long duration it is necessary to calculate the probability for the n-th sample to exceed a given value y_s and all previous samples to be > 0, i.e.:

$$\begin{aligned}&P([\boldsymbol{y}(n) > y_s] \cap [\boldsymbol{y}(n-1) > 0] \cap [\boldsymbol{y}(n-2) > 0] \cap \ \ldots \ \cap [\boldsymbol{y}(2) > 0] \cap [\boldsymbol{y}(1) > 0]) = \\ &= \int_{y_s}^{\infty} \int_0^{\infty} \overset{n-1}{\cdots} \int_0^{\infty} f_{\boldsymbol{y}(n),\boldsymbol{y}(n-1),\,\ldots\,,\boldsymbol{y}(2),\boldsymbol{y}(1)}(y_n, y_{n-1}, \ldots, y_2, y_1)\, \mathrm{d}y_n\, \mathrm{d}y_{n-1} \ldots \mathrm{d}y_1 \\ &= \int_{y_s}^{\infty} \int_0^{\infty} \overset{n-1}{\cdots} \int_0^{\infty} f_{\boldsymbol{x}}(y_n - y_{n-1}) \cdot \ldots \cdot f_{\boldsymbol{x}}(y_2 - y_1) \cdot f_{|\boldsymbol{x}|}(y_1)\, \mathrm{d}y_n\, \mathrm{d}y_{n-1} \ldots \mathrm{d}y_1 \end{aligned} \tag{12}$$

This n-fold integration can be re-arranged in a similar way as shown in **Eq. 8** for the first $n-1$ integrals and the same recursive scheme of **Eq. 9** for the first $n-1$ steps can be used except for the last n'th step. The highest possible value of $\boldsymbol{y}(n)$ is $y_{\max} = 2n \cdot \Delta x \ \forall n$, which equals the upper limit of the last integral. Thus, the whole scheme can be calculated numerically and two results are shown **Fig. 3**.

Daniel Opitz
ASKON Consulting, Münsterstr. 246, 40470 Düsseldorf, Germany

Calculation of synthetic camera images from simulated fire scenarios for algorithm development, refinement and validation

Abstract

A novel approach to generate synthetic fire test video sequences from numerically simulated fire scenarios is outlined.

This new method is expected to be a valuable extension for the development, refinement and validation of algorithms for video-based fire detection systems.

It will lead to a reduction of real fire and non-fire tests and therefore to longer-term savings in time and costs. Due to the larger possible volume of fire test sequences, it enables faster and easier development and maturing of video-based fire detection algorithms. The approach also makes the simulation of scenarios possible which are extremely difficult or impossible to realise in real fire or non-fire tests.

1. Introduction

Video-based fire detection is a rather new and promising technique. A camera, possibly combined with a dedicated illumination device for enhanced smoke detection capabilities, registers time series of images of the area to be monitored. The captured images are then further processed and evaluated to extract the relevant fire signatures.

An overview concerning video-based fire detection with special respect to its pros and cons is given in [1].

Video-based systems provide data of a fire or non-fire situation in very good spatial and temporal resolution and quality. Unlike spot detectors, information is captured simultaneously from the whole observation area (volumetric fire detection system). Smoke does not have to penetrate the detection device to be detected. Instead, it can be detected directly at its source or nearby. Therefore, video technology is especially useful in installations, where conventional systems are not properly applicable (e.g. in large buildings with high ceilings or in open areas) or if very early or fast smoke detection is needed.

However, as video-based fire detection systems do not perform signal capturing in a isolated measuring chamber, nuisance alarm sources can be suppressed only to small extent by mechanical means.

As video-based fire detection algorithm basically have to rely on and evaluate what they "see" (which is the entity of the surrounding scene (background image) and the superimposed, visual representation of the fire or non-fire phenomenon), all fire and non-fire scenarios should be tested as close as possible to *real* installations and conditions.

It is of great importance, that the tests "look real" to the camera, i.e. that the test-cases provide a very similar image compared to that of real fire- or non-fire-cases. For example, it is not sufficient to model solely smoke particle properties in an artificial environment, like in a smoke tunnel or a similar installation.

The challenges in the development of video-based fire detection systems as outlined above give rise to a large number of different test cases/scenarios for development, testing and validation/qualification purposes which have to be set-up in precise congruence to reality. This may consume a lot of time and money for test set-ups, necessary reconstructions and system re-installations and thus require large investments in money, manpower and time.

To enhance the current situation, a new approach is proposed to calculate synthetic video sequences of simulated fire scenarios. This new technique is expected to be most useful for the simulation of room fires like e.g. in storages, hangars, churches and (aircraft) cargo compartments and also for the simulation of open-air facilities, where (large-scale) fire-testing and the realisation of nuisance alarm sources like fog, dust is elaborate or even impossible.

This approach leads to a reduction of real fire tests and therefore to long-term savings in time and costs. Due to the larger possible volume of fire test sequences, it also helps to further develop and mature the state-of-the-art of video-based fire detection algorithms.

Last but not least, there are – due to the very special characteristics of video-based fire detection systems - *some* fire and non-fire scenarios which are extremely difficult to model in real-fire tests, e.g. the (sudden) formation of fog in aircraft cargo compartments or (movement of) fog and dust in open-air facilities.

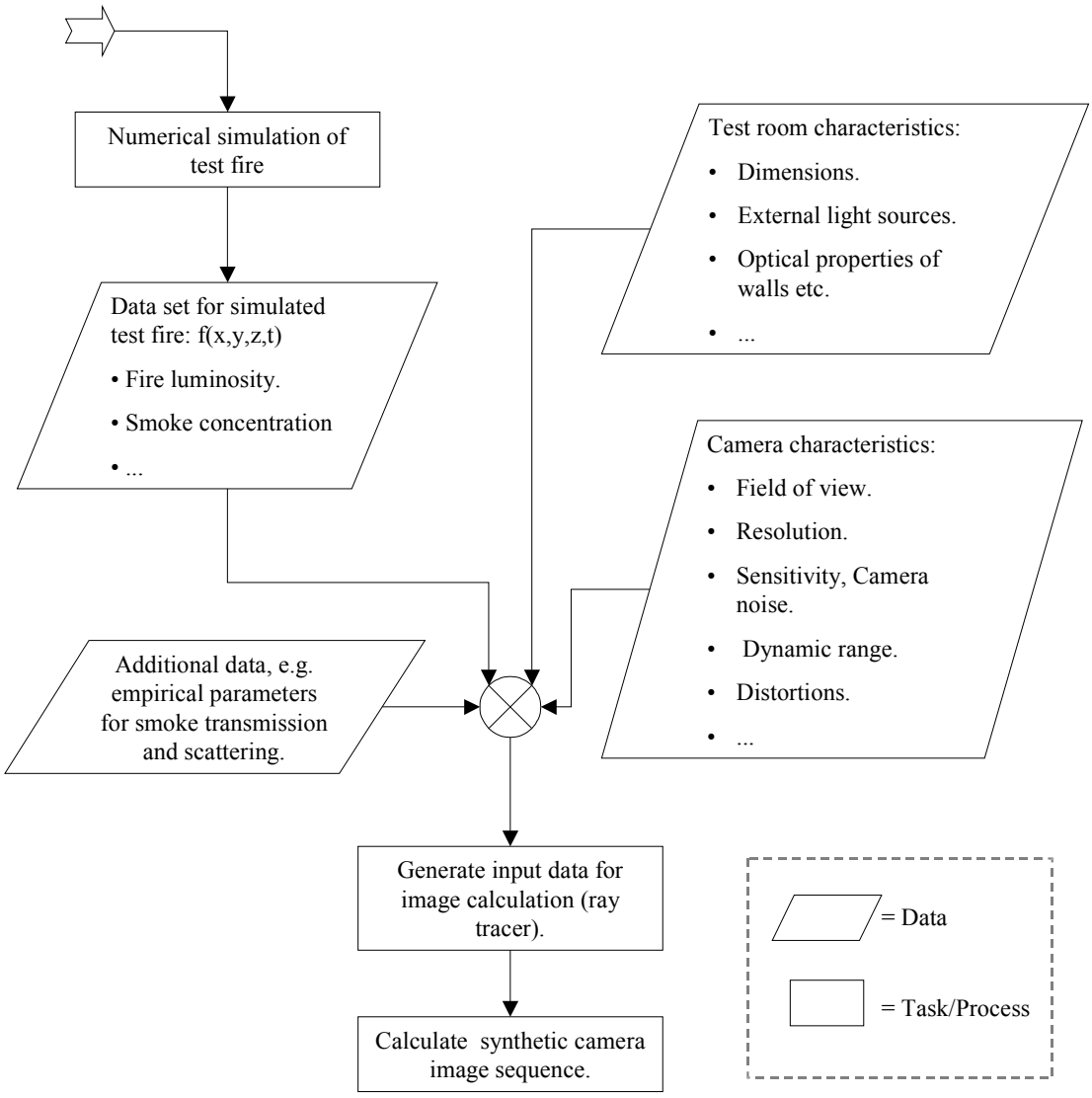

Fig. 1: Flow diagram for calculation of synthetic camera images.

2. Approach

The proposed approach divides into 3 main tasks and processes (Fig. 1):

1. Numerical simulation of the test fire within test scenario (room dimensions, etc.).
2. Generation of input data for the image calculation process by joining the data of the test fire simulation with the characteristics of the test room (dimensions, light sources, optical properties of walls, etc.) and the camera characteristics (sensor resol-

ution, sensor sensitivity and noise, dynamic range and field of view), and additional data.

3. Calculation of synthetic image sequences. Calculation can be done with adopted open source ray-tracing software like the impressive POV-Ray [2].

Fig. 1 shows a flow diagram of the image calculation process, more detail on the above listed calculation steps are provided in the following chapters.

3. Numerical Simulation of Test Fire within Fire Scenario

A common technique for the simulation of non-reactive and reactive (*i.e.: fire*) flows is the use of field models, which divide the simulated volume into a three-dimensional grid of tiny cells. The field model then calculates changes in each grid element by using fundamental equations of fluid dynamics (so called Navier-Stokes-Equations [3]).

This process of solving the fundamental fluid dynamics with the aid of computers is commonly referred to as Computational Fluid Dynamics (CFD). The field model calculates in a recursive process the physical condition of each cell with respect to its neighbouring cells.

As a general advantage, field models rely minimally on empirical correlations. Thus, they are capable of simulating scenarios without the limitations associated with such simplifications. The disadvantage bound up with that is that they require a good understanding of fluid dynamics and combustion processes. This point is qualified to some extent, because the tricky part in the course of the simulation process is to set up a proper simulation model of the fire, which has to be done only once for a specified fire type. To change e.g. the room geometry later is, generally spoken, of much smaller effort.

The simulation of large-scale, non-reactive flows as outlined above is a quite complex task. However, in the case of fire various sub-models have to be incorporated in order to make simulations possible, e.g.:

- In most cases, a turbulence model [3] for the prediction of the (buoyancy driven) turbulent flow (e.g.: k-ε model, Reynold-stress model, Large eddy simulation (LES) model) [4].
- A combustion model to simulate the course of combustion (e.g.: Eddy Dissipation Model, Flamelet model) [3].
- A radiation model to simulate the thermal (and visible light) radiation (e.g.: Monte-Carlo-Methods, Discrete-Transfer, Rosseland-model, P1-model).

- A soot model (e.g.: Magnussen soot model [5]) which models the formation of soot ("smoke") during combustion and yields the particle density. Some information about particle properties and characteristics like e.g. the size distribution have to be fed into these models.

3.1. Turbulence

Turbulence is characterised by spatial and temporal irregularity and randomness. The turbulent motion follows the fundamental laws of conservation, given by the so-called Navier-Stokes-equations [3]. These equations are basically a set of three-dimensional, time dependant, non-linear partial differential equations and express the conservation of mass, momentum and energy.

Vortices are created in the flow and dissipate their kinetic energy while becoming smaller and smaller until they vanish when they become smaller than the Kolmogorov length-scale, which is the size of the smallest element found in the flow.

Thus, these length scales – simplified the size of the vortices – are very important for the description of the turbulent flow.

Two approaches have become more and more accessible in the recent past due to enhanced availability of computational power: Direct Numerical Simulation (DNS) and Large Eddy Simulation (LES).

The Direct Numerical Simulation (DNS) method resolves the whole turbulent range of length scales (turbulence spectrum) from the smallest eddies to the largest whirls and solves the Navier-Stokes-equations directly without simplification [3]. Therefore, DNS calculation are model-free with respect to the turbulence structure and therefore physically precise, but extremely complex and laborious - due to the fact that the grid cell size has to be at least the size of the smallest length scale (Kolmogorov length) present in the flame. This method has proven to be very fruitful for the simulation of rather small-scale flames [6], but is - at this point in time – not applicable to large-scale scenarios.

A state-of-the-art approach for the computation of the turbulence structure in large flows is the Large Eddy Simulation (LES) method ([7], [8]).The main difference to DNS is, that, for vortices smaller than a certain limit, a turbulence model is incorporated. For larger eddies, the Navier-Stokes-equations are solved directly like in DNS. The big advantage with this technique is, that the computational grid size can now be chosen independ-

ent from the Kolmogorov length and therefore large enough to make also large-scale-simulations possible, whilst preserving a satisfying simulation accuracy.

The FDS-Package from BFRL [9] also allows the use of a LES-model, an example for a numerical simulation with this package is given in Fig. 2.

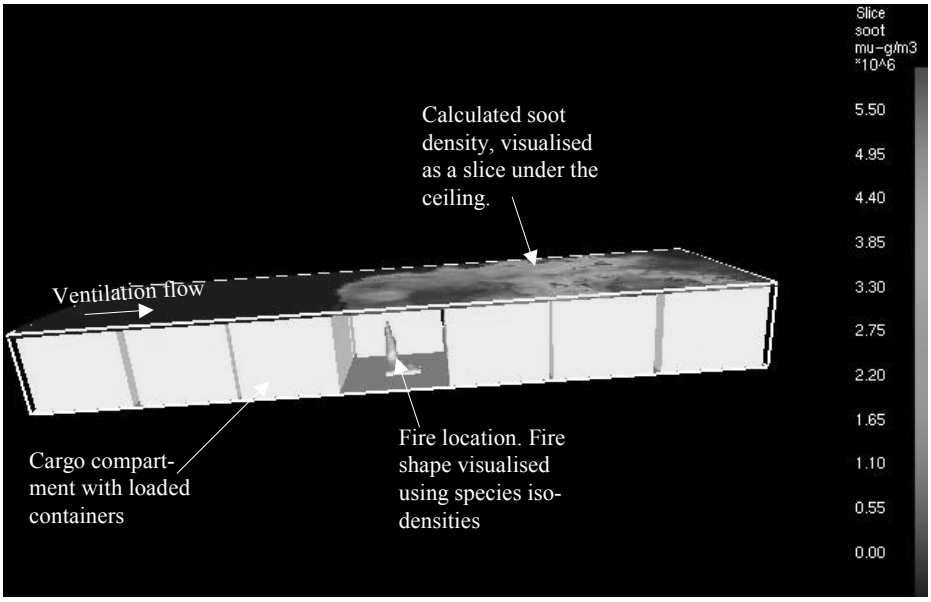

Fig. 2: Example for a numerical simulation, performed with FDS2-package (LES-simulation, number of grid elements (L x W x H) 200 x 60 x 50). Visualised with Smokeview2.

- *Heptane-fire in an aircraft cargo compartment (loaded with containers, ventilation flow rate 4.8 m³/min).*
- *Dimensions of compartment: Length 14.6 m, Width 4.2 m, Height 1.7 m.*
- *Shown is the soot density distribution in a horizontal slice under the compartment ceiling (37s after start of fire).*

3.2. Combustion model

Another very important sub-model is the combustion model. Combustion is a process including the transfer of mass and energy.

A fuel (the combustible substance) reacts with oxygen in an exothermic reaction, forming products that have lower chemical bond energies than the reactants. The difference in chemical bond energy (reaction enthalpy) is transformed to i.e. thermal energy (heat) and visible radiation (flame luminosity).

Combustion is a chain reaction process involving a large sequence of single (elementary) reactions, ending up with a set of products, for hydrocarbons typically carbon monoxide, carbon dioxide and water. These reaction networks are extremely complex.

Even in the combustion of the simplest hydrocarbon, methane, multi-step reactions with far over 40 different elemental chemical reactions take place.

The use of a combustion model allows to simulate the fuel-oxidiser mixing process. This implies that the heat release can be referred to volumes where the appropriate conditions for combustion exist, for example presence of reactants. This way, the combustion model makes it possible to predict and simulate phenomena such as flame lengthening under ventilation or due to wind influence.

3.3. A minimum set of data

Taking into account what is essentially needed for the image calculation process, the following *minimum set of data* is derived:

1. Mass Combustion rate, from which the fire's radiation in the visible spectra range can be approximated (refer e.g. to [10]).
2. The smoke distribution, which - with some assumptions on the smoke properties (refer to [11], [12], [13], [14]) - yields the transmission values of the atmosphere and the intensity of scattered light.

It is important to remember, that the more accurate and detailed the calculations are performed, the more precise and reliable the synthetic images will be.

4. Calculation of synthetic camera images

For the calculation of the synthetic camera images, so called rendering methods (and software) can be used.

In fact, these methods are basically the same as these which make dinosaurs walk and clown fishes swim on screen.

One well-known method is ray tracing, which is perhaps one of the most straightforward ways to model our 3-D world on a 2-D monitor. It is quite possibly the most used technique in film and television to achieve computer special effects, because it is so precise. From the eye or camera, light rays are traced in backwards direction through a pixel in the image plane and it is determined, what is hit by the rays. The image pixel is then set to the colour or brightness value returned by the corresponding ray (Fig. 3). This procedure is performed successively with each image pixel to yield a complete image.

This way of modelling the image formation process is close to its physical nature. Some minor simplifications are usually made, i.e. the ignoring of light-wave polarisation

(which is not registered by humans or standard video cameras) or the quantum behaviour of light photons.

The main drawback of the ray tracing method is the need of comparable large computational power.

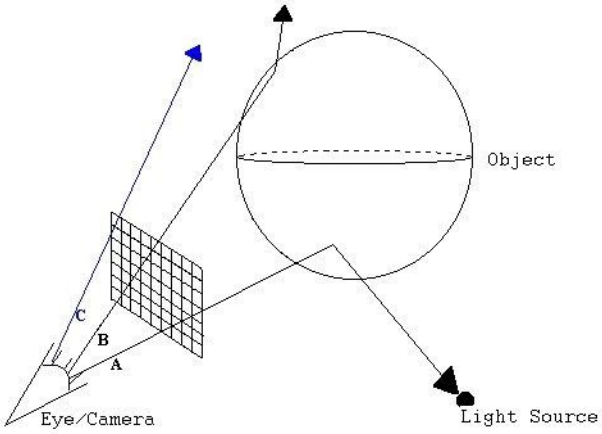

Fig. 3: Basic principle of ray tracing.
Light paths are computed from the imaginary eye/camera through the pixels on the screen until an object is intersected (rays A and B) or it leaves the scope of the model (ray C) without interaction. The image point corresponding to ray A will appear brighter than B because it has a relatively direct connection to a light source, while that one corresponding to ray C will appear black.

For this approach, however, the necessary computer performance can be significantly reduced by evaluating in which quality and preciseness the images have to be calculated.

For our purpose, the images don't have to be *photo-realistic*. Instead, they have to appear *physico-realistic to the detection algorithms*, which shall mean in this context, that they show the relevant signatures and effects in a physically precise 2D-projection.

For example, objects, especially their surfaces, don't have to appear natural in all cases. A fire detection algorithm will not examine whether a wooden cupboard looks realistically beech. It is fully sufficient that important characteristics of the surfaces like reflections, scatter, or e.g. a pattern which could confuse the algorithm, are modelled. This makes scene modelling easier and image computation much faster.

Now, it becomes clearer where extensions or adoptions to standard ray-tracing procedures appear necessary:

1. Introducing the open flame, there is an additional light source of quite complex shape. This light source has to be defined in terms of size and shape, brightness, directional properties, and colour when using a colour camera.

2. Smoke and its transmission and scattering properties. The smoke which is produced by a fire fills up the modelled area (e.g. a room) and counteracts with the ray traces in two ways:
    - The light rays are partially absorbed by the smoke particles, thus a lower brightness value is assigned to the corresponding image pixel.
    - The smoke scatters the light and acts therefore as a secondary light source.

    These effects are modelled to some degrees also in state-of-the-art ray tracing software. However, the intention of these models is the generation of a well-looking image rather than the implementation of a physically precise description of the underlying processes. Thus, the existing models would have to be checked and perhaps a new model would have been to be implemented.
3. Adoption to non-ideal camera. There are some imperfections of a real camera that have to be taken into account:
    - Noise and sensitivity.
    - Limitations due to dynamic range. Blooming. Smearing.
    - Lens system imperfections, lens aberrations.
    - Frame interlacing effects.
4. The output of the used ray-tracing process should be given in standard radiometric dimensions. This ensures the yield of a quantitative measure e.g. for the introduction of the camera characteristics or the evaluation/comparison of different cameras.

5.Summary and Outlook

A new method to yield video test sequences, especially for algorithm development and verification purposes, has been demonstrated.

This approach combines the numerical simulation of a fire (or non-fire) scenario with the use of computer graphics to generate synthetic, physico-realistic video sequences of fire and non-fire cases.

It has been demonstrated by analysis and also by proof-of-concept-work, that all necessary tools are available for use or can be adapted to it. For each outlined task, there is open source software available, which makes changes and extensions of the tools more easy, because they can be based on a proofed and well-documented source code base.

However, the realisation of the above outlined approach is not trivial and would bind a lot of different competences and professions together, i.e. software engineering, numerical simulation, fire engineering - to mention a few. Therefore, it can prove useful and economically worthwhile to access technical consulting companies like e.g. Askon [15] which can provide the required expertises on short notice and also limited to the – in some cases relatively short – periods of time where these specific professions are needed.

6. References

[1] Opitz,D., Willms,I., *Videobasierte Rauch- und Flammenentdeckung - Einsatzgebiete, Stärken und Schwächen*, s+s report, **2**, 2004

[2] http://www.povray.org

[3] Warnatz,J., Maas,U., Dibble,R.W., *Technische Verbrennung*, Springer Berlin, (2001)

[4] Ferziger,J.H., Perić,M., *Computational Methods for Fluid Dynamics*, Springer Berlin Heidelberg, (1997)

[5] Magnussen,B.F., Hjertager,B.H., *On mathematical modelling of turbulent combustion with special emphasis on soot formation and combustion*, in: Proc. Sixteenth Symp. (Int.) on Combustion (1976)

[6] Staus, St.; Schönbucher, A., *Modelling transient irradiation intensities of pool flames*, in: Scientific Computing in Chemical Engineering II (Keil,F., Mackens,W., Voss,H., Werther,J.(Eds.)), Springer Berlin (1999)

[7] Baum,H.R., *Large eddy simulations of fires: From concepts to computations*, Fire Protection Engineering, **40**, 2000

[8] Inagaki,M., *Large eddy simulation as a powerful engineering tool for predicting complex turbulent flows and related phenomena* , R&D Reviews of Toyota, **39**, 2004

[9] http://fire.nist.gov

[10] Hamins,A., Kashiwagi,T., Burch,R.R., *Characteristics of pool fire burning*, in: ASTM STP 1284 (Totten,G.E., Reichel,J(Eds.)), American Society for Testing and Materials (ASTM), Philadelphia, PA. (1996)

[11] Tamm,E., Mirme,A., Sievert,U., Franken,D., *Aerosol particle concentration and size distribution of test-fires as background for fire detector modelling*, in: Proc. AUBE '99 (1999)

[12] Loepfe,M, Ryser,P., Tompkin,C., Wieser,D., *Optical properties of fire and non-fire aerosols*, Fire Safety Journal, **29**, 1997

[13] Mulholland,G.W., *Smoke production and properties*, in: SFPE Handbook of Fire Protection Engineering (DiNenno,P.J. et al.(Eds.)), (1986)

[14] Mulholland,G.W., Croarkin,C., *Specific extinction coefficient of flame generated smoke*, Fire and Materials, **24**, 2000

[15] http://www.askon.de

Giuseppe Marbach[1], Markus Loepfe, Thomas Brupbacher
Siemens Building Technologies AG, CH-8708 Männedorf, Switzerland

An Image Processing Technique for Fire Detection in Video Images

Abstract

This paper presents an image processing technique for automatic real time fire detection in video images. The underlying algorithm is based on the temporal variation of fire intensity captured by a visual image sensor. The full image sequences are analyzed to select a candidate flame region. Characteristic fire features are extracted from the candidate region and combined to determine the presence of fire or non-fire patterns. Fire alarm is triggered if the fire pattern persists over a period of time.

1. Introduction

The progress on video surveillance and monitoring equipment technology in the last decade has increased the presence of Closed Circuit Television (CCTV) cameras in many public and private areas. Their presence has opened the CCTV market to the opportunity to perform, besides monitoring and storage, automatic event detection, e.g. real time video fire detection.

Image processing algorithms for automatic video fire or smoke detection have been developed in the past for applications in tunnels, aircraft hangars, fighting ships, etc. [1, 2, 3]. But none of the algorithms presented in the past are so robust and flexible as to face all of the problems typical in the CCTV automatic video fire detection. These problems are

- Lighting conditions (day and night, artificial lights, light reflections, shadows),
- Image quality (poor camera resolution, poor camera contrast, poor signal transmission, dirty lens, vandalism affecting the image quality),
- Scene complexity (moving objects and people: different velocities and sizes),
- Processor performance (real time detection, processor speed and memory)
- System installation (friendly configuration and parametrisation)

[1] Corresponding author, giuseppe.marbach@siemens.com

Great flexibility and high reliability are required from the fire detection algorithms to reduce the false alarm rate and to decrease the alarm reaction time. Moreover the detection algorithms must not disturb the performance or reduce the quality of the monitoring and storage task.

The method presented in this paper uses the temporal accumulation of time derivative images to extract the *best candidate fire region*. The temporal accumulation and the candidate fire region are described in section 2. The subsequent analysis for the detection of fire is evaluated with the data of the best candidate fire region. Characteristic fire features are extracted from the image data of this region, as described in section 3. These features are used to compute the *fire indicator*, see section 4, whose pattern describes the presence of fire or non-fire in the video sequence. Fire alarm is triggered if this fire pattern persists for a critical time. In section 5, the sensitivity parameters of the algorithm are introduced and their effect on the false alarm rate and alarm reaction time are explained. Finally, in section 6, the response of the algorithm towards a series of tests in different environments is discussed.

2. Candidate Fire Region

Fire has the property to flicker, increasing and decreasing the intensity of the emitted light. From the point of view of a camera, this flicker causes an increase and decrease in the luminance of the video images. The typical fire flicker frequency is in the 1 to 10 Hz range. Moreover, fire is, typically, the strongest source of light, thus the luminance of the pixels near the fire tends toward the maximal value allowed by the camera, reaching in most cases the saturation level. These two proprieties of the fire, to flicker and to reach maximal luminance, are used to model the algorithm presented in this paper.

The YUV representation of the video data is here assumed. The luminance component is represented by $Y_{ik}(t)$ and the chrominance by its two components $U_{ik}(t)$ and $V_{ik}(t)$, where t is the time and the indices i, k are the horizontal and vertical pixel position.
The time derivative of the luminance $Y_{ik}(t)$ is zero for the stationary scene regions, and is non-zero for moving objects. Thus the time derivative of the video images will track a moving object. The sum of the absolute value of the derivatives increases if the object

moves periodically around a region. In case of a fire scene, the property of the fire to flicker increases permanently the pixels value near the fire region. This sum of derivatives is represented by:

$$M_{ik} = \sum_t D_{ik}(t), \quad t_0 \le t < t_n$$

where $[t_0, t_n)$ is the discrete summation interval and $D_{ik}(t) = |\partial_t Y_{ik}(t)|$ is the absolute value of the luminance time derivative, e.g. the discrete approximation is:

$$D_{ik}(t) = |Y_{ik}(t) - Y_{ik}(t-1)|.$$

A more efficient and robust way to express the sum $M_{ik}(t)$ is to introduce the *cumulative time derivative matrix* $A_{ik}(t)$, expressed by the recursive formula

$$A_{ik}(t) = \alpha \cdot A_{ik}(t-1) + (1-\alpha) \cdot D_{ik}(t),$$

where α represents the cumulative strength, $0 \le \alpha \le 1$. The matrix $A_{ik}(t)$ describes approximately the mean of the time derivatives $D_{ik}(t)$ in the time interval $[t-N, t]$ with $N + 1 = N/\alpha$. Contrary to the sum M_{ik}, the cumulative time derivative matrix $A_{ik}(t)$ has the advantage to be recursive and the values of $A_{ik}(t)$ increase or decrease exponentially according to the cumulative strength α, converging to finite values:

$$\min\{D_{ik}(t)\} \le A_{ik}(t) \le \max\{D_{ik}(t)\}.$$

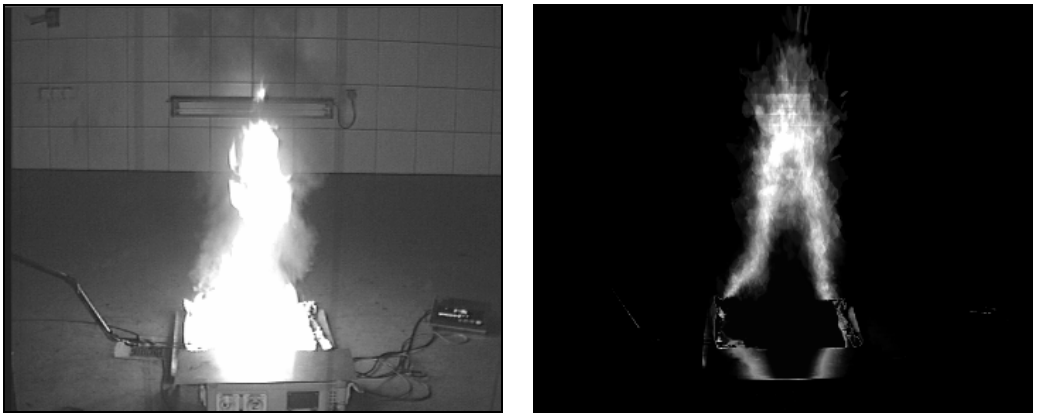

(a) (b)

Figure 1. Typical fire video image (a) and its cumulative matrix (b).

Figure 1.b shows a typical cumulative time derivative matrix $A_{ik}(t)$ of a fire video sequence. The values of $A_{ik}(t)$ are scaled to fit an 8 bits luminance image.

In fire scene, the cumulative matrix $A_{ik}(t)$ will have high values at the borders of the flame region and otherwise values nearly zero. For persistent fire, the values of $A_{ik}(t)$ near the flame region converge as a geometric series to the temporal mean of $D_{ik}(t)$. In the center of the fire, most luminance pixels are saturated, their time derivative is zero, and they do not contribute to $A_{ik}(t)$.

In order to improve robustness of the cumulative time derivative matrix towards false alarms, the time derivative $D_{ik}(t)$ is multiplied by a weight matrix $W_{ik}(t)$:

$$A_{ik}(t) = \alpha \cdot A_{ik}(t) + (1-\alpha) \cdot D_{ik}(t) \cdot W_{ik}(t).$$

To enhance the property of the fire of having pixels with maximal luminance and to suppress those having low luminance, the weight matrix $W_{ik}(t)$ is chosen to be proportional to the luminance. This condition is expressed by

$$\text{if } Y_{ik}(t) \geq \delta \quad \text{then } W_{ik}(t) = Y_{ik}(t), \quad \text{else } W_{ik}(t) = 0,$$

where the luminance threshold $\delta(\lambda_1,\lambda_2)$ depends from two empirical constants λ_1 and λ_2. These empirical constants ensure that the threshold δ is always between the maximal fire luminance and the scene mean luminance, suppressing most of the non-fire pixels of the scene.

Pixels in the cumulative time derivative matrix $A_{ik}(t)$ with high value represent pixels with high probability of being fire pixels. Thus, to extract the *best candidate fire region* Ω_{ROI}, the pixel with maximal value in the cumulative matrix is chosen:

$$(i_{ROI},k_{ROI}) = \{ (i,k) \mid \max\{A_{ik}(t)\} \}.$$

The region Ω_{ROI}, is defined in the algorithm implementation as a 32×32 pixels neighborhood of (i_{ROI},k_{ROI}).

The method presented here uses only one Ω_{ROI} region to detect the presence of fire. Obviously, it is possible to choose more than one non-overlapping candidate fire region.

3. Features Extraction

In the second part of the detection, the analysis is focussed only on the candidate fire region Ω_{ROI}: characteristic fire features are extracted and combined to evaluate the presence of fire or non-fire patterns.

To extract the six features used for the fire detection, the notion of the *active pixels* of the Ω_{ROI} region is introduced: it is defined as the pixels (i,k) of Ω_{ROI} whose values $A_{ik}(t)$ are greater than or equal to a threshold η_1, where $0 \leq \eta_1 \leq 255$ for $A_{ik}(t)$ quantized to 8 bits. The set of active pixels of Ω_{ROI} is thus

$$\pi_{ROI} = \{ (i,k) \in \Omega_{ROI} \mid A_{ik}(t) \geq \eta_1 \}.$$

The luminance of the active pixels in the Ω_{ROI} region provides the basis for the extraction of three main features:

- the luminance of the active pixels: $l_{ROI}(t)$
- the frequency of $l_{ROI}(t)$: $f_{ROI}(t)$
- the amplitude of $l_{ROI}(t)$: $a_{ROI}(t)$

The luminance of the active pixels is thus

$$l_{ROI}(t) = \{ \text{mean}\{ Y_{ik}(t) \} \mid (i,k) \in \pi_{ROI} \}.$$

The features $f_{ROI}(t)$ and $a_{ROI}(t)$ are estimated analyzing the luminance curve $l_{ROI}(t)$ over the time t.

The second set of three features is related to the numbers of pixels:

- the number of active pixels, $r_{ROI}(t)$
- the number of saturated pixels, $s_{ROI}(t)$
- the number of fire-color pixels, $c_{ROI}(t)$

The number of active pixels $r_{ROI}(t)$ is defined as the size of the set π_{ROI}:

$$r_{ROI}(t) = \| \pi_{ROI} \| = \{ \text{number of } (i,k) \in \Omega_{ROI} \mid A_{ik}(t) \geq \eta_1 \}.$$

Thus $r_{ROI}(t)$ is in the range $0 < r_{ROI}(t) < N_{ROI}$, where N_{ROI} is the total number of pixels in the region Ω_{ROI}. The feature $r_{ROI}(t)$ acts as a measure of the number of pixels in Ω_{ROI} that fulfill the fire properties described by the cumulative time derivative matrix $A_{ik}(t)$.

The second feature of this group, $s_{ROI}(t)$, represents the number of luminance pixels that are saturated, i.e. pixels whose value is bigger than or equal to a threshold η_2:

$$s_{ROI}(t) = \{ \text{number of } (i,k) \in \Omega_{ROI} \mid Y_{ik}(t) \geq \eta_2 \},$$

where $\eta_2 < 255$ and $\eta_2 >> 0$. This feature acts as a measure of the number of pixels in Ω_{ROI} that fulfill the condition that fire pixels have maximal luminance value.

The feature $c_{ROI}(t)$ is defined as the number of chrominance pixels in the region Ω_{ROI} falling in a chrominance sector Ω_c divided by all the *active chrominance pixels* in Ω_{ROI}:

$$c_{ROI}(t) = \{ \text{ number of } (i,k) \in \Omega_{ROI} \mid (V_{ik}(t), U_{ik}(t)) \in \Omega_c \text{ and } \left\| (V_{ik}(t), U_{ik}(t)) \right\| \geq \varepsilon \text{ and } A_{ik}(t) \geq \eta_1 \} / \rho(t),$$

where (U,V) represents the chrominance vector, and $\rho(t)$ is the number of active chrominance pixels in the region Ω_{ROI}:

$$\rho(t) = \{ \text{ number of } (i,k) \in \Omega_{ROI} \mid \left\| (V_{ik}(t), U_{ik}(t)) \right\| \geq \varepsilon \text{ and } A_{ik}(t) \geq \eta_1 \},$$

where ε is typically $0 < \varepsilon < 20$. The first inequality in $\rho(t)$, $\left\| (V_{ik}(t), U_{ik}(t)) \right\| \geq \varepsilon$, ensures that the pixels near the grey scale are eliminated. The second inequality ensures that chrominance pixels that are not active pixels are not considered. This feature measures the presence of fire pixels in Ω_{ROI} using the color propriety of fire. For monochrome cameras and poor color cameras, this feature can be switched off, as described in section 5, or its contribution to the final fire pattern attenuated.

The chrominance sector Ω_c is in the algorithm implementation represented by two lines, dividing the chrominance space in two sectors, see figure 2. The fire sector is around the color red and is chosen wide enough, so that chrominance analysis for poor quality color cameras or cameras with slight color shift can be still done.

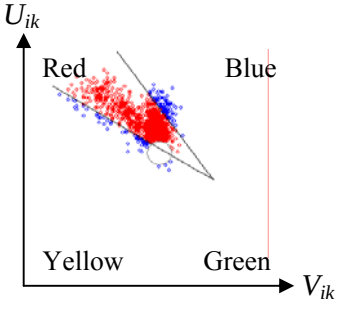

Figure 2. Qualitative representation of the chrominance sector Ω_c and the chrominance pixels $(V_{ik}(t), U_{ik}(t))$ for a typical fire video sequence.

In order to have robust and continuous feature values, each feature is accumulated over the time using the efficient recursion method:

$$\underline{\mathbf{x}}_{ROI}(t) = \beta \cdot \underline{\mathbf{x}}_{ROI}(t-1) + (1-\beta) \cdot x_{ROI}(t),$$

where $x_{ROI}(t)$ is the feature value, e.g. the active pixels feature $r_{ROI}(t)$. β is the accumulation strength and $\underline{\boldsymbol{x}}_{ROI}(t)$ is the resulting *cumulative feature* value. The strength β is chosen so that it reproduces a time integration over 1 second, i.e. $\beta = 0.96$ for a video frame rate of 25 fps.

4. Fire Pattern

Each of the six features, $\underline{\boldsymbol{x}}_{ROI}(t)$, is associated with an indicator, $\boldsymbol{I}(\underline{\boldsymbol{x}},t)$, as follow:

$$\boldsymbol{I}(\underline{\boldsymbol{x}},t) = 1, \text{ if } \mu_{low}(\underline{\boldsymbol{x}}) \geq \underline{\boldsymbol{x}}_{ROI}(t) \geq \mu_{high}(\underline{\boldsymbol{x}})$$

$$\boldsymbol{I}(\underline{\boldsymbol{x}},t) = 0, \text{ else.}$$

The values of the thresholds $\mu_{low}(\underline{\boldsymbol{x}})$ and $\mu_{high}(\underline{\boldsymbol{x}})$ are determined empirically. All these indicators are combined together to build the *fire indicator* $\boldsymbol{I}_F(t)$, which describes the presence of fire or non-fire. An intuitive and easy way to represent $\boldsymbol{I}_F(t)$ is to multiply all the six indicators $\underline{\boldsymbol{x}}_{ROI}(t)$:

$$\boldsymbol{I}_F(t) = \boldsymbol{I}(\underline{\boldsymbol{l}},t)\cdot\boldsymbol{I}(\underline{\boldsymbol{f}},t)\cdot\boldsymbol{I}(\underline{\boldsymbol{a}},t)\cdot\boldsymbol{I}(\underline{\boldsymbol{r}},t)\cdot\boldsymbol{I}(\underline{\boldsymbol{s}},t)\cdot\boldsymbol{I}(\underline{\boldsymbol{c}},t).$$

Obviously, more sophisticated representations of $\boldsymbol{I}_F(t)$ are possible, e.g. the combination of the features $\underline{\boldsymbol{x}}_{ROI}(t)$ to a neural network.

The fire pattern is recognized if the fire indicator $\boldsymbol{I}_F(t)$ is equal to 1. Fire alarm is triggered if this fire pattern persists for a critical time. This is expressed by the integrator $\boldsymbol{Q}(t)$, which increments or decrements according to the value of $\boldsymbol{I}_F(t)$:

$$\boldsymbol{Q}(t) = \boldsymbol{Q}(t-1) + \nu(2\cdot\boldsymbol{I}_F(t)-1),$$

where ν represents the decrement and increment strength. The integrator $\boldsymbol{Q}(t)$ increases by a factor ν if $\boldsymbol{I}_F(t)$ is equal 1, else it decreases.

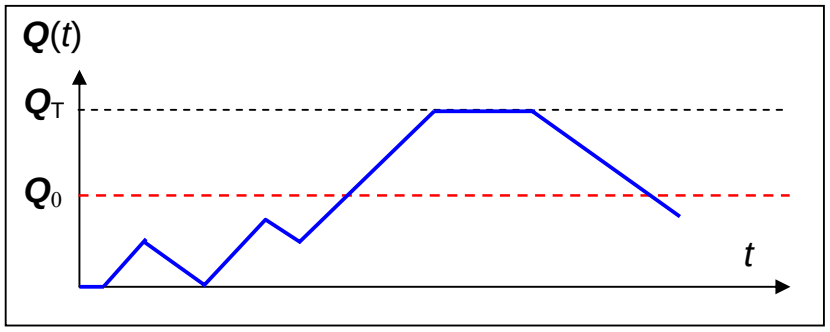

Figure 3. Typical $\boldsymbol{Q}(t)$ for fire pattern, alarm is triggered if $\boldsymbol{Q}(t) \geq \boldsymbol{Q}_0$.

In order to prevent an endless decrement or increment, $\boldsymbol{Q}(t)$ is saturated to 0 on the bottom and by the threshold $\boldsymbol{Q}_T$ on the top. Alarm is then triggered if the integrator $\boldsymbol{Q}(t)$ reaches the threshold $\boldsymbol{Q}_0$: $\boldsymbol{Q}(t) \geq \boldsymbol{Q}_0 \Rightarrow$ fire alarm, where $0 \leq \boldsymbol{Q}_0 \leq \boldsymbol{Q}_T$. Figure 3 shows a typical $\boldsymbol{Q}(t)$ pattern, where fire has been detected.

5. Sensitivity

The scene environment and the application requirements – e.g. outdoor scene with low false alarm rate – demand high flexibility from the algorithm. Internal parameters need to be adapted without affecting seriously the detection performance and reliability.

Four sensitivity parameters have been introduced to modify the algorithm's internal parameters according to the requirements and needs:

- $\boldsymbol{S}_r$, time reaction sensitivity,
- $\boldsymbol{S}_l$, luminance sensitivity,
- $\boldsymbol{S}_m$, motion sensitivity,
- $\boldsymbol{S}_c$, chrominance sensitivity,

The **S** are in the range: $0 \leq \boldsymbol{S} \leq 1$ and the default value, or standard configuration, of $\boldsymbol{S}$, with the exception of $\boldsymbol{S}_c$, whose default value is 1, is 0.5. The change of one or more sensitivity parameters has an immediate impact on a set of corresponding internal parameters.

The time reaction sensitivity $\boldsymbol{S}_r = \boldsymbol{S}_r(\nu, \boldsymbol{Q}_0, \boldsymbol{Q}_T)$ affects the parameters ν, $\boldsymbol{Q}_0$ and $\boldsymbol{Q}_T$, defined in section 4. Increasing the sensitivity parameter $\boldsymbol{S}_r$, decreases the algorithm's reaction time: less time is needed to trigger the fire alarm.

The luminance sensitivity $\boldsymbol{S}_l = \boldsymbol{S}_l(\lambda_1, \lambda_2, \eta_1, \eta_2, \beta)$ influences the internal parameters λ_1, λ_2, η_1, η_2 and β, defined in sections 2 and 3. It is coupled to the light condition of the environment scene: luminance, contrast, saturation, etc.

Increasing the sensitivity $\boldsymbol{S}_l$ increases the algorithm's reaction to small changes of the scene's light condition.

The motion sensitivity $\boldsymbol{S}_m = \boldsymbol{S}_m(\alpha)$ controls the build-up of the cumulative matrix $A_{ik}(t)$ by affecting the internal parameter α. Higher values of $\boldsymbol{S}_m$ mean that the algorithm is more sensitive to moving objects, e.g. tree's leaves, snow flakes, light reflections, ...

The chrominance sensitivity $\boldsymbol{S}_c$ weights the chrominance indicator $\boldsymbol{I}(\underline{\boldsymbol{c}},t)$, in such a way that if $\boldsymbol{S}_c$ is equal to 0, no color analysis is considered; if it is equal to 1, the chrominance indicator is weighted with the same strength as the other indicators. In the case of a monochrome camera or a poor color camera, $\boldsymbol{S}_c$ is set to 0.

The sensitivity parameters – except $\boldsymbol{S}_m$ – can be adjusted by analyzing offline the values of the features for a representative time interval. A special software simulator tool has been developed to analyze offline the features data and to estimate good values for the sensitivity parameters. False alarm rate and reaction time can be tuned by changing the sensitivity parameters directly on the software tool.

6. Tests and Conclusions

The algorithm has been implemented on an Equator MAP-CA™ digital signal processor (DSP). CCTV cameras have been installed in different indoor and outdoor environments and connected to the DSP board. The video images have been down-sampled to the CIF format (288x352 pixels) before being analyzed at 25 fps

The tests have been subdivided in two phases: a training or learning phase – where the algorithm's parameters are tuned to the scene environment – and an operating phase – where the detection was operative.

During the training phase, which lasted between 15 to 20 days, the algorithm ran with the default sensitivity parameters. Every ca. 30 seconds (ca. 750 frames) all the features values of one frame were written on a file. Thereafter, the software simulator tool, which delivers the false alarm statistics, analyzed the collected data. It simulates offline the change of the false alarm statistics according to the change of the sensitivity parameters.

In our tests, the sensitivity parameters have been changed in order to have at least 2 false alarms in 10 days. First the time reaction sensitivity, $\boldsymbol{S}_r$, was adjusted to have maximal 60 seconds reaction time. Then the luminance sensitivity, $\boldsymbol{S}_l$, was adjusted according to the environment light condition, with the intent of reducing the remaining false alarms. Motion and chrominance sensitivity, $\boldsymbol{S}_m$ and $\boldsymbol{S}_c$, were not changed. If still some false alarms were present, the time reaction sensitivity was decreased again to reach the desired compromise between the false alarm rate and the reaction time.

In the operative phase, the algorithm has been reconfigured with the new sensitivity parameters. The tests in the operative phase lasted for ca. 25 to 40 days.

The algorithm has been tested in different environments. As expected, in the operative phase, the algorithm detected less than one false alarm per week in almost all environments. In one case, the particular environment as well as the position of the camera and the type of the moving object have generated an unfavorable constellation so that the false alarm rate was under specific lighting conditions, very high.

In general, the tests showed that the method proposed here works under a variety of conditions. It has a high reliability and a strong robustness towards false alarm, also in most critical environments. Moreover, the reaction time and the sensitivity of the algorithm can be adjusted according to the scene complexity and light condition, increasing the flexibility of the method. Tests with true fires in the laboratory showed a fast reaction of the algorithm. Other tests with true fires in non-laboratory environments – working rooms, high rack warehouses – are in progress.

7. References

[1] Lloyd, D., "Video Smoke Detection (VSD-8)", Fire Safety Engineering, Jan. 2000

[2] D. Wieser and T. Brupbacher, "Smoke Detection in Tunnels Using Video Images", 12th International Conference on Automatic Fire Detection, March 2001, Gaithersburg, USA

[3] S. Y. Foo, "A rule-base machine vision system for fire detection in aircraft dry bays and engine components", Knowledge-Based Systems, Vol. 9, 1996

A. FREILING, U. STORM, K. SCHMOET ER
Airbus GmbH, Bremen, Germany

Re uirements and Image ayout for ideo-Based Fire Detection in Commercial Aircraft

Abstract

This paper describes what the main aircraft requirements for a video based fire detection system are as well as a proposed layout for display in the cockpit.
It has been identified that video based fire detection brings advantages for aircraft application. Lower deck cargo compartments are inaccessible during flight. A video based system would provide the pilot with a view inside the compartment to assess the urgency of the situation in case of a smoke warning.

Introduction

Image based fire detection/verification has been investigated as feasible 1, 2, 3, 4, 5 .
The aircraft cargo compartment imposes tough requirements on fire detection instruments because the environment changes continuously. Temperature, humidity and pressure gradients in the compartment can lead to fog formation. Furthermore, freight can lead to emissions of dust or similar nuisance sources. Unknown reflections are other examples for challenges of video based systems in aircraft application.

As the system shall be used for fire verification, the detection performance must be at least as good as that of the spot type detectors in the way they are installed in the cargo compartments.
During extinguishing agent discharge (currently halon) the system has to fulfil the function to monitor the compartment for the remainder of the flight in order to determine if the suppression was successful.
The design of the graphical layout of the video image and control panel has to take into account the cockpit philosophy and pilots needs. The interface has to be user friendly

without providing too many control functions, so that it can be easily handled in a critical or stressful situation.

The cockpit crew will switch on the video image after the spot type smoke detection system has issued an alarm. A replay function [6] that allows to look back in time is an essential part of the system because it enables to assess how the alarm event had developed and what the scene looked like. Another benefit of the replay function is that with the indication of the Extinguishing agent discharge event, it can be verified that the agent has reached the compartment inside.

A clear indication of the camera position and the field of view is mandatory.

Re uirements

Two kinds of requirements have to be distinguished for image based fire detection instruments designated for application in an aircraft cargo compartment. The first set of requirements is derived from the environmental conditions under which the system has to operate, such as ambient temperature, vibrations, shock and EMI (Electro Magnetic Interference). These requirements can be found in [7] and [8]. The second set is focused on the required performance characteristics of such a system in the aircraft context, taking into account the special geometrical and physical constraints of the cargo compartment. Some of the latter requirements shall be reflected.

If applied as a fire verification system, an image based system is used after a smoke alarm detected by conventional smoke detectors has been given. One requirement for example is that a verification system shall provide the necessary information one second after the smoke alarm.

The conditions that lead to false alarms have to be well understood for the design of an aircraft fire verification system. [9] lists possible false alarm sources. The main reasons for false alarms can be summed up as follows:

- Condensation/fog formation: This phenomenon can have 2 reasons. One is the transportation of e.g. vegetables that emit moisture. The other reason can be the opening of the cargo compartment door in a hot and humid area after a long dis-

tance flight. The aircraft interior usually holds 2-5% relative humidity after these kinds of flight.

- Dust clouds caused by animals in the cargo compartments or dusty containers
- Oily vapour that can egress out of the Auxiliary Power Unit in certain failure cases
- Exhaust air from other aircraft queuing after each other on the runway
- Exhaust gases from ground service trucks
- Forest fires that occur within the route of the aircraft
- Other recorded events are of singular characteristic and are e.g. wet paint, leaking substances from cargo like battery acid etc.

The cases that led to false smoke warnings in the past are poorly reported and can hardly be used to assess the definite condition under which the alarm was issued.

The geometrical conditions in an aircraft cargo hold are a further challenge for an image based system. Even if the aircraft is not moving, there is a 1.7 inch gap between the top of the cargo containers and the ceiling of the compartment. As the aircraft structure is not stiff, bending can occur during flight or an effect called fish tailing if the aircraft gets into turbulences. The video sequence to be used for image processing will like this not be static.

Cargo is not only transported in containers, also pallets are allowed which are usually wrapped with plastic foil of non-predictable shape. Figures 1 to 4 show different examples of aircraft cargo which might challenge an image based system. Figure 4 for example shows a Lower Deck Mobile Crew Rest Container in which the cabin crew can sleep during long distance flight an which can be removed during one Turn-Around-Time. It is accessible from the cabin. Access hatches block the line of sight of image sensors, so respective system design precautions have to be taken.

Fig. 1: palletized cargo before loading

Fig. 2: palletized cargo loaded inside a lower deck cargo compartment

Fig. 3: Cargo Container in use

Fig. 4: Lower Deck Mobile Crew Rest Compartment

Another goal of the use of a fire verification system is the avoidance of unnecessary extinguishing agent discharge. To date, halon is used for fire suppression in commercial aircraft. Dedicated working groups and different vendors investigate the possibility to replace this ozone-layer depleting agent. If the cockpit crew is unsure about the fire/smoke situation in the cargo compartment, they will discharge the extinguishing agent. The requirement to a verification system is to monitor the situation also after the agent has been released.

Man-Machine-Interface

The Man-Machine (or Human-Machine) – Interface described in the following paragraphs is the result of an assessment between system designers and flight crew representatives. It focuses on ease of use and congruence with the cockpit philosophy, which is to have a "dark" cockpit (no lights on) if all systems are working properly. Furthermore, it is important to select appropriate colours for the Graphical User Interface (GUI) because colours code the urgency of the situation for the pilot (e.g. green amber and red). The components of the man-machine-interface are a control panel and a display.

Replay function

The replay function is an essential part of Fire Verification. For every image sensor, pictures are taken every e.g. 5 seconds and stored in a memory. This is done for e.g. 10 minutes. The result is a fast motion film that allows to assess the situation before the event occurred. The cockpit crew has to take immediate decisions after a smoke warning and information has to be provided in a clear way. The duration of the fast motion film has been assessed by cockpit crew specialists and it has been estimated that a duration of 15 seconds for 10 Minutes is appropriate for the scenarios that were investigated. The time interval 5 minutes prior to and after the first smoke event is stored separately and is not overwritten in order to provide this critical sequence for the rest of the flight.

Control functions

Besides control of the replay function, general functionalities for selecting the image sensors in the cargo compartments are provided to the flight crew. This includes a selector switch for selecting the compartment in which the event occurred and a pushbutton for switching the image sensors in this compartment.

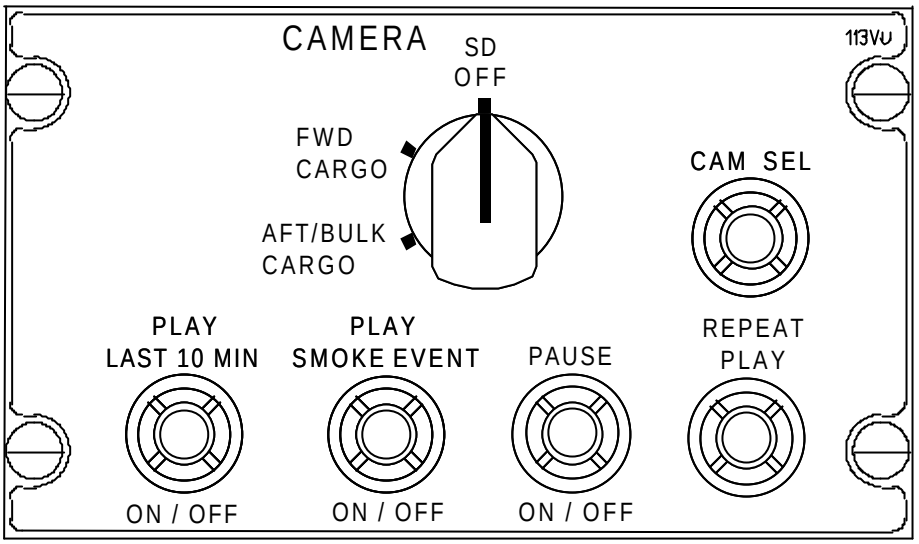

Fig. 5: Cockpit controls Design

Several control mechanisms have been evaluated in order to find the most appropriate solution for controlling the replay function.

The lower row of 4 pushbuttons in Fig. 3 shows the control of the replay function. With the “PLAY LAST 10 MIN” function, the crew can activate the replay function to always play the last 10 minutes prior to the current time within e.g. 15 seconds. If the button is pressed again, the replay mode is left and a life image is displayed. The PLAY SMOKE EVENT function provides a similar functionality, only that here, the pilot will always see the 10 Minutes around the first smoke event for the remainder of the flight. The “PAUSE” button can be used to stop the replay film for deeper assessment of the situation. The replay film will stop at the end. In order to see the same film again, the “REPEAT PLAY” function can be used.

Graphical User Interface (GUI)

The picture and its overlays are split into 4 different areas. The following picture areas are to be distinguished, see Fig. 4:

- System Information Area
- Video Image Area
- Pictogram Area
- Replay Area

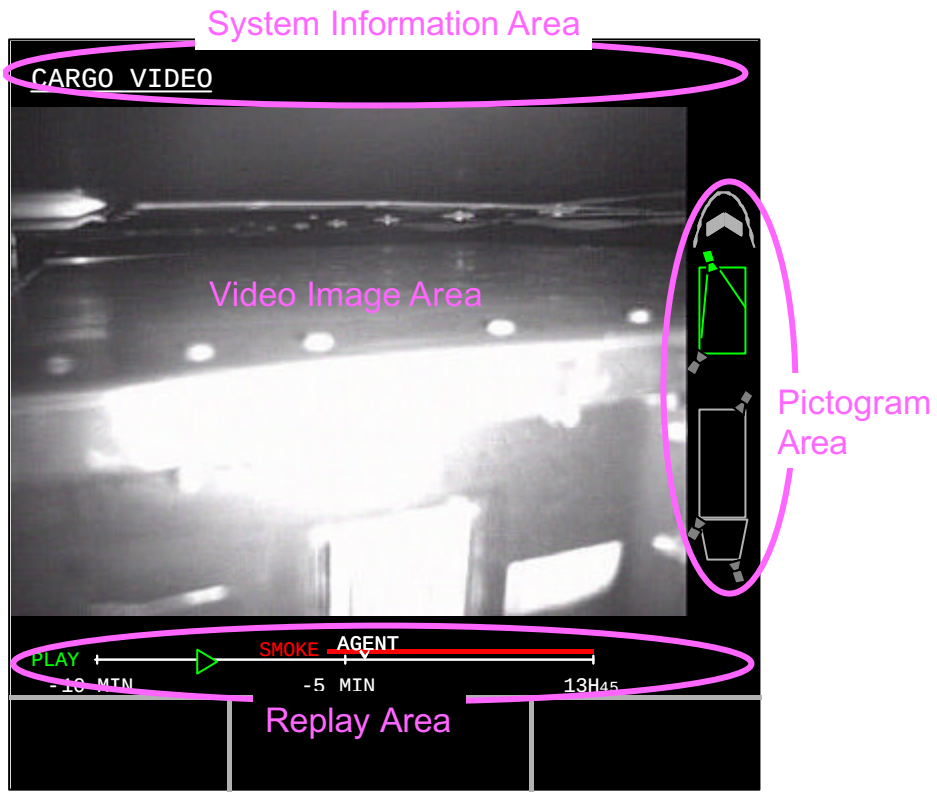

Fig. 6: Graphical User Interface

The System Information area displays the name and status of the system. The following states are possible:

- The text CARGO VIDEO or similar is displayed anytime when the CFVS is powered and operative.

- The text SMOKE CONFIRMED or SMOKE NOT CONFIRMED is displayed additionally if the CFVS confirms or unconfirms a fire or smoke situation in the compartment.

- The text CONFIRMATION NOT AVAIL is displayed additionally if a failure condition has occurred which prevents the CFVS from being able to output a confirmation information.

Replay Area

In the Replay area, a time bar is displayed when in Replay mode, representing the last 10 minutes before the current time. The Replay time bar can have an exemplary layout shown in Figure 1. The time interval displayed on the time bar is frozen as long as the Replay function is ON. The text AGENT is displayed above the time bar together with an appropriate graphical symbol to mark the extinguishing agent discharge point on the time bar.

Aircraft Pictogram Area

The camera configuration as well as the image sensor positions are displayed in the aircraft pictogram area. The selected image sensor is displayed in green. If an image sensor indicates smoke, then this sensor is displayed in red. The field of view of the selected image sensor is displayed with lines. Any camera that is not selected is displayed in grey, selected ones in green as well as the selected compartment. Any faulty camera is displayed in amber or similar.

Video Image Area

A video image from the selected image sensor will be displayed in the Video Image Area.

Conclusion and utlook

Requirements for image based fire detection instruments for aircraft application have been defined and a Man-Machine-Interface (MMI) comprising a graphical user interface and control panels has been developed under involvement of pilots and system designers. The MMI is in congruence with the overall cockpit philosophy and gives the pilot a decision aid in case of a smoke alarm in order to distinguish between a true and a false fire warning. In a further step, if image processing algorithms of video fire detectors are mature enough, a logical connection between the conventional smoke detection system and the verification system might be reachable. Currently, the pilot himself is performing the decision process of diverting the aircraft or not.

References

1 Boucourt, G., Two dimensional multi detection fire sensor, system architecture and performance, Proceedings of the 12th international conference on automatic fire detection, March 26-28 2001, Gaithersburg, Maryland, USA; 677-688

[2] K. Schm tzer; Cargo Compartment Fire Verification System - Image based fire/smoke detection (Video-detection); International Aircraft Systems Fire Protection Working Group; Meeting in London, UK, on June 13-14th, 2002; http://www.fire.tc.faa.gov/pdf/systems/CargoFireVerification.pdf

3 Boucourt, G., Fire Detection and visualization Systems for aircraft application, Proceedings of the VdS conference Videodetection, May 27th –28th, Cologne, Germany

4 akrzewski, R. Video based Cargo Fire Verification System for Commercial aircraft, see this book of conference

5 Leisten, V., Camera based Fire Verification System (CFVS) for Aircraft components, see this book of conference

6 Freiling, A, Schm tzer, K; Patent pending, Deutsches Patentamt, A 102004024884.2, Applied 19. Mai 04

5 Freiling, A.; Requirements for Fire Detection in civil aviation; Proceedings of the VdS conference Gas Sensors for Fire Detection, November 15-16, Cologne, Germany

8 Environmental conditions and test procedures for airborne equipment, RTCA DO160, RTCA, Washington, USA

9 Mangon, P., Fire Detection for Aircraft cargo compartments, reduction of false alarms; Proceedings of the 12th international conference on automatic fire detection, March 26-28 2001, Gaithersburg, Maryland, USA; 653-664

Christian SCHMID, Klaus SCHMOETZER
Airbus, Bremen, Germany

System Design: Smoke Detectors interfaced by a deterministic CAN bus Network

1. Abstract

Smoke detectors are installed in various areas overall in the aircraft's pressurized zones like lavatories, equipment bays, cargo compartments and rest rooms. The electrical network to interface the detectors varies between the applications. Some equipment require a dedicated power supply and provide information on an analogue current loop, while others use digital busses or discrete I/Os for information exchange. A proprietary bus system incorporating a complex power and signal multiplexing method is also widely utilized. All methods have pros and cons, but there is the industrial need to standardize the electrical interfaces to minimize the number of derivates.

The CAN bus was originally developed by the German company Robert Bosch GmbH for use in the automobile industry. Nowadays CAN is being used in an increasing number of applications in the automotive industry and in many other industrial applications. Some manufacturers of smoke detectors have also developed equipment with CAN bus interface. As the CAN bus defines only layers 1 and 2 of the OSI communication model, additional higher layer features are necessary to achieve the level of operational assurance required for a safety critical application, namely smoke detection on an aircraft.

This paper is particularly focused on the development of a deterministic CAN bus network with strict configuration control of smoke detectors in the scope of an aircraft application. International airworthiness authorities have approved the application in the frame of the Airbus A318 Type certification.

2. Introduction

The objective of the new Smoke Detection System was to replace the proprietary current modulated supply and communication loop with an open, non-proprietary bus standard. The overall system reliability and performance was to match or surpass the existing architecture while keeping development and purchasing costs at a comparative level.

The latter was feasible by reusing the existing smoke detector in a new smoke detector featuring an altered communication and power interface.

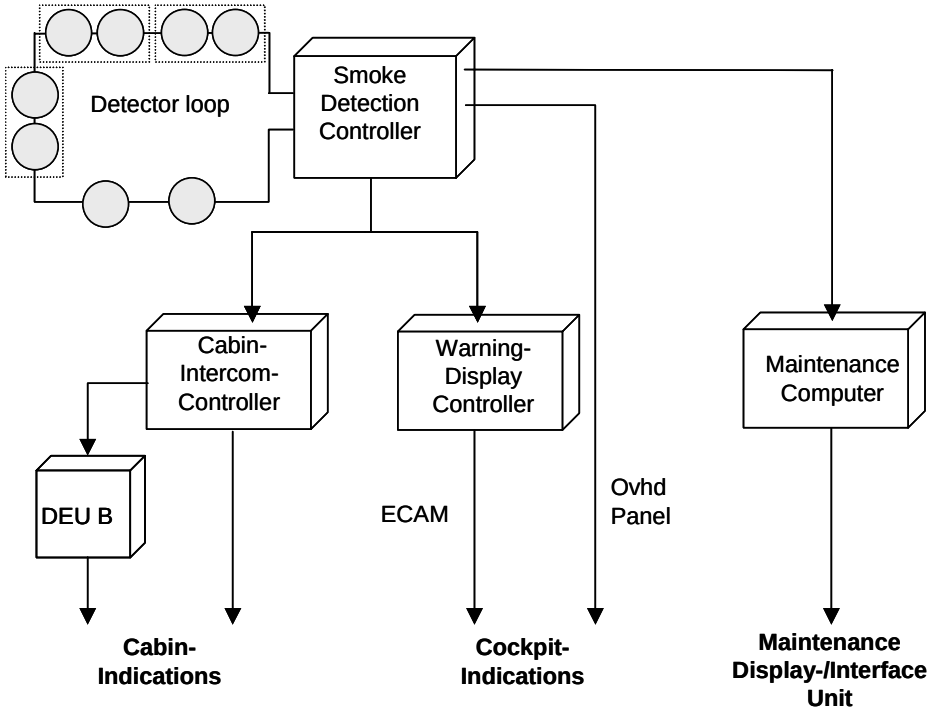

Smoke Detection System using proprietary detector supply & communication loop

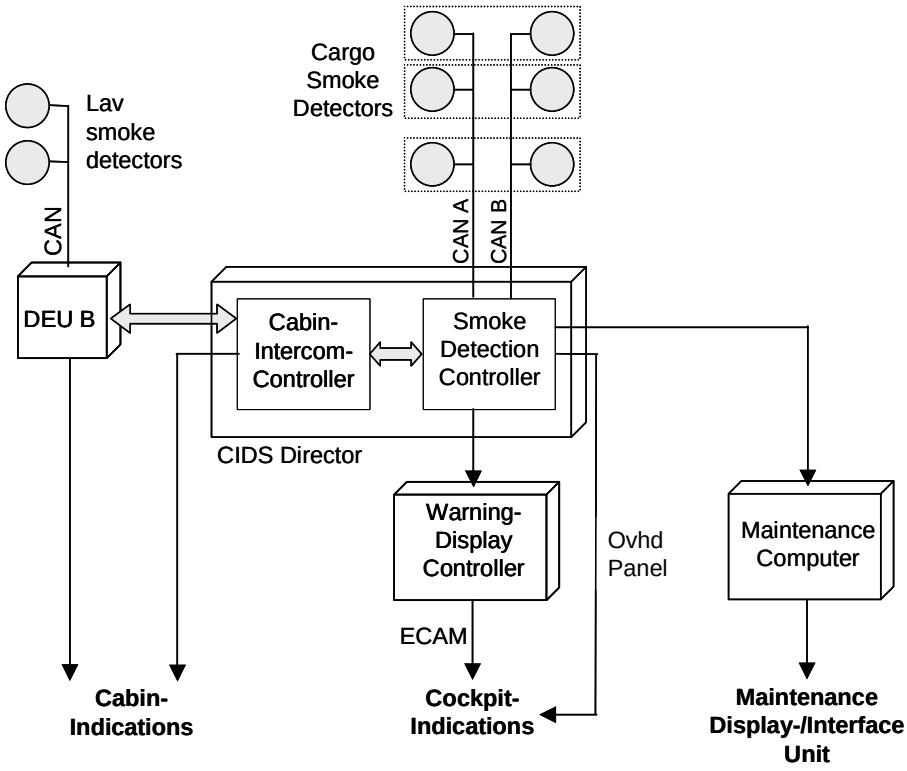

Smoke Detection System using an open standard CAN bus to interface detectors

The communication medium had to meet a number of requirements for eligibility in a safety-critical application:

- Advanced data integrity, and error detection features
- Deterministic behavior
- Operability in challenging EMC environments
- High degree of flexibility in choice of network size and topology

Considering the 30-year design life of a modern passenger aircraft, the long-term availability of electronic components was scrutinized in order to minimize equipment redesign resulting from component obsolescence throughout the life cycle of the aircraft.

The CAN (Controller Area Network) bus was deemed the most suitable communication medium capable of fulfilling the above requirements.

3. Protocol

The CAN protocol, as defined in ISO 11898 [1], covers layers 1 and 2 of the OSI communication model. The remaining layers up to layer 7 have to be managed by the application. Various standardized higher layer protocols such as CANopen are available and widely used in industrial applications. Instead of selecting a generic high layer protocol, a specific to-type application layer protocol was developed and documented in a System Interface Document [2] in order to ease compliance with RTCA/DO-178 [3] guidelines.

Analysis of the communication needs resulted in the following protocol requirements:

- Every individual smoke detector on the network must be uniquely identifiable
- Message generated by a smoke detector must contain information about its identity
- Support a Master-Slave communication model

CAN Identifier

The 29 bit extended identifier is utilized, and partitioned into the following sub fields:

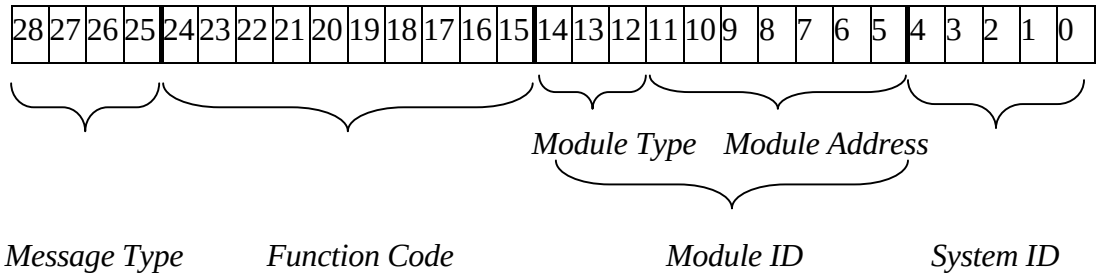

Message Type (bits 28..25)

The purpose of the *Message Type* is to categorize messages according to their overall relative priority and indicate whether the *Module ID* contains a transmitter or receiver address. Two classes of *Message Type*, Process Data Object (PDO) and Service Data Object (SDO) are instantiated either as Transmit or Receive objects; T_PDO and R_PDO as well as T_SDO and R_SDO respectively. A Transmit Data Object (T_xDO) denotes the *Module ID* contains the network address of the transmitter, whereas a Receive Data Object (R_xDO) contains the network address of the intended receiver in the *Module ID* field.

Function Code (bits 24..15)

Every application function is designated a unique *Function Code* within its respective *Message Type*. In addition to describing the next level of arbitration priority, the Function Code is used to transport logical data without the use of the actual CAN data fields. In this case the Data Length Code (DLC) is 0, enabling efficient use of data bandwidth, particularly for R_PDOs and R_SDOs which contain mostly status requests directed at smoke detectors and don't carry any further information than the request itself.

Module ID (bits 14..5)

The *Module ID* field contains the unique network identification of the CAN node. This may also be a broadcast identification when a message is directed at several nodes simultaneously. Two sub fields *Module Type* and *Module Address* split the *Module ID*

into equipment classes and their individual addresses. The entire *Module Address* space may be reused for every *Module Type* on the network.

System ID (bits 4..0)

The *System ID* is used to tag the CAN identifier with a unique system identification code. All smoke detectors and other fire protection components are assigned a fixed value.

Data Frames

A Data Frame is generated by a transmitter to transfer application data to one, or in the case of a broadcast, several receivers. Within the Data Frame, the Data Field consisting of 1-8 bytes carries the application data. A Data Frame may contain an empty Data Field (DLC = 0). In this case, data is carried through the *Function Code* alone.
A smoke detector's 8-byte status Data Field is as follows:

Data byte	MSB	LSB	Description Comment	Format
1	7	5	spare / not used	-
	4	4	Detector Warning	Discrete
	3	3	Prefault threshold exceeded	Discrete
	2	2	Detector standby	Discrete
	1	1	Detector alarm	Discrete
	0	0	Detector failure	Discrete
2	7	0	Trouble shooting data	Binary
3	7	2	spare / not used	-
	1	0	MSB contamination level	Binary
4	7	0	LSB contamination level	Binary
5	7	2	spare / not used	-
	1	0	MSB smoke level	Binary
6	7	0	LSB smoke level	Binary
7	7	2	spare / not used	-
	1	0	MSB temperature	Binary
8	7	0	LSB temperature	Binary

Definition of smoke detector status bits in data byte 1

Designation	bit	
Failure	0	The smoke detector is no longer able to detect smoke or to communicate this information in a reliable manner
Alarm	1	Smoke is detected and confirmed
Standby	2	The smoke detector is able to detect smoke and communicate this information in a reliable manner
Prefualt	3	The smoke detector optical cell contamination level has exceeded the internal threshold for triggering a corresponding maintenance message
Warning	4	The CAN TX error counter has exceeded 96

4. Network Management

It is of utmost importance that the system configuration and availability of resources (smoke detectors) is known to the network master. Lack of configuration control through the network master device would jeopardize safety and disqualify the system. From a safety assessment point of view, the worst case is an undetected configuration error leading to an incorrect compartment designation incase of fire; an alarm reported in the forward cargo compartment while the real fire occurrence is in the aft cargo compartment and vice versa. Such a case is classified as catastrophic and must be ruled out with a defined level of confidence. Therefore, various network management mechanisms are necessary to ensure proper system configuration during initialization and normal operation.

Power Up Configuration Control

The normal expected configuration of smoke detectors is fixed in a lookup table within the network master's operational software. At power up or system initialization, the current configuration is compared with the expected through a mechanism called Configuration Check Request. During the Configuration Check Request process, the network master broadcasts the Configuration Check Request as an R_PDO with the broadcast *Module ID* to all smoke detectors. These in turn reply with T_PDOs containing

their individual *Module Address*, enabling the network master to make a comparison of the received replies with the expected replies, and thereby detecting the following failure cases:

- Incorrect configuration of network master for the intended installation
- An expected smoke detector has not replied (missing smoke detector on network)
- An unexpected smoke detector has replied (excessive smoke detector on network)

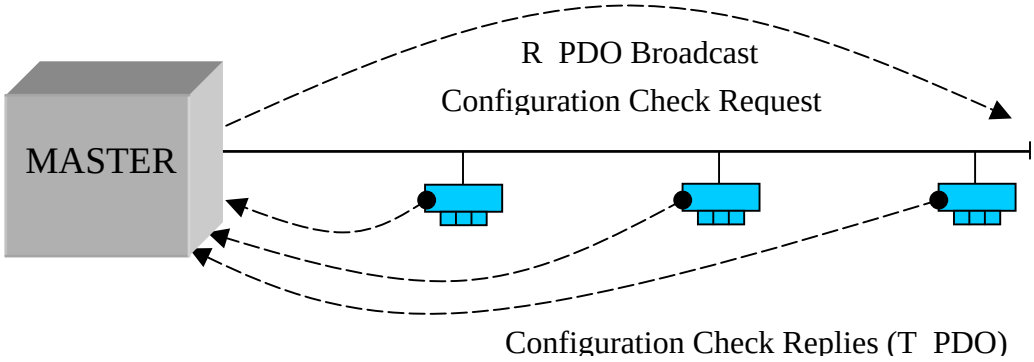

Normal Configuration Check Request / Reply Process

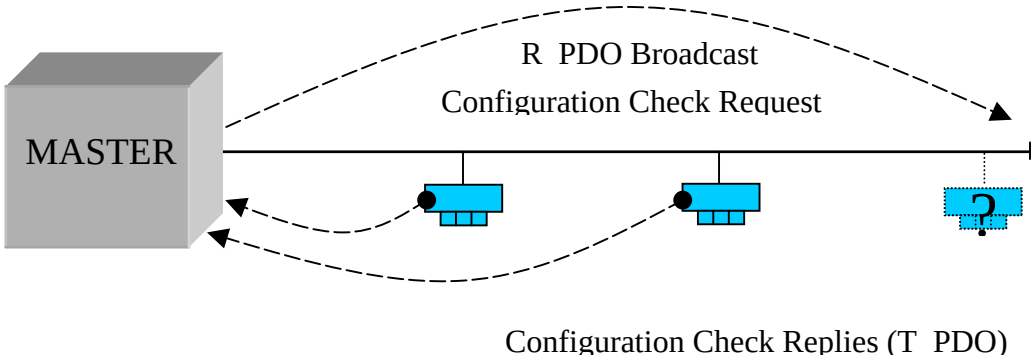

Failure of Expected Smoke Detector to Reply

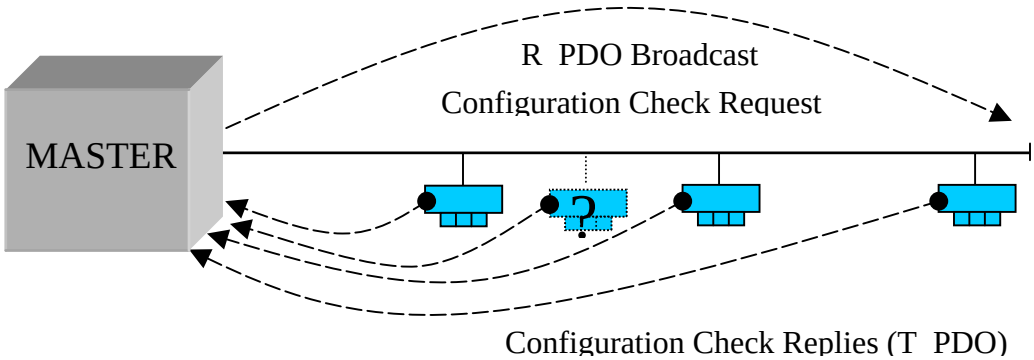

Unexpected Smoke Detector Reply

Normal Polling Operation

The CAN bus is operated in Master-Slave mode. The network master cyclically acquires the status of each smoke detector by an explicitly addressed request frame. Not to be confused with CAN remote request frames, the request message is a regular data frame of type R_PDO containing the individual *Module ID* of the subject smoke detector, and is replied to by a T_PDO data frame containing the *Module ID* of the replying transmitter.

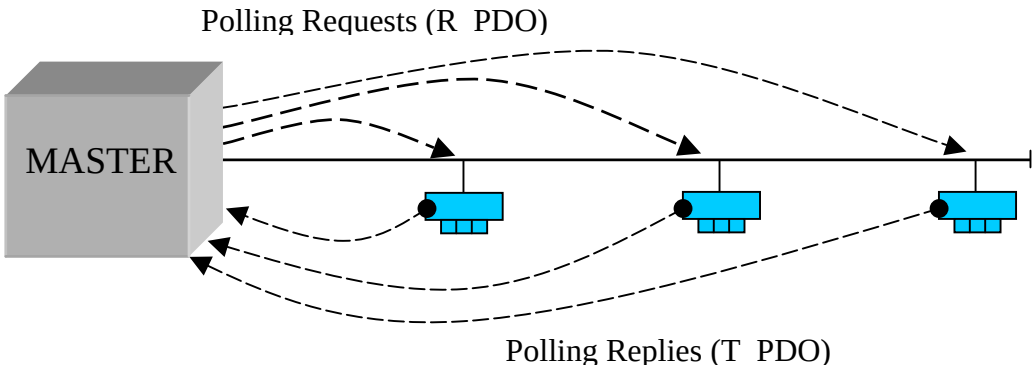

Each polling request is monitored by a timeout in which the reply is expected. The polling cycle is repeated every 2 seconds.

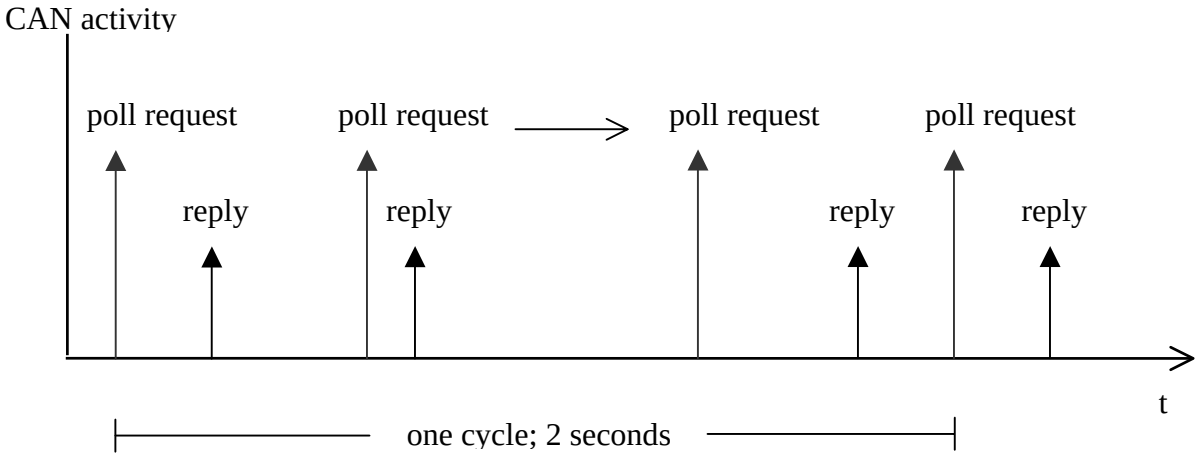

The response time of the smoke detector is 60ms, including internal processing time and retry mechanisms inherent to CAN. A reply is considered timed out by the network master when not received within the following polling cycle; 2 seconds later. An outstanding reply increments a counter C in the network master. Once the counter reaches 5 outstanding replies (10s), the smoke detector is declared inoperable and is no longer polled. The reception of a normal polling reply while the counter is $1 \leq C < 5$ leads to a reset of the counter to 0 and the smoke detector is restored to normal operation. Determinism is ensured through the request-reply time window and the polling cycle:

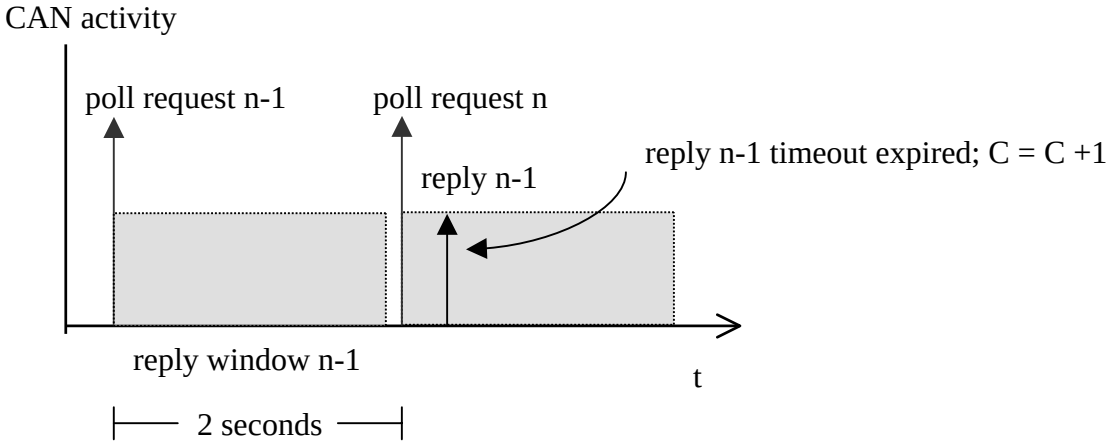

In summary, the polling process abides by the following rules:

- Only expected smoke detectors are polled
- A smoke detector is no longer polled when declared failed
- A smoke detector is no longer polled following 5 consecutive timeouts
- A smoke detector determined missing during power up is not polled

Smoke Detector Monitoring

In addition to the network based configuration and time monitoring, the smoke detector is monitored for proper functional behavior by the network master. Normally the smoke detector is in the standby condition (bit 2 on data byte 1 is TRUE). In case of alarm, the *standby* bit becomes false while the alarm condition (bit 1 on data byte 1) is TRUE. These conditions are by definition mutually exclusive and are therefore be monitored for proper behavior. If two consecutive polling replies are received with neither the *standby* nor the *alarm* bit set to TRUE, or both bits set to TRUE, the smoke detector is declared failed and is no longer polled. In Boolean terms: $Failed = (\text{alarm} * \text{standby}) + (\overline{\text{alarm}} * \overline{\text{standby}})$

5. Network Topology

The smoke detectors are connected with the network in a linear bus topology with stubs departing from a central bus line. Bus termination is accomplished through resistors implemented within the network master at one end of the network, and the last smoke detector at the other end. Each item of equipment is qualified to operate on a CAN bus of length 150m, with 32 nodes connected through 2m long stubs to main bus line.

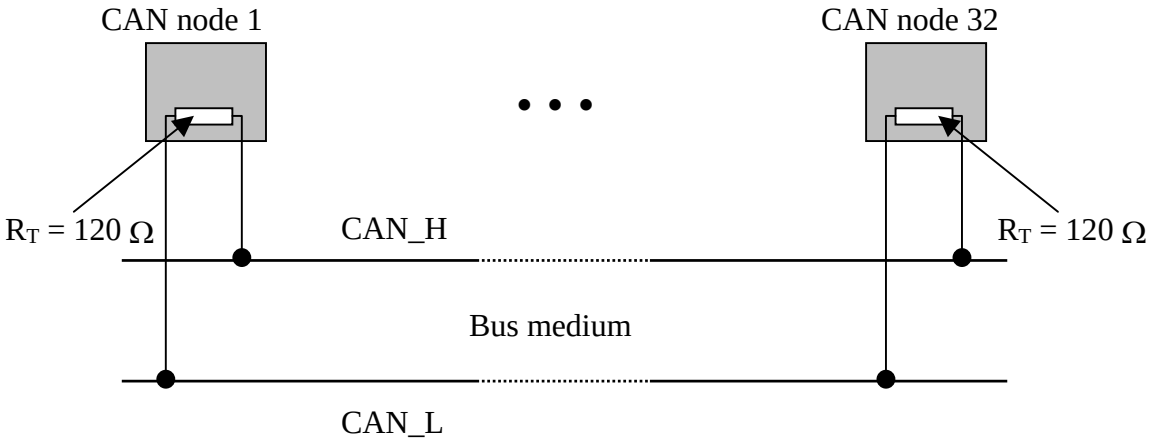

Depending on compartment being monitored, either a single or dual-redundant bus line is incorporated depending on the reliability requirements and whether the compartment is accessible or not during flight. The dual redundant architecture implies two smoke detectors at each location within a compartment. This is the case for the cargo compartments in the lower deck of the aircraft. Each lavatory, on the other hand, is fitted with a single smoke detector.

6. Conclusion

Through clever system design and network management, a CAN bus based safety critical smoke detection system with deterministic behavior capable of fulfilling the safety and reliability requirements was developed, and approved by airworthiness authorities and is in commercial service since mid 2003.. The robustness and reliability of CAN in an aircraft application is being closely monitored, with some 400,000 accumulated flight hours (including multiple equipment factor) having been accumulated in the period between mid 2003 and April 2004.

7. References

[1] ISO11898 AMENDDMENT 1 Road vehicles – Interchange of digital information-Controller are network (CAN) for high-speed communication

[2] Schmid, C. SID 2616DD100 “ATA26 CAN Application Layer Protocol”, Issue 2

[3] Radio Technical Commission for Aeronautics (RTCA) Washington D.C., RTCA/Do-178B Software Considerations in Airborne Systems and Equipment Certification

Radoslaw R. Zakrzewski, Mokhtar Sadok, and Bob Zeliff

Goodrich Corporation, Vergennes, Vermont, USA

[radek.zakrzewski, mokhtar.sadok, bob.zeliff]@goodrich.com

Video-based Cargo Fire Verification System for Commercial Aircraft

Abstract

The Cargo Fire Verification System was developed to address the problem of frequent false smoke alarms that are of particular concern in long range flights of passenger aircraft. The system uses low-cost CCD cameras operating in the near infra red range to directly detect fire and hotspots. In addition, LED illumination units are appropriately switched on and off, and the obtained images are analyzed to detect smoke. Fusion of image processing results with temperature and humidity readings allows reliable detection of true fires and elimination of false alarms due to fog and dust.

Introduction

Development of the Cargo Fire Verification System (CFVS) was motivated by the need to reduce the incidence of false alarms of conventional smoke detection systems used in cargo bays of commercial aircraft. Upon an alarm, the crew is typically required to release fire suppressant and to divert to the nearest airport. Each emergency landing due to a false alarm incurs significant cost to the air carrier. In addition, diversion to a small remote airport may itself pose significant danger to the passengers or the aircraft. In case of long range flights over polar regions, the nearest airport may lack the necessary facilities, so safe take-off may be questionable in harsh weather environment. It is therefore desirable to reduce the false alarm rate and give the crew a method to assess the state of the cargo compartment prior to and after fire suppression. The CFVS was designed to address this issue in long range Airbus A340 wide body aircraft.

The CFVS was designed as a verification system, intended to confirm or unconfirm alarms issued by the primary system. While suppression would still be performed following a smoke alarm, the decision to divert would be based on the actual state of

the cargo bay. The digital video recording function of the CFVS allows visual inspection of the bay to check if fire conditions indeed existed at the time of the alarm. However, visibility in a fully loaded cargo hold may be restricted to very narrow gaps between containers and the bay's ceiling and walls, thus making such visual assessment of limited utility. To address this difficulty, the CFVS uses image processing to detect and differentiate phenomena invisible to the naked eye in raw video feed. Image features calculated from multiple frames are fused with non-video data to obtain a final diagnosis that maximizes rejection of false fire alarms without affecting true ones.

As suggested by Airbus, the CFVS was developed to meet performance requirements based on EN54 fire detection standard, which are significantly more demanding than the usual smoke detection tests used for aircraft certification purposes.

The use of computer vision constitutes a breakthrough in aircraft fire detection. From the performance standpoint, the CFVS can be used as a stand-alone system. Its smoke detection capability matches, and fire detection surpasses, that of traditional smoke detectors. It is also much less sensitive to such common false alarm sources as fog or dust. It also gives the crew greater confidence by presenting the diagnosis in a visual form overlaid over the actual images of the cargo bay. Installed either in new aircraft or as a retrofit, it offers greatly improved detection and false alarm immunity.

System architecture

The core of the CFVS are CCD cameras operating in the near infrared (NIR) band. Two cameras are located in opposite corners of each cargo bay, providing full visibility of the entire bay. In order to make them immune to external illumination sources, the cameras use optical filters that block visible light. Typically, cargo bays are equipped with fluorescent lighting with no emissions in the NIR band. Therefore, the CFVS operation does not depend on whether the cargo bay light is on or off. Each camera is equipped with its own controlled NIR LED illumination source. Additional NIR illumination units are installed in the ceiling of the bay. Through appropriate switching of those illumination sources, the system obtains different views of the scene, as described in a following section. An example of placement of cameras and overhead illumination sources in A340 cargo bays is shown in Figure 1.

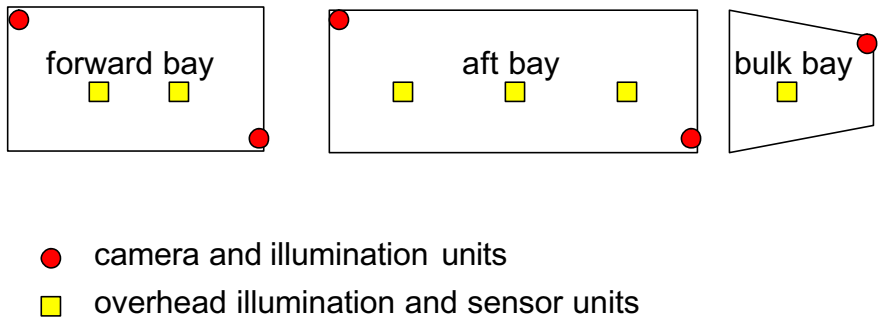

Figure 1. Example of camera and illumination placement in cargo bays; top view

Each camera is equipped with a DSP processor to analyze captured images and to calculate their various numerical features, which are then sent to the central control module. Additionally, the CFVS collects temperature and humidity measurements from sensors placed within cameras and overhead illumination units. These values are used to assess possibility of a false alarm-inducing scenario such as ascent-related fog. The central processing unit analyzes video and non-video data and upon an alarm issued by the primary system produces confirmation or unconfirmation diagnosis, together with the appropriate highlighting of the images sent to the cockpit video display.

In addition to decision making, the central unit acts as a digital video recorder. Output of each camera is recorded at a lower frame rate, so that it can be viewed at any time at push of a button. This allows the crew examining the state of a cargo bay before and after a primary alarm. In the present implementation, the CFVS stores the most recent 10 minutes of video from each camera. With addition of memory chips or adjustment of recorded frame rate, the length of this time window may be modified as needed.

Light switching sequences

To detect various visual aspects of fire and smoke and to differentiate it from non-fire aerosols such as fog and dust, the CFVS analyzes different views obtained under different illumination conditions. In the current implementation, four distinct views are used. Figure 2 shows examples of these four views through a simulated 4.3 cm gap above a container, acquired in University of Duisburg Fire Detection Laboratory.

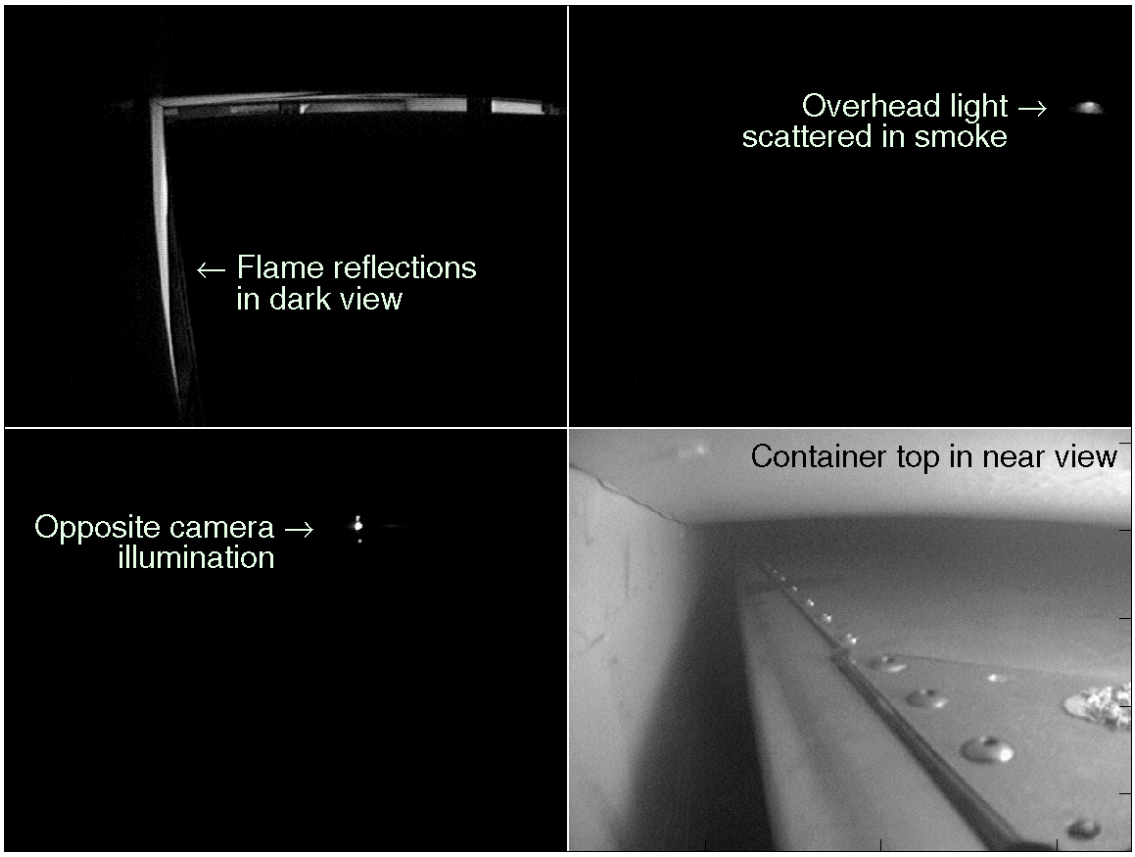

Figure 2. Four views with different illumination, same geometric configuration

In the dark view, all illumination sources are turned off, so that the presence of any high intensity image areas indicates a heat source, as illustrated in the upper-left part of Figure 2. This view is used for flame and hotspot detection, which is sufficient in majority of fire cases. However, in a fully loaded cargo bay, flames may be hidden behind containers. Similarly, for smoldering fires similar to EN54 fires TF2 and TF3 no flames may be visible. In such cases, the system must use the alternate smoke detection mode. For this, the remaining three illuminated views are used.

In the overhead view, the cameras' LED sources are switched off, while the overhead illumination units are turned on. In presence of smoke, their light is scattered, resulting in brighter image areas, as illustrated in the upper-right part of Figure 2. In many cases, the overhead light provides quickest smoke detection.

In the opposite view, all illumination sources are turned off, except for the LED of the opposite camera. In absence of smoke the opposite light is well visible, as seen in the

lower-left part of Figure 2. With smoke, the light gets absorbed and the image becomes smaller and dimmer until it may disappear completely. It may be noted that the CFVS operating in opposite view mode acts as a very long optical smoke detector, whose length comprises the entire bay. A pair of cameras placed on opposite ends of the bay replaces, and offers detection superior to, an entire set of multiple conventional point smoke detectors. For this mode to work, however, there must be a clear gap between the top of the cargo (containers) and the ceiling, e.g. as stated in Airbus loadability conditions. Presence of any cargo obstructing visibility of the opposite light may make this view useless from the detection point of view. However, the system may analyze such situation prior to take-off and switch to alternate backup detection modes.

The last of the illuminated views is the so-called near view, in which the only light turned on is the one collocated with the camera that is acquiring images. It is the near view that is fed to the central unit and recorded for later use by the crew. An example of a near view image is shown in the lower-right portion of Figure 2. Smoke may be visible in the near view through scattering of light by an aerosol cloud.

Performance requirements

The main challenge in design of the CFVS image processing and decision making algorithms was to specify clear and verifiable performance criteria. On one hand, the CFVS must always detect true fire or smoke prior to the primary system, so that when the latter issues its alarm the CFVS is ready with a confirmation decision. On the other hand, the common false alarm scenarios should be recognized as such. This required detailed characterization of the most common false alarm causes. We used available public domain studies such as [1], as well as proprietary false alarm statistics provided by Airbus. In addition, an advisory group of university and industrial experts was formed and asked to determine which false alarm scenarios are prevalent in practice and may be successfully distinguished from true smoke or fire. A conclusion of this study was that the overwhelming majority of false alarms is most likely caused by fog. For example, fog may form through super-saturation of humid air due to rapid pressure decrease and adiabatic cooling during take-off and ascent. Fog may also form during the flight near moisture-emitting cargo such as vegetables or animals. The second most

probable false alarm cause was determined to be dust lifted from dirty containers, or perhaps produced by cargo such as pollinating plants or agitated animals.

In view of these findings, the CFVS was designed to address fog and dust as primary non-fire scenarios. For performance in fog, the system was tested in a pressure chamber, in which rapid depressurization was used to produce dense fog. For performance in dust, a specialized dust generator was used with standardized ISO dust.

Densities of both fog and dust were chosen such that they caused the conventional smoke detectors to alarm. The success criterion for the CFVS was to diagnose a non-fire case and to unconfirm the primary system's alarm.

For fire detection, it was agreed that a super-set of EN54 test fires would be useful. Since the EN54 tests were originally designed for point smoke detectors with focus on building environment, they had to be appropriately adapted and scaled, so that they more closely correspond to cargo bay conditions. These modifications are described in detail in the accompanying paper [2]. The CFVS was required to reach a confirmation decision for each test fire prior to the primary system's alarm.

Detection and discrimination algorithms

Image processing is performed by DSP chips located within each camera. Therefore, it is done on a single frame basis – i.e. each frame is analyzed independently. Then the calculated values of image features are sent over a low-bandwidth digital link to the control unit which then performs data fusion and makes a fire/non-fire decision.

Different image processing algorithms are used for the four different views. Although state of the art DSP chips are used, the processor cycles are still at premium, which is a typical situation in image analysis applications. Therefore the priority was given to computationally inexpensive image features well known in literature [3]. Among those, mean pixel intensity and its standard deviation were found particularly useful.

$$\mathrm{mean}(X) = \frac{1}{MN}\sum_{i=1}^{M}\sum_{j=1}^{N} X(i,j)$$

$$\mathrm{stdev}(X) = \sqrt{\frac{1}{MN}\sum_{i=1}^{M}\sum_{j=1}^{N}\left(X(i,j) - \mathrm{mean}(X)\right)^2}$$

These two image statistics provide useful information about global intensity level and its variability, but do not allow any inference about its spatial distribution. This maybe achieved by analyzing second order moments

$$\mathrm{M}_{20}(X)=\frac{1}{MN}\sum_{i=1}^{M}\sum_{j=1}^{N}(i-\mathrm{X}_c)^2\,X(i,j)$$
$$\mathrm{M}_{02}(X)=\frac{1}{MN}\sum_{i=1}^{M}\sum_{j=1}^{N}(j-\mathrm{Y}_c)^2\,X(i,j)$$
$$\mathrm{M}_{11}(X)=\frac{1}{MN}\sum_{i=1}^{M}\sum_{j=1}^{N}(i-\mathrm{X}_c)(j-\mathrm{Y}_c)\,X(i,j)$$

where X_c and Y_c are the center of mass coordinates for the intensity field, given by

$$\mathrm{X}_c(X)=\frac{1}{MN}\sum_{i=1}^{M}\sum_{j=1}^{N}i\,X(i,j)\qquad \mathrm{Y}_c(X)=\frac{1}{MN}\sum_{i=1}^{M}\sum_{j=1}^{N}j\,X(i,j)$$

The above image statistics may be applied to raw images, as captured by the camera, or after suitable transformations designed to extract the specific aspects of interest. For example, edge detection transformation may be performed. Then, mean intensity of the edge image describes “edginess” or detail level of the original image. A fairly simple transformation that describes image sharpness is gradient norm, given by:

$$G_1(i,j)=X(i+1,j)-X(i,j)$$
$$G_2(i,j)=X(i,j+1)-X(i,j)$$
$$G_N(i,j)=\sqrt{G_1^{\,2}(i,j)+G_2^{\,2}(i,j)}$$

The mean value, standard deviation and second order moment statistics may be applied to the gradient image. For example, a decrease in mean gradient norm may indicate decrease in contrast associated with presence of fog.

For hotspot analysis we applied standard image segmentation algorithms to detect connected, space- and time-wise, regions of elevated intensity.

To reduce influence of spurious noise effects on detection, each feature is appropriately filtered. The simplest option is to use a first order filter

$$y_{filt}(t)=(1-\alpha)y_{filt}(y,t-\Delta)+\alpha y(t)$$

where $y(t)$ is the most recently calculated image feature, $y_{filt}(t)$ is its filtered value, α is the filtering constant, and Δ is the time interval between acquisition of consecutive images. Setting of initial conditions and possible re-initialization of image feature filters had to be carefully considered.

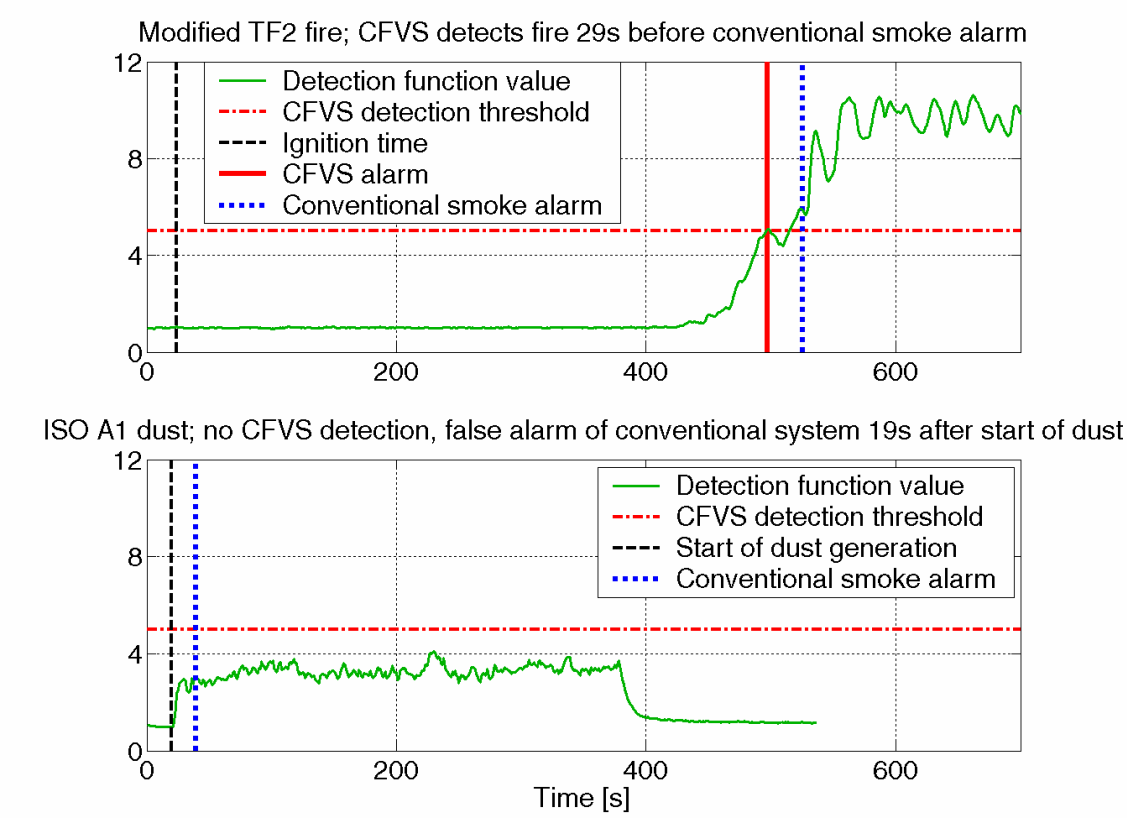

Figure 3. CFVS performance compared to conventional A340 detectors

The filtered image features are sent by the cameras to the central processing unit, which compares them and their most recent values against detection thresholds and performs final decision making. In its simplest form, a decision function may involve checking whether a filtered image feature crossed its associated threshold

$$D_i = \left(y_{filt\,i} > t_i \right)$$

A more complicated form may involve a linear combination of image features

$$D_i = \left(\sum_{j=1}^{k} a_j y_{filt\,j} > t_i \right)$$

Then the final decision may be a Boolean function of multiple elementary decisions D_i. Other more involved decision making methods may also be used, such as optimal Bayesian reasoning. They fuse image data with non-image measurements such as temperature, humidity or flight phase status to obtain the best decision.

The choice of the particular image features and decision functions is based on experimental video database. While certain guidance may be gathered from the general nature of the observed images, such as fading, loss of contrast, or light blooming, the

final selection can only be made based on the actual video data. The decision functions and their thresholds are chosen in such a way so that correct classification of all true fire cases is always assured, but the incidence of false alarms is minimized.

Figure 3 shows two typical examples of CFVS performance compared to actual behavior of production A340 smoke detectors. The decision function shown is based on analysis of the overhead view. For a smoldering fire, the CFVS is ready to confirm almost half a minute prior to the conventional smoke alarm. In the dust test, the CFVS detection threshold is never crossed, while the conventional system issues an alarm only 19 seconds after start of smoke generation. In this case the CFVS would unconfirm the smoke alarm as false. This illustrates the improved immunity of the CFVS to common false alarm causes.

System development status

The CFVS image processing algorithms and their specific parameters were developed based on a large video database, involving smoke, fog, dust and other aerosols. The primary experimental location was in University of Duisburg Fire Detection Laboratory. Fire and smoke experiments were also conducted in a cargo bay mock-up in Trauen, Germany, for accurate simulation of a fully loaded cargo bay. Fog and smoke data in simulated take-off conditions were collected in a National Technical Systems pressure chamber in Boxborough, Massachusetts, USA. Finally, smoke experiments were also conducted on the ground in an A340 aircraft made available by Airbus. The collected database was used to define the exact image features, filtering constants and detection threshold values to be used in the CFVS software.

At present, the CFVS camera and overhead illumination units are fully developed and packaged, meeting all Airbus and FAA/JAA requirements. The control unit along with its software is also fully developed. The system is currently ready for deployment.

Conclusions

The CFVS constitutes a major advancement in the state of the art of aircraft of fire detection. While the concept of video-based detection is well known and was

practically used in buildings or tunnels [4], [5], the CFVS is the first vision system suitable for actual deployment in a commercial aircraft. In performance tests, the CFVS detected all fire cases 20 to 350 seconds before the conventional A340 smoke detection system. The hardware meets all DO-160D environmental specifications and software has been developed according to DO-178B guidelines. As such the CFVS is fully certifiable. Although it was developed with Airbus A340 in mind, it may be modified for other aircraft as well – either as original equipment or as a retrofit option.

The advantage of the CFVS over conventional smoke detection is twofold. Firstly, it is able to detect flames and hotspots directly from NIR images. Therefore, it may detect low-smoke fires much faster than traditional smoke detectors. Secondly, the system makes use of the distributed nature of video information. Instead of a small number of discrete points, a camera image integrates data from a large volume, which enables earlier detection. Use of switched lighting allows analysis of different features of smoke and non-smoke aerosols, thereby providing means of fire/non-fire differentiation absent in conventional detectors. The result is a detection system that meets or exceeds all fire detection requirements with greatly improved false alarm immunity.

References

[1] P. Mangon, “Fire Detection for Aircraft Cargo Compartments, Reduction of False Alarms”, in: K. Beall, W. L. Grosshandler, H. Luck, Eds., *Proceedings of 12th International Conference on Automatic Fire Detection "AUBE '01"*, pp. 653-664, 2001.

[2] W. Krüll, I. Willms, J. Shirer, “Test Methods for a Video-Based Cargo Fire Verification System”, in *Proceedings of 13th International Conference on Automatic Fire Detection "AUBE '04"*, elsewhere in this volume, 2004.

[3] R. C. Gonzalez, R. E. Woods, *Digital Image Processing*, Prentice Hall, 2002.

[4] R. Maegerle, “Fire Protection Systems for Traffic Tunnels Under Test”, in: K. Beall, W. L. Grosshandler, H. Luck, Eds., *Proceedings of 12th International Conference on Automatic Fire Detection "AUBE '01"*, pp. 324-337, 2001.

[5] D. Wieser, T. Brupbacher, “Smoke Detection in Tunnels Using Video Images”, in : K. Beall, W. L. Grosshandler, H. Luck, Eds., *Proceedings of 12th International Conference on Automatic Fire Detection "AUBE '01"*, pp. 79-90, 2001.

Wolfgang Krüll, Ingolf Willms
Universität Duisburg-Essen, Campus Duisburg, Germany
Jeff Shirer
Goodrich Corporation, Vergennes, Vermont, U.S.A.

Test methods for a video-based Cargo Fire Verification System

Abstract

A video-based fire and smoke detection system for cargo bays of airplanes has been developed. It was necessary to create a suite of fire sensitivity and false alarm immunity tests applicable to these vision based fire detection systems. This paper will concentrate on testing aspects and test cell modifications.

Introduction

Against the background of high costs caused by false alarms of smoke detectors in cargo bays of airplanes, a video-based smoke detection system (**C**argo **F**ire **V**erification **S**ystem - **CFVS**) has been developed. Currently, if a smoke alarm occurs, the crew must activate the extinguishing system and land at the nearest suitable airport. High costs are caused by flight diversions, landing costs and loss of the cargo load. The pilot has no capability to verify if the alarm is real or false. Possible reasons for false alarms of traditional smoke detectors are mist, dust, oil particles. Additional problems in cargo compartments are environmental conditions such as temperature variation and air pressure variation. The objectives of the Cargo Fire Verification System are to provide the aircrew with images of the conditions in the cargo bay, to detect fire earlier than conventional smoke detectors, and to greatly reduce false alarms.

Aircraft cargo compartments

Cargo compartments of passenger aircraft are located below the passenger cabin and are not easily accessible during flight. They are a difficult area to view with video cameras because the gap between the cargo and the cargo bay ceiling can be as small as 4.3 cm. For reference, the size of an Airbus A340-500 aft compartment is 10.4 m long, 4.2 m wide, and 1.7 m high. The A340-500 contains 3 cargo compartments, referred to as the

Forward (in front of the aircraft), Aft, and Bulk cargo bays (behind the wing boxes). Figure 1 shows how the cargo compartment can be nearly completely filled with cargo containers.

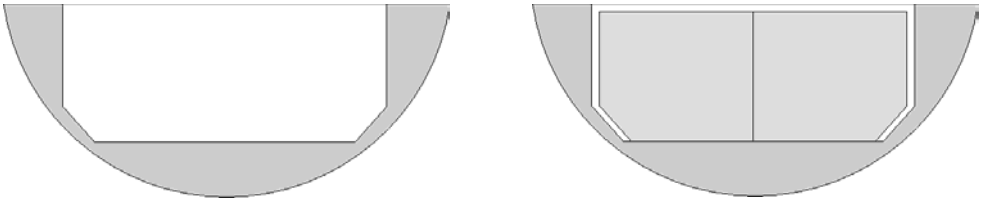

Fig. 1 Section views of a cargo compartment without (L) and with (R) containers

Video-based detection system

The functional objectives of the Cargo Fire Verification System are to provide the aircrew with images of the conditions in the cargo bay, to detect fire and smoke faster than conventional smoke detection systems, and to be immune to typical false alarm sources. Thus, the CFVS primary detection must be video based [1].

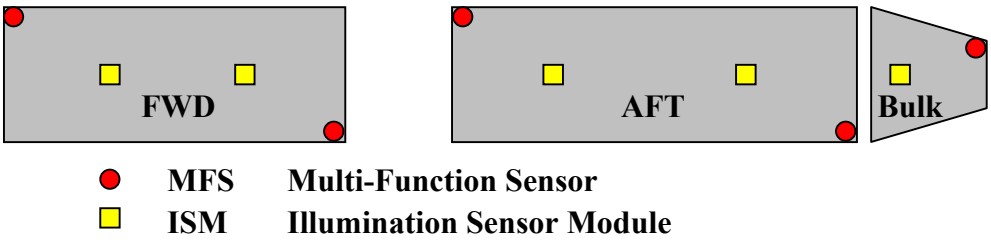

Fig. 2 Example CFVS aircraft installation, top view

The CFVS was developed by Goodrich Corporation. It consists of Multi-Function Sensors (MFS), Illumination Sensor Modules (ISM), and a Cargo Fire Verification Control Unit (CFVCU). The MFS includes a near-infrared filter and CCD video camera, integrated LEDs for illumination, a Digital Signal Processor for image analysis, and a lens window heater to prevent condensation in the field of view. Near-infrared functionality ensures operation without visible lighting in the cargo bay. The MFS provides real time video and image statistics to the CFVCU. The MFS's are mounted in the cargo compartment to maximize volumetric coverage of the compartment.

The ISM consists of near-infrared illumination LED's, a temperature sensor, and a humidity sensor. Sensor data is provided to the CFVCU. ISM's are mounted in the ceiling of the cargo compartment. The CFVCU provides system operation control, sensor data fusion, smoke alarm decision making, video storage for replay, and cockpit display interfaces. The CFVCU is typically installed in an avionics bay. Figure 2 shows a representative CFVS installation, and Figure 3 is an image of the gap between a cargo container and the top of a cargo bay from an MFS.

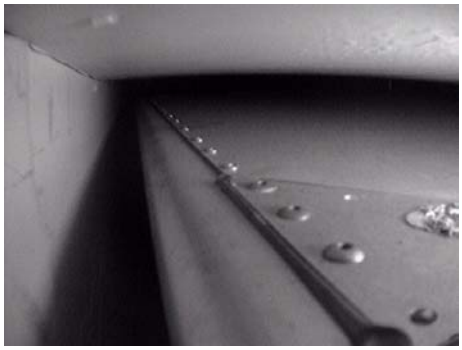

Fig. 3 Typical view of a camera behind containers

Testing of video-based systems

The existing testing guidelines and standards for qualification of current smoke detection systems were formulated mainly to address the case of traditional detection technologies, e.g., optical-based smoke detectors. In many cases, the qualification tests were derived from the EN-54 [2] fire sensitivity tests, which were originally developed for testing smoke detectors in buildings. In short, the EN-54 tests have different types of smoke sources at the center of the floor of a large test chamber. During the tests, the smoke density at the location of the smoke detector and the alarm time of the detector are measured. The geometry and contents of the test chamber are not critical to the smoke detectors if the smoke density increases within the EN-54 guidelines.

However, for a video-based detection system, the scene geometry and contents are critical. The scene should closely represent the actual application. For an aircraft cargo bay application, the fire test room should resemble an actual cargo bay, including cargo obstructions in the camera field of view. The tests should also retain the repeatability aspects of the EN-54 tests. Possible candidates for the testing of the CFVS included:

- Special testing aircraft
- A reconstruction of a cargo compartment
- A modified EN-54 test room

Testing in an aircraft has many of disadvantages, e.g., high costs, limited test times, and restricted test options (no open fires and dust tests are permitted). Figure 4 is an image from a video recording of a smoke test in an A340-600 aircraft.

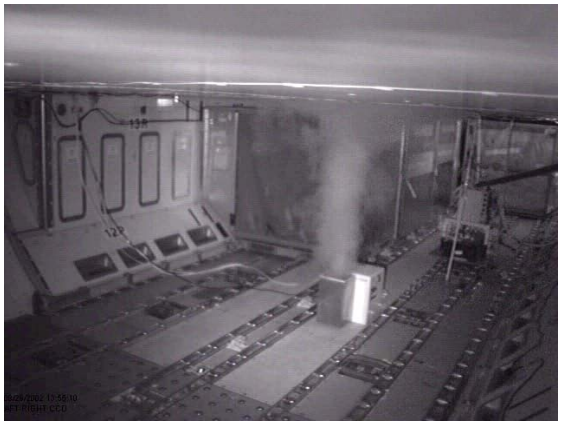

Fig. 4 Smoke generator test in A340-600 aircraft

Fig. 5 A340-500 cargo bay mock-up in Trauen, Germany

Tests in a reconstruction of a cargo compartment, such as the A340-500 cargo bay mock-up in Trauen, Germany, have the advantage that the geometry is very close to the actual cargo bay, Figure 5 shows the mock-up. The main drawbacks of the Trauen mock-up are the difficult adaptation to a special compartment type, high construction effort, and the required space only for this application. Furthermore, no comparative EN-54 tests are possible because of the smaller volume of the mock-up, the uncontrollable environmental conditions, and the lack of required instrumentation. Because of the disadvantages listed above, the tests were performed in the fire detection lab of the University Duisburg-Essen, which is traditionally used for EN-54 tests.

Fire room configuration

The Duisburg fire lab exhibits an EN-54 like test cell with the option of changing the height of the cell by moving the ceiling in a wide range. Advantages of the Duisburg fire lab are controlled environmental conditions, a wide range of measurement possibilities, and a significant better probability for “repeatable” tests than other testing options.

The fire room was modified so that it more closely resembled a cargo bay in the following ways (see Figure 6, Figure 7, and Figure 8):

- Aluminium side wall plates were hung from the ceiling to reduce the room width to that of a cargo bay. The side walls hung down 95 cm from the ceiling at a distance of 210 cm from the centerline of the fire room, emulating a cargo compartment width of 420 cm. To enhance the realism of the side walls, the plates were covered with DuPont Tedlar PVF Film as in an actual cargo bay.

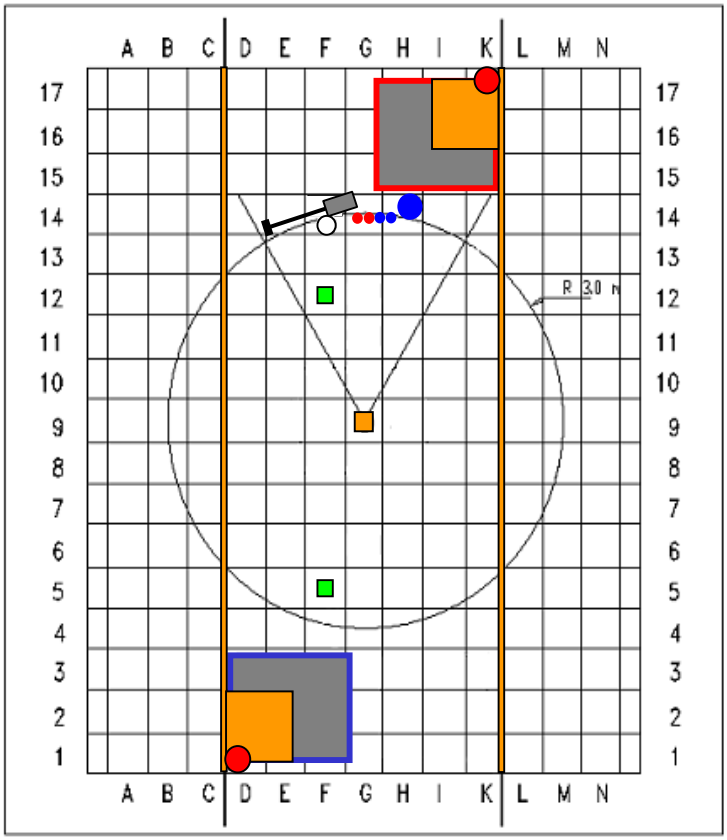

Fig. 6 Modified Duisburg Test Cell – Top View

- A single 1 m² sheet metal plate covered with the cargo bay lining material was mounted on the ceiling near the cameras in order to provide realistic optical conditions near the cameras.
- Fire and non-fire sources were placed on a platform, so that the distance between the source and the fire room ceiling was 1.7 m, which is the floor to ceiling distance in a cargo bay. A platform was required to raise the source because the ceiling cannot be lowered closer than 2.87 m from the fire room floor.
- LD-3 cargo containers were placed in front of the cameras to limit the field of view to the gap between the top of the container and the ceiling. Both containers were set on platforms so that the gap between the container and the ceiling was in the worst case at a minimum value of 4.3 cm. The containers were located according to existing cargo loading standards.

- The test cell observation windows were covered so that outside light did not enter the test cell. In addition, the test cell lights were turned off during the tests.

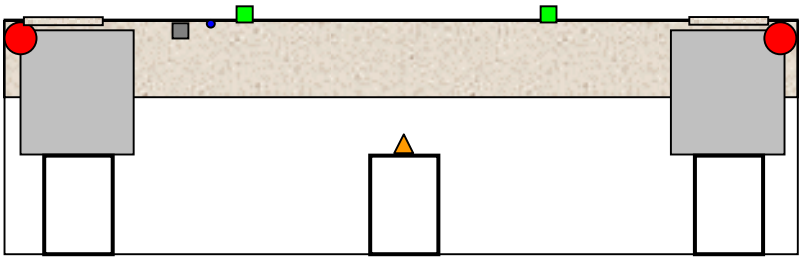

Fig. 7 Modified Duisburg Test Cell – Side View

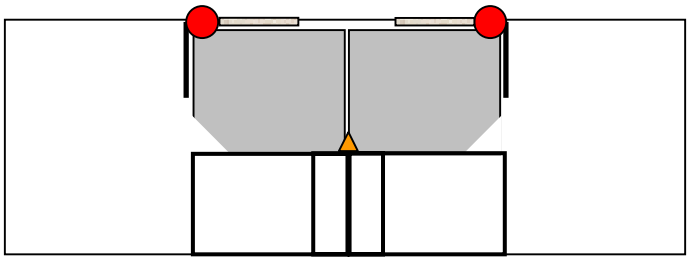

Fig. 8 Modified Duisburg Test Cell – Front View

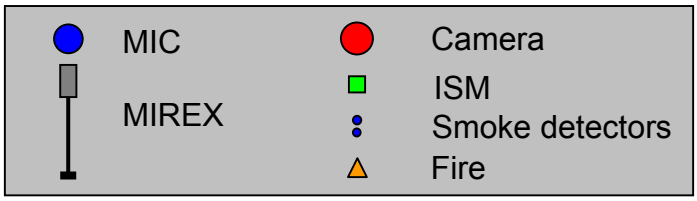

Fire tests

A suite of fire sensitivity tests applicable to vision based fire detection systems was then developed by Goodrich Corporation and the Universität Duisburg-Essen. The objective was to scale the standard EN-54 fire sensitivity tests [2][3] for the reduced volume of the modified test cell as described above. Fire and smoke tests were performed in the A340-500 cargo bay mock-up in Trauen and in Duisburg. At the Duisburg Fire Detection Lab tests were performed in three major types of scenarios, see Table 1:

- Standard EN-54 test fires.
- Modified test fires without test cell modifications, but with camera obstructions by containers.

- Modified test fires with test cell modifications (for Forward, Aft, and Bulk compartment configurations), including camera obstructions by containers. The test cell was modified to more closely resemble an actual cargo compartment, and the test fire material was reduced to account for the reduced test cell volume.

		Modified test fire		EN-54 test fire	
TF	Material	Amount	Pan size	Amount	Pan size
1	beech wood	40 pieces	-	72 pieces	-
2	beech wood	16 pieces	-	30 pieces	-
3	cotton	54 wicks	-	108 wicks	-
4	polyurethane	2 mats	-	4 mats	-
5	n-heptane	120 g	12cm*12cm*2cm	650 g	33cm*33cm*5cm
6	alcohol	850 g	33cm*33cm*5cm	2300 g	50cm*50cm*5cm
7	decalene	75 g	10cm*10cm*2cm	170 g	12cm*12cm*2cm

Table 1 EN-54 and modified test fires

Even though the room geometries of both test cells (the reconstruction of a cargo compartment in Trauen and the Duisburg fire lab) are completely different, the results are comparable by using a simple scaling factor. If smoke density (via the MIREX instrument) over time values measured in Duisburg (without side walls) are multiplied with a factor “3” the values are comparable with Trauen results. Figure 9 compares the Duisburg test cell and Trauen mock-up.

The Duisburg test cell volume was 293 m^3 (10.5 m * 9.0 m * 3.1 m) and the Trauen mock-up volume was 103 m^3 (15.0 m * 4.2 m * 1.71 m). Figure 10 compares smoke density values for TF2 runs at both locations and scaled values.

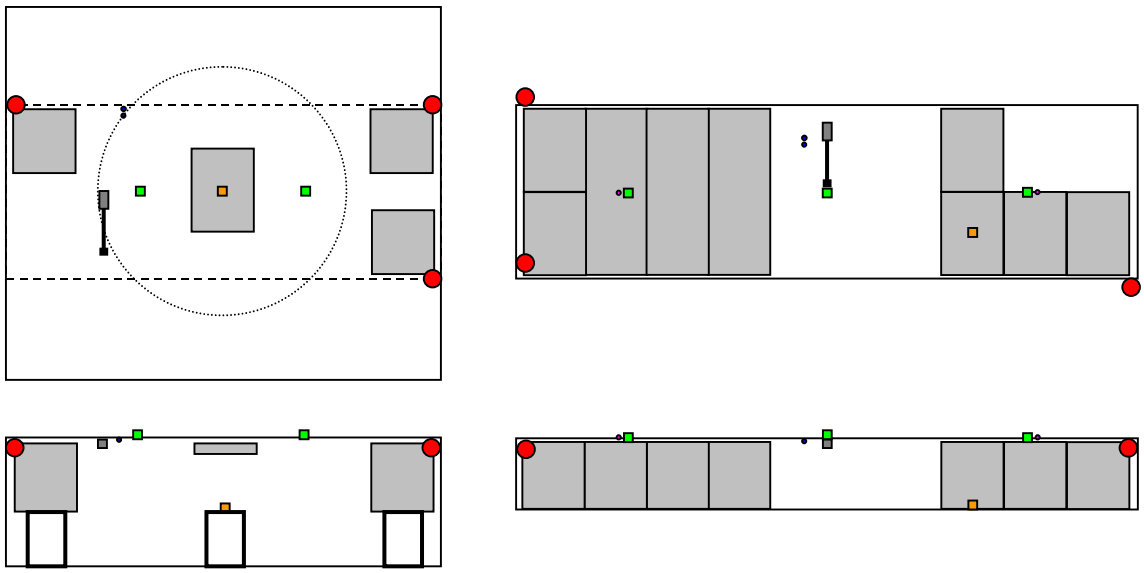

Fig. 9 Comparison of Duisburg top view (upper left), Trauen top view (upper right), Duisburg side view (lower left), and Trauen side view (lower right)

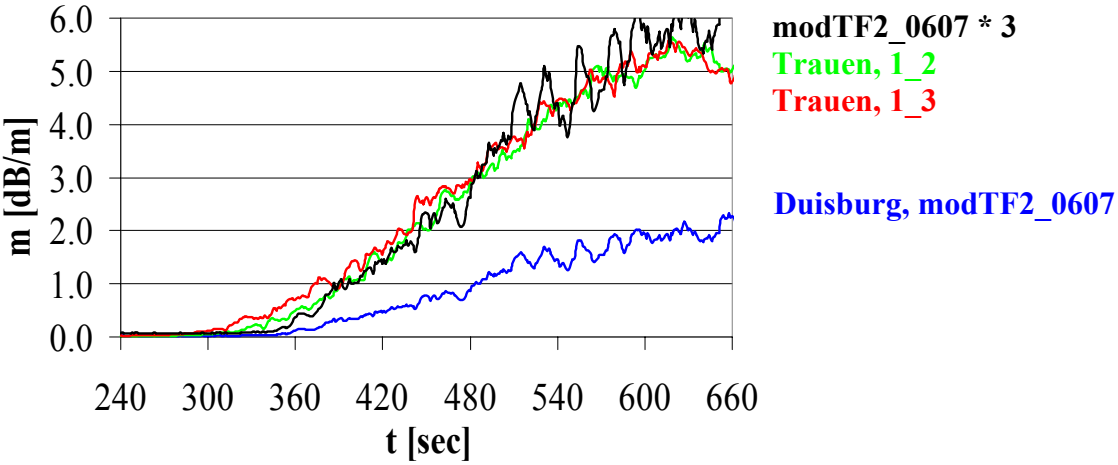

Fig. 10 MIREX values of modified TF2, measured in Trauen and in Duisburg (without side walls) and scaled values

Further tests with side walls in Duisburg show very good results with respect to the reconstruction of a cargo compartment in the Trauen - it is still a simple scaling factor to approximate the results from Trauen. A scaling factor of “1.5” shows a good approach to Trauen data bay (see Figure 11).

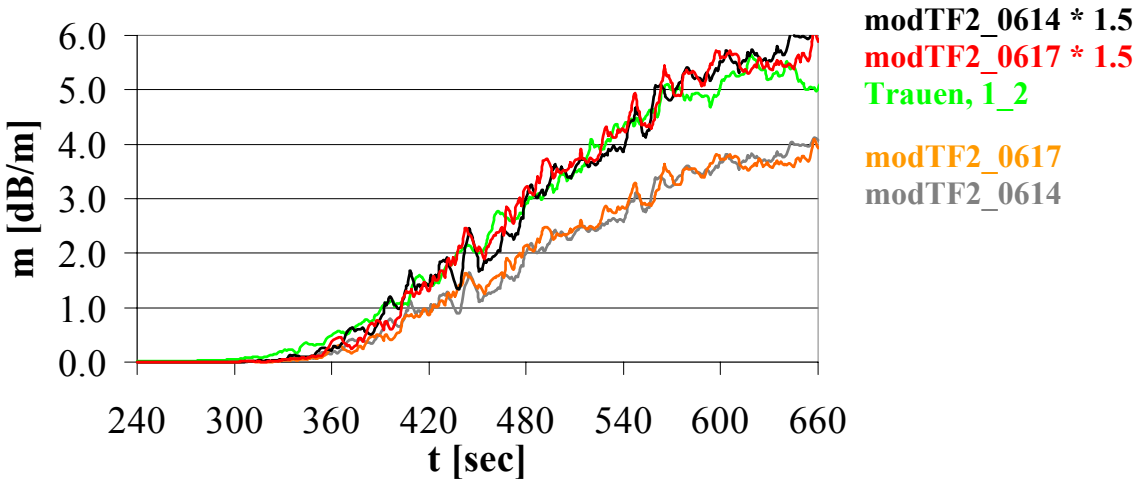

Fig. 11 MIREX values of modified TF2, measured in Trauen and in Duisburg (with side walls) and scaled values

Traditional smoke detectors were also part of the preliminary scaling experiments, and the smoke densities at which they alarmed were determined for each test fire type. The CFVS was required to detect the test fires at a lower smoke density than the traditional smoke detectors.

Dust tests

In addition to fire tests, non-fire tests with dust were set-up and performed. Dust is known to cause problems with optical smoke detectors and not only in cargo bays. Depending on the dust type and the dust production it may look similar to smoke on video. Thus the discrimination of dust and smoke in video-based systems is a challenge in its own. Therefore special consideration was given to dust tests and measures in order to provide a high degree of repeatability.

The dust tests used the test cell configuration modified to mimic a cargo bay, as described above. Figure 12 shows the set-up for the dust test. The key factors in the dust tests included the type of dust, the rate of dust introduced into the test cell, and amount of time that dust was generated, and the location of the dust generator.

Dust is typically defined as *"small solid particles, conventionally taken as those particles below 75 µm in diameter, which settle out under their own weight but which may remain suspended for some time"* [4]. Standardized dust particles are designated in several groups [5] and two of them were used for testing in Duisburg:

- A1 dust: Ultrafine, dust particles with nominal size 0-10 µm
- A2 dust: Fine, dust particles with nominal size 0-80 µm

The small particles in these dusts remain airborne longer than large particles and are more likely to be detected as smoke. They also are close to the particle sizes found in wood smoke, which makes it difficult for detection systems to distinguish between smoke and dust.

A dust generator was used to introduce dust into the test chamber. The generator adds the dust to a compressed air stream which is then directed by a nozzle into the test cell. The dust was expelled at a constant rate of 140 g/s. The dust nozzle was directed vertically towards the ceiling. By adjusting the compressed air pressure and the height of the dust generator, it was possible to create a dust cloud just below the ceiling. This put the dust cloud directly into the CFVS field of view. This type of dust generation is also analogous to the smoke generation of the test fires described above.

Fig. 12 Set-up for the dust test

In the test fires, the smoke rises in a vertical stream and then forms a cloud beneath the ceiling. Making the dust generation mimic the smoke generation is a challenging false alarm immunity test for the CFVS.

The total amount of dust injected into the test cell was controlled by the on-time of the dust generator. The on-time was used as the key metric for determining a system's immunity to dust. The dust levels in the test cell were measured with a separate particle counter, whose inlet tube was placed in the ceiling of the test cell. The particle counter values were used to verify that the dust generation was valid.

In preliminary testing, the dust generator was placed in several locations in the attempt to satisfy two objectives:

1. Subject the traditional smoke detectors and the CFVS to the same dust environment.
2. Determine the amount of dust generator on-time to trigger a smoke alarm from the traditional smoke detectors.

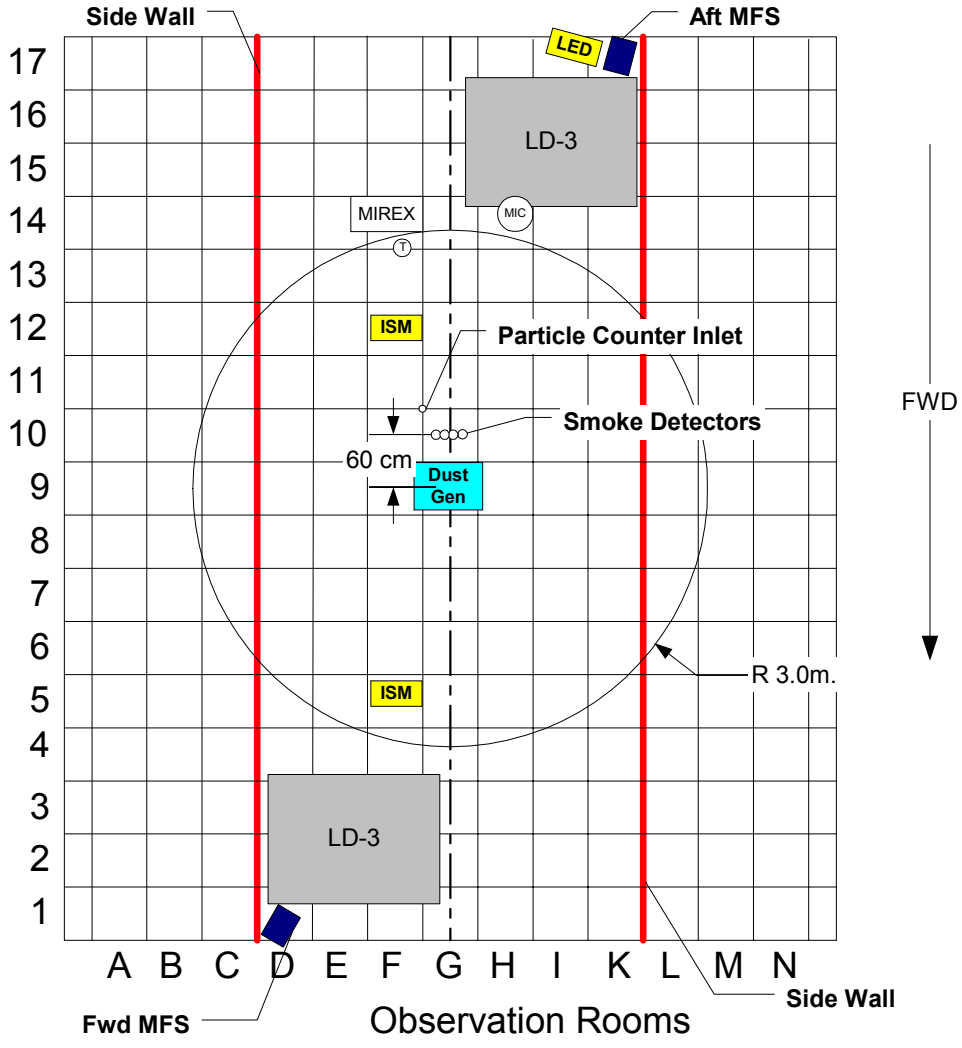

Fig, 13 Test cell set-up for Forward and Aft bay dust tests

The preliminary tests led to the definition of the CFVS dust-immunity tests. Figure 13 is a top view of the test chamber for the Forward and Aft bay configuration tests. Figure 14 is the same view for the Bulk bay configuration tests. In the Forward and Aft bay configuration, the test cell includes sidewalls and reflective plates, as did the modified test cell for the test fires. The dust generator was placed on a platform in the center of the test cell, in the same location as the test fire source. LD-3 cargo containers on platforms limited the view of the video cameras to the 4.3 cm gap between the containers and the ceiling.

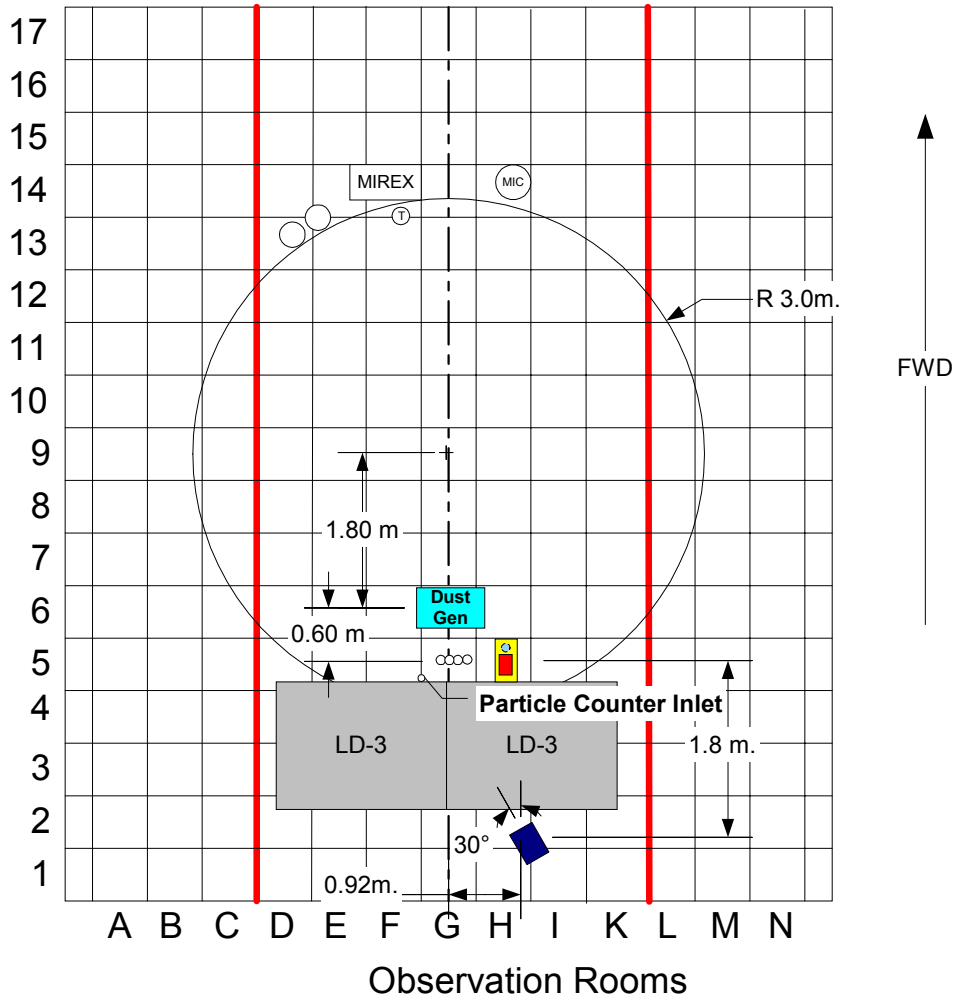

Fig. 14 Test cell set-up for Bulk bay dust tests

In the Bulk bay configuration, the dust generator was moved closer to the lone video camera in response to the smaller size of the Bulk compartment. The camera field of view was obscured by LD-3 containers.

The main CFVS dust-immunity requirement is that the CFVS must not indicate a smoke alarm for a given time after the start of dust generation. That critical time was far beyond the time at which a traditional smoke detector would issue a false alarm.

Conclusions

The existing testing guidelines and standards for qualification of current smoke detection systems were formulated mainly to address the case of traditional detection technologies. It was necessary to develop a suite of fire sensitivity tests, non-fire tests with dust and test room modifications applicable to vision based fire detection systems. Modified tests with room modifications in the Duisburg fire lab show good match with tests performed in a cargo mock-up.

References

[1] R. Zakrzewski, M. Sadok, and B. Zeliff, “Video-based Cargo Fire Verification System for Commercial Aircraft”, in *Proceedings of 13th International Conference on Automatic Fire Detection "AUBE '04"*, 2004.

[2] EN-54, Part 9, Fire Sensitivity Tests, BSi Standards, 1984.

[3] CEA, GEI 1-049, Test Methods For Multisensor Smoke Detectors, 1997.

[4] ISO 4225:1994, Air quality – General aspects – Vocabulary, 1994.

[5] ISO 12103-1:1997, Road vehicles – Test dust for filter evaluation – Arizona test dust, 1997.

Volker Leisten, Ingo Bebermeier, Carsten Oldorf
m.u.t Aviation-Technology GmbH, Tempowerkring 6, 21079 Hamburg, Germany

Camera-based Fire Verification System (CFVS) for Aircraft Cargo Compartments

Abstract

At present a very high rate of false fire alarms caused by smoke detectors installed in aircraft cargo compartments is resulting in unnecessary emergency landings, high additional cost for airlines as well as a high degree of distrust by the pilots. A camera-based multi-sensor system using proper software algorithms for detection of fire and smoke events is presented, which can provide substantially improved information to the flight crew and supports the decision making process in case of real fire and smoke events. The CFVS has already reached the prototype level and is undergoing an intensive test phase including preparation for a trial installation on an AIRBUS long range aircraft or similar test rig.

Introduction

Especially onboard of aircraft fire and smoke events have to be considered extremely safety critical. A lot of people and sensitive equipment are packed inside of a small volume, there are no emergency exits available while airborne, fire fighting resources are very limited and pilots have only few and risky options at hand. Therefore, any fire and smoke incident creates a high psychological stress situation, since it may lead to loss of aircraft and/ or loss of human lives. For that reason lavatory areas and cargo compartments of all larger aircraft are outfitted with smoke detectors and fire suppression systems. In order to allow an early detection of fire and smoke and to conform with international regulations these smoke detectors have to have a high sensitivity and a short response time of less than 60 seconds, [1] and [2]. However, these desirable features lead to a high ratio between false and real alarms. According to an FAA study only one out of about 200 fire alarms is a real one [3], thus resulting in a high number of unnecessary emergency landings associated with high cost and loss of image for both airlines and aircraft manufacturers. For the time period 1974 to 1999 the same FAA study

found more than 1.300 fire incidents in cargo compartments of US registered aircraft only, almost all of them caused by electric sources, i.e. malfunctioning electrical equipment or short circuits in wiring.

Figure 1 shows an inverter of a Boeing B737-700 which overheated and created large amounts of toxic smoke and damage to the aircraft [4].

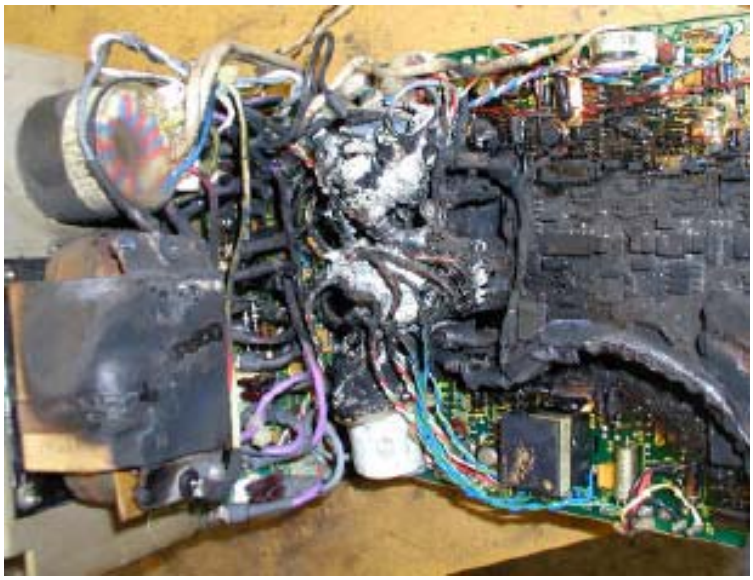

Figure 1: Inverter of Boeing 737-700

However, the aircraft landed safely and nobody was injured. Other fire incidents ended less luckily like the ValueJet accident in 1996 (110 fatalities, [5]), the FedEX freighter in 1996 (no fatalities, but aircraft & cargo lost, at 300 Mio.$, [6]) or Swiss Air Flight 111 in 1998 (231 fatalities, [7]). In addition, cargo compartments represent a significant portion of each larger passenger aircraft (approx. 40% of the total volume) and they are completely inaccessible during flight. Therefore, pilot organisations like ALPA (Air Line Pilots Association) require state-of-the-art improvements which can detect “initial signs of ignition” within less than today’s 60 seconds and provide more information than the present quote: “idiot lights” in the cockpit [8].

But there are also economical reasons which call for improvements in the fire and smoke detection systems. Airlines identify a growing demand for long distance flights lasting 18, 20 or even more than 22 hours non-stop, resulting in diversion times beyond today’s regulation of 180 minutes. With present smoke detectors onboard the increased flight time will inevitably come along with an increased probability of false alarms per

flight, thus reaching a level which would neither be acceptable to the authorities nor the airlines. An AIRBUS publication of 2002 dealing with the concept of Long Range Operations (LROPS) identifies false cargo fire warnings as “significant reason or unnecessary diversions” and estimates cost per diversion to “anything from $1m to $3m depending upon the location of the diversion airfield”,[9]. This situation was the starting point for intense discussions with AIRBUS, Deutschland in 2002/ 2003, finally resulting in a development programme initiated by m.u.t Aviation-Technology GmbH and partially funded by the “Luftfahrtforschungsprogramm” of the City of Hamburg.

System Concept

When looking for an improved fire and smoke detection system, one has to recall how human beings react, if they presume a fire. Almost all of them will try to see the fire, thus being able to *locate* it and to *assess* its size and the impending hazards. Seeing a fire also means being able to select appropriate countermeasures and to monitor the efficiency and sustainability of those measures, in other words, pilots would be able to respond to fire alarms as required by the regulations, but would also be supported in making the correct and less risky decisions during and after the incidents.

One has to keep in mind, fire and smoke incidents are 3-dimensional occurrences, nonetheless, present smoke detectors are based on *spot-like* sensors only, as a matter of principle they cannot provide spatial resolution or even a visual impression of the incident.

It was a logical consequence to support both natural human behaviour and the demand for more and conclusive information by:

- installation of video cameras in cargo compartments
- using additional light sources to provide illumination and to make smoke and fog/ aerosol incidents visible by scattering of light
- using additional sensors which help to distinguish between fog/ aerosols and real smoke events
- develop appropriate software algorithms for
    - image processing to allow recognition of fire and smoke
    - merging and evaluation of additional sensor data
    - provision of unambiguous outputs on displays in cockpit

A typical CFVS configuration for an aircraft comprising three cargo compartments is depicted on **Figure 2**.

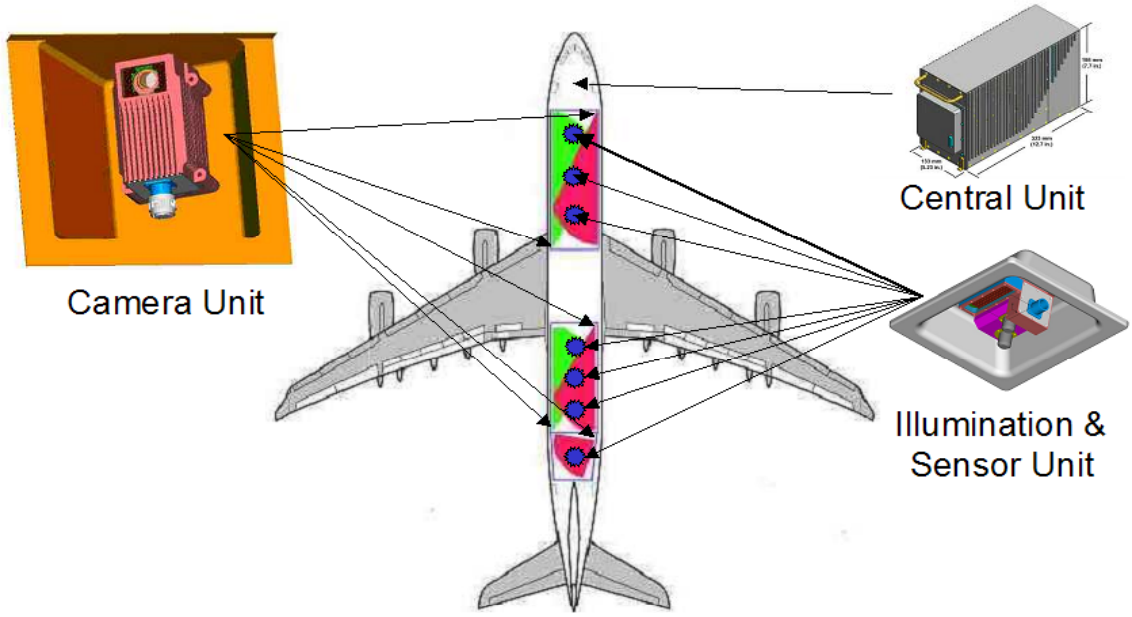

Figure 2: CFVS Components Allocation

However, development activities concentrated on the Camera Unit, the Illumination & Sensor Unit and software algorithms for detection of fire and smoke events as well as discrimination between smoke and fog events. The Central Unit is simulated by using a high-end PC being able to manage communication with all units via CAN Bus as well as to perform video data acquisition and image processing.

The Camera Units will be installed inside of special cavities close to the ceiling of the cargo compartments. Installation will be made such that a maximum field of view can be obtained and two cameras of one compartment will be able to “see each other” in a diagonal view.

The key features of each Camera Unit (see **Figure 3**) can be summarised as follows:

Figure 3: Prototype of Camera Unit

- Provision of NTSC quality Near-Infrared (NIR) Video Images
- Image Processing by internal software for “Hot Spot” / Fire Detection as well as pre-processing of parameters for detection of smoke, dust, fog/ aerosols
- Internal NIR Lighting, 2 groups for near and far range
- Built-in Test Equipment (BITE)
- CAN Bus Interface
- Mass < 1,5 kg
- MTBF ca. 50.000 h (BELLCORE)

In addition to the Camera Units Illumination & Sensor Units will be installed inside of special cavities in the ceiling of the cargo compartments. The main functions of those units are:

- to provide NIR-illumination for direct views into the cargo compartments
- to make smoke and aerosol / fog events visible to the Camera Units by scattering of NIR light
- to support discrimination between smoke and fog / aerosols events, thus reducing the number of false alarms

This discrimination between smoke and fog / aerosol events will be achieved by precise measurement of two additional parameters in combination with dedicated software algorithms:

- actual temperatures including monitoring of temperature trends
- actual dew point temperature including monitoring of dew point temperature trends

Nearly all aircraft applications require a design which provides high precision, long term stability, no or very low need for maintenance and low cost. While concepts and hardware used for temperature measurement can achieve these goals, measurement of dew point temperature requires a more sophisticated approach. State-of-the-art dew point sensors are

- either relatively cheap with a broad effective range, but showing a drift of approx. 2% per year thus requiring regular re-calibration or limiting the shelf life in an unacceptable way
- or quite expensive with a narrow effective range, but providing the desired long-term stability.

In order to get out of this dilemma the development work at m.u.t Aviation-Technology aimed at a new sensor which combines the positive properties of both sensor types. Tests performed on the new sensor included in the prototype of the Illumination & Sensor Unit as depicted on **Figure 4** demonstrated, that this goal is successfully achieved.
The quantity of Illumination & Sensor Units and their installation positions were selected in a way that a maximum of the volume of the cargo compartment (in loaded and unloaded conditions) can be illuminated. The key features of each Illumination & Sensor Unit can be summarised as follows:

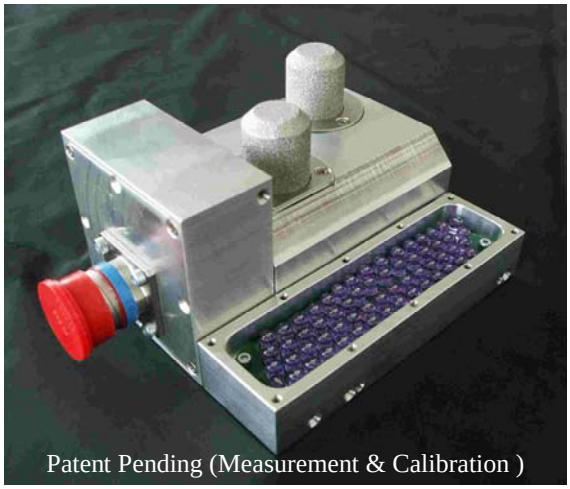

Figure 4: Illumination & Sensor Unit

- Near-Infrared Illumination by Solid State Emitters
- Temperature Measurement, ranging from –55°C to +85°C
- Drift Free Measurement of Dew Point and Relative Humidity, 5 to 100%
- CAN Bus Interface
- Built-in Test Equipment (BITE)
- Mass < 0,750 kg
- MTBF ca. 120.000 h (BELLCORE)

Test Results

Test activities can grossly be divided into two major groups hardware related tests and verification of software functions. In order to be able to detect the onset of a fire or smoke event within significantly less than 60 seconds, the camera has to provide both the highest possible sensitivity and images which are not altered by automatic image correction functions as usually included video chips. Even more, the typical non-uniformity of the individual pixels of a video chip has to be determined and to be taken into account by appropriate software algorithms. The utilisation or modification of already available camera modules like those used for door surveillance or in-flight entertainment systems is immediately ruled out by these requirements. **Figure 5** shows the test images obtained from a calibrated black body heat source (+300°C, top left to +330°C, right bottom, with 10°C increments), demonstrating the capability to detect hot spots at temperatures which are far below the level visible to the human eye (approx. 600°C) or even open flames (starting at approx. 900°C).

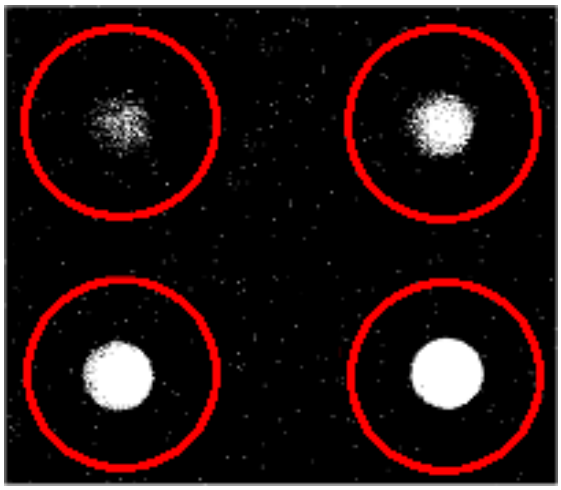

Figure 5: Hot Spots, +300°C to +330°C

Tests using a small tea warmer candle showed that detection is also possible if the heat source is hidden in dense (artificial) smoke, **Figure 6** or even behind cargo containers, **Figure 7**.

Figure 6: Small Fire in Dense Smoke

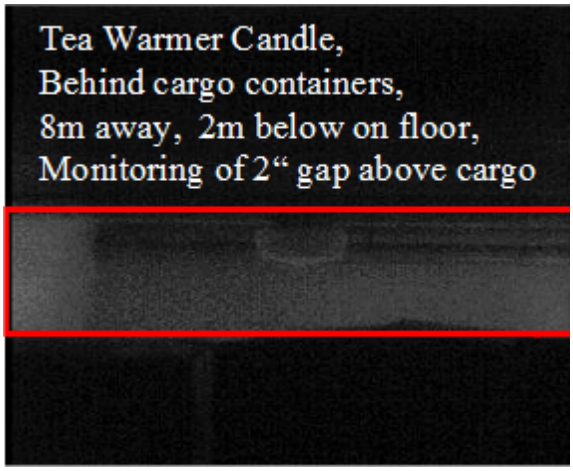

Figure 7: Small Fire behind Cargo

A dedicated software test bed operating under Windows is being used for development of software algorithms needed for detection of hot spot/ fire and smoke/ aerosol incidents respectively.

This approach turned out to be faster, more comfortable and very cost efficient in comparison to directly using embedded software on the Camera Units. In addition, the test bed was configured such that it can process either live images or videos recorded during test campaigns. **Figure 8** shows the results of a smoke test performed in accordance with EN54, scaled Test Fire TF2, Smouldering Wood.

For detection of smoke entering the gap above the containers one Camera Unit has switched on its NIR light and the second Camera Unit is taking images which are analysed by a set of dedicated software algorithms, which generate an output (detection) signal as displayed on the lower halve of **Figure 8**. Even small amounts of smoke already lead to a significant change of the detection signal and within less than 5 seconds a smoke alarm is generated.

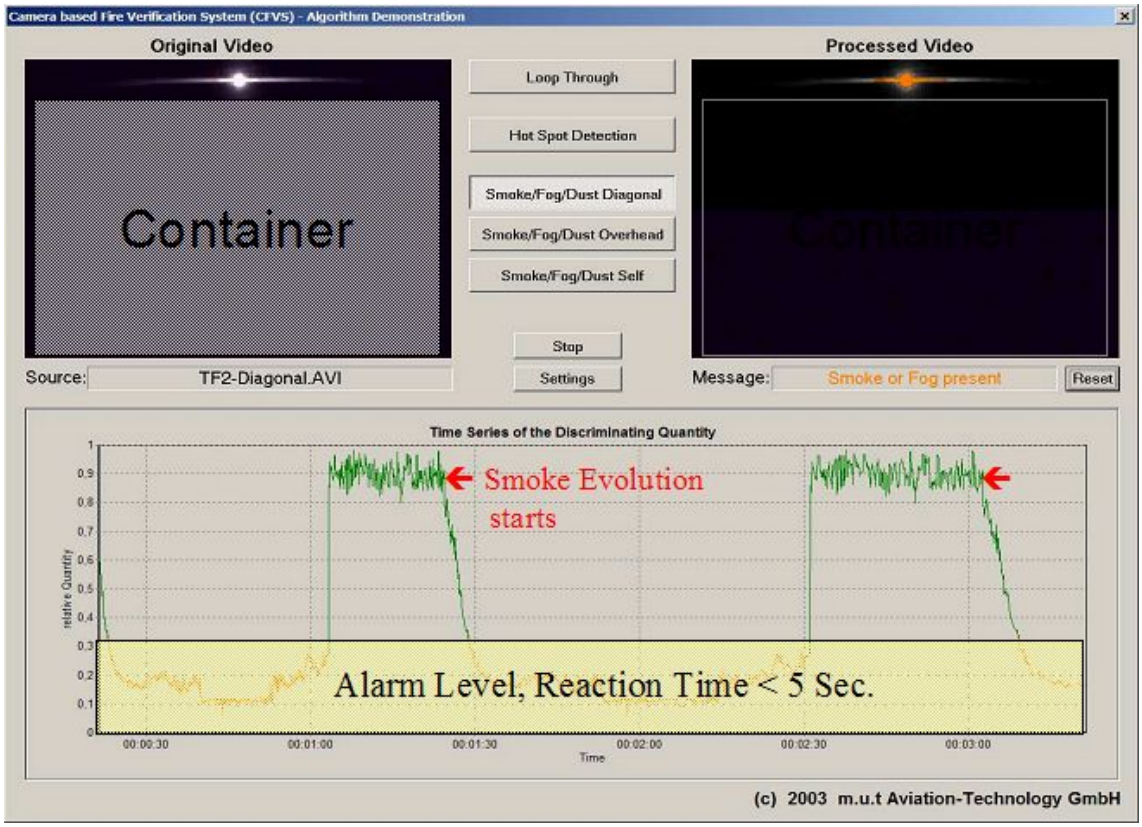

Figure 8: Software Test Bed, Detection of Smoke above Cargo Container

Summary

Key hardware elements as well as a set of software algorithms required for an image-based system allowing both fire and smoke detection as well as verification of alarms generated by conventional smoke detectors have been developed by m.u.t Aviation-Technology GmbH. As of today these components are being thoroughly tested and a set of hardware is prepared for a trial installation and tests on an AIRBUS long range aircraft or similar test rig by mid of 2004.

Literature

[1] JAR/FAR 25.858, Requirements for Fire Detection Systems

[2] AUBE´01, K. Schmoetzer, “Aircraft Fire Detection: Requirements, Qualification and Certification Aspects”, March 2001

[3] Federal Aviation Administration, DOT/FAA/AR-TN00/29, David Blake, “Aircraft Cargo Compartment Smoke Detector Alarm Incidents on U.S.-Registered Aircraft, 1974-1999”, June 2000

[4] BFU Report No. 5X016-0/13, November 25, 2003

[5] Aviation Safety Network Message, McDonnell Douglas DC-9-32, ValueJet, Message #47377/496, May 11, 1996

[6] Aviation Safety Network Message, McDonnell Douglas DC-10, FedEX, Message # 47809/191, Sep. 05, 1996

[7] Civil Aviation Authority, CAA Paper 2002/01, DOT/FAA/AR-02/50, September 06, 2002, R.G.W. Cherry, “A Benefit Analysis for Enhanced Protection from Fires in Hidden Areas on Transport Aircraft”

[8] ALPA (Air Line Pilot Association) Letter Response to FAA, NPRM-97-10, “Revised Standards for Cargo or Baggage Compartments in Transport Category Airplanes”, September 11, 1997

[9] AIRBUS Publication, Magazine FAST, Number 28, October 2002

U. STORM, A. FREILING, K. SCHMOETZER
Airbus – Bremen – Germany

C.-D. KOHL
Institut für Angewandte Physik (IAP) – Giessen – Germany

Fire Gas Detectors for Aircraft Application

Abstract

Aircraft applications require high system performance. The reduction of false alarms and the improvement of safety and reliability figures are therefore major criteria for the fire/smoke detection system. There are several approaches to reach these targets, whereas the application of semiconducting gas sensors is one of them. Changing environmental conditions like temperature, airflow, pressure and humidity put a burden on gas sensors. Immunity against multiple false alarm sources, vibrations, electromagnetic effects, high reliability and simple maintainability are challenges for such devices. Qualification and certification of fire gas detectors in aircraft application are in some areas still open issues.

This paper is focused on fire gas detectors for aircraft application. The requirements are described and results of measurements with several commercial semiconducting gas sensors under aircraft-similar conditions are summarized. The results are a summary of contracted work packages to *RST Rostock System Technik GmbH*, *Institut für Angewandte Physik* (Giessen) and *Gesellschaft für phys. Technologie und Elektronik mbH* (Viersen).

Introduction

Aircraft have to be protected against fire. This fire protection concept is combined of passive and active methods: on one side the usage of non-burnable materials and burn-through protected construction and on the other side the fire/smoke detection and fire extinguishing [1,2].

Permanently occupied areas are “equipped” with the best fire/smoke detectors – the human nose and eyes of crew and passengers, whereas areas that are not or not permanently occupied (i.e. cargo compartments, electronic compartments, lavatories crew rest compartment, etc.), have to be equipped with electronic smoke/fire detectors. These detectors are installed in/under the ceiling (see figure 1) or in the air extraction

ducts [2] and are working on the principle of optical particle detection or ionisation method.

Figure 1: Two smoke detectors in a cavity for installation in the ceiling of a cargo compartment

Both methods are able to provide a safe and reliable fire/smoke detection, but they have a common weakness: a cross sensitivity to some non-fire events, which can lead to false smoke alarms [3]. An activation of the fire extinguishing system (i.e. halon discharge), unscheduled flight diversion and evacuation of the aircraft are the result of a false alarm. There are different approaches to overcome this weakness: video-based systems [4], gas detectors, and multi-criteria detectors [10] are some of them. This paper is particularly focused on semiconducting gas sensors in the scope of smoke/fire detection in pressurized areas of aircrafts.

Performance of Smoke/Fire Detectors for Aircraft Application

The intended function of a fire/smoke detector is to detect all types of fire/smoke events. The detection shall be within 60 seconds after a start of a fire and not be inhibited by environmental conditions (i.e. pressure, temperature, humidity, acceleration, etc.). On the other side, smoke/fire detectors shall not trigger alarms in case of non-smoke/-fire events. This performance leads to a compromise between fast/sensitive and immune/insensitive detectors. Selectivity is the keyword for this behavior, but it is at the same time a big challenge, because of the strong requirement to detect <u>all</u> smoke/fire events and not to miss any fire. The validation and verification of the sensor performance become therefore very important tasks.

Environmental Conditions

Semiconducting gas sensors are working on the principle of adsorption and desorption of gas molecules [5]. The sensor characteristics depend on the partial pressures, temperature, flow rates and last but not least the sensor history. During ground and flight phases on an aircraft, most of these parameters are not stable, so that it is a challenge to extract the gas-sensing signal from the raw sensor data.

Environmental Temperature

The temperature category for a smoke detector, which is installed in a cargo compartment, is specified as cat A3 according to ABD0100 [6] and RTCA/DO-160D [7]. That means operation in the range of –40°C ≤ T ≤ +85°C and storage at –55°C ≤ T ≤ +85°C. The temperature variation is specified as 5 K/min.

Resistive gas sensors are heated up to temperatures between 100°C and 1000°C depending on sensor material and target gas to improve the desorption of gas molecules from the sensor surface and the diffusion effects. A change of the environmental temperature leads to a change in sensor temperature and behavior. Stabilizing the temperature by controlling the heating power of the sensor can mitigate this effect, but there are some limitations due to sensor layout, i.e. backside heater or buried heater, which leads to temperature gradients within the sensor structure. The temperature on the sensor surface remains therefore dependent on the environmental temperature.

To overcome this problem, a gas sensor array has been designed with radiation heaters in hybrid technology (see Figure 2). Tests in a climatic chamber have shown that the stabilization of the surface temperature can be improved by this concept. But the bigger size of the sensor array increases the power consumption to about 7W – 11W (dependent on the environmental temperature).

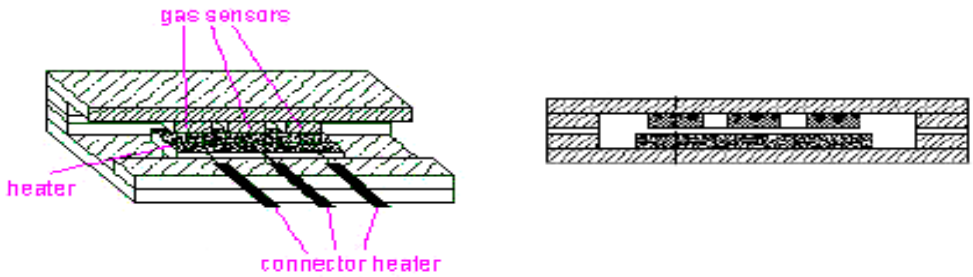

Figure 2: Gas sensor array with radiation heater. 3D view and cross section.

Airflow

The variation of the sensor temperature due to changing environmental temperatures is increased by the influence of the airflow on the sensor temperature due to changing heat convection. Coming back to the installation locations of smoke/fire detectors in air extraction ducts, close to air outlets and in ventilated cargo compartments, it becomes clear that the measurement and stabilization of the gas sensing layer temperature is an important task for such devices in aircraft application.

A sensor cell with forced airflow and a sensor array in a small bypass-channel (see Figure 3) has been built up to mitigate this dependency.

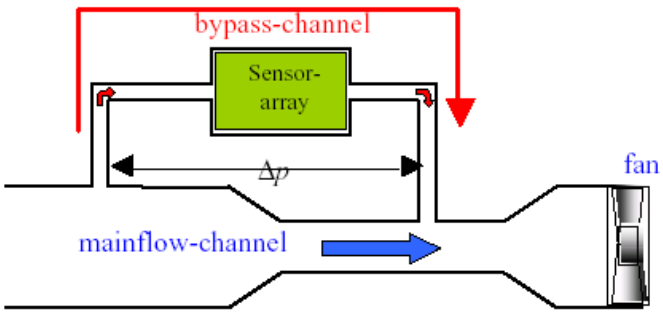

Figure 3: Sensor cell with sensor array in bypass-channel

The airflow through the bypass-channel was tested under different incoming flow rates and angles. The dependency of the airflow through the bypass-channel is significantly decreased by the cell arrangement and the sensor signal is leveled out due to defined steady-going airflow over the sensor surface. But, in spite of the orthogonal bypass inlet, it is necessary to use a filter for the sensor cell due to deposition of dust in the main-flow channel under very dirty environmental conditions. The flow through the filter (i.e. through the main-flow channel) is in the range of some l/min, which leads to large filter surfaces and/or short maintenance intervals. Therefore the design with a main-flow / bypass has been changed to a serial arrangement (see Figure 4).

The flow through the filters decreases to few 10 ml/min so that the filter size and maintenance intervals can be improved, but the dependency on the external airflow is degraded.

Considering the pros and cons, the serial arrangement seems to be the best solution, if the general philosophy of a forced airflow over the sensor surface should be followed.

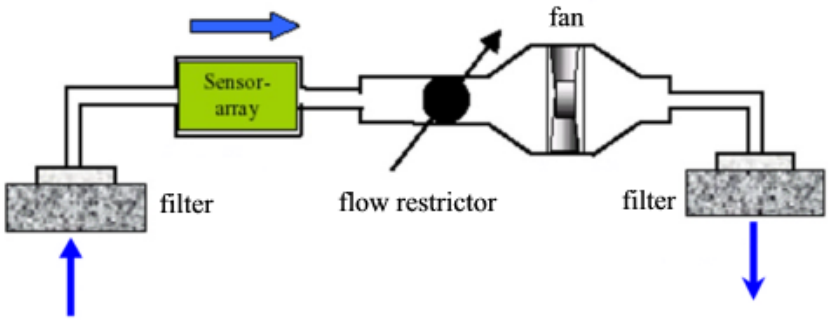

Figure 4: Serial arrangement of sensor cell

Pressure

The specified absolute pressure for a smoke/fire detector in aircraft application is about 571 mbar < P < 1069 mbar (limits are dependent on the type of the aircraft). Measurements with 12 different semiconducting gas sensors from FIS Inc (Japan), UST Umweltsensorik (Germany) and Figaro (Japan) have shown that the environmental pressure has no significant influence on the sensor behavior. It is assumed that the sensor surface is saturated with oxygen at pressures of several percents of the normal pressure. A relatively small change (less than one dimension) shows therefore nearly no influence on the gas sensor signals.

Humidity

For optical smoke detectors there are two different requirements in the specification for Airbus aircraft. First is to run several temperature cycles between 55°C and 38°C under high humidity conditions. Afterwards the detector has to function without faults. This requirement is focused on possible accumulation of water inside the equipment due to condensation effects during normal aircraft operation. The second requirement is directly related to condensation/fog effects, which can appear, if a cargo door is opened e.g. in Singapore after a long flight (cold compartment and warm/wet environment): A cold detector has to be put in a warmer atmosphere with high humidity. During this test, the detector is not allowed to generate any nuisance alarm.

Both requirements are related to condensation/fog effects. These are problems for optical and ionization type detectors as particles are formed (or transported into) the measurement chamber. Semiconducting gas sensors are heated for operation; therefore there should be no problem with condensation of water on the sensor surface.

Anyway, some of the tested gas sensors have shown strong influence of the humidity on the gas sensor signal. This effect can be explained by adsorption of OH-groups on the sensor surface, which has a direct effect on the sensor signal and additionally indirect effects by influencing the adsorption and reaction of other gas molecules on the sensor surface. High changes in humidity are therefore a difficult parameter for gas sensors in aircraft applications.

Further False Alarm Sources

Special attention has to be paid also on further false alarm sources: Different fluids like cleaning fluids, insecticides and de-icing agents are some of them [6,7]. Also sand and dust particles and salt spray are potential candidates for degradation and/or false alarms in the region of stormy deserts or seas. Last but not least, the smoke/fire detection should work after fire agent discharge (halon), to monitor the success of the fire extinguishing release. All this conditions have to be tested for fire gas detectors in aircraft application.

Vibration / Acceleration

Resistance against different mechanical stressing is a further requirement related to aircraft application. High constant acceleration up to 13g, and different high vibration curves due to engine fan blade loss and landing gear tire burst have to be survived [6]. This high mechanical stressing is a challenge for hybrid sensor arrays (see Figure 2) and for systems with moving mechanical components (see Figure 3 and Figure 4). Also gas sensor chips, which are hung-up in the sensor socket for thermal isolation [5], may have problems with these hard requirements.

Electromagnetic Environmental Requirements

Airliners become more and more densely packed electronic aircrafts. The requirements related to radiation of electromagnetic power and susceptibility against it will be therefore more and more tightened [6,7]. A way to fulfill these requirements is to put al the electronics in a shielded box and to filter all the electronic in- and outputs (“dirty box”). For gas sensors this approach may have some problems, as the box needs in and outlets for the gas. Additionally, the usual concept to drive gas sensor heaters by power pulses can lead to electromagnetic radiation. This can be mitigated by analog heater supply. Last but not least there are also some effects in the scope of susceptibility,

which may cause some problems:Resistive gas sensors are sensitive to high electrical fields [5]. All of these effects have to be considered during the design phase and compliance with the requirements has to be shown.

Reliability and Maintainability

A further problem is the reliability of gas sensors. The expected operation time of a smoke/fire detector is 100 000 but at least 15 000 operating hours without any scheduled maintenance task. During this interval the detector has to compensate the drift and the change of sensitivities, but drift compensation shall not influence functionality.

Possible contamination and blocking of gas sensitivities, which lead to blindness of the smoke detection system, should be avoided, but have at least to be detected by a built in test equipment (BITE) without the need of further external test tools. It is not acceptable to test the functionality of the gas sensors in short intervals like months with a test gas from a pressurized dispenser.

High reliability and low effort on maintainability of the gas sensors is absolutely essential for the integration of fire gas detectors into aircrafts. This can only be reached by the selection/development of gas sensors with low drift and intelligent self-monitoring capability.

Weight

Equipment weight is always an issue in aircraft application. Each gram has to be reviewed, if it can be saved to increase the payload of an aircraft. Smoke/fire detectors are relatively light equipment, but there are about 40 detectors installed in a large aircraft, so that the total mass of all smoke/fire detectors comes in the range of more than 15 kilograms. Additionally there is the weight for the electrical installation - the cables - as the detectors have to be supplied by electrical power. The more power has to be provided to the detectors the larger is the diameter of the cables and the heavier is the weight for the installation. Large aircrafts have a length of about 80 m so that the total length of the cables comes in the range of km.

On one hand, smoke/fire detectors with semiconducting gas sensors may have the potential to decrease the number of equipment and therefore the total weight, but on the other hand, they may be heavier and need more electrical power and therefore heavier

additional installation. These effects have to be further analyzed and tested at least in full size mock-ups of aircraft compartments.

Qualification and Certification

The requirements for qualification and certification of the smoke detection system are detailed elsewhere [1]. But it should be added, that there are some problems for fire gas detectors. The accepted qualification test standards like the EN54, designed for optical and ionization point-type sensors, cannot directly be applied to the gas sensor technology. There is the request to issue a new test standard to ensure the detection capability of fire gas detectors by a limited amount of fire and non-fire tests.

A similar problem appears for the integration test in the aircraft. It has to be shown that under worst case conditions the smoke detection system triggers an alarm in the cockpit within 60 seconds after ignition of a fire. This is actually done with a so-called “smoke generator”: Paraffin is vaporized in an amount that the effect on a conventional smoke detector is the same as the effect of a certain amount of smoke. This is usefully and accepted by the authorities for particle detectors, but it is vaporized paraffin and no real smoke, least of all a representative amount of fire gases. The certification of fire gas detectors in aircraft application is therefore not clarified until today and needs further definition.

Measurements

Different commercial semiconducting gas sensors have been compared with respect to sensitivity and selectivity to fire and non-fire events under different aircraft-like environmental conditions. Table 1 shows a summary for 17 different gas sensors.

It should be pointed out that these data are the outcome from different partners and are reflecting measurements with up to 10 exemplars for some sensor types and long-term experience for others. Some of the sensors have been sorted out in an early phase, because of low capability for fire gas detection in aircraft application due to high cross sensitivities to environmental conditions, other sensors have participated in further test campaigns with gas emission from smoldering wood, overloaded electrical cables, heptane fires, oranges, broccoli, ethanol, ethylene and ozone.

Sensor	Pros	Cons
FIGARO TGS 800		Fire detection capability depends on environmental conditions
FIGARO TGS 813		Fire detection capability depends on environmental conditions
FIGARO TGS 2620		High cross sensitivities / Fire detection capability depends on environmental conditions / Heater not controllable
FIS SB-AQ4	High fire detection capability / Low sensitivity to disturbances / High linearity	Cross sensitivity to H_2
FIS SB19	High fire detection capability / Low sensitivity to disturbances	Cross sensitivities to all tested disturbances
FIS SP-MW0		Sensitive to ethanol and ethylene
FIS SP-MW1		Low detection of fires
FIS ST-MW1		Low fire detection capability / Cross sensitivities to all tested disturbances / Heater not controllable
FIS ST-MW2		Sensitive to ethanol and ethylene
FIS ST-MW3	High fire detection capability / Low sensitivity to disturbances	Cross sensitivity to H_2 / Heater not controllable
UST CuPC	High fire detection capability / Low cross sensitivity to disturbances / Low cross sensitivity to humidity	Slow behaviour
UST GGS 1330		Low detection of fires
UST GGS 2015		Low detection of fires
UST GGS 5530	Fast detection behaviour / Low cross sensitivity to disturbances / Stable behaviour	Fire detection depends on environmental conditions / Sensitive to oranges
UST GGS 6330		Fire detection depends on environmental conditions / Sensitive to ethanol and ethylene
UST GGS 7330		Fire detection depends on environmental conditions
UST GGS 7530	High fire detection capability / High linearity	Cross sensitivity to O_3 and NH_3 / Cross sensitivity to humidity

Table 1:Fire detection capability of different gas sensors under conditions similar to those prevailing in aircrafts

Conclusion

The measurement results (see Table 1) show that most of the semiconducting gas sensors have cross sensitivities to non-fire events and/or changes of environmental conditions. Some sensors have generally a low sensitivity to fire gases, as they are designed for other applications, but there are also some potential candidates for fire gas detection. Based on the measurement results and our experience, a set of three gas sensors has been selected for further analysis of fire gas detection in aircraft application: FIS SB-AQ4, UST GGS 5530 and UST CuPC. These sensors have been integrated into a conventional optical smoke detector from *AOA apparatebau gauting* and the signals have been evaluated by pattern recognition.

Further work has now to be done by definition of a representative test-set of fire and non-fire tests to verify the required detection of all fires in aircraft application and the false alarm immunity. Also the certification of fire gas detectors in aircraft application is not clarified until today and needs further definition. Last but not least there is a lot of work to do, to reach a high reliability and low effort on maintainability for the fire gas detectors to get market acceptance. All of these tasks are essential for the integration of fire gas detectors into commercial aircraft.

References:

[1] K. Schmoetzer: *"Aircraft Fire Detection: Requirements, Qualification and Certification Aspects"* Proceedings of AUBE'01 - 12th International Conference on Automatic Fire Detection – March 2001 – pp. 630-640

[2] A. Freiling: *"New Approaches to Aircraft Fire Protection"* Proceedings of AUBE'01 - 12th International Conference on Automatic Fire Detection – March 2001 – pp. 641-652

[3] P. Mangon: *"Fire Detection for Aircraft Cargo Compartments – Reduction of False Alarms"* Proceedings of AUBE'01 - 12th International Conference on Automatic Fire Detection – March 2001 – pp. 653-664

[4] A. Freiling, U. Storm, K. Schmoetzer: "*Requirements and Image Layout for Video-Based Fire Detection in Commercial Aircraft*" - See proceedings of this conference.

[5] U. Storm, O. Bartels, J. Binder: "*A resistive gas sensor with elimination and utilization of parasitic electric fields*" Sensors and Actuators B77 (2001) pp. 529-533

[6] Airbus Directives (ABD0100) "*Equipment - Design - General Requirements For Suppliers*", Issue E

[7] Radio Technical Commission for Aeronautics (RTCA) Washington D.C.; DO-160D *"Environmental Conditions and Test Procedures for Airborne Equipment*"

[8] D. Kohl, J. Kelleter, H. Petig: "*Detection of Fires by Gas Sensors*" Sensors Update, Wiley-VCH, Weinheim, Vol 9, 2001, pp. 161-223.

[9] Freiling, A.: *"Requirements for Fire Detection in civil aviation"* Proceedings of the VdS conference Gas Sensors for Fire Detection, November 15-16, Cologne, Germany

[10] Schmoetzer, K.: *"Multi Criteria Fire/Smoke Detector for Cargo Holds"* International Aircraft Systems Fire Protection Working Group Meeting in Phoenix AZ on March 26-27th, 2003

http://www.fire.tc.faa.gov/pdf/systems/MultiCriteria%20Fire%20Detector_L2610PR0301202_v1%20IASFPWG%20Phoeni.pdf

Hanspeter Schlatter
Schweizerische Bundesbahn (SBB AG), Bern, Switzerland
Joëlle Vouillamoz
BLS Lötschbergbahn AG, Bern, Switzerland

Stationäre Detektion brennender Züge

Abstract

In Switzerland, there are 2 long railway tunnels under construction: the 57 km long Gotthard base tunnel and the 35 km Loetschberg base tunnel. They will be in operation in 2014 and in 2007, respectivly. The two base tunnels are the core part of the future European high-speed railway network (passengers and freight traffic) between the North of Europe and the South.

After the catastrophic events in the last years in long road tunnels in Austria, France and Switzerland a special focus of the safety measures for tunnels is put to the problem of fire detection discussed here. Another aspect is to find a solution for the detection of dangerous goods (release of toxic gases) not discussed here in detail, although there are some analogies with fire detection.

The focus lies not only on the damage of persons, but also damage due to an operational breakdown is to be taken in consideration.

The most important guideline in a tunnel safety philosophy can be expressed by the slogan "no sick train in a tunnel". So a burning train must be stopped before it enters a tunnel, and a burning train in the tunnel should drive out of it whenever possible.

To be independent of the rolling stock (problem of open access of trains in Europe), a stationary detection of fire was looked for. A stationary detection will also be much cheaper than a detection system on the trains.

After "looking around the world", there was no existing system for our problem. The detection of a fire in road tunnels is completely different to the detection of a fire in railway tunnels. So the two Swiss rail companies BLS and SBB made a few tests during the last 2 years to check the technical feasibility: In the old tunnel of Loetschberg (built 100 years ago, 15 km long) the detection of a fire with the power of 0.5 MW on a train with a speed up to 110 km/h (maximum speed in this tunnel) was tested. The goal was

to detect a fire in the beginning, so there is enough time for an intervention. In contrast to a burning car, a burning train can drive a long distance in most of the cases.

Because fire has a lot of phenomena which can be detected, a lot of types of detection systems as flame detectors, infrared detectors, gas detectors (CO, CO_2) and smoke detectors, of different providers were tested. The fire was simulated with a propane burner, the smoke with special simulators from the fire brigades, the heat with hot plates.

The result after the first tests was, that the detection of CO in combination with CO_2 and a third system, probably smoke detection, will give the best response: all the test courses could be detected, and there were no false alarms.

A problem similar to the road tunnels is the pollution of the detectors. In a long time test was proved, that this problem can be solved with adequate maintenance.

In addition to these tests, a lot of theoretical reflections and calculations were necessary to account for the test results, to define threshold values etc.

After finishing these tests, the following findings can be summarised as follows:

- There is no stationary detection system of fire on trains on the market.
- The technical feasibility of stationary detection of fire on trains is proved.
- The detection will be based on the detection of CO and CO_2, with eventually one more system (redundancy).
- A stationary detection system should be as simple as possible (high reliability, low cost).
- Crude estimations show, that a system with a good cost-benefit effect will be possible.

In the next step the operational feasibility will be proved. These tests are in preparation and will be implemented presumably 2004 and 2005.

1. Zusammenfassung

Der Bau und Betrieb sehr langer Eisenbahntunnels bringt eine ganze Reihe von Herausforderungen mit sich, die gelöst werden müssen. Eine dieser Herausforderungen stellen die speziellen Risiken dar, die sich durch einen Brand auf einem fahrenden Zug oder durch Freisetzung von Gefahrgut ergeben können. Die Tunnelunfälle der letzten Jahre – insbesondere in Strassentunnels – zeigten deutlich auf, welche verheerenden Folgen ein Brand in einem Tunnel haben kann. Grundsätzlich ist das Ziel, brennende bzw. Gefahr-

gut verlierende Züge vor Einfahrt in einen langen Tunnel abzufangen. Die stationäre Detektion bietet gegenüber Detektionsanlagen am Rollmaterial sowohl aus einer Gesamtbetrachtung als auch aus Sicht des Infrastrukturbetreibers diverse Vorteile. Eine praktikable Lösung für die stationäre Detektion indes fehlt bisher. Daher haben die BLS Lötschbergbahn AG (BLS) zusammen mit der Schweizerischen Bundesbahn (SBB) Versuche für die Detektion von kleinen Bränden auf bzw. an fahrenden Zügen durchgeführt. Im folgenden Artikel werden diese Versuche beschrieben und die wesentlichen Ergebnisse vorgestellt.

2. Einleitung

In der Schweiz sind zur Zeit zwei lange Eisenbahnbasistunnels durch die Alpen im Bau: der 37 km lange Lötschbergbasistunnel (geplante Inbetriebnahme 2007) sowie der 57 km lange Gotthardbasistunnel (geplante Inbetriebnahme 2014). Bis dahin soll ein stationäres Detektionssystem vorliegen, das fahrende brennende Eisenbahnzüge detektieren kann. Nebst der Entwicklung von Detektoren auf dem Rollmaterial wird eine *stationäre* Lösung aus folgenden Gründen angestrebt:

- Der Netzbetreiber will die Sicherheit seines Netzes unabhängig vom Rollmaterial garantieren, dies insbesondere im Hinblick auf den "Open Access" im europäischen Bahnnetz.
- Die Kosten eines stationären Systems dürften im Vergleich zur Ausrüstung des gesamten Rollmaterials wesentlich geringer ausfallen.
- Die Intervention im Störungsfall liegt in der Hand des Infrastrukturbetreibers.

Ebenso soll der Austritt von Gefahrgut aus fahrenden Gefahrgutwagen festgestellt werden können. Im vorliegenden Artikel wird nur die Branddetektion besprochen. Wesentliche Erkenntnisse können aber direkt für die Detektion von austretendem Gefahrgut genutzt werden.

3. Ziel

Das Ziel ist letztlich, einen brennenden Zug wenn immer möglich erst gar nicht in den Tunnel einfahren zu lassen ("keine kranken Züge in Tunnels"). Falls ein Zug erst im Tunnel zu brennen beginnt, soll er wenn immer möglich aus dem Tunnel fahren. Falls das nicht möglich ist, ist ein gezielter Halt an den vorgesehenen Nothaltestellen vorgesehen. Das Detektionssystem soll also v.a. ermöglichen, einen brennenden Zug *vor* der

Einfahrt in den Tunnel zu erkennen und anzuhalten. Die Anlagen müssen somit in (natürlich vorhandenen) vorgelagerten Tunnels installiert werden. Durch Detektionsanlagen im zu schützenden langen Tunnel selbst soll zudem die Möglichkeit geschaffen werden, den Lok-Führer rechtzeitig zu informieren, damit er in Zusammenarbeit mit der Betriebsführung im Brandfall optimal reagieren, d.h. wenn immer möglich aus dem Tunnel gelangen kann.

Die Brandleistung, die detektiert werden soll, beträgt 0.5 MW. Dieser Wert entspricht einem Brand im Anfangsstadium, also einem vergleichsweise kleinen Brand. Entsprechend ist das Ziel anspruchsvoll. Die Detektion einer so kleinen Zielgrösse ist aber notwendig, da ein Brand in einem frühen Stadium erkannt werden soll, um eine Reaktion zu ermöglichen.

Als Beispiele für Brandleistungen sind hier ein paar typische Zahlenwerte aus der Literatur zusammengestellt:

- Ein PW im Vollbrand hat eine Leistung von ca. 2 bis 5 MW.
- Ein grosser LKW, wie er etwa im Montblanc-Tunnel gebrannt hat, entwickelt 100 MW und mehr.
- Der Güterzugnormbrand (Mineralölganzzug, 4 Kesselwagen betroffen) erreicht nach 40 Minuten 240 MW und verbleibt dann ca. 90 Minuten auf etwa diesem Niveau.

4. Charakteristik eines Brandes auf einem fahrenden Zug

Brände in Eisenbahntunnels sind aus verschiedenen Gründen völlig unterschiedlich von Bränden in Strassentunnels oder Gebäuden (Kinos, Hotels etc.). Einige dieser Unterschiede können anhand der Abbildung 1 erklärt werden.

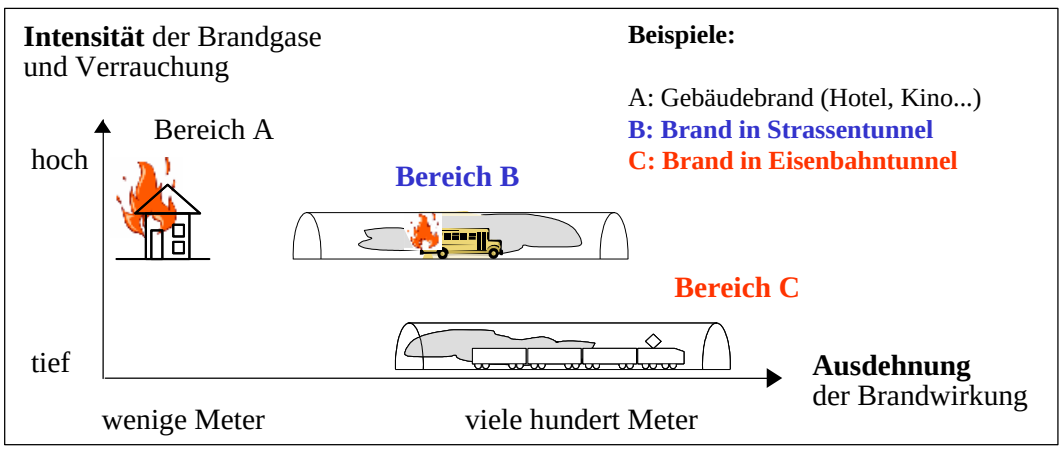

Abbildung 1: Verschiedene Typen von Bränden unter den Aspekten Ausdehnung des Brandes sowie Intensität der Brandgase und der Verrauchung

Die drei Bereiche A bis C werden kurz einzeln diskutiert.

Bereich A, stationärer Brand in Gebäuden ("Normalfall"):
Die Ausdehnung des Brandes beschränkt sich auf wenige Meter. Typischer Fall ist ein Gebäudebrand. Die Intensität der Brandgase und der Verrauchung nimmt rasch zu und erreicht kritische Werte. Eine rasche Flucht aus diesen Räumen ist lebenswichtig.
Bereich B, stationärer Brand im Tunnel (Brand im Strassentunnel):
Die Ausdehnung des Brandes beschränkt sich auf wenige Meter. Typischer Fall ist ein Strassenfahrzeugbrand im Tunnel. Im Gegensatz zu einem brennenden Eisenbahnzug hält ein brennendes Strassenfahrzeug in der Regel sofort an. Die Intensität der Brandgase und der Verrauchung der direkten Umgebung der Tunnelröhre nimmt zu, breitet sich im Falle eines grösseren Fahrzeuges (Lieferwagen, Lastwagen) schnell aus, kann bald einige hundert Meter erreichen und schnell kritische Werte annehmen. Bei grösseren Brandlasten ist eine rasche Flucht aus der Röhre lebenswichtig.
Bereich C, bewegte Brandquelle im Tunnel (Brand im Eisenbahntunnel):
Eine Brandquelle auf einem Eisenbahnzug bewegt sich weiter, unter Umständen über viele Kilometer, da sie in manchen Fällen nicht sofort entdeckt wird und die Züge über eine gewisse Notlaufeigenschaft von einigen Minuten verfügen. Die Intensität der Brandgase und Verrauchung ist selbst in einem Tunnel gering. Sie erreicht auch bei grösseren Bränden bei Weitem keine kritische Werte, solange sich der Zug bewegt. Nicht zuletzt darum ist es das Ziel, unter allen Umständen zu verhindern, dass ein solcher Zug unkontrolliert in einem Tunnel zum Stehen kommt.

Ausserdem sind in einem Strassentunnel aufgrund der Verbrennungsmotoren der Fahrzeuge mögliche Parameter, die für die Branddetektion in Frage kommen (z.B. Brandgase wie CO oder CO_2, Sichttrübung), bereits im Normalfall in jenem Messbereich oder sogar weit darüber, den eine bewegte Brandquelle in einem Eisenbahntunnel hervorrufen würde. Zusammenfassend kann daher gesagt werden, dass zur Detektion eines Brandes auf einem fahrenden Zug ganz andere Messtechniken und Auswertealgorithmen gefragt sind als in der Gebäudetechnik und in Strassentunnels z.Zt. angewandt werden.
Als Messgrössen für die Detektion eines Brandes kommen grundsätzlich folgende Kenngrössen in Frage: Brandgase, Sichttrübung, Wärme, Flamme (Flackern).

5. Versuche

Im Verlaufe der Jahre 2002 und 2003 wurden im bestehenden Lötschberg-Scheiteltunnel mit Unterstützung von Siemens-Cerberus Schweiz mehrere Versuchsfahrten durchgeführt (Abbildungen 2 und 3). In der Mitte des Tunnels wurden in einer Nische verschiedenste Sensoren, die grundsätzlich einen Brand entdecken können, von diversen Herstellern installiert:

- Gasmelder (Brandgase CO und CO_2)
- Sichttrübungsmesser (Rauch)
- Infrarotkamera (Wärme)
- Flammendetektoren (Flackern der Flamme)

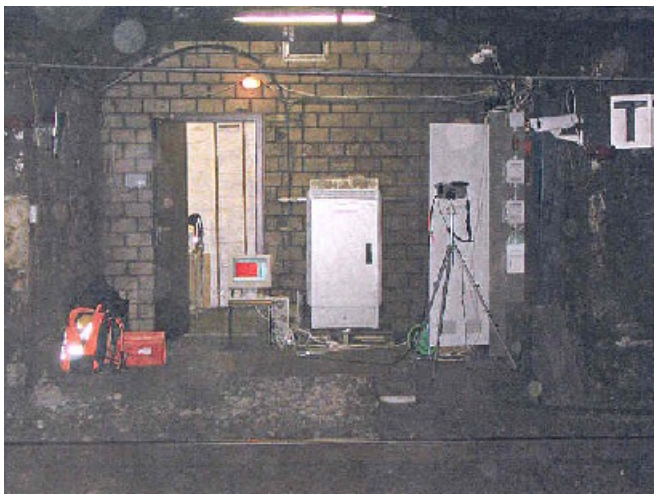

Abbildung 2: Nische in der Mitte des Lötschberg-Scheiteltunnels mit verschiedenen Detektoren

Im parallel geführten Langzeitversuch wurden diese Geräte auf ihr Verhalten in der Tunnelumgebung hin geprüft. Fragen zu Wartungsintervallen und zur Zuverlässigkeit konnten damit beantwortet werden. Ebenso wurden Informationen zu Täuschungsgrössen während des normalen Tunnelbetriebs gewonnen. Auf diesen Versuch wird an dieser Stelle nicht weiter eingetreten.

Als Versuchszug diente ein Autoverladezug (Abbildung 3). Darauf wurde der Brand mit folgenden Mitteln simuliert: Mit zwei verschieden grossen Flammen (Propan-Brandsimulator mit rund 0.2 MW Brandleistung, Propanbrenner mit rund 0.5 MW Brandleistung) konnten 3 Brandgrössen simuliert werden (Rauchgase, Wärme und Flamme zum Testen der Gasmelder, der Infrarotkamera und der Flammendetektoren). Rauchgassimulatoren, wie sie z.B. im Theater Verwendung finden, testeten die Sichttrübungsmesser, Kochplatten die Infrarotkamera.

Die Versuche wurden jeweils in den Nachtstunden durchgeführt, damit einerseits der übrige Zugbetrieb möglichst wenig eingeschränkt wurde und andererseits möglichst viele Versuche ungestört gefahren werden konnten.

Abbildung 3: Stimmungsbild vom Autoverladezug, der mit den Brand- und Rauchsimulatoren sowie Kochplatten bestückt ist.

Die Versuche wurden sukzessive vereinfacht und fokussierten auf jene Detektortypen, die sich als zielführend herausstellten. Zudem konnten bei den letzten Versuchsfahrten auch Geräte in einer zweiten Nische stationiert werden, die 400 m von der ersten entfernt war. Dies diente insbesondere folgenden Zwecken:

- Zwei weitgehend unabhängige Messungen stehen zur Verfügung.
- Die Fahrtrichtung des Zuges kann erkannt sowie seine Geschwindigkeit abgeschätzt werden.
- Eine Entwicklung des Brandes ist allenfalls erkennbar.

6. Resultate

Die erfolgversprechendsten Resultate wurden mit Kohlenmonoxid (CO) erreicht. Aus diesem Grund werden im Folgenden diese Resultate vertieft dargestellt. In der folgenden Abbildung 4 sind die Verläufe von vier CO-Detektoren während einer der drei Versuchsnächte zu sehen. Je zwei Detektoren waren in jeder Nische.

In Abbildung 4 ist folgendes eindeutig zu erkennen:

- Auf der x-Achse ist die Zeit dargestellt. Die Versuche wurden zwischen 1:00 Uhr und 4:00 Uhr durchgeführt. Auf der y-Achse ist die CO- Konzentration in ppm dargestellt. Es sind die Aufzeichnungen von vier Geräten wiedergegeben.
- Die Grundkalibrierung ist bei allen Geräten verschieden. Dies ist für diese Versuche nicht relevant, weil v.a. die *Anstiege der CO-Konzentrationen* und nicht die absoluten Werte interessieren.
- Die Werte bewegen sich in einem sehr tiefen Bereich, der weit unterhalb von gesundheitsgefährdenden Werten liegt.
- Die Konzentrationssanstiege infolge der Versuchsfahrten sind markant und verweilen einige Minuten bis ca. eine Viertelstunde auf erhöhtem Niveau. Dann sinkt die Konzentration wieder allmählich auf den Anfangswert.

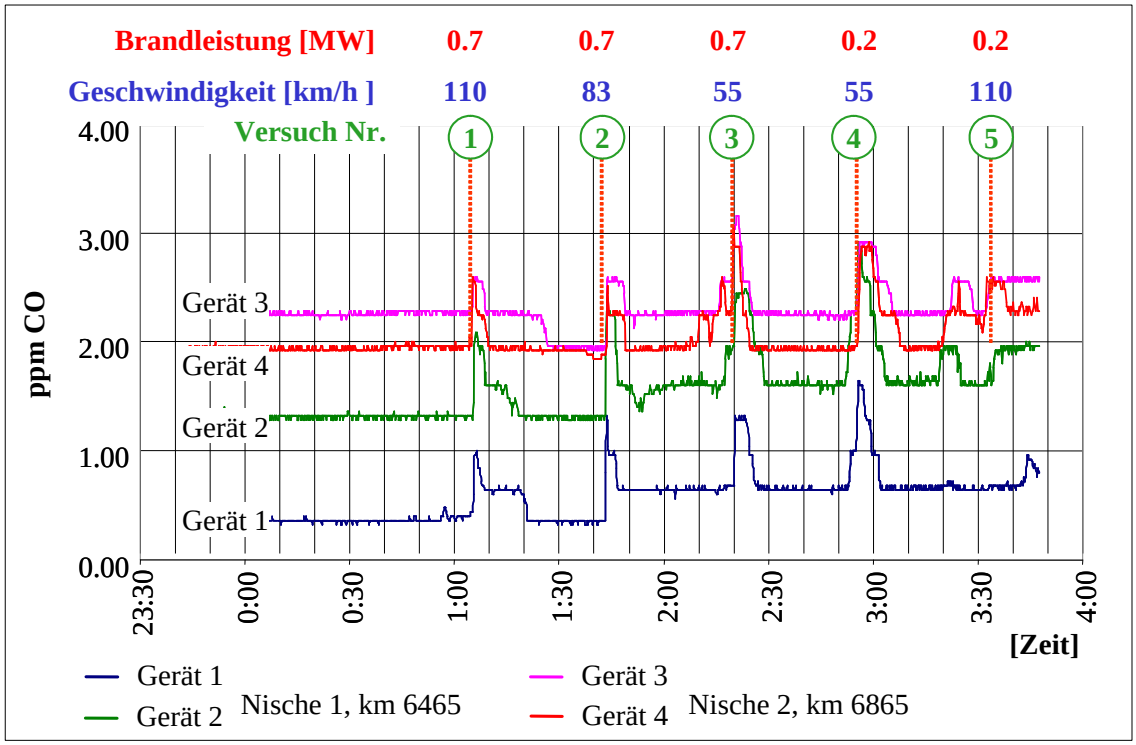

Abbildung 4: Verlauf von vier Messkurven der CO-Konzentration während einer der Versuchsnächte über rund 4 Stunden (Erklärung siehe Textteil).

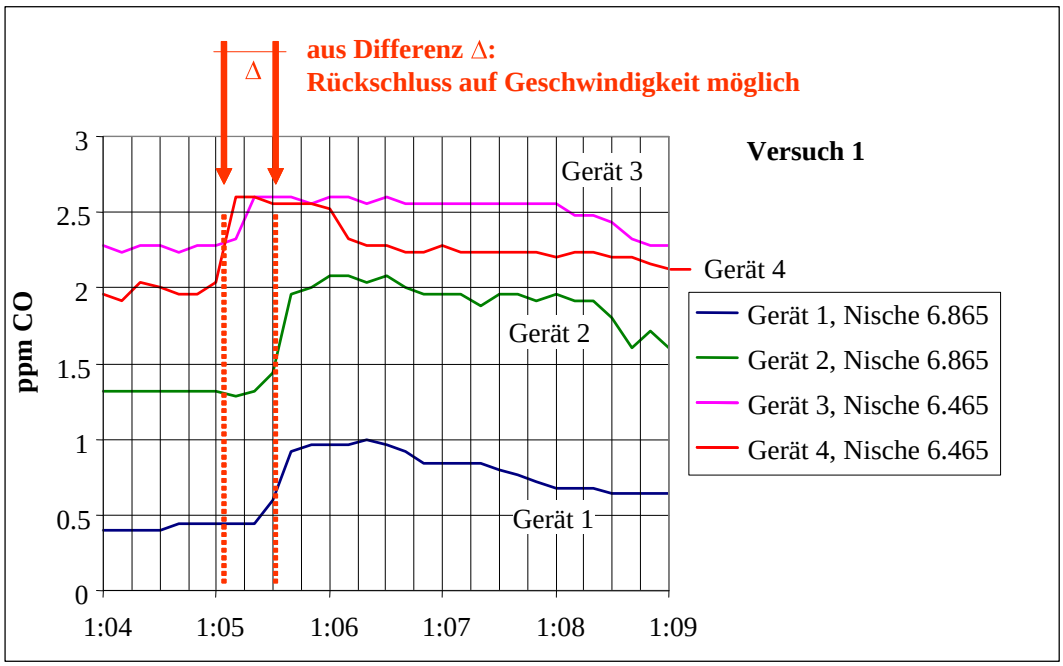

Abbildung 5: Vergrösserter Ausschnitt aus Abbildung 4 (Versuch 1): Die Zeitdifferenz der Anstiege bei den Geräten in den beiden Nischen ist gut erkennbar: Er beträgt ca. 15 s. Das ergibt bei einer Distanz von 400 m eine Geschwindigkeit des Zuges von knapp 100 km/h. 110 km/h war im Versuch für diese Fahrt vorgesehen und wurde effektiv auch gefahren.

- Die ersten vier Versuchsfahrten wurden von allen vier Geräten gut erkannt. Bei den letzten, anspruchsvollsten Versuchsvoraussetzungen (hohe Geschwindigkeit, kleine Brandleistung) geben nur drei von vier Geräten einen eindeutigen Anstieg wieder.
- Kleine Anstiege, die nicht von Versuchsfahrten herrühren, sind auf Fahrten von fahrplanmässigen Zügen zurückzuführen (Fehlerquelle nach mehreren Versuchsfahrten, vgl. z.B. um 3:20)
- Auf dieser "gequetschten" Darstellung kaum erkennbar ist, dass die Anstiege der beiden unteren Kurven (blau und grün, Nische 6465) nicht genau gleichzeitig mit jenen der beiden oberen (lila und rot, Nische 6865) erfolgen. In Abbildung 5 ist daher für Versuch 1 ein vergrösserter Ausschnitt von 5 Minuten wiedergegeben: Dort ist dieser Zeitunterschied gut erkennbar.

Die Vorteile der Detektion des CO sind zusammenfassend:
- CO entsteht bei praktisch jedem Brand.
- CO kann in geringen Mengen mit genügender Trennschärfe detektiert werden.
- Die gemessenen Werte können rechnerisch überprüft werden.
- Im Normalfall (d.h. Umgebungsluft) ist die Konzentration des CO praktisch Null.
- Die Spuren, die hinterlassen werden (erhöhte CO-Konzentration), sind auch Minuten nach der Durchfahrt noch vorhanden (dies z.B. im Gegensatz zum Flackern, dessen Detektion innert Sekundenbruchteilen erfolgen muss).
- Auch Brände im Wageninnern von Reisezügen sollten ab einer gewissen Grösse genügend CO entwickeln, das durch die Lüftung nach aussen gelangen und so detektiert werden kann.

Herausforderungen:
- Trotz grundsätzlich bekannter Störgrössen (Bauarbeiten im Tunnel, Kühlgeräte auf transportierten LKW, Dieselloks, rauchende Personen), die vom Tunnelbetreiber vorgängig geplant werden, besteht ein Fehlalarmpotenzial.

7. Berechnungen

Aufgrund der ersten Versuche konnten auch die im Vorfeld angestellten Abschätzungen der zu erwartenden Messresultate im Bereich der Rauchgase CO und CO_2 überprüft und die Berechnungen genauer durchgeführt werden. Mit den Parametern Tunnelquerschnitt, Zugsgeschwindigkeit und Brandleistung konnten die erwarteten Anstiege der Konzentration dieser Gase recht genau abgeschätzt werden[1]. Umgekehrt kann nun auch aufgrund der Höhe der Anstiege der Gaskonzentrationen auf die Brandleistung geschlossen werden. Diese Werte werden für die Bildung der Algorithmen (Einstellung der Alarmwerte etc.) benötigt.

[1] Insbesondere diese Erkenntnisse, die grundsätzlich für Gase gelten, dienen direkt auch der Lösung für die Detektion von austretenden gasförmigen Gefahrgutstoffen.

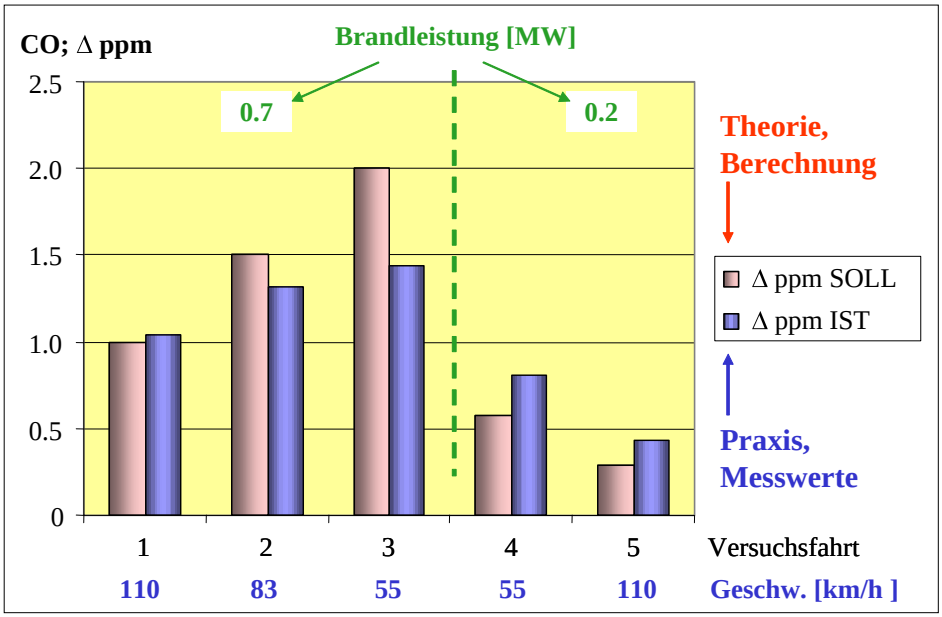

Abbildung 6: Vergleich der berechneten und der gemessenen Werte einer Versuchsnacht: Die Werte stimmen gut überrein.

8. Fazit

Mit den durchgeführten Versuchen und Berechnungen konnte ein Konzept für die stationäre Branderkennung von Bränden auf fahrenden Zügen gefunden werden. Die technische Machbarkeit wurde gezeigt. Als Basis dient die CO-Messung. Noch offen ist z.Zt. der definitive Entscheid, welche Geräte zusätzlich zu CO-Detektoren zum Einsatz gelangen sollen: Einerseits soll ein Brand eindeutig erkannt werden. Daher sollte das Zuschalten weiterer Geräte, z.B. eine Sichtrübungs- oder CO_2-Messung, dank weiterer Brandkenngrössen ein eindeutigeres Resultat liefern. Andererseits muss das System so einfach wie möglich sein, damit auch die Algorithmen und die darauf basierende Intervention transparent und einfach bleiben. Weiter darf die Wartung des Systems nicht aufwändig sein.

Je nach Kosten des Systems ist künftig auch der Einsatz für die bestehenden langen Tunnels im Bereich ab vielleicht 6 bis 8 km zu prüfen.

In einer nächsten Phase, die zur Zeit in Bearbeitung ist, wird die operative Machbarkeit geprüft. Die BLS und SBB wollen in Zusammenarbeit mit der Industrie in dieser Phase ein marktreifes Produkt herstellen. Die Interventionsprozesse sind zu definieren. So sollten aus heutiger Sicht bei Inbetriebnahme des ersten der beiden langen Basistunnels (Lötschberg) im Jahre 2007 die Bahnen auch aus dieser Sicht bereit sein.

T. Ono∗, H. Ishii∗, K. Kawamura∗, H. Miura∗, E. Momma∗, T. Fujisawa∗, J. Hozumi∗∗
∗Nihon University, Tokyo, Japan, ∗∗Koito Industries,Ltd., Japan

Application of Neural Network to Analyses of CCD color TV-camera Image for the Detection of Car Fire in Expressway Tunnel

Introduction

In this paper, the detection of a car fire using a Neural Network (NN), which uses features of flame images in a simulation fire as input elements, is considered. As the initial step of the study, the simulation fire is photographed with a CCD color TV camera, simulating a surveillance camera in a tunnel, to provide a dynamic image.

This study aims to investigate the effectiveness of the early detection of a car fire occurring in an expressway tunnel using surveillance cameras.[1] [2] [3] Road and rail tunnels need to be built in mountainous areas, in order to provide the effective distribution of goods. A fire in a tunnel can endanger human life as the heat flow and smoke increase rapidly in such a long enclosed space.[4] In addition, it can significantly affect social economies owing to a stagnation of the distribution and the breakdown of the distribution network.

A series of this study is performed taking into consideration the NN which applies features of the flame images, which is taken from the dynamic image, for detection. The features of the flame images are extracted from a rectified image which considers the difference in distance from the CCD color TV camera to the fire source.

Simulation fire experiment

The simulation fire experiment of a car fire in a tunnel considered the following situations.

1. A burning car has stopped.
2. A burning car is moving.
3. A following car or an oncoming car is approaching the burning car in situation 1.

Fig. 1 is the outline of the simulation fire experiment. There are simulated lane lines, a simulated tunnel wall, the CCD TV camera, the fire source and cars.

The lane lines divide the road into a slow lane and a fast lane, separated by 3.5m, on a concrete road surface.

By creating the simulated tunnel wall in a position just under a high-pressure-sodium-lamp light source (from the right line to 1.6m), a reflection from a tunnel wall is reproduced.

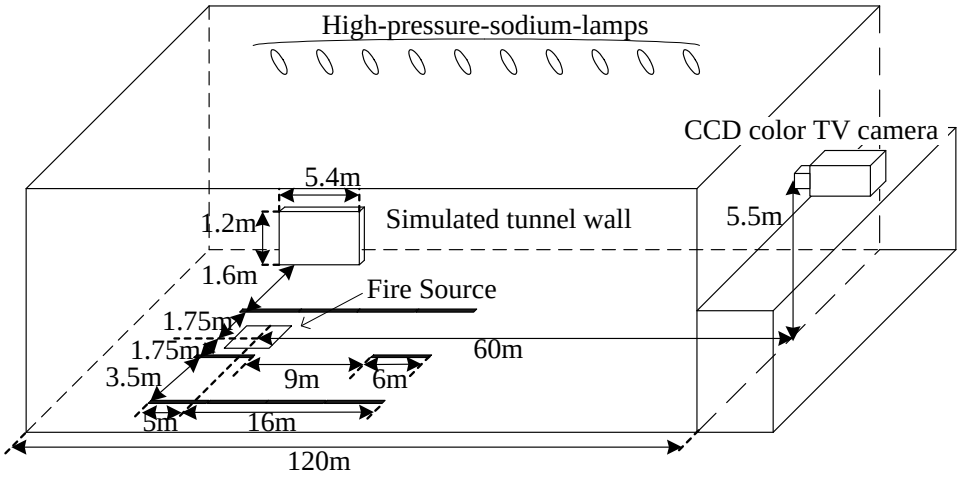

Figure 1: Arrangement outline of equipment for the experiment

Figure 2: Simulation fire experiment

The CCD color TV camera is placed in the position 60m away from the fire source simulating the established surveillance camera(a height of 5.5m) . Further more, the focal length in The CCD color TV camera is adjusted to make appropriate dynamic images which are 37.5-225m away from a fire source.

The fire source simulates a burning car and consists of gasoline in a 50cm square fire bowl which is filled with water (In order to avoid too much boiling of liquid fuel and to keep the combustion state uniform). The fire bowl is placed on the fast lane in the case of situation 3 and placed on the slow lane in the other situations.

A saloon car and a station wagon which has a revolving emergency light attached (red and yellow) are assumed to be a general car and an emergency vehicle, respectively.

Fig. 2 is the image of situation 3 and the station wagon which has the revolving emergency light and the emergency flasher on is moving towards the fire source at approximately 20 km/h.

Flow of processing

The car fire is detected by image processing and NN from the photographed dynamic image taken. Since a dynamic image is a group of 30 frames per second, one image is taken from every frame.

Fig. 3 is the flow of fire detection for a one-frame image.

An image in the state where there are neither cars nor flames is used as the background image. Since flame in an image has the feature that its Red intensity is generally high, red intensity differences between the background image and each frame are calculated. The zone estimated to be flame is then extracted by the labelling method.

Next, after standardising this zone by expansion and reduction, quantiles of its histogram and its area are calculated as feature parameters.

Finally, the car fire is judged by the hierarchical type NN (one input layer, one middle class, and one output layer) with the feature parameters as input elements. The above processing method is repeated to all the zones estimated to be flame.

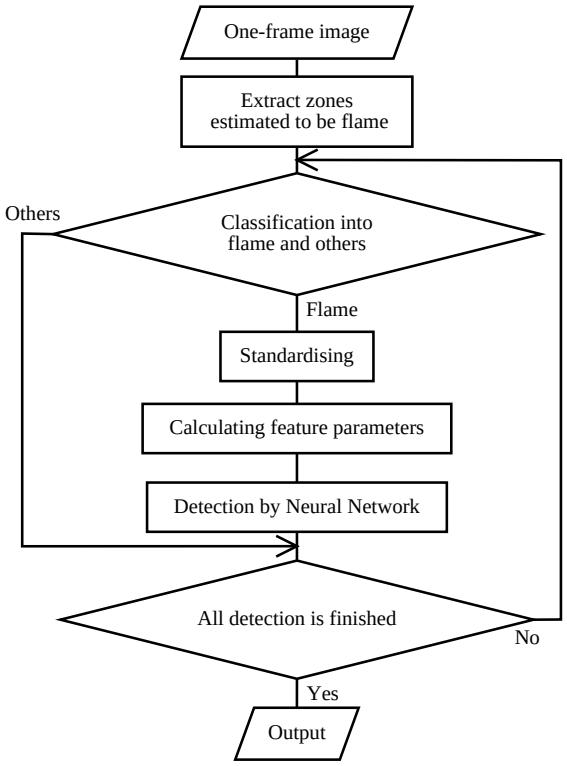

Figure 3: Flow of processing

Extraction of flame image

The zones estimated to be flame are extracted by comparing and categorising. To begin with, the one-frame image is compared with the background image on Red

intensity by calculating its difference. After the labelling method and categorising of colors, the zones estimated to be flame are classified into flame and others.

For comparison, a value of each color in a pixel (x, y) in the one-frame image f_N is defined as $f_N(x, y)$ (formula (1)). A value in the background image is similarly defined as $f_B(x, y)$ (formula (2)), and these difference values $f_{out}(x, y)$ are calculated by formula (3). However, Th is the threshold defined by considering noise. This processing for the all pixels extracts pixels estimated to be flame.

$$f_N(x,y) = (R_N(x,y), G_N(x,y), B_N(x,y)) \quad (1)$$

$$f_B(x,y) = (R_B(x,y), G_B(x,y), B_B(x,y)) \quad (2)$$

$$\begin{cases} f_{out}(x,y) = f_N(x,y) & if R_N(x,y) - R_B(x,y) > Th \\ f_{out}(x,y) = (0,0,0) & if R_N(x,y) - R_B(x,y) \leq Th \end{cases} \quad (3)$$

Fig. 4 is an example of results which changed the threshold to the same image. Image (a) is situation 3, a car and an emergency vehicle are stopping in front of the flame and image (b) is the background image. Image (c) and (d) are the results of the incorrect extraction and the correct. On one hand the cars and the road surface are extracted by the influence of noise with $Th = 0$, on the other hand the flame is extracted exactly with $Th = 30$. As a result of using the suitable threshold, the flame is extracted although other luminescent objects besides the flame (a headlight, a revolving emergency light, a brake lamp, road surface reflection of a headlight) are also included. Thus the threshold is set to $Th = 30$.

With respect to the pixels estimated to be flame, in order to eliminate small noise, the continuation zone is extracted by the labelling method, with the proviso that its area is more than 10 pixels.

For the classification into flame and others, the value of each color in the pixels is investigated. From our present study, the distinctive relation between Red intensity and Green intensity in the case of a car fire flame is known. Fig. 5 is the relation of the pixels. It shows the value is distributed in a specific zone.

To identify the range of flame on the Red-Green plane, the boundaries of Fig. 5 are approximated to formula (4) and formula (5) respectively. Red intensity is defined as R and Green intensity, G, is consequently derived, the range of flame is defined by formula (6).

$$G_{sup} = 34.8 \times \exp(0.0084 \times R) \quad (4)$$

$$G_{inf} = 11.7 \times \exp(0.012 \times R) \quad (5)$$

$$\begin{cases} 34.8 \times \exp(0.0084 \times R) - G_{sup} \leq 0 \\ 11.7 \times \exp(0.012 \times R) - G_{inf} \geq 0 \end{cases} \quad (6)$$

Fig. 6 is the result of plotting the value of a revolving emergency light, brake lamps and flame. Although all brake lamps were judged to be a non-fire, some revolving emergency lights were judged to be flame. Thus, to provide a more exact judgement, the NN is applied.

(a) Situation3 (b) Background image

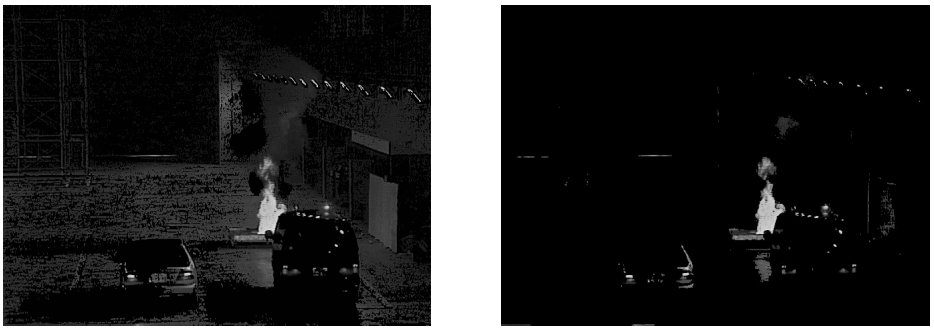

(c) Incorrect extraction(Th=0) (d) Correct extraction(Th=30)

Figure 4: Extraction of flame by difference processing

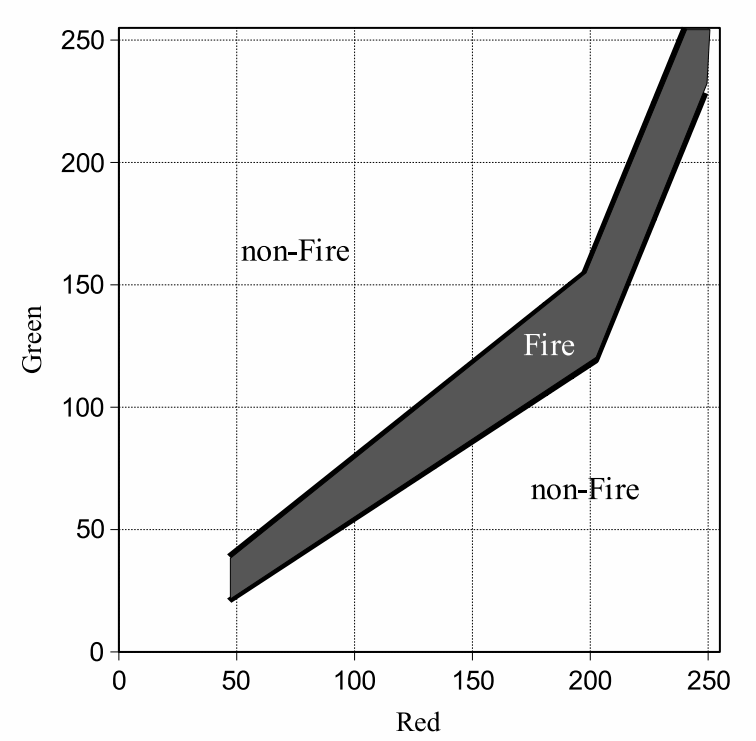

Figure 5: Color area of flame

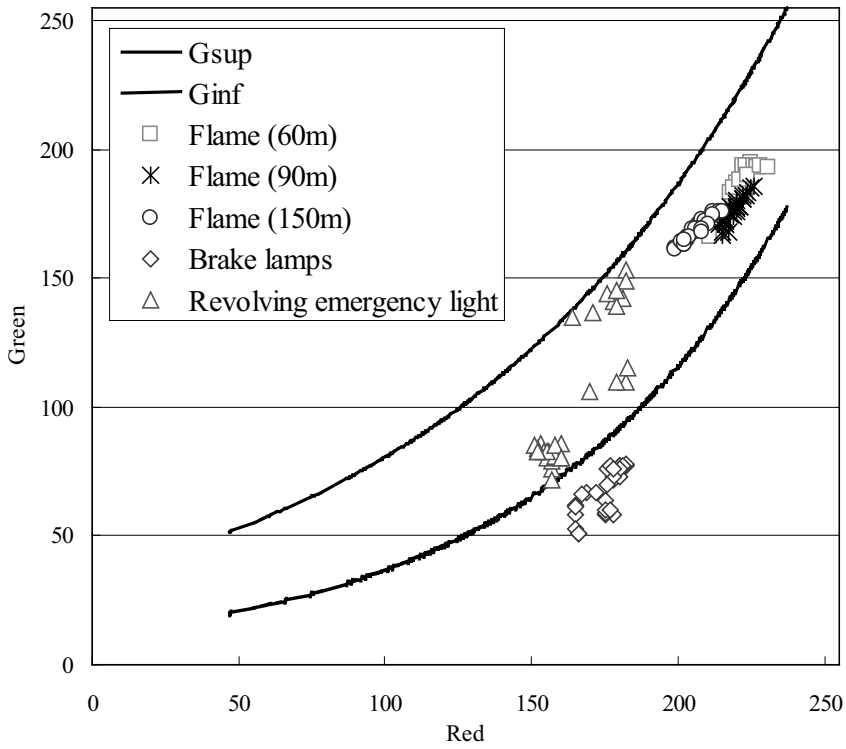

Figure 6: Approximation of color area

Extraction of the feature parameters

To apply the NN to this detection, feature parameters as input elements of the flame are considered.

For detection of the fire, use of a surveillance camera fixed in a tunnel is assumed. Surveillance cameras are installed at intervals of 150m, therefore, the maximum distance between a flame and a camera which must be detected is 150m. Before finding feature parameters, it is necessary to standardise the image.

The standardisation is to expand or reduce the zone estimated to be flame into a size based on a standardisation distance. The standardisation distance is set to 60m and this process is performed with linear interpolation.

Fig. 7 shows the images at which the distance of the fire source and the camera is equivalent to 60m, 90m, and 150m, and the images after the standardisation. From the images after the standardisation, feature parameters are calculated

Since detection of the fire should be fast, the feature parameters are calculated using the area and the color information of the zone estimated to be flame. If the intensity and histogram are used as input elements for color information, learning by the NN will take time and the accuracy of the judgement will worsen. Moreover, the area of flame is not fixed and the intensity is usually saturated. Therefore, the distribution, the skew, or the kurtosis showing a form of the histogram are not suitable to be used as the feature parameters.

Therefore, as the feature of a histogram, quantile $Q(x)$ is used. $Q(x)$ is the value which occupies $x \times 100\%$ of the whole histogram area. Fig. 8 is the histogram and

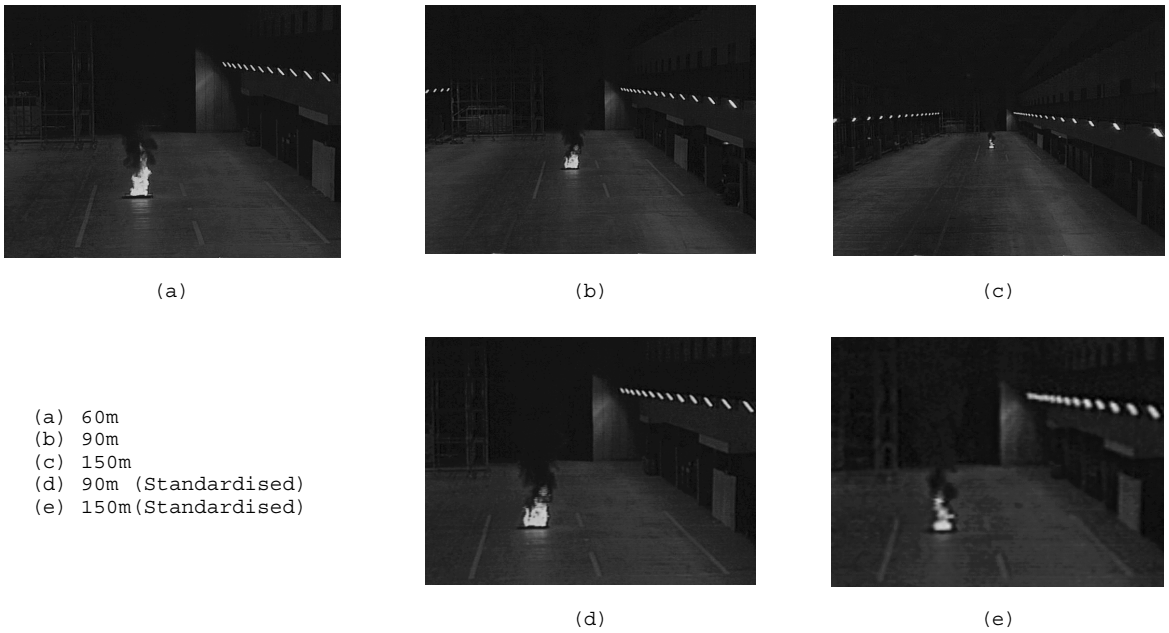

Figure 7: Standardisation of picture by alignment interpolation

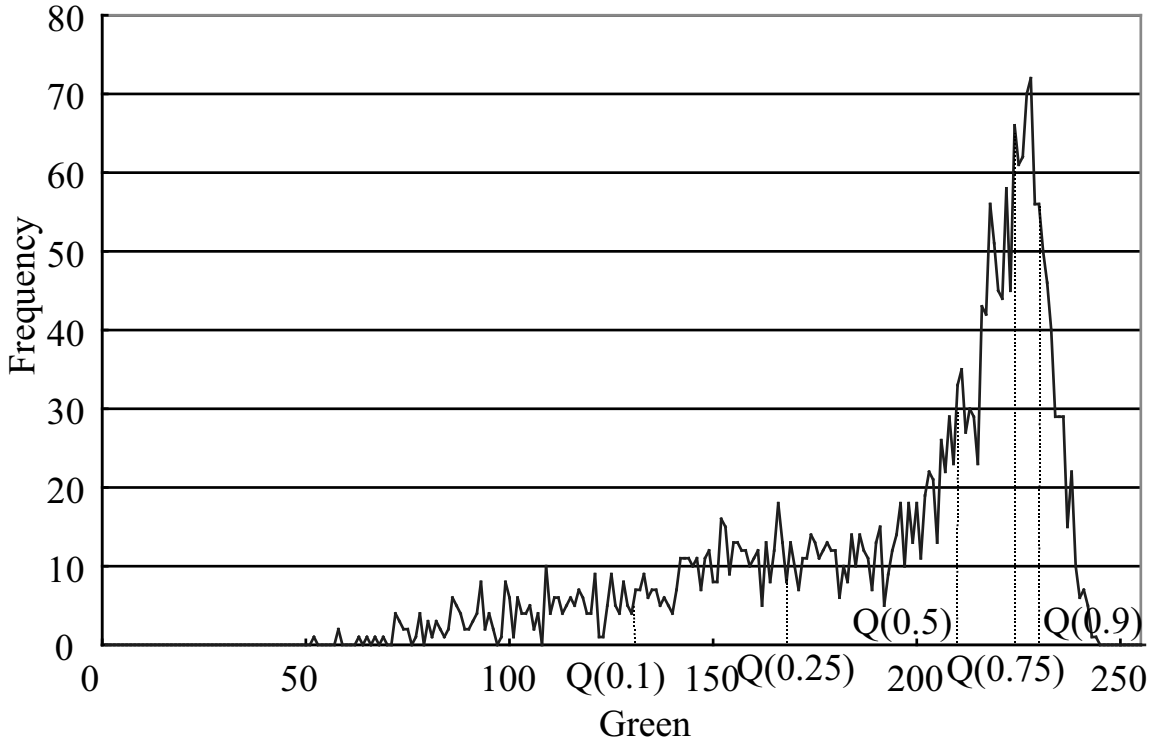

Figure 8: Histogram and quantile of Green intensity of flame

quartile ($Q(0.25)$, $Q(0.5)$, $Q(0.75)$), and quantile ($Q(0.1)$, $Q(0.9)$) of Green intensity of the flame. The input element to NN regarding color information is the value which normalised the quartile and quantile of Red, Green, and Blue intensity. The input element to NN regarding the area of flame is the normalised area. The NN using these feature parameters will be able to extract the flame at high speed from just one frame.

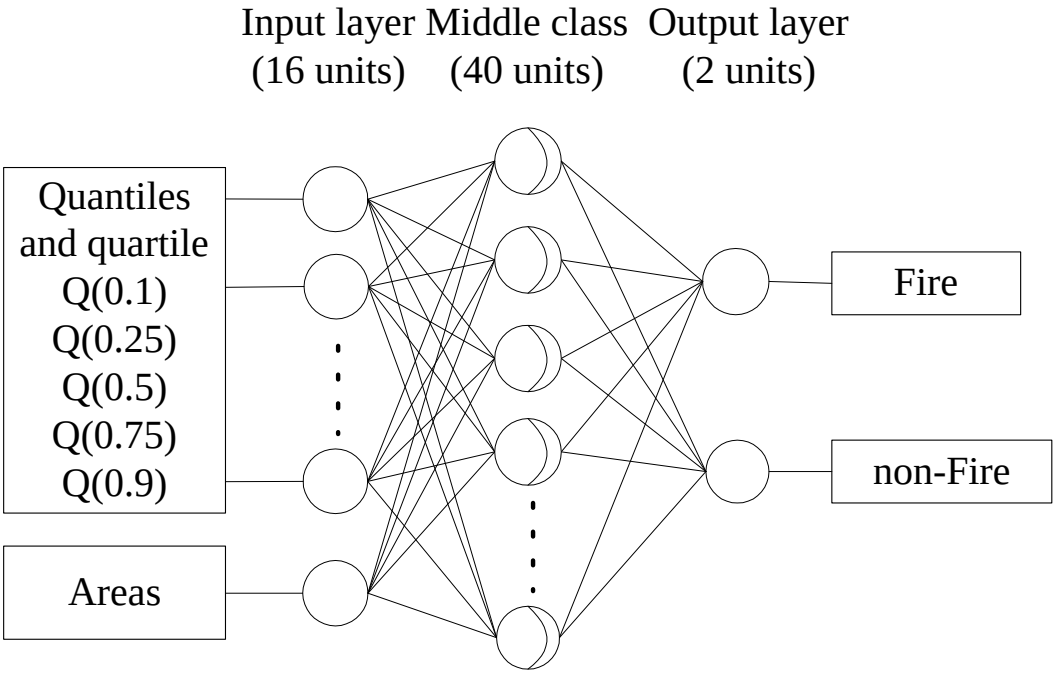

Figure 9: Outline of a hierarchical type NN

Fire detection by NN

The car fire is judged by the hierarchical type NN with the feature parameters as input elements. Fig. 9 is the outline of the hierarchical type NN used for this detection. As for the number of the input layer, the middle class, and output layers, NN is one each, and input data is a total of 16 units of the quantiles and the quartile of Red, Green and Blue, and the normalised area. The middle class is 40 units and the output layer is two units of a fire output and a non-fire output. The error reverse spreading method is used by the NN to determine the following:

- A flame which has changed brightness with the iris diaphragm of the camera and a ND filter
- A Brake lamp
- A Headlight
- Road surface reflection of a headlight

- A Revolving emergency light

If a fire output is 0.7 or more and a non-fire output is 0.3 or less, it is defined as the fire and its opposite is defined as a non-fire. Moreover, with other outputs, it is defined as judgement being impossible.

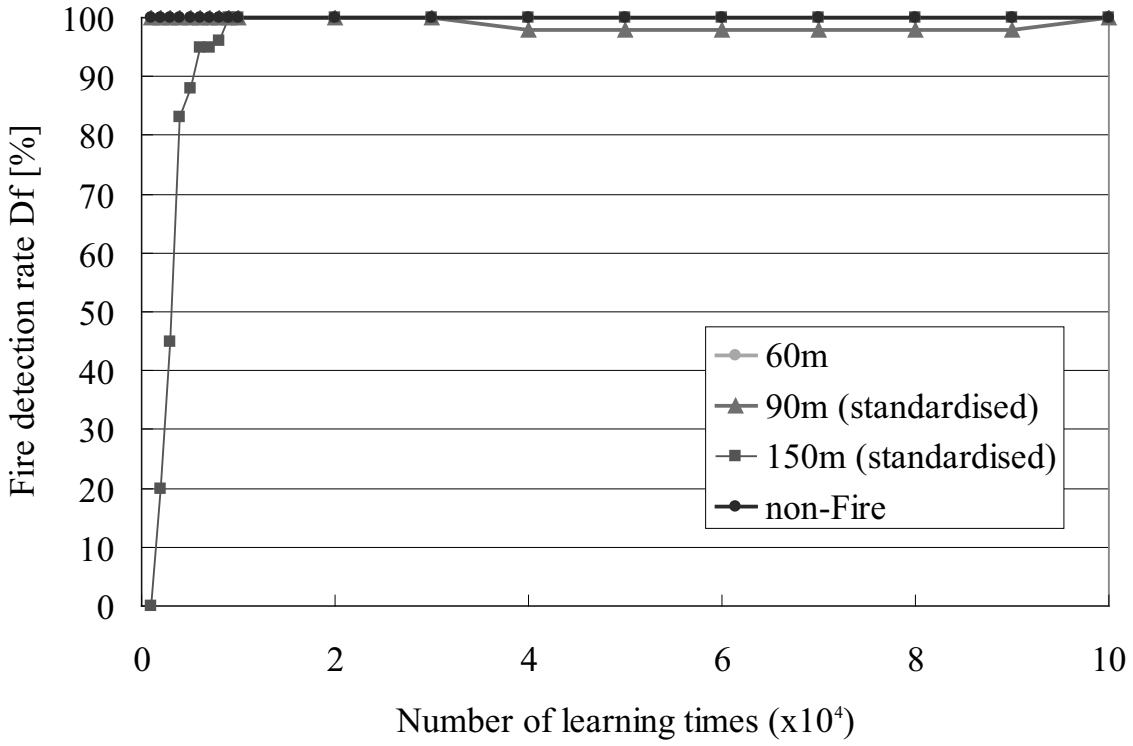

Figure 10: Relation between learning times and fire detection rate

Fig. 10 shows the fire detection results of various conditions in the NN comparing the number of learning times and the fire detection rate D_f (formula (7)). 10,000 plus learning times showed the detection rate at nearly 100% in all fires. Moreover, the detection rate of a non-fire was 100%. Therefore, it became clear that a car fire is detectable with this method.

Table 1: Result of detection

Distance from camera	Detecting target	D_f
60m	Fire bowl fire	100%
90m	Fire bowl fire	93%
	Standardised Fire bowl fire	100%
150m	Fire bowl fire	3%
	Standardised Fire bowl fire	100%

Table 1 shows the significance of distance standardisation with regard to the fire bowl fire (∼50cm height) resulting from the NN feed back consisting of 30,000

learning times. It became clear from standardisation, having raised the detection rate to 100%, that it is very effective especially when the distance from the camera is far.

$$D_f = \frac{\text{The number judged correctly}}{\text{The tested number}} \times 100[\%] \tag{7}$$

Conclusion

The results are clarified as follows.

1. A car fire which occurred less than 150m far from a surveillance camera is detectable by standardising the distance.

2. A car fire with a height of 50cm is clearly detectable using the NN which uses color and area information as the input elements.

From the above results, it is shown that the detection of a car fire is possible by applying the image information obtained from the CCD color TV camera to the NN.

The following are raised as future areas of research.

1. Detection of a small flame in the first stage of car fires

2. Improvement on the detectable distance

3. Examination of the features of the fluctuation of a flame as an input element to NN etc.

4. Correlation to cars using new technologies, such as a fuel cell

References

[1] K. Takahashi, M. Kawano, E. Momma, T. Ono, H. Ishii, and J. Hozumi. Fire detection by ccd-tv camera in high-speed automobile tunnels. In *JAFSE Annual Symposium 2001*, pages 284–285, 2001.

[2] K. Takahashi, E. Momma, T. Ono, H. Ishii, and J. Hozumi. Fire detection of car in highway tunnel by using optical flow. In *JAFSE Annual Symposium 2002*, pages 298–299, 2002.

[3] H. Ishii, K. Kawamura, T. Ono, H. Megumi, and A. Kikkawa. A fire detection system using optical fibers for utility tunnels. In *Fire Safety Journal*, volume 29, pages 87–98, 1997.

[4] A. N. Beard, D. D. Drysdale, and S. R. Bishop. Model of fire in a tunnel. In *Bull. Inst. Mathematics and its Applications*, volume 32, pages 139–142, 1996.

Stefan Brügger
Securiton AG, Special Fire Detection Systems, Zollikofen, Switzerland

Performance behaviour of line type heat detectors in road tunnels

1 ABSTRACT

For most tunnel experts, the necessity of a tunnel fire detection system is undisputed, but about the features, not only positive views are held. Very often it is also said that fire detection systems are too slow in the first place, and that alarming occurs via other communication channels anyway.
This report wants to prove the opposite. It will give an overview of the requirements and performance of a tunnel fire detection system, and also answers the question of reliability and talks about the topic of false alarms.

2 EINFÜHRUNG

Branddetektion in Strassentunnels ist ein Spezialgebiet, das auf Grund von verschiedener grösserer Katastrophen[1] vermehrt in das Blickfeld der Öffentlichkeit geraten ist.
In diesem Bericht geht es darum, die Anforderungen an eine Tunnelbrandmeldeanlage aufzuzeigen sowie das Leistungsvermögen der meist eingesetzten Linienförmigen Wärmemelder aus der Praxis näher zu bringen.

3 ANFORDERUNGEN AN TUNNELBRANDMELDEANLAGEN

3.1 Extremste Umweltbedingungen

Die Umweltbedingungen in einem Strassentunnel sind mit die Extremsten, die es in der Technik gibt. Aggressive Abgase und Streusalznebel, Dieselruss und Staub vermischen sich mit der oft herrschenden Feuchte zu äusserst korrosiven Säuren und Basen; Witterungseinflüsse (im Portalbereich) kommen dazu. Entsprechend darf in Tunnels z.B. nur Montagematerial der besten Qualität (V4A Stahl) eingesetzt werden.

[1] Eine interessante Zusammenstellung findet sich z.B. in http://home.no.net/lotsberg/artiklar/brann/en_tab.html oder in http://www.etnfit.net/content/database/index.html Database 1.

3.2 Massnahmen welche durch Tunnel Brandmeldeanlage ausgelöst werden

- Tunnelzentrale alarmieren (wenn vorhanden)
- Lichtsignalanlage auf „rot“, um Einfahrt von weiteren Fahrzeugen zu verhindern
- Lüftungsanlage auf Programm „Entrauchung“ stellen
- Feuerwehr alarmieren
- Löschanlage auslösen (wenn vorhanden)

3.3 Notwendige Detektionseigenschaften

Die für Tunnelbrandmeldesysteme zu erzielenden Detektionseigenschaften richten sich vor allem nach den Schutzzielen und den automatisch auszulösenden Massnahmen. Dabei sind nicht nur die Ansprecheigenschaften auf ein Schadenfeuer wichtig, sondern ebenso wichtig ist die Zuverlässigkeit des Systems mit möglichst kleiner Fehlalarmrate.

3.3.1 Schnellstmögliche Branddetektion

Von der „World Road Association PIARC“ wurden Empfehlungen herausgegeben, bei welchen Brandlasten resp. bei welchen Ereignissen ein Tunnelbrandmeldesystem einen Alarm auslösen soll. Demgemäss soll ein Vollbrand eines grossen Personenwagens (Brandlast ca. 5 MW) innert 60 sec erkannt werden.
Ein guter Überblick zum Thema findet sich in der Literatur[2] resp. das Basismaterial in[3].

3.3.2 Kleinstmögliche Fehlalarmrate

Das ungewollte Auslösen der vollautomatischen Steuerungen in einem Tunnel kann verheerende Konsequenzen haben:

- Durch die Lichtsignalanlage wird ein Stau ausgelöst, welcher einen Folgeunfall auslösen kann. Ein Fehlalarm in einem Citytunnel während der morgendlichen Rushhour kann eine gesamte Stadt lahm legen!
- Das Hochfahren der Lüftungsanlage benötigt in einem grossen Tunnelbauwerk Energie in der Grössenordnung des Energieverbrauchs einer Kleinstadt.
- Häufige ungewollte Alarmierungen der Feuerwehr demotivieren die Einsatzkräfte.
- Eine ungewollte Auslösung einer Löschanlage im Tunnel kann Unfälle verursachen.

---

[2] An Overview of Vehicle Fires in Tunnels, Haukur Ingason, SP Swedish National Testing and Research Institute

[3] Fires in Transport Tunnels: Report on full-scale tests, EUREKA-Project EU499; Firetun, Studiengesellschaft Stahlanwendung e.V. D-40213 Dusseldorf, 1995.

3.3.3 Kompromiss zwischen Geschwindigkeit und Auslösesicherheit

Zwischen der Anforderung „schnellstmögliche Detektion“ und der Anforderung „möglichst keine ungewollten Alarme“ gibt es aber einen Konflikt, der ausgetragen werden muss, indem die tolerierte Rate der ungewollten Alarme definiert wird (Je nach Sichtweise (Tunnelbetreiber – Feuerwehr – Anlagenerrichter) ergeben sich zudem unterschiedliche Definitionen eines ungewollten Alarms).

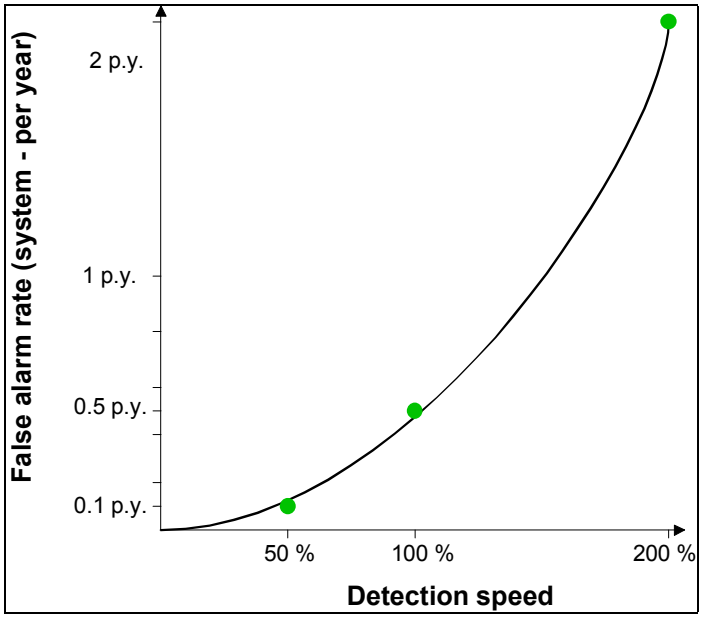

Abhängigkeit der Fehlalarmrate von der Detektionsgeschwindigkeit

3.3.3.1 Alarmrate von Brandmeldesystemen in Tunnels

Bisher gibt es leider keine konkreten Anforderungen an die Fehlalarmrate in Tunnels. Aufgrund von langjährigen Beobachtungen in der Praxis liegt die Fehlalarmrate ca. bei 0.5 Fehlalarmen pro Anlage und Jahr (= 1 Fehlalarm in 2 Jahren). Wünscht der Tunnelbetreiber nun eine doppelt so hohe Detektionsgeschwindigkeit, so muss dies mit einer erhöhten Fehlalarmanfälligkeit erkauft werden.

3.3.3.2 Vergleich Alarmrate von Brandmeldesystemen in Gebäuden

Als Vergleich kann die Rate der ungewollten Alarme von Brandmeldesystemen in Gebäuden herangezogen werden. Der Verband der Errichter von Sicherheitsanlagen erarbeitet zusammen mit dem Schweizerischen Feuerwehrverband und den 6 Berufsfeuerwehren der Schweiz eine jährliche Alarmstatistik[4]. Daraus geht hervor, dass die Rate der ungewollten Alarme pro Anlage bei ca. 0.7 Alarme pro Anlage und Jahr liegt. Die Rate der echten Alarme liegt bei ca. 0.14 Alarme pro Anlage und Jahr.

[4] Alarmstatistik SES/SFV – Siehe unter www.sicher-ses.ch

3.3.4 Ortgenaue Lokalisierung des Brandherdes

Bei der Ansteuerung einer Lüftungsanlage mit Halbquerlüftung sind ca. alle 20 m Lüftungsklappen an der Decke angeordnet, welche bei Bedarf angesteuert werden. Deshalb ist eine ortgenaue Lokalisierung des Brandherdes auch unter erschwerten Bedingungen notwendig (keine Sicht wegen Rauch, Stromausfall, etc.).

3.4 Anforderungen an Verfügbarkeit

Jeder Anlagenbetreiber wünscht sich zwar eine Verfügbarkeit der Systeme von 100%; jedem ist aber auch klar, dass dies nur mit grösstem Aufwand zu erreichen ist, der dann nicht mehr bezahlt werden kann.

3.4.1 Definitionen Verfügbarkeit

Definitionen:

- MTBF = Mean Time Between Failure = mittlerer Ausfallabstand τ
- MTTR = Mean Time To Repair = mittlere Reparaturzeit
- V = Verfügbarkeit = $\frac{MTBF}{MTBF + MTTR} \times 100\%$
- λ = Ausfallrate = 1 / MTBF

3.4.2 Verfügbarkeit von Tunnelbrandmeldeanlagen

Bisher werden von den Tunnelbetreiber kaum Anforderungen an die Verfügbarkeit eines Brandmeldesystems gestellt. Auf Grund von Praxiserfahrungen kann für Tunnelbrandmeldeanlagen eine Verfügbarkeit von ca. 99.5 % angenommen werden, was einer MTTR von 43.5 h pro Jahr entspricht. Wird eine Verfügbarkeit von 99.8% (MTTR von 17.8 h) gefordert, sind dazu erhöhte Massnahmen im Bereich der Vorortlagerung von Ersatzteilen und der Verfügbarkeit von Werkzeugen (z.B. Hebebühne) notwendig.
Wichtig ist, dass dabei die gesamte Kette vom Sensor bis zur Alarmweiterleitung gleichwertig betrachtet wird. Eine redundante Auslegung des Sensor macht keinen Sinn, wenn die Auswertung durch eine nicht redundant ausgelegte Zentraleinheit vorgenommen wird.

3.4.3 Ausfallverhalten - redundante Systemauslegung

Einige Tunnelbetreiber haben angefangen zu fordern, dass ein System auch nach einem Unterbruch des Sensors weiterfunktionieren soll. Dies mit dem Hintergrund, dass mechanische Beschädigungen an einem Sensorkabel vorkommen können (Die Erfahrung zeigt aber, dass ein solches Ereignis höchstens alle 10 –20 Jahre auftritt) oder dass das System durch den Brandfall selbst zerstört wird und eine Detektion von weiteren Bränden (Sekundärbrände) noch gewünscht wird.

Hier muss davon ausgegangen werden, dass die Temperatur an der Tunneldecke erst bei Jahrhundert-Bränden mit > 25 MW so hoch wird, dass das System zerstört wird. Als Lösung dienen entweder beidseitige Abtastung eines Sensorkabels oder, noch besser, die vollständige Redundanz durch ein zweites System, dass parallel verlegt wird.

3.5 Wartung

Das Brandmeldesystem darf keine aktiven Elemente im Fahrbahnbereich aufweisen, welche einen Unterhalt benötigen.

3.6 Anschluss an übergeordnete Leitsysteme - Ausgabe Temperaturprofil

Das Tunnelbrandmeldesystem hört nicht bei der Alarmübertragung auf. Integration in übergeordnete Leitsysteme mittels Modbus, Profibus, OPC, SCADA, etc. sind Standard; ebenso wie die Visualisierung der Temperaturwerte.

3.7 Einfache Montage/Inbetriebnahme

Da die Tunnelbrandmeldeanlage meist erst kurz vor Eröffnung des Tunnel als letztes technisches Werk eingebaut wird, ist eine einfache und flexible Montagemöglichkeit Voraussetzung.

3.8 Preis

Obschon der Preis keine Anforderung im technischen Sinn darstellt, soll er hier doch erwähnt werden, da das Tunnelbrandmeldegeschäft sehr preissensitiv ist. Das Preisniveau liegt (Stand 2004) bei ca. 16-20 k€ pro km Brandmeldesystem (inkl. Auswertung).

3.9 Normative Anforderungen

Bisher hat praktisch jedes Land im Bereich der Tunnelausrüstung mit Brandmeldeanlagen eigene Normen, die mehr oder weniger voneinander abweichen; zum Teil sogar von Objekt zu Objekt, von Ingenieur zu Ingenieur. Aufgrund der bekannten Katastrophen in letzter Zeit sind nun aber in den einzelnen Ländern sowohl Überprüfungen der Tunnel und der Normen im Gange wie auch auf europäischer Ebene die sehr zu begrüssende Vereinheitlichung der Normen[5], die aber erst in einige Jahren abgeschlossen sein dürfte. Interessant ist auch, dass von Seiten des CEN TC 72 in der EN 54-Normenserie eine Norm für linienförmige Wärmemelder in Arbeit ist; worunter auch die in Tunnels eingesetzten Brandmelder fallen werden. Diese Norm (hEN 54-22) dürfte in ca. 2-3 Jahren in Kraft treten.

[5] Siehe Projekte FIT, UPTUN, European Tunnel Safety

3.10 Bauproduktrichtlinie

Da Tunnelanlagen als Bauprodukt gelten, dürfen in Zukunft nur noch Produkte eingesetzt werden, welche gemäss einer hEN geprüft wurden.

4 ÜBERBLICK DER BRANDMELDESYSTEME

Nach dieser Einführung in die Anforderungen folgt ein Überblick über die in der Praxis eingesetzten Systeme.

4.1 Wärmemelder

Aufgrund der hervorragenden Resistenz gegenüber den erwähnten widrigen Umgebungseinflüssen, werden zur Hauptsache Wärmemelder im Tunnel eingesetzt.

4.1.1 Wärme ist komplexer als einfach nur Temperaturmessung

Wärmeübertragung ist ein komplexes Zusammenspiel zwischen Wärmestrahlung, Wärmeleitung und Wärmeausbreitung. Vielfältige Einflussfaktoren wie Umgebungsbedingungen, Windverhältnisse (Einfluss sowohl auf Abbrandverhalten (Sauerstoffzufuhr) wie auch auf Wärmeausbreitung), Feuchte, Druckverhältnisse, Materialen (Reflexionsverhalten, Wärmeleitung, etc.) sowie die Brandlast selbst beeinflussen die Ausbreitung. Deshalb wird die Leistungsfähigkeit der Wärmemelder oftmals zu Unrecht unterschätzt!

4.1.2 Punktförmige Wärmemelder

Punktförmige Wärmemelder waren früher Standard, werden heute aber aufgrund der Fehlalarmanfälligkeit und des grossen Aufwandes für die Installation und die Wartung nicht mehr verwendet.

4.1.3 Linienförmige Wärmemelder

Als Brandmelder werden heute zur Hauptsache linienförmige Wärmemelder eingesetzt. Aufgrund der hohen Windgeschwindigkeiten im Tunnel, betragen die Temperaturerhöhung an der Tunneldecke selbst bei relativ grossen Brandlasten z.T. nur einige Grad und überschreiten die Auslöstemperaturen für Temperaturmaximalmelder oder Sprinkler nicht. Deshalb ist in Tunnels nur ein Wärmemelder nach dem Differentialprinzip geeignet. Die einfachen sog. digitalen oder analogen Sensorkabel sind für die Brandmeldung in Tunnel nicht geeignet!

4.1.3.1 Einteilung Linienförmige Wärmemelder

Definition:

- Melder, bei dem das Detektionselement eine linienförmige Ausdehnung hat.

Einteilung:

- Lineare Wärmemelder:
  Melder, welcher über die gesamte Länge eine kontinuierliche Detektion vornimmt.
- Mehrpunktmelder (Sensorsystem):
  Melder welcher mehrere linienförmige Sensoren enthält.

4.1.3.2 Temperatursensorkabel

Temperatursensorkabel haben in regelmässigen Abständen Temperatursensoren integriert, welche eine präzise Angabe der herrschenden Temperaturen ermöglichen. Zusammen mit intelligenter Auswertesoftware lassen sich so die schnellsten Wärmemelder mit frei programmierbarem Ansprechverhalten konfigurieren.
Zudem sind die Sensorkabel relativ kostengünstig und schnell zu reparieren.
Aufgrund der zentimetergenauen Lokalisierung ist es in der Praxis einfach, fehlalarmanfällige Stellen (LKW-Stau unter Brandmeldesystem) unempfindlicher zu schalten.

4.1.3.2.1 Vergleichsversuche Hagerbachstollen

Im folgenden soll das Leistungsvermögen eines Temperatursensorkabels anhand von Brandversuche im Versuchsstollen Hagerbach aufgezeigt werden:

4.1.3.2.2 Versuchsanordnung

Der Versuchsstollen Hagerbach bei Sargans, in der Schweiz, ist ein idealer Ort um sogenannte „Fullscale Brandversuche“ durchzuführen.
Dabei werden in einem realen Tunnel Brandlasten gezündet, welche denen eines richtigen Tunnelbrandes entsprechen.

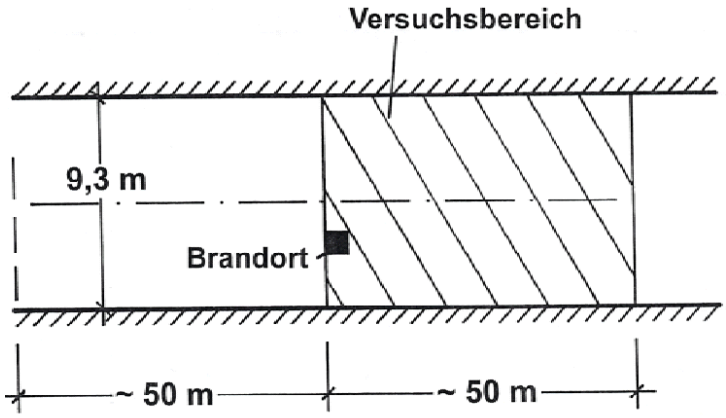

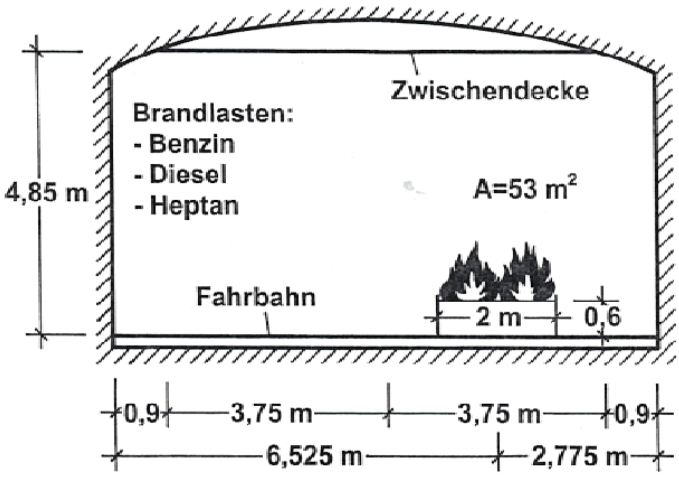

4.1.3.2.3 Ergebnisse

			Alarmzeit [s]			
Versuch		Energie-menge	Max. Temp. (Sensor 1)	System 1 (copper-tube)	System 2 (Sensor)	System 3 (Sensor)
1	(20 l Benzin 2m² mitte)	4.4 MW	64° nach 4 min	7	28	ca. 45
2	(20 l Benzin 4m² mitte)	8.8 MW	82° nach 3 min	13	21	ca 35
3	(20 l Diesel 2m² rechts)	3.6 MW	48° nach 4 min	21	74	???
4	(20 l Diesel 4m² rechts)	7.2 MW	69° nach 4 min	20	32	ca. 50
5	(20 l Heptan 4m² links)	Ca. 8 MW	31° nach 3 min (44° Sensor 3)	15	21	ca. 45
6	(20 l Heptan 2m² links)	Ca. 4 MW	32° nach 3 ½ min (39° Sensor 3)	21	37	ca. 50
7	(20 l Heptan 1m² links)	Ca. 2 MW	30° nach min (34° Sensor 3)	51	170	???

Tabelle: Brandversuche im Hagerbachstollen

4.1.3.3 Interpretation

- Die eingesetzten Linienförmigen Wärmemelder weissten alle ein schnelles Ansprechverhalten auf.
- System 1 war das schnellste System (copper-tube System)
- System 2 war schneller als System 3; dabei fällt auf, dass System 2 auf einem sehr dünnwandigen Sensorkabel basiert, welches einen niedrigen Wärmeübergangskoeffizienten aufweist.

Der Alarm wurde durchwegs auf Grund des Differenzialverhaltens der Melder ausgelöst.

- Ein Maximalmelder hätte nie Alarm ausgelöst; entsprechend hätte auch ein Sprinkler nicht ausgelöst.
- Das Temperaturmaximum ist nicht immer direkt über dem Brandherd sondern um einige Meter in Windrichtung verschoben.

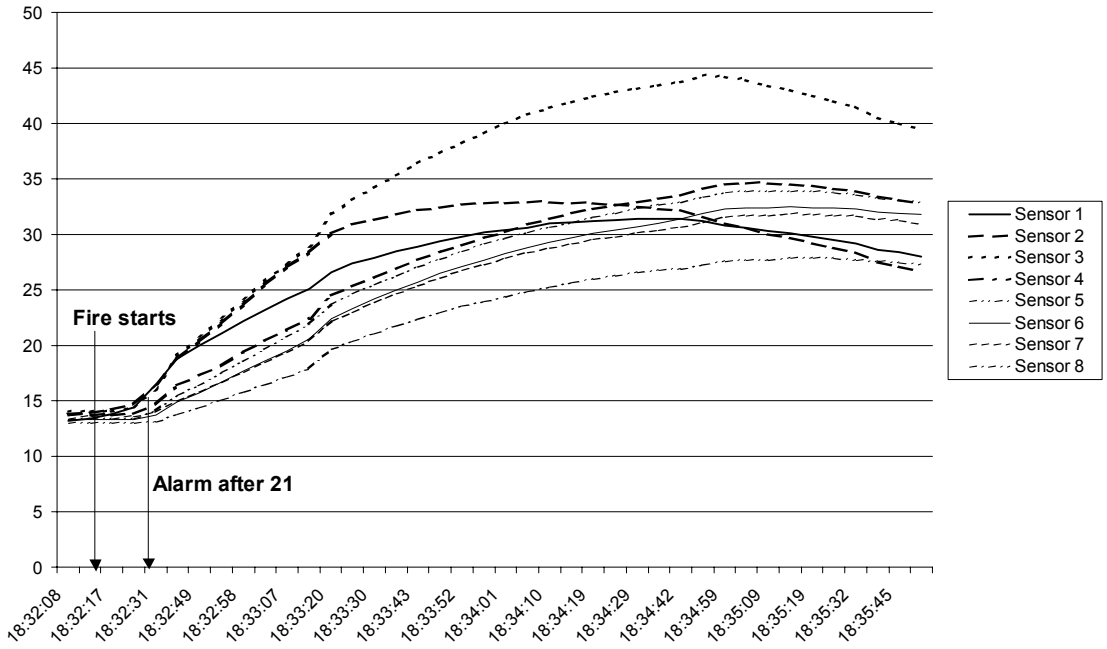

Temperaturkurven eines Sensorsystems im Test – man beachte, dass ein Maximalmelder nie ausgelöst hätte!

4.1.3.4 Glasfasersysteme

Ursprünglich für die Hot-Spot Messung in Energiekabel verwendet, werden Glasfaser-Temperaturmesssysteme auf Basis des OTDR oder OFDR[6] Messverfahrens auch als Tunnelbrandmeldesystem eingesetzt. Das Ansprechverhalten der OTDR Systeme kommt den Sensorsystemen nahe, OFDR Systeme haben systembedingt (FFT) ein langsameres Ansprechverhalten.

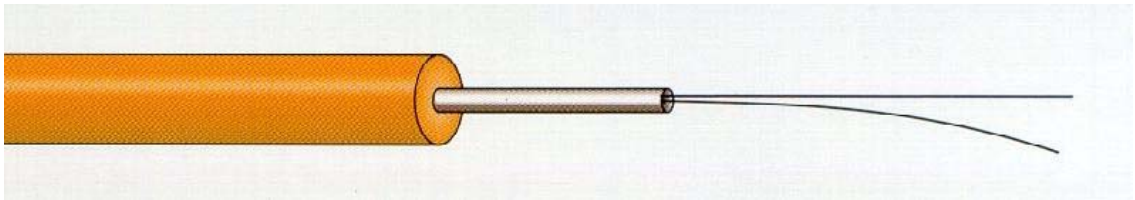

Bsp eines OFDR Glasfasersystems

[6] OTDR = optical time domain reflectometry;
OFDR = optical frequency domain reflectometry

4.1.3.5 Pneumatische Systeme (copper-tube system)

Beschreibung:

- Pneumatisches System
- Überwachungssegmente von ca. 100m
- Detektionsgeschwindigkeit: Sehr hoch

Weitere Merkmale:

- Bewährtes System
- Sehr hohe Zuverlässigkeit
- Günstiger Preis

4.1.4 Ansaug-Rauchmelder

Versuche mit Ansaug-Rauchmelder in Tunnels sind im Gange. Als Vorteil muss die sehr hohe Detektionsgeschwindigkeit angesehen werden; Probleme sind aber die hohen Bau- und Wartungskosten (Verschmutzung der Systeme; ergibt zugleich beschränkte Verfügbarkeit) sowie die noch zu hohe Fehlalarm-rate.

4.1.5 Videobrandmelder

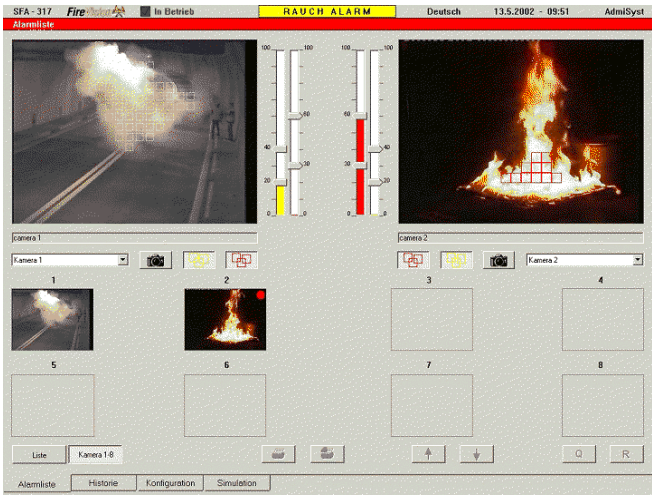

Nach dem Motto: „Video hat es eh in einem Tunnel“ werden Videobrandmelder mit viel Vorschusslorbeeren bedacht. Es sind denn schon einige Systeme vorgestellt und im Testeinsatz. Die Erfahrungen sind aber noch nicht ganz zufriedenstellend; ein Ersatz der bestehende Systeme ist zur Zeit noch nicht möglich. Die Alarmrate beträgt je nach System und Einstellung ca. 1 pro Woche bis 1 pro Monat, was eindeutig zu hoch ist. Zudem ist die Verfügbarkeit abhängig vom Vorhandensein von Licht und sauberen Linsen, was gerade beim Einsatz von Streusalz im Winter zu grösseren Problemen führen kann.

Die Videobrandmelder sind aber eine der wichtigsten Erfindungen der neusten Zeit. Im Moment dienen diese System als zusätzliche Information, überall dort, wo eine rund um die Uhr besetzte Kontrollstelle vorhanden ist und wo der Operateur gewarnt werden kann.

4.1.6 Sichttrübungsmessung zur Vorinformation

Beschreibung:

- Optische Sichttrübungsmessung ist ohnehin in Tunnel eingebaut
- Grosse Abstände
- Detektionsgeschwindigkeit:
- Raucherkennung, Abhängig von Ort

Weitere Merkmale:

- Ungenaue Lokalisierung
- Dient nur als Zusatzinformation

4.1.7 Flammenmelder

Beschreibung:

- Detektiert Flammen im IR/UV Bereich
- Punktförmiger Melder, in Abständen von 20 – 25 m angeordnet
- Detektionsgeschwindigkeit: hoch

Weitere Merkmale:

- Wird nur in Japan eingesetzt

4.2 Überblick

System	Detektionsgeschwindigkeit	Zuverlässigkeit	Verfügbarkeit
Temperatursensorkabel	hoch	hoch	hoch
Glasfasersysteme	mittel	hoch	Hoch
Ansaug-Rauchmelder	sehr hoch	mittel	mittel
Video	hoch	tief	tief
Sichttrübungsmessung	hoch	tief	tief
Flammenmelder	sehr hoch	tief	mittel

Tabelle Eigenschaften Tunnelbrandmeldesysteme

5 SCHLUSSWORT

- Linienförmige Wärmemelder als Tunnelbrandmeldeanlagen sind in der Lage, einen Brand zuverlässig und schnell zu erkennen und können Steuerungen vollautomatisch vornehmen.

- Die Detektionsgeschwindigkeit ist hoch und entspricht den von den Tunnelbetreibern geforderten Werten.
- Die Umgebungsbedingungen in Tunnels sind sehr hart und können nur von den wenigsten Systemen eingehalten werden.
- Videobranderkennungssysteme werden immer zuverlässiger und sind gut geeignet zur Vorinformation
- Sollen Löschanlagen automatisch angesteuert werden, ist eine redundante Ansteuerung mit zwei unabhängigen Systemen ins Auge zu fassen.

6 REFERENTENBESCHRIEB

Stefan Brügger, El.-Ing. HTL/FH, Wirtschaftsingenieur STV. Internationaler Product Manager für Sonderbrandmeldetechnik der Securiton AG in Zollikofen/Schweiz. Obmann der Fachkommission „Bewährung von Brandmeldeanlagen“ des Verband Schweizerischer Errichter von Sicherheitsanlagen SES; Convenor der TC 72 WG 18 (Line Type Heat Detectors) des CEN (Comité Européen de Normalisation).

Florence Daniault, Oliver Linden
Wagner Alarm- und Sicherungssysteme, Langenhagen, Germany
http://www.wagner.de

Brandfrühesterkennung in Tunneln

Einleitung

Das seit einigen Jahren vermehrte Auftreten von Tunnelbränden ist Kennzeichen der verkehrstechnischen Entwicklung unserer Zeit. Trotz allgemein gestiegenen ökologischen Bewusstseins werden mehr und mehr Gütertransporte von der Schiene auf die Straße verlegt. Zusätzlich hat der Individualverkehr aufgrund erhöhter beruflicher Mobilitätsanforderungen an Fahrleistung stetig zugenommen. Als Resultat ist die Gefahr durch Tunnelbrände in hohem Maße gestiegen. Durch diese Erhöhung der Faktoren 'Eintrittswahrscheinlichkeit' und 'potentielle Ereignisschwere' hat sich das Risiko eines Tunnelbrandes im Vergleich zu früheren Jahren deutlich vergrößert. Experten sind sich einig, dass die gerade stattgefundene EU-Osterweiterung besonders in Deutschland zu einer weiteren Zuspitzung der Situation führen wird. Schließlich ist neben der zusätzlichen Verkehrsbelastung zu erwarten, dass in hohem Maße Lkw aus Osteuropa einreisen werden, die den westeuropäischen Sicherheitsstandards bei weitem nicht genügen.

Es besteht also vermehrter Handlungsbedarf auf westeuropäischen Straßen. So können beispielsweise verkehrsleitende Maßnahmen dabei hilfreich sein, die Unfallwahrscheinlichkeit zu verringern. Dennoch lassen sich Unfälle wie auch andere technische Brandursachen auf der Straße und im Tunnel nie ganz vermeiden. Für diese Fälle gilt es, die Schadenschwere über einen adäquaten Brandschutz zu begrenzen und damit Personen und Sachwerte zu schützen. Dabei ist der Erfolg jeder Brandschutzmaßnahme durch nichts mehr bestimmt als durch den Faktor Zeit.

Der Faktor Zeit

Sobald in einem Tunnel ein Brand oder ein Unfall bzw. eine andere potentielle Brandursache entdeckt wird, können geeignete Brandbekämpfungs- und Löschmaßnahmen ergriffen werden. Mindestens eben so wichtig ist es aber, weitere Fahrzeugführer davon abzuhalten, in den Tunnel einzufahren und dort:

- selbst in Lebensgefahr zu geraten,
- entgegenkommende, flüchtende Personen zu gefährden,
- mit ihrem Fahrzeug weitere Brandlast in den Tunnel einzubringen und
- mit Ihrem Fahrzeug für Lösch- und Rettungsaktionen fatale Barrieren zu errichten.

Um dies zu verhindern, sehen die Richtlinien für die Ausstattung und den Betrieb von Straßentunneln [RABT 2003] vor, dass Tunnel ab einer Länge von 400 m mindestens mit einer Gefahrenwarnung in der Tunnelzufahrt oder aber mit einer Möglichkeit der Tunnelsperrung ausgestattet sein sollen.

Berücksichtigt man, dass innerhalb weniger Sekunden mehrere Reisebusse und/oder Gefahrguttransporter in einen Tunnel einfahren können, so ist klar, dass die Gefahrenmeldung so schnell wie möglich geschehen muss. Dies zu gewährleisten ist Aufgabe des eingesetzten Branderkennungssystems - eine *frühest mögliche Branderkennung* ist erforderlich.

Trotz der hohen Bedeutung des Zeitfaktors werden immer noch zahlreiche Tunnel mit Wärmemeldern ausgestattet. Der deutsche Feuerwehrverband (DFV) hat diesen Widerspruch schon lange erkannt und deshalb bereits im Jahre 2000 in einer Veröffentlichung mitgeteilt [DFV 2000]:

"Entscheidend für die Personenrettung ist die
frühzeitige Erkennung eines Brandes"
und
"Die Erkenntnisse, insbesondere auch aus dem Brand im
Mont-Blanc-Tunnel, machen deutlich, dass herkömmliche
Brandmeldeanlagen zu spät auslösen."

Brandfrühesterkennung mit Rauchansaugsystemen

Der Einsatz von Rauchansaugsystemen[1] erstreckt sich mittlerweile über ein weites Gebiet von Applikationsbereichen und deckt technologisch Einsatzgebiete von Reinsträumen bis zu Müllverwertungsanlagen ab. Dabei werden Rauchansaugsysteme insbesondere in solchen Applikationen eingesetzt, in denen konventionelle Brandmelder aufgrund von extremen Umgebungsbedingungen und/oder hohen Ansprüchen an die Ansprechsensibilität nicht erfolgreich eingesetzt werden können.

Folgt man der Empfehlung des Deutschen Feuerwehrverbandes, so zählen Tunnel eindeutig zu diesen Problembereichen. Um bei der Branderkennung einen möglichst hohen Zeitvorteil zu erzielen, genügt es schließlich nicht, den Vollbrand eines Pkw zu detektieren. Wie die Tunnel Task Force des Bundesamts für Straßen richtig feststellt, werden "große Brände ... in der Regel von allen ... Branddetektoren erfasst. Sogenannte 'kalte Brände', die nur einen geringen Temperaturanstieg an der Tunneldecke erzeugen, ... sind schwieriger zu orten" [TTF 2000]. Aber gerade die frühzeitige Detektion dieser Feuer bietet die Möglichkeit, Personenschaden zu vermeiden und Sachschaden so wie Betriebsausfallzeiten des Tunnels zu minimieren. Bild 1 verdeutlicht diesen Zusammenhang vor dem Hintergrund allgemein anerkannter Erkenntnisse aus dem Bereich der Brandschutztechnik. Demnach werden Feststoffbrände i.A. über ausgedehnte Brandentstehungsphasen eingeleitet. Mit einer rechtzeitigen Detektion besteht so die Möglichkeit, die Brandentwicklung noch deutlich vor dem "Flash Over" zu stoppen.

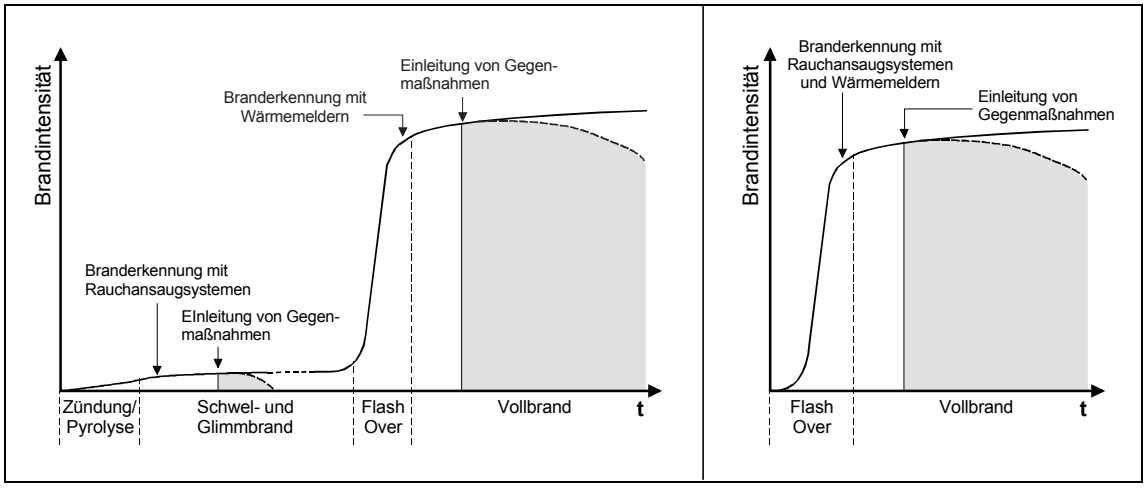

Bild 1: Schematisierter Brandverlauf eines Feststoffbrandes (links) und eines Flüssigkeitsbrandes (rechts), modifiziert nach [LINDEN 2003]

[1] Bezeichnung nach VdS Schadenverhütung: "Ansaugrauchmelder"

Aufbau und Funktion eines Rauchansaugsystems sind in Bild 2 schematisiert dargestellt. Das System besteht aus 2 bzw. 3 Teilen: dem Ansaugrohr(system), dem Detektor und einem optionalen Filtermodul für den Einsatz in Applikationsbereichen, in denen (wie bei Tunneln) mit einem hohen Verschmutzungsgrad gerechnet werden muss.

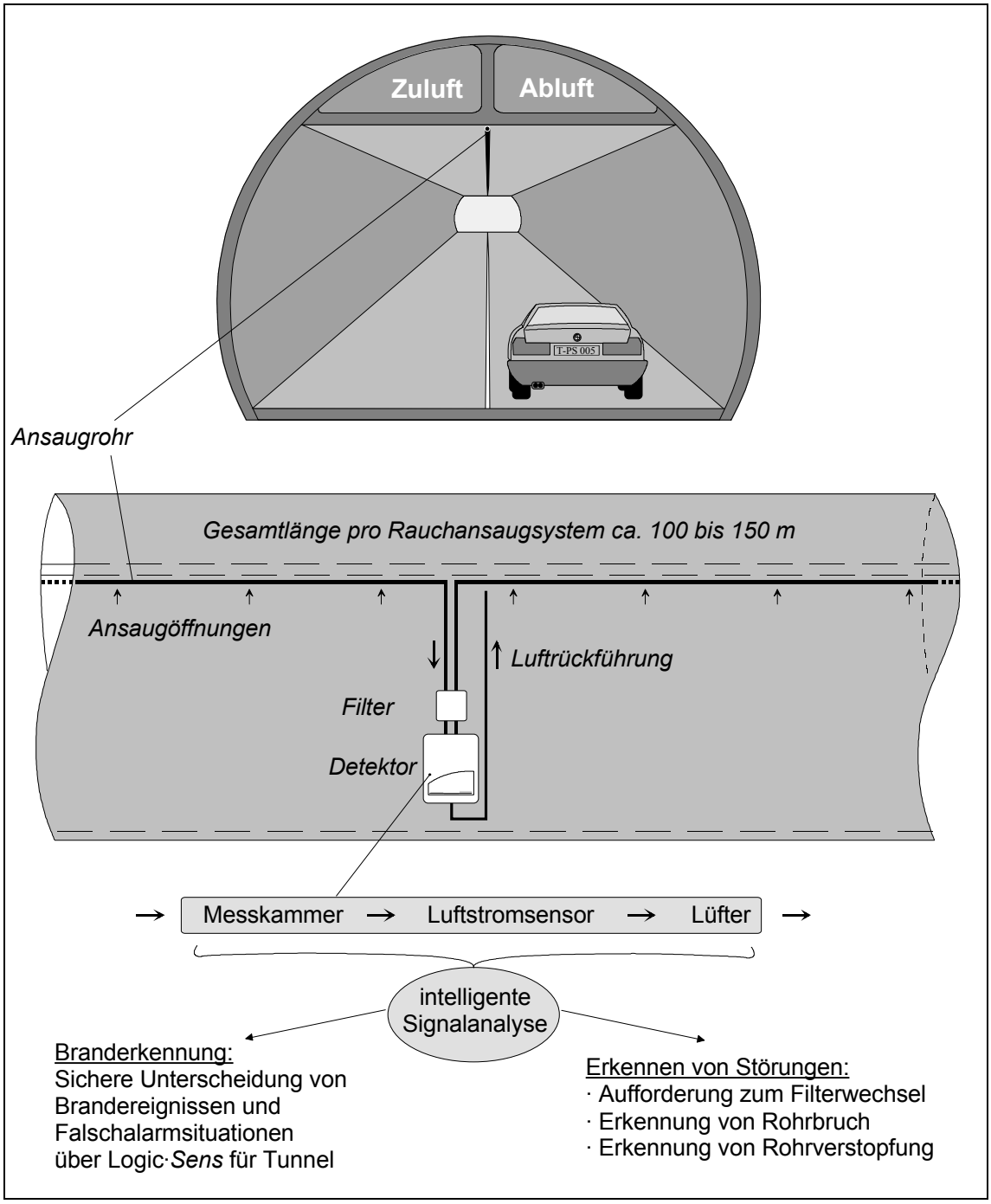

Bild 2: Aufbau und Funktion eines Rauchansaugsystems am Beispiel einer Tunnel-Applikation, schematisiert

Im Detektor befinden sich die Messkammer, ein temperaturkompensierter Luftstromsensor, ein Lüfter sowie die Auswertelektronik. Das dargestellte Rauchansaugsystem verfügt über 2 Messkammern zur Überwachung zweier getrennter Bereiche oder für die Realisierung einer Zweimelderabhängigkeit nach DIN VDE 0833 [VDE 0833]. Das Ansaugrohr ist mit Öffnungen zur Ansaugung der Probenluft versehen. Dabei entspricht der max. Überwachungsbereich einer Ansaugöffnung i.A. dem max. Überwachungsbereich eines punktförmigen Rauchmelders (120 m² in allgemeinen Anwendungsbereichen).

Rauchansaugsysteme zeichnen sich im Wesentlichen über folgende Vorteile gegenüber konventionellen punktförmigen Rauchmeldern aus:

- Aktive Ansaugung der Probenluft

  Die Probenluft wird zwangsweise durch die Messkammer geführt. Eine Abhängigkeit des Eindringverhaltens von Luftströmungen im Raum ist nicht vorhanden.

- Einsatz von Filtern

  In Bereichen mit hoher Staubbelastung wird dem Detektor ein Filter vorgeschaltet, der Staubpartikel zurückhält und (kleinere) Brandaerosole durchlässt. Auf diese Weise wird eine gegenüber punktförmigen Rauchmeldern deutlich verbesserte Signal/Noise-Ratio erzielt.

- Sammeleffekt

  Jeder Öffnung eines Ansaugrohres ist ein festgelegter Überwachungsbereich zugeordnet. Durch gleichzeitige Beaufschlagung mehrerer Öffnungen eines Rohres kommt es zum Sammeleffekt, wodurch sich die Rauchkonzentration am Detektor vervielfacht.

- Hohe Sensibilität

  Punktförmige, optische Rauchmelder verfügen i.A. über eine Ansprechschwelle bei einer Lichttrübung von ca. 3 %/m. Durch den Einsatz einer 'High-Power-Light-Source' kann die Sensibilität eines Rauchansaugsystems bis zu 0,001 %Lichttrübung/m betragen. Die Auswahl der Alarmschwelle wird dabei den Anforderungen der Applikation angepasst.

- Unempfindlichkeit gegenüber Umwelteinflüssen

  Rohrsystem und Detektor eines Rauchansaugsystems können räumlich getrennt werden. Das Auftreten von Umwelteinflüssen wie starker elektromagnetischer Strahlung und kondensierender Feuchte im Überwachungsbereich stellt daher für das System kein Problem dar.

- Wartungsfreundlichkeit

  Punktförmige Rauchmelder müssen zu Wartungszwecken einzeln ausgelöst werden. Bei Rauchansaugsystemen, die bis zu 48 Rauchmelder ersetzen können, wird lediglich der zentrale Detektor an einer gut zugänglichen Stelle geprüft.

Visualisierung und Nutzung von Branddaten

Der Einsatz von Rauchansaugsystemen ermöglicht die Aufteilung eines Tunnels in Überwachungszonen von ca. 50 bis 100 m Länge. Durch den standardmäßigen Einsatz eines Wärmesensors im Detektor werden dabei neben den Rauchdichteinformationen auch örtlich aufgeschlüsselte Temperaturdaten in rettungsrelevanter Raumhöhe gewonnen. Beide Datenströme können online visualisiert werden und bieten somit Tunnelbetreiber und Feuerwehr jederzeit ein genaues Abbild der vorherrschenden Gefahrenlage. Bild 3 veranschaulicht die Online-Aufbereitung der gewonnenen Daten beispielhaft über die schematisierte Darstellung eines Feststoffbrandes in einer Tunnelröhre.

Aus der zeitlichen Entwicklung des Brandszenarios lässt sich der weitere Brandverlauf prognostizieren. Vor diesem Hintergrund können dann entsprechende Schutzmaßnahmen für die Einsatzkräfte sowie Rettungs- und Löschmaßnahmen eingeleitet werden.

Die Tunnel Task Force [TTF 2000] wie auch Feuerwehrverbände fordern seit Jahren die vermehrte Erfassung und Auswertung von Bränden in Tunneln. Zu diesem Zweck ist u.A. eine adäquate Nachbereitung der Brandereignisse notwendig. Auch in dieser Hinsicht birgt der Informationsgehalt der Daten aus Bild 3 neue Möglichkeiten. Brandszenarios lassen sich damit ort- und zeitdiskriminiert nachvollziehen und helfen bei der Brandursachenforschung und somit bei der Klärung von Haftungsfragen. Des Weiteren lassen sich darauf aufbauend ggf. Strategien entwickeln, mit denen das Risiko ähnlicher Brandszenarien in der Zukunft gemindert werden kann.

Bild 3: Schema der Visualisierung eines Feststoffbrandes in einer Tunnelröhre - örtliche und zeitliche Diskriminierung von Rauch- und Wärmeinformationen

Erfahrungen aus der Praxis

Als erfolgreiches Anwendungsbeispiel für den Einsatz von Rauchansaugsystemen in Tunneln kann der Plabutschtunnel angeführt werden. Der 10 km lange Straßentunnel ist mit einem Durchsatz von ca. 20.000 Fahrzeugen pro Tag einer der meistbefahrenen Tunnel Österreichs. Nach Gesprächen mit Fachleuten für Tunnelsicherheit und der raschen Durchführung von Vorstudien und Analysen wurde das Objekt mit Rauchansaugsystemen der Firma Wagner ausgestattet. Seit Januar 2004 läuft nun das Gesamtsystem absolut frei von Täuschungsalarmen. Die besondere Eignung des Systems zur Früherkennung von Bränden wurde im Prüfbericht vom Institut für Brandschutztechnik (IBS) in Linz bestätigt.

Die Funktionsfähigkeit des Rauchansaugsystems wurde unter Anderem über einen Brandversuch mit 8 brennenden Polyurethan-Matten überprüft. 1:11 min nach Zündung (bzw. 00:37 min nach Vollbrand) wurde der Hauptalarm ausgelöst. Bereits nach 00:28 min war die Infoalarmschwelle erreicht und die ständig besetzte Stelle für die Tunnelüberwachung wäre informiert worden. Aufgrund der vorherrschenden Luft-

strömung im Tunnel stellte sich über die gesamte Branddauer unter der Tunneldecke keine ausreichende Temperaturerhöhung ein, um den zu Vergleichszwecken installierten linienförmigen Wärmemelder auszulösen. Die besondere Tauglichkeit des Rauchansaugsystems zur *Brandfrühesterkennung* wurde durch die schnelle Detektion geringer Mengen Rauches demonstriert, die mittels Rauchgenerator erzeugt wurden. Der Hauptalarm wurde dabei bereits nach 01:22 min ausgelöst.

Fazit

Mittlerweile besteht unter Fachleuten ein breiter Konsens darüber, dass herkömmliche Brandmeldeanlagen keinen ausreichenden Schutz für die Sicherheit von Straßentunneln und anderen Tunneln bieten. Zwar können insbesondere mit linienförmigen Wärmemeldern Vollbrände von Pkw zweifelsfrei erkannt werden, jedoch versagt diese Technik bei der Früh(est)erkennung von Feststoffbränden. Reifenbrände, "Schleifbrände", Frachtbrände aber auch Vergaserbrände können lediglich über die Erkennung von Rauch (und Gasen) noch während ihrer Entstehungsphase erkannt und rechtzeitig unterbunden werden. Hier lassen sich mit modernen Rauchansaugsystemen wertvolle Sekunden und Minuten gewinnen - Zeit, die aus vielen Gründen Leben rettet:

- *Lösch- und Rettungsmaßnahmen können frühzeitig eingeleitet werden.*
  Feststoffbrände können auf diese Weise im Einzelfall noch deutlich vor dem "Flash-Over" gelöscht und das Schadensausmaß somit minimiert werden
- *Fahrzeugführer können rechtzeitig davon abgehalten werden, in den Tunnel einzufahren.*
  ... und selbst in Lebensgefahr zu geraten, flüchtende Personen zu gefährden, mit ihrem Fahrzeug weitere Brandlast in den Tunnel einzubringen oder fatale Barrieren für Lösch- und Rettungsaktionen zu errichten.
- *Über eine geeignete Visualisierung der Daten kann sich die Feuerwehr ein genaues Bild über die im Tunnel vorherrschenden Rauch- und Wärmebedingungen machen.*

  Aus der örtlichen und zeitlichen Entwicklung des Brandszenarios lässt sich der weitere Brandverlauf prognostizieren. Entsprechende Schutzmaßnahmen für die Einsatzkräfte sowie Rettungs- und Löschmaßnahmen können eingeleitet werden.
- *In der Nachbereitung eines Brandfalls kann das Brandszenario ort- und zeitdiskriminiert nachvollzogen werden.*
  Mit dieser Analyse kann ein wichtiger Beitrag geleistet werden zur Brandursachenforschung bzw. zur Klärung von Haftungsfragen, wie auch zur Entwicklung geeigneter Bekämpfungsstrategien für zukünftige Brandfälle.

Literatur

DFV 2000	n.n: "Brandschutz in Tunnelanlagen"; DFV-Empfehlung, Fachempfehlung Nr. 1/2000, Deutscher Feuerwehrverband, 2000
LINDEN 2003	Oliver Linden: "Entwicklung von Prüfmethoden zur Sicherstellung der Schutzfunktion von Brandmeldern mit Gassensoren"; ISBN: 3-936050-05-8; VdS Schadenverhütung; Reihe "Wuppertaler Berichte zum Brand- und Explosionsschutz", Nr. 4, 2003
RABT 2003	n.n.: "Richtlinien für die Ausstattung und den Betrieb von Straßentunneln (RABT)"; Forschungsgesellschaft für Straßen- und Verkehrswesen, herausgegeben vom Bundesministerium für Verkehr, Bau- und Wohnungswesen, Ausgabe 2003
TTF 2000	n.n.: "Tunnel Task Force - Schlussbericht"; Bundesamt für Straßen, 2000
VDE 0833	n.n.: "Gefahrenmeldeanlagen für Brand, Einbruch und Überfall - Teil 2: Richtlinien für Brandmeldeanlagen (BMA)", DIN VDE 0833 Teil 2, Februar 2004

David Blake
Federal Aviation Administration Technical Center, Atlantic City, New Jersey, USA
Jill Suo-Anttila
Sandia National Laboratories[◊], Albuquerque, New Mexico, USA

Aircraft Cargo Compartment Fire Detection and Smoke Transport Modeling

Abstract

The U.S. Federal Aviation Administration, along with other regulatory agencies, requires that cargo compartments on passenger carrying aircraft be equipped with fire detection and suppression systems. Current regulations require that the detection system alarms within one minute of the start of a fire and flight tests are required to demonstrate compliance with these regulations. Due to the high costs of flight tests, extensive ground tests are typically conducted to ensure that the detection system will meet the time to alarm requirements during the flight tests.

A transient computational fluid dynamics computer code for the prediction of smoke, heat and gas species transport in cargo compartments has been developed as a simulation tool to be used in the detection system certification process. This simulation tool couples heat, mass, and momentum transfer in a body fitted coordinate system in order to handle a variety of cargo bay shapes and sizes. Ideally, such a physics-based CFD simulation tool can be used during the certification process to identify worst case locations for fires, optimum placement of detector sensors within the cargo compartment, and sensor alarm levels and algorithms needed to achieve detection within the required time. Validation of the CFD model is in progress and comparison of the predicted results with the results obtained from full-scale fire tests in a variety of actual aircraft cargo compartments provides insight into the model capabilities.

A standardized flaming fire source consisting of plastic resin pellets molded into a small block has been developed. The fire source uses a small quantity of heptane ignited on the top surface as well as an embedded length of nichrome wire to produce a consistent, representative, and repeatable fire. This fire source has been proposed as the standard to

[◊] Sandia National Laboratories is a multiprogram laboratory operated by Sandia Corporation, a Lockheed-Martin Company, for the United States Department of Energy under Contract DE-AC04-94AL85000.

be used for cargo fire detection. The heat release rate, mass loss rate, and smoke and gas species generation rate from this fire source are used as an input to the CFD model. The model can then predict the time that detection will occur with the given boundary conditions and detector alarm criteria.

Validation testing is being conducted at the FAA Technical Center. The code was developed by Sandia National Laboratories. Funding for the model development was provided by the National Aeronautics and Space Administration (NASA) Glenn Research Center under the Aviation Safety Program.

1. Introduction

The objective of this project is to standardize the certification of aircraft cargo compartment fire detection systems and to improve the reliability of those systems. The U. S. Federal Aviation Administration (FAA), along with other regulatory agencies throughout the world, require that cargo compartment fire detection systems provide a visual indication to the flight crew within one minute of the start of a fire [1]. An inflight demonstration is also required to show compliance with this regulation. Historically, a variety of smoke sources have been permitted during the inflight demonstration and the quantity of smoke generated has also varied. Due to safety considerations from igniting actual fires inflight, artificial “smoke” sources have been widely used with properties that could be very different from those of actual smoke [2].

The detection systems most commonly used in aircraft cargo compartments has predominately been reflected-light photoelectric smoke detectors and to a lesser extent ionization smoke detectors. This equipment is prone to false alarms from other airborne particles present in cargo compartments, such as dust and water vapor. The ratio of false alarms to the detection of the rarely occurring actual cargo compartment fires is on the order of hundreds to one [3]. Existing regulations do not preclude the use of any detection technology other than smoke particle detection or in combination with smoke particle detection. However, this method of fire detection has been the technology of choice by the aircraft manufacturing industry for at least the last 30 years. The FAA publishes guidance material in the form of Advisory Circulars (AC) that, although not

required, are generally used by aircraft manufacturers during the certification process. AC 25-9A addresses cargo compartment fire detection and is written in a way that assumes fire detection is performed using smoke detectors [4]. Guidelines do not currently exist for detection systems that respond to signatures from a fire other than smoke.

To address some of the issues outlined above, the FAA Technical Center has developed a standardized fire source as a result of this ongoing project. The details of the fire source and initial testing along with a description of the smoke transport code have previously been presented in the AUBE 2001 conference [5]. Initial fire source testing focused on a block of compressed plastic pellets in either a smoldering or flaming mode. This fire source produced a quantity of smoke that was similar to the quantity previously used in some aircraft smoke detection certification tests in small cargo compartments. Subsequent testing determined that the flaming mode better replicates the standard fire that was desired for detection because, not only was the smoke quantity sufficient, but it also produced detectable levels of other fire signatures that could be used to discriminate between actual fire and false alarm sources. Testing was then conducted with this fire source in a cone calorimeter with Fourier Transform Infrared (FTIR) mass spectroscopy gas species measurement capability. The diagnostic was used to characterize the heat release rate, mass loss rate, and production rate of smoke and gas species. The test data from both the cargo compartment and the cone calorimeter testing showed very good repeatability. Concurrent with the FAA testing, Sandia National Laboratories has developed a computational fluid dynamics model to predict the transport of smoke, heat and gas species throughout a cargo compartment. The FTIR data are used as the fire source term in the transport model.

Along with the introduction provided above and a basic description of the smoke transport code, this paper presents the first phase of validation, including experimental data and corresponding model simulations.

2. Transport Solver

A detailed description of the working transport equations and numerical procedure used in the FAA smoke transport code has been previously presented [6]. The computer code draws upon detailed experimental data that are designed to provide time-varying boundary conditions for mass and heat sources. The determination of the transient transport of species that are evolving from the fire source at different rates can therefore be accomplished. It is anticipated that the simulation tool can be extremely advantageous to the threshold design testing of new detection sensors. Moreover, much physical insight can be gained by the visualization of the smoke transport.

3. Baseline Validation Experiments

A series of 15 baseline validation experiments were conducted in the forward cargo compartment of a Boeing 707 fuselage to compare experimental results with code predictions. The experiments consisted of a 300 second duration flaming resin block fire near the center of the compartment. The cargo compartment was instrumented with forty ceiling thermocouples, six smoke obscuration meters and a movable gas probe plumbed to low range CO and CO_2 gas analyzers. Figure 1 shows the cargo compartment and the instrumentation locations. The gas probe was moved to three different locations for five tests at each location during the series. Two of the locations were in recessed pans in the ceiling of the compartment, similar to the location where smoke detectors in actual compartments are typically located. The third location was at the ceiling level in the corner of the compartment.

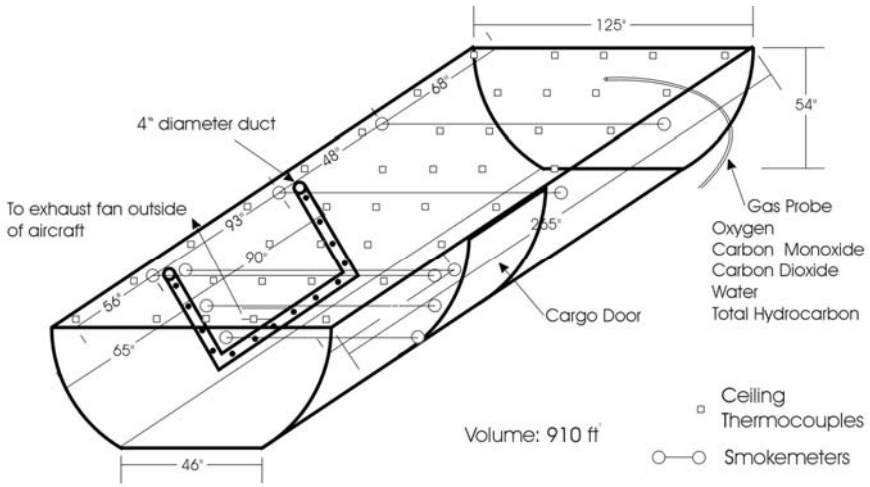

Figure 1. B707 Cargo Compartment

It is desirable to select scalar quantities for comparing experimental data to computational simulations; thus, the following validation metrics were selected after a review of the baseline test results. The chosen metrics are as follows:

-Ceiling temperature and gas species concentration rise from 0-60 seconds, 0-120 seconds and 0-180 seconds

-Light transmission (smoke obscuration meter)

-30 and 45 seconds (ceiling and all vertical)

-60 seconds (vertical- high, mid, low)

-120 seconds (vertical- mid and low)

-180 seconds (vertical- mid and low)

4. Baseline Validation Simulations

Smoke transport model simulations were performed for comparison to the baseline experiments to facilitate validation of the computational model. A flaming fire event occurring over 300 seconds was simulated using the computational model. The computational mesh consisted of 20 x 40 x 30 nodes and the geometry of the cargo compartment was accurately represented by the body-fitted coordinate system of the computational model. The ability of the user to place the fire in the correct location is limited by the cell sizes within the computational mesh. This constraint can result in a slight variation from the actual fire location in the experiments. The center of the experimental fire location was approximately 0.075 m (3") different than the computational fire location in two dimensions. For each time step, at each of the 24,000 cells, the user has access to values for the velocity (u, v, w), density, temperature, turbulence parameters, soot, CO, and CO_2. An example of the temperature results within a plane (at the centerline of the fire source) of the computational domain is shown in Figure 2. The computational model runs on a standard personal computer, Linux workstation, and Solaris workstation. The simulations presented here were run using a 1.8 GHz Dell Latitude laptop requiring approximately 1 hour of computational run time for each minute of real time.

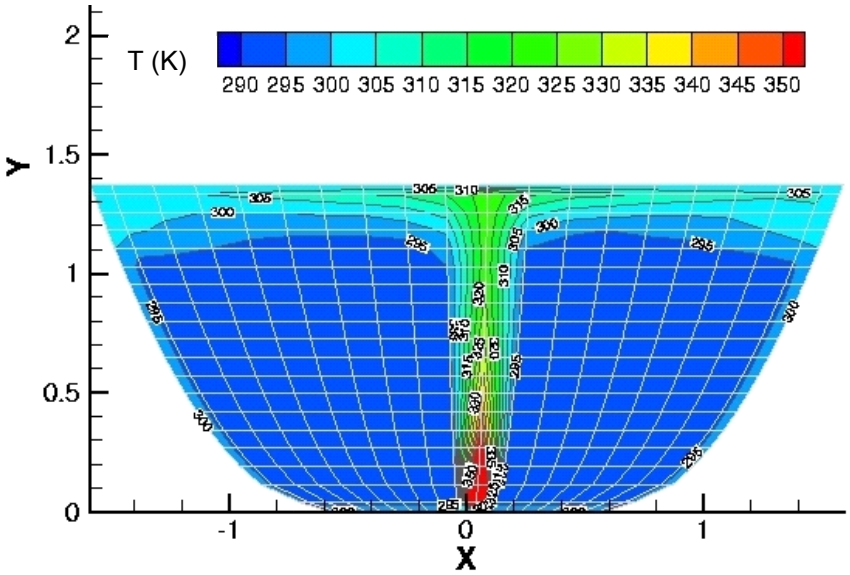

Figure 2. Computational Temperature (K) Distribution at the Fire Centerline

5. Comparison and Analysis of Experimental and Computational Results

The experimental and computational results were compared for each validation metric identified in the previous section. Due to space limitations, the comparison of three representative metrics will be described, but the rest of the comparisons can be found in a related document [6].

Ceiling Temperatures

At 60 seconds after ignition, the computational temperatures (solid and dotted lines) at the thermocouple locations are plotted with the experimentally acquired temperatures (symbols with error bars) in Figure 3. The distribution of temperatures in the compartment predicted by the model are similar to the experimental data. Although the trends in both the experimental data and the computational results for all the temperature validation metrics were very similar, the magnitudes of the computational temperatures were consistently higher by several degrees for the simulations with no heat loss to the walls (solid line). The code has the ability to transfer heat to the walls while the walls remain at a constant temperature. The results of the simulation with heat loss (dotted line) are lower than the experimental results. It is encouraging that the experimental results lie between these computational extremes, but more information about the heat transfer to the walls is required. It is proposed that heat flux and

temperature gauges be installed to provide data to aid in the future development of a sub model (one-dimensional wall conduction) that more closely predicts the thermocouple temperatures. In addition, it was noticed that some thermocouple beads were covered by an insulating sheath. Further experiments revealed that the covered beads significantly influenced the recorded temperatures; therefore, the initial validation experiments must be followed by additional experiments with the sheath removed to expose the bead and obtain accurate temperature data for model validation.

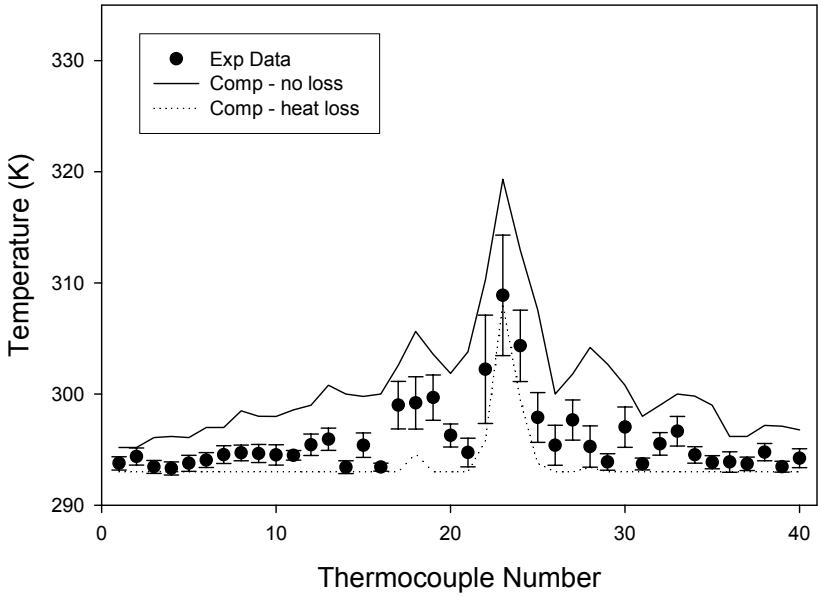

Figure 3. Preliminary Comparison of Temperature at 60 sec

Gas Concentrations

The computational gas concentrations were extracted from the simulation domain at locations corresponding to the gas analyzer locations. Mid and aft concentrations were obtained in the recessed area, which is currently not modeled; therefore, those predicted concentrations were obtained just below the ceiling level. The corner gas sampling location was very close to the experimental sampling location. The agreement in the magnitudes of the CO gas concentrations (shown in Figure 4) is fair at 60 seconds after ignition, although the trends are different. At later times not shown, the agreement of the trends is better, but the magnitudes are less favorable (especially for CO_2). Overall, the gas concentration predictions were not satisfactory.

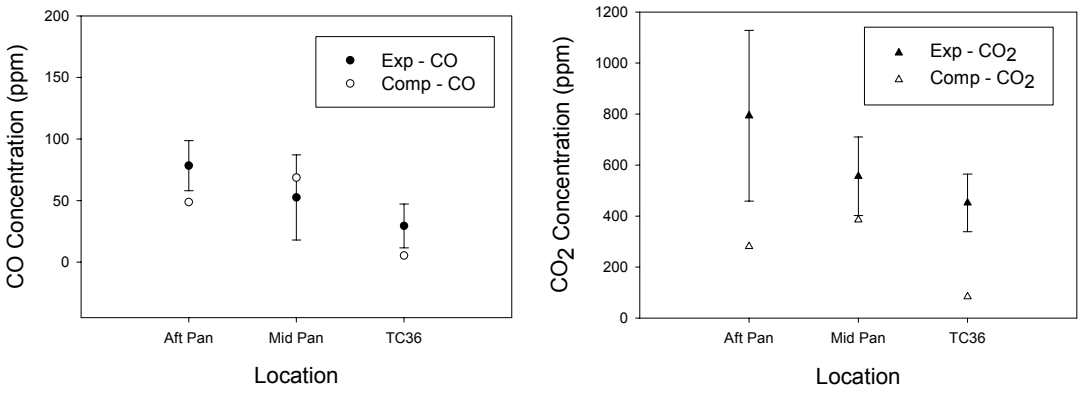

Figure 4. Preliminary Comparison of Gas Concentrations at 60 sec

The first potential reason for the discrepancy is that the recessed areas are not currently being modeled; instead, code predictions are presented one cell below the ceiling. Previous studies have shown the recessed areas impact the flow field. Therefore, the recessed areas are being added to the model. Secondly, it was observed that some items in the cargo compartment may be impacting the flow and transport of smoke (i.e. floor lamp and large gas sampling line). It is likely that the line for the gas sample is considerably affecting the transport of smoke and gas species since it is quite large and is attached to the ceiling. An indication of this effect is evident in the trends of the gas readings. The experimental gas concentrations in the aft pan are consistently higher than the mid pan. This result is counter-intuitive because the mid pan is closer to the fire source. It is possible that the ceiling jet flow interacts with the line causing the smoke to be transported differently than if the line was not present. To improve the next set of validation data, the gas analyzer line was modified to collect samples from a fitting in the recessed area while the entire line was routed through the area above the cargo compartment, thus keeping the ceiling free of obstructions.

Light Transmission

The smoke meter model predictions agree with the experimental measurements very well in both trends and magnitude, as shown in figure 5. Note that the computational data for the ceiling smoke meters are presented at y = 1.32 m, which is approximately 0.01 m (0.4″) higher than the experimental measurements, but it is likely that this minor

discrepancy in computational measurement locations would not result in a deviation from the experimental measurements within the error bounds. Potential sources for uncertainty in the experimental measurements, such as beam steering and collection of soot on the optics, were investigated and were shown to be negligible.

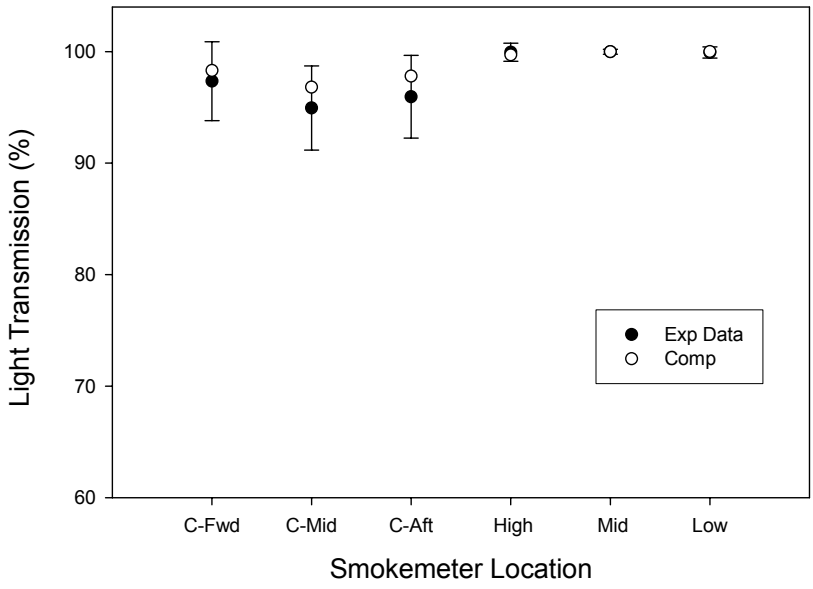

Figure 5. Preliminary Comparison of Ceiling Light Transmission at 30 sec

6. Recommendations for Future Validation Experiments

Several items have been identified as likely contributing to the differences between the experimental data and the code predictions; therefore, modifications will be made prior to repeating the validation exercise. On the experimental side, the gas sampling probe was rerouted and the sheaths were removed from the thermocouples. In addition, a small lamp illuminating the resin block was removed to eliminate the potential for inducing an additional flow pattern not included the model. On the computational side, the code was modified to include the recessed areas in the ceiling of the cargo compartment and heat transfer to the walls and ceiling of the compartment. The location of the fire source and instrumentation were modified such that exact duplication is possible in the modeled domain. In addition, the next round of validation comparisons will contain mesh sensitivity calculations.

7. Conclusion

Initial comparisons of code predictions with experimental data were reasonably good but there is room for improvement. A number of potential modifications to the experimental instrumentation and the transport code have been identified. These improvements will be implemented and the validation experiments will be repeated. The results of these validation comparisons will be published in the near future.

Acknowledgements

The authors would like to acknowledge the contributions of the following individuals: Walt Gill and Louis Gritzo for technical guidance, Carlos Gallegos, Jim Nelson, and Stefan Domino for code development, Bob Filipczak and Louis Speitel for source characterization, and Rick Whedbee and Frank Gibbons for conducting the validation experiments. In addition, the support of NASA Glenn Research Center is also gratefully acknowledged.

References

[1] Code of Federal Regulations 14 CFR Part 25.858

[2] Suo-Anttila, J., Gill, W., Gritzo, L. Comparison of Actual and Simulated Smoke for the Certification of Smoke Detectors in Aircraft Cargo Compartments, DOT/FAA/AR-03/34, November 2003.

[3] Blake, D. Aircraft Cargo Compartment Smoke Detector Alarm Incidents on U.S.-Registered Aircraft, 1974-1999, DOT/FAA/AR-TN00/29, June 2000.

[4] DOT/FAA. Smoke Detection, Penetration, and Evacuation Tests and Related Flight Manual Emergency Procedures, AC 25-9A, January 1994.

[5] Blake, D., Domino, S., Gill, W., Gritzo, L., Williams, J., Initial Development of Improved Aircraft Cargo Compartment Fire Detection Certification Criteria, AUBE ’01 Conference Proceedings, March 2001.

[6] Suo-Anttila, J., Gill, W., Gallegos, C., Nelson J., Computational Fluid Dynamics Code for Smoke Transport During an Aircraft Cargo Compartment Fire: Transport Solver, Graphical User Interface, and Preliminary Baseline Validation, DOT/FAA/AR-03/49, October 2003.

D.O. Odigie
Yamen Systems Services, P.O. Box 562 Fordham Station, Bronx NY 10458 USA

STOCHASTIC MODELING OF THE SPREAD OF SMOKE IN BUILDINGS.

1. ABSTRACT

In this paper, due to the instability and variability in the process the spread of smoke in a building is simulated using a stochastic process, the Markov chain. The spread of smoke is approximated by a discrete Markov chain with very small time unit step. The simulation was done using the most relevant of the factors affecting flow. The basis for the choice of the factors used is presented. Equations of flow are developed. The effect of buoyancy pressure on the spread of smoke was first investigated. The result indicated that buoyancy pressure does not play significant part in the spread of smoke beyond the fire room. Hence a deterministic model that excludes effect of buoyancy pressure and a stochastic model were then developed and used for the simulations. The stochastic model attempts to represent the variation in the medium of spread. Input data from the fire is from that used by previous modelers. The building considered for the simulation is a ten storey with a stairwell, corridors and compartments. The simulation is limited to spread in the stairwell, corridors on the floors and between levels. A deterministic model was first developed then converted to a stochastic model by approximating the process by a Markov chain.

Results of the simulation include carbon dioxide concentrations with respect to time in various parts of the building. The paper illustrates the feasibility of the Markov chain methodology in modeling the spread of smoke. The uncertainty in the estimates of the signatures of fire can be addressed by this stochastic method. The signatures of fire were presented with their probabilities of occurrence. Realistic knowledge of the signature of fire and their distribution is prelude to the evaluation of fire and air control systems in buildings.

Keywords: Stochastic, probability, smoke spread, fire, Markov chain.

2 Introduction

A stochastic process X(t) is defined by the following quantities [1]: (a) State space, (b) Index parameter (time), and (c) Statistical dependencies between the random variables (r.vs) X(t) for different values of the index parameter t.

The state space is the set of possible values (or states) that X(t) may take. We have a discrete-state process if the values that the process may take are finite or countable. In smoke spread, a particle can occupy any of the infinity of positions about it, hence the process cannot be discrete. The possible positions of the smoke particles, in this case, are over a finite or infinite continuous interval. The spread is thus a continuous-state process.

The index (time) parameter at which changes may occur is anywhere within a set of finite or infinite intervals on the time-axis; hence it is a continuous-parameter process.

The flow of smoke is considered as a stochastic process. This is due to the instability and variability in the process. One of the stochastic processes that can describe this is the Markov process. The Markov property assumes that the future behavior of a sequence of events is uniquely decided by a knowledge of the present state only. In essence, given the state of the process at any time, the Markov process assumes that its subsequent behavior is independent of its past history. The Markov process with discrete parameter space is referred to as a Markov chain. Smoke spread does not occur in discrete time hence it can only be modeled approximately as a Markov chain.

Consideration will be given to the concentration of species only. A deterministic model will be converted to a non-deterministic model as a Markov chain process. Data from a chosen model will input into the model.

3 Flow between nodes on a level

Consider a network of nodes. At a given time t, node A is in some initial state with species concentration x of mass m_1 and of temperature t_1 and node B with species concentration y of mass m_2 and of temperature t_2. Assume there is a link (opening)

between the two nodes such that smoke flows from node A to B. For small infinitesimal time *dt* there is some additional quantity of smoke flowing from node A to B resulting in increase in temperature and species concentration in node B.

At time t

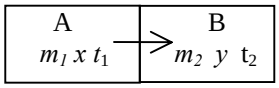

Fig 1 Flow from node A to B.

4 Deterministic Model

The first step in developing a stochastic model is to develop a deterministic process that describes the spread of smoke. This can then be converted to a stochastic process. Flow in deterministic processes is defined mainly by known input parameters. For instance, the spread of smoke is mainly due to differential pressures. Difference in pressure could be due to many factors.

4.1. Factors affecting flow Pressure

The pressure difference Δp , causing the flow can be due to many factors. These include stack, buoyancy, wind and mechanical devices. The relevance of any or a combination of these will depend on the location of the fire, height of building or number of levels, and the building configuration. Each of these is discussed below. Buoyancy is the effect of the pressure difference between hot gases from a fire compartment and its surroundings. The effect of buoyancy pressure will depend largely on the gas temperature distribution along the levels of the building. Buoyancy pressure was only significant on the floor of the fire but did not have much effect for locations far from the fire source in initial simulations. Hence it can be assumed that the effect due to buoyancy for flows in this simulation is not significant in the flow of gases.

Stack pressure is caused by the difference in temperature between the outside environment of the building and the inside. When the outside is colder there is an upward lift of flow (normal stack effect), while the reverse is the case when the outside is warmer (reverse stack) [Federic et al, 2]. Stack action can be due to the temperature of the fire and to the difference in temperature between the inside and outside of the

building. While the first acts only on the fire floor, the later acts over the entire height of the building [Tamura 3].

The expression for stack pressure differences at standard atmospheric pressure is given as

$$\Delta p_s = ks\ (1/TT - 1/TTs)\ H \qquad (1)$$

Where

p_s = Pressure difference from shaft to outside (Pascal)

TTs = Temp of inside air in stair shaft (K), TT = Temp of outside air (K)

H = Height above neutral plane in m, Ks = 3460 N.K.m^{-3} Coefficient.

The effect of wind is not considered here for simplicity and to correspond with the conditions of the experiment and data available for verification [4]. The building is made of concrete and external openings are closed. Only the openings in the corridor in the outside wall are opened. The input data does not include the situation where a window is broken. It is taken that the effect is not consequential in this case.

4.2. Species Concentration

Considering figure 1 again, the following could be derived.

The quantity of species flowing from node A to B in (t, $t+dt$) =

$$\left[CA\sqrt{\rho\Delta p}\right]x dt = \left[CA\sqrt{\rho\Delta(p_b + p_s)}\right]x dt \qquad (2)$$

where

ρ = Gas density, A = Area of orifice (e.g. door)

C = Coefficient of orifice, Δp = Pressure difference between A and B

x = Concentration in previous node (A), y = Concentration in current node (B)

p_b = Pressure due to buoyancy effect, P_s = Pressure due to stack effect.

Similarly, the quantity of species flowing out of node B in (t, $t+dt$)

$$= \left[CA\sqrt{\rho\ \Delta p}\right]y dt = \left[CA\sqrt{\rho\ \Delta(p_b + p_s)}\right]y dt$$

The quantity of species in node B at time $t = m_2 y$

and the quantity of species in node B in time $t+dt$ =

$$m_2 y + \left[CA\sqrt{\rho\ \Delta(p_b + p_s)}\right]xdt - \left[CA\sqrt{\rho\ \Delta(p_b + p_s)}\right]ydt$$

The concentration of species in node B at time $t+dt$ can then be shown to be given by

$$\frac{dy}{dt} = \frac{(x - y)}{m_2} CA\sqrt{\rho\Delta(p_b + p_s)} \tag{3}$$

For horizontal flow, effect due to buoyancy can be assumed to be insignificant. Going by the assumption that the openings are of the same size, equation (3) above becomes:

$$\frac{dy}{dt} = \frac{(x - y)}{m_2} CA\sqrt{\rho\Delta p_s} \tag{4}$$

By the above expression, the rate of increase in concentration with time in node B depends on the difference in concentration between the two nodes, the pressure differences due to buoyancy and stack, and the mass of gas in the node. Pressures due to buoyancy and stack are functions of temperature. The area of openings is assumed to be the same. Otherwise the expression needs to be modified.

4.3. Discretizing the Model

The spread of smoke is a continuous process. This must be discretized in order to be able to simulate the process. Let the unit step of time in discretizing be h.

Equation (4) above can also be discretized as follows

$$y_{n+1} - y_n = \frac{CAh\sqrt{\rho\,\Delta p}(x_n - y_n)}{m_2} \tag{4}$$

where $\Delta p = \Delta(p_b + p_s)$

The above equation will be used in computing species concentration at different locations in the building. In computing the species concentration in the corridor, it is taken as one compartment. The corridor can be subdivided into smaller units and the equation modified. If the corridor is subdivided then the flow will be horizontal and equation (3) developed earlier will be applicable.

5 Source of Data

Data used for validation of the model is from Hokugo and Hadjisophocleous [4]. The experiments were conducted in the NRCC ten-storey experimental smoke spread tower. The fire is by the door to the stairwell on the second floor. Hence there is flow of smoke into the stairwell on the second floor. This is used as input to the model. The data has been used in validating the NRCC smoke spread model. The data will be input into this model.

6 Results of Simulations for Deterministic model

The following figure is a typical result of the simulations of the spread of smoke in the NRCC building for the deterministic model. The deterministic model does not incorporate uncertainties. Results for the stochastic models are presented later in the paper.

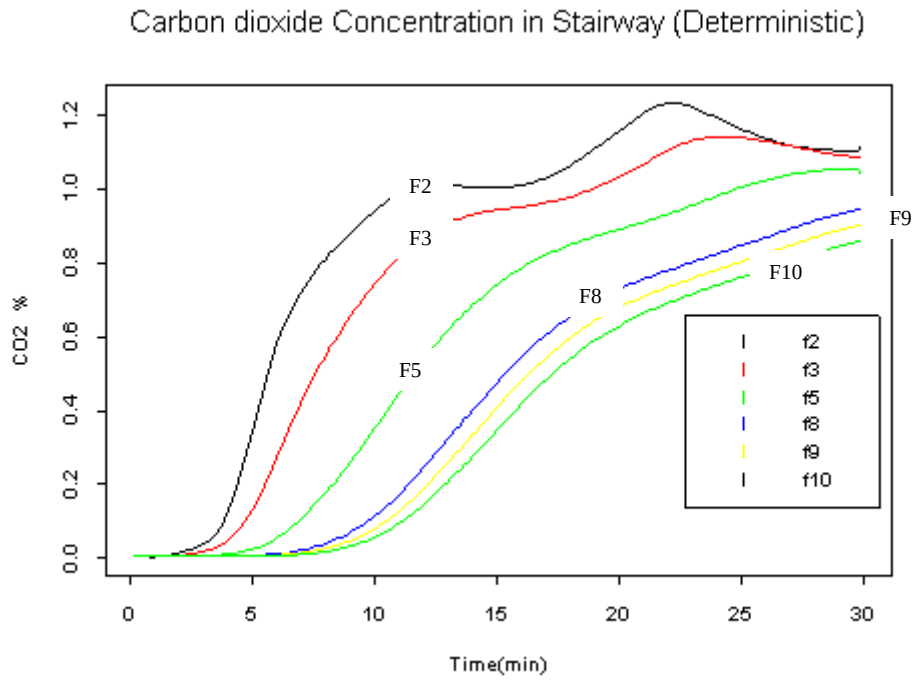

Fig 2 Carbon dioxide distribution for the stairway of the NRCC building. (F2 – Level 2)

The above model can be turned into a stochastic model that induces variability with the objective of incorporating some fluctuations in the process due to some unpredictable events.

7. Stochastic Model

It is not possible to predict the exact outcome of an event that is described by a random variable (RV). It can only be estimated by a probability. Smoke spread is a highly variable stochastic process. Though a continuous process, smoke spread can be approximated by a discrete process. Continuous processes are difficult to simulate in practice.

7.1 Species Concentration

Let α be the discretizing parameter that is the unit step of the stochastic jumps. If the probability of the change in the phenomenon being investigated (in this case, concentration of smoke) is β, then the probability of no increment in the concentration will be $1 - \beta$. This can be expressed as follows:

Let

$$\frac{CA\ \alpha\sqrt{\rho\Delta p}}{m_2}(x_n - y_n) = E(\Delta y) = k$$

(The above follows from equation 4 of the deterministic model).

$$P_\alpha = P\{\Delta y = \alpha\} = \beta \quad (5)$$

$$P_0 = P\{\Delta y = 0\} = 1 - \beta$$

$$E(\Delta y) = \alpha P_\alpha + 0P_0 = \alpha P_\alpha = \alpha\beta = k$$

Hence

$$\beta = \frac{k}{\alpha} \quad (6)$$

The variance of the process is given as

$$Var(\Delta y) = \alpha^2\beta(1-\beta)$$

The coefficient of variation of the process is given by

$$CV = \frac{Std.Dev(\Delta y)}{mean(\Delta y)} = \sqrt{\frac{\alpha}{k} - 1} \quad (7)$$

The above expression implies that for a constant mean increment (k) the variation in the process increases with increasing values of the discretizing parameter (α). The magnitude of α indicate the extent of variability in the process.

7.3 Results of Simulations for Stochastic model

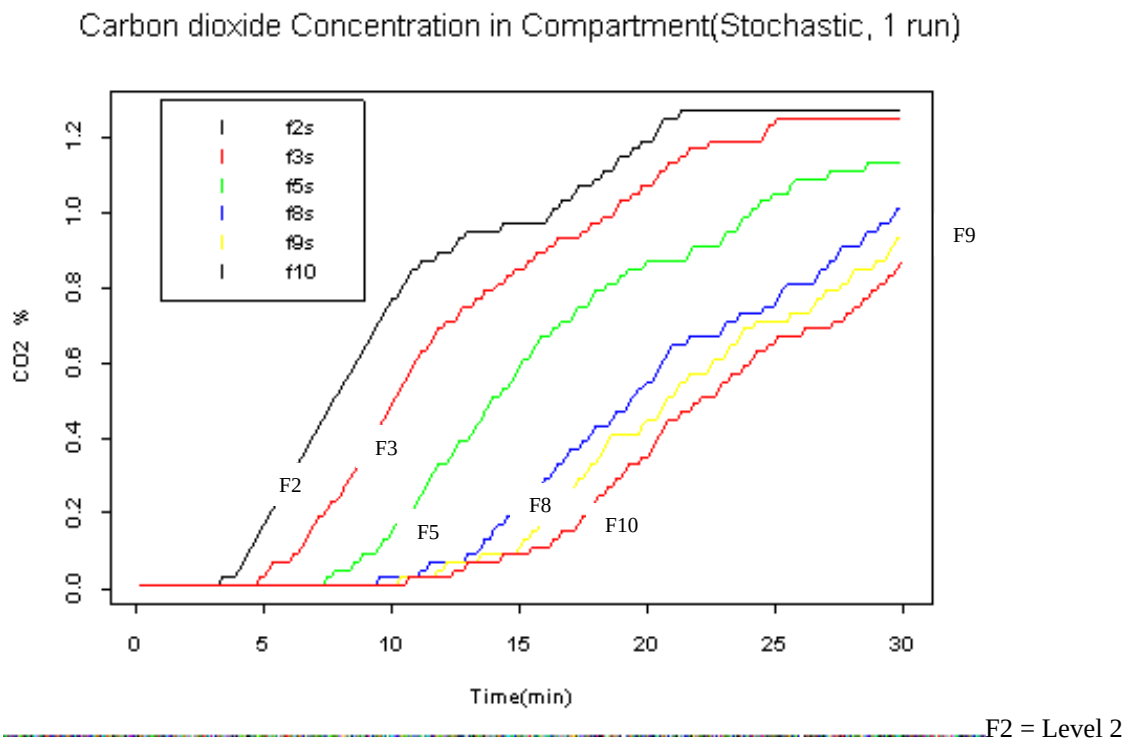

Fig 3 Plot of Carbon dioxide concentration variation with time for the respective stairway floor levels (NRCC building) for a stochastic simulation.

The above figure is comparable to that of the deterministic in Fig 2. The stochastic model is able to estimate the probability of occurrence of the results by running the model a number of times. The value of α used in the above simulations was 0.03. The probability of the change, β, in the phenomenon was determined by Bernoulli trial, giving either a 0 or 1. For each trial the change may (1) or may not occur (0). A value of 1 gives a jump while a 0 does not. The simulation was performed 1000 times. The Markov chain modeling methodology is able to estimate the spread of smoke. Below is the result of a run of the stochastic model for the species concentration in the stairway. It is now possible to determine the condition of an occupant moving from one location to another in a bid to escape the effects of smoke.

The 29th minute of the process was taken and results from the runs were analyzed. Analytical results for chosen floors are as presented in the table below.

Table 1 : Descriptive analytical result for the 29th minute for the 8th floor (Carbon dioxide concentration):

Staircase level 8				
Max	**Min**	**Mean**	**Std Dev**	**Var**
1.09	0.85	0.97632	0.037447	0.001402

The above result is for the stochastic run of the model. A time unit step of 10 seconds was used. The values obtained for each staircase is representative of all possible scenario for the assumed conditions. The choice of the number of classes ensures that not too much detail is lost and the shape of the distribution is easily seen. Although nothing could be said about the individual values the histogram does give the necessary probabilities for a range of values necessary for future estimates.

The above results in Table 1 can be compared with that of the real life fire experiment conducted by Hokugo et al [4] for the 29th minute presented below.

	F8s
Stochastic mean	0.97632
Hokugo	0.945

The experimental mean lies within one standard deviation of the mean of the simulation.

The cumulative relative frequency of a particular class is the proportion of concentrations that fall below the upper limit of that class. From it the probability at or to the left of each

point χ can be specified. The cumulative relative frequency distribution graph (ogive) of the smoke concentration for the 29th minute after the start of fire for the staircase on the third floor of the building concerned is presented below.

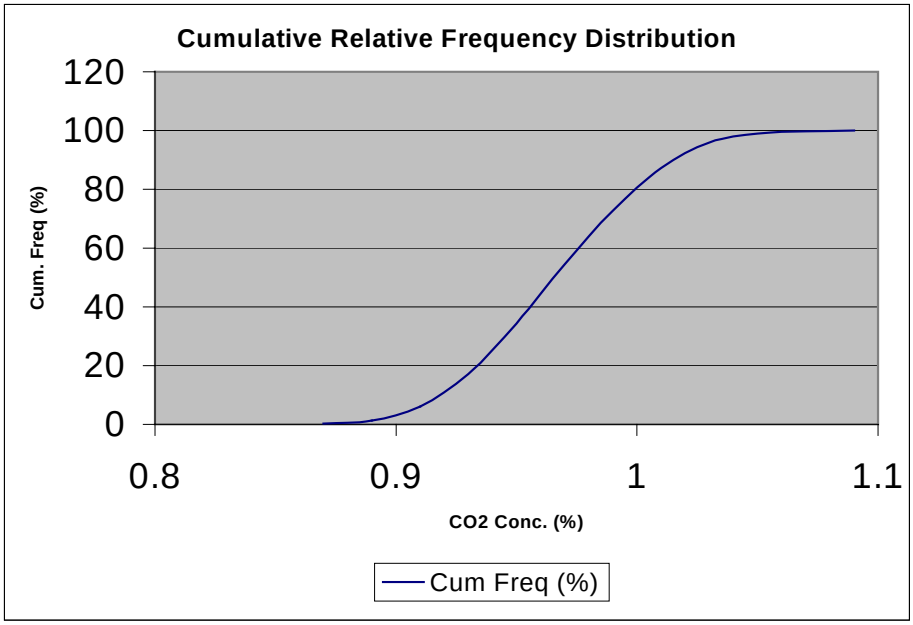

Fig. 4 Cumulative Relative Frequency Distribution for the Carbon dioxide Concentrations for the 29th minute after the start of Fire on the eighth level of the Stairway.

The same result can be done for any other signature of the fire that can be approximated by similar mode of spread, Markov chain. Gases like hydrogen cyanide (HCN) and carbon monoxide (CO) could be of interest. The combined effect of the gases can then be evaluated. The distribution of the time to effective incapacitating dosage (EID) can be obtained for an occupant moving from say the tenth to the third floor.

8 Conclusion

The spread of smoke in a building was simulated using a stochastic process, the Markov chain. The spread of smoke was approximated by a discrete Markov chain with very small time step unit. The extent of accuracy depends on the fineness of the time unit step that is stipulated by the modeler.

The simulation was done using the most relevant of the factors affecting flow. The basis for the choice of the factors used was presented. Equations of flow were developed.

A deterministic model was first developed with a stochastic model given and used for the simulations. The stochastic model attempts to represent the variation in the medium of spread. Input data from the fire was from that used by previous modelers. The building considered for the simulation is a ten storey (NRCC building) with a stairwell, corridors and compartments. The simulation was limited to spread in the stairwell, corridors on the floors and between levels.

The above illustrates the feasibility of the Markov chain methodology in modeling the spread of smoke. The uncertainty in the estimates of the signatures of fire can be addressed by this stochastic method. Knowledge of expected species concentration in locations in a building would be useful in developing measures and devices that assist occupants' safety.

REFERENCES:

1. Parzen E. "Stochastic Processes", Holden day series in probability and statistics, San francisco, 1962.

2. Frederic B., and Clarke B. "Physiological Effects of Smoke: Managing Escape", ASHRAE Winter Meeting Technical Program, January 25-29, 1997, Philadelphia.

3. Tamura G.T. "Smoke Movement & Control", National Fire Protection Association, Inc., USA, 1994, ISBN: 0-87765-401-8.

4. Hokugo A., Yung D. and Hadjisophocleous G.V. "Experiments to validate the NRCC smoke movement model for fire risk-cost assessment", The Fourth International Symposium on Fire Safety Science, 1994, pp 805-816.

P. Andersson and J. Blomqvist
SP Fire Technology, Borås Sweden and Siemens Fire Safety, Sweden

Early Smoke Detection in High Buildings

Abstract

Some results from two projects carried out 2001-2003 are presented in this paper. The paper focuses on the full scale experiments conducted in two different industrial building and the CFD simulations conducted of these test.

Introduction

Many industries today rely heavily on the detection system to be fast enough and give such early warning that the rescue service arrives in time to extinguish the fire before the damage is severe. In some cases they also trust that the detection system gives such early warning that the smoke does not cause any damage like smell and corrosion on the goods stored. If the system fails to do so, the company will loose customers and good-will in these days of just in time production.

Early detection in high industrial buildings is a difficult task. The smoke movement at an early stage of the fire, i.e. when it is only smouldering, is controlled by the airflow pattern in the building before the fire. This airflow pattern is normally not known, it is determined by the ventilation system, other heat sources in the room, moving machines or forklifts, open gates etc. Obtaining data from all this and simulating the airflow is very time consuming. Furthermore, the smoke production and velocity and temperature profile from such small fires is usually not known.

It is desirable to be able to determine whether the detection system will give early warning enough and to determine the best placement of the detectors. It is possible to test this in existing buildings by creating a fire of the same magnitude that one wants to be able to detect and see if one gets alarm. But this is not an option in a non-existing building e.g. during the design phase of a building. In addition it is difficult to determine beforehand what will happen if changes are made to geometry, ventilation system etc. Therefore computer simulations could be an alternative. However, in order to be able to determine when a detector will be activated in a scenario one needs to know the smoke production and the detectors sensitivity to that smoke. The detector

sensitivity will depend on the particle size of the smoke aerosol and its velocity, but such information is not easily available. On the other hand, the soot models in CFD codes still needs development and usually one does not know what fuel is involved in the fire. Therefore an approach by letting the smoke aerosol in as a conserved scalar with neutral density that follows the air or by using a prescribed soot source where the soot source is defined as a certain amount of soot (unit kg/s) can possibly be useful.

Some results from two projects sponsored by BRANDFORSK are presented in this paper. The projects included measuring the smoke production from different package materials and electrical material such as cables and lighters for fluorescent lamps since the smoke production from these materials is not reported in the literature. The sensitivity for different smoke detectors against these fires was investigated in an EN54 room. The ventilation systems used in today's industry were investigated by means of discussions with manufacturer of ventilation systems. CFD simulations were carried out for buildings with two different types of ventilation system, i.e. one displacement and one well-stirred system. In addition full-scale experiments were carried out in the same type of buildings. This paper focuses on the full-scale experiments and the simulations of these, for information on the other parts the reader is referred to the complete reports[1,2].

Different types of ventilation systems

The ventilation systems used in industries can be divided into two main different types, i.e. mixing systems, which is a "well stirred reactor" type of system where the temperature is the same in the whole room, and displacement systems, where a temperature gradient is maintained in the room with high temperatures close to the ceiling, i.e. cold air is supplied at floor level and warm air is extracted higher up. The velocities close to the air supplies can be substantial in the former case while the temperature gradient causes problem in the latter case. It is also common with mixtures of the two different types of ventilation in a room. In many cases there is also a dead volume close to the ceiling that does not take part in the ventilation flow. For ventilation purposes it is the climate rather close to the floor where people are present that is interesting. Ventilation designers often do not need to care about what happens closer to the ceiling. This makes it difficult to get data on the temperature etc. close to the ceiling without measuring at the site.

Full scale experiments

Full-scale experiments were conducted in two different industrial buildings. One series was conducted at Fläkt woods in Enköping and one at IKEA in Jönköping. In both cases the experiments were performed during normal operation of the facility i.e. normal working activities were going on. It means that the experiments were not controlled, for instance gates were opened and closed, machines started and switched off, forklifts were driving around etc.

Displacement System – Fläkt Woods

Fläkt Woods has a displacement ventilation system i.e. a temperature gradient is maintained in the building. The temperature gradient was measured during the experiments. The air velocity in the room was measured to be between 0.1 and 0.2 m/s, however close to the air inlets the velocity was somewhat higher. The room is 171 x 90 m with a room height of 7.25 m. During the tests the smoke concentration was measured at three different places with laser diodes with a wavelength of 670 nm. 13 optical point detectors (DO1151/APS006) and one sampling system (ASD using a DO1153 with parameter set APS071, alarm at 0.25%/m) were mounted as well. The point detectors were mounted in pairs, one close to the ceiling and the other 90 cm below that. Two computers registered the output from all detectors. In total 13 tests were conducted. Three different smoke generators were used; the TF2 fire according to EN54-7, the SG3000 and one called AG2000 that is under development by Siemens Fire Safety.

Studying the results the following observations can be made:

- The smoke concentration measured with the lasers and detectors are in reasonable agreement with each other.
- The sampling system gave alarm first followed by the detectors close to the fire.
- The detectors gave alarm in a order that differed from the order first predicted by the ventilation staff. This was, however, a question that caused a lot of discussion and after discussion with other ventilation consultants they concluded that the air should not drift in any direction.
- There was a slight tendency that the lower detectors gave alarm and warning before the detectors close to the ceiling. However, for time to pre-alarm it was

the other way around.

- The TF2 fire was difficult to detect. In one test only warnings were achieved. In test 13 the fire was moved about 1 m. In this test the smoke took another route compared to the other tests, i.e. the route that was first predicted by the ventilation staff. The smoke kept hanging in the air and moved downwards to the people working in the building.
- Comparing test 3 (AG2000 2.2 kW) and test 10 (AG2000 4.6 kW) shows that a higher heat results in better possibility to detect the fire. This is partly due to that the smoke production increases with the applied heat in the AG2000 but still there is a tendency for the smoke to reach higher if the heat applied increases.

The fact that the smoke took a different route in test 13 is probably not so much due to that the fire was moved 1 meter to the side in this case. The smoke took a slightly different route also in test 1. This is probably caused by changes in the airflow pattern due to gates being opened etc. Before the test series started all air inlets were reset to the airflow they were planned to have according to the ventilation staff. Walking around the second day showed however that the production staff had changed the ventilation by means of e.g. corrugated cardboard to eliminate draught at their workplaces.

Mixing system – IKEA

The experiments were conducted in a room 165 x 200 m. The ceiling height was 11.8 m. The building has a total mixing ventilation system. The temperature gradient in the room was measured during the tests together with the air velocity below one of the inlets. The smoke concentration was measured at three different places with laser diodes with a wavelength of 670 nm. 12 optical point detectors (DO1151/APS006), four CO/optical detectors (DOTE/APS216), four beam detectors, a video and one sampling system (ASD) were mounted as well.

The point detectors were mounted in pairs, odd numbers close to the ceiling and even numbers 1.5 meter below that. Computers registered the output from all detectors. Three different smoke generators were used, these were the TF2 fire according to EN54, the SG3000 and AG-2000. The fires were placed at different locations.

Studying the results the following observations can be made:

- The measured smoke concentrations were rather low in all tests.
- The sampling system gave alarm/warning first.
- The detectors closest to the fire gave alarm/warning earlier than the detectors more far away
- There was a tendency also in these tests that the detectors placed 1.5 m below the ceiling gave higher smoke signals then those placed close to the ceiling.
- In some cases the DOTEs mesured CO but no smoke in other cases it was the other way around
- Comparison of the time to warning, pre alarm and alarm for the tests indicates that time to warning and pre-alarm is longer for the DOTEs while time to alarm is slightly shorter for the DOTEs.
- The beam detectors 1.5 m below the ceiling gave alarm in most tests.
- The agreement between the sampling system and the beam detector closest to it is very good except for test 7 and 10 where the sampling system shows less obscuration and test 1 where the beam detector signals show a bit less obscuration.

Simulations of the tests

The tests using the SG3000 were simulated using the CFD-code Sofie[3], i.e. test 1, test 2 and test 7. These were simulated in a 20 m wide and 15 m deep room. The room height is 7.3 m. The simulation was run using 311 000 cells, the largest cell size was 0.3 x 0.3 x 0.2 m^3. The smoke was let in as a conserved scalar through a hole 0.2 m squared with a velocity of 1.5 m/s and a temperature of 340 K in two cases; one case using the normal k-ε model and one case using the modified k-ε suggested by Bill and Nam[4]. The smoke source was set to 10 dB/m up to time 10 seconds. At time 10 seconds it was assumed to increase linearly with a factor of 7/350 starting at 0.1. In addition, a third simulation was run, where the SG3000 was modelled as a volumetric source. In this case the source was 0.2 by 0.2 m in area and 0.1 m high. The enthalpy source was 400 000 W/m^3 which results in a total heat release of 1600 W. The smoke source was set to 10 g/s for the first 10 seconds and then increasing linearly from 0.1 g/s up with a factor of 7/350 g/s.

In order to be able to simulate the smoke source as accurate as possible the velocity and temperature above the source was measured[5]. These results were then compared with the results from different ways of representing the smoke source and the best representation was selected. This proved however to be a time consuming task.

Table 1 Comparing the simulated and measured obscuration, %/m.

Detector/laser	Simulation	Simulation Nam and Bill	Volumetric source	Test1	Test2	Test7
Detector1	6.7	5.8	1.8		6	0
Detector2	5.6	5.2	1.4		3.6	0
Detector 3	4.0	3.4	0.9		0.2	0
Detector4	1.6	1.4	0.5		0.2	0
Detector5	2.8	2.4	0.7		0.7	0
Detector 6	1.0	1.2	0.3		0.5	0
Detector7	4.2	3.6	0.8	0.4	2	0.2
Detector8	1.6	1.7	0.5	0.5	0.1	0.1
Detector 9	3.0	2.1	0.7	1.9	2	1.4
Detector10	1.8	1.4	0.6	3	3	2.8
Detector11	2.7	2.3	0.7	4.2	4.6	0.5
Detector 12	1.4	1.3	0.3	0.1	0.2	1.5
Detector 14	2.7	2.3	0.7			11.4
Laser1	14.3	11.7	2.8	57	56	58
Laser2	1.0	1.3	0.3	4.3	3.2	0.14
Laser3	1.4	1.4	0.3	8.2	1.4	0.088

Studying the table and comparing the three experiments it is obvious that these are very stochastic experiments, a feature that CFD simulations cannot capture. The results from test 2 are in better agreement with the simulations than the other tests. Comparing the laser signals with the simulation is somewhat doubtful since the laser measures over one meter while the simulation values are in a single point taken at the middle of the laser measuring beam.

The order of magnitude is about the same in the experiments and simulations except for laser 1 and the volumetric source. The simulations do not, however, capture the variation in smoke levels between the different detector locations. For instance the smoke level at detector 7 and 8 differs significantly from the level at detector 3 and 4 in one of the experiments while it does not in the simulation.

The ratio between different detector locations is about the same in all three

simulations. The different magnitude in smoke obscuration in the volumetric source calculation can to some extent be due to inaccuracy in transforming the smoke obscuration to a soot mass source rate due to uncertainties in the volumetric flow rate estimation in the plume.

The simulation shows a more "traditional" smoke layer than the experiments, this is partially due to that the simulation does not take into account air movements from the ventilation system, the only disturbance included is the beam and the temperature gradient. It is not possible to include all "disturbances" such as local velocities and temperature distribution on walls etc., it is too time consuming and it can also be very difficult to get input data for it. In addition the velocity in the volumetric source case was found to be too high as compared with the experiments.

The tests conducted at IKEA were also simulated. These simulations showed similar problems.

Discussion

It is clear that the simulations did not reflect the experiments satisfactorily. There are a number of possible reasons for this:

- The grid used in the simulations was too coarse. The parametric study indicates, however, that the solutions were grid independent. The grid used for simulating the experiments were similar to the grid used in the parametric study.
- The time step was too large. The time step used was 1 s in all simulations. The simulation time varied between 2 and 14 days using a PC (1 GHz) for the different simulations. Decreasing the time step with a factor of 10 would increase the total simulation time a factor of 10. A simulation time longer than several months is hard to justify for such a simplified problem.
- The scenarios were simplified. In the Fläkt Woods case all machines, air inlets etc. were not included in the simulation as obstructions or heat and air flow producers. The only disturbance included was the temperature gradient. For the IKEA case it was only the air inlet and outlets that were modelled. The workshop and measuring room were not included. On the other hand, it seems unlikely that the inclusion of the workshop and measuring room would change the results considerably. Of course there can be other sources that produce air

currents that we did not identify before and during the experiments.

- The smoke source was not modelled correctly. The velocity and temperature profile in the centre above the smoke source was measured experimentally and then the smoke source was tuned in to fit these values. This turned, however, out to be very time consuming and difficult. After a couple of weeks it was decided to use the best fit found so far. This process could, maybe, have been improved by measuring the velocity and temperature profile in more points over the smoke source and then representing the smoke source as several small sources with different temperature and velocity. Or, preferably, if there was a function available that automatically determined the best representation of a source with a certain temperature and velocity profile in the plume.
- The turbulence model used was not appropriate. The k-ε model was used for all simulations. In some cases the factors used were those recommended by Nam and Bill[4]. This did improve the air entrainment in the plume to some extent but was still not good enough.
- Sofie is not useful for such a small fire. The only CFD code used in this project was Sofie. Sofie is developed for use on larger fires than those studied in this project. Perhaps another code more intended to simulate indoor climate or air currents would have been more successful.
- The problem is not suitable to be solved with CFD. If all other reasons have been investigated without any improvement of the result then the only explanation can be that the problem is not suitable to be solved with CFD simulations.

It has not been possible to determine what reason(s) is the main explanation for the poor result of the simulations within this project.

Conclusions

There are two main different types of ventilation systems used in industries, one is maintaining a temperature gradient in the room, the other uses a total mixing concept. All kinds of mixtures between the two exist as well. In addition can a "dead volume", where no air enters, exist close to the ceiling. Ventilation system manufacturers do not

bother about the temperature etc. close to the ceiling, their concern is the climate close to people working and material produced or stored.

The full-scale experiments showed that what way the smoke moves differs from each test. Even when all parameters are the same the differences in the smoke field are substantial between each test. This behaviour can never be captured with a CFD simulation unless the CFD simulation would have every single small detail in it.

The simulations of the full-scale experiments were not very successful. The simulations showed a more traditional smoke layer than the experiments. This is partly due to that the geometry of the room and disturbances was simplified. In addition, the turbulence model used is known to give to narrow a plume i.e. the air entrainment is under predicted. Adjusting the model by using the constants suggested for fire plumes by Bill and Nam[4] did improve the simulations to a limited extent. Furthermore, the difficulties with the simulations can to some extent be due to that the SG3000 differs from a fire and Sofie is mainly intended for simulation of fires. The SG3000 has a higher velocity but lower temperature profile than fires normally have. In addition, one could suspect that the density of the smoke will increase due to coagulation and thus cannot be modelled as a conserved scalar.

The experiments showed a slight tendency for more smoke at the detectors placed a bit below the ceiling, which indicates that it can be useful to place detector about 10 % from the ceiling (or just below ceiling beams) together with detectors placed in the ceiling.

The CFD simulations can be used for studying trends, but this can be accomplished by using empirical plume formulas for the temperature gradient case. Since CFD simulations visualizes the problem better than empirical formulas for people not so involved in fire problems they can be useful in the construction phase of the building or when planning the detection system at a building not yet built or where it is impossible to conduct full scale experiments.

It is very difficult and time consuming to choose the parameters of the smoke inlet so that the velocity and temperature profiles are similar to the experimental profiles. A tool where one could give the profile as input and get the smoke source as output would be useful. SG3000 is useful as a smoke generator since it does not smell and can be used also in sensitive areas. The question is, however, how well the SG3000

reflects a possible small fire. The temperature and velocity profile is not known for small fires, the question is, is the profile similar to the SG3000?

Another problem is how small fire must be detected. Little work has been done on small fires, probably because it is a difficult problem. Whether a smouldering fire continues to grow or is self extinguished is difficult to predict. Will the fire continue to glow for a long time and then suddenly start to increase or will it start to increase immediately. The glowing fire maybe already has caused severe damage in a sensitive environment before it starts to grow.

Finding the optimal placement of detectors is an almost endless project both using simulations or experiments since so many different airflow patterns and fires must be covered. The smoke from a larger fire reaches higher than the smoke from a smaller fire. The airflow pattern depends on the time of the year and day, the activity going on in the building, which machines are in operation, what doors are opened etc. A possible solution is placing sensitive detection at several heights. If point type smoke detectors are used they may have to be so sensitive that they are outside the normal sensitivity range allowed within EN54-7. Using such sensitive detectors requires an intelligent system to minimize false alarms.

Acknowledgement

This work was sponsored by BRANDFORSK which is gratefully acknowledged.

References

[1] Andersson, P. and Blomqvist J. "Smoke detection in buildings with high ceilings" SP Report 2003:33, Borås 2003, downloadable at www.sp.se

[2]Andersson, P. and Ingason, H. "Smoke Production and Detection" SP Technical Note 2001:35 Borås 2001

[3]Rubin, P., "SOFIE V 3.0 Users guide," School of Mechanical Engineering, Cranfield University UK, 2000.

[4] Nam, S. and Bill, R. "Numerical Simulation of Thermal Plumes", Fire Safety Journal Vol. 21, No. 3, pp. 231-256, 1993.

[5] Conte, F. "CFD simulations of smoke detection in rooms with high ceilings" SP Technical Note 2002:30, Borås 2002.

ZHENG Xin, YUAN Hongyong and FAN Jun
State Key Laboratory of Fire Science, University of Science and Technology of China
P.O. Box 4, Hefei, 230037, Anhui, P.R. China

A Laboratory Emulator for Smoke Plume Study in Atrium Space

Abstract

With development of national economic and advance of building-construction techniques, more and more atriums with extended height or larger space have been or are being built in China for recent years. While admitting merits and advantages of the atrium space, a difficult problem should be aware by fire protection engineers is the effect of conventional spot type smoke or heat detectors installed in the ceiling of the atrium are hardly expected because the atmospheric stratification created by the HVAC system or solar radiation etc prevents the smoke plume from impinging the ceiling or make them dilute to be undetectable before they reach the detectors in the fire incipient stage.

Although a few computational models have been developed, the effect of atmospheric stratification on the rise and dispersion of smoke plume in the atrium space is far from fully understood.

Now estimating the effect is still experimentally subjective and analytically difficult. However the experiments in the full scale atrium space are difficult to implement and the cost and time of large number of full scale experiments is too great to afford. For our studying the effect, we designed an emulator in State Key Laboratory of Fire Science (P.R. China) to reproduce the atmospheric stratification of the atrium. In addition, the laser sheet with high speed camera is applied to visualize and record the quick rise and dispersion of smoke plume. In the emulator the rise and dispersion of smoke plume generated by the test fires of EN54 presented similar form of progress with the full scale experiment.

Besides the main function of it, the emulator has proven to be a flexible design. Other instruments can be easily added according to the requirement of experiments. In some case, we have observed the difference of rise and dispersion between some gas production such as carbon monoxide and smoke particles in the atmospheric stratification, the carbon monoxide can rise higher than particles to impinge the ceiling

of atrium. Now, we are preparing for a full scale experiment concerning the difference. If the phenomenon proved to be appliance for engineering, we may provide a new selection for early fire detection in the atrium.

The emulator is a type of flexible device for studying the effect of atmospheric stratification on the rise and dispersion of the smoke plume in the atrium. As we know, no similar device has been covered in the publication. In this paper, we introduce the design and operation of the emulator, compare the experiments in the emulator with the full scale experiments, describe some special phenomena in the atmospheric stratification important for fire detection and give prospect about the application of the emulator and study on the effect of atmospheric stratification on the rise and dispersion of smoke plume in atrium space.

Claudia Rexfort

Universität Duisburg-Essen, Duisburg, Germany

Combination of a Fire Model and a Fire-Sensor Model

Abstract

An interface between a fire model and a fire-sensor model has been developed. For the realisation of the combined fire and fire-sensor model, output parmeters of the fire model have to be converted into input parameters of the sensor model. The developed model gives the opportunity to simulate the response of a fire-sensor from the beginning of the fire up to the output signal of the fire-sensor. Results of numerical simulations of the combined model are presented and discussed.

Introduction

The principle of an over-all modelling in automatic fire detection was stated by Luck [2] at the AUBE'99 conference. The idea of this over-all modelling is to simulate the process of automatic fire detection from the beginning of the fire up to the alarm decision at the output of the fire detector. This over-all model can be divided into three parts. The first part is the observed environment where a fire or a non fire situation exists. The second part of the model represents the fire-sensor including its housing, where the conversion from the physical properties observed in the environment to electrical signals takes place. The third part is the detector unit where the sensor signal is processed and the alarm decision is made. For this different parts of the over-all fire model separate realizations exist, but the interfaces between the different model parts are still missing. This paper deals with the realization of an interface between a fire model and a fire-sensor model [4]. This interface is a first step to develop an over-all model for automatic fire detection.

fire model	sensor model
smoke mass density	particle number concentration geometric mean particle diameter geometric standard deviation
flow velocity	flow velocity
temperature	temperature
-	complex refractive index

Table 1: Results of the fire model and input parameter of sensor model

Fire and Fire-Sensor Model

For the fire simulations the 'Fire Dynamics Simulator (FDS)' software of the National Institute of Standarts and Technology is used [5]. The basis of the FDS is a computational fluid dynamics model specialized for fire simulations. Compared to other fire simulation programs the FDS gives the possibility to define the combustion material and a combustion reaction to calculate the different combustion products. This is important for a detailed simulation of the smoke development during the fire.

The model of a fire-sensor in its housing has been developed at the University Duisburg-Essen [1]. The model output gives the signal of a fire-sensor determined by a given fire situation. This fire situation is defined by the input parameters given to the model. With this simulated sensor signal the detector unit can decide whether there is a fire situation or not. Different types of sensors can be simulated with the sensormodel.

In this paper emphasis is given to smoke sensors. To simulate smoke sensors severall input parameters are needed for the sensor model. These parameters are usually taken from measurements and shall now be simulated by the FDS. Table 1 shows the output parameters of the fire model and the necessary input parameters for the smoke sensor models. The flow velocity and the temperature can be simulated with the FDS program directly. Looking at the smoke properties the FDS only calculates the mass density as mass per volume, while the sensor model needs informations about the particle size distribution. Therefore a model has been developed to obtain the particulate smoke properties from the

smoke mass density. Also processes which affect the particle size distribution but not the mass density of smoke and which are therefore not considered in the fire simulator have been implemented. The complex refractive index of the smoke particles, needed for the simulation of optical smoke sensors, can not be simulated so far and has to be taken from other studies.

Particle Number Concentration

The particle number concentration shall be computed from the results given by the FDS. A log-normal size distribution of the particle sizes is assumed.

$$n(v,t) = \frac{N}{3\sqrt{2\pi}\cdot \ln(\sigma_\mathrm{r})v} \exp\left(\frac{\ln^2(v/v_\mathrm{g})}{18\ln^2\sigma_\mathrm{r}}\right) \tag{1}$$

where v_g is the geometric mean volume of the particles and $\ln\sigma_\mathrm{r}$ is the geometric standard deviation of the distribution. As shown in table 1 the FDS gives the smoke mass density as a result of the simulation. The smoke sensor model needs the particle number concentration, the geometric particle diameter and the standard deviation as input parameters. The particle number concentration can be computed from the smoke mass density using the first order moment of the distribution. The relation between the particle size distribution and the smoke mass density is given by

$$N_0 = \frac{\rho_\mathrm{smoke}}{\rho_\mathrm{part}} v_\mathrm{g}^{-1} \exp\left(-\frac{9}{2}\ln^2\sigma_\mathrm{r}\right). \tag{2}$$

Where ρ_smoke is the smoke mass density and ρ_part is the specific density of the smoke particles, which is a material property. Figure 1 shows the simulated particle number concentration compared with measurement results. It can be seen that the amplitudes of the results are nearly the same, but after the fire burned out at about 200s the measured particle number concentration decreases strongly, while the simulated one decreases very slowly.

Implementation of Coagulation

With eq.(2) the particle number concentration is calculated from the smoke mass density, assuming that the specific soot density, the geometric mean volume and the standard

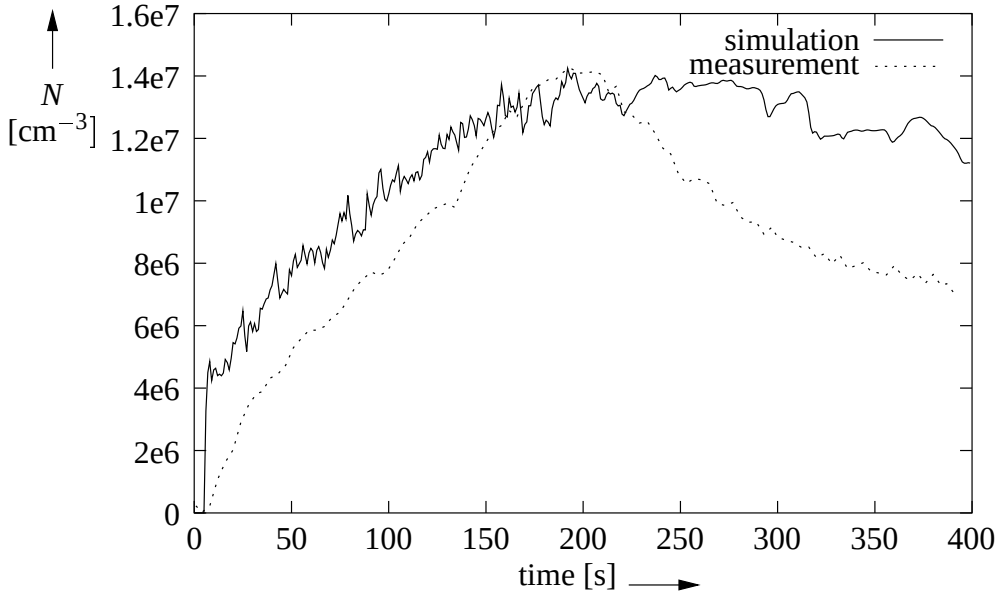

Figure 1: Particle number concentration

deviation of the particle size distribution are known. The reason for the decrease of the particle number concentration after the fire burned out is the coagulation of the smoke particles. Due to relative movements collisions between particles occur and with a certain probability these colliding particles coagulate to one particle. The coagulation has no effect on the smoke mass density, therefore the coagulation is not considered in the fire model and can not be considered using eq. (2). In the following an approach for implementing coagulation in the calculation of the particle number concentration N and the geometric mean volume v_g is given. The given solution holds for polydisperse particles. A continuous particle size distribution is considered, and it is assumed that the probability that two particles which collide also coagulate to one particle is equal to 1. The decay of the particles due to coagulation can be written as follows [2]

$$\frac{\partial}{\partial t} n(v,t)_{\text{coag}} = \frac{1}{2}\int_0^v \beta(u, v-u) n(u,t) n(v-u,t)\,\mathrm{d}u - n(v,t)\int_0^\infty \beta(u,v) n(u,t)\,\mathrm{d}u, \quad (3)$$

where $\beta(u,v)$ is the so called coagulation kernel.

In this paper a solution for particles which are large compared to the molecules of the surrounding gas is given. In this case the coagulation kernel $\beta(u,v)$ in eq. (3) is given as [2]

$$\beta(u,v) = K_c(u^{1/3} + v^{1/3})\left(\frac{1}{u^{1/3}} + \frac{1}{v^{1/3}}\right), \quad (4)$$

with $K_c = 2kT/(3\mu)$ the collision coefficient, k is the Boltzmann constant, T the temperature and μ the dynamic viscosity.

One method to solve eq. (3) is the moments method [2]. With this method eq. (3) is expressed in terms of the moments of the particle size distribution.

This method leads to the following solutions for the particle number concentration $N(t)$, the geometric mean particle volume $v_g(t)$ [2].

$$\frac{N(t)}{N_0} = \frac{1}{1 + [1 + \exp(\ln^2 \sigma_{r,0})] \cdot K_c N_0 t}, \tag{5}$$

with the initial values $N(0) = N_0$ and $\ln \sigma_r(0) = \ln \sigma_{r,0}$. Furthermore, the solution for the change of the geometric mean particle volume [2] is given as

$$\frac{v_g(t)}{v_{g,0}} = \frac{\exp(9\ln^2(\sigma_{r,0})/2) \cdot [1 + \{1 + \exp(\ln^2 \sigma_{r,0})\} K_c N_0 t]^{3/2}}{[2 \cdot (1 + \{1 + \exp(\ln^2 \sigma_{r,0})\} K_c N_0 t) + \exp(9\ln^2 \sigma_{r,0}) - 2]^{(1/2)}}, \tag{6}$$

with $v_{g,0} = v(0)$ the initial geometric mean particle volume for the lognormal distribution. The variable t of the equations is the particle age.

Simulation Results

The initial particle number concentration depends on the initial particle volume respectively on the initial particle diameter, which goes into calculation by the power of three, so it has to be chosen attentively. The initial particle diameter can be taken from measurements, but this measured diameter is influenced by the measurement procedure to a certain degree and the measured particles are already grown due to coagulation. Therefore, a variation calculus was made to find the suitable initial diameter. Simulations of the particle number concentration were compared to measurement results and a value of 68nm was found for the initial particle diameter for the simulation of an EN 54 part 9 n-heptane fire. Figure 2 shows the simulated and the measured particle number concentration for n-heptane fire following EN 54 part 9. The simulated particle number concentration has a sudden increase at the beginning of the fire but reaches the maximum at nearly the same time as the measured one does.

The sudden increase can be explained by the fact that in the case of liquid fires, like n-heptane, the whole surface starts burning at the moment the liquid is ignited and a smoke

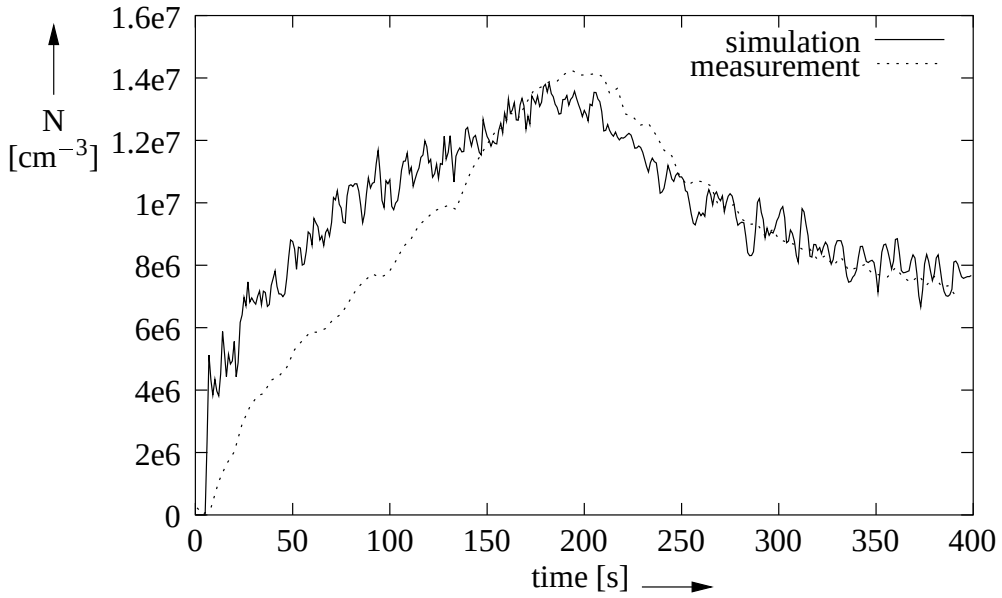

Figure 2: Simulated and measured particle number concentration for an n-heptane fire

cloud arises from the burning surface . At the measurement the smoke is sucked through a tube, diluted by clean air and then supplied to the measurement apparatus. During this process a certain amount of particles will deposit in the tube and there also may be other effects that influence the measurement results. In the simulation of the fire the smoke mass density, from which the particle number concentration is calculated, is computed at a chosen position in the environment of the fire. No effect of any measurement equipment or housing is considered in the simulation, which gives the opportunity to investigate their influence on measurements .

Figure 3 shows that the simulation of the geometric mean diameter for n-heptane fires gives reasonable results. For the measured as well as for the simulated geometric mean particle diameter there is a sudden increase at the beginning of the fire. After the fire burned out both diameters start to increase. This is caused by the fact that the particles become larger due to coagulation, but no new smaller smoke particles are produced.

Results of Sensor Simulations

In the following part simulation results for a scattered light sensor and an ionization chamber are given, whereby the input parameters of the sensor model are simulated with the

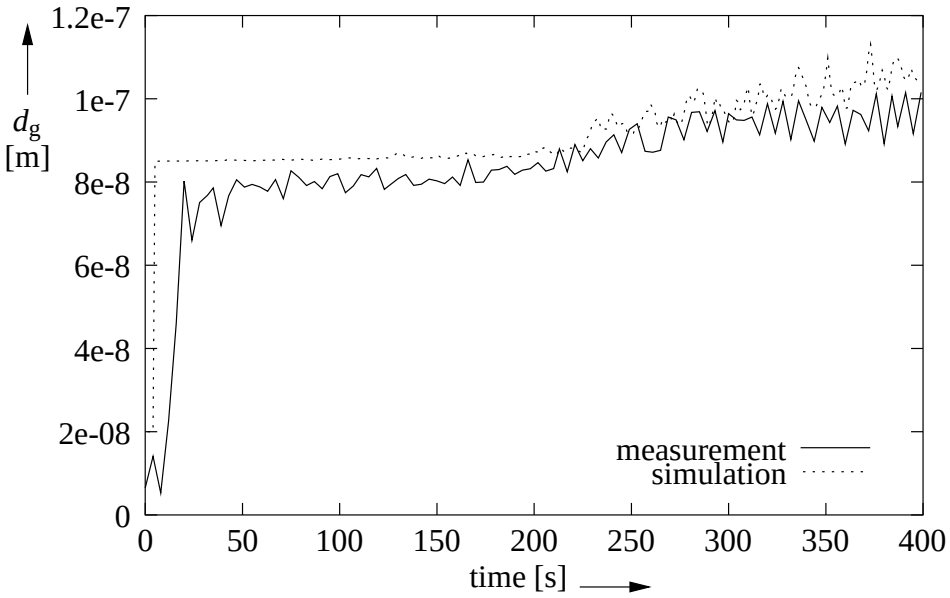

Figure 3: Simulated and measured geometric mean particle diameter for an n-heptane fire

introduced model. The scattered light sensor is sensitive to small changes in the input parameters, for it measures the intensity of the light that is scattered in a defined direction, which is a very small part of the incoming light. This way even small changes in the particle number or size have strong effects on the sensor signal. Figure 4 shows a correlation between the measured intensity and the simulated one at the very beginning of the fire. Both signals show a sudden increase in the beginning. But after a short period of time the simulated intensity starts to increase at a higher degree than the measured one. At about 180s both signals reach nearly the same value. The results show that after the fire burned out (200s) the scattered intensities show the same progression.

The results of the chamber current are measured with a measurement ionization chamber (MIC) at the fire detection laboratory at the University Duisburg-Essen. The simulation of the chamber current of a MIC monitoring an n-heptane fire (see figure 5) gives good results compared to measurements. Especially in the starting phase of the fire. At the beginning of the fire the measured chamber current as well as the simulated chamber current show a sudden increase. From the beginning of the fire up to 200 seconds the measured chamber current and the simulated chamber current have nearly the same progression.

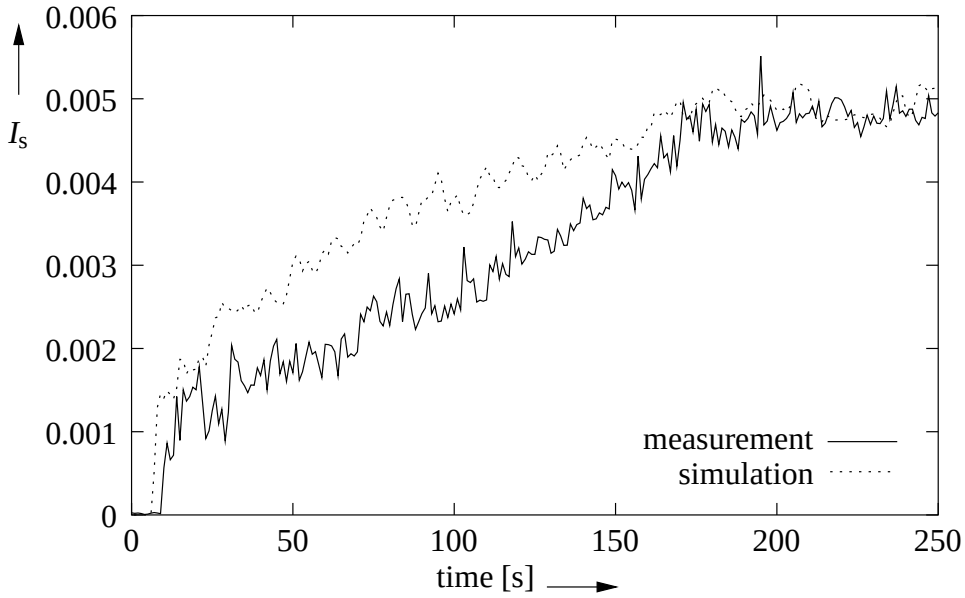

Figure 4: Assessed scattered intensity for n-heptane fire

When the fire burns out (200s) the over-all simulated current starts to increase, while the measured one stays nearly the same. This could be caused by the measurement procedure of the MIC.

Conclusion

A combination of a fire model and a smoke-sensor model is introduced. The simulation results of the presented fire and fire-sensor model give good results compared to measurements. The developed model gives the opportunity to simulate different smoke sensors from the fire up to the output signal of the smoke sensors. Contrary to measurements the simulations allow to investigate the influence of a single environmental parameter on the sensor output. In addition to the presented simulations of a fire, the model gives the opportunity to simulate defined non-fire situation, which can lead to a false alarm of a smoke detector. This gives the possibility to investigates this non-fire situations to prevent such false alarms. With development off the combined fire and smoke-sensor model a first is made to an over-all model for the automatic fire detection.

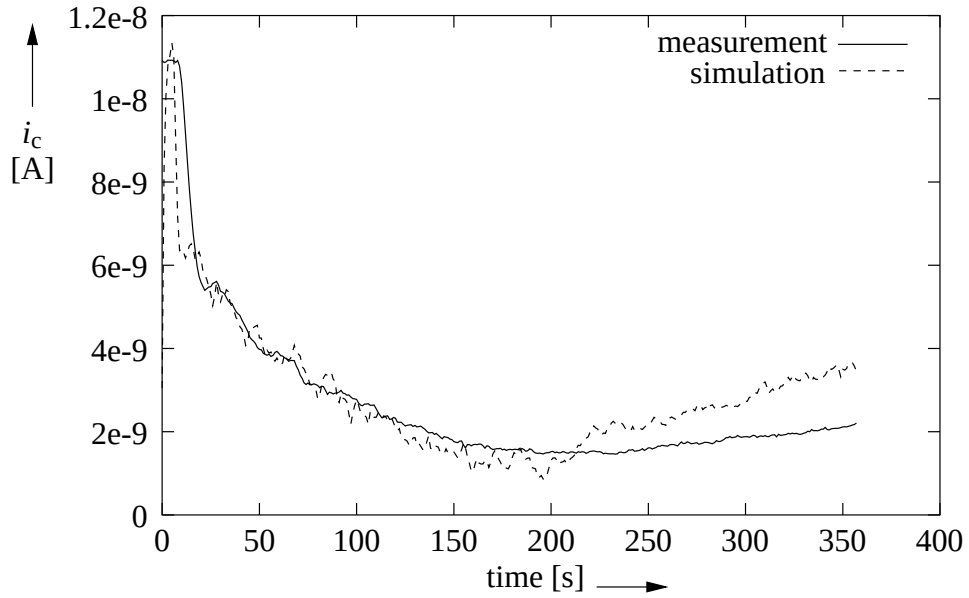

Figure 5: Chamber current for n-heptane fire

References

[1] Gockel F., Ein allgemeines Modell für Brandsensoren im Gehäuse PhD Thesis, University-Duisburg Essen, Duisburg, Germany, 2001

[2] Lee K.W., Change of Particle Size Distribution during Brownian Coagulation, Journal of Colloid and Interface Science 92:315-325, 1983

[3] Luck H., Sievert U., Does an Over-All Modeling Make any Sense in Automatic Fire Detection, Proceedings AUBE'99, Universität Duisburg-Essen, Germany 1999

[4] Rexfort C., A Contribution to Fire Detection Modelling and Simulation, PhD-Thesis, University-Duisburg Essen, Duisburg, Germany, 2004

[5] Fire Dynamics Simulator - Technical Reference Guide, NIST, Gaithersburg, USA, 2001

O. Keski-Rahkonen
VTT Technical Research Centre of Finland, P.O. Box 1803, FIN-02044 VTT, Finland

Model of time lag of smoke detectors

Abstract

Earliest possible detection of fires has been the goal of active fire prevention through ages by any possible means. Since the introduction of numerical room fire simulation codes there has been detailed tools to predict conditions and times for fire detector response. Majority of these tools treat phenomena outside the detector. The long chain from the incipient fire to detector has been modelled at different degrees of sophistication starting from experimental plume models combined with zone type room fire models and ending with various kinds field model simulations.

While for heat detectors reliable models are available existing time lag theories for smoke detectors are unsatisfactory. Traditional scaling model by Heskestad works well for larger flow velocities, but it fails to explain the critical velocity threshold observed experimentally by Brozovsky. This situation is encountered for smoldering fires, and is observed in quiescent environments as long delays for many commercial smoke detector systems. The author showed earlier that fluid dynamic phenomena cannot explain in an acceptable manner that observed behaviour.

The key point is smoke penetration into the detector. A smoke detector has partially permeable walls separating the gas volume in the detector from the volume around it. Using general theory of filtering a new model is proposed for time lag, where small smoke particles partially separate from the carrier fluid while penetrating into the smoke detector. Walls of commercial detectors consist mostly of mesh, or perforated plates. In each form they delay fire detection as compared to a fully open detector. At small flow velocities the separation seems so effective that detection time is delayed much or smoke may remain undetected totally. The theoretical model and some sample calculations of particle penetration probability through a mesh as a function of flow velocity for different diameters of smoke particles are shown in the paper. Since only scattered direct experiments are available for comparison, and no resources for own measurements were avialable at this phase, the model is presented for fire science community to be tested and evaluated.

Kurt Müller, Markus Loepfe, Dieter Wieser
Siemens Building Technologies AG, CH-8708 Männedorf, Switzerland.

Optical simulations for fire detectors

Abstract

In this paper, we present the method for optical simulation that we have successfully applied to new designs of fire detectors, with a focus on scattering smoke detectors. Our simulation is based on a commercially available software tool for non-sequential ray-tracing and on measurements of the differential scattering cross-section of test fire aerosols. With optical simulation, we succeeded in predicting the main characteristics of a scattering smoke detector, the zero-smoke signal and the response signal to test fires with sufficient precision.

1 Introduction

The life cycle of every new generation of fire detectors is shortened, following a general trend. Correspondingly, the time available for design and realization of a new innovative product decreases. To illustrate this fact, we consider a scattering smoke detector. A scattering smoke detector has a labyrinth, which acts as a light trap that reduces unwanted light. The efficiency of a labyrinth critically depends on its geometry and the optical parameters of its surfaces. Therefore, prototypes have to be fabricated using the molding tools employed later for mass-production of the detector's plastic parts. In order to optimize the labyrinth, several prototypes are usually necessary, improved step by step. Every new prototype calls for a modification of the very complex mold. As a consequence, the process of optimization is costly and time consuming.

A remedy can be found by full optical simulation of the smoke detector and by so-called "virtual prototyping". In the case of a scattering smoke detector, this includes precise modeling of all optically relevant components including the labyrinth and the smoke of the test fires. Foremost, simulation allows for the search, visualization, and elimination of blazing spots in the labyrinth. Blazing spots transport large amounts of parasitic light from the source to the detector without any scattering at smoke particles. Furthermore, simulation enables one to calculate the main characteristics of a scattering smoke

detector from scratch, i.e. the detector's zero-smoke signal and its response to the presence of the smoke of test fires.

Optical simulation allows for the investigation of as many versions, called the virtual prototypes, of the CAD-geometry of a smoke detector as is necessary. The most adequate version only will be realized as a mold and just one real prototype will be assembled from molded plastic parts and tested with test fires according to the European norm EN-54.

2 Optical simulation method

To demonstrate the simulation method applied, we consider a scattering smoke detector. Fig.1 shows an opened labyrinth of a scattering smoke detector with two LEDs, a photodiode (bottom) and a lens with several light rays crossing the scene and disappearing in the lamellas of the labyrinth. When smoke permeates the labyrinth, the light of the sources is scattered in all directions by the smoke particles, and a small amount of scattered light hits the photodiode. In the absence of smoke particles, the light, except for a small residual which is called the zero-smoke signal, is absorbed by the black colored plastic of the labyrinth.

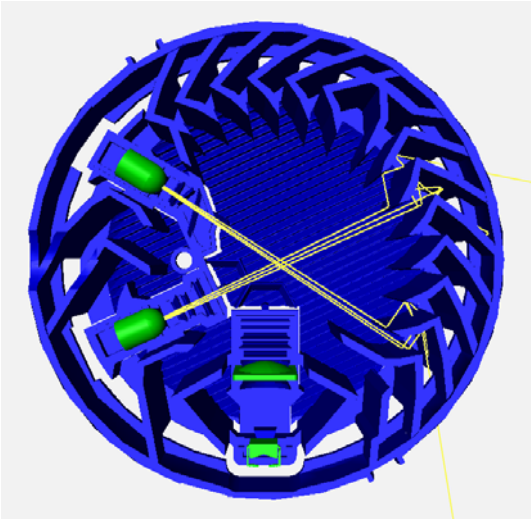

Fig.1: Labyrinth with two sources (left), several light rays, a lens and a receiver (bottom).

A light ray on its way through the labyrinth does not encounter a predefined sequence of optical elements. Therefore, we have chosen a so-called "non-sequential ray-tracing

tool" [1] for optical simulation and analysis. This tool can handle the complex CAD-geometry of the labyrinth as a solid object and can trace the light rays through the labyrinth and model the optical properties of all parts involved, including the scattering characteristics of smoke, in a realistic way. A simulation consists of tracing 10^7-10^8 rays of light emerging from the source and diffusing through the labyrinth, of registering the trajectory of every single ray, and of recording the light intensity impinging on the photodiode and on exposed lamellas vis-à-vis the source (see fig.1).

3 Optical model of the LED

As an example for optical modeling, we present a detailed model of an LED. Fig.2 shows a conventional wired LED from the outside. Fig. 3 shows a close-up view of the cup and the chip inside together with some light rays emerging from the chip. The optical properties of all parts of the LED, used in the model, are taken from data sheets.

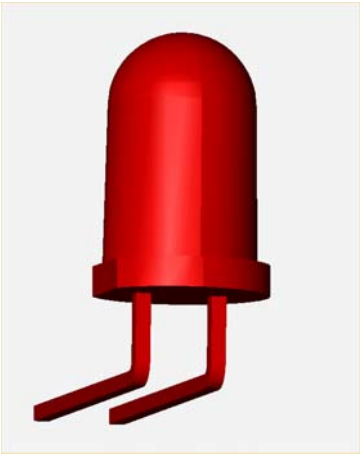

Fig.2: Wired LED

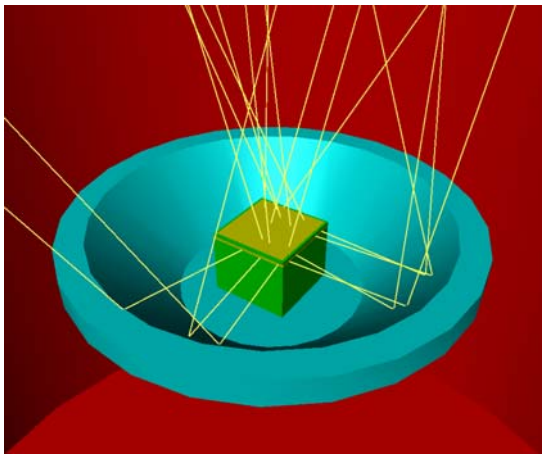

Fig.3: Chip and cup inside the LED, with a couple of emitted light rays.

To validate the LED model we considered the polar intensity diagram. Figs.4 and 5 represent the simulated (left) and the measured (right) polar intensity diagram of the LED. The agreement of simulation and measurement is satisfactory.

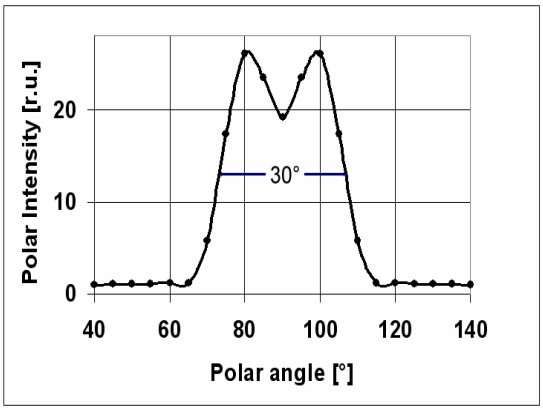

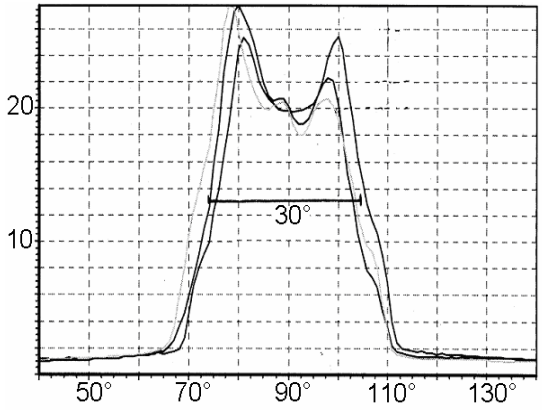

Fig.4: Simulated Polar Intensity of the LED.

Fig.5: Measured Polar Intensity of the LED.

4 Elimination of blazing spots in the labyrinth

A new design for a scattering smoke detector normally comprises exposed blazing spots in the labyrinth; these push the zero-smoke signal to an intolerably high level. Therefore, it is essential to track down and to eliminate the blazing spots. Without simulation means, we are forced to get rid of the blazing spots by testing real prototypes and modifying the mold in each case. On the contrary, with the aid of optical simulation, blazing spots can be visualized and easily removed.

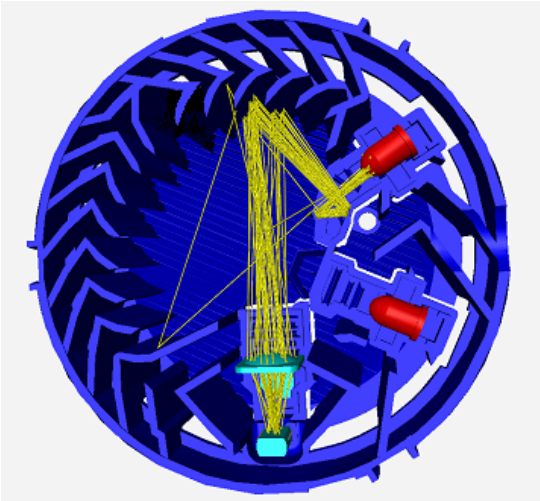

Fig.6: Labyrinth with two blazing spots at the housing of the upper LED.

Fig. 6 shows a bundle of light rays, which make a substantial contribution to the zero-smoke signal for an early, not yet fully optimized version of the labyrinth.

The problematic zone next to the upper LED is visualized and accessible to a correction. In a short time, several subsequent versions of the CAD-geometry can be implemented and checked for their zero-smoke signal by simulation. This procedure, called “virtual prototyping”, gives a substantial reduction of cost and time of development.

We get an impression of the balance of a design with a statistical analysis of the number of reflections a traveling ray encounters in the labyrinth before hitting the photodiode, and thereby making a contribution to the zero-smoke signal. That can be seen from fig.7 and fig.8, which show the occurrence of the number of reflections (# =1,2,3…) at the plastic of the labyrinth, together with the associated power of the accordant light transported to the receiver for an unbalanced and a balanced design of the labyrinth.

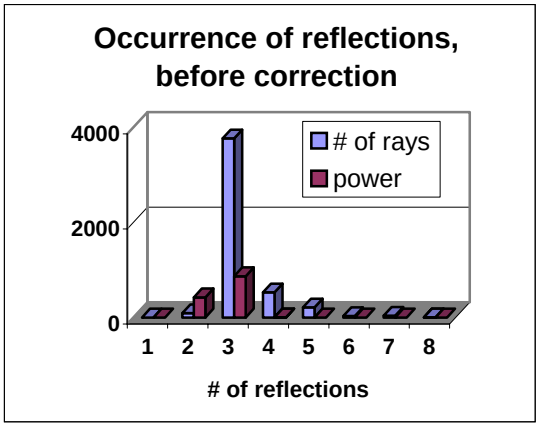

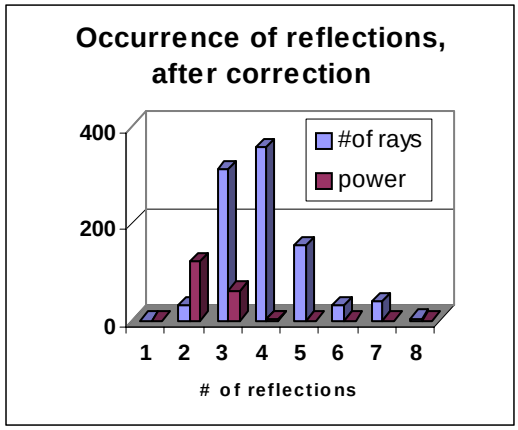

Fig.7: Unbalanced design of a labyrinth, showing an outlier.

Fig.8: Balanced design after optimization

Fig.7 stands for the early version of the labyrinth in fig.6 with two blazing spots, which result in an outlier at the # of reflections equal to 3. Fig.8 shows the result at the end of the optimization process. The distribution in fig.8 has an intuitively acceptable shape and smaller amplitude compared to that of fig.7.

5 Simulated zero-smoke signal

The zero-smoke signal, as mentioned above, is the residual signal of the photodiode for the case where no smoke is present in the labyrinth. The labyrinth, made from black plastic, typically absorbs 95% of the incident light; the remaining 5% are found in diffuse and mirror-like reflections. Starting with a typically emitted power of the LED

of 100mW in short pulses, we get a simulated zero-smoke signal in the optimized labyrinth of 100pW, a level 10^9-times smaller than the input power.

Simulation reveals that the zero-smoke signal strongly depends on the reflection parameters of the labyrinth, a fact depicted in fig.9. Fig.9 represents the zero-smoke signal in the labyrinth as a function of the reflection parameter of the plastic used. The zero-smoke signal approximately follows a polynomial of degree 2.5.

In the case that the labyrinth is uniformly brightened by settled dust, the zero-smoke signal can drastically increase. A change of the average reflection parameter of the plastic from 5% to 15% multiplies the zero-smoke signal with a factor of 16, as can be seen from fig.9.

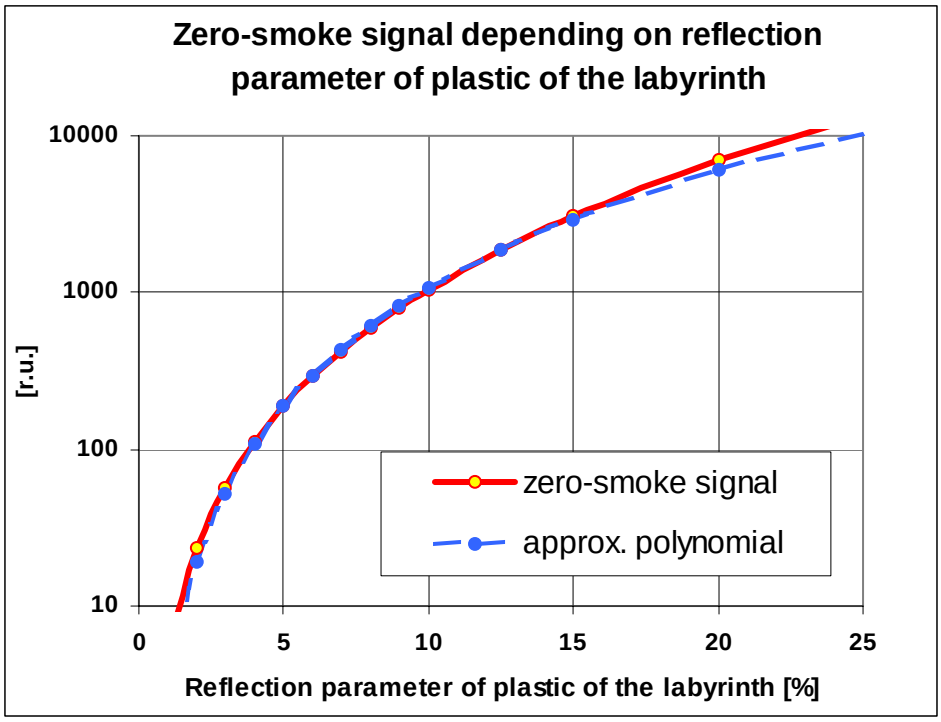

Fig.9: Dependence of the zero-smoke signal on the reflection parameter of the plastic of the labyrinth.

6 Simulated signal at presence of smoke

For a simulation of the response signal of a scattering smoke detector to permeating smoke, the differential and the total scattering cross-section of the corresponding smoke are necessary ingredients. Measurements of the scattering properties of the aerosols of diverse test fires and of the paraffin aerosol, used for calibration purposes, are published [2-6]. Fig.10 shows the scattering cross section of the paraffin aerosol and of the EN-54

test fires TF1-TF5. A.Keller et al. [6] have recorded these data using a Diesel Particle Scatterometer, described by A.J.Hunt et al. [7]. The wavelength of the light source was 520 nm. The optical smoke density was 1dB/m in each case, recorded with a Sick equipment for extinction measurements. Furthermore, Keller has collected the distribution of the mobility diameter of the paraffin aerosols using a Scanning Mobility Particle Sizer System [8]. With these data, he calculated the refractive index of the paraffin aerosol particles on the basis of Mie theory as $1.47 + i \cdot 0.03$.

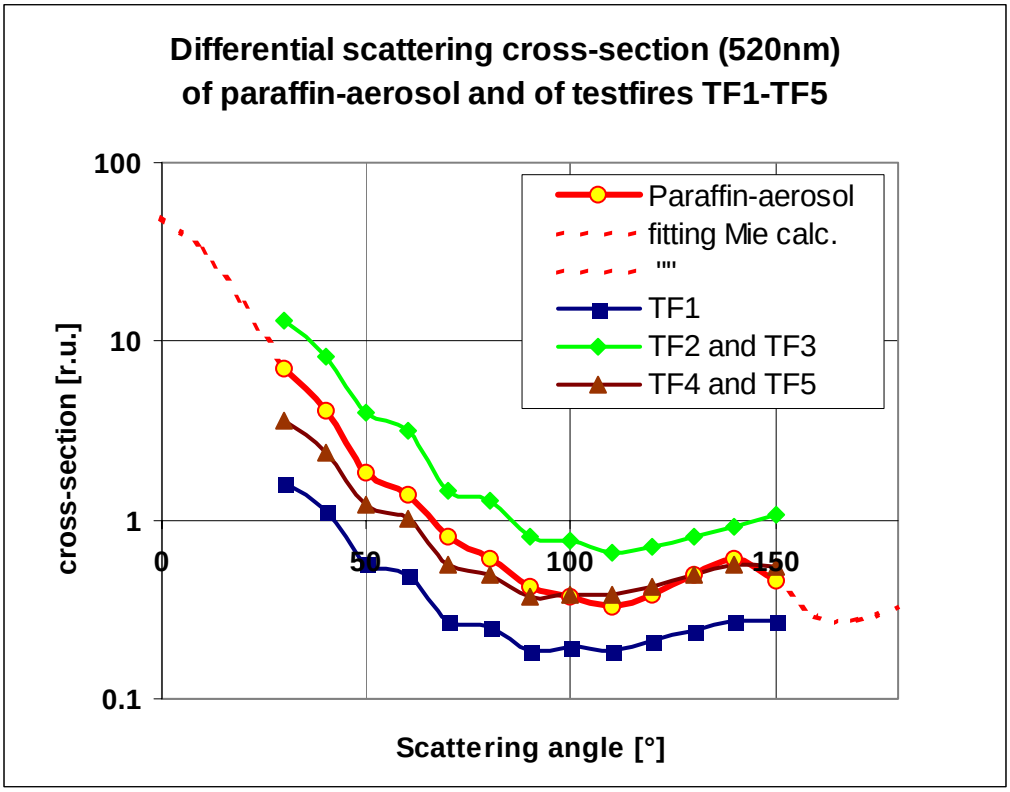

Fig.10: Measured differential scattering cross-section of paraffin aerosol and of aerosols of the EN-54 test fires TF1-TF5.

In Fig. 10, measurement data for low and high scattering angles are missing. Using the results of Keller, we complemented the curve for the scattering cross-section of the paraffin aerosol [6] (here we presume Mie theory [9] can be applied) and we got the missing data for the scattering angles 0-30° and 150-180°. With the completed curve, we calculated the total scattering cross-section by integration; this is a necessary input parameter for simulation. In a next step, we calculated the signal of the detector at

presence of paraffin aerosol with an optical density of 6%/m extinction, a figure typically used for calibration of detectors, and we got a signal of approx. 10nW at a scattering angle of 60°. Thereby, we neglected the small absorption of the paraffin and equated the total scattering cross-section with the extinction at 6%/m. The simulated signal of 10nW for paraffin defines the alarm threshold of the detector for the test fires TF1-TF5.

Finally, we can get all the signals for the test fires TF1-TF5 by simply scaling the simulation result for paraffin, i.e. by replacing its differential scattering cross-section with the one of the test fire considered for the same scattering angle. Let's take the smoldering fire TF2 as an example. TF2 at a scattering angle of 60° exhibits a differential scattering cross-section, which is about two times higher than the differential scattering cross-section of the paraffin aerosol. Therefore, the detector will release an alarm at a smoke density two times smaller than for the paraffin aerosol, i.e. at 3%/m extinction in place of 6%/m at calibration. - This conclusion is strictly valid only for a wavelength of light of 520 nm and with negligence of the entry lag of the smoke into the labyrinth.

7 Conclusions

We have optimized the labyrinth of a scattering smoke detector by optical simulation. Thereby, we replaced traditionally used real prototypes with a sequence of CAD-geometries improved step-by-step, the so-called "virtual prototypes".

Further, we have calculated the optical characteristics of a scattering smoke detector, i.e. the zero-smoke signal, and the response signal to test fires TF1-TF5 with sufficient precision. We have succeeded in reducing the zero-smoke signal to an extremely low level. The ratio of a typical smoke signal to the zero-smoke signal reaches a comfortable value of about 50.

Two restrictions remain to be mentioned in the end: The results above are only approximately valid when taking into account wavelengths different from 520 nm, and we have disregarded the entry lag of the smoke into the labyrinth of a detector.

8 References

[1] Commercially available software tools are: OptiCad, ASAP, LightTools, TracePro, SPEOS, and others.

[2] M.Loepfe, P.Ryser, C.Tompkin, D.Wieser: *Optical Properties of Fire and Non-fire Aerosols,* Fire safety Journal 29 (1997) 185-194.

[3] J.Zhu, M.Y.Choi, George W.Mulholland, and L.A.Gritzo, *Soot Scattering Measurements in the Visible and Near-Infrared Spectrum*, Proceedings of the Combustion Institute, Vol.28, 2000, 439-446.

[4] Weinert, D., Th.Cleary and George W.Mulholland. *Size distribution and light scattering properties of test smokes*, Proceedings of the International Conference on Automatic Fire Detection AUBE01, March 26 (2001), 58-70.

[5] Widmann, J.F., J.C.Yang, T.J.Smith, S.L.Manzello, George W.Mulholland. *Measurement of the optical extinction coefficient of post-flame soot in the infrared*, Combustion and Flame 134 (2003) 119-129.

[6] Keller, A., H.Burtscher, M.Loepfe, P.Nebiker, R.Pleisch. *Online determination of the refractive index of test fires,* Proceedings of the International Conference on Automatic Fire Detection AUBE04, Sept. 14 (2004).

[7] Hunt, A.J., M.S. Quinby-Hunt, and I.G.Shepherd. *Polarized light scattering for diesel exhaust particulate characterization*, "Proceedings of the DOE Diesel Engine Emissions Reduction Workshop", Costine, MA, July 6-9 (1998).

[8] Scanning Mobility Particle Sizer System (CPC model 3022A and DMA model 3080) from TSI Inc., Particle Instruments, St.Paul, MN, USA.

[9] Bohren, C.F. and D.R.Huffman (1983). *Absorption and scattering of light by small particles,* (Wiley Science, New York, USA).

Daisuke Kozeki*, Hiroyuki Tamura*, Yoshinori NIshiue**
* National Research Institute of Fire and Disaster, Tokyo, Japan
** New Cosmos Electric Co., Ltd., Osaka, Japan

Development of Residential Fire Detection System installed in Air Conditioning Unit

Abstract

In Japan the victims in residential fires occupy about 80% within the total fire victims, according to the Japanese fire statistics. Only very few fire detectors are however installed in Japanese residences due to such reasons as false alarms, installation cost and maintenance troublesome. In order to reduce those victims, we have been developing a new residential fire detection system which is highly reliable to detect residential fires with less false alarms, considering easy installation, easy maintenance and operation stability which cover the long period of time of the system. For this purpose, we used the technology of the home electric appliances such as air conditioner or smoke neutralizer whose accumulation of know-how of those issue area is extremely abundant. The air conditioner which possesses the function which does fire detection and room air pollution monitoring with temperature sensor, humidity sensor etc. which are included in these equipment, and smoke particle sensor and gas sensors (the carbon monoxide sensor and the hydrocarbon sensor) was made on an experimental basis. Many tests have been made to verify the function of the system.

Introduction

We developed a residential fire detection system in a form that would encourage its voluntary installation in homes and make its maintenance easy, to reduce the number of deaths in residential fires that account for 80% of all fire-related deaths. In this development effort, we paid particular attention to the long-term operational stability and ease of installation of the system. Technologies to satisfy these requirements have been typically accumulated and applied in the area of civilian equipment such as air conditioning units and air cleaner units. Therefore, utilizing those technologies and

taking advantage of the thermal sensor, humidity sensor, as well as smoke particle sensor and gas sensors (carbon monoxide sensor and hydrocarbon sensor) that are also incorporated in these units, we made two prototypes of air conditioning units that are capable of detecting fire, monitoring the home environment, and setting off an alarm, if necessary.

Overview of the Residential Fire Detection System installed in Air Conditioning Unit

In developing the Residential Fire Detection System installed in Air Conditioning Unit, we tried to achieve the ease of voluntary installation and maintenance in homes, in addition to excellent fire-detecting performance.

(1) Fire-detecting Performance

A good fire detection system must deliver high fire sensitivity and low likelihood of false alarms, a contradictory pair of requirements. It is expected that if one can develop a sensor that detects phenomena unique to fire, the performance of a fire detection system will greatly improve. However, at present, the possibility is slim for such a sensor to be created. Therefore, we modified the existing sensor algorithm for fire detection to improve the fire-detecting sensitivity and to lower the likelihood of false alarms of our prototypes of the Residential Fire Detection System installed in Air Conditioning Unit.

a) Fire-detecting Sensors

The Residential Fire Detection System installed in Air Conditioning Unit uses a thermal sensor, humidity sensor, smoke particle sensor, carbon monoxide gas sensor and hydrocarbon gas sensor to monitor the heat, smoke, and

Table 1: Sensors Used in the Residential Fire Detection System installed in Air Conditioning Unit

Sensor	Monitoring Range	Comment
Thermal sensor	0 to 60 °C	Outputs thermistor resistance
Humidity sensor	10 to 95 %	Outputs change in resistance
Smoke particle sensor	Detects particles of about 1 μm or larger	Outputs voltage signal proportional to the particle count
CO gas sensor	0 to 150 ppm	Constant-potential electrolytic sensor; outputs voltage
HC gas sensor	0 to 200 ppm	Hot-wire semiconductor sensor; outputs voltage

concentrations of combustion gases. Table 1 shows the overview of each of these sensors.

Of the sensors listed in Table 1, the thermal, humidity, carbon monoxide gas, and hydrocarbon gas sensors that we used are widely used for industrial instrumentation.

As for the smoke particle sensor, we used a "dust sensor" that is typically used in air cleaning units (Figure 1). As shown in Figure 2, this smoke particle sensor uses a photo transistor to monitor the diffuse light generated by the passage of smoke particles in the LED light beam, obtains the number of particles per unit volume, and outputs a voltage signal that is proportional to the number of particles.

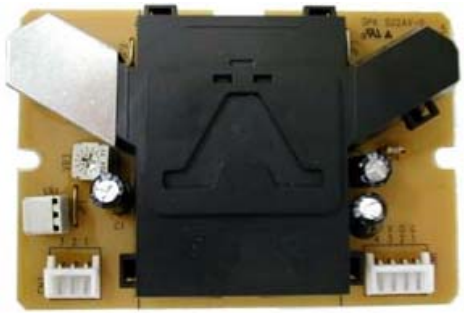

Fig. 1: Smoke particle sensor

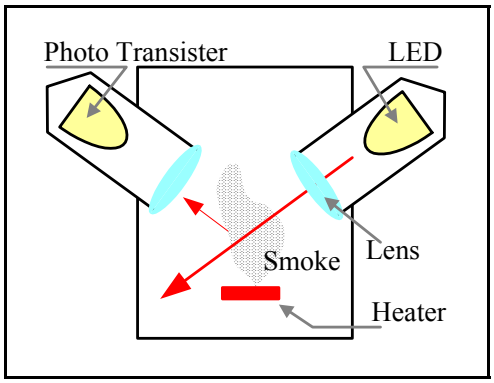

Fig. 2: Internal structure of the smoke particle sensor

The carbon monoxide sensor is a constant-potential electrolytic sensor. This sensor causes the electrolysis of the carbon monoxide gas at a constant potential, monitors the electrolytic current generated, and deduces the gas concentration. Figure 3 shows the sensor structure. By maintaining a constant potential, the direct electrolysis is caused at the working electrode located at the surface boundary between the atmosphere and the solution. The following chemical reactions take place at the working electrode and counter electrode to generate the electromotive force.

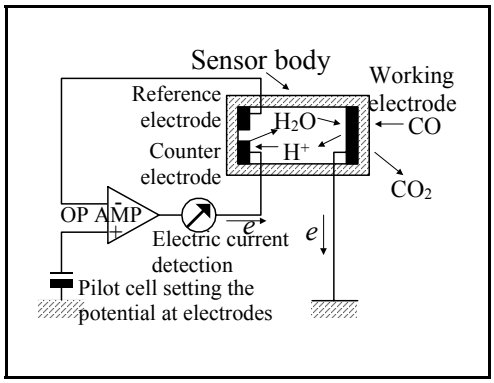

Fig. 3: Standard circuitry of the constant-potential electrolytic CO gas sensor

Working electrode .... $CO + H_2O \rightarrow CO_2 + 2H^+ + 2e^-$

Counter electrode ..... $\frac{1}{2}O_2 + 2H^+ + 2e^- \rightarrow H_2O$

The concentration of the carbon monoxide gas can be obtained by measuring the electric current that is generated at this time.

The hydrocarbon gas sensor is a hot-wire semiconductor type gas sensor. This sensor measures the changes in the resistance at both ends of the platinum coil and obtains the changes in thermal conductivity and electrical conductivity caused by electron donation from the combustible gases on the metal oxide semiconductor (SnO_2) surface. Figure 4 shows the structure and standard circuitry of the hot-wire semiconductor sensor.

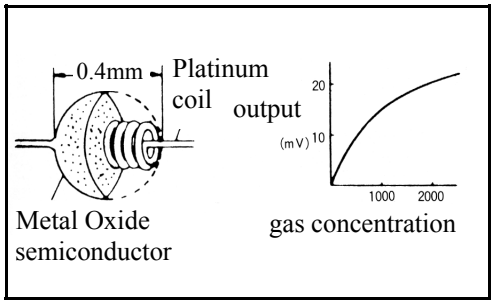

Fig. 4: Structure and standard circuitry of the hot-wire semiconductor sensor

b) Fire-detecting Algorithm

The presence of fire is determined by any signal from any of these sensors exceeding its threshold value, in which case the alarm goes off. To automatically select the appropriate threshold values in accordance with the room environment where the air conditioning unit is installed, an algorithm based on a statistical analysis using Mahalanobis Distance[1)] is used to detect anomalies in sensor data. This enables selecting the threshold values for fire detection that match the environment of installation[2)].

(2) Dissemination of Fire Detection Systems to Homes

Even if excellent fire detection systems are developed, if they are not purchased, installed, or regularly operated in good condition in homes, the number of deaths from residential fires will not decline. We therefore listed below the points that need to be considered to ensure the dissemination of fire detection systems to homes and the maintenance of these systems, good condition.

a) Guaranteed Ease of Installation

The heat and smoke from a fire is best detected at a higher part of the room. Therefore, the sensors should be installed on the ceiling, or on a wall near the ceiling, or on top of a piece of furniture such as a closet. However, ceiling-mount or wall-mount installation may have issues of appearance and the inevitable damages to the ceiling or wall by nail/screw holes, which some people may feel should be avoided. Moreover, there is the issue of electrical wiring to secure power supply, and this may become a deterrent against the purchase/installation of such systems. Considering the above, we concluded

that a fire detection system that is likely to be voluntarily purchased and installed would be the type that can simply be placed on top of a piece of furniture, such as a closet, or the type that can be incorporated in other appliances that are ordinarily mounted on a higher part of a wall, such as an air conditioning unit, or a wall-mount clock. Therefore, in this research, we made two prototypes of air conditioning units, within which the above-described set of sensors and signal processing unit are incorporated to act as a comprehensive residential fire monitoring system. Figure 5a shows Prototype 1, with the sensors and signal-processing unit externally mounted on the air conditioning unit. Figure 5b shows Prototype 2, with the sensors and signal-processing unit internally embedded.

Fig 5a: Comprehensive Residential Fire Monitoring System- Prototype 1

Fig. 5b: Comprehensive Residential Fire Monitoring System - Prototype 2

b) Maintenance and Management

To ensure that the comprehensive residential fire monitoring system operates in good condition, it is imperative that the user should notice any abnormal behavior of the system whenever such behavior starts showing, and request a maintenance or repair service promptly. Any fire detection system that sets off the alarm at the time of a fire is normally silent when there is no fire, and therefore, there is the danger that malfunctions of the system are overlooked. With respect to the automatic fire alarm systems that are required by law to be installed in office buildings, etc., regular inspections are also required by law to ensure the malfunctions of the systems are promptly discovered. However, the comprehensive residential fire monitoring system would be voluntarily installed in homes, and it is impossible to make regular inspections mandatory. To

counter this dilemma, we designed a scheme with which to check the condition of the sensors and signal-processing unit through their normal operation, by incorporating a function to send alarm messages alerting the users to air pollution and necessity of ventilation under non-emergency circumstances.

c) Improvement of the Product Appeal to Promote Purchase

As was explained in the above chapter on maintenance and management, if the system is only for fire detection, consumers would consider it dormant under ordinary circumstances, which will discourage them from purchasing the system. However, the comprehensive residential fire monitoring system has the function to alert the users to air pollution and necessity of ventilation under ordinary circumstances, and the consumers will consider the system as a home appliance of high value that works round-the-clock.

(3) Improvement of the Alarm Message Communication

The Residential Fire Detection System installed in Air Conditioning Unit has not only the fire-detecting function, but also the ability to monitor air pollution under ordinary circumstances. A simple alarm tone will not be sufficient to communicate much information. Therefore, we equipped the system body with a light-emitting display and a voice alarm capability, and further enabled it to communicate wirelessly with a TV set to display the alarm on the screen, and with the telephone network to alert the authorities to an emergency. For impaired and elderly users who might have difficulties hearing the fire alarm, we are further considering an interlocked operation of an olfactory fire alarm system, in which a particular smell alerts the user to a fire.

a) Light-Emitting Display and Voice Alarm Capability

This capability is delivered by the EL character display and speaker installed in the air conditioning body unit. There are two voice alarm messages: one for deterioration of the comfort level and/or possible gas intoxication in the room judged from the monitoring of the room temperature, humidity, and air pollution; and the other for a fire. The alarm tone is adjustable by changing the sound source data to change the volume and tone color. This is to ensure the alarm tone does not hinder the comfort, and can be set to match the characteristics of the auditory sense of elderly people.

b) Alarm Display on the TV Screen

This function alerts the users to air pollution or a fire, while they are watching the TV, by indicating the alarm message on the TV screen. The prototype system uses a personal computer that has the TV viewing capability. The communication is wireless between the comprehensive residential fire monitoring system and the PC with TV viewing capability. So long as wireless communication is not hindered, the PC with TV viewing capability can receive the alarm message anywhere in the home. Figure 6a shows the TV screen displaying the air pollution alarm, and Figure 6b shows the TV screen displaying the fire alarm.

Fig. 6a: Air pollution alarm displayed on the TV screen

Fig. 6b: Fire alarm displayed on the TV screen

c) Interlocked Operation of the Olfactory Fire Alarm System

Light and vibration may be effective to alert hearing-impaired users to a fire, but there are issues of directivity and shielding of the light and the portability of the vibrating component of the vibration alarm system, leading to common occurrences of the users being out of the reach of the alarm. In addition to light and vibration alarm systems, we are developing olfactory fire alarm systems. The same concept has been most widely implemented as a form of gas leak alarm for fuel gases including the city gas. Smell is a result of diffusion of odorant substances, and is not affected by directivity or shielding, and does not require any special portable reception terminal. It is considered highly effective to alert people in a building to a fire. Currently we are in the process of selecting the type of smell suitable for fire alarm, and studying the storage method of odorant substances as well as their diffusion method when the alarm is set off.

Fire Detecting and Room Environment Monitoring Tests

In order to verify the fire detection capability of the prototype air conditioning unit, we installed it in the Residential Fire Detection Test Room(6.8m x 4.5m x 2.5m; approximately 14 tatami mats) in the Structure Fire Prevention Research Building of the National Research Institute of Fire and Disaster and performed a fire detection tests with various fire sources. Table 2 shows the fire sources used in the tests, the operational status of the air conditioning unit, and the results of the fire detection tests.

Table 2: Fire sources used in the fire detection tests and the test results

Fire type	Material burnt	Ignition Method	A/C on/off	Fire detection result
Wood flaming fire	5mm x 5mm x 120mm, cedar, 6 rods x 20 layers	Ignited paper under the wood	OFF	Fire alarm: True
			ON	Fire alarm: True
Wood smoldering fire	5mm x 5mm x 120mm, cedar, 10 rods	Heated steel pan on which the wood was placed	OFF	Fire alarm: True
			ON	Fire alarm: True
Cotton smoldering fire	Panya cotton cushion	Ignited it with a cigar lighter, then blew out the flame	OFF	Fire alarm: True
			ON	Fire alarm: True
Liquid fuel flaming fire	n-heptane in, 10cm x 10cm pan	Ignited it with a cigarette lighter	OFF	Fire alarm: True
			ON	Fire alarm: True
Cigarette smoke	3 cigarettes	Three people smoked in a normal manner	OFF	Air pollution alarm: True
Fumigation insecticide	1 fumigation insecticide	Fuming by water	OFF	**Fire alarm: False**
Deep-frying oil flaming fire	Cooking oil 20cc	Heating by electric heater	OFF	Air pollution alarm (True); followed by fire alarm (True) after the oil caught fire

In the fire tests, one or more of the sensors sensed the monitored value(s) exceeding the threshold for detecting fire and subsequently set off the alarm, in all of the wood flaming fire tests (see Figure 7a, b): wood smoldering fire test, cotton smoldering fire test (see Figure 8a, b), and liquid fuel flaming fire test. In the non-fire tests, the system set off the air pollution alarm only in the cigarette smote test (see Figure 9), and stopped short of a fire alarm. In the fumigation insecticide test, a relatively high concentration of carbon monoxide was detected, resulting in a false fire alarm. With a deep-frying oil test, an air pollution alarm went off first caused by the soot, followed by a fire alarm after the oil caught fire. The smoke particle sensor that was used in the prototype detected over-the-scale monitored value from cigarette smoke, and therefore, we were

unable to set the threshold for fire detection. Lowering of the sensitivity of the smoke particle sensor or widening of its monitoring range is required to counter this problem.

Conclusion

We developed the Residential Fire Detection System installed in Air Conditioning Unit as a residential fire detection system in the form that would encourage its voluntary installation in homes and make its maintenance easy, to reduce the number of deaths in residential fires. The fire detection tests on the fire-detecting capability of the prototype

Fig. 7a: Wood flaming fire test

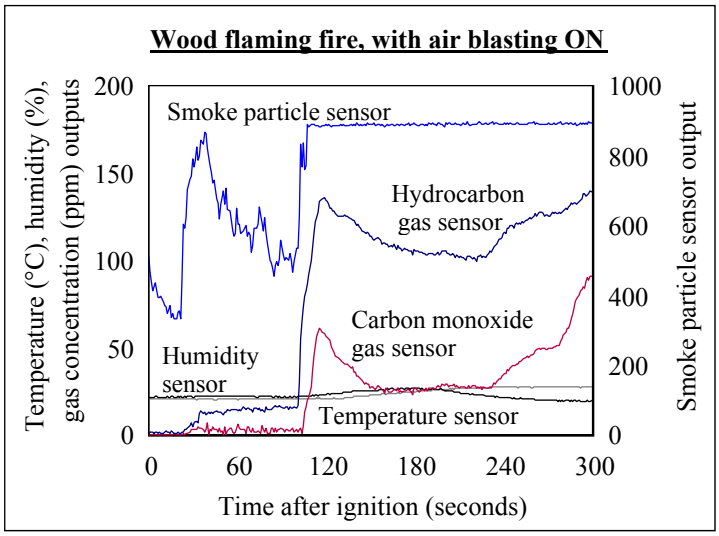

Fig. 7b: Sensor outputs of the wood flaming fire test

Fig. 8a: Cotton cushion smoldering fire test

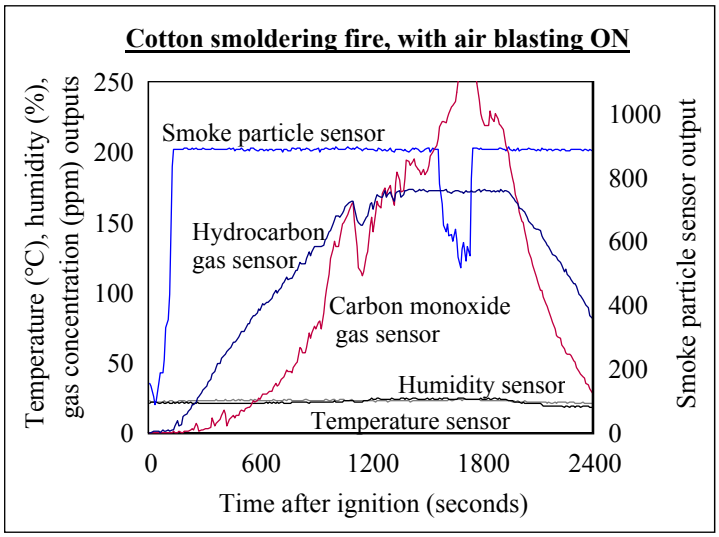

Fig. 8b: Sensor outputs of the cotton cushion smoldering fire test

air conditioning units indicated that thermal, humidity, smoke particle, and gas (carbon monoxide and hydrocarbon) sensors on the system could effectively detect a fire. However, as the test with a fumigation insecticide showed, we were unable to completely eliminate the possibility of false fire alarms. We need to further study the system through a long-term operational test before commercialization. We also found that the smoke particle sensor used in the prototype needed to be modified to lower the sensitivity or widen the monitoring range.

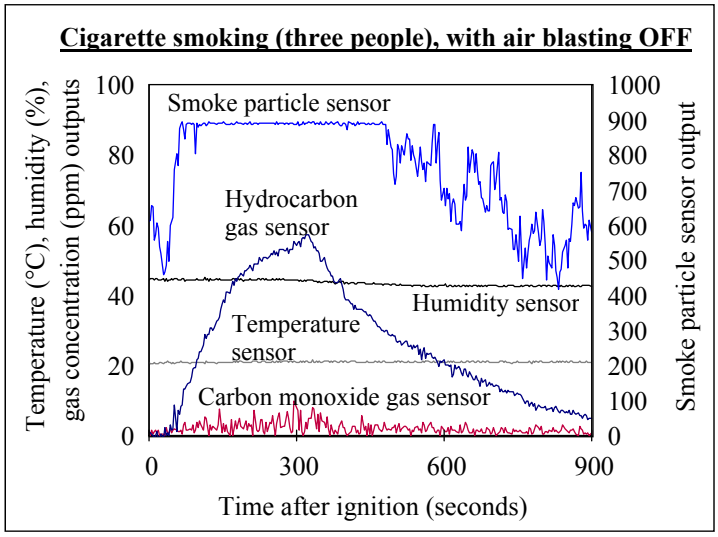

Fig. 9: Sensor outputs of the cigarette smoking test

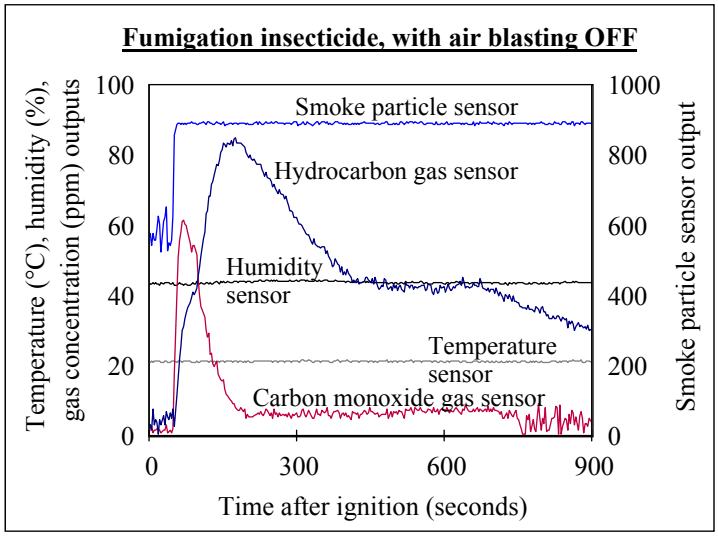

Fig. 10: Sensor outputs of the fumigation insecticide test

5. Bibliography

1) The Japanese translation of Multivariate Statistical Methods: A Primer by B. F. J. Manly; translated by Masayasu Murakami and Masaaki Taguri; printed by Baifukan Co., Ltd.; 1992.

2) Discrimination of In-Ordinal State in Room Temperature Based on Statistical Analysis: authored by Daisuke Kozeki, Ken-ichi Takanashi, Yoshiyuki Matsubara; published in Report of National Research Institute of Fire and Disaster vol. 90; September 2000.

U. Glombitza, Henrik Hoff
LIOS Technology GmbH, Schanzenstrasse 6 -20, 51063 Cologne, Germany

Fibre Optic Radar System for Fire Detection in Cable Trays

Abstract

With the development of heat and radiation sensitive cable designs and further development of the optical OFDR Raman radar measuring method with high location resolution and high temperature accuracy a fire detection system for fire monitoring in cable trays has been successfully realised. Complex measurement of Raman back-scatter light, calculation of the Raman back-scatter curve from the Fourier transformation of the measurement signal and application of the mathematical correspondence between frequency and location-space for correction of disturbance variables are the unique exclusive features of OFDR Raman technology. Based on these special qualities the OFDR Raman technology has technical and also economic advantages compared to all commercial fire detection systems. This new fibre optic radar system contains the possibility to detect thermal overloading of cables in the first phase of initial damage (build-up phase) prior to or during the early pyrolysis phase.

2. Introduction

The LIOS Technology Company, founded in early 2000, is developer and producer of fibre-optic radars which monitor temperature as a function of location and time via silica fibre (optic) cable over a distance of many kilometres. The invention is based on development of a novel optical radar monitoring process awarded second prize in the Cologne Innovation competition [1]. Basic development was supported financially by the Federal Ministry for Education, Science, Research and Technology (BMBF) technical training program "Microsystems Technology" [2]. In cooperation with a leading world company in the field of fire prevention, Siemens Building Technologies Ltd, the product was successfully launched under the name FibroLaserII for fire monitoring in road tunnels. The monitoring system has been optimized in recent years and developed to series production models now available for further innovative applications. Since early 2004 a total of 500 systems have been installed worldwide using optical fibre cable lengths providing monitoring ranges of some 1000km.

Application for early fire detection in cable trays with which this paper deals is on the other hand new and is still under development. Currently field trials under authentic environmental conditions are under way.

Greater and greater demands are being placed on fire prevention. On the one hand the operator wants real value protection and on the other public authorities demands the greatest possible protection of the general public from systems fraught with risk. Retention of function of important monitoring units over a specific timescale (fire detection equipment, escape route signalling etc.) and cost-intensive operational units (e.g. computer centres, control rooms etc.) are additional fire prevention system requirements which must also be met by modern fire detection systems.

Cabling systems are important components of building infrastructure in communications, decentralised data processing and electrical equipment power supplies. By laying cables in cable trays the risk of an undetected fire and fire spreading to other areas of the building increases. It is true that by bundling cables in cable trays great ease of installation is achieved, at the cost however of a greater risk of fire through cables overheating in the absence of adequate heat dissipation or ventilation. In addition to spontaneous cable ignition cable systems also run the risk that the naked flame will jump across and spread uncontrollably through the building.

If there is cable ignition the flames can very rapidly spread to all cables in the tray. The spread rate is highly dependent on the cable insulation characteristics. Cable insulation burnout is associated with strong smoke generation with toxic fumes. Due to access routes and the seat of the fire being shrouded in smoke the fire services are unable to efficiently combat the fire.

In this paper initially some background facts regarding the cause and generation of cable fires is provided. Subsequently the specification profile of fire prevention systems for fire monitoring of cable networks from the viewpoint of the operator and the emergency rescue services management is dealt with. There then follows a product overview of commercially available fire and smoke detections including a comparison of the

technical and economic advantages of fibre-optic Raman-based temperature sensors. The operating principle and technical improvement to a heat and radiation-sensitive optical fibre cable with the associated evaluation processor unit is presented which meets the technical demands of cable tray fire monitoring. The paper ends with a summary with an outlook for the future.

2. Generation of Fire in Cable Tray Electrical Cabling

Electrical cables transmit energy for power supply and control of electrical equipment. During energy transmission current-dependent losses occur in the conductors, metal sheathing and cable armouring plus current-dependent losses within the insulation. These losses are dissipated to the cable surface via the cable's thermal resistance and from there to the atmosphere. Maximum cable loading is determined by the cable's electrical and thermal stability and heat dissipation from cable surface to the surrounding atmosphere. If there are several cables in a cable trough or tray they affect one another mutually. The consequence is an additional heat influx. For this reason in cable bundlings thermal bottlenecks occur which must be taken into account at the planning stage by a current reduction of the overall installation. Conditioned by high assignment densities in cable ducts there is a risk of heat build-up, especially during subsequent installations. Errors in laying, e.g. mechanical damage to insulation, kinks etc. may give rise to initial cable damage which greatly reduces the thermal capacity of the cable.

The operator of electrical equipment must ensure at all times that the permissible temperature is not exceeded, otherwise accelerated cable-aging results. In the worst-case scenario thermal breakdown occur leading to destruction of the power cable. For cross-linked polyethylene (XLPE) cables VDE regulations state that permissible cable temperature is 90ºC.

Point of origin for every occurrence of fire is the thermal loading of oxidizable compounds, which for the most part have a carbon or hydrocarbon content, leading to spontaneous combustion of the material. In this process even in the build-up phase various mutational processes in the material may be observed - note that we only

consider plastics as cable insulation materials [5]. An injection of heat into the insulation material up to some 80-90°C leads initially to no appreciable change - most types of insulation are designed for a continuous operating temperature of up to 90°C (s. table 1).

Material	PVC	PE	LDPE	HDPE	PP	PA	FEP	PTFE	PFA
Max. operating temp (°C)	85	90	70	100	100	105	180	260	260
Breakdown Temp (°C)	120	100	100	120	180	140	290	327	327

Table 1: Thermal Characteristics of Typical Plastics

A continuous operating temperature of just under 90°C however leads to accelerated aging a associated mutation processes leading to increasing brittleness of the material. Above the continuous operating temperature the material markedly softens. Significant in the case of plastics is the absence of any discrete softening point - one refers rather to softening range characterized by the break-up of intermolecular bonds - as a rule van der Waals bondings. The degree of softening and reduction in viscosity depends inter alia on the macromolecule chain length. The spectrum above the so-called breakdown point (100-120°C) is characterized by break-up of intermolecular bonds. Pyrolysis follows initially with oxygen deficiency leading primarily to fragmentation of the macromolecules with associated of unsaturated and radical compounds (crack process). Other products of pyrolysis may be CO, HC1, HCN and soot. Pyrolysis is a process in flux and depending on heat input, availability of oxygen, the material and the morphological state of the insulation the most widely varying - mostly toxic and combustible - pyrolysis gases result which add significantly to the problems of fighting fires in cable trays:

- Intense smoke emission during cable insulation burn-down filling rescue routes and fire teams approach routes.
- Long-term damage and high clean-up costs following combustion of halogen-compound cable insulations [6].
- Human health danger from toxic fumes and fire residues.

- "Flash-over" via escaping pyrolysis gases following intense pre-heating by a secondary fire.

If the critical heat flow density, i.e. that heat flow density at which a material does not ignite after an infinite period, is exceeded the insulation material ignites, the consequence being an open fire. A realistic critical heat flow density is around 13 kW/m^2.

The cause of cable fires in the final analysis is the limited thermal stability of the electrical cable insulations. In the event of short circuits at the operator's site, incorrectly set power limits, inadequate heat extraction or cable damage electrical cables may be so intensively heated that the maximum permissible cable temperature is exceeded and thermal damage set in motion. This first phase of initial damage (build-up phase) subsequently moves on to the pyrolysis phase and if heat continues to be added leads to spontaneous ignition of the cable.

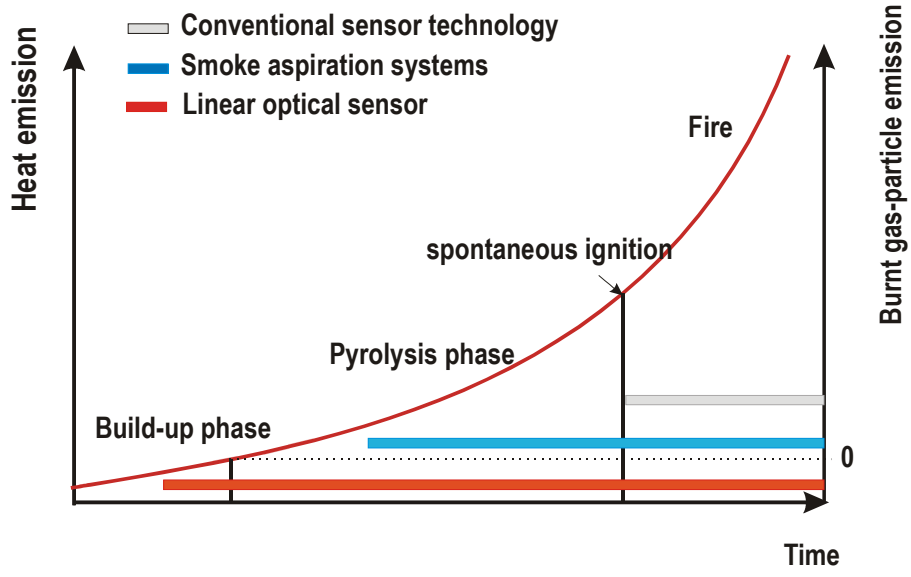

Diagram 1: Fire process profile and detection limitations of various detection technologies

If one considers the problems of the pyrolysis phase in particular with a view to fire prevention in cable trays then a compelling precondition is earliest possible early fire warning prior to or during the early pyrolysis phase. The main problem is prompt

monitoring and localization of these spatially very limited points of overheating of the cable (e.g. at cable crossings, insulation damage sites etc.).

Electrical equipment is combustible to a greater or lesser degree depending on the material used so that even with a fire which has broken out at another location there the combustible insulation is a contributory factor to the fire occurrence and the fire can spread out as with an explosive fuse to unaffected areas of the building. The upshot is that there is optimum fore prevention for cable trays if fire early detection, fire localization and fire fighting is covered by one single fire monitoring and alarm system. A precondition is uninterrupted (without gaps) temperature monitoring in the immediate vicinity of the electric conductors as a function of the site where the cables are laid.

3 Catalogues of Specifications from Operator and Rescue Services Management Perspective

From the viewpoint of operator and rescue services management the requirements list for the fire detection system for cable trays is very clear-cut and concise:

- Prompt reliable detection at the early stage (if possible prior to pyrolysis)
- Simplicity of installation and low maintenance costs
- Location of the seat of the fire to within a metre with clear correlation within the building
- Information regarding spread of fire and smoke (fire progress monitoring)
- Automatic interactions, e.g. signalling, shutdown of faulty conductors etc.

Further requirements are listed in Chapter 4.2.

4 Cable Tray Fire Monitoring

4.1 State of the Art

Below are outlined the advantages and disadvantages of currently established cable tray fire detection techniques:

4.1.1 Classical Smoke Detectors

4.1.1.1 Optical Smoke Detectors: Characteristic feature is the drop in intensity of IR source by absorption in the radiation pathway.

4.1.1.2 Ionisation Detectors: "Geiger counter" with constantly radiating ^{60}Co radiation source.

Advantages:

- Low procurement costs.
- Simple technology proven in buildings fire protection.

Disadvantages:

- For cable trays inadequate false alarm performance (dust exposure).
- Inadequate sensitivity, no detection possible in early pyrolysis phase.
- Maintenance costly - if not impossible - in inaccessible locations.
- Low monitoring density.

4.1.2 Classical Heat Detector

4.1.2.1 Heat Detector: Measurement of temperature rise within and interval or measurement of maximum temperature. This group includes heat-differential detectors and heat-maximum detectors.

4.1.2.2 Flame Detection: Measurement of radiations given off by the fire (infrared, visible spectrum ultraviolet) IR and UV flame detectors primarily used with this method.

Advantages:

- Low procurement costs.
- Simple technology proven in buildings fire protection.

Disadvantages:

- Sensitivity too low, no detection possible in early pyrolysis phase.
- Maintenance costly - if not impossible - in inaccessible locations.
- Low monitoring density.
- Flame detection requires an unobstructed radiation field, which is not guaranteed in cable trays with corners.

4.1.3 Linear Fire Detectors

4.1.3.1 Smoke Extraction System: The monitored object ambient air is extracted via pipework to a special detector unit. There then takes place evaluation of incoming air (smoke quality). If needed filter boxes may be fitted before the detector unit (in the case of extreme exposure to dust) or condensation filters (where there are condensation problems).

Advantages:

- High sensitivity due to extraction system's cumulative effect - therefore fire detection in the early pyrolysis phase.
- By comparison with discrete detectors a high monitoring density is realizable.

Disadvantages:

- Detector site not clearly identifiable.
- High maintenance costs due to filter replacement.
- After many years of operation lower sensitivity possibly to be feared.

4.1.3.2 Linear electronic heat detectors: These are mostly a thick cable in which discrete addressable sensors are fitted at freely optional intervals and therefore represent a hybrid between discrete and genuine linear fire detector technology.

Advantages:

- Simple installation.
- Sturdy low-cost technology.

Disadvantages:

- Low monitoring density.
- Too insensitive, no advanced early warning possible.

4.1.3.3 Other linear detector systems: One very robust technology is measurement of temperature variation by means of pressure changes within a copper tube. A further possibility is measurement of the electrical resistance of a cable as a marker for temperature variations. Both techniques are too insensitive for advanced early warning

in cable trays and are associated with high installation and maintenance costs.

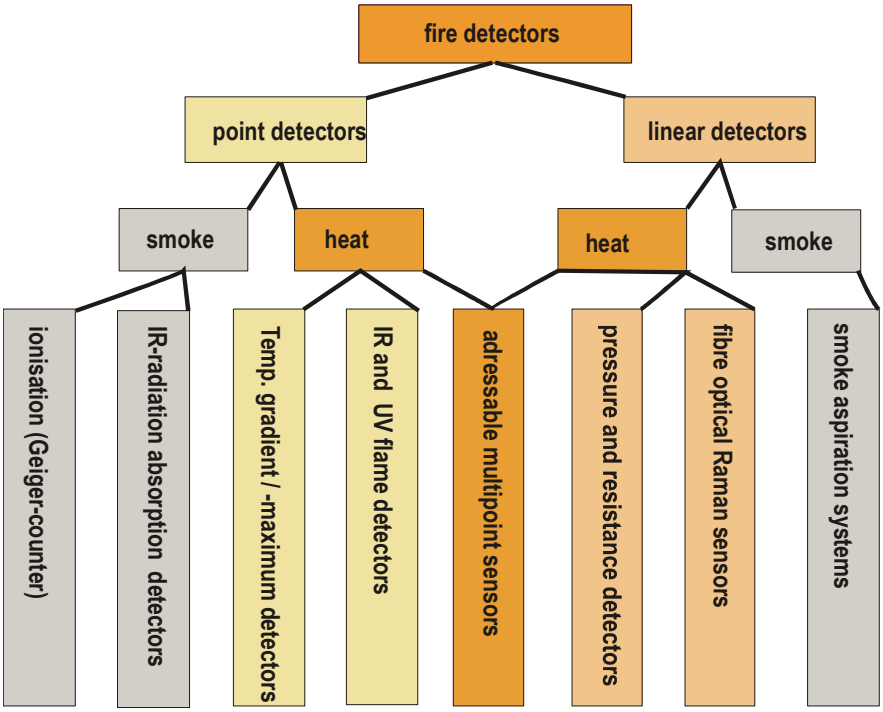

Diagram 2: Classification according to various fire detection technologies

4.2 Linear Optical Fire Detectors - Basis for Optimum Fire Protection in Cable Trays.

Cable trays are long and extensive objects, and are difficult to access so that the installation and maintenance expenditure involved with classical heat detectors cannot be justified on economic grounds. Even the linear fire detectors presented here do not fulfil the requirement for continuous temperature sensing. This requirement is only met by a linear optical fire detector (see Diagram 2). The linear optical fire detector is based on a fibre-optic Raman back-scattering procedure. The actual heat detector (temperature sensor) is a heat and radiation-sensitive optical fibre cable. With the addition of an evaluation set (optical Raman reflectometer radar) temperature values in the cable fibre optics can be determined broken down by location.

Optical fibre cables have a very low attenuation. The minimal attenuation of optical fibre is limited by the Rayleigh scatter of the light, which is caused by the amorphous

structure of the optical fibres. In addition to Rayleigh scatter, when affected by heat an additional scattering takes place in fibre-optic material, so-called Raman scatter. Temperature variations induce grid oscillations in the silica glass fibre molecular bond. If light falls on these thermally excited molecular oscillations the result is an interaction between the light particles (photons) and the electrons of the molecule. In the fibre-optic cable a temperature-dependent light scatter occurs (Raman scatter) which is spectrally displaced vis-à-vis the incidental light by the amount of the grid oscillation resonance frequency (Diagram 3). Raman scatter possesses - in comparison to Rayleigh scatter - only a very small, inter alia negligible degree of scatter and can be measured using the classical OTDR technique.

The intensity of the Anti-Stokes bandwidth is temperature-dependent, whereby the Stokes bandwidth is practically independent of the temperature. Measurement of the local temperature at any given point along the fibre-optic cable is derived from the relative intensities of the Anti-Stokes and Stokes light. A feature of this Raman technique is direct temperature measurement with a Kelvin scale. By using an optical Raman back-scatter procedure the temperature along the fibre optic can be measured as a function of location and time. The most familiar back-scatter procedure is OTDR (Optical Time Domain Reflectometry). It operates on the principle of a pulse-echo procedure whereby the echo time difference between transmission and detection of the light impulse determine the level of scatter and the scatter site. In comparison to Rayleigh scatter in the case of Raman light scatter measurement the signal is less by a factor of 1000. A locally assigned Raman temperature sensor with OTDR is therefore only viable with powerful (expensive) pulse laser sources (in general solid state lasers) and rapid, similarly expensive signal communication techniques. The OFDR (Optical Frequency Domain Reflectrometry) technology developed by LIOS Technology does not work as does OTDR in the time range, but in the frequency range. With OFDR a statement regarding the local temperature pattern when the back-scatter signal detected over the entire measurement period is measured as a function of the frequency and therefore subjected to complex measurement (complex transfer function) and subsequently goes though a Fourier transformation.

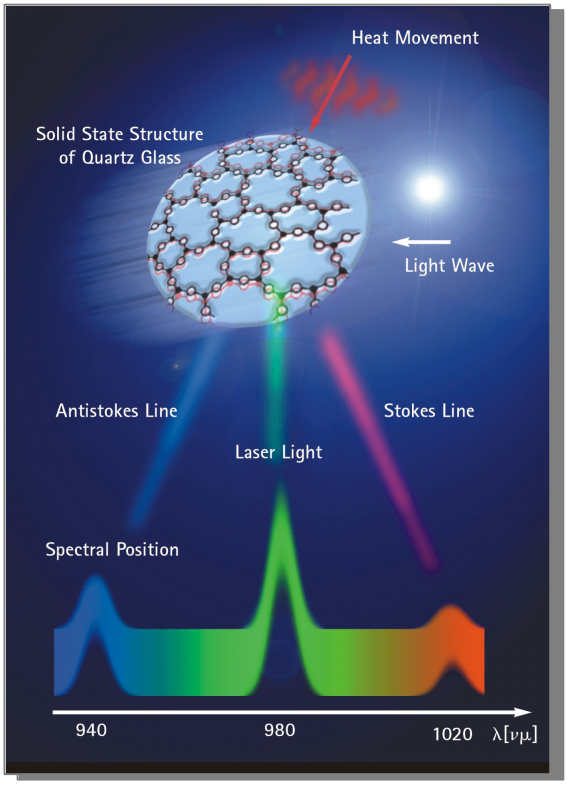

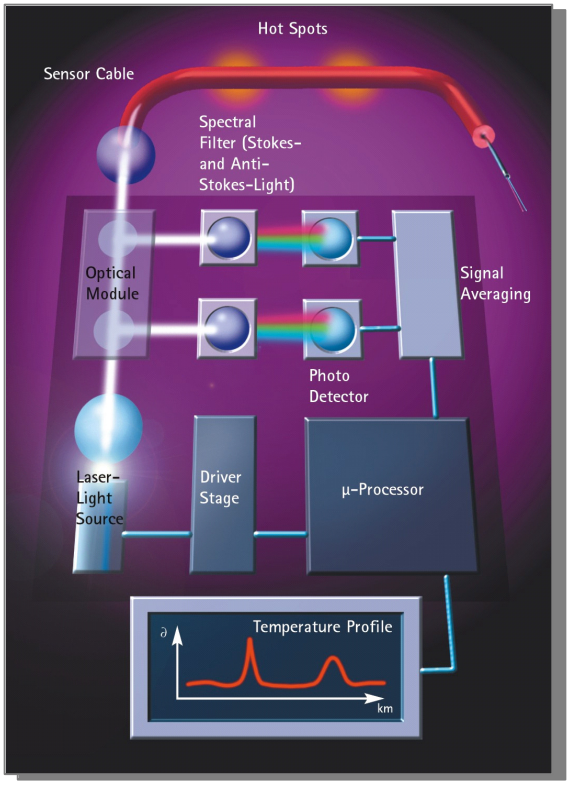

Diagram 3: a) Raman Spectrum, b) Linear Optical Heat Detector

The unique exclusive features of the OFDR Raman Technique are:

1. Complex measurement of Raman back-scatter light as a function of the laser frequency
2. Calculation of the Raman back-scatter graph using the Fourier transformation rule
3. Use of a clear mathematical mapping rule between frequency and location-space with the option of online disturbance variable correction

In relation to these unique exclusive features of OFDR Raman technology the result is a series of technical and commercial advantages as against OTDR Raman technology which are listed below and briefly elaborated on:

A) Technical Advantages of OFDR Raman as against OTDR Raman Technology:

1. Higher SNR: Through the almost continuous-wave operation of the laser and the narrow-band detection of the optical back-scatter signal with OFDR technology a distinctly higher signal-to-noise ratio is achieved than with pulse technology.

2. Greater Range: Conditioned by the better SNR achievable distinctly greater ranges may be monitored with the identical fibre-optic type. Without using optical amplifiers with OFDR measured sections exceeding 30km in extent can be monitored [8].

3. Longer working life of the cw Raman Light Source: For fibre optic Raman backscatter measurement laser light sources of some 100 milliwatt light output or pulse light sources of some kilowatts output are used. The thermal loading of the laser medium is clearly less with the cw laser and therefore the working life is clearly longer than that of pulsed light sources.

4. Less interference from optical Fresnel reflections: The lower optical power of the OFDR laser source (mW instead of kW) clearly reduces the widely known "dead zone" OTDR interference effect of optical overloading of the receiver phase by Fresnel reflections (e.g. in the case of plug-and-socket connectors).

5. Better local measuring accuracy: As against the OTDR measuring signal the OFDR measuring signal has a narrower spectral bandwidth. Signal distortions caused by fibre optic dispersion effects are less strongly pronounced so that greater locational accuracy is achieved.

6. Simple signal averaging technique: With the OFDR method digital signal processors are used to compute the Fourier transformation. The FT algorithm corresponds to a numeric signal averaging which is technically considerably simpler and more elegant as against the OTDR technology electronic boxcar integrators.

7. Application of system theory algorithms to improve signal quality: To improve measuring time and signal quality with OFDR efficient and generally applicable numeric computing algorithms may be used such as for example the FFT averaging method or the window function for noise suppression.

8. Simple online calibration of the fibre optic measuring instrument (frequency calibration): Calibration data (frequency data) can be very simply ascertained on the basis of device-specific frequency and location-space parameters without the need for access to the measuring instrument.

9. Simple automatic recalibration of the fibre optic measuring instrument (field calibration): On the basis of device-specific frequency and location-space parameters correction data (frequency data) can be calculated which make possible precise determination of the spectral attenuation per unit length of the optical fibre. Based on these correction data one achieves a simple automatic recalibration of the fibre optic OFDR measuring instrument (field calibration).

B) Economic Advantages of OFDR Raman as against OTDR Raman Technology:

1. Use of less costly system components: By using semi-conductor laser diode, use of comparatively "slow" electronic modules, application of numeric signal averaging techniques including the option of single-end measurement less costly system components can be used by comparison with OTDR Raman technology.

2. Greater reliability: The OFDR laser light source works in virtual cw mode. The working life, longer than with pulse operation, also means greater reliability of the overall system.

3. Simpler maintenance schedule: Due to the complex OFDR measurement of Raman back-scatter light and the clarity of the Fourier transformation mapping rule between frequency and location-space new possibilities for a simple, automated and field unit calibration of the fibre optic temperature measurement system.

These technical and economic advantages of OFDR Raman technology are countered by the technically difficult measurement of Raman back-scatter light (complex measurement by amount and phase) and expensive signal processing using the FFT calculation with higher linearity demands on electronic modules.

Diagram 3b shows the schematic configuration of the linear optic heat detector. It consists of an evaluation unit including frequency generator, laser, optical module, receiver and microprocessor unit plus a (silica) fibre optic cable as linear temperature sensor.

In accordance with the OFDR method the laser is sine wave modulated within a measuring time interval and chirped into the frequency. The frequency deviation is a direct measure for the locational resolution of the reflectometer. The frequency modulated laser light is launched into the fibre optic (Diagram 3b). At every location along the fibre Raman scatter light is produced which radiates in all spatial directions. A proportion of this Raman scatter light travelling in a reverse direction reaches the evaluator unit. The back-scattered light is spectrally filtered and converted to electrical signals in the measuring channels by means of photodetectors, amplified and electronically processed further. The µ-processor performs the Fourier transformation calculation. As an interim result the Raman back-scatter curves are received as a function of cable length. The amplitudes of the back-scatter curves are proportional to the intensity of prevailing Raman scatter. From the relationship of the back-scatter curves the fibre temperature along the length of the fibre optic cable. The technical specifications of the Raman temperature-sensing system can be optimised in line with the application by adjustment of unit parameters (range, locational resolution, temperature precision, measuring time etc.). Example: The temperature profile of a 4km fibre optic cable run can be measured to a temperature accuracy of ±2K and a location resolution of 3m in 12 seconds overall measuring time.

The fibre optic cable can similarly be adapted by variations in the respective application configuration. The thermal stability of the glass fibre coating limits the fibre optic cable's maximum temperature range. Standard fibres for information transmission are provided with an acrylic type or UV-hardened coating and are designed for a temperature range up to some 80°C.are With for example polyamide glass fibre coatings these can be used up to a maximum of 400°C.

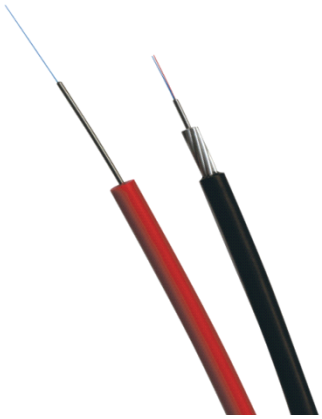

Diagram 4: Sensor cables (standard cables)

For fire monitoring in road tunnels stainless steel tubes are used as the basic element of the sensor cable in which the fibre optic cable is then housed. The stainless steel coating can be adapted to requirement regarding wall thickness (8mm and 5mm external diameter) and choice of coating material (HDPE, HM4) - left side cable sample in Diagram 4). For applications requiring a high degree of mechanical resilience, e.g. fire monitoring in explosion risk areas aluminium or stainless steel armouring can be inserted between the stainless steel tube and the extrusion sheathing (right side cable sample Diagram 4).

For fire advance early warning in cable trays there are more stringent system requirements by comparison with fire monitoring in subterranean tunnels. Consequently both evaluation units and the sensor cable must be further developed and optimised in line with the following aims:

- Greater location resolution (≤ 0.5m, measurement of hotspots with small longitudinal dimensions)
- Reduced evaluation unit measuring times (to meet DIN EN 54 Class 1A)
- More rapid response characteristic in the sensor cable (to meet DIN EN 54 Class 1A)
- Fire detection system multi-channelling (option of simultaneous monitoring of different fire sectors or cable trays)
- Graphic display of temperature occurrences along the length of the cable trays

Diagram 5 shows the fire detection system (radar) and associated fibre optic cable. Vis-à-vis the cable design in Diagram 4 there is a clearly improved heat and radiation sensitivity. In contrast to both standard cables the new cable design has a lower heat capacity, an improved temperature response and a larger effective cross-section.

Diagram 5: Fire detection system and fibre optic cables for fire advance early warning in cable trays.

These characteristics were achieved by a reduction in the cable diameter, insertion of good heat conductors between tube and outer sheathing plus a radiation-absorbing sheath. Comparison of the response characteristic of both fibre optic cables is illustrated in Diagram 6. A silica glass fibre as a reference point, being the most rapid possible response characteristic of the heat detector is similarly depicted in Diagram 6.

In this trial the cable samples including the bare optical fibre were simultaneously heated in an oven with a maximum temperature gradient of 3K/min. On reaching the maximum permissible temperature of the samples used the cable samples were spontaneously cooled by opening the oven door. In the top curve the hotspots of individual samples over the location range at a point in time. The bottom curve shows the development over time of the respective samples. As expected the bare optical fibre shows a very spontaneous response characteristic and follows the ambient temperature gradient with virtually no time lag. (Diagram 6b top curve). The standard cable responds clearly later, follows the gradient only hesitantly and reaches a maximum

temperature of barely 70°C when an ambient temperature of 90°C is reached (Diagram 6b bottom curve). The middle curve in the time lapse clearly shows the successful optimisation of the sensor cable.

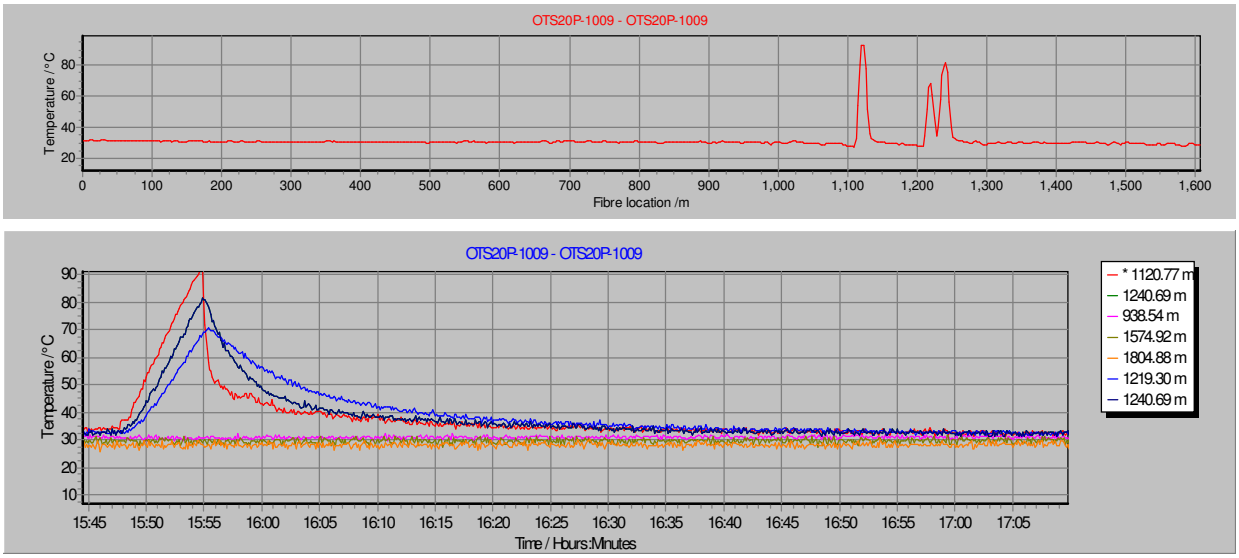

Diagram 6: a) Temperature as Function of location, oven area with three fibre optic sensor runs (1121m), standard cable (1220m) and EN54 cable (1240m)
b) Temperature as function of time, selected points inside and outside the oven

In further series of experiments it was confirmed that with improved cable design the requirements of DIN EN 54 Class A1 are met. DIN EN 54 relates to the response characteristic of point heat detectors. Transferred to the linear optical heat detector this means that with a 2km long sensor run and a location resolution of 0.5m all 4000 of these measuring points meet the requirements of DIN EN 54. Or, expressed differently, the linear optical heat detector is equal in terms of its monitoring function to 4000 point heat detectors.

With the OFDR Raman back scatter method the temperature profile is received as a function of time and cable location. By computer-assisted evaluation of the temporal and spatial temperature variations the fire can be located to one metre accuracy and tracked along the cable tray. Similarly in the temperature pattern the spread of hot fumes can be clearly recognised, so that even fume spread is captured. An example of

visual display of a temperature occurrence for building monitoring is shown in Diagram 7.

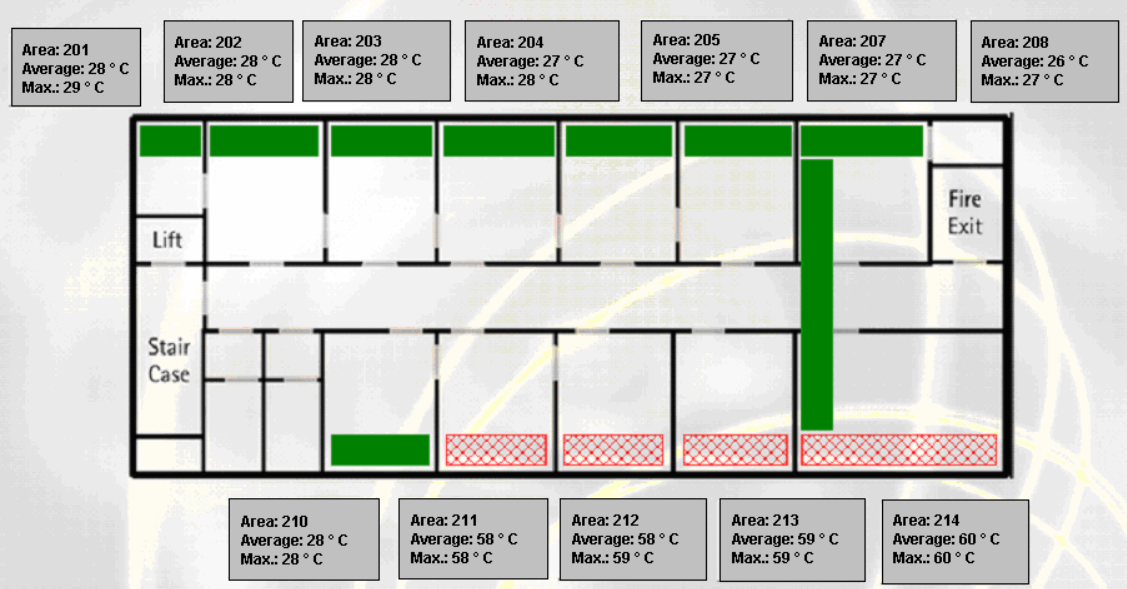

Diagram 7: 2D Visual Display of Temperature Occurrences

The fire detector cable was installed inside the cable duct of one floor. The sections of each office were combined in fire detection groups and the maximum and mean temperature values were calculated. If as the result of a temperature anomaly one of the three detection criteria is triggered there is a change in the colour/structure of the zones concerned. With an evaluation unit location resolution of 50cm the information density is very high so that the local trigger point and the direction of fire spread can be determined extremely precisely and rapidly.

To conclude the Chapter customer and operator requirements in respect of the linear optical heat detector for fire monitoring in cable trays are listed and broken down by the parameters of fire detector system sensor and evaluation unit, design and cost effectiveness (Table 2). These requirements are set against the LIOS products' technical system characteristics. This presentation may serve as an aid to decision-making in the choice and appraisal of fire detector systems.

Customer and operator requirements	System Requirement / Fire Detector Specifications
Fire detection system (sensor cable):	
- High reliability	Fibre optic in protective tubing with sheath
- Simple installation	Temperature sensor in the form of a cable
- Rapid response	Small cable diameter, metal sheath
- Good radiation sensitivity	Black radiation-absorbing cable sheath
- Simple connection	Standard fibre
- Long working life	Fibre optic cable with additional length in protective tubing
- Large temperature measurement range	Fibre optic cable with special coating
- Long sensor range	Standard fibre with low attenuation
Fire detection system (evaluation unit):	
- Distributed sensing without gaps	Use of back-scatter method
- Fire tracking	Use of back-scatter method
- Redundant design	Loop configuration with optical switch
- Great temperature precision	Calibratable measurement system,
- Open system	Standard interface with standard protocols
- Autonomous system	µ-processor system
- Event recorder (black box)	EPROM, non-volatile storage
- Data archiving	µ-processor system
- Battery backup	DC supply
Design:	
- User-oriented field calibration	Automatic and simple measurement procedure
- User-oriented evaluation	Project oriented parameterisation by PC
- Automatic interactions	Interconnection with conductors (see open system)
- Approved as fire detection system	Classification to DIN EN54
- Simple installation technology	19" rack housing
- Data visual display	Open software package
Cost Effectiveness:	
- Low overall system price	Use of economically priced unit technology
- Low operating and maintenance costs	System-conditioned self-test
- Low installation costs	Economically priced mounting system
- Low repair costs	Established connector technology
- Low consequential costs after damage	Modular design, exchangeable system components

Table 2: Comparison of customer with the fire detection system requirements.

5 Summary and Outlook

Cable systems are increasingly important components in building infrastructure for communications, decentralised data processing and electrical equipment power supply. By laying cables in cable trays increased ease of installation is achieved whilst on the other hand the risk of an undetected cable fire is increased.

By comparison with classical fire monitoring there are more stringent requirements for fire monitoring of cable trays. In the early stage cable overheating (e.g. at cable crossings, damaged insulation etc.) is limited to a very short section of cable (<1m) so that the cable heating is only measurable in the immediate vicinity of the point of damage site. If this increasing overheating is recognised too late cable ignition results and therefore the fire will jump across to neighbouring cables in the tray, this being associated with intense smoke formation. By filling the access routes and the seat of the fire with smoke efficient fire fighting by the fire service is not then possible. Therefore there is a strong interest in locating instances of cable overheating during the build-up phase in order to be in a position to initiate damage limitation measures (e.g. switching off electrical power supply before ignition of the cable takes place so that no risk of smoke formation arises. Since cable trays are lengthy and extensive monitoring objects difficult to access more than a thousand measuring points (detectors) are needed. No fire detector systems for cable trays are available on the market which meets an optimum asset value and personal protection from economically justifiable points of view.

With the development of heat and radiation sensitive cable designs and further development of the optical OFDR Raman radar measuring method a fire detection system for fire monitoring in cable trays, which meets the requirements of plant operators and rescue service management, has been successfully realised:

- Rapid, reliable sounding in the early stage (if possible prior to pyrolysis)
- Simple installation and low maintenance costs
- Seat of fire location to within one metre with clear correlation within the building
- Information regarding spread of fire and smoke (fire tracking)

- Automatic interactions, e.g. signalling, disconnection of faulty conductors etc.

Highlighted is the important requirement of advance fire recognition. Related to fire detection in cable ducts and false ceilings this means the possibility of recognising cable fires as early as the build-up phase and determining the direction of spread early and with great precision. In the early stage damage limitation measures may be initiated which not only save human lives but also prevent great physical damage and damage by fire-fighting water. In addition to the high information density by comparison with other technologies further advantages of the method are worthy of note, such as simplicity of installation, great range and the maintenance-free sensor cable, which permits laying in areas no longer accessible. Therefore a synergy of largely conflicting aspects has been successfully achieved, in which a high technological demand is combined with economic justifiability.

The unique exclusive features of OFDR Raman technology are the complex measurement of Raman back-scatter light, the calculation of the Raman back-scatter curve from the Fourier transformation of the measurement signal and the application of the mathematical correspondence between frequency and location-space for correction of disturbance variables.

Compared to OTDR Raman technology OFDR Raman technology possesses the following technical and economic advantages:

- High SNR
- Great range
- Long working life of laser source
- Low interference from optical Fresnel reflections
- Possibility of using algorithm to improve signal quality
- Simple online (frequency) calibration of fibre optic measuring instrument
- Simple recalibration of fibre optic measuring instrument (field calibration)

- Use of economically priced system components

- Greater reliability
- Simplified maintenance schedule.

At present further field trials are taking place with our customers. Under investigation are solution designs regarding the optimum laying of the fibre optic cable in cable trays with a high cable density. A further development objective is technical realisation of a multi-channel optical fire detection system for buildings monitoring in order to cover several fire sectors with a single monitoring system.

6 References

[1] U. Glombitza, *Sensorische Nutzung integrierter Lichtwellenleiter in Energiekabeln und Leitungen*, Innovations in Microsystems Technology, Vol. 58, VDI/VDE Technology Centre Information Technology GmbH, Teltow, March 1998

[2] U. Glombitza, F&G Energietechnik AG, *Faseroptisches Temperaturmeßsystem FibroLaserII,* 2nd Prize at Cologne Innovation Competition 1998

[3] Montanari, G. C., Simoni. L., *Aging Phenomenology and Modelling,* IEEE Transactions on Electrical Insulation, Vol. 28 (1993), S. 755-776

[4] U. Glombitza, R. Willsch, *Faseroptische Temperaturmessung zur Überwachung elektrischer Betriebsmittel,* VDE Symposium: Sensor Technology and Local Information Processing in Energy Technology, ETG-Specialist Report, Vol. 64, Dortmund, March 1997

[5] Will, J.; Hosser, D.; Siegfried, W., *Experimentelle Untersuchung zum Brandverhalten von Kabelanlagen,* IBMB Research Report, TU-Braunschweig, 1998

[6] Directive, *Instandsetzungsarbeiten an elektrischen Anlagen auf Brandstellen,* BGI 766, May 2000

[7] Directive, *Brandschutzleitfaden für Gebäude besonderer Art oder Nutzung,* Federal Ministry for Traffic System, Building and Housing Construction Nov. 1998, 2nd Ed.

[8] Emir Karamehmedovic, U. Glombitza, *Fibre-Optic Distributed Temperature Sensing Using Incoherent Optical Frequency Domain Reflectometry*, The International Society for Optical Engineering, Photonics West, 2003

M. Debliquy, Materia Nova and A. de Haan, Faculté Polytechnique de Mons
Rue de l'Epargne, 56
7000 Mons (Belgium)

F. Groulard Sochinor, Sochinor
Faubourg de Mignault, 17
7070 Le Roeulx (Belgium)

Fire protection based on gas sensors for dusty industries. Validation tests in a cement factory.

Abstract.

Sochinor together with the Faculté Polytechnique de Mons and Materia Nova (research Centre in Mons) have developed gas sensors based on semiconductors for fire detection in dusty industries. These specific sensors are commercially called Pyros-F.

The project consisted in installing an experimental system for fire detection based on Pyros gas sensors in the production plant in CBR Antoing.

The detection system consists of groups of detectors strategically placed linked to an Central Information Processing Unit (Siemens automat). The communication between the detectors and the Central is achieved with Profibus DP via optical fibres to insure the quality of the data transfer. The states of the detectors are displayed in the Control Room on the process control screens.

During the 10 months test period, the system showed its reliability for the detection in closed buildings although very dusty. No important evolution of the sensors was stated. For outdoor applications, the system showed good reliability but needs a periodic maintenance.

1. The project.

It is well known that classical fire detection based on the detection of particles is not usable in dusty places. Unfortunately, a lot of dangerous industrial processes like heat treatments in furnaces take place in dusty environments. In general, the problem is that you cannot protect the really hot spots of the process and the factory has to invest in a fire detection system installed precisely where nothing never happens.

The only way to get rid of this problem, is to use gas sensors as detection elements[1,2,3,4]. Different systems were proposed these last years based on commercially available gas sensors like CO sensors [5] or metal oxide [6] or organic semiconductors [7].

The project consisted in installing an experimental system for fire detection based on gas sensors using an organic semiconductor as a sensitive layer. The prototype system was tested in a Belgian cement production plant (CBR in Antoing).

The system was continuously followed for 10 months in order to observe the behaviour of the detectors and their evolution in the course of time. Indeed, in these very particular conditions, the experience in domestic use is no longer valid. The detection thresholds need to be adjusted and the lifetime is unknown.

2. Working principle of the detectors.[7,8,9]

The detectors exploit the signal of a gas sensor (semiconductor type) called Pyros-F developed by Sochinor and the Faculté Polytechnique de Mons.

The sensors consist of an organic semiconductor film (copper phthalocyanine CuPc), deposited by thermal vacuum deposition on an insulating alumina substrate provided with gold electrodes (figure 2.1).

The signal consists in measuring the conductivity of the film (in practice, the resistance of the film between the electrodes). This resistance depends on the composition of the surrounding atmosphere.

Like other well known semiconductor gas sensors, the basic working principle is that the gases in the surrounding atmosphere can adsorb on the surface of the sensitive layer and modify the number of charge carriers in the sensitive layer thanks to an electron transfer.

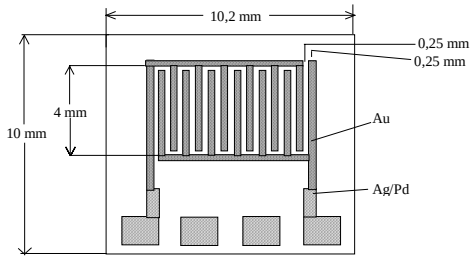

Fig. 2.1. Schematic of the interdigitated electrodes on the insulating substrate.

When the film is exposed to ambient air : acceptor gases present in ambient air (like O_2, SO_2, NO_x) adsorb on the surface of the film or in the bulk and give a extrinsic p-type character to the phthalocyanine film. When exposed to acceptors (oxidants), the number of positive charges inside the film increases and logically, the conductivity increases. When contacting with a donor gas like NH_3, H_2S, in normal conditions (after a contact with ambient air), we observe a conductivity decrease due to the cancellation of the effects of acceptor gases already adsorbed. The amplitude of the conductivity variations depends, of course, on the concentrations of the gases and on their redox character [10,11]. The useful signal is thus the electrical resistance of the sensitive layer between the electrodes.

For fire detection, the sensitivity of a phtalocyanine layer to gases emitted during a combustion is exploited. This sensitivity is reflected by important variations of the conductivity of the phtalocyanine film (eg resistance of the sensor). For instance, the response of the sensor to normalised TF5 fire (smouldering wood) is an increase of resistance of about 2 decades and the response to TF2 (heptane) fire is a decrease of the resistance of a factor 4 to 10.

Moreover, this type of sensor permits the distinction between a fire with flames and a smouldering fire : indeed, during a smouldering fire, the combustion is not complete and emits essentially gases with an electron donor character. The adsorption of these gases on the film will decrease drastically the conductivity. The contrary goes for flame fires.

These sensors, in contrast with the other sensors proposed on the market [12,13] work at **room temperature** and are **not sensitive to combustible gases like methane, heptane, alcohols, aromatics.** It is a advantage for the use in industrial environments.

The sensors placed in a normal atmosphere present resistance fluctuations due to the influence of the atmospheric changes. This resistance variation is directly linked to the concentration variations of polluting gases present in minute quantities in atmosphere like nitrogen and sulphur oxides, ozone and humidity. [13]

These fluctuations, which could be quite large in amplitude (typically a factor 4 peak to peak on the resistance), prevent the use of a simple resistance threshold for the switching of an alarm. These unavoidable natural variations are eliminated by a signal

processing based on the dynamic of the phenomena to be detected. Indeed, fluctuations in the ambient air, although sometimes important, are slow compared to those recorded during a fire (different time scale : hours <>minutes).

This observation led us to consider not the absolute values of the resistance but its variations dR/dt. The detection criterion is now based on a dR/Rdt variation threshold.

In that optic, we defined the concept of «ratio » $r = \frac{R(t)}{R(t-15s)}$

R(t) is the resistance of the sensor at time t and R(t-15) is the resistance of the sensor at time t-15 seconds.

For residential fire detection, we usually consider the following alarm thresholds :

r<0,85 : alarm fire with flames.

r>1,20 : alarm smouldering fire.

3. Description of the system.

3.1. General set up.

Sochinor's system consists in groups of detectors positioned in strategic places all connected to a Central Information Processing Unit (figure 3.1). The communication between the detectors, all addressable, and the CIPU is insured by Profibus DP. In Control Room, the state of the various detectors are displayed in a monitoring page. The different states of the detectors are : alarm smouldering fire, alarm flame fire, absence of the detector, failure (failed detector, communication interrupted or temperature too high for instance).

For a validation phase, the system was installed in 3 different places :

The first line of detectors consists of 9 detectors distributed along the solid fuel transport belt feeding the oven (the belt is completely covered). The fuel is a mixture of finely ground carpet, paper, plastic waste or even animal food. This solid fuel is very smelly and sticky.

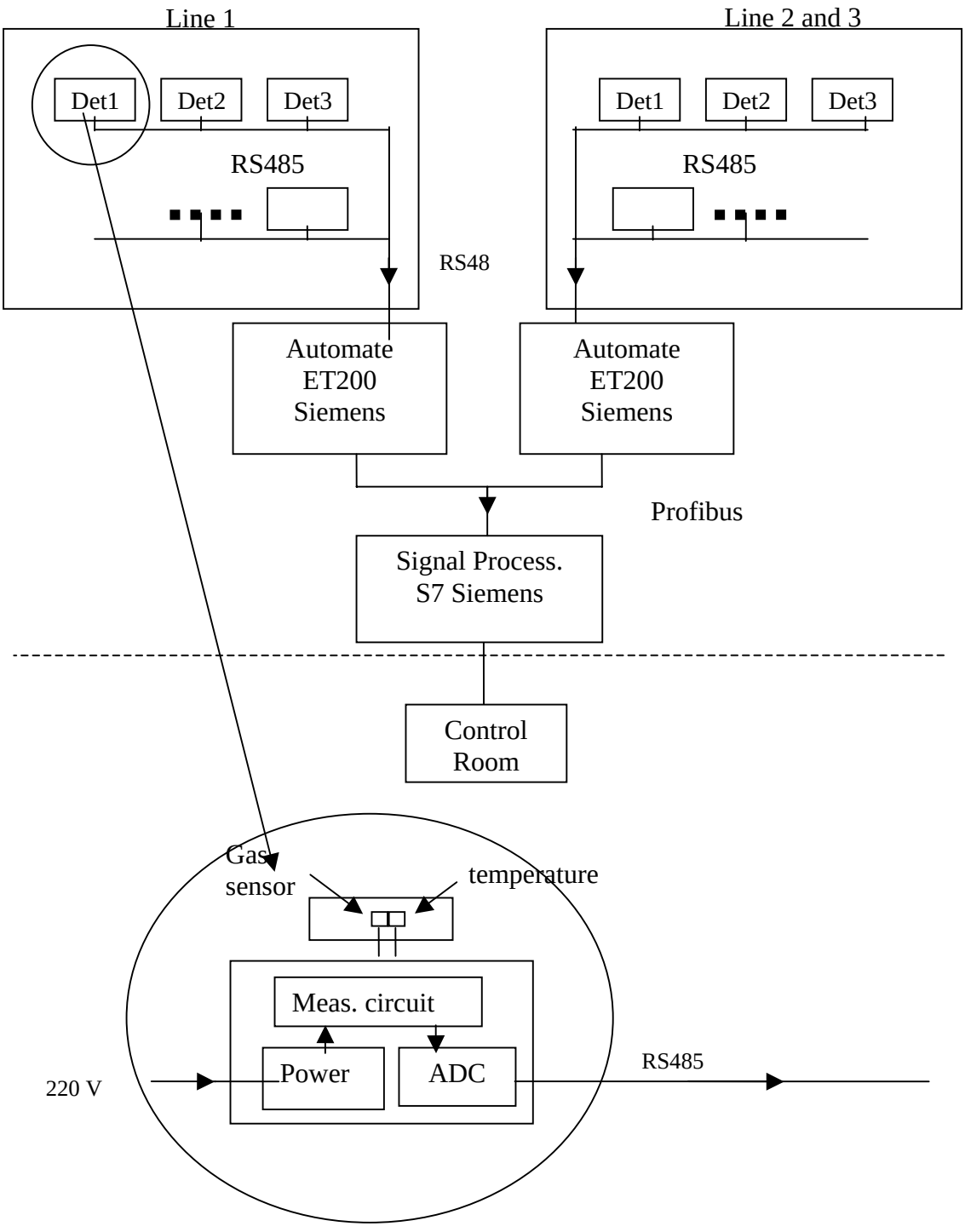

Fig. 3.1. General layout of the installation.

The second line consists of 4 detectors in open air surrounding the inlet of the furnace at the end of the transport belt.

The third line consists of 4 detectors in an electrical substation (fairly dusty). In this zone, a conventional detection system already exists but with a lot of false alarms.

3.2. The detectors.

The detectors consist of 2 parts :

1. Removable head including the gas sensor and a temperature sensor.
2. Fixed metallic box including the electronic boards for the measurements and the communication.

The detectors are supplied with 220 V AC (according to the desire of CBR).

The philosophy of the system is that the detectors are addressable and send raw values of the useful signals to the Central Signal Processing Unit (PLC S7 Siemens). No intelligence was put in the detectors. This permits to change easily the thresholds or even the detection algorithm if needed.

The temperature sensor in the head is additional to the detection of flame fires. Its signal is used as complementary information in the detection algorithm as a thermic and thermovelocimetric detector.

A second temperature sensor was placed in the box to control if the temperature conditions are compatible with the good working of the electronics (-15 °C to 60 °C). Some detectors were placed outdoors near the main furnace and the temperatures could be very high in summer.

3.3. Communication and signal processing.

The detectors of the same group (line) communicate via RS485 (2 wires) with a local automate (ET200 Siemens) which permits the RS485/Profibus conversion and the communication between the CSPU (S7 Siemens) and the detectors. The local automates communicate with the CSPU via Profibus DP supported on optical fibres.

The CSPU insures the following functions :

a. Data acquisition (CSPU is the Master for the communication.
b. Communication of the data (R,T, alarms, failures) on Profibus DP.
c. Calculation program and signal processing. Definition of the states of the detectors.
d. Portable PC Interface for the start and test phases.
e. Ethernet link to the Control Room.

4. Experimental Results.

The system was followed continuously for about 10 months in order to learn about the behaviour of the sensors and their evolution in the course of time. The first point is necessary to set the alarm thresholds (a priori unknown for this type of environment). The second point allows to evaluate the drifts and the life time of the detectors in that particular environment. After this test, we were able to define the periodicity of the maintenance for these detectors.

Fire tests were carried out on the detectors placed in line 2 (detectors in precalcination tower round the solid fuel inlet of the furnace). These tests were meant to evaluate the thresholds in this worst case.

4.1. Detectors in the electrical substation UCD4 (line 1).

This closed room is similar to what can be encountered in residential fire detection and presented no surprise nor difficulty. To prove that, 4 detectors were placed and followed during 10 months. The data were recorded and checked periodically. Figure 4.1 shows a typical result of the evolution of the resistance of the sensors during 17 days.

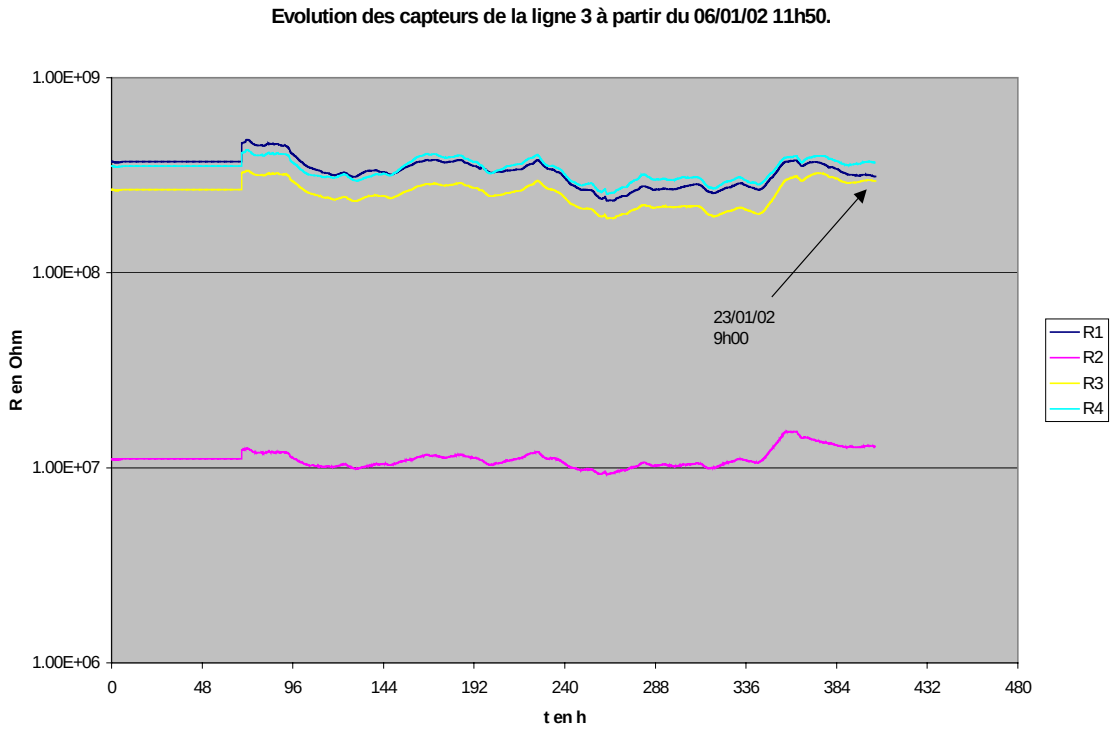

Fig. 4.1. Evolution of the resistance of the sensors placed in substation UCD4.

We observe that the resistance evolves slowly and weakly.

* Sensor 2 is of a different family than the other usual sensors. It's a modified sensor as used in line 2 (see below).

Since the beginning of the tests (October 23th, 2001), with the usual thresholds for residential fire detection no false alarm was noticed although another already installed commercial system did. Moreover, the drift in the mean resistance R_m after 10 months is weak (of the order of natural fluctuations in ambient air) (table 4.1).

Time (months)	Rm (in MOhm)	Rm (in MOhm)	Rm (in MOhm)	Rm (in MOhm)
0	700	16	1950	800
2	590	10	240	340
4	400	12	280	390
6	520	20	545	380
8	650	38	920	440
10	1160	57	1660	1140

Tab. 4.1. Evolution of the mean baseline resistance of the sensors.

The life time in these conditions is more than 10 months which is better than the already installed commercial system that has to be replaced every 3 months.

4.2. Detectors on the solid fuel feed belt (line 2).

The detectors are placed in caissons above the transport belt feeding the main rotating furnace in substitution solid fuel. The solid fuel is a mixture of carpet, rubber, plastics shreds and even animal food. Detector 1 is at the end and 9 is near the inlet drum. This environment is extremely dusty. Moreover, for detectors 8 and 9 showed a rapid corrosion of the metallic compounds. This important corrosion is due the humid atmosphere and the gases emitted by the hot fuel itself. For future models, this corrosion problem will taken into account. Note that the sensor itself was not destroyed.

Usually, dust does not lead to major problems for Sochinor's technology but in that particular case, because of the high humidity, the dust becomes sticky and after a certain time, the gases can not penetrate the detection head. Therefore a periodic maintenance is needed. A replacement of the detection heads every 3 months seems reasonable seen the aggressive environment.

The other problem met is that the fuel itself emits an very strong odour (putrefaction). Moreover, slow smouldering fires (considered as normal by the production engineers) can occur because of natural fermentation. These factors generate donor gases which cause the increase of the baseline resistance to unusual values and caused false alarms. The usual sensors were then replaced by less resistive sensors which are less sensitive to these donor gases but still sensitive to oxidants. Furthermore, only the flame fires were taken into account in the algorithm of detection.

Unfortunately, for evident practical reasons, real scale fire tests could not be carried out on these detectors. Laboratory tests were although performed to simulate the conditions in which the detectors are placed. These test consisted in confining the detector in a small caisson geometrically similar to those used on the transport belt and put fire to a small quantity of the same solid fuel as used in the industrial process. The ventilation conditions are also similar to the real situation.

After adjustment of the new thresholds, the false alarms disappeared.

4.3. Detectors round the fuel inlet of the furnace (line 3).

4 detectors were installed round the fuel inlet of the furnace.

Remark : The wind dilutes and deviates the combustion gases. These could pass aside the detectors which then don't « feel » anything. This problem is solved by multiplying the number of detectors. For our lay out, the number of detectors was not enough but it was just to study the behaviour of the system in difficult situations.

Some real fire tests were performed to specify the thresholds. 3 tests were organised by CBR consisting in putting fire to paper and cardboard in a metallic bucket (flame

fire). The bucket is placed 2 m below and at the vertical of the detector during 30 s. This unnormalised fire is representative of the fire intensity they want to detect in this environment. The thresholds were adapted to this « intensity » and were close to those used for residential applications. We must notice that during the process small smouldering fires may appear (solid fuel falling on hot plates round the furnace inlet), these, quite frequent, small and not dangerous (at least at this stage) fires are not taken in consideration by the production managers although they are detected by our system.

The major problem met in this environment are the wind and the rain. The rain penetrating in the detection head caused important noise and false alarms. Therefore, it was needed to add a protection cap, a vertical cylinder in PVC (10 cm in diameter and 10 cm height which is 1.5 times the height of the detection cap) to avoid this water penetration. This protection does not influence the detection has the fires come from bottom to top but limit the area of the protected zone. It involves a multiplication of the number of detectors.

With protection, no false alarms were detected (except smouldering fires not taken into account).

5. Conclusions.

Our system showed its reliability for the detection in closed buildings, even very dusty. No significant drift was stated during the test period which means that the maintenance period is longer than 1 year.

For the detectors placed outdoors round the inlet of the furnace, the design of the detection head is very important in order to avoid problems with the rain. After the redesign, the detectors proved to be reliable for flame fires (the detection of smouldering fires was not taken into consideration because it is considered normal for this process).

For the detectors placed along the solid fuel, a maintenance (replacement of the sensor head) every 3 months is needed because of the concentrated sticky dust that blocks the arrival of gases on the sensor. During the operational period, the detection was proved to be reliable for flame fires (smouldering fires are considered normal in this application).

References.

1. M. A. Jackson and I. Robins, “Gas sensing for fire protection : Measurements of CO, CO2, H2, O2 and smoke density in European Standard Fire Tests”, Fire Safety Journal, Vol. 22, pp. 181-205 (1994).

2. J. Riches, A. Chapman and J. Beardon, “The Detection of Fire Precursors Using Chemical sensors”, 8th International Fire Science and Engineering Conference, Edinburgh (1999).

3. BS. Rodricks, “Fire Detection Systems for the Millennium”, Trans ImarE, Vol. 113/1, pp 24-36 (2001)

4. Z. Liu, AK Kim, “Review of recent developments in fire detection technologies”, Journal of Fire Protection Engineering, Vol. 13/2, pp.129-149 (2003).

5. R. Barett, “CO Fire Detection”, Fire Safety Engineering, August 2000.

6. H. Petig, J. Kelleter,and Dieter Schmitt, “Gas Sensor Fire Detectors prove effective in Coaling Plants”, Allianz Report 4/99.

7. M. Debliquy, PhD Thesis, « Etude des films minces de phtalocyanine : application à la détection d’incendie », 1999.

8. Sochinor, Technical folder “Pyros-F sensors”

9. M. Debliquy, A. de Haan, « Influence of the morphology of copper phthalocyanine films on their sensitivity for gases », Conférence Internationale Semiconductor Gas Sensors à Ustron, Pologne, 25-29 septembre 1998.

10. M. Bouvet, E.A. Silinsh and J. Simon, Mol. Mat., Vol. 5 p255 (1995).

11. J.D. Wright, Gas adsorption on phthalocyanines and its effects on electrical properties, Progress in Surface Science, Vol. 31, pp. 1-60 (1991).

12. Moseley P, Norris J, Williams D., Techniques and Mechanisms in Gas Sensing, The Adam Hilger Series on Sensors, 1991.

13. Figaro, Technical folder, Taguchi Gas Sensors.

14. A. de Haan, M. Debliquy and A. Decroly, « Influence of atmospheric pollutants on the conductance of phtalocyanine films », Sensors and Actuators B, 1-3 69-74 (1999).

Liu Weihua Li Xiangyang

Gulf Security Technology Co., Ltd., inhuangdao, Hebei Province, PRC

Mei hibin Pan Gang

Shenyang Fire Research Institute, Shenyang, Liaoning Province, PRC

erformance Tests and Analysis on Aspirating Smoke Detectors in Typical Applications

Abstract

Aspirating smoke detectors have been widely used in many special areas for its active sampling of air and high sensitivity. As a new type of detector, there isn t a general standard to evaluate its performance, or installation codes to guide its applications. To gain further knowledge of this type of detector, we designed several tests to test application features of aspirating detectors in typical environments. Our results indicated that the structure of air sampling pipes, numbers of holes and diameters of these holes are the key factors to determine the sensitivity of aspirating smoke detection system. We suggested that the configuration of air sampling pipe networks should be taken into consideration when an aspirating detector was tested or evaluated.

1. eneral

In order to describe application features of aspirating smoke detectors, we designed three tests to measure response threshold values of air sampling holes under typical office environment. We chose two samples from two different manufacturers, S1 S2. Their specifications are as follows.

	S1	S2
Sensitivity Range(%obs/m)	0.03%FSD 25%obs/m	0.005% 20% obs/m
Sensitivity Resolution (%obs/m)	0.0015%obs/m	0.005%obs/m
Maximum Sampling pipe Length	200m	100m
Single Pipe Maximum Length	100m	--
Sampling Pipe Inlets	4	4

The atmospheric conditions for testing are as follows.

Temperature: (18 to 25) C

Relative humidity: (35 to 45) %

Air Pressure: (100 to 105) kPa

All pipes and sampling holes are designed with the software provided by manufacturers. The test equipment is Trutest smoke detector sensitivity tester, which is UL268 listed. Smoke density provided by the tester is Min=0%obs/ft, Max=6.00%obs/ft, and accuracy is 0.01%obs/ft.

Note: Smoke generated velocity from aerosol generator is 0.50%obs/ft per minute. Measuring at maximum responding time of 120s, maximum tolerance should be less than 1.00%obs/ft.

- **Typical application under office en ironment**

We chose S1 in testing. Sampling is done by four pipes. Pipe 1 is parallel with pipe 2 and pipe 3 is parallel with pipe 4. Sampling holes are placed as in Table 1.

Table 1 Parameters of Sampling pipes

	Total Pipe Length (m)	Inner Diameter (mm)	Spacing of Sampling Hole (m)	uantity of Sampling Hole
Pipe 1	22	21	5	4
Pipe 2	22	21	5	4
Pipe 3	27	21	5	5
Pipe 4	27	21	5	5

We tested response threshold value at sampling points on pipe 1 and 3 with the manufacturer recommended sensitivity setting. Measured results are as in Table 2 and Fig. 1.

Table 2 Test result of four-pipe network

Number of Sampling Holes		1	2	3	4	5
Pipe 1	Diameter of Hole (mm)	3	3	3	3	
	Response Threshold Value (%obs/ft)	3.6	4.1	4.16	4.98	
Pipe 3	Diameter of Hole (mm)	3	3	3	3	3
	Response Threshold Value (%obs/ft)	3.64	3.97	3.98	4.55	4.73

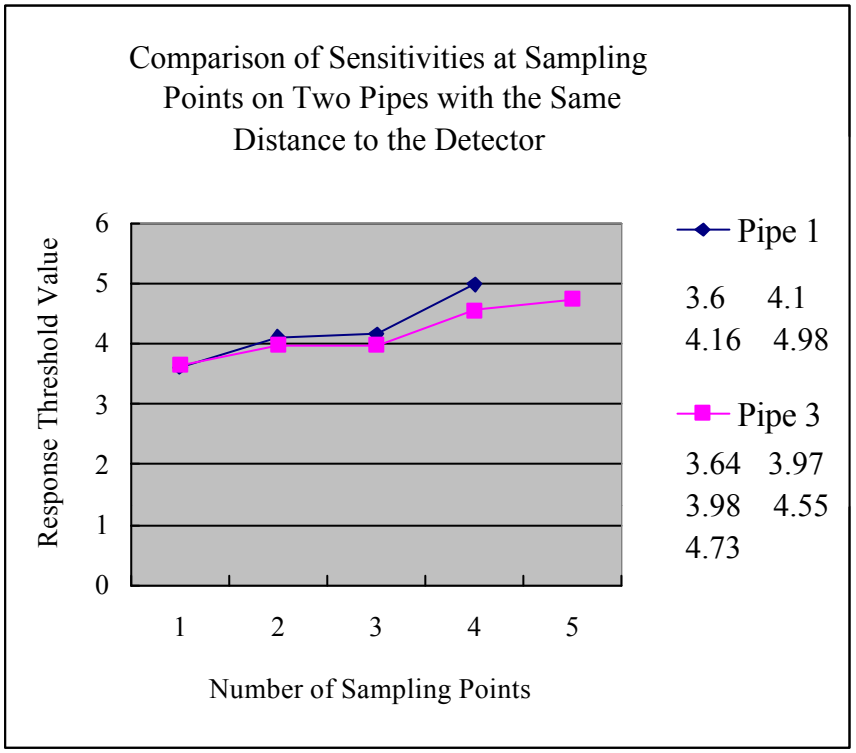

Fig. 1 Comparison of sensitivities at sampling points on two pipes

Brief summary: When sizes of sampling holes on the same pipe are the same, the farther a sampling hole is from detector main unit, the lower its sensitivity is. In the same zone, for two holes on two pipes of the same design, sensitivities of holes at the same position are almost the same.

. **Test on ma imum pipe length**

Select S1 and S2, measure response threshold values at different sampling holes with manufacturer recommended sensitivity level.

Test 1: Sampling with a single straight pipe. Maximum pipe length is 96 meters. Pipe setting: inner diameter is 21mm, sampling holes spacing is 6m, and quantity of sampling holes is 16.

Test 2: Sampling with a single pipe. Maximum pipe length is 96 meters. The pipe layout is shown in Fig. 2. Pipe setting: inner diameter is 21mm, sampling hole spacing is 6m, and quantity of sampling holes is 16.

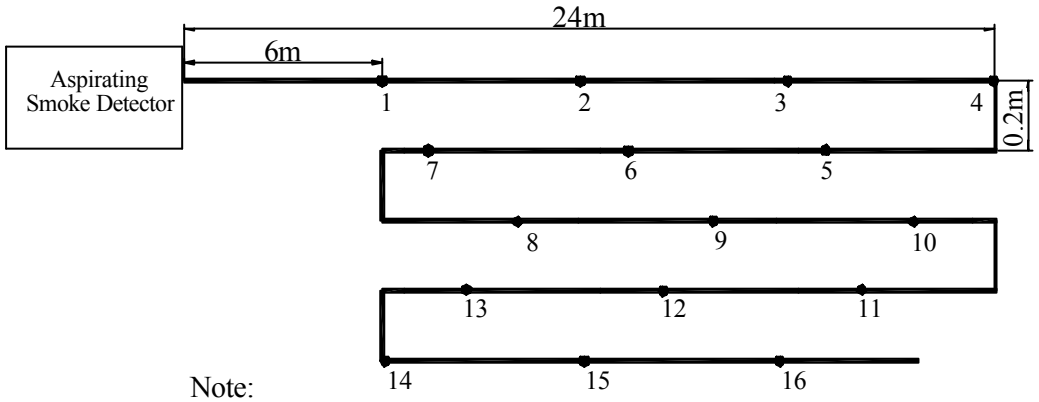

Note:
1. Spacing between neighboring sampling holes on main pipe is 6 meters.
2. Total pipe length is 96 meters.

Fig. 2 Bended pipe system and layout of sampling pipe

Results of Test 1 and Test 2 are shown in Table 3.

Table 3 Results of Test 1 and Test 2

<table>
<tr><td rowspan="3">Number of Sampling Point</td><td colspan="3">S1</td><td colspan="3">S2</td></tr>
<tr><td colspan="2">Straight Pipe</td><td>Bended Pipe</td><td colspan="2">Straight Pipe</td><td>Bended Pipe</td></tr>
<tr><td>Diameter of Sampling Hole (mm)</td><td>Response Threshold Value (% /ft) in Fire 1</td><td>Response Threshold Value (% /ft) in Fire 1</td><td>Diameter of Sampling Hole(mm)</td><td>Response Threshold Value (% /ft) in Fire 1</td><td>Response Threshold Value (% /ft) in Fire 1</td></tr>
<tr><td>1</td><td>3.0</td><td>3.10</td><td>3.26</td><td>3.0</td><td>0.87</td><td>0.87</td></tr>
<tr><td>2</td><td>3.0</td><td>3.49</td><td>3.61</td><td>3.0</td><td>1.06</td><td>1.04</td></tr>
<tr><td>3</td><td>3.0</td><td>3.86</td><td>4.26</td><td>3.0</td><td>1.29</td><td>1.25</td></tr>
<tr><td>4</td><td>3.5</td><td>4.26</td><td>4.73</td><td>3.5</td><td>1.53</td><td>1.43</td></tr>
<tr><td>5</td><td>3.5</td><td>4.53</td><td>4.98</td><td>3.5</td><td>1.87</td><td>1.51</td></tr>
<tr><td>6</td><td>4.0</td><td>4.75</td><td>5.55</td><td>4.0</td><td>1.94</td><td>1.66</td></tr>
<tr><td>7</td><td>4.0</td><td>4.97</td><td>5.60</td><td>4.0</td><td>2.02</td><td>1.84</td></tr>
<tr><td>8</td><td>4.0</td><td>5.13</td><td>5.79</td><td>4.0</td><td>2.26</td><td>1.94</td></tr>
<tr><td>9</td><td>4.0</td><td>5.45</td><td rowspan="7">When smoke density reaches 5.98, aerosol generator is stopped and no sampling point alarms fire 1.</td><td>4.0</td><td>2.44</td><td>2.42</td></tr>
<tr><td>10</td><td>4.0</td><td rowspan="7">When smoke density reaches 5.98, aerosol generator is stopped and no sampling point alarms fire 1.</td><td>4.0</td><td>2.95</td><td>2.51</td></tr>
<tr><td>11</td><td>4.0</td><td>4.0</td><td>3.16</td><td>2.87</td></tr>
<tr><td>12</td><td>4.0</td><td>4.0</td><td>3.24</td><td>3.06</td></tr>
<tr><td>13</td><td>4.0</td><td>4.0</td><td>3.58</td><td>3.22</td></tr>
<tr><td>14</td><td>4.0</td><td>4.0</td><td>4.16</td><td>3.24</td></tr>
<tr><td>15</td><td>4.0</td><td>4.0</td><td>4.27</td><td>4.45</td></tr>
<tr><td>16</td><td>4.0</td><td>4.0</td><td>4.29</td><td>5.09</td></tr>
<tr><td>Remarks</td><td colspan="2">Sensitivity level is 2 (Range allowed is 0 8); airflow velocity is 16.</td><td>Fire 1 is set at 0.08obsc/m; airflow velocity is set at 10.</td><td colspan="2">Sensitivity level is 2 (Range allowed is 0 8); airflow velocity is 16.</td><td>Fire 1 is set at 0.08obsc/m; airflow velocity is set at 10.</td></tr>
</table>

Comparison of results between test 1 and 2 is shown in Fig. 3.

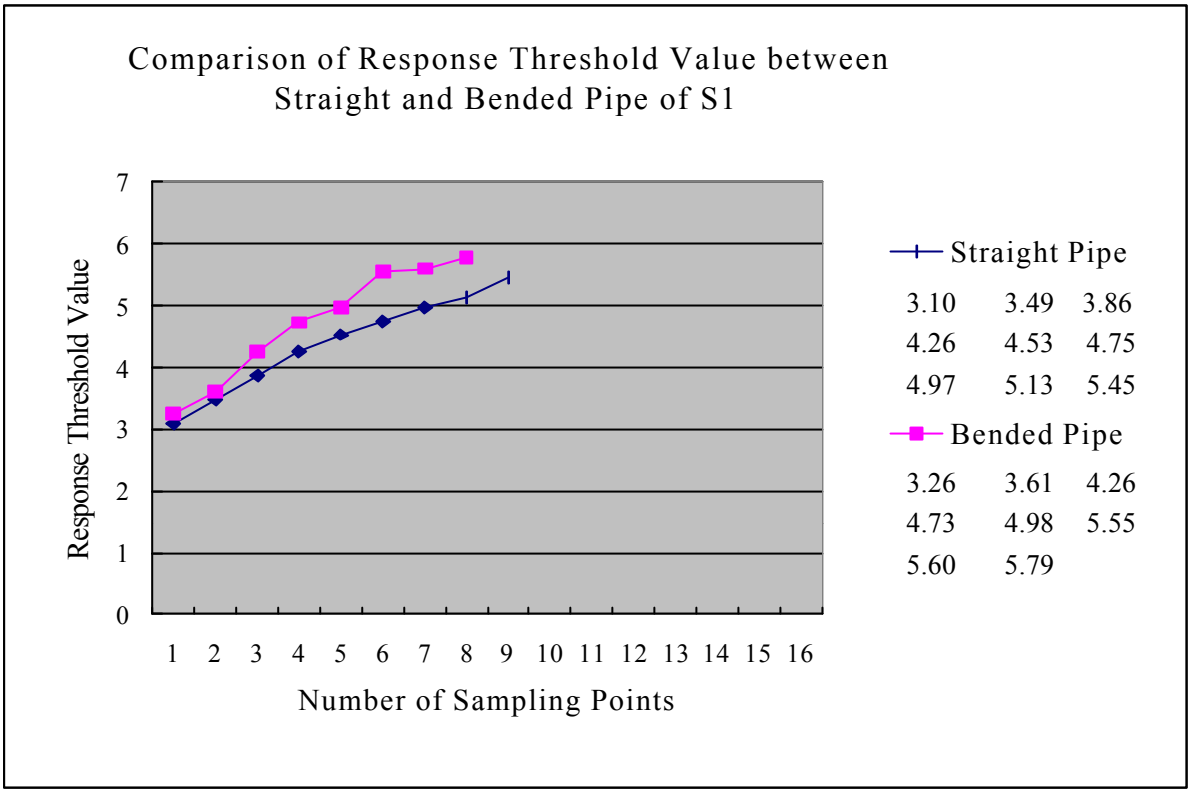

(a) S1

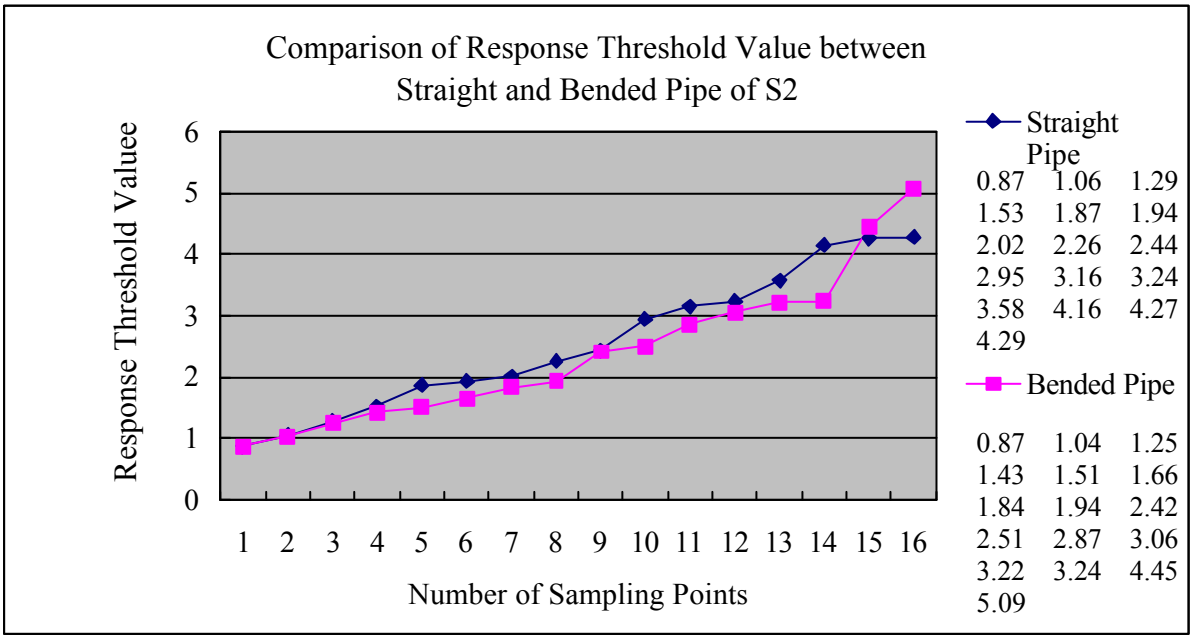

(b) S2

Fig. 3 Comparison of different features between straight pipe and bend pipe systems

Brief Summary: When pipe length reaches the maximum value provided by manufacturers, if diameters of holes along the pipe are not optimized, the difference of sensitivities at the nearest and farthest point is significant. In systems of S1, sensitivity of a sampling hole on bended pipe is less than that of the hole with the same position on straight pipe, while there is not much difference for S2 systems.

. **Test in simulated pressure difference en ironment**

As shown in the following figure, put two pipes on S1, and one sampling point on each pipe. Sampling point B is connected with air source where air pressure is adjustable to provide pressure difference between the two pipes.

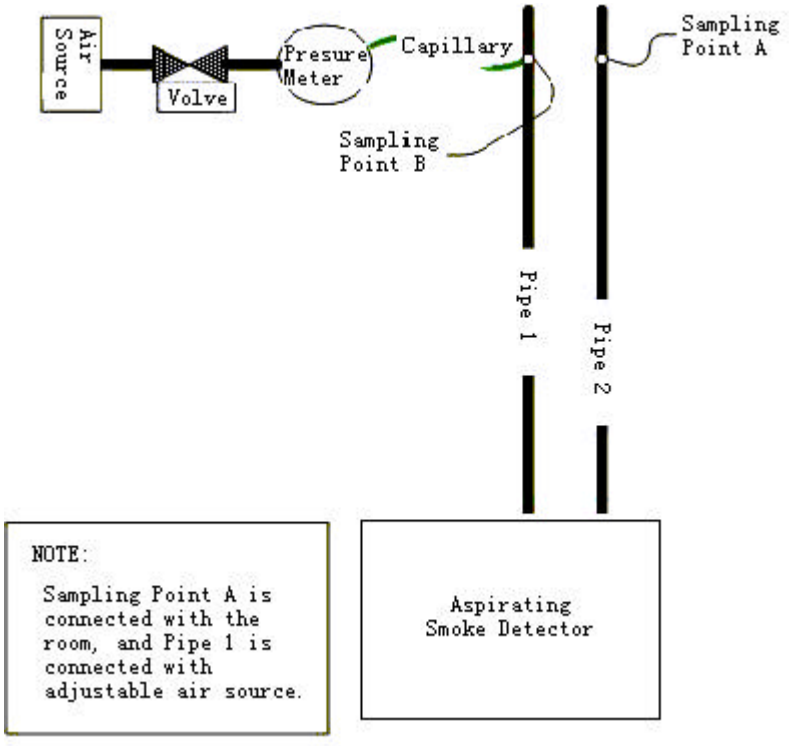

Fig. 4 System configuration

Under different pressure difference, measure response threshold value at point A. Results are as follows.

Table 4 Test result in simulated pressure difference environment

No.	Pressure Difference between Pipe 1 and Pipe 2（MPa）	Response Threshold Value % /ft (Point A) (Pipe Length 6m)
a)	0	3.1
b)	0.025	3.17
c)	0.05	3.28
d)	0.075	3.38
e)	0.1	3.72

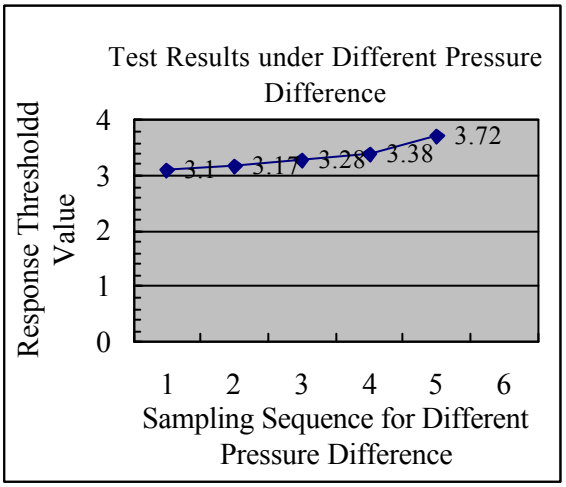

Fig. 5 Test Results under Different Pressure Difference

Brief summary: When the two pipes sample together, pressure difference between different pipes will affect sensitivity of sampling hole, which is lower at lower pressure side.

. **Summary from the abo e tests**

The test results indicated that the structure of air sampling pipes, numbers of holes and diameters of these holes are the key factors to determine the sensitivity of an aspirating smoke detection system. We suggested that the configuration of air sampling pipe

networks should be taken into consideration when an aspirating detector was tested or evaluated.

Whereas the sensitivity range of aspirating smoke detectors is so wide and the fire detection system might get different sensitivities on different sampling pipe networks, we suggested that this type of detectors should be graded according to sensitivity, and regulations on pipe structure of each grade should be established.

The test results also indicated that the sensitivity might be reduced by pressure difference between different pipes. So it might be important to limit the scope of application of aspirating smoke detector in Code of practice for system design, installation and maintenance.

Reference:

No Climb Products Ltd.

, Date 03/31/00

Fang Jun,Yuan Hong-Yong
State Key Laboratory of Fire Science, University of Science and Technology of China,
Hefei, Anhui, People's Republic of China,230027

Experimental Measurements, Integral Modeling and Smoke Detection of Early Fire In Thermally Stratified Environments

1. Introduction

In modern large volume buildings with high ceilings, due to the thermal load of solar radiation, air conditioning system and translucent glass structure, hot air with different temperature gradient often exists under the ceiling to form a thermally stratified environment. Sometimes the hot air layer is very thick and the temperature gradient is big. Due to the buoyant effects, the early fire smoke cannot breakthrouth the stratified environments and may terminate at a maximum height to disable the traditional spot or beam smoke detectors under the ceiling.

The previous work of fire smoke movements in large spaces mainly focused on smoke filling and settlement process of a large fire by experimental measurements or zone modeling for smoke exhaust or egress time analysis[1-3]. In NFPA 92B for the stratification consideration[4], the maximum smoke rise equation which only depends on the convective heat release rate and the ambient temperature variation in the space was derived by Morton, Taylor and Turner in 1956 [5] using an integral model as equation (1) describes.

$$Z_{\max} = 5.54 Q_c^{1/4} \left(dT_a / dZ\right)^{-3/8} \tag{1}$$

where $Z_{\max}$ is the maximum height of a smoke plume(m),Q_c is the convective portion of the fire heat release rate(kW),T_a is the ambient air temperature(K), Z is the vertical coordinate.

Equation (1) often takes the following form which is usually used to analyze the bubble movements in the stratified water[6-8].

$$Z_{\max} = 3.8 B_0^{1/4} N^{-3/4} \tag{2}$$

where B_0 is the thermal buoyant flux(m^4/s^3), N is Brunt-Vaisälä buoyant frequency(Hz)as below

$$N = \left(-\frac{g}{\rho_{a0}} \frac{d\rho_a}{dZ} \right)^{1/2} \tag{3}$$

where, ρ_{a0} is the reference air density(kg/m^3), taken as the ambient air density near the fire source, ρ_a is the ambient air density (kg/m^3), g is the gravitational acceleration.It is easy to prove that the above equation (1) and (2) are equivalent by substituting $B_0 = gQ_c / \rho_{a0} C_p T_{a0}$ and $\rho_a = 0.003484 P / T$ into (2), here C_p is the heat capacity at constant pressure (J/(kg K)), T_{a0} is the ambient air temperature near the fire source, P is the constant atmospheric pressure(Pa).

The above maximum rise equations were not verified in real fire scenarios, further the temperature gradient is not always linear and the influences of light or heavy smoke were not considered. In this paper, we conducted many experiments with different fire materials in a small enclosure,and the integral equation was discussed and improved to agree with the experimental and CFD results. Finally an optical section image smoke detection method was proposed to detect the early fire in large volume spaces.

2. Experiments

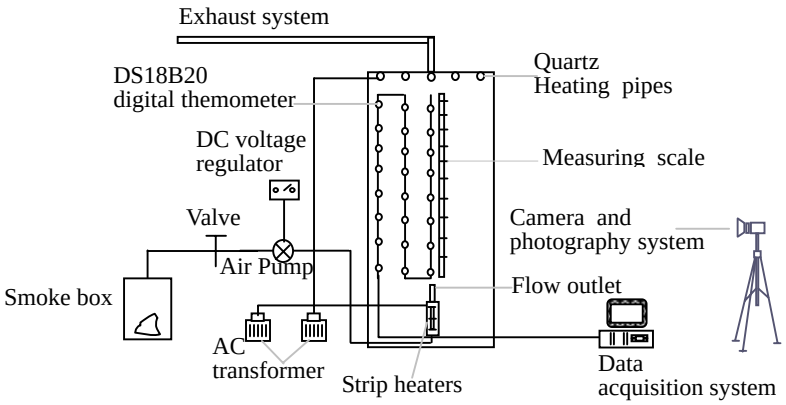

Fig.1 Schematic plan of the experimental setup

The experimental room is a small scale enclosure which is 1.2 m long, 1.2 m wide and 2 m high enclosed by organic glass materials and coated with black cloth materials leaving a front face for observation and a vent for smoke exhaust as Fig.1 shows. In the bottom of the experimental setup, there are small air laps connected with the outer environment to keep a constant atmospheric pressure. There is a measuring scale located along the axial direction to mark the different heights for later maximum heights analysis. The stable linearly thermally stratified air environments were accomplished by pre-heating the enclosure air with fifteen quartz heating pipes with even space put under the ceiling of the enclosure.

The test fire materials are cotton rope which is one of the Europe standard fire materials and standard A55 diesel oil, they can produce light smoke and heavy smoke typically.

The outlet velocities were obtained with the help of a high speed camera (SPEEDCAM Pro-Lt) working at 100 frames per second by using its own image analysis software to calculate the ratios of two frontal surface height values of a rising plume to the needed time. The maximum heights of the plume were obtained by analyzing the plume images captured by a digital camera. The axial temperatures and the ambient air temperatures of the smoke plume were obtained by three rows of digital thermometers (DS18B20) suspended respectively in the middle and at one side in the vertical direction of the enclosure.

For the smoke outlet in the small enclosure, two schemes were adopted. One is that the fire smoke from the smoke box was pumped through a PVC pipe into an outlet device with strip

heaters inside. The outlet device surface was thermally insulated to avoid thermal diffusion into the ambient environment and the outlet device was put in the middle of the enclosure bottom. The outlet flow fluxes were adjusted with different heating powers, pump powers and different outlet diameters. The advantages of this scheme are that it not only can obtain different smoke rises of the same fire materials in different outlet conditions and different stratified environments, but also can obtain different maximum rises of different fire materials in the same outlet conditions and stratified environments to get more information than what NFPA 92B can give.

The initial outlet flow and thermally stratified environment parameters for smoldering cotton rope and flaming diesel oil smoke of scheme 1 are listed as table 1 shows.

Table 1 Initial outlet conditions and thermal environments of scheme 1

Case no.	Outlet ambient temperature (C)	Outlet smoke temperature (C)	Outlet velocity (m/s)	Outlet thermal buoyant flux (m^4/s^3)	Stratified intensity (Hz)	Gr	Re
a	18.0	22.25	0.521	1.1077820E-05	0.451103159	3771.5	387.097
b	17.5	25.0125	0.4	1.7462582E-05	0.48466414	2568.3	507.425
c	18.1	23.125	0.5125	1.4049425E-05	0.446978899	1255.0	559.781
d	17.5	30.0625	0.5971	4.2650424E-05	0.484613324	1000.6	625.031
e	18.5	30.0625	0.6667	4.0478616E-05	0.595809563	12048.0	358.565
A	17.5	19.5	0.18	9.8579551E-06	0.49849529	28112.0	653.529
B	17.6	24.7125	0.3333	5.35113360E-05	0.509281455	28015.6	464.249
C	18.5	25.625	0.2411	3.35707E-05	0.628627741	39953.7	580.931
D	19.1	29.125	0.3077	6.08497E-05	0.651868276	23553.5	478.373
E	18.1	23.875	0.2411	3.19966E-05	0.519990808	2129.8	514.144

In scheme 1 for the lower case letters of a,b,c,d,e, the outlet diameter is 1.5cm, for the upper case letters of A,B,C,D,E, the outlet diameter is 3cm. For each case, the outlet conditions and stratified environments are the same for smoldering cotton rope and flaming diesel oil smoke.

Scheme 2 is that the smoke box was put in the middle of the enclosure and the fire smoke entered the enclosure through a 2.5cm diameter outlet directly.

Table 2 Initial outlet conditions and thermal environments of scheme 2

Case no	Material and combustion	Outlet ambient temp.(°C)	Outlet smoke temp.(°C)	Outlet velocity (m/s)	Outlet thermal buoyant flux (m^4/s^3)	Stratified intensity (Hz)	Gr	Re
1	Smoldering cotton rope	24.25	48.5	0.1052	3.6285E-05	0.6201	35477.05	147.26
2		24.25	47	0.1221	4.1040E-05	0.5457	35643.34	171.49
3		25.56	64	0.1334	7.1328E-05	0.6213	47829.14	171.03
4		24.50	56.3	0.1302	6.0391E-05	0.5655	43477.13	175.95
1	Flaming diesel oil	24.4	74.2	0.135	7.5899E-05	0.7376	52472.13	167.08
2		24.4	72.8	0.131	7.4064E-05	0.6440	52090.63	162.77

The initial outlet flow and thermally stratified environment parameters for smoldering cotton rope and flaming diesel oil smoke of scheme are listed as table 2 shows.

3. Analysis and comparisons

Fig.2 Typical experimental photograph (left) and simulated contour (right) of a cotton rope smoke mushroom

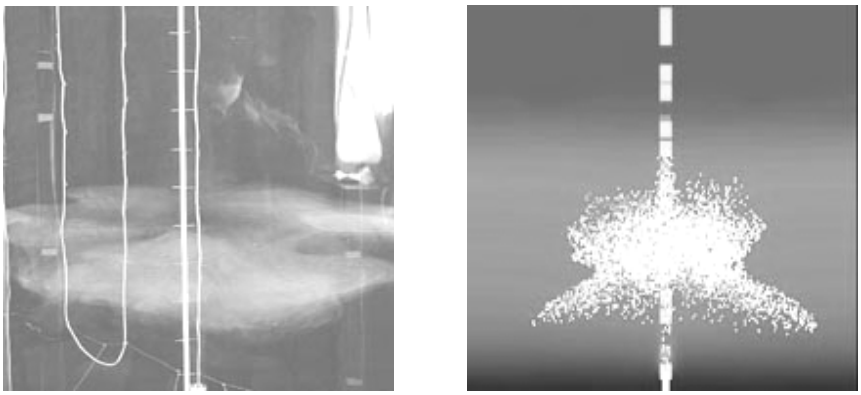

Fig.3 Typical experimental photograph (left) and simulated contour (right) of a diesel oil smoke mushroom

The experimental observations found that in the early time the smoke plume affected the ambient temperature gradient a little and the smoke plume flowed out of the outlet and gradually expanded its radius due to the entrainment of the ambient air, and finally spread horizontally and terminated at a maximum height like a mushroom shroud.

To obtain more information about the smoke movements in thermally stratified environments, CFD simulations were finished by adopting large eddy simulation(LES) technique, the cotton rope smoke and diesel oil smoke were both assumed to be a gaseous mixture with different molecular weights and the radiation and combustion effects were neglected. For cotton rope and diesel oil smoke in scheme 1 and 2, the simulated axial and ambient temperatures, the axial velocities and the maximum heights agree well with the experimental observations.

The typical experimental and simulated mushrooms of cotton rope smoke and diesel oil are as Fig.2 and Fig.3 show. And the typical axial velocity, axial and ambient temperature are

illustrated as Fig.4 shows.

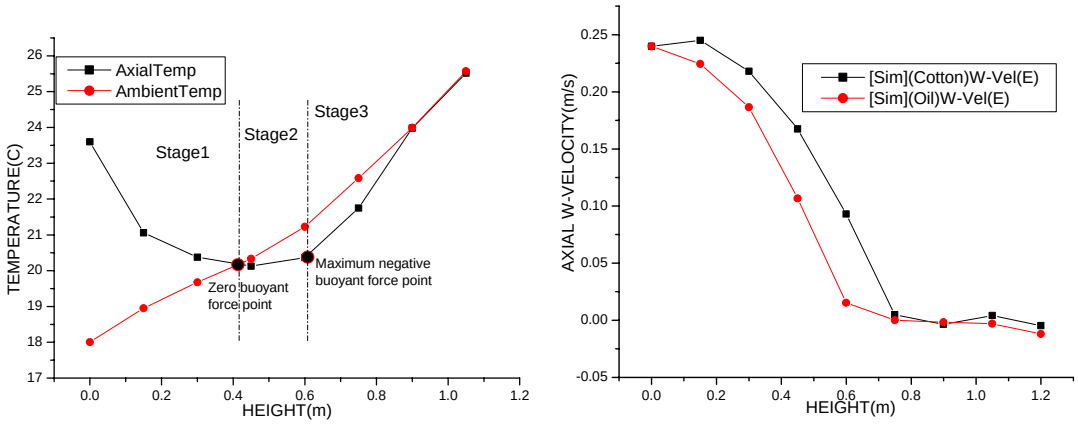

Fig.4 Typical profile of axial and ambient temperatures (left) of scheme 1 and 2, and axial velocities (right) of cotton rope and diesel oil smoke in scheme 1

To verify the integral model equation (2), the experimental and simulated maximum heights of different test materials in scheme 1 and 2 are as Fig.5 and Fig.6 show.

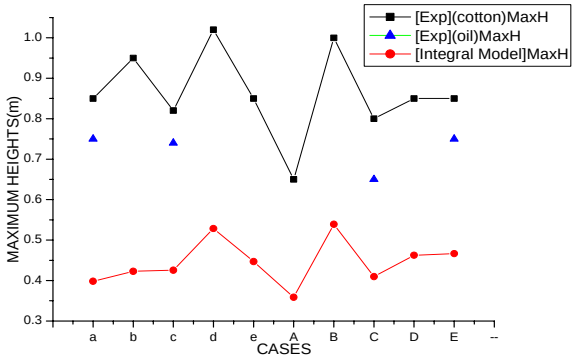

Fig.5 The experimental and integral equation maximum heights of cotton rope and diesel oil in scheme 1

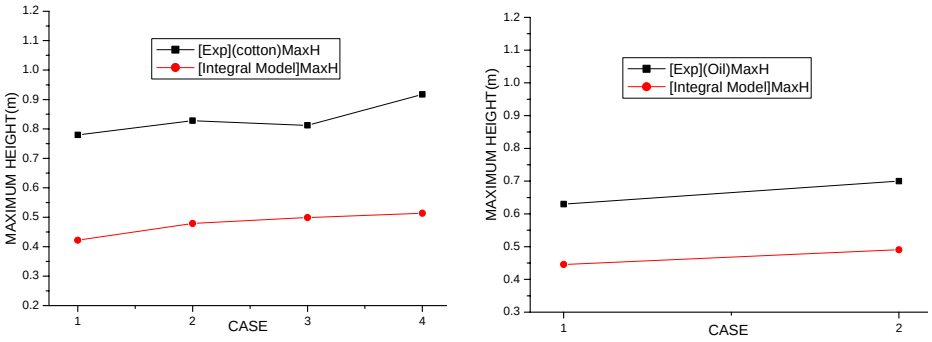

Fig.6 Experimental and integral maximum heights of cotton rope and diesel oil in scheme 2

From Fig.4 to Fig.6 we can see, it is obvious that the integral model is invalid to obtain the actual higher maximum heights of the test materials and is unable to predict the differences of the cotton rope smoke and diesel oil smoke movements. The main reason may result from that the integral model supposes that the plume is fully developed turbulent and self-preserving in

the distributions of the vertical velocities, and the gaseous smoke of different fire materials is all assumed to be air.

4. Improved integral equation

As described above, the failure of the previous integral equations in predicting the actual maximum rises is first due to the self-similarity of a fully developed turbulent smoke plume. For a smoke plume induced by early fire, there is often a laminar or transitional flow near the fire source and there is a certain distance proportional to the fire source size to satisfy the self-preserving distributions of the vertical velocities and smoke concentrations [9].

Furthermore, for the same convective heat flux of a fire smoke plume with different smoke densities in the same thermally stratified environment, there may be some differences in the maximum rises for the light smoke or heavy smoke plume.

Table 3 Maximum heights and correction factors of cotton rope smoke of scheme 1 and 2

Material and scheme	Case	Outlet diameter d_0(m)	Experimental maximum rise(m)	Integral maximum rise,Z_{max}(m)	Self-similarity factor, k_2	Gr	Re
Cotton (Scheme 1)	a	0.015	0.85	0.398	30.1145	2129.8	514.14
	b	0.015	0.95	0.423	35.141	3771.5	387.10
	c	0.015	0.82	0.405	27.628	2568.3	507.43
	d	0.015	1.02	0.528	32.753	1255	559.78
	e	0.015	0.85	0.447	26.87	1000.6	625.03
	A	0.03	0.65	0.279	12.370	12048	358.56
	B	0.03	1	0.589	13.696	28112	653.53
	C	0.03	0.8	0.410	13.009	28015.6	464.25
	D	0.03	0.85	0.463	12.913	39953.7	580.93
	E	0.03	0.85	0.466	12.775	23553.5	478.37
Cotton (scheme 2)	1	0.025	0.78	0.422	11.918	35477.05	147.26
	2	0.025	0.83	0.479	11.639	35643.34	171.49
	3	0.025	0.81	0.499	10.439	47829.14	171.03
	4	0.025	0.92	0.514	13.453	43477.13	175.95

Table 4 Maximum heights and correction factors of diesel oil smoke of scheme 1 and 2

Material and scheme	Case	Outlet diameter d_0(m)	Experimental maximum rise(m)	Integral maximum rise,Z_{max}(m)	Self-similarity factor, k_2	Smoke density factor k_1	Gr	Re
Diesel oil (scheme 1)	a	0.015	0.75	0.3983	30.11	0.74892	2129.8	514.14
	c	0.015	0.74	0.4056	27.63	0.80275	2568.3	507.43
	C	0.03	0.69	0.4097	13.01	0.73152	28015.6	464.25
	E	0.03	0.75	0.4667	12.78	0.78574	23553.5	478.37
Diesel oil (scheme 2)	1	0.025	0.63	0.4456	11.2	0.78	52472.1	167.08
	2	0.025	0.70	0.4904	12.1	0.82	52090.6	162.77

So, to consider the influences of different densities and the requirements of self-similarity of a smoke plume, equation (1) and (2) are modified as equation (4) and (5) respectively.

$$Z_{\max}' = k_1 \cdot \left[5.54 Q_c^{1/4} \left(\frac{dT_a}{dZ} \right)^{-3/8} \right] + k_2 \cdot d_0 \tag{4}$$

$$Z_{\max}' = k_1 \cdot \left(3.8 B_0^{1/4} N^{-3/4} \right) + k_2 \cdot d_0 \tag{5}$$

where k_1 is the smoke density correction factor, k_2 is the self-similarity correction factor,d_o is the equivalent diameter of a fire source size.

The maximum heights and correction factors of cotton rope and diesel oil smoke in our small scale experiments are as table 3 and table 4 show. From them we can see, the self-similarity factors are mainly related to Grashof number.

In a real large volume space, the temperature gradient in the vertical direction is often illustrated as Fig.7 shows. As the thermal buoyant flux in a homogeneous environment keeps constant, the real maximum heights in the constant temperature and convective zone of a fire smoke can be written as equation (6) and (7) show.

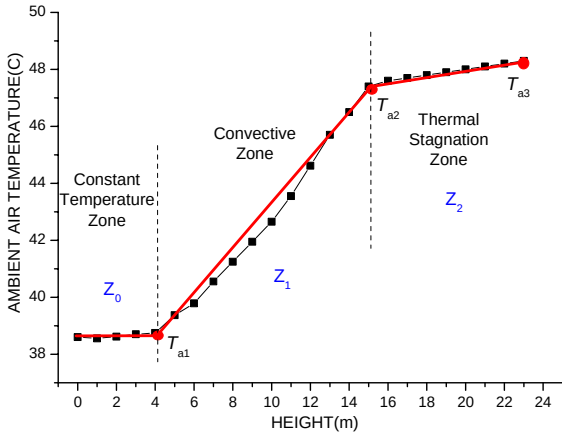

Fig.7 Temperature gradient in a large volume space

$$Z_{\max}'' = Z_0 + k_1 \cdot \left[5.54 Q_c^{1/4} \left(\frac{dT_a}{dZ} \right)^{-3/8} \right] + k_2 \cdot d_0 \tag{6}$$

$$Z_{\max}'' = Z_0 + k_1 \cdot \left(3.8 B_0^{1/4} N^{-3/4} \right) + k_2 \cdot d_0 \tag{7}$$

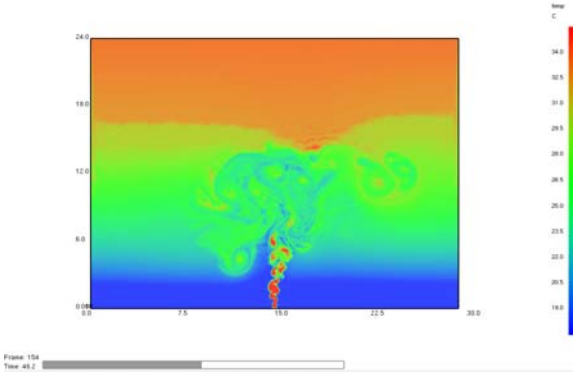

Fig.8 Typical smoke contour in a large space with a sectional linear air temperature gradient

Equation (6) is proved to be right for many fire induced smoke plumes in a 30m×30m×24m big space with different sectional linear air temperature gradient environments by CFD simulations typically as Fig. 8 shows.

5. Early fire smoke detection in large volume spaces

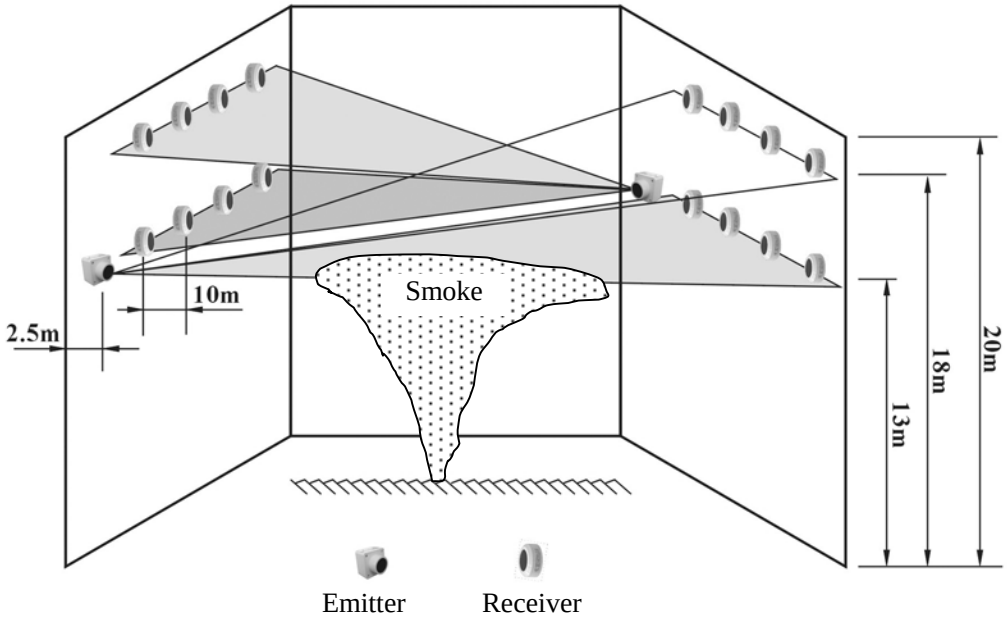

Fig.9 Typical optical section image smoke detection layout

As the early fire smoke may suspend at a maximum height in a high large volume spaces, the conventional spot and light beam smoke detectors under the ceilings are difficult to detect the smoke effectively. So we propose an optical section image smoke detection system that is our patented invention as Fig.9 shows. This system consists of light emitters/receivers and a signal processing unit. The light emitters are a lot of infrared illuminators and the corresponding receivers are several infrared cameras. When the fire smoke flows across the infrared light beam, the facula in the pictures taken by the cameras will get weak in luminosity. Then the host computer can analyze these pictures using a certain algorithm to judge whether a fire has happened and give a signal to the interlock controller to activate fire suppression facilities such as water guns.

For high large volume spaces, there can be emitters and receivers in more than two planes to form a three dimensional optical smoke detection network to guarantee immediate response of a fire in the early time.

6. Summary and conclusions

A detailed study of smoke plumes of smoldering cotton rope smoke and flaming diesel oil in linearly thermally stratified environments was investigated by small scale space experiments and CFD simulations. The reasonably good agreements of the experimental and simulated results show that the thermally stratified environment intensified the decreases of the axial

temperatures and velocities of a fire smoke plume until made it terminate at a certain height. By analyzing the differences between the maximum heights of the cotton rope smoke and the diesel oil smoke plumes with the same thermal buoyant flux and the same stratification conditions, as well as the great differences between the experimental and integral results, the previous integral equation was improved to consider the influences of the stratified environment, smoke property and plume turbulence for its better applications in real large volume spaces.

To avoid missing and false alarms of early fire smoke in high large space buildings, an optical section image smoke detection method with a three-dimensional observation net was proposed to overcome the shortcomings of conventional spot and beam smoke detectors.

Acknowledgements

The authors deeply appreciate the support of the China NKBRSF project (No.2001CB409608).

References

[1] Frederick W. Mowrer. “Enclosure Smoke Filling Revisited”. Fire Safety J. 1999,33: 93-114.

[2] W.K. Chow,et al. “Natural Smoke Filling in Atrium with Liquid Pool Fires up to 1.6 MW”. Building and Environment. 2001,36:121-127.

[3] W.K. Chow,et al. “On the Use of Time Constants for Specifying the Smoke Filling Process in Atrium Halls”. Fire Safety J. 1997,28:165-177.

[4] NFPA, “Guide for Smoke Management Systems in Malls, Atria, and Large Areas”, NFPA 92B-2000,National Fire Protection Association, Quincy, MA, 2000.

[5] Morton,B.R.,Taylor,Sir Geoffrey,and Turner,J.S. “Turbulent Gravitational Convection from Maintained and Instantaneous Sources”.Proc.Royal Society A. 1956,234:1-23.

[6] Fischer,H.B.,et al. “Mixing in Inland and Coastal Waters”.Academic.1979.

[7] Turner,J.S. “Buoyancy Effects in Fluids”.Combridge University Press.1973.

[8] J.S.Turner. “Turbulent Entrainment:the Development of the Entrainment Assumption,and its Application to Geophysical Flows”.J.Fluid Mech,1986;173:431~471.

[9] B.R.Morton, “Forced Plumes”,J.Fluid Mech.,1959,5:151-163.

Rajko Rothe
Institut für Sicherheitstechnik/Schiffssicherheit e.V., Rostock, Germany

Detection reliability of different fire detector principles – Results from investigations of the fire hazards under real conditions in cabins aboard seagoing vessels

Abstract

The predominant conditions in seafaring make special demands on the active and passive fire fighting. The fast and reliable fire detection is particularly important because of this. It stands at the beginning of every defensive measure. The effective fire detection is indicated by a detection reliability of 100% within the first three minutes as well as by a false alarm frequency of approximately zero.

Investigations were carried out at conventional as well as at new technologies in the context of a research project sponsored by the country of Mecklenburg-West Pomerania. A particular aim was to test the present performance of the detection technologies under real operating conditions. A ship cabin was manufactured and installed in the fire test laboratory of the Institut für Sicherheitstechnik/Schiffssicherheit e.V. to proof the effectiveness of the different sensor strategies. This trial construction was built up after an original cabin. For the investigations different sensors and sensor systems were used: optical smoke detectors, air sampling systems and gas detection systems.

Fire and emission sources were used which are actually utilized in the equipment of real cabins. The fires were burned in two scenarios, as open fires and smouldering fires. The tests were carried out with and without ventilation and every test was repeated 3 times.

After evaluation of all available results the following statements can be made concerning the detection reliability:

The present used or available technology of fire detection in cabins on seagoing ships is characterised by a very high stability against false alarm activation. In no case there was a detection of the typical interfering substances (steam, tobacco smoke, cleaning agents etc).

The determined detection times aren't acceptable with respect to the special requests of seafaring. Primarily the optical smoke detectors respond on average clearly too late. The gas analysis or the air sampling technologies are real alternatives at least from the view of effectiveness.

1. Einführung

Die vorherrschenden Bedingungen in der Seeschifffahrt stellen besondere Anforderungen an die aktive und passive Brandabwehr. Schiffsbrände sind immer Spezialbrände, bedingt durch bauliche und lüftungstechnische Gegebenheiten, durch die hohe Komplexität und Integrität der technischen Anlagen und nicht zuletzt durch organisatorische Bedingungen.

Eine besondere Rolle kommt daher der schnellen und zuverlässigen Branderkennung zu, steht sie doch am Anfang jeder Abwehrmaßnahme. Die aktuellen Statistiken zeigen, dass zwar die Anzahl der Schiffsbrände nicht steigt, aber zunehmend mit höheren Schadensumfängen gerechnet werden muss, wenn es zu einem Brand kommt. Das belegen sowohl Havarieauswertungen auf Schiffen, hervorgerufen durch Brandereignisse, als auch durch Mitarbeiter unseres Hauses selbst angefertigte offizielle Gutachten. Es zeigt sich auch immer deutlicher, dass die Zeitspannen zum wirksamen Reagieren immer kürzer werden. Die Ansprüche an die Wirksamkeit der Abwehrtechnik wachsen zunehmend.

Die Forderung nach einer schnellen und zuverlässigen Branderkennung ist aufrecht zu erhalten, wobei eine Ansprechwahrscheinlichkeit von 100% in den ersten drei Minuten nach Ausbruch eines Brandes angestrebt werden muss. Dabei soll die Falschalarmhäufigkeit nahezu „NULL“ betragen.

2. Zielstellung

Im Rahmen eines vom Land Mecklenburg-Vorpommern geförderten Forschungsprojektes konnten Untersuchungen an herkömmlichen sowie an neuartigen Melderprinzipien bzw. –systemen durchgeführt werden. Ein Ziel war, den gegenwärtigen Leistungstand der Technik unter Bedingungen zu testen, die dem realistischen Einsatz sehr nahe kommen. In dieser Forschungsarbeit wurde sich dabei beispielhaft auf Brände in Aufbautenbreichen von Schiffen bezogen.

Die Arbeiten wurden gemeinsam mit verschiedenen Partnern durchgeführt. Beteiligt waren die Firmen W.I.S. Engineering als Projektant und Errichter von Schiffskabinen sowie die Firma WMA Airsense Analysetechnik GmbH als Hersteller von Gasanalysetechnik.

3. Versuchsaufbau

Zum Nachweis der Wirksamkeit verschiedener Sensorkonzepte wurde eine Schiffskabine gefertigt und im Brandlabor des Institutes für Sicherheitstechnik/Schiffssicherheit e.V. errichtet. Dieser Versuchsaufbau wurde maßstabsgerecht einer Original-Schiffskammer nachempfunden. So besteht die Versuchskammer aus einem 2,76m x 3,25m Aufenthaltsraum und einer innen liegenden Sanitärzelle von 1,34m x 1,25m. Es wurde eine aktive Be- und Entlüftung installiert, die den tatsächlichen Bordgegebenheiten entspricht. Das heißt, dass ca. 70% des Zuluftstromes über die verschließbare Sanitärzelle abgesaugt werden und ca. 30% der Zuluft über die Eingangstür (siehe dazu auch Abbildung 1: Skizze des Versuchsaufbaus, Draufsicht und Abbildung 2). Die Druckverhältnisse wurden mit einem geeichten Bargraphen den Kabinenbedingungen auf Passagierschiffen angepasst.

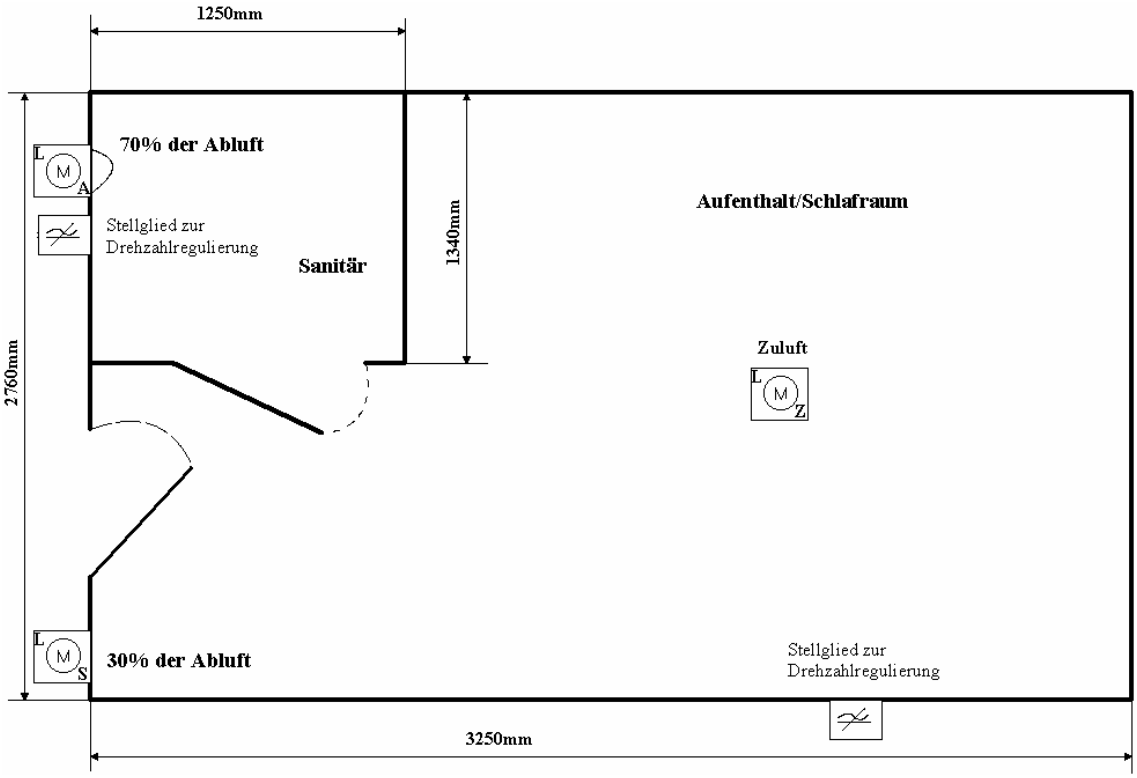

Abbildung 1: Skizze des Versuchsaufbaus, Draufsicht

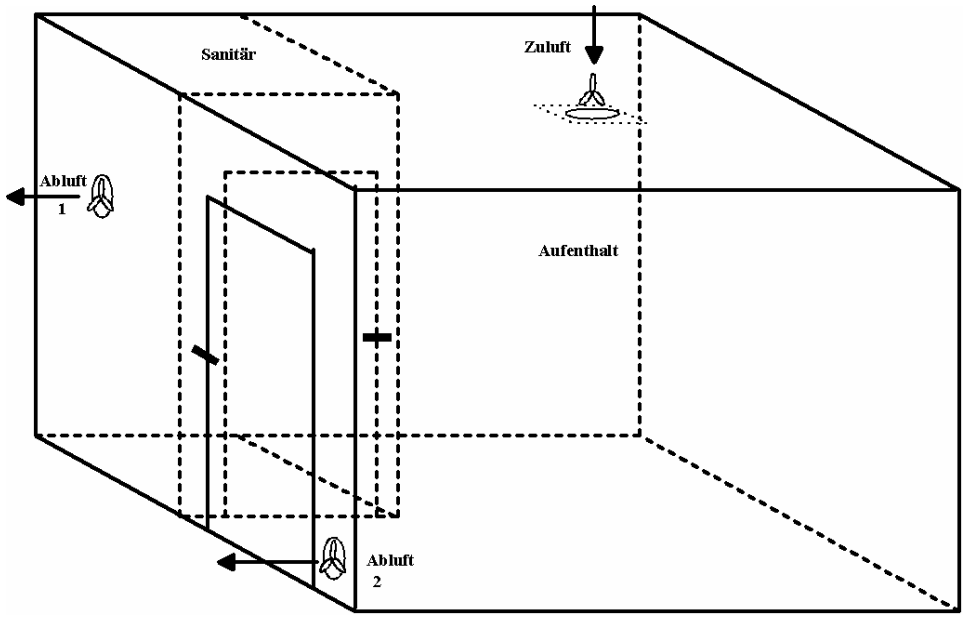

Abbildung 2: Skizze des Versuchsaufbaus, räumliche Darstellung

Sensoren

Für die Untersuchungen wurden folgende Sensoren und Sensorsysteme verwendet:

- 2 Frühwarnsysteme, FWS1 und FWS2 auf Gasanalysebasis
- 4 Punktmelder, die im Schiffbau eingesetzt werden, dabei waren zwei Melder reine Streulichtmelder (M1, M3) und zwei weitere Multisensoren mit Streulicht- bzw. Wärmediffentialmeldern (M2, M4)
- 1 Luftansaugsystem LAS mit optischer Auswertung

Die Anordnung der Melder bzw. Systeme erfolgte entsprechend den Regeln der Technik.

Unmittelbar an der Zuluftöffnung wurden ein Punktmelder (M3), die Frühwarnsysteme sowie die am weitesten von der Auswerteeinheit entfernte Ansaugstelle des LAS installiert. Weitere vier Ansaugstellen befanden sich außerhalb der Kabine und nahmen somit ausschließlich unbelastete Luftproben.

Weitere Punktemelder wurden wie folgt eingebaut:

M1	im Sanitärtrakt, unter der Decke, unmittelbar an der Abluftöffnung
M2	unter der Decke, in der Nähe der Eingangstür
M4	unter der Decke, in der Raumecke

Die Anordnung der weiteren Ansaugstellen des LAS erfolgte entsprechend Abbildung 3.

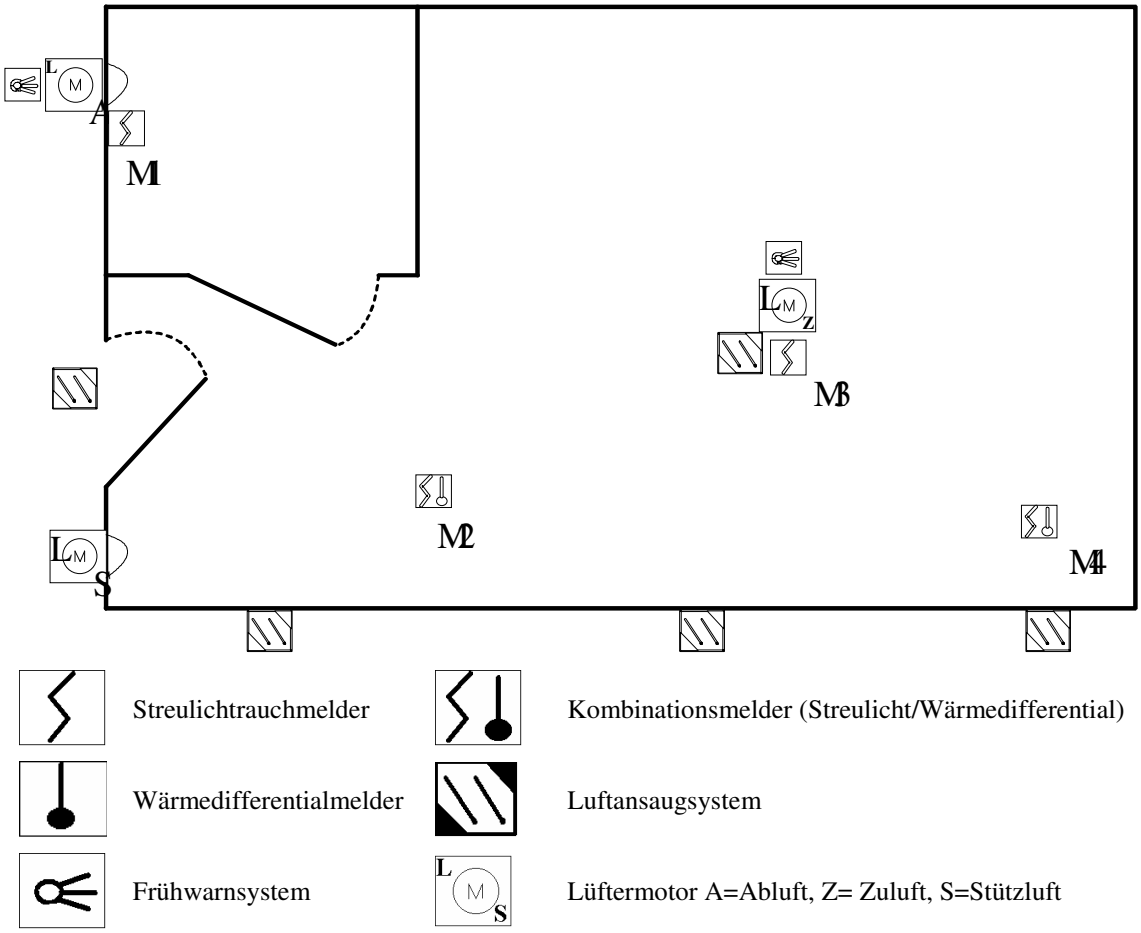

Abbildung 3: Skizze der Sensorpositionierung

Brand-/Emissionsstoffe

Um die Realitätsnähe zu wahren, wurden Brand- und Emissionsstoffe verwendet, die im Schiffbau und bei der Ausrüstung von Kabinen tatsächlich zum Einsatz kommen. Das waren im Einzelnen:

Brandstoffe	**Emissionsstoffe (Störgrößen)**
Fußbodenbelag	Reinigungsmittel
mit Papier gefüllter Abfallbehälter	Wasserdampf
Möbelholz	Körperspray (Deodorant/Haarfestiger)
Gardinen und Wandverkleidungen	Zigaretten/Zigarre/Pfeife
Möbeltextilien (Stuhl-, Sesselbezüge)	
Kabel	
E-Installationsmaterial	
Brandbeschleuniger	

Die Brand-/ Emissionsherde befanden sich an verschiedenen Stellen der Räume.

4. Versuchsbedingungen

Die Versuche wurden in dem Zeitraum Januar und Februar 2003 durchgeführt. Die äußeren Bedingungen waren relativ konstant, d.h. der Luftdruck lag durchweg bei mehr als 1023hPa und die Temperaturen zwischen –8°C und +3°C. Die rel. Luftfeuchte bewegte sich zwischen 45 und 60%.

5. Versuchsdurchführung

Die Brandstoffe wurden in verschieden Szenarien, offenen Bränden und Schwelbränden, verbrannt und die Emissionsstoffe entsprechend appliziert. Die Durchführung der Versuche erfolgte je drei Mal mit und ohne Ventilation.

Mit folgenden Brand-/Emissionsstoffen und Szenarien wurden die Sensorsysteme getestet:

Brandlast	Brandszenarios
gefüllter Papierkorb	verdeckter offener Brand
Fußbodenbelag	Schwelbrand, Entzündung mit Brandbeschleuniger, glimmende Zigarette
Dekostoffe	Schwelbrand, offenes Feuer ohne und mit Brandbeschleuniger
Möbeltextilien	Schwelbrand, Feuer mit Brandbeschleuniger
Zigaretten	1 Stück, 5 Stück
Wasserdampf	reine Emission
Körperspray	reine Emission
Kombination Fußbodenbelag / Benzin	reine Emission
Elektrokabel	Schwelbrand durch Stromüberlast
Steckdosen	Schwelbrand durch Stromüberlast
Möbelholz	Schwelbrand; Feuer mit Brandbeschleuniger
Reinigungsmittel	reine Emission
Kombination E- Kabel/ Wasserdampf	
Kombination Möbelholz/ Wasserdampf	

Die analogen Signale der Frühwarnsysteme wurden via RS 232 Schnittstelle und Datenkabel zu je einem Laptop bzw. PC geführt. Die Daten der adressierbaren Punktmelder gelangten über einen Zweidraht-BUS an eine Brandmeldezentrale. Das Luftansaugsystem entnahm die Luftproben über Luftansaugöffnungn und führte sie über ein Rohrsystem einem optischen Sensor in der Auswerteeinheit zu.

Insgesamt wurden 125 Versuche durchgeführt. Die Ansprechzeiten und, wo möglich, wurden die Signalverläufe erfasst. Zur Veranschaulichung wurde jeder Versuch per Video aufgezeichnet.

6. Auswertung

Bei der Auswertung der durchgeführten Versuchsreihen sind zwei Aspekte von besonderer Bedeutung – die Ansprechwahrscheinlichkeit innerhalb einer definierten Zeit sowie die Falschalarmhäufigkeit.

Im Folgenden sind einige Versuchsergebnisse auszugsweise dargestellt. Zu sehen sind die mittleren Ansprechzeiten der versch. Sensorsysteme bei diversen Brandversuchen (s. Abbildung 4, Abbildung 5und Abbildung 6).

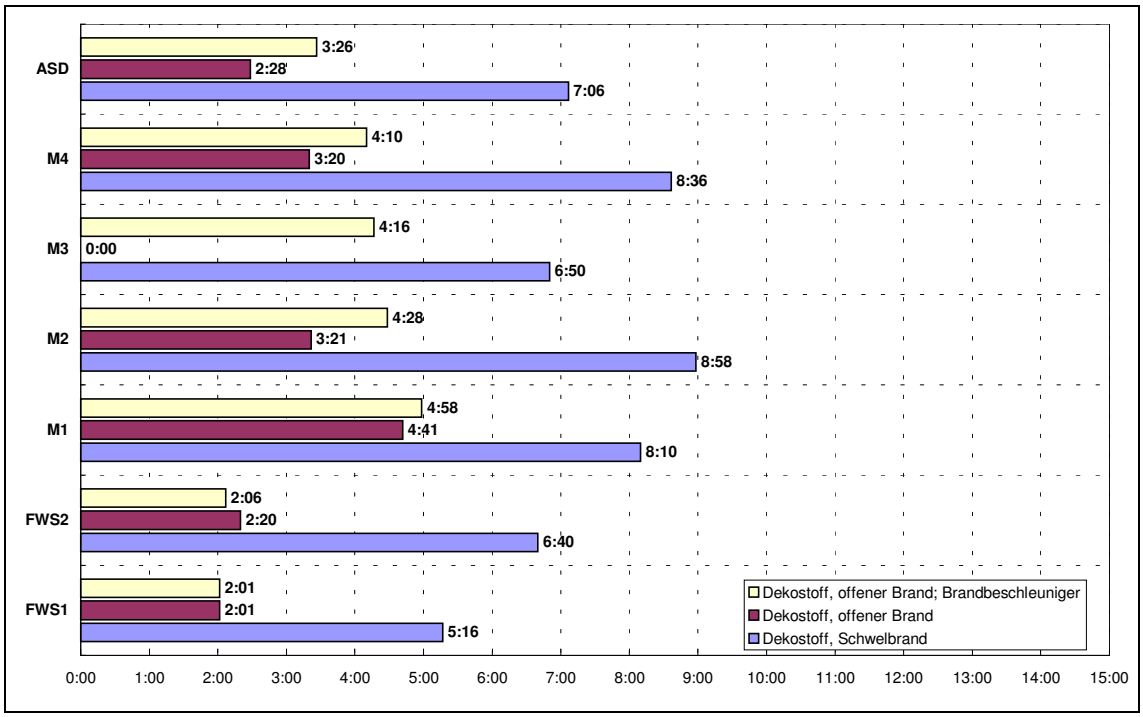

Abbildung 4: Darstellung der mittleren Ansprechzeiten bei Brandversuchen mit Dekostoffen

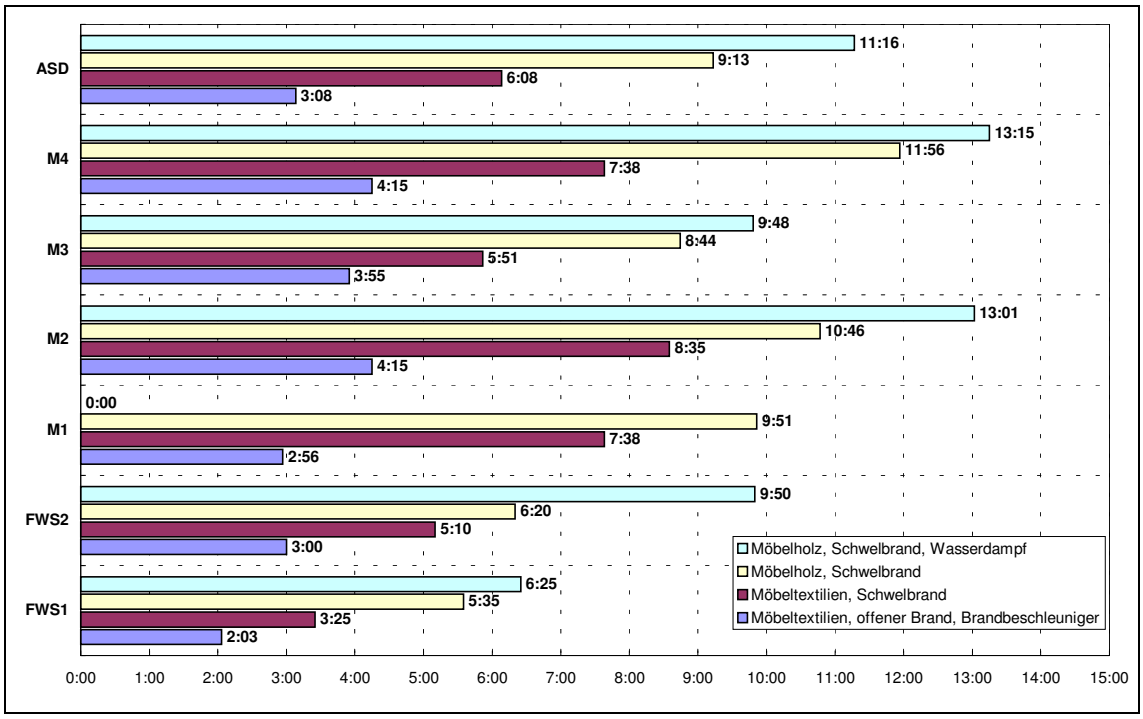

Abbildung 5: Darstellung der mittleren Ansprechzeiten bei Brandversuchen mit Möbeln

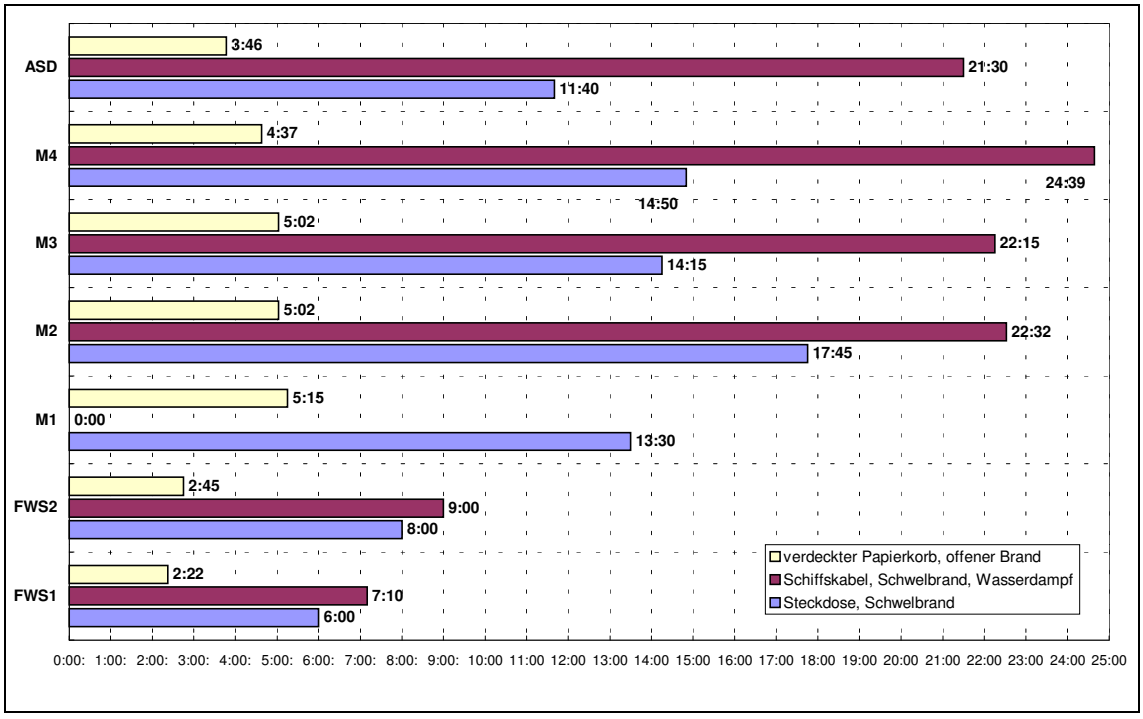

Abbildung 6: Darstellung der mittleren Ansprechzeiten bei Brandversuchen mit Kabel- und Papierbränden

Bei Auswertung **aller** verfügbaren Ergebnisse lassen sich folgende Aussagen zur Ansprechwahrscheinlichkeit machen:

1. Die mittleren Ansprechzeiten aller Sensoren liegen in einem Bereich von ca. 2,5min bis ca. 24min. Dabei werden offene Brände schneller erkannt, während die Detektion der schwachen Schwelbrände deutlich länger dauert.
2. Die mittleren Ansprechzeiten der Melder M1-M4 sind am höchsten, die Frühwarnsysteme sprechen am schnellsten an. Die mittleren Ansprechzeiten des Luftansaugsystems liegen dazwischen.
3. Der Einfluss der Lüftung ist vernachlässigbar, d.h. die mittleren Ansprechzeiten waren bei den Versuchen mit Lüftung um durchschnittlich 10s erhöht bei den an/in der Abluft installierten Sensoren.
4. Die Falschalarmhäufigkeit ist unter Berücksichtigung der verwendeten Störgrößen sehr klein, es erfolgte von keinem Sensorsystem eine charakteristische Detektion.

7. Fazit

Die gegenwärtig eingesetzte bzw. verfügbare Technologie zur Branderkennung im Kabinenbereich auf Seeschiffen zeichnet sich durch eine sehr hohe Stabilität gegen Falschalarmauslösung aus. Es kommt in keinem Fall zu einer Detektion der typischen Störgrößen (Wasserdampf, Tabakrauch, Reinigungsmittel u.ä.).

Die festgestellten Ansprechzeiten sind in Hinsicht auf die besonderen Anforderungen der Seeschifffahrt nicht akzeptabel. Vor allem die Punktmelder detektieren im Mittel deutlich zu spät. Zumindest aus Sicht der Wirksamkeit wären hier die Luftansaug- bzw. die Gasanalysetechnologie vernünftige Alternativen.

Im Vergleich zu einer früheren Untersuchung (Untersuchungen zur Ansprechwahrscheinlichkeit von Branderkennungsensoren unter realen Bedingungen im Schiffsbetrieb, Vortrag auf der AUBE ´95) ist eine Entwicklung der Branderkennunsgtechnik eindeutig festzustellen. Das betrifft hauptsächlich die Falschalarmhäufigkeit. Aber ebenso ist die Weiterentwicklung neuer Technologien zu verzeichnen. Vor allem diese haben das Potenzial, die nötige Zuverlässigkeit und Wirksamkeit für diesen speziellen Anwendungsfall zu erbringen.

Zurzeit erscheint es sinnvoll, auch aus ökonomischer Sicht, eine Kombination der verschiedenen Systeme zum Einsatz zu bringen. Voraussetzung dafür ist die vorausschauende Risikoanalyse und -bewertung der Brandgefährdung auf Seeschiffen.

Charles D. Litton, Kirk R. Smith, Rufus Edwards, and Tracy Allen
Pittsburgh Research Laboratory, Pittsburgh, PA 15236, USA

Combined optical and ionization techniques for measurement and characterization of sub-micrometer aerosols

Abstract

Previous research has indicated, and it is generally accepted, that ionization-type smoke sensors respond better to smaller smoke particles produced during the flaming stages of fire while photoelectric-type smoke sensors respond better to the larger particles produced from smoldering fires. Litton[1] has reported a series of detailed experiments that demonstrate and quantify these effects for a range of flaming and smoldering fires and for particles produced from the exhausts of diesel engines. This paper develops the theory that explains the previous experimental results and then presents the results of a series of experiments to define ionization and optical responses to sub-micrometer aerosols of known size distributions and mass concentrations. In the experiments, simple combination ionization/photoelectric smoke detectors were modified so that continuous signals could be measured for both the ionization and optical components. The sensors (3) were then exposed to narrowly-distributed aerosols produced by a standard laboratory aerosol generating system with number mean diameters that varied from about 90 nm to 600 nm with GSD's typically in the range of 1.4 to 1.5. During the experiments, mass concentrations and particle size distributions were measured independently. The results of these experiments indicate that a simple theory is adequate to describe the operation of the sensor and presents correlations and techniques that will allow the sensor to be used for measurement and characterization of aerosols over a broad spectrum of possible applications related not only to fire detection but also to environmental measurements of combustion-generated aerosol mass concentrations, surface concentrations and particle sizes.

[1] Litton, C. D. The Use of Light Scattering and Ion Chamber Responses for the Detection of Fires in Diesel Contaminated Atmospheres. Fire Safety Journal, vol. 27, pp. 409-425, 2002.

Thomas G. Cleary
Building and Fire Research Laboratory
National Institute of Standards and Technology
Gaithersburg, MD 20899 U.S.A.

Time Resol ed Si e Distributions of Test Smokes and uisance Aerosols

Abstract

An electrical low-pressure impactor (ELPI) has been used to measure the size distribution of various test smokes and nuisance aerosols generated in the fire emulator/detector evaluator (FE/DE). Previously reported size results were time-averaged values with sampling times on the order of five minutes required to collect a weighable amount. The ELPI is a 12-stage cascade impactor that separates particles between an aerodynamic diameter size range of 0.03 μm to 10 μm, which covers a wide range of particle sizes of interest in smoke alarm research. A complete size distribution is recorded every 10 s. The size distributions of several test smokes including: propene soot, smoldering cotton, and smoldering wood smoke were measured throughout smoke alarm exposure tests. The size distribution of several nuisance aerosols including: dust, cigarette smoke, and cooking smokes were also measured. Additionally, comparisons were made between the ELPI results and results from a tapered element oscillating microbalance and the measuring ionization chamber.

Introduction

Smoke alarm response is a function of the amount of aerosol present in the sensing volume, and the properties of that aerosol. The particle size distribution of an aerosol is a characteristic that influences the response of photoelectric (light scattering alarms), ionization alarms, and light extinction-based alarms. Size distribution information has been gathered on smokes used in fire alarm studies and test methods 1-4 . The range of the size distributions of all aerosols of interest covers nanometer sized particles to particles potentially greater than 10 micrometers, or upwards of 4 orders of magnitude. Low-pressure impactors can cover a range from the largest size of interest, down to less than 50 nanometers. Here, the response of an electrical, low-pressure impactor (ELPI), developed at the Tampere University of Technology, 5 was used to measure temporal

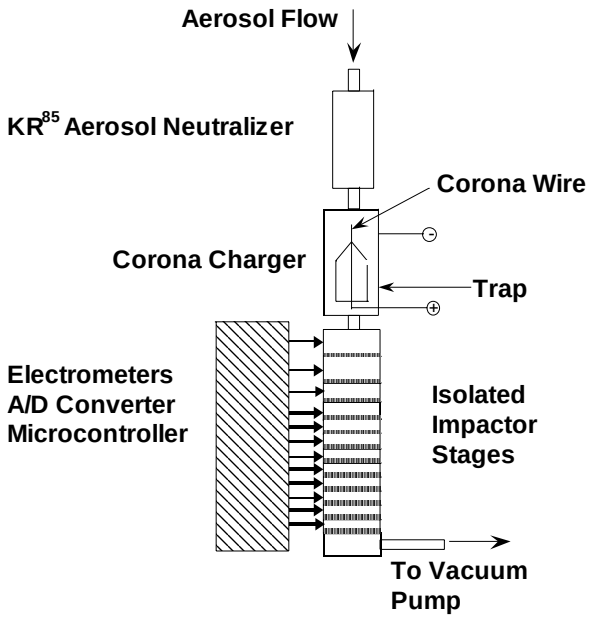

Figure 1 Schematic of the I

size distributions of several test smokes generated in the fire emulator/detector evaluator. It measures the size distribution over an aerodynamic diameter size range of 0.03 – 10 μm in 12 discrete channels. It has a temporal resolution on the order of 5 s. A schematic diagram of the instrument is given is Figure 1, and it is commercially available from DEKATI LTD[1].

A performance evaluation of the instrument was conducted, and results of the number distribution compared favorably with another standard aerosol sizing instrument 6 . The instrument consists of a 12-stage multi-orifice, low-pressure impactor that classifies particles according to their aerodynamic size (equivalent diameter unit density sphere.) Beginning at the first stage, particles of a narrow size range (defined by a cut-off size) impact on that stage s collection plate, while smaller particles move on to the next stage. The process repeats itself until the last stage is reached. The flow through the instrument is 10 l/min. Typically, cascade impactors rely on a gravimetric determination of the amount of particles collected on any stage, thus the sampling time must be sufficient to gather a weighable amount of material on each stage. This impactor is unique in that it detects particles that impact on the different stages by measuring the charge transferred to the stage from the elemental charges carried by the particles. Aerosol particles will achieve a statistically average charge level based on particle diameter, initial charge state, and exposure to charging mechanisms. The ELPI conditions the aerosol to such a state by a two-step process. The initial charge state is forced to an equilibrium, Boltzmann charge distribution by passing the aerosol through

[1] Certain commercial products are identified to adequately describe the experiment. This in no way implies endorsement from NIST.

a charge neutralizer (external to the ELPI). Then, a high-voltage corona wire unipolar charger puts known a excess charge on the aerosol particles based on their size and the residence time the aerosol remains in the charging section. Excess ions and very small charged particles are removed by an ion trap just past the charger. Each impactor stage is electrically isolated and connected to an electrometer. As aerosol particles impact on the various stages, they transfer their charges and a current is measured. From the current measurement, impactor stage cut-off sizes, flow through the instrument, and the relationship between the particle size and average charge, the number of particles that impact each stage is computed and the number size distribution is characterized. The number distribution can be converted into diameter, surface area, or mass distribution, etc., and the total number, or mass (assuming spherical unit density particles) can be computed.

perimental

All aerosols were generated and sampled from the fire emulator/detector evaluator, described in detail elsewhere 7,8 . Briefly, it is a single pass wind tunnel that is used for smoke alarm research. The aerosols were isokinetically sampled from the center of the duct in the test section, below the measuring ionization chamber, which in turn, was mounted on the duct ceiling. The aerosol passed through a Kr^{85} neutralizer then was split between the ELPI and other aerosol measurement instruments including a tapered-element, oscillating microbalance (TEOM), an instrument that records real-time mass concentration of the aerosol. The TEOM has an estimated standard uncertainty of 0.5 mg/m^3.

The test aerosols examined include soot from the propene smoke generator attached to the FE/DE. Smoldering cotton and smoldering beech wood block smokes similar to the smolder sources in EN 54 part 9 9 were generated. Nuisance aerosols included cigarette smoke from two lit cigarettes placed inside the FE/DE, ISO test dust injected into the FE/DE from a constant dust feeder, and smoke from bread toasting in a toaster placed inside the FE/DE duct. Full details on the methods of smoke and nuisance aerosol generation are provided in 8 .

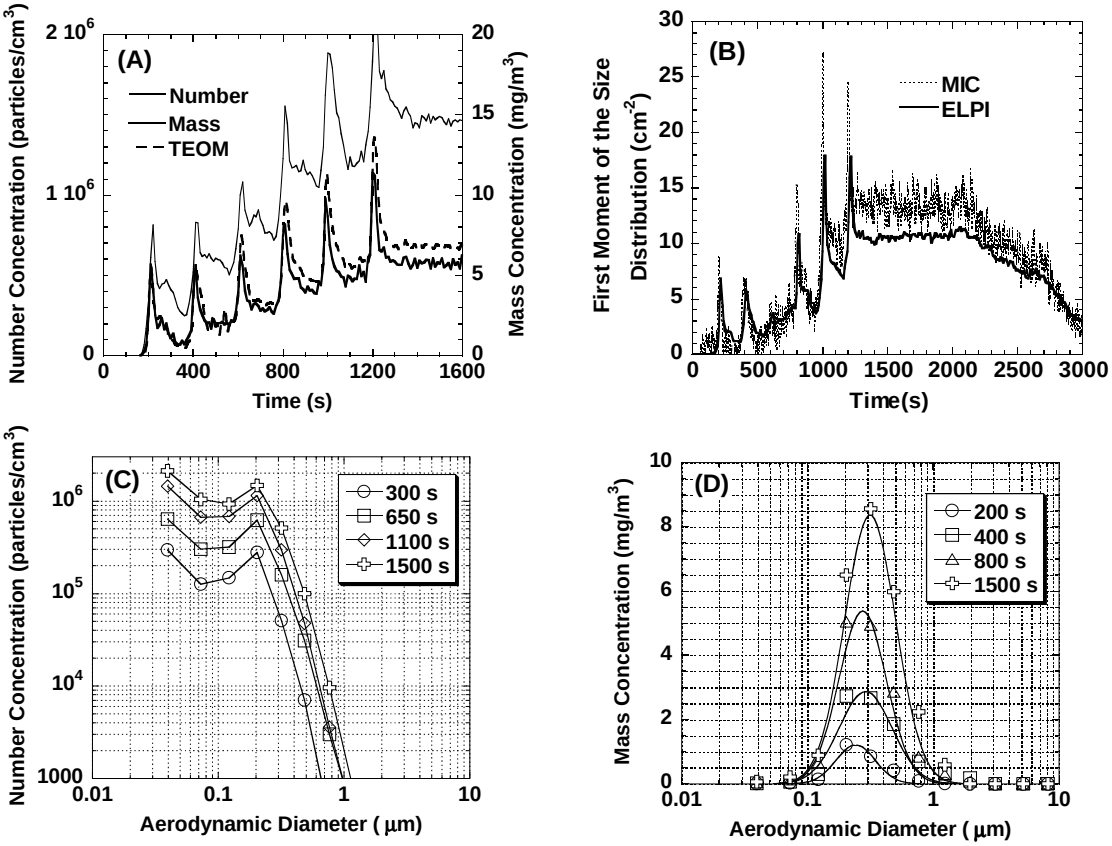

Figure Results for cotton smolder smoke

Results and Analysis

Figure 2 shows the results for cotton smolder smoke. At 200 s intervals, sets of wicks (two wicks for the first four intervals, and four wicks for the next two intervals) were ignited. Figure 2A shows the number and mass concentration from the ELPI, and the mass concentration (aerosol density assumed to be 1.0 g/cm^3 here, and likewise the same for subsequent aerosols, except ISO dust) from the TEOM. The ELPI mass concentration follows the TEOM mass concentration trend, though it recorded a lower value. Figure 2B shows a comparison of the measuring ionization chamber (MIC) results and the ELPI diameter averaged size distribution. The MIC results were converted into the first moment of the size distribution (the first moment is equal to the sum of all particle diameters, and on a unit volume basis it has the units of length $^{-2}$.) from the correlation provided by Fissan, 10 and their chamber constant of 0.033 cm^2 (standard uncertainty 0.005 cm^2.) The ELPI data reduction program was used to compute the first moment of the size distribution. The MIC first moment was slightly

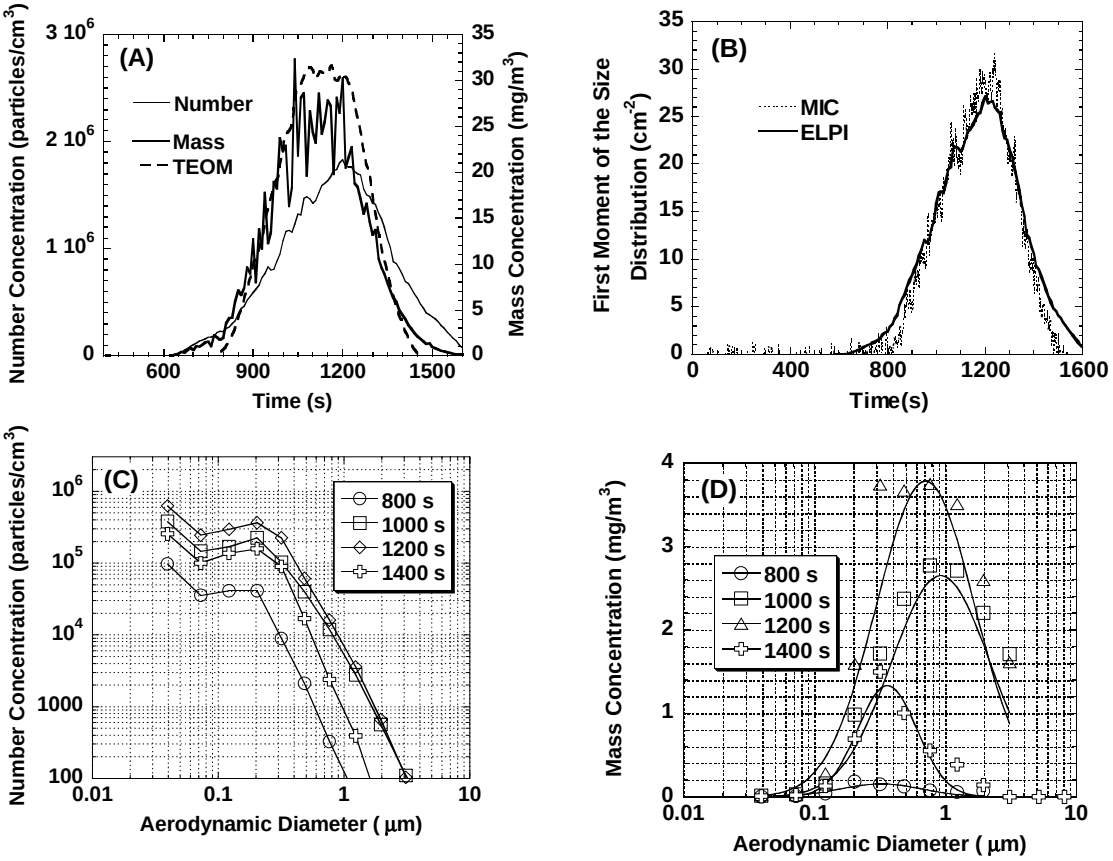

Figure Results for ood smoke

higher than the ELPI first moment, but it is within the uncertainty of the estimate. The difference could be due in part to the fact that the ELPI does not count particles below 30 nm. Figure 2C shows the number distribution at four discrete times. The number of particles (per unit volume) that were impacted on a particular stage are plotted against the geometric midpoint of the stage cutoff size and the stage above it. The shapes of the four distributions are similar suggesting the size distributions were similar, and only the concentrations were different. The data also suggest the size distribution is bimodal with a number peak at a size range below the lowest resolvable size. Figure 4D shows the mass distribution at four discrete times. The smooth curves through the data points are best-fit curves fitted to a lognormal size distribution. The mean size and the width of the distribution appear essentially constant at those times.

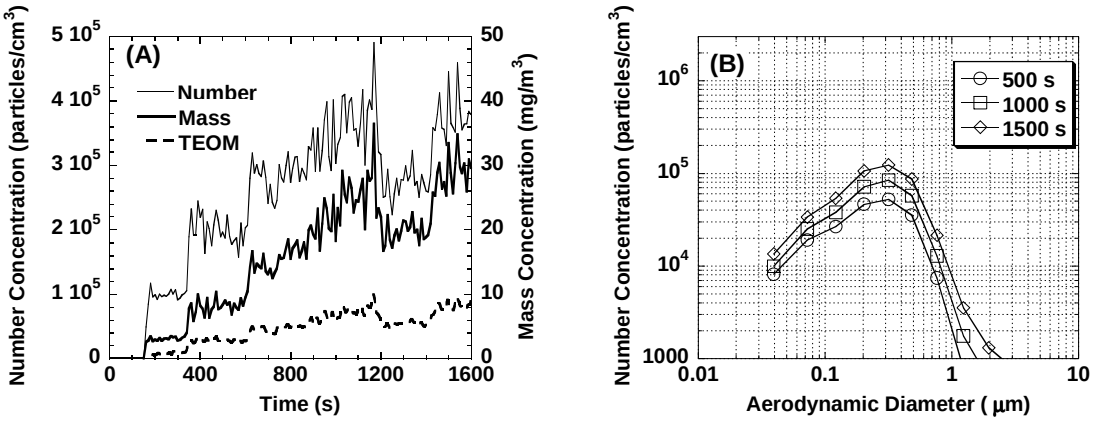

Figure Results for soot

Figure 3 shows the results for wood smoke. Figure 3A shows the ELPI mass peak was lower than the TEOM peak, but the trends were the same. Figure 3B shows that the first moment calculations were similar. The number distribution at four different times is plotted in Figure 3C. Similar to the cotton smolder smoke, the wood smoke appears to have a bimodal number distribution. Figure 3D shows the mass distribution at four times. The mass mean diameter appears smaller at the beginning and end of the smoke production (800 s and 1400 s), and overall was larger than cotton smolder values.

Figure 4 shows the results for soot. Figure 4A shows that the ELPI and TEOM mass concentrations differ by upwards of 200 %. Figure 4B show the number distribution at three discrete times for reference. There are several issues concerning measuring soot in the ELPI. First, soot is characterized as a fractal agglomerate made up from a number of primary particles typically on the order of 30 nm in diameter 11 . Using a cascade impactor for soot agglomerates is much more unforgiving than for more compact aerosols. The gross size of an agglomerate is larger than its aerodynamic size even though the bulk density of soot primary particles is close to 2 g/cm^3 12 . So, even if the aerodynamic diameter is known, an apparent density is needed to compute the particle mass from the aerodynamic diameter. Furthermore, ELPI software assumes the net charge carried by a particle is determined by the spherical size of the particle. Soot agglomerates tend have a higher charge state than what is estimated by their aerodynamic diameter, which leads to an over-prediction of the number of soot

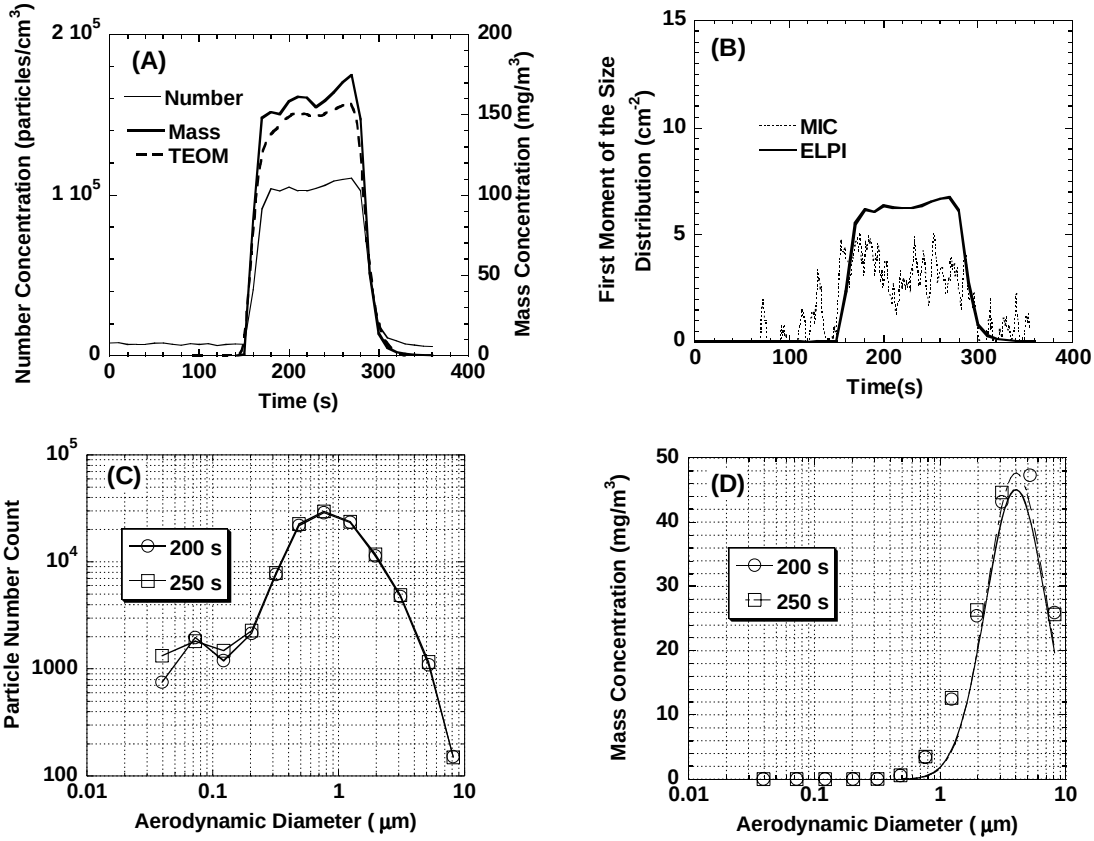

Figure Results for IS test dust

particles impacted on a stage for a given current reading 13 . Van Gulijk ., describe a model that, with further development, could improve the ELPI data reduction scheme for soot 13 .

Figure 5 shows the results for ISO fine test dust. The ELPI data was reduced using the known particle density of 2.65 g/cm^3 for the ISO dust. The ELPI and TEOM mass concentrations were nearly identical. The MIC first moment tended to be less than the ELPI first moment, which could be due to differences in concentration arising from the two sampling heights and the uncertainty in the calculated values. The number distribution shows a large peak at about 0.8 μm, which is attributed to the dust, and a flat section at smaller sizes, which was probably due to ambient aerosol in the FE/DE flow. The mass distribution shows a peak a 4.0 μm.

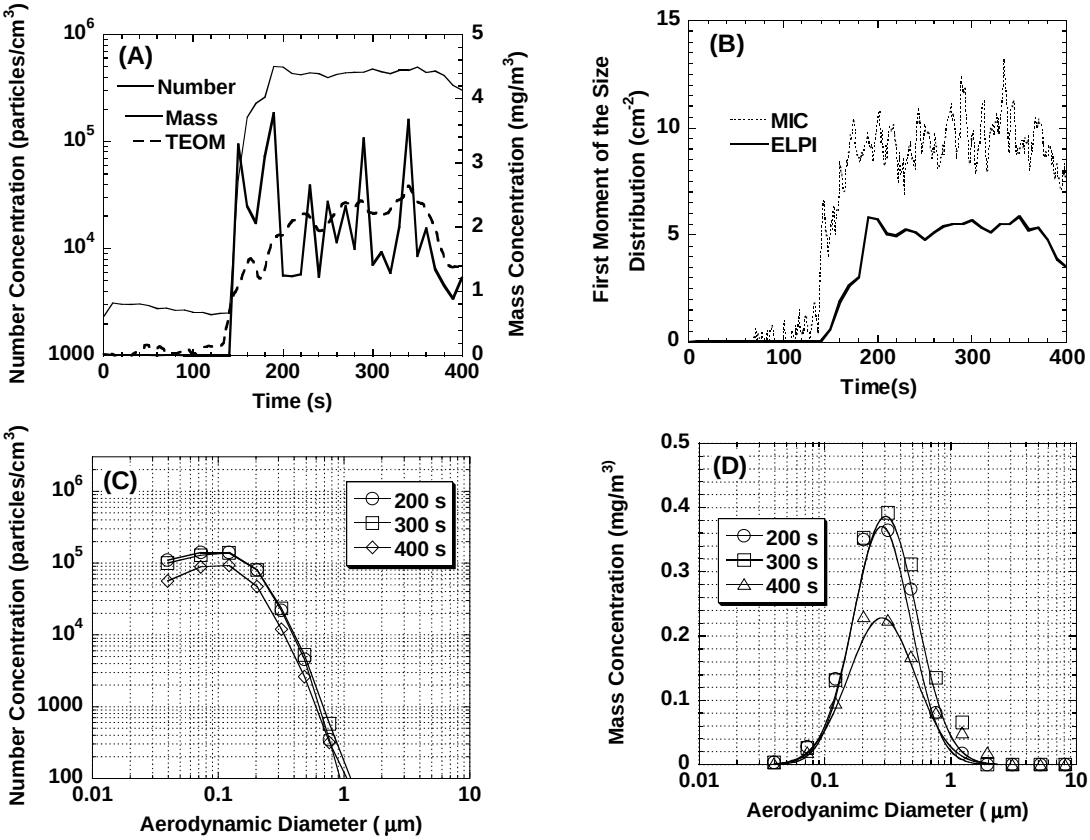

Figure Results for t o cigarettes

Figure 6 shows the results for cigarette smoke from two lit cigarettes placed inside the FE/DE. The ELPI and TEOM mass concentrations were similar; the fluctuations in the ELPI mass concentration were most likely due to the ELPI electrometer gain selection. The MIC first moment was larger than the ELPI value. Figure 6C shows that the number concentration from the ELPI misses a lot of particles smaller than 0.03 μm, which is probably main the cause of the moment differences. The mass mean diameter for the cigarette smoke was about 0.3 μm.

Figure 7 shows the results for one slice of white bread toasting in a toaster. The ELPI and TEOM mass concentrations are quite different before 300 s. The ELPI indicated mass earlier than the TEOM. After 300 s the two instrument mass concentration measurements agreed much better. The first moment calculations were far apart until about 320. Clearly, the nature of the toasting bread aerosol was causing problems with

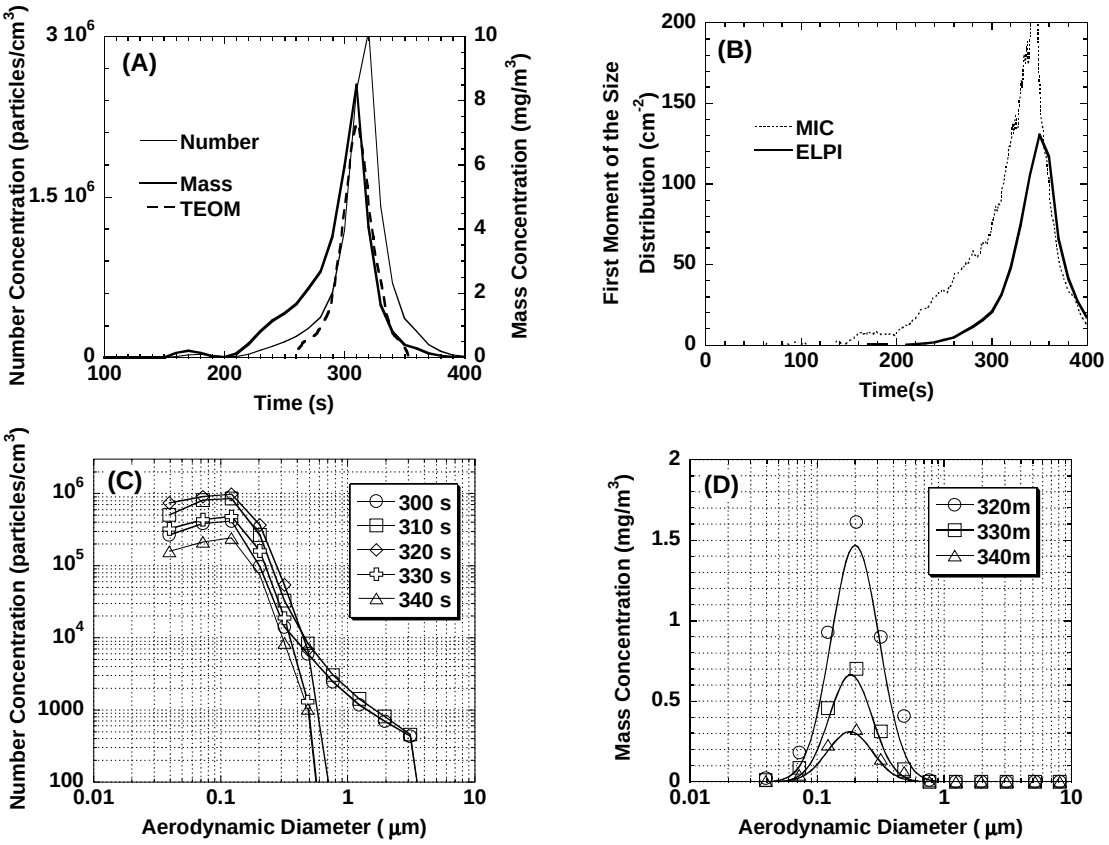

Figure Results from toasting bread

the instrument data reduction scheme. The number distribution shows the effects of this error. A tail at large particle sizes was evident at times below 330 s, which leads to the mass concentration and first moment errors. Figure 7D shows the mass distribution using the data from stages with a cut-off size less than 1 μm.

Conclusions

The ELPI showed that it could measure the size distributions of several test aerosols used in smoke detector research. It provided temporally resolved results, and in many cases compared favorably with other measurements. While the ELPI covers a very wide size range, the fact that it does not measure the size distribution below 30 nm means some aerosols are not fully characterized. The commercial ELPI does have the provision of an extra 13th stage back-up filter that collects all particles below 30 nm, and which would provide more quantitative information on the concentration of the

small particles. There were some problems with soot aerosol, and the early aerosol produced from the toasting bread, that led to suspect results. For the most part, careful attention to the operation of the instrument, and interpretation of the results, yields valid size distribution information.

References

1 Helsper, C., Fissan, H., Muggli, J., and Scheidweiler, A., "Particle Number Distributions of Aerosols from Test Fires," J. Aerosol Sci., Vol. 11, pp. 439-446, 1980.

2 Tamm, E., Mirme, A., Sievert, U., Franken, D., "Aerosol particle concentration and size distribution measurements of test-fires as background for fire detector modeling," 11th International Conf. on Automatic Fire Detection AUBE 99, Duisburg, Germany, pp. 150-159, 1999.

3 Weinert, D., Cleary, T., and Mulholland, G., "Size distribution and Light Scattering Properties of Test Smokes," 12th International Conf. on Automatic Fire Detection AUBE 99, Gaithesburg, MD, USA , pp. 58-70, 2001.

4 Weinert, D., Cleary, T., Mulholland, G., and Beever, P., "Light Scattering Characteristics and Size Distribution of Smoke and Nuisance Aerosols," Seventh International Symposium on Fire Safety Science, ed. Evans, D., pp. 209-200, 2002.

5 Keskinen, J., Pietarinen, K., and Lehtimaki, M., "Electrical Low Pressure Impactor," J. Aerosol Sci., Vol. 23. No. 4, pp. 353-360, 1992.

6 Marjamaki, M., Keskinen, J., Chen, D., and Pui, D., "Performance Evaluation of the Electrical Low-pressure Impactor (ELPI)," J. Aerosol Sci., Vol. 31, No. 2, pp.249-261, 2000.

7 Cleary, T., Donnelly, M., and Grosshandler, W., "The Fire Emulator/Detector Evaluator: Design, Operation, and Performance," 12th International Conf. on Automatic Fire Detection AUBE 99, Gaithesburg, MD, USA , pp. 312-323, 2001.

8 Bukowski, R., Peacock, R., Averill, J., Cleary, T., Bryner, N., Walton, W., Reneke, P., and Kuligowski, E., "Performance of Home Smoke Alarms," NIST Tech. Note 1455, 2003.

9 EN 54: Components of Automatic Fire Detection Systems, European Committee for Standardization, Parts 1-9, 1988.

10 Helsper, C., Fissan, H., Muggli, J., and Scheidweiler, A., "Verification of Ionization Chamber Theory," Fire Technology, Vol. 19, No. 1, pp. 14-21, 1983.

11 Samson, R., Mulholland, G., and Gentry, J., "Structural Analysis of Soot Agglomerates," Langmuir, 3, pp. 272-281, 1987.

12 Cleary, T., "Measurement of the Size Distribution, and Aerodynamic Properties of Soot," MS Thesis, University of Maryland, 1989.

13 Van Gulijk, C., Marijnissen, J., Makkee, J., Moulijn, J., and Schmidt-Ott, A., "Measuring Diesel Soot with a Scanning Mobility Particle Sizer and an Electrical L-Low-Pressure Impactor: Performance Assessment with a Model for Fractal-like Agglomerates," J. Aerosol Sci., Vol. 34, pp. 633-655, 2004.

Chen Nan

Fire Protection Engineering Dept., The Chinese People's Armed Police Force Academy

Langfang Hebei 065000, China. E-mail: chen.pro@263.net

A Smoke Particle Measuring Method of Laser Scattering and It's Applied Researches

Abstracts

According to the requirement of the detecting intelligence in fire detecting and alarming systems, the laser scattering processing method of small smoke particles in earlier fire parameters is analyzed in this Paper. The artificial intelligence detecting arithmetic of earlier fire detecting data is put forward, and the testing project and the currently products of the earlier fire detecting and alarming system are introduced.

Introduction

In the fire developing process, the smoke particle concentration is the very important characteristic parameter. It can be realized for the fire detecting and alarming to adopting the photoelectric smoke detecting principle[1]. It has obtained the great progress in engineering applications which is the analysis technique of the particle size and concentration based on the laser detecting method since 1970's, but the laser diffraction detecting method of the particle measurement is only suitable to particles whose size is over 5 micron and can't satisfy with the small particle measurement of earlier fire smoke granules[2]. When measuring earlier fire smoke particles, it is provided with the practicability to adopt the method of the sensitive laser smoke fire detection based on the Mie scattering principle [3].

The measuring principle of smoke particles in earlier fire parameters

Based on the scattering ray characteristic of the tiny smoke particle, the laser detecting technique is efficiently adopted to measure the concentration of smoke particles in

initial fire. If the granule group of all M entries granule in the forepart fire smoke is divided into L grades in terms of the granule size, the granule group in every grade i ($i=1,2,\ldots,L$) has the granule number M_i , the granule size d_i and the same granule shape. Then the particle distributing characteristic of all M entries smoke granule in random is provided with the following predigesting simultaneous equation[4].

$$I_{sc} = C_1 \sum_{i=1}^{L} d_i^2 M_i Q_{sc}(a_i, m) \tag{1}$$

$$\ln\left(\frac{I_0}{I}\right) = C_2 \sum_{i=1}^{L} d_i^2 M_i Q_{ex}(a_i, m) \tag{2}$$

Where, I_{sc} is the intensity of the scattering ray; I_0 is the intensity of the incidence ray; I is the intensity of the permeation smoke ray; C_1 and C_2 is the constant correlated with the length of laser carry; a_i is the scale parameter of the scattering particle in grade i; m is the refractive index; $Q_{sc}(a_i, m)$ is the scattering efficiency factor; $Q_{ex}(a_i, m)$ is the extinction efficiency factor.

The smoke granule distribution [$M_1, M_2, M_3, \ldots, M_L$] and its concentration can be obtained by measuring the real parameter I_0, I and I_{sc}, and computing the simultaneous equation (1) and (2). The software which analyzes the granule size distribution and concentration of the smoke particle may subsequently be compiled.

The detecting arithmetic of earlier fire detecting data

In the fire signal disposal process, basing on the laser scattering measuring principle of the smoke particle concentration and synthesizing the detecting request and the parameter variety, for example the temperature etc., in initial fire locale, the fire detecting intelligence can be realized using the neural network configuration in Fig.1 which bases on traditional the three layer BP neural network model[5,6] reconstructed by the wavelet analysis method.

In Fig.1， the signal x_1 and x_2 of the input layer IN represent separately the smoke concentration output of the laser scattering smoke detector and the temperature output of the semiconductor temperature detector in the unitary value, which its region is in

0~1; the signal y of the output layer OT is the probability of the fire occur; the connotative layer IM is the wavelet neural cell, which adopts the non-linearity wavelet radix instead of the non-linearity Sigmoid[6] function in the traditional BP neural network model. Between the connotative layer IM and the output layer OT, if the w_j is the authority value and the t_{ij} and d_{ij} ($i=1,2$; $j=1,2,...,N$; the N is the node number of the wavelet radix) represent separately the translational factor and the flexible factor, the signal can be imitated as follows by using the wavelet radix $\psi(t,d,x)$.

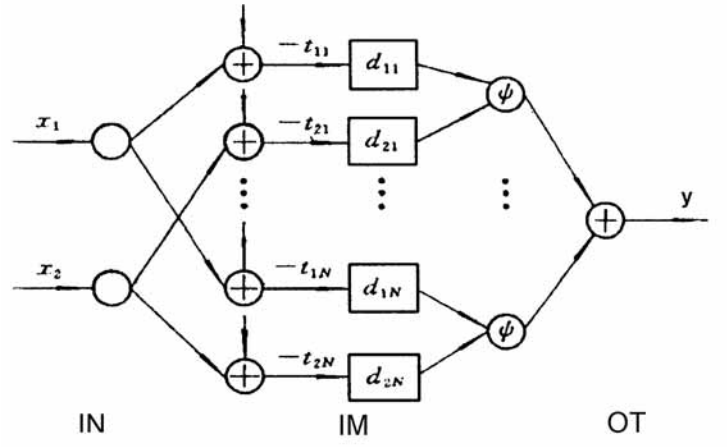

Fig. 1 The neural network based on the wavelet analysis method

$$\tilde{y} = \sum_{j=1}^{N} w_i \psi\left(t_{1j}\left(x_1 - d_{1j}\right) \cdot t_{2j}\left(x_2 - d_{2j}\right)\right) \tag{3}$$

In the formula (3), following the mother wavelet $\psi(x)$ and the energy function E of the least mean-square error are used.

$$\psi(x) = x^T x \cdot \exp\left(-x^T \cdot x/2\right) \tag{4}$$

$$E = \frac{1}{2}\sum_{j=1}^{T}\left(y - \tilde{y}\right)^2 \tag{5}$$

Where, the T is the sample mode number. While the w_j, t_{ij} and d_{ij} are optimized using the conjugate gradient method in the same time, a better configuration of the initial neural network can be obtained till the E is less than certain scheduled error or the cycle of the operation program is end.

The testing project of the smoke particle detecting arithmetic

Through training and testing the above initial neural network by the standard fire in Europe Standard EN54 Part9, the result is very similar as the reference [7], which the mean-square error of the wavelet neural network is less than the BP neural network. Analyzing the experiment result of the wood fire shown in Fig.2[7], in which the broken line and real line of the graph (a) represent separately the unitary output value of the smoke detector and the temperature detector, and the graph (b) is the variety of the fire probability, it is obvious that the fire probability increases and is in favor of the earlier fire detection.

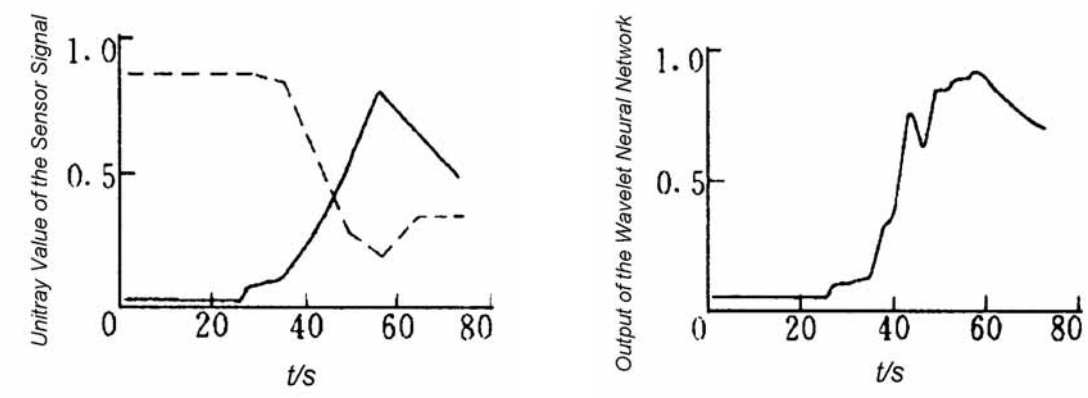

(a) (b)

Fig.2 The experiment result of the wood fire by Europe standard

The product analysis of earlier fire detecting and alarming systems

GO-DEX high sensitivity aspirating smoke detection system (Thereinafter shortened form: GO-DEX System) is one of the typical systems, which adopts the smoke detecting principle of the laser scattering, the active air sampling method of the detecting environment, the intelligent fire detecting arithmetic of the neural network and the dust identify technique of detecting parameters. The working principle of GO-DEX System is shown in Fig.3, in which the filtrated sampling air of the detecting region is sent into the testing room, the parallel laser beam of the LASER irradiates the air and gives birth to the scattering ray of the smoke particle and the laser receiver at high

sensitivity receives the scattering light of the concave mirror and produces photoelectric signals. Afterwards, the reliable fire information can be obtained by use of the similar formula (1)~(3).

The influence of the environment temperature and air current and dust pollution is compensated in course of the GO-DEX System's fire detecting process. Using the special chip of the artificial neural network arithmetic and the appropriative analysis software of GO-DEX Classifire^{TM}-3D, which can efficiently deal with the scattering light signal of the smoke particle, the environment temperature parameter and the dust pollution information, GO-DEX System can provide the very accurate and reliable sensitivity setting which its range is from 0.0015% Obs/m to 5% Obs/m, and can output the fire alarming signal in the different grade.

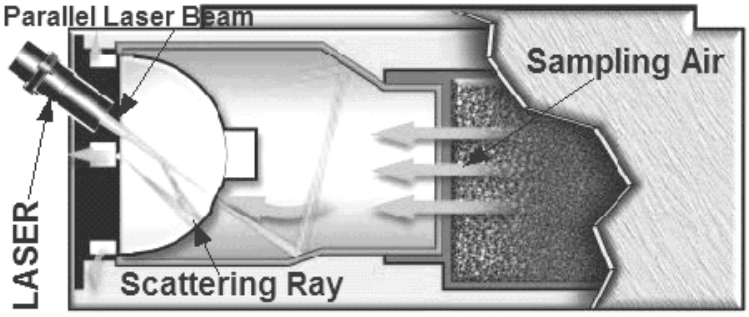

Fig.3 Sketch of the elemental working principle in GO-DEX System

For example, the smoke concentration characteristic of the smoke contaminated environment at the manufactory, the tunnel and the microwave room is shown in Fig.4, and the smoke concentration characteristic of the clean environment at the telecom room, the pharmacy factory and the nonexistent dust room is shown in Fig.5. Basing on the stretch mean of the smoke particle concentration in fire detecting region and combining with the deviation value lain on the environment factor, GO-DEX System can automatically compensate for the environment influence by means of the following formula：

$$S_e = k \times D \tag{6}$$

Where, S_e is the excursion value of the laser detector output signal; k is the compensable extent which is confirmed by the fire detecting arithmetic; D is the deviation value which lain on the environment factor.

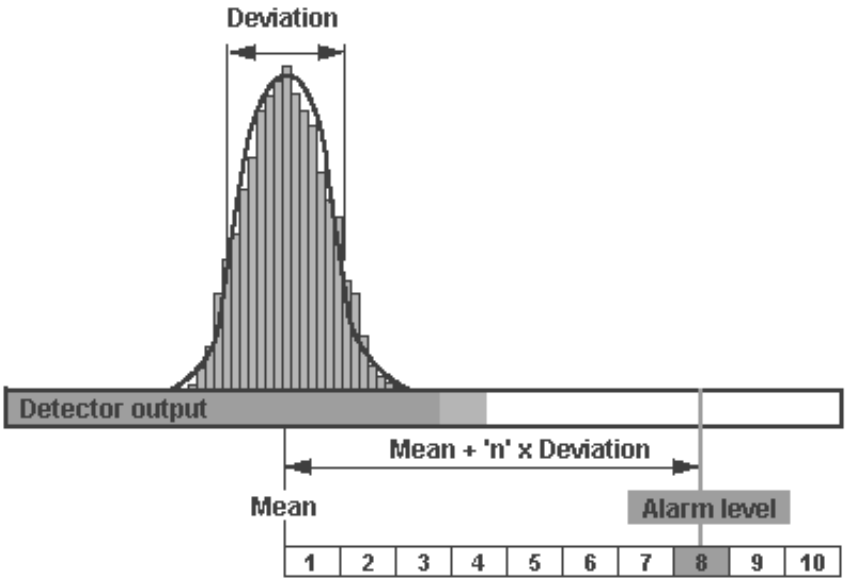

Fig.4 Sketch of the concentration distributing curve in the smoke contaminated environment

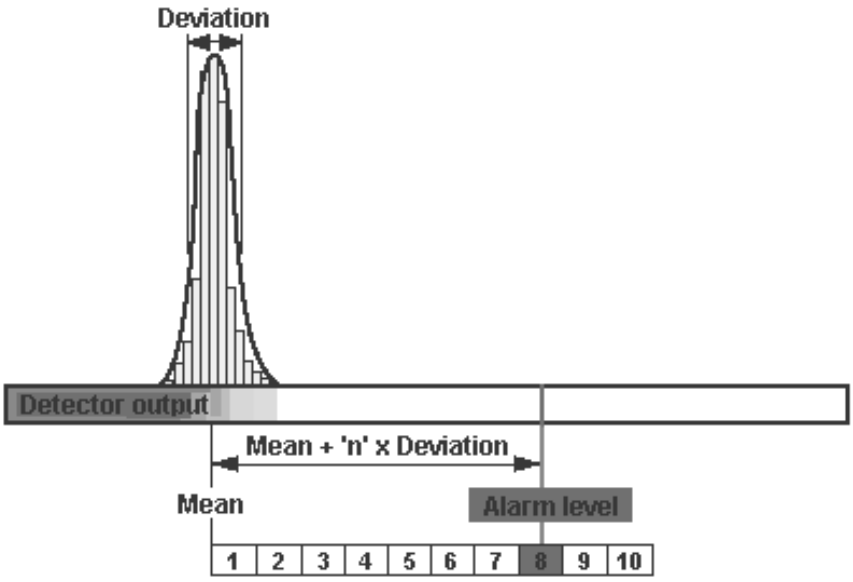

Fig.5 Sketch of the concentration distributing curve in the clean environment

According to the compensable extent of above, GO-DEX System can choose the fire alarm threshold or level, distinguish the smoke contaminated environment with the clean environment, and then adjust the sensitivity of fire detection and alarm so as to make the fault-alarming ratio tend to zero.

Conclusion

Summing up above all, basing on the laser scattering measurement of the smoke particle concentration, the active air sampling of the monitoring environment and the fire detecting arithmetic of the wavelet neural network, the intelligent earlier fire detecting and alarming system can be constructed and used in the high hazard or high expense locale, the tall space and other special site. It is provided with the very doughty surroundings adaptability, the study ability, the fault-tolerant ability and the management ability of parallel signals.

References

[1] M.Loepfe, et al. Optical Properties of Fire and Non-fire Aerosols[J]. Fire Safety Journal, 1997, 29:185~194.

[2] Ren Zhongjing, The Headway of The Modern Laser Particle-analyzing Technique and Its Application[J]. Physics, 1998, 27(3):163~166.

[3] H.C.van de Hulst. Light Scattering by Small Particles[M]. New York:wily, 1957.

[4] Zhao Jianhua, et al. Experimental Study on the Laser Detection of Concentration and Particle Size of Smoke[M]. Laser & Infrared, 2000, 30(5):277~279.

[5] Zhang Q, Benveniste A. Wavelet Network[J]. Proc. IEEE Trans. on Neural Network, 1992, 3(6):889~898.

[6] Han Liqun. The Theory, Design and Application on Artificial Neural Network[M]. Beijing: Chemical Industry Publishing Company, 2002.

[7] Wang Haoran, et al. The Application of a Wavelet Neural Network on Fire Detection[J]. J.Huazhong Univ. of Sci. & Tech., 1998, 26(11):1~3.

MEI Zhibin, SONG Liwei, LI Jian, WANG Zhuofu, LI Ningning
Shenyang Fire Research Institute of the Ministry of Public Security, Shenyang, China

Data Acquisition and Characteristic Analysis of the Early Fire Smoke Aerosol Information

Abstract

This paper illuminates the goal and design of the information acquiring system for early fire smoke aerosol. This system, based on multi-thread message mechanism which is comprehensively integrated with various parameters measuring equipment, has realized acquisition and processing of kinds of such data as particle concentration, particle diameter, temperature and various gas composition and concentration of the early fire. It also analyzes changing features of a different test fire in the realm of time and space, the Matlab Environment when the sensors are mounted on the ceiling of the standard fire test laboratory at different places or different heights, furthermore the system offers basic data for establishing a multi-thread intelligent fire detection platform.

1. Introduction

The early detection of any fire conduction is one of three critical links in achieving fire suppression and extinguishing techniques. [1] Along with the economic and social developments, hazards and loss caused by fire to the society of mankind are more and more serious. The objective of fire detection is just to achieve a reliable time for fire extinguishing and emergency escape. In order to reduce fire loss to the minimum, it is very important to detect fires as earlier as possible. According to statistics, there are 5,000 to 6,000 thousands of fire detectors installed in the nation’s buildings each year, about eighty percent among them are smoke detectors. It is found from practice that phenomenon of false, miss and delay alarms often occur from the conventional fire detection methods which generally detect fires in a way of a single physical parameter threshold value type [2], and the fact shows that a large quantity of fire incidents causing life injures and deaths and property loss are related to detection reliability. Therefore, it is necessary to make a study of early characteristics of fires with its focus in developing multi-thread intelligent fire detection methods based on fire products and process so as to make the early detection of fire to become possibility.

In recent years, Shenyang Fire Research Institute of the Ministry of public Security has designed and established a multi-thread data acquisition system of smoke aerosol characteristics of the early fires under the fund support of the national item ‘973’ Derivative and Preventive Base of Fire Dynamics and other related Items, which has promoted study of multi-parameter and multi-criterion fire detection methods through successively acquiring fundamentally dynamic data on early fire products and process.

2. Design of the multi-thread data acquisition system

2.1 Design thinking

A fire is a complicated physical change and chemical reaction process .As pyrolytic and combustion products, smoke aerosol is the main phenomenon and basic feature occurred in the early duration of a fire. The multi-thread data acquisition system of the early fire smoke aerosol mainly performs a real-time acquisition of the parameters, the basic objective information such as composition and concentration of produced gases involved in smoke aerosol, particle concentration, particle diameter and heat [3] output, there combined change process in the realms of time and space and etc.

2.2 Comprehensive integration of multi-thread data communication techniques

Due to diversification of present fire detection principles and difference of smoke concentration measuring modes, thus various sensing and measuring equipment shall be applied in acquisition of the early smoke and gas parameter information of a fire. The following table 1 shows type selection of equipment for acquiring data about the early smoke and gas characteristics of a fire.

The data acquiring, measuring and sensing equipments had originally their own systems with different information output forms and more output variety. Especially the three smoke detectors had different bus communication formats and protocols and could only communicate with corresponding fire alarm control units, and had no capability to return detection analogue information in real time in the communication with a computer. Therefore, these equipments had no way to be combined together and couldn’t uniform management and communication coordination becomes a critical technique to be achieved by this data acquisition system.

According to the forms of their information output, these data acquiring, measuring and sensing equipment are grouped as follows:

<table>
<tr><td colspan="2">Smoke and gas parameters</td><td colspan="3">Measuring and sensing equipment</td></tr>
<tr><td colspan="2" rowspan="6">Solid granule parameter</td><td rowspan="4">Particle concentration</td><td rowspan="3">Smoke detector</td><td>Ionization smoke detector USC4701</td></tr>
<tr><td>Forward scattering photoelectric smoke detector JTF-GOQM-HST8140</td></tr>
<tr><td>Backward scattering photoelectric smoke detector JTF-YW-TL2101</td></tr>
<tr><td rowspan="3">Measuring equipment</td><td>Measuring ionization chamber</td></tr>
<tr><td>Obscuration meter</td></tr>
<tr><td>Condensation Particle Counter(CPC3022A-S)</td></tr>
<tr><td>Particle size and distribution</td><td colspan="2">SMPS system--Scanning Mobility Particle Sizer(SMPS3936L22)</td></tr>
<tr><td colspan="2" rowspan="2">Heat parameter</td><td colspan="3">Thermocouple (T type)</td></tr>
<tr><td colspan="3">High-temperature thermocouple (K type)</td></tr>
<tr><td rowspan="4">Gas parameter information</td><td>CO</td><td colspan="3">CO Infrared gas analyzer (QGS-08B)</td></tr>
<tr><td>CO_2</td><td colspan="3">CO_2 Transducer</td></tr>
<tr><td>H_2O</td><td colspan="3">Moisture content scalor(hmp233d)</td></tr>
<tr><td>O_2</td><td colspan="3">O_2 sensor (MF010-0)</td></tr>
<tr><td colspan="2">Gas composition analysis</td><td colspan="3">FT-IR spectroscopy (Avatar370)</td></tr>
</table>

Table1. List of multi-thread data acquiring equipment for the early fire smoke aerosol characteristics

A thermocouple, CO analyzing instrument, CO_2 sensor, humidity and moisture content measuring instrument, oxygen sensor which give a standard output current signal of 4 to 20mA by using a high speed data acquiring card are put under one acquisition sub-group.

Design communication transfer loop board corresponding to detection bus/bus RS485 and respectively transfer digital analogue output in formation from the three smoke detectors into RS485 signal which are forming an acquisition sub-group by using switch RS232/RS485.

MIC and AML whose output are parallel BCD code digital signal are forming an acquisition sub-group by using a photoelectrical isolating data input card.

A precision electron balance which can measure mass of combustion products (burning materials) is independently forming an acquisition sub-group.

Because particle counter/ particle dimension distribution and FT-IR have special communication software and interface and a long period of data acquisition, so they can separately communicate through other computers.

Since information output form of each sub-group are different and their acquired data output speed are not the same too, multi-threading is adopted in data acquisition, i.e. a parallel working mode by which every data acquisition sub-group possesses a thread to acquire data, this mode can improve the system's data acquisition efficiency quite a lot. At the same time, multithreading is also adopted in calculation, transformation, memory and display of acquired data. In this way we can make full use of computer resources, integrally raise processing efficiency of data acquisition.

Therefore through different communication and interface modes of computers, these measuring equipments are classified and combined to perform a parallel acquisition and processing, we have achieved our goals that the system structure is compact, acquisition parameters and sensing equipment can be extended flexibly, speedily and reliably respond to the design objectives. The multi-thread data acquisition system structure of the early fire smoke aerosol characteristics is shown as in the Figure 1.

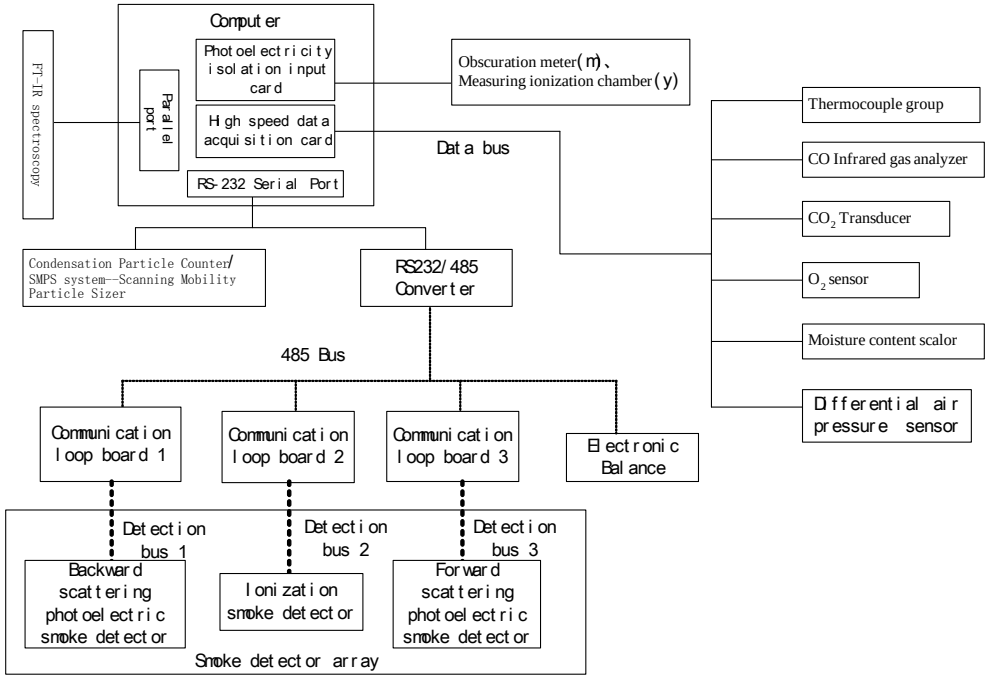

Figure 1. Block diagram of multi-thread data acquisition system structure for the early fire characteristics

3．Design of the test methods

3.1 Test fire

A fire has a dual law of certainty and randomness [1]. For the fire protection of the general civil architecture and industrial buildings, solid fires and liquid fires (confined space, igniting source) are our primary research objects, also the main forms of test fires in the standards of testing fire detectors performance. Due to operability of standard test fires is intensive, and every type has a typical significance, so we have used seven types of test fires selected in standards to perform tests for comprehensively acquiring information of the early fire smoke aerosol characteristics as shown column 2 of the table 2.

3.2 Experimental conditions and methods

Tests were proceeded in the fire testing lab of the China National Quality Supervision and Testing Center of Fire Electronic Products .Because situation of fire detectors installed in sites are possibly different, thus data of every test fire was acquired in multi-group respectively in the ceiling heights of 3m, 4m and 6m, so as to benefit test data complete and valid. Arrangement of materials used fires and measuring equipment, igniting methods and conditions of test fires ended were all to refer to the related specifications of the relative standards, and a video synchronistic record was taken to each group of testing processes, and ignition time and was accurately recorded to benefit data comparison and analysis.

4. Test conclusions and analysis

According to the above test conditions and methods, data acquired from the above tests in different fire types, ceiling heights and groups were picked up and analysed by using software tool Matlab [4], and the characteristic curve of the corresponding output were plotted and result preparatory analysis are as follows:

4.1 Gas composition analysis of the early fire aerosol

Composition of gases produced in combustion processes of seven kinds of standard test fire were measured and analysed by using FT-IR. Gas composition spectrograph of a smoldering cotton fire wick produced in a test room with a ceiling 3m height seen from figure 2.

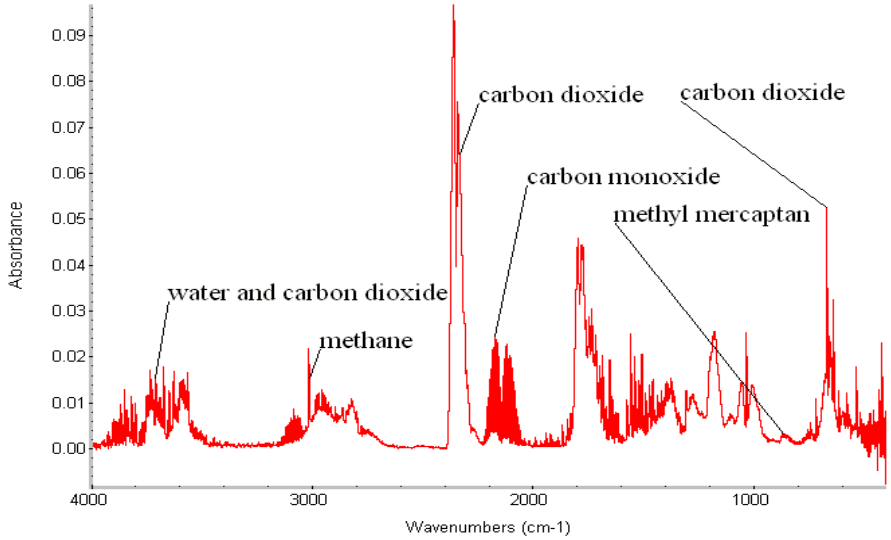

Figure 2　Gas composition spectrograph of a smoldering cotton wick fire in a test room with a ceiling of 3m heights

It is obviously marks given in the figure that CO_2、CO、H_2O、CH_4 and CH_3SH were generated in smoldering process of cotton wicks. Through measuring and analyzing composition of aerosol and gases produced in the seven kinds of standard test fire, we can reach the following conclusions:

There equally exist CO_2、CO and　H_2O produced in the early fire, so CO_2 or CO can be regard as one of fire detection parameters, but H_2O shouldn't be regarded as a fire detection parameter due to its two-way production state. For the major gases produced in the early fires i.e. CO_2 and CO, CO_2 is generated earlier than CO in the developing process of a smoldering fire, but its production intension is much less than CO.

4.2 Test conclusions and analysis of solid smoke particles in the early fires

Particle size and distribution in early fire was tested by using dynamic particle size analysis instrument and particle counter, the result of test in a test room with a variable height (locations for installing detectors) are shown in table 2.

With the development of a fire, the average particle size of each test fire generally tend to enlarge, among them open cellulose (wood) fire demonstrates most obviously (see figure 3) next ones are smoldering (pyrolysis) wood fire and glowing smoldering cotton fire. When every test fire is reaching to the criterion at the end, the average micro particle size of liquid (methylated spirits) fire is minimum (less than 100nm, in common), the average particle size of other test fires is between 150nm and 250nm.

4.3 Test conclusions and analysis of smoke concentration and heat characteristics in the early fires

After acquiring and processing smoke parameter data of each test fire, by using scientific operation superiority and flexible plot output of tool software-Matlab, these data are plotted into corresponding output curve to be analysed according to different contrasted objectives. A comprehensive variation curve for smoke parameter data of open cellulose (wood) fire in a test room with a ceiling height of 3m is shown in the figure 4.

Table 2.Test result of solid smoke particles for each test fire

serial No.	Test Fire	Height of the Ceiling (m)	Particle concentration (per cm^3)		Average value of particle diameter (nm)	
			Value at the end	Value at the start	Value at the end	Value at the start
1	Smoldering (pyrolysis) wood fire ISO-7240-7/GB	3	1.6e+6	1.82e+5	181	89
		4	1.12e+6	9.81e+4	159	90
		6	9.8e+5	2.51e+4	146	83
2	glowing smoldering cotton fire ISO-7240-7/GB	3	2.54e+6	6.01e+4	216	93
		4	2.28e+6	8.71e+4	183	108
		6	1.59e+6	2.66e+4	180	77
3	flaming plastics (polyurethane) fire ISO-7240-7/GB	3	5.17e+6	4.57e+5	226	184
		4	3.51e+6	4.6e+5	217	173
		6	1.64e+6	7.84e+4	201	183
4	Flaming liquid (n-heptane) fire ISO-7240-7/GB	3	4.93e+6	2.6e+5	220	202
		4	3.47e+6	5.23e+5	223	201
		6	3.10e+6	2.64e+5	203	192
5	low temperature black smoke (decaline) liquid fire ISO7240-15	3	9.58e+5	1.82e+5	246	232
		4	2.99e+6	3.68e+5	236	210
		6	8.3e+5	1.65e+5	231	223
6	Liquid (methylated spirits) fire EN54-1	3	2.37e+5	6.57e+4	77	76
		4	1.69e+5	2.09e+4	77	85
		6	8.94e+4	4.49e+4	67	65
7	open cellulose(wood) fire EN54-9	3	2.84e+6	3.5e+5	202	42
		4	2.24e+6	2.87e+5	186	56
		6	2.1e+6	2.32e+5	178	50

Note: Value at the start in the table is particle data acquired at the time a flaming fire is ignited or after one minute when visible smoke appears in smoldering fire, Value at the end in the table is particle data acquired when the test fire is reaching to the criterion at the end.

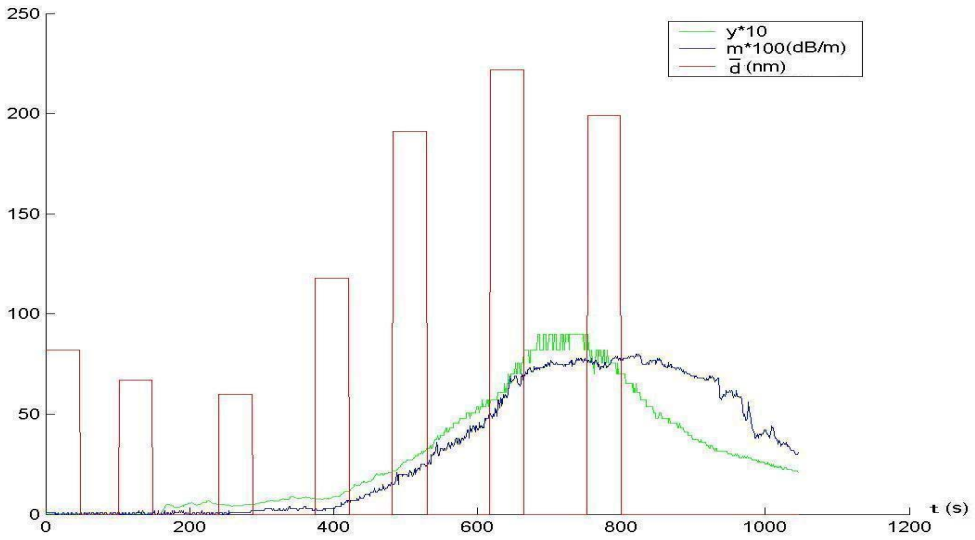

Figure 3 The average smoke particle size variation of open cellulose (wood) fire compared with y-value and m-value (in a test room with a ceiling height of 4m)

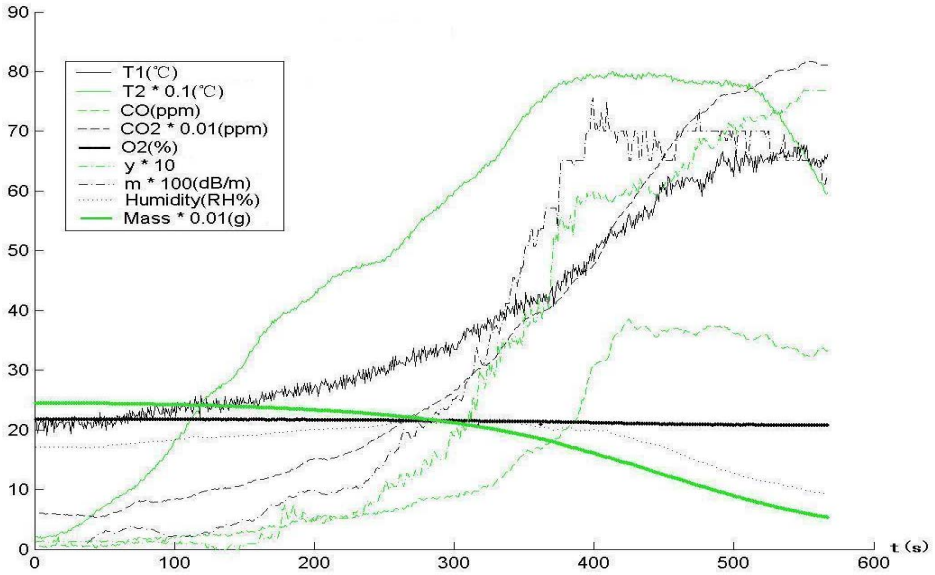

Figure 4 A comprehensive variation curve for smoke parameter data of open cellulose (wood) fire (in a test room with a ceiling height of 4m)

Y-value and m-value of variation character of different test fire and three kinds of smoke detectors response to actual fire indicate that backward scattering photoelectric smoke detectors and ionization smoke detectors have good responsive uniformity to each test fire (except flaming methylated spirits fire). Forward scattering photoelectric smoke detectors have no good responsive performance to black smoke. For a smoldering fire, rise of m-value and is more obvious than that of y-value, so the photoelectric smoke detector is superior to the ionization smoke detector in detecting a smoldering fire. Concentration of particles produced by liquid (methylated spirits) fire is too low to make smoke detectors to effectively respond.

All test fires have generated CO gas in their early process, take a ceiling height of 4m as an example, where CO concentration of a glowing smoldering cotton fire is the highest (about 220ppm), that of a smoldering (pyrolysis) wood fire comes second, and that of liquid (methylated spirits)fire is the lowest(about 18ppm). The above fact accurately shows that the CO gas has a basic characteristic of its production intensity varied with burning intensity of an early fire, in the meantime, concentration of a CO_2 gas generated in a fire also varies with burning intensity, concentration of the CO_2 gas generated in a flaming fire is higher than of a smoldering fire, among them, the highest for the methylated spirits fire (about 7200ppm), the second for the open cellulose (wood) fire, and the least one for the smoldering wood fire (about 780ppm). Moreover, for the same test fire the concentrations of CO and CO_2 gas detectable correspondingly reduce if the more the ceiling is high and the more the space is large.

Characteristic of CO_2 against CO concentration ratio. For the flaming fires, the concentration ratio of CO_2 and CO gases generated in a fire is approximately 10:1 to 1000:1, i.e. the difference of both is one to three orders of magnitudes. For the smoldering fires, intensity of CO gas production is more than that of CO_2 gas production, hence concentration ratio of CO_2 and CO gases generated is roughly similar at the same order of magnitude.

Under a condition of the same ceiling height, temperature rise of flaming liquid (n-heptane) fire and liquid (methylated spirits)fire are the fastest, and that of flaming plastics(polyurethane) fire and open cellulosic (wood)fire comes the second , temperature rise of other test fires are slow, which accord with varying character of heat production intensity in the early fires. For test flaming fire with notable temperature rise distinct, when the ceiling heights and space herein are changed, the detectable

temperature rise will be different obviously. So temperature detection is unfavourable for early discovery of fire in a room with a large space and a high ceiling.

When the ceiling is lower , smoke particles can easily rise to the detector locations where the particle concentration is thicker, therefore the installing height of smoke detectors can influence their detection effect.

5. Conclusions

Detection of single sensor and method of traditional criterion has its limit, which has no way to detect all kinds of fires at the same time, even causes missing of alarms. This research group has establish a set of comprehensive information acquiring equipment reliable in performance and usable for a long term for the study of characteristics of smoke and gases in the early fires, at the same time, data out of near one hundred of test fires have been acquired to now. It is intended that information characteristics of various environmental backgrounds will be tested and acquired in our next working plan so as to form a complete comprehensive information and data base on the process of the early fires. With continuous proceeding of the research, test data can be acquired and added, enabling the contents of this multi-thread database to be richer and to supply sufficient data support for the purpose of realizing intelligent identification and effective detection of the early fires.

Acknowledge

The authors would like to acknowledge the financial support by sub item of national project ‘973’- “Multi-sensoring and intelligent identifying at early fire stage (2001CB409608)” and commonweal project of MOST.China -“Evaluating of fire detective algorithm”.

References

[1]. Fan Weicheng Recommondation of the Project ‘Plan of the National Major Basic Research Development’ Sep., 2001 p1,p8

[2]. Thomas J.McAvoy, James Milke, and tekin A. Kunt. Using Multivariate Statistical Methods to Detect Fires. Fire Technology, Vol. 32, No. 1, 1st Quarter, Jan./Feb., 1996

[3]. Richard W. Bukowski and Paul A. Reneke. New Approaches to the Interpretation of Signals from Fire Sensors. NIST Building and Fire Research Laboratory, BFRL Publications - false alarms p291-p298

[4]. Qingyuan Computer Studio MATLAB6.0Elements and Applications, Mechanical Industry Publishing House, 2001, p114-p132

T. Fujisawa, T. Suzuki, Y. Yoshikawa, S. Ohkuma
Nittan Company Limited, Tokyo, Japan

Optical Smoke Detector Using Dual Light Spectrum

Abstract

An optical smoke detector with scattering light principle is today taking over the place once an ionization smoke detector held in the market, because the use of radioactive material for ionization smoke detector has been more regulatory controlled and restricted for its use and handling as year go by. In generally speaking, the scattering light technology used for the commercial detectors is however not able to discriminate larger size of particles like a steam or dust that are major causes of false alarms. Furthermore the optical detector is insensitive against the flaming fires when compared to the ionization type of detector. To overcome to the later of these weak points on optical detectors, a multi-sensor technology has been recently used as a most common solution. For instance, heat sensor is supplementary used to discriminate the fire by sensing temperature rise to be combined with smoke signal by scattering light with a specific algorithm.

As a quite different approach to solve these problems, we focused on the Theory of Gustave Mie. The theory suggested the possibility to discriminate smoke particles from non-combustion particles by estimating the relative difference of particle size from calculating the ratio of two scattering light by different wavelength of light sources. We expected that it would be possible to eliminate the most of false alarms caused by steam and dust discriminating large particles. By the discrimination of particle size, it would be possible to make detectors more sensitive against flaming fires with shifting of the alarm threshold level when the ratio of two scattering light showed particles being in the category of smallest size as a smoke particle.

In this paper, we wish to present the various experimental results of which we obtained using a unique optical chamber to get the ratio of two different spectrums of scattering light and coupled with the basic algorithm for the detector based on these results.

1. Introduction

In 1990s, a blue light LED was developed for general commercial and industry use by the significant work by Shuji Nakamura in Nichia Chemical in Japan. The combination of this new LED and conventional Infra-Red LED enabled us to construct the widest difference of two wavelengths of light sources. Fig.1 shows the unique optical chamber which contains two light sources (Blue LED and IR LED) and one light receiving photo diode. Both LEDs light on alternatively and a photo diode receives two different wavelength of scattering light in a short duration of time. The angle between the light beam and the view axis of Photo diode is so designed to be same for the both LEDs.

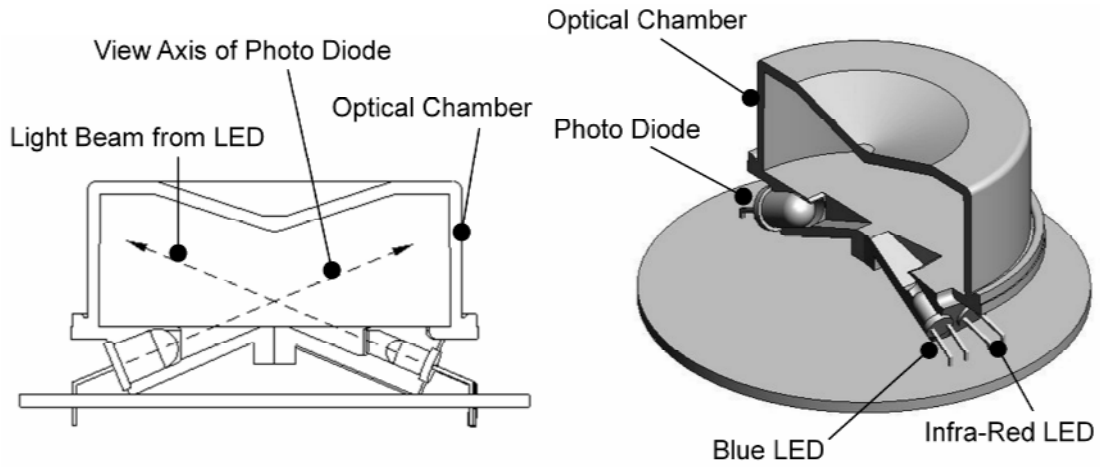

Fig 1 Optical Chamber containing dual LEDs and a single Photo Diode

The peak wavelength is actually 945 nm for Infra-Red LED and 470 nm for Blue LED.

When the particle's diameter is very small such as under 1/10 of wavelength of light in which region Rayleigh Scattering Theory is valid, scattering coefficient (Kscat) is inverse proportion to the wavelength of light source to the fourth. Therefore, in this region of particle size, if the intensity of light is same for both wavelengths, the ratio of Scattering Coefficient will be in principle:

$$(\mathrm{Kscat})_{\mathrm{BL}} / (\mathrm{Kscat})_{\mathrm{IR}} = \frac{1/470^4}{1/945^4} \fallingdotseq 16$$

In the region of particle's size where the theory of Mie is valid, if particle's diameter is much larger than wavelength the Scattering Coefficient is not influenced by the wavelength. Therefore the ratio in this region will be: $(\mathrm{Kscat})_{\mathrm{BL}} / (\mathrm{Kscat})_{\mathrm{IR}} \fallingdotseq 1$

The ratio of Scattering Coefficient for various sizes of particles by Blue LED and Infra-Red LED was calculated with parameters of the particle of water and polystyrene sphere particles according to the equation of Mie. Fig.2 shows the results of the calculation using on-line service for "Scattering Calculation" by Oregon Medical Laser Center in USA.

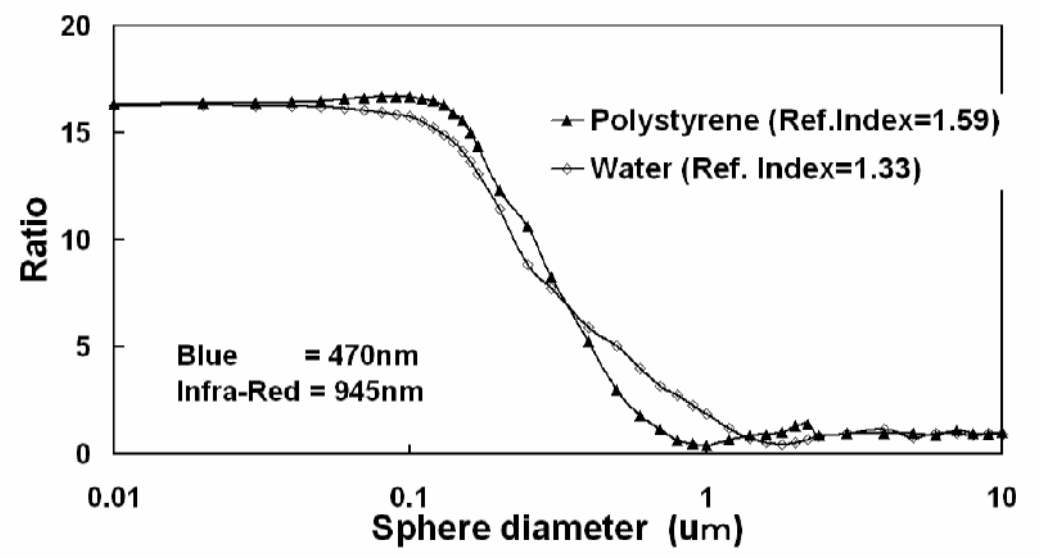

Fig. 2 Ratio of Scattering Coefficient by Blue and IR (Theoretical)

From Fig.2, it was expected that the actual ratio of scattering light received by the Photodiode would be significantly influenced by the size of particles between 0.1 um and 1.0 um in diameter. The calculation for the ratio of scattering light intensity with 45 to 90 degree of scattering angle showed similar curve between 0.1 um and 1.0um of particle size. .

2. Matching of spectrum for LED and photo diode

It should be considered for measuring two different spectrum of light that the sensitivity of the photo diode was not the same for all spectrum of light as shown in Fig. 3. Fig.3 shows that the sensitivity of Photo Diode to the Blue LED is almost one fourth with respect to the sensitivity to the Infra-Red. This difference of sensitivity was compensated for measuring the scattering light by changing the light intensity of each LED, by adjusting the current through LED in the circuit shown in Fig. 4.

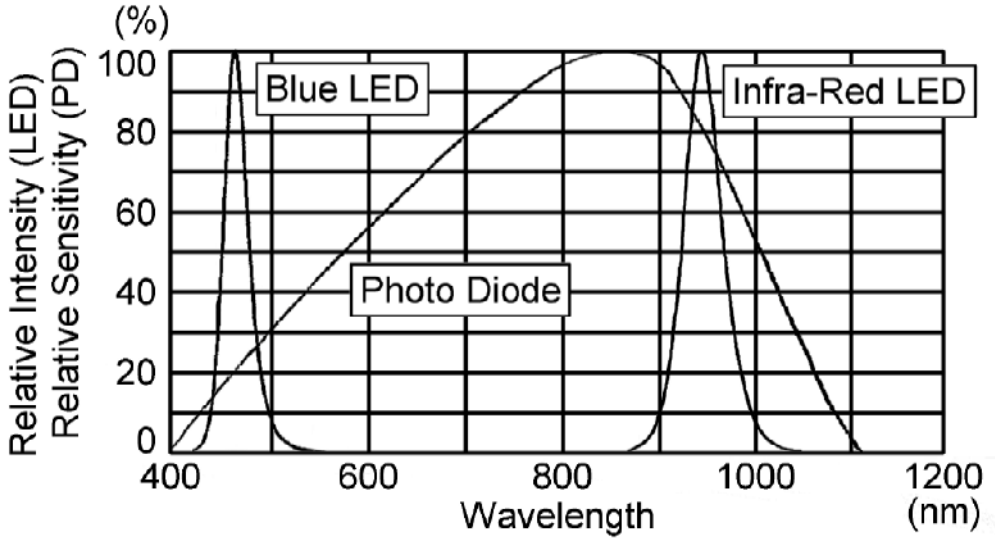

Fig 3 Spectrum Characteristics of Optical Devices

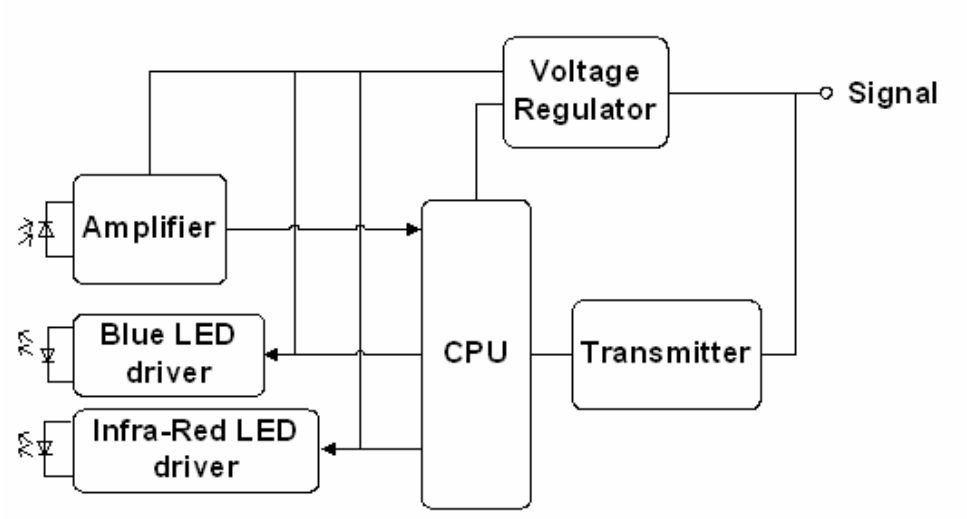

Fig 4 Circuit Diagram for Optical Detector with Dual Spectrums

The calibration was carried out in a certain concentration of sufficiently large size of particles, in which the intensity of scattered light will not be theoretically influenced by the wavelengths and, therefore, the ratio of the output of the photo diode is to be calibrated to 1.0 in this condition.

3. Measurement of the ratio of scattering light by dual spectrum

The ratio of scattering light by dual spectrum was measured with several sizes of polystyrene sphere particles referring to the theoretical simulation of scattering coefficient. The intensity

of scattering light was measured alternatively within 5 milliseconds for each light source with 3 to 4 seconds of sampling interval.

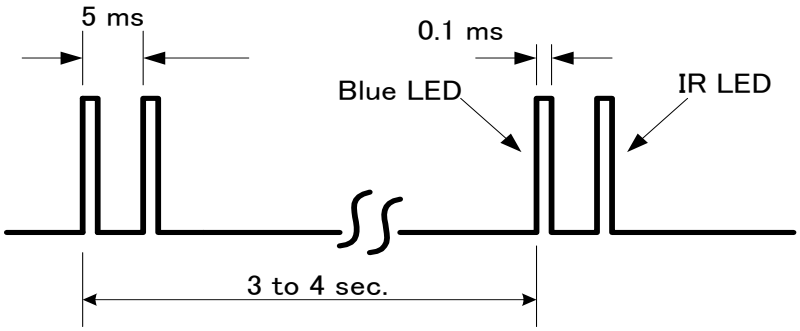

Fig. 5 Timing for sampling of scattering light intensity

The result of experimental measurement is shown in Fig.6, in which the theoretical ratio of scattering coefficient is also shown with dotted line as reference.

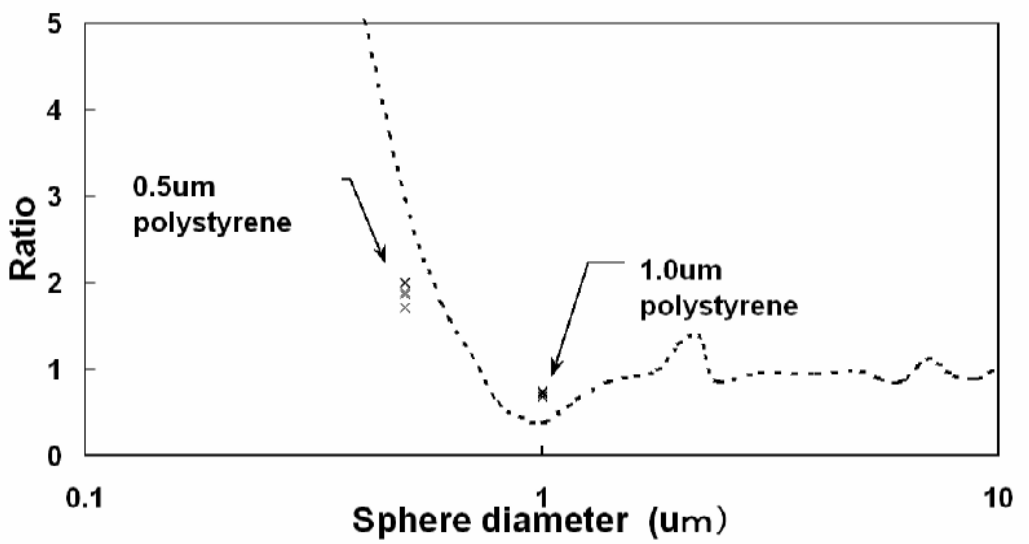

Fig.6 Ratio of Scattering Light by Blue and IR (using polystyrene)

4. Measurement of the Ratio by Test Fires

Test Fires specified by CEN and ISO Catalogue for Full Scale Fire Test, N290 by ISO/TC21/SC3, are considered to cover a majority of fires with combustibles representing those in the practice including wood (cellulosic materials), plastics and liquids, and with burning and smoldering. Therefore the detector is considered to be the most ideal if it is operated at the adequate level in all test fires. Optical smoke detectors is basically sensitive

to large and gray combustion particles by TF2 (Smoldering wood fire) and by TF3 (Smoldering cotton fire) and less sensitive to small combustion particles by TF1 (Open wood fire) and black particles by TF5 (Liquid fire). Fig 7 shows the outputs of Photo Diode by Blue and Infra-Red scattering light and also the ratio of these outputs (Blue / IR) under the Test Fire TF1. Fig 8 shows those under the test fire TF2.

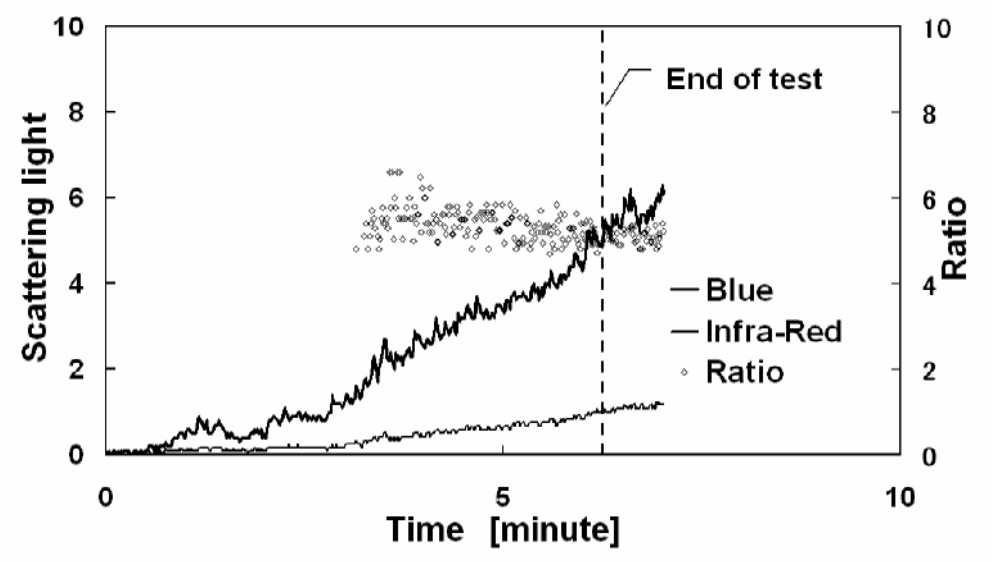

Fig.7 Scattering light signal by Blue and IR and the Ratio on TF1

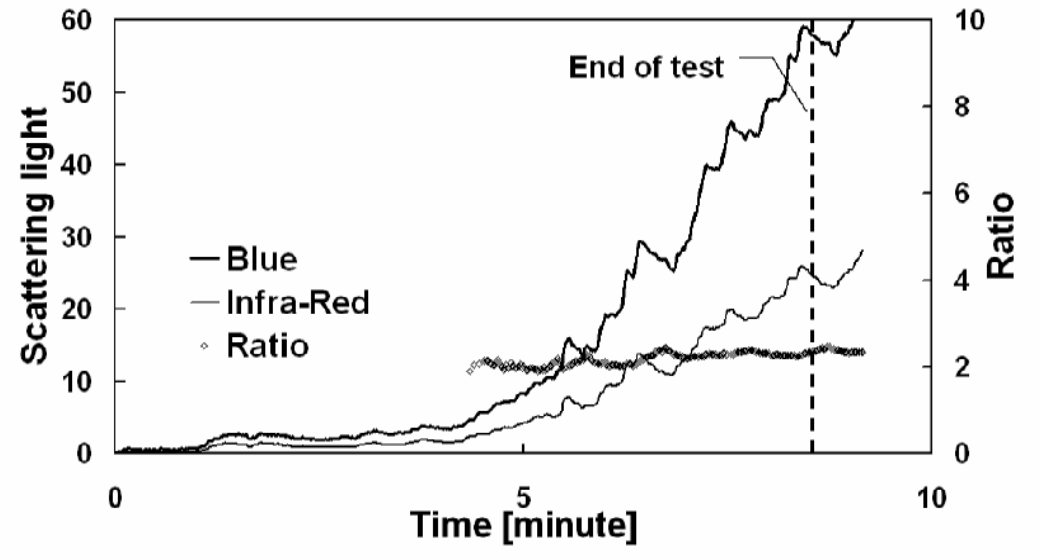

Fig.8 Scattering light signal by Blue and IR and the Ratio on TF2

Before the measuring, the scattering light signals by both LEDs were adjusted to 10.0 in the 10 %/m of obscuration rate (m=0.46) by using more than 5 um diameter of particles.

The frequency of the ratio through the test was calculated for each test fire. Fig 9 shows the frequency calculated for each ratio of dual (Blue and IR) spectrum for TF1 to TF5.

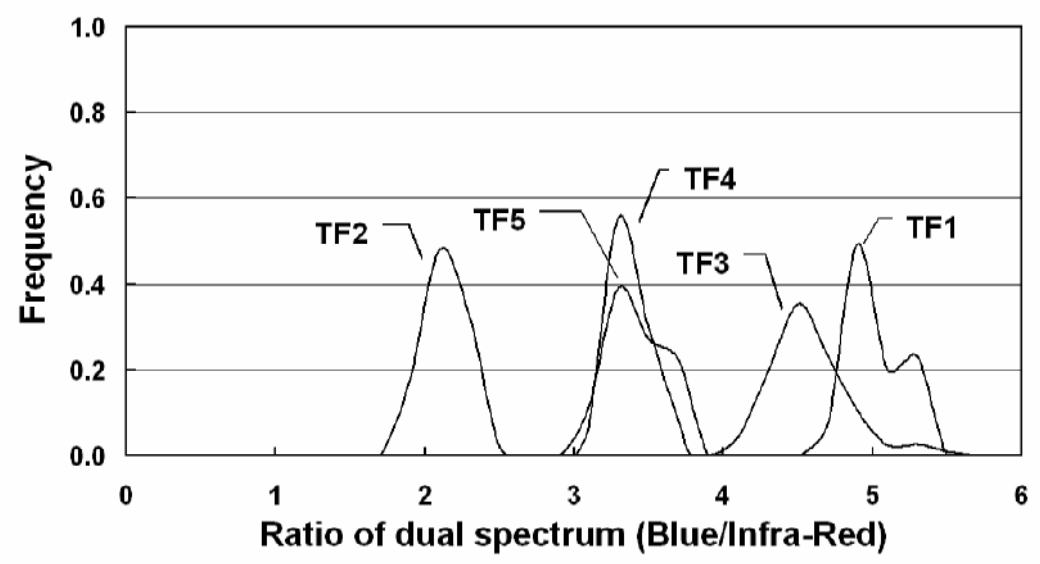

Fig.9: Frequency to Ratio of dual spectrum for TF1 to TF5

5. Measurement of the ratio by particles other than combustion materials

The ratio of dual spectrum was measured also with particles other than combustion materials.

Fig. 10 shows the result of measurement for steam, Fly Ash (specified by JIS Z8901, Class 5) as a substitute of dust particles and hair spray. These are major representatives of the causes of false alarms for optical smoke detectors.

The graph shows that scattering light of these particles is not influenced by Blue and Infra-Red, and the ratio is almost 1.0, probably due to their diameter being considerably larger than the wavelength of both spectrums.

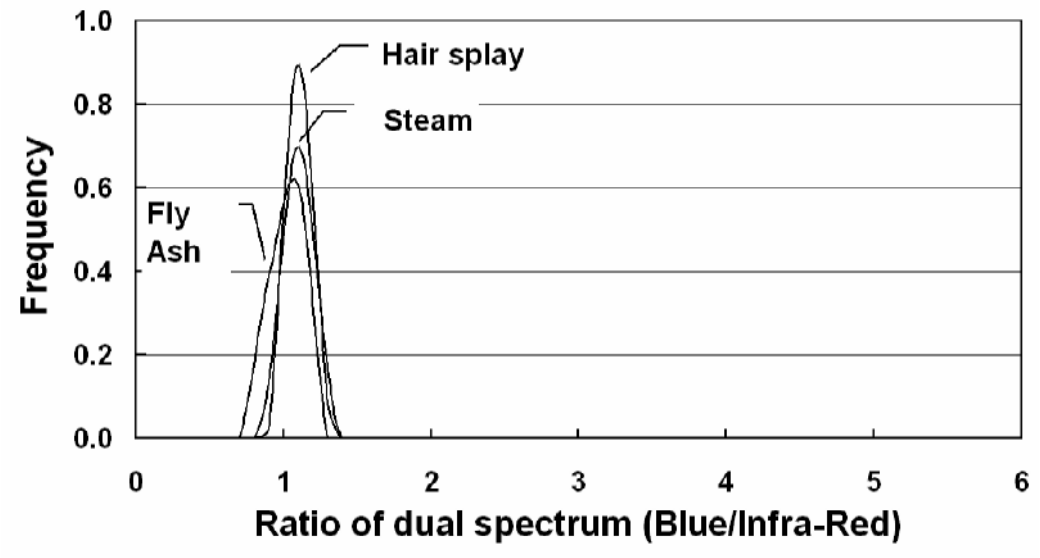

Fig.10: Frequency to Ratio of dual spectrum for various particles

6. Algorithm for ideal smoke detectors using dual light spectrum

Fig.9 and Fig.10 indicate that the discrimination of smoke and other larger particles by steam, dust and hair spray would be possible by using the ratio of dual spectrums (Blue and Infra-Red) of scattering light. The detector with the algorithm implemented was introduced into the market in 2003. Some of our field experiments showed that the detector was very efficient even in the room closed to bathroom.

Fig.11 is a general flow chart representing the logic of the discrimination.

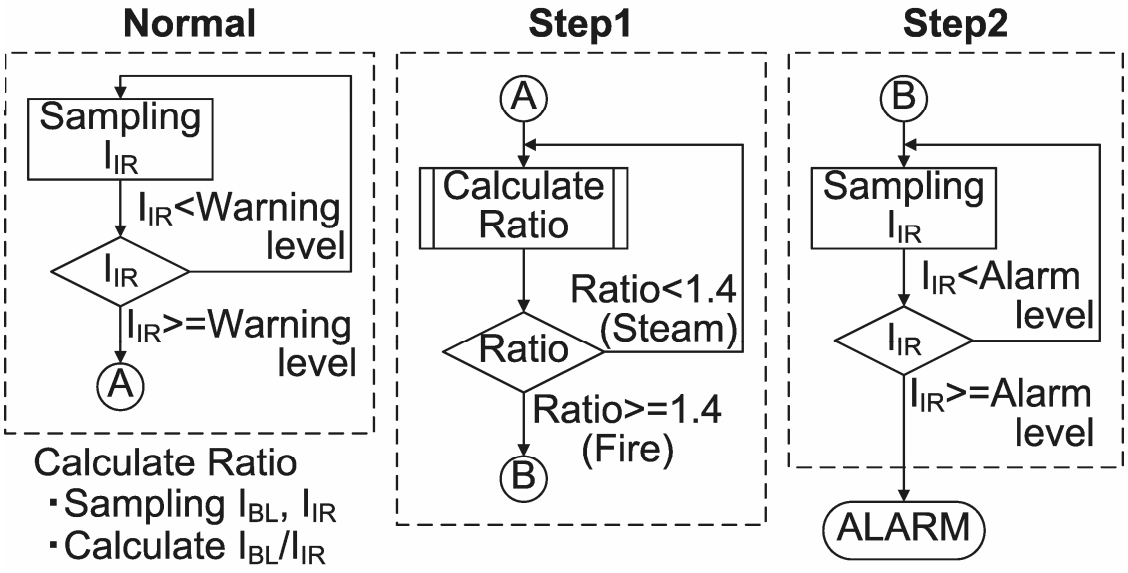

Fig.11: Algorithm to discriminate smoke to steam or dust

In this detector, the scattering light signal by Infra-Red was mainly used for determination of the threshold value of fire. Blue light was only used to calculate the ratio of dual spectrum.

The second version of the detector used Blue light for the threshold value of fire to make it more sensitive to the smaller particles. For flaming wood fire TF1, it did not perform satisfactorily comparing to an ionization type of detector.

Fig. 12 shows the level of scattering light signals by Blue (solid line) and Infra-red (dotted line) reached to 3 classes of smoke level by test fires TF1 to TF5.

The scattering light signal is adjusted for measurement to certain level separately for each spectrum, as expressed as 10 in the graph, by the 10 %/m of obscuration rate (which is equivalent to 0.46 by m-value) with the smoldering paper.

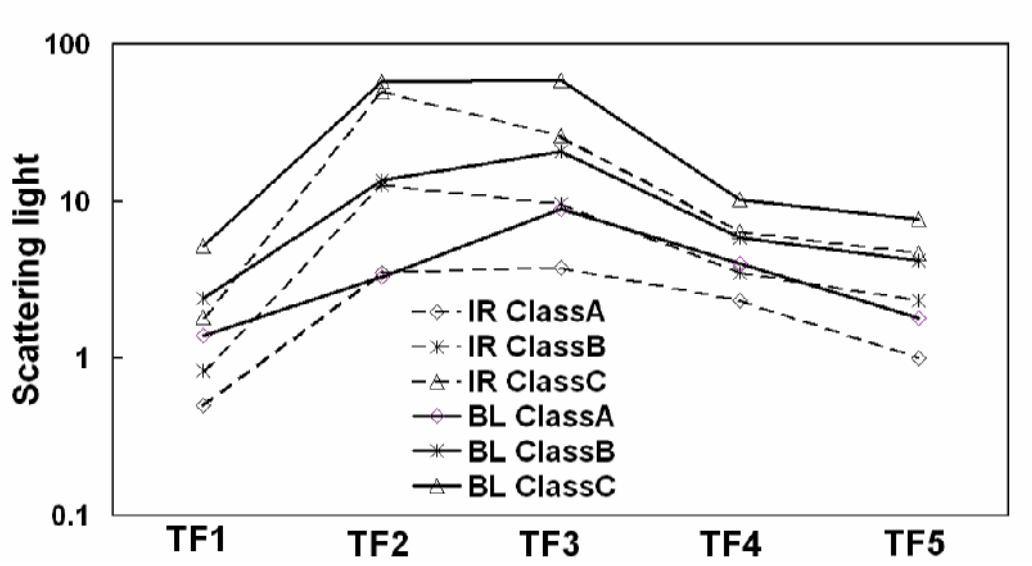

Fig.12 Output of blue scattered light for various Test Fires

These graphs show that the use of blue light improves the sensitivity to TF5, but not TF1.

The new algorithm (Fig.13) has been developed from the above results. The algorithm quite that of utilizes also the ratio of dual spectrum to compensate the sensitivity differences by various test fires.

On the step2 in the flow chart, smoke is classified to 3 types from the ratio of scattering light signals and the signal is multiplied by the value decided according to the ratio as shown in Fig13.

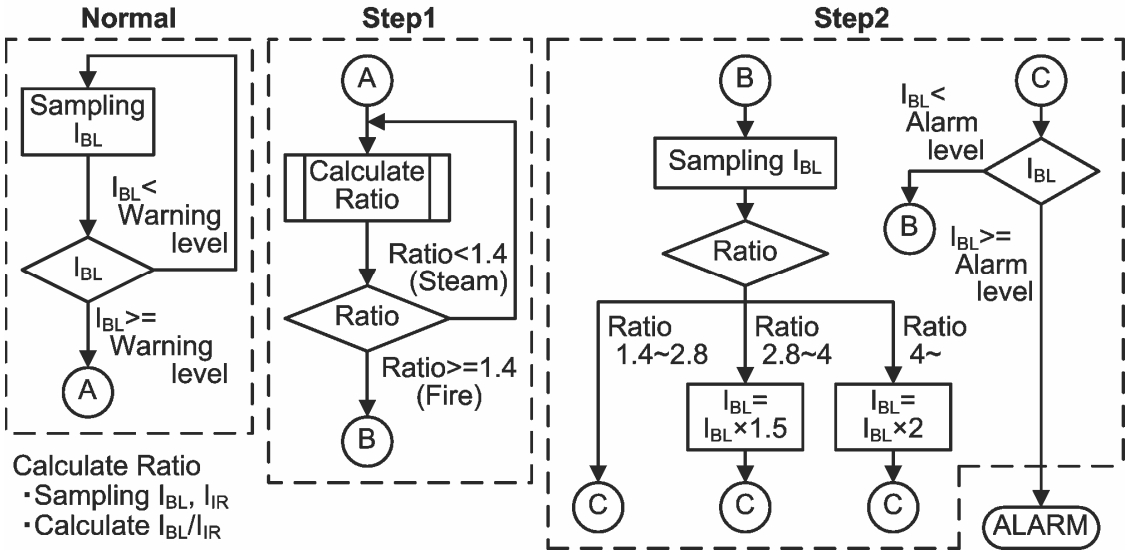

Fig.13 Algorithm with the compensation of sensitivity to TF1

7. Conclusion

The ideas to measure multi spectrum of scattering light or obscuration coefficient by different sizes of particles have been reported by many people to verify the Theory by Rayleigh and Mie. Their efforts have made enable us to produce the practical detector with the dual spectrum technology with the Blue LED. This technology can be expected for further improvement to close to the ideal fire detector by its capability to discriminate particle sizes: smoke and other particles as well as classification of the types of smoke.

References

1. Atsuyuki Hirono, Akio Takemoto, Yoshiaki Kanbe: "Discrimination between fire smoke and non-fire with extinction coefficients by three wavelengths", Research Presentation in Japan Fire Academy, 1990, National Research Institute of Fire and Disaster

2. A.J.Cox, Alan J.DeWeerd,Jennifer Linden: "An Experiment to measure Mie and Reileigh total scattering cross sections", Am. J. Phys., Vol. 70, No.6,June, 2002, University of Redland,

3. ISO/TC21/SC3, N290, "ISO Catalogue for Full Scale Fire Test for Smoke and Fire Detectors of Fire Detection and Alarm Systems", 1996

4. Gustave Mie: "Beiträge zur Optik trüber Medien, speziell kolloidaler Metallosungen" Ann.der Phys., 25, 1908

5. The page of website by Oregon Medical Laser Center, "Scattering Calculation"

6. Kanji Takahashi: "Basic Aerosol Engineering", 1972, Kyoto University

Shu Xue-ming，Yuan Hong-yong，Fang Jun，Su Guo-feng
State Key Laboratory of Fire Science, University of Science and Technology of China, Hefei 230026, P.R.China

A New Method of Laser Sheet Imaging-Based Smoke Particles Detection

Abstract

An optical non-intrusive measuring method to detect smoke particles based on laser sheet imaging was developed in this paper. A set of experimental apparatus to capture smoke particles were designed, which included three parts: the smoke passage system, light scattering system and particle imaging system. From the experimental apparatus and image processing algorithm, particle images, particle sizes as well as their distributions of different fuels were acquired. This method provided us with not only the smoke particle morphology but also its size and distribution, which maybe benefit for the research of smoke technology.

Key Words: Fire Detection, Smoke Particles, Laser Sheet Imaging, Light Scattering, Particle Size.

1. Introduction

Fire detection is one of the most important aspects in the research of fire science and fire-protection engineering. Usually, smoke appears much earlier than the flame of combustion, so fire smoke characteristics are the foundation of fire detection [1,2]. According to statistics, more than 80 percent of fire detectors in China are smoke-type, such as ionization smoke detectors and photoelectric smoke detectors [3]. However, both the ionization smoke detectors and photoelectric smoke detectors could only detect the variation of smoke concentration, and may cause false alarms
in the environment of dust, vapor, oil smoke, wind and electromagnetism, etc[4]. One of the major factors of false alarm is come from the influence of particle size and its distribution. The smoke particle characteristics of different materials, especially the particle image characteristics may provide us such information of particle size and its distribution.

Based on the Mie scattering theory about the interaction between laser and smoke particles, an optical nonintrusive detecting method for fire smoke by laser sheet imaging was developed. A set of experimental apparatus was designed to capture smoke particles, which included three parts: the smoke passage system, light scattering system and particle imaging system. Particle parameters such as particle size, number and coordinates were obtained. The results were analyzed in histograms. From the experimental apparatus and image processing algorithm, particle images of different fuel types and the particle size as well as its distribution were obtained [5～7].

2. Experimental Study

2.1 Experimental Apparatus

An optical nonintrusive detecting method for fire smoke by laser sheet imaging was developed in our laboratory. By capturing fire smoke particle images from the smoke passage and processing with image processing software, particles geometric characteristic information was obtained, such as smoke particle morphology, particle size and distribution. From the geometry characteristics' of the fire smoke and the non-smoke aerosol, as flour or dust, the differences were obvious and the results could be quickly computed with the image processing algorithm, which provided an effective method to distinguish fire smoke from non-fire aerosols in the early fire detection.

The experimental apparatus included three parts, and the first part was smoke passage system, which provided a stable and uniform smoke current of burning materials. The second part was the light scattering, which contained a laser sheet beam for scattering on smoke particles and CCD camera for receiving the scattering signals at a certain angel. The third was the particle imaging system, which gave the particle geometry characteristic information.

In the first part of the experimental apparatus, smoke passage system included inlet, adjusted section, stable section, measurement section, fan and outlet. The schematic construction of smoke passage system was showed in figure 1.

In order to keep the smoke current stable and uniform in this passage, an adjusted passage was designed which section was from small to large. Its length could be

changed according to the definition of the captured images. Two dozens of uniform slender pipes were installed along the axis line in the stable section, which were 800 cm long with a diameter of 10 cm. The speed of exhaust fan can be adjusted according to the definition of particles image, too.

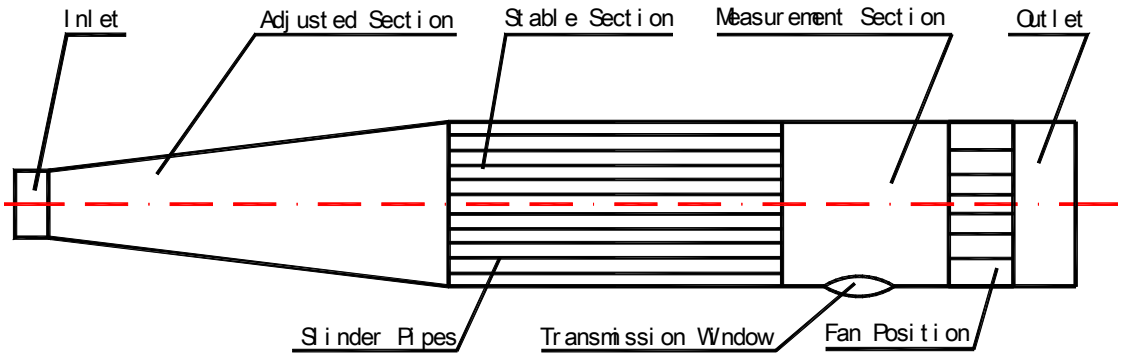

Figure 1. Schematic Construction of Smoke Passage System

There will be intensity scattering on the smoke particles when the laser wavelength was about the order of the particle size due to the interaction between laser and smoke particles [8,9]. At the second part of the experimental apparatus, a laser light with a wavelength of 635nm was selected as the incidence light. In order to avoid the overlapping effects of smoke particles, the laser light was manipulated to be 1 mm around thickness of laser sheet by using a semi-cylindrical lenses, which made the scattering light in horizontal direction extend enough for a camera to record smoke particle images separately. The overlapping phenomenon of particles was avoided by this way.

In order to obtain a simple way to conduct such studies, an XTD-06 type microscope was installed in the forward 30 degree of the light scattering pathway. As the particle size was at the sub-micron level, battery of lens with image multiplication function in the microscope were used in order to acquire clear images of smoke particles.

To capture smoke particle images, a high-resolution charge-coupled device (CCD), named IK-204 type camera was installed in the forward 30 degree direction of the light

transmission pathway, same as the direction of the microscope. At mean time, the exposure time of single image and particle image's long tail was shorten by using an electric shutter to control the sampling rate, which made the camera record sequential images in very short time with high spatial resolution.

In this experiment apparatus, an XTD-06 type microscope, battery of lens and IK-204 type camera were used to realize the close range image shot, and the scattering light was imaging on the CCD target. An OK-C20 type image acquisition card was selected to capture the smoke particle images by a high performance PC computer rapidly, which was installed in the computer and connected with the camera.

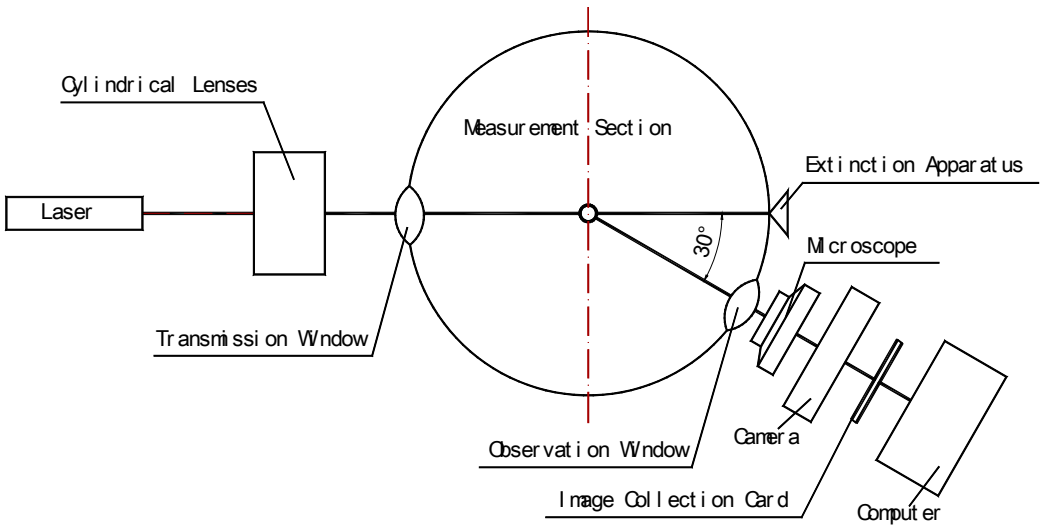

Figure 2. Schematic of Experimental Setup

In the third part, a set of software was made to process the captured particle images by mathematical correlation analysis on a cluster of particles and powerful particle image processing algorithms.

2.2 Experiment Test

In order to distinguish the fire smoke particles from non-fire aerosols, contrast experiments were conducted. Some particle images of fire smoke materials were captured, such as that of polyurethane, beech wood, cotton wick, and non-fire aerosols of land plaster or dust.

Those particle image characteristics were analyzed to find out the differences between fire smoke and non-fire aerosol. Particle images of land plaster and smoke of different materials were showed in figure 3.

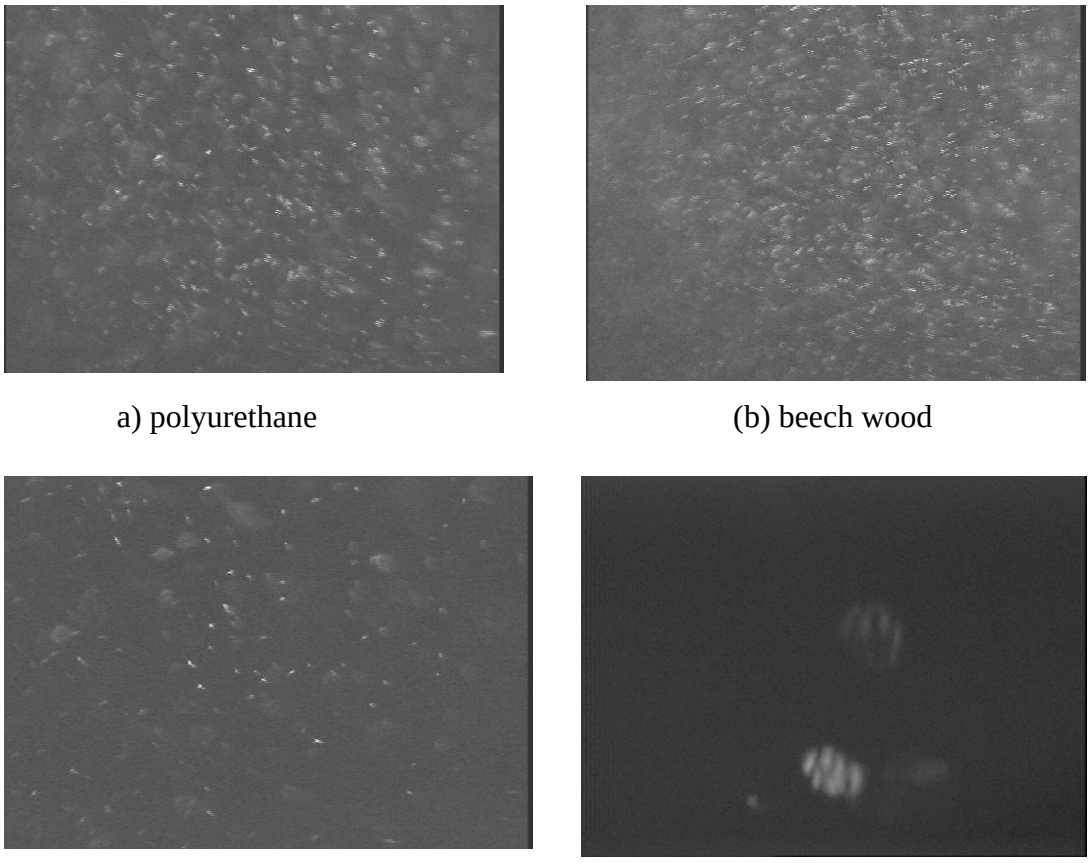

a) polyurethane (b) beech wood

(c) cotton wick (d) land plaster

Figure 3. Particle images of land plaster and smoke of different materials

3. Image processing and Result Analysis

The smoke particle images were real-time captured and displayed on the computer indicator through the light scattering system and particle imaging system from this experimental apparatus. Particle images were saved by the acquisition program in the camera automatically or by manual acting. The memorized particle images provided the particle geometry information by the image processing algorithm.

The first procedure was image preliminary processing. The captured particle images were saved in bitmap documents of 24-bit color style, then turned into 256 grey maps by the preliminary processing software.

The second step of image process was two-value processing of grey map. In order to de-noising of particle images, two-value processing of grey map was a popular technology in image processing. In this experiment, we selected a fixed thresholds of 128 to turn the grey map into black and white images.

The third process was image calibration. As the image was acquired in the forward 30 degree of the light scattering pathway, the observation direction was not perpendicular to the direction of laser light transmission, and the particle images on the camera's target didn't show the true ones, but deformed images through central projection [10]. It was designed of a set of object and image transformed coordinates system to calibrate the captured pictures.

The fourth processing was statistic algorithm of particle size. In order to get the particle number and particle size on black and white images, it need to mark the connectivity area of cluster of particles, scan the particle images line-by-line with a certain sequence, from the top to bottom, and left to right, and calculate every pixel element, particle circumference, area and particle size.

The last step of particle image processing was experimental data processing and result output, which was showed in figures 4(a), 4(b), 4(c), and 4(d) as below.

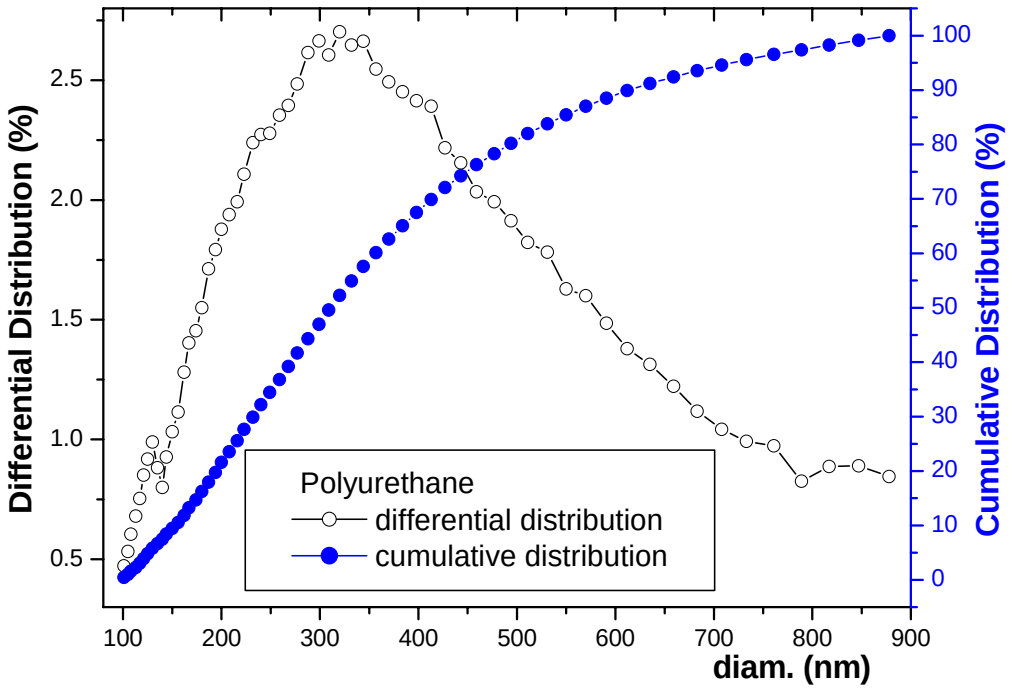

Fig. 4(a) Histogram of smoke material "Polyurethane"

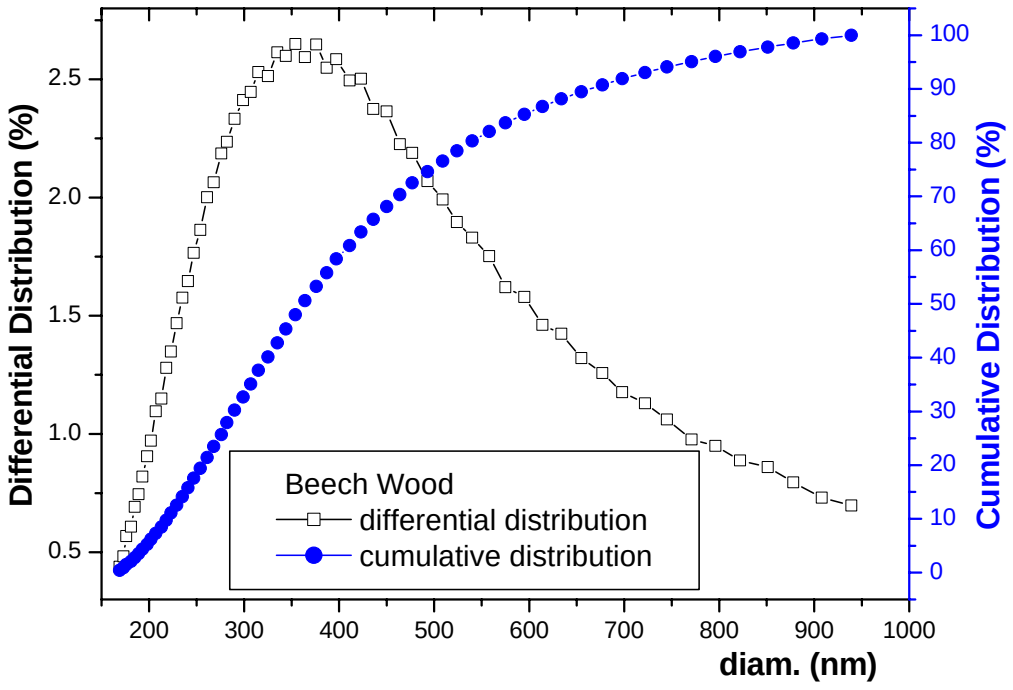

Fig. 4(b) Histogram of smoke material "Beech Wood"

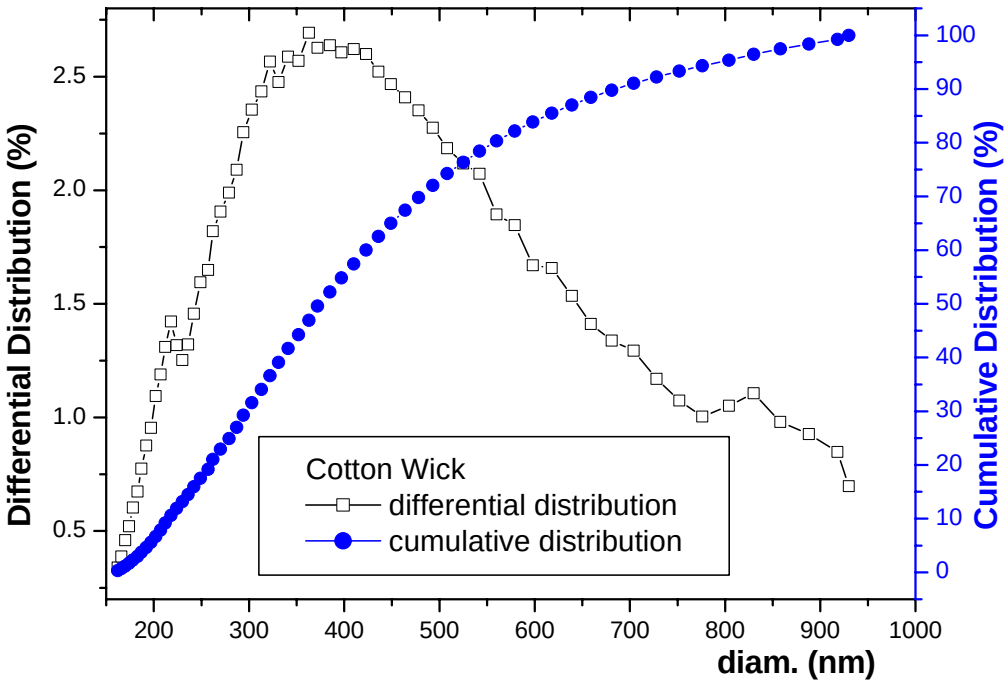

Fig. 4(c) Histogram of smoke material "Cotton Wick"

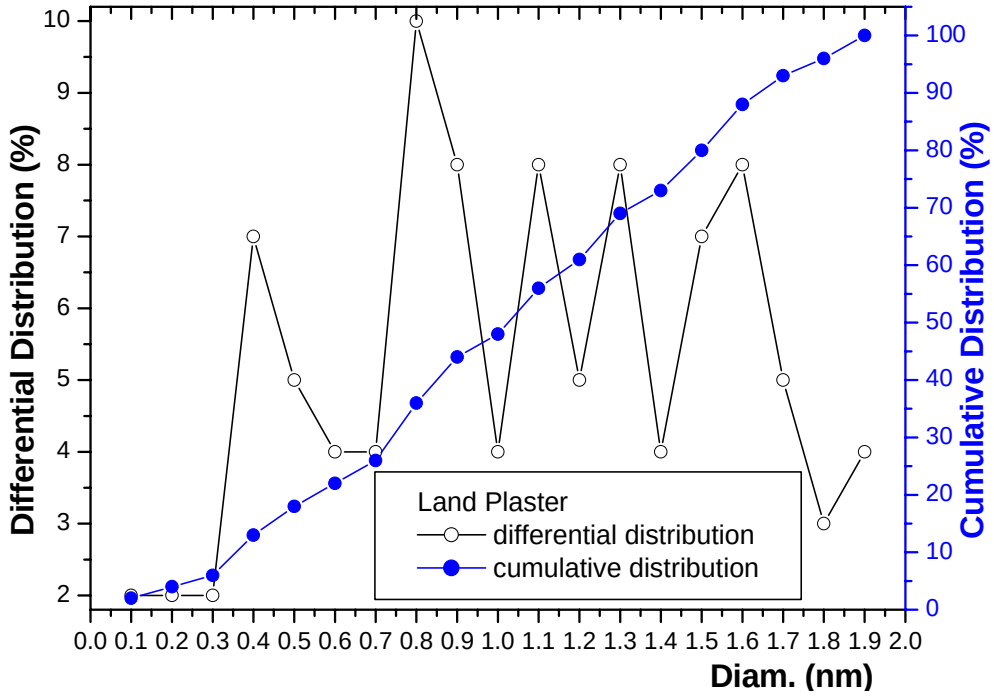

Fig. 4(d) Histogram of smoke material "Land Plaster"

From above histograms of several smoke materials and land plaster, the differences can be seen among the varieties of materials. In the figure 4(a), there is a peak in the differential distribution of polyurethane at about 320 nanometers. In the figure 4(b), the beech wood's differential distribution curve has a peak value at 350 nanometers, and its integral distribution curve is quite smooth. In the figure 4(c), the maximum of the differential distribution curve of cotton wick is about 360 nanometers. In the figure 4(d), land plaster's differential distribution is much random, and its distribution extension is also much more fluctuant than that of others, and the integral distribution curve is not so steep as the others. So, according to the processing result of captured images, the particle size and its distribution of different materials were acquired.

4. Conclusion

In this paper, an optical nonintrusive measuring method to detect smoke particles based on laser sheet image was developed. From the experimental apparatus, several kinds of fire smoke particle images were acquired. By particle image processing system, the information of particle size, distribution and morphology of different material smokes were obtained. From contrast experiments, the differences were also acquired between burning smoke and non-fire aerosol in particle size and its distribution.

It could be seen that the detection method of laser sheet imaging-based smoke particles detection was viable. The method could not only obtain the morphology of particles, but also the particles size and its distribution. The work of this paper tried to seek an advanced fire smoke detection which might be more sensitive to fire smoke and more effective in the ambient environments with dust or other interference sources.

Acknowledgements

This paper was supported by the Fire Dynamics and Fundamental of Fire Protection (FDFFP) Program. (Grant No: 2001CB409608). The authors deeply appreciate the supports.

References

1. FAN Wei-Cheng, WANG Qing'An, et al. (1995). Fire Science Foundation. University of Science and Technology of China Press, Hefei,1995: 243-330 (in Chinese).
2. WU Long-biao, YUAN Hong-yong. (1999). Fire Detection and Controlling Engineering. University of Science and Technology of China Press, Hefei,1999: 12-136 (in Chinese).
3. MEI Zhi-bin, SONG Li-wei, et al. (2003). Data Collection System Design of Multi-information of Character of Early Fire Smoke. 2003 International Symposium on fire science and fire-protection engineering proceedings. Beijing, 2003: 320-324 (in Chinese).
4. ZHAO Jian-hua, YUAN Hong-yong, et al. (2001). Study of Fire Smoke based on Multi-wavelength Laser Extinction. Applied Laser,2001,21(2):79-81 (in Chinese).
5. SHU Xue-ming, YUAN Hong-yong, et al. (2002). Photoelectric Dectector and its Application to Fire Detection. Journal of Fire Science and Technology， 2002,1:31-33 (in Chinese).
6. SHU Xue-ming, YUAN Hong-yong, et al. (2003). Study of Fire Smoke Detection based on Sheet Laser. 2003 International Symposium on fire science and fire-protection engineering proceedings. Beijing, 2003: 337-340 (in Chinese).
7. ZHAN Fu-ru, XU Qiong, et al. (2002). The Fire Detection of Multi-angle Laser Scattering with CCD Imaging. Fire Safety Science. 2002,11(1): 52~56 (in Chinese).
8. H.C.Van de Hulst．(1957) .Light Scattering by Small Particles．New York: John, Wiley & Sons Inc．London, Chapman & Hall, Ltd. 1957,62-380.
9. WANG Shao-qing, REN Hong-jing, et al.(1997). Study of Mie Scattering Coefficient Calculate Method. Applied Optical, 1997,18(2):4-9 (in Chinese) .
10. XU Qiong, YUAN Hong-yong, et al. (2003). Measurement of Smoke Particle Size Distribution by the Near-Forward Scattering Light of Laser Sheet. Fire Safety Science. 2003,12(2): 95-99 (in Chinese).

A. Keller, H. Burtscher
University of Applied Sciences, North-Western Switzerland, Windisch, Switzerland

M. Loepfe, P. Nebiker, R. Pleisch
Siemens Building Technologies Ltd, Fire & Security Products, Männedorf, Switzerland

Online determination of the refractive index of test fires

Abstract

The performance of smoke detectors depends largely on the characteristics of the smoke produced in a fire situation. A better knowledge of the properties of the aerosol particles originating in fires will therefore help to improve the performance of existing detectors, reduce the amount of false alarms, and serve as guideline in the development of new measuring techniques. Here, we present a study of the optical properties of the standard EN54 test fires. The measurements were done using the diesel particle scatterometer [1]. This instrument measures the angular distribution of the Mueller scattering matrix elements S_{11}, S_{12}, and S_{34} [2] with a time resolution faster than 1 Hz. The size distribution and the complex refractive index of the particles can then be determined by fitting the data with Mie-scattering calculations. The optical information was complemented with the aerosol size distribution measured using a SMPS system. Our results show that the simultaneous measurement of several scattering-matrix elements can serve as a good discrimination criterium for the different types of fire (flaming and smoldering). In contrast, no appreciable differences were present in the size distribution data.

Introduction

Optical methods play an important role in the monitoring and characterization of aerosol particles. Among them, non intrusive methods have the advantage of not disturbing the aerosol sample by collection, avoiding changes like selective losses, coagulation, and evaporation of volatile compounds. Most of these optical methods rely on light scattering and are therefore very sensitive to particle shape and composition. Thus, in order to use them it is important to have good knowledge of the optical

properties of the relevant aerosols. Here, we present a study of the optical properties of several fire-originated aerosols. Our data is applicable to a broad area of practical application extending from environmental control to automatic smoke detection systems as well as to theoretical calculations.

Theoretical background

In this section, we will give a description of the formalism needed for the analysis of our optical data. Please refer to [2], [3] and [4] for an exhaustive description and a better insight into the details of light scattering as a tool for the characterization of small particles.

Scattering matrix formalism

The scattering intensity and polarization state of a light beam can be described by means of the Mueller scattering matrix [2], [3], hereafter scattering matrix. The scattering matrix relates a set of four parameters defined in terms of the complex electric fields $\mathbf{E}_\parallel$ and $\mathbf{E}_\perp$, parallel or perpendicular to the scattering plane, by

$$\begin{aligned} I &= \mathbf{E}_\parallel \mathbf{E}_\parallel^* + \mathbf{E}_\perp \mathbf{E}_\perp^* \\ Q &= \mathbf{E}_\parallel \mathbf{E}_\parallel^* - \mathbf{E}_\perp \mathbf{E}_\perp^* \\ U &= \mathbf{E}_\parallel \mathbf{E}_\perp^* + \mathbf{E}_\perp \mathbf{E}_\parallel^* \\ V &= i(\mathbf{E}_\parallel \mathbf{E}_\perp^* - \mathbf{E}_\perp \mathbf{E}_\parallel^*) \end{aligned}$$

through

$$\begin{pmatrix} I_{\text{sca}} \\ Q_{\text{sca}} \\ U_{\text{sca}} \\ V_{\text{sca}} \end{pmatrix} = \frac{1}{k^2 r^2} \begin{pmatrix} S_{11} & S_{12} & S_{13} & S_{14} \\ S_{21} & S_{22} & S_{23} & S_{24} \\ S_{31} & S_{32} & S_{33} & S_{34} \\ S_{41} & S_{42} & S_{43} & S_{44} \end{pmatrix} \begin{pmatrix} I_0 \\ Q_0 \\ U_0 \\ V_0 \end{pmatrix}. \tag{1}$$

Where I, Q, U, and V are the so called Stokes parameters. I describes the total intensity of the light beam, Q the amount of the parallel and perpendicular polarized light, U the $\pm 45^\circ$ polarization, and V the circular polarization. $k = 2\pi/\lambda$ is the wavenumber, and r the distance from the scattering point to the observer. The S_{ij} form the elements of the scattering matrix. All these elements can be measured directly by selecting different polarization states for the incoming light and analyzing the polarization state of the

scattered light. They all provide a direct measure or are indicative of the physical properties of the scattering medium. Their definition can be found under [2].

In the most general case, the scattering matrix has 16 non-zero elements but can be simplified using several symmetry relations. For our current purposes, it is sufficient to know that a cloud of randomly oriented, non-optically active particles is represented as

$$M = \begin{pmatrix} S_{11} & S_{12} & 0 & 0 \\ S_{12} & S_{22} & 0 & 0 \\ 0 & 0 & S_{33} & S_{34} \\ 0 & 0 & -S_{34} & S_{44} \end{pmatrix}, \tag{2}$$

thus reducing the amount of independent matrix elements from 16 to 6. Quinby-Hunt *et al.* [5] describes them as:

S_{11} transformation of total intensity of incident light; gives general size information;

S_{12} (S_{21}) depolarization of linearly polarized light parallel and perpendicular to the scattering plane (S_{21} the converse); depends on size, shape, and complex refractive index of the scatterers;

S_{22} transformation of linearly polarized incident light (parallel and perpendicular) to linearly polarized scattered light (parallel and perpendicular); $S_{22} = S_{11}$ for spherical particles;

S_{33} (S_{44}) transformation of linearly polarized incident light at $\pm 45^\circ$ (circularly polarized in the case of S_{44}) to linearly polarized scattered light at $\pm 45^\circ$ (circularly polarized for S_{44}); $S_{33} = S_{44}$ for spherical particles;

S_{34} (S_{43}) transformation of circularly polarized incident light to linearly polarized scattered light ($\pm 45^\circ$) (S_{43} is the converse); this element is strongly dependent on size and complex refractive index of the scatterers.

Since we are assuming that the particles have no preferred orientation, each of the elements of the scattering matrix is a function of the scattering angle, although not the orientation of the scattering plane.

General scattering theory

The most commonly used approach to predict the expected scattering for particles is the Mie calculation. It is based on the solution of the Maxwell's equations for a homogeneous sphere and is discussed in detail by [2] among others. This analytical solution is restricted to particles with a spherical shape. For this special case $S_{22} = S_{11}$ and $S_{33} = S_{44}$. It can be applied to real particles, though it must be emphasized that most particles are non-spherical. A poor agreement between observations and Mie calculations has been reported for a S_{22}/S_{11} ratio below 0.9 [6], [7].

The Mie solution for a sphere involves writing down expansions for the incident, internal and scattered waves and finding a solution by applying the electromagnetic boundary conditions. As a consequence, the resulting scattering-matrix elements have the form of the product of convergent infinite series. The rigorous solution of scattering problems is complicated and tend to involve a considerable amount of computer time and storage even for small particles and simple geometries. There are, however, some approximations for certain particle sizes and refractive indexes that not only provide a simple solution but give also some insight into the scattering process.

One of these approximations exists for the so called Rayleigh scattering, which applies to particles where $|m|x \ll 1$. Here m is the complex refractive index of the particle, $x = \pi d_p/\lambda$ the size parameter, d_p the particle diameter, and λ the wavelength of the incoming light. With these considerations, the corresponding scattering matrix is [2]

$$M(|m|x \ll 1) = \frac{9}{4}|a|^2 \begin{pmatrix} \frac{1}{2}(1+\cos^2\theta) & \frac{1}{2}(\cos^2\theta - 1) & 0 & 0 \\ \frac{1}{2}(\cos^2\theta - 1) & \frac{1}{2}(1+\cos^2\theta) & 0 & 0 \\ 0 & 0 & \cos\theta & 0 \\ 0 & 0 & 0 & \cos\theta \end{pmatrix}, \qquad (3)$$

where a is defined as

$$a \equiv \frac{i2x^3}{3}\frac{m^2-1}{m^2+2}. \qquad (4)$$

This gives the typical shape of the Rayleigh scattering, where the scattered light is totally polarized at 90°. It also shows that, for small ($x \ll 1$) or weakly scattering particles, $S_{34} = S_{43} = 0$.

Methods

We focused on the analysis of the aerosol particles (smoke) originating in different test fires produced in accordance with the EN54 norm for fire detection and fire alarm systems [8]. The test fires studied in this work were:

TF1 flaming wood fire (EN54 standard),

TF2 smoldering wood fire (EN54 standard),

TF3 smoldering cotton fire (EN54 standard),

TF4 flaming foam fire (EN54 standard),

TF5 flaming *n*-heptane fire (EN54 standard), and

DC flaming decalin, $C_{10}H_{18}$ (non-standard test).

The measurements were done in a $10\times6\times4$ meters room (length$\times$width$\times$height). The procedure of the tests is well described by the norm and will not be mentioned here. The non-standard DC fire was done in a similar way to the other flaming liquid fire, TF5, but using pure decalin instead of the *n*-heptane mixture.

During the tests, air was sampled from the ceiling of the room at the position were the fire detectors should be located. The sample was then diluted by a factor of 10, to reduce particle coagulation and other processes that may alter the sample, and analyzed by our measuring system. We used a fast flow rate after dilution (30 liters/min) to ensure a short residence time (1 second) before the analysis. Special care was taken to avoid the particle-free dilution air from entering the test room.

The measurement of the optical properties was made using the diesel particle scatterometer (DPS) developed by Hunt *et al.* [1]. This instrument measures the angular distribution of the scattering-matrix elements S_{11}, S_{12}, and S_{34}. The instrument uses a 532 nm laser as a light source and 13 photomultipliers, fixed at different angles between 30° and 150°, as detectors. 30° is the angle closest to the forward scattering (i.e. 0°), while 150° the closest to back scattering (180°). The detector located at 130° is slightly modified with respect to the others in order to measure S_{22} instead of S_{12}. This is used as an indicator of the sphericity aerosol particles.

In order to obtain the different matrix elements, the state of polarization of the laser beam is modulated at a frequency of approximately 50 kHz. The state of polarization of the scattered light is then analyzed on-line with a computer by means of a Lock-In

technique. The 13 different angles are measured simultaneously and the system delivers a full set of scattering-matrix elements in less than one second.

Using the measured matrix elements, the size distribution and the complex refractive index of the particles can be determined by fitting the data with modelled scattering calculation using a Levenburg-Marquardt optimization technique. For this, we used a translation to C [9] of the Bohren and Huffman code for Mie scatterers [2], which we adapted for a Log-Normal size distribution.

The particle size distribution was measured using a scanning mobility particle sizer (SMPS). The instrument classifies the particles according to their electrical mobility by means of a differential mobility analyzer (TSI DMA Model 3080) and then counts them optically using a condensation particle counter (TSI CPC model 3022A). The SMPS system is automated with a personal computer that controls the individual instruments and performs data reduction. It was set to register a complete spectrum in 55 seconds and start a new measurement every minute.

Discussion

The SMPS is a relatively slow system that provides a size distribution spectrum by scanning the particle diameter and counting the number of particles for every size. It is designed to measure steady or slowly changing aerosol concentrations. These requirements are, of course, incompatible with the dynamics of a test fire, where the particle concentration is usually increasing with time. Still, the SMPS system delivers valuable information about the particle size. In our case, its measurements can be interpreted by keeping simple guidelines in mind. During all of our tests, the scans were done from small to large particle sizes. A scan was completed in 55 seconds. This means that the number of particles with $d_p = 20$ nm (lower end of the concentration) refers to the concentration at the start of the scan, whereas the number of particles on the upper end represents the concentration 55 seconds later. For an increasing concentration, the number of particles at the upper end will be exaggerated in comparison to the lower end. This will make the geometrical mean diameter, d_{pg}, appear larger. The opposite will happen for a decreasing concentration, leading to a smaller d_{pg}.

Figure 1 shows the evolution in time of the size distribution spectrum for all the test

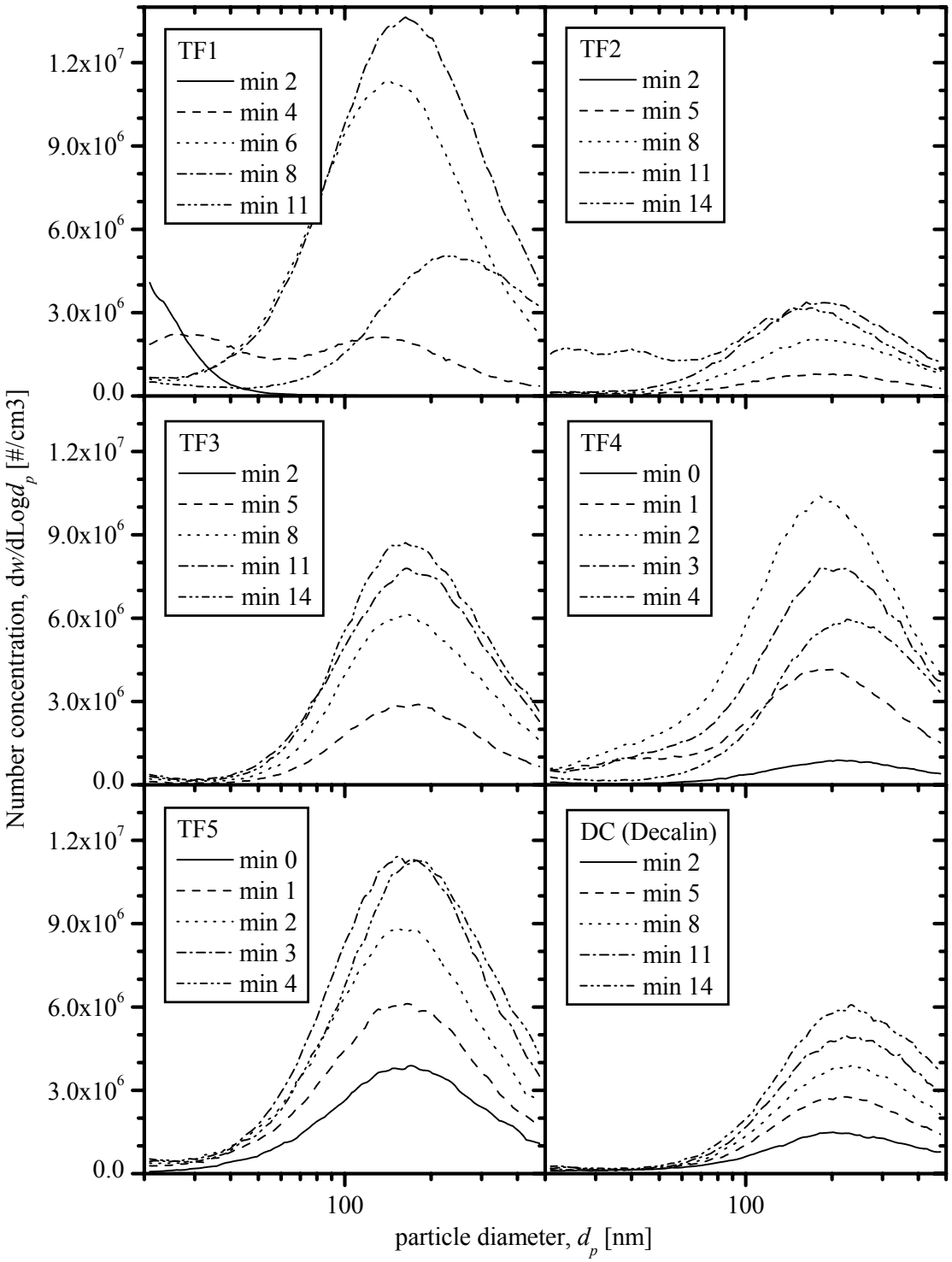

Fig. 1. Size distribution for all test fires as measured with the SMPS system. The time given for each curve marks the start of the measurement. In every test, a complete spectrum was registered every minute.

fires. A complete spectrum was registered every minute but, for visualization reasons, only five samples are shown from every test. In the case of TF4 and TF5, the figure covers the complete test, which lasted just a little over 5 minutes.

The size spectra of all test fires look very similar. This is, in most of the cases, they have a log-normal size distribution and their size parameters, d_{pg} and σ_g, do not vary significantly. There are just few exceptions, like at the end of the TF2 (smoldering wood) where a second smaller peak is present at minute 14. The peak appears at the same moment where the smoldering material catches fire due to the high temperature. Therefore, the bimodal distribution is most probably caused by a mixed combustion where the small particles originate in the open combustion and the large particles in the smoldering. A similar situation can be seen at minute 11 from the TF1 (flaming wood), when the flame disappears and the smoldering starts. The particle concentration decreases and the distribution is shifted towards larger particles. Also in TF1, during minute 2, a small peak is present at the left of the spectrum, showing the presence of very small particles. The peak is still present at minute 4 and disappears afterwards. This corresponds to the particles generated by the flaming combustion of alcohol used to start the test. The peak disappears when the alcohol is totaly combusted.

When removing the spectra of the special cases (the mixed combustion phases and the particles originating from the alcohol fire) the rest of the curves can be well fitted by a log-normal size distribution. Figure 2 shows a plot of the fitted parameters for our set of test fires. The figure shows that no conclusion can be drawn out about the origin of the particles, smoldering or flaming, by simply looking at the size distribution. The same statement can be made about the quantity measured by the commercial photoelectric (scattering) detectors: the total scattered intensity of unpolarized light at a fixed angle, $I_{\mathrm{sca}}(\theta)$. Particles originated in smoldering fires scatter light more efficiently than particles originated in flaming fires. However, a second parameter, like number concentration, is needed in order to discriminate between the different fires.

From equation 1 follows that $I_{\mathrm{sca}}(\theta) \propto S_{11}(\theta)$ for unpolarized light. Therefore, $I_{\mathrm{sca}}(\theta)$ is one of the parameters measured by the DPS. Figure 3 shows the evolution in time of $I_{\mathrm{sca}}(30^{\circ})$ for two very different fires, TF1 and TF2. It can be seen that the maximum scattering intensity for TF2 is one order of magnitude larger than for TF1 even if the maximum particle number concentration for the latter is about 4 times larger than for

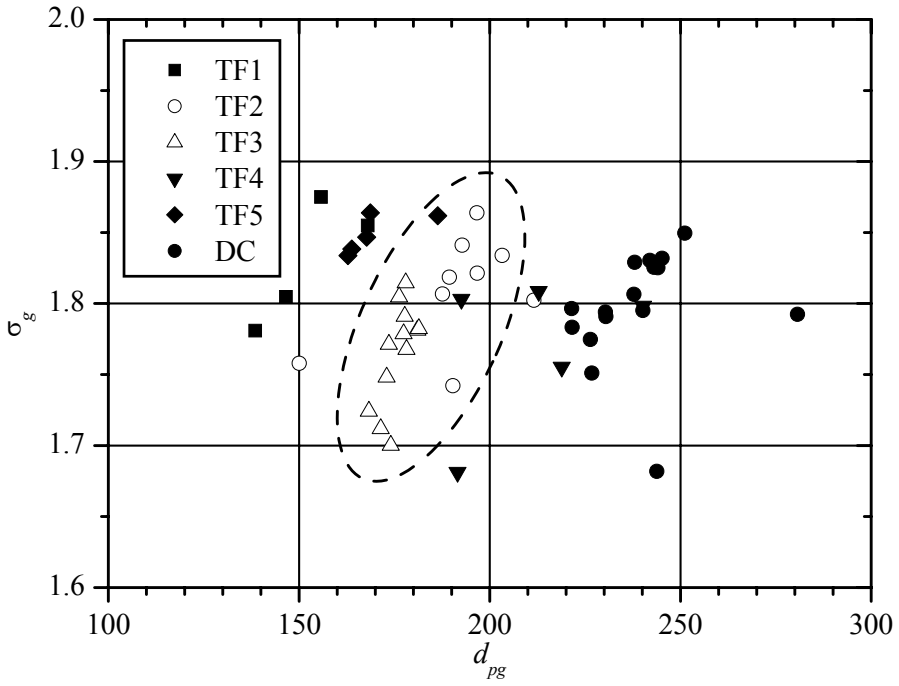

Fig. 2. Geometrical standard deviation, σ_g, and mean geometrical diameter, d_{pg}, for all test fires at different moments during the test. The parameters where obtained from a Log-Normal fit to the particle size distribution. The ellipse marks the area where most of the points corresponding to the smoldering fires are located (open symbols).

TF2. Also in figure 3, it is interesting to see that the optical data clearly marks the point of transition from smoldering- to flaming combustion in the TF2 test (the other way around in the case of TF1) by a steep decrease (increase) in $I_{\mathrm{sca}}(\theta)$.

On the other hand, we can distinguish the type of combustion by looking at the complete set of scattering-matrix elements measured by the DPS. Figure 4 shows an example of this. For an easier interpretation, the values of S_{12} and S_{34} are normalized by S_{11}. The curves for the different test fires are clearly separated according to their origin into smoldering and flaming.

At this point, it is worth to emphasize that no assumption whatsoever is made in order to obtain the different scattering-matrix elements. They are the result of an analysis of the polarization state of the scattered light for different states of polarization of the incoming light. Their value results entirely from the properties of the scattering media and not from an approximation to a special case.

Loepfe *et al.* [10] measured the degree of polarization for the EN54 test fires. Their

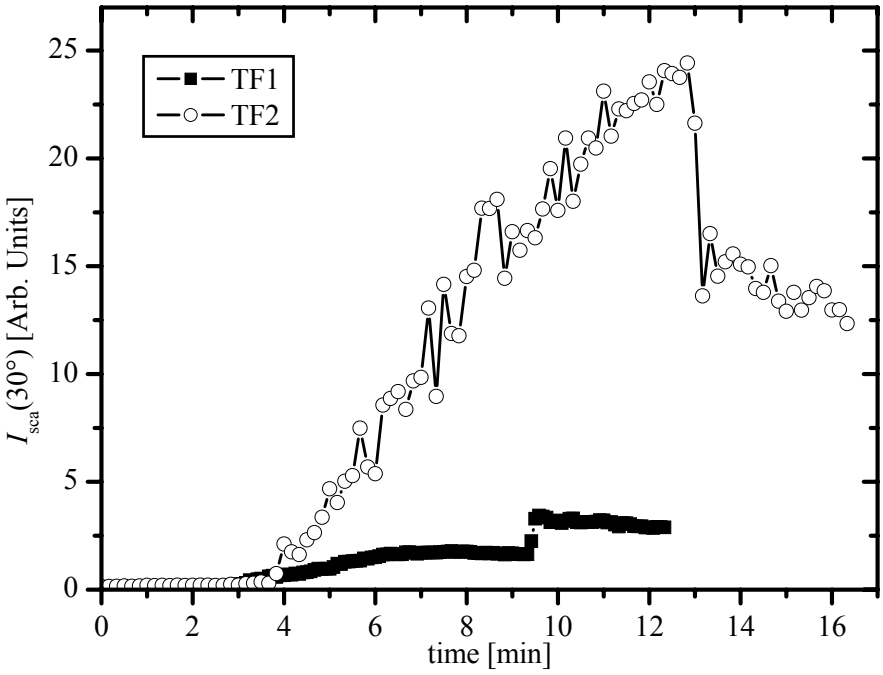

Fig. 3. Evolution of the scattering intensity at 30° during a flaming (TF1) and a smoldering test fire (TF2).

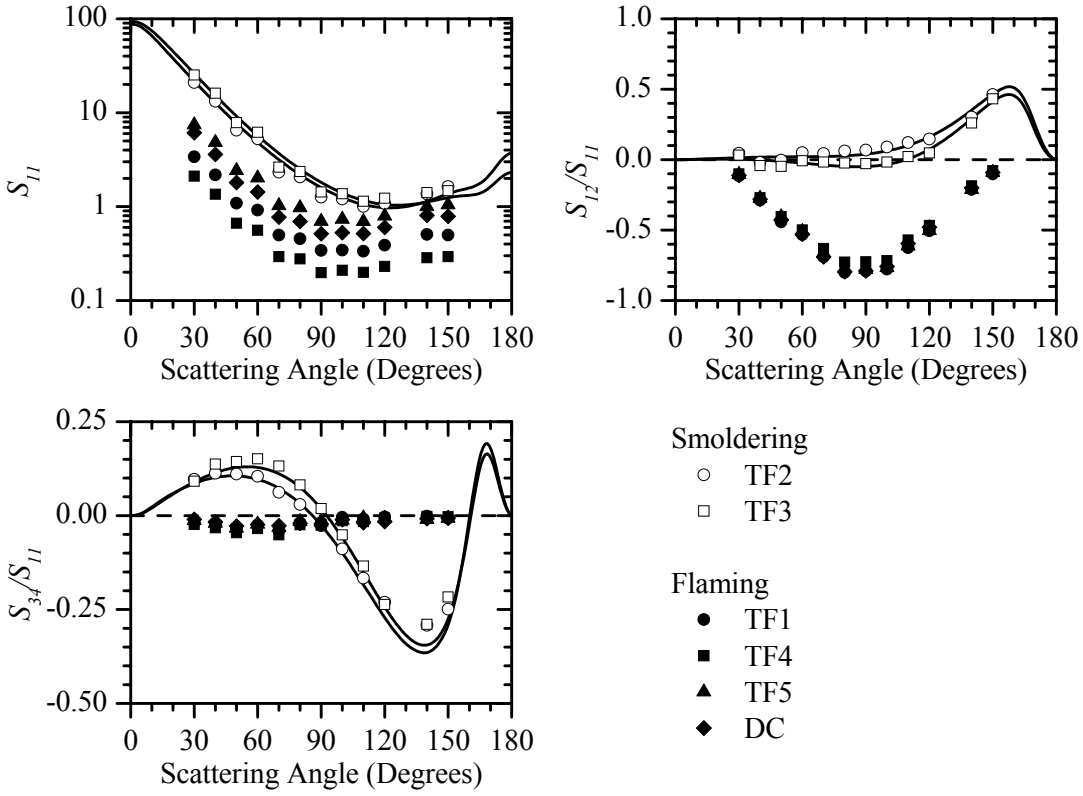

Fig. 4. Snapshot of the scattering-matrix elements for all test fires. The lines are fits to Mie scattering calculations (only available for smoldering test fires).

data is equivalent and very similar to our S_{12}/S_{11} measurements. In their work, Loepfe *et al.* compared the shape of the S_{12}/S_{11} curve for flaming fires to the typical shape produced by Rayleigh scatterers and concluded that particles originating in flaming fires have smaller diameters. Our SMPS measurements give us further insight to this and show that the particles originating in EN54 flaming fires are not Rayleigh scatterers. The difference in the polarization state must therefore come from the shape and/or complex refractive index of the particles.

It has been reported that particles originating in flames are aggregates with fractal dimension smaller than 2 (see, e.g., [11]) and that their scattering is well described by the Rayleigh-Debye-Gans approximation [4]. This assumption is compatible with our measurement of the S_{22} scattering-matrix element at 130°. We found the ratio S_{22}/S_{11} to be closer to unity ($S_{22}/S_{11} = 0.9$) in the case of smoldering than in the case of flaming fires ($S_{22}/S_{11} \approx 0.7$).

A Mie analysis (lines in figure 4) was only possible in the case of particles originating in smoldering fires. The reason for this is that a great amount of volatile material condenses on these particles giving them a compact structure [12] which is close to the ideal spherical shape. No reasonable fit was possible for the flaming fire particles. This was to be expected, given their low fractal dimension and small S_{22}/S_{11} ratio. Rayleigh scattering is a special case of the Mie theory. Therefore, the fact that no Mie analysis was possible for this kind of particles shows once more that the flaming-fire particles are not Rayleigh scatterers.

Figure 5 shows the comparison of the size distribution parameters calculated through the Mie analysis with the SMPS data for the TF2 test. The information obtained through both techniques is very similar. Before minute 7, σ_g shows a much wider distribution in the case of the Mie analysis. This can be caused by a few large particles that are not seen by the SMPS, or simply by a poor fit due to the low particle number concentration, N, of the diluted aerosol. After minute 13, the ignition produces a bimodal size distribution with a first peak around 30 nm and a second around 170 nm. This is seen by the SMPS system and results in a sharp drop of the total d_{pg}. At this point, the test room is completely filled with the smoke of the smoldering phase, which scatters light more efficiently than the flaming-fire particles. This is the reason why the Mie analysis only corresponds to the second peak (open circles in figure 5).

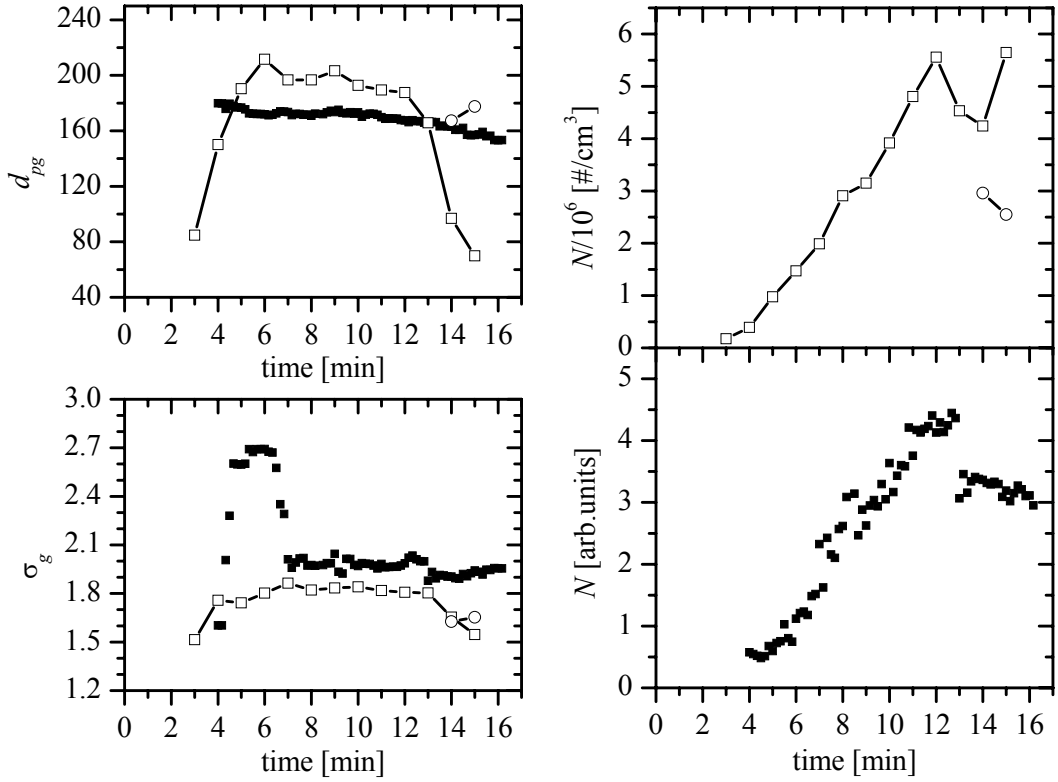

Fig. 5. Comparison of the size distribution parameters for the TF2 test, as calculated from the SMPS data (open squares) and the DPS data (solid squares). After minute 13 a bimodal size distribution was used to fit the SMPS data. The open circles represent the resulting d_{pg} and σ for the second peak of the bimodal distribution.

The ignition is seen by the Mie analysis as a sudden drop in N, which is also seen by the SMPS for the second peak.

We found the average refractive index, m, of the smoldering fires to be $m = 1.57 - 0.01i$ in the case of TF2 and $m = 1.55 - 0.02i$ for TF3. These values have a very small imaginary part, smaller than the reported value for a typical urban aerosol: $m = 1.56 - 0.087i$ [13]. They are however in accordance to the study for forest fires by Patterson and McMahon [14], where they assumed a fixed size distribution and a fixed real part of the refractive index ($\mathrm{Re}(m) = 1.53$) and arrived at an imaginary part in the range $0.004 \leq |\mathrm{Im}(m)| \leq 0.07$.

Summary

We measured the size distribution and the S_{11}, S_{12}, S_{34}, and S_{22} scattering-matrix elements for the aerosol particles originating in several standard EN54 test fires and the non-standard flaming decalin fire. The size distribution measurements showed no marked differences regardless of the combustion type (flaming and smoldering). Only differences in the total number of particles were observed. On the other hand, we observed that the simultaneous measurement of several scattering-matrix elements serves as a good discrimination criterium for the different types of combustion.

The smoldering-fire aerosols are well described by the Mie theory, whereas flaming-fire aerosols are not. In the case of the smoldering fires, the size distribution parameters obtained through a Mie analysis are very similar to ones measured by the SMPS system.

The characteristic S_{12} fingerprint of the flaming-fire aerosols is similar to those of particles much smaller than the wavelength of light (Rayleigh scattering). However, both techniques, the optical analysis and the SMPS data, show that the particles originating in the EN54 flaming-fires are not Rayleigh scatterers (at $\lambda = 532$ nm).

References

[1] A. Hunt, M. Quinby-Hunt, and I. Sheperd, "Polarized light scattering for diesel exhaust particulate characterization," in *Proceedings of the DOE Diesel Engine Emissions Reduction Workshop*, Castine, MA, July 6-9 1998.

[2] C. Bohren and D. Huffman, *Absorption and scattering of light by small particles*. Wiley Science Paperback Series, New York, U.S.A., 1983.

[3] A. Jones, "Light scattering for particle characterization," *Progress in Energy and Combustion Sci.*, vol. 25, pp. 1–53, 1999.

[4] C. Sorensen, "Light scattering by fractal aggregates: A review," *Aesorol Sci. Technol.*, vol. 35, pp. 648–687, 2001.

[5] M. Quinby-Hunt, P. Hull, and A. Hunt, *Polarized light scattering in the marine environment.* Academic Press, 2000, ch. 18, pp. 525–554.

[6] ——, "Predicting polarization properties of marine aerosols," in *Proc. SPIE*, vol. 2258, 1994, pp. 735–746.

[7] M. Quinby-Hunt, L. Erskine, and A. Hunt, “Polarized light scattering by aerosols in the marine atmospheric boundary layer,” *Appl. Opt.*, vol. 36, pp. 5168–5184, 1997.

[8] *EN54: Components of automatic fire detection systems*, European committee for standarization, 1987.

[9] P. Flatau, http://atol.ucsd.edu/∼pflatau, 1998.

[10] M. Loepfe, P. Ryser, C. Tompkin, and D. Wieser, “Optical properties of fire and non-fire aerosols,” *Fire Safety J.*, vol. 29, pp. 185–194, 1997.

[11] H. Kim and M. Choi, “In situ line measurements of mean aggregate size and fractal dimension along the flame axis by planar laser light scattering,” *J. Aesorol Sci.*, vol. 34, pp. 1633–1645, 2003.

[12] D. Steiner, H. Burtscher, and H. Gross, “Structure and disposition of particles from a spark-ignition engine,” *Atmos. Environ.*, vol. 26A, pp. 997–2003, 1992.

[13] W. Hinds, *Aerosol Technology*, 2nd ed. John Wiley & Sons, 1999.

[14] E. Patterson and C. McMahon, “Absorption characteristics of forest fire particulate matter,” *Atmos. Environ.*, vol. 18, no. 11, pp. 2541–2551, 1984.

Paul Drake CEng MIEE, Principal Engineer, Electronic Test Laboratory
Building Research Establishment, Watford, United Kingdom

The Future of Technical Appro als of Security uipment ithin the uropean conomic Area

Abstract

The acceptance and use of national standards for the security industry throughout Europe is in a state of flux. In the United Kingdom for example, the arrival of EN50131-1 and the imposed withdrawal date of the British standard that it replaces has sent the various factions of the security industry – manufacturers, installers, trade associations and accrediting bodies - into a state of high confusion. Other influential players, such as the Association of Chief Police Officers (ACPO) and their policy for reducing the number of false alarms, have added to the complexity.

This situation is replicated, to a greater or lesser extent, throughout Europe. Of course the long gestation period of the new standards, coupled with the news that a revision is already on the horizon, has not helped.

Market drivers such as the need to maintain and improve quality within the industry coupled with the potential influx of low-cost product from other parts of the globe – particularly wireless systems that can easily be self installed – mean that a widely applied and accepted European security standard can only be of benefit to the industry and the consumer. Likewise the problem of false alarms is driving the market to innovate new technology solutions – either at the detector, panel or system level or in operational procedures. An additional confirmed alarm feature and capability may be difficult to test, approve and integrate with the published European standards.

This paper discuses the applicability of the newly emerging European security standards and examines the various approaches to controlling false alarms in a number of European countries. Through discussion with the various influential players across the continent – some national, some global some parochial and even protectionist in their attitudes - the future path of technical approvals is envisioned.

Introduction

The European security and safety market is today estimated today to be in excess of 20 billion.

Insurance requirements have helped to ensure that the vast majority of commercial and public sector buildings have some form of alarm system installed. Intrusion into commercial premises is a significant problem. The European intruder alarms market is well developed, with a wide range of equipment and systems available.

Three areas of intruder detection that will be changing rapidly over the next year or two will be:

- European Standards and Technical Specifications
- Interconnection methods – wireless systems
- Control of false alarms

The arrival of the EN 50131 series of European standards for intruder detection is imminent. Some standards are already released as full EN (standard) status whilst some are released as technical specification (TS) which although not a full standard, will allow interested parties to prepare for the future.

The increasing popularity of wireless intruder detection systems coupled with a number of new wireless technologies from 802.11 to Bluetooth and the newer igbe (lower cost) technology will result in the standard for interconnection developing to keep in line with practice.

The accidental activation of alarm systems, whether caused by poor installation, malfunctioning equipment or user error has been problematic for both the end-user and the police. Today s modern alarm systems have the ability to integrate confirmation technology which can significantly reduced the incidence of false alarms. Certain countries have developed their own national standards to deal with this particular problem by controlling the system build and installation and covering procedural issues

when an alarm is raised. These techniques may prove problematic in reconciling this area with the European standards.

In the following sections the background and current situation of the European standards is considered, followed by a review of the various pan European influencing bodies – Euralarm, and the European Fire and Security Group (EFSG). The current operational practice in a number of European countries is then considered with specific reference to any control systems for false alarms. Although wireless systems are not directly considered, it must be born in mind that an increasing number of self installed systems (allowed to be connected to alarm receiving centres (ARCs) in some countries), will inevitably lead to higher levels of false alarms.

01 1 - The uropean standard for intruder detection systems

One of the most significant objectives of the new European Standard for intruder detection is to make a single standard for Europe. In doing so it is envisioned that equipment manufacturers will be able to work in a single European market; installers will be able to work in any country and customers will have a clearer picture of the quality of products from a single approval

However the reality is that different countries in Europe have standards of widely varying quality and different practices. Despite many years of work, the process of creating the EN documents is far from complete.

EN 50131 is the top level number designated for intruder detection. Within EN 50131 there are the following sub sections:

- EN 50131-1 – General System Requirements
- EN 50131-2 - Intrusion Detectors
- EN 50131-3 - Control and Indicating Equipment (i.e. the control panel and keypads)
- EN 50131-4 - Warning Devices (i.e. bells and sounders)
- EN 50131-5 - Interconnections (i.e. how detectors talk to panels)
- EN 50131-6 - Power Supplies

- EN 50131-7 - Application Guidelines (i.e. installation and maintenance)

The first documents were published in the late 1990 s.

The governing body for these standards (CENELEC) have decided to put some momentum back into the process by publishing several of the available documents in a form that is not quite a full standard. These are called Technical Specifications or TS s. The plan is that TS documents become full EN documents after a period of two years for review, but in the meantime they can be bought by the public and put to use.

an uropean influencing bodies

There are two main collectives in Europe concerned with the area of electronic intruder detection – Euralarm and the European fire and security Group (EFSG). Both these organisations, one representing the manufacturers and the other the approval bodies and test laboratories, have as one of their goals the multiple certification from a single test based on a set of harmonised European standards.

Euralarm is the association of European manufacturers and installers of fire and security systems. Founded in 1970 its members are national associations of 14 European countries. These associations collectively represent around 700 companies or approx 70 % of the total European market.

Euralarm represents - via their National Associations - the needs of European manufacturers and installers in electronic Fire and Security and aims to influence the positive growth of the market and the added value of the companies serving the market.

Euralarm s strategic objectives are:

- multiple certification from a single test performed on the base of European standards or agreed technical specifications.
- multiple certification to ISO 9000 from a single audit.
- the availability of a consistent set of European Standards and agreed technical specifications.

EFSG are a European group of approval bodies and test laboratories covering the certification of products, materials, systems and services in the fields of fire protection, security and loss prevention.

EFSG member approval bodies are:

- Centre National de Pr vention et de Protection (CNPP) - France
- Building Research Establishment (BRE) – formerly LPC - UK
- VdS Schadenverhütung - Germany
- Svensk Brand Säkerhets Certifiering AB (SBSC) - Sweden
- AFNOR Certification (AFNOR) - France
- ICIM S.p.A. - Italy
- Schweizerisches Institut zur F rderung der Sicherheit (SI) - Switzerland
- Forschungs- und Prüfgemeinschaft Geldschränke und Tresoranlagen (FuP) - Germany
- Danish Institute of Fire and Security Technology (DIFT) - Denmark

EFSG is concentrating on the procedure for Multiple Certification. Within the harmonization of the European market, EFSG is working to establish a common approach to product certification and testing. This is to ensure that all member bodies including their associated laboratories are operating on a common basis.

eographic agaries in the regulation installation and operational procedures of Intruder Detection Systems IDS

There are varying approaches to the regulation, installation and operation of electronic intruder detection systems adopted by different European countries, particularly with regard to the control of false alarms. The following section gives an overview of the various approaches taken in each country drawing on research carried out by the BSIA1.

nited ingdom

Although there are no specific figures for false alarms in the UK the police claim it is unacceptably high. The ACPO policy[2] outlines three levels of police response to security systems.

- Level 1- Immediate
- Level 2 – Routine (attendance may be delayed)
- Level 3 – Response withdrawn

If the security system suffers two false alarms in a twelve month period the response will be downgraded from level 1 to level 2. Five false alarms and the system is downgraded to level 3

The UK security industry has taken an active role in the development of British and European standards through various trade associations and inspectorates ; however widespread knowledge of EN 50131 did not occur until the publication of the first documents in the UK in 1997 and 1998. With the publication of these documents and an associated guide it became possible to use the European Standard for an installation in the UK. This guide - Scheme for the application of European Standards for intruder alarm systems is published by BSi and numbered PD 6662: 2000 .

European rules concerning the issue of standards determine that the existence of a European standard covering the same subjects as a national standard means that the national standard must be withdrawn after a period of overlap. It was decided (originally) to withdraw the BS 4737, BS 7042, etc in September 2003. However, the fact that the EN documents are not complete means that complying with the requirements of EN 50131-1 proved to be difficult. Secondly the application in the UK of practices, such as alarm confirmation according to DD 243 (a BSi Draft for Development giving recommendations for the design installation and configuration of intruder alarms incorporating confirmation technology), meant that equipment sold in the UK was specially adapted for UK use (i.e. BS 4737 and DD 243) not EN. It was decided that a longer period would be needed to enable equipment to be designed and

manufactured that allowed for a UK style of EN installation (for example, EN 50131-1 with DD243: 2002). As a result a decision was taken not to withdraw the British Standards until the spring of 2004.

PD 6662:2000 is currently in the process of being updated and will become PD 6662:2004 when published. The development work is being based on an advanced copy of the revised EN 50131-1. DD243 is also in the process of being updated (although with relatively minor changes) and is due for publication in September 2004. The aim is for manufacturers and installers to be using the new EN standards by September 2005.

France

The false alarm rate in France is high – more than 90 percent of the alarms received by ARCs in France are false. This is in spite of more reliable products and improved installation procedures being brought in over the last ten years.

The root cause of the majority of false alarms is attributed to user error.
The method employed in France to combat this high incidence is audio confirmation. Up to 45 percent of all installations now use some form of audio link. ARCs in France are generally smaller establishments leading to a close working relationship between monitoring staff and clients.

The typical security product in France is a complete package including installation, maintenance, monitoring and response. The alarm company provides first response, the police are not involved until the cause of the alarm is known. This method of operation coupled with a fine of approximately 300 if the police are called to a false alarm, leads to good cooperation and ownership of the problem by both the service provider and the client.

What is surprising is that in France a user can self install an alarm system and then log on to an ARC to initiate monitoring. These systems actually generate a relatively low level of false alarms.

ermany

Germany is a highly regulated market and both security products and companies are required to meet strict criteria. The VdS is the umbrella organisation of the German insurance industry and are responsible for carrying out test and certification of security components and systems plus the installation of the system as well. Certified systems must be installed as certified with no substitution of alternative components for reasons of price or availability. Successful products and companies are then added to an authorised list.

A significant difference in the operation of the German security industry compared to the UK is the training of the security company s employees at the laboratory where the product and system are tested. This results in a standardised method of installation which is generally of high quality. The installed systems are inspected only if and when there are some reported problems and the installing company, if found to be at fault, is then removed from the list of approved companies. Reinstatement to the list is not straightforward.

The VdS lists of approved components and systems are a widely recognised reference work for potential buyers, but it is not compulsory to use VdS certified products / systems. On the other hand, from a marketing point of view it is essential for suppliers that their names and products appear in such directories because this is demanded by private and public consumers due to strict insurance rules.

Generally the influential bodies in the German market support the introduction and use of EN standards in Germany although it is unclear as to how the European standards will be used. It is likely that they will be used as a basis for a VdS approval scheme that encompasses the European standards but also adds additional requirements specific to the German market.

Germany enjoys a low false alarm rate and this is credited in part to the use of the Blockschloss system where access to a premises is only possible when the alarm system is deactivated – effectively reducing the possibility of user error. Traditionally a mechanical lock (rarely used today), the modern equivalent is applied in electronic form using special installation techniques on window and door sensors adding cost.

The German police also have a policy for containing the number of false alarms. From 2003 onwards new systems will not be allowed to generate an alarm unless the cause can be verified. Moreover only three ARCs are authorised to pass alarms to the police from banks and similar organisations. All other ARCs must use private response agencies.

Belgium

In Belgium the subject of false alarms is taken very seriously and a law was introduced in 1990 requiring alarm companies to pay an indemnity of between 8,000 to 16,000 against their occurrence. The effect of this law has resulted in high quality, well designed security equipment being installed and the numbers of authorised installers fell by nearly 50%.

In addition the Government can impose swingeing fines and various penalties such as mandatory inspections if a system is found to suffer from false alarms or other procedural failures. Persistent infringement of the rules can lead to the system being placed under the control of a state authorised body with compulsory remedial action.

A ministerial committee is required to approve products following laboratory testing in all cases where the system is to be connected to an ARC. Installation standards are maintained by compulsory training of managers and technicians.

In the Belgian market INCERT is the organisation that is involved in the use of standards and comprises representation from manufacturers, distributors, installers, insurers, consumer organisation, certification bodies and test labs. INCERT is a voluntary certification programme which will use the new EN s and TS s but as long as the available European documents are complete INCERT will also continue to use local standards.

ANPI

The National Association for the Protection against Fire and Intrusion (ANPI-NVBB) is a non-profit association established at the initiative of the Belgian insurance companies.

BOSEC is the organisation which deals with security certification.

S eden

Sweden introduced a system for limiting the effect of false alarms as early as 1990. The system was based on an A/B alarm confirmation principle whereby the activation of any one detector is classed as a B alarm by the ARC. On receiving the B class alarm the ARC then informs the user. The alarm is upgraded to a class A alarm if a second signal from a different detector is received within 30 minutes of the first signal. On receipt of a class A signal the ARC then calls the police.

Information from 1997 indicates that 8.6 per cent of alarms were in the A category and interestingly over a quarter of these were cancelled within five minutes. Of the remainder over 31 percent were indeed crime related.

Following the publication of EN 50131-1 the police are now insisting that ARCs use additional confirmation techniques to additionally vet the A class signals.

Trade associations in the intruder detection sector have their own regulations for professional alarm systems, applicable in the Nordic countries and in many other countries, setting out requirements for the various components of the systems, such as the CIE, power supply, detectors etc. Although compliance with the regulations is voluntary, there are obvious advantages in marketing certified products.

Certification bodies refer increasingly in their regulations to common European standards, which mean that, in the longer term, the test material and results can be used as a basis for certification in several countries.

SP, the Swedish National Testing and Research Institute, offers advisory services, complete testing and examination of system elements for various types of systems. SP claim their test reports are accepted as a basis for certification in Sweden, Norway and Denmark.

Italy

The Italian government is committed to on-going investment in the security industry within the country s infrastructure, with particular emphasis on utilisation of new technologies.

In terms of false alarms Italy provided some revealing information regarding the user attitudes to alarm systems – 83 percent were unsure of using their alarm keypad fearing they could instigate a false alarm. This apparent lack of interest in the systems is further illustrated by the fact that 67 percent did not read the instruction manual and preferred personal instruction and 92 percent would call the ARC rather than responding to any message on the keypad themselves.

As with France, in Italy first response is provided by the security companies; hence users are at no risk of losing police cover.

The use of an electronic key to set and unset the system from outside the premises (similar to the German Blockschloss) is a popular option.

Denmark

In Denmark there is no legal regulation of the security market. The security market is mainly grey (no approvals) or driven by insurance companies. The mutual organisation for insurance companies – SKAFOR has changed its name to Forsikring og Pension abbreviated to F P. F P have a well established business with approval of security equipment, and listing of some other security products. The approval is done according to a set of local standards (SKAFOR or AIA catalogue). These approvals would be recognized in Norway and partially in Sweden. It is expected that F P will change to use EN s and TS s as and when they appear, and they will probably accept certification from European accredited certification bodies. Denmark has a tradition for accepting other EU counties approvals. It is expected in some areas that the Scandinavian countries will accept certification from each other.

astern urope

It is not possible in this paper to cover the entirety of the Eastern European markets and therefore Lithuania is used as a representative example.

It is difficult to accurately estimate the value of the security market in Lithuania, because of the lack of accurate statistics. According to expert estimations, the value of security services purchased in 2001 was about 28-35 million EUR.

According to Lithuanian legislation, security products sold in the country should meet approved EU standards. European standards on intrusion detection (EN 50131) are valid and as far as can be ascertained there are no local standards in place. As Lithuania is now a member of the EU it is keen to be seen to adapt to all EU standards.

Conclusion

There is no doubt that the long awaited arrival of common security standards across Europe is welcomed by most parties whether they be end-user, manufacturer, tester or approver.

The pan-European trade associations are pursuing the ultimate prize of a single European quality mark for intruder detection systems or at least test reports that can and will be accepted by sister organisations. In truth one stop certification may still be some distance away with the Scandinavian countries appearing to be the most forward thinking and advanced in this area.

There are areas of development ahead for the intruder alarm market and the technology that serves it; which is only to be expected in a thriving and growing business area.
A number of approval bodies still see holes in the new standards and it is hoped that the use of the standards – albeit as technical specifications - will either allay the fears and/or enhance the standards to a point where they are more universally acceptable.

At this time the best that can be hoped for is that EN 50131 et al will be seen as a good baseline to build on. A lowest common denominator if you will, that will allow a test report from an accredited test laboratory to be acceptable across Europe. It may be that

in certain countries supplemental testing will be required, particularly in the area of false alarms, before approval to national requirements is granted.

There seems to be a feeling in the industry that we have turned a corner and that with the imminent issuing of the component standards to sit under the general requirements standard, albeit as technical specifications, the industry finally has something to work with.

References

1 BSIA – False Alarms July 2001 – www.bsia.co.uk

2 ACPO Policy on Police Response to Security Systems April 2004 www.acpo.police.uk/policies

Tsigros C.; Huysmans W; Juste P.
ANPI
Louvain-La-Neuve, Belgium

Large scale testing of intrusion detectors: an alternative test method to the walk test?

1. Introduction

ANPI has developped, fifteen years ago, a method for the measurement of the coverage pattern of intrusion detectors.

This method uses an AGV (Auto Guided Vehicle). A heated target (representing a human being) is mounted on the AGV and can rotate in one meter diameter circles on the AGV. Before 1998, tests were made in a 15 m long test room. After 1998, around 380 tests have been made in a new test room of 28 meters long, 11 meters large and 4 meters high.

This paper describes the test facility : the AGV, the targets, the room and the test method.

It analyses the reproducibility and the calibration of the system.

2. Presentation of the test facility

2.1. Description of the AGV

The dimensions of the AGV are the following: 150 x 120 x 67 (L x l x h) cm^3.

It is powered by six batteries of 12 V; 26 Ah, combined to give an 24 V; 78 Ah power source.

The AGV is stationned on floor pick-up pads where the batteries are charged during at least two hours.

The AGV emits 27 MHz ON/OFF signals to the base station. It receives signals at around 1,2 kHz and 1,4 kHz frequency (for longitudinal and transversal displacement) from wires integrated in the floor.

A laptop on the AGV manages the internal control routines for the charging, security aspects, control of the rotationnal speed, and deals with the programmed test paths.

The composition of the AGV is given on figure 1.

General layout of the test system (figure 1)

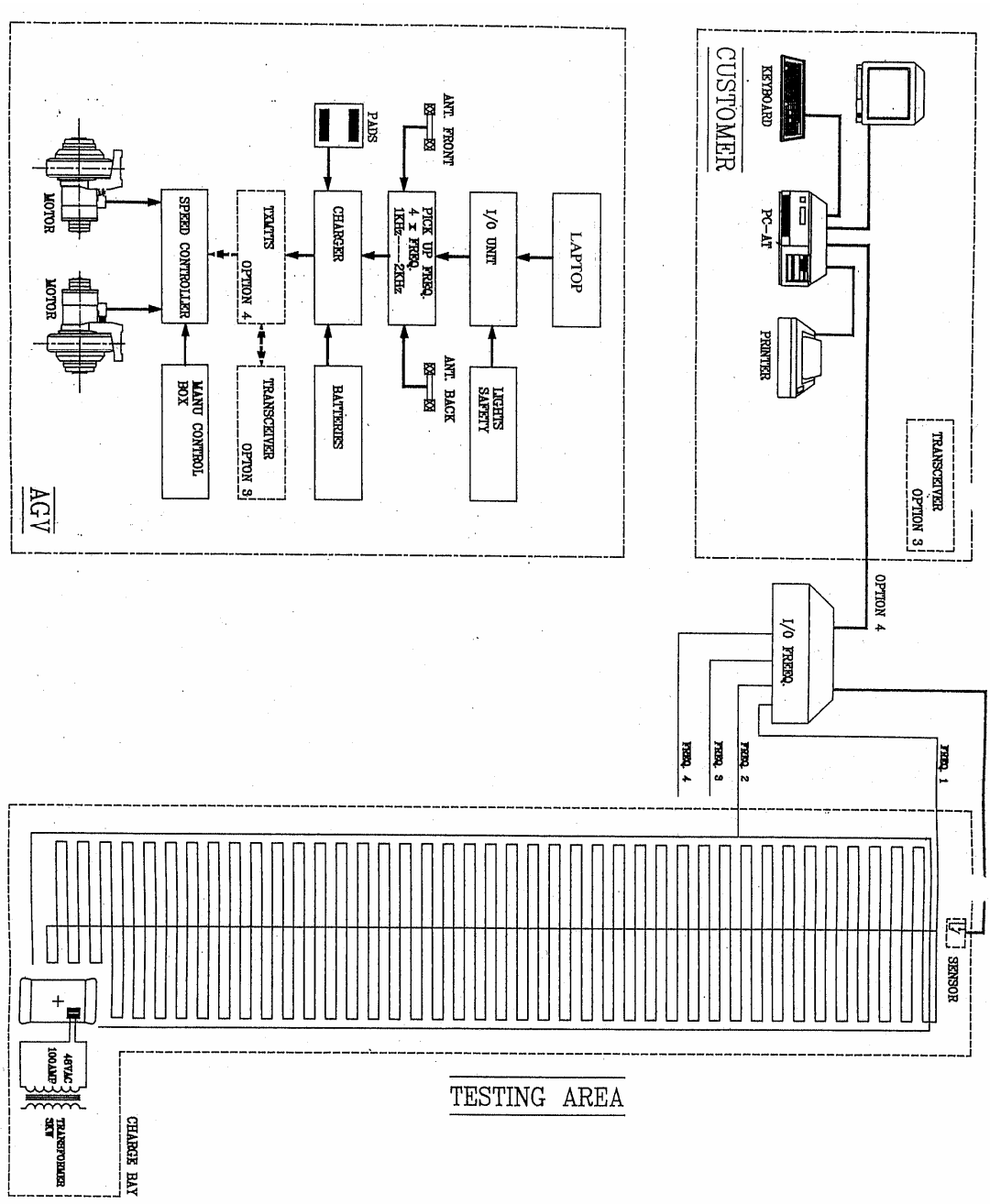

2.2. Description of the Room

The dimensions of the room are the following: 28 x 11 x 4 (L x l x h) m^3.

The temperature is maintained between 18 and 24 °C. The maximum variation of the temperature on the surface of all the walls and floor is 1°C. The maximum variation of the temperature on the surface of the walls in face of detector and floor is 0.7°C.

This is achieved thanks to:

- Climatisation systems that allows renewing of the air and which is shut off during the working days.
- Plaster plates with 5 cm glass wool, 8 cm air gap and concrete blocks.
- The room is partially under the ground level and not directly exposed to solar light.

2.3 Description of the targets

2.3.1 The large target

The dimensions of the large target are the following: 30,5 x 24,5 x 150 (L x l x h) cm^3.

Figure 2 shows the way the wire is bobinated on the target. The target is made, from inside to outside, by a wooden structure, isolation plates, heating wire bobinated horizontally on the height of the target, aluminium plates and a cotton tissue covers the entire target. A temperature regulator achieves a temperature difference of 4 °C higher than the background temperature. The temperature variation on the surface of the target is not more than 1°C.

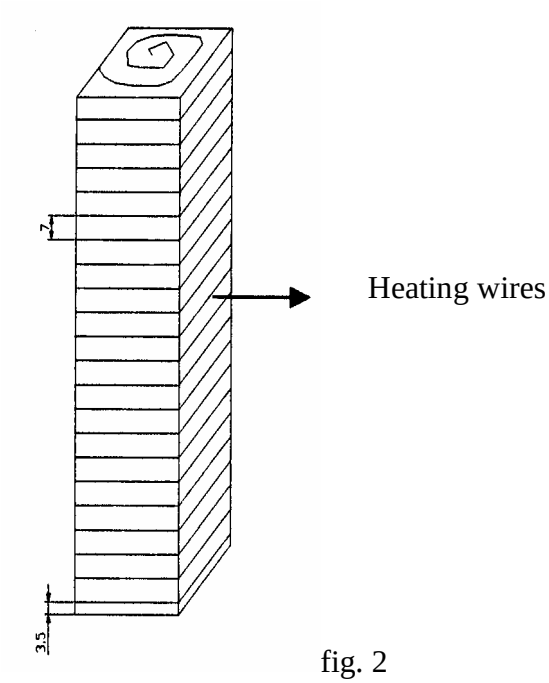

fig. 2

2.3.2. The small target

The dimensions of the small target are the following: 15,4 x 9,6 (L x section) cm^3.
It is composed of a series of electrical resistances that are powered by a constant voltage regulator. No temperature regulator is needed to achieve a temperature difference of 4 °C higher than the background temperature. It is used to simulate small domestic animals.

2.4. Total possibilities and characteristics of the system

- Large scale Test of PIR; PIR+MW; PIR+US intrusion detectors; both wall and ceiling mounted.
- Measurement of the complete detection angle.
- Target rotation speed up to 3 m/s.
- Duration of test: 1h20 (for 15 m path).
- Total measurement time of "15 m; 90°" PIR detector: 5 hours.
- X;Y coordinates of the detection point at RS-232 output.
- Additionnal battery set for continuous operation.

3. Description of the test sequence

a) Inputs: range and coverage angle of the detector (from the manufacturer's specification).
b) Outputs: number of tests needed and path.
c) Do test: the AGV moves from one test point to the other (see figure 3). Then it stops and the target rotates at the programmed speed (0.3 m/s; 1 m/s or 3 m/s). During the rotation the status of the detector is acquired by the base station, see figure 3. After the test the AGV returns to its charging pads.
d) Output of the test : one or more files corresponding to the mounting angle, (each file gives the association between the position of the room and the status of the detector).
e) Compilation of all the files and comparison to the manufacturer's data, see figures 4 & 5.

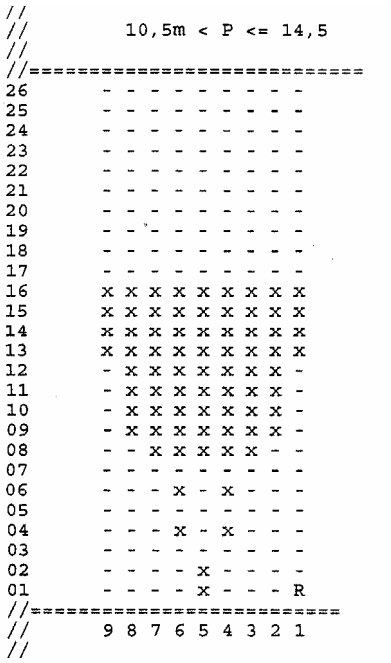

fig. 3

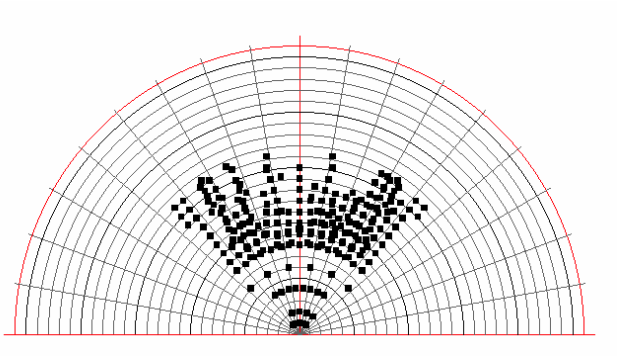

fig. 4

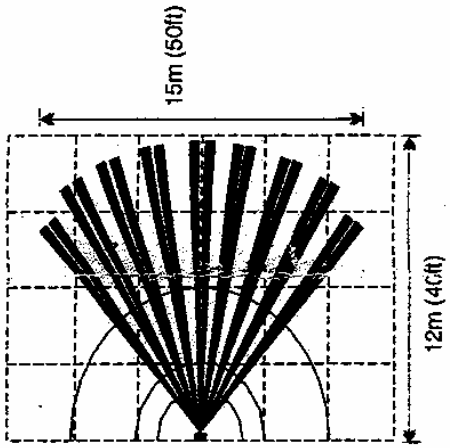

fig. 5

4. Analysis of the method

December 2002 and April 2004: three main grid (Run 1; Run 2 and Run 3) of our three "Reference" detectors were performed within the same day without moving them from their support. The test plan is as follows : detector 1 on position 3, detector 2 on position 5 and detector 3 on position 7. The position is the mounting place of the detector on the support (see figure 6).

The position 5 corresponds to a mounting where the detector faces to the longitudinal direction of the room (mounting angle = 0°) . In the position 3, the mounting angle is 38° and in position 7 the mounting angle is –38°.

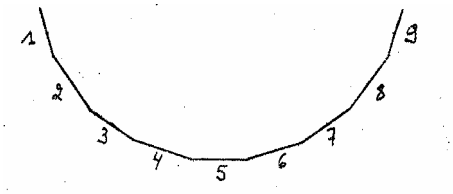

fig. 6

4.1 Repetability

The results shows the number of detection points for each distance from the detector. The graphs show that there is maximum 2 meters difference between the same detector-position in three tests performed the same day.

Test 12 December 2002 (Position 3)

	run 1	run 2	run 3	mean position
Distance (m	Position 3	Position 3	Position 3	
1	0	0	0	0,00
2	1	1	1	1,00
3	0	0	0	0,00
4	1	2	1	1,33
5	0	0	0	0,00
6	2	2	2	2,00
7	0	0	0	0,00
8	4	4	4	4,00
9	3	3	3	3,00
10	5	5	6	5,33
11	5	5	5	5,00
12	5	4	5	4,67
13	2	2	3	2,33
14	2	1	1	1,33
15	1	1	1	1,00
16	0	0	0	0,00
sum	31	30	32	

Test 28 April 2004 (Position 3)

	run 1	run 2	run 3	mean position
Distance (m	Position 3	Position 3	Position 3	
1	0	0	0	0,00
2	1	1	1	1,00
3	0	0	0	0,00
4	1	2	2	1,67
5	0	0	0	0,00
6	1	2	1	1,33
7	0	0	0	0,00
8	4	4	4	4,00
9	3	3	3	3,00
10	4	5	5	4,67
11	3	4	4	3,67
12	2	4	3	3,00
13	2	2	2	2,00
14	1	1	1	1,00
15	1	1	0	0,67
16	0	0	0	0,00
sum	23	29	26	

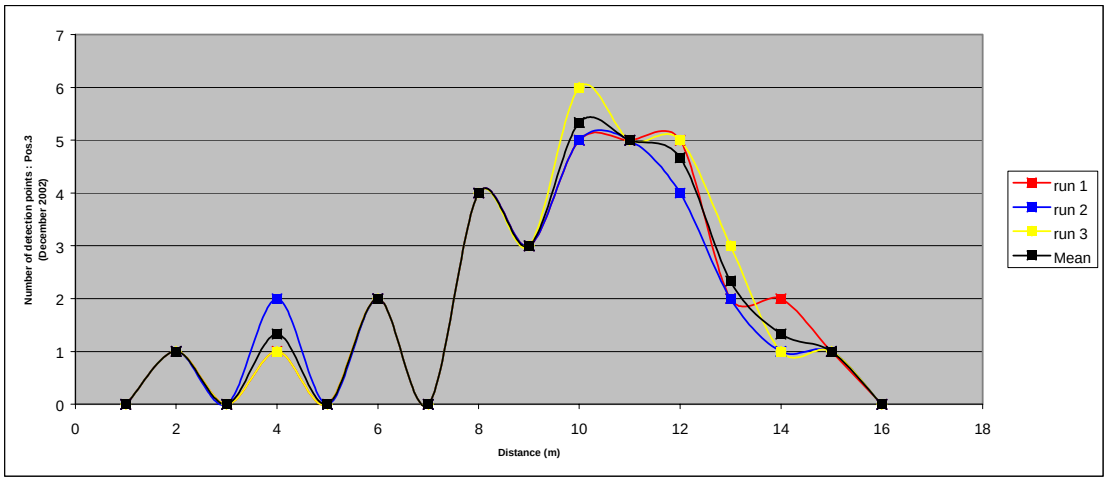

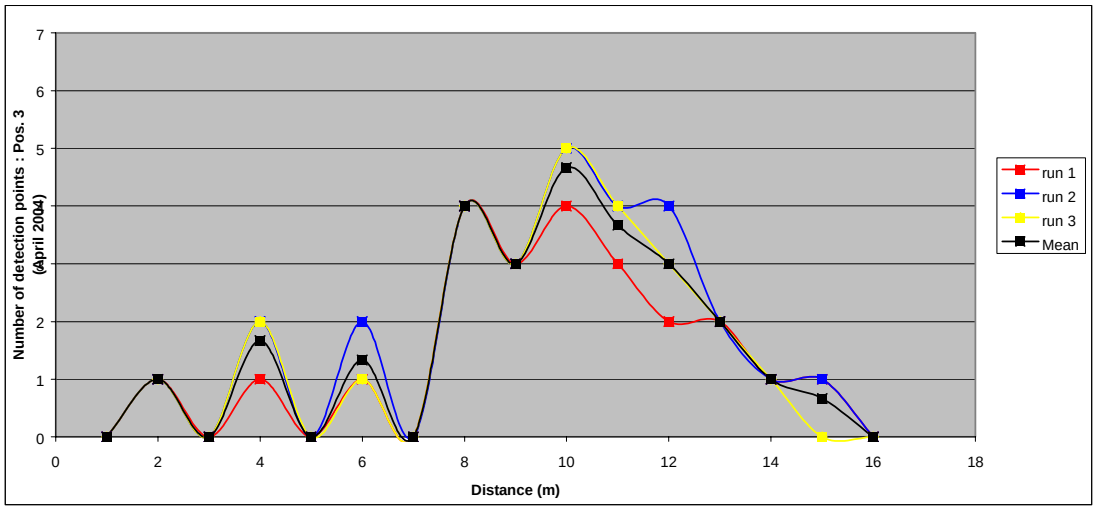
Number of detection points : Pos. 3 (April 2004)
Distance (m)
run 1
run 2
run 3
Mean

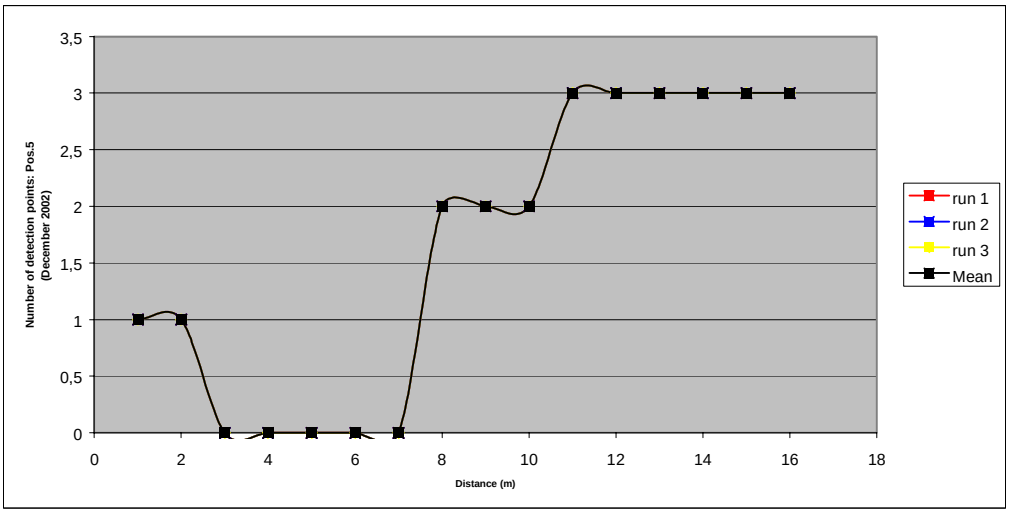
Number of detection points: Pos.5 (December 2002)
Distance (m)
run 1
run 2
run 3
Mean

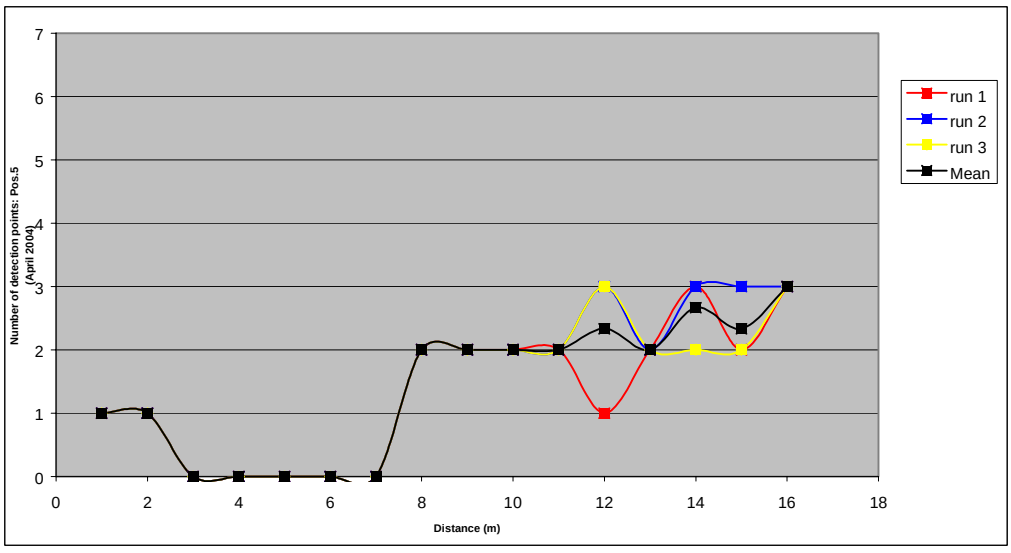
Number of detection points: Pos.5 (April 2004)
Distance (m)
run 1
run 2
run 3
Mean

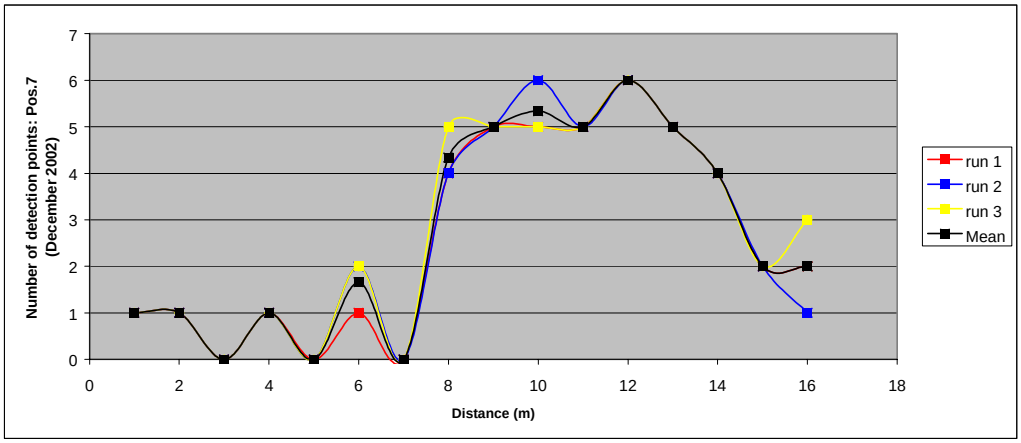

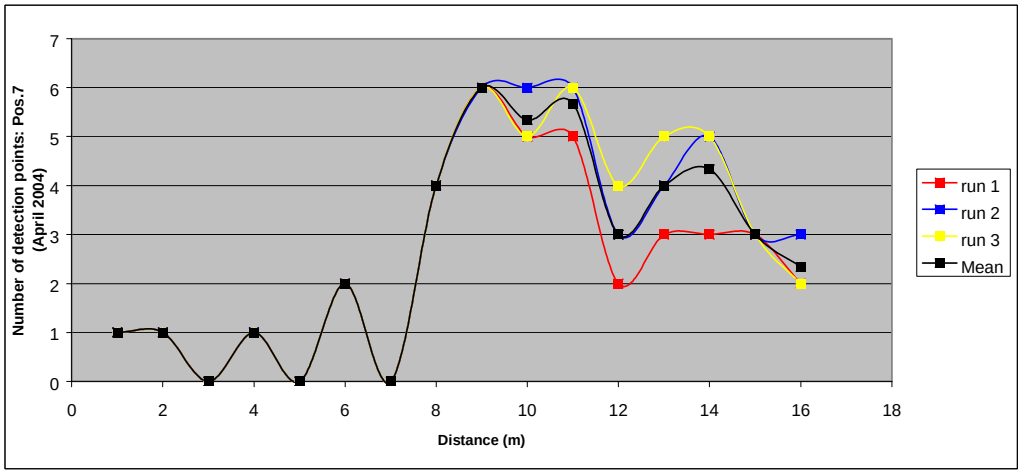

4.2 Reproducibility

The mean value of the detection points for each detector-position at a given distance from the detector is shown in the following graph.

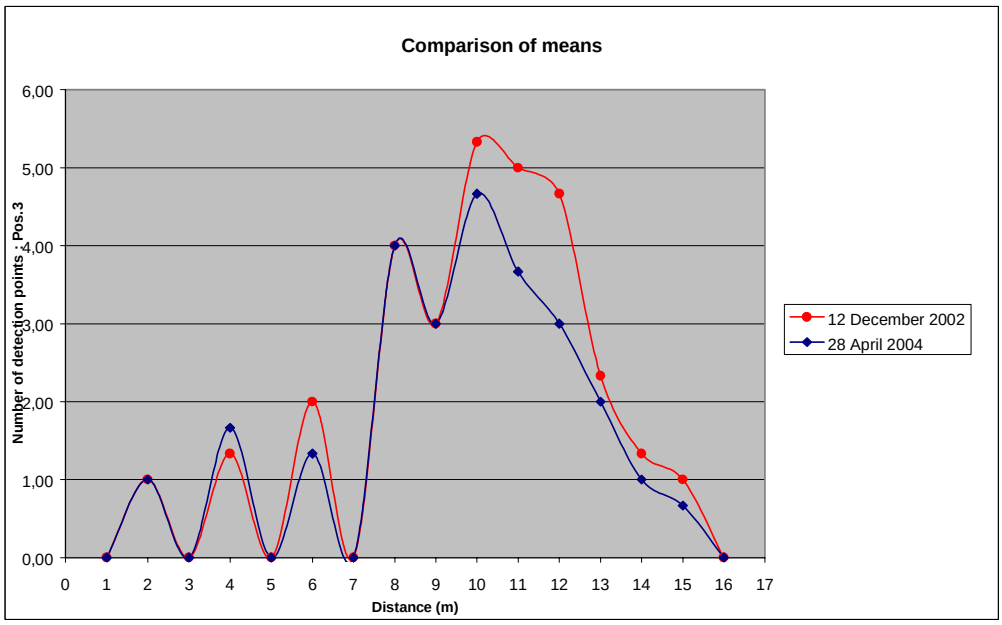

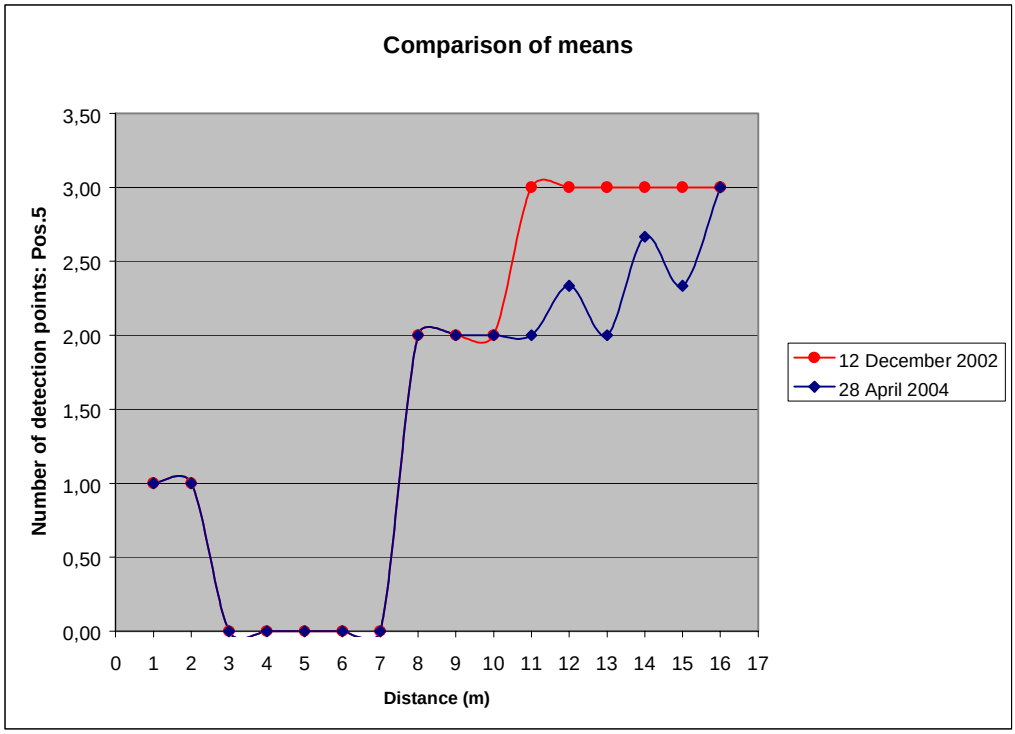
Comparison of means
Number of detection points: Pos.5
3,50
3,00
2,50
2,00
1,50
1,00
0,50
0,00
0 1 2 3 4 5 6 7 8 9 10 11 12 13 14 15 16 17
Distance (m)
12 December 2002
28 April 2004

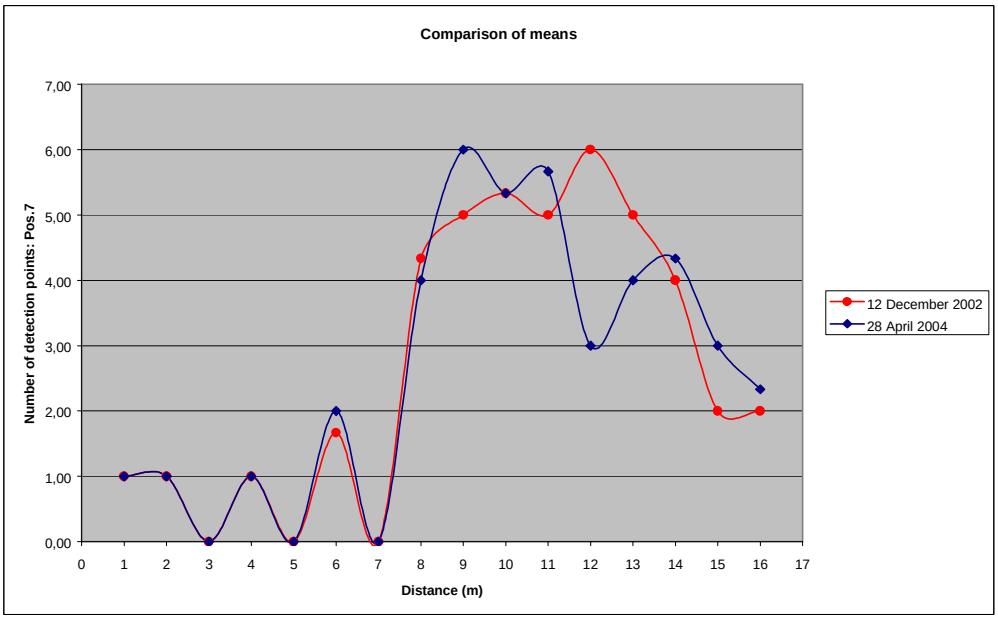
Comparison of means
Number of detection points: Pos.7
7,00
6,00
5,00
4,00
3,00
2,00
1,00
0,00
0 1 2 3 4 5 6 7 8 9 10 11 12 13 14 15 16 17
Distance (m)
12 December 2002
28 April 2004

5. Calibration

5.1 Temperature of the room and the target

The temperature of the room is measured with a non-contact measuring thermometer.
It is calibrated by comparison with thermocouples placed on the target, on the wall and on the floor. If necessary, the calibration error is calculated and taken into account during the measurements with the non-contact thermometer.

5.2 Rotating speed

In order to achieve linear speeds of 0.3 m/s, 1 m/s and 3 m/s the rotation speed is set to the following values 0.0955 turn/s; 0.3183 turn/s and 0.9549 turn/s respectively.
The calibration is made by measuring the time needed to make 10 turns for 0.3 m/s and 1 m/s and 20 turns for 3 m/s.

6. Comparison with walking tests

Walking tests have been performed according prTS 50131-2-2. At 0° detection angle, a man is walking at 1 m/s with angles of 45° and –45° on 3 meter distance, at 12 m; 15 m; 16 m and 17 m from the detector.
Figure 4 shows that for a 0° detection angle, a detection occurs up to 15 m from the detector. The walking test gives a detection up to 16 m from the detector. The difference can be explained from the different temperature difference between the target and the man. The target has a difference of temperature of 4°C relative to the background, the man has a difference of temperature of 9°C relative to the background.

7. Conclusion

We show that with a room and target temperatures under control, and with a detection stimuli principle consisting of a rotating movement as a composition of linear movement in order to control the speed, a reproducible method can be used for the verification of the detection area announced by manufacturers of intrusion detectors.
All this contributes to reduce the time and the costs of the tests.
We have good hope that, in the future, this method could be used for new detector technologies like image comparison, video motion detection, etc…

Ole Olsen

DELTA Danish Electronics, Light & Acoustics, Hørsholm, Denmark

The Intrusion Detector Test System – The IDT test equipment, the test methods and the application of the test methods in type approval testing

Abstract

This paper will present the IDT, Intrusion Detector Test System. We start where the need for a reproducible test method that could quantify the sensitivity of intrusion detectors of different technologies was recognized by the international standardisation authorities. We will shortly see how this problem was addressed by creating an international consortium supported by the European Union, a consortium that should develop methods for this test equipment and later a prototype of the equipment.

The result of the R&D work of the consortium, the IDT equipment, will be explained. Late in this development process, the IDT was utilised for practical intrusion detector test in the same way as it was intended for use in type approval testing. The test results from these tests will be discussed.

A proposal for the implementation of the test method in the CENELEC intrusion detector standards will be presented and, finally, a brief status of the IDT and its impact on the standardisation work in TC79, WG2 will be given. To some extent, the equipment is in commercial service at DELTA.

Introduction

In the late 80'es, the work in the standardisation group WG2 in TC79 in CENELEC recognised the need to be able to assign a figure designating the sensitivity of an intru-

sion detector to test samples of intrusion detectors.

This problem had already been recognised in the CEN work for type approval testing of fire detectors, heat and smoke detectors, covered in the EN54 family standards. The problem in this context was to assign a figure to test specimens of fire detectors that described the sensitivity of the detector. This problem was addressed by the construction of the test tunnel described in the standards EN54-5 and EN54-7. The test tunnel enables the test house to measure the Response Threshold Value (RTV) for a smoke detector, and the Response Time for a heat detector. These values relate to specific conditions during the testing described in the two standards. Most of the measured sensitivities are treated as relative measurements, e.g. before and after environmental tests. Consequently, these measurements of a reproducible sensitivity enabled the standardisation working groups to define a limit for the maximum change of sensitivity during exposure to environmental tests, i.e. define accept criteria for detector stability.

The test tunnel is a rather big and complicated instrument if it complies with the requirements in the EN54-5/7 standards, but the test tunnel is, however, of crucial importance for type approval testing of fire detectors today.

It is not surprising that the working group, WG2, concerned with test of intrusion detectors, encountered the same type of problem during the writing of the first intrusion detector standards. Different approaches had been made to the construction of an instrument which could serve as reference test equipment in the intrusion detector standards, but none of them seamed to solve the problems. Eventually, it was decided that the work was too complicated to be performed within the scope of the WG2 group, and a consortium of nine parties representing detector manufacturers, test houses and a university was established and supported by the European Commission under the framework programme: "Research and Technological Development, RTD". The project was proposed late in 1996 and was started in the beginning of 1998.

The participants in the consortium were:

VdS	ANPI
SIEMENS	SECURITON
CNPP	BRE
GE-Interlogix	DELTA
Gerhard Mercator Universität, Duisburg	

Bench marking test of prototype II

The final result of the industrialised model was tested by the partners at the site of VdS in Köln in Germany in March and April 2002.

Table 1

Description of Environmental test (EnvT)
Dry Heat 55 °C; 16 hrs
Cold -10 °C; 16 hours
Damp Heat 40 °C; 93 % RH; cyclic 2 days; according CEI 60068-2-30 variant 1
SO_2 25 °C; 93 % RH; 25 ppm; 21 days
Vibration endurance 10 to 150 Hz; 9,81 m/s^2; 20 cycles at 1 octave/min in 3 axes(1)
Shock Peak acceleration : A=100-20xM (gn); 6 ms sinusoïdal pulse Directions : 6; Shock/direction : 3(1)
Electrostatic Discharge 6 kV contact; 8 kV air; at least 2 points; 10 discharges/point
Electrical Fast Transient 1 kV; duration : 1 min

In this bench mark test, a large amount of intrusion detectors of 26 different types, submitted by the consortium partners and representing all the detector technologies mentioned in the beginning of this presentation were tested. The conditioning of the test specimens was performed by VdS. The operation of the IDT equipment was performed by representatives of the partners in the consortium. The representatives commented this experience in reports. No major obstacles were encountered due to the IDT equipment, and the test equipment received mainly positive comments and some last proposals for improvements in the final report from the partners.

The tests were performed as a subset of the test which would be made during a type approval test including the application of the IDT test equipment.

The tests included repeatability test (repeated RTV test on the same test specimen), reproducibility test (measurements of RTV variation within the same production lot) and stability test (RTV test of detectors before and after environmental conditioning).

As an example of the obtained results in the bench mark test, the stability of a list of anonymous detectors conditioned in environmental test will be given below.

The environmental conditioning during the bench mark test is listed in table 1.

The SO_2 test was supplementarily performed according to the VdS standard.

The results of the RTV measurements before and after the conditioning were listed and the ratio between the values were calculated and are given in the table 2 below (the ratio 1.0 means no change during conditioning).

Table 2

	Detectors						
Test environment	A	B	C	L	M	N	Y
Dry heat	1,210	1,047	1,025	1,044	1,088	1,084	
Dry cold	1,167	1,071	1,165				
Damp heat	1,515	1,036					
Corrosion_VdS				1,372	3,201	1,049	
Corrosion_IEC	1,294	1,244					1,165
Shock	1,172	1,564					1,000
Vibration	1,184	1,043					1,165
ESD	1,248	1,080	1,060				1,014
Burst	1,442	1,086	1,023	1,097	1,200	1,020	1,113

As it can be seen from the table, good detectors will only change a few percent in sensitivity during mild tests, but some detectors will change several hundred percent during a rough corrosion test. The detectors that changed sensitivity more than 50% in a test are marked with grey colour in the table.

Proposals for application of the IDT equipment in European standards

Based on the assumption that a standard requirement should be easy to fulfil for a "good" commercial detector and only unstable detectors should fail the requirement, a proposal for requirements of tests performed with the IDT equipment was given in the final report of the IDT project. The test requirements were proposed for the CENELEC standard product family for intrusion detectors, EN50131-2-x in the document: "Proposals for application of the IDT equipment in European standards".

The document included requirements concerning the following tests:

- Repeatability test
- Reproducibility test
- Requirements for maximum change of RTV during environmental test

The build standard of the IDT equipment

The final hardware of the IDT test apparatus (prototype II) was integrated in two parts and consisting of the following subsystems:

A. The measurement chamber including an electronic control unit (ECU) and IQ modulator units. These two subsystems are placed in separate EMC tight cassettes at each end of the test chamber as illustrated in the graphic below. The ECU which was a separate rack in prototype I is shown in the schematic at the right side of the test chamber. This ECU cassette contains:
    1. A PCB containing the interface between the PC and the electronic systems in test chamber, infrared emitter driver and IQ modulator box.
    2. A PCB containing the driver electronics for the three stepper motors in the test chamber.
    3. Linear power supplies for all devices in the test chamber including the IQ modulator box, the ECU box and the infrared emitter driver PCB.
    4. Control panel containing test connectors and indicators.
B. A personal computer equipped with interface cards for producing and acquiring analogue and digital signals at defined input and output rates.

In the left side of the schematic, the IQ modulator cassette is shown. This cassette contains the IQ modulators for MW K-, S- and X-band modulation.

An infrared driver PCB for activating the stimulus for PIR detectors is integrated between the two aluminium plates that form the bottoms of the test chamber, close to the 1.0 m infrared emitter platform. In the test chamber, the detector to be tested (DUT) is fixed at a suitable position using a special mounting plate. The DUT position can be aligned under computer control. The detector is then stimulated by means of IR, US, MW signals or combinations of these stimuli. All of these signals are produced by means of 64 D/A channel converters, contained in the ECU.

In the end opposite to the detector, a linear motion unit for mounting of Doppler anten-

nas (US and MW) is situated. This unit enables displacement of the active antenna to measure effect of standing waves in the measurement chamber.

Three platforms for mounting of the infrared emitter array for stimulus of PIR detectors are provided in the test chamber. The 0.5 m platform is used for simulating the walk test target for short range PIR, the 1 m platform is used for normal range PIR and the 1.6 m platform is used for long range devices.

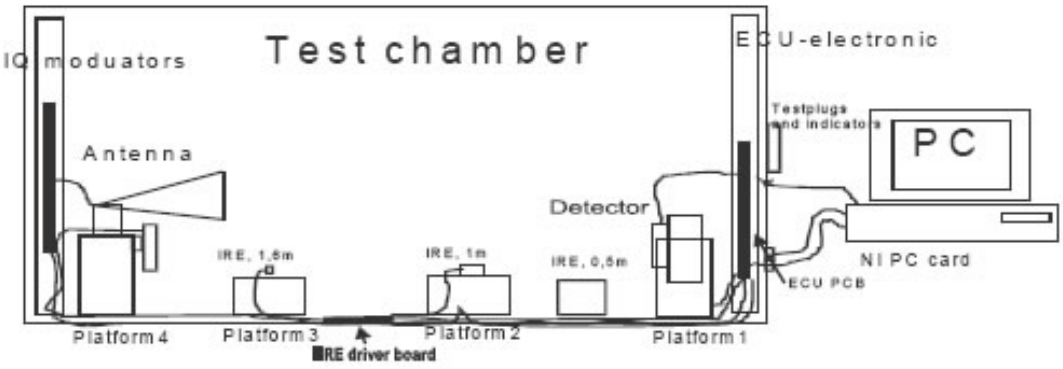

FIG. 1 Structure of the test system

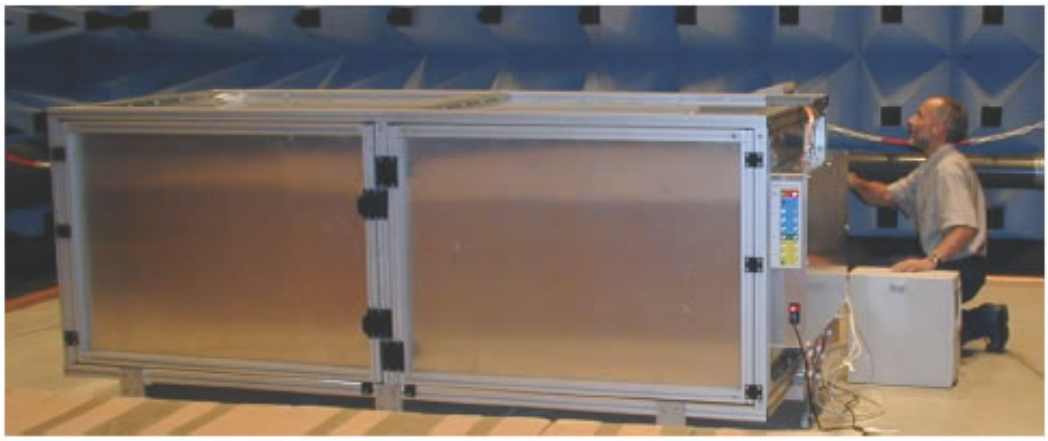

PHOTO 1 IDT test equipment during test

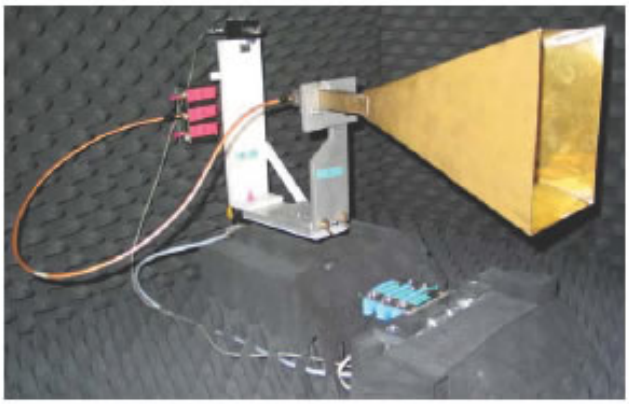

The set-up shows the X-band MW antenna connected to the IQ modulator output.

PHOTO 2 Linear motion platform inside the measurement chamber

PHOTO 3 Two-dimensional rotation unit for mounting of the detector under test.

This unit performs the specified positioning of the rotation and declination of the detector during the test.

Next to the white plate intended for mounting of detectors under test, the analogue instrument for measurement of infrared emitter intensity is visible.

The damping material on all the internal surfaces is visible.

User interface

The IDT equipment is set up for the relevant measurement or utility routine guided by a Windows-look-a-like interface programmed in Labview.

The menus of the PC software offer a variety of options for specify detailed measurements for different detector types, equipment test and calibration routines.

The most important measurement type is the RTV measurement. Basically, this measurement type simulates the walk test target at a speed of 1 m/s passing the detector under test. The test stimulus is created in different ways depending on the detector technology. For PIR detectors, the stimulus is created by successive heating of a group of infrared emitter arrays consisting of 60 emitters.

For US detectors, the Doppler signal corresponding to the passage of the walk test target is simulated in the Labview guided A/D converters and is then analogically modulated on the recorded detector carrier wave. For the MW detector types (X, S and K-band), the modulation of the Doppler signal is performed in the microwave IQ-modulator part of the equipment.

Different magnitudes of stimulation are presented to the detector under test. To find the RTV, the level of stimulation which exactly triggers the alarm condition of the DUT,

the stimulus is presented in a successive approximation scheme. To improve the noise tolerance of the detection routine, the successive approximation is performed with an overlap of 20%.

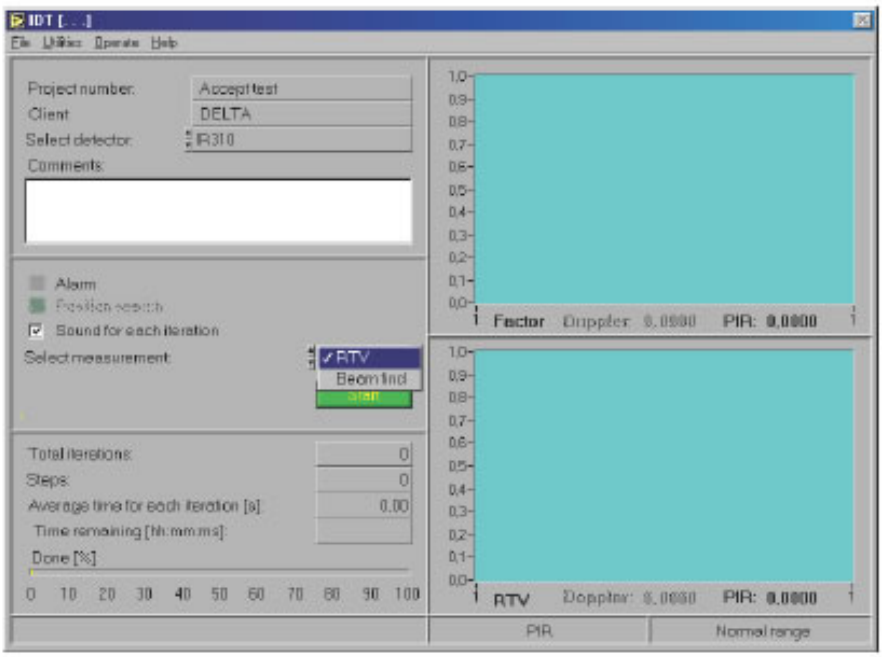

FIG. 2 PC measurement window for set-up of RTV test user interface

Further development of the IDT equipment

After the finalisation of the EU project mentioned in the beginning of this presentation, further work to improve the IDT system has been performed.

At DELTA a program for automatic recording of sensitive zones of PIR detectors has been created. This program benefits from the IDT hardware function for automatic movement of the detector under test and records, in programmable steps, if a certain spatial angular of the DUT is sensitive to IR stimulation. In its present form, the program records the zone as sensitive or not. No sensitivity value (RTV) is referenced to the zone.

If the set-up for this measurement is programmed with a high spatial resolution, the amount of measurements will be considerable and the measurement can be time consuming. The set-up for this measurement, as for the other measurement types, contains estimated measurement times to help the user tailor the right set-up. Though this measurement can last from half an hour to many hours, it is performed fully automatically and can run overnight. The result from the program, called: "Beamfind" is a printable

file, mapping the sensitive zones graphically in a coordinate system with axes labelled "Rotation" and "Declination". An example of the mapping of sensitive zones for a PIR detector is given below.

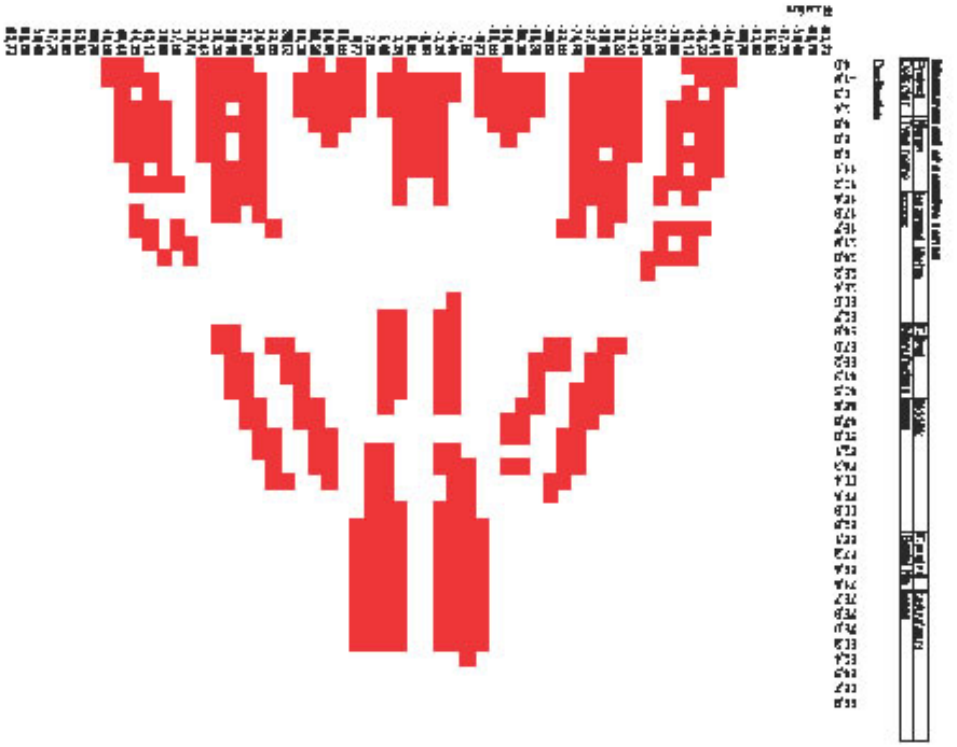

FIG. 3 Sensitive zones plot of a PIR detector automatically recorded with the "Beamfind" program.

Mechanical Doppler generation

At Mercator University, a unit for pure mechanically generated Doppler modulation has been constructed.

The mechanical Doppler unit provides Doppler modulation for US and MW detectors. This unit is more versatile than the electronic system, as the Doppler modulation is rather independent of frequency band and, thus, does not require different set-up for e.g. new MW bands. Furthermore, the mechanical design is rugged and cheaper to build than the electronic system.

The new mechanical unit can be included in the existing IDT measurement chamber.

The mechanical Doppler unit is constructed in a way that simulates the effect of a walk test target extremely well. The magnitude of the Doppler stimulation is guided from the IDT software during the RTV measurement by adjustment of the window size exposing the moving surface to the DUT.

PHOTO 4 Mechanical Doppler unit in front of IDT measurement chamber (not installed)

Status of the IDT application in CENELEC standards

During the development of the IDT equipment, contact to the TC79 WG2 working group was kept through official and unofficial channels. The final result of the IDT project was first presented to WG2 at a meeting in June 2002. At this time, WG2 had encountered big problems in the approval of the detector standards written by the group. Furthermore, some members of the working group considered the IDT to be too expensive to introduce in the standards. This in spite of a price level of the IDT equipment, which was estimated to be at the same level as the cost of a test tunnel for test as described in the EN54 standards. Consequently, many members of the working group were reluctant to implement the IDT equipment in the standards. As an alternative measure for pre and post environmental test, a very simple device was introduced in the standards for BDT (basic detector test). This test is not intended to quantify the sensitivity of the DUT but rather confirm that some detection capability still exists in the DUT after conditioning.

The detector standards from WG2 are now being published as Technical Specifications, and the experience from using them in practical testing will show the need for corrections when the TS's will be voted for as standards (EN's) in two years.

However, in more cases, DELTA has utilised the IDT equipment on commercial terms for supplementary tests on new detector devices in order to predict or improve their quality for the benefit of individual manufacturers, products and end users.

Thomas G. Cleary
Building and Fire Research Laboratory
National Institute of Standards and Technology
Gaithersburg, MD 20899 U.S.A.

Residential uisance Source Characteristics for Smoke Alarm Testing

Abstract

Nuisance scenario tests were performed in the manufactured home used in the Home Smoke Alarm fire test series. The scenario selections were based on what are commonly thought to be causes of residential nuisance alarms, and were designed to mimic normal activities (i.e. no intentional food burning, with the exception of toasted bread.) The bulk of the scenarios were related to cooking activities including: frying, deep-frying, baking, broiling, boiling, and toasting. In addition, cigarette smoking and candle burning were included. Smoldering fire scenarios were examined for comparative purposes. Aerosol concentrations, temperature, humidity, flow velocity and analog output from several photoelectric, ionization and carbon monoxide sensors were gathered. It was observed that nuisance alarms in residential settings were affected by the properties of the aerosol produced, its concentration, the location of an alarm relative to the source, and the air flow that transports smoke to an alarm. This study provides a detailed set of data that can be used to address several issues involving nuisance alarms and reinforces current suggested practices.

Introduction

Smoke alarms are susceptible to alarming when exposed to non-fire aerosols. In residential settings, this typically involves cooking activities or transient, high humidity conditions (i.e., “show steam”). The objective of this research, performed as part of the Home Smoke Alarm project 1 , was to develop a basis for standard residential nuisance source testing. The approach taken was to define a set of nuisance scenarios, replicate the events that cause nuisance alarms, and quantify the important variables that cause nuisance alarms. Translating the results to a set of nuisance source conditions reproducible in a suitable test-bed (i.e., a test room or the fire

emulator/detector evaluator) would allow for more comprehensive detector performance testing.

perimental

Nuisance scenario tests were performed in the manufactured home used in the Home Smoke Alarm fire test series 1 . The selections were based on what are commonly thought to be causes of residential nuisance alarms, and scenarios were designed to mimic normal activities (i.e. no intentional food burning, with the exception of toasted bread). No consideration was given to the probability of occurrence for any given scenario; the objective was to gather data on a number of scenarios. The bulk of the scenarios were related to cooking activities including: frying, deep-frying, baking, broiling, boiling, and toasting. Cigarette smoke and candles were included. Smoldering fire scenarios (smoldering polyurethane foam, beech wood blocks and cotton wick) were examined for comparative purposes.

A schematic of the manufactured home is shown in Figure 1. Its exterior dimensions were 20.1 m long and 4.2 m wide, with and interior ceiling that was pitched from the centerline height of 2.4 m to a height of 2.1 m at the long exterior walls. The dark shaded areas were closed off. During these tests, all external doors and windows were closed. Most scenarios were repeated with and without a floor fan blowing air from the master bedroom into the kitchen/living room area.

Aerosol concentrations, temperature, humidity, flow velocity and analog output from photoelectric, ionization and carbon monoxide sensors were gathered. Figure 1 shows the approximate ceiling location of all the measurement positions. Details of the measurement are given in NIST TN 1455 1 .

Two portable aerosol instruments were used to gather aerosol number and mass concentrations during the tests. Number concentration was recorded with a TSI model 3007 portable condensation particle counter (CPC) . This instrument is capable of

---

Certain commercial equipment are identified in this paper in order to accurately describe the experimental procedure. This in no way implies recommendation by NIST

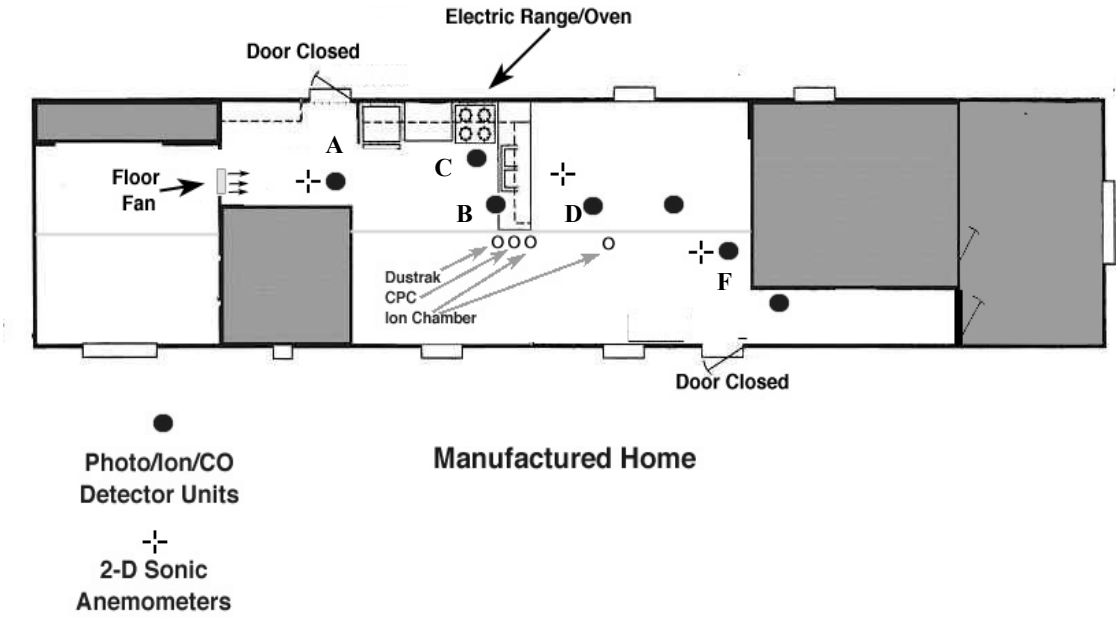

Figure 1 Schematic of the test home

counting particles greater than 10 nanometers up to concentrations of $5x10^5$ particles/cm^3 with an uncertainty of 10% of the reading. The upper concentration limit of the instrument is insufficient for many fire and nuisance conditions so the air sample was diluted with a fixed amount of clean air prior to entering the CPC resulting in an approximate 20 to 1 dilution ratio of the sample. The dilution ratio for each test was obtained by measuring undiluted and diluted background room aerosol prior to the start of the test. The uncertainty in the dilution corrected number concentration is estimated to be 12%. A TSI model 8520 "Dustrak" portable aerosol mass monitor was used to gather the aerosol mass concentration. This device consists of a light scattering photometer that analyzes the laser light scattered at an angle of 90^o from particles flowing through the device. Its default calibration is set to the respirable fraction of standard ISO 12103-1 A1 test dust. It has a range from 0.001-150 mg/m^3. The effective particle size measurement range is 0.1 μm up to 10 μm. The device can be calibrated for any aerosol with scattering properties different from the test dust provided the true mass concentration is determined. Here, the default calibration was used, so any given mass concentration measurement reported are relative to an

equivalent mass of test dust. Since the device in not calibrated to each of the aerosols produced in the nuisance tests, the uncertainty in the measurement in not determined. However, the results are proportional to the mass concentration and correspond directly to the scattering signal strength of photoelectric detectors with an equivalent amount of aerosol in its sensing region.

Seven dual photo/ion smoke alarms were modified at NIST to provide continuous analog output of photoelectric, ionization, carbon monoxide, and temperature sensor values [1]. Each detector was calibrated in the FE/DE with the cotton wick smoke, and the sensor values are presented in engineering units of extinction coefficient (m^{-1}), volume fraction of CO, and temperature in Celsius. The positions of the sensor packages are indicated on Figure 1 and represented in the results by the letters A-G. Carbon monoxide and temperature sensor data are not presented here. All of the data collected in this test series is available in the NIST Report of Test FR 4019 [2].

The time to reach photoelectric and ionization alarm points was determined from ion and photoelectric sensor calibration test data, and estimated alarm sensitivities appropriate for the FE/DE cotton wick smoke. Estimated high, medium and low sensitivities for both photoelectric and ionization alarms in terms of extinction coefficient and obscuration are given in Table 1. These values cover the range expected for residential smoke alarms for each sensor type.

Sensor	High sensitivity m^{-1}, (%/ft)	Medium sensitivity m^{-1}, (%/ft)	Low sensitivity m^{-1}, (%/ft)
Photoelectric	0.05, (1.5)	0.083, (2.5)	0.117, (3.5)
Ionization	0.016, (0.5)	0.033, (1.0)	0.050, (1.5)

Table 1 Alarm sensitivity for photoelectric and ionization sensors

Results and Analysis

The results presented here are for selected tests showing the time to alarm for each photoelectric and ionization sensor at the three sensitivity levels, and the aerosol mass and number concentration at a central ceiling level location. Location E only had an

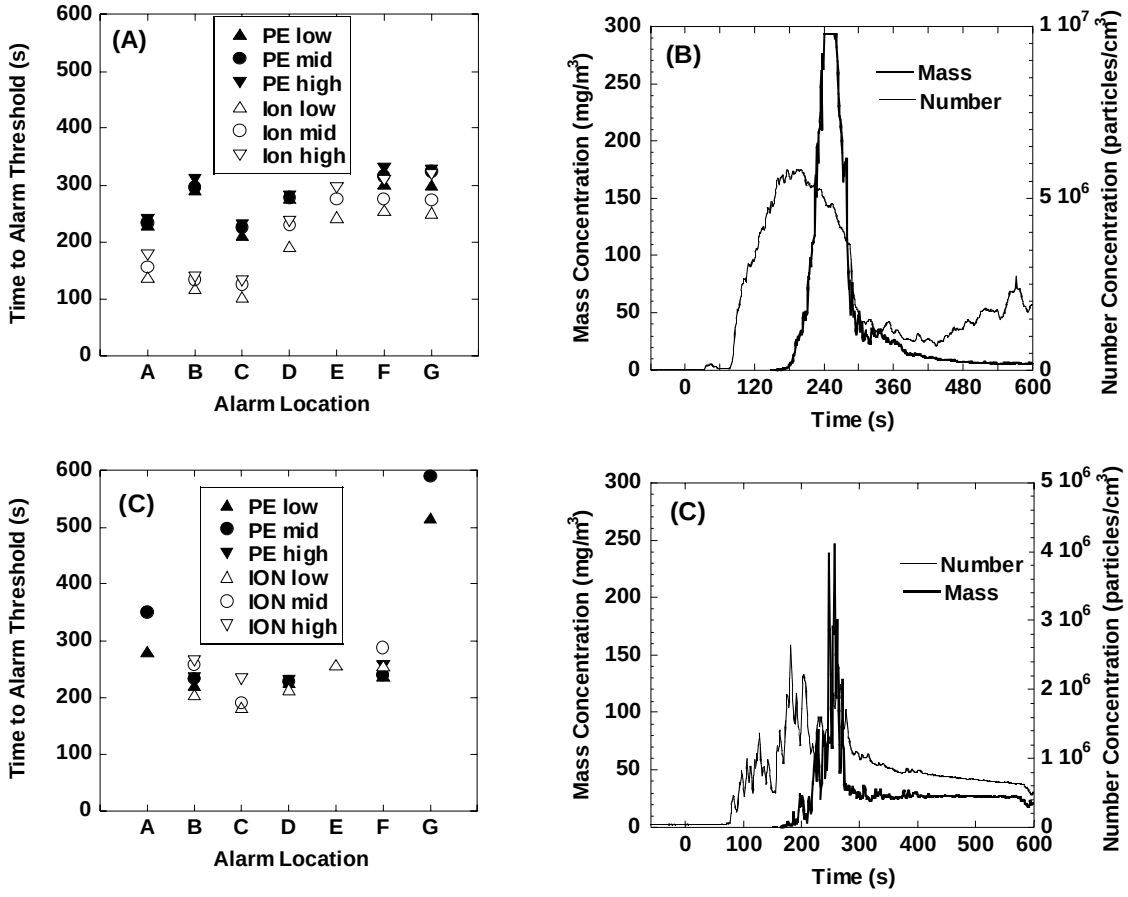

Figure Results for toasting bread Figures labeled A and B are for the test ith no fan and figures labeled C and D sho repeated test results ith the fan on

ionization smoke sensor. Nominal repeat tests are shown without the floor fan on (labeled A and B) and with the floor fan turned on (labeled C and D.)

The toasted bread results are shown in Figure 2. The toaster with two slices of bread was placed on the counter to the left of the range. It was turned on at time = 0 and turned off 250 s later. With no fan flow, the ionization alarms tended to reach their threshold levels before photoelectric alarm. The time to reach the threshold increased as the distance of the toaster from the alarms increased. The number concentration reached its peak before the mass concentration began to rise, and started to fall before the mass concentration peak was reached. With the fan turned on, fewer alarm thresholds were met, and contrary to the no fan case, some photoelectric alarm thresholds were reached before the ionization thresholds, and at some locations the

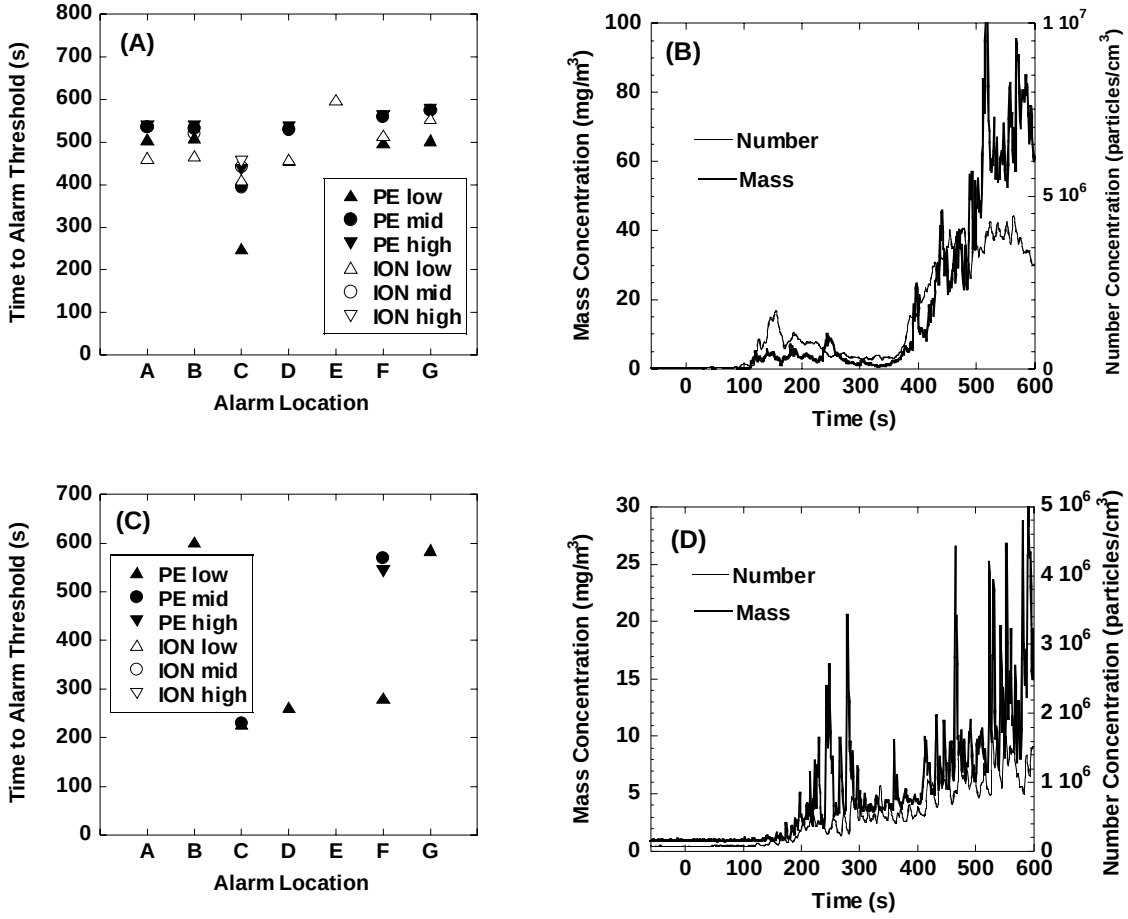

Figure Results for frying hamburgers A and B fan off C and D - fan on

ionization alarms never reached their low threshold. The number and mass concentration trends were similar to the no fan case, but the levels were lower.

Three 110 g frozen hamburgers were fried in an aluminum skillet pan on an electric range. With no fan flow, all locations reached photoelectric and ionization alarm thresholds, most within 100 s of one another. The photoelectric sensor closest to the electric range reached a threshold first. The number and mass concentration increased steadily after 350 s. With the fan on, no ionization alarm thresholds were reached, and photoelectric alarm thresholds were reached at all locations they were present except location A. The number and mass concentration started to increase at 150 s and the mass concentration showed brief sharp increases periodically.

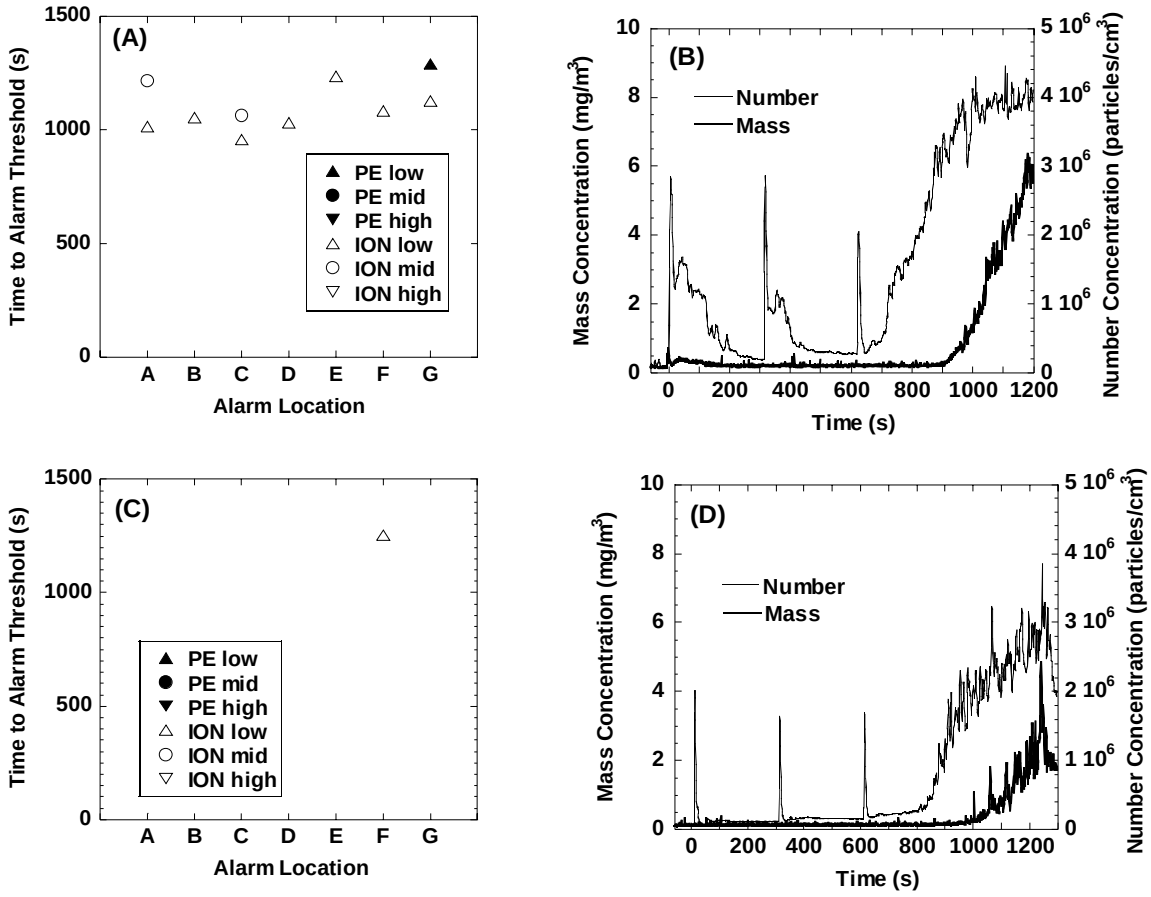

Figure Results for pi a cooking A and B fan off C and D - fan on

A small (158 g) frozen cheese pizza was cooked on a pan in the oven. To begin, the oven was pre-heated to 350 ^{o}F, the pizza was placed in the oven, then baked. The oven door was opened twice during baking time to check the pizza. After 630 s, the oven broiler element was turned on and the door was left slightly open. Figure 4 shows the results for the pizza cooking tests. With the fan off, all locations reached an ionization threshold, and only one location reached a photoelectric threshold. The number concentration results show three spikes at the time the oven door was being opened. The mass concentration doesn t start to increase significantly until about 900 s. With the fan on, only one location reached an ionization alarm threshold, and it was at a location some distance from the oven. The number concentration showed three spikes due to the door opening, but both the number concentration and mass concentration were lower compared to the fan off case.

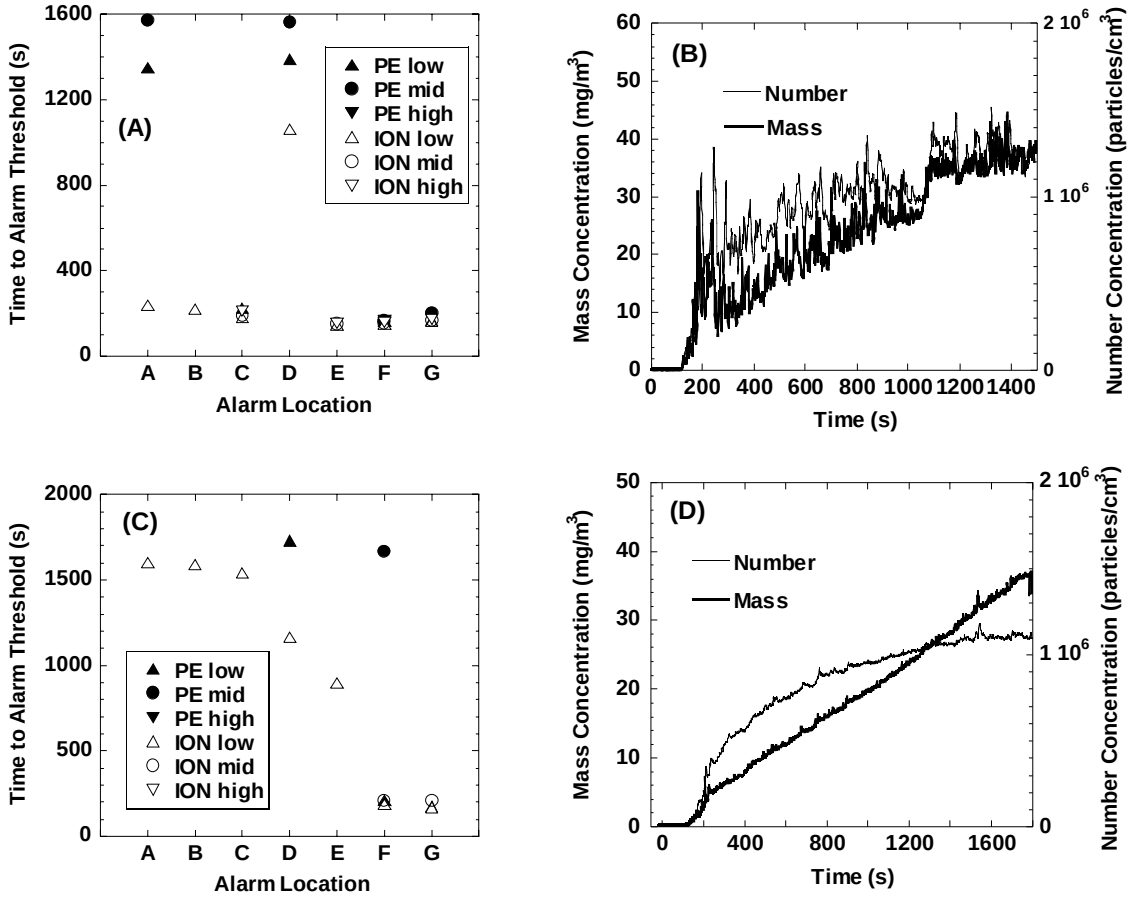

Figure Results for smoldering icks A and B fan off C and D - fan on

The cotton smolder smoke was generated with the staged wick ignition device 3 placed on the floor in the living room area. After an initial delay of 30 s, 8 sets of 4 wicks were ignited with 12 s delay times between sets. With no fan flow, ionization alarm thresholds were reached at all locations. Photoelectric alarm thresholds were reached at the locations nearest the source first, then much later at locations further from the source (Location B did not have a working photoelectric alarm during this test.) The number and mass concentration began to increase around 150 s, and steadily increased during the test. With the fan on, the two ionization alarms closest to the smoldering wicks reached thresholds, followed by the locations further from the source. Only two locations reached photoelectric alarm thresholds. The number and mass concentration began to increase around 150 s. The mass concentration steadily

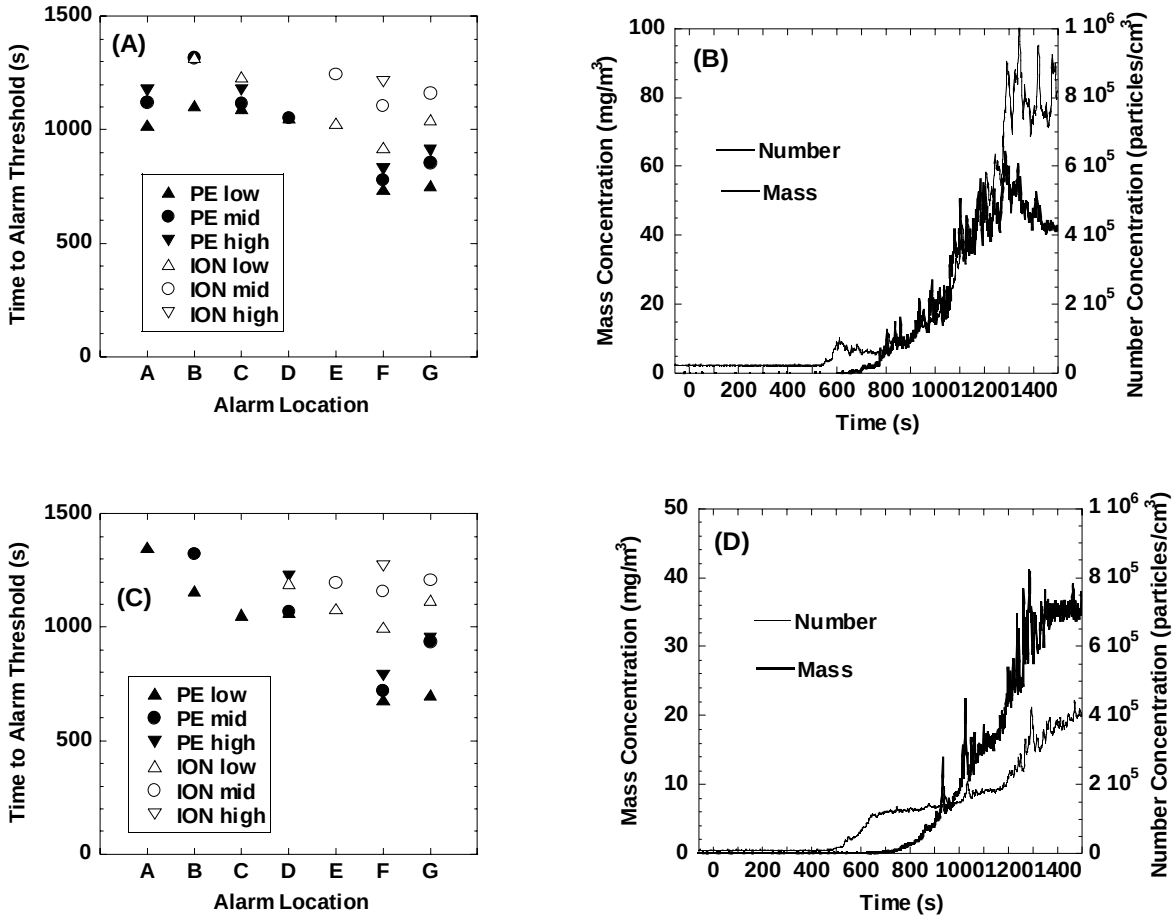

Figure Results for smoldering ood A and B fan off C and D - fan on

increased during the test, while the number concentration rate of rise started to decrease after 200 s.

Wood smoke was produced by placing eight 3.5 cm by 2.0 cm by 1.0 cm beech wood blocks on a 750 W electric hot plate. The hot plate was located on the living room floor, and at the beginning of the test the hot plate was turned on. For the fan off case, the photoelectric alarms reached their thresholds before the ionization alarms at all locations. The number and mass concentration started to increase between 500 s and 600 s, and both increased steadily until the hot plate was turned off at 1200 s. For the case with the fan on, all locations that have photoelectric alarms reached threshold values, and ionization alarms closest to the source reached threshold values. Results were similar to the no fan case. The number concentration started to increase at about

500 s, while the mass concentration started to increase at 700s; the concentration levels were below the no fan case.

Conclusions

The results presented for nuisance source tests and comparative smoldering tests here display several characteristics related to nuisance alarms. Nuisance alarms in residential settings from typical cooking activities, smoking or candle flames were affected by the properties of the aerosol produced and its concentration, the location of an alarm relative to the source, and the air flow that transported smoke to an alarm. These conclusions hold for the additional tests from this series 1 . Threshold adjustment to lower sensitivities reduced the number of nuisance alarms in some cases, but in others, the rate of smoke production was so great, that all threshold levels were reached in a short period of time. With ventilation air flow, dilution of the aerosol as it was dispersed throughout the home tended to reduce the smoke levels below alarm threshold values. This study provides a detailed set of data that can be used to address several issues involving nuisance alarms and reinforces current suggested practice of moving alarms as far away from cooking appliances as practical. Additionally, the results are being programmed into the fire emulator/detector evaluator to reproduce the nuisance source conditions, which will allow for more comprehensive detector performance testing.

References

1 Bukowski, R., Peacock, R., Averill, J., Cleary, T., Bryner, N., Walton, W., Reneke, P., and Kuligowski, E., "Performance of Home Smoke Alarms," Natl. Inst. Stand. Technol., Techical Note 1455, 2003.

2 Cleary, T., "Home Smoke Alarm Project, Alarm Responses to Nuisance Sources," Natl. Inst. Stand. Technol., Report of FR 1419, 2003.

3 Cleary, T., Donnelly, M., and Grosshandler, W., "The Fire Emulator/Detector Evaluator: Design, Operation, and Performance," 12th International Conf. on Automatic Fire Detection AUBE 99, Gaithesburg, MD, USA , pp. 312-323, 2001.

Li Jian[1,2]，Dong wenhui，Mei zhibin

Shenyang Fire Research Institute Ministry of Public Security, China[1]

Dalian University of Technology[2]

Evaluating fire detectors using fuzzy analytic hierarchy process

Abstract

The main objective of this paper is to present a new approach to evaluating fire detector's performance based on fuzzy analytic hierarchy process. The importance and purpose of fire detectors evaluation and evaluating flow are briefly described and it is justified that the evaluation process should be formulated as a multiple criteria decision-making problem under uncertainty. The characteristic of fire detectors including fire detective、surroundings applicable and immunity to false alarm or nuisance sources is proposed as decision attribute using in basic analytic hierarchy process. Detailed test is designed to achieve scores of alternative under multiple criteria. The proposed fuzzy method uses triangular fuzzy number as pairwise comparison judgements rather than exact numerical values to cope with uncertain weights , thus adapting to domain experts' natural languages. A example, illustrating the application of this method to evaluating two kinds of intelligent fire detectors, is given.

Key words: Fire detectors；performance evaluation；analytic hierarchy process；triangular fuzzy number

Introduction:

Fire detectors, which determine actual fire by responding fire resultant such as smoke、gases、flame or change of temperature, are playing important roles in fire automatic detection and alarm systems. The worth of a fire detector is determined as much by its ability not to respond to stimuli that are generated from non-threatening sources as to respond in a timely manner to an actual fire[1].

With the development of technology, a lot of research work has been done to test fire detectors performance.

Cleary[2] use a test bed named as fire-emulator/detector-evaluator(FE/DE) to examine fire detector's performance especially the ability that immune to stimuli not associated with a fire threat. Gockel[3] propose a modular model for fire sensors so as to know exactly how fire sensors' working. Another reason relating to special evaluation maybe associate with end-users who perhaps pay more attention to select the suitable detectors for their application. So we can conclude that the fire detectors evaluating is important and useful. By some well-chosen designed experiments, multiple aspects of a detector's performance can be demonstrated and this maybe give end-users a references to select better products.

In order to point out fire detectors performance, multiple factors, which act mutually and co-adapt in the whole evaluating process, must be distinction to insure the validity and scientific of the final result.

The remainder of this paper is organized as follows: Section 2 describes the main factors in the evaluating process. Section 3 describes the basic framework of the Analytic Hierarchy Process and discusses the uncertainty pairwise comparison in actual application. Section 4 contains the brief of experiments. Section 5 describes fuzzy method uses triangular fuzzy number as pairwise comparison judgements rather than exact numerical values to cope with uncertain weights , thus adapting to domain experts' natural languages. Section 6 provides a evaluating example to demonstrate this method. Section 7 contains a summary and describes the need to be addressed in the future.

2 The main factors in the evaluating process

There are at least three factors that can influence the final evaluation result. First and foremost, fire detectors are used to find out fire when it is at early stage. So, fire detective is the name we called to present the characteristic associated with detectors ability to detect fire at early stage. Secondly, some buildings, especially in some representative location such as concourse、bibliotheca、shopping mall, have their own unique background signal that fire detectors explore. It is known that the sensor signal

in clean air may change over the life of the detector. Such changes may becaused, for example, by contamination of the sensing chamber with dust or by other long-term effects such as component ageing[4]. We use surroundings applicable to indicate stability of detectors working in different buildings with long-term effects. Thirdly owing to the performance when detectors are exploring in some nuisance circumstance such as smoking、cooking、bathing and so on ,we call it immunity. So we take into account the three main factors when we discuss the problem of evaluating performance of fire detectors.

3 The evaluation work flow

The evaluation work flow is illustrated as Fig.1. Before we carrying out detailed test, Data sample that is sampled from typical applicable surroundings must be gained. Fortunately, an elaborate project by Shenyang Fire research Institute, which funded by National government, has collected useful data , therefore a database has been build to support us as applicable information.

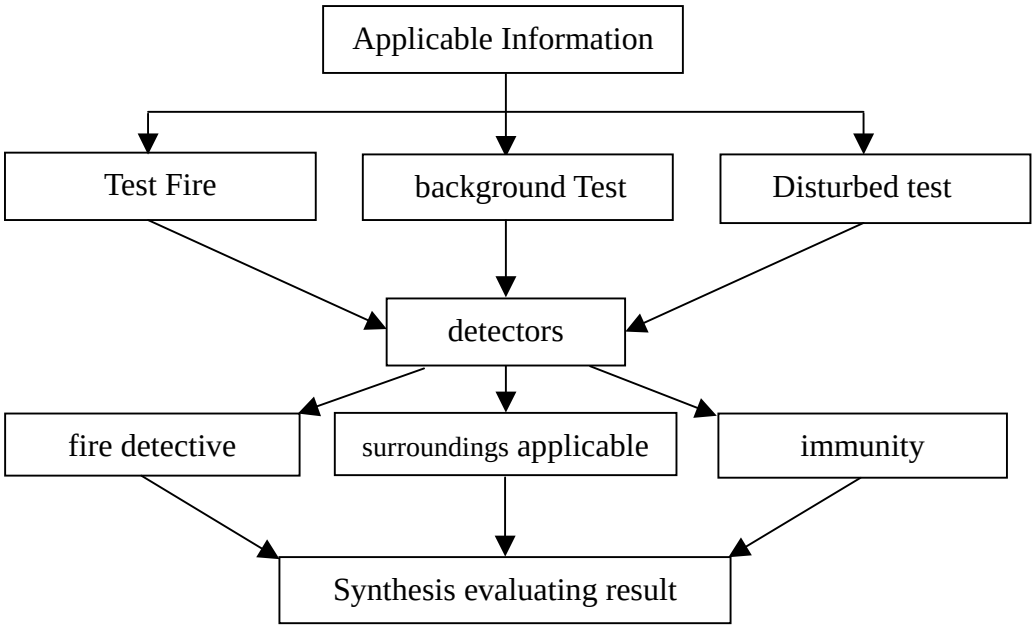

Fig.1 Flow Chart of the evaluation pattern

Some test has been designed to get each scores from the above three aspect. Needless to say, every aspect includes a series test. Finally, synthesis evaluating result is alluring to

us, but how can we take order with so many attribute weights? Obviously, it should be formulated as a multiple criteria decision-making problem under uncertainty.

4 Brief of experiments

The experiments used in the evaluation process include two parts. On the one hand, standards including ISO/EN,UL and GB , especially fire test , are adopted. On the other hand, some experiments must be designed for certain purpose such as water mist,dust,and cooking or smoking. First and foremost, scores, which indicating the result of a experiment must be obtained through detailed design and try. Next, Adopting standards test insure those experiments more creditable and consistent.

5 The basic and extended framework of the Analytic Hierarchy Process

The AHP divides the decision problem into the following main steps[5]:

1. Problem structuring.
2. Assessment of local priorities.
3. Calculation of global priorities.

In the AHP the decision problem is structured hierarchically at different levels, each level consisting of a finite number of decision elements. The upper level of the hierarchy represents the overall goal, while the lower level consists of all possible alternatives. One or more intermediate levels embody the decision criteria and sub-criteria. The weights of the criteria and the scores of the alternatives, which are called local priorities, are considered as decision elements in the second step of the decision process. The decision-maker is required to provide his preferences by pairwise comparisons, with respect to the weights and scores. The values of the weights v_i and scores r_{ij} are elicited from these comparisons and represented in a decision table. The last step of the AHP aggregates all local priorities from the decision table by a weighted sum of the type

$$R_j = \sum_i v_i r_{ji} \qquad (1)$$

The global priorities R_j thus obtained are finally used for ranking of the alternatives and selection of the best one.

The first and the last steps of the AHP are relatively simple and straightforward, while the assessment of local priorities, based on pairwise comparisons is the main constituent of this method.

The pairwise comparison in the AHP assumes that the decision maker can compare any two elements E_i , E_j at the same level of the hierarchy and provide a numerical value a_{ij} of the ratio of their importance. In such a way a positive reciprocal matrix of pairwise comparisons A is constructed.

$$A=\begin{bmatrix} a_{11} & a_{12} & \cdots & a_{1n} \\ a_{21} & a_{22} & \cdots & a_{2n} \\ \vdots & \vdots & & \vdots \\ a_{n1} & a_{n2} & \cdots & a_{nn} \end{bmatrix} \qquad (2)$$

A local priority vector $w = (w_1, w_2,\ldots , w_n)^T$ may be obtained from the comparison matrix A, by applying some prioritisation techniques, such as the Eigenvalue method, the Least Squares method and so on .

However, in most practical situations the decision-maker's evaluations a_{ij} are not consistent, they are only estimations of the exact but unknown ratios .So we introduce triangular fuzzy number as pairwise comparison judgements rather than exact numerical values to cope with uncertain weights, thus adapting to domain experts' natural languages. A triangular fuzzy number can represented as $N = (X_l, X_m, X_u)$, and it's membership function is illustrated as Fig.2.

$$\mu_A(x)=\begin{cases} 0, & x < X_l \\ \dfrac{x-X_l}{X_m-X_l}, & X_l < x < X_m \\ \dfrac{X_u-x}{X_u-X_m}, & X_m < x < X_u \\ 0, & x > X_u \end{cases} \qquad (3)$$

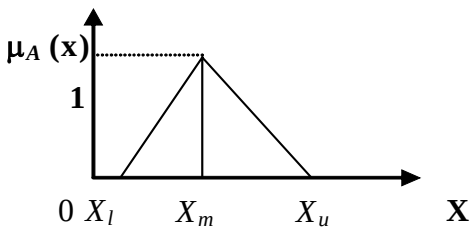

Fig.2 Triangular fuzzy number N and membership function

The elements in matrix of pairwise comparisons *A* ,as it mentioned above, can be replaced by triangular fuzzy number(l_{ij}, m_{ij}, u_{ij}).So, the matrix of pairwise comparisons *A* transfer into fuzzy matrix *A*'.

By applying sum-product method[6] and operational formula of triangular fuzzy number, $\bar{b}_{ij} = (\bar{l}_{ij}, \bar{m}_{ij}, \bar{u}_{ij})$ can be obtained ：

$$\bar{l}_{ij} = \frac{u_{ij}}{\sum_{k=1}^{n} u_{kj}} \quad (2) \qquad \bar{m}_{ij} = \frac{m_{ij}}{\sum_{k=1}^{n} m_{kj}} \quad (3) \qquad \bar{u}_{ij} = \frac{l_{ij}}{\sum_{k=1}^{n} l_{kj}} \quad (4)$$

From $\bar{b}_{ij} = (\bar{l}_{ij}, \bar{m}_{ij}, \bar{u}_{ij})$, $\bar{\omega}_i$ can be induce：

$$\bar{\omega}_i = \sum_{j=1}^{n} \bar{b}_{ij} \quad (5) \qquad \omega_i = \frac{\bar{\omega}_i}{\sum_{i=1}^{n} \bar{\omega}_i} \quad (6)$$

Normalize $\bar{\omega}_i$ to sum of one，deduce ω_i，It is the number *i* of vector *w*，In such a way the priority vector *w* , representing the importance of elements each other, can be gained.

From above discussion, this fire detectors evaluation process can be divide into the following steps:

1、The actual test result from fire detective、surroundings applicable and immunity to false alarm or nuisance sources should be obtained through experiments.

2、The evaluating committee will be grouped by fire detective domain experts.

3、Matrix of pairwise comparisons *A* ,representing $A_1,\ldots,A_n$ elements , is constructed by domain experts, according to the characteristic of location and some special fire requirement.

4、Calculating the priority vector w. based on equation (6).

5、Matrix of pairwise comparisons A' is ascertained by expert under element A_i in terms of certain fire detectors.

6、Calculating the priority vector *w'*. based on equation (6).

7、Calculating the total score by W⊙W' （⊙,multiplication of triangular fuzzy number）. The total score will distinguish fire detectors from different manufacturers

at a global view.

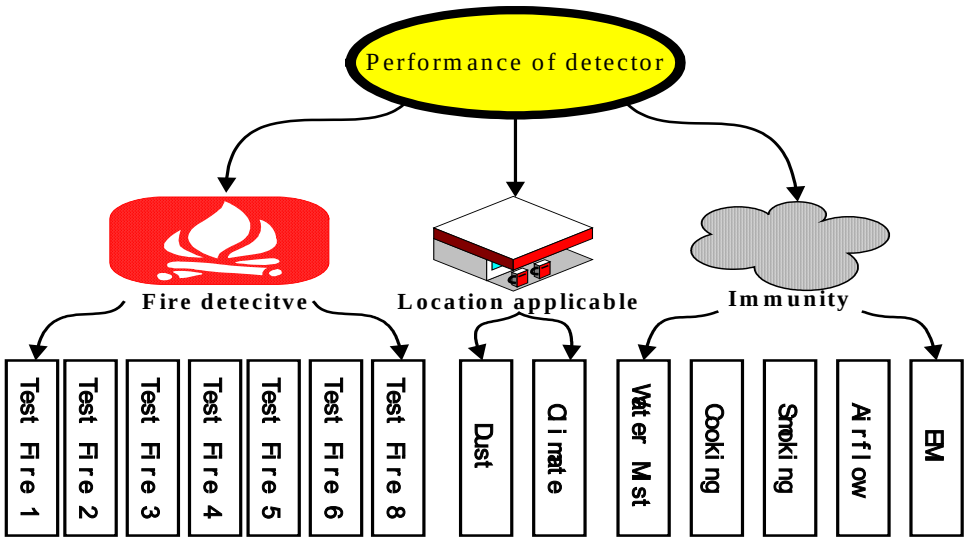

Fig.3 AHP structure model for evaluating of fire detectors

6 Illustrative example

In order to demonstrate the application of the fire detector evaluating method, we will consider an example where the decision-maker has to make a compare between two kinds of point-type photo-electric smoke detectors in terms of suitability for certain application. Fig.3 denotes the whole AHP model. This model mainly concerns of technology and application, while others elements such as cost、maintenance、operation are not included. Therefore, they are also can be added to the model with the same theory.

The solution process is based on Section 4. Matrix of pairwise comparisons A and A' by the committee of experts are as follow. In the next step of the decision making process the weights of the criteria are to be derived from (2) to (6). Fig 1 to Fig 3 display the weights and final results of the two detectors.

$$A=\begin{bmatrix} (1,1,1) & (6,7,8) & (5,6,7) \\ \left(\frac{1}{5},\frac{1}{3},1\right) & (1,1,1) & \left(\frac{1}{3},1,\frac{3}{2}\right) \\ \left(\frac{1}{6},\frac{1}{4},1\right) & (4,5,6) & (1,1,1) \end{bmatrix} \quad \overline{A}=\begin{bmatrix} (0.33,0.63,0.73) & (0.43,0.54,0.72) & (0.53,0.75,1.11) \\ (0.06,0.21,0.73) & (0.07,0.08,0.09) & (0.04,0.13,0.24) \\ (0.05,0.16,0.73) & (0.26,0.38,0.55) & (0.10,0.13,0.16) \end{bmatrix}$$

ω_1=（1.29,1.69,2.56） ω_2=（0.17,0.42,1.06） $\omega 3$=（0.41,0.67,1.44）

Tab.1.Weights on items

	Fire detective	surroundings applicable	immunity
weights	0.25,0.61,1.37	0.04,0.15,0.57	0.22,0.24,0.28

Tab.2.Weights on sub-items and fuzzy scores of the two detectors

	weights	detector Ⅰ	detector Ⅱ
Open cellulosic fire	0.08, 0.20, 0.34	0.20, 0.64, 0.98	0.10, 0.32, 0.57
Pyrolysis Wood	0.29, 0.65, 1.08	0.21, 0.57, 1.01	0.20, 0.36, 0.68
Smouldering cotton	0.19, 0.48, 0.79	0.09, 0.54, 0.89	0.08, 0.56, 0.87
Polyurethane	0.09, 0.40, 0.76	0.10, 0.58, 1.12	0.13, 0.55, 1.11
n-heptane	0.23, 0.54, 0.65	0.30, 0.55, 0.78	0.23, 0.65, 0.86
Alcohol	0.01, 0.30, 0.56	no response	no response
Decalene	0.20, 0.34, 0.64	0.12, 0.54, 0.99	0.07, 0.34, 0.58
Dust accumulation	0.23, 0.67, 0.98	0.14, 0.65, 0.99	0.12, 0.23, 0.38
Atmosphere	0.10, 0.30, 0.45	0.23, 0.45, 0.78	0.24, 0.53, 0.96
vapour	0.16, 0.41, 0.70	0.20, 0.34, 0.67	0.30, 0.58, 1.03
Cooking aerosol	0.12, 0.21, 0.56	0.02, 0.30, 0.78	0.23, 0.67, 0.91
Smoking	0.11, 0.19, 0.34	0.12, 0.45, 0.97	0.27, 0.56, 0.89
EMI	0.09, 0,17, 0.40	0.26, 0.65, 1.21	0.10, 0.32, 0.79
airflow	0.08, 0.12, 0.35	0.17, 0.59, 0.98	0.24, 0.37, 0.86

Tab.3.Values of the two detectors

detector Ⅰ	detector Ⅱ
0.196, 1.472, 3.137	0.160, 1.253, 3.389

From Tab.3 and Fig.4, with operating method of Triangular fuzzy number ,we can point out that detector Ⅰ is more suitable than detector Ⅱ.

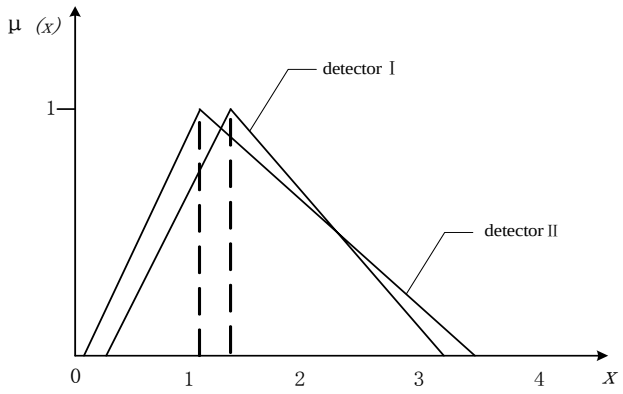

Fig.4 Values of the two detectors

7. Summary and Conclusions

In this paper we have studied the process of evaluating performance of detectors .It is shown that the evaluation process should be formulated as a multiple criteria decision-making problem under uncertainty. An AHP-based model is proposed to derive global priorities of multi-aspects of the attributes of a detector. To deal with the uncertainty ,triangular fuzzy number is introduced to copy with the judge of experts. A illustration demonstrate the whole flow of the method. In terms of implementation, the scores of evaluating is only a reference to end users and it only represents this evaluating architecture.

Acknowledge

The authors would like to acknowledge the financial support by sub item of national project ‘973’- “Multi-sensoring and intelligent identifying at early fire stage (2001CB409608)” and commonweal project of MOST.China -“Evaluating of fire detective algorithm”.

References

[1] Cleary,T., Grosshandler,W., and Chernovsky, A., Smoke Detector Response to Nuisance Aerosols. Proceding of AUBE 99', Duisburg Germany, 1999 , 3.

[2] Thomas Cleary,Michelle Donnelly, and William Grosshandler.The Fire Emulator/Detector Evaluator: Design, Operation, and Performance. Proceedings of AUBE 01', Duisburg Germany, 2001 , 3.

[3] Frank Gockel. Fire Sensor Modeling and simulation. Proceedings of AUBE 01', Duisburg Germany, 2001 ,3.

[4] Annex L. detection and alarm systems —Part 7:Point-type smoke detectors using scattered light, transmitted light or ionization. ISO/FDS 7240-7:2003(E).

[5] Thomas L Saaty. Multi-criteria Decision Making ：The Analytical Hierarchy Process. RWS Publication，1980.

[6] Hun Y Q，Guo Y H. Tutorial of Operation Research. Beijing：Tunghua University Publication，1998，6.

[7] Didier Dubois ,Henri Prade. Fuzzy sets and systems: theory and applications. New York: Academic Press,1980.

Svein Skogstad
Autronica Fire and Security AS, Trondheim, Norway

Automatic alarm test and self-verification of fire-detectors

Abstract

The traditional concept of manual testing of fire detectors (smoke, heat, gas and flame detectors) and interfaces is a time consuming procedure, which involves a number of inherent problems and unreliability. Unwanted alarms and disruption of system operation often occur. Service engineers may not have access to particular areas or the detectors may be out of reach. Mistakes can easily be made if detectors are not installed according to the plan. Test gas or smoke is rarely used in calibrated quantities during manual tests, and even a heavily polluted detector will eventually react if its chamber is filled with enough smoke.

The automatic self-verifying technology ensures that the system completely checks all detectors and interfaces. All parts and components in the detector responsible for processing the alarm signal are verified without human intervention, providing increased safety, integrity and reliability. The technology not only tests whether a detector is capable of provoking an alarm – it even verifies the sensitivity of every detector with a calibrated signal. The system ensures that each detector will always respond to the correct alarm level.

SINTEF, the Norwegian Fire Research Institute and Autronica Fire and Security AS developed the AutroSafe SelfVerify® fire-detection system with the support of NTNF's (The Research Council of Norway) KAPOF programme and major international oil companies.

The target was to develop a fire-detection system with a high reliability and lower life-cycle cost. In the SINTEF report it is calculated, with critical failure rates, that in a combination of 1) visual inspection with automatic self-verifying and 2) visual inspection with manual testing, the first combination is better, and far less time-consuming and costly.

Increased safety and integrity are the most important benefits of the automatic self-verifying technology.

This development of self-testing and verification will push the market forward in a future standard requirement for self testing and verifying systems. The new technology will require development of new references and standards for testing since there are no existing technical specifications coping with this technology.

Introduction

Autronica Fire and Security AS (AFS), a Norwegian company developing fire detectors and panels, was in the early 1990s approach by oil company superintendents forwarding some ideas regarding more reliable and cost efficient fire detection systems. At the time there also was a funding program through the Norwegian Research Council (NFR), the KAPOF program, where the oil companies contributed to the industrialization process of product ideas for the offshore industry. Based upon the ideas presented to AFS, there was a research project performed by the SINTEF group in Trondheim Norway, resulting in a report that showed a great potential in increased reliability and life cycle cost savings for the SelfVerify principle of detector testing. The ideas, together with the SINTEF report, was presented to the KAPOF program and was accepted with four oil companies contributing both technically and financially to the SelfVerify project.

Effect of testing

Based upon offshore field data together with some expert judgements, the critical failures both of physical and functional nature, has been split into 6 types/categories. The term used to define the critical and dangerous failures is: Fail To Operate (FTO) due to physical and functional failures. To detect these failures, we look at different test and inspection strategies.

- **Inspection**: Walk-through to inspect all detectors to see that they and their surroundings are OK.
- **Manual testing:** Existing manual functional testing using gas/smoke/heat etc.
- **Self-verification:** Built in self-verification to stimulate the detection chamber until the alarm limit is reached. This test-alarm message is transferred to the panel for validation of signal path.

In addition there will in most cases be a continuous **automatic self-test** detecting failures of the basic sub-system functions, i.e. loop polling, checksums, HW-tests etc.

Table 1 is showing the failure categories as found combining field data and expert judgement. For each type of test, the coverage is assessed, with respect to each of these failure types. Coverage for each failure category also has been assessed by expert judgement.

Table 1: Failure categories and coverage of individual tests.

Failure category		**% of all failures**	**Coverage of individual tests**		
			Inspection (i)	**Manual (ii)**	**SelfVerify (iii)**
Physi-cal	Detector chamber and electronics failure	40%	0%	95%	98%
	Transmission from detector to central system	5%	0%	98%	98%
	Detector cover failure (by mistake painted over)	5%	90%	95%	0%
Func-tional	Detector wrapped (room cleaning/painting)	1%	95%	85%	0%
	Detector left inhibited (i.e. outputs not enabled)	45%	0%	98%	99%
	Blockage of line of sight	4%	80%	50%	0%
	Total	**100%**	**9%**	**95%**	**89%**

The statistics in Table 1, combining field data and expert judgements, shows that there are two major problem areas connected to the reliability of fire detection systems.

Undetected failures of the chambers and electronics in the detectors (40%) and the transfer lines (5%) to the panel, and the problem of parts of the system being left inhibited (45%) after manual test. Together they represent 90% of all failures in the fire detection and alarming system. Overall coverage is assessed for each test. Observe that self-verification obtains an overall coverage of 89%. The main reason for not getting a higher value is that in total 10% of the failures are assumed not to be detected by self-verification. Observe that inspection complements self-verification in a very nice way. The inspection has a very low coverage (9%), but is effective exactly against those failure categories that are not detected by the self-verification.

In Table 2 we look at the combinations of tests. A simple assumption is used to give the maximum coverage of the tests for the different categories. It is observed that the combination of self-verification and inspection is assigned the same overall coverage as the combination of self-verification and manual testing (i.e. 97%), and that the combination of manual test and inspection has a lower coverage (i.e. 96%).

Table 2: Failure categories and coverage of test combinations.

Failure category		**% of all failures**	**Coverage of test combinations**		
			SelfVerify & Inspection	**SelfVerify & Manual**	**Inspection & Manual**
Physi-cal	Detector chamber and electronics failure	40%	98%	99%	95%
	Transmission from detector to central system	5%	98%	98%	98%
	Detector cover failure (by mistake painted over)	5%	90%	95%	95%
Func-tional	Detector wrapped (room cleaning/painting)	1%	95%	85%	95%
	Detector left inhibited (i.e. outputs not enabled)	45%	99%	99%	98%
	Blockage of line of sight	4%	80%	50%	80%
	Total	**100%**	**97%**	**97%**	**96%**

Measures on Safety and Availability

To quantify the safety and availability a CSU-value is calculated.

CSU – Critical Safety Unavailability.

The probability that the function is unable to operate, i.e. no alarm is given when gas/smoke/heat etc is present and an alarm should have been initiated.

The value calculated in the SINTEF report may be compared to the term PFD used in IEC 61508 for Safety Integrity Levels. PFD – Probability of Failure on Demand.

Five test schemes are evaluated and compared. The test schemes are combinations of the above mentioned test methods, and the tests are assumed to be performed with different time intervals.

Table 3: Coverage for tests and combinations of tests

Test	**Coverage**	**Test scheme**
Inspection	9%	
Manual testing	95%	I
Self-verification	89%	
Inspection & manual	96%	II
Inspection & self-verification	97%	III
Manual & self-verification	97%	IV
Inspection & manual & self-verification	98%	V

Table 4: Definition of test schemes

Type of test	Test intervals, τ				
	Test scheme I	Test scheme II	Test scheme III	Test scheme IV	Test scheme V
Inspection	-	3 months	12 months	-	12 months
Manual	3 months	3 months	-	12 months	12 months
Self-verification	-	-	24 hours	24 hours	24 hours
Autom. self-test	Continuous	Continuous	Continuous	Continuous	Continuous

The CSU is calculated from the formula

$$\mathbf{CSU = \lambda \bullet C_1 \bullet \tau_1/2 + \lambda \bullet (C_2 - C_1) \bullet \tau_2/2 + \ldots + \lambda \bullet (1 - C_k) \bullet \tau_D/2 + TGF \bullet d/\tau_m + TIF + d_s/\tau_s}$$

Where λ represents the failure rate estimated to 3.0 per 10^6 hours and τ is the test intervals from table 4. C is the coverage from table 3. Where combined tests are applied C_2-C_1 represents the additional coverage. (1-C_k) represents the contribution from random failures not detected in any test. TGF is the probability of Test Generated Failures for manual test only (typically leaving parts in inhibit mode) and TIF is the probability of Test Independent Failures, i. e. the probability of having a failure even when the detector is fully tested and apparently fault-free. The last term represents the unavailability due to self-verification testing.

Autronica Fire and Security AS is a manufacturer of fire, gas and flame detection systems and the CSU-calculations has been made for both smoke, heat, flame and gas detectors. The results are shown in table 5.

Table 5: CSU values

Detector	Test scheme	CSU				
		$\lambda \bullet C \bullet \tau/2$	TGF	TIF	d_s/τ_s	Total
Flame	I	0.0045	$1.1 \bullet 10^{-4}$	0.0051	-	0.010
	II	0.0042	$1.1 \bullet 10^{-4}$	0.0051	-	0.009
	III	0.0019	-	0.0052	$7 \bullet 10^{-5}$	0.007
	IV	0.0019	$3 \bullet 10^{-5}$	0.0052	$7 \bullet 10^{-5}$	0.007
	V	0.0017	$3 \bullet 10^{-5}$	0.0052	$7 \bullet 10^{-5}$	0.007
Gas	I	0.0045	$1.1 \bullet 10^{-4}$	0.0101	-	0.015
	II	0.0042	$1.1 \bullet 10^{-4}$	0.0101	-	0.015
	III	0.0019	-	0.0102	$7 \bullet 10^{-5}$	0.012
	IV	0.0019	$3 \bullet 10^{-5}$	0.0102	$7 \bullet 10^{-5}$	0.012
	V	0.0017	$3 \bullet 10^{-5}$	0.0102	$7 \bullet 10^{-5}$	0.012
Smoke	I	0.0045	$1.1 \bullet 10^{-4}$	0.0011	-	0.006
	II	0.0042	$1.1 \bullet 10^{-4}$	0.0011	-	0.005
	III	0.0019	-	0.0012	$7 \bullet 10^{-5}$	0.003
	IV	0.0019	$3 \bullet 10^{-5}$	0.0012	$7 \bullet 10^{-5}$	0.003
	V	0.0017	$3 \bullet 10^{-5}$	0.0012	$7 \bullet 10^{-5}$	0.003
Heat	I	0.0045	$1.1 \bullet 10^{-4}$	0.0101	-	0.015
	II	0.0042	$1.1 \bullet 10^{-4}$	0.0101	-	0.015
	III	0.0019	-	0.0102	$7 \bullet 10^{-5}$	0.013
	IV	0.0019	$3 \bullet 10^{-5}$	0.0102	$7 \bullet 10^{-5}$	0.013
	V	0.0017	$3 \bullet 10^{-5}$	0.0102	$7 \bullet 10^{-5}$	0.013

Main conclusion:

The overall safety performance of test schemes III, IV and V are very similar. So it does not matter much whether the self-verification test is combined with inspection, manual testing or both. Thus, having a combined test scheme of self-verification and manual testing **or** inspection, it is not much to be gained by including also the third test in the test scheme.

Life Cycle Cost (LCC)

The SelfVerify development project had its offspring from the oil producing operations on the Norwegian Continental Shelf. When the SINTEF report now continues to calculate life cycle costs, a total fire and gas system is the basis for the calculations. The calculations are split in a smoke/heat part and a gas/flame part. The report looks into both non-addressable and addressable systems, but here we only look at addressable systems.

LCC is calculated from the following formula:

LCC = LCA + CIR + k•T•CYCyear

Where

LCA = acquisition cost incl. detectors, loop modules, cabling, installation and commissioning

CIR = investment for operation (training) and maintenance (spare parts)

k is a discount factor = 0.72 (cost increase and interest rates etc, see ref. II)

T = projected lifetime = 15 years

CYCyear = operation and maintenance cost per year of operation

(SelfVerify equipment and spare parts cost are assumed to be 10% higher than non-SV)

Table 6: Number of detectors and loops

Detector type	Addressable	
	No. of detectors	No. of loops
Gas	800	32
Flame	400	16
Smoke/heat	700	28
Total	1900	76

Table 7: Man-hours for testing and inspections

	Man-hours per detector/test
Manual (functional) testing	1
Inspection	0.1

For the offshore industry the man-hour cost was in the report set to USD 200,-.

CYCyear is calculated in table 8 for 3 months and 12 months test intervals.

Table 8: Yearly maintenance cost, manual testing and inspection

Detector	Number of detectors	CYCyear in USD million	
		3 month test interval	12 month test interval
Gas	800	0.70	0.18
Flame	400	0.35	0.10
Smoke/heat	700	0.62	0.15

Finally, in table 9 we find the LCC according to the above formula comparing test scheme II (no SV, 3 months interval) and test scheme V (with SV, 12 months interval).

Table 9: LCC costs

Example	Detectors	Costs in USD million, without self-verification (test scheme II)			Costs in USD million, with self-verification (test scheme V)		
		Primary invest-ment	Operat./ mainten-ance	Total LCC	Primary invest-ment	Operat./ mainten-ance	Total LCC
Gas and Flame	800 gas	5.88	7.60	13.48	6.02	1.90	7.92
	400 flame	3.95	3.80	7.75	4.10	0.95	5.05
	Total	9.83	11.40	**21.23**	10.12	2.85	**12.97**
Smoke/ Heat	700 smoke/heat	4.47	6.67	**11.14**	4.50	1.67	**6.17**
Combined	In total 1900	14.30	18.07	**32.37**	14.62	4.52	**19.14**

It was found that the LCC was rather similar for addressable and non-addressable systems when self-verification is not applied.

However, going from addressable systems without SelfVerify to addressable systems with SelfVerify imposes a considerable reduction in life cycle cost. The LCC of all detectors is reduced from USD 32.37 million to USD 19.14 million (see last line of table 9).

Testing requirements and standards

Today the authorities and approval bodies are describing testing requirements as a combination of manual testing and inspection. To be able to have the full benefit of increased reliability and reduced life cycle costs with SelfVerify, the technology has to be recognised by

the authorities and approval bodies to be included in the testing requirements and standards. Autronica Fire and Security AS is present in many different market segments including maritime and offshore oil industry, with different requirements and standards for system testing. As an example; there are requirements to test 10% of the detectors each year, which means that it might be 10 years before a faulty detector is found. The SelfVerify technology will, with its calibrated alarm test, give a fault warning within 24 hours. Authorities and approval bodies are invited to study and discuss the SelfVerify technology and take part in a possible development of new references and standards towards increased safety, integrity and reliability.

References:

I. SINTEF Report STF48 F93033 Self-Verifying Detectors

II. SINTEF Report STF75 A89024 Life Cycle Cost Prediction Handbook

Wang Yinbin Wang Aizhong Ji Fuyi
Gulf Security Technology Co., Ltd.

Fire Test Room Environment Supervision System

Abstract

This article briefly describes the requirement on environmental supervision of fire test room, analyzes the hardware composition, communication protocol, software module function of the environmental supervision system, provides test data of the system in supervising smoldering (pyrolysis) wood fire under two kinds of abnormal test conditions and draws a conclusion.

Key words: environmental supervision; digital field bus; communication controller; smoldering (pyrolysis) wood fire

1. Introduction

As people's demand for fire protection increases and more and more fire protection regulations goes into effect, the market of fire protection products are flourishing, which brings good chances for fire protection industry. Stability is a key factor of a product's quality as well as the focus of competition. For this purpose, manufacturers are developing intelligent fire detector by integrating fire algorithms into its microprocessor(s). A fire test room provides a test environment for responding performance of fire detectors, and a necessary test facility for the study of fire algorithm, thus playing a more and more important role in improving product quality.

2. Environmental Requirements on Fire Test Room

China national standard *GB4715-93 Technical requirements and test methods for point type smoke fire detectors* provides all dimension and technical requirements on fire test room. A fire test room should consist of a monitoring room and a fire room.

Monitoring room is used to operate and observe the test, and Fire room is to provide the test environment.

Detailed requirements are as follows:

Before test, the fire room should meet following requirements: Temperature T=23°C± 5°C; relative humidity H=45%~75%; barometric pressure P=86Kpa~106Kpa; Obscuration m<0.05dB/m; Ionization chamber y<0.05.

During test, validity of test fire should conform to G6 of Annex G, H5 of Annex 5, I5 of Annex I and J5 of Annex J5 of EN54-7: 2001.

3. Introduction of GST'S Fire Test Room

3.1 Functions of Monitoring System

The test environment monitoring system is able to collect environmental data, to control temperature and smoke exhausting, and to analyze and process data. Furthermore, to improve test efficiency, it can also automatically ignite a fire, adjust environmental control devices according to results of collected data, judge conditions to stop a test fire and its validity, and provide sensitivity level of test samples.

Environmental data to be collected include: humidity information (H), barometric pressure output information (P), CO density information during a fire (N), Output information of Optical Density Meter (m), information from MIC (y), Temperature information (T, 3 channels), information from detector samples being tested (s, 8 channels), Weight information of flaming material (G); Environment control includes automatic control of air conditioner, smoke exhaust, fresh air, igniter, light, and video monitoring equipment; Data processing includes display of fire test curve, automatic judgment of finish of test, sensitivity level, validity, generation of database, and easily searching, checking, printing and sharing test data.

3.2 Equipments of a Fire Test Room

The system consists of the following four parts: computer (PC), communication controller, environmental data sampling module and environmental control module, sensors and controlled devices. System composition is shown as figure 1.

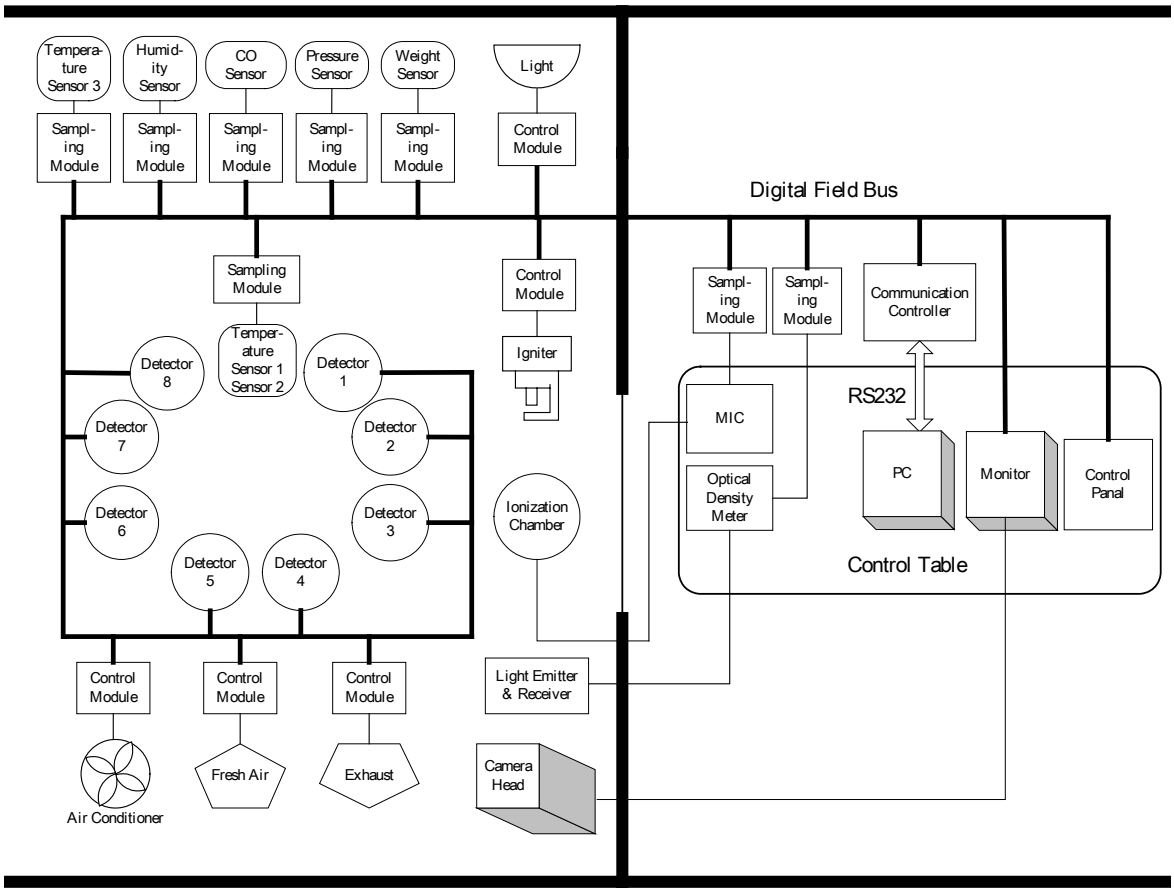

Fig. 1 System composition

In Fig. 1, PC communicates with communication controller through RS232, and the communication controller communicates with modules through digital field bus. Sampling modules translates standard signals of the sensors (4mA~20mA current, 0V~5V Voltage, and BCD code) into digital signals to realize digital field bus communication, and through which the control module transforms control commands from PC into input signal acceptable by controlled devices to realize control of these devices.

Digital field bus is newly developed by GST. Its protocol stipulates the physical layer, link layer and application layer. Physical layer is formed by main device and slave devices. Descending Information applies power cable carrier wave mode: high level is 24V and low level is 0V; Upgoing information is by 4mA~20mA current loop. Link layer can be realized by two modes: main device to one slave device or main device to all slave devices. Devices share the bus by polling mode.

If the address codes of two devices are mis-programmed the same, they can still be distinguished by its other features.

The system integrates bus devices like sampling modules, control module into a platform. Each module has its own logic address, which represents the sensor or controlled device it's connected with. By polling, communication controller can receive digital signal processed by sampling module, give command to control module to control connected devices.

Although there are various types of sensors, which output different signal, and they have to be connected with controlled devices by different interfacing mode, the PC main unit can integrate them into one system through field data bus, thus reduces system cost, and provides good expandability for both the sensors and connected devices. The locally processed sensor signal has very good anti-interference ability without distortion.

3.3 Functional Modules of System Software

Fire test environmental monitor system is the latest software system, realizing sampling and analyzing of data and automatic control. It processes, organizes, manages, and controls received data by sampled project to set up a fire test database.

System software mainly consists of project management module, sampling control module, data processing and displaying module, database and data interfacing module.

3.3.1 Project Management Module

The fire test database takes sampled projects as its management unit. Project

management module includes project information input module and sampled data searching module. To easily manage and search data, the module requires operator to input information of name of the test, name of operator, test date, file number, editing password, sample model, test condition, monitoring mode, and sampling interval. Further analysis and processing can be made to former test data through searching function of sampled data searching module.

3.3.2 Data Sampling and Control Module

Screen of data sampling and control module is shown in Fig. 2.

Fig. 2 Screen of data sampling and control module

Data sampling and control module mainly provides sampling and control command, and displays sampled data and status of controlled devices. The system can both automatically control the fire tests according to results of data sampling, status of

controlled devices, and conditions for starting and ending the tests, or manually control the tests by connected control panel.

3.3.3 Data Sampling and Displaying Module

Data sampled by sampling module will be saved into data file regularly. Data processing system can automatically judge condition for ending the test, and sensitivity level. Under graphic displaying mode, vertical axis displays output signal of m, y, T and s, and horizontal axis displays time. Different curves can be distinguished by color, which can be selected by operator. Any curve can be shielded, and different display screens can be switched among each other. Thus you can compare and analyze environmental data from terminal devices and data sampled from test sample to acquire their relationships during fire test.

3.3.4 Data Interfacing Module

The system supports data output and printing functions. Because data processing function of the system is not as strong as other specific softwares, it offers date output function.

The data output is compatible with other softwares such as Excel and Origin, so that in-depth analysis can be done with the aid of other softwares. The system can print out some real time information or data to be saved by file format, such as real time curves and data tables.

3.3.5 Database

The system applies Microsoft Access2000 Database. It saves information of tested projects with database, and searches them by its searching module, avoiding the problems of a large database and slow system running due to data accumulation.

4. Results of Fire Test

Airflow within fire room and smoothness of its ceiling may greatly affect the diffusion and flow of smoke, which will be directly displayed by data validity curve sampled by

optical density meter and MIC. We will present examples of smoldering (pyrolysis) wood fire, and put forward test curve under normal and abnormal conditions.

4.1 Effect on Smoke Sampling Data by Airflow

Adjust temperature by an air-conditioner, and start test before airflow becomes stable. Shape of rising smoke and its changing process is shown in Fig. 3.

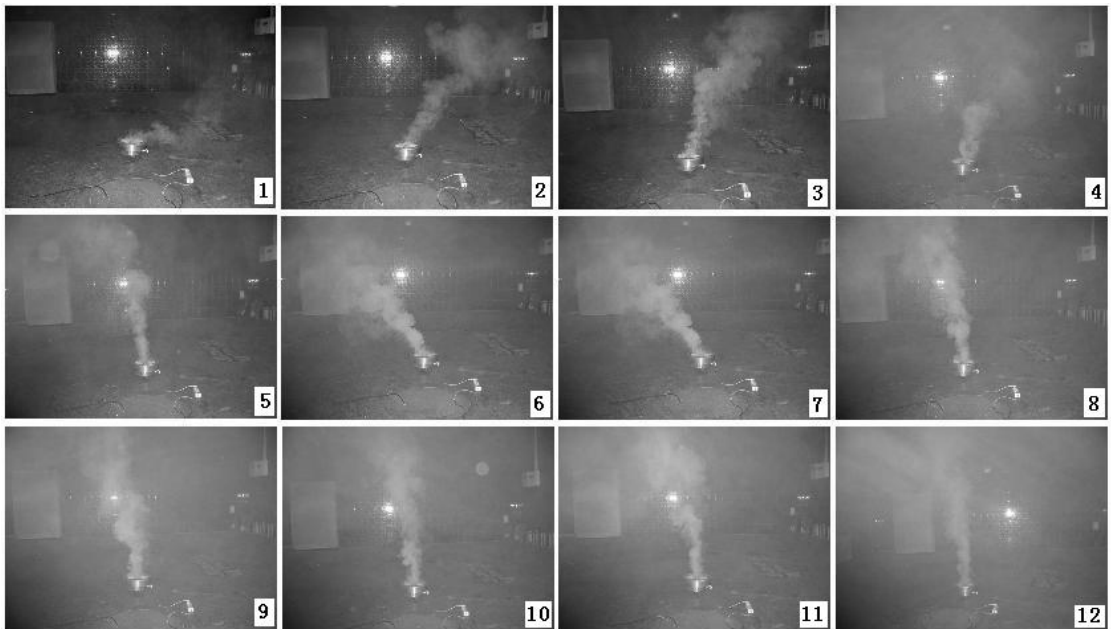

Fig. 3 Shape of rising smoke and its changing process

From Fig. 3, we can see that smoke doesn't rise vertically.

There is an obvious deviation. But as time passes, the deviation will become smaller and smaller, until it disappears.

Effect on smoke sampling data by environmental airflow is shown in Fig. 4.

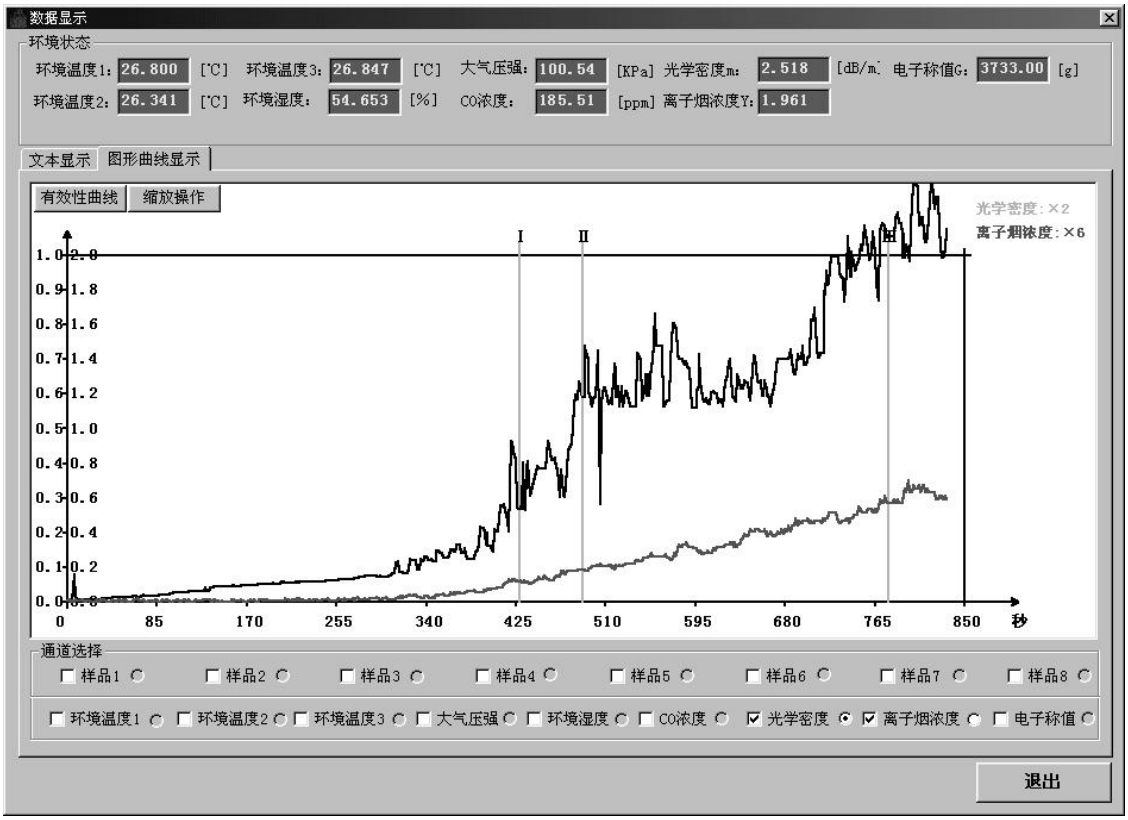

Fig. 4 Effect on smoke sampling data by environmental airflow

We can also see from Fig. 4 that the sampled value by optical density meter is greatly affected by airflow, rising irregularly. While the MIC is less affected because it is connected with a vacuum pump generating negative pressure. And, due to the airflow, data sampled from different position of the fire room varies greatly.

As airflow will affect sensitivity test results, if you changed environmental data by devices like air-conditioner, then before a test, you must wait until air flows stably. According to our experience through tests, adjusted airflow will become stable after 15 minutes.

4.2 Effect on Smoke Sampling Data by Obstruction on the Ceiling of Test Room

Mount a loop girder on the ceiling, taking smoke rising point as its center.

Its radius is 3 meters, height 8cm and thickness 10cm. Position data sampling sensors and test samples on the girder. Then start fire test.

Effect on smoke sampling data by ceiling smoothness is shown in Fig. 5.

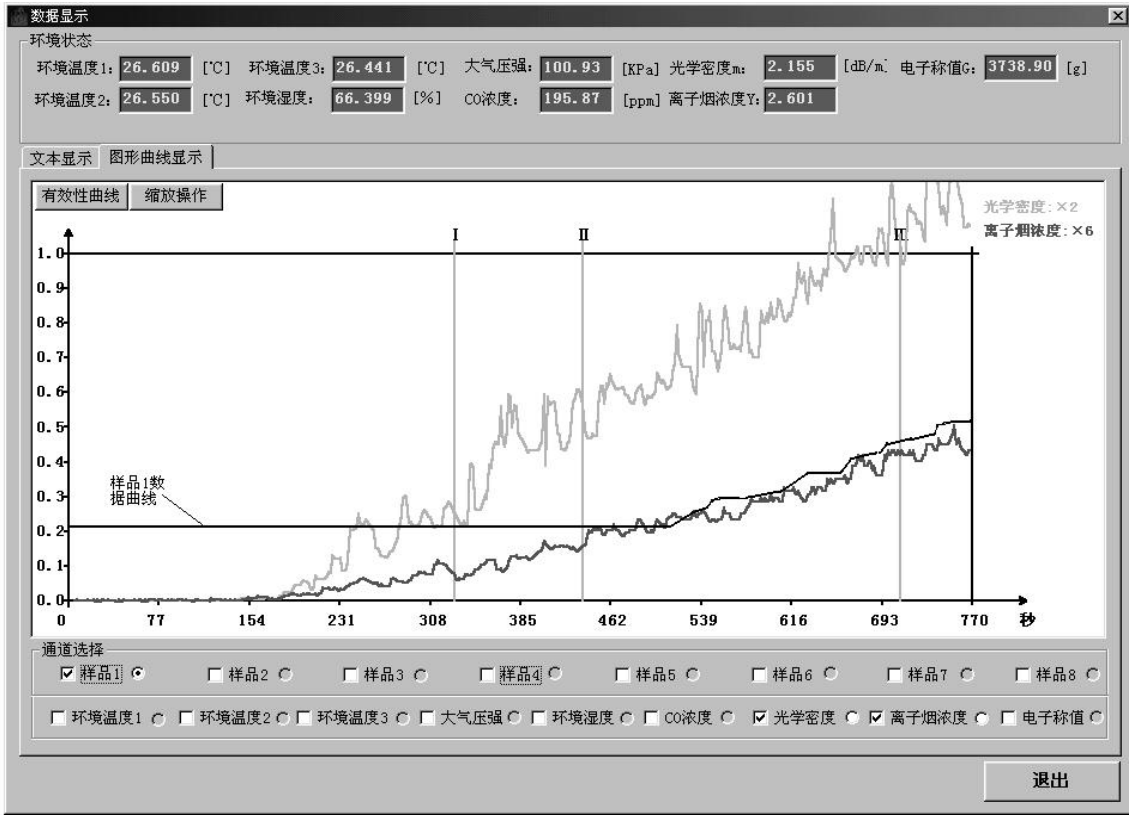

Fig. 5 Effect on smoke sampling data by ceiling smoothness

The figure 5 shows the analogue data of test sample No. 1. It's obvious that the variation of data of test sample No. 1 is much slower than that of optical density meter and MIC.

When smoke with higher temperature diffuses to the girder along the ceiling, its diffusing direction slants to a downward direction because of the obstruction of the girder and heat interchange. The result is that at the initial stage of the test, smoke cannot reach chamber of smoke detector mounted on the girder. With the increase of smoke density and balance of heat transfer, gradient pressure of smoke is also increased, and smoke will be gradually diffused to the chamber.

During the whole smoke rising process, the presence of the girder affect little to data sampling by optical density meter and MIC because of their relatively lower position.

4.3 Test Data and Result Under Normal Condition

After removing all environmental effects and after test verification, the system meets all specification requirements by *GB4715-93 Technical requirements and test methods for point type smoke fire detectors*.

Fig. 6 (a), 6 (b), 7 (a) and 7 (b) show respectively the test curve for smoldering (pyrolysis) wood fire (SH1) and heptane fire.

From Fig. 6 (a) and Fig. 7 (a), you can find the m-t curve and m-y curve of the two test fires conform to requirements in section I.5 of EN54-7: 2001 Annex I. The test fires are valid. From Fig. 6 (b) and Fig. 7 (b), you can see directly the alarming position of test sample 1, thus judge its sensitivity level.

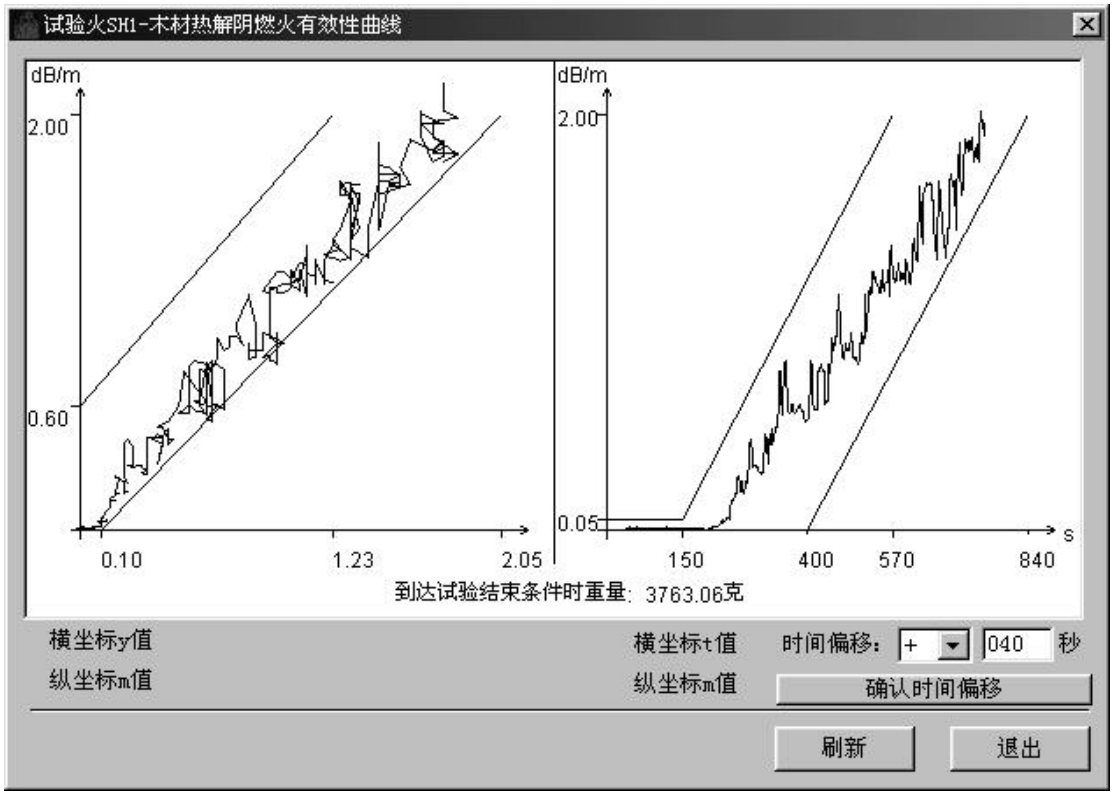

Fig. 6 (a) Validity curve of smoldering (pyrolysis) wood fire

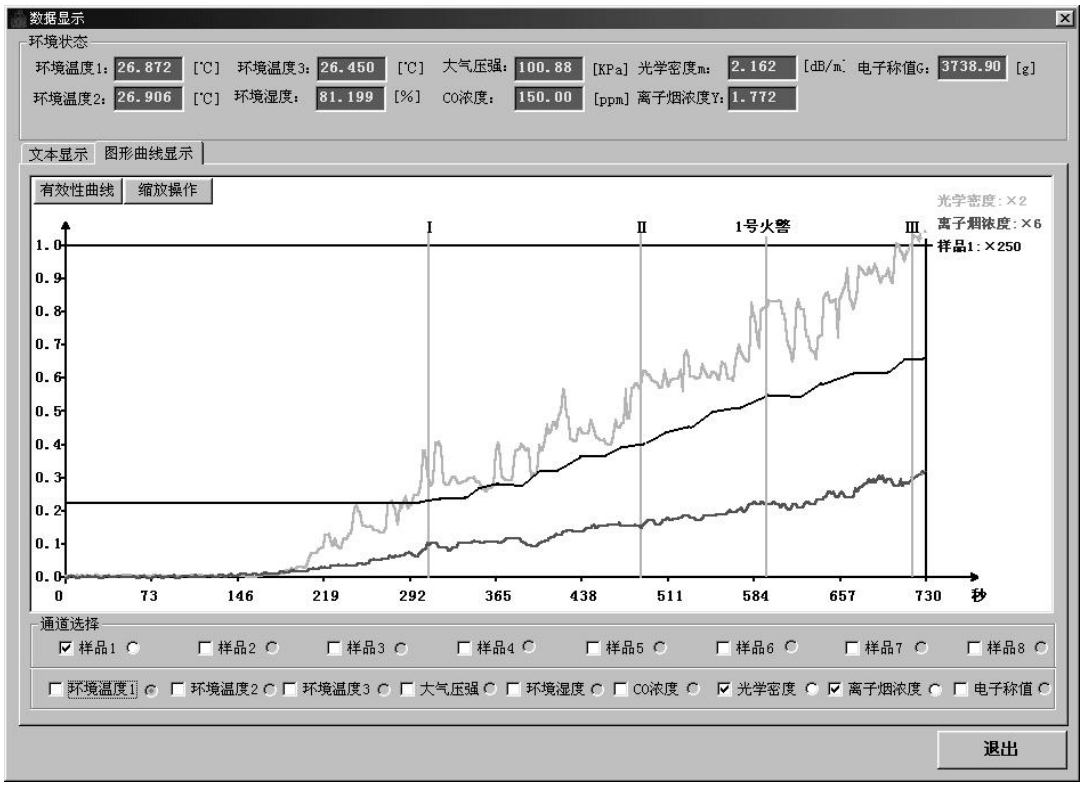

Fig. 6 (b) Sampling data curve of smoldering (pyrolysis) wood fire

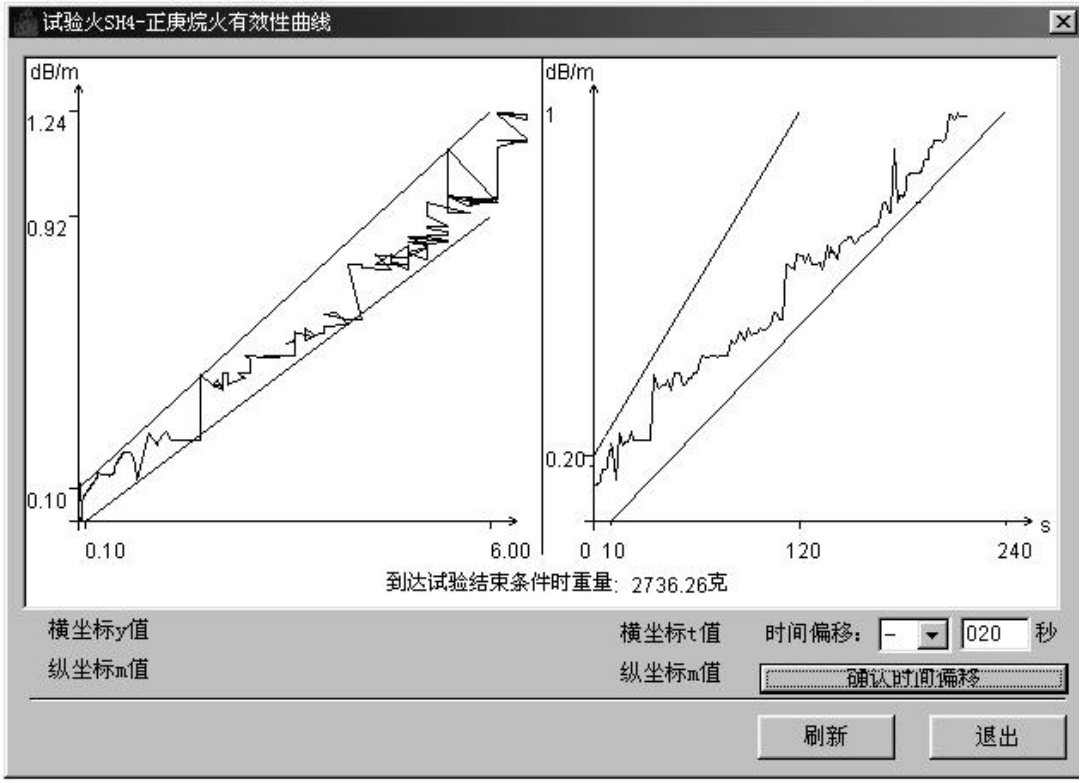

Fig. 7(a) Validity curve of heptane fire

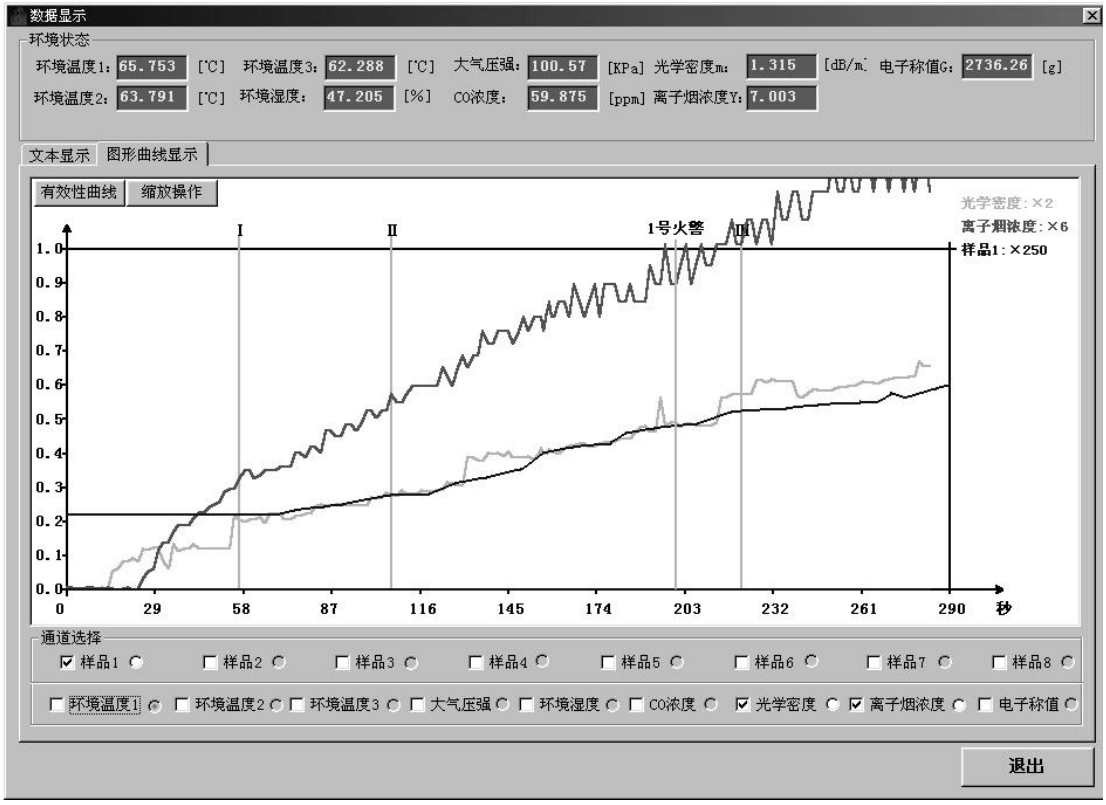

Fig. 7 (b) Sampling data curve of heptane fire

5. Conclusion

This system innovatively integrates fire test environmental monitoring devices by field data bus. The fire test room meets all specifications required by *GB4715-93 Technical requirements and test methods for point type smoke fire detectors*.

On this basis, it realizes functions like automatic ignition, automatic judgement of the condition to end a test, automatic judgement of sensitivity of detectors, and automatic save of test data into database, enables share of test data and printing of test results. It increases the efficiency of fire sensitivity test, which has built a good foundation for the study of fire algorithm.

The system has also been completed with its expected aim of low cost, simple wiring, good expandability and compatibility.

Reference

[1] Yang Xianhui *Field Bus Technology and Its Applications* Beijing Tsinghua University Press 1999. 16~19

[2] Jiao Xingguo GB 4715-93 *Technical requirements and test methods for point type smoke fire detectors* China Standard Press 1993. 19~24

[3] EN54-7:2001 Fire detection and fire alarm systems. London：BSI，2001. 39~46

Wang Aizhong, Wang Ji, Yang Zhanlin, and Zu Mingyan
Gulf Security Technology Co., Ltd., Qinhuangdao, Hebei Province, PRC

Research on Dust-proof Performance of Photoelectric Smoke Detector

Abstract

This article discusses the false alarm problems of photoelectric smoke detectors in application, put forwards the authors' viewpoint that dust-proof performance is very important for this kind of smoke detector. Then it offers methods to solve this problem by design of sensing chamber, fire algorithm and maintenance of the detector, and introduces progresses made.

Key Words

False alarm Dust-proof performance Sensing chamber

1 General Introduction

Comparing with ionization smoke detectors, photoelectric smoke detectors have such advantages as no radioactive pollution, being less affected by airflow and environmental humidity and low cost. As time passing, there is a growing trend that photoelectric smoke detector will gradually replace ionization smoke detectors. Our company has over 3 million photoelectric smoke detectors running in different projects. We did some initial study on reasons of false alarm and found that 70% are that the detector's chamber is polluted by dust. So we started the work to improve the dust-proof performance of photoelectric smoke detector and made some progresses.

2 Principle for False Alarm Caused by Dusts

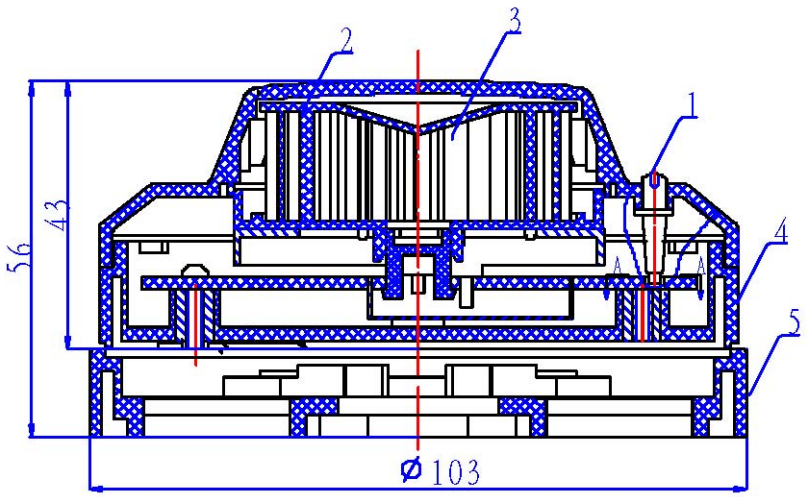

Fig. 1 Structure of photoelectric smoke detector

1 -- Light Pipe 2 -- Sensing Chamber 3 --Sensitive Space

4 -- Enclosure 5 -- Base

The principle for false alarm caused by dusts is that: If there is no smoke particle in the sensitive space of the sensing chamber, environmental light is obscured by the chamber from entering the sensitive space. So the IR LED can only receive light that have been reflected many times by the inner surface of the chamber, which we call background light. When smoke particles enter the sensitive space housed by the chamber (Fig. 1), they absorb the incoming light and scatter it with the same wavelength. Some of the scattered lights are received by the IR LED to become photoelectric current. When the photoelectric current increases to a certain value, the detector will alarm. When there is no smoke particle, the surface is almost black (Fig. 2) that can absorb IR light, so that the lights that are able to reach IR LED is rare due to multiple reflection by the inner surface of the chamber. With dust pollution to the chamber, its color becomes lighter and lighter (Fig. 3), and it can absorb less and less IR light, and background light becomes stronger and stronger. When it exceeds the alarm threshold, the detector will generate false alarm.

Fig. 2 A clean chamber

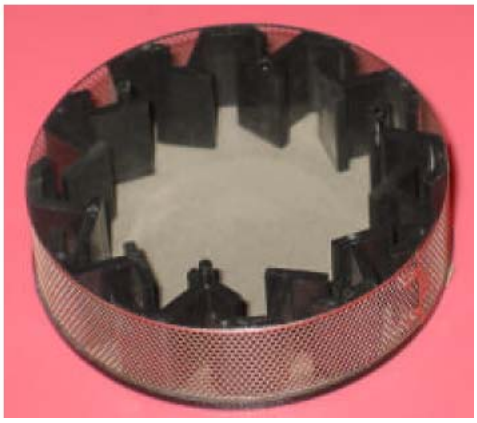

Fig. 3 A polluted chamber

3 Main Reasons for False Alarm Caused by Dusts

3.1 Pollution to the chamber during production stage

Sensing chamber is an important part of photoelectric smoke detector, which is molded with plastic. Plastic foreign material and dusts in the molding workshop may enter the chamber. During assembly process, dusts in workshop especially fibers from PCB boards may also enter the chamber to pollute it.

3.2 Pollution to the chamber during installation stage

Some construction works haven't been completed after the detectors have been installed into a building. Dusts enter the chamber to caus e pollution before commission.

A typical example is the project of Tianjin Taida. In project commission, false alarm rate exceeds 30%. After field checking, it was due to pollution to the chamber. The wall was still being whitewashed, and the protectio n covers to some detectors were not mounted.

Those without protection cover were seriously polluted. Mr. Wayne D. Moore, chairman of NFPA72 National Fire Alarm Code technical committee said that the main reason of false is poor installation and pollution during installation. This is also the case in China.

3.3 Pollution to chamber after running

1) Re-construction to the whole building or some room after the detectors go into running, and are not properly protected.
2) During detector running, room cleaning and sandstorm weather will also cause dust entering the chamber. Especially in western cities like Yinchuan and Taiyuan, such weather is very common.
3) Dust accumulation during long-time running. Detectors mounted on corridors, lobbies, near air-conditioners and air-inlet are specially been polluted.

4 Measures Prevent Dust-caused False Alarm

Because of the reasons for false alarm mentioned above, we find that it's a series of work to reduce such false alarm involving not only R&D stage, but also production, project design, installation, maintenance and establishment of standards.

4.1 Product Design

Improving structure of sensing chamber by using dust-resistant material; Adding digital filtering and dust compensation algorithm; using combination sensors which are no sensitive to dusts; Developing special-purposed dust-proof detectors; adding dust indication and detector cleaning indication functions of fire alarm control panel to reduce false alarm and indicate user to clean the detector when it's polluted to a certain level.

4.2 Production

Sensing chamber molding and processing workshop should be kept clean. Packing of the sensing chamber should be sealed to prevent foreign material, and the color of plastic powder should be controlled. Processing workshop should also be clean. The chamber should be cleaned by high pressure before processing, and there should be testing stage to test pollution of chamber.

4.3 Project Design

A good product should be properly installed to get good performance. A most important factor in project design is to choose appropriate type of detector. For example, smoke detector is not appropriate for an environment with lots of dust.

If smoke detectors are used in garages, workshop for selecting soyabean, steel factory of underground tunnels, frequent false alarm will surely occur. Training of project designer, study of *"Code for Installation and Acceptance of Fire alarm System"* and field research are good measures.

4.4 Installation

Dust pollution during installation is a main reason for false ala rm. People doing installation do not know the importance of protection detector from dusts, and put them without enough caution, or take down the protection cover or even paint on surface of the detector. Detector manufacturer should explain in product manual how to protect the etector from dusts and should train installation people to improve their sense to protection detector during installation.

4.5 Maintenance

Pollution to the detector by dusts after long-time running is unavoidable. Regular test and clean to the detector is an important step to ensure reliable running of a project. Product manufacturer should provide detailed method of cleaning the sensing chamber and training of operators. Indication of cleaning to the detector is also a effective way to reduce dust-caused false alarm. Besides good products, qualified maintenance personnel are also an important factor to reliable running of a project.

4.6 Establishment of standard

How to evaluate dust-proof ability and dust-proof performance in trail running and make technical requirement of smoke detector's dust-proof ability is also a compulsory way to reduce false alarm.

5 Initial Study on Improving Dust-proof Ability and Test Results

We researched in two ways: improving design of sensing chamber and improving dust compensation algorithm.

5.1 Improving Design of Sensing Chamber

1) Material selection: Selecting appropriate material and surface processing technology to make the chamber not sensitive to dusts or make dusts difficult to accumulate. The sensitive parts of our detectors used to be ABS material, which is changed to plastic powder with static power resistant ingredients. This kind of material greatly reduced dust accumulation by the effect of static power.

2) Improve optical structure of sensing chamber: This method is to reduce the affect of sensing chamber's inner surface to background light while maintaining sensitivity, especially affect by the part easy to accumulate dusts, in order to reduce sensing chamber's sensitivity to environment.

Main methods are:

The height of sensing chamber used to be not very high, light from IR LED goes directly to the bottom of the chamber, where dusts easily accumulate, making its color light. Large amount of light are reflected to the photodiode greatly increasing background light as shown in Fig. 4.

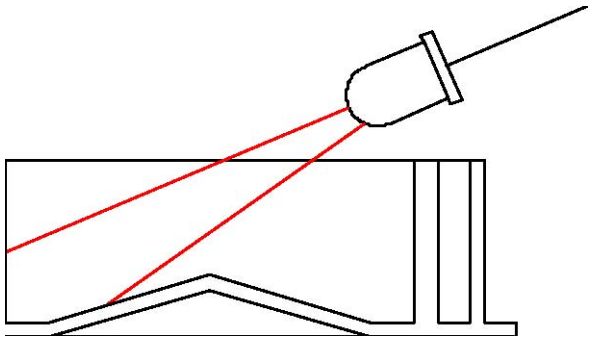

Fig. 4 Light path in short sensing chamber

We added the height of chamber by 4mm. The light from IR LED goes to the wall of chamber where dusts do not easily accumulate. Less reflected light reduced false alarm caused by dusts as shown in Fig. 5.

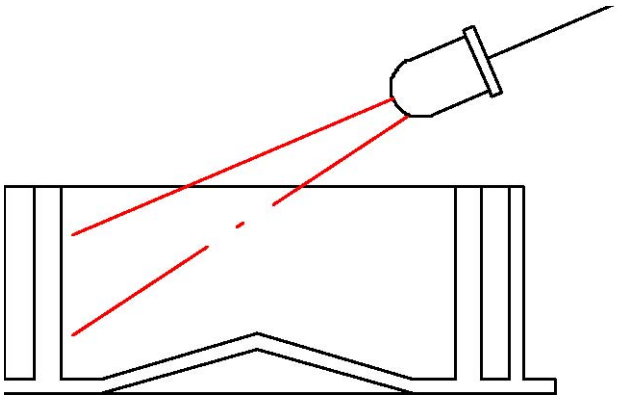

Fig. 5 Light path in high sensing chamber

Test method for evaluation and compare of dust-proof performance:

a) Take one detector with high chamber and one with short chamber, measure their background light and make records. Put the two detectors into dust test box as shown in Fig. 6.

b) Put 1000 g cement powder into the clean dust test box. Air pressure is 0.3 MPa, run three hours, and stop for two hours to wait for dust completely fall down. Measure background light of the detectors.

c) Repeat step b). When output of short chamber's background light becomes saturated, take it out and put another clean short chamber in.

d) Repeat step b). When output of high chamber's background light becomes saturated, the test is completed.

Fig. 6 Dust test box

Test results:

a) The test was done twice, the tested data are shown in Table 1.

b) From the results, the dust-proof performance improves greatly by design improvement. A clean high chamber and short chamber were put into the dust test box together. When the first short chamber alarms dirty, background light of high chamber is only one third of that for alarming dirty. Then put the second short chamber into the test box. When the second chamber alarms dirty, background light of high chamber is two third of that for alarming dirty. Put the third short chamber into the text box, the third short chamber and the high chamber alarm dirty simultaneously.

Therefore we can assume that cleaning period of high chamber is three times of short chamber, and dust-proof ability of the chamber has been greatly improved.

Times of pollution	Background light magnitude increment of high and short chamber			
	High chamber Unit mv	Short chamber 1 (Unit mv)	Short chamber 2 Unit mv	Short chamber 3 (Unit mv)
1	250	264		
2	824	1520		
3	1320	2280		
4	1380	2480		
5	1600	3560 (alarm dirty)	300	
6	1680		1380	
7	1740		2080	
8	1780		2720	
9	1940		3020	
10	2180		3460 (alarm dirty)	324
11	2300			712
12	2560			2480
13	2820			3000
14	3160			3300
15	3380			3500 (alarm dirty)
16	3520 (alarm dirty)			3500 (alarm dirty)

Table 1 Results of first test

5.2 Dust compensation:

Drift is a phenomenon that the system cannot be stabled at zero point (initial point) due to variation of environment and temperature. Zero point here refers to the detector's reference value, which is set before delivery by measuring background light and recorded into its EEPROM. Drift mainly includes time drift and temperature drift. For detectors in fire alarm system, time drift is a main factor, which is related to time, especially slow accumulation of dust. If dust accumulation makes background light

exceeding pre-set alarm threshold value, false alarm will occur. Therefore, it is important to realize drift compensation to detectors in fire alarm system.

Drift compensation is to analyze background light of a detector, find whether it's drifted, to calculate the variation between running background light and initial background light, which is called drift value. And then compensate the alarm threshold with this drift value, to keep detector's alarm sensitivity unchanged in order to reduce false alarm. In a stable environment, background light should be kept at a certain value (with very small variation). Because pollution by dusts, after a long time, the background light of the detector may be different from the value while the detector was delivered. This variation is the drift compensation value.

Method: Judge whether signal data is within the followed range, and whether its difference is less than the most possible variation. Sum this value with the followed values (totally m values), minus the first in followed value, then find the average value of the sum. The difference between the average value and reference value is drift value.

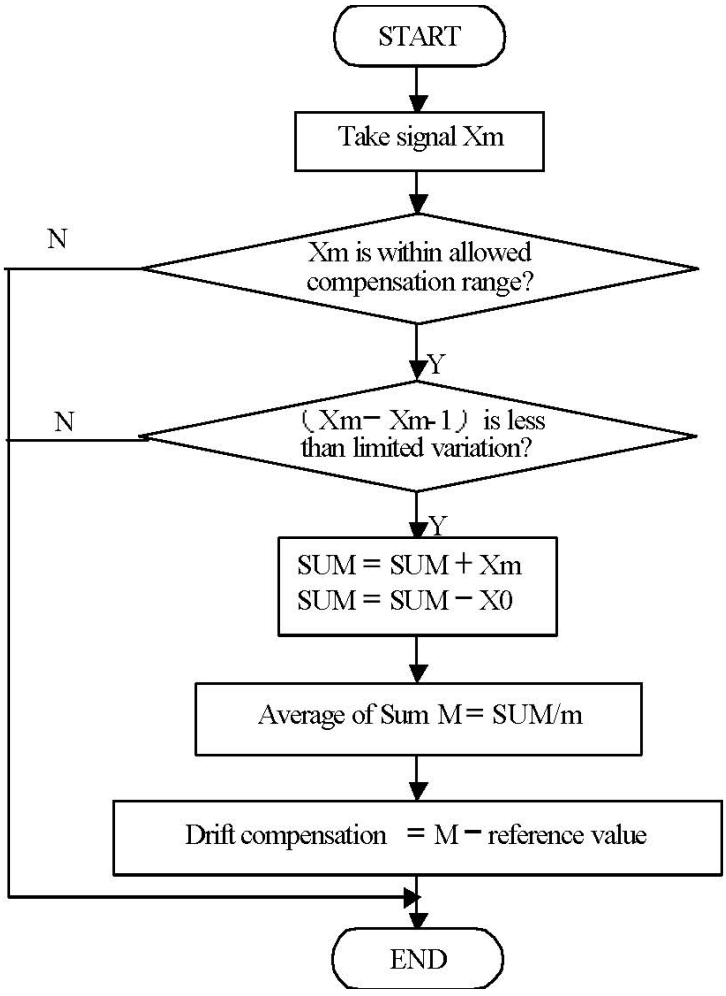

6 Conclusion

We can gain following conclusion from the above:

1) Reducing false alarm caused by dusts is a serial of works involving product manufacturer, system designer, installer, and ma intenance personnel of the user.

2) Optimize product design is a main way to solve this problem.

3) Evaluating dust-proof performance by standard and how to reduce dust-caused false alarm by implementing product standards is a subject valuable to study.

Reference

David S. Bernstein, The end of false alarms? NFPA Journal, July/February 1998, 47~49

Leander Mölter, Dipl.-Ing. (FH) u. Patricia Keßler, M.A.
Palas® GmbH, Karlsruhe, Germany

Zuverlässige Aerosol-Testkomponenten zum schnellen, preiswerten und eindeutigen Test von Rauchmeldern (Reliable aerosol test components for the fast, economical and clear test of smoke detectors)

Zusammenfassung (Abstract)

Smoke detectors are used with success in the most diverse danger places. They can protect human beings e.g. in houses, hospitals, hotels, etc. or also products in factory buildings.

Depending upon the environment, where a smoke results from fire, the smoke will be different in the

- particle size and particle concentration,
- particle shape and particle material,
- electrical charge of the particles,
- temporal stability of these parameters.

The operate behaviour of the smoke detectors depends predominantly on the physical measurement principle, its realisation and on the geometrical structure of the smoke sensor. Due to these facts, smoke detectors should be tested with different test aerosols.

A test aerosol should be clearly characterised with regard to the above mentioned parameters and should be able to be manufactured reproducibly.

For a high-resolved particle size measurement and a time-resolved particle size and particle volume measurement, the white light aerosol spectrometer welas® has proved of value.

In this paper, we will point out the advantages which are possible with clearly characterised aerosol-technological components (e.g. aerosol generators, dilution systems, optical aerosol spectrometers, condensation nucleus counters) and with a practical measuring strategy in order to accomplish economically and reliably the further development and/or the quality assurance of smoke detectors.

Furthermore, we will show how the further development of a smoke detector with regard to the operate behaviour and the geometrical structure of the sensor can be accomplished at a simple test channel.

We are also going to demonstrate how the production supervision for smoke detectors with different lower detector response can be accomplished reliably with only one aerosol generator.

1. Einleitung

Rauchmelder werden mit Erfolg an den verschiedensten Gefahrenstellen eingesetzt. Sie können Menschen schützen, z. B. in Wohnhäusern, Krankenhäusern, Hotels usw., aber auch Produkte in Fabrikhallen.

Je nachdem, in welcher Umgebung ein Rauch entsteht und durch was er verursacht wird, unterscheidet sich der Rauch

- in der Partikelgröße und Partikelkonzentration,
- in der Partikelform und im Partikelmaterial,
- in der elektrischen Ladung der Partikel,
- in der zeitlichen Konstanz dieser Parameter.

Das Ansprechverhalten von Rauchmeldern hängt überwiegend vom jeweiligen physikalischen Messprinzip und dessen technischer Umsetzung sowie vom geometrischen Aufbau des betreffenden Rauchsensors ab. Aufgrund dieser Tatsachen kann es sinnvoll sein, Rauchmelder mit unterschiedlichen Prüfaerosolen zu testen.

Jedes Prüfaerosol, das zum Test von Rauchmeldern eingesetzt wird, sollte bezüglich der o. g. Parameter eindeutig charakterisiert sein und reproduzierbar hergestellt werden können.

Weitere entscheidende Kriterien für die Auswahl eines geeigneten Prüfaerosols werden durch die konkrete Testaufgabe nach der jeweiligen Zielvorgabe des Prüfenden bestimmt. Beispiele für eine Zielvorgabe sind

- der Vergleich von Rauchmeldern nach EN 54
- die Qualitätssicherung der Produktion

- die Optimierung der unteren Nachweisgrenze (Konzentration)
- die Optimierung des geometrischen Aufbaus
- die Entwicklung eines neuen Rauchmelders.

Angesichts der unterschiedlichen Zielvorgaben beim Test von Rauchmeldern ist es sowohl aus technischer als auch aus wirtschaftlicher Sicht sinnvoll, je nach Zielvorgabe des Prüfenden unterschiedliche Testsysteme einzusetzen.

In Abb. 1 ist das Funktionsprinzip eines Testsystems dargestellt. Das schwächste Glied in diesem System bestimmt die Qualität der Messung. Erfüllt nur eine der Komponenten nicht den gewünschten Qualitätsanspruch, so kann auch die Mittelwertbildung mehrerer Messungen die Qualität des Messergebnisses nicht verbessern.

Abb. 1: Aufbau eines Testsystems

In Prüfkanälen, Zuführungsleitungen und Aerosolmessgeräten können Partikel durch **die folgenden vier aerosolphysikalischen Phänomene** abgeschieden werden:

1. Koagulation, d. h. das Zusammenstoßen und Aneinanderhaften von Partikeln. Durch die Koagulation wird der Partikeldurchmesser größer, die Partikelanzahlkonzentration sinkt bei gleichbleibender Massenkonzentration. Die Zeitdauer, in der sich die Partikelanzahlkonzentration aufgrund von Koagulationseffekten um die Hälfte verringert, bezeichnet man als Halbwertszeit $t_{1/2}$.

C_{n0} [1/cm³]	$t_{1/2}$
10^{14}	20 µs
10^{12}	2 ms
10^{10}	0,2 s
10^{8}	20 s
10^{6}	33 min
10^{4}	55 h
10^{12}	2331 Tage

Tabelle: Halbwertszeit verschiedener Partikelanzahlkonzentrationen

Zigarettenrauch hat z. B. eine Anzahlkonzentration von $>10^{12}$ Partikel pro cm³, das heißt, dass nach ca. 2 ms die Anzahl um die Hälfte absinkt.

2. Sedimentation $\sim \rho \cdot d^2 \cdot t$

3. Trägheit $\sim \rho \cdot d^2 \cdot v = \sim \rho \cdot d^2 \cdot s/t$

4. Diffusion $\sim (t/d)^{1/2}$

ρ = Dichte des Partikelmaterials
d = Partikeldurchmesser
t = Zeit (Verweildauer)
v = Partikelgeschwindigkeit

Auch die notwendige Messtechnik ist von der Zielvorgabe des jeweiligen Tests abhängig. Es ist leicht vorstellbar, dass die Messtechnik für die Neuentwicklung eines Rauchmelders aufwändiger sein muss als z. B. ein Messgerät zum Vergleichen von Rauchmeldern nach Norm oder zur Produktionsüberwachung. Daher können sich je nach Zielvorgabe die Anschaffungskosten und die Betriebskosten für das benötigte Testsystem erheblich unterscheiden, so dass sich eine differenzierte Betrachtung geeigneter Testsysteme und ihrer Einzelkomponenten (von der Aerosolerzeugung über die Verdünnung bis zur Charakterisierung des Prüfaerosols) lohnt.

2. Methoden zur Erzeugung von Testaerosolen

Der erste Schritt zum eindeutigen Test von Rauchmeldern nach entsprechender Zielvorgabe besteht in der Erzeugung des geeigneten Testaerosols.

In der VDI Richtlinie 3491 sind Methoden zur Herstellung von Prüfaerosolen beschrieben, die u. a. zur Kalibrierung von Aerosolmessgeräten oder zur Abscheidegradbestimmung eingesetzt werden können. Die dort empfohlenen Herstellungsverfahren, deren Beschreibung „eine einheitliche Durchführung der Verfahrensschritte sicherstellen“ soll (Zitat VDI Richtlinie 3491 Blatt 2), können auch für die Aerosolerzeugung zum Test von Rauchmeldern Geltung beanspruchen.

Testaerosole sollten, wie bereits in der Einleitung erwähnt, eindeutig charakterisiert sein. Der zu ihrer Erzeugung benötigte Aerosolgenerator sollte reproduzierbar herzustellen sein und muss bei jedem einzelnen Betriebszustand eindeutig charakterisiert sein, da sich in Abhängigkeit des Volumenstromes durch den Aerosolgenerator die Partikelgrößenverteilung und/oder die Partikelkonzentration ändern.

2.1 Erzeugen von Tröpfchenaerosolen

Bei der Aerosolerzeugung zum Test von Rauchmeldern nach der zur Zeit gültigen EN 54 und zur Produktionsüberwachung hat sich besonders das Vernebeln von Flüssigkeiten, z. B. von Paraffinnöl, bewährt. Die Verwendung von Paraffin als Prüfaerosol ist nach EN 54 vorgeschrieben.
Besondere Vorteile für diese Anwendung bieten die Aerosolgeneratoren AGF 2.0 und UGF-2000, da sie durch Kaltvernebeln des Paraffins eine sehr feine und sehr schmale Verteilung des Tröpfchenspektrums liefern. Beide Generatoren werden seit Jahren mit Erfolg zum Testen von HEPA und ULPA-Filtern nach EN 1822 und VDI 2083 weltweit eingesetzt.

2.1.1 Aerosolgenerator der AGF-Serie

Abb. 2: AGF 2.0

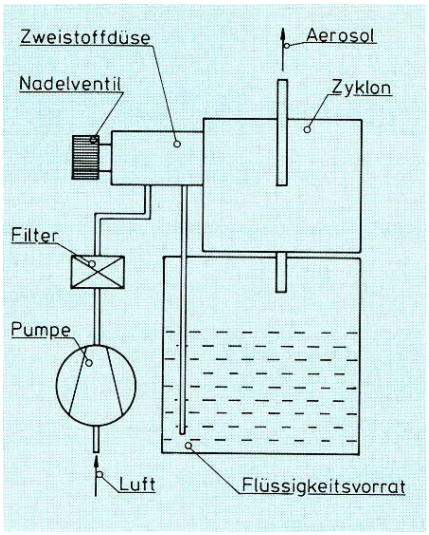

Abb. 3: Funktionsprinzip AGF 2.0

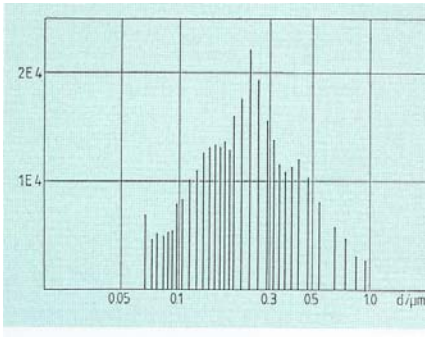

Abb. 4: Anzahlhäufigkeitsverteilung von DEHS gemessen mit dem LAS-X der Fa. PMS

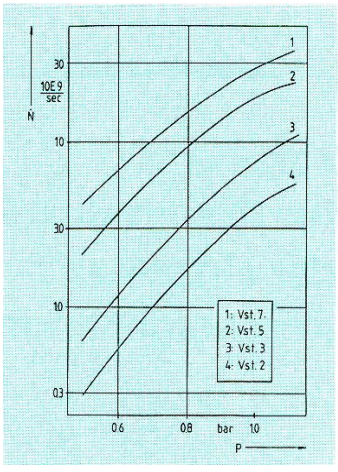

Abb. 7: Abhängigkeit des Partikelstroms vom Vordruck

Der Partikelmassenstrom des AGF 2.0 kann von ca. 500 mg/h bis 2000 mg/h eingestellt werden.

2.1.2 Aerosolgenerator UGF-2000

Abb. 8: UGF-2000

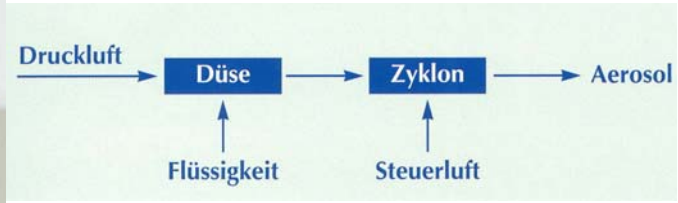

Abb. 9: Funktionsprinzip UGF-2000

Der Partikelmassenstrom des UGF-2000 kann von ca. 200 mg/h bis 1500 mg/h eingestellt werden.

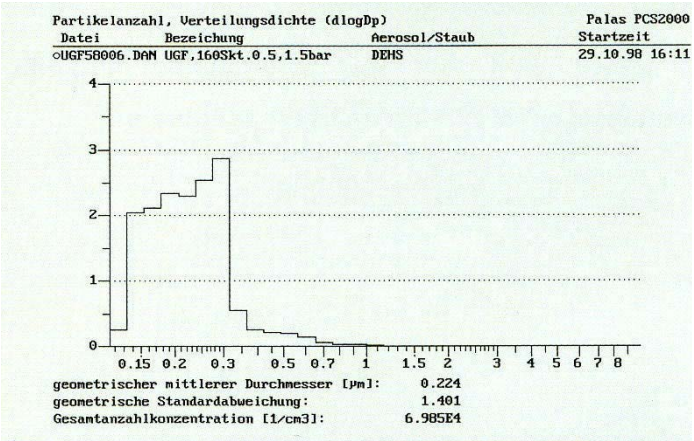

Abb. 10: Anzahlhäufigkeitsverteilung von DEHS, gemessen mit dem welas®-1100

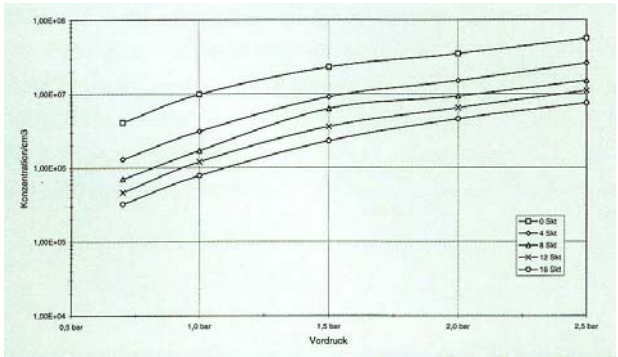

Abb. 11: Abhängigkeit der Partikelanzahl-konzentration von Vordruck und Steuerluft

2.2 Erzeugen von rußähnlichen Testaerosolen

Zum Erzeugen von rußähnlichen Partikeln mit niedrigen Massenströmen bietet der Funkengenerator GFG-1000 nach VDI 3491 Blatt 16 besondere Vorteile.

2.2.1 Aerosolgenerator GFG-1000

Abb. 14: GFG-1000

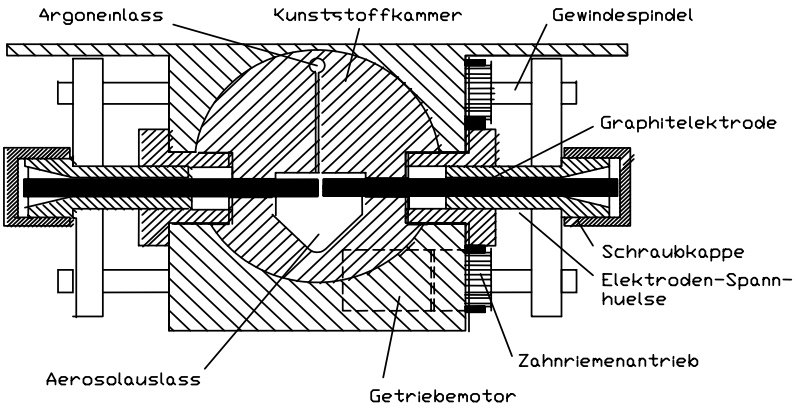

Abb. 15: Funktionsprinzip des GFG-1000

Der Massenstrom kann von ca. 0,07 bis 7 mg/h eingestellt werden. Zum Verhindern von Koagulation kann direkt im Generator mit Verdünnungsluft verdünnt werden.

2.3 Erzeugen von Testaerosolen im Verbrennungsprozess

Zum Erzeugen von Rußpartikeln, die durch einen Verbrennungsprozess definiert hergestellt werden, bietet der neue Variable Soot Generator nach Dr. Wahl besondere Vorteile.

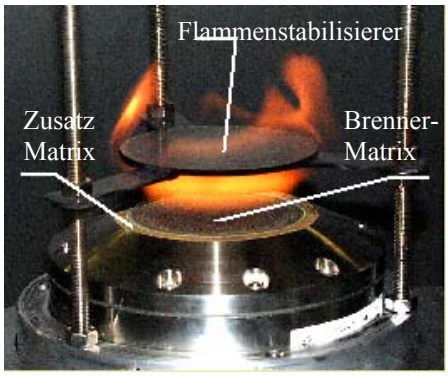

Abb. 16: Variable Soot Generator

Rußpartikeldurchmesser: 5 nm bis 200nm

Größenverteilung: Lognormal

Brenner: Coflow Matrix Brenner

Brennstoff: vorgemischtes Ethen (C_2H_4)/Luft

Zusatz: Stickstoff

Druck: Außenluftdruck

Der Massenstrom kann variabel eingestellt werden.

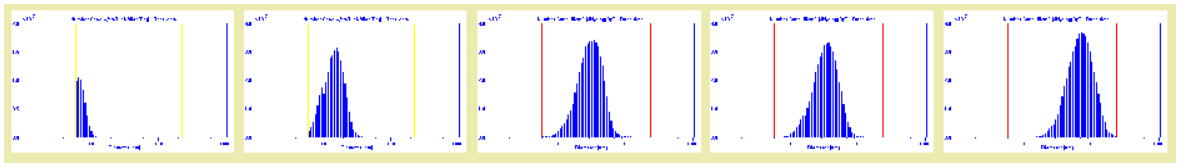

Durchmesser d = 7,5 nm	Durchmesser d = 15,2 nm	Durchmesser d = 32,8 nm	Durchmesser d = 36,7 nm	Durchmesser d = 76,3 nm

Abb. 17

3. Verdünnen von Prüfaerosolen

Die Anzahlkonzentrationen von Prüfaerosolen zum Test von Rauchmeldern liegen oft bei 10^5 bis 10^6 Partikeln pro cm³. Für verschiedene Aerosolmessverfahren sind diese Konzentrationen für die direkte Messung jedoch viel zu hoch, so dass in diesen Fällen die Verwendung eines Verdünnungssystems notwendig ist.
In der VDI Richtlinie 3491 Blatt 15 sind Verdünnungssysteme beschrieben. Eine Grundlage für die Erarbeitung dieser Richtlinie bildete das **Palas® Verdünnungssystem VKL-Serie**, das zum Verdünnen hochkonzentrierter Aerosole besondere Vorteile bietet.

3.1 Verdünnungssystem VKL-Serie

Abb. 18: zwei VKL-10 im Koffer

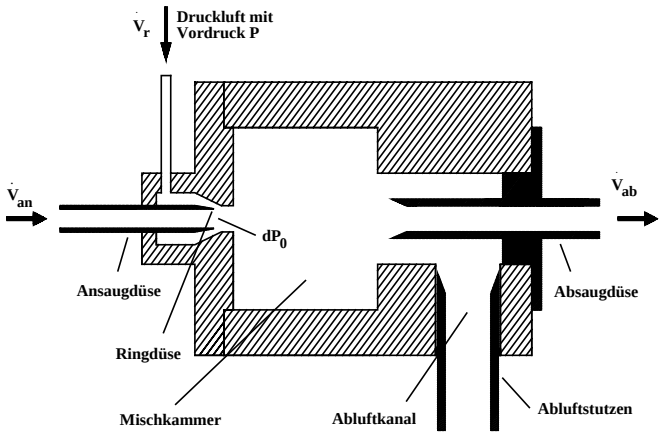

Abb. 19: Funktionsprinzip der VKL-Serie

Formel des Verdünnungsfaktors:

$$W = (\dot{V}_r + \dot{V}_{an}) / \dot{V}_{an}$$

Der Verdünnungsfaktor kann durch die Kaskadierung mehrerer VKL-10-Systeme erhöht werden.

Verdünnungsstufen	Verdünnungsfaktor
1	10
2	100
3	1000
4	10 000
5	100 000

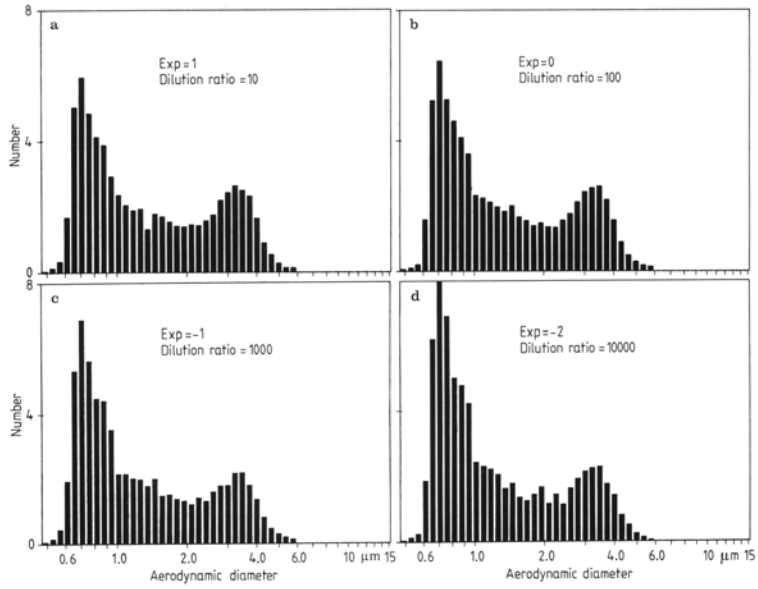

Bild 9 a–d. Größenverteilung eines Testaerosols gemessen mit dem APS nach 10facher (**a**), 100facher (**b**), 1000facher (**c**) und 10 000facher (**d**) Verdünnung

Abb. 20: Partikelgrößenverteilung eines Testaerosols für verschiedene Verdünnungsfaktoren

Ein Vorteil der Kaskadierung mehrerer VKL-10-Systeme besteht darin, dass durch die Kaskadenschaltung die benötigte Verdünnungsluft um ein vielfaches verringert wird.
Will man z. B. pro Minute zwei Liter Aerosol ansaugen und um den Faktor 10 verdünnen, so beträgt der Verdünnungsluftverbrauch 18 l/min. Mit einer Kaskadenschaltung von vier Einzelverdünnern (W = 10) lässt sich eine Verdünnung um den Faktor 10 000 mit einem Luftverbrauch von nur 72 l/min erzielen – gegenüber einem Verbrauch von 20 000 l/min bei einem einstufigen System mit gleichem Verdünnungseffekt.

4. Charakterisierung von Prüfaerosolen

Eine Voraussetzung für den sinnvollen Test von Rauchmeldern ist die eindeutige Charakterisierung des verwendeten Prüfaerosols. Die VDI Richtlinie 3489 Blatt 1 enthält eine Übersicht über Methoden zur Charakterisierung und Überwachung von Prüfaerosolen, die mit Hilfe von Aerosolgeneratoren unter Laborbedingungen erzeugt werden.
Aerosolmessverfahren können wie folgt eingeteilt werden:

Messverfahren	**Messgerät**
• Messung am Partikelkollektiv	⇨ z.B. Photometer
• Messung am Einzelpartikel	⇨ optisches Aerosolspektrometer
(zählendes Verfahren)	⇨ Kondensationskernzähler (CNC)

In der derzeit gültigen Norm nach EN 54 ist zur Charakterisierung eines Prüfaerosols für den Test von Rauchmeldern die Partikelmessung mit einem **Photometer** vorgeschrieben. Photometer eignen sich zur Messung von hohen Konzentrationen. Die Ände-

rung des Photometersignals kann allerdings sowohl durch Schwankung der Partikelgrößenverteilung als auch durch Konzentrationsschwankungen hervorgerufen werden. Nur unter der Voraussetzung, dass die Partikelgrößenverteilung stabil ist, kann mit dem Photometer die Konzentration eindeutig bestimmt werden.

Mit dem **Kondensationskernzähler CNC** können sehr kleine Partikel eindeutig gezählt werden. Der CNC kann aber nur die Partikelmenge zählen. Die Partikelgrößeninformation geht durch den Kondensationsprozess verloren.

- $C_{max} \approx 10^3$ Partikel/cm³
- dp ≈ 5 nm bis 1000 nm

Vorsicht beim Betrieb des CNC im Photometermode: Nach VDI 3489 Blatt 2 kann in diesem Mode bis zu 80% falsch gemessen werden!

Optische Aerosolspektrometer basieren wie der CNC auf einem **zählenden Messverfahren**. Aerosolspektrometer eignen sich zur gleichzeitigen Bestimmung der Partikelgröße *und* der Partikelmenge.

- Maximale Konzentration $C_{max} \approx 10^5$ Partikel/cm³
- Partikeldurchmesser dp ≈ 180 nm bis 4000 nm

4.1 Das optische Aerosolspektrometer welas®-System

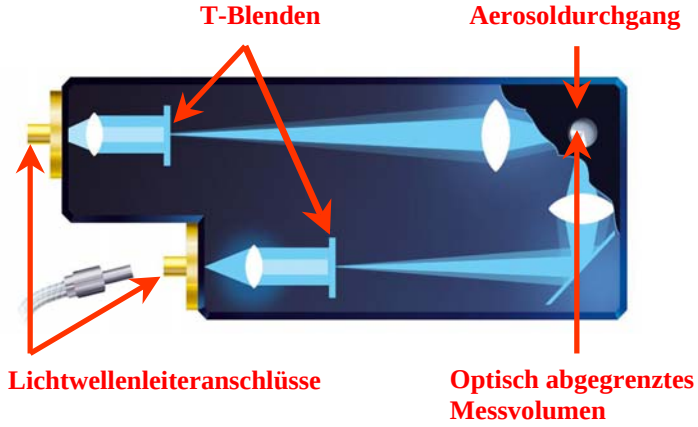

Abb. 21: Querschnitt durch den welas® Sensor

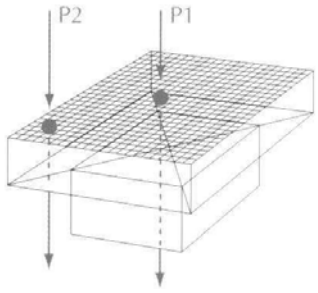

Abb. 22: T-Blenden-Technik des welas®-Systems

Das Weißlicht-Aerosolspektrometer welas® von Palas® misst die Konzentration und den Durchmesser der Partikel.

Das welas®-System bietet dem Anwender folgende Vorteile:

- ein hohes Auflösungsvermögen
- eine gute Klassifiziergenauigkeit
- eine eindeutige Kalibrierkurve
- eine Messung ohne Randzonenfehler
- eine Koinzidenzerkennung

Diese Vorteile werden durch **Weißlicht**, **90° Streulichtdetektion**, ein **homogen ausgeleuchtetes Messvolumen** und die patentierte **T-Blenden-Technologie** erreicht.

Da das Messverfahren des welas®-Systems auf der „wahren" Mie-Theorie beruht und somit die Tröpfchengröße und Tröpfchenmenge exakt bestimmt, kann mit diesem einfachen und robusten Aerosolspektrometer der Vergleich von verschiedenen Rauchmeldern im Prüfkanal nach EN 54 unter Verwendung eines Tröpfchenaerosols wie Paraffinölnebel sehr exakt durchgeführt werden.
Mit dem welas®-System kann nicht nur das Prüfaerosol Paraffin eindeutig charakterisiert werden, auch die untere Nachweisgrenze eines Rauchmelders lässt sich mit diesem Aerosolspektrometer wesentlich genauer bestimmen.

4.2 Vergleichsmessung: Rauchmelder und Aerosolspektrometer welas®

In einer Vergleichsmessung konnte gezeigt werden, dass das zählende Messverfahren des welas®-Systems wesentlich empfindlicher die verschieden eingestellten Aerosolkonzentrationen messen kann.
Die Messung fand mit folgendem einfachen Testaufbau statt:

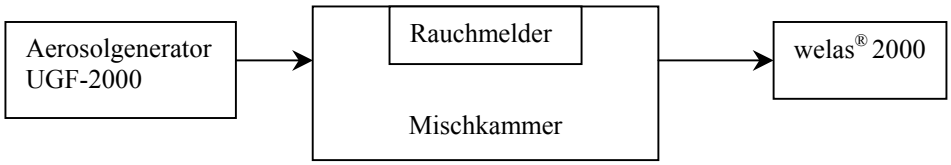

Messwerte Rauchmelder dB/m	Partikelzahl welas® P/cm³
0,002	450
0,004	730
0,015	3740

Die Ergebnisse zeigen, dass selbst bei einem derart einfachen Testaufbau mit dem Ae-

rosolspektrometer welas® 2200 der Nachweis der Partikelkonzentration sehr genau bestimmt werden kann, da auch niedrigere Konzentrationen mit weniger als 450 Partikel pro cm³ eindeutig gemessen werden können.

Um beim Test eines Rauchmelders im Strömungskanal nach EN 54 weitere Messfehler zu vermeiden, muss überprüft werden, ob die Partikelkonzentration und die Partikelgrößenverteilung über den gesamten Querschnitt des Kanals konstant ist. Diese Überprüfung ist mit dem welas® sehr einfach, schnell und zuverlässig durchzuführen.

Die nähere Betrachtung der verschiedenen Messverfahren zur Partikelcharakterisierung beim Test von Rauchmeldern zeigt, dass die bereits in der Einleitung erwähnte Forderung, je nach Zielvorgabe das geeignete Testsystem einzusetzen, insbesondere auch für diese Testkomponente sinnvoll ist. So kann das Photometer, das in der aktuellen EN 54 zur Messung vorgeschrieben ist, nur unter bestimmten Voraussetzungen eindeutige Messergebnisse liefern.
Je nach Messaufgabe ist auch ein kombiniertes Partikelmesssystem, bestehend aus einem Kondensationskernzähler und einem optischen Aerosolspektrometer, ideal. Von Friehmelt wurde dies in /11/ vorgeschlagen.

5. Zusammenfassung

Wie in diesem Vortrag gezeigt wurde, ist es sowohl aus technischer als auch aus wirtschaftlicher Sicht sinnvoll, je nach Zielvorgabe des Tests unterschiedliche aerosoltechnische Komponenten einzusetzen.
Wichtig ist, dass alle einzelnen Komponenten – wie z.B. Aerosolgenerator, Aerosolmessgerät und evtl. Verdünnungssystem – eindeutig charakterisiert sind.
Ebenso wichtig ist, dass auch die Aerosolzuführung konstant ist. Außerdem müssen die Partikel bezüglich der Größe und der Konzentration über den Kanalquerschnitt gleichmäßig verteilt sein.
Die vorgestellten Palas®-Testkomponenten sind für jeden Betriebsparameter eindeutig charakterisiert. Daher kann der Betreiber im Falle von Unsicherheiten einen möglichen Fehler im Testsystem selbst finden.
Die Palas®-Komponenten zeichnen sich durch ihren robusten Aufbau, ihre hohe Zuverlässigkeit und ihre geringen Anschaffungskosten aus.

Mit eindeutig charakterisierten aerosoltechnologischen Komponenten können Testsy-

steme für Rauchmelder z.B.

- zur Optimierung
- zur Produktionsüberwachung
- zum Vergleich nach Norm

zuverlässig und wirtschaftlich aufgebaut werden.

Literatur

/1/ Blattner, J., Dilution System for Aerosol Measurements with Optical Single Particle Counters at Very High Concentrations, Filtration & Separation 5, 1996.

/2/ Evans, D. E., Harrison, R. M., Ayres, J. G., The Generation and Characterisation of Elemental Carbon Aerosols for Human Challenge Studies, Journal of Aerosol Science 8, 2003.

/3/ Helsper, C., Mölter, L., Haller, P., Representative Dilution of Aerosols by a Factor of 10.000, Journal of Aerosol Science 1990.

/4/ Kirchner, U. u.a., Single Particle MS, SNMS, SIMS, XPS, and FTIR Spectroscopic Analysis of Soot Particles during the AIDA Campaign, Journal of Aerosol Science 10, 2003.

/5/ Lindenthal, G., Mölter, L., New White-Light Single-Particle Counter - Border Zone Error Nearly Eliminated, Proceedings of Partec 1998.

/6/ Saathoff, H. u.a., The AIDA Soot Aerosol Characterisation Campaign 1999, Journal of Aerosol Science 10, 2003.

/7/ Schütz, S., Mölter, L., Accurate Particle Counting of Vacuum Cleaner Emissions. Filtration & Separation 9, 2003.

/8/ VDI-Richtlinie 3489 Part 1, Particulate Matter Measurement. Methods for Characterisation and Monitoring of Test Aerosols Survey, 11/ 1986.

/9/ VDI-Richtlinie 3491 Part 15, Particulate Matter Measurement. Generation of Test Aerosols. Dilution Systems with Continuous Volumetric Flow, 12/ 1996.

/10/ VDI Richtlinie 3491 Part 16, Particulate Matter Measurement. Generation of Carbon Aerosols using a Spark Aerosol Generator, 11/ 1996.

/11/ Friehmelt, R., Aerosol-Meßsysteme. Vergleichbarkeit und Kombination ausgewählter on-line Verfahren, Diss. 1999.

Xie Qiyuan, Yuan Hongyong, Su Guofeng

State Key Laboratory of Fire Science, USTC, Hefei, Anhui, P.R. China

The Influence of High Smoke Velocity on Sensitivity of Smoke Detectors

Abstract

The objective of this work was to evaluate the sensitivities of spot-type photoelectric and ionization smoke detectors in different smoke velocities at the Fire Emulator/Detector Evaluator (FE/DE), which was developed recently by SKLFS. This was accomplished through a series of experiments using smoldering cottons as the smoke source, with the smoke velocity 0.5m/s, 1.0m/s, 1.5m/s, 2.0m/s, 2.5m/s, 3.0m/s, 3.5m/s, 4.0m/s, 4.5m/s, 5.0m/s and 5.5m/s, respectively. In this way, the different responses of spot-type photoelectric and ionization smoke detectors in different smoke velocities can be easily observed. The experimental results indicate that the sensitivity of the photoelectric smoke detector decreases sharply when the smoke velocity around it increases, with nearly the same smoke density around. In contrast, under the same condition, the sensitivity of the ionization smoke detector does not fall down as sharply as the photoelectric detector, but still maintains high sensitivity even when the smoke velocity around is as high as 5.5m/s. Finally, there is another point worthy of our notice. The *code for design of automatic fire alarm system* (GB50116-98, Chinese standard code) recommends that photoelectric smoke detectors should be selected in the places with air velocity exceeding 5.0 m/s. But according to the experimental results, the ionization smoke detectors are much more sensitive to the smoke than the photoelectric ones in high smoke velocity. Due to this, the author intends to do further researches, involving smoke detectors produced by more companies and in more types of smoke.

1. Introduction

The fire smoke is motivated by the buoyancy force when fires happened in common places with small air velocity [1, 2]. Hence, the fire detectors mounted there are required to respond sensitively to smoke in environments of low air velocity. However, in some special places, such as trains, subways, and some special large workshops where the air

must be replaced with fresh air several times per hour, the air velocity is probably much higher. When a fire happens in such places, the combustion behavior and the characteristics (e.g. size distribution) of smoke particles generated would be different from those generated in environments of low air velocity. Therefore, it is required that the fire detectors mounted there should respond sensitively to smoke under the condition of high smoke velocity. Nevertheless, within the author's inspection of literature, little research has been found on evaluating the response sensitivity of fire detectors in different smoke velocity environments. The basic aim of the present work was to experimentally evaluate two kinds of most widely used fire detectors, i.e. forward-scattering photoelectric and ionization smoke detectors, in various smoke velocity environments at the Fire Emulator/Detector Evaluator. The experimental evaluation results were helpful for the design of automatic fire alarm systems in those special places with high air velocity.

2. Experimental

2.1 Experimental Apparatus

All the experiments were conducted in the FE/DE, which was developed by State Key Laboratory of Fire Science (SKLFS) in University of Science and Technology of China (USTC). The FE/DE is for emulating a wide range of fire and non-fire scenario to which a spot-type fire detector could be exposed. The concept of FE/DE is first introduced by Grosshandler[3]. The FE/DE in the SKLFS is a 0.4m high by 0.4m wide cross-section flow tunnel designed to reproduce the time-varying temperature, speed and concentration (gas and particulate) expected at detector locations in the early stages of fire (Figure.1-a). The inside and outside walls of the tunnel are made of stainless steel, and the interlayer is the asbestos, which is heat insulating. As can be seen in Figure.1-a, this apparatus can work at either open-style or circle-style by merely changing the states of the three valves. In this paper, the open-style work-mode is selected during all the experiments. The FE/DE employs a variable speed blower and electrical heaters to

control velocities ranging from 0.02m/s to greater than 5m/s, and temperatures from 20 ℃ to 100℃. The blower is controlled by the transducer with a feed-back velocity. Water mist produced by the centripetal humidifier may be sprayed into the flow after the heater section to fix the humidity between the ambient room and saturation conditions depending on the spray flow. CO, CO_2 or other gas blends may be introduced into the flow via electronic mass controllers. Not only the fire scenario but also the nuisance alarm scenario can be emulated in the FE/DE. The dust with different diameters may be metered into the flow. In addition, some types of smokes and non-combustion aerosols also can be immitted into the flow, including the cooking fumes, smoldering smoke, flaming soot and nebulized liquid mists through the hood (see Figure.1-a). As is mentioned above, the FE/DE at SKLFS can be operated in the open-style and circle-style work-modes, which can be easily switched to one another. Here lies the most distinct difference between the FE/DE at the SKLFS and the one at NIST [4, 5]. The adding of a circle-style work-mode has made it easier to simulate the processes of increasing of some fire signals (smoke or gas concentration, temperature etc.) in a wider range. For example, in order to evaluate a heat detector, we should simulate an increasing process of temperature in the test section. Obviously, in doing so, it is necessary to increase the power of heater when the FE/DE is at open-style. However, when the FE/DE is switched to the circle-style, although the power of heater is unchanged, the temperature in test section keeps increasing. Therefore, at the circle-style, the temperature can be simulated in a range much wider than that at the open-style. The same is with the processes of increasing smoke or gas concentration.

The spot-type fire detectors to be evaluated, as well as the measurement instruments, were mounted at the test section (see Fig.1-b). Here commercially available digital addressable point smoke detectors were used, including forward scattering photoelectric detectors and ionization detectors. The digital output value from a detector ranges from 0 to a maximum of 255. The detector manufacturer's instruction book recommended that a threshold level of 115 units for photoelectric and 170 units for ionization would

be appropriate fire alarm triggers with common sensitivity, respectively. The real-time outputs of the smoke detectors were displayed and recorded through the communication between the control panel and the personal computer using a terminal program. Air temperature, humidity and velocity were recorded at the test section by thermal resistances, humidiometer and thermo-anemometer, respectively. CO and CO_2 concentrations were monitored by the non-dispersive infrared (NDIR) analyzer.

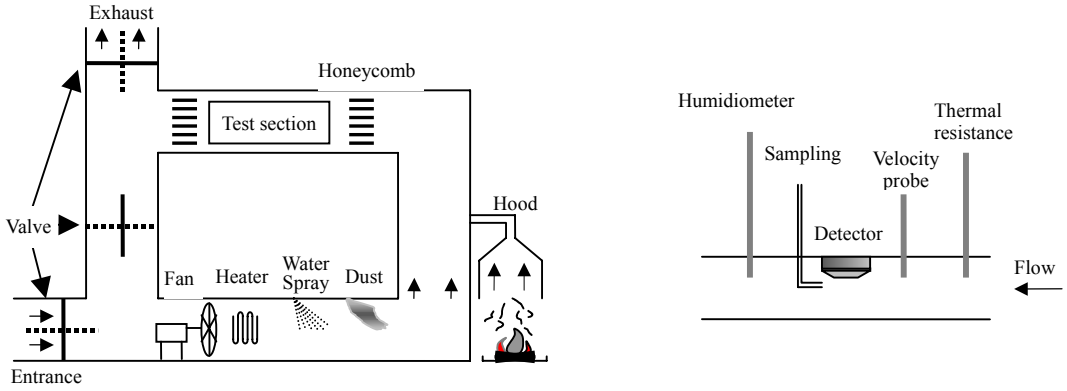

Fig.1-a. whole schematic

Fig.1-b. side view of test section

Fig.1 The schematic of Fire Emulator/Detector Evaluator
Valves located at the dashed line state: open-style work-mode;
Valves located at the real line state: circle-style work-mode;

2.2 Experiments description

With the purpose of comparing the response sensitivity of the scattering photoelectric and ionization smoke detectors in various smoke velocities, the experiments were designed as follows.

Just as indicated above, here all experiments were carried out in the open-style work-mode of the FE/DE. In the FE/DE, the rotational speed of the fan could be changed by adjusting the frequency of the converter. At the beginning of every experiment, the rotational speed could be changed for the air velocity in the test section to reach a certain value. Eleven experiments were conducted with the smoke velocity in the test section 0.5m/s, 1.0m/s, 1.5m/s, 2.0m/s, 2.5m/s, 3.0m/s, 3.5m/s, 4.0m/s, 4.5m/s, 5.0m/s, 5.5m/s respectively. A minimum of two runs was carried out for each smoke velocity. If the results of the two runs were significantly different, a third run was made.

For the sake of more convenient comparisons, in each experiment, 60 smoldering standard cottons [6] were used as the same smoke source, i.e. the same smoldering cottons were placed at the entrance of the FE/DE no matter how high the smoke velocity in the tunnel is. Before each experiment, a 100 second baseline was taken to record the initial conditions. After that, the 60 smoldering cottons were placed at the entrance of the FE/DE for about 300 seconds to produce smoke in the tunnel, and were then moved away to stop supplying smoke.

From the above description of the experiment process, it is obvious that the only difference of experimental conditions among these eleven experiments was the smoke velocity inside the tunnel of the FE/DE. Hence it is helpful to compare the different response sensitivity of the two kinds of smoke detectors in different smoke velocity.

3. Results and Discussion

With 60 smoldering cottons as the same smoke source, Figures 2-6 show the outputs of the forward scattering photoelectric and ionization smoke detectors with the smoke velocity in the test section 1.0m/s, 1.5m/s, 2.0m/s, 3.0m/s and 4.0m/s, respectively.

As can be seen from Figures 2-6, the shapes of the two curves in these five figures are similar to each other. Namely, while the smoke velocities are different, the outputs of both kinds of smoke detectors increased sharply as soon as the smoke had been supplied by the smoldering cottons, and approximately remain at some certain values while the smoke was being supplied for about 300 seconds. Finally, the outputs fell down sharply to the original values when the smoke supplying was stopped, namely, the smoldering cottons were moved away. For a convenient comparison of the response sensitivity of

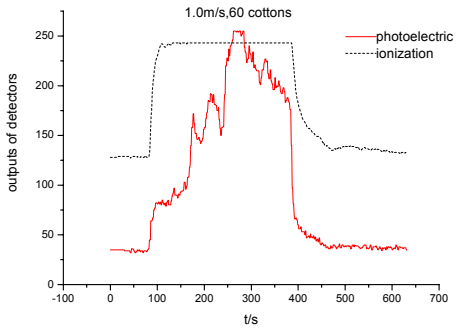

Fig.2 outputs of detectors (1.0m/s,60 cottons)

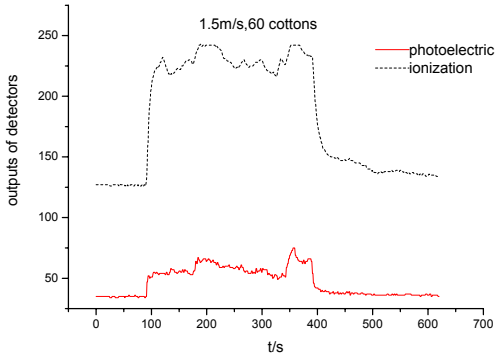

Fig.3 outputs of detectors (1.5m/s,60 cottons)

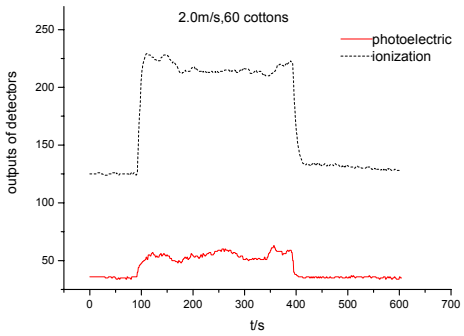

Fig.4 outputs of detectors (2.0m/s,60 cottons)

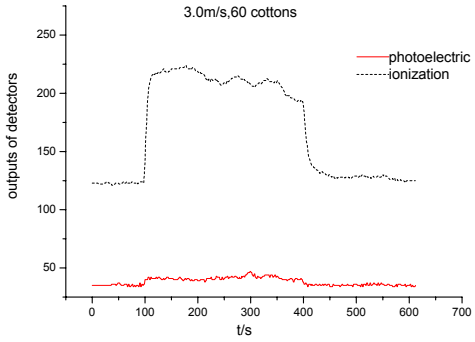

Fig.5 outputs of detectors (3.0m/s,60 cottons)

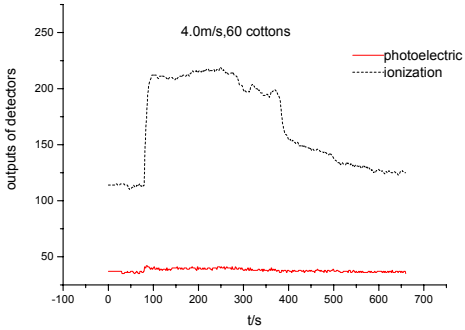

Fig.6 outputs of detectors (4.0m/s,60 cottons)

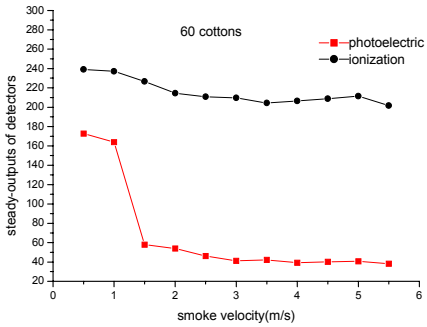

Fig.7 the steady-outputs of detectors vs. velocities

smoke detectors in different smoke velocity, here the arithmetic mean of the outputs of smoke detectors during these 300 seconds was named steady-output of smoke detectors under the according experimental conditions. The steady-outputs of the two kinds of smoke detectors, corresponding to different smoke velocities in the test section, were given in Figure 7.

It can be seen from the Figures 2-6 and Figure 7 that, as regards the photoelectric smoke detectors, the steady-outputs decreased when the smoke velocities around the detectors increased, while the smoke source (i.e. 60 smoldering cottons) kept unchanged. In the case of the smoke velocity being 1.0m/s, as is shown in Figure 2, the outputs of the photoelectric smoke detector sharply increased as soon as the 60 smoldering cottons were placed at the entrance of the FE/DE. And the fire alarm signal was soon given out. However, with the smoke velocity increased, as can be seen in Figures 3-6, the steady-outputs of photoelectric smoke detector decreased with the same smoldering cottons as smoke source. As is particularly shown by Figure 6, with the smoke velocity in the test section 4.0m/s, the steady-output of photoelectric smoke detector was nearly equal to its original value, namely, its outputs when no smoke was around it. This trend of change was particularly obvious in Figure 7, which gave the steady-outputs of smoke detectors with the smoke velocity from 0.5m/s to 5.5m/s and the step 0.5m/s. This preliminary experimental data suggested that the response sensitivity of the photoelectric smoke detector was influenced by the smoke velocity around it. Hence, in this case, the photoelectric smoke detectors may fail to give out fire alarms when a real fire happens in an environment of high air velocity.

However, as for the ionization smoke detectors, from the corresponding curves of Figures 2-7, their response sensitivity was much less affected by the smoke velocity around them. Although the steady-output of the ionization smoke detectors did decrease a little when the smoke velocity increased, the degree of decreasing was much less than that of the photoelectric smoke detectors. In addition, as can be seen from the comparison of the two curves in Figure 6, when the smoke velocity in the test section was 4.0m/s, the photoelectric smoke detectors almost gave no response to the smoke while the ionization smoke detectors still remained highly sensitive to the smoke and quickly gave out fire alarm signals.

Also, as is shown by Figure 7, with the smoke source unchanged, the outputs of the ionization smoke detectors still increased obviously and quick gave out fire alarm

signals even when the smoke velocity in the test section was as high as 5.5m/s.

According to the above analysis and comparison, the response sensitivity of the photoelectric and ionization smoke detectors, which are most popularly used at present, reflect quite differently to the smoke velocity around them. The photoelectric smoke detectors had good smoke sense ability in the low smoke velocity environment. However, when the smoke velocity exceeded a certain value (the value attained here was about 1.5m/s, as can be seen from Figure 7), they showed much less response sensitivity under the condition of the same smoke source and even may not work well in detecting a fire. As for the ionization smoke detectors, they kept highly sensitive to the smoke with the smoke velocity from as low as 0.5m/s to as high as 5.5m/s. That is to say, their sensitivity was much less affected by the smoke velocity than photoelectric smoke detectors. The ionization smoke detectors showed a great sensitivity in high smoke velocity environments, hence they are more suitable to be chosen used in those places with high air velocity.

There exist lots of factors that led to the different response sensitivity to the smoke velocity between the photoelectric and ionization smoke detectors. A preliminary analysis suggested that the result was mainly due to the differences in smoke-sensing principles and smoke tunnels' inner structures between this two kinds of smoke detectors. In addition, another factor is that increasing the flow velocity in the vicinity of smoldering cottons decreases particles size. That is because it decreases the residence time for particles to grow by coagulation [7].

4. Conclusion

In some special places where possibly exist high air velocity, such as trains, the fire detectors mounted there are required to keep a good sensitivity in high smoke velocity environments. This work experimentally evaluated the two kinds of most commonly used smoke detectors at present, i.e. photoelectric and ionization smoke detectors, in various smoke velocities using the smoldering cottons as the smoke source. According

to the experimental results, the following preliminary conclusions can be drawn:

1) The photoelectric smoke detectors had a high sensitivity in sensing the smoke in low smoke velocity environment. Yet their smoke sense ability apparently decreased when the smoke velocity exceeded a certain value (the experiments here indicated that it was about 1.5m/s) with the same smoke source, i.e. 60 smoldering cottons.

2) The response sensitivity of the ionization smoke detectors was much weakly affected by the smoke velocity. They showed a high sensitivity in high smoke velocity environments, hence they were more suitable to be used in those places with high air velocity.

3) The code for design of automatic fire alarm system (GB50116-98, Chinese standard code) recommends that photoelectric smoke detectors should be selected in the places with air velocity exceeding 5.0 m/s [8]. But according to the experimental results here, the ionization smoke detectors were much more sensitive to the smoke than the photoelectric ones in high smoke velocity. Namely, the experimental results here were surprisingly different to the code. Due to this, the author intended to do further research, involving more smoke detectors produced by other companies and in more types of smoke. Also, the influence of the air velocity on the smoke particle size distribution remains to be a very interesting topic of future work, because the response sensitivity of photoelectric and ionization smoke detectors was greatly affected by the particle size distribution of the smoke generated [9, 10].

Acknowledgments

This paper is supported by Fire Dynamics and Fundamentals of Fire Protection (Grand No: 2001CB409608). The authors deeply appreciate the supports.

References

[1] Chow WK, Yin R Free boundary conditions for simulating air movement in a big hall induced by a "bare cabin" fire J FIRE SCI 17 (2): 111-147 MAR-APR 1999

[2] Cooper LY Calculating combined buoyancy- and pressure-driven flow through a shallow, horizontal, circular vent: Application to a problem of steady burning in a ceiling-vented enclosure FIRE SAFETY J 27 (1): 23-35 JUL 1996

[3] Grosshandler, W.L., "Toward the Development of a Universal Fire Emulator/ Detector Evaluator," Fire Safety Journal 29, 113-128, (1997).; also in AUBE '95 Proceedings, pp. 368-380.

[4] Cleary, T., and Donnelly, M., and Grosshandler, W., "The Fire Emulator/Detector Evaluator: Design, Operation, and Performance," Proceedings of the 12th International Conference on Automatic Fire Detection "AUBE '01", March 26-28, 2001, National Institute of Standards and Technology, Gaithersburg, MD, USA, Grosshandler, W., Ed., 2001.

[5] Cleary, T., Grosshandler, W., and Chernovsky, A., "Smoke Detector Response to Nuisance Aerosols," Proceeding of the 11th International Conference on Automatic Fire Detection "AUBE '99", March 16-18, 1999, Gerhard Mercator University, Duisburg, Germany, Luck, H., Ed., pp 32-41, 1999.

[6] GB 4715-93 Technical requirements and test methods for point type smoke fire detector[S], 1993.

[7] Lee, T.G.K. and G. Mulholland, “Physical properties of Smoke Pertinent to Smoke Detector Technology,” NBSIR 77-1312, National Bureau of Standards, Washington, D.C. (1977)

[8] GB 50116-98 Standard of the Design of Automatic Fire Alarming Systems[S], 1998

[9] Fleming, J; Photoelectric vs. Ionization Detectors – A Review of the Literature; Proceedings Fire Suppression and Detection Research Application Symposium, February 25-27, 1998, Natl. Fire Protection Association, Quincy, MA, 1998, pp.18-59.

[10] Qualey, J, Desmarais, L, and Pratt, J.; Fire Test Comparisons of Ion and Photoelectric Smoke Detector Response Times; Fire Suppression and Detection Research Application Symposium, Orlando, FL, February 7-9, 2001.

Jeffrey C. Owrutsky, Susan Rose-Pehrsson, and Frederick W. Williams
Naval Research Laboratory, Washington, DC, 20375, USA
Daniel A. Steinhurst and Christian P. Minor
Nova Research, Inc., Alexandria, VA, 22308, USA
Daniel T. Gottuk
Hughes Associates, Inc., Baltimore, MD 21227, USA

Long Wavelength Video Detection of Fire in Ship Compartments Abstract

In this report we describe progress using filtered, long wavelength video image-based detection (LWVD) of events in laboratory tests and full scale fire testing within the Volume Sensor Task at the U.S. Naval Research Laboratory (NRL). Another part of the program is to evaluate and use video image detection (VID) systems based on cameras that operate in the visible region. The latter were initially developed for detecting smoke, but have recently been adapted to detecting fire. The VID systems are not as effective at detecting fire outside the direct line of sight of the camera. Our studies demonstrate that long wavelength imaging achieves effective detection of reflected flame emission compared to visible video images. A system that combines visible and long wavelength image capabilities may be more accurate and sensitive than either alone.

Our LWVD approach exploits the long wavelength response of standard CCD arrays used in many cameras. A long pass filter (typically in the range 700-900 nm) increases the contrast for flaming and hot objects and suppresses the normal video image of the space, thereby effectively providing a degree of thermal imaging. There is more emission from hot objects in this spectral region than in the visible region (<600 nm). Testing has demonstrated the detection of objects heated to 400^{o} C or higher. A simple luminosity-based algorithm was developed and used to evaluate camera/filter combinations for fire, smoke, and nuisance (false) event detection and response times.

Introduction

We report recent progress in using long wavelength video image-based detection (LWVD) of fire that has been developed in the Volume Sensor (VS) Task at the U.S. Naval Research Laboratory (NRL). In the VS Task, which is a component of the

Advanced Damage Countermeasures Program in the Platform Protection Future Naval Capability, the primary goal is to employ optical detection methods for inexpensive, remote and real-time monitoring of ship spaces, including the detection of fire and smoke. Previous efforts at NRL have demonstrated significant improvements in accuracy, sensitivity and response time in fire and smoke detection using multicriteria approaches which combine various sensors and utilize neural network algorithms [1,2]. The response time of these methods, however, is inherently limited by their reliance on point detection sensors (e.g., of heat, smoke or gases, such as CO or CO2), which depend on molecular or thermal diffusion from the fire or smoke source to the sensor. Optical sensors do not depend diffusion, so they can provide stand-off detection, achieve faster response and more quickly identify a fire or other hazardous conditions.

The central element of the VS Task is the identification of fire, smoke, and other conditions using video image detection (VID) systems in which the images are analyzed by machine vision algorithms. Progress in this area, which includes testing of commercial systems, is being reported in other contributions at this meeting [3,4]. These video fire detection systems are most effective at identifying smoke and direct line of sight (LOS) fire and are less successful for identifying small or obstructed flames from reflected emission or hot objects. Video detection systems can respond quickly, but a common limitation is that that they require a direct LOS between the source and detector for optimum performance. It is not feasible for practical or economical reasons to deploy enough sensors to ensure complete direct LOS coverage throughout the compartment space, especially in crowded spaces that are typical for Navy ships. A possible remedy being explored is to detect reflected radiation as described below using LWVD. In addition, other kinds of sensors are being incorporated into the VS system as described in elsewhere at this meeting [4]. The LWVD is one component of the multisensor, data fusion-based VS system currently under development at NRL.

There may be at least one VS system deployed in every compartment of Navy ships, therefore it is important to minimize the unit cost. The goal of developing an inexpensive yet effective system motivated using near infrared imaging. The LWVD method uses commonly available, inexpensive cameras. These can be simple surveillence cameras (<$100) or commercial camcorders (<$1000), both of which cost much less than mid infrared cameras (3-12 microns, >$5000). The latter are almost

certainly better for thermal imaging. For example, they have a much lower minimum detectable temperature and can distinguish between body temperature and room temperature. Although mid infrared cameras outperform LWVD, the latter provides a desirable trade off between cost and performance for the applications described here.

Long wavelength or near infrared (NIR) emission radiation detectors have been used previously for fire detection. Lloyd et al. [5,6,7] reported and patented approaches intended to detect reflected near infrared emission using several narrow band detectors without any imaging capability. The results demonstrated the feasibility of detecting reflected NIR emission. In addition, NIR image detection has been applied in background free environments, such as for monitoring forest fires from terrestrial based [8] and satellite images [9], tunnels [10], as well as aircraft cargo surveillance [11]. The latter study includes a detailed characterization of using CCD cameras operating in the NIR for remote temperature measurement and demonstrated a minimum detectable termperature of about 350° C. NIR detection of forest fires and other quiescent environments is effective in part because there are few if any interferences or nuisances to complicate the detection. A narrow band filtered (1140 nm) NIR imaging technique that includes image analysis has been patented as method for improved fire and hot object detection by reducing false alarms in protected areas [12].

In our LWVD approach to fire detection, we use a long pass filter (LPF) positioned in front of a camera that has a standard CCD array. The LPF transmits light with wavelengths longer than a cutoff, typically between 700 and 900 nm, which increases the contrast for fire, flame, and hot objects by suppressing the normal video images of the space. This provides modest thermal imaging. There is more emission from hot objects in this spectral region than in the visible (<600 nm). Nightvision videos are demonstrated to be particularly beneficial for providing high contrast and therefore straightforward LOS detection for flames and hot objects, where the latter includes bulkheads heated by obstructed fires, and for identifying obstructed fire and flame based on reflected light.

Approach

The LWVD method is implemented by acquiring long wavelength images in real time and from digital recordings with various long pass filters (typically, 720-850 nm) using

both a Sony camcorder (DCR-TRV27) in Nightshot mode and inexpensive “bullet” cameras (Si-SPECO (CVC-BOR)). This report will focus on results from full scale fire testing in the CVNX and VS1 test series conducted aboard the ex-USS *SHADWELL* in April 2003 [13] and tests conducted at the facilities of Hughes Associates, Inc, in Baltimore, MD in 2003-2004 [14].

The video signal from a nightvision camera was converted from analog to digital video (DV) format with a Firewire video adapter (Dazzle Hollywood DV Bridge) or to digital AVI format with a USB video adapter (Belkin USB VideoBus II) for suitable input into a computer. A program coded in Mathworks' numerical analysis software suite, MATLAB v6.5 (Release 13), was used to control the video input acquisition from the cameras and to analyze the video images. The latter was carried out using a straightforward luminosity-based algorithm developed at NRL explicitly for analysis of nightvision images. The design goal of the luminosity algorithm was to capture the enhanced sensitivity of the nightvision cameras to the thermal emission of fires, hot objects, and especially flame emission reflected off walls and around obstructions from a source fire not in the field of view (FOV) of the camera, thereby augmenting the event detection and discrimination capabilities of the VID systems. This goal was achieved by tracking changes in the overall brightness of the video image. Further details of the luminosity algorithm are available in an NRL report [13]. Alarms were indicated in real time and alarm times were recorded to files for later retrieval and compilation into a database. A background video image was stored at the start of each test, as well as the alarm video image when an alarm occurred. Luminosity time series data were recorded for the entire test.

Results

As a result of several test series conducted during the VS Task, there have been more than 300 tests of fire and smoke sources and nuisances in real or simulated ship compartments. These tests have included heated bulkheads due to fires in the adjacent spaces, flaming fires, both in an out of the field of view, smoldering sources, and various nuisance events, such as grinding, welding, and activity and motion within the compartment. The LWVD approach has been useful for sources typical of Navy environments, especially for reflected fire emission and hot objects. Also, LWVD-

detected luminosity was correlated with thermocouple temperature measurements of a heated bulkhead to demonstrate detection of objects hotter than 400º C.

Several general capabilities of the LWVD method were apparent from visual inspection of the video streams as the tests were being conducted. First, flaming fires are detected with greater sensitivity with filtered nightvision cameras than with regular cameras because there is more emission from hot objects at the longer wavelengths detected by the nightvision cameras. NIR emission from flames is easily visible to the nightvision cameras, which is not always the case for regular video cameras. The point is demonstrated in Figure 1, which consists of several panels of images extracted from the

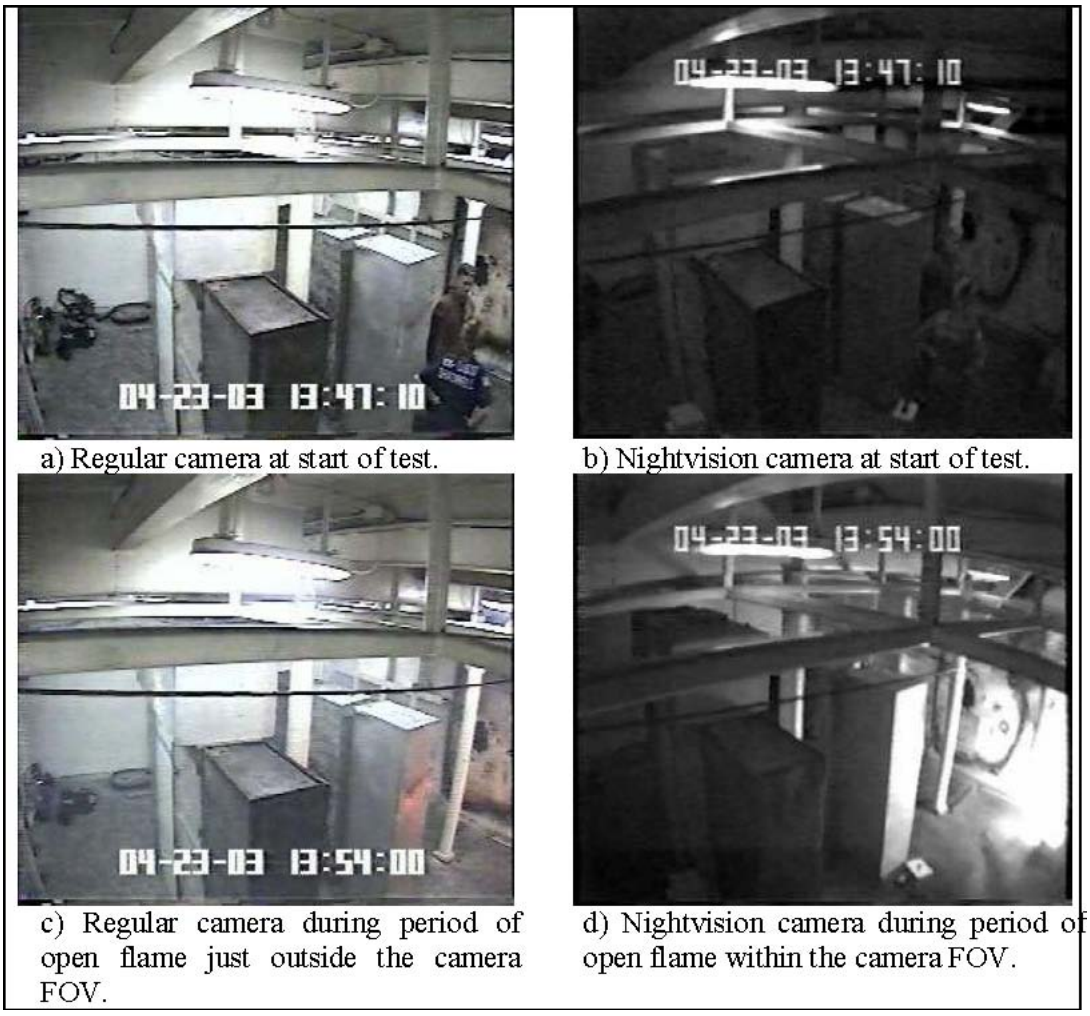

Fig. 1 – Camera video from a test on the ex-USS Shadwell. Regular and nightvision still images before and during a flaming event.

videos from a test. Panels a) and b) show images from a test aboard the ex-USS Shadwell for the regular and the filtered nightvision cameras, respectively, prior to

source ignition. The images in panels c) and d) are from the same cameras several minutes later while the cardboard box flaming source is burning in the lower right hand corner, within the camera FOV for the nightvision camera and just out of the camera FOV for the regular camera. The flame is evident in both types of video. Emission from the flame can be seen on the surface of the nearest cabinet in the regular video image, but a more dramatic change is observed in the nightvision camera image, in which the lower righthand quadrant is brightly illuminated. Although this example is somewhat biased because the fire is in the FOV of the nightvision camera and not the regular camera, it nevertheless demonstrates the high sensitivity of filtered LWVD. The LWVD images are more informative so that less is required of the image analysis for detection and identification. A simple luminosity algorithm would be much less effective for regular video images.

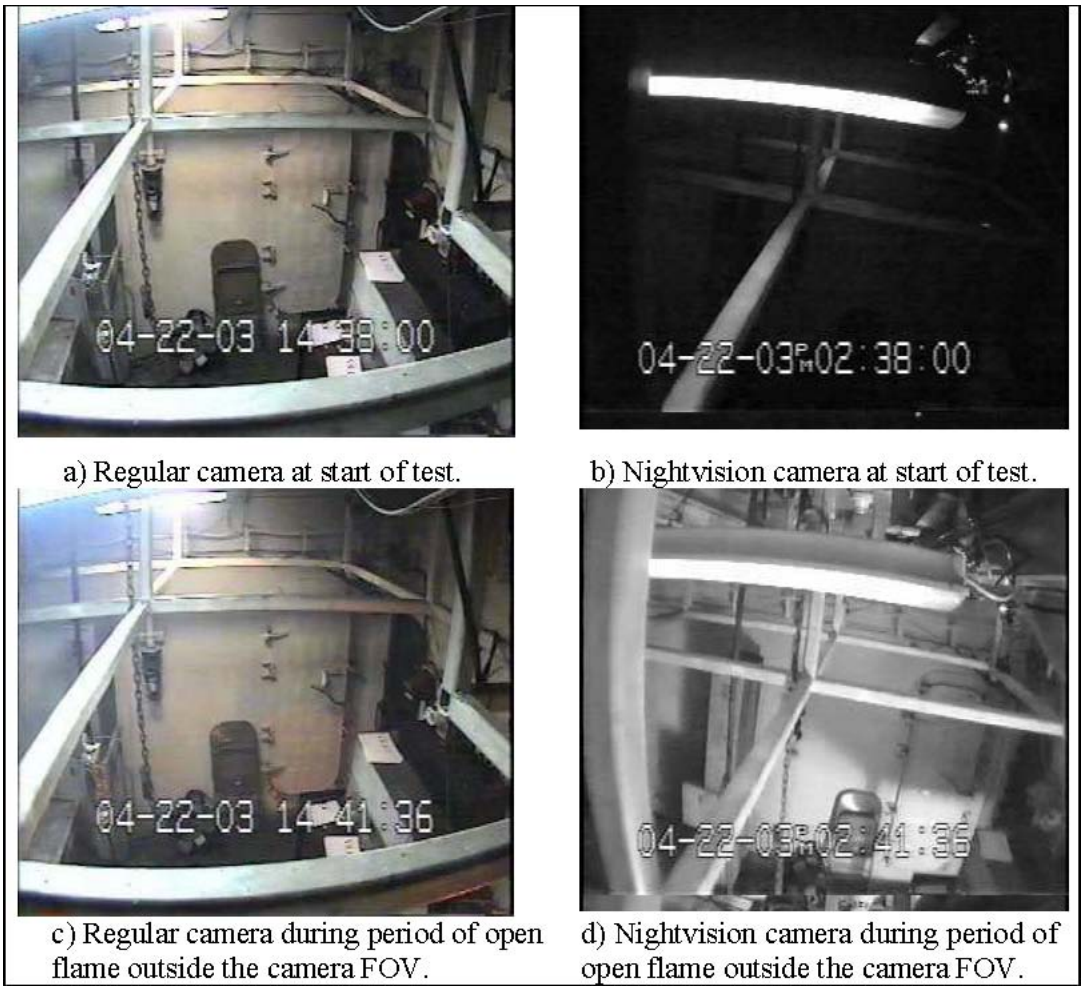

Fig. 2 – Regular and nightvision images before test ignition and during a flaming event outside the camera FOV

Another example is shown in Figure 2 for a source that is completely outside the FOV of all cameras. The source for this test was several cardboard boxes placed on the deck against the aft bulkhead. This position is below and behind the FOV of the camera. Panels a) and b) show images obtained prior to ignition of the source from the regular and nightvision cameras, respectively. The images in panels c) and d) were acquired several minutes after ignition when the source was fully engulfed in flame. Little or no difference can be seen between the regular images, with the exception of what appears to be smoke in the upper left-hand portion of the image. There is, however, a marked difference between the two nightvision images. NIR emission from the flame illuminates the entire area within the camera FOV. In the nightvision video, the NIR illumination fluctuates with the same temporal profile as the flame itself. This suggests that reflected NIR light could be used to detect flames that are out of the camera FOV based on time-series analysis of the camera video alone.

A second general observation is the ability of the nightvision cameras to act as an inexpensive form of thermal-imaging camera. In fact, they worked so well that during the CVNX test series the ex-USS *SHADWELL* control room crew used the nightvision cameras as monitors for the progress of tests involving fires in adjacent compartments. For several tests in the CVNX test series, heptane spray fires were set up outside the test magazine and directed at a magazine bulkhead to simulate a fire in an adjacent compartment. If the bulkhead behaves similar to a blackbody emitter, the NIR emission from the bulkhead should increase with increasing temperature. In addition to monitoring the luminosity with the LWVD system, the bulkhead temperature was measured with thermocouples attached to the bulkhead. Figure 3 contains several still images from the nightvision camera as the bulkhead temperature increased during the test. NIR emission of the bulkhead is seen to grow in both size and intensity as the temperature increased. Before ignition (in panel a)), the image is dark. After 279 seconds as shown in panel b), a small illuminated region is seen and the maximum temperature of the bulkhead is 370º C. In b) and c), 737 and 1243 seconds after ignition, respectively, the luminosity is higher and the temperatures measured are 540º C and 565º C. There is no indication from the regular video images (not shown) that the bulkhead temperature is elevated. Hot object identification is a capability of LWVD that cannot be achieved with regular video.

The results of a hot bulkhead test for which images are shown in Figure 3 were used to estimate the minimum detectable temperature (Tmin) of the LWVD system using the luminosity algorithm. Tmin was found to be about 400º C by comparing the luminosity (intensity) measured for a small area of the images to the actual bulkhead temperature as recorded by thermocouples (TC),. The results for the shipboard test were verified in laboratory measurements carried out using a blackbody emission source using the LWVD system and a narrowband filtered (at 800 nm) single element detector. The Tmin of about 400º C is similar to the value reported in the study by Sentenac et al. using CCD camera temperature sensing for hangar bay surveillence [11].

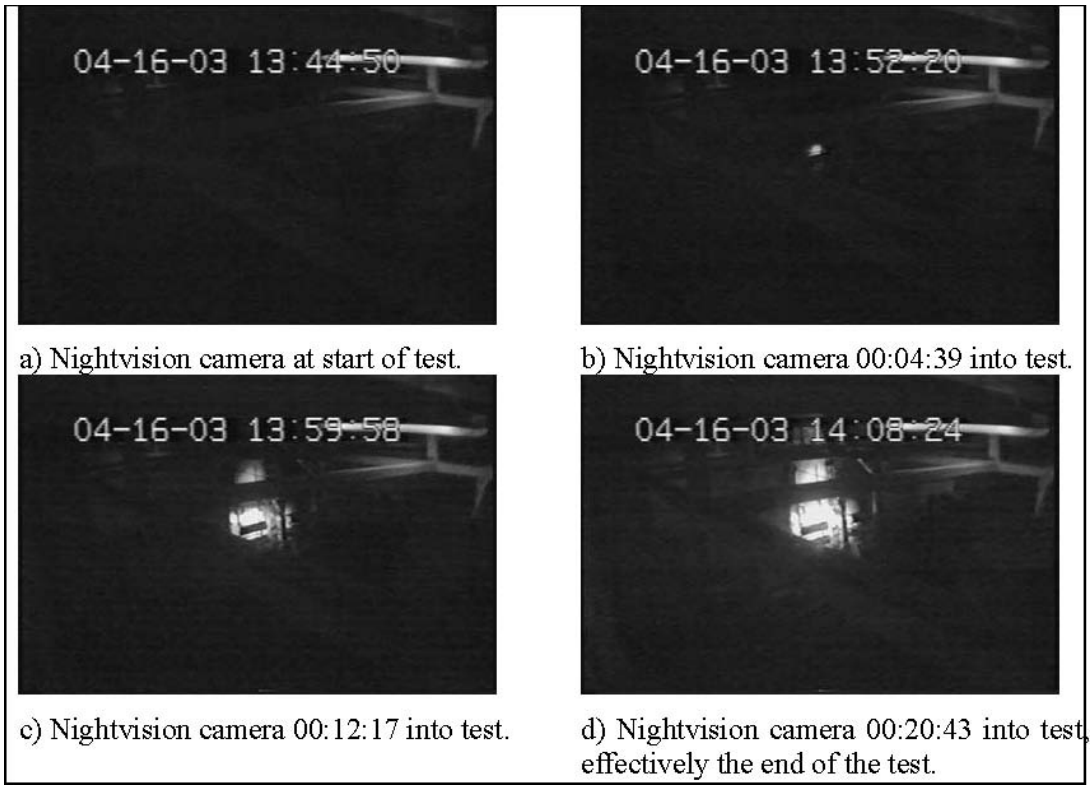

a) Nightvision camera at start of test.

b) Nightvision camera 00:04:39 into test.

c) Nightvision camera 00:12:17 into test.

d) Nightvision camera 00:20:43 into test, effectively the end of the test.

Fig. 3 – Still images of nightvision video from test of a hot bulkhead before and at three times during the test

A final general observation is that there is tradeoff in flame and hot object detection with smoke detection, depending on the long wavelength filter used. While the nightvision cameras are more sensitive to flames and other hot objects when longer wavelength LP filters are used, they suppress more of the visible image and increase the contrast for NIR emission, and consequently they degrade the sensitivity for detecting

smoke. There is actually some flexibility in how one might utilize the enhanced NIR sensitivity in imaging applications. One perspective on this is whether the approach would be to use one camera or two. For a single camera version, increased sensitivity in the NIR while retaining the image for smoke detection would be implemented with light filtering (shorter wavelength LP filter, perhaps 650-750 nm). An approach that would yield more sensitivity albeit with more complexity would be to use two cameras, one in the visible for smoke and a heavily (>900 nm) filtered LWVD for better contrast and more effective hot object and reflected flame detection. Another advantage to heavy filtering is that it could be used in spaces where privacy is an issue (e.g., berthing compartments), i.e., where images of people might not be desirable, but video fire protection would still be beneficial.

Conclusions

LWVD offers an attractive and cost-effective augmentation to the standard implementation of VIDS technologies as seen in currently available commercial systems. The NRL LWVD system emphasizes detection of fire and hot objects both within the camera FOV and outside the camera FOV. The NIR radiation from flaming and hot objects is sufficiently intense in the observation band of the nightvision cameras (700 – 1000 nm) to quickly detect fires and hot objects such as overheated cables and ship bulkheads heated by a fire in an adjacent compartment. As part of the NRL LWVD system, a simple total luminosity-based, machine vision algorithm has been developed to support the nightvision camera development. Since LP filters suppress the visible image detected with nightvision cameras, smoke is not easily detected by the LWVD system. The LWVD system already shows promise as an inexpensive pseudo-thermal imaging system for remote monitoring of surface temperatures. Both spatial and time-series analysis will be incorporated into an enhanced version of the LWVD algorithm in a parallel effort to the planned testing.

References

1. Rose-Pehrsson, S. L., Hart, S. J., Street, T. T., Williams, F. W., Hammond, M. H., Gottuk, D. T.,Wright, M. T., and Wong, J. T.: "Early Warning Fire Detection System Using a Probabilistic Neural Network," Fire Technology, 39(2), 147-171 (2003).
2. Pfister, G.: “Multisensor/Multicriteria Fire Detection: A New Trend Rapidly Becomes State of the Art”, *Fire Technology Second Quarter*, Vol 33, No. 2 (1997), 115.
3. Gottuk, D. T., et al.: AUBE ’04, Proceedings of the 11th International Conference on Automatic Fire Detection, Duisburg, Germany.
4. Rose-Pehrsson, S., et al.: AUBE ’04, Proceedings of the 11th International Conference on Automatic Fire Detection, Duisburg, Germany.
5. Zhu, Y.-J., Lloyd, A., Sivathanu, Y., and Gore, J., “Experimental and Numerical Evaluation of a Near Infrared Fire Detector,” Fire Research and Engineering, Second (2nd) International Conference, (ICFRE2), Slaughter, K.C., Editor, p. 512, 1998.
6. Lloyd, A.C., Zhu, Y.J., Tseng, L.K., Gore, J.P. and Sivanthanu, Y.R.: “Fire Detection Using reflected Near Infrared Radiation and Source Temperature Discrimination,” NIST GCR 98, 747 (1998).
7. Sivathanu, Y., Joseph, R.K., Tseng, L., Gore, J.P., and Lloyd, A.: “Flame and Smoke Detector,”United States Patent 6,111,511, August 29, 2000.
8. Thomas, P.J.: “Near-Infrared Forest-Fire Detection Concept,” Appl. Opt. 32, 5348 (1993).
9. Lasaponara R., Cuomo V., Macchiato M.F., Simoniello T.: “A self-adaptive algorithm based on AVHRR multitemporal data analysis for small active fire detection,” International Journal of Remote Sensing, 24, 1723 (2003).
10. Wieser, D., Brupbacher, T.: “Smoke Detection in Tunnels Using Video Images,” NIST SP 965, February 2001.
11. Sentenac, T., Le Maoult, Y., and Orteu, J.-J.: “Evaluation of a charge-coupled-device-based video sensor for aircraft cargo surveillance,” Opt. Eng. 41, 796-810 (2002).

12. Chan, William S. and Burge, John W.: “Imaging flame detection system,”United States Patent 5,937,077, August 10, 1999.
13. Steinhurst, D.A., Minor, C.P., Owrutsky, J.C., Rose-Pehrsson, S.L., Gottuk, D.T., Williams, F.W., and Farley, J.P.: “Long Wavelength Video-based Event Detection, Preliminary Results from the CVNX and VS1 Test Series, ex-USS SHADWELL, April 7-25, 2003,” NRL/MR/6110—03-8733, December 31, 2003.
14. Lynch, J.A., Gottuk, D.T., Rose-Pehrsson, S.L., Owrutsky, J.C., Steinhurst, D.A., Minor, C.P., Wales, S.C., Williams, F.W. and Farley, J. P.: “Volume Sensor Development Test Series 2 – Lighting Conditions, Camera Settings, and Spectral and Acoustic Signatures,” NRL/MR/6180—04-XXXX , June 2004.

Thomas G. Cleary
Building and Fire Research Laboratory
National Institute of Standards and Technology
Gaithersburg, MD 20899 U.S.A.

ideo Detection and Monitoring of Smoke Conditions

Abstract

Initial tests have been performed to assess detection limits and smoke obscuration monitoring for a video scene under different lighting and smoke concentration conditions. An illuminated exit sign located in the fire emulator/detector evaluator duct was used as the scene. A fixed gain, black and white CCD camera, coupled to a manual-focus, manual-iris video zoom lens was used. The lens itself was attached to a rigid boroscope, which penetrated the duct and viewed the exit sign from a distance of 2 m. Flaming soot, smoldering wood smoke, and ISO test dust were used to obscure the scene. Repeated tests were performed with the external scene lighting turned on or off. Scenes ranged from smoke/dust free conditions to a completely obscured exit sign. Analysis of the data shows that a CCD camera pointed at a continuously illuminated source, like an exit sign, can provide an indication of obscuring aerosols in the scene (i.e. detection). Furthermore, an assessment of the visibility conditions can be obtained from the scene under fixed lighting conditions. Analysis of the loss of contrast between the illuminated letters and the background of the sign provides a more general assessment of visibility conditions.

Introduction

Building video surveillance via human monitoring of multiple locations was the norm just a few years ago. Now, automatic video image processing and decision algorithms exist for many conditions including, traffic control, perimeter security, and even facial recognition. Essentially, any routine decision that a human observer makes can be replaced with some level of success by a dedicated machine vision system. Fire detection schemes employing video cameras have been developed and deployed in various environments. Security concerns will only increase the use of video monitoring in buildings, so it make sense to maximize that infrastructure investment. Augmenting

existing fire detection systems with video detection may increase sensitivity to real fire events. Another potential benefit would be real-time assessment of visibility conditions in fires to help with egress and search and rescue. There is little quantitative data in the literature relating the video image properties to smoke obscuration levels.

Wieser and Brupbacher 1 , give a brief description of a design based on loss of contrast due to smoke. They also discuss calibration issues, and the challenges of deploying a design in a road tunnel. Jin s work on visibility through smoke related the amount of smoke to the visibility distance of internally illuminated and reflecting signs 2 . He also postulated the main reasons for decrease in visibility through smoke as (1) a reduction in light intensity of the object (sign) and background due to the obscuring smoke, and (2) scattered light off smoke particles from other light sources that reach the subject s eye. Collins 3 studied exit sign visibility in clear and smoke obscured conditions and observed that sign luminance, and to some extent uniformity and contrast, are important in sign visibility in smoke. Ouellette s 4 study on exit sign visibility in smoke examined the effects of ambient illumination and suggested that brighter exit signs are needed to compensate for the luminous veil created by ambient lighting when smoke is present, or lighting along lines of sight to exit signs should be reduced when smoke is detected.

The experiments conducted in this study were designed to assess the ability to use video images to detect the level of different types of smoke and dust in the path from a viewing location to a constantly illuminated target, and to predict the visibility conditions over that path length.

perimental

The fire emulator/detector evaluator 5 was used to provide different volumes of uniform smoke concentration. The test section was modified to allow viewing of an internally lit exit sign through the smoke. A schematic of the test section is shown in Figure 1. Smoke enters from the right and exits through a 90^{o} elbow at the left side. A diode laser beam (635 nm) travels from the end of the duct to a mirror located above the center of the exit sign back to a photodetector. The light transmission path length is

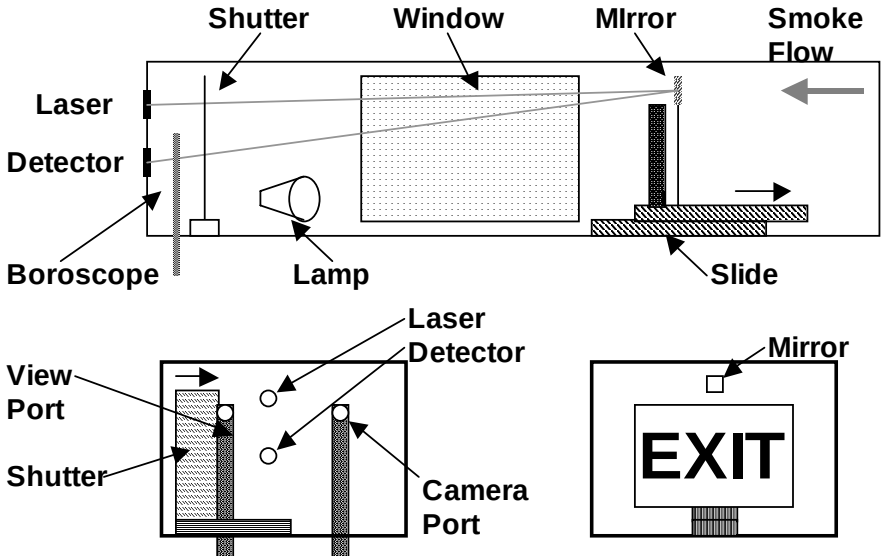

Figure 1 Schematic of the perimental Setup

4.30 m. The exit sign scene is viewed through boroscopes that extends into the duct at the far end. One boroscope is reserved for a CCD camera and one is used for human observation. The boroscopes provide a wide-angle view with a magnification of 0.20X. The distance from the boroscope viewing port to the exit sign is 1.92 m, thus the sign appears to be 9.6 m from the viewer. A 150 W incandescent lamp was placed slightly forward of the boroscopes to illuminate the exit sign with external lighting. Room lights were turned off during testing to reduce the ambient light entering the test section windows to a negligible amount. In addition, laser light extinction measurements were taken when the exit sign and external lighting were extinguished. The sign was an internally illuminated exit sign 31 cm by 19 cm with a red colored semi-transparent insert (i.e., red-lettered sign). Letter widths were approximately 20 mm, and the sign contained an11w incandescent bulb.

Images were taken with a 1/3 inch type black and white CCD camera module with a manually adjusted gain setting (the gain setting remained the same for all tests shown here.) One boroscope was coupled to a video zoom lens attached to the CCD camera module. The gain was set such that the brightest pixel intensity was less than the maximum for the brightest (externally-lit) scene. The dynamic range of the CCD

camera is such that the background details are not apparent unless the exit sign is over-exposed. Images were acquired with an image acquisition card once per second.

Three different types of smoke: propene soot, wood smolder smoke, and cotton wick smoke were produced for the tests, in addition, ISO Fine test dust was also used to obscure the exit sign. Details on the properties of these smokes and dust are available in another paper in these proceedings [6].

Results and Analysis

The laser transmittance data was used to compute the average extinction coefficient over the viewing path length. The extinction path length of 4.30 m was used to compute the extinction coefficient (k, m^{-1}). The standard uncertainty in the extinction coefficient is estimated as 2% of the value up to 1.0 m^{-1} [5]. Random fluctuations due to varying smoke concentration along the path length are larger than the uncertainty. An apparent extinction coefficient (k_a) was computed using the apparent distance from the sign to the viewing location and the equality below.

$$\left(\frac{}{0}\right) = (1.92) = (9.60) \qquad (1)$$

The apparent extinction coefficient is the value that would yield the same light transmittance over a path length equal to the apparent sign distance; it is equivalent to the observed extinction coefficient times the boroscope magnification value (0.20). Values of extinction coefficients at alarm activation typically range from 0.03 m^{-1} to 0.1 m^{-1} (1%/ft to 4 %/ft) for cotton smolder smoke.

The CCD image consists of pixels of varying levels of brightness over a range spanning 0 to 255 (8 bit). Brightness is a relative measure proportional the luminance or intensity of the visible radiant energy from the sign. For the purposes here, pixel brightness is considered to be a measure of normalized (non-dimensional) luminance. Thus, contrast measurements may be computed from the pixel brightness values. Three metrics were used to characterize the image change under smoke conditions. First, the

average pixel brightness for a region of interest, defined here as the area covering the exit sign, the Weber contrast, and the Michelson contrast. The Weber contrast (C_W) is typically used to characterize contrast between an object and a uniform background, and it is defined as:

$$= \quad / \quad -1 \tag{2}$$

Where L_o and L_b are the object and background brightness respectively. Here the object was the illuminated sign letters and the background was the non-illuminated portion of the sign. The Michelson contrast is typically used to characterize periodic variations in luminousity, and it is defined as:

$$= (\quad \text{max} - \quad \text{min}) / (\quad \text{max} + \quad \text{min}) \tag{3}$$

Where L_{max} is the mean pixel brightness of the letters and L_{min} is the mean pixel brightness of the surrounding sign area.

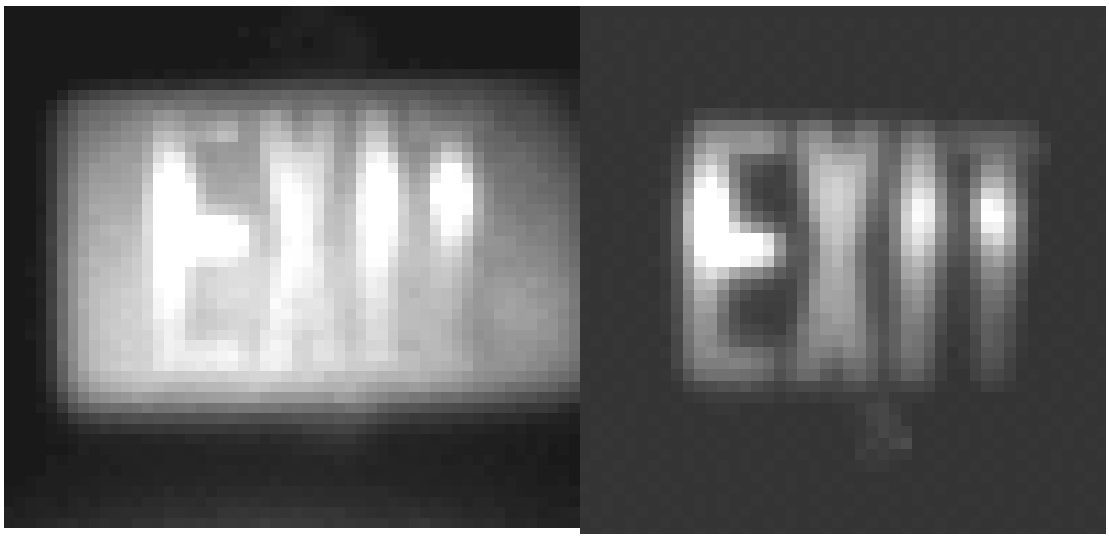

Figure o smoke sign images ith and ithout ambient lighting

Figure 2 shows the two images of the sign in clear conditions with and without external lighting. The sign letter width in on the order of 4 pixels. The non-uniform letter intensities were caused by uneven illumination related to the location of the lamp inside the sign.

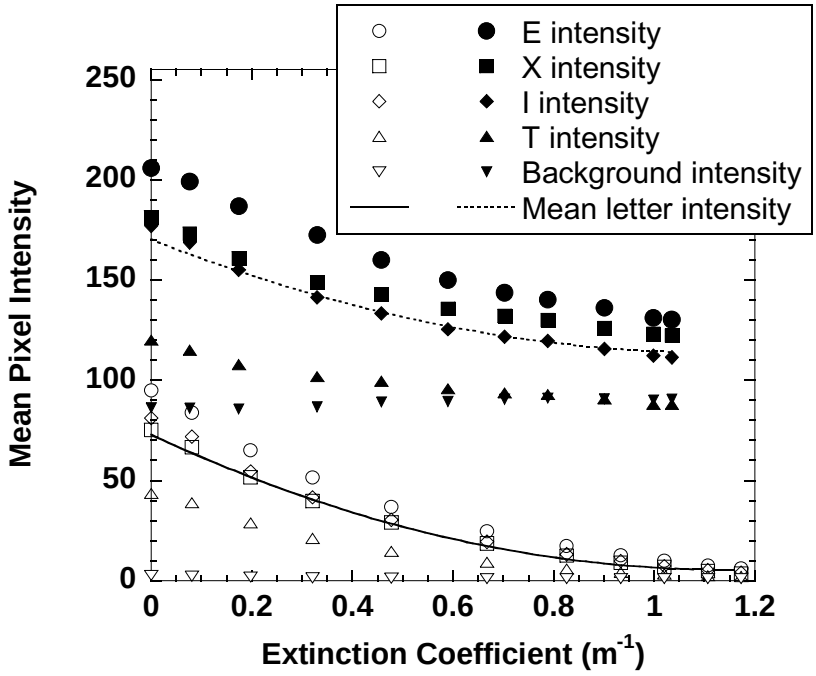

Figure Mean pi el intensity for indi idual letters and background for ood smoke obscuration pen symbols no ambient lighting closed symbols ambient lighting

Figure 3 shows the mean pixel intensities of each letter and the background for two tests, with and without external lighting, and wood smoke obscuration. In clear conditions, the variation in the mean letter intensity was 75% with external lighting and over 100% without external lighting. Without external lighting, the mean background intensity was about 3.0 to start, and decreased as the smoke extinction increases. With ambient lighting, the background intensity actually rose slightly as the smoke extinction increased due to the scattered ambient light. The mean letter intensities are given by the smooth curve that connects the arithmetic mean of the individual letter values at different extinction coefficient values. Figure 4 shows two images with external scene lighting. The left image shows the clear conditions and right image shows the luminous veil produced by wood smolder smoke light scattering at an extinction coefficient of 1.0 m^{-1}. The initial dark boundary surrounding the sign plus the illuminated and non-illuminated portions of the sign approach the same luminance.

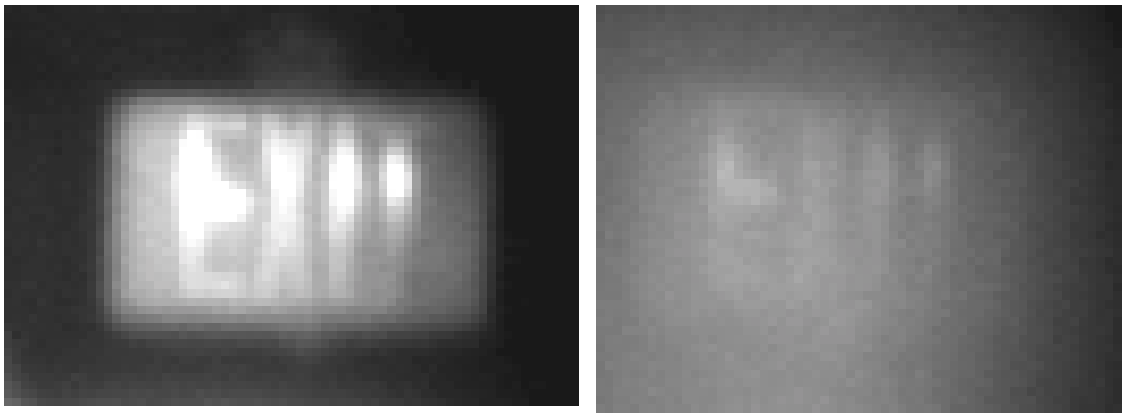

Figure ternally illuminated sign in clear conditions left image and in ood smoke ith an e tinction coefficient of 1 0 m^{-1} right image

Figure 5 shows the mean pixel intensities for the region consisting of the sign for all three smokes and ISO test dust. The externally illuminated sign had an initial mean pixel intensity of about 120 units, without external illumination the initial mean pixel intensity was about 35 units. For the case without external illumination, as the extinction coefficient increased the decrease in the mean pixel intensity drops off more rapidly than transmittance expected from an extinction meter (eq. 1) which is represented here as a curve with an initial value of 35. This was due to the large non-illuminated area of the sign, which factored into the average. The results for the externally illuminated sign show that dust, wood, and wick smolder smokes are similar, with an initial drop in the mean pixel intensity followed by a flattening out due to the luminous veil. The mean pixel intensities in soot smoke, on the other hand, continued to drop as the extinction coefficient increased. Soot scatters much less light than the smolder smokes or ISO dust at any given extinction value, where light absorption is the main mechanism for extinction. In terms of smoke detection, a marked decrease in pixel intensity at an extinction coefficient of 0.1 m^{-1} was observed. For this scene that appears to be 5 m away, this yielded an apparent extinction coefficient of 0.02 m^{-1} which is sufficiently sensitive for smoke detection. The only caveat is that the smoke must fill the path between the camera and the sign.

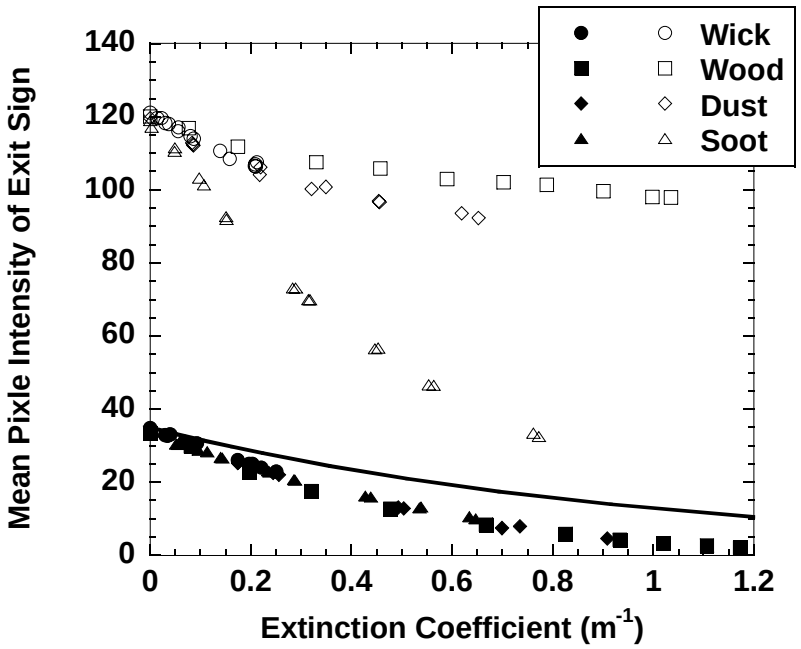

Figure Mean pi el intensity of the e it sign for all smoke and dust pen symbols ambient lighting closed symbols no ambient lighting Cur e represents light transmission e tinction meter results

Figure 6 shows the results of the contrast calculations for the cases with no external illumination. The Weber contrast for all three smokes and ISO dust were similar and showed a decline with increasing extinction coefficient. The Michelson contrasts were also similar for all three smokes and the ISO dust, remaining relatively flat up to about 0.6 m^{-1}, then decreasing. The observed Weber contrast over the entire extinction coefficient range, and the Michelson contrast up to 0.6 m^{-1} can both be explained by the fact that the mean letter intensity decreased while the background remained consistently low. The observation that the Michelson contrast rolls off above 0.6 m^{-1} was an artifact caused by the constraint that the mean pixel intensity of the background was not allowed to drop below 1.

Figure 7 shows the results of the contrast calculations for the cases with external illumination. The Weber contrast for the two smolder smokes and ISO dust showed a similar rate of decline with increasing extinction coefficient, while the Weber contrast trend for soot showed a slower rate of decline. The Michelson contrast trend for the

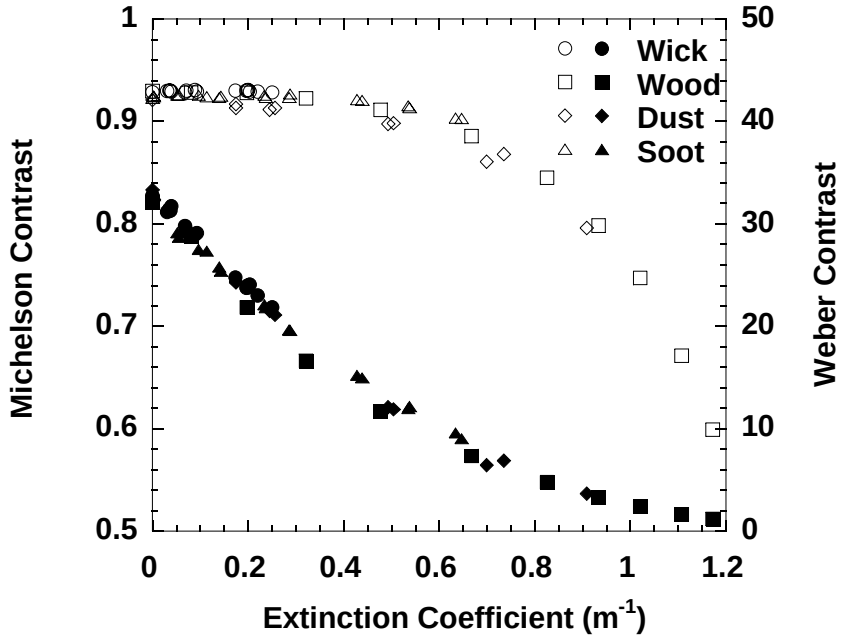

Figure Contrast measurements for e periments ithout e ternal lighting pen symbols Michelson contrast closed symbols eber contrast

two smolder smokes and ISO were similar and continued to drop as the extinction coefficient increased. For the smolder smokes and ISO dust, both contrast measures continued to decline as the extinction coefficient increased, while the mean pixel intensities of the sign were observed to decline at a much slower rate due to the luminous veil. Michelson contrast trend for soot was markedly different. It was observed to increase from the initial clean air value. This increase in contrast apparently was due to a preferential reduction in the sign background intensity due to reduction of light reflecting off the sign relative to the reduction in the illuminated letter intensities.

Conclusions

(1) Pixel intensity measurements can be used to detect the presence of obscuring aerosols including fire smokes.

(2) Weber contrast measurements can indicate visibility degradation in cases with and without external illumination.

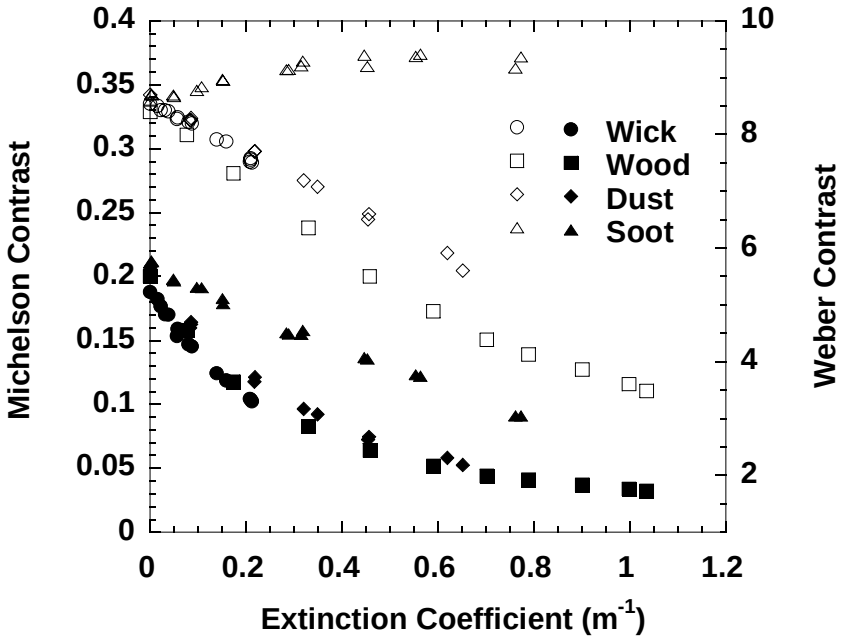

Figure Contrast measurements for e periments ith e ternal lighting pen symbols Michelson contrast closed symbols eber contrast

(3) Together, the Michelson and Weber contrast measurements with external illumination can distinguish black soot smoke from smolder smokes and dust.

References

1 Wieser, D., and Brupbacher, T., "Smoke Detection in Tunnels Using Video Images," AUBE 01, Proceeding, Gaithersburg, MD, Grosshandler, W., Ed., 2001.

2 Jin, T., "Visibility Through Fire Smoke," J. of Fire and Flam., 135, Vol.9, 1978.

3 Collins, B., Dahir, M., and Madrzykowski, D., "Evaluation of Exit Signs in Clear and Smoke Conditions," NISTIR 4399, NIST, Gaitherburg, MD, 1990.

4 Ouellette, M., "Exit Signs in Smoke," Lighting Res. and Tech, Vol. 20, No. 4, 1988.

5 Cleary, T., Donnelly, M., and Grosshandler, W., "The Fire Emulator/Detector Evaluator" AUBE 01, Proceeding, Gaithersburg, MD, Grosshandler, W., Ed., 2001.

6 Cleary, T., "Time Resolved Size Distributions of Test Smokes and Nuisance Aerosols," AUBE 04, Proceedings, Duisburg, Germany, Luck, H., Ed. 2004.

S. Dunkelmann, I. Bebermeier, C. Oldorf and V. Leisten
m.u.t Aviation-Technology GmbH, Hamburg, Germany

Comparison of NIR, MIR and LWIR cameras for video based detection of fire

Abstract

The common approach in video-detection of fire relies on the thermal radiation and smoke generated by the fire. The major part of thermal radiation belongs to the infrared wave band, which is partially atmospheric opaque and partially atmospheric transparent. Therefore the imaging detectors support the three atmospheric windows Near Infrared NIR (0.8-1.4µm), Midrange Infrared MIR (3µm-5µm) and Long Wave Infrared LWIR (8µm-12µm), but which range is best? Unfortunately there is no easy answer and the best choice varies depending on the application and its special conditions. This article collects imaging features, shows our own experimental results and discusses several special conditions and applications, which may be used as a decision guidance.

Introduction

Standard video systems working in the visible range loose considerable amount of image information, when fog, dust or smoke is present. The objects of the monitored scene may even vanish. Using spectral ranges in the infrared is a powerful method to overcome this monitoring problem [1][2].

Unfortunately it is impossible to achieve optimal monitoring of the scene and optimal visualization of smoke and flames at the same time and wave band. This conflict is the main reason, why the best choice is strongly depending on the application and its special conditions.

The radiation theory of light based on Planck's law and extended to grey body model, which includes reflection and transmission, is a good starting point to discuss thermal radiation and imaging. Since fog, dust or smoke particles scatter the radiation, the theoretical part should also contain some scattering theory. Therefore the next section briefly presents radiation and scattering theory reduced to the results required to detect fire.

Theoretical Background

To begin with an idealised radiator, which is in thermal equilibrium and does not reflect nor transmit background radiation, shall be considered. This radiator will absorb radiation from the background, when it has a lower intensity than the background, or will emit radiation to the background, when it has a higher intensity than the background. In fact absorption and emission share the same physical concept. Since total absorption is combined with black, such radiators are also called black bodies.

Planck's law of radiation describes the intensity of a black body as a function of temperature T in Kelvin and wave length λ:

$$I(\lambda,T)=\frac{2\pi hc^2}{\lambda^5}\left[\frac{1}{\exp(hc/\lambda kT)-1}\right],$$

where h is Planck's constant, k is Boltzmann's constant and c is the vacuum speed of light [3].

When the wave band is kept constant, the intensity is strictly monotonic increasing with the temperature giving a one-to-one relationship between temperature and intensity. This relationship may be extended to summed intensities of an arbitrary wave bands weighted with some temperature independent detector sensitivity. Thus intensities measured by detectors may be expressed as black body temperatures and vice versa.

Integrating the black body intensity by the wave length gives the following surprisingly short Stefan-Boltzmann formula:

$$I(T)=\sigma T^4,$$

where σ is the Stefan-Boltzmann constant [3]. This formula is widely used to define effective temperatures.

The black body model does not deal with reflection nor transmission effects, but the grey body model will. Any material has the ability to absorb, emit, transmit and reflect, where the appropriate coefficients may depend on temperature and wave length. These coefficients are named absorption α, emission ε, reflection ρ and transmission τ.

According to Kirchhoff's results absorption and emission share the same coefficient, yielding:

$$\varepsilon(\lambda,T)=\alpha(\lambda,T),$$

where the wave length λ and temperature T are arbitrary [3]. This generalises the aforementioned black body behaviour.

The conservation of energy implicates, that emission, transmission and reflection are balanced to 1:

$$\varepsilon(\lambda,T)+\rho(\lambda,T)+\tau(\lambda,T)=1,$$

wave length λ and temperature T are arbitrary again [3].

The detectable intensity of an object is established by the weighted sum of all three effects:

$$I(\lambda,T)=\varepsilon(\lambda,T)I_{\varepsilon}(\lambda,T)+\rho(\lambda,T)I_{\rho}(\lambda,T)+\tau(\lambda,T)I_{\tau}(\lambda,T),$$

where I_{ρ} describes the intensity of the reflected background, I_{τ} describes the intensity of the scene buried by the object and I_{ε} describes the undisturbed emission from the object, which is equivalent to the black body intensity in thermal equilibrium by definition.

The gray body model simplifies the coefficients in assuming, that all coefficients are not depending on wave length nor temperature. This approximation is known to be mostly justifiable. Applying the Stefan-Boltzmann formula to the previous equation yields:

$$T_D{}^4 = \varepsilon T_{BB}^4 + \rho T_{BG}^4 + \tau T_{BS}^4 ,$$

where the index BB is an abbreviation for black body and the indices D, BG and BS are used to denote effective temperatures for detection, background and buried scene.

The optimisation conflict mentioned in the introduction is implied by the last equation, since the optimal monitoring of the buried scene requires the transmission part to be dominant and the optimal monitoring of the object requires the same part to be negligible.

The last equation must be reapplied for tracking the radiation through media. As a consequence the transmission is squared, when the thickness of the media is doubled. This generalizes for homogenous media to the typical exponential decay:

$$\tau(d)=\exp(-\kappa\cdot d),$$

where d is the thickness of the media and κ a material depending damping factor measured in reciprocal thickness units.

Flame Detection

The camera system has been placed to monitor a candle in a distance of about 0.5 m. The temperature variation within the flame is expected to range from 800°C to 1400°C [5].

Figure 1: Greyscale image of the candle used as a source for flame detection

The NIR camera has shown a clear visible flame with high intensity. A black body equivalent temperature of about 700°C has been measured indicating the dominance of emission.

The MIR and LWIR camera have shown a barely visible flame (temperature increase of the background less than 1°C), but the burning wick for both camera systems. Applying the grey body model this experiment indicates the domination of transmission for both spectral ranges. This feature is very useful for monitoring and fire fighting [1][2], but circumvents flame detection.

Smoke Detection

In a chamber of about 10 m length, 2.2 m width and 2.5 m height the camera systems have been placed to monitor a scene across the chamber at the opposed wall including a rectangular black body reference with controlled 60°C temperature. The chamber has been fumigated by a standard fog machine used in theatre.

The NIR camera has shown visible wads of smoke. Although the range of sight has been reduced to some centimetres after some time, a distant candle has remained visible. Thus forward scattering is obviously dominating.

Figure 2: NIR image shows a candle in spite of the low range of sight

The MIR camera has shown a blurred image of the scene. Illuminating the scene with a tungsten-halogene lamp the video images have exhibited scattering effects like flares and multiple reflections. The transmission has been calculated to 0.39.

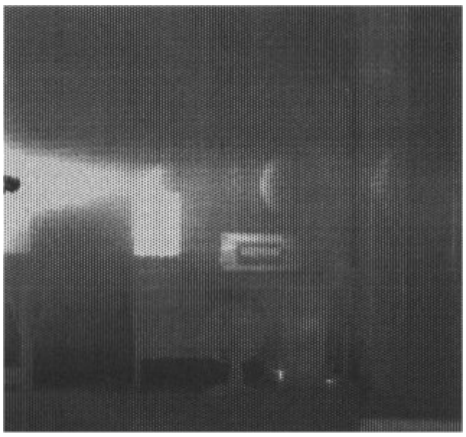

Figure 3: MIR-Image of smoke filled chamber shows reflections when illuminated

The LWIR camera has delivered high-contrast video with barely noticeable loss of contrast. Applying the known reference source to the gray body equation mentioned in section “Theoretical Background” the transmission has been calculated to a very high value of 0.83. Therefore the smoke filled chamber has appeared almost transparent, thus the

density fluctuation and movements of the smoke have been practically invisible on the video. This excellent transmission supports fire fighting.

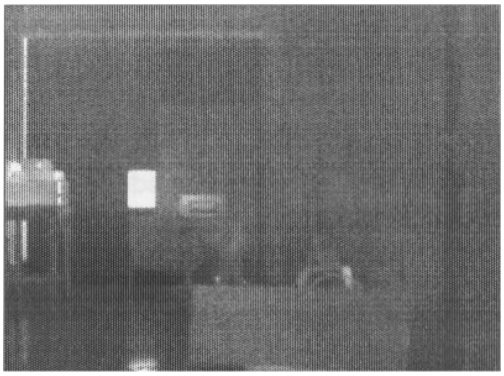

Figure 4: LWIR-image of smoke filled chamber shows no evidence of the smoke

Using the exponential decay from the section “Theoretical Background” MIR and LWIR ranges could be compared. Increasing the distance by a factor of 5 for the LWIR range would give the same value as the MIR range.

These experiments are in agreement with the general scattering theory of electromagnetic waves on spherical particles, also called Mie Theory, which predicts for particle sizes smaller than the scattered wave length, that the transmission losses are decreasing while the wave length is increasing [4]. This result is applicable, since smoke particles are expected to have sizes smaller than 1µm [7]. Furthermore Mie Theory predicts a boost of forward scattering for wave length comparable to the particle size, which explains the special behaviour for NIR observed above.

The results of this section are extendable for all phenomena consisting of small particles like fog and dust.

Hot Spot Detection

MIR and LWIR cameras are suitable to measure surface temperatures below 0°C as a special benefit. Thus monitoring the surface and analysing the temperature changes allows the early detection of fire, where hot spots beyond the surface are noticed at the surface due to heat transfer [1][2].

It is possible to build thermal cameras using the NIR range [6], but the minimal temperature is higher compared to MIR and LWIR cameras. Presenting a black body source to several NIR cameras in a dark room we have measured minimal temperatures from 280°C to 350°, which is still considerably lower than temperatures detectable by the human eye.

Detection of Hidden Fire

In the same chamber used for the smoke detection (see section “Smoke Detection”) the camera systems have been placed to monitor a candle of same size used for flame detection (see section “Flame Detection”). This candle has been put to the floor across the chamber. A pack of boxes leaving a gap of 0.2m to the walls and ceiling of the chamber have been placed between the candle and the monitoring cameras.

Figure 5: Greyscale image shows set-up for hidden fire experiments.

The MIR and LWIR cameras have shown no evidence of the burning candle. This result may be reasonable, since flames are almost transparent for MIR and LWIR and the

heated candle wax and the wick provide much lower radiation energy than the flames. Furthermore the reflection of walls is very low in the MIR and LWIR range.

In contrast the NIR camera has shown clear evidence for the burning candle, since the much higher radiation energy of the candle flame has been reflected by the walls and ceiling. The flickering of the candle has also been visible due to changes in total brightness of the scene.

Figure 6: NIR-image indirectly shows the candle flame due to reflections on the walls

Day-and-night Operation

MIR and LWIR images taken in darkness or daylight are barely changing their contrast. Therefore these spectral ranges are widely used in military applications to monitor enemy units at day-and-night and at all-weather conditions.

NIR imaging is strongly depending on the illumination, since most sensitive hot spot detection is demanding darkness, however if the application allows higher thresholds, a certain level of illumination is acceptable. In contrast smoke detection is demanding some kind of NIR illumination, which may be artificial or natural.

Conclusion

The LWIR camera provides early fire detection and superior monitoring and fire fighting capabilities when fog, dust or smoke is present, but flames, smoke and hidden fires cannot be detected.

The MIR camera provides hot spot and early fire detection and smoke detection, but no flame information. Furthermore MIR cameras are only able to support fire fighting for short distances.

Outdoor surveillance and early fire detection using NIR are difficult, but can be achieved by high-level image processing and complex software algorithms respectively. In addition NIR is the only range, where the detection of hidden fires and flames detection could be achieved.

From the commercial point of view, hardware needed for NIR systems is by orders of magnitudes cheaper than hardware required for MIR or LWIR systems. However, this significant advantage of NIR systems is partially compensated by additional cost for software development.

Any range NIR, MIR or LWIR has its drawbacks and benefits, but NIR detection systems offer most attractive commercial solutions, thus any surveillance application should be attempted with NIR technology first. Only if support of fire fighting or detection of hot spots lower than 300°C are definitely required, MIR or LWIR technologies have to be used.

References

[1] R. Braun and H. Weidener, *The Early Detection of Fires in Waste Bunkers using Infrared Thermography: Restrictions and Validation.* VGB Kraftwerktechnik 77 No 12, 1997.

[2] W. von Borries and H. Katzer, *Frühzeitige Erkennung von Brandentwicklungen im Abfallbunker.* VGB Kraftwerktechnik 74 No 10, 1994, p. 873-874.

[3] W.L. Wolfe and G.J. Zissis *The Infrared Handbook.* revised edition, Office of Naval Research Department of the Navy, Arlington VA, 1985.

[4] M. Born and E. Wolf, *Principles of Optics*. 7th edition, Cambridge University Press, Cambridge, 2003.

[5] S.E. Dillon and A. Hamins, *Ignition Propensity and Heat Flux Profiles of Candle Flames for Fir Investigation*. Proceedings of Fire and Materials 8th International Conference, San Francisco, 2003, p. 363-376.

[6] K. Höppner, patent DE 38 12 560 C2, current patent holder m.u.t GmbH, published 1998.

[7] P.J. DiNenno et. al (editors), *The SFPE Handbook of Fire Protection Engineering*. 2nd Edition, Society of Fire Protection Engineers, 1995, p. 2-221.

Meenakshi Gupta*, Ravi Shankar, R K Rajora and J C Kapoor
Centre for Fire, Explosives & Environment Safety (CFEES),
Defence Research and Development Organization (DRDO),
Brig. S K Majumdar Road, Timarpur,
Delhi – 110054, INDIA

Development of Real-Time Signal Acquisition based Fire Detector

Abstract

The dynamic states of temperature and smoke density form most important and crucial signals for fire detection systems. Conventional fire detectors monitor parametric value at a particular moment of time with no reference to the temporal variations. This value if exceeds the preset trigger value, alarm is actuated. This conventional logic does not take into account the dynamic trends of temperature and smoke concentrations and therefore, are highly prone to false alarms. This paper describes the work carried out on development of a dual- sensor fire detector based on dynamic monitoring of temperature and smoke density profiles.

During the development of the detector, two major facilities

- (i) Simulation Facility for Test-fires (SIFT) for generation of unique fire signatures and for evaluating the behaviour of detectors to real fire and non-fire sources, and
- (ii) Smoke Tunnel Test Facility (STTF) for environmental testing and dynamic performance evaluation of detectors, were developed and these are also described in the paper.

Test results on the 20 prototypes carried out in the SIFT and STTF indicate that combining smoke and temperature signatures in an intelligent decision specific detection algorithm not only results in nearly zero level false alarms, but also enhances the sensitivity of detector to real fires and improves the response time to a few seconds. The detector gives correct and rapid alarms for both smoldering (response time 130-150 sec) and open flaming fires (response time - 15 to 30 sec). The paper also describes the test methods on these detectors and discusses the results.

Development of Real-Time Signal Acquisition based Fire Detector

1.0 Introduction

Most commonly used current generation of fire detection systems are based on measurement of smoke, heat or the electromagnetic radiations generated during the smoldering or flaming combustion. These systems operate on fixed threshold i.e. they monitor a parametric value at a moment of time with no reference to the signal history . This momentary value is compared to a preset trigger value, which if exceeded, actuates the alarm. This conventional logic does not take into account the dynamic trends of temperature and smoke and therefore, are prone to false alarms. In fact, the dynamic states of temperature and smoke density are important parameters conveying crucial information to fire detection systems. Advancement in microelectronics, sensors and signal processing in recent years has enabled the monitoring of dynamic trends of the smoke and temperature with a response time of few milliseconds and very high accuracy. This has resulted in significant improvements in fire detection system performance especially on two counts (i) to identify the fire in its early stage and (ii) very low false alarm frequency.

At Centre for Fire, Explosives & Environment Safety , a project was taken up to develop a fire detection system based on dynamic monitoring of temperature and smoke optical density. The main goal is to provide faster response to real fire threats while providing better nuisance alarm immunity compared to conventional heat or smoke detectors. This has been accomplished by combining milli-second responses from highly sensitive laser based smoke optical density sensor and temperature sensor in a decision specific algorithm which utilizes a unique fire/non-fire signature database and also some prediction logic based on the observed signal pattern. The software logic takes care of the ongoing temporal changes in the dynamic behaviour of its respective sensor and data trends which indicate possible fire situations, i.e. rapid increase or continued rise in smoke or temperature slope.

The overall experimental work plan involved the design, development and testing of a detector prototype combining smoke optical density / temperature sensing mechanisms; design and development of a facility for generation of unique fire signatures for incipient fire and nuisance sources; design and development of fire detection alarm algorithm and testing of the response of the fire detectors to fire and non-fire sources;

and design and development of Smoke Tunnel Test Facility as per BS-5445 standards for the testing and evaluation of the performance of the detector under dynamic conditions.

The developed fire detector gives correct and rapid alarms for both smoldering (response time 130-150 sec) and open flaming fires (response time - 15 to 30 sec). These advanced and accurate detectors are highly suitable for (i) critical applications where response time and accuracy of the response are highly critical like shipboard applications, telecommunication facilities, airport, mutiplexes etc., and (ii) hostile applications where conventional detectors are a failure viz. , warehouses, chemical plants, paint industries, cement industries etc.

2.0 Development of Fire Detector:

Combination of smoke sensor and a temperature sensor results in the best combination for giving good response to a wide range of fires. The fire detector employs smoke optical density measurement and heat development measurement in a single housing and the analog signals generated are constantly monitored by a microcontroller based electronics unit. The signals from the two sensors are acquired by the processor (personal computer) and further processed by the specific software program to arrive at a decision of fire or no-fire condition. This signal processing and fire detection algorithm compares these signals with the database of fire signatures generated by wide range of experiments performed on a range of fire and non-fire conditions and stored into the computer in the form of correlations database.

2.1 The Detector Design:

In the design of the sensor head, rate of increase of smoke measurement was combined with rate of temperature to cover a wider range of fires. This also enabled the defining of fire signatures in a more comprehensive and effective manner because the smoke and temperature are the most important of the several parameters that indicate the growth of fire.

For smoke detection, the principle of light extinction by smoke particulate was utilized. To optimize light extinction measurement sensitivity, a monochromatic source of light i.e. a laser diode (center wave length of 650nm) has been used and, the path length

through the smoke was increased by multiple reflections inside the sensor head as shown in **Fig 1**.

Light attenuation caused by smoke particulates is measured as analog output of the photodiode which is continuously monitored by the microcontroller of the control module. The optical density is calculated using Lambert-Beer's law [10] which can be simplified as follows:

$$m = \frac{10}{d} \log_{10} \frac{I_0}{I}$$

where I_0 = Initial intensity of light

I = Intensity of light after it passes through smoke

d = path length of light through smoke

m = measure of light attenuation or smoke optical density in dB/m

Measurement of rate of temperature rise is carried out using an appropriate temp sensor (AD 590) inserted in the entry of smoke such that it does not obstruct the laser beam. Temperature sensor AD 590 has a linear output over a wide operating range, 0 - 155°C, in terms of current and has high sensitivity of 1μA/°K.

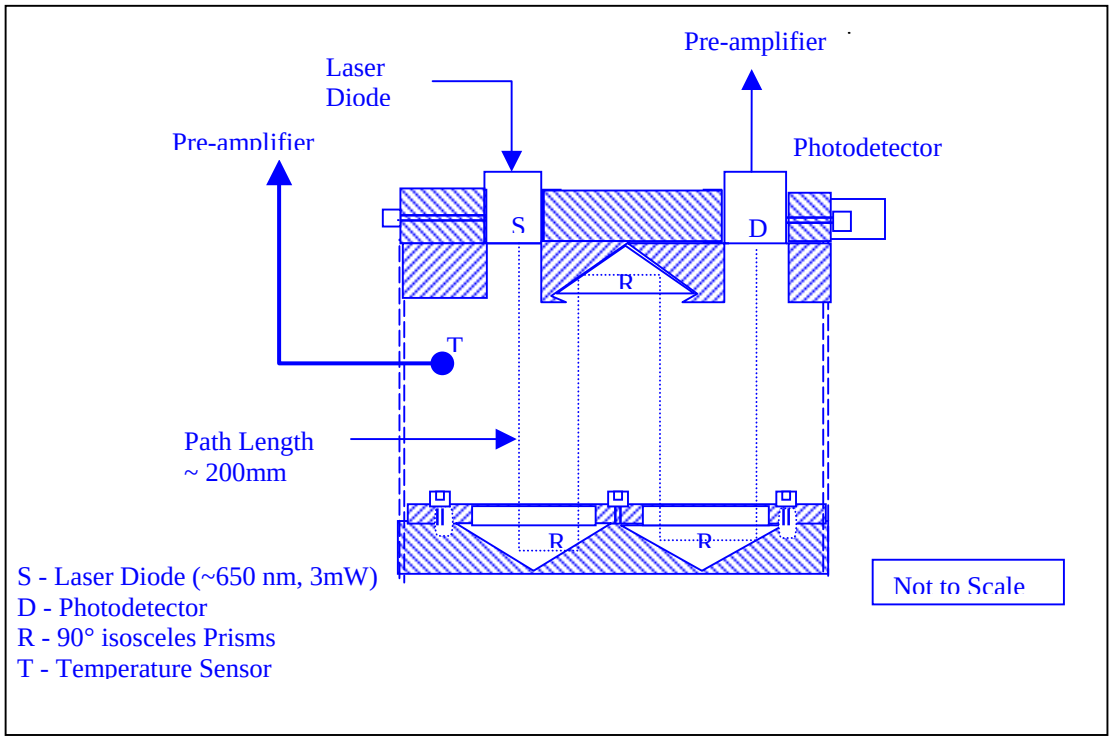

Fig. 1 Fire Detector Prototype – schematic diagram

The prototype fire detection system mainly consists of two types of modules – detector modules and control module. Four nos. of detector modules are connected to one main control module via RS-485 interface and the main control module is interfaced to the computer via RS-232 interface. **Fig 2** gives the schematic block diagram of the fire detector units with the control unit. A shielded twisted pair of cables with wire conductor of dia 1.00 mm (multi-stranded) is used to connect the detector modules with the main control unit.

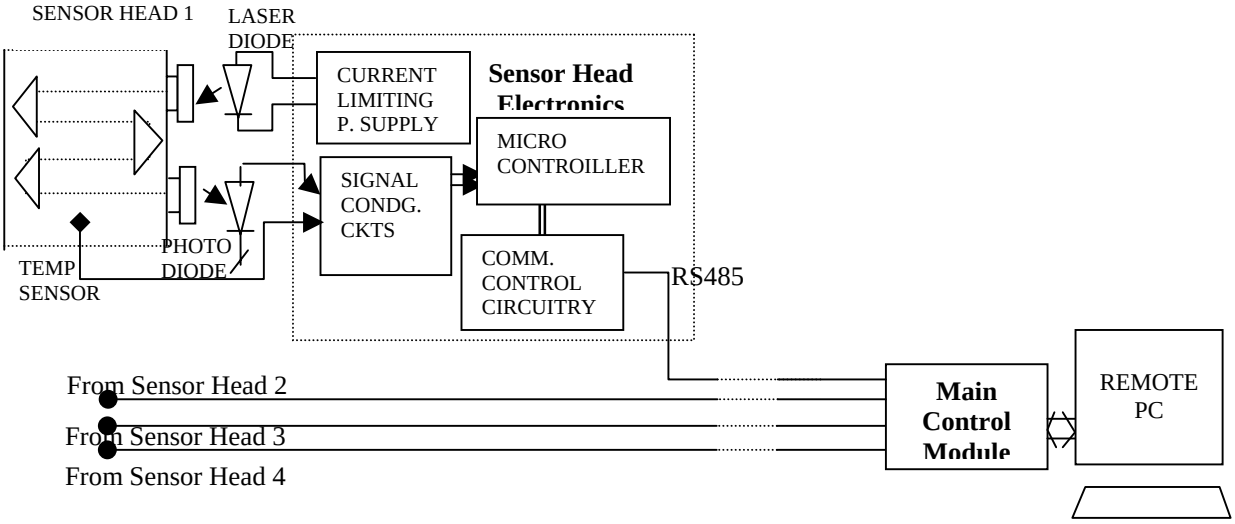

Fig. 2 Schematic arrangement of the fire detection prototype system

2.3 Fire Alarm Detection Algorithm

The key to reliable fire detection is the fire detection algorithm, which effectively combines the smoke optical density output with that of heat development such that nuisance alarms are eliminated and detector sensitivity to real fires is subsequently improved over current smoke/heat detectors. Decision making algorithm is tested experimentally along with the sensor prototype by exposing to a range of fire sources, from smouldering cotton wicks, poly-urethane foam and flaming n-heptane to cooking fumes and cigarette smoke.

Reading from the sensors are acquired every 500 ms. Fire decision loop performs statistical analysis on the data received for 2 sec and extends it upto 10 sec. This involves analysis of the sensors' signals for a typical growth pattern similar to that observed for a real fire condition. This growth pattern of smoke opacity and temperature

is defined as unique fire signature and is utilized by the analysis software for differentiating a real fire condition from nuisance condition. . **Fire alarm** condition is prefixed with two pre-alarm signals – **Alert** and **Pre-alarm** to provide confirmed decision on a real fire condition. A set of rules have also been employed in the detection algorithm for example, averaging of data for very weak or slow growing fires upto 30 sec and setting a threshold of this averaged value to give the first level of alarm. Two next level of alarm conditions, Pre-alarm and Fire alarm are given when the increasing trend of the smoke OD signal or temp rise signals continues.

Short and long term variations in the ambient temperature, RH and dust concentrations, which define the background noise are accounted for, in the software by initializing the threshold reference of these parameters every one hour.

The software also generates diagnostic information – environmental and internal and provides pre-emptive alarms that indicate the sensors or associated components getting close to critical condition before an actual failure occurs. The program also keeps a record of the sensors' history information such as hours of operation, day and time of installation, environmental conditions during installation etc.

2.4 Generation of unique fire and non-fire signatures

Unique fire signatures defined by regression slope of the growth profile of smoke optical density and temperature, forms the firm basis for differentiating a real fire condition from the nuisance condition. Reliability of the fire detectors in terms of nuisance signal rejection is thus enhanced greatly. Fire signatures generated for the followingtest fires as specified in the EN-54 standards -

TF1 - Open cellulosic fire (wood)

TF2 - Smoldering pyrolysis fire (wood)

TF3 - Glowing Smoldering fire (cotton)

TF4 - Open plastic fire (Polyurethane)

TF5 - Liquid fire (n-heptane)

TF6 - Liquid fire (methylated spirit)

These test sources were selected as they encompass the hazards due to many expected threats. Experiments were performed in a Simulation Facility for Test-Fires (SIFT) developed in-house to study the development profiles for temperature and smoke

along with the smoke particle size distribution, smoke emission factor and rate of fuel loss in the early stages of fire.

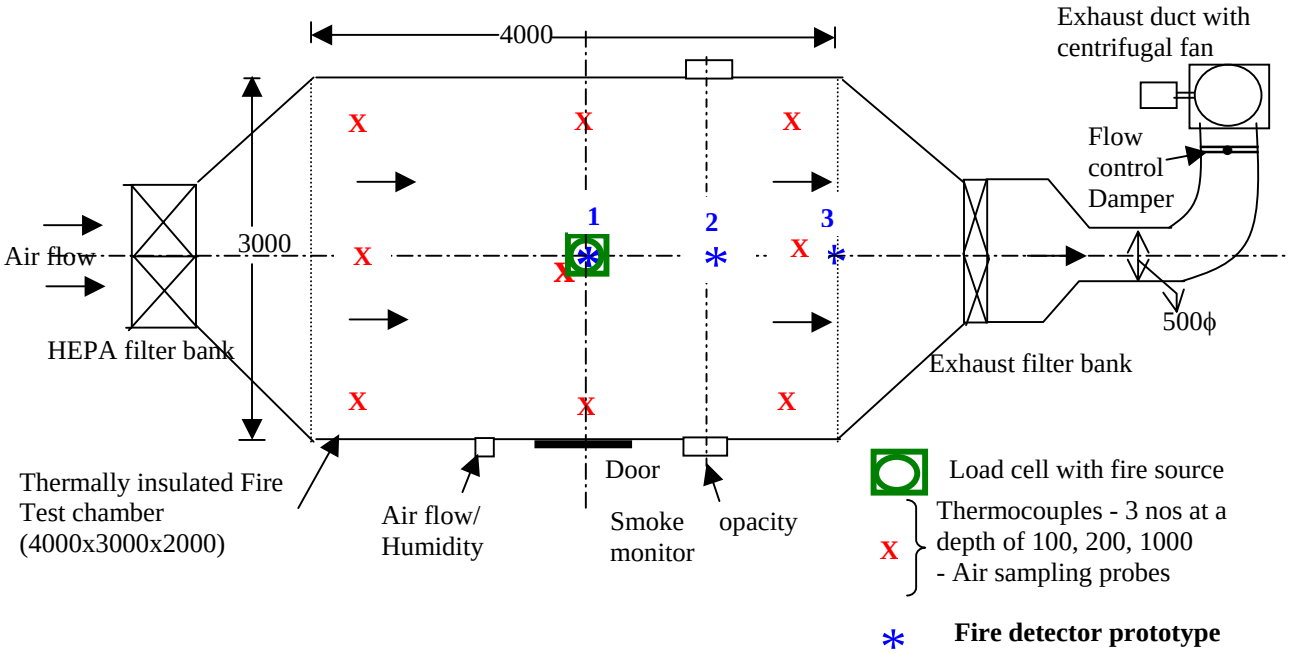

Fig 4.0 - Experimental setup plan

SIFT consists of a thermally insulated test chamber of approx. 25 m^3 volume (4m x 3m x2m) with various instruments for control, monitoring and recording of parameters during the fire test. The details of the experimental set-up are shown in the fig 4.0. One side of the test chamber is fitted with HEPA filter bank assembly and the opposite side is connected to a duct head (500mm dia) via an induced draft fan with damper control. The draft fan serves the purpose of exhausting the test chamber of any smoke or other particulates and also for maintaining a constant air flow in the chamber (0.01 to 0.2m/s). A number of thermocouple probes to measure the temporal as well as spatial profiles of temperature and a smoke opacity monitor to record the spatially averaged smoke opacity have also been installed in the test chamber. Samples of the smoke from the chamber are also drawn for the analysis of particle size distribution and various gaseous components like CO, CO_2, total HC and NOx. The fuel was placed in the center of the test chamber on the load cell of a dynamic weighing balance for recording the fuel loss every second. The fire detector prototypes were mounted at the ceiling on the top of the

fire source, at distance of 1 m and 2m away from the centre line. The access door to the test compartment, which is located in the front wall, remains closed during all tests.

Series of tests were conducted with various types of test sources in natural ventilation as well as in forced ventilation (0.1m/s). The tests were divided in two series, the real fire sources and nuisance sources. Real fire sources include smouldering cotton wicks, polyurethane foam and flaming liquids like methylated sprit and n-heptane (first column of Table I), and nuisance sources were cigarette smoke and smouldering incense sticks.

2.5 Results and analysis of growth characteristic of Test- fires

Experiments were carried out to generate unique fire signatures for all standard fire sources as per EN54. On the basis of the results obtained a software logic which yields high response – time performance of the detectors with very high reliability in terms of nuisance signal rejection was developed. Development of final alarm algorithm necessitated carrying out extensive experimental work with the test fires and nuisance sources to establish the criteria.

Smouldering cotton wicks corresponds to a smoke generating source with virtually no development of heat and slow rise of smoke to the ceiling. Flaming liquids like n-heptane and methylated spirit are fire sources with very fast heat development. In case of n-heptane pool fire, fast heat release is accompanied with very high and fast smoke development causing considerable change in smoke optical density. Flaming PU-foam generates both smoke and heat with lower development rate than flaming n-heptane. In all test cases, known amount of test fuel normalized to the size of SIFT chamber was burnt to monitor the enhanced response of the detectors during initial burning conditions. The smaller size of the test sources ensures comparatively slow rise of smoke and temperature signatures as observed in the early stages of actual fire and also maintain experimentation time to the minimum. Non-fire sources were taken as cigarette smoke and smouldering incense sticks.

Response of the detector as observed for various test fire and non-fire sources at 3 different locations varied from quick, 10 sec (when 100 ml flaming n-heptane in a tray of dimensions 10” x 18” was just below one of the detector prototype) to a slowest, 300 sec when smoldering cotton wicks source was kept 2 m away from the centre line of the detector prototype. The response time was measured from the moment of ignition of the

fuel. It includes the delay involved in the smoke travel to the detector location. The detector prototype does not respond at all to the agarbatti smoke and cigarette smoke even when the sources were kept just below the detector.

Results of average response time for various test conditions along with the coefficient of regression obtained is summarized in **Table 1**.

Table 1 Summary of detector prototype's response-time performance for various test sources

S. No.	Test source	Test Quantity	Detector Location (refer fig 3.0)	Coeff of Regression		Avg. Res. Time (Sec.)
				Smoke OD	Temp.	
1	n-heptane	100 ml	# 1 # 2 #3	0.1-0.12 0.08 – 0.1 0.05 – 0.06	1.8 – 2.0 1.6-1.7 1.5-1.6	6-15 18-25 25-38
2	Methylated Spirit	100 ml	#1 #2 #3	0.001 0 0	1.2 1.15 1.10 – 1.15	30-40 45-55 58-65
3	PU foam	~50 gm	#1 #2 #3	0.008–0.012 0.004-0.006 0.002-0.004	0.05-0.06 0.05 0.04	45-65 128-135 230-250
4	Cotton wicks (dia - 6 mm)	~100 nos.	#1 #2 #3	0.008 – 0.01 0.004-0.006 0.002-0.004	0 0 0	55-72 150-170 280-300
5	Cigarette Smoke	2 nos. continuously smoked	#1 #2	0.001 0	0	No alarm
6	Smoldering Incense Sticks	Bunch of 10 nos.	#1 #2	0.002 0	0	No alarm

Analysis of the test results shows that the response of the detectors is very much dependent upon the rate of change in the smoke optical density and temperature at the detector location. So, farther the source from the detector, larger will be the response time of the detector. The added sensor for detection of the temperature rise gives an advantage for the detection of all types of fires – smouldering or flaming - with high response time and accuracy. For the test cases where heat development is also

accompanied with the significant smoke emissions as in n-heptane and PU-foam, detection of rate of rise in smoke optical density (OD) was faster than the detection of rise in temperature and significant change in smoke OD factor initiates the alarm condition. The coverage of the detector can be calculated on the basis of the required response time or the critical nature of the protected area.

The elimination of false signals for cigarette smoke or incense stick smoke have been achieved using the detection logic, which monitors and detects a steady rise of the smoke optical density or temperature rise.

3.0 Performance Evaluation of Detectors as per EN-54 / BS-5445 Standards:

The fire detectors are required to be subjected to various basic and environmental tests to ensure their capability both for normal service and for probable exceptional conditions. The European standard series (EN-54 or BS-5445) specifies requirements, test methods and performance criteria for point-type fire detectors that operate using temperature rise or smoke detection using scattered light, transmitted light, or ionization (part 7) and for temperature detectors (part 5) but there are no specifications for testing the dual mode detectors. Therefore, to carry out the performance of the dual mode fire detectors, new test regime was developed by combining the requirements of the two tests . For this purpose, a modified smoke tunnel system has been designed and developed to specially fulfill the requirements of EN-54 or BS 5445 standards. This smoke tunnel incorporates provisions for evaluation of the basic characteristics of the fire detector such as (i) production homogeneity (similarity of response threshold), (ii) operational ability and reliability under normal service conditions, (iii) repeatability, (iv) immunity against environmental effects, and (v) durability in service.

In evaluating all the above characteristics, the quantitative criterion used is the variation of the response threshold value of smoke density and temperature rise rate within a specified limit, except for the immunity against false alarms. This threshold value may vary within the set of the test unit or it may change due to an environmental exposure on a single detector.

Fig 5 shows the photographic view of the Smoke Tunnel Test Facility (STTF) for measuring the response threshold values and evaluation of performance of dual mode fire detectors. The smoke tunnel is a thermally insulated duct having dimensions of

500mm Iϕ x 1200mm of total length, made of Stainless steel. The tunnel comprises of unit for generating, controlling and measuring the air flow in the duct, heater unit for controlling the air temperature, pressurized air operated aerosol generator for producing artificial smoke, detector test chamber and necessary instrumentation for the smoke density, number concentration and temperature measurements.

The important characteristics of the smoke tunnel facility are as follows :

(i) Test aerosols are introduced such that in the measuring section, a homogeneous dispersion of aerosol density is obtained over the cross-section.

(ii) The smoke tunnel is capable of generating averaged air velocities between 0.1m/s and 10m/s.

(iii) The air temperature in the wind tunnel can be raised from 20°C to 60°C at a rate of ≤ 1°C/min.

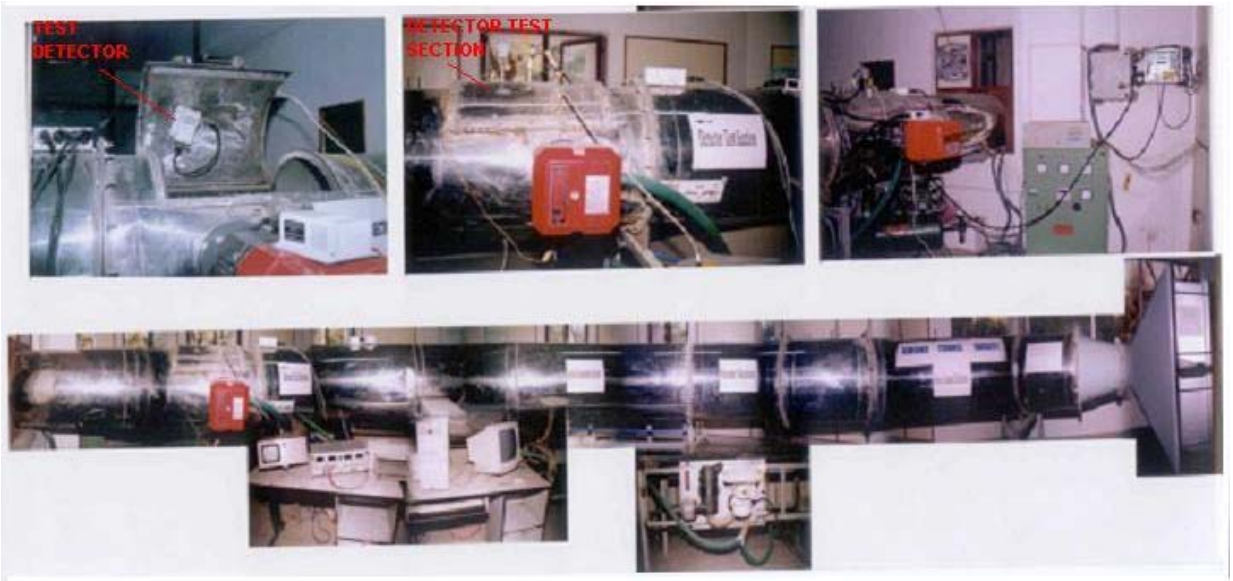

Fig 5 SMOKE TUNNEL TEST FACILITY

The present smoke tunnel system is an open loop system where the measuring zone receives the fresh stabilized aerosols at each time and thus minimizing the problems associated with agglomeration and aging of the aerosol as encountered in the closed loop tunnel system.

3.1 Test Method

The detector under test is installed in the smoke tunnel's detector test section with fastenings provided for this purpose. The detector is connected to its control module kept outside the tunnel. The fire alarm detection software loaded on the computer is executed and the dynamic response of the detector to the aerosol concentration and the temperature variations is continuously monitored.

The response of the detector is monitored for 20-30 min for stabilizing its output before commencing the test experiments by varying temperature; smoke aerosol concentration or air flow. Air velocity in the proximity of the detector is 0.1 – 0.2 m/s for all the tests unless a different value is explicitly indicated. Air temperature in the wind tunnel is 23 ± 5° (normally ambient), unless a different value is expressly indicated, e.g. in the high ambient temperature test.

Before commencing each measurement, it has been ensured that the smoke tunnel and the detector being tested are free from any aerosols by running the induced draft fan for atleast 15 min. Test aerosol is fed into the tunnel at a rate such that rate of change of smoke optical density, $\Delta m/\Delta t$ in the test chamber, is less than 0.2 dB/m per min.

Initially selected rate of increase in aerosol density is kept similar for all measurements in the smoke tunnel. Poly-dispersive aerosol generated using pneumatically operated nebulizers operating at 1 –2 bar, has been used as the test aerosol. The maximum of its particle size distribution is between 0.1 to 1 μm under these conditions and is very much similar to that for smouldering cotton wicks smoke (**Fig 6.0**). The liquid paraffin oil of density ~ 0.845 ± 0.015 gm/cc, kinematic viscosity – 30 cS was used for generating mists.

Air temperature in the tunnel is raised from 20°C to 50 °C at a rate <1°C/min. Value **m** (smoke optical density) from smoke optical density monitor and temperature as indicated by various thermocouples inserted in the test detector zone is recorded, at the moment of recording the response.

For the verification of the response threshold of the detector, the response profiles of the test detector is compared with that of reference detector in the clean air, before and after each test. If there is a discrepancy of more than 0.02 dB/m between the two, the measurements are repeated.

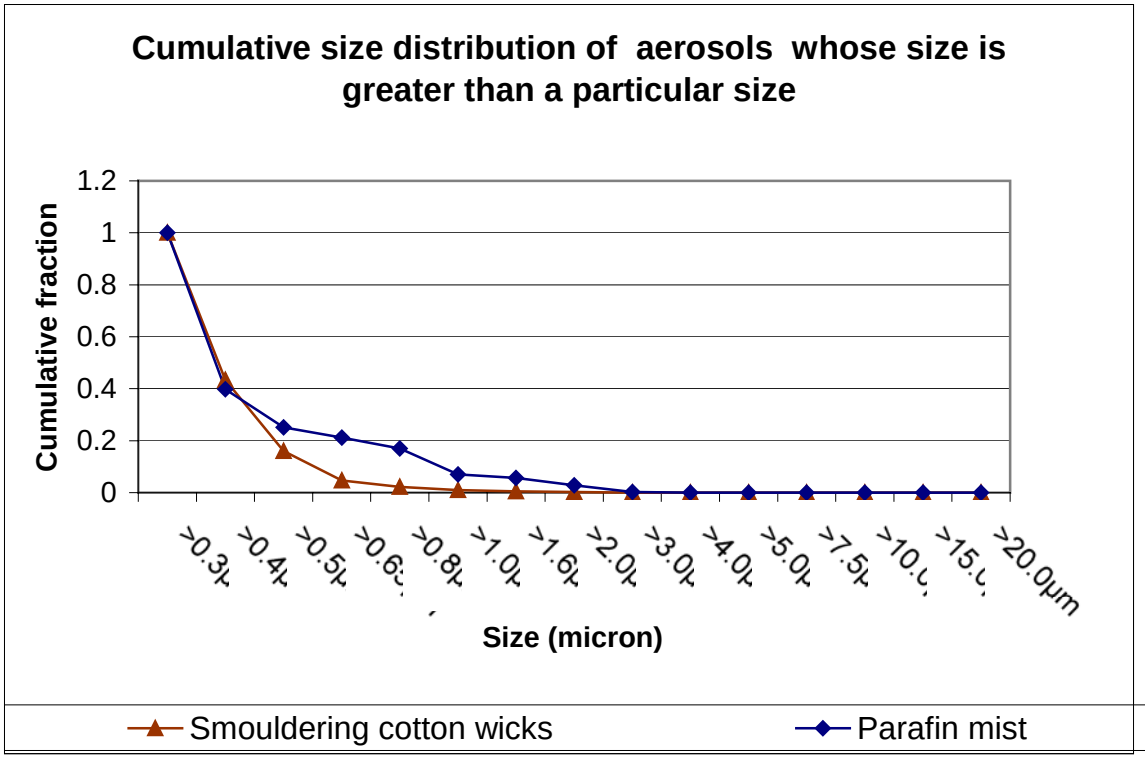

Fig 6.0 Cumulative size distribution of smouldering cotton wicks smoke aerosols and aerosols generated using paraffin mist as measured by GRIMM aerosol monitor model 1.108

3.2 Result and analysis

Table - 2 gives the details of the tests carried out on the detector prototypes in the Smoke Tunnel Test Facility and their output results.

The results of the tests carried out in the smoke tunnel facility show that the threshold of the detection lies at 0.1 ± 0.02 dB/m. This has been tested and verified for all the tests as listed in the **Table –2**. The response accuracy can be improved further using a high bit resolution analog to digital conversion in the sensor heads.

Tests carried out on 20 prototypes developed in the SIFT and STTF indicate that combining smoke and temperature signatures in an intelligent decision specific detection algorithm not only results in false alarm level approaching zero, but also enhances the sensitivity of detector to real fires and improves the response time to a few seconds. The detector gives correct and rapid alarms for both open flaming fires (response time - 15 to 30 sec) and smoldering (response time 130-150 sec)

Table 2 : Details of tests carried out in Smoke Tunnel Test Facility

Sl.no.	Test	No. of Detector Prototypes tested	Test freq.	Remarks
1.	Switch-on test	2	10 10	Variation within - 0.02 dB/m and +0.04 dB/m
2.	Variation in Supply Voltage Test	1	2	Variation within - 0.02 dB/m and +0.04 dB/m
3.	High Ambient Temperature Test	1	10	Variation within - 0.02 dB/m and +0.04 dB/m
4.	Repeatability	2	10	Variation within - 0.02 dB/m and +0.04 dB/m
5.	Reproducibility	4	5	Variation within - 0.02 dB/m and +0.04 dB/m
6.	Directional Dependence (8 directions of air vel.)	2	5	Variation within - 0.02 dB/m and +0.04 dB/m
7.	Test for sensitivity to air movement : (i) Response behaviour (ii) False Alarm behaviour	2	10	Response time increased with increased airflow in No False Alarm
8.	Test for sensitivity to Smoke puff	2	30	First level alarm observed for few cases, not confirmed by the 2nd and final alarm level
9.	Drop Test	1	1	Variation within - 0.02 dB/m and +0.04 dB/m

4.0 Conclusion:

The intelligent fire detector developed and discussed in this paper has demonstrated high reliability and better response – time performances as an added advantage over the conventional detectors as it is based on the rate of growth of two fire parameters (smoke and temperature) and not on threshold values as in conventional detectors. Use of the online comparison of signatures for various kinds of fires and non-fire stimuli with actual real time signal provides reliable basis for differentiating fire and non-fire phenomena. This, combined with the smoke and temperature signatures in specific alarm detection algorithm reduces the false alarms to nearly zero and response time to few tens of seconds.

The intelligent fire detector prototype developed is associated with electronics and digital signal processing techniques to provide better signal to noise ratio and eliminate EMI interferences, environmental effects and log term drifts. Fire detection based on intelligent algorithm also includes diagnostic information for both environmental and internal drifts- may provide preemptive alarms that indicate a part of the system is getting close to a critical condition before an actual failure occurs. This intelligence helps avert costly system downtime.

Detector prototypes developed are immune to background conditions and thus are suitable for any type of application environment, whether it is a chemical lab, process plant or a clean sophisticated installations.

Our future research work is focused on addition of third dimension to the fire detection by incorporating a carbon monoxide sensor in the same detector and utilizing the pattern recognition and neural logic to further increase the discrimination between real fire situations from non-fire conditions for achieving ZERO false alarm frequency with better response time performance.

5.0 References:

(i). Antti I. Ahonen and Pauli A. Sysio, " A wind tunnel system for testing of smoke detectors", Research report, Technical Research Centre of Finland, 1983

(ii). Ahonen, Antti I., Sysio, Pauli A. , " A run-in test series of a smoke test room", Technical Research Centre of Finland, 1983

(iii). Blake D. et al. , " Aircraft Cargo Area Fire Detection", Brief comments of a meeting held among officials of Federal Aviation Administration, British Airways, Boeing Company headed by Thomas Cleary of NIST and david Blake of FAA.

(iv). Conforti F., "Multi-sensor, multi Criterion detectors are better", AUBE '99 – Proceedings of the 11th International Conference on Automatic Fire Detcetion, 1999

(v). Daniel T. Gottuk et al., "Advanced fire detection using multi-signature alarm algoritms" Fire Safety Journal 37, 2002

(vi). EN 54/ BS 5445: Components of Automatic Fire Detection Systems; Part 1. Introduction, European Committee for Standardisation, April 1988.

(vii). EN 54/ BS 5445: Components of Automatic Fire Detection Systems; Part 5, Heat sensitive detectors - point detectors containing a static element , European Committee for Standardisation, April 1988.

(viii). EN 54/ BS 5445: Components of Automatic Fire Detection Systems; Part 7. Point-type smoke detectors; Detectors using scattered light, transmitted light or ionization, European Committee for Standardisation, April 1988.

(ix). EN 54/ BS 5445: Components of Automatic Fire Detection Systems; Part 9. Fire Sensitivity test, European Committee for Standardisation, July 1982

(x). Grosshandler, William L. , "A Review of Measurements and candidate signatures for early fire detection", 1995

(xi). Grosshandler, William L. . "An Assessment of Technologies for advanced fire detection", 1992

(xii). Heskestad G, Newman JS. "Fire detection using cross-correlations of sensor signals", Fire Safety Journal, 1992; 18(4): 355-374.

(xiii). Ishii H, Ono T, Yamauchi Y, Ohtani S.. "An algorithm for improving the reliability of detection with processing of multiple sensors' signal" Fire Safety Journal 1991;17; 469-84

(xiv). Kuo H. C., Chang H.K., "A real-time shipboard fire detection system based on grey-fuzzy algorithms", Fire Safety Journal 38, 2003

(xv). Letian W, Cheghua Z, Wag J. "A new type of intelligent point photoelectric smoke-heat combined fire detector". AUBE '99 – Proceedings of the 11th International Conference on Automatic Fire Detection, 1999.

(xvi). Milke JA, McAvoy Tj. "Analysis of signature patterns for discriminating fire detection". Fire Technology 1995

(xvii). Mulholland, George W., "Smoke production and properties", SFPE Handbook for fire protection engineering 2nd Ed. NFPA, Quincy, Mass. 1995

(xviii). Pfister G. , "Multisensor/multicriteria fire detection: a new trend rapidly becomes state of the art". Fire Technology, Second Quarter 1997

(xix). Richard W. Bukowski and Paul A. Reneke, "New approaches to the interpretation of signals from fire sensors", Building and Fire Research Laboratory, NIST, Gaithersburg, MD, USA, May 1996

(xx). Ronald K. Mengel, "Industry advances in fire detection technology", Pittwat Systems Technology Group, 2002

(xxi). Liu Z., Kim A. K., "Review of recent developments in fire detection technologies", Journal of Fire Protection Engg. V-13, No.2, May, 2003

(xxii). William C. Hinds, "Aerosol Technology - Properties, behaviour and measurement of airborne particles", John Wiley & Sons, Inc.

Thorsten Schultze, Ingolf Willms
University Duisburg-Essen, Campus Duisburg, Germany

Smoke and dust monitoring by a microscope video sensor

Abstract

Fire detection on the basis of an analysis of video sequences is an upcoming technology and is used in a growing number of applications. There are several success factors for this development. One of the reasons is the availability of sufficient and modestly cheap computing power in the form of PC's or special cards using DSP chips for video signal processing. Still a fire alarm installation with video cameras can only be cost effective in applications where conventional fire detectors are facing severe problems such as in large or high halls.

But the application of video analysis is used in many other areas apart from video surveillance of large areas or large volumes. One example is the video analysis of colloidal solutions for the determination of water quality. In this application video sequences showing a small illuminated volume are automatically analysed.
In the paper it will be discussed in which way a video camera might be used for the characterisation of aerosols with an application in fire detection.

Introduction

Video based fire detection is an upcoming technology, mostly used for the surveillance of large areas or volumes, or areas were cameras already are installed. Different methods for the detection of flames and smoke are known, basing on various principles like image contrast changes, colour distribution or fire dynamics. Video technology also finds application in process automation, e.g. monitoring of chemical processes by analysing suspensions or by measuring flow velocity fields with the PIV (Particle Image Velocimetry) technique. Industrial solutions for the micro-optical waste water analysis, filter control or the PIV are available.
This study tries to combine fire detection with the micro-optical video analysis. Not

only static characteristics but also the dynamic behavior of fire products and tests aerosols shall be recorded and evaluated, providing information for the discrimination between fire and non-fire scenarios. The first step of the project was the design of an appropriate measuring system for the data acquisition, which was installed directly under the ceiling of a compartment with fire.

The prototype setup basically consists of a system of lenses (or a microscope for extra high magnification) equipped with a camera connected to a processor unit, where the image processing takes place. Different from most industrial systems not the usually implemented extinction microscopy is applied, but the backscattering microscopy. This technique allows a greater distance between the analysed volume and the microscope lens, minimising the influences of the measuring system on the measured volume. Further on, future fire detectors based on such a technique could be mounted directly on the ceiling, although the measurement takes place some centimeters below.

Experimental setup

The experimental setup consists of a microscope equipped with a high sensitive CCD camera connected to a PC. For the first experiments a miniaturised experimental setup has been chosen, in order to maintain the system flexible for changes. The aerosol-generator and the light source are in-vitro, assuring a controllable aerosol distribution and flow characteristics. The aerosol is suspended in air using a fan. Fire products are created with a small wood bar wrapped with a resistance wire (2 W power). In the next figure 1 the experimental setup is shown.

Two different light sources have been used for the analyses. One high-power (5 W power) LED with a special optic for the optimal illumination of the measured volume, due to the high optical losses in the microscope. Another reason for the choice of a high-energy LED is the fact that high flow velocities imply short exposure times. As the light sensitivity of the CCD chip is a constant, the quantity of light has to be increased to drive the sensor. The second light source is a gas lamp (flash lamp). This lamp unifies both needed characteristics, high energy and short flash period. This light

source is however not appropriate for video sequences, as the time period between two flashes is too long for the motion analysis.

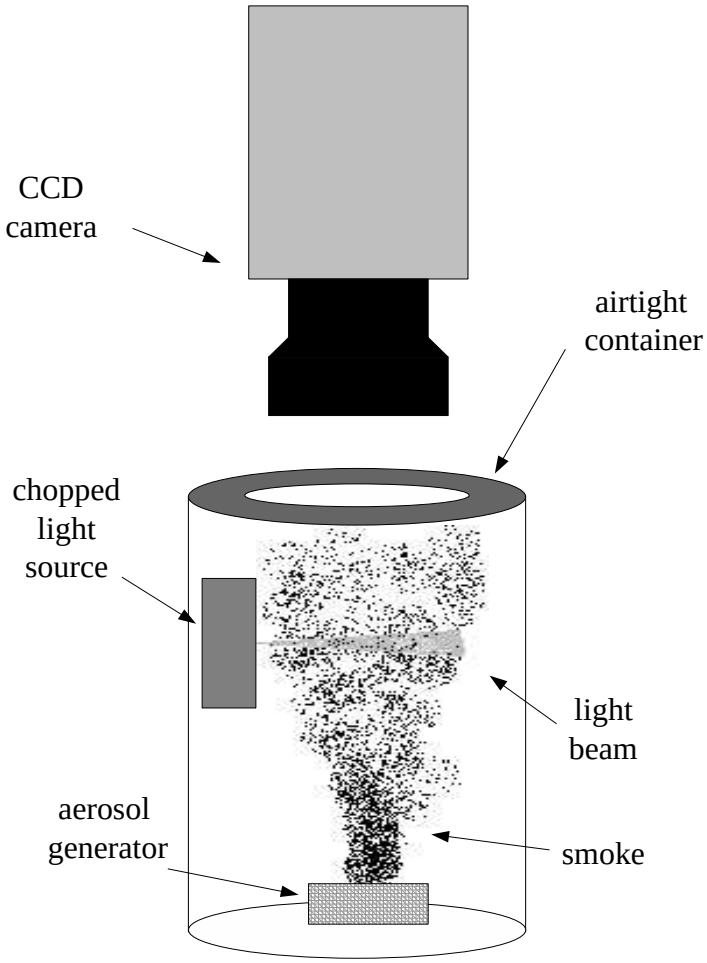

Figure 1: The experimental setup

First results

The next three figures show snapshots from experiments done in-vitro. Smoke from a small smouldering wood bar, as well as two different dust types, i.e. ISO 12103-1-A2 of the type fine and ultra-fine, were recorded through a microscope.

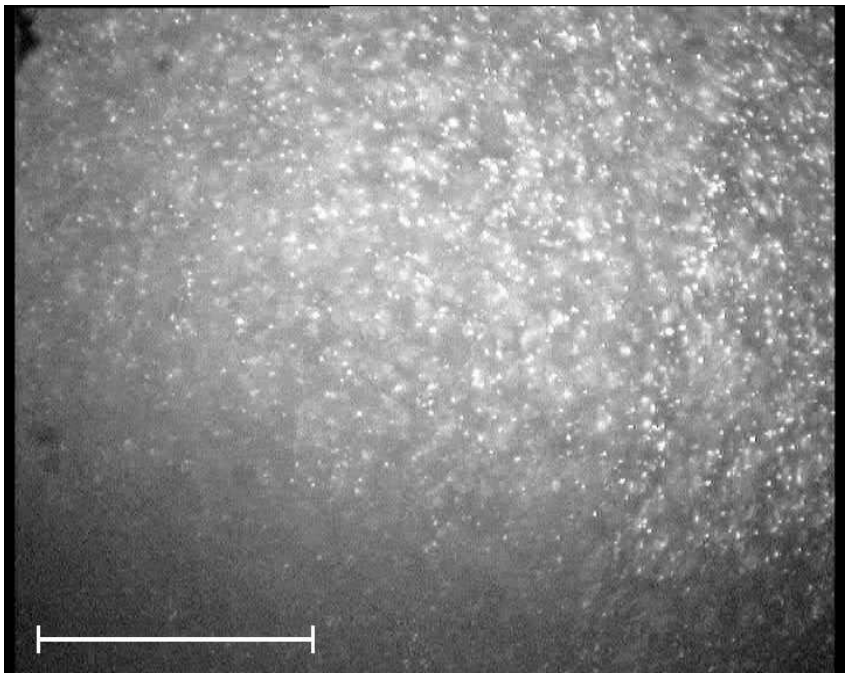

Figure 2: Snapshot of smoke, in-vitro

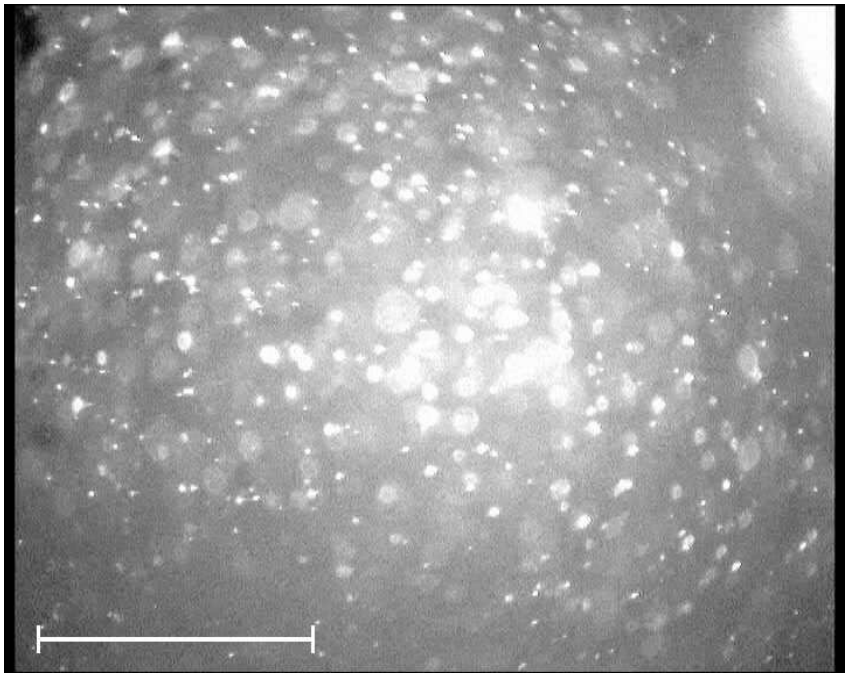

Figure 3: Snapshot of ultra-fine dust type, in-vitro

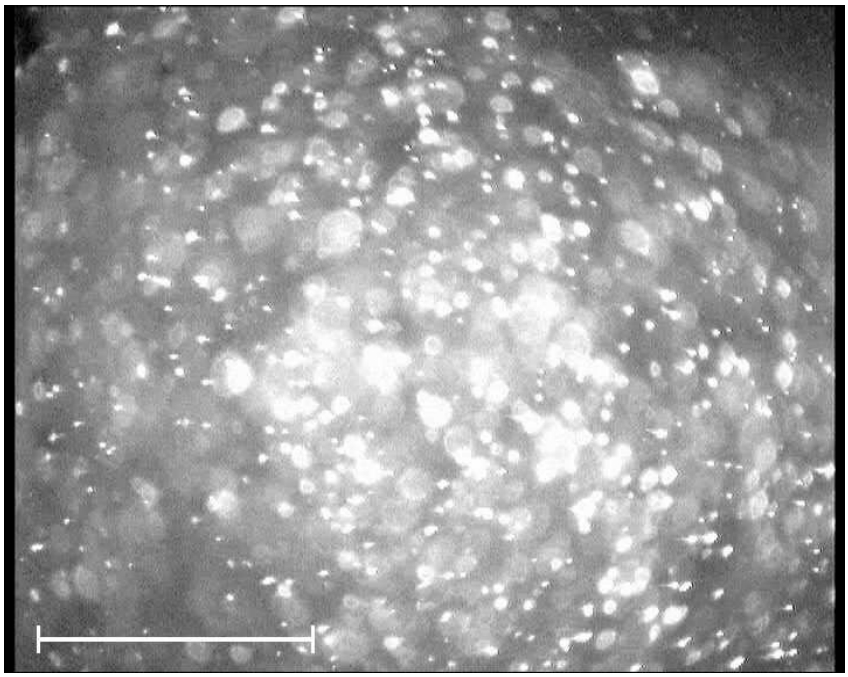

Figure 4: Snapshot of fine dust type, in-vitro

The illumination was carried out by a gas lamp with a power of about 2 Ws, located at the right-hand side of the pictures. Due to the short and bright light flash of the lamp, it was possible to record the images with minimal motion blur. The white dash at the bottom of the left side of the figures correspond to 1 mm.

Figure 2 shows smoke and it is interesting to note that many small spots have been recorded. Their nature has not been determined till now, however it is probable that figure 2 shows water droplets arising from the smouldering wood stick. Greater areas with less brightness fill the background of the picture. These areas arise from smaller particles and unsharp reflections from other particles, as the illuminated area is thicker than the depth of focus of the camera.

For fire detection it is important to compare these results with typical non-fire scenarios, recorded under the same conditions. Therefore snapshots with two standardised dust types have been recorded. In figure 3 the ultra-fine ISO dust type and in the figure 4 the dust of type fine was used.

Comparing these two figures with the figure 2 it is eye-catching that the size distribution of the dots is different. In the two dust figures also small dots can be seen, however the number of bigger sized spots is considerably larger than in the image showing smoke. As expected, it is possible to distinguish between both dust types by analysing the results. In figure 4 (fine dust type) the size distribution of the dots is shifted towards greater values, compared to figure 3 (ultra-fine dust type). By this analysis it is therefore possible to draw conclusions about the particle size distribution of the measured aerosol.

As the in-vitro analyses showed convincing results, first tests under real conditions have been performed in the fire detection laboratory, but without using a microscope. A camera with magnifying lens was fixed on the ceiling and perpendicular to it a high-power LED has been installed to illuminate the measured area. Under normal conditions, i.e. no smoke or dust, only sporadic dots are to be seen. For the analyses the test-fire TF3 of the EN54 Part 9 (a cotton wick smoldering fire) and the described dust types have been evaluated. The results show that the air turbulences and the flow velocities increase significantly. However the same characteristics as documented in figures 2 to 4 can be observed, allowing therefore a good discrimination between fire and non-fire scenarios.

Conclusion and Outlook

The results show that it is probably possible to distinguish between fire and non-fire scenarios by the analysis of the air under the ceiling using a video camera. For the design of a fire detector based on this concept, it is however necessary to make further tests with different types of fire and non-fire scenarios. The next steps will comprise to improve the hardware and the computer-aided evaluation of the recordings.

References

[1] Lourenco, L. et al *Proceedings of the International Conference in Applications of Lasers to Fluid Mechanics*, TRUE Resolution PIV: A Mesh-free Second Order Accurate Algorithm, Lisbon, 2000

[2] Raffel, M., Willert, C., Kompenhans, J. *Particle Image Velocimetry. A Practical Guide.*: Springer, 1998

[3] Törnblom, Olle *Introduction course in particle image velocimetry* [El. doc.], 2004

[4] Ulaby, F. et al *Microwave remote sensing. Active and passive.*: Addison-Wesley Publishing Company: Massachusetts, 1981

Dachuan Wang, Ingolf Willms
University Duisburg-Essen, Duisburg, Germany

Automatic flame detection using video sequence analysis

Abstract

In this paper an image-processing algorithm for flame detection in video sequences is presented. Some existent video fire detection algorithms need infrared camera to remove non-fire objects; others detect flames by observation of contrast variation in images or by colour and luminance variation of pixels. The algorithm described here uses normal commercial video cameras as visual sensor, and analyses colour, flickering frequency and motion characteristics. The luminance difference of frame sequences are determined from the original colour frame sequences and turned into a binary frame sequence for motion analysis. In addition flame detection is based on colour and frequency criteria.

1 Introduction

At present video surveillance applications are growing quickly. In more and more big buildings, traffic-centers, depots, docks, tunnels and other places such systems are installed. In most cases the purpose is surveillance. Video surveillance significantly helps the operators in a remote control center in dealing only with possibly important events. This development in security applications also contributed to the development of video fire detection as an additional function to surveillance.

Another development has to do with component features and prices. For standard definition video and other usual applications, cameras prices dropped significantly, HDTV cameras are on the way. Other features of cameras have been improved over the years. Colour cameras need only a fraction of that illumination needed a few years ago. Some black&white cameras are not very far away from the sensitivity of the human eye.

CMOS imaging sensors show improvements over CCD chips in terms of dynamic range, speed and other features.

In addition to such developments cameras and the corresponding electronics are getting smaller and smaller. The one-chip video camera is on the market. Other cameras are equipped with DSP chips for improving the sensitivity or performing functions such as motion detection. In addition the calculation speed of digital signal processors increased year by year. Dedicated media processors are on the market. The size of future self-contained video fire detectors, which are made up of a video sensor and a DSP chip or a media processor, could be as small as a conventional fire detector. Only the power supply still remains as a problem.

Thus improved and cheaper imaging sensors will drive the development also in fire detection applications. The next chapters describe in detail the onsets and the associated criterions applied for a flame detection algorithm.

2 The colour criterion

Colour images captured by a video camera are resolved in red, green, and blue (RGB) components. In order to detect flames based on colour feature extraction, the distribution of colour components of flames has to be studied. These distributions were analyzed in three steps.

- Templates containing only flame images were chosen
- Colour components were introduced into the distribution diagram
- A mathematical description of RGB regions of the colour distribution was determined

In such a diagram each colour corresponds to a point in the three dimensional colour space. Figure 1 shows the two colour distribution diagrams on which the colour criterion was based.

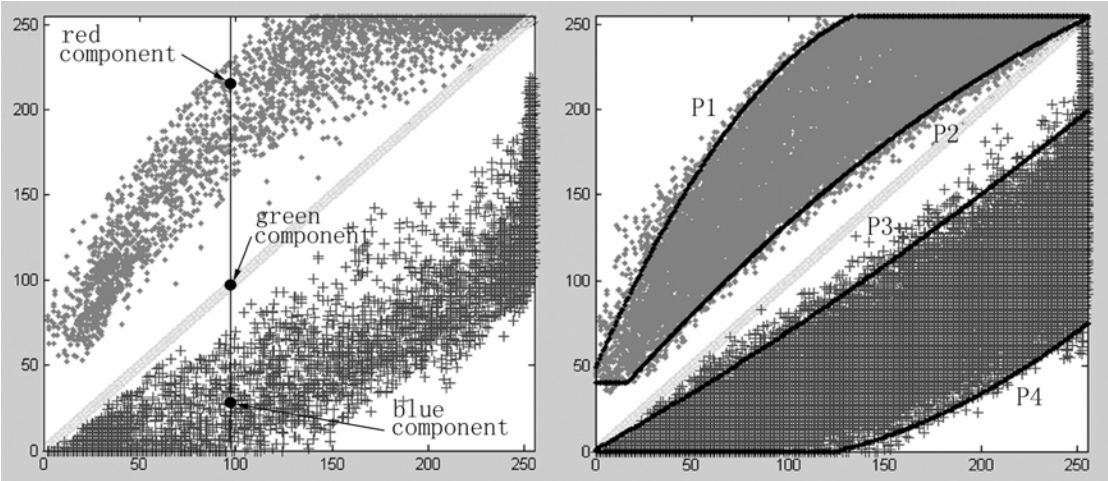

Figure 1: Colour distribution of flame and boundary functions

In these two dimensional colour distribution diagrams the horizontal coordinate shows the green component values, and the vertical coordinate shows the values of red and blue components. In addition also the green component is plotted over itself giving just a line. So in these distribution diagrams each flame pixel of the template gives three points in the diagram. As usual RGB component values are in range of 0 to 255 due to 8 bit coding. So both horizontal and vertical coordinates show values in that range. Below and above the green line the areas of red points (in the upper half) and blue points (in the lower half) are to be seen.

Colour distribution diagrams obtained from different flames are not quite the same. Therefore diagrams from different flames were merged into a total colour distribution diagram. In this total distribution diagram the relations between colour components could still be distinguished clearly. Still the red area was above the green line, due to significant red components in flames. Blue components were found to be always smaller than green components. The boundaries of red and blue areas could be represented by exponential functions resulting in quick calculations.

Using such boundary functions as the basis of a colour criterion a fire detection algorithm can determine whether each pixel exhibits a typical flame colour or not by locating the colour components in the distribution diagram.

3 The frequency criterion

In order to check the frequency of pixels in a frame, the colour frames are converted into luminance frames by computing the weighted mean of three colour components. For turbulent flames a flickering frequency in the range of 1 Hz to 8 Hz can be assumed. Based on this feature flames can be distinguished from many objects. The same holds for frame areas with a constant background and objects with brightness changes and frequencies above 8 Hz. The filter needs 7 luminance frames as input data, therefore the system will always keep the 7 latest frames in memory. After the filtering the resulting luminance frames contain to a high degree only such pixels inside the frequency band of 1 Hz to 8 Hz.

4 The motion criterion

The human vision is more sensitive to moving or varying objects than to still objects. Flames show high luminance values, this means that normally a high contrast to the background exists. Flames are flickering, their size and shape are varying in subsequent video frames. So motion is another criteria for detection. For the application of this criterion binary frames, which contain the motion information of the original luminance frames are used. They are obtained by computing the difference between subsequent luminance frames and by quantifying the luminance differences.

The following figure 2 shows a comparison between a luminance frame and a binary frame. In the binary frame the interframe motion of a flickering flame (object A) and of a moving man (object B) are visible.

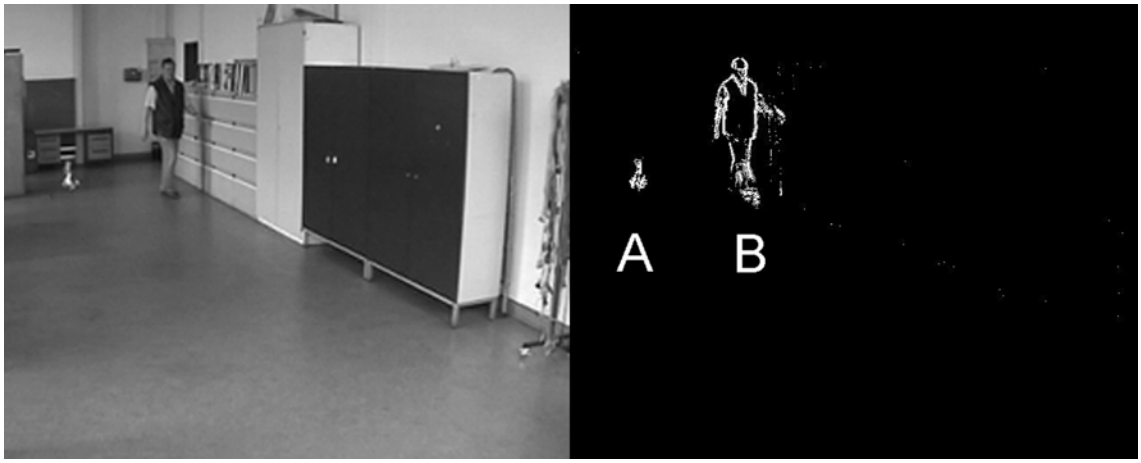

Figure 2: luminance frame (left) and binary frame (right)

The binary operation removes the motionless background, so that the recognition is simplified for recognition of the interframe motions of the flame in the binary frame. In binary frames of complex scenes there are many interframe motions from various objects and some tiny spots. In order to detect a flame reliably, the difference between the interframe motions of flames and other objects has to be considered.

4.1 Difference between interframe motions of flame and other objects in the binary frame

Interframe motions from non-flame objects are classified into 5 types. These classes comprise moving objects with a constant shape, objects with a fixed position and varying shapes like trees or flags, blinking lights and reflected lights, and some tiny spots caused by noise in the video capturing process.

In order to detect a flame in the binary frame sequence, two methods, which can distinguish the flame from these 5 types of interframe motions by using their visual difference, are presented in the following paragraph. Both methods use the luminance frame sequence as input data and find objects with motion characteristic similar to a flame.

4.2 Method 1

This method divides the binary frame into blocks of 32 rows and 36 columns. Each block exhibits 18 rows and 20 columns of pixels. The size of each block has to be set smaller than the size of the smallest detectable flame.

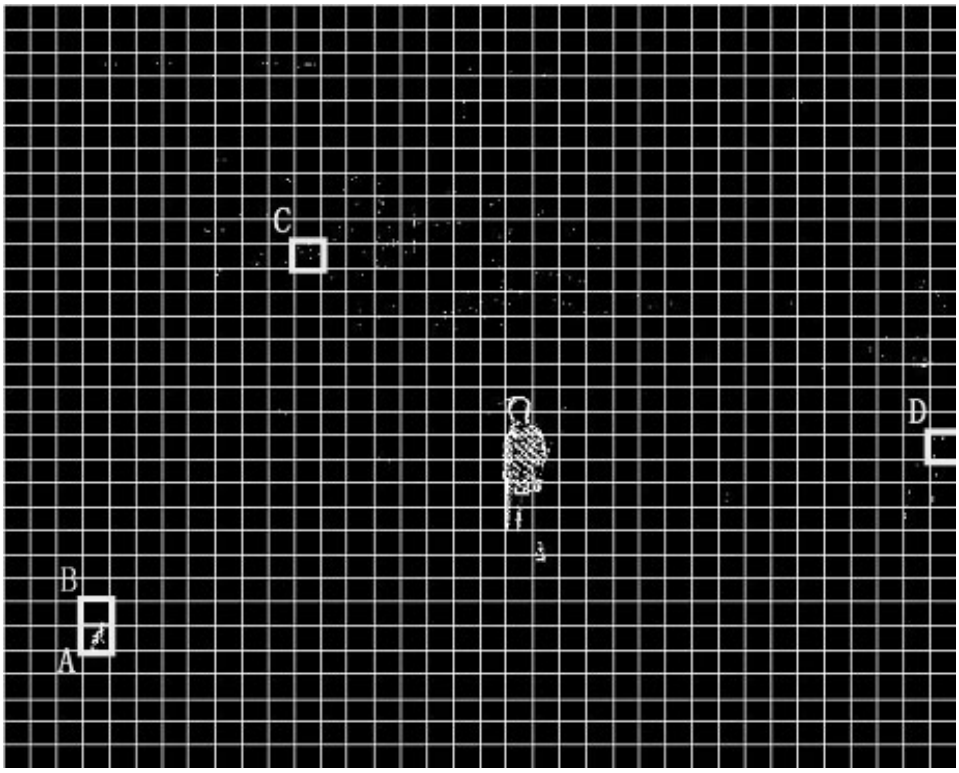

Figure 3: Blocks of a binary frame

In figure 3 block A is the main part of the flame, block B contains flickering parts of it. Block C and D are left from the removal of the background and contain some small spots. In the center of the binary frame a walking man can be recognized. Obviously the number of white pixels in those 4 blocks and the blocks covered by the walking man are quite different.

Figure 4 presents a plot of the number of interframe motion pixels in blocks A to D. The vertical coordinate gives the number of frames analysed. In block A the quantity is in most cases bigger than 40, and it shows a large dynamic range from 16 to 73.

In block B the quantity has a mean value of less than 15, but several peaks go up to 30. In blocks C and D the interframe motion pixels have a mean of less than 10 without showing any significant peaks.

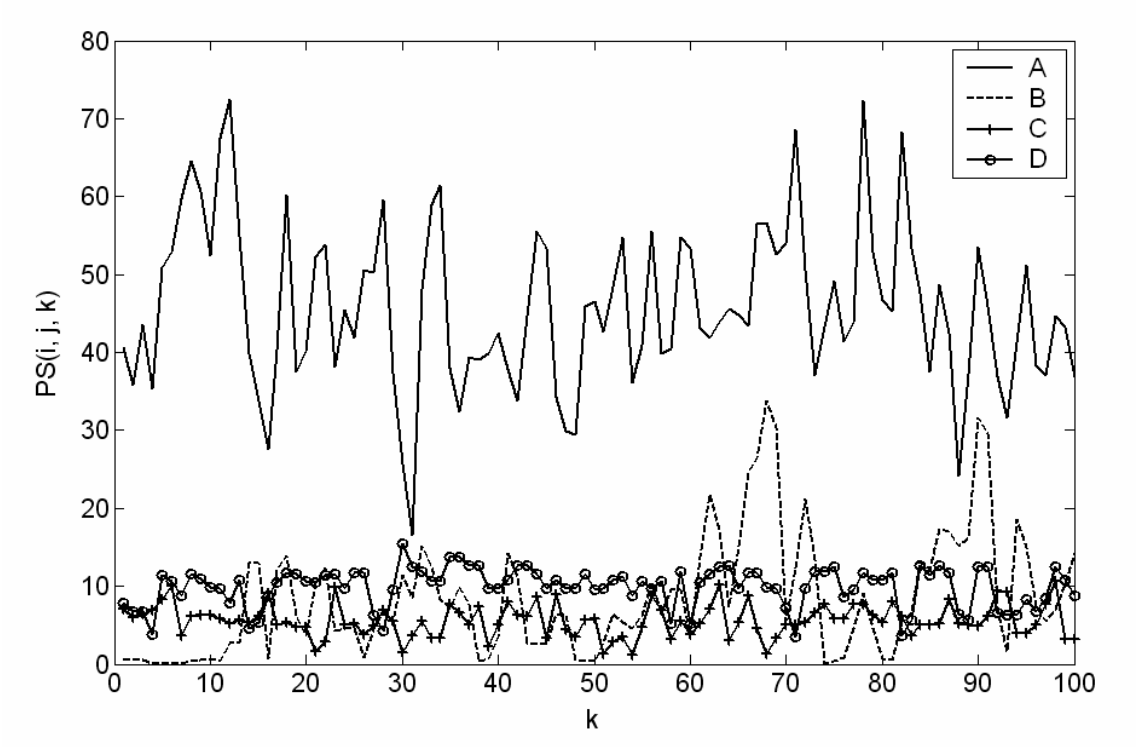

Figure 4: Quantities of interframe motion pixels in block A, B, C and D

The quantity of interframe motion pixels in the blocks due to the walking man is similar to block A, but after some time the quantity in this block will drop to 0. This happens after the walking man moves out of the frame. The combination of features of block A and block B indicate a possible flame.

4.3 Method 2

This method gathers the interframe motion pixels in the binary frame into groups corresponding to respective objects. First an erode operation eliminates the large numbers of tiny spots in the binary frame, and then a dilate operation connects the adjacent interframe motion pixels by enlarging them.

According to their connectivity groups of interframe motion pixels corresponding to the objects are obtained. Those spots, which are not eliminated by the erode operation will be found by counting the quantity of interframe motion pixels in each group.

But the motion of such pixel groups in the binary frame is not in all cases the same as the motion of real objects. Although special movements like a rotation of objects was not taken care of, the application of method 2 for flame recognition was found to be very useful.

Figure 5 shows the grouping result from the frame in figure 2. The system clusters interframe motion pixels into 2 groups and locates the groups using rectangular boxes. For each frame the grouping operation is performed, so that the trajectories of the boxes of each object in a frame sequence can be obtained.

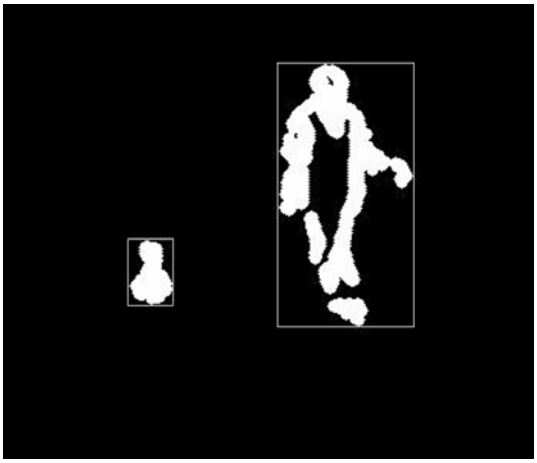

Figure 5: Pixel groups for a flame and a walking man

In this algorithm it is assumed that flames do not move. Still the upper border has a bigger dynamic range than the other borders. Thus moving objects can be distinguished from flames. This procedure prevents that pixel groups of blinking lights are detected as flames.

So the second method contains the following steps:

- Erode the single spots in the binary frame;
- Connect pixels from one object by using a dilate operation, and locate the groups with rectangular boxes in each frame to obtain the box trajectories;
- Find boxes which constantly appear, show a fixed center, and which exhibit motion of their upper border.

5 Overview on the algorithm

In order to detect flames reliably all three mentioned criteria are used in the algorithm. First of all one of the two methods performing motion analysis is carried out to find a possible flame in the binary frames. The system then determines a slightly enlarged rectangular area for each possible flame. In addition the sub-frame sequence of this area is stored and analyzed using the colour and flickering frequency criteria. Compared with the method of checking colour and frequency first, computing time and memory usage are saved.

In the sub-frame sequence the colour criterion and the frequency criterion eliminate the non-flame pixels separately. Then the number of remaining pixels is compared with the number of all pixels in the sub-frame.

6 Conclusion

In this paper an algorithm for detecting flames in video sequences captured by commercial colour video-cameras was presented. The algorithm assumes that flames stay at fixed positions and uses the criteria of colour, frequency, and motion to distinguish flames from various other objects in the scene. Experiments have shown that the algorithm is able to detect flames in both indoor and outdoor scenes.

Further work will concentrate on improving the analysis of the shape of flames in order to enhance sensitivity and false alarm rejection.

7 References

/1/ C. Cedras, M. Shah, “Motion based recognition: A survey”, Image and Vision Computing, vol. 13, no. 2, pp. 129-155, 1995

/2/ O.A.Plumb, R.F.Richards, “Development of an economical video based fire detection and location system”, Department of Mechanical and Materials Engineering, Washington State University, 1996

/3/ I. Willms, “Digitale Video-Analyse in der automatischen Brandentdeckung”, Simedia Forum Videoüberwachung, Frankfurt am Main, Germany, June 28-29, 2001

/4/ Foo., S. Y., “A rule-based machine vision system for fire detection in aircraft dry bays and engine compartments”, Knowledge-Based Systems, vol. 9 pp. 531-41, 1995

/5/ Walter Phillips III, Mubarak Shah, Niels da Vitoria Lobo, “Flame Recognition in Video”, Computer Vision Laboratory, School of Electrical Engineering and Computer Science, University of Central Florida, 2002

/6/ T. Kulessa, M. Hoch, “Efficient Color Segmentation under Varying Illumination Conditions”, Proceedings of the 10th IEEE Image and Multidimensional Digital Signal Processing (IMDSP) Workshop, July 12-16, 1998

/7/ T. Wittkopp, C. Hecker, D. Opitz, 2001, “The Cargo Fire Monitoring system (CFMS) for the visualisation of fire events in aircraft cargo holds”, 12th International Conference on Automatic Fire Detection (AUBE’01), National Institute of Standards and Technology, Gaithersburg, March 25-28, 2001

Thorsten Kempka, Thomas Kaiser and Klaus Solbach
Universität Duisburg-Essen, Duisburg, Germany

Microwaves in fire detection

Abstract

Continuing our previous paper [2] published at AUBE '01, the issue of fire detection by means of microwave radiation is further discussed. First a concept for this task is presented, along with a short repetition of the physical fundamentals of thermal radiation, electromagnetic wave propagation and attenuation.
In the second part the microwave receiver will be presented, which allows to carry out experiments in Duisburg's fire detection lab. The receiver is able to measure thermal radiation in a frequency region from 2 GHz up to 40 GHz, where the superheterodyne technique enables a rather flexible measurement range among arbitrary frequency bands with width of 100 MHz.
The receiver is controlled by a normal PC, which makes the measurement setup configurable, i. e. one can choose any combination out of the 380 x 100 MHz frequency bands for a single measurement. A graphical tool can be used to configure and to control the measurements. This facilitates the set up of the desired frequency bands and to carry out the data logging. In the last part of our contribution we are going to present and discuss the results of measurements of selected standardized European test fires according to ISO 7240 (EN 54 Part 9).

Introduction

Today, typical smoke and flame detectors and also imaging cameras are based upon thermal radiation in the infrared (IR) region. IR radiation itself is a special kind of an electromagnetic wave for the wavelength range $750\,\text{nm} \leq \lambda_{IR} \leq 1\,\text{mm}$. The question arises wether electromagnetic radiation with other wavelengths λ can be used for fire detection. Without doubt, most of the thermal power radiated by the fire belongs to the IR spectrum. So, the first choice for a *radiometer,* this is a device which measures the radiated power of

the fire, is the IR spectrum. Examples for such radiometers are flame detectors (e. g. see [8]) or the above mentioned IR cameras. However, from scattered light or light extinction detectors we know that the attenuation of this radiation due to smoke is rather high. In fact, those detectors *exploit* the high attenuation of smoke or the high scattering due to smoke in the fire case and *not* the emitted radiation power of the fire. Because of this it is reasonable to look for a region of the electromagnetic spectrum where the attenuation is less than in the IR region although the emitted power is even lower. In the micro- and millimeterwave region, this means for a wavelength range 1 mm $\leq \lambda_{\mathrm{MW}} \leq$ 187 mm or the corresponding frequency range 1.6 GHz $\leq f_{\mathrm{MW}} \leq$ 300 GHz, such characteristics are given. Hence, exploiting thermal radiation in the microwave region (MW radiation for short) for fire detection purposes is the topic of this contribution.

Concept

Fig. 1 represents one concept for the use of microwave radiation in fire detection. Because

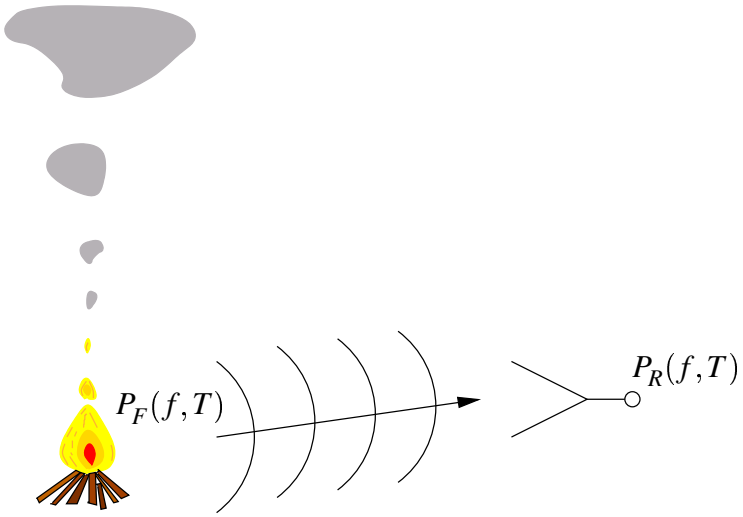

Figure 1: Concept

of its temperature unequal to zero a fire emits electromagnetic radiation, The radiation power $P_{\mathrm{F}}(f,T)$ depends on the observed frequency f and certainly on the fire temperature. The idea is, that a receiver measures the thermal radiation $P_{\mathrm{R}}(f,T)$ within the room. If there is no fire within the room it will measure the room temperature. If a fire is present,

the received thermal radiation power is increased.

To proof this simple concept, already used in the infrared region of the electromagnetic spectrum, the thermal radiation power of a fire $P_{\mathrm{F}}(f,T)$ has to be known. Also the radiation power $P_{\mathrm{R}}(f,T)$ at the receiver has to be known. The propagation of electromagnetic waves and the interaction of waves have to be taken into account because they impact $P_{\mathrm{R}}(f,T)$.

Fortunately, all of these phenomena are well investigated from other areas. PLANCK´s law of radiation gives an upper bound for the thermal radiation power of a fire. For propagation effects we can apply the free space propagation model for simplicity (known e.g. from wireless communications) and the interaction with matter is described by MIE-theory and RAYLEIGH-scattering, respectively. In the following paragraphs these physical fundamentals are briefly revisited (For more information see e. g. [1], [7], [11], [12]).

The thermal radiation power of the fire $P_{\mathrm{F}}(f,T)$ can be calculated from the RAYLEIGH-JEANS-law and the emissivity $w_{\mathrm{E}}(f,T)$. The RAYLEIGH-JEANS-law is an approximation of PLANCK´s law in the microwave region, which describes the thermal radiation power of a black body. The emissivity $w_{\mathrm{E}}(f,T)$ is a normalized material parameter which depends on the frequency as well as the temperature. It holds

$$0 \leq w_{\mathrm{E}}(f,T) \leq 1 \quad \forall \quad f,T$$

and

$$\mathrm{d}P_{\mathrm{F}}(f,T) = \frac{2A\,\mathrm{k}\,T}{\mathrm{c}_0^2} w_{\mathrm{E}}(f,T)\, f^2\, \mathrm{d}f, \tag{1}$$

with BOLTZMANN constant k, speed of light in vacuum c_0, and surface and temperature of the fire A,T, respectively. For the received power $P_{\mathrm{R}}(f,T)$ at the antenna it follows under free space propagation [6], [13]

$$\mathrm{d}P_{\mathrm{R}}(f,T) = \frac{A_{\mathrm{e}}(f)}{4\pi d^2}\,\mathrm{d}P_{\mathrm{F}}(f,T),$$

which leads to

$$P_{\mathrm{R}}(f,T) = \frac{\mathrm{k}AT}{2\pi\,\mathrm{c}_0^2\,d^2}\int A_{\mathrm{e}}(f)\, w_{\mathrm{E}}(f,T)\, f^2\,\mathrm{d}f = \frac{\mathrm{k}AT}{8\pi^2 d^2}\int G(f)\, w_{\mathrm{E}}(f,T)\,\mathrm{d}f, \tag{2}$$

with the distance between fire and antenna d, the effective area of antenna $A_\mathrm{e}(f)$, and the antenna gain $G(f) = \frac{A_\mathrm{e}(f)\,f^2}{\mathrm{c}_0^2}$. For a narrow frequency band with center frequency f_c and bandwidth Δf we obtain

$$P_\mathrm{R}(f_c, \Delta f, T) = \frac{\mathrm{k} A\, T}{2\,\pi\,\mathrm{c}_0^2\, d^2}\, w_\mathrm{E}(f_c, T)\, A_\mathrm{e}(f_c)\, f_c^2\, \Delta f = \frac{\mathrm{k} A\, T}{8\,\pi^2\, d^2}\, w_\mathrm{E}(f_c, T)\, G(f_c)\, \Delta f.$$

The attenuation of the thermal radiation by smoke or other matter is discussed in the following. Since thermal radiation is an electromagnetic wave, the attenuation of electromagnetic waves by dielectric particles is of relevance.

The attenuation of electromagnetic waves includes two effects, absorption of energy by particles and scattering of energy by particles. Both effects lead to attenuation or extinction of the incident electromagnetic wave. The general solution to this problem was given by MIE and is denoted as MIE-theory or MIE-scattering (see e.g. [3], [7]). MIE assumed, that the dielectric particles are spheres with a fixed diameter d_p and the collisions are elastic, i.e. the kinetic energy remains unchanged. The approximation for particles small compared to the wavelength λ of the incident wave is called RAYLEIGH-scattering, which is valid for

$$\frac{d_\mathrm{p}}{\lambda} < \frac{1}{10}.$$

The particle size distributions of smoke in fires are in the range from 4.2 nm to 7.5 μm (see [10]). The wavelength of microwaves varies between 1 mm $< \lambda <$ 187 mm, so for the maximum ratio holds

$$\left(\frac{d_\mathrm{p}}{\lambda}\right)_\mathrm{max} = 0.0075.$$

Hence, RAYLEIGH-scattering is reasonable and the scattered intensity $I(\lambda)$ is strongly dependent on the wavelength λ, to be more precise proportional to λ^{-4} in this case. So, for the comparatively long wavelengths in the microwave region in contrast to the infrared region, this scattering is quite small and hence neglectable. This is one distinct advantage when using the microwave region of the spectrum for fire detection.

Microwave receiver

This section describes the microwave receiver we built up to measure the thermal radiation power of fires. Currently it is able to measure between 2 - 40 GHz. The receiver is designed according to the superheterodyne principle, which has two major advantages. First, the receiver can easily be enlarged to deal with other frequency bands and second, it is able to amplify the thermal power at an intermediate frequency, where succeeding amplifiers are easier to build. Fig. 2 shows a principle sketch of our receiver.

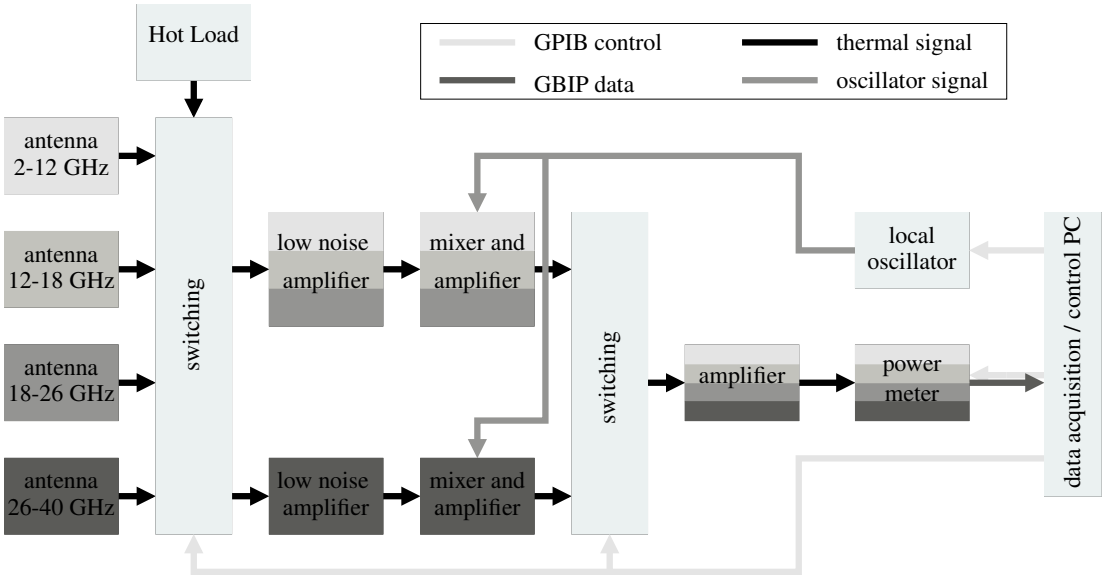

Figure 2: Schematic diagram of the microwave receiver

The four broad-band antennas cover the frequency bands 2-12 GHz, 12-18 GHz, 18-26 GHz and 26-40 GHz and are followed by a switching stage, where each of the antennas or a "Hot Load" could be selected. The Hot Load with a constant temperature of 100 °C is used to calibrate the complete measurement device. After the switching stage two low noise amplifiers (LNA) amplify the received thermal radiation power with a gain of $G_{\mathrm{dB}} = 30\,\mathrm{dB}$ and a noise figure F less than 3 dB over the whole frequency range. The latter is needed to achieve a satisfactory temperature resolution ΔT_{m}, where [9]

$$\Delta T_{\mathrm{m}} = \frac{T_{\mathrm{m}} + T_{\mathrm{r}}}{\sqrt{\Delta f\ \tau}},$$

with the radiometer bandwidth Δf, the measurement time τ, the temperature of the measured object T_{m}, and the noise temperature of the receiver T_{r}. Tab. 1 represents some

typical values for ΔT_m for this microwave receiver.

T_m / °K	300	600	2000
ΔT_m / °K	0.4	0.6	1.5

Table 1: Temperature resolution ΔT_m of the microwave receiver

The measurement time τ is limited to a few seconds because the receiver should be able to track the variation of the thermal radiation of a starting fire. In this receiver it can be chosen as $\tau = n \cdot 25\,\mathrm{ms}$ with $n \in \mathbb{N}$.

The mixers shift the input signal to the intermediate frequency $f_\mathrm{IF} = 150\,\mathrm{MHz}$ and limit the bandwidth to 100 MHz. A local oscillator generates the mixing frequency f_LO, which is equal to the center frequency f_m of each 100 MHz wide measuring band minus the intermediate frequency f_IF. The desired measuring band is chosen by tuning the mixing frequency f_LO.

The noise temperature T_r could be expressed by the receiver noise figure F_r [4]

$$T_\mathrm{r} = \left(10^{(0.1 \cdot F_\mathrm{r})} - 1\right) \cdot 290\,^\circ\mathrm{K}.$$

For the noise figure of concatenated systems holds [5]

$$F_\mathrm{g} = F_1 + \frac{F_2 - 1}{G_1} + \cdots + \frac{F_n - 1}{G_1 \cdot G_2 \ldots G_n} = F_1 + \sum_{\nu=2}^{n} \frac{F_\nu - 1}{\prod_{\mu=1}^{\nu-1} G_\mu}, \qquad F_\nu \geq 1, G_\mu > 0,$$

where G_μ is the gain of the μ-th system. From this follows, that the receiver noise figure F_r is always greater than the noise figure F_1 of the LNAs. However, the noise figures of the succeeding stages, which follow the LNA are not so important, because they are divided by the gain of 30 dB ($G_1 = 1000$) of the LNAs.

The mixers are followed by further amplifiers and a second switching stage is used to select one of the two front-ends for either the frequency range $2 - 26\,\mathrm{GHz}$ or $26 - 40\,\mathrm{GHz}$. Before the thermal power is measured with a conventional power meter, it is further amplified by 60 dB at the intermediate frequency f_IF.

A data acquisition and control computer collects the measurement data of the power meter. It controls all the switching as well as the local oscillator. It is connected via the

general purpose interface bus (GPIB), which is a derivation of the HEWLETT-PACKARD-Interface Bus (HPIB). This bus allows the remote control of different measurement devices, like power meters, wave generators, or oscilloscopes.

Some limitations of our microwave receiver should be mentioned also. Because of the design goal to measure over a wide frequency range a bulky receiver has to be build up. Furthermore, all microwave components are manufactured for narrowband applications so that this microwave receiver is an assembly of many narrowband receivers with different properties in different frequency bands, e.g. the total amplification $G_{\mathrm{MR}}(f)$ depends on frequency. Hence, it is useful as a relative measuring device only, that compares the measured thermal radiation power $P_{\mathrm{M}}(f,T) = G_{\mathrm{MR}}(f) \cdot P_{\mathrm{R}}(f,T)$ of fire to non-fire situations for each frequency band respectively. The evaluation of the absolute value of $P_{\mathrm{M}}(f,T)$ requires further calibration efforts and will not be discussed here.

Another drawback is the rather complex control of the receiver, that follows from the broadband setup also. Because of this, the duration between two consecutive measured values may vary, if several frequency bands are measured simultaneously. In this case a configurable number of samples will be measured in one frequency band. Then the receiver changes to the next frequency band and takes the samples for the new frequency band. After all selected frequency bands are measured, the receiver will measure the first band again. The duration of frequency band changes depends on switching times for the different switches and the settling time of the local oscillator. The time between measurement samples in the same band depends on the number of measured bands and this can take some seconds. This is the reason why measurement results (see next section) for multiple frequency bands are drawn over the sample number instead of time.

In the next section, results from measurements carried out in Duisburg's fire detection lab are presented in order to gain more insight about microwave emission of fires.

Experiments

In this section some fire test results are presented. The distance between the receiver and the fire was approx. 1 m for all experiments. The test fires TF1 and TF2 out of the European standard EN 54 Part 9 (old version) are used for the measurements.

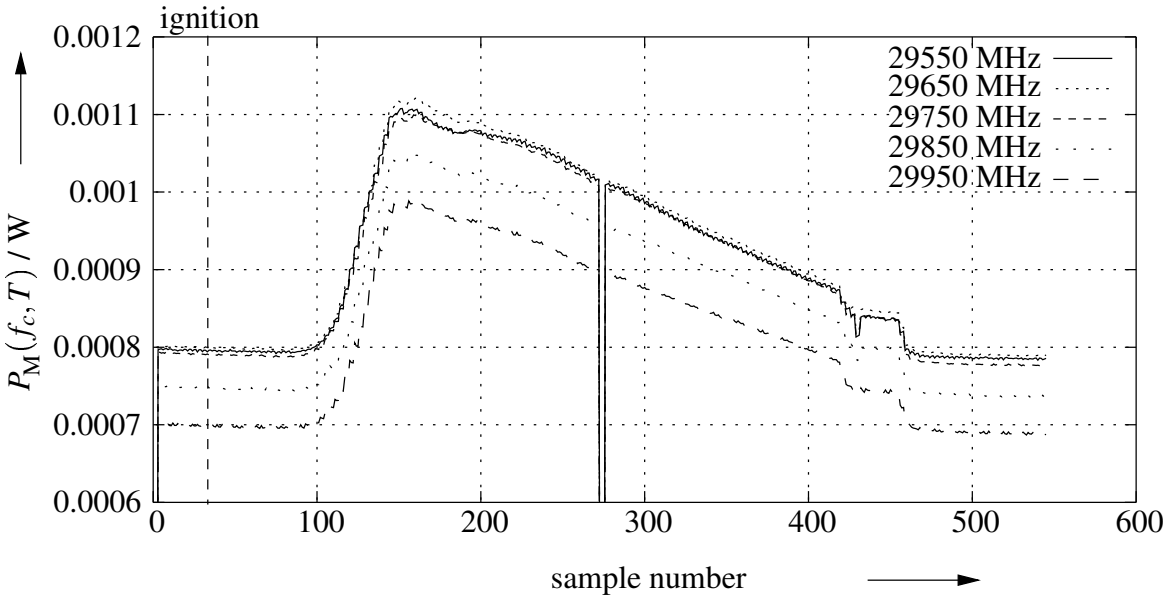

Figure 3: Measured thermal radiation power $P_{\mathrm{M}}(f,T)$ of a TF1 for different frequencies

TF1 is an open wood fire where beechwood is burned. Fig. 3 presents the measured thermal radiation power $P_{\mathrm{M}}(f,T)$ of this fire for different frequencies. The ignition of the wood took place at about $n = 30$ samples and is marked by the dashed line. At about $n = 100$ samples the measured power begins to rise in a nearly exponential manner up to the maximum at approx. $n = 150$ samples. After that time the radiation power drops of linearly. At about $n = 280$ samples a calibration took place. Therefore the power of the Hot Load was measured instead of the fire power. The two jumps between $n = 400$ and $n = 500$ follow from mopping the remaining wood out of the observed area. This measurement was done for the frequency range of 26 GHz - 40 GHz. The results of the other frequency bands within this range are very similar so they will not be shown here.
In order to get an impression of the time behavior, a measurement for a single frequency band (center frequency $f_c = 33.75\,\mathrm{GHz}$) was carried out. The result of this measurement is depicted in Fig. 4.
The fire was ignited at 240 s, which directly led to a small peak in the measured thermal radiation power $P_{\mathrm{M}}(f,T)$. The reason for this peak is possibly related to the used automatic ignition method. Thereby, a guncotton is electrically heated until it explodes.

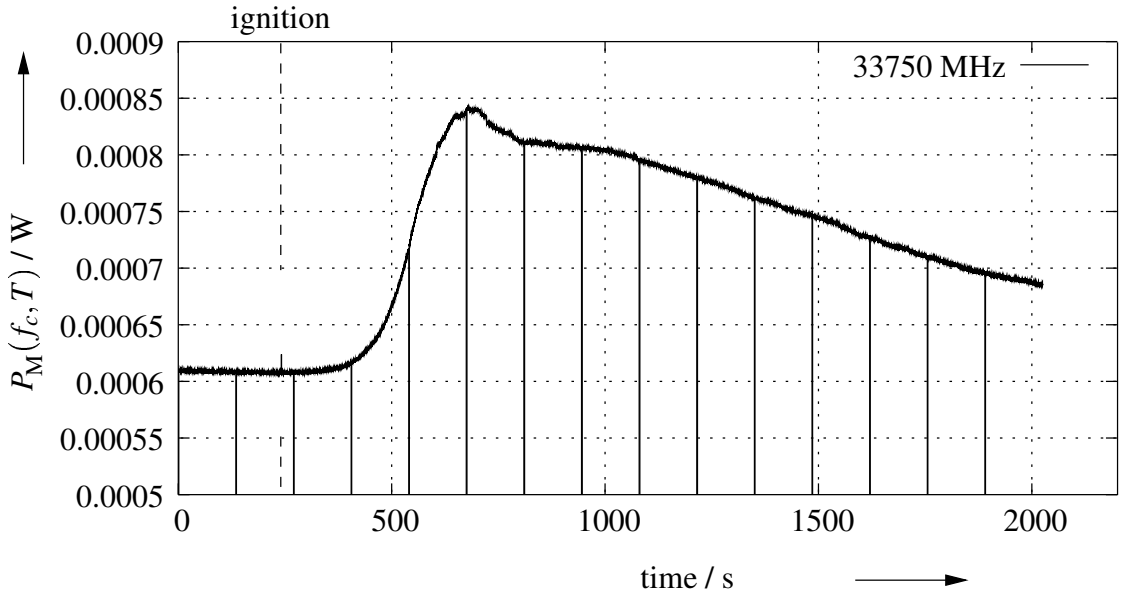

Figure 4: measured thermal radiation power $P_{\mathrm{M}}(f,T)$ of a TF1

A rise in the measured power can be observed at about 330 s. Hence, 90 s after ignition changes in the measured radiation power become visible, which is in agreement with data taken form ionization chamber (MIC), extinction light sensor (MIREX), CO-, and CO_2-measurements. The jumps in the end of the fire are missing, because nobody mopped the remaining wood out of the observed area.

The same measurements were carried out for TF2, which is a smouldering wood fire. The beechwood is placed upon a heater, which heats up to 600 ° C.

The frequency range of 26 GHz - 40 GHz is considered again. Because the results are very similar in the different frequency bands of this region only the time-dependent measurement for the center frequency $f_c = 31.75\,\mathrm{GHz}$ is represented in Fig. 5.

The heater was switched on at 120 s after the beginning. At 200 s the received thermal radiation power $P_{\mathrm{M}}(f,T)$ begins to rise. This is a much faster reaction than MIC, MIREX, CO-, and CO_2-measurements show. In these measurements it takes around 360 s before changes are observerable, because the wood must heat up to a temperature at about 300 ° C until it starts to produce smoke. (Fig. 6 represents normalized MIC, MIREX, CO-, and CO_2-measurements for convenience.) The maximum is reached at 800 s and it is followed by a smooth drop off. In the end at about 1700 s the remaining wood is mopped out of

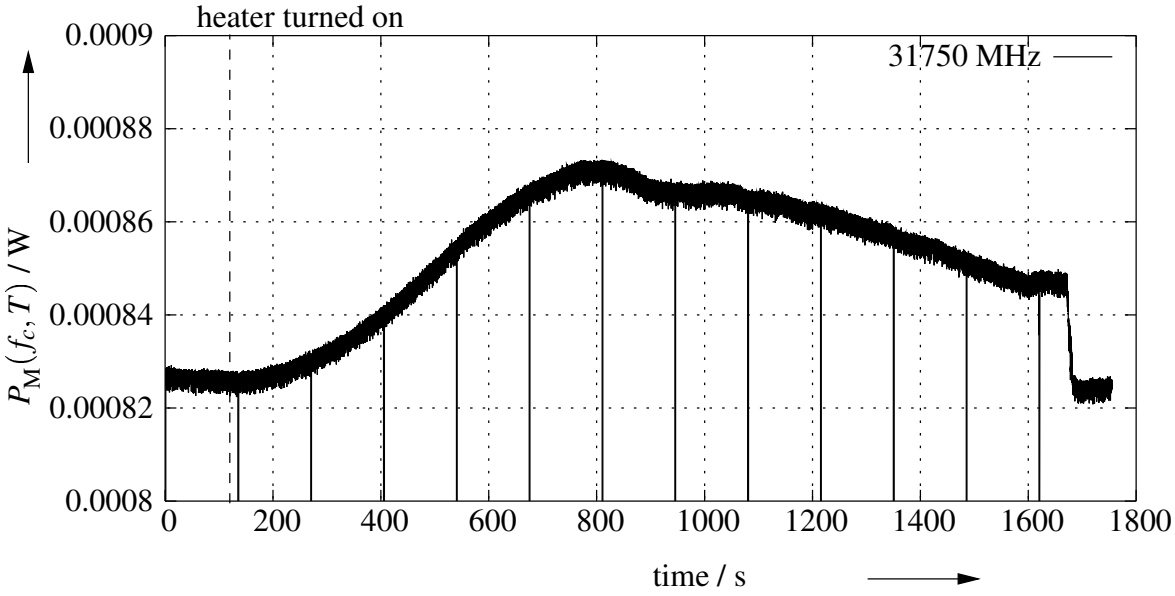

Figure 5: Measured thermal radiation power $P_{\mathrm{M}}(f, T)$ of a TF2

the observed area. The jump in thermal radiation can be seen very clearly, although there was little wood remaining after pyrolysis.

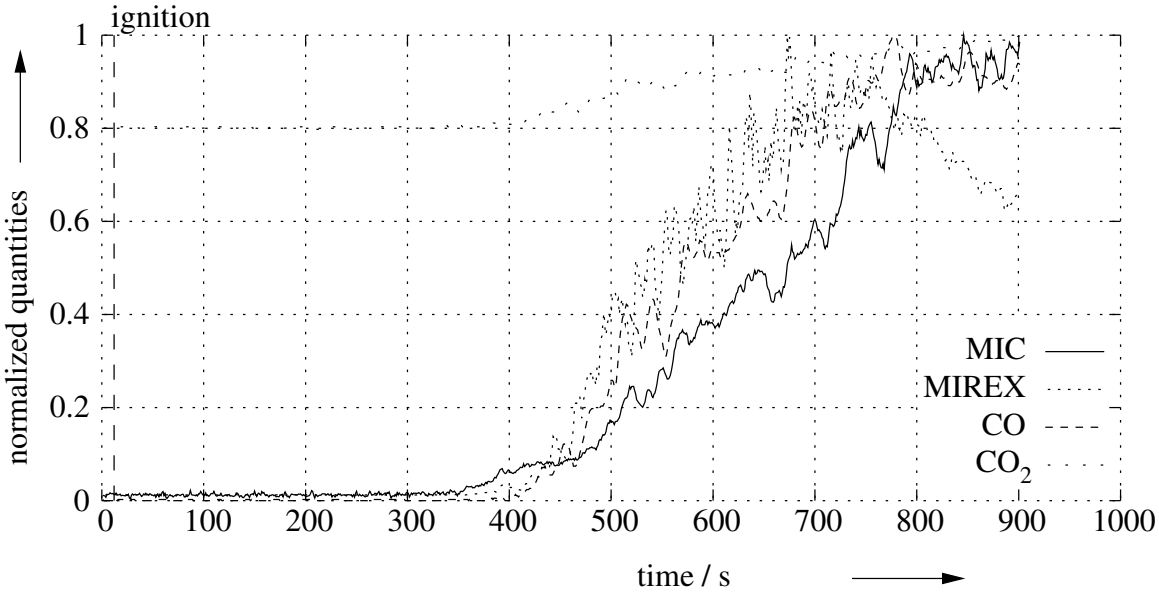

Figure 6: Normalized MIC, MIREX, CO-, and CO_2-measurements of a TF2

The last figure represents measurements of TF2 within the same frequency range for a

different measuring setup. This time there was a tile of the mineral fibre ceiling placed between the microwave receiver and the fire. The tile has a thickness of 2 cm and covered up the antenna completely. Hence, the fire was observed *through* an artificial ceiling. Comparing Fig. 7 to data recorded without the tile yields that the curves are very similar to each other at a first glance, but there are some slight differences. The reaction time is about 33 % longer, which yields to a reaction time of about 120 s if the tile is present and the maximum is approx. 33 % lower. However, in general, the fire is still detectable from the measured data. Note that this relevant observation is only based on a measurement bandwidth of 100MHz, i.e. by averaging over frequency the signal to noise ratio can be further improved.

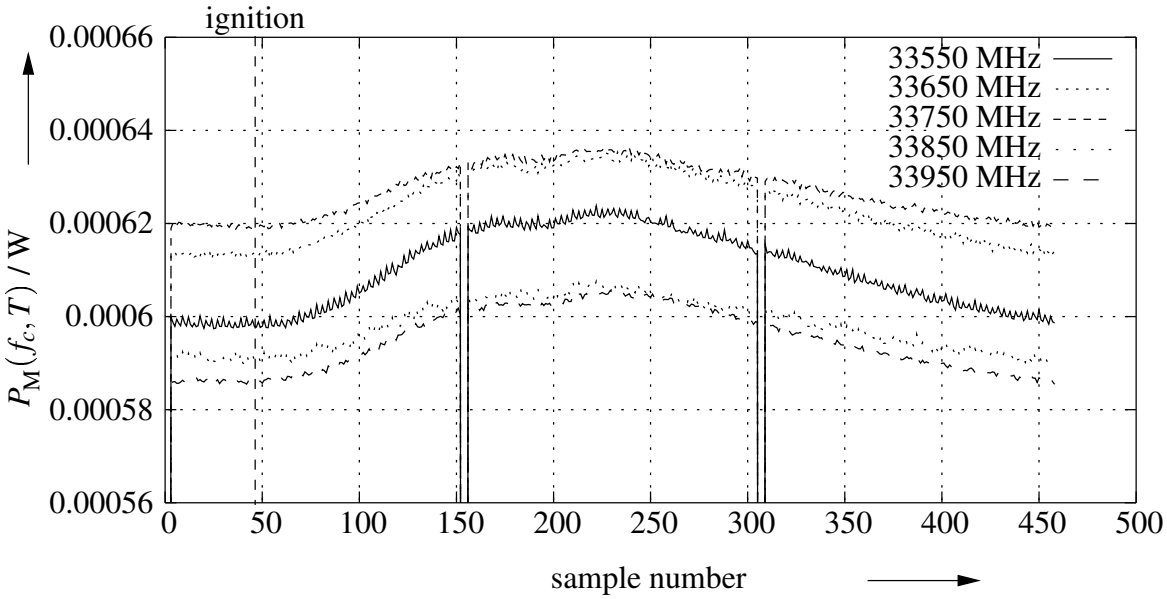

Figure 7: Measured radiation power $P_{\mathrm{M}}(f,T)$ of a TF2 behind ceiling tile

Conclusion

The idea of using microwaves for fire detection along with the underlying physical theory was presented at AUBE '01 conference ([2]). This time a receiver for thermal radiation in the microwave region of the electromagnetic spectrum is shown. Data taken from two European standardized test fires confirm the basic functionality of this approach. Hence,

thermal microwave radiation is a measureable quantity to detect fires. The measurements of TF2 indicate that in some cases it is possible to detected fires earlier than with optical- or gas-sensors. A further advantage is the penetration of non-metal materials by microwaves, which allows detection even behind walls.

Acknowledgment

The authors thank "Deutsche Forschungsgemeinschaft (DFG)" for supporting this project.

References

[1] C. Gerthsen, "Physik" , Springer-Verlag 1966.

[2] T. Kaiser, T. Kempka, "Is Microwave Radiation Useful for Fire Detection?", Proceedings of 12th International Conference on Automatic Fire Detection AUBE '01, 26.-28.3.2001, Gaithersburg, NIST Special Publication 965.

[3] M. Kerker, "The scattering of light and other electromagnetic radiation" , Academic Press 1969.

[4] R. Lentz, "Rauschen in Empfangsanlagen", UKW-Berichte 3 , 1975.

[5] H. Luck, "Grundlagen der Nachrichtentechnik 1-4" , Vorlesungsskript Universität Duisburg-Essen, 2003.

[6] H. Meinke, F.W. Gundlach, "Taschenbuch der Hochfrequenztechnik Bd1-3" , Springer-Verlag 1986, ISBN 3-540-15394-2 (Bd.1), 3-540-15395-0 (Bd. 2), 3-504-15396-9 (Bd. 3).

[7] C. R. Nave, "HyperPhysics" , http://hyperphysics.phy-astr.gsu.edu/hbase/hframe.html.

[8] R. Siebel, "Ein LOW-COST Flammenmelder mit guten Alarm- und Falschalarmeigenschaften" (in German), Proceedings AUBE '99 zur 11. Internationalen Konferenz über Automatische Brandentdeckung, 16.-18.3.1999 in Duisburg, Heinz Luck (Ed.), Agst Verlag, Moers 1999, ISBN 3926875313

[9] B. Schiek, H.-J. Siweris, ”Rauschen in Hochfrequenzschaltungen” , Hüthig Buch Verlag 1990, ISBN 3-7785-2007-5.

[10] E. Tamm, A. Mimre, U. Sievert, D. Franken, ”Aerosol Particle Concentration and Size Distribution Measurements of Test-Fires as Background for Fire Detection Modelling“, H. Luck (Herausgeber), Tagungsband der 11. Internationalen Konferenz über automatische Brandentdeckung AUBE ’99, Duisburg, März 1999, Agst Verlag Moers 1999, S. 150-159.

[11] F. T. Ulaby, R. K. Moore, A. K. Fung, ”Microwave Remote Sensing Vol.1 Fundamentals and Radiometry” , Addison-Wesley, 1981, ISBN 0-201-10759-7.

[12] B. Vowinkel, ”Passive Mikrowellenradiometrie” , Friedr. Vieweg & Sohn, Braunschweig / Wiesbaden, 1988, ISBN 3-528-08959-8.

[13] O. Zinke, ”Lehrbuch der Hochfrequenztechnik 1” , Springer-Verlag 1990, ISBN 3-540-51421-X.

Ingolf Willms, Thomas Kaiser
University Duisburg-Essen, Duisburg, Germany
H. Sachs
TU Ilmenau, Ilmenau, Germany

UWB enhanced Microwave Fire Detection

Abstract

Microwave Fire Detection is a passive detection technique and relies on the increased radiation of hot spots due to PLANK's law. However, the received microwave power depends both on the objects temperature and the material, namely its surface emissivity. Conducting materials like metallic objects or foils e.g. might hide a hot spot due to blocking of its radiation.

In this respect Ultra-Wide Band (UWB) radar measurements might help in some aspects. This active measurement technique could help in detecting areas with metallic objects thus identifying areas being uncovered by passive microwave fire detection. In addition, UWB measurements could lead to a rough characterisation of the objects material with respect to its electrical properties.

The paper gives an overview on UWB radar technology and its possible application in the detection and localisation of a fire and shows results from recent experiments of UWB radar measurements of test fires. Unfortunately, UWB radar measurements are influenced by the incidence angle at the point of contact of waves and object in addition to the surface roughness. The paper describes concepts how to treat such influences.

Introduction

The detection of hot spots using the measurement of microwave power for the frequency band 2 GHz to 40 GHz is subject of current investigations.

Using this technique PLANK's law is practised for microwave fire detection in the form of a passive detection principle [1]. First results are promising.

They show a temperature resolution of some degrees for sufficiently large hot objects in relation to the microwave antennas opening angle.

One problem of microwave fire detection is that a hot spot could be hidden by metallic objects, even by metallic foils. But also other materials could impact the radiation. If some information about the material would be known, the received microwave power to some extent could be adjusted for with respect to different emissivities.

A method of obtaining additional information about the electrical properties of objects is UWB Radar. It is an active method which relies on microwave backscattering. This happens at material boundaries essentially due to different dielectric and magnetic properties.

Backscattering always takes place if electromagnetic waves pass through media with different wave resistance values**.** The value for free space is:

$$Z_0 = \sqrt{\frac{\mu_0}{\varepsilon_0}} = 377\Omega\,.$$

Essentially the wave resistance is a function of the relative dielectric constant ε_r with $\varepsilon = \varepsilon_r \varepsilon_0$ for materials which are not ferro- or ferrimagnetic. For non-magnetic materials the relative permeability μ_r with $\mu = \mu_r \mu_0$ is close to 1. If waves propagate through air and hit an object, the different wave resistance values, i.e. when different from 377Ω, lead for perpendicular incidence to a reflection at the material boundary according to the reflection coefficient p with

$$p = \frac{Z_W - Z_0}{Z_W + Z_0} \quad \text{and} \quad Z_W = \sqrt{\frac{\mu}{\varepsilon}} = Z_0 \sqrt{\frac{\mu_r}{\varepsilon_r}}\ .$$

Thus, the wave transition from air to an arbitrary non-magnetic material is always connected with a negative *p*-value. Metals cause a full reflection with $p = -1$.

If the waves pass through the object (and if still the boundary material-air is given) once more a reflection takes place, this time with a changed sign of p but with the same amount.

For other materials than air, the wave resistance is determined by the fraction ε_r / μ_r . Figure 1 show this relation for fractional values in the range of 1 to 60.

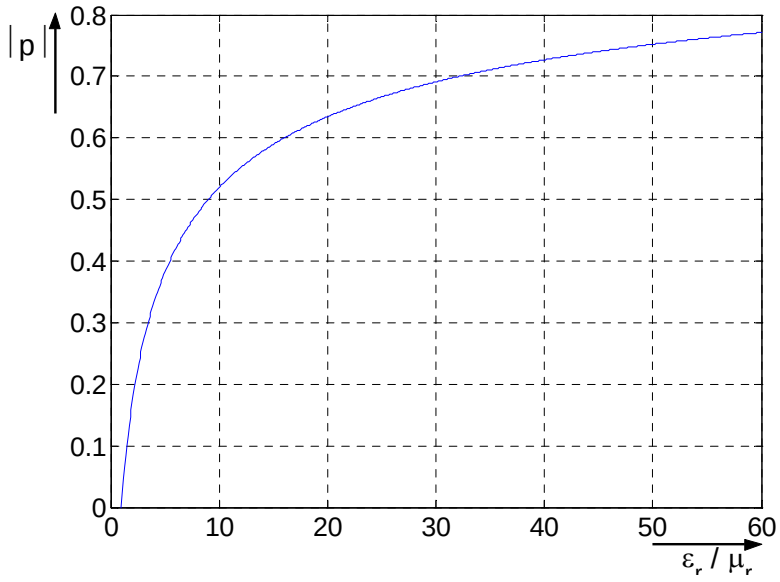

Fig. 1 Plot of $|p|$ over ε_r / μ_r

The property of classifying materials on the basis of microwave reflections is used in a number of applications like Ground Penetration Radar (GPR) and related Imaging Radar techniques. The application cover very different areas such as:

- Mining (locating of coal) [2]
- Road maintenance (non-destructive inspection of weak layers in the ground) [3]
- Archaeological investigations (determining hidden or inhomogeneous structures in historical buildings and monuments) [4]
- Agriculture (determination of soil humidity) [5]
- and several other applications (e.g. anti personnel mine removal, localisation of hidden persons, localisation of metallic bars in concrete, rain radar)

The UWB radar technolgy is described in the following chapter.

UWB Principle for Radar Sensing

Signals with an ultra-wide spectrum can be produced based on different approaches. Using a classical carrier modulation a suitable (stepped or continuous) frequency modulation can be applied. Another method is to emit short impulses of adequate energy. Both approaches suffer from disadvantages. A third method combines advantages of the first two onsets without suffering from major drawbacks. Due to the availability of digital circuits with clock rates above 1 GHz, UWB signals for radar applications can be cost effectively realised. These are periodic signals exhibiting a power spectral density (PSD) with dominant values spread in an ultra-wide band.

Such a UWB signal is then transmitted to the objects to be analysed.

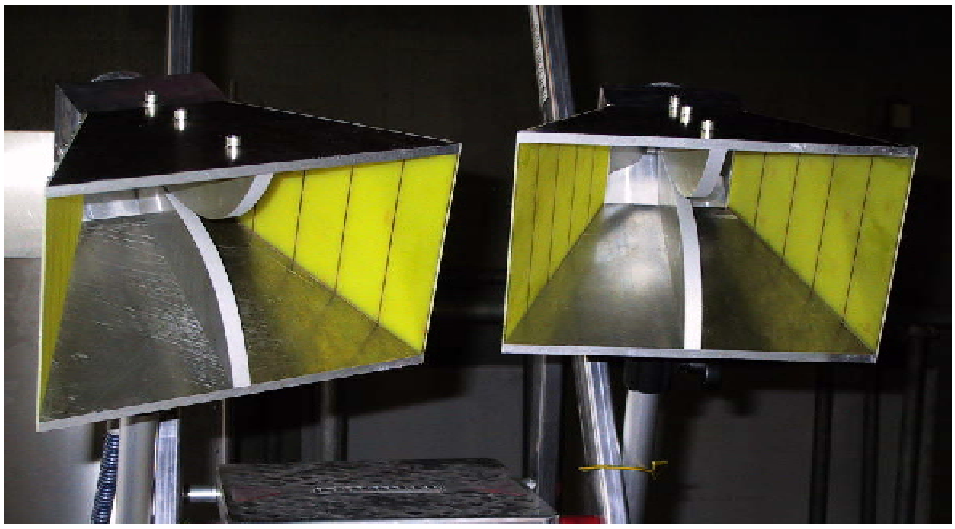

Fig 2 UWB antennas for the range 1 – 18GHz

The path from the transmission antenna to the receiving antenna across the object to be analysed can be thought of as an LTI system. Its properties are fully determined by its impulse response *h(t).*

It is a well known approach to exploit a so called M-Sequence for estimating *h(t).* Certain sequences with a sufficiently high order *n* give an auto-correlation function of the antenna signals used which comes close to a Dirac impulse sequence. A direct and preferred way of producing sequences is to use feedback shift-register circuits.

For certain feedback combinations the Maximum Length Binary Sequence (or short M-sequence) results. Figure 3 shows an example of an M-sequence with the order of *n = 4* in the time and frequency domain.

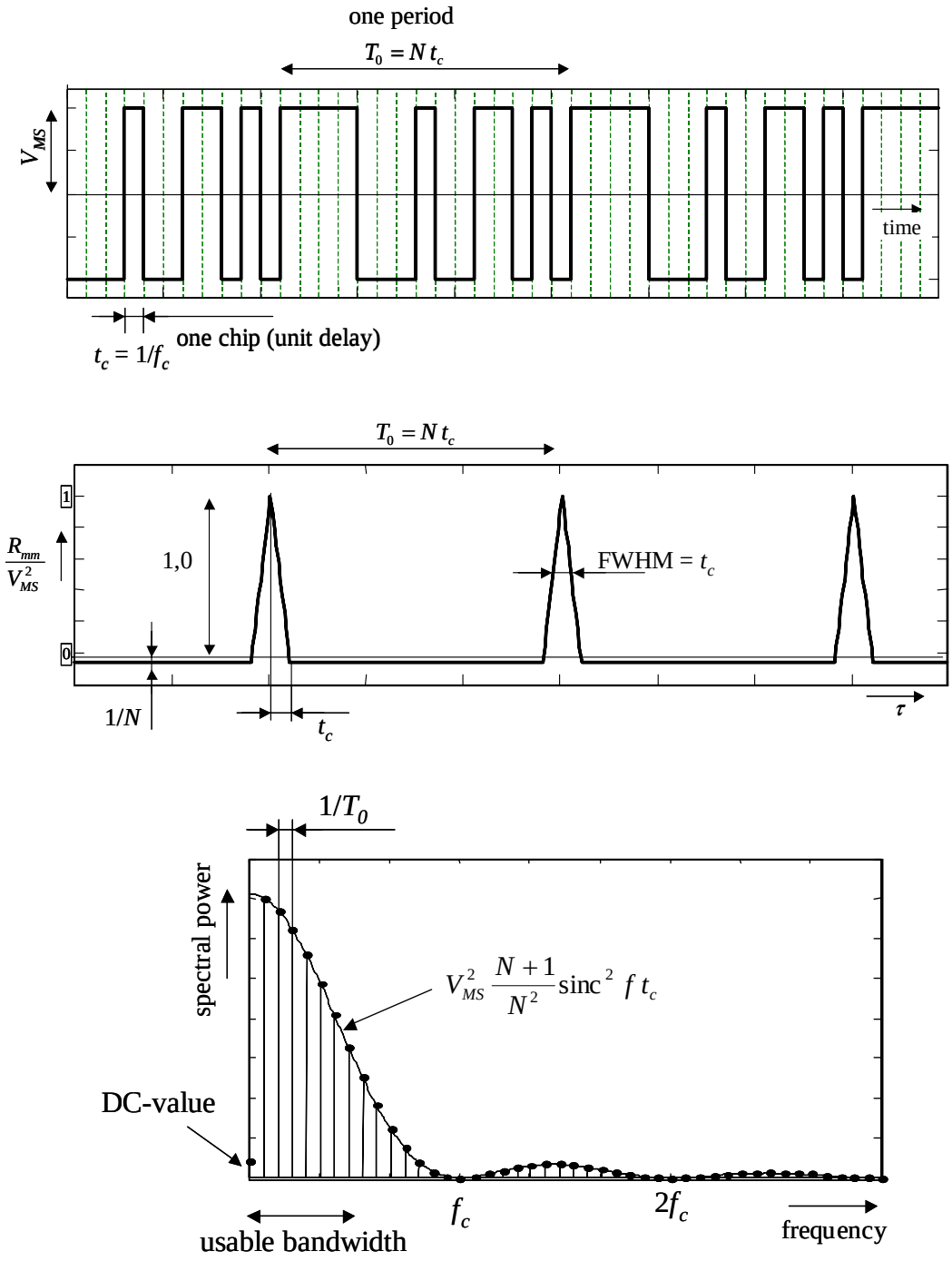

Figure 3 M-Sequence signal, its shape, auto-correlation function and spectrum

The M-sequence is produced on the basis of a highly stable clock and an n-stage shift register. Without additional modulation or signal processing the binary output signal of the shift register is then fed to an UWB antenna. Another antenna of the same kind then receives the back-scattered signals [6]. Here, the LTI-system is denoted with device under test (DUT). In this case, the device under test covers the antennas and the scenario to be monitored.

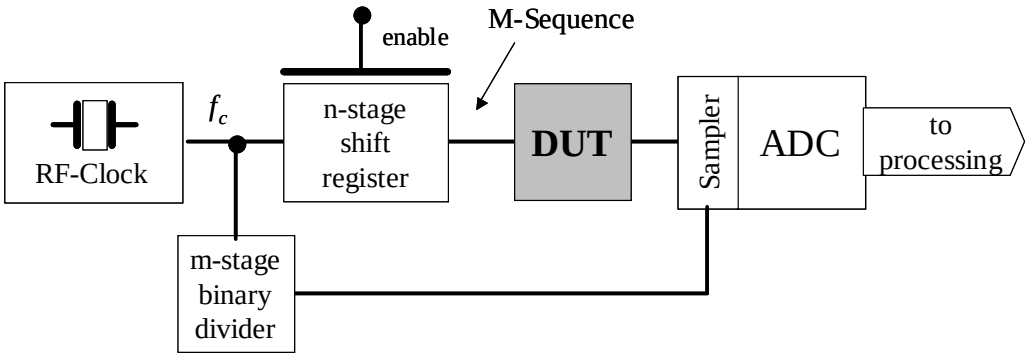

Figure 4 Basic structure of an M-Sequence radar system

It should be mentioned that according to the Nyquist criteria, the sampling of the back-scattered signal would normally be performed at the clock frequency f_c . Fulfilling the demand according to the Nyquist criteria leads to a sampling rate in the GHz frequency range with all associated problems.

If the objects analysed does not (or only to a sufficiently low extent) change properties over time the impulse response can be gained by distinct undersampling. According to figure 4 this is realised by an m-stage divider giving an undersampling factor of 2^m. In the present realisation of the UWB radar sensor the clock rate is set to 9 GHz and 512-times undersampling is performed. Due to direct coupling of the sampling control signal with the system clock the usual jitter and drift problems are reduced. The highly reduced sampling rate has also a positive impact for all following signal processing components. Thus, normal DSP chips or a more convenient PC can be used for the subsequent analysis.

Concepts for UWB enhanced microwave detection of hot spots

The objective of improving microwave fire detection by UWB radar measurements is to help detecting metals or other conducting materials which might prevent electromagnetic waves from reaching the sensor.

A second objective is to obtain information about an object which is a potential hot spot due to previous radiometric measurements showing an increased electromagnetic radiation. The aim is here to determine very roughly the class of the material in order to compensate for to some extent different surface emissivities of the objects. This would contribute to improved measurement results especially in those cases where a limited range of materials is expected.

For such an application UWB sensors are very well suited. If frequency bands match, the UWB antennas could be used for the radiometric measurements too. UWB and radiometric meassurements could even share many other components. The transmit antenna needs to be switched off and just a different processing of antenna signals needs to be performed.

There is also another aspect where UWB radar measurements might improve the capabilities of microwave fire detection sensors. This improvement is related to the advantages of UWB technologies for the localisation of the fire. With UWB devices objects or other UWB devices can be precisely localised.

It has to be taken into account that in a typical situation a classical fire detection system will hardly benefit from UWB radar sensors. The additional information provided by the UWB sensor on the existence of metallic objects influencing microwave fire detection will hardly lead to moving away the corresponding object or to find a new improved position for the microwave sensor.

This situation would be different for special application areas. Such an application is the area of fire detection based on mobile sensors, e.g. on robots. In such a situation the robot could move to another position which gives a clearer “view” on possible hot spots.

The ability to move the sensor position is also extremely useful for taking into account different incidence angles. Smooth surfaces (in terms of the microwave wavelength) only lead to reflections in the direction of the receiver antennas with suitable incidence angles. So a robot could perform measurements at optimised angles. If on the other hand, rough surfaces are analysed, microwaves are scattered in a wide angle and a certain reflectivity pattern does exist. The idea is here to use again the robots motion for measurements at difference incidence angles and thus to estimate the material class of the object.

Finally also the size of objects matter. Here the use of antennas with a small opening angle could be used to reduce the dependency of backscattering on objects size.

Tests performed in the fire lab

Of course the question arises to what degree the UWB radar sensor on its own is able to detect a fire or to distinguish burning from normal material. In order to obtain a first impression on the properties of UWB sensing of fires a test series in the fire detection lab of the University Duisburg-Essen was performed. The tests essentially included a few open fires and smouldering wood fires.

Tests with open fires revealed no response of the radar sensor to flames, which means no back-scattering was observed. Obviously this is due to a too low concentration of charged particles in the plasma of the flame. Although useless for flame detection this feature could be exploited for locating persons behind large fires.

Another objective was to see whether burnt pieces of wood could be distinguished from unburnt pieces. For this reason TF2 test material (beech wood) was partially burnt on the EN54 hotplate and then analysed by means of the UWB radar sensor in a couple of tests. Both transmitter and receiver antennas have been of the double-ridged horn type featuring a slightly frequency dependant opening angle of about 45°.

The experiments started with reference measurements. In these initial experiments only backscattering from the test set-up itself, essentially from a fire resistant board, wooden bars and some metallic construction elements were expected.

Figure 5 shows just the back-scattered data for all experiments with TF2 material. The data was recorded without wood pieces, with wood pieces and with carbonised wood pieces. All data in figure 5 are plotted on top of each other. Due to the band-pass character of the DUT, i.e. mainly the antennas, the signals are showing damped oscillating waveforms.

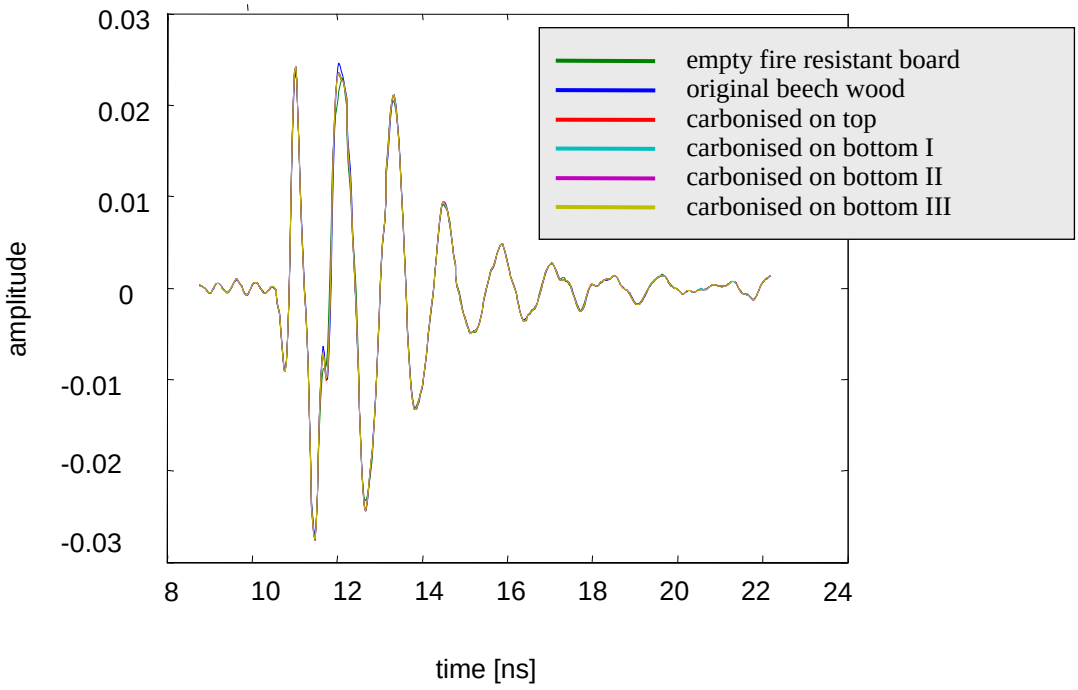

Figure 5 Original data

Apart from the point in time of about 12 ns all plots are quite close. A more closer look at the effect of backscattering due to wood pieces is given in the figures 6 and 7, which show the difference of several tests in comparison to the reference set-up.

Figure 6 shows that the signal amplitudes gained with burnt material are reduced about 1/3 compared to amplitudes for unburnt material. This can be explained by different dielectric constants of wood and the burnt material of which it is assumed to have a dielectric constant value close to that of char coal. For dry wood the dielectric constant value is in the range of 2 - 6. For charcoal the range is 1.2 – 1.8. The measurements were found to be very reproducible, 3 tests using the same set-up gave nearly identical results.

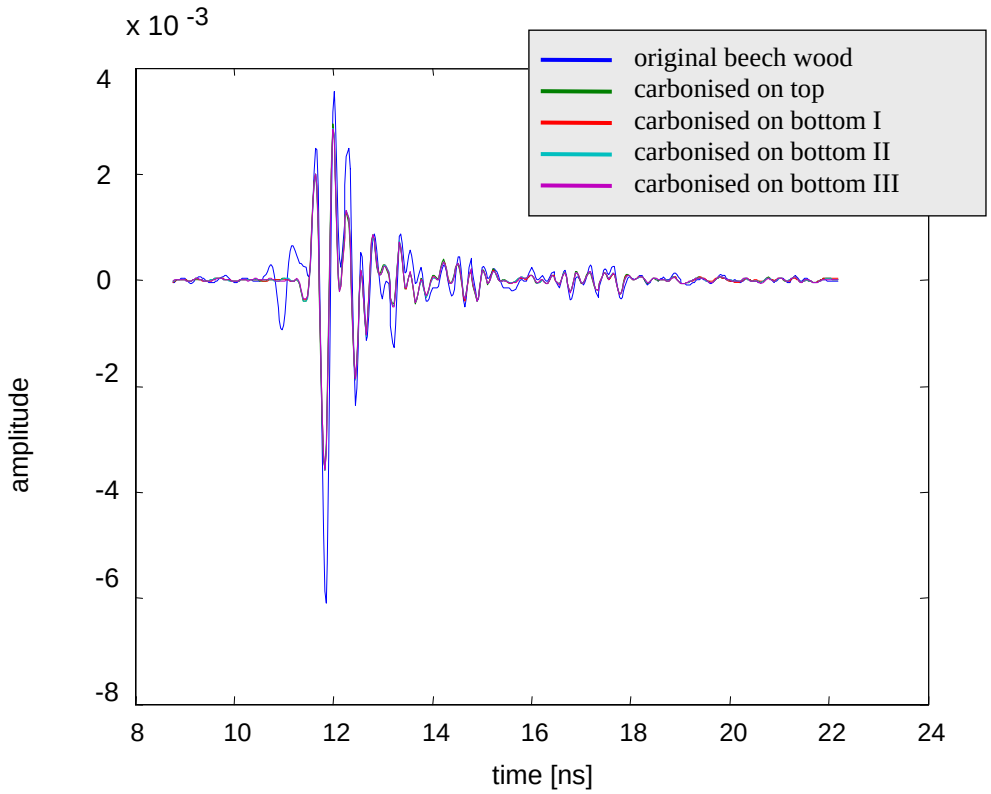

Figure 6 Difference signals (signals gained with burnt material vs. reference signal)

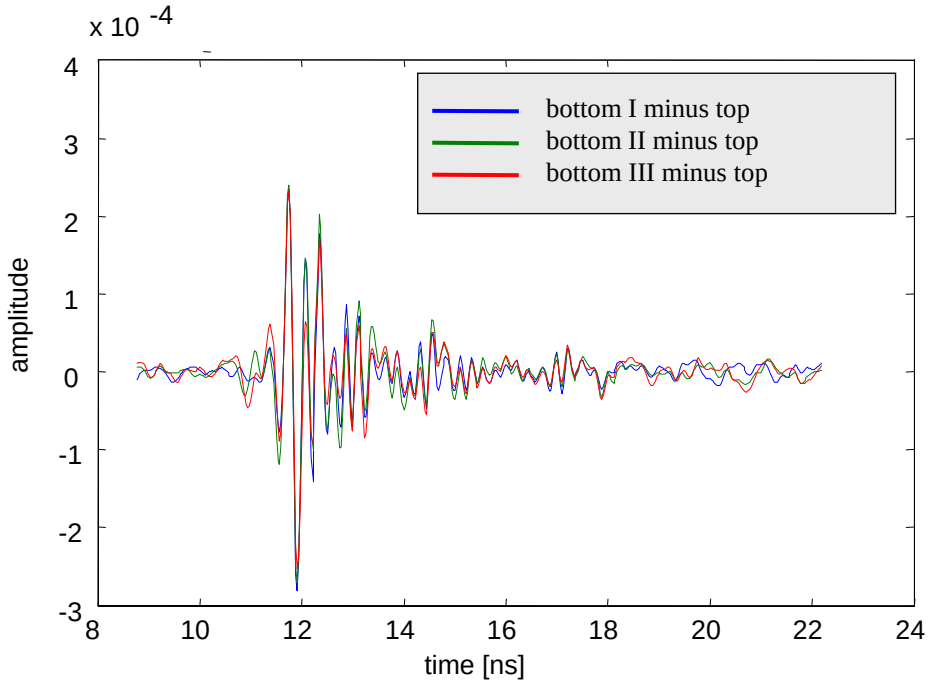

Figure 7 Difference signals for burnt side on top vs. burnt side on bottom

The UWB radar sensor could even distinguish between the different distances (about 5 mm difference) of the carbonised part of the wood to the antenna. Although very small, the signal differences can clearly be observed in figure 7.

Conclusion and outlook

UWB sensors might enhance the detection of hot spots in terms of determining possibly uncovered areas and in terms of roughly classifying the materials scanned. UWB radar technology is a supplement for microwave fire detection insofar as a common set of components can be used. UWB radar technology most probably will not penetrate the market for classical fire detectors. The advantages of UWB radar sensing can be better exploited in a scenario with new mobile sensors.

UWB radar technology in such an application has to take into account different kinds of influences on measurements. So a lot of work needs to be done on methods for compensating as far as possible various effects due to different object size, inclination angle and surface roughness. Concepts of such methods have been described for the application area of mobile sensors.

Recent experiments in the fire lab have indicated the potential of UWB radar technology for precise resolution concerning the localisation of objects. In the (of course) artificial environment of a fire detection lab, burnt from unburnt pieces of TF2 material could be clearly distinguished.

Improved results in terms of spatial resolution (with reduced backscattered signal width) can be expected if the impulse response of the antenna is taken into account by means of deconvolution. Thus the data of scattered signals would indicate dielectric boundaries of even thinner components than those used in the tests.

References

[1] T. Kaiser, T. Kempka, ”Is Microwave Radiation Useful for Fire Detection?”, Proceedings of the 12th International Conference on Automatic Fire Detection AUBE '01, 26.-28.3.2001, Gaithersburg, NIST Special Publication 965

[2] R.L. Chufo, W.J. Johnson, ”A radar coal thickness sensor”, IEEE Transactions on Industry Applications, Vol. 29, No. 5, Sept./Oct. 1993

[3] Homepage of Geophysical Survey Systems, Inc. http:// www.emcgeophysics.com

[4] Homepage of the GPR Laboratory, http://radio.stu.neva.ru/a263/gpr_pict.htm

[5] C.A. Laymon, W. Belisle, T. Coleman, W. Crosson, A. Fahsi, T. Jackson, A. Manu, P. O’Neill, Z. Senwo and T. Tsegaye, ”An experiment in ground-based microwave remote sensing of soil moisture, Journal of Remote Sensing, Vol. 20, No. 4, 1999

[6] J. Sachs, P. Peyerl, R. Zetik, S. Crabbe, "M-Sequence Ultra-Wideband-Radar: State of development and Applications”, Radar 2003, Adelaide, Australia, September 3-5, 2003

Ma Suihua and Yuan Hongyong

State Key Laboratory of Fire Science

University of Science and Technology of China, Hefei, P.R. China

Character of liquid crystal light valve in image fire detection

Abstract

Image fire detection is effective and important to large space safety protection, which is based on the infrared radiation measurement, but the main component to implement infrared filtering are optic glass or liquid crystal light valve. Liquid crystal light valve is a good method because crystal light valve has two-state feature which can integrate the fire safety monitor and guard monitor system. Twisted Nematic liquid crystal light valve is a simple component, but its characters in image fire detection need further studying.

The infrared light-wave can be transmitted in whichever state of TN liquid crystal light valve, but the visible-light is cut in black-state and is transmitted in transparent state. This character of TN liquid crystal valve was studied based on the candle combust experiment, with the result that the polarizer of the light wave can not only polarize the visible light wave but let out the infrared light wave. Another experiment will tell that light intensity loss comes from polarizer, liquid crystal layer or glass base sheet, and how to evaluate the image quality in two-state of image fire detection. All this is important to make a special fire liquid crystal light valve.

The effect of the fire image detection is analyzed in this paper resulting from the visual angle and the light transmission ratio of light valve, and some problems in project are pointed out when using the TN liquid crystal light valve as the light switcher.

1. Introduction

Image fire detection is based on the infrared radiation of flame to detect fire now, and image fire detection system identifies the fire using the image intensity, increasing image area and irregular flame wedge angle [1].

In the engineering application, three devices are used to distill the infrared radiation, which are optical glass, PCTS liquid crystal light valve and Twisted Nematic liquid crystal light valve. Optical glass is a high pass optical filter which has sharp filtering curve and cut-off wave length at 860nm, but it can not be used to implement the fire monitor and guard monitor integrating in the engineering, so in large and important space monitor system, two cameras must be equipped, accordingly, the cost is increased.

Liquid crystal light valve is a special optical device, which has two states that are black state and transparent state. Infrared light can transparent the light valve at two states with a high intensity. But the visual light is entirely different that it is cut at black state and transmits at transparent state. So in the image fire detection system, the liquid crystal light valve can be used to implement the infrared light distilling for its special optical properties, which make the CCD camera capture the infrared radiation of flame and get the infrared flame image.

PCTS liquid crystal light valve has not polarizing film, so its transmitting intensity of visual light at transparent state is higher than TN liquid crystal light valve, but its transmitting intensity of infrared light at black state is smaller than TN liquid crystal light valve.

2. Special optical properties of LCLV

2.1 Principle of LCLV

The usually used LCLV is TN black-type liquid crystal light valve, TN LCLV has two polarizing film and a crystal box. The linearly polarized light generates the double refraction in anisotropic crystal box, the polarizing direction of input light rotates 90 degree angle through the optical axis of crystal molecular, so the input light is cut at the back polarizing film which has the same polarizing direction as the fore polarizing film.

When the square electric wave is pressed on LCLV, all molecular are uniformly arranged and the molecular axis is the same direction as the electric field, and the light

will not twist. Rotation disappears and all light can pass the blank polarizing film.

If the TN LCLV of 90 degree angle wants to control the switch of visual light, it must satisfy the follow inequity:

$$|\Delta nd / \lambda| >> 0.5 \quad (1)$$

In that, Δn is the coefficient of double refraction of liquid crystal material; d is the thickness of liquid layer, that is the 1/4 pitch; λ is the wavelength of visual light in vacuum.

The optical transmittivity of a black-type TN LCLV is

$$T = \sin^2[\pi(1+u^2)^{1/2}]/(1+u^2) \quad (2)$$

In that, $u = 2d\Delta n / \lambda$. When $u = \sqrt{3}, \sqrt{15}, \sqrt{35}, \sqrt{63}\ldots$, and $T = 0$.

Usually, the pitch P of liquid layer is lager than the wavelength of visual light, and the representative value of Δn is from 0.1 to 0.2. If the LCLV want to satisfy the inequity (1), the liquid layer must be thicker, so that the response speed of LCLV is also slower. In the manufacture, $|\Delta nd / \lambda|$ can only be greater than 0.5, when it equals to 0.5, the view angle is biggest.

Although the optical transmittivity and cut-off wavelength of TN LCLV of different manufacturer are different, almost all TN LCLV can transmit infrared light. The 90 degree optical rotation of TN liquid box to visual light is depend on the two polarizing film, but the infrared light doesn't rotate. The follow experiment explains why the TN LCLV produces different effect for the infrared light and visual light.

Experiment materials are candle flame, CCD camera (light spectrum from 400nm to 1100nm), TN LCLV LV47F and optical glass HWB4 (high pass optical filter from 800nm to 2500nm), using these materials we test the optical selectivity of polarizing film.

Fig.1 is the image produced by CCD camera of candle flame of experiment 1 in which the flame transparent the single LCLV. Fig.2 is the image of candle flame of experiment 2 in which flame transmits two LCLV; In experiment 3, two LCLV is laid orthogonal, and candle flame transmits the HWB4 first, then transmit the two LCLV, Fig.3 is the result image; In experiment 4, two LCLV is laid orthogonal also, but candle flame directly transmit the two LCLV, Fig.4 is the result image of experiment 4.

Fig.1 Flame image of single LCLV

Fig.2 Flame image of two LCLV

Fig.3 Flame image of infrared light

Fig.4 Flame image for two orthogonal laid LCLV

From the four experiments, we found that the two orthogonal laid LCLV did not rotate the infrared light which produced by the optical glass HWB4, and the polarizing film has not the entirely polarizing effect to infrared light. In another experiment, we let the incandescent light transmit the two orthogonal laid LCLV, and the result image is entirely black.

So we can know from experiment that the 90 degree angle TN LCLV can not make the infrared light rotate, but it can decrease the intensity of infrared light.

2.2 The effect to fire detection of optical property of LCLV

From experiment 1, we know that TN black-type LCLV can not make the visual light from 400nm to 750nm entirely cut-off at transparent state, because the liquid layer can make only one special wavelength exactly rotate 90 degree angle. The spectrum

transmitivity of single LCLV LS-043a-2 is displayed in Fig.5.

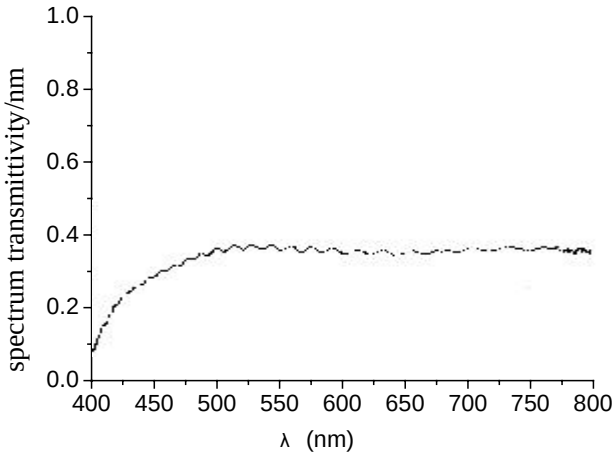

Fig.5 Spectrum transmittivity of single LCLV LS-043a-2

CCD camera has high sensitivity to visual light, so we must use two TN liquid crystal light valves (LV47) which are parallel bonded to reduce the leakage of visual light that results the false infrared image. The spectrum transimittivity of two LV47 is displayed in Fig.6. In the Fig.6, curve 1 is the spectrum transimittivity at transparent state, and curve 2 is the spectrum transimitivity at black state. Apparently, two LCLV can cut off the visual light entirely at black state, and the transimittivity of infrared light is almost same at both black and transparent state. This character exactly satisfies to integrate the infrared fire detection and guard monitor.

Two LCLV has four polarizing film and increase the optical distance which make the intensity of visual light reduced large at transparent state, so that the signal-noise ratio of CCD image are decreased. But in engineering, the image quality and the sensitivity that is millisecond degree of rise-time and fall-time of LCLV can entirely satisfy the guard monitor. The infrared radiation is reduced with the distance, so in image fire detection engineering, we should use the smaller relative aperture, small view angle and long focus lens to increase the sensitivity to infrared image of the image fire detection system using LCLV.

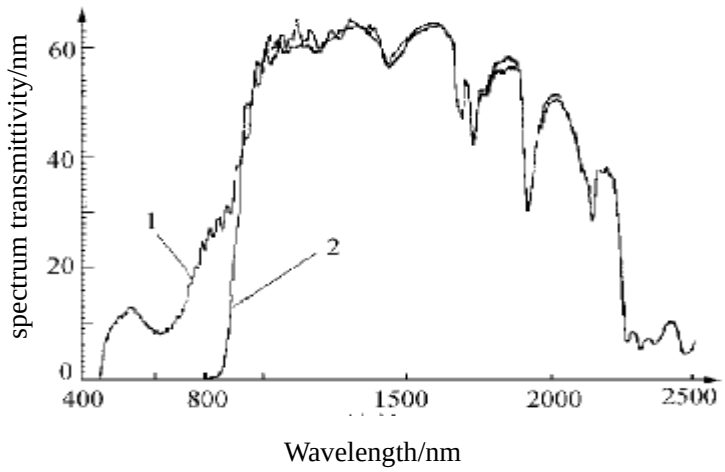

Fig. 6 Spectrum transmittivtiy of two LV47

2.3 The view angle of TN LCLV

The view angle of TN LCLV depend on $\Delta n \cdot d$, the biggest horizontal view angle of LV47 is 60 degree and the biggest vertical view angle is 40 degree, so the view angle of CCD camera and lens should not exceed 60 degree. If the view angle of lens exceeds 60 degree, the image of CCD camera has four black spot at transparent state and the area of black spot increases with lower electric pressure. If increasing the electric pressure, the black spot decreases, and if increasing the frequency of electric pressure, the black spot move to edge, when increasing electric pressure to 8 volt and 300HZ, the black spot disappear. Fig.7 gives the curve of transmittivity with view angle [3]. In that, Cr is the contrast, when Cr is small than 2, the image is entirely indistinctness, and when it is bigger than 3, the quality of image is better. From Fig.7, we can found the area that Cr is bigger than 3 is limited in area of the biggest horizontal view angle and vertical view angle. In image fire detection, the detection area is decreased for view angle of LCLV.

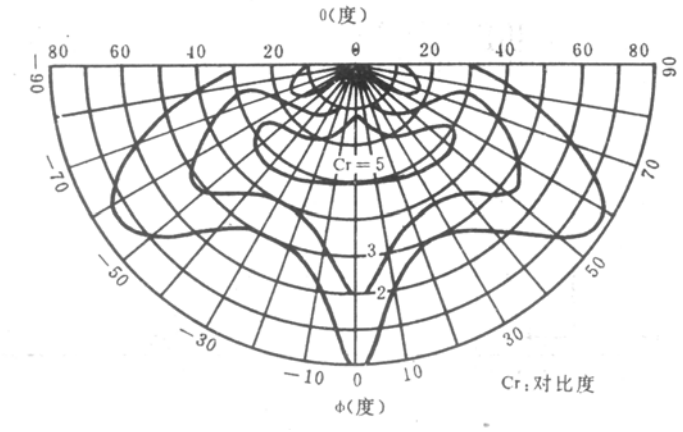

Fig.7 View angle- transmittivity curve

3. Conclusion

Image fire detection is important to large space fire safety monitor, and the image fire detection system using TN LCLV can implement to integrate the image fire detection and guard monitor which is easily control. Because the limit of LCLV, such as view angle and transmittivity, we should use two LCLV, the smaller relative aperture, small view angle and long focus lens. We have successively used this image fire detection and guard monitor system in other school. With the further study of liquid crystal material and polarizing film, a special LCLV for image fire detection will be developed.

References

1. Wu longbiao, Song weiguo, Lu jiecheng. The application of liquid crystal light shutter in fire detection. Optical Technique. 1999, No.1. (in Chinese)
2. Fan zhixin, the technology basis of liquid crystal device,2000.(in Chinese)
3. Wang qingbing, Studies and Application of Transmittance-Wavelength Dependence of Normal-Mode PCTS shutters. Liquid crystal and displays, 1999, No.3 Vol.14.(in Chinese)

D.T. Gottuk, J.A. Lynch
Hughes Associates, Inc., Baltimore, Maryland USA

S.L. Rose-Pehrsson, J.C. Owrutsky, F.W. Williams
Naval Research Laboratory, Washington D.C. USA

Video Image Fire Detection for Shipboard Use

Abstract

The objective of this work was to evaluate the effectiveness of commercial video image fire detection systems for small, cluttered spaces as would be found on navy ships. The primary goal was to establish an understanding of the performance sensitivity and limitations of the video image detection (VID) systems to various setup and environmental conditions that may occur onboard ship while exposed to a range of flaming and smoldering fire sources and potential nuisance alarm sources. The response of the VID systems was benchmarked against standard fire alarm systems using addressable ionization and photoelectric smoke detectors.

Introduction

Computer processing and image analysis technologies continue to improve significantly, which has allowed the recent development of effective video image fire detection systems. Typically, these systems have been designed and used in large facilities, outdoor locations and tunnels. However, the technologies are also proving effective in smaller, cluttered compartments found on ships and in commercial and industrial sites. With the increasing move to use onboard video for surveillance and security, there are advantages in using the video images for other functions, such as fire detection. In addition, video image recognition technology has the potential for personnel tracking, flooding detection and physical damage assessment.

This work represents part of an ongoing multi-year program to identify, evaluate and adapt video image detection (VID) technologies for improved situation awareness and damage control assessment onboard navy ships [1]. Three commercial video image fire detection systems were evaluated in multiple full-scale test programs with a range of

flaming and smoldering fire sources and potential nuisance alarm sources. The primary objective of the last test series and the focus of this paper, was to establish an understanding of the performance sensitivity and limitations of the VID systems to various setup and environmental conditions that may occur onboard ship. Toward this end, 280 full-scale tests were conducted in a mockup of a shipboard compartment and passageway to evaluate the performance of the detection systems under various background, lighting and camera setting configurations while exposed to a range of flaming and smoldering fire sources and potential nuisance alarm sources. Conditions that were evaluated consisted of white and gray bulkheads (walls) and dim to bright white lighting, as well as red illumination. Camera settings were systematically varied to include optimal images, out of focus and poor contrast images. The response of the VID systems was benchmarked against standard fire alarm systems using addressable ionization and photoelectric smoke detectors. Due to the limited space in this report only highlights of the experimental setup and results are provided. Full details of the extensive test program are discussed in Reference [2].

Experimental Setup and Procedures

Test Spaces

The tests were conducted in a 10 m x 10 m x 3 m high (33 ft x 33 ft x 10 ft) test facility that was divided into three compartments and a passageway. As shown in Figures 1, only the 5.9 m (19.5 ft) x 8.8 m (29.0 ft) compartment and the adjacent 10.0 m (33.0 ft) long by 1.2 m (4.0 ft) wide passageway were instrumented with detection systems and used as locations for fire and nuisance sources during the tests. Though the other spaces were not directly used, the doorways between all spaces were open during the tests, but the multi-room facility was closed and isolated from the lab. No active ventilation was used during the testing.

The compartment contained “overhead beams” constructed of steel sheeting, These simulated “beams” created visible obstructions (camera line of sight) as well as physical obstructions to smoke travel in the overhead. The simulated beam obstructions were secured to the overhead with a spacing of 1.2 m (4ft) and depths of 30 cm (12.0 in), the passageway had a smooth overhead. The compartments contained multiple visual

obstructions such as electrical cabinets, chairs, tables, office equipment, cable trays and ductwork.

Consistent with the range of various lighting conditions on U.S. Navy ships, four nominal conditions were studied in this work: 1) 7 footcandle (Fc), 2) 14 Fc, 3) 28 Fc and 4) red illumination. Lighting was installed in general accordance to the military standard (DoD-HDBK-289) in the overhead of the test compartments to provide the illumination comparable to various spaces onboard naval ships. Commercial 20-Watt, 120 VAC fluorescent light fixtures [Lithonia model number LB 2 20 120 LPF] were suspended approximately 0.3 m (12 in) below the overhead, making them flush with the overhead beams. Two 20-Watt fluorescent bulbs [General Electric model number F20T12/CW] were used with each light fixture. The 28 Fc light level included the additional use of halogen lamps. The red illumination was accomplished by covering the fluorescent bulbs at the 14 Fc setup with colored sleeves [Arm-A-Lite Safety Sleeves model number TP312W/R/T12]. Photometric surveys were conducted to ensure the uniformity and level of illumination at 0.76 m (30 in.) above the deck as defined in the military standard. The nominal illumination levels determined per the U.S. Navy guidelines were slightly less than desired, for example the calculated 14 Fc level had an initial value of 12.2 +/- 2.0 Fc across the space.

In addition to the changes in illumination and camera settings, different colored bulkheads were evaluated to analyze the video systems performance to various background colors typical of naval ships. Based on ship visits and design specifications, two colors were selected to provide a range of conditions. The test spaces were painted a standard Navy ship interior color of white and gray. The colors were matched by Sherwin-Williams to be indistinguishable by the naked eye to DOD-E-24607A chlorinated alkyl enamel paint color white (FED-STD-595 color No. 27880) and bulkhead gray (FED-STD-595 color No. 26307). The forward and port bulkheads were painted gray while the aft and starboard bulkheads in Compartment 1 were painted white.

Instrumentation

The primary instrumentation consisted of three video image fire detection systems and two commercial, smoke detection systems (referred to as Spot-1 and Spot-2) used to provide a benchmark of state-of-the-art, spot-type fire alarm equipment performance. Two of the three VID systems utilized both smoke and flame alarm algorithms; the third system used only a smoke algorithm. One of the systems with flame alarms utilized two different flame algorithms: one for fires in the field of view of the camera and an "offsite" algorithm for detecting the reflections of flames that are out of the field of view of the camera. All three of the video image detection (VID) systems used the same cameras located in the test spaces. Each camera image was sent to each VID system as well as a digital or VHS recorder via an amplified splitter.

The Spot-1 system smoke detectors were monitored using a corresponding manufacturer alarm panel with default alarm sensitivity levels, which were the least sensitive settings at 11.0%/m (3.5%/ft) for the photoelectric units and 5.1%/m (1.6%/ft) for the ionization units. The Spot-2 system detectors were controlled using a corresponding manufacturer alarm panel set to 6.76%/m (2.12%/ft) for the photoelectric units and 5.62%/m (1.75%/ft) for the ionization units.

The detector types and their respective locations in each test compartment were chosen to allow the response of the different detection methods to be compared based upon complete systems with full space coverage. The smoke detectors were installed to industry standards (i.e., NFPA 72 [3]). The VID systems were setup per the recommendations of each manufacturer. These systems received images from six cameras located around the periphery of the space as shown in Figure 1. These camera locations did not necessarily represent the optimum placement. Rather, the cameras were setup to provide a range of views that covered the entire test area. The optimum number of cameras and placement were evaluated by assessing the performance of different groupings of cameras within the spaces. Two models of standard CCD color cameras (Sony SSC-DC14 and Sony SSC-DC393) were used with Pentex manual iris 3.5 to 8 mm, variable focus lenses.

Fire and Nuisance Sources

Twelve fire and eleven potential nuisance sources were created to expose the detection systems to a range of scenarios. Small smoldering and flaming fires were used to challenge the detection systems and to provide performance results for early detection. The sources were located throughout the test spaces as shown with the numbered squares in Figure 1. Fire sources included smoldering and flaming cables and mattresses, various cardboard box fires and trash fires, and smoldering computer monitors and printed circuit boards. Potential nuisance sources were developed with a focus on the video detection systems as opposed to the spot-type smoke detection systems. These included, various numbers of people working and smoking within the space, waving white material, spray aerosol, overdone toast, welding, grinding steel, burst of sunlight, flash lights and flash bulbs.

Procedures

The focus and iris settings of the cameras were systematically varied for individual cameras to yield optimally set images, dark and light images, and out of focus images.

The focus and iris of the cameras were adjusted to provide video images that were not optimal, yet still within tolerable conditions, in other words, conditions that may not evoke the need for immediate adjustments. The iris controls the amount of light into the camera; it is used to maximize and sharpen the division between dark and light objects (i.e., the contrast). If the iris is closed too far, the contrast will be very dark with loss of detail in parts of the image. If the iris is opened too far, the contrast decreases causing the image to become over exposed.

After baseline conditions were established for all camera settings and detection systems, sources were initiated and testing commenced. The test was terminated after all alarms had occurred or after conditions were deemed to have reached a maximum or steady-state level, such that no other detection alarms were anticipated.

Results and Discussion

A set of tests was conducted with all six cameras collocated at Camera Location 1 such that they had essentially the same view but different camera settings to yield a range of

optimal to out of focus and off-contrast images. The response of each algorithm (smoke and flame) was monitored individually for each VID system. Overall, the systems demonstrated the ability to detect smoke and fire for numerous camera settings and lighting conditions. Compared to VID system performance with the cameras set to provide optimal video images, the dark contrast and low illumination levels generally resulted in better detection of flaming fires, while the light contrast and high illumination levels resulted in improved detection of smoke. Although the VID systems demonstrated the ability to alarm to various camera settings and light levels, specific combinations of illumination, camera setting and VID system algorithm did result in undetected fires. The smoke algorithms for two of the systems generally did not alarm when cameras set to dark contrast were located in a compartment under red illumination. The flame algorithm for one of the same systems would not produce an alarm when the Sony SSC-DC393 cameras were in a compartment with red illumination. No problems were observed for the other model camera. With exception to these relatively extreme cases (cameras with dark settings at 14 Fc and then subjected to red illumination which made the images even darker), the VID systems were able to consistently produce alarms. These results indicate that the VID systems taken as a whole (i.e., considering the combined performance of both the smoke and flame algorithms) are not very sensitive to camera settings as long as reasonable video images are obtained; this includes images that are slightly out of focus and with non-optimal contrast.

The results collected indicate that the effect of potential shipboard background color on VID system fire detection performance is insignificant. The type of fire source and relative location to the field of view of the camera played a greater role in detection capability and activation times. For example, when a flaming fire is within the line of sight of the camera the VID-1 and VID-2 systems readily detected the fire source with the flame algorithms. When the fire was moved to an obscured location the flame algorithms became ineffective. The exception was the VID-1 offsite algorithm, considered an indirect flame algorithm, which maintains the ability to detect obscured flaming fires via detection of reflections. The tests indicate that the offsite algorithm may only be effective in circumstances where relatively bright or sizable reflection

areas are in the video image. In circumstances where the fire is across the room from the camera, fully behind obstructions, the general flickering illumination from the fire may not be sufficient. This diminished performance was observed for the flaming box fires, where the offsite algorithm did not pick up the fire when it was on the other side of the compartment. Additional work in the broader program [1], has shown that the use of near infrared video with luminosity algorithms are more sensitive to these lower intensity reflections [4].

An analysis was performed to assess the performance of the VID systems as a function of the number of cameras in the space. This analysis was based on a set of 83 tests in which the six cameras, set for optimal images, were distributed around the test compartment as shown in Figure 1. Figure 2 shows the percent of fires detected versus the percent of nuisance alarms as a function of the number of cameras used in the space for each VID system. As shown in the figure, using any two-camera combination in the test space, the two multi-algorithm VID systems alarmed to a range of fire sources and source locations with average alarm rates of 93% and 94%, respectively. The corresponding nuisance alarm rates were 33 and 17 percent, respectively. The third VID system did not perform as well detecting only 63% of the fires when considering any two-camera combination system in the space.

The commercial VID technologies clearly demonstrated the ability to alarm to more sources faster than the spot-type detection systems during the series of 83 multiple source fire tests. Based on the analysis above, Cameras 1 and 4 were selected as a representative two-camera system for the space. The performance of each VID system using this two-camera combination was compared to each of the spot-detection systems. Two aspects of detector performance were compared: number of fire sources detected and speed of detection. Table 1 presents the number of fire sources detected by each VID and spot-detection system. The VID-1 and VID-2 systems demonstrated comparable ability in detecting flaming fires to the Spot-1 and Spot-2 ion detection systems. The VID-3 system and the photoelectric detectors did not perform as well, detecting only 35 to 62% of the flaming fires. The VID-1 and VID-2 systems also detected more smoldering fires than the photoelectric spot-detectors, detecting 92% and 95% versus 76% and 71%, respectively. The results from the smoldering and flaming

fire tests were combined to give the overall performance of the systems. The VID-1 and VID-2 systems detected 95% and 96% of the fires, whereas the next best performance was the Spot-1 ion system, alarming in 67 of the 83 fires or 81%.

The VID systems and spot-type detection systems alarm times were compared on a test-by-test basis to identify detection performance as it pertains to speed of detection. In general, the Spot-1 ion detectors produced the quickest alarm times in a majority of the flaming fires while the VID systems produced quicker alarm times for the majority of the smoldering sources. When the Spot-1 ion detectors did produce a quicker alarm during a flaming fire, it was nearly 2 minutes before the VID systems. When the VID systems produced quicker alarms during the smoldering sources it was approximately 4 to 7.5 minutes before the spot-type detectors (ion or photo). One notable deviation from the general trend is this; the VID-1 system alarmed faster to more fires than all of the VID and spot-type detection systems, with faster alarm times independent of source type and type of spot detector.

The passageway provided a space with a different aspect ratio than used in any prior tests. The change in dimensions narrowed the field of view of the cameras. In general, the VID systems had similar alarm responses to fires, such as the flaming boxes and smoldering cable fires, in the passageway and in the compartment. Overall, the passageway did not present any clearly identifiable issues for the VID systems that were not identified in the compartment tests for either fires or nuisance sources.

Conclusions

Real-scale fire tests in mock ship compartments were conducted to evaluate the fire detection performance of three commercially available video image fire detection systems under various lighting and camera setting configurations. The VID systems demonstrated the ability to detect smoke and fire for numerous camera settings and lighting conditions, indicating reliable performance for sub-optimal video images. Using a two-camera system in the same compartment with two spot detectors, the VID systems generally detected more fires and also detected fires, particularly smoldering, faster than the spot-type detection systems.

References

1. Rose-Pehrsson, S.L, Owrutsky, J.C., Wales, S.C., Farley, J.P, Williams, F.W., Steinhurst, D.A., Minor, C.P., Gottuk, D.T., and Lynch, J.A., "Volume Sensor for Damage Assessment and Situation Awareness, *AUBE '04 – Proceedings of the 13th International Conference on Automatic Fire Detection*, Duisburg, Germany, September 14-16, 2004.
2. Lynch, J.A., Gottuk, D.T., Rose-Pehrsson, S.L., Owrutsky, J.C., Steinhurst, D.A., Minor, C.P., Wales, S.C., Williams, F.W., and Farley, J.P., "Volume Sensor Development Test Series 2 – Lighting Conditions, Camera Settings, and Spectral and Acoustic Signatures," NRL/MR/6180—04-XXXX, June 2004 (in review).
3. National Fire Protection Association, "NFPA 72 – National Fire Alarm Code, 2002 Edition," National Fire Protection Association, Quincy, MA, 2002.
4. Owrutsky, J.C., Steinhurst, D.A., Minor, C.P., Rose-Pehrsson, S.L., Gottuk, D.T and F.W. Williams "Long Wavelength Video Detection of Fire in Ship Compartments," *AUBE '04 – Proceedings of the 13th International Conference on Automatic Fire Detection*, Duisburg, Germany, September 14-16, 2004.

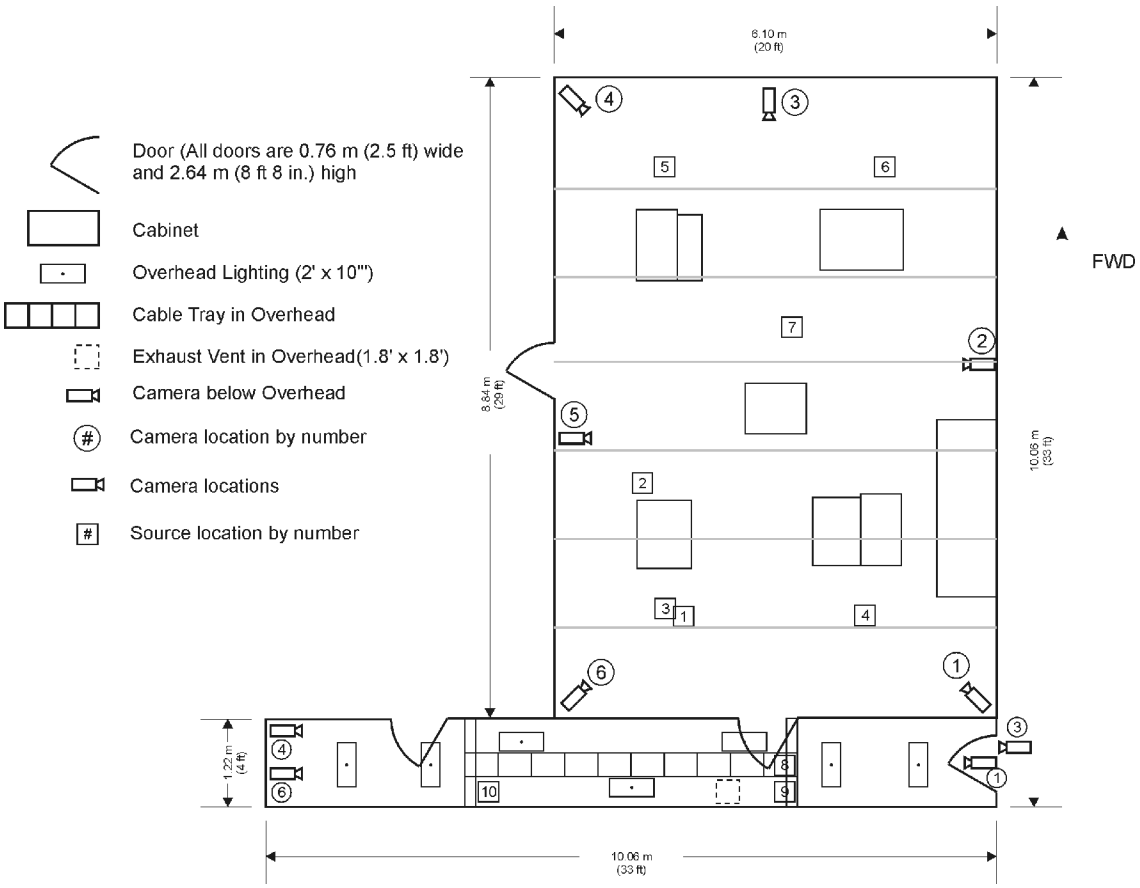

Figure 1. Schematic of experimental setup

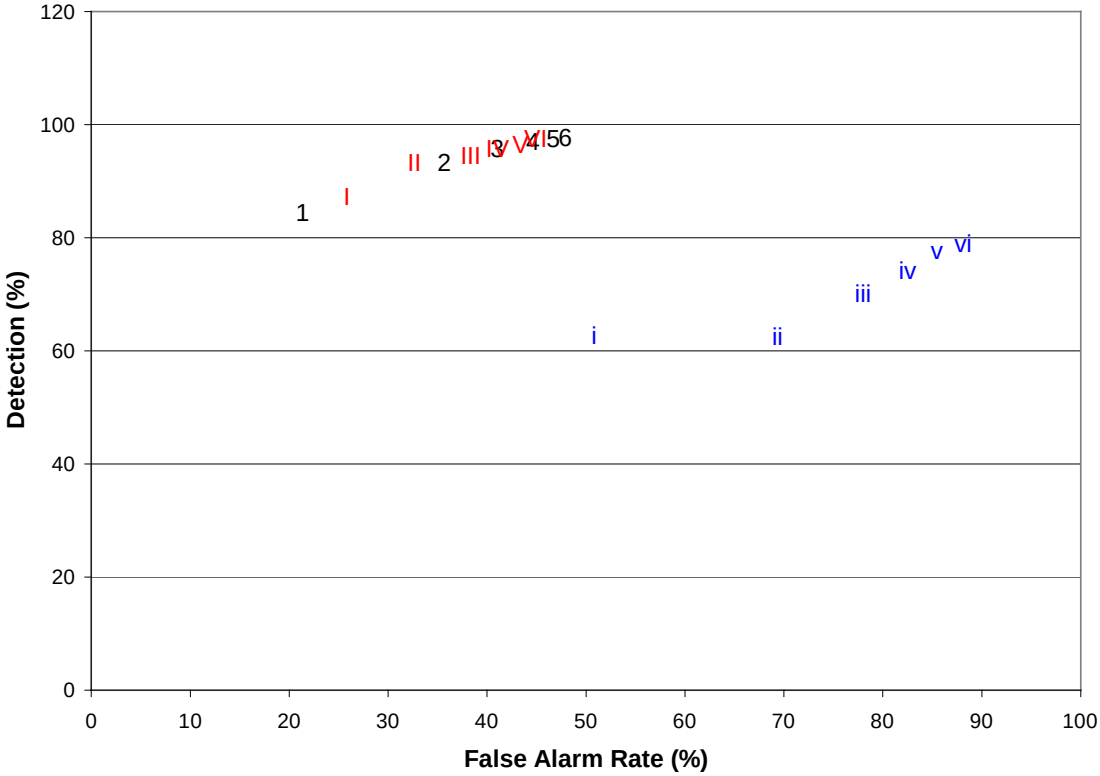

Figure 2. A plot of the percent of fire sources detected versus the percent of nuisance sources detected for various numbers of cameras in a VID system. The numbers indicate the quantity of cameras in a system. The color and font identify the system: black (1,2) is VID-1, red (I, II) is VID-2, and blue (i, ii) is VID-3.

Table 1. Ratios and percentages of sources detected by each detection system to the total number of sources tested for smoldering and flaming fires.

	Number of Flaming Tests	Number of Smoldering Tests	Total Number of Tests	% Alarm Activation (Flaming)	% Alarm Activation (Smoldering)	% Alarm Activation (All Tests)
VID-1	34/34	45/49	79/83	100%	92%	95%
VID-2	33/34	47/49	80/83	97%	96%	96%
VID-3	21/34	31/49	52/83	62%	63%	63%
Spot-1 Ion	34/34	33/49	67/83	100%	67%	81%
Spot-1 Photo	12/34	37/49	49/83	35%	76%	59%
Spot-2 Ion	34/34	19/49	53/83	100%	39%	64%
Spot-2 Photo	15/34	35/49	50/83	44%	71%	60%

R. Lüttenberg

VdS Schadenverhütung, K ln, Deutschland

urop ische ormen

Die neue orm 1 0 -1 00 f r automatische elektrische Steuer- und er gerungseinrichtungen

Abstract

Fire detection and fire alarm systems are linked to other systems e.g. especially fire protection systems. Often a connection is provided to fire extinguishing systems, whereas the triggering and control of gas extinguishing systems is special case. The perfect functioning of an extinguishing system as part of a whole fire protection concept is of high importance.

The activation of a gas extinguishing system requires a set of parameters to be taken into account. To ensure the functioning of a whole installation, requirements were established for a reliable activation of the extinguishing system, taking into account necessary life safety aspects.

The result of these considerations is the standard EN 12094-1 for electrical automatic control and delay devices (e.c.d.). Such a device may be inserted into a control and indicating equipment (c.i.e.) of a fire detection system or may be constructed as a separate device, to be connected by wires. The standard was developed following the standard EN 54-2 for c.i.e s, so that its structure is similar to the structure of EN 54-2 consisting of mandatory requirements, which have to be provided for each e.c.d. and options with requirements, which may be provided and possibly reflect national peculiarities. The mandatory functions are restricted to

-the receipt of triggering signals (from a c.i.e. or manual triggering devices)

-the undelayed activation of alarm devices

-the undelayed transmission of the extinguishing signal (e.g to a solenoid valve)

for each flooding zone.

The mandatory functions are supplemented by a number of options with requirements. In addition, the e.c.d. shall be provided with technical means to detect faults, to disable and enable certain functions and to indicate each condition, corresponding to the different events in a clear and unambiguous way. Detailed information, as far as possible, is given on the

functional operating sequence and the interaction between the c.i.e. and the e.c.d and on the connected peripheral devices, representing the whole fire protection installation.

inleitung

Ortsfeste L schanlagen mit gasf rmigen L schmitteln werden heute häufig über automatische Brandmeldeanlagen angesteuert und über l schanlageneigene Steuer- und Verz gerungseinrichtungen gesteuert. In der Norm EN 54-1 ist der Aufbau eines Brandmeldesystems mit seiner zu erwartenden Peripherie schematisch dargestellt. Neben der Ansteuerung von Alarmierungseinrichtungen zur Warnung von Personen, der bertragung einer Brandmeldung an die Feuerwehr wird auch die Aufgabe der Ansteuerung von automatischen Brandschutzeinrichtungen (G) von einer Brandmeldeanlage ausgeführt. Dabei stellt (G) die Steuereinrichtung für automatische Brandschutzeinrichtungen dar. Was sich zeichnerisch sehr einfach darstellen lässt, kann jedoch in der realen Umsetzung sehr komplex werden. Dies trifft insbesondere bei L schanlagen mit gasf rmigen L schmitteln zu, bei denen Personenschutzmassnahmen sicher zu stellen sind. Die Anforderungen an eine Steuer- und Verz gerungseinrichtung einer solchen Gas-L schanlage sind in der neuen EN 12094-1:2003 zu finden.

Das Gesamtkonzept einer BMA in Verbindung mit einer L schanlage, einschl. der Aufgabenstellungen, lässt sich wie folgt darstellen.

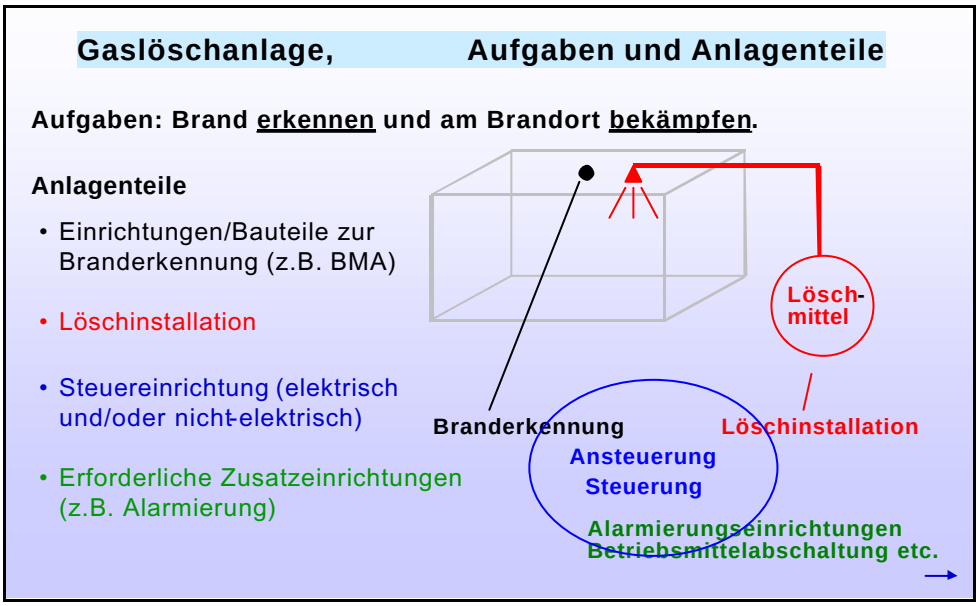

1 0 -1

Für den berblick über den Aufbau und die Systematik sind insbesondere die folgenden Punkte wichtig:

- -Anwendungsbereich
- -Umweltklassen
- -Verbindliche und wählbare Funktionen
- -Berücksichtigung von Einbereichs- und Mehrbereichssteuerungen
- -Anhang A

An endungsbereich

Der Anwendungsbereich bezieht sich auf elektrische Steuer- und Verz gerungseinrichtungen (EST) für CO_2-, Inertgas- und Haloncarbongas- Feuerl schanlagen. Die Steuereinrichtung kann dabei Bestandteil einer Brandmeldeanlage, eingesetzt in eine Brandmelderzentrale (BM), oder der Feuerl schanlage sein. u beachten ist, ob an die EST auch direkt Brandmelder angeschaltet werden sollen, da sich dann der Anforderungsumfang an die EST um die EN 54-2 erweitert.

Anwendungsbereich:

- Elektrische Steuer- und Verzögerungseinrichtungen (für Gaslöschanlagen), die in Brandmeldeanlagen oder Gaslöschanlagen eingesetzt werden. (EST)

- **Separate Einrichtung** oder **in einer BMZ integrierte Funktionen**

Eine separate EST erhält Eingangssignale immer von einer BMZ.

Werden an das Gerät auch Brandmelder angeschaltet, ist das Gerät eine BMZ mit integrierter EST und muss auch EN 54-2 entsprechen.

m eltklassen

Im Gegensatz zu der für BM vorgesehenen Anwendung in sog. sauberen und trockenen Räumen (Einsatztemperaturbereich von –5 °C bis 40 °C), ist der Einsatzort einer EST vergleichbar mit dem Einsatzort anderer peripherer Geräte für Brandmeldeanlagen. In der

Tradition der Europäischen Normen für L schanlagen ist für die Peripherie hier jedoch der Temperaturbereich –20 °C bis 50 °C vorgesehen. usätzlich wird auch der Einsatz in korrosiver Atmosphäre unterstellt. Es sind vier Umweltklassen vorgesehen.

-Klasse A	-5 °C	bis	40 °C	
-Klasse B	-20 °C	bis	50 °C	
-Klasse C	-5 °C	bis	40 °C	plus korrosiver Atmosphäre
-Klasse D	-20 °C	bis	50 °C	plus korrosiver Atmosphäre

Der Hersteller einer EST muss sich also entscheiden, für welche Umgebungsbedingungen sein Gerät vorgesehen sein soll. Die Umweltprüfungen sind weitestgehend identisch mit denen, die in der Norm für Brandmelderzentralen EN 54-2 vorgesehen sind. Allerdings ergaben sich nderungen aufgrund der vorgesehenen Umweltklassen bei den Prüfungen „Feuchte Wärme", „Kälte" und „Schwingen". Für EST nach den Klassen C und D ist eine zusätzliche Korrosionsprüfung vorgesehen

erbindliche und hlbare Funktionen

Wie schon bei Brandmelderzentralen gestaltete sich auch hier die Normungsarbeit als schwierig. Grund: In mehreren europäischen Ländern lagen schon Anforderungen an EST vor, die sich jedoch signifikant unterschieden. Daher wurde der gleiche L sungsweg wie bei der Normierung von BM beschritten. Es wurde unterschieden zwischen verbindlichen und wählbaren Optionen, wobei nur wenige verbindliche Funktionen fest-geschrieben wurden. Bereits national vorliegende Anforderungen an solche Einrichtungen und damit verbundene unterschiedliche Philosophien wurden analog zu EN 54-2 in Optionen mit Anforderungen widergespiegelt. Für den Hersteller einer solchen Einrichtung bedeutet dies Informationszwang zu den in den einzelnen europäischen Ländern geforderten Funktionen für eine EST, damit er die entsprechenden in der Norm aufgeführten Optionen auswählen kann, wenn er einzelne Märkte mit seinem Produkt bedienen will. Sieht er Europa als einen Markt an, tut er gut daran, alle aufgeführten Optionen für sein Produkt vorzusehen. Optionen sind immer mit Anforderungen verbunden, die zu erfüllen sind.

Verbindliche Funktionen

Die verbindlichen Funktionen beschreiben die Mindestanforderungen an die Funktionalität der EST. Diese beschränken sich auf den Empfang von Eingangssteuersignalen und die nachfolgende unverz gerte Ansteuerung eines Alarmgerätes und eines elektrischen Elementes in der L schinstallation. Wenn die EST für mehrere L schbereiche vorgesehen ist, gelten die Mindestanforderungen pro L schbereich. Generell sind wie in EN 54-2 für BM in jeder EST – unabhängig vom Ausbau – berwachungsfunktionen zur St rungserkennung, Bedienelemente zur Ab – und Einschaltung bestimmter Funktionen sowie Anzeigelemente zur Anzeige der verschiedenen Betriebszustände vorzusehen. Die verbindlichen Funktionen sind nachstehend aufgeführt und bildlich dargestellt:

1) Empfang und Verarbeitung eines Eingangssteuersignals von einer BMA (BM)

2) Empfang und Verarbeitung eines Eingangssteuersignals von einer direkt anschlie baren Handansteuereinrichtung (manuelle Ausl sung der EST)

3) bertragung eines Ausl sesignals an die L schinstallation

4) Aktivierung von Alarmierungseinrichtungen

5) Anzeige des jeweiligen Betriebszustandes

6) bertragung der Information über den Ausl sezustand

7) bertragung der Information über den St rungsmeldezustand

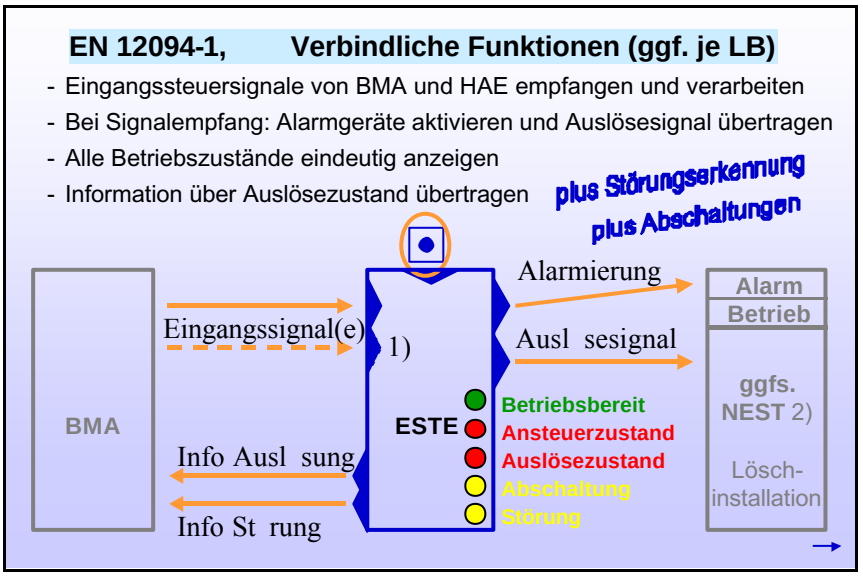

1) In einigen Ländern (z.B. Frankreich) sind zwei unabhängige bertragungswege für zwei Eingangssteuersignale gefordert

2) NEST = Nicht-elektrische Steuer- und Verz gerungseinrichtung (gegebenenfalls vorzusehen)

Wählbare Funktionen (Optionen mit Anforderungen)

Die wählbaren Funktionen kann der Hersteller vorsehen, muss es aber nicht. Wenn er sich jedoch für eine Option entscheidet, muss er alle jeweils zugeh rigen Anforderungen erfüllen. Die Optionen decken nicht nur technisch ein breiteres Anwendungsspektrum von EST ab, die auf die vielfältigen Belange der Ansteuerung von Gasl schanlagen abgestimmt sind, sondern stehen zum Teil auch für nationale Eigenheiten. Dazu geh ren

Steuerfunktionen (Ansteuerung-Steuerung-automatische Abschaltungen-Reaktionen)

- weitere unverz gerte Ansteuerungen (z.B. für Reservebatterien oder zu weiteren Geräten innerhalb der Feuerl schanlage oder auch für Betriebsmittel au erhalb der Feuerl schanlage, die im Falle einer Ausl sung zur Sicherstellung der L schwirkung unbedingt erforderlich sind)
- verz gerte Ansteuerungen zur Berücksichtigung von notwendigen Verz gerungszeiten (z.B. zum wecke der Personensicherheit)
- Flutzeitsteuerungen (Dauer der Flutung oder Steuerung einer Halteflutung z.B. Für CO_2 - Niederdruck-Anlagen)
- Einleitung einer Nachflutung (z.B. Für CO_2 - Niederdruck-Anlagen)
- Ansteuerung von Alarmierungseinrichtungen mit unterschiedlichen Signalen
- Rückmeldung L schmittelfluss
- L schmittelfreigabe für ausgewählte L schbereiche (mit automatischer Abschaltung anderer L schbereiche)

sowie

Sicherheitsfunktionen (Personensicherheit) und berwachungen (auf Funktionsfähigkeit)

- Anschluss eines Stopp-Tasters (Unterbrechungs- Funktionen eines bereits eingeleiteten Steuervorganges
- Anschluss eines Not-Aus-Tasters (Unterbrechungs- oder Abbruch-Funktionen eines bereits eingeleiteten Steuervorganges
- Wechsel vom automatischen/manuellen Modus zum rein manuellen Modus
- berwachung des ustandes/der Position von Bauteilen der L schinstallation

berwachung ustand/ Position von nichtelektrischen Blockiereinrichtungen

Nachstehend sind die wesentlichen wählbaren Optionen zweigeteilt in Steuerfunktionen und Sicherheitsfunktionen/ berwachungen bildlich dargestellt:

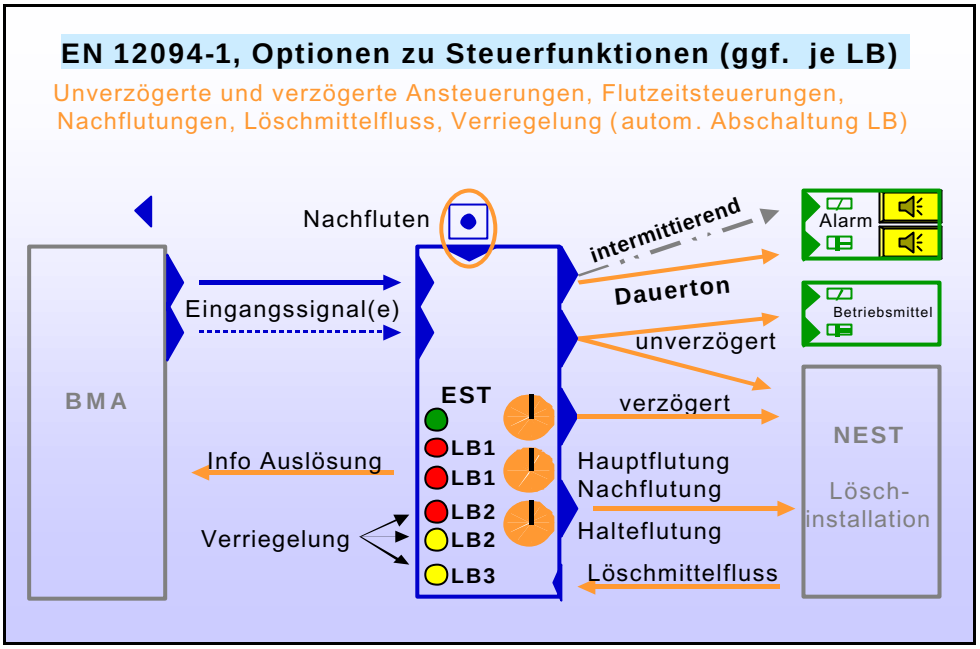

Die dargestellte Verriegelung (automatische Abschaltung von L schbereichen nach Erreichen des Ausl sezustandes für einen L schbereich) zeigt die Anzeigen für die automatische Abschaltung der L schbereiche LB2 und LB3, wobei für LB2 der Ansteuerzustand aufgrund des Empfangs eines Eingangssteuersignals für diesen LB2 vorliegt. LB1 befindet sich im Ausl sezustand.

In der nachfolgenden bildlichen Darstellung zu den Sicherheitsfunktionen ist auch angegeben, welche Länder sich bezüglich der Anwendung dieser Sicherheitsfunktionen in die Normierung eingebracht haben. Daraus folgt natürlich, dass auch andere Länder, die nicht unmittelbar an der Erstellung der Norm mitgearbeitet haben, m glicherweise diese Funktionen nutzen oder fordern. Die nachfolgende bildliche Darstellung ist daher nicht ersch pfend. Der Hersteller einer EST ist gehalten, sich zu informieren.

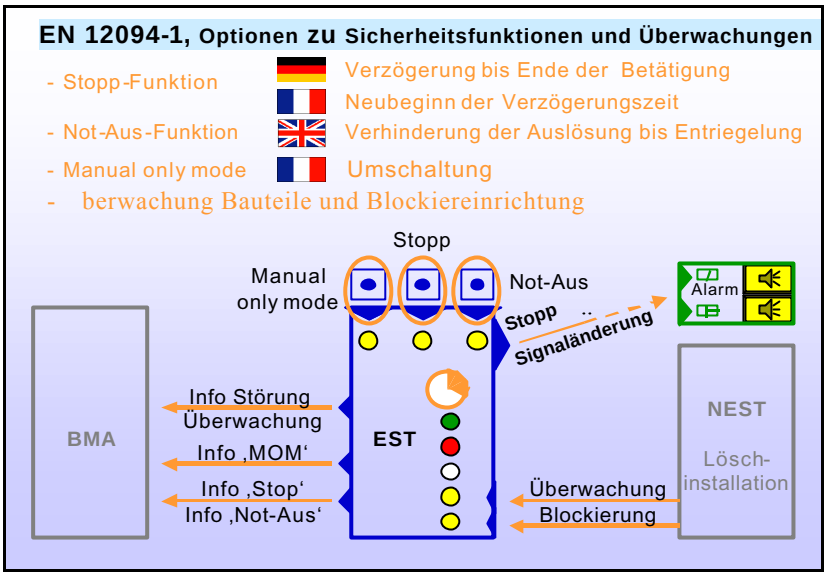

Breiten Raum nehmen die Anforderungen an die Funktion der EST mit den Anforderungen an die Signalverarbeitung und den geforderten Anzeigen für die verschiedenen Betriebszustände sowie der Bedienbarkeit ein.

Ber cksichtigung on inbereichs- und Mehrbereichssteuerungen

Eine EST kann einen L schbereich oder mehrere L schbereiche steuern. Wenn mehrere L schbereiche gesteuert werden ist sicher zu stellen, dass die verbindlichen Funktionen, wie o.g. angegeben, pro L schbereich vorzusehen sind, wobei die bertragung der Informationen zum St rungsmeldezustand und zum Ausl sezustand als Sammelmeldung erfolgen kann.

Wählbare Funktionen (Optionen mit Anforderungen) k nnen einzelnen L schbereichen zugeordnet werden. Die Norm ist nicht so zu verstehen, dass wählbare Funktionen immer für alle L schbereiche vorgesehen werden müssen. Es macht z.B. keinen Sinn, die Option „Steuerung der Flutungszeit" für einen L schbereich zu fordern, wenn für den Anlagentyp des L schbereiches ausschlie lich CO_2-Hochdruck vorgesehen ist. In einer modular aufgebauten EST k nnen daher durchaus Module für L schbereiche vorhanden sein, die sich in der Auswahl der Optionen unterscheiden. Deutlich wird dies für den Leser der Norm im Anhang

A.3, wo für die CE-Kennzeichnung je L schbereich die Kennzeichnung der zur Verfügung gestellten Optionen verlangt wird.

St rungen eines bertragungsweges oder die Systemst rung bei softwaregesteuerten EST für Mehrbereichssteuerungen dürfen sich in Analogie zu den Anforderungen an BM nach EN 54-2 nur auf einen L schbereich auswirken.

Anhang A

Bei der Norm EN 12094-1 handelt es sich um eine harmonisierte Norm, der Anhang A ist vorhanden. Das hei t, die Einschaltung einer Notifizierten Stelle zum wecke der Konformitätsbewertung ist zwingend erforderlich. Der Anhang A bezieht sich auf alle Anforderungen der Norm.

Gemä Ver ffentlichung im EU Amtsblatt: C67 vom 17.03.2004

CE M glich ab 01.02.2004
Gesetzlich vorgeschrieben ab 01.05.2006

Schlussbemerkung

Die vorliegenden Ausführungen beinhalten natürlich keine umfassende Darstellung der Norm EN 12094-1 mit allen Anforderungen und Anhängigkeiten. Deshalb: Eine detaillierte Information gibt nur die Norm selbst.

Thomas Brupbacher
Convenor of CEN TC72 WG12
Siemens Building Technologies AG, Fire and Security Products
8708 Männedorf, Switzerland
thomas.brupbacher@siemens.com

Standardising Multi-Phenomena Fire Detectors – Status Report from CEN TC72 WG12 –

Abstract

The standardization process for multi-sensor/multi-phenomena detectors is a slow one; it has been going on for about fifteen years and is still going on. After many twists and turns, another effort is now underway at CEN TC72, and is making progress towards a standard for multi-phenomena detectors that is open to new, unknown technologies.

This paper will describe the current status of the standardization effort, the difficulties that we face, and the proposed solutions. As this is still very much work in progress, there will be no firm answers presented, but suggestions that we believe have a good chance of working in practice.

1. Introduction

1.1. Historical background

With the advent of the first smoke/heat fire detectors in the early 1990s, the need for a new standard also arose. In 1993 a working group, CEN TC72's WG12 for the EN54-15, was formed to this end. When ISO started a multi-sensor standardization effort as well, CEN dropped its work in favour of the ISO effort. In 2001, CEN TC72 decided to re-form the multi-sensor working group because of a perceived lack of progress in the ISO working group. This re-forming of the WG 12 is in violation of the Vienna agreement and, thus, was reluctantly done.

By the time the WG 12 was re-formed, products using several new detection prin-

ciples had started to appear on the market, or at least in sales literature: namely gas detectors. Therefore, the scope of WG12 was opened up by TC 72 to include other, undefined sensor principles. This open scope of the standardization effort has been debated since the inception of WG12 but was confirmed by TC 72 in October 2002 and in April 2004, and remains unchanged. The main point of this ongoing debate is the technology agnosticity of the current work: the parties opposing the open scope would rather include only well known and understood technologies. The counter argument is that in the past innovation was stifled, in effect, by such technology-centred standards and that this is clearly in no-one's interest.

In the mean time, the ISO working group picked up again and have produced a standard for smoke/heat detectors that was sent out for vote in 2003. This standard, ISO 7240-15 [3], could also be promoted to an European Norm (EN) simply by the addition of an annex ZA, but CEN TC 72 decided against that.

1.2. Expectations for a multi-sensor detector

In order for the customer to be willing to pay a premium for a multi-sensor/multi-phenomena detector, it has to fulfill the expectation that it be better than a state of the art fire detector. For the WG, we have identified the following expectations:

- Fewer false alarms with better detection reliability
- Better response to a broader range of fires
- Extend range of usage (e.g. hotel bedrooms)

Therefore, the detector is a *general purpose* detector that is suitable for environments that are difficult to handle with a single sensor/phenomenon detector.

1.3. Current scope

The scope as it stands today is:

> The European Standard EN 54-15 specifies requirements, test methods, and performance criteria for point-type multi-sensor fire detectors

for use in fire detection systems installed in buildings (see EN54-1:1996) incorporating in one mechanical enclosure sensors which detect more than one physical or chemical phenomenon of a real fire. The overall fire performance is determined utilising a combination of the detected phenomena.

Examples of physical or chemical phenomena of a real fire are:

- Aerosol, i.e. smoke
- Heat
- Combustion gases
- Electromagnetic radiation
- Sound

For other types of multi-sensor fire detectors, this standard should only be used as a guidance. Multi-sensor fire detectors with special characteristics and developed for specific risks are not covered by this standard.

Compared to earlier standardization efforts, the emphasis has changed from specifying *sensors* to specifying *phenomena*. The reason behind this is the difficulty of defining a sensor, as it becomes very plausible to include sensors for different phenomena on the same physical, highly-integrated device. For example, arrays of gas sensors are known and have been used in fire detectors, and it is unclear whether each of these gas sensors should be counted as an individual sensor, or whether the whole array should be counted as one single sensor. The definition *via* phenomena removes this ambiguity by counting all gas sensors as detecting one phenomenon. Furthermore, would the gas array include a temperature sensor, the new definition would count that as a separate phenomenon.

As a side note, it should be understood that this definition is not new compared to that for conventional smoke detectors: nobody cares about the signals coming from the photo diode detecting the scattered light, we only care that the detector raises an alarm at a given smoke concentration. How the detector does that is entirely up to the manufacturer.

2. General principles of the standard

In general, the current draft version of the standard tries to re-use procedures from existing EN54 standards such as EN54-5 [2] and EN54-7 [1] as often as possible. By

doing so, it is hoped that the experience with existing standards can be leveraged and the cost of new equipment for all parties involved can be kept low.

On the other hand, this implies also that we have to keep less satisfactory solutions instead of designing better ones. This last point is illustrated by the test fires where we keep the measurement ionization chamber (MIC) because it would be a lot of work to change the test fires to use something like CO/CO_2 concentrations for the envelopes, even though everybody agrees that the MIC is undesirable.

2.1. A model for the multi-sensor/phenomena detector

In order to understand the difficulties faced by the working group, it is useful to use a simple model for the multi-sensor/phenomena detector:

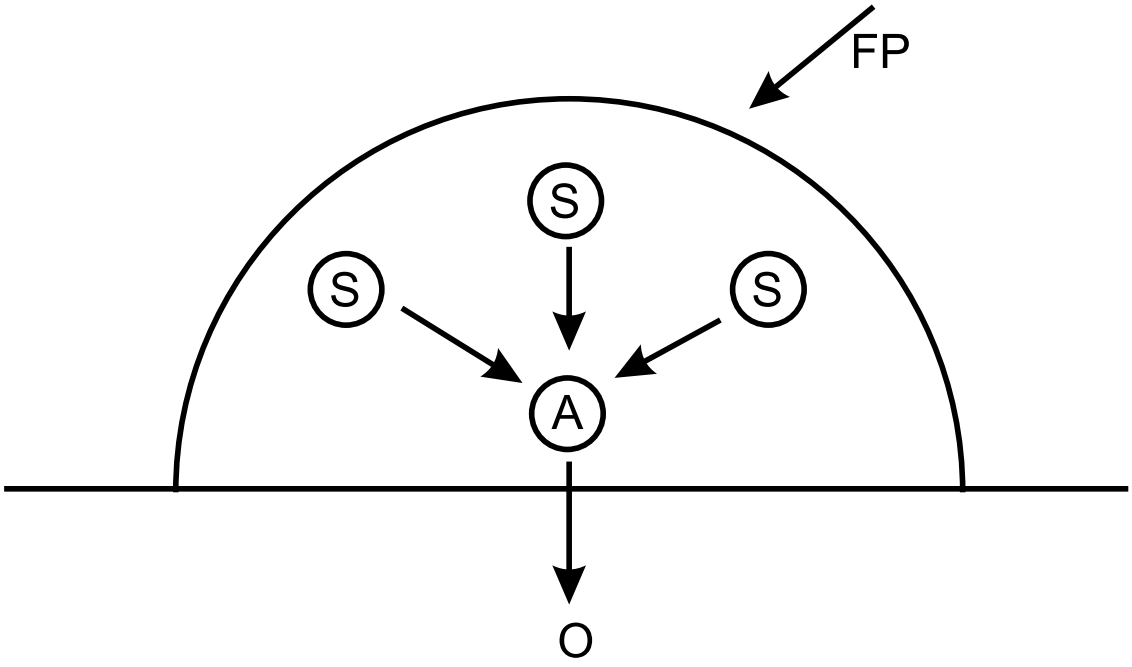

Figure 1: Model for the multi-sensor/multi-phenomena detector.

The enclosure of the detector contains several sensors (S) detecting different fire phenomena (FP). The outputs of these sensors are combined in an algorithm (A) that generates a single output (O). For the sake of assessing the quality of the detector, only the output O is taken into account.

2.2. Grey box/glass box

Once we have the model, we can discuss the assessment of the detector. Since we have to include the algorithm in the test, the *glass box*, or *grey box*, method is used. The detector is treated as a box with one single output: the alarm output. Only this alarm output is used in judging the quality of the detector. We do not care what the algorithm inside the box does, as long as it causes the detector to detect a fire in time. Because we require that the detector includes sensors for several different phenomena, the manufacturer has to specifiy the nature of the sensors inside. So, the black box is transparent and is, therefore, a glass box.

2.3. General testing

Because the scope of the standard is open, only real fires are used to stimulate the detectors when measuring their performance.

The fire performance of the detector is assessed by subjecting the detector to the test fires TF 1 to TF 5 plus TF 8. It is required that the detector passes all six test fires; additionally there are tests under consideration to make to detector respond more "evenly" to fires. Another consideration is to have no-alarm tests that would stimulate the detector with only one non-fire phenomenon, such as paraffin aerosols, and require the detector to not raise an alarm at low levels.

For assessing the ability of the detectors to withstand harsh environmental conditions, the detectors are subjected to TF 2 and TF 5 *after* conditioning, and their response is compared to that in the fire tests. A certain degradation of performance is allowed, but the details are not yet fixed.

3. Selected difficulties and their proposed solutions

In this section, a few of the key difficulties encountered in the drafting of the standard will be presented alongside with the WG's currently proposed solutions. Mostly, the difficulties stem from the scope of the standard that includes inherently an algorithm as a key element of the detector.

3.1. Dry heat test

The intent of this test is to check the detector's ability to function at high temperatures. Starting from the conditions in EN 54-7, similar test conditions were derived, mainly conditioning the detector at a temperature of 50°C and then running the test. The main difficulty with this test is the fact that the detector should not be subjected to a negative temperature gradient, because this would be a strong indication for a non-fire situation. Therefore, it is not possible to condition the detector in a climate chamber and then transfer the detector to the ceiling. So, a housing has to be constructed that keeps the temperature constant until the fire starts.

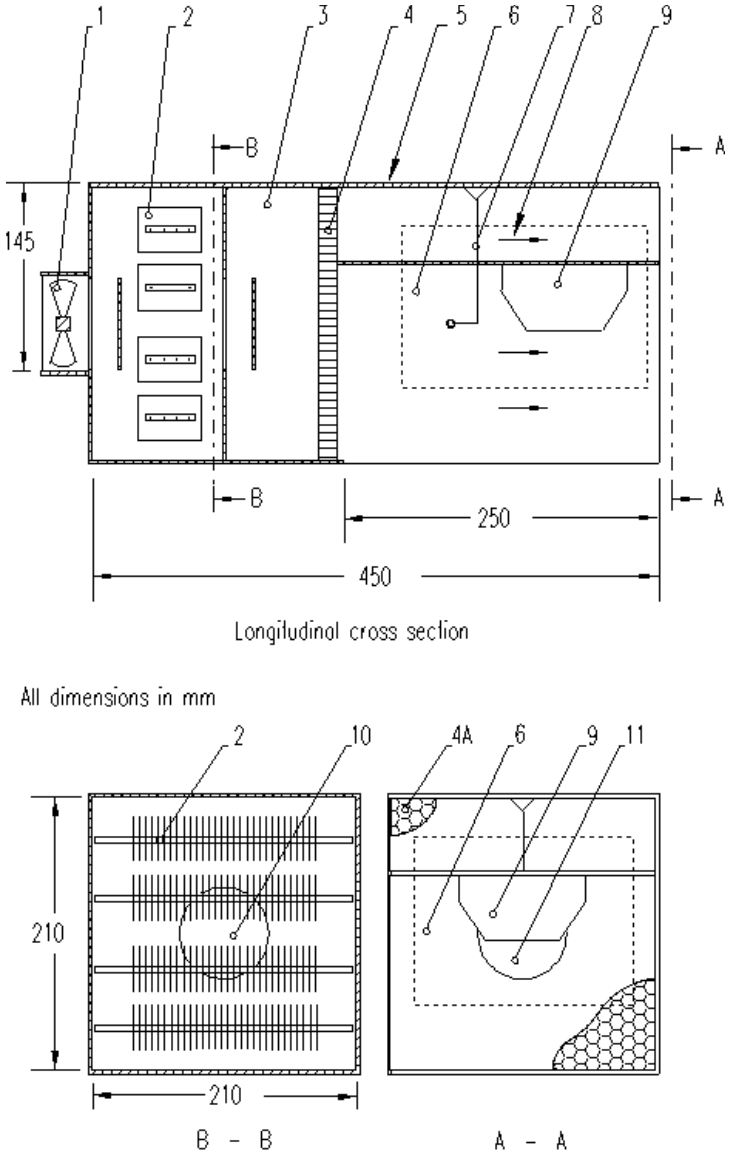

Figure 2: Schematic of the prototype dry heat tunnel.

A schematic of the solution accepted for now is depicted in figure 2. It consists of a small section of a tunnel that is to be mounted at the ceiling of the fire test room. A fan is aspirating the fire gasses and aerosols, they are passing over a heating element and then flowing past the detector. An optional opening at the bottom of the tunnel allows for windows in order to allow for sensors detecting electromagnetic radiation, such as flame detectors. So far, one prototype has been built and the actual implementation is shown in figure 3.

Figure 3: Photo of the prototype dry heat tunnel as mounted in the fire test room.

This prototype was exposed to a series of fires at Siemens in Männedorf using a detector with analogue read-out capabilities. This allowed for an assessment of the disturbances introduced by the heated housing and also of the conditions inside the tunnel. From the results, it is clear that the housing has no large negative effects on the overall reproducibility of the test fires and that the conditions in the unheated tunnel are similar enough to the conditions outside *i.e.* that the detectors report the same smoke densities. When in heated mode, the temperature profile measured at the detector is bad in the sense that the thermal mass of the housing leads to a very slow increase of the temperature for TF5 (heptane fire). Recent tests with

a modified set-up seem to indicate that the problem can be solved by a different arrangement of the fan and heaters.

3.2. Humidity tests

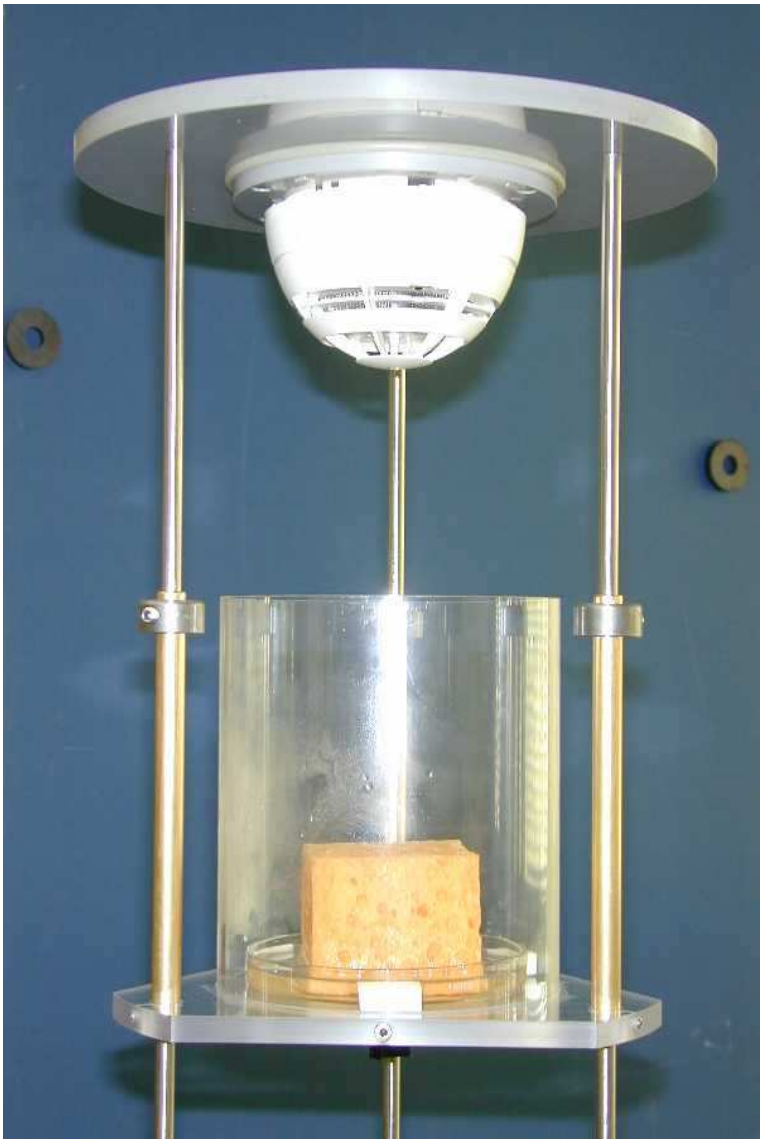

Figure 4: Photo of the prototype apparatus used for the humidity tests. Visible on top is the mounted detector; below is the movable chamber containing a jar with a saturated salt solution. To condition the detector, the chamber would be slid over the detector.

To test the detectors under different humidity conditions, an approach similar to the dry heat test is considered: again we will try to construct an apparatus to

condition the detector properly that can be mounted at the ceiling of the fire test room. The problem is simple in comparison to the dry heat test problem in that a negative gradient of humidity is not a very strong indication for a non-fire situation. Therefore, the solution proposed is to condition the detector and then to transfer the detector quickly to normal relative humidity just before the fire is lit. Figure 4 shows a photo of the current prototype.

The apparatus consists of a sealed chamber in which a constant relative humidity is produced using a saturated salt solution. After the conditioning/stabilization period, the apparatus is mounted at the ceiling of the fire test room and a test fire is performed. Just before the fire is lit, the chamber is lowered away from the detector, allowing the fire aerosols and gasses to flow freely around the detector. So far, no tests using real fires in the fire test room have been made, but no big problems are expected.

3.3. Slowly developing fires

The name of this test comes from the respective test in EN54-7. Its objective is twofold: first, to test that slowly developing fires are detected and second, to test that the detector still detects a fire even if it is at the limit of compensation for individual sensors. The difficulties encountered in designing the test are typical for the testing of multi-phenomena detectors in the sense that they come from the interplay between sensors with an algorithm.

At the point of this writing, the WG is considering a combination of software inspection and simulation of the algorithm inside the detector.

4. Conclusion and outlook

In this paper, the status of the work in CEN TC72's WG12 has been illustrated, a selection of the difficulties encountered and proposed solutions shown. The work is far from complete, but progress is being made on all fronts and there are no problems that seem unsolvable today.

By the end of this year, a first rough draft will go out to CEN TC72 in order to illustrate the work done so far and to give TC72 an understanding of where the work will lead. By the end of 2005, the standard should be ready for first enquiry;

a goal that is abitious, but doesn't seem to be unreachable today.

References

[1] CEN-TC 72, "EN54: Fire detection and fire alarm systems – Part 7: Smoke detectors – Point detectors using scattered light or ionization", Brussels, 2000, and Annex 1, 2002.

[2] CEN-TC 72, "EN54: Fire detection and fire alarm system – Part 5: Heat detectors – Point detectors", Brussels, 2000, and Annex 1, 2002.

[3] ISO TC 21/SC 3, "ISO 7240: Fire detection and alarm systems – Multisensor fire detectors – Part 15: Point type fire detectors incorporating a smoke sensor (using scattered light, transmitted light or ionisation) in combination with a heat sensor", Geneva, 2004.

Martin Hesels
VdS Schadenverhütung GmbH, Germany

Multiple Sensor and Multiple Criteria Fire Detectors
Current and Future Test Procedures in the VdS Fire Test Laboratories

1 Abstract

VdS Schadenverhütung, the German test house for fire detecting and fire alarm systems, offers test procedures and approvals for multisensor/multicriteria fire detectors.
Since there are still no national or European standards available for such detectors, other rules and guidelines, or even test agreements between the test house and the manufacturer form the basis for a VdS type testing and approval.
Besides the presentation of the current VdS methods for type testing, a brief outlook is given to show the new approach of a CEN TC 72 working group, which has been introduced recently to develop a general product standard for multisensor/multicriteria fire detectors.

2 Introduction

For many years now multisensor/multicriteria fire detectors can be found on the European market. The two most important reasons for the development of such a detector may be identified as follows:

1. Multisensor detectors promise a reduction of false alarm rates
2. Multisensor detectors shall allow the detection of a wide range of different fires

Although a lot of such products can be found on the market, the current EN 54 series of valid standards does not cover multiple sensor / multiple criteria fire detectors. So, in European standards no common requirements and test procedures are available at present. Only CEA, the Committee of European Assurances, established a specification in 1999 for multisensor detectors, which respond to smoke and heat, and smoke detectors with more than one smoke sensor (see 4.1). This specification therefore does not cover all conceivable types of multisensor detectors.

For some special multisensor/multicriteria fire detectors organisations and test houses have produced appropriate guidelines. Other detectors, which are not covered by these rules, are currently tested in accordance with individual test agreements between test houses and manufacturers.
All in all, an acceptable solution for all existing multisensor detectors is still missing.

3 Definitions

Multiple sensor and multiple criteria fire detector:

A multisensor/multicriteria fire detector can be considered as a detector which contains at least two different sensors in a common housing.
Examples for such detectors are:

- flame detector with two sensors, each detecting a different wavelength
- combination of optical smoke detector and heat detector
- scattered light smoke detector with two different scattering angles
- combination of gas sensors, sensitive on different combustion gases
- combination of a gas sensor and a heat sensor
- combination of a smoke sensor and a gas sensor

It has to be mentioned, that in EN 54-1 a multisensor fire detector is defined as follows: “A detector which responds to more than one phenomenon of fire.”

Sometimes it is difficult to distinguish between a multiple sensor detector and a multi criteria detector. A multiple criteria fire detector may in addition to the processing of the signals from the different sensors also include other criteria (e.g. time) for the alarm decision.

4 Current test methods and requirements for multiple sensor / multiple criteria fire detectors used in the VdS fire test laboratory

Despite the lack of national or European standards for multisensor / multicriteria fire detectors, most of the test houses offer test and approval procedures for such devices.
Often tests can be conducted in accordance with guidelines and regulations which have been introduced by different organisations or even the test houses themselves.
In other cases test houses and manufacturers can agree on an individual test schedule which describes all necessary tests and requirements. Usually these test schedules origin on existing standards for similar products as far as possible. Finally the certification body is able to approve the product on the basis of this test schedule.

4.1 Multisensor Smoke detectors according to CEA 4021

CEA (Comité Européen des Assurances) is the European federation of national insurance associations, which represents the common interests of the European insurance industry.
CEA has published requirements and test methods for multisensor smoke detectors. Multisensor smoke detectors in the sense of CEA 4021 are detectors with at least one smoke sensor. The tests described in CEA 4021 are primarily based on proving the stability of each single sensor and the assumption that the behaviour of the complete detector is sufficiently stable if the performance of the single sensors is stable within defined limits.
There are three cases under consideration:

a) Detectors with more than one smoke sensor according to EN 54-7

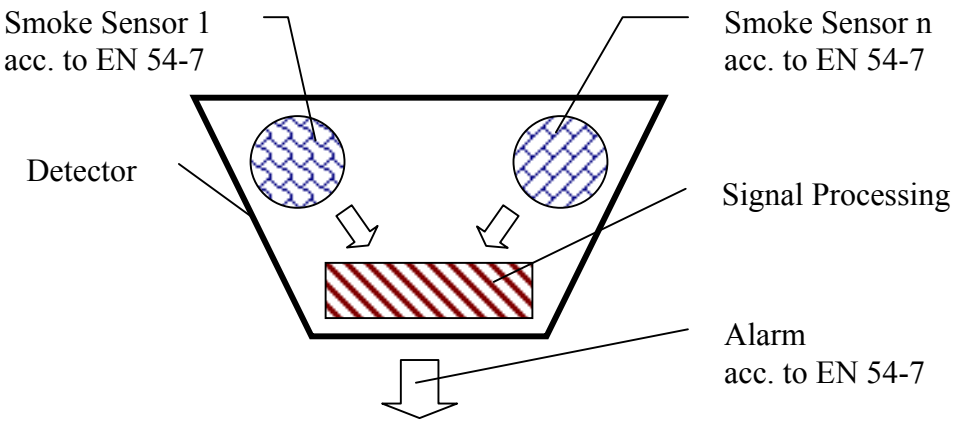

b) Detectors with at least one smoke and heat sensor, where the heat sensor(s) enhances the smoke response characteristics

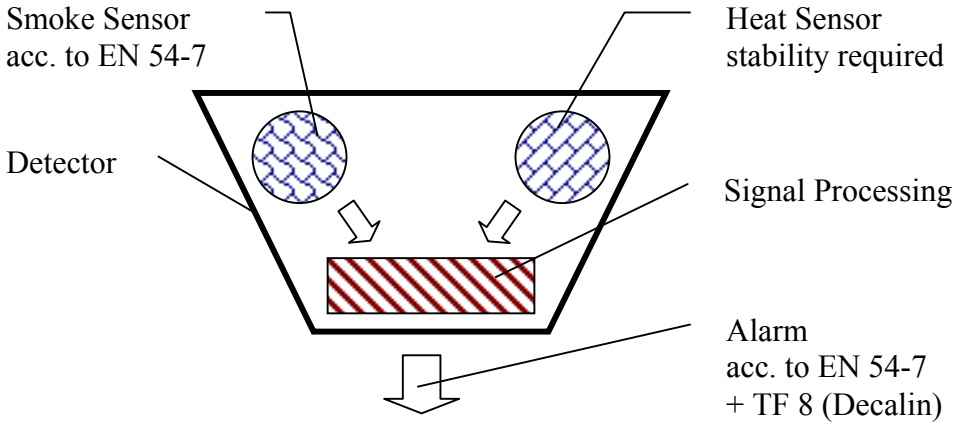

c) Detectors with at least one smoke and heat sensor, where each sensor with its circuitry fulfils the relevant part of the European Standards EN 54-7 and EN 54-5).

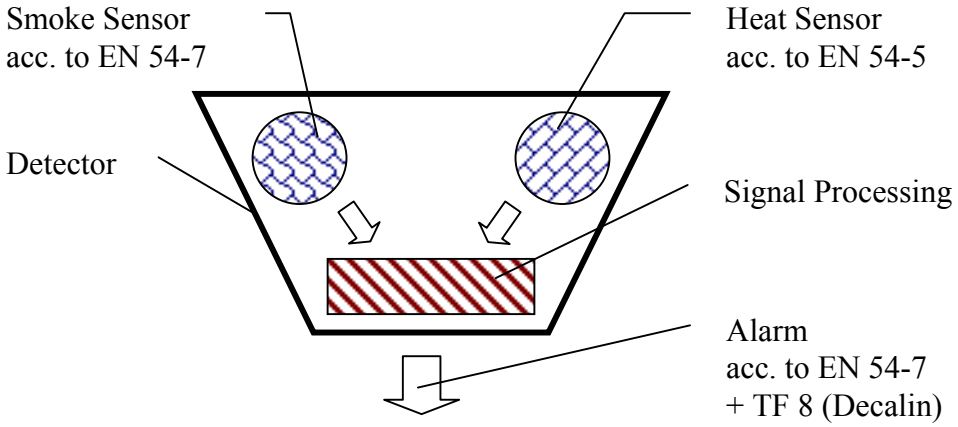

The stability of each single sensor is measured and assessed either according to the appropriate EN 54 standard or, for the case that a heat sensor is not intended to comply with EN 54-5, as described in CEA 4021.

The idea behind this method is as follows: If the single sensor under test stays stable within well defined limits, the overall performance of the multisensor detector is assumed to be also sufficiently stable.

Not only the detector stability, but also the fire performance is an important aspect of CEA 4021. Beside the test fires TF2 to TF5, required in EN 54-7, a Decalin test fire is mandatory for multisensor smoke detectors containing a heat sensor.
This is to prove the capability of the smoke sensor to respond sufficiently sensitive without the primarily contribution of the heat sensor.

Advantages of the CEA 4021 test method:

- Equipment is already available in the test houses and in the labs of the manufacturers
- Well known test methods of EN 54-5 and EN 54-7 are applicable
- Performance of the stability tests is quite precise
- Process could be adopted to other sensor principles (gas, radiation, …)

Disadvantages of the CEA 4021 method:

- The effort of testing rises with the number of sensors
- Output signals must be available for each sensor
- Definition of a sensor: Is a sensor array a single or a multiple sensor?
- Provision of means to stimulate each sensor independently
- Algorithm is not tested: stable sensor ≠ stable detector behaviour
- The detector is forced to respond with a certain sensitivity to smoke only

4.2 Fire gas detectors according to VdS 2806

In cooperation with the German industry VdS Schadenverhütung has developed a guideline for testing fire gas detectors used in fire detection and fire alarm systems. These fire gas detectors are intended to detect combustion gases or gaseous products of thermal decomposition.

The fundamental test principle is as follows:

VdS test lab is equipped with a gas mixing apparatus to produce a gas mixture of CO_2, CO, H_2 and NO_2, diluted in synthetic air. If required, additional gases can be added to the mixture.

This apparatus allows testing fire gas detectors with one or more gas sensing elements. The aim of the tests is again to prove the stability of the single sensors and to show the capability of a fire gas detector to detect a specified range of real test fires.

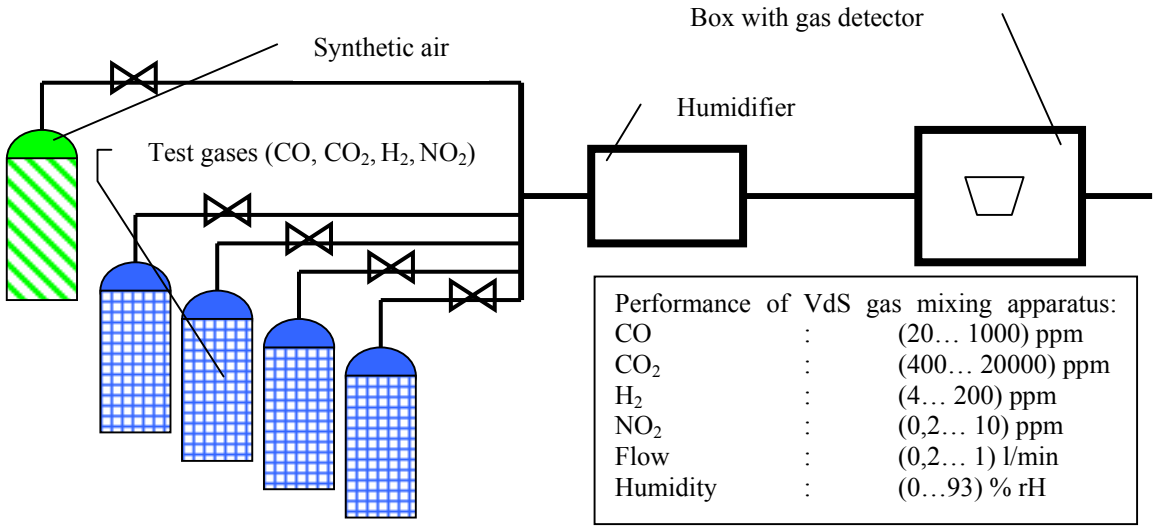

Performance of VdS gas mixing apparatus:		
CO	:	(20… 1000) ppm
CO_2	:	(400… 20000) ppm
H_2	:	(4… 200) ppm
NO_2	:	(0,2… 10) ppm
Flow	:	(0,2… 1) l/min
Humidity	:	(0…93) % rH

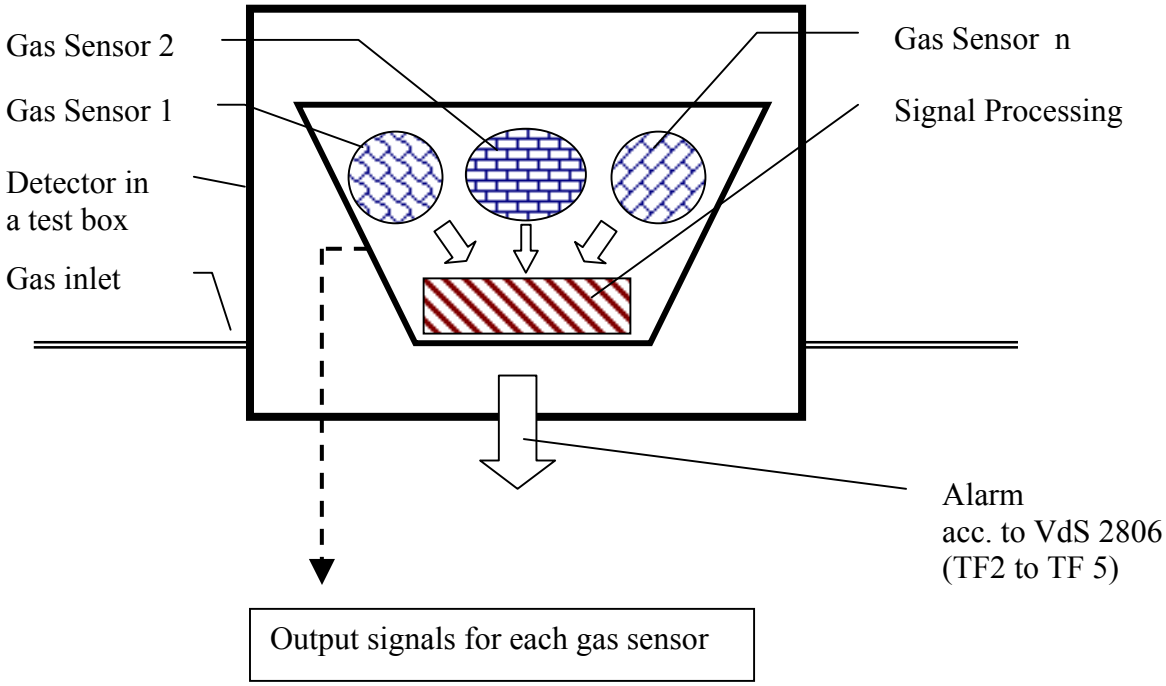

Advantages of the VdS 2806 method:

- Possibility of simultaneous stimulation of more than one sensor
- Open for all gas sensing principles
- Open for additional gases beside the leading gases CO_2, CO, H_2 and NO_X
- Performance of the stability tests is quite precise
- A sensor array with only one output can be stimulated completely

Disadvantages of the VdS 2806 method:

- Output signals must be available for each sensor
- Algorithm is not tested: A stable sensor does not guaranty stable detector behaviour.
- New equipment is required
- Cross sensitivities may influence the performance of a single sensor

4.3 Smoke detectors with more than one smoke sensor (EN 54-7:2000 / prA2:2003)

For smoke detectors, which contain more than one smoke sensor, a CEN working group (CEN TC 72 WG 5) has prepared an amendment EN 54-7:2000 / prA2:2003 which deals with additional requirements, following also the principle, to assess the single sensor stability.

Primarily the complete detector has to fulfil all requirements of EN 54-7. Furthermore, the repeatability, the directional dependency and the stability of each single smoke sensor shall be assessed separately.
The manufacturer shall provide means which allow measuring the output signal of each sensor. The output signals shall be recorded up to a certain level, predefined by the manufacturer.
The repeatability, directional dependency and stability of the single sensors shall be determined by measurement of the output signals followed by a comparison.

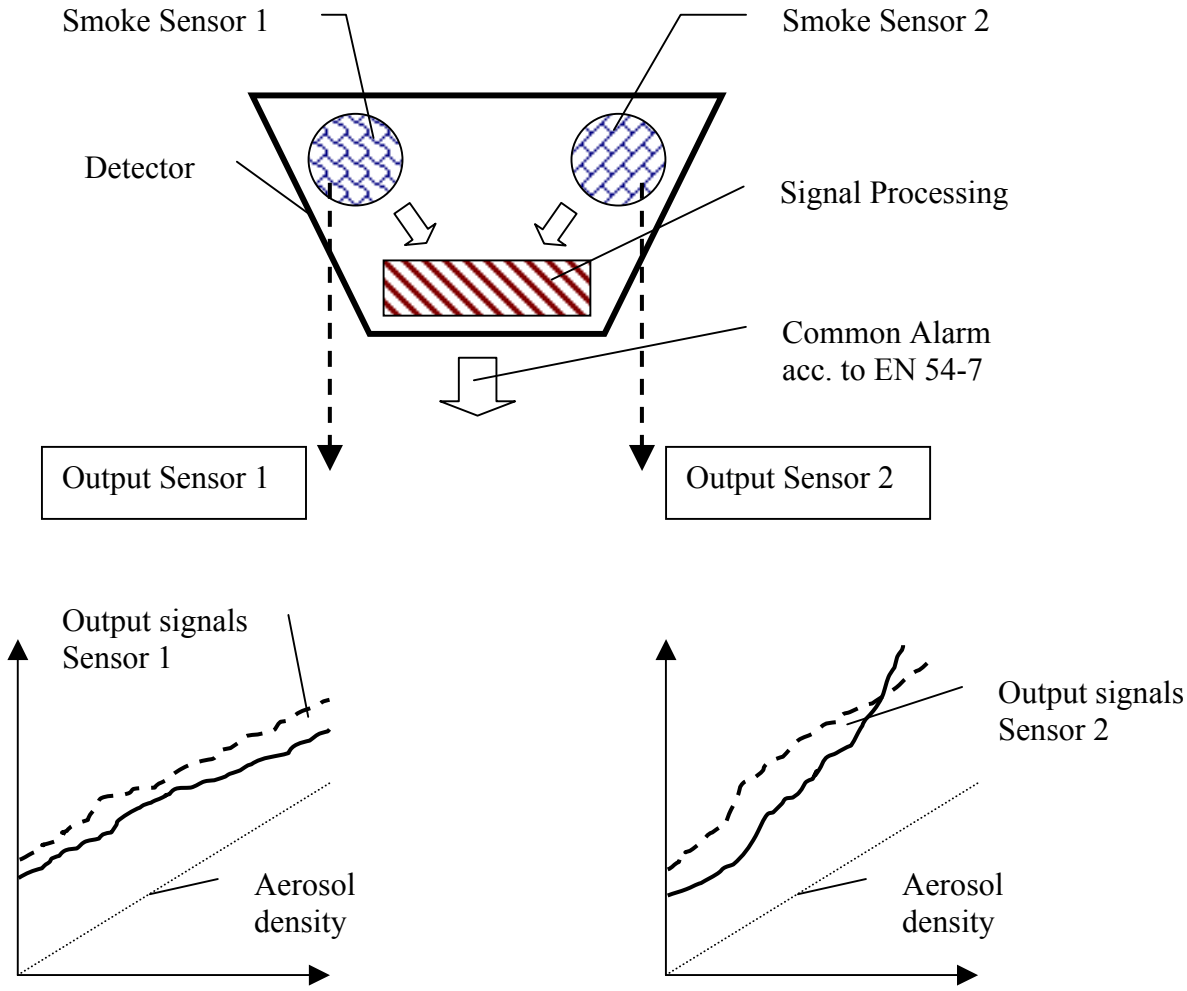

Output signals are shown before and after environmental testing.

4.4 Testing of other sensor combinations based on a test agreement

As mentioned before, for most of the possible sensor combinations no regulations have been developed so far.

In cooperation with the manufacturer the test house may set up a test schedule which contains all important details for the intended test procedure. Usually this test schedule reflects the test methods defined in standards or guidelines for similar products. Example: A test schedule for a multisensor fire detector with a heat and gas sensing element would probably have the structure of CEA 4021 (Multisensor smoke detector) and consist of appropriate tests and requirements of EN 54-5 (heat detectors) and VdS 2806 (fire gas detectors).

5 Future test methods for multiple sensor / multiple criteria fire detectors:

Driven by the demand of the fire detection industry, CEN TC 72 has opened a new work item to create a European standard for multi-sensor fire detectors. In October 2001 WG 12 of CEN TC 72 started their work, developing a new part in the EN 54 standard series.

The new multi-sensor standard shall be based on the following scope:

> The European Standard EN 54-15 specifies requirements, test methods, and performance criteria for point-type multi-sensor fire detectors for use in fire detection systems installed in buildings (see EN54-1:1996), incorporating in one mechanical enclosure sensors which detect more than one physical or chemical phenomenon of a real fire. The overall fire performance is determined by utilising a combination of the detected phenomena.
>
> Examples of physical or chemical phenomena of a real fire are:
>
> - Aerosol, i.e. smoke
> - Heat
> - Combustion gases
> - Electromagnetic radiation
> - Sound
>
> For other types of multi-sensor fire detectors, this standard should only be used for guidance. Multi-sensor fire detectors with special characteristics and developed for specific risks are not covered by this standard.

The scope of this new standard is not limited to any technologies or any sensor principles. This is different to EN 54-7, which allows only certain technologies. The new standard shall focus on the detection of different fire phenomena (e.g. aerosols, heat,…). It will be a big challenge to create sufficient test methods and requirements to cover all possible sensor combinations which are already in the market and which will occur in the future.

Consequently and also to overcome several problems with the current test methods (e. g. high costs for sensor by sensor testing, no testing of the detection algorithm, how to test integrated sensor arrays?) one goal was, to test the stability of the whole detector in one step. The single sensors shall not longer be investigated individually.

As already introduced in other standards (e.g. EN 54-7) the type testing shall be roughly divided in two parts: stability testing and performance testing.

For stability testing a detector is exposed to a certain number of real test fires in the standard fire test room before (in some cases also during) and after environmental conditioning. The detector under test is expected to release an alarm signal before the specific end of test criterion of the test fire is reached. There is no longer any response ratio required between tests before and after environmental conditioning. The response to the test fires is considered to be sufficient.

Performance testing takes also place in the standard fire test room. The detector is exposed to the known test fires TF 1 to TF 5 and TF 8.

Conducting all tests in the fire test room seems to be the most promising way to get rid of several weaknesses we find in the current fire detector standards. However, the decision to go this way caused a lot of new problems which have to be solved. Tests, which can be done pretty good in a test tunnel or a limited volume, seem to be impossible in a large fire test room. For example the dry heat test, humidity tests, dazzling test, air velocity and directional dependence test have to be adapted to the new situation.

Advantages of the new EN 54 approach:

- Open for all current and future sensing principles
- Simultaneous stimulation of the complete fire detector is more efficient
- No artificial stimulation is required
- No separate outputs from single sensors are required
- Behaviour of the signal processing is part of the testing
- Sensor arrays without single outputs do not cause any problems

Disadvantages of the new approach:

- Partly new equipment necessary
- Tests in the fire test room are less precise
- Probably not all sensors are assessed sufficiently
- Specific weaknesses of single sensors will probably not be considered

6 Conclusion

Multiple sensor detectors are available on the market for many years now. Especially detectors with a smoke and heat sensor combination are well established and have so far successfully been tested according to the CEA 4021 specifications.

But in the last few years more and more manufacturers have been going to implement gas sensing elements and to develop higher sophisticated fire detectors to satisfy the market demand for a further reduction of the false alarm rate.

Actually, the time has come to produce a new EN 54 series product standard which allows a reliable but not to expensive testing and approval of all modern fire detectors with more then one sensing element.

VdS Schadenverhütung is in line with this development in order to support an improved fire protection technology for the future.

Oliver Linden
University Duisburg-Essen, Duisburg, Germany

Function-Based Testing Procedure for Multi Sensor Fire Detectors

Abstract

Within the past years fire detection technology has developed at a high speed of innovation. Computerisation and the use of sophisticated fire detection algorithms gained more and more importance at taking advantage of the wide range of opportunities multisensor detectors show. Despite this development testing methods still remain to be the same. European testing standards and testing equipment that have been created for fire detectors decades ago are undergoing adoption to state of the art of fire detection technology step by step. Against this background a new testing concept for multisensor fire detectors has been developed at the section Communication Systems at University Duisburg-Essen. The testing concept provides the opportunity of performing a function-based stability test of multisensor fire detectors while showing a high grade of repeatability. As a main advantage compared to the traditional testing concept, not just the single sensors are tested, but the whole detector can be evaluated as one system including the influence of data processing. In comparison to an earlier approach of University Duisburg-Essen significant changes have been made in order to enhance the testing repeatability at low purchasing costs. Several testing houses and manufacturers already possess the main parts of the equipment needed.

1 Introduction

Since decades testing technology lags behind the technological evolution in the field of fire detection. While fire detection technology is characterised by an increasing use of multi-sensor technologies and more and more sophisticated data processing, the current testing concept is still basing on antiquated standards. However, the EN 54 [EN 54-7] was an adequate solution for being able to test fire detectors according to the state of the art thirty years ago. But it did also put up barriers for future developments due to its technology-based concept. Also the new testing approach of the CEA 4021 guideline

[CEA 4021] for multi sensor fire detectors did not show any fundamental changes for it mainly was an instruction how to combine parts 5 and 7 of EN 54.

Although if up to now not everybody involved is willing to support a fundamental change of testing philosophy there is an unambiguous directive of ISO/IEC concerning the "Rules for the structure and drafting of International standards" [ISO/IEC 2001] explicitly demanding a "Performance Approach":

> *"Whenever possible, requirements shall be expressed in terms of performance rather than design or descriptive characteristics. This approach leaves maximum freedom to technical development."*

Following this directive the new European standard for multi sensor fire detectors shall base on a concept which is almost open to future demands. In this spirit the responsible CEN working group (TC72/WG12) intends to go a new way by establishing a non-technology based testing standard which shall be applicable to all kinds of fire sensors.

2 Stability Test

However, special demands need to be fulfilled depending on the aim of a test. So a fire sensitivity test is generally expected to show all criteria of real fires like they occur in practice - the repeatability demands have always been of secondary importance in this respect. In contrast to the fire sensitivity test the stability test shall meet totally different demands for it is not just used to qualify a detector's property, but to *quantify* the repeatability of a sensor's or detector's response behaviour. Therefore, a bad repeatability would go against the basic idea of the test.

Within the past year a project has been carried out at the University Duisburg-Essen to elaborate a low-cost stability test procedure for multisensor fire detectors. The resulting "*multi criteria tunnel*" is a testing & development tool which is able to produce highly defined and repeatable test conditions while giving the opportunity to separately adjust the ratio of different fire criteria (particle density / fire gases / heat). Optionally, synthetic gases can be let into the tunnel by means of flow controllers. Thus, the new procedure is suitable to force an alarm release of a wide variety of multi sensor fire

detectors using the alarm point as test criterion. In this paper the *multi criteria tunnel* is compared with a stability test concept using *test fires*.

2.1 Single signal evaluation or detector evaluation?

Generally, all concepts for the stability test of multisensor fire detectors can be divided up into eighter following the traditional "single signal evaluation" or relying on the *function-based* concept of "detector evaluation" using the detector's alarm threshold.

However, it should be recognised that the old-fashioned EN 54 testing concept originally *did* already base on "detector evaluation". The stability test of smoke and heat detectors has been performed by submitting the test item to a permanently increasing concentration of a fire criterion (smoke or heat) until the alarm is released - principally the same concept as it is used for the "multicriteria tunnel" presented in this paper.

As mentioned before, the current testing procedures do not take into account the technological revolution regarding computerisation, data processing and (multi) sensor technologies. Fortunately, there is now almost common sense about the need of a future-oriented testing concept basing on detector evaluation.

Why do we need a "detector evaluation"-based testing concept?

Up to now multisensor fire detectors need to be tested in a highly time consuming and costly way. So today a fire detector e.g. with a smoke, a heat and a gas sensor has to be submitted to three different test procedures (smoke tunnel, heat tunnel, test bench for gas sensors[1]) to achieve an approval (picture 1). However, some gas sensors (and so the whole detector) are still not testable according to existing guidelines because they react to substances which are unknown or which would have to be produced synthetically with too high financial efforts.

Moreover, the current test procedure does not take into account the sensor's weight for the alarm release. This means that a gas sensor which might be evaluated in a fuzzy way

[1] According to the VdS guideline for testing gas sensor based fire detectors

by trend analysis currently has to fulfil the same testing demands like a much more sharply evaluated sensor which has the major influence on the alarm decision (e.g. a light scattering smoke sensor).

Both reasons lead to the current situation that the use of many sensors which might contribute to a lower rate of false alarms is *practically excluded*. Thus, a potential barrier for future developments has been made up. Further problems with the current test procedure are described in [LINDEN 2003].

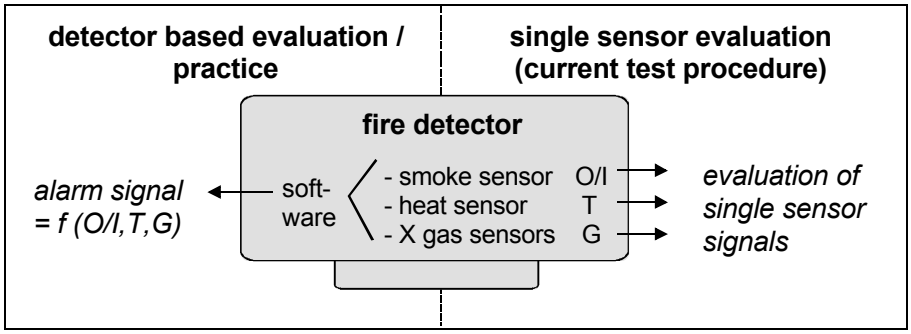

Picture 1: Detector based evaluation / single signal evaluation

2.2 Detector evaluation based testing concepts

Actually there are two different approaches for a function-based stability test for multi sensor fire detectors:

1) Test Fires
   Several fire detectors shall be subjected to test fires at the same time.
2) Multi Criteria Tunnel
   Fire Detectors are subjected separately to a mixture of fire criteria (particles, heat, fire gases) at a concentration which is increased almost linearly.

In the following the advantages and disadvantages of both concepts will be illustrated and compared to each other.

2.2.1 The test fire concept

Following the test fire concept multi sensor fire detectors are submitted to the products of test fires at a fire room. This concept has two main advantages:

1. Theoretically many detectors can be tested with on fire at the same time. This way testing time and money could be saved. However, this advantage cannot be put into practice for reasons which will be discussed closer later on.
2. The fire detectors are submitted to the whole bandwidth of fire criteria. Thus, the testing procedure is principally suited for all kinds of fire sensing technologies.

The main disadvantages of the concept are:

1. In general fires show a chaotic burning behaviour. At each kind of fire clouds appear causing a non-predictable increase of fire criteria under the ceiling which is absolutely non-linear but determined by peaks instead.
2. The experience shows that the course of - also well-defined - fires depends on various environmental parameters:
   - The spread of smoke (especially at smouldering fires) is highly influenced by temperature differences between the walls and/or between ground and ceiling.
   - The conglomeration behaviour of the smoke particles is influenced by
     - the room temperature
       (through a difference in thermal buoyancy, the resulting velocity of particles and - as a consequence - a non-repeatable age of particles in the measuring zone) and by
     - non-repeatable climate conditions regarding humidity and pressure.

Picture 2 shows both the chaotic burning behaviour of a well-defined test fire (TF 2) and the effect of varying test parameters regarding the seasonal dependency on climate conditions. Evaluating some series of TF 2 test fires which have been carried out at an EN 54-conform fire room it turned out that the major pattern of the course of fire showed a seasonal dependency. This dependency is probably caused to a high amount by differences in temperature between the ground, the ceiling and/or the walls.

As a result there are actually two different TF 2 test fires showing their own characteristics[2]: a *summer TF 2* and a *winter TF 2*. *However, without conditioning the climate parameters of the fire room the repeatability of any smouldering or glowing fire is not sufficient for the stability test because of its strong dependency on predominant air streams*. Thus, at least a stability test which has to be carried out before and after a 6 months long-term environmental test would be out of the question.

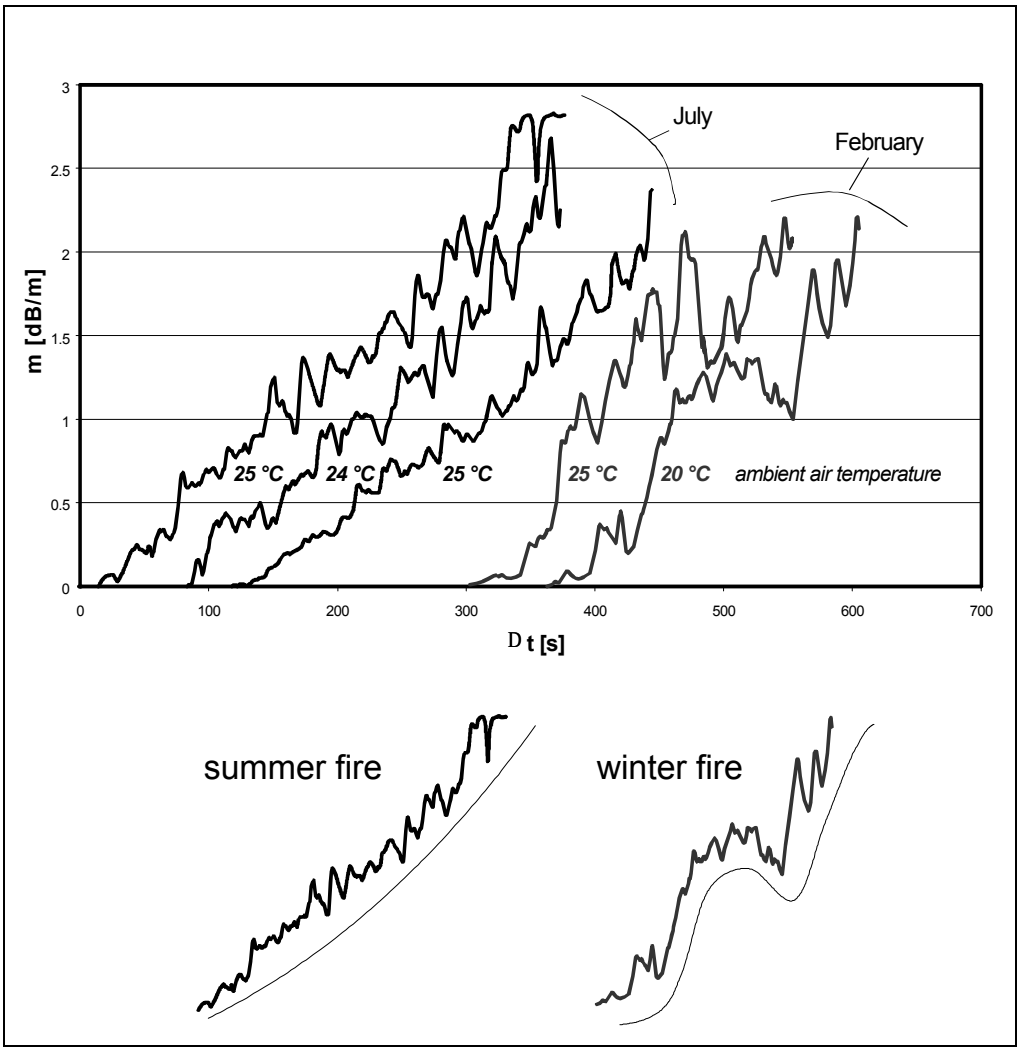

Picture 2: Upper diagram: Confrontation of different courses of the test fire TF 2 in summer and winter (selection); lower diagram: illustration of recurring patterns regarding the dependency of the TF 2 on seasonal influences

[2] Test fires carried out in other fire rooms might show different characteristics.

An other problem arises by the *non-circular expansion of the fire emissions*. Experience shows that even 4 detectors (which are mounted side by side under the ceiling of the fire room) show time-shifted signals. This phenomenon is illustrated in Picture 3. Due to prerequisites regarding room structure and climate a certain (non-stable) pattern of smoke expansion arises. *As an inevitable result the measuring points at the 3m radius under the ceiling of the fire room are reached with a changing time delay*. This further means that signals of the measuring equipment do not show a direct reference for the fire detector signals. For this reason the detector's response behaviour cannot be evaluated properly (see chapter 2.2.3).

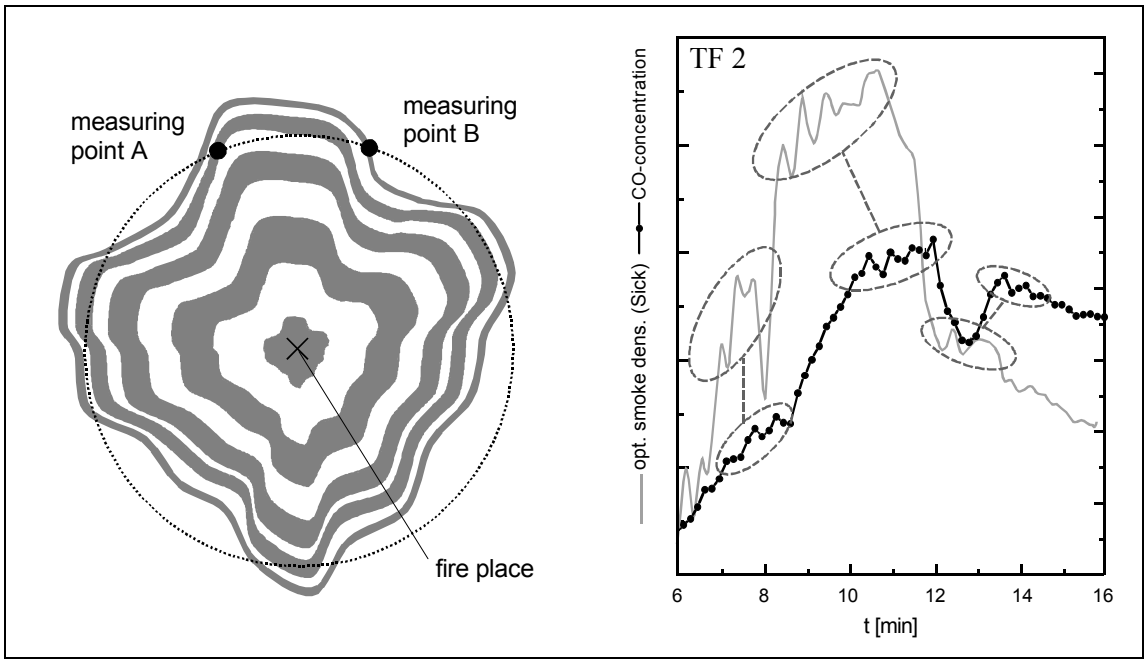

Picture 3: Smoke spread & sensor signals: left diagram: spread of wads of smoke under the ceiling (top view, schematic); right diagram: correlation of signals during a TF 3 test fire: CO and Sick reference (measured signals) [LINDEN 1998]

2.2.2 The multi criteria tunnel concept

The multi criteria tunnel concept (picture 4) bases on the EN 54 smoke tunnel. At the time being the concept covers the following test phenomena:

- Particle density

  The particle density is produced by means of a paraffin oil generator.

- Heat

  The tunnel is provided with a heating option (like it almost common use). With respect to the heat development of a moderate burning open fire (e.g. test fire TF 1) a heat ramp of at least 4 K/min is realised.

- Gases

  The fire gases are produced by real fires (e.g. a cotton wick fire) by means of a simply constructed burning chamber; the smoke particles are filtered out. Additionally, there is the option to inject synthetic gases into the tunnel.

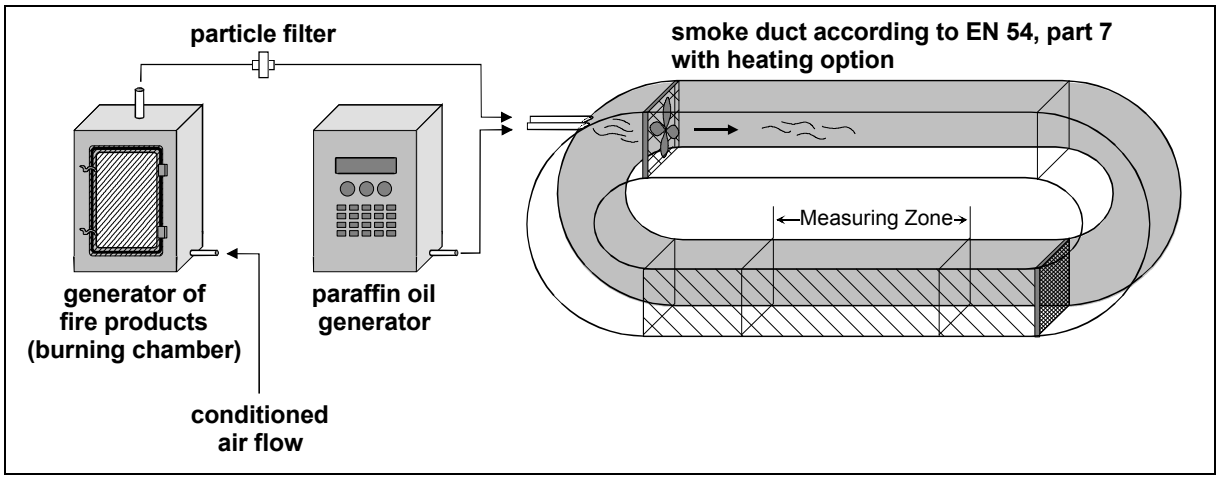

Picture 4: Multicriteria tunnel - basic setup

Why still using paraffin oil vapour?

Investigations at University Duisburg-Essen have shown that the smoke density in the measuring area depends on various environmental parameters which are difficult to control[3]. *Both the burning process and the coagulation behaviour of the smoke particles depend on the climate parameters air pressure, temperature and humidity*. Although the testing conditions are much easier to control within a small burning chamber compared

[3] At the multi criteria tunnel as well as at the fire room

to the fire room, the results in the test tunnel have not been satisfactorily so far. So, instead of going a sophisticated way to exclude the climate influences it was decided to chose a fast, cheap and actually repeatable solution by using a paraffin oil generator. This solution shows crucial advantages:

- The paraffin oil generator is already used for testing smoke detectors. Each company possessing an EN 54 smoke tunnel also has this generator and a lot of experience has been gained concerning the handling of the generator.
- The generation of paraffin oil vapour is highly repeatable.
- Paraffin oil does not contaminate the test tunnel at a great extend.
- The conglomeration behaviour of paraffin oil is highly independent from the predominant environmental conditions.

However, both heat ramp and gas concentrations (CO and CO_2 have been measured at a first step) can already be produced highly repeatable. At earlier investigations at University Duisburg-Essen a repeatability of CO and CO_2 was reached showing a maximum deviation of factor 1.15 over the whole testing time.

The fire phenomena are offered at an almost linear rising concentration. Because of buffering effects, the resulting gradients are smoothened to a great extend. The main effects determining the rise of gas concentrations in the measuring zone are illustrated in picture 5.

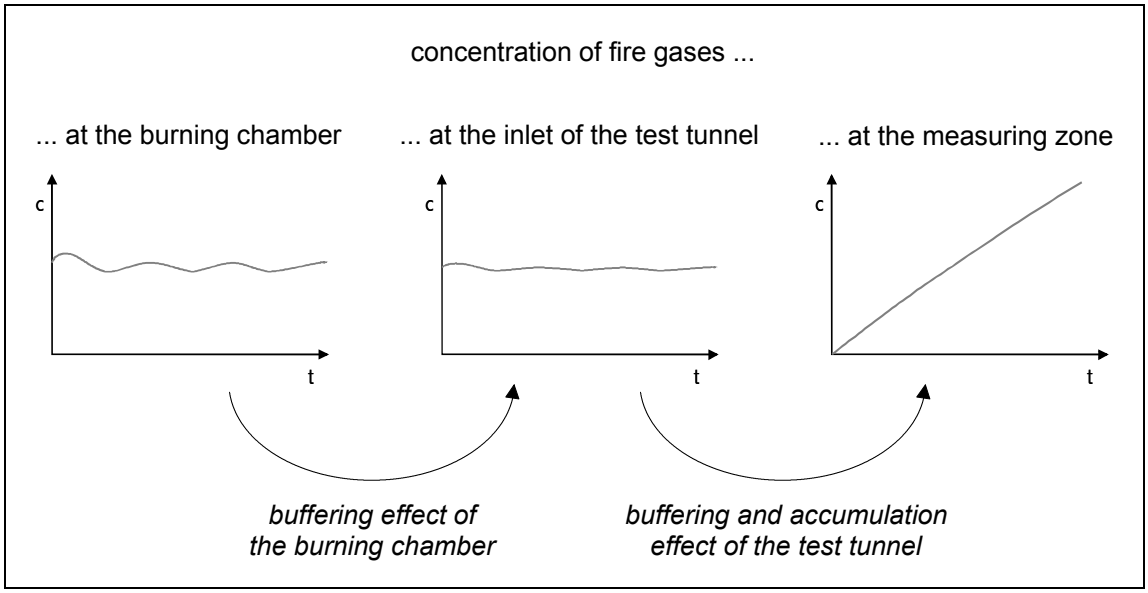

Picture 4: Buffering and accumulating effects of the multi criteria tunnel (schematic illustration)

2.2.3 Evaluating the detector signals

The main advantages and disadvantages of the presented detector-based testing concepts appear at trying to evaluate the signals. In this regard the most important aspects are *the course of signal rise* and *the coincidence of the detector's signal and the reference signal(s)*.

Course of signal rise

As mentioned before, the test fire concept shows a course of signal rise which is very much determined by peaks, due to an always chaotic burning behaviour and strong dependencies on predominant air streams and environmental factors. Thus, test fires are - as a matter of principle - not repeatable enough to derive *quantitative* results. An example of what may appear at evaluating the signal is given in Picture 5. On the other hand picture 5 (lower diagram) also illustrates the evaluation of the smoothened and almost linear rising signals with the multi criteria tunnel concept.

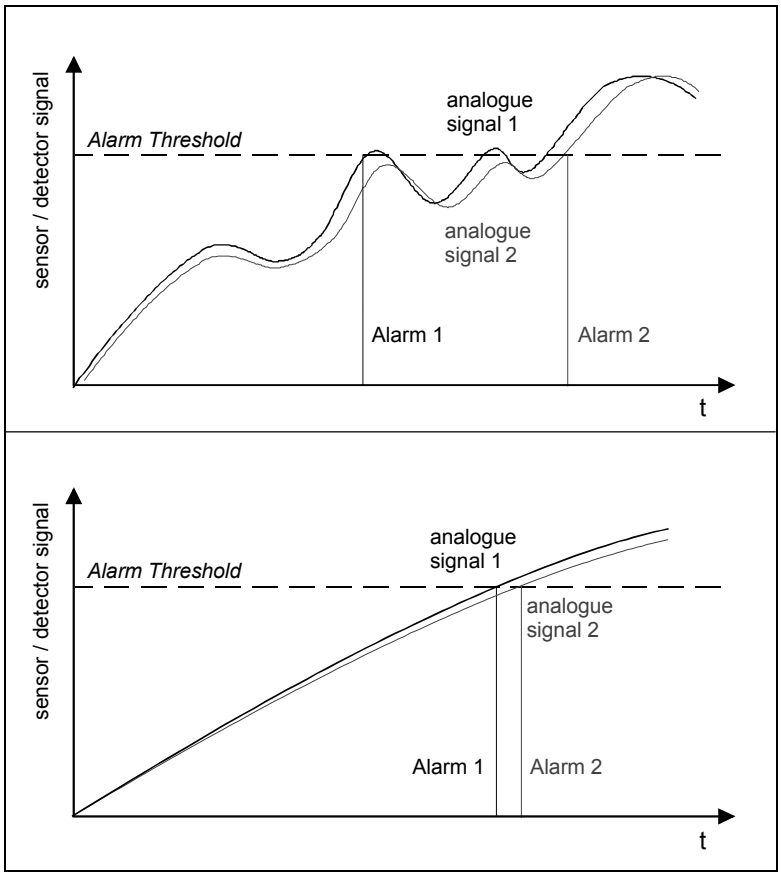

Picture 5: Potential effects of marginal differences at repeating the stability test by means of test fires (upper diagram) and by means of the multi criteria tunnel (lower diagram)

Coincidence of the detector's signal and the reference signal(s)

Because of the non-circular expansion of fire emissions the test fire concept shows a non-predictable and non-stable time-shift of detectors' and reference signals (see chapter 2.2.1). For this reason *no direct coincidence* of both signals is given so that there is no appropriate reference to quantify the detector's response behaviour (picture 6). However, at the tunnel concept the detector and the measuring equipment are mounted in a way which provides a coincidence of signals at a high degree (picture 7).

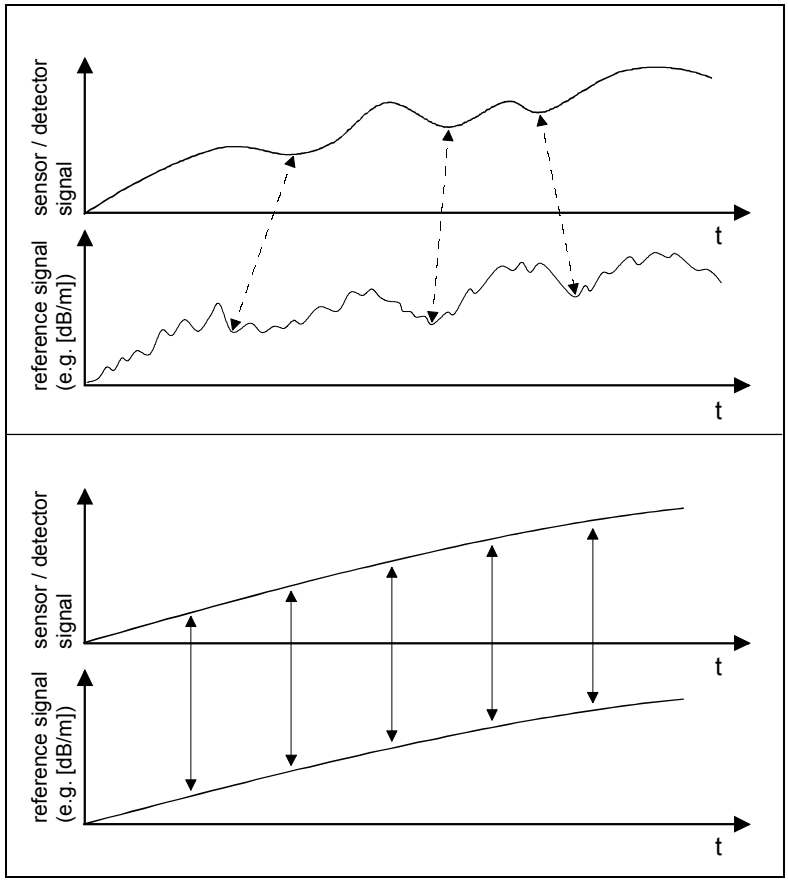

Picture 6: Coincidence of signals: test fire concept (upper diagram) and multi criteria tunnel concept (lower diagram)

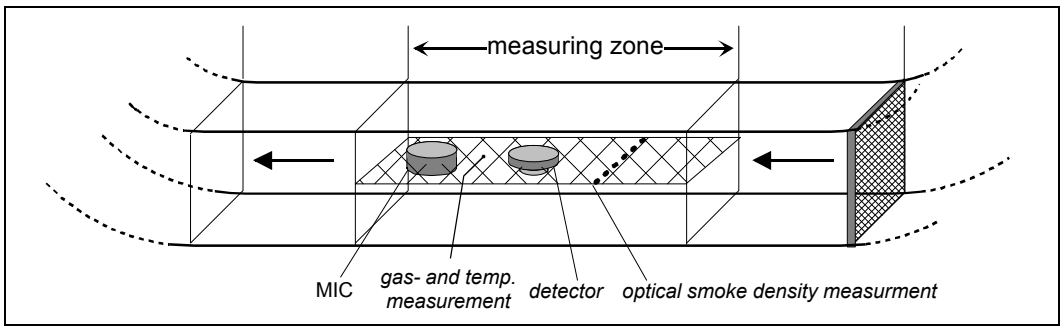

Picture 7: The measuring zone at the multi criteria tunnel

3 Conclusion / Outlook

In this paper a low-cost test procedure was introduced which allows to carry out the stability test for multi sensor fire detectors in a highly repeatable way. However, the appropriate test bench originally was developed and built up at University Duisburg-Essen as *a tool for developing multi sensor fire detectors*. As such it is foreseen to be used for current and future projects. Furthermore, the University Duisburg-Essen has talks with international manufacturers of fire detectors concerning the purchasing of an optimised test tunnel which is described closer by Müller et. al. [Müller 2004].

In comparison to the use of test fires the 'multi criteria tunnel concept' shows crucial advantages concerning repeatability and signal evaluation which are inherent in the concept. Nevertheless, a possible way to improve the properties of test fires for quantifying test purposes to some extend is to control the climate parameters of the fire room. But the degree of success of such a costly alteration is not predictable.

However, the independence from technologies is a weighty argument for the 'test fire concept'. The test tunnel would need to be modified first in order to test fire detectors using radiation or video sensors. But what is the probability for such sensors to appear on the market being implemented in multi sensor fire detectors? The combination of e.g. a video sensor and a conventional fire sensor might make no sense just because of the different areas of surveillance. It needs to be asked:

> *Shall every multi sensor fire detector be submitted to a stability test procedure of minor quality just because of the possible future use of technologies which might never come up?*

A possible solution for this problem could be to follow a bipartite strategy: only those detectors would be submitted to the 'test fire stability test' which are not testable at the tunnel. This provisional regulation could be applied until the multi criteria tunnel is modified adequately (if it makes economic sense). Nevertheless, in case of a 'test fire stability test' the current demands on the stability of fire detectors regarding environmental impacts (factor 1.6 according to EN 54) would need to be weakened. Weakening the demands by the extend of uncertainty of the test fires might result in a max. factor of deviation amounting to 2.0 or higher.

4 References

CEA 4021 n.n.: "Specifications for fire detection and fire alarm systems: requirements and test methods for multi sensor detectors, which might respond to smoke and heat, and smoke detectors with more than one smoke sensor"; CEA Guideline 4021, EFSAC-endorsed document, Paris, 1999

EN 54-7 n.n.: "Fire detection and fire alarm systems - part 7 smoke detectors - point detectors using scattered light, transmitted light or ionisation"; European Committee for Standardisation, Brussels, 2000

ISO/IEC 2001 n.n.: "Rules for the structure and drafting of international standards"; ISO/IEC directives, part 2, fourth edition, 2001

LINDEN 1998 O. Linden: "Untersuchungen zur Eignung von Gassensoren für die Brandmeldetechnik"; Diploma Thesis at University Wuppertal, section Fire and Explosion Protection, 1998

LINDEN 2003 O. Linden: "Entwicklung von Prüfmethoden zur Sicherstellung der Schutzfunktion von Brandmeldern mit Gassensoren"; ISBN: 3-936050-05-8; VdS Schadenverhütung; Series "Wuppertaler Berichte zum Brand- und Explosionsschutz", No. 4, 2003

MÜLLER 2004 U. Müller, O. Linden, W. Krüll, I. Willms: "Test Tunnel for Multi Sensor Fire Detectors"; AUBE- Proceedings 2004

Ulrich Müller, Oliver Linden, Ingolf Willms and Wolfgang Krüll
Department of Communication Systems, Duisburg-Essen University,
D-47058 Duisburg, Germany

Test Duct for Multi Sensor Fire Detectors

Abstract

In the course of developing a testing concept for multisensor fire detectors and multi-sensor aspirating systems a new test bench has been built up at the department of Communication Systems at the University Duisburg-Essen. Main part of this test bench is a duct which provides the opportunity of performing a stability test of multisensor fire detectors while showing a high grade of repeatability. It needs to be stressed that the test bench has been developed to be used for carrying out a function-based stability test which allows the fire detector to be evaluated as one system including the influence of data processing. However, the new multi criteria duct can also be used for development purposes and/or to simulate potential conditions of deceptive alarm.

Introduction

The new test duct has a similar application area as the NIST´s Fire Emulator / Detector Evaluator FE/DE. However, the main task of the FE/DE is to simulate reality-like fire and non-fire scenarios and not to perform stability tests in order to quantify the response behaviour of fire detectors. In contrast to the open duct principle of the FE/DE the presented multicriteria duct is self-contained and provides for an improved repeatability and for linear rising concentrations of fire phenomena. It can be used for fire and non fire tests. The new test duct is applicable for detector design, development and test.

Within the multi criteria duct defined mixtures of a) smoke / particles b) gases and c) heat can be generated at flow streams between 0,1 m/s and 3,0 m/s. The single fire (and non-fire) phenomena can be generated the following ways:

a) smoke / particles:
- by leading in fire emissions *or*
- by leading in paraffin oil *or*
- by leading in (dust) particles as potential sources of false alarm

b) gases: - by leading in fire emissions *and/or*
- by leading in single gases or gas mixtures from gas cylinders optionally water vapour can be injected (if necessary)

c) heat: - by heating up the duct material by means of heating cables *and*
- by simultaneously leading in hot air to heat up the air in the duct

This paper shall show the setup of the new test bench as well as results of repeatability measurements regarding smoke density, gas concentrations and temperature.

Technical Background of implemented features

For testing multi sensor fire detectors with gas sensors it is important that the combustion gas mixture is not changed by the test equipment to a greater extend. So the new test duct uses a low temperature heating concept due to the reason that zones of high temperature might promote chemical reactions among the gases. Furthermore, the presence of silicone compounds has a potentially poisoning effect on some gases which might result in a non-reversible change of the sensing properties. Another unwanted effect has been excluded or minimised by the use of teflon-coated stainless steel. However, the use of chemical elements like zinc or copper might promote chemical reactions with the combustion gases. In addition further positive effects are reached due to the choice of the duct material: the metal is protected against oxidation, the whole duct can easily be grounded and the danger of water condensation at the heated metal surface is almost excluded.

The multi criteria duct is self-contained in order to reach a high grade of repeatability and almost linear rising concentrations of fire phenomena. A sheet metal of not more than 1 mm thickness is used to achieve a low heating time constant for the duct material. The maximum temperature rise of the duct (4 K/min) has been chosen with respect to the development of the moderate burning open test fire TF 1.

The testing of heat detectors according to EN 54–5 is not realised yet. For this purpose the heating concept would have to be upgraded to achieve a temperature rise of 30 K/min. However, this feature is not relevant for testing multi sensor fire detectors.

To achieve a homogeneous heating of the test duct the aerosol inside the duct and the duct material are heated up by different heaters. The whole surface of the duct is heated by 290 meters of heating cable, the inspection windows are heated by using heatable window panes. Currently the duct air is heated by means of a hot air blower. In the next time the blower will be replaced by a heater which will be mounted inside the duct. First experiments with the hot air blower have shown a bad influence on both linearity and repeatability of the rise of fire phenomena.

Figure 1 visualises a simulation of the heating concept. The left curve of Figure 1 shows the temperature rise of the air at the measuring zone being produced by the hot air blower working at a flow-rate of $\dot{V} = 200l/\min$ and a temperature of $T = 60°C$. The temperature rise of the duct material is shown in the right curve of Figure 1. It is produced by 290 meters of heating cable being operated at $P = 5500W$.

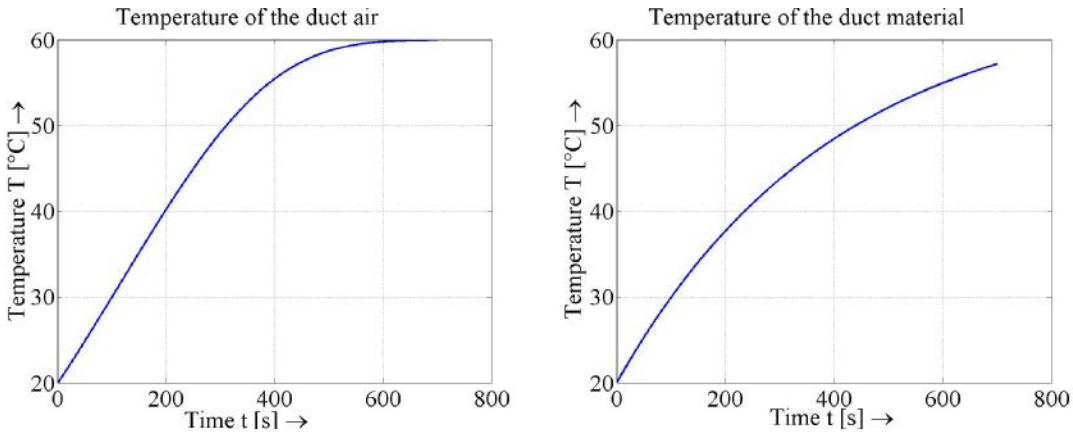

Figure 1: Simulated temperature of the duct air (left curve) and the duct material (right curve)

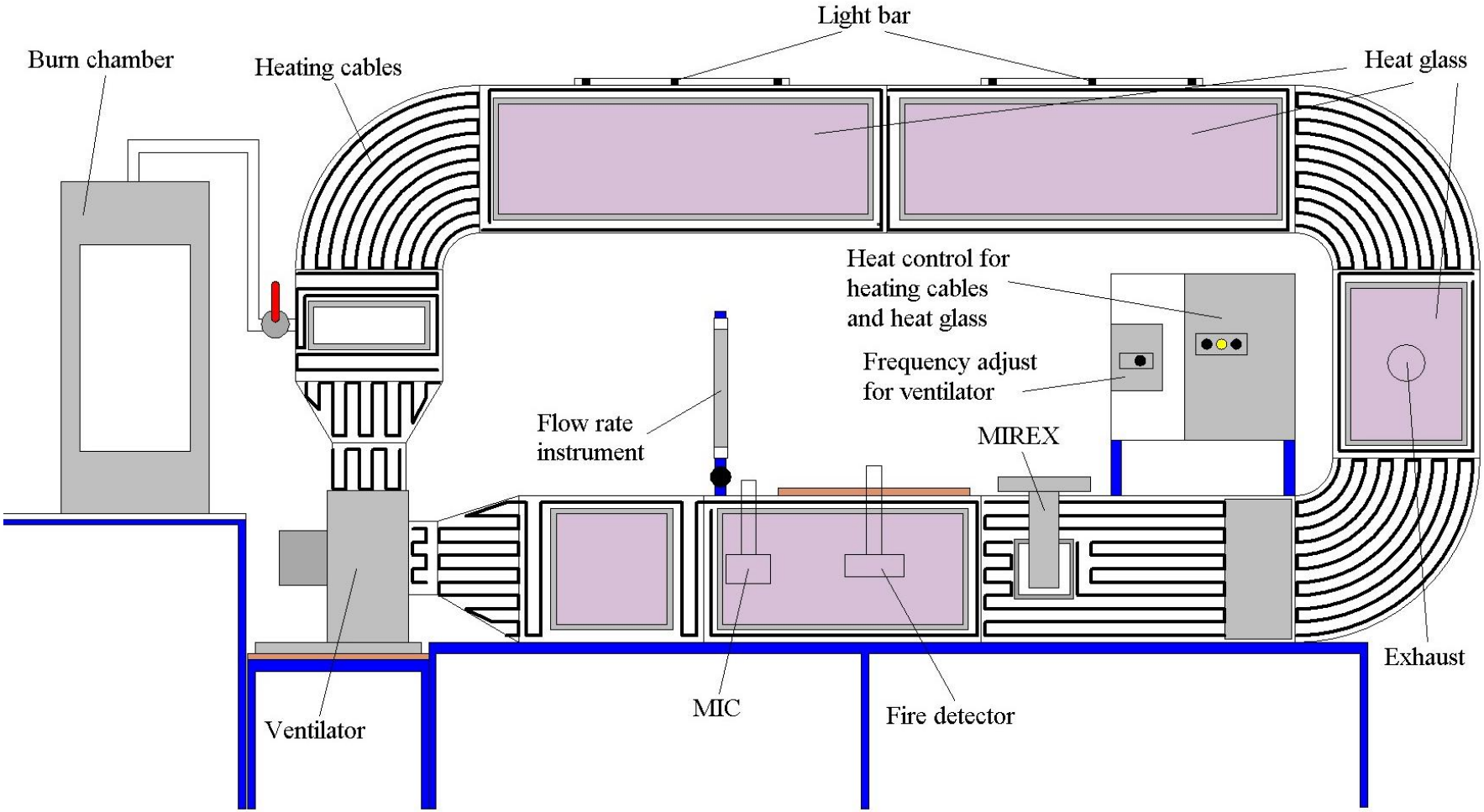

Figure 2: Setup of the test bench

The test bench setup

The setup of the test bench is printed in Figure 2. The technical data of the test bench is given below. Up to date photos of the test duct are pictured in Figure 3 and in Figure 4.

Technical data of the test duct:

Function:	Testing of fire detectors with smoke-, heat- and / or gas-sensors		
Temperature range:	20…60°C		
Wind velocity:	0,1…3,0 m/s		
Inserted substances:	user-defined		
Temperature rise:	0…4 K/min		
Max. heat power:	8 kW		
Measurement :	- smoke density:	Transmitted light:	MIREX
		Ionisation chamber:	MIC
	- gas concentrations:	Infrared photometry:	Uras 14
	- temperature:	PT 100	
Volume:	1200 l (Mean airway 7,5 m; Cross section 0,4 m x 0,4 m)		
Principle:	self contained duct		

Figure 3: Test duct

Figure 4: Measurement equipment

Results of repeatability measurements

Particle density:

A Lorenz AGW paraffin oil generator was used to produce a defined rise of particle density within the duct. For first evaluation studies the following parameters have been chosen:

Frequency of the internal valve:	1.5 Hz
Total flow rate:	50 l/min and
Paraffin oil temperature:	100°C

With these parameters the following rise of smoke density can be measured in duct:

$$\frac{\Delta m}{\Delta t} \cong 0.07 \frac{dB}{m \cdot min}$$

The gradient fulfils the specifications for testing smoke detectors according to EN 54-7:

$$0.015 \frac{dB}{m \cdot min} \leq \frac{\Delta m}{\Delta t} \leq 0.1 \frac{dB}{m \cdot min}$$

The measured data is graphed in the Figure 5 to Figure 7. The studies have been carried out without using the heating system.

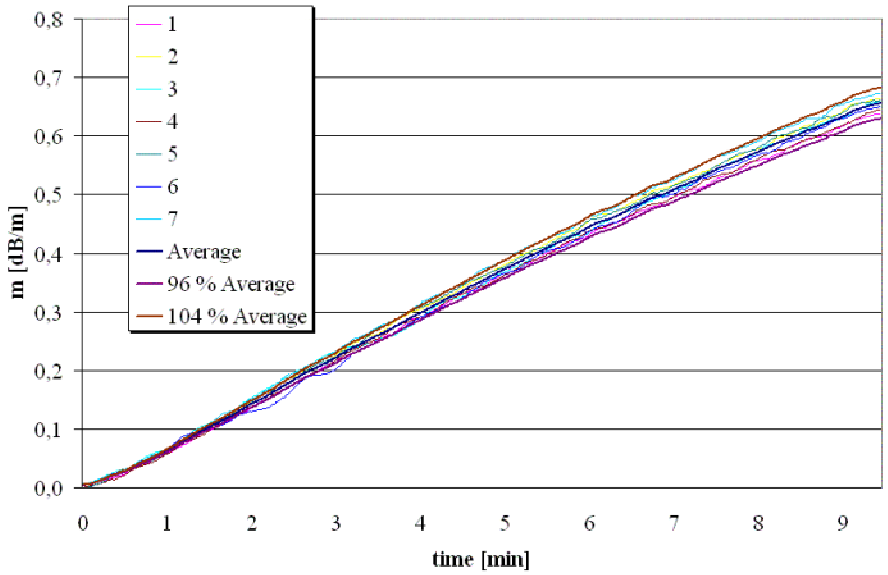

Figure 5: Smoke density measurement with the MIREX

Figure 5, Figure 6 and Figure 7 show a very high grade of repeatability. The rise of smoke density is almost linear. The repeatability factor for the MIC and the MIREX is $\frac{1.04}{0.96} = 1.08$. It describes the maximum factor of deviation regarding the highest and the lowest value being measured at the same point of time.

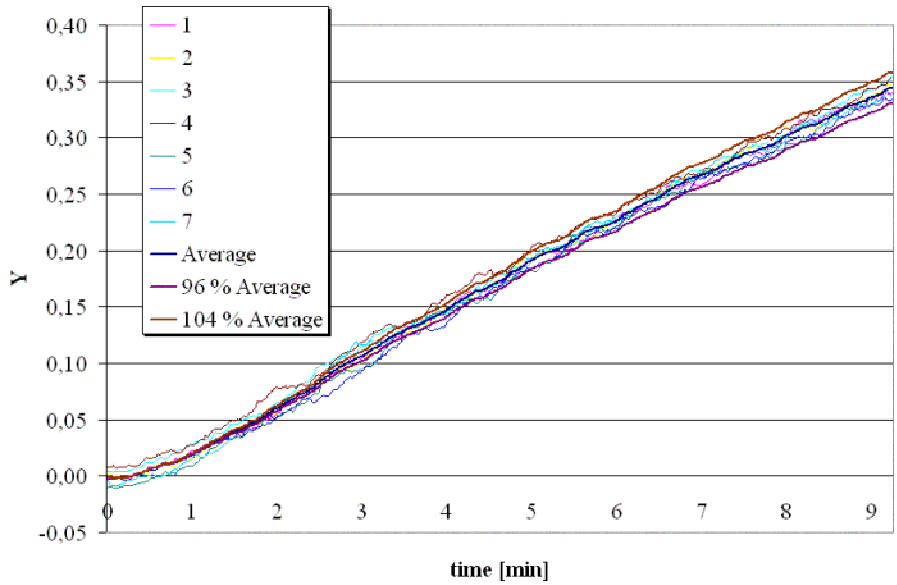

Figure 6: Smoke density measurement with the MIC

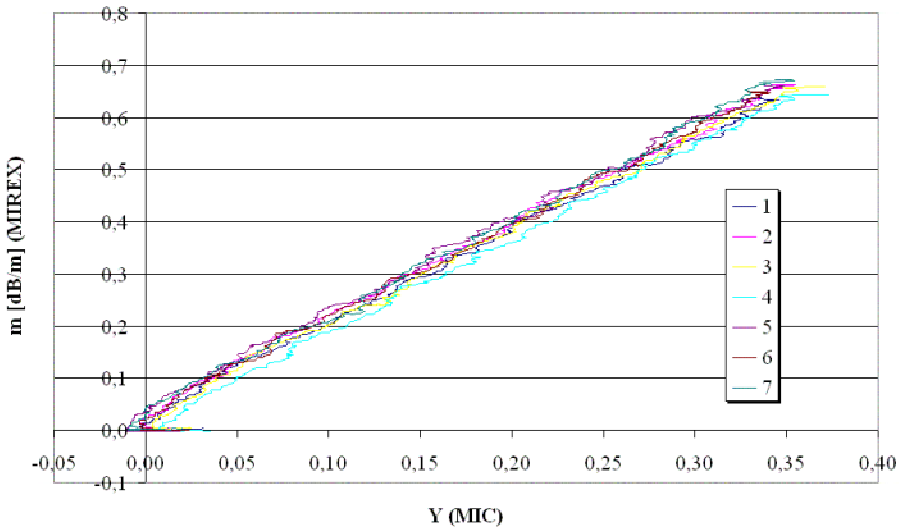

Figure 7: Plot of the function m = f(Y)

Temperature rise:

The temperature rise in the measurement zone shows the function of the heating system (Figure 8). Until the end of the test a temperature rise of $\Delta T \cong 27K$ was reached. The presented evaluation studies already show a high repeatability (repeatability factor: 1.04). However, currently no kind of heating control is implemented. A later implementation of a heating control is planned to obtain a high grade of flexibility for future investigations.

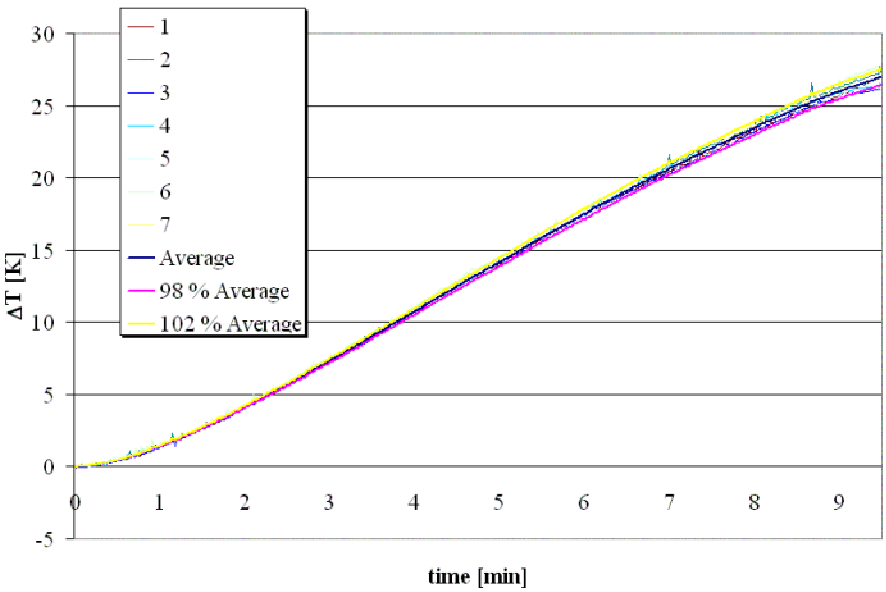

Figure 8: Measurement of the temperature rise inside the test duct

Rise of gas concentrations:

For generating combustion gases 3 cotton wicks have been burned down in the burning chamber which was provided with clean air at a constant flow rate of 42 l/min and a relative humidity of 50 %. The concentrations of carbon monoxide and carbon dioxide have been measured (see Figure 9 and Figure 10).

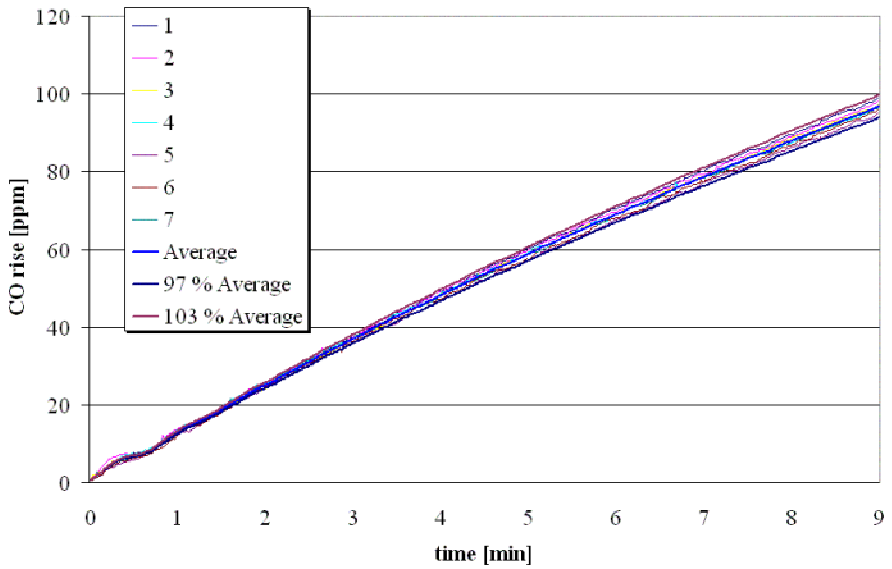

Figure 9: Measurement of carbon monoxide concentration

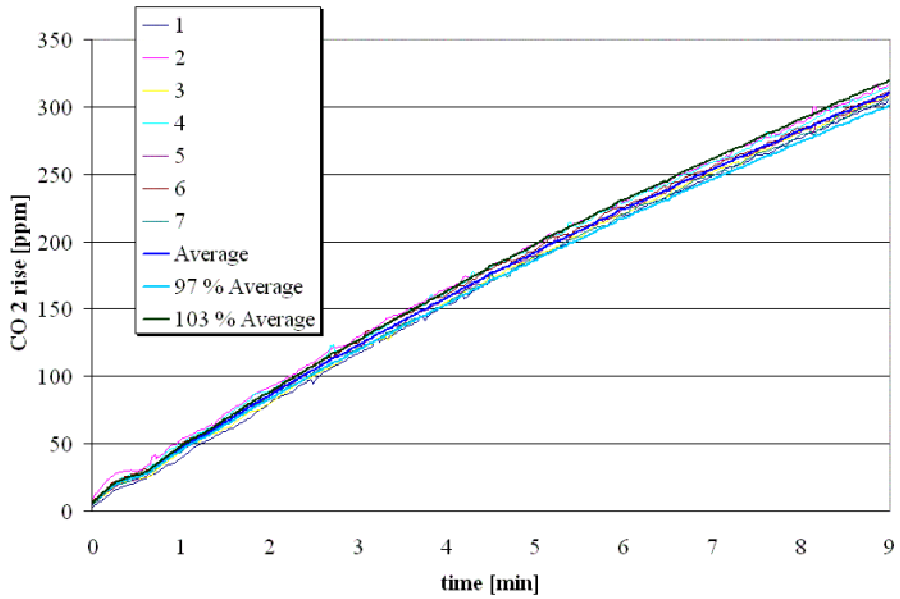

Figure 10: Measurement of the rise of carbon dioxide concentration

Former investigations at University Duisburg-Essen have already shown a high repeatability of gas concentrations being generated by cotton wicks being burned under defined conditions. According to the expectations also the current test results presented in the Figure 9 and Figure **10** show a low grade of deviation and a highly linear rate of rise. For both carbon monoxide and carbon dioxide a repeatability factor of 1.06 was reached. The studies have been carried out without using the heating system.

Conclusion

The first evaluation studies which have been performed with the new multi criteria test duct have shown absolutely promising results. Both the rate of rise and the repeatability of the generated fire phenomena already meet the initial objectives at a very early stage. These objectives have been set up in order to perform a defined and repeatable stability test for multi sensor fire detectors. The repeatability factors which have been achieved regarding the rise of temperature, particle density and gas concentrations are smaller than 1.1. This is far below the permitted max. change of response behaviour (factor 1.6) a detector may show according to EN 54. However, additional tests need to be performed for final conclusions concerning all repeatability issues.

In the future more automatic functions have to be integrated. Magnetic valves and the heating option shall be controlled by PC in order to allow fully automated testing. Furthermore, it is intended to implement a continuously adjustable temperature control (0…4 K/min) and a complex humidity measurement / control unit. Further work will also be done on the implementation of vapour and dust generators and tests concerning slowly developing fires. Beyond that the basic concept of the new duct shall serve as low-cost testing concept for multi sensor fire detectors by providing the opportunity to upgrade existing EN 54 - test benches with low financial efforts.

References

/1/ O. Linden, Entwicklung von Prüfmethoden zur Sicherstellung der Schutzfunktion von Brandmeldern mit Gassensoren, Dissertation, Bergische Universität Wuppertal, February 2003

/2/ U. Müller, Konzeption einer Prüfeinrichtung zur Bestimmung der Ansprechschwelle von Multisensor-Brandmeldern für Brand- und Nichtbrandsituationen, Diploma thesis, Universität Duisburg-Essen, December 2003

/3/ U. Müller et al., Design and functionality of a new test duct for multi sensor fire detectors, Proceedings of EUSAS-Workshop on "Multiple Sensor based (Fire-) Detectors; Design and Testing", Lübeck/Germany, June 2004

PDG Massingberd-Mundy
Vision Systems (Europe) Ltd, Hemel Hempstead, UK

M Serveau ; DEF, France
F Daniault ; Wagner, Germany
J-P Dhaine ; CNPP, France

Development of the prEN54-20 for Type Approval of Aspirating Smoke Detectors

Abstract

This paper describes the development of the new standard prEN54-20 which is founded on the requirements of EN54-7 and includes several new test fires for the type approval of Aspirating Smoke Detectors (ASDs). Typical applications for ASDs are outlined and provide the reasoning behind the introduction of three ASD Classes which is fundamental to the new standard. The essential requirements of the new standard are reviewed and the challenges in developing a new range of test fires outlined for high sensitivity ASDs.

Introduction

The many benefits of Aspirating Smoke Detectors (ASDs) are now widely recognised and the technology is used in many applications. In support of this CENTC72 was mandated to write a standard for the type approval of this well established technology. This paper reviews the main drivers for installing ASD systems, as opposed to other fire detection solutions, which leads into a description of the classification system developed by the CEN Working Group (WG16). Following a review of the importance of the EN54 series of standards in the European and International framework, this paper describes the essential objectives of a Type Testing standard and outlines the thinking of the WG in selecting the various test and performance requirements.

Undoubtedly the biggest challenge for the working group has been the development of fire tests to test the performance of the high sensitivity ASDs in order to verify their capability as fire detectors. EN54-7 (ref 1) provides for the type approval of point type smoke detectors using standard test fires TF2, TF3, TF4 and TF5, these test fire are not

directly suitable for testing the early response capabilities of high sensitivity ASDs. Never-the-less, these test fires have been used successfully in the certification of ASDs by arranging for significant dilution of the smoke sample taken from the fire test room - for example, installing 1 hole in the test room and 39 holes outside thereby proving the fact that ASD detectors perform as least the same as a point detector based on a "point per sampling hole" design concept. However, due to their advanced sampling technology, ASDs can perform much better which creates a need for alternative test fires. The development of a set of reduced test fires is outlined in this paper but the full details are provided elsewhere (ref2).

Finally this paper introduces the value of performance based testing to verify the on-site performance of enhanced and high sensitivity ASDs. Reference is made to standardized hot wires tests currently available and current work in the area is outlined concluding in a proposal for the formation of a group to co-ordinate the work.

What is an ASD?

It continually draws air samples by means of an aspirator or fan through one or more sampling pipes (or more formally a *sampling device*) to a central detector where the samples are analysed for the presence of smoke. This method allows one detector to examine air from many places within the fire zone. Also, where the detector is highly sensitive it can detect very low levels of smoke.

The formal definition of ASD in prEN54-20 includes the sampling device. However, for the purposes of this paper the term *ASD* shall be used to describe the central detector unit (most typically containing the aspirator, sensing elements, displays and controls/signalling capability) and the expression *"ASD system"* shall be used to include the sampling device (see figure 1).

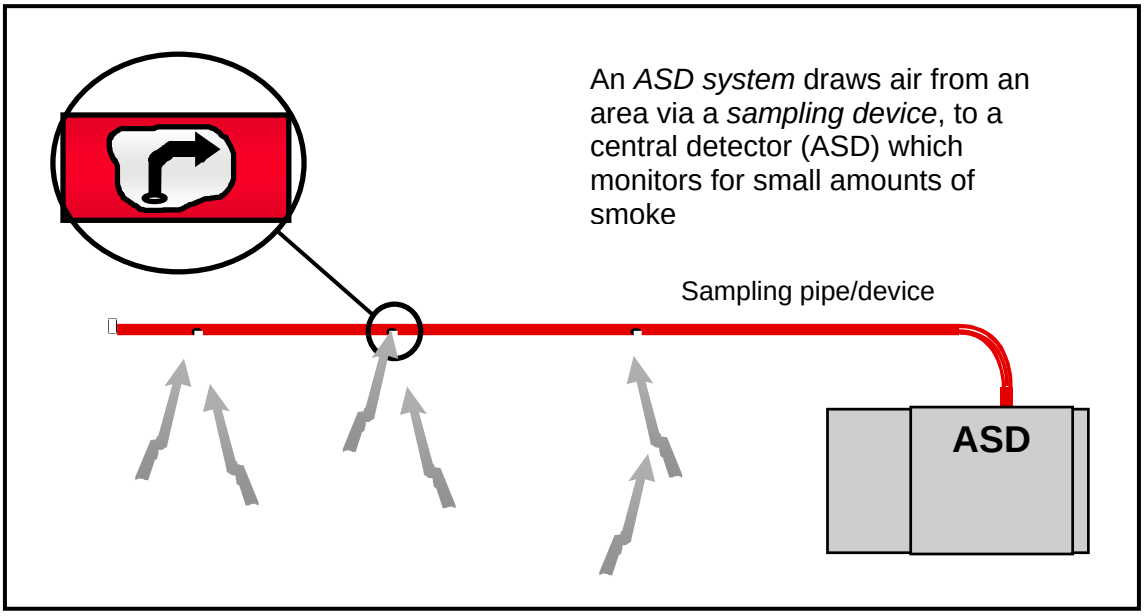

Figure 1 – ASD system showing the detector (ASD) and *sampling device*

The drivers for using ASD systems

During the first meeting of TC72WG16 in Paris in September 1999 the applications for ASD systems were considered. The following seven drivers encompass the main reasons for installing an ASD system.

- Environmentally challenging areas
- Aesthetics and concealed detection are important
- Maintenance access is limited
- Smoke is difficult to detect (e.g. high airflows, high ceilings or open areas)
- Earliest detection to enable business continuity
- Extra time is required for safe evacuation
- Unnecessary suppression release must be avoided

As a result ASD systems are installed in a wide range of applications, from clean rooms, computer suites and telecommunication facilities to heritage buildings, prisons, shopping complexes and industrial facilities. Today, ASD have also been widely used to provide innovative detection system design and meet performance based design requirements as acceptable alternative design in applications where normal point detectors are tranditionally used.

Essentially these seven drivers break done into three core attributes of the ASD technology:

- early warning/high sensitivity,
- cumulative sampling providing enhanced coverage and protection
- flexibility of design and applications.

The needs for ASD Classification

It was recognised that attitudes to ASD differ across Europe with some markets using the technique primarily for its flexibility in difficult or inaccessible applications while other markets capitalise on the early warning capabilities of the technology. These attitudes are reflected in the products that dominate in the various markets – either standard sensitivity systems using point detector technology integrated into a fan enclosure or bespoke high sensitivity detections system capable of very early warning. To accommodate these stark differences in technology it was necessary for the working group to define a Classification system and three levels were identified:

- Class A – super enhanced sensitivity
- Class B – enhanced sensitivity
- Class C – normal sensitivity

These essentially address the three core attributes identified above and have enabled TC72WG16 to develop a standard that covers the whole range of aspirating systems.

The cumulative effect

To have confidence that the detection performance of an ASD system is effective, it has been usual to demonstrate that the detection performance of a single hole is equivalent to a point detector. In view of this, the scenario of smoke only entering one hole is considered and it must be recognised that ASD systems have an inherent dilution whereby smoke entering one active hole is diluted by clean air entering other holes. Therefore, to achieve the necessary performance, the central detector must be more sensitive than a standard point detector.

However, when viewed for a different perspective, this *dilution* effect is, in fact, one of the unique benefits of an ASD system and gives them the ability to reliably detect lower concentrations of smoke than a normal point detector – not only because the single central detector typically incorporates more advanced stable technology than a low cost point detector - but also because ASD systems effectively become *more* sensitive *when* smoke enters more than one sampling point. In any real fire scenario, it is highly unlikely the smoke will only enter one hole. When smoke enters more than one hole the smoke concentration at the central detector is less diluted. As a result, ASD systems have a natural ability to detect "diluted" smoke in the space – the more dispersed or diffused the smoke becomes the more sampling holes it enters and the higher the effective sensitivity of the ASD becomes. This positive feature essentially reverses the natural dispersion and diffusion of smoke in a volume and is often referred to as the *cumulative* effect by ASD manufacturers.

Standards, approvals and type testing

Whatever the technology, the value of independent 3rd party verification of performance cannot be disputed. Essentially, the aim of 3rd party testing is to demonstrate the performance and robustness of a particular technology in consideration of its application.

The importance of 3rd party testing is particularly relevant to ASD systems where the complexities of dilution mean that misleading claims can be made due to manufacturers/installers mistakenly using normal sensitivity point detector to cover many holes. In recognition of this CEA developed type testing guidelines for ASD systems which was first published as GEI 1-048 in January 1997(ref 3). The latest version of this document was published as a specification CEA 4022 in December 1999 (ref4) and has been endorsed by EFSAC (European Fire and Security Advisory Council – www.efsac.org). This standard (and it's derivatives such as the ONorm F3014 (ref5)) is developed from EN54-7 requirements and has been the cornerstone of ASD approval throughout most of Europe . The only exception is the Norm Francaise, NFS61950 (ref6) which includes specific requirements for *détecteur multiponctuel* which include a Go/No-go smoke test using a piece of cellulose burnt in test tunnel. This test does not

include measurement of the smoke concentration and is a relatively crude open loop test requiring that the detector responds before the cellulose has totally burned. As a result it has not been adopted outside France.

With the establishment of the Construction Products Directive (CPD) (ref7) and the specific decision to make Fire related products subject to Level 1 attestation in order to affix the CE mark, the need for a harmonised standard for the type approval of ASD systems was identified and TC72 was mandated to produce a standard.
TC72WG16 adopted CEA 4022 as the basis for prEN54-20

Type Testing of a product includes:

- testing for reliability, repeatability, robustness (including environmental and EMC testing).
- Testing for performance in operation - the challenge; a representative cross spectrum of smokes/fires within realistic costs,

By adopting the CEA standard, the tests for reliability, repeatability and robustness were largely defined and are based on the same requirements as EN54-7. Table 1 shows a summary of the tests required and includes a convenient comparison with EN54-7. It is clear that the differences are minimal.

The principal difference is that prEN54-20 requires that the flow monitoring capability of the ASD is checked at appropriate stages during the testing to verify that it is reliable. Specifically the detector shall signal a flow fault when the volumetric flowrate is reduced or increased from the normal flow by 20%.

Test	Test sensitivity...	Requirement	Check Flow	EN54-7
Repeatability	6 times on 1 sample	$N_{max}/N_{min}<1.6$	N	Similar *
Reproducibility	on 8 samples	$N_{max}/N_{mean}<1.3$ $N_{mean}/N_{min}<1.5$	Y (each unit)	Similar *
Variation of supply voltage	min, nominal & max	$N_{max}/N_{min}<1.6$	as smoke	Similar *
Dry heat (55ºC for16 hours)	B, D & A	$N_{max}/N_{min}<1.6$	D & A	Same expect only 2h
Cold (–10ºC for 16 hours)	B, D & A	$N_{max}/N_{min}<1.6$	D & A	Same
Damp heat, (40ºC, 93%RH for 4 days)	B, D & A	$N_{max}/N_{min}<1.6$	D & A	Same
Damp heat, (40ºC, 93%RH for 21 days)	B, D & A	$N_{max}/N_{min}<1.6$	D & A	Same
SO_2 corrosion (25ppm for 21 days)	B & A	$N_{max}/N_{min}<1.6$	A	Same
Shock ($10 \times (100 - 20M)$ m s^{-2})	B & A	$N_{max}/N_{min}<1.6$	A	Same
Impact (0,5 J)	B & A	$N_{max}/N_{min}<1.6$	A	Different
Vibration (10-150 Hz, 5 m s^{-2})	B & A	$N_{max}/N_{min}<1.6$	A	Same
Vibration (10-150 Hz 10 m s^{-2})	B & A	$N_{max}/N_{min}<1.6$	A	Same
EMC - Immunity tests (EN50130-4)	B & A	$N_{max}/N_{min}<1.6$	A	Same

Key : N=response threshold, B=before, D=during, A=after

* the only difference is that EN54-7 includes an additional requirement that $y_{min}>0.2$ and m_{min} >0.,05dBm

Table 1 – prEN54-20 environmental requirements compared with EN54-7

Another difference between EN54-7 and prEN54-20 is that the former includes maximum sensitivity requirement for point detectors to prevent poor quality products becoming approved by simply increasing the gain to pass the more challenging fire tests (typically TF4 and TF5 for optical detectors) because such actions increase the risk of unacceptably high false alarm rate in the field. However, for ASD systems such a maximum sensitivity requirement contradicts their value as early warning detectors and is not included in prEN54-20.

Finally, two further differences between the two standards, namely the 16 hour “hot” test and new impact test reflect the larger size of an ASD compared to a point detector. In all other aspects the requirements of prEN54-20 are essentially the same as EN54-7 including; individual alarm indications, threshold adjustments, response to slowly developing fires, software assessment, marking and data/documentation.

Development of Fire tests

It is beyond the scope of this paper to describe the details of the new *reduced* fire tests for verifying the performance of Class A, B and C detectors. (see ref 1) but the following paragraph provides an overview.

Fundamentally, the challenge is that the test fires in EN54-7 and CEA 4022 are intended for standard point detectors. While these tests are suitable for Class C ASD systems they cannot be used to verify the performance of enhanced (Class B) or high sensitivity (Class A) systems. However, simply scaling down the existing tests to produce less smoke is not practical due to the low thermal energy, lack of lift and resulting chaotic nature of the smoke which leads to results with very poor repeatability. A proposal to introduce forced movement of the air in the Fire test room using a simple duct and fan positioned about 1.5m above the fire was successfully developed into a new range of reduced tests. Fuel quantities and end of test conditions have been developed by the members of TC72WG16 and CNPP to correspond with the three classes A, B & C. The use of a fan essentially disperses the smoke throughout the fire test room so that the chaotic effects of relying on a smoke plume are avoided.

Verifying installed performance

Product that are approved are only reliable and effective in the field if they are specified and installed correctly. In the case of point detectors, various prescriptive national standards exist across Europe which effectively provide clear recommendations on the frequency and positioning of point detectors. For example, for optical and ionisation point detectors ; VdS 2095 (ref9) recommends an area coverage of 60-110m² for each detector depending on the ceiliing height, BS5839-1 (ref 10) basically recommends a radius of coverage of 7.5m and the French APSAD R7 rules (ref11) recommend area coverage of 60-120m² depending on ceiling height and incline. [It should be noted that the R7 rules specify the maximum area coverage of an ASD sampling hole as 35m² - but requirement must be considered in conjunction with the NFS61950 requirements mentioned above]

The recommendations for the spacing of point detectors are based on years of experience and an assumption that the detectors meet a minimum criteria (e.g. EN54-7). In many cases smaller areas of coverage are defined for specific risks such as high air flows – as detailed in BS6266 (ref12) and VdS 2095 (ref9).

The same prescriptive rules can be applied for Class C ASD systems because individual holes have been approved as meeting the minimum criteria for a point detector. Unfortunately, for Class A & B detectors the installation *rules* are not well defined. However, since such systems are invariably provide better detection capability than normal Class C systems it is reasonable to space the holes in accordance with the rules for point detectors and be assured of meeting the minimum requirement. Where verification of the improved performance capabilities of class A & B systems is required the best option is to specify a performance test. BS6266 is unique in this regard and, by reference to the BFPSA code of Practise for Aspirating Systems (ref13), defines hot wire tests and a smoke pellet test which are often used to verify the performance of high sensitivity and enhanced sensitivity ASD systems. Performance tests are also specified in the APSAD R7 rules (ref 11) but these typically release large quantities of smoke and are intended for testing point detectors (and by inference Class C ASD systems). Clearly more work is required to develop a full range of performance tests suited to the wide range of environments into which ASD systems are installed. There are some various national groups in various organisations working to develop installation recommendations and performance tests for ASD systems – either specifically or as part of a more general guide for the installation of fire detectors. Clearly any such performance tests must consider the applications, the associated risks and performance requirements - which is not an easy task. A joint European or international working group to develop and co-ordinate the specification of on-site performance tests would be more efficient and build on the successful work of TC72WG16 in creating prEN54-20..

Conclusion

TC72WG16 has successfully written prEN54-20, a type testing for ASD systems. The standard has been developed from EN54-7 by the introduction of specific requirements for ASD systems and introduces three sensitivity classes to define high sensitivity ASD systems – reflecting the increasing adoption of ASD as a detection solution in a wide range of applications. In support of these classes a new series of reduced test fires has been developed to provide repeatable low concentrations of smoke in the EN54 fire test room. Ongoing development of performance based tests for use in the field will continue to ensure that ASD technology is correctly installed and applied.

Acknowledgements

This paper and the standard prEN54-20 would not have been possible without the following people:

- the joint authors of this paper and other members of TC72 WG16 who were key to the development of prEN54-20.
- Vision Fire and Security in supporting the development of this important standard
- John Northey (TC72) for supporting the inclusion of ASD in the CEN mandate 109 and for his guidance through the final stages editing.
- Richard Philips (LPCB) for his support and comments during the development of the reduced fire tests.
- Claude Jouis (CNPP) who performed the test and presented the results during the development of the fire tests.

References

1. prEN54-20
2. EN54-7:2001 Fire detection and fire alarm systems – Part 7: Smoke detectors – point detectors using scattered light, transmitted light or ionization.
3. Paper: New fire tests for aspirating smoke detectors. J-P Dhaine, CNPP. AUBE '04 Conference, Duisburg, September 2004
4. Comité Européen des Assurances. GEI 1-048, 30-01-97. Guidelines for fire detection and fire alarm systems. Test methods for Aspirating Smoke Detectors
5. Comité Européen des Assurances. CEA 4022 :1999-12. Specifications for fire detection and fire alarm systems. Requirements and test methods for Aspirating Smoke Detectors
6. ÖNORM F 3014 Ausgabe: 1999-02-01 Rauchansaugsysteme in Gebäuden und Bauwerken Raumschutz und Lüftungs-leitungsschutz (Aspirating smoke detectors in building constructions – Indoor protection and protection of ventilation pipes)
7. NFS61-950 Novembre 1985 Matériel de détection d'incendie. Détecteurs, tableaus de signalisation et organes intermédiaires
8. Construction Products Directive 89/106/EEC
9. VdS 2095 : 2001-3 (05) VdS-Richtlinien für automatische Brandmeldeanlagen – Planung und Eunbau
10. BS5839:1 : 2002 Fire detection and fire alarm systems for buildings – Part1 : Code of practice for systems design, installation, commissioning and maintenance.
11. ADPAD R7 Règle d'installation. Detection automatique d'incendie
12. BS6266 : 2002 Code of practice for fire protection for electronic equipment installations
13. BFPSA – British Fire Protection Systems Association Code of practice for category 1 aspirating detection systems

J-P Dhaine
Centre National de Prévention et de Protection (CNPP), Division Electronique de Sécurité (DES), Vernon, France

New fire tests for aspirating smoke detectors

Abstract

New fire tests for aspirating smoke detectors, developed by CNPP and TC72-WG16 in the frame of the project prEN 54-20, are presented. These tests allow the evaluation of the sensitivity of the aspirating smoke detectors.

Introduction

The TC72 working group 16 was set up with the assigned task to define requirements for aspirating smoke detectors (ASD). This has been made with the project prEN 54-20. According to their sensitivity, prEN 54-20 classes the ASD into three classes. From the most to the less sensitive, these classes are: A ("super enhanced sensitivity"), B ("enhanced sensitivity"), C ("normal sensitivity"). A class C ASD is a detector which, submit to the fire sensitivity tests TF2 to TF5 (the same as those defined in EN 54-7) shall succeed to the corresponding requirements. So, the working group 16 considered that class A and B ASD shall respond to the same variety of types of smoke than class C ASD, but, in order to verify there higher sensitivity, that new fire tests producing lower levels of smoke concentration had to be defined.

Preliminary orientation

The choice was made, for the definition of reduced-fire tests, to use, as far as it is possible, the test apparatus used for point smoke detectors (i.e. detectors complying with EN 54-7), first the fire test room.

This is justified by two aspects. First, the method for testing the fire sensitivity of point smoke detectors has been defined and is used for decades. The corresponding tests are well known and accepted by manufacturers, laboratories and users. So, the new fire tests for enhanced and super enhanced sensitivity shall respect the "philosophy" of the tests defined in EN 54-7 for normal sensitivity. Secondly, the financial aspect is concerned. It

is important that all laboratories interested might use the new tests, and not only laboratories which could afford to buy the potential new test apparatus. This is especially true with ASD, since the number of such detectors tested by laboratories is not, and will probably not, be so important to justify the purchase by a laboratory of a totally new test equipment dedicated to these detectors.

Ventilation system

ASD has a particularity compare to point detectors: the aerosols produced by the fire are mechanically conveyed from the sampling point (inside the fire test room) to the sensing element (outside the fire test room). So, to avoid the direct sucking by the sampling network of the ASD of the aerosols produced by the fire, it is necessary to dilute these aerosols in the test volume (fire test room). For this purpose, a ventilation equipment has been designed (see Fig. 1). It is constituted of a square section tunnel located in the fire test room as shown in figure 2. The air speed at the output of the tunnel is tuned at 1 m/s and maintain constant during the tests (to have a stable air movement in the fire test room).

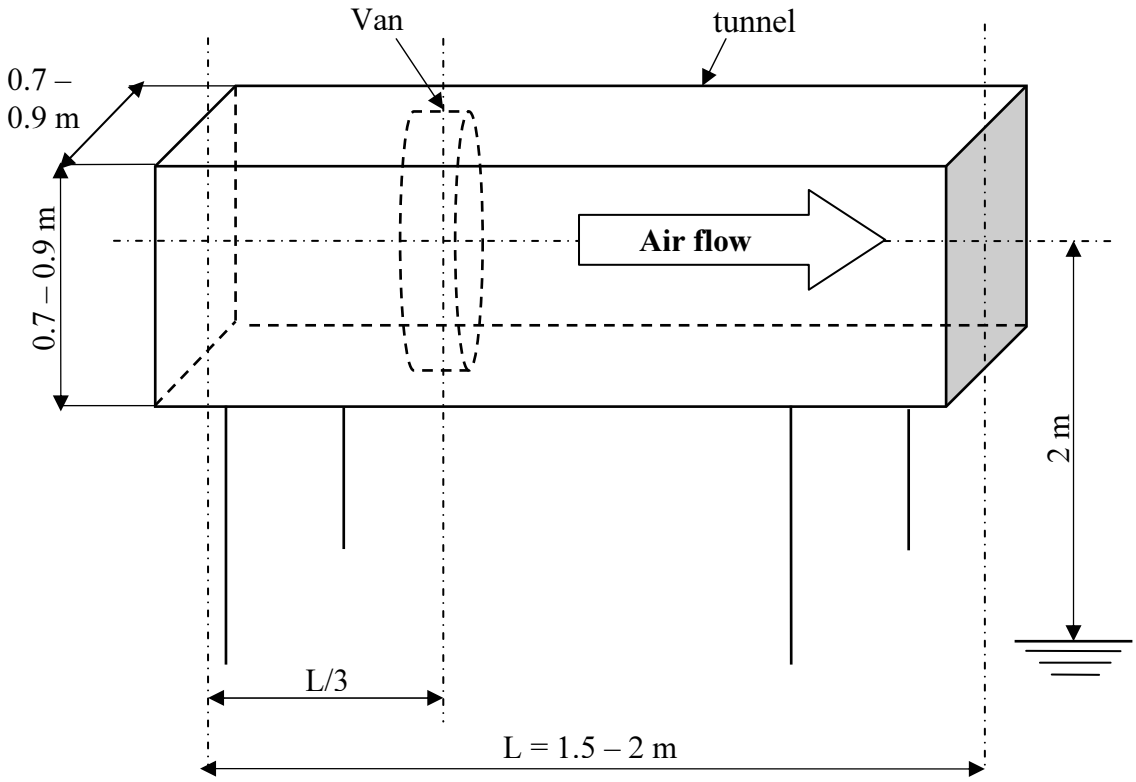

Fig. 1 Ventilation system

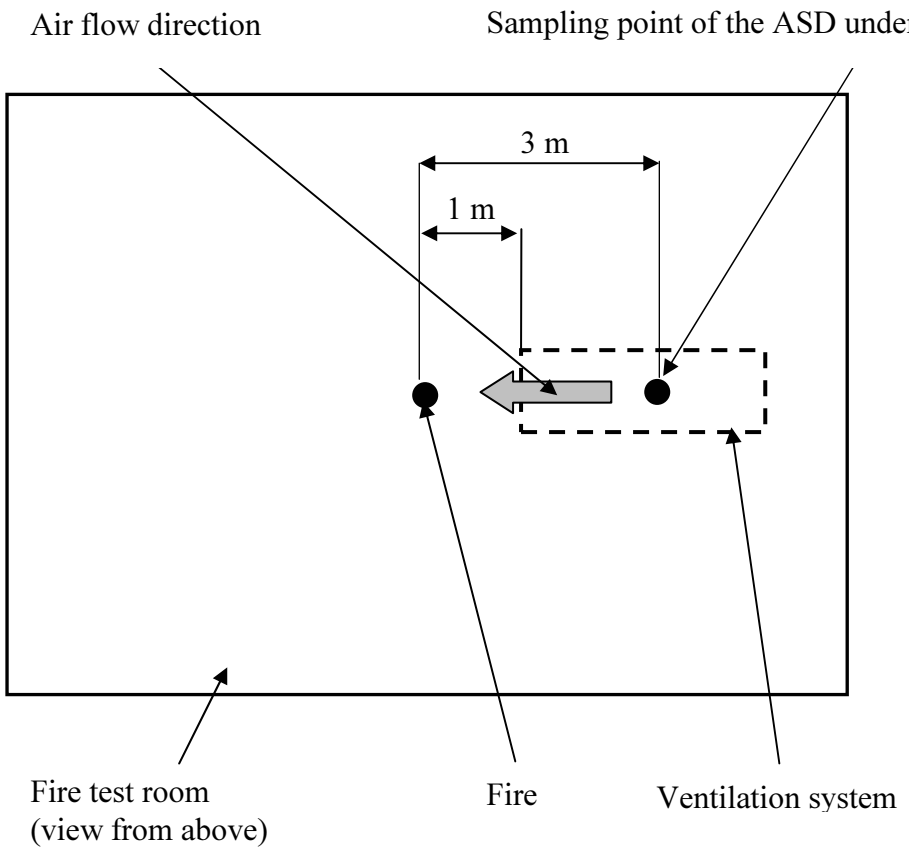

Fig. 2 Location of the ventilation system in the fire test room

Common characteristics of reduced fire tests

The objective of the new fire tests is to generate a very low quantity of smoke with a slope m=f(t) the most constant as possible ("m" is the smoke density (optical) in the fire test room). The main restraint is then the stability of the fire, which is directly in correlation with the repeatability of the test. The parameters adjusted to achieve the objective have been the arrangement of the fire test and the quantity of fuel.

Concerning the initial "m" value, the one defined in EN 54-7 (0,02 dBm^{-1}) was found sufficient by the TC72-WG16. The object of fire tests is actually to show that the detector has adequate sensitivity to a broad spectrum of smoke types as required for general application in fire detection systems for buildings and other applications as applicable to the Class of Detector. In other words, we are talking about fire detection, not about protection of clean rooms. This brings to a crucial point: the precision of the

measuring equipment used for testing the fire sensitivity of detectors according to EN 54-7 is sufficient.

On the other hand, the temperature of the fire test room is an important parameter for reduced fires. Tests made at CNPP shown, particularly for reduced-TF2, that a temperature below 20°C brings to an important peaking of the curve m = f(t) (see Fig. 3 and 4). So the initial air temperature for the fire sensitivity test is 23°C +5/-3 in prEN 54-20 (compare with 23°C +/- 5 in EN 54-7).

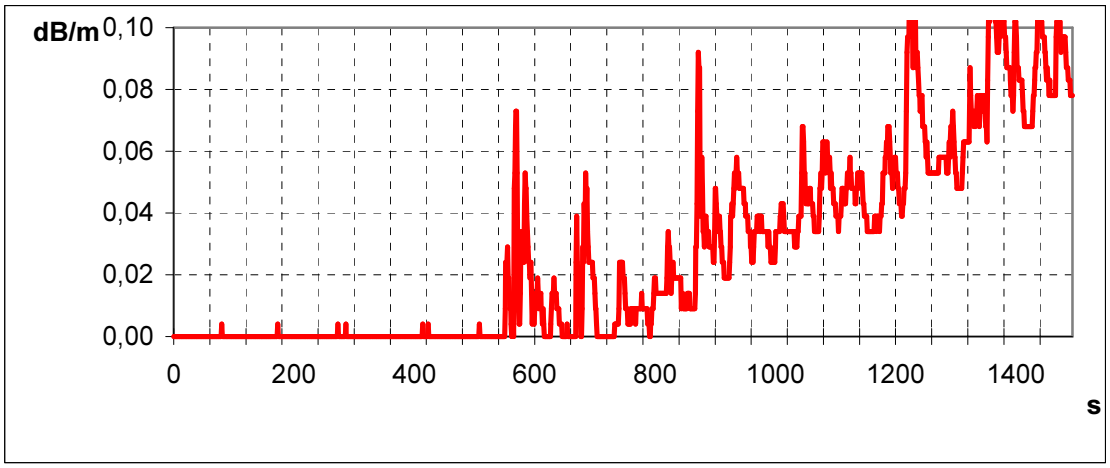

Fig. 3 m against time for a reduced-TF2 (3 wood sticks, hot plate temperature limited at 500°C, temperature of the fire room below 20°C)

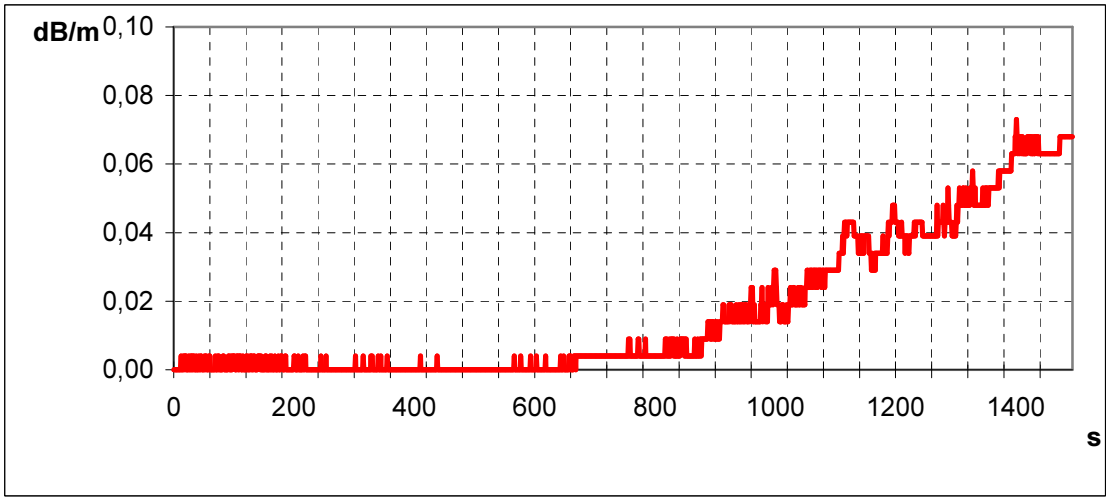

Fig. 4 m against time for a reduced-TF2 (3 wood sticks, hot plate temperature limited at 500°C, temperature of the fire room above 20°C)

Y parameter dropped out for reduced test fires

As enhanced sensitivity (i.e. class B) and super enhanced sensitivity (i.e. class A) ASD are detectors which have a clear objective to detect very early smouldering fires, m parameter was deemed to be convenient and representative to verify the performances of these detectors. So, y parameter is not used to define the end of test conditions of reduced fire tests. Y parameter is, of course, maintains in the end of test conditions of the "normal" fire tests (used for class A ASD, which shall pass the same fire tests as those defined in EN 54-7). What is more, prEN 54-20 requires that class A and B detectors shall pass TF4 to ensure they have capability to detect y dominated fires.

Definition of the end of test (EOT) conditions

The EOT conditions of each new fire test have been defined from the double point of view of the class of the detector and of the size and colour of the aerosols particles ("optical / ionic smokes").

Concerning the class of the detector, the working group 16, considering typical applications of ASD and experience of members of this group, defined the limits between classes A, B and C in term of opacity ("m" parameter) bringing to an alarm condition.

The definition of EOT was then completed with the following approach to take into account the size and colour of the aerosols particles:

1 - For a given ASD class, the EOT defined (expressed in term of opacity) are different for "ionic" and "optical smokes" (as the EOT defined for the EN 54-7 fire tests);

2 – The ratio between the EOT (expressed in term of opacity) corresponding to classes A and B, which is equal to 3, is the same whatever the fuel is.

For the need of this paper, the EOT conditions are presented before the tests themselves, but it is obvious that the definition of the EOT conditions and of the fires were made simultaneously, often by successive approach and with a lot of reversals!

TF2 reduced tests

To define the reduced TF2 (called TF2A and TF2B), two parameters were modified, compare to the "normal" TF2 (TF2 as it is defined in EN 54-7): the number of wood sticks and the maximal temperature of the hot plate.

The decreasing of the number of wood sticks has two limits. First, the maximal amount of smoke generated by the fire can not be sufficient to be detected by the equipment under test. Secondly, wood, as most of natural materials, is not homogeneous. So, the less wood sticks we use, the less repeatable the fire test will be: from the point of view of the overall density of smoke produced, a large number of wood sticks compensates the non homogeneity of each individual wood stick.

So, in addition of reducing the number of wood sticks, the maximal temperature of the hot plate was reduced from 600°C (as in EN 54-7) to 500°C. The consequence is that, for a given number of wood sticks, the slope of the curve m=f(t) decreases again.

The EOT conditions for TF2A and TF2B are the following (see Fig. 5):

- TF2A (for class A ASD): m = 0,05 dBm^{-1}; t = 1440 s (24 minutes)
- TF2B (for class B ASD): m = 0,15 dBm^{-1}; t = 2000 s (33 minutes)

Frames have been defined for the evolution of m against time. The amount of fuel has to be adjusted to respect the EOT conditions and the frames m against time (approximately 4 or 5 sticks).

TF3 reduced tests

Cotton wicks fire as the particularity to produce nearly no heat. For this reason, the smoke produced by this fire test is often qualified of "cold smoke". When you reduce the number of wicks, compare to the number defined for TF3 in EN 54-7, the small amount of smoke combined with the quasi-absence of heat bring to a difficulty for this smoke to achieve the ceiling and then to be detected.

A first approach to solve this problem was to put the cotton wicks directly inside the ventilation system (see Fig. 3). So, doing this way, we reduce the distance the aerosols have to cover from the fire to the ceiling and, what is more, we emphasize the dilution of these aerosols in the volume of the fire test room. But these gains are counterbalanced by two things. First, we inject in the volume of the fire test room large particles from the burning cotton wicks. This changes the nature and the size of the particles generated by the fire test, and then its result. Secondly, this way of doing is different of the one use for the other fire tests, as well as the "normal" TF3 than the other reduced tests, which are made on the ground, at the centre of the fire test room.

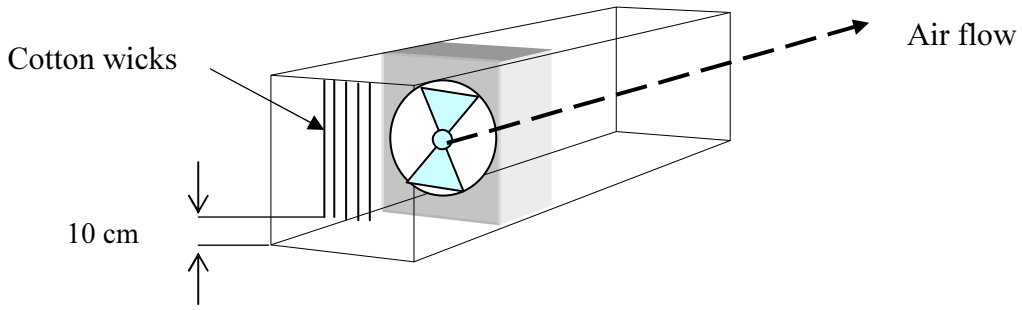

Fig. 3 First approach for the reduced TF3 arrangement

So, this solution was abandoned and the working group 16 come back to the arrangement of the "normal" TF3. This arrangement consists of building a chimney with the cotton wicks. The effect of this chimney is to help the small amount of fumes generated by the fire test to achieve the ceiling. As with the reduced fire test we have a small amount of wicks, the chimney was artificially constituted by completing the wicks with a piece of metal (see Fig. 4).

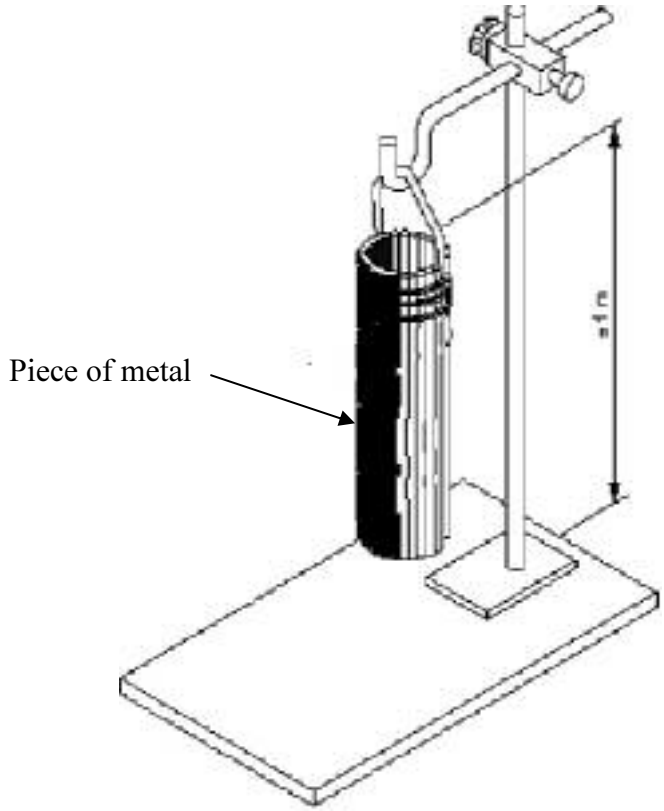

Fig. 4 TF3A and B arrangement

The EOT conditions for TF3A and TF3B are the following (see Fig. 5):

- TF3A (for class A ASD): m = 0,05 dBm^{-1}; t = 1200 s (20 minutes)
- TF3B (for class B ASD): m = 0,15 dBm^{-1}; t = 1200 s (20 minutes)

Frames have been defined for the evolution of m against time. The amount of fuel has to be adjusted to respect the EOT conditions and the frames m against time (approximately 30 wicks for TF3A and approximately 40 wicks for TF3B).

TF5 reduced tests

Reduced-TF5 was the easiest fire to develop. The slope of the curve m against time is mainly dependant of the area of the tank and the duration of the test is mainly dependant of the height of the tank (in fact, the volume of fuel).

The differences with the “normal” TF5 are the following:

- The use of toluene in the n-heptane is not accepted in reduced fire: the presence of toluene in the fuel will significantly modify the behaviour of the fire, particularly at the beginning of the test, giving an initial peak burn.
- The tank shall be put on a base plate acting as a heat sink to avoid boiling of the n-heptane. Actually, it was observed during investigations than, due to the small quantity of fuel, the n-heptane boiled and splashed about.

The n-heptane (purity about 99%) is put in a tank with dimensions approximately:

- TF5A: 100mm x 100mm x 100 mm (for approximately 200 ml of fuel);
- TF5B: 175mm x 175mm x 100 mm (for approximately 300 ml of fuel).

The EOT conditions for TF5A and TF5B are the following (see Fig. 5):

- TF5A (for class A ASD): m = 0,1 dBm^{-1}; t = 1200 s (20 minutes)
- TF5B (for class B ASD): m = 0,3 dBm^{-1}; t = 1020 s (17 minutes)

TF4 reduced tests

The initial objective of the working group 16 was to have four fuels for the reduced tests, to have the same approach than EN 54-7. Unfortunately, polyurethane is a non-homogenous material and reduced fires using this fuel, whatever the arrangement was, have turned out to be non-repeatable fires.

Considering these results, the ambition to develop a reduced-TF4 was abandoned. This is not a blockage point: reduced-TF2, 3 and 5 allow the evaluation of the sensitivity of an ASD in a broad spectrum of smoke type:

- Smouldering fires (optical behaviour): reduced-TF2;
- Open fires (ionic behaviour): reduced-TF5;
- Fires at the limit between optical and ionic behaviour (reduced-TF3).

And it shall be noted that this broad spectrum is severe for enhanced sensitivity and super enhanced sensitivity ASD: these detectors have been developed to detect very early the beginning of a fire, i.e. a smouldering fire.

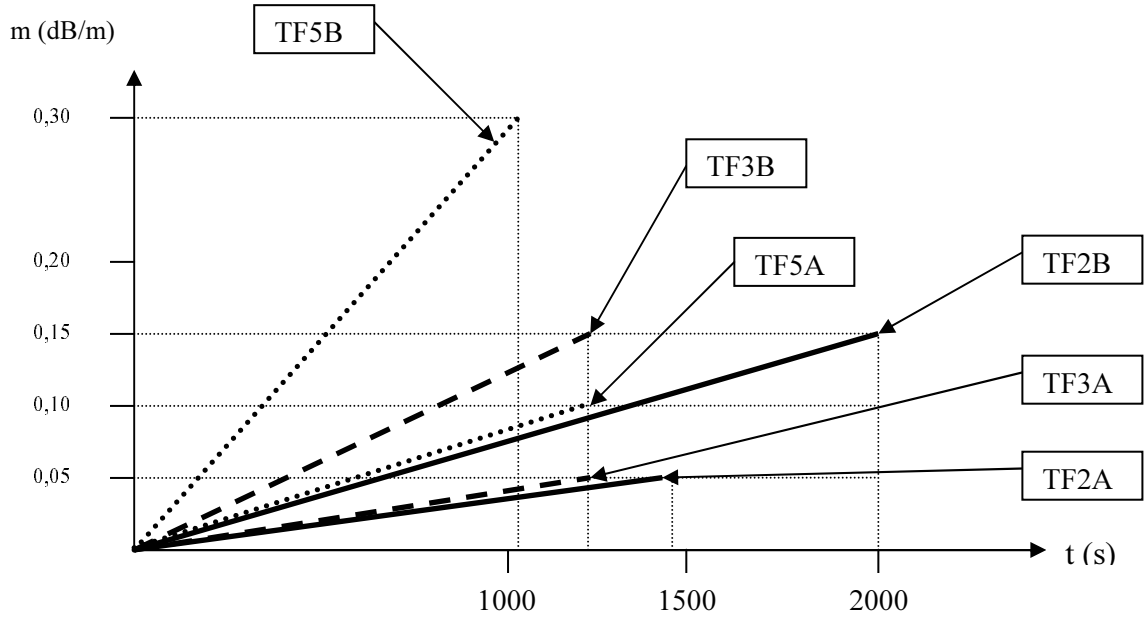

Fig. 5 Graphic representation of the end of test conditions of the reduced fire tests

Conclusion

Two sets of reduced fire tests have been defined, based on the "standard" fire tests TF2 to TF5 defined in EN 54-7. These new fire tests allow the classification of the ASDs according to their sensitivity, in compliance with prEN 54-20 which defines three classes:

- Class C detectors, tested with TF2 to TF5 (already defined in the existing EN 54-7);
- Class B detectors, tested with TF2B, TF3B and TF5B;
- Class A detectors, tested with TF2A, TF3A and TF5A.

We can note that TFx for class C ASD are not called TFxC but as they are called in EN 54-7, to avoid confusion and highlight the fact that they are the same fire tests.

The new fire tests use the same fire test room as the one defined in annex F of EN 54-7. The only new apparatus defined is the ventilation system, which is necessary to mix the aerosols with the ambiance of the fire test room before the equipment under test suck up a sample of this ambiance. So, in addition to be repeatable, and because they are based on existing means and ability, the new fire tests are easily usable by all laboratories and have an acceptable cost for the end user.

P. Basmer, G. Zwick
Forschungsstelle für Brandschutztechnik an der Universität Karlsruhe (TH),
Ansyco GmbH, Karlsruhe

Messung des Giftgascocktails bei Bränden mit der FT-IR Messmethode

Abstract

More than 60 % of all casualties in fires are caused by the intake of toxic effluents, such as CO. While CO would be expected in high concentration in most fires esp. smouldering fires, burning of e.g. plastics will result in a cocktail of other toxic gases including hydrogen cyanide (HCN), hydrogen chloride, (HCl), ammonia (NH_3), nitric oxides (NO_x) and many other gases and particulates. Therefore the protection of firemen and population with respect to toxic effluents of fire is important. At the „Forschungsstelle für Brandschutztechnik" (FFB, Research Centre for Fire Protection Technology) at the University of Karlsruhe (Germany), series of laboratory scale smouldering fires with defined materials as well as room fires in real scale were conducted to determine online the concentrations of gases with the mobile FT-IR Analyser GASMET.

Most organic and inorganic gases show characteristic IR- signals and can be measured by the IR method (except O_2, Cl_2, H_2S). Using FT-IR, spectra are rapidly recorded in the Infrared wavelength range. The GASMET FT-IR analyser is a system including a special spectral evaluation software, which takes the strong band overlap into account. The concentrations of 31 single gases were calculated, including inorganic gases (CO, HCl, HCN, NH_3, SO_2, NO, NO_2, N_2O, COS, CS_2, H_2O, CO_2) and organic gases (formaldehyde, acroleine, phosgene, benzene, toluene, xylenes, ethylbenzene, styrene, phenole, chlorobenzene, ethanole, acetone, acetic acid, methane, ethane, ethene, acetylene) and the trend of concentrations recorded.

Comparing the measured peak concentrations of gases such as CO, HCN, HCl, NH3, NOx with existing Permissible Exposure Limits (PEL or MAK) and other more critical concentrations (which lead to unconsciousness or death), it was demonstrated, that the toxic gas cocktail of fires is sufficient, to acutely endanger the life or health of anyone exposed. The FT-IR analysis of fire gases using the mobile GASMET- FTIR- analyser and the patented evaluation algorithm enables a direct reading, continuous measurement of the concentrations of relevant volatile toxic gases of fires. The toxic potential inherent in fire gases can be assessed.

Giftige Gase bei Bränden

Mehr als 60 % aller Toten bei Bränden sterben durch Vergiftung mit akut toxischen Gasen. Bei jedem Feuer entstehen große Rauchgasmengen, die in erster Linie das unsichtbare, geruchlose und äußerst giftige Kohlenmonoxid (CO) enthalten. Bei Vorhandensein von Kunststoffen wird zusätzlich ein Giftgascocktail mit Blausäure (HCN), Salzsäure (HCl), Ammoniak (NH_3), Stickoxiden (NOx) und vielen weiteren Gasen gebildet. Deshalb ist der Schutz von Einsatzpersonal und Bevölkerung vor den akut-toxischen und weiteren, latent gefährlichen Giftstoffen äußerst wichtig.

Die Feuerwehr benötigt während des Einsatzes übersichtliche und mit Bewertung versehene Auskünfte über mögliche Brandprodukte und deren Zersetzung. Für die Messung der Konzentrationen von Brandgasen werden zwar viele Messmethoden wie Messröhrchen, elektrochemische Sensoren, Explosimeter, PID, IR u.a. verwendet.[1)] Jedoch stellt die oft fehlende Selektivität und damit die begrenzte Aussagekraft der Ergebnisse ein Problem dar. Die recht teuere und aufwendige GC-MS Methode eignet sich gut zur Identifizierung unbekannter organischer Schadkomponenten.[2)] Zur Messung der Konzentrationen der akut-toxisch relevanten anorganischen Gase CO, HCl, HCN, NOx, NH_3 und SO_2 wurde bei den hier beschriebenen Versuchen ein mobiler FT-IR Analysator [3)] eingesetzt. Hiermit wurden auch die zeitlichen Konzentrationsverläufe ermittelt.

Testpyrolysen und Brände mit Gasmessung

An der Forschungsstelle für Brandschutztechnik (FFB) der Universität Karlsruhe (TH) wurden in einer kleinen Brandkammer Pyrolyse- und Brandversuche durchgeführt. Zuerst wurden Modellpyrolysen mit definierten Materialien wie PVC, Wolle und einer Elektronikplatine durchgeführt. Die Bildung der Gase aus diesen Materialien sollte bestimmt werden.

Außerdem wurde noch ein großer Brand- und Löschversuch an einem Modellzimmerbrand durchgeführt, der begleitend gemessen wurde. Ergebnisse dieser Versuchsserie sind in [4)] dokumentiert.

Die FT-IR Messmethode

Die FT-IR Messmethode, die seit etwa 30 Jahren im Labor verwendet wird, erlaubt auch die Messung von Gasgemischen. Bei der FT-IR Methode werden Spektren im Infrarot-Bereich schnell gemessen und alle darin enthaltenen Signale ausgewertet. Die meisten organischen und anorganischen Gase zeigen charakteristische Absorptionssignale und können deshalb erfasst werden (außer O_2, Cl_2, H_2S). Mit dem GASMET Analysator steht nun auch ein mobiles FT-IR Messsystem mit geeigneter Software zur Verfügung. Die zugehörige CALCMET Software bietet aufgrund eines neuen, patentierten Rechenvorgangs eine effektive Möglichkeit, die Konzentration von Gasen in Gemischen und deren Konzentrationsverlauf sofort anzuzeigen. Der Analysator ist mit 16 kg zwar mobil, aber nicht tragbar. Das System wird relativ einfach über einen Notebook PC bedient.

Die Schwierigkeit bei dem Einsatz von Infrarotanalysatoren liegt darin, dass sich die Signale vieler Messkomponenten überlagern. Die Software des FT-IR Analysators wertet alle vorhandenen Gase aus, um Bandenüberlagerungen im Spektrum zu kompensieren. Nur so sind selektive Ergebnisse zugänglich. Bei der Auswertung wurden hier die Konzentration von 31 Einzelkomponenten berechnet.

Bei jedem Brandversuch bildete sich neben CO_2 immer giftiges Kohlenmonoxid und die hochflüchtigen und leicht brennbaren Gase Methan, Ethan, Ethen und Acetylen (als C1-C2 bezeichnet, ein oder zwei Kohlenstoffatome im Molekül) sowie je nach Brandgut weitere gefährliche Brandgase.

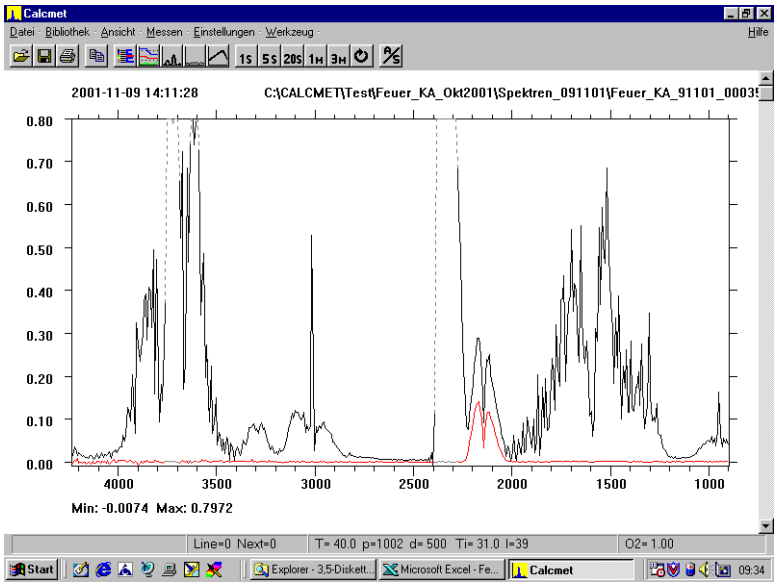

Ein FT-IR Spektrum während eines Zimmerbrandes.
CO Vergleichsspektrum (hellere Linie).
CO = 2050 – 2250 cm $^{-1}$
Methan = bei 3018 cm $^{-1}$
Ethen = bei 957 cm $^{-1}$
Große Signale von CO_2 und Wasser in anderen Bereichen des Spektrums.

Pyrolyse von PVC

3 Hart-PVC Stäbe wurden auf einer Heizplatte für 50 min bis auf 400 °C erhitzt. Die Entwicklung von Gas und Rauch setzt bei einer Temperatur der Heizplatte von etwa 300 °C ein. Bei der Pyrolyse von Hart-PVC entstanden sehr hohe Konzentrationen von mehr als 1 %-Vol. (10.000 ppm !) an Chlorwasserstoff. Die Spitzenkonzentrationen der aromatischen Kohlenwasserstoffe lag bei 350 ppm, bei einem Maximalwert von 200 ppm Benzol, 70 ppm o-Xylol und 50 ppm Ethylbenzol sowie 17 ppm Formaldehyd. Der CO-Gehalt erreichte max. 270 ppm und die leicht brennbaren Gase wie Methan, Ethan und Ethen zusammen ca. 410 ppm.

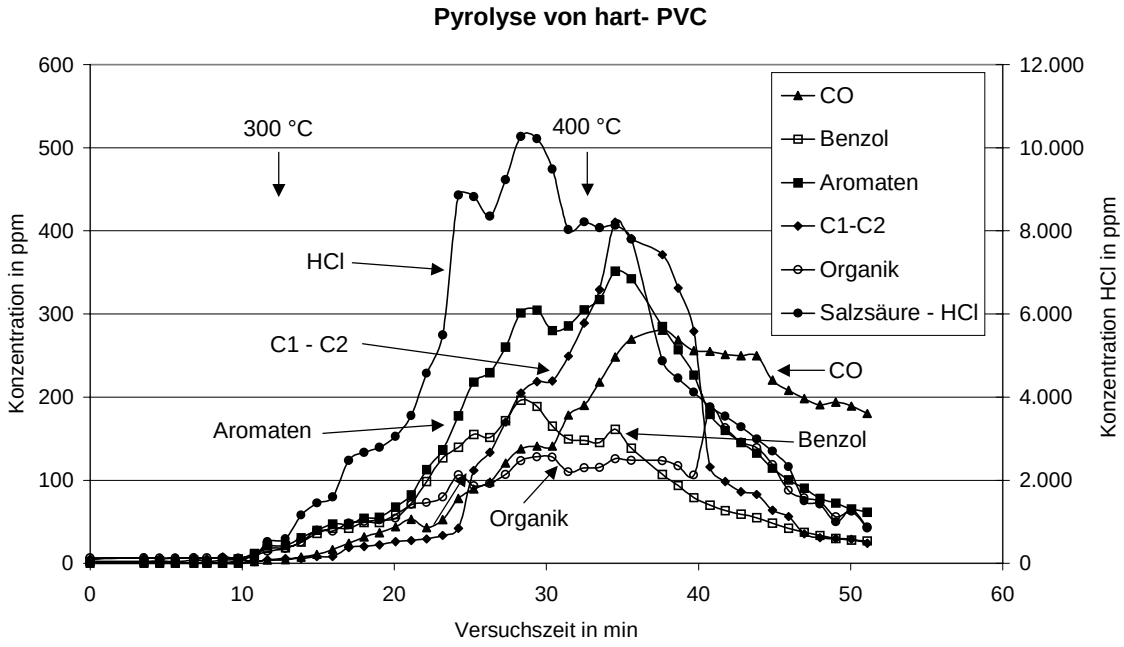

Pyrolyse von Wolle

50 g Longhair-Mohair (60% Mohair, 40 % Acryl) wurden für 18 min bis auf 285 °C erhitzt.

Bei der Pyrolyse von Wolle setzt schon bei einer Temperatur von etwa 160 °C die sichtbare Gasentwicklung ein. Es wurden vor allem stickstoffhaltige Gase wie Ammoniak (max. 250 ppm), Blausäure (63 ppm) und Stickoxide (16 ppm) gemessen. Zusätzlich wurden schwefelhaltige Gase wie COS (42 ppm), SO_2 (3 ppm) und CS_2 (2 ppm) analysiert. Brennbare organische Komponenten wie Methan, Ethen, Ethan erreichten 90 ppm. 14 ppm 2,5-Dimethylfuran wurden ebenfalls gemessen. Der CO-Anteil erreichte 75 ppm und die Aromaten bildeten sich bis zu einer Konzentration von 21 ppm, bei einem Gehalt von max. 4 ppm für Benzol.

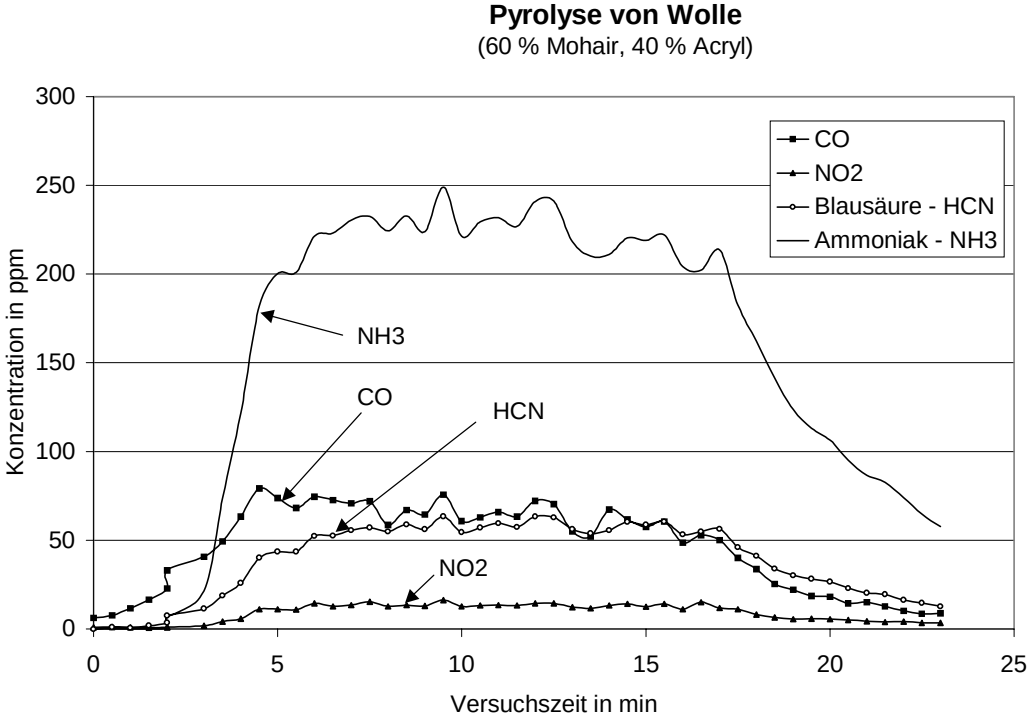

Pyrolyse einer Elektronikplatine

Eine PC-Graphikplatine wurde für 35 min bis auf 325 °C erhitzt. Die merkliche Bildung von Rauch und Gas beginnt bei einer Temperatur von ca. 250 °C. Neben ca. 70 ppm CO wurden hauptsächlich organische Komponenten gemessen u.a. 10 ppm Methan, 15 ppm Ethen, 24 ppm Ethan, 5 ppm Acetylen sowie 15 ppm Ethanol, 40 ppm Aceton und 3 ppm Essigsäure. An Aromaten wurde 16 ppm Benzol, 14 ppm o-Xylol und 4 ppm E-thylbenzol gemessen. Die Konzentration von mehr als 60 ppm Phenol fiel besonders auf.

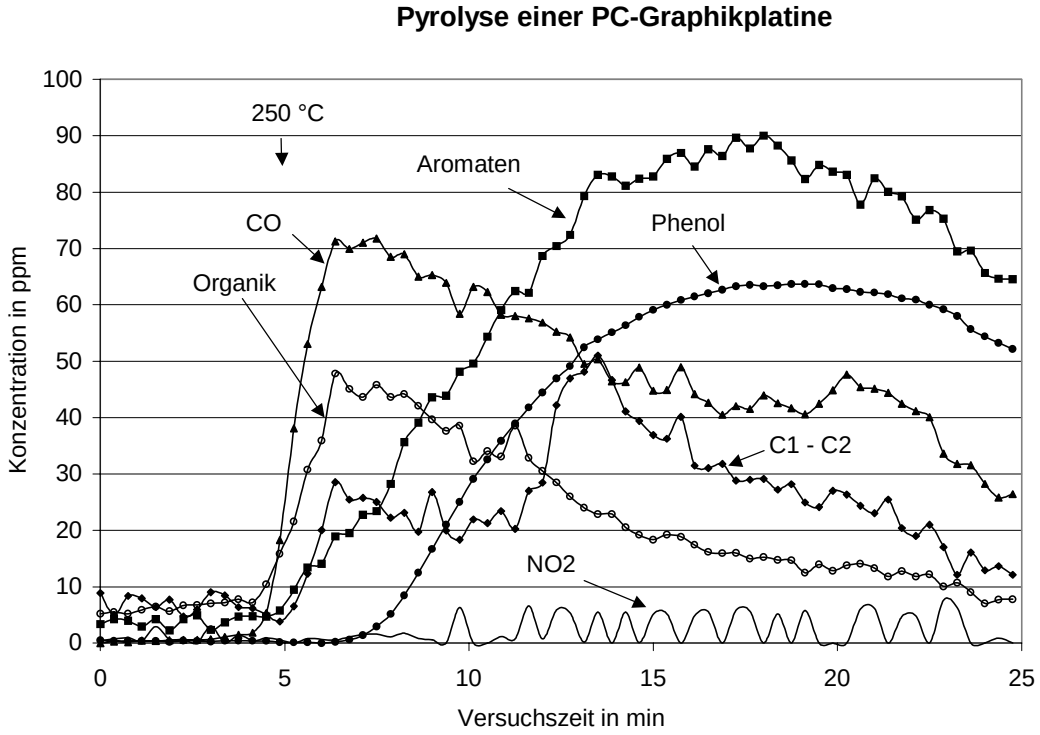

Modellbrand eines Zimmers im Realmaßstab

In der Brandhalle der FFB wurde der vorhandene Modellbrandraum im Realmaßstab möbliert. Das Inventar mit einem Gesamtgewicht von 730 kg bestand u.a. aus Sitzgruppe, Regal, Schrank, Tisch, Holz und Zeitungen. Der Brandraum selbst hat die Maße von 5 m x 5 m x 2,6 m und steht auf einer elektronischen Waage in der 12 m hohen Versuchshalle.

Die Zündung des Musterzimmers erfolgte neben einer offenen Schranktür mit Hilfe von 0,5 Liter Brennspiritus. Die Probennahme erfolgte zu Beginn der Messung im Brandraum direkt über der Sitzgruppe. Aufgrund der großen Hitze im Zimmer war bei der angewandten Probennahme über einen Schlauch nach einer gewissen Zeit keine weitere Probennahme möglich. Deshalb wurde nach etwa 10 Minuten auf die Probenahmestelle über dem Brandraum umgeschaltet, um die Brandgase oberhalb des Modellzimmers in der Halle zu analysieren. Die Temperatur an der Zimmerdecke betrug bereits nach 6 Minuten nahezu 1000 °C. Nach einem Abbrand von insgesamt 290 kg (40 %) wurde nach einer Versuchsdauer von 17,5 Minuten das Feuer gelöscht.

Die folgende Grafik zeigt die Konzentrationsverläufe einiger Brandgase während des Brandversuches.

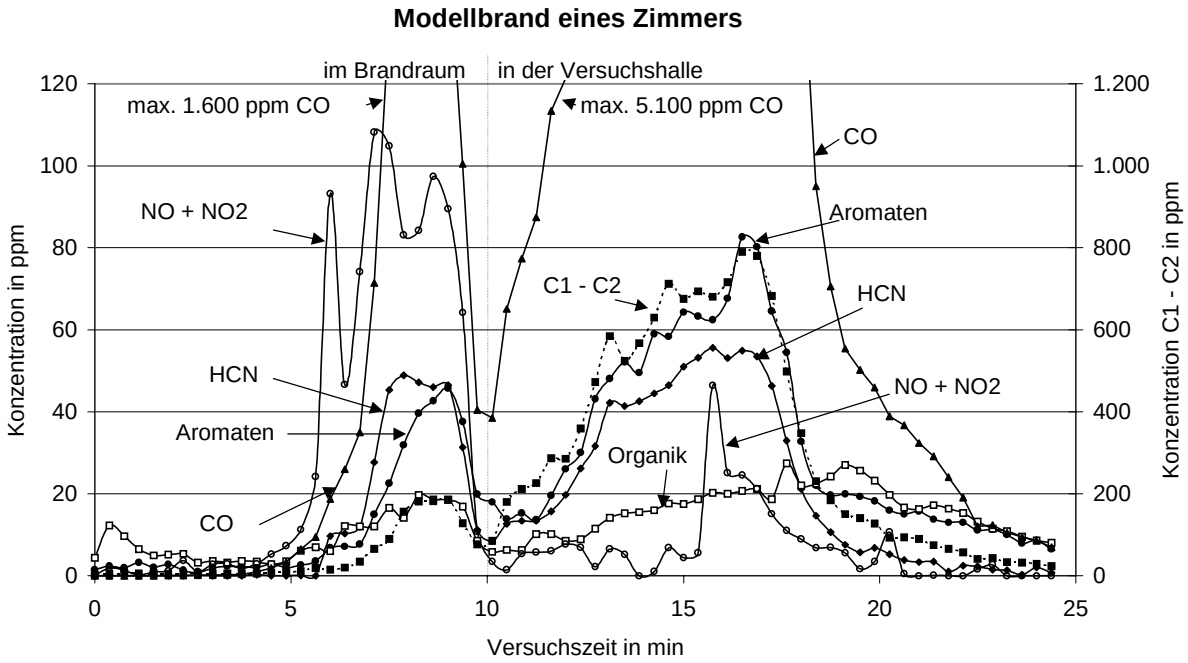

In der Zeit zwischen 5 und 9 Minuten stiegen die Konzentrationen im Zimmer stark an. Die Stickoxide erreichten Konzentrationen bis 110 ppm, Blausäure bis 49 ppm, SO_2 bis 96 ppm, Salzsäure bis 1 ppm, Benzol bis 15 ppm und CO bis 1600 ppm.

Die bei den hohen Temperaturen entstehenden Pyrolysegase verbrannten teilweise innerhalb und auch außerhalb des Brandraumes. Die sehr großen Mengen des dabei entstandenen Brandgasgemisches sammelten sich unterhalb der Hallendecke und wurden im weiteren Verlauf des Versuches der vorhandene Abgasreinigung zugeführt.

In dem Gasgemisch unter dem Hallendach wurden in der Versuchszeit zwischen 11 und 19 Minuten maximale Konzentrationen von 44 ppm Stickoxide, 55 ppm Blausäure, 10 ppm SO_2, 4 ppm Salzsäure, 43 ppm Benzol, 5 ppm Formaldehyd und 5100 ppm CO gemessen. Dieses Gasgemisch enthielt zusätzlich größere Mengen von unverbrannten flüchtigen C1-C2 Komponenten (bis 800 ppm).

Zusammenfassung und Bewertung

In der folgenden Tabelle sind die gemessenen maximalen Konzentrationswerte zusammengestellt (Werte über 1 ppm; der Modellbrand Holz/PVC ist nicht detailliert enth.).

Brandgase		Modellpyrolysen / Brand				Zimmerbrand	
		Hart-PVC	Wolle	PC-Platine	Holz/PVC	Messstelle innen	außen
		in ppm				in ppm	
Kohlenmonoxid	CO	270	75	70	2700	1600	5100
Chlorwasserstoff	HCl	10000	0	0	11	1	4
Blausäure	HCN	5	63	5	3	49	55
Ammoniak	NH3	3	250	1	8	0	1
Schwefeldioxid	SO2	7	3	1	3	96	10
Nitrose Gase	NOx	10	16	7	11	110	44
Kohlenoxidsulfid	COS	0	42	1	3	4	1
Formaldehyd	CH2O	17	2	1	8	1	5
Acrolein	C3H4O	0	1	0	0	3	2
Phosgen	COCl2	4	0	2	4	0	0
Benzol	C6H6	200	4	16	19	15	43
Phenol	C6H6O	7	1	63	5	14	1
Aromaten		350	21	90	33	45	80
C1 - C2		400	90	50	1350	180	800
Organik		180	53	48	750	20	28

Für die anorganischen Gase CO, HCl, HCN, NH_3, SO_2, NOx und die organischen Gase Formaldehyd, Acrolein, Benzol, Phenol bestehen aufgrund der Giftigkeit Regelungen über die maximal zulässigen Grenzwerte am Arbeitsplatz (MAK). Die Gruppen Aromaten und Organik enthalten weitere Komponenten mit individuellen Grenzwerten.

In der nächsten Tabelle werden eine Reihe von Grenzwerten (MAK) und kritischen Konzentrationen aufgelistet. Die Spalte „30 min Rettung" bedeutet, dass bei der angegebenen Konzentration nach 30 Minuten Bewusstlosigkeit eintritt und damit keine Selbstrettung mehr möglich ist. In der Literatur [5), 6), 7), 8)] sind z.T. unterschiedliche Werte angegeben.

Gefährliche Brandgase Grenzwerte für die einzelnen Gase in ppm					
		MAK-Wert	**30 min Rettung**	**5 min Tod**	**60 min Tod**
Kohlenmonoxid	CO	30	1.500	12.000	4.600*
Blausäure	HCN	1,9	100	250	100
Chlorwasserstoff	HCl	5	100	14.000	1.000
Ammoniak	NH3	20	500	5.000	
Nitrose Gase	NOx	5			300
Schwefeldioxid	SO2	0,5	100		500

* =30 min Tod

Schwerflüchtige Schadstoffe wie z.B. Dioxine, Furane, PAK treten zusätzlich auf. Sie sind meist partikelgebunden und stellen vor allem ein Problem in den Brandrückständen dar. Sie werden hier nicht behandelt und müssen auch mit anderen Methoden analysiert werden (Dioxine und Furane z.B. mit gaschromatischer Auftrennung - gekoppelt mit hochauflösenden Massenspektrometern als Detektoren).

Kein Zweifel kann daran bestehen, dass Brandrauch sehr gefährlich ist.[9)] Ein Vergleich der hier gemessenen Maximalwerte mit den Grenzwerten bzw. den kritischen Konzentrationswerten zeigt, dass die Konzentrationen in den Giftgascocktails ausreichen, das Leben von Menschen akut zu gefährden bzw. um gesundheitsschädliche Folgen hervorzurufen.

Nicht zu unterschätzen sind zusätzliche Kombinationswirkungen wie z.B. Sauerstoffmangel im verrauchten Bereich, zusammen mit vermindertem Sauerstofftransport im Blut durch CO-Vergiftung und verminderte Verwertung des Sauerstoffs in den Körperzellen durch Blausäurevergiftung, die zu verstärkter Schädigung mit fatalen Folgen führen.

Deshalb ist bei dem Einsatz während eines Brandes die Verwendung von schwerem Atemschutz Pflicht. Besonders nach Tunnelbränden und Bränden in Lagerhallen muss an der noch warmen Brandstelle noch mit sehr gefährlichen und schädlichen Konzentrationen toxischer Brandgase gerechnet werden.

Die FT-IR Messung mit dem mobilen GASMET-Analysator und der patentierten Auswertemethode ist geeignet, eine Gefahrenbeurteilung von relevanten flüchtigen toxischen Gase wie z.B. CO, HCl, HCN, NH_3, SO_2, NOx sowie einer Reihe von organischen Komponenten durchzuführen.[10)] Sicherlich sind noch weitere Untersuchungen mit der vorgestellten FT-IR Messtechnik notwendig, um die Ergebnisse zu verfeinern bzw. um Möglichkeiten und Grenzen des Einsatzes im Brandfall zu ermitteln.

Literatur:

1. Rönnfeldt; Messtechnik im Feuerwehreinsatz, Kohlhammer Verlag (1995)
2. Föhl, Basmer, Schwarz; Forschungsbericht Nr. 106, Arbeitsgemeinschaft der Innenministerien der Bundesländer, Arbeitskreis V - Ausschuss für Feuerwehrangelegenheiten
3. Modell GASMET Dx-4000, Herstellers TEMET Instruments Oy, Helsinki (Finnland), Bezugsquelle bei Ansyco GmbH, Karlsruhe
4. Basmer, Zwick; FFZ Feuerwehr Fachzeitschrift, Heft 3 (2002), Seite 176 – 180
5. MAK Liste (2003)
6. Greim, Buff; Zivilschutzforschung, Band 25, (1997), Bundesamt für Zivilschutz
7. Roth, Weller; Chemiebrände, Ecomed Verlag, (1986)
8. Finnische Brandforschungsstelle, Espoo, Finnland, (Private Mitteilung)
9. Widetschek; BLAULICHT 12-99
10. Basmer, Zwick; Forschungsbericht Nr. xyz, „Einsatzmöglichkeiten eines mobilen Vielkomponenten-FT/IR-Gasanalysators“, Arbeitsgemeinschaft der Innenministerien der Bundesländer, Arbeitskreis V – Ausschuss für Feuerwehrangelegenheiten

H. Fissan[1], M.K. Kennedy[1], T. Krinke[1], R. Ligman[2], S. Campbell[2], F.E. Kruis[1], B.R. Mehta[3]

[1]Universität Duisburg-Essen, Process- and Aerosol Measurement Technology Division, Bismarckstr. 81, 47057 Duisburg, Germany
[2]University of Minnesota, Faculty of Electrical and Computer Engineering, Minneapolis, Minnesota 55455, USA
[3]Thin Film Laboratory, Department of Physics, Indian Institute of Technology,
Hauz Khas, New Delhi 110016, India

Development of nanostructured multi-gas sensors for fire detection

I. INTRODUCTION

One way of fire detection is to detect the change in the composition of the gas phase in a room caused by a starting fire. Of interest is the possibility to be able to follow not only a single component, but several components of the changing gas mixture.

Nanoparticles, smaller than 100 nm, have many properties which differ from the corresponding bulk material, thereby making them attractive for many new electronic, optical or magnetic applications. Making use of these properties of semiconducting materials leads to new or at least improved devices, such as optical sensors, gas sensors, light emitting diodes, solar cells, quantum dot laser, single electron transistors and memory units.

Using nanoparticles as building blocks for functional layers provides one possible route to create these kind of new devices together with substrates based on silicon technology. Substrates with interdigitated electrode configuration are now built using microsystem technology methods (Chung et al., 2000). This structure is suitable for thin films because the large contact area and short distance between the electrodes reduce the overall resistance and response time of the film compared with other two-point arrangements.

The production of functional layers can be divided into different areas of investigation. Depending on the synthesis method and conditions, different composition, shape and sizes of particles will be produced, which should affect the functional properties of the particles.

The deposition process defines the arrangement of the particles on the substrate. Contacting the obtained structures electrically opens the possibility to investigate the electrical characteristics of the electronic device.

The investigation of the sensing mechanism together with material structure requires certain steps. The first step is to control the microstructure of the sensing layer and to provide suitable substrates, depending on the application to build a full device. For determination of possible improvements of such a device the material structure such as stoichiometry, film density and crystal structure have to be analyzed. Additionally, the results have to be compared with electrical measurements to understand the operation of the sensor and possible effects of the nanostructured layers on sensor properties. For gas sensors this includes sensitivity, selectivity, stability (SSS) and dynamics.
The goal of this work is to find ways to exploit the size-depending sensing properties of a device where the sensing layer is produced by an aerosol-synthesis method. Additionally, possible ways are presented to fabricate multi sensing devices.

II. Synthesis of nanoparticles and thin particle layers

In this investigation a gas-phase synthesis method originally devised for forming PbS nanoparticles was used (Kruis et al., 1998). It was modified for the preparation of crystalline, quasi-spherical, monodisperse SnOx particles by introducing an additional oxidation step (Kennedy et al., 2000). The method is based on particle formation by homogeneous nucleation induced by cooling down of SnO vapor and subsequent aggregation by Brownian motion, followed by a size-fractionation step and a sintering/crystallization step. The experimental setup is depicted in Figure 1. It contains six elements: a nanocrystal source in the form of a sublimation furnace, a radioactive β -source (Kr85) which acts as bipolar aerosol charger, a Differential Mobility Analyzer (DMA) (Model 308500, TSI, Minneapolis, USA) (Chen et al.,1998) used as a size-classifier, a second tube furnace for sintering and crystallization of the SnO aggregates, a deposition chamber, and a particle size measurement system (DMPS) consisting of a DMA and a condensation nucleus counter (Model 3025, TSI, Minneapolis, USA). Nitrogen obtained from liquid evaporation and purified by passing it through a getter (MonoTorr PS4-MT3-

N2, SAES Getters, Cologne, Germany) is used as carrier gas. In the second half of the sintering/crystallization furnace a flow of O_2 is added in order to oxidize the SnO nanoparticles to SnO_x nanoparticles, with $1 < x < 2$.

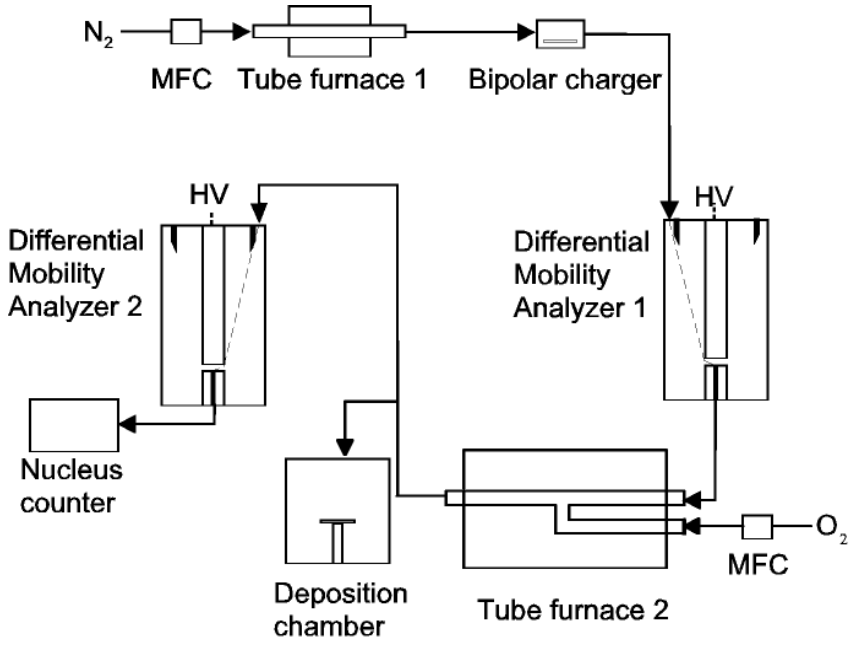

Fig. 1: Experimental setup for the synthesis of monodisperse tin oxide nanoparticle films.

The particles are introduced with the gas flow into a deposition chamber, where they are deposited on a substrate sticking into the flow.

The production of electronic devices containing nanoparticles as building blocks depends on the ability to guide the particles to the places on the substrate were they are needed. In case of aerosols the particles have to be guided from the random distribution in the gas phase on specific areas on the substrate surface. The particles deposition in a homogeneous electric field and the microscopic aspects of the particle arrangement on flat substrate surfaces has been investigated in detail experimentally and theoretically (Krinke et al., 2002).

It is also possible to use low pressure impaction to create a more dense structure. If inertia is the dominant force, particles resist following the streamline and, if the deviation from the streamline is large enough, they can be delivered onto surfaces.

III. Gas sensing properties

Particle and thin layer characterization

In a detailed study to understand the performance of the device and its dependence on particle properties, the particles have to be well characterized. For gas sensing analysis the control of the microstructure of SnO_x nanoparticle layers is of great importance. Therefore intensive studies have to be made to obtain information about the chemical composition. TEM and AES studies have been carried out to analyze the thin particle films. The TEM micrographs of SnO_x nanoparticles produced via the above mentioned gas-phase synthesis process indicate a narrow size distribution ($\sigma < 10$ %).

The annealing of as-deposited SnO particles oxidize the particle surface nearly to stoichiometric SnO_2, depending on the initial oxygen content. The surface stoichiometry is not found to change with the particle size (Ramamoorthy et al., 2003).

Substrate Configuration

In order to analyze the electrical properties of functional particle layer, a sufficient substrate has to be provided. For measurements of electrical properties a higher resistance compared to the functional layer must be guaranteed. An adequate electrode structure depending on the requirements and especially for the measurement of gas-sensing properties additional layers which can be used for heating up the entire sensing film, so called microhotplates, are needed. To enable electrical measurements of the gas-sensitive properties of the deposited SnO_x nanoparticle films having higher resistivities, a 1 mm^2 structure consisting of 160 interdigitated fingers with a width of 2 μm and an identical separation was fabricated on a microhotplate of 3 mm x 3 mm size. The electrodes are buried in phosphor-doped silicate glass (PSG). If the electrodes are not buried, they influence the particle deposition and a region of low particle concentration appears close to the electrodes (Prost et al., 1998). This would also hinder the electrical transport. The microhotplates are bonded to a DIL8 chipcarrier. A poly-Si layer is imbedded in the structure and serves as heating element, allowing a maximum surface temperature of 350 °C at these conditions. Resistance measurements of the nanoparticle layer are carried out in an automated gas sensor set-up using a Picoamperemeter with internal voltage source (model 487, Keithley, Germering, Germany) (Kennedy et al., 2003).

Gas-sensing Properties of Tin Oxide Nanoparticle Layers

The gas-sensing properties in terms of sensitivity and dynamic behavior were determined by measuring the time-dependent changes in resistance upon changing the gas environment in the measurement cell at substrate temperature varying from 100 °C to 300 °C.

Prior to gas-sensing measurements, SnO_x nanoparticle films were annealed at 300 °C for about 2 hours in 1000 ppm ethanol in synthetic air. The annealing will lead to the formation of sintering necks. This is supported by the fact that during the annealing process the resistance of SnO_x nanoparticle samples decreased by several orders of magnitude. Figure 2 compares the response transients of nanoparticle films at 300 °C having D_{ms} = 10 nm, 20 nm and 35 nm at an ethanol concentration of 1000 ppm. It can be clearly seen that the sensitivity to ethanol increases as the particle size decreases. Furthermore, the value of the measured response time τ decreases with decreasing particle size, τ =10 s for D_{ms} = 10 nm and τ =38 s for D_{ms} = 20 nm. For a sample with a particle diameter of D_{ms} = 35 nm, τ was not measured due to insignificant change in the resistance on gas exposure. It can be seen that the sensitivity increases with decreasing particle size. Increasing the temperature leads also to an increase in the sensitivity. Similar results were also obtained by changing the mean particle size between 5 nm and 32 nm via the calcination temperature and by using metal additives (Xu et al., 1991). In addition to the wide particle size distribution observed in these samples, the process parameters responsible for size control must have caused microstructure and composition variations. On this account the conclusion about size dependence of gas sensitivity could be misleading in the above investigation. It may be emphasized again that in our studies the size distribution was narrow and the particle size was the only variable.

Additionally, the microstructure of the films of different particle sizes was comparable and did not change due to the annealing. It is clear that the variation of *S* and τ observed in the present study is purely a consequence of nanoparticle size dependence. As the size becomes small, concentration and energy position of absorption sites in the band gap of the semiconductor are also affected significantly. Together, these factors result in an improved response of the nanoparticle films to the gas molecules in terms of higher sensitivity and low response time at smaller particle sizes (below 20 nm) (Kennedy et al., 2003).

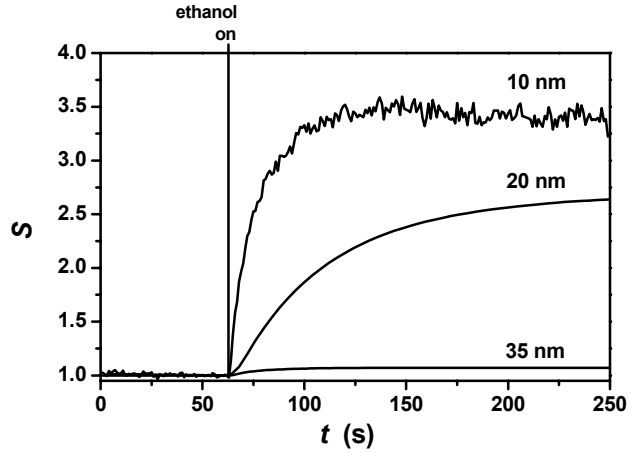

Fig. 2: Response transient curves for different particle sizes. Gas: 1000 ppm ethanol in synthetic air, T_{op} = 300 °C, estimated film thickness: 1.5 µm

IV. Multi-sensor arrays

Reduction of size of the sensing layer

Figure 3 shows a schematic of a multi-sensor microhotplates, having a heating layer and a temperature sensitive resistance. The four interdigitated electrode pattern can have for instance different electrode widths, (1) 30 nm, (2) 100 nm, (3) 500 nm and (4) 2 µm to investigate percolation effects of the conductivity. Another possibility is to fabricate equal electrode width and deposit size-selected nanoparticles with different sizes on each electrode pattern. Consequently, if different particle size cause different sensitivity values and dynamic behavior, only one operating temperature is necessary.

Particle deposition experiments were carried out on unbonded microhotplates consisting of four interdigitated electrode patterns on a 4 mm^2 area. The four interdigitated electrode pattern can have different electrode widths, (1) 30 nm, (2) 100 nm, (3) 500 nm and (4) 2 µm. The diameter of the deposition spot turned out to be in the range of 400 µm.

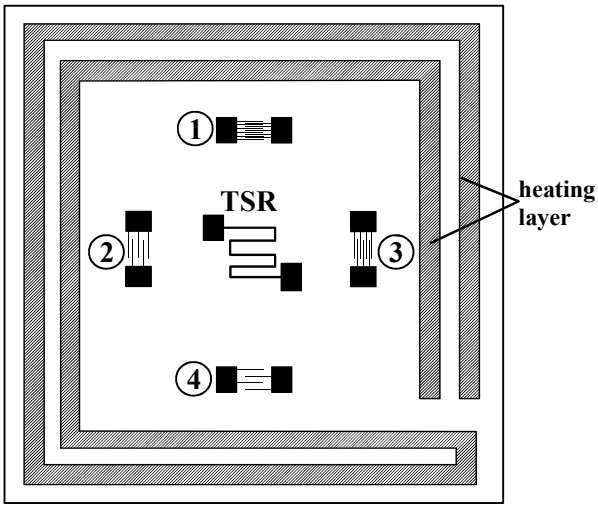

Fig. 3: Schematic of the top view of a fabricated multi sensor having a heating layer and temperature sensitive resistance (TSR). The four interdigitated electrode pattern have different electrode widths, (1) 30 nm, (2) 100 nm, (3) 500 nm and (4) 2 µm.

Contact Charging – Parallel Production

For mass production of sensors parallel processing has to be developed. For the transducer, conventional microtechnology, is used, which is a parallel technique. The sensing layer made out of nanoparticles produced in the gas phase has to be restricted to the area of the electrodes of each sensor arranged in a plane.

In order to realize defined shapes of the sensing layers, the controlled deposition of charged nanoparticles from the gas phase was investigated. By applying surface charges on the substrate by means of contact charging (Krinke et al., 2001) an electric microfield can be established which guides the particles to the desired areas on the substrate surface. In order to investigate the structured deposition of particles on oxidized silicon substrates, charge patterns were applied on the substrate surface by contact charging with different PDMS-stamps (Jacobs et al., 2001, Krinke et al., 2002). The two main goals were to show whether it is possible to transfer complex charge patterns onto oxidized silicon substrates using a stamp, and whether the charge density within these patterns is sufficient to selectively deposit nanoparticles on the desired areas of the substrate. The principle of charge printing

is that a stamp is moved gently up and down by a piston in order to touch the substrate without applying pressure. The substrates were p+ doped silicon (100) with 0.01 to 0.02 Ωcm resistivity, with thermally-grown wet oxide. This leaves a highly planar surface. The oxide thickness was chosen to be either 500 nm or 50 nm. During contact between the metal layer of the stamp and the substrate, charges cross the interface between the two materials. In order to be able to control the charge transfer and to enhance the charging effect, a voltage of ± 20 V was applied between the stamp and the back side of the substrate, depending on whether negative or positive charge patterns were created. The charging procedure was carried out in a glove box flooded with ultra clean nitrogen, in which an electrostatic precipitator (ESP) is installed as well. Thus, contact of the substrate with ambient air during and after charging is avoided.

Fig. 4 shows as an example spot like patterns of 30 nm gold particles. This structure has been created by using a PDMS-stamp with a microscopic dot structure, having a pitch of 520 nm. The diameter of the circular contact areas was approximately 150 nm. The stamp had a diameter of 5 cm. A bias of –20 V was applied to the stamp during charging a substrate with a 50 nm thick oxide layer. The sample was placed in the ESP and 30 nm gold particles, which were carrying a single positive charge were deposited for 120 min. An additional homogeneous electric field of 50 kV/m was applied in the ESP to enhance the particle deposition. The particles were deposited in spot like patterns which correspond to the structure of the stamp, which was in contact with the substrate. Between these spots no deposition of particles takes place.

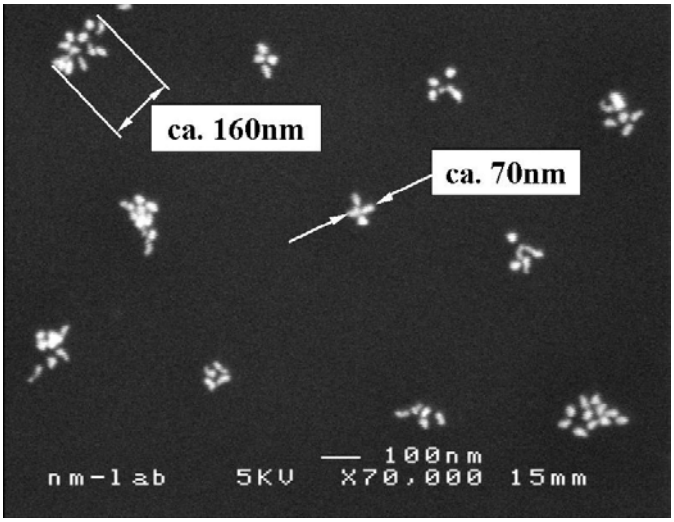

Fig. 4: SEM-image of spot like patterns of 30 nm large gold particle, after deposition on charge pattern. Substrate: 50 nm SiO_2 on Si.

V. Existing and expected developments

In this paper we demonstrated the development of a semiconducting gas sensor based on a microhotplates with interdigitated electrode patterns covered with a thin layer of equal sized SnO_x nanoparticles. The evaluation of the device leads to basic knowledge about the performance of gas sensors but we also found ways to adjust the improved sensing properties by particle size and chemical composition. The properties are easily controlled by process parameters.

For analysis of gas mixtures a set of different sensors is needed. Steps are taken towards smaller interdigitating structures which allows the parallel arrangement of several sensors on one microhotplate. A parallel particle deposition process based on creating charged areas on the surface with the potential to be used for microhotplates was developed. We estimated that 15000 sensing structures can be fabricated in parallel on one 300mm wafer. Using particles with different sensing properties the parallel production of multi-sensor arrays compatible with microelectronic technology seems to be possible.

VI. Acknowlegdements

We like to thank Dr. Werner Prost (Solid-State Electronics Department, Gerhard-Mercator-University Duisburg, Germany) for helping us to develop special substrates for electrical measurements. The authors would like to thank Lars Samuelson, head of the Nanometer Consortium, and Knut Deppert, head of the Aerosol Group of the Division of Solid State Physics, Lund University, Sweden, for the support of the experimental investigation of the deposition processes. These projects were funded by the German National Science Foundation (DFG) in the framework of the special research program (SFB 445) 'Nanoparticles From The Gas-Phase: Formation, Structure, Properties', by the ESF program NANO and the EU-TMR project CLUPOS.

References

Chen D.R., Pui D.Y.H., Hummes D., Fissan H., Quant F.R. & Sem G.J. 1998. Design and evaluation of a nanometer aerosol differential mobility analyzer (Nano-DMA). J. Aerosol Sci. 29, 497-509.

Chung W.Y., Lim J.W., Lee D.D., Miura N. & Yamzoe N. 2000. Thermal and gas-sensing properties of planar-type micro gas sensor. Sensors and Actuators B64, 118-123.

Diéguez A., Romano-Rodríguez A., Morante J.R., Weimar U., Schweizer-Berberich M. & Göpel W. 1996. Morphological analysis of nanocrystalline SnO_2 for gas sensor applications. Sensors and Actuators B31, 1-8.

Dixkens J. & Fissan H. 1999. Development of an electrostatic precipitator of off-line particle analysis, Aerosol Sci. Technol., 30, 438-453.

Jacobs H.O. & Whitesides G.M. 2001. Submicrometer Patterning of Charge in Thin-Film Electrets. Science 291, 1763-1766.

Jiménez V.M., Caballero A., Fernandez A., Espinós J.P., Ocana M. & González-Elipe A.R. 1999. Structural characterization of partially amorphous SnO_2 nanoparticles by factor analysis of XAS and FT-IR spectra. Solid State Ionics, 116, 117-127.

Krinke T.J., Deppert K., Magnusson M.H. & Fissan H. 2002. Nanostructured deposition of nanoparticles from the gas phase. Particle & Particle Syst. Charact. 19, 321-326.

Krinke T.J., Deppert K., Magnusson M.H., Schmidt F. & Fissan H. 2002. Microscopic aspects of the deposition of nanoparticles from the gas phase. J. Aerosol Sci. 33, 1341-1359.

Krinke T.J., Fissan H., Deppert K., Magnusson M.H. & Samuelson L. 2001. Positioning of nanometer-sized particles on flat surfaces by direct deposition from the gas phase. Appl. Phys. Let. 78, 3708-3710.

Kennedy M.K., Kruis F.E., Fissan H. 2000. Gas phase synthesis of size selected SnO_2 nanoparticles for gas sensor applications. Mater. Sci. Forum, 343-346, 949-954.

Kennedy M.K., Kruis F.E., Fissan H., Mehta B.R., Stappert S. & Dumpich G. (2003). Tailored nanoparticle films from monosized tin oxide nanocrystals: particle synthesis, film formation, and size-dependent gas-sensing properties. J. Appl. Phys., 93, 551-560.

Kruis E.F., Fissan H., Peled A. 1998. Synthesis of nanoparticles in the gas phase for electronic, optical and magnetic applications – a review. J. Aerosol Sci., 29, 511-535.

Kruis F.E., Nielsch K., Fissan H., Rellinghaus B. & Wassermann E.F. 1998. Preparation of size-classified PbS nanoparticles in the gas phase. Appl. Phys. Lett., 73, 547-549.

Nagel R., Hahn H. & Balogh A.G. 1999. Diffusion processes in metal/ceramic interfaces under heavy ion irradiation. Nuclear Instruments and Methods in Physics Research, B148, 930-936.

Prost W., Kruis F.E., Otten F., Nielsch K., Rellinghaus B., Auer U., Peled A., Wassermann E.F., Fissan H. & Tegude F.J. 1998. Monodisperse aerosol particle deposition: prospects for nanoelectronics. J. Microelect. Eng., 41/42, 535-538.

Ramamoorthy R, Kennedy M.K., Nienhaus H., Lorke A., Kruis F.E., Fissan H. 2003. Surface oxidation of monodisperse SnOx nanoparticles. Sensors and Actuator B: chemical, in press

Sánchez-López J.C. & Fernández A. 2000. TEM study of fractal scaling in nanoparticle agglomerates obtained by gas-phase condensation. Acta Materialica 48, 3761-3771.

Wada K. & Egashira M. 2000. Hydrogen sensing properties of SnO_2 subjected to surface chemical modification with ethoxlsilanes. Sensors and Actuators B62, 211-219.

Wise K.D., Angell J.B. & Starr A. 1970. An integrated-cicuit approach to extracellular microelectrodes. IEEE Trans. Biomed. Eng. BME-17 (3), 238-247.

Xu C., Tamaki T., Miura N. & Yamazoe N. 1991. Grain size effects on gas sensitivity of porous SnO_2-based elements. Sensors and Actuators B3, 147-155.

Jörg Kelleter
GTE Industrieelektronik mbH, Viersen, Germany

Detection of smoldering fires in dust loaded areas by sensing of specific gas emissions

Schwelbranddetektion in staubbelasteten Räumen durch Sensoren für brandspezifische Gase

Abstract

In buildings with high dust loads gas sensor based fire detectors show benefits in comparison to conventional smoke detectors. Optical smoke detectors are affected by soiling and interference by dust particles or dew. The advantages of fire gas detectors are insensitivity towards particles, aerosols or water and the capability of detecting a broad variety of smoldering fires or open flames. Even covered smoldering fires with no or a reduced emission of smoke aerosols can be detected by sensing released combustion gases.

The advantages of several years lifetime, durability even at high variations of temperature or humidity are obtained by the application of semiconductor type gas sensors. A combination of three sensors proved to be suitable for a lot of applications. These sensors were optimized for the detection of hydrocarbons, H_2 and CO. The hydrocarbon sensor shows a high sensitivity on products of decomposition of coal and wood (especially methoxy-phenoles). Main applications are industrial buildings with high, even dust explosive loads. For EX zones 20 or 21 an ATEX approved version of a fire gas detector is available. The dust protection is achieved by a sintered metal cap screwed in an aluminium die-cast housing.

A first application example is the monitoring of wood and straw pellets in storage halls for biomass powered electricity plants. These halls are considered as EX zone 20. Here not only fire detection but also indication of a beginning fermentation process can be provided. A second example is monitoring in coal mining; To prevent from loss of production excavators and the transportation system are equipped with gas sensor for early detection of smoldering coal.

1. Grundlagen

Die Detektion eines Brandes kann je nach Art und Ausbreitungsphase anhand der Brandkenngrößen „Gas“, „Rauch“ und „Temperatur“ erfolgen. Ein Brandgasmelder hat im Vergleich zu konventionellen Rauchmeldern eine Reihe von Vorteilen: So ermöglicht er die frühzeitige Detektion von solchen Bränden, die in der Entstehungsphase zunächst kaum Rauch freisetzen [1]. Weiterhin lassen sich Gassensor basierte Melder sehr gut gegen Umgebungseinflüsse wie Stäube, Nebel oder mechanische Beeinträchtigungen schützen. Rauchmelder reagieren auf Staub oder Partikel mit Verschmutzung oder Fehlalarmen. Da Brandgase per Diffusion zu den Sensoren gelangen, eignen sich hier verschiedenartige Filter, um Schmutz oder Staub abzuhalten. Auch wenn sich auf der Melderoberfläche trockener Staub abgesetzt hat, wird die Detektion nicht beeinträchtigt. Sogar durch eine Schicht von einigen Millimetern diffundieren Brandgase zu den Sensorelementen innerhalb weniger Sekunden.

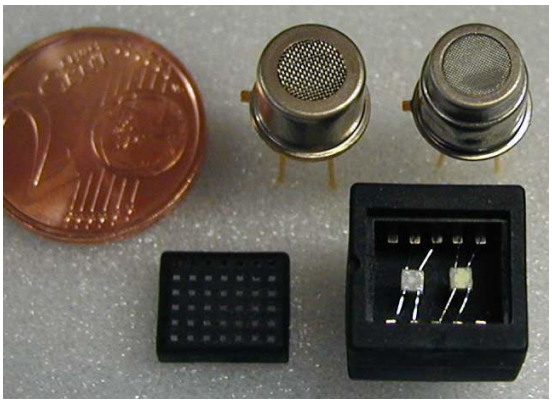

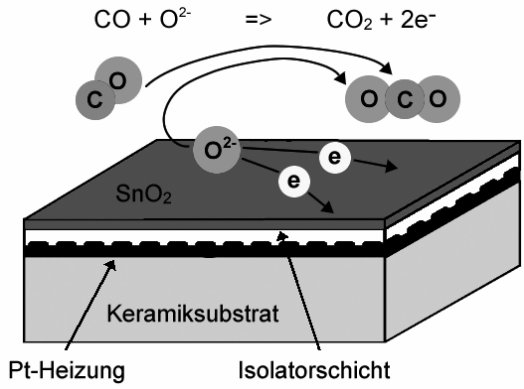

Abbildung 1

Halbleitergassensor (-array): Bauformen bei abgenommener Kappe sind die gasempfindlichen Elemente zu erkennen.

Detektionsschema: Bei einer Reaktion (hier von CO) auf der geheizten Oberfläche ändert sich der elektrische Widerstand der Oberfläche.

In vielen Fällen ist es erforderlich, zwischen Brandgasen und Gasen anderer Quellen zu unterscheiden. Je nach Applikation spielen dabei Ausgasungen des gelagerten oder zu überwachenden Materials (Kohle, Holz, Biomasse) oder Abgase von Kraftfahrzeugen

eine Rolle. Der Einsatz mehrerer unterschiedlicher Gassensoren liefert die gewünschte Selektivität bei hoher Empfindlichkeit.

In dem ADICOS Melder kommen Sensorelemente zum Einsatz, die bezüglich Selektivität für folgende Gase oder Gasarten optimiert wurden:

- Kohlenwasserstoffe: Methoxy-Phenole und Furane [2]
  Entstehung bei allen unvollständigen Verbrennungen von organischen Materialien, insbesondere von Holz und Papier, auch bei Kohle
- Kohlenwasserstoffe: Ketone und Aldehyde
  Entstehung bei allen unvollständigen Verbrennungen von organischen Materialien
  Auch als Hintergrund bei Biomasse (Zersetzungsprodukte)
- Kohlenmonoxid (CO)
  Entstehung bei jedem Schwelbrand von organischem Material,
  aber auch als Abgas oder bei kalter Oxidation von Kohle
- Wasserstoff (H_2)
  Entstehung bei jeder Glut bei Anwesenheit von Feuchtigkeit, insbesondere bei Glut von Holz, Papier, Kohle und Metall,
  aber auch bei elektrischer, chemischer oder katalytischer Umsetzung von Wasser (Akkuladung, Korrosion, Wassergasgleichgewicht bei Kohle) und als Abgas.
- Stickoxide (NO_x)
  Entstehung bei allen Flammen, aber auch im Verbrennungsmotor als Abgas

2. Brandgasmelder

2. 1. Geräteausführung

Je nach Anforderung und Anwendungsgebiet stehen die Melder „GSME-L3“ oder „GSME-HC“ in einem robusten Aluminiumgehäuse oder der Melder „GSME-L1“ (zur Aufschaltung auf SIEMENS Sigmasys: „SDG 3800“) bzw. GSME-FG in einem Kunststoffgehäuse für Montage in Bajonett-Melderfassungen zur Verfügung.

Der Melder GSME-L3/-HC ist in Schutzart IP 64 ausgeführt, eine Sinterbronzekappe dient als staubdichter aber gasdurchlässiger Schutz für die darunterliegenden Sensoren.

Wasser wird aufgrund seiner Oberflächenspannung daran gehindert, einzudringen. Lediglich andauerndes Spritz- oder Strahlwasser kann durch die Poren eindringen. Ein Industrie-Bajonett-Stecksystem ermöglicht die unkomplizierte Montage und Installation auch unter schwierigen Bedingungen. Der Melderzustand „Betrieb“, „Alarm“ oder „Störung“ wird mit 3 LED’s am Gehäuse angezeigt [4].

Bei dem Melder GSME-L1 wurde der Design-Schwerpunkt auf Kompatibilität zu herkömmlichen Rauchmeldern gelegt. Daher ist die komplette Sensorik und Auswerte-elektronik in einem „standard“ Kunststoff-Meldergehäuse zum Einsatz in einen Bajonett-Meldersockel integriert.

Die Anzeige des Melderzustands erfolgt über eine Zweifarben-LED (Betrieb: grün, Alarm: rot oder Störung: orange). Zur Detektion dient ein Array mit Sensorschichten zur Erfassung von unterschiedlichen Kohlenwasserstoffen und Stickoxiden.

2. 2. Detektionseigenschaften

Die ADICOS Brandgasmelder sind in der Lage, sowohl Glimm- oder Schwelbrände nahezu aller organischen Materialien, als auch Brände mit offenen Flammen zu detektieren. Hier kann man die Anforderungen der EN 54, Teil 7 (für punktförmige Rauchmelder) heranziehen. Als Erprobungstest für automatische Brandmelder sieht diese Norm die Testfeuer TF2 (Buchenholz-Schwelbrand), TF3 (Lunten-Glimmbrand), TF4 (Polyurethan-Matten-brand) und TF5 (n-Heptan-Flüssigkeits-Brand) vor. Methoden für eine weitergehende Überprüfung durch den VdS werden z. B. in [3] diskutiert.

Die Detektionseigenschaften werden selbst durch mehrere Millimeter dicke Staubschichten nicht beeinträchtigt.

Abbildung 2

ADICOS GSME-L1 nach einem Jahr Betriebsdauer in einem Getreidelager; Der Melder ist trotz Verschmutzung voll funktionsfähig. Eine Reinigung ist nicht erforderlich.

Eine Reinigung der Melder ist nicht erforderlich; Eine unsachgemäße Reinigung kann sogar einen negativen Effekt haben, indem dann die Filterporen verstopfen.

Tabelle 1: Beispiele für Einzelsensorsignale bei Testfeuern des Erprobungstests nach EN 54, Teil 7; Fett gedruckt sind Sensorsignale und korrespondierende Referenzmesswerte zum Zeitpunkt der Alarmauslösung

	GSME-L3			***Referenzmessung***		
TF	***S(H2)***	***S(CO)***	***S($_{KW/NOx}$)***	***m***	***Y***	***Δ T***
2 „Buchenholz“	***1,5***	***70***	***50***	***0,3***	***0,7***	***-***
„Brandende“	8	>100	70	2	1,9	-
3 „Lunten“	***3***	***25***	***20***	***0,01***	***0,2***	***-***
„Brandende“	22	>100	40	2	2,9	-
4 „PU-Schaum“	***0,5***	***7***	***-10***	***0,5***	***1,6***	***4***
„Brandende“	1	28	-16	1,7	6	20
5 „n-Heptan“	***0,5***	***6***	***-10***	***0,35***	***1,5***	***20***
„Brandende“	3	65	-27	1,3	6	58
BRK „Braunkohle“	***2***	***60***	***3***	***0,03***	***0,19***	***-***
Nach 1 h 10 min	7,5	28	5	0,1	0,3	-

(m: Lichttrübung; y: rel. Ionisationsstrom, Δ T: Temperaturanstieg; GSME-L3: mit typ. Kohlenkraftwerksparametrierung)

2. Explosionsschutz-Variante GSME-EX

Bei vielen Anlagen für Transport oder Lagerung brennbarer Stoffe treten während des Betriebes Stäube auf. Je nach Ausführung der Anlagen und Eigenschaften der Stäube kann sich explosionsfähiges Staub–Luft–Gemisch bilden. In diesem Fall erfolgt eine Einstufung der Anlagen in verschiedene Zonen; Für den Staub-EX Bereich sind dies die Zone 20 („... explosionsfähige Atmosphäre ... ständig oder langzeitig oder häufig ...“), Zone 21 („... in dem damit zu rechnen ist, dass explosionsfähige Atmosphäre ...“) oder Zone 22 („... bei Normalbetrieb nicht damit zu rechnen ist, dass explosionsfähige Atmosphäre ... auftritt, wenn sie aber doch auftritt, dann nur kurzzeitig.“) [5]. Für Bereiche, die als Zonen 21 oder 20 deklariert sind, dürfen nur elektrische Betriebsmittel eingesetzt werden, die entsprechend der Richtlinie 94/9/EG ATEX ausgelegt und durch ein akkreditiertes Institut (in Deutschland z. B. die DMT oder PTB) geprüft worden sind. Zusätzlich zur Baumusterprüfung unterliegt der jeweilige Produktionsbetrieb einer Überwachungsauditierung durch das Prüfinstitut.

Für die Brandgasmelder der GSME-Reihe wurden Varianten entwickelt, bei denen u. a. durch besondere Maßnahmen bei der Gehäusekonstruktion die geforderte Schutzart erreicht wird.

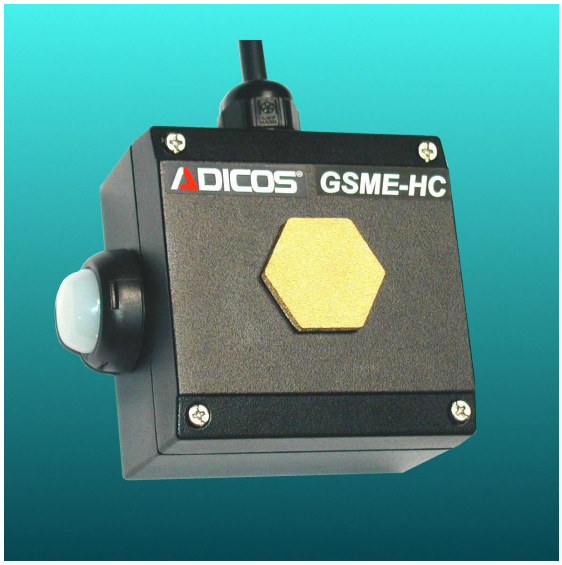

Abbildung 3

ADICOS Brandgas-Melder GSME-HC-EX) für den Einsatz in Staub-Ex-Zone 20/21:

Ex II 1D T100°C EEx ia
(Konform mit RL 94/9/EG ATEX)

Zugelassen mit Prüfnummer
DMT 03 ATEX E 050

3. Applikation

3. 1. Allgemeines

Förderanlagen für z. B. Kohle, Holz- oder Strohpellets, Getreide etc. stellen an die automatische Branddetektion eine hohe Anforderung. So herrschen in diesen Anlagen in der Regel eine hohe Staubbelastung, z. T. sind solche Bereiche auch als Ex-Bereich (Zone 22 bis 20) zu deklarieren. Hier sind ADICOS Brandgasmelder prinzipiell geeignet. Weiterhin sind Luftströmungen sowohl von der Betriebsart als auch von klimatischen Einflüssen abhängig. Deshalb muss der Installationsort geeignet gewählt und ggf. eine melderspezifische Einstellung vorgenommen werden.

Zur Installation sind ähnliche Regeln zu beachten, wie sie auch für Rauchmelder gelten; Diese sind z. B. in der Richtlinie VdS2095 (VdS-Richtlinien für automatische Brandmeldeanlagen: Planung und Einbau) zu finden. Dort findet man neben Aussagen zu Überwachungsflächen in Abhängigkeit von Raumgröße und Deckenhöhe als zentrale Regel:

„Automatische Brandmelder sind so anzubringen, dass die Brandkenngröße sie ungehindert erreichen kann."

Daraus resultiert die besondere Aufgabe des Errichters, Melder so zu positionieren, dass im Brandfall die Brandgase den Ort der Melder erreichen können. Sollen Schwelbrände in einem frühen Stadium detektiert werden, muss berücksichtigt werden, dass diese mit nur geringer Wärmeentwicklung ablaufen und somit praktisch keine Thermik erzeugen. Die Brandgase (und auch der Rauch) breiten sich dann nur zusammen mit der vorherrschenden Luftströmung aus. Besonders zu berücksichtigen sind daher Gebäudeöffnungen (Tore, Fenster oder weiterführende Fördereinrichtungen) sowie Zwangsbelüftung.

3. 2.Melder auf einem „Braunkohlenbagger"

Sehr hohe Anforderungen an einen Brandgasmelder findet man u.a. in „Braunkohlen-baggern" (korrekt werden diese Maschinen mit „Großgerät" bezeichnet). Hier kommen hohe wechselnde Staubbelastung zusammen mit extremen Klimaschwankungen und Betauung vor. Eine Herausforderung bei dieser Applikation ist die Weiterleitung der

Alarmmeldung. Bislang sind Melder in dieser Applikation an eine konventionelle Brandmelderzentrale angebunden. Diese leitet eine Meldung weiter an das Betriebspersonal des Großgeräts. Eine Übertragung an eine Feuerwehr oder andere Stellen erfolgt dann per Funk. Zur Zeit wird eine Einbindung der Technik in ein Funknetzwerk diskutiert, so dass eine Fernübertragung von Meldungen oder Fernservice ermöglicht wird.

Abbildung 4: Einsatz von ADICOS GSME-Meldern in einem Braunkohlen-bagger; Oberes Teilbild: Montageort innerhalb des Turms.

4. 2. Melder in einem Lager für Strohpellets

Mittlerweile sind eine Reihe von Großanlagen zur thermischen Verwertung (Verbrennung) von nachwachsenden Rohstoffen in Europa errichtet worden. Um eine automatische kontinuierliche Beschickung der Kessel mit Holz, Stroh oder anderen Biomasse-Produkten zu gewährleisten, ist ein System aus Anlieferung (z. B. per Schiff), Transport mit Förderbändern und Zwischenlagerung erforderlich. In den großen

Lagerhallen werden die in der Regel in Form von Pellets (Preßlingen) vorliegenden Brennstoffe z.T. über mehrere Monate trocken gelagert. Hier kann es leicht zu Schwelbränden kommen. Insbesondere Vorgänge, die zur Selbstentzündung führen können, sind zu beachten. So können gelagerte Stroh- oder Holzpellets bei Eindringen von Feuchtigkeit anfangen zu gären. Bei guter thermischer Isolierung innerhalb der Schüttung werden so rasch Temperaturen erreicht, die zu Schwelvorgängen führen. Aufgrund der z.T. hohen Staubbelastung sowie der EX-Zonen-Einteilung in Zone 20 kommen zur Detektion von Schwelbränden ADICOS Melder vom Typ GSME-EX zum Einsatz. Auf Anregung der Betreiber sind bei dieser Anlage einige Zusatzfunktionen realisiert. Dazu gehören eine automatische Empfindlichkeitsumschaltung bei Befahren der Lagerhallen mit Fahrzeugen mit Verbrennungsmotor oder eine Zusatzauswertung, die einen Gärungsprozess detektiert und eine Vorwarnung ausgibt.

Abbildung 5: *Einsatz von ADICOS GSME-EX Brandgasmeldern in einer Lagerhalle für Strohpellets;*

Versetzte Montage im Bereich der Dachkonstruktion

Literatur

[1] *D. Kohl, J. Kelleter and H. Petig* Detection of Fires by Gas Sensors; p. 161 – 223 in Sensors Update; Editors: H. Baltes, J. Hesse and J. G. Korvink; Vol. 9; 2001; Wiley-VCH

[2] *D. Kohl and A. Eberheim* Selective Recognition of Smoke from Spruce and Beech Wood by Gas Sensors; AUBE 2004 Proceedings

[3] *O. Linden* Function-based Testing Procedure for Multi Sensor Fire Detectors; AUBE 2004 Proceedings

[4] *H. Petig, A. Lechte, D. Kohl und J. Kelleter* Neuer Gassensor-Brandmelder mit Monitoring System; Allianz Report 4/99, S. 244-250

[5] *N.N;* EN50281-1-2; Elektrische Betriebsmittel zur Verwendung in Bereichen mit brennbarem Staub;

Carsten Oldorf, Ingo Bebermeier, Volker Leisten
m.u.t Aviation-Technology GmbH, Hamburg, Germany

Thomas Steinbeck
m.u.t GmbH, Wedel, Germany

Early fire detection based on semiconductor laser gas detection

Abstract

An overview of the actual state of the art and newest developments of semiconductor lasers for gas detection is presented. Actual industrial applications frequently use near infrared (NIR) diode lasers in the 750nm to 2000nm wavelength range, where still new laser types are under development. Laboratory laser gas spectrometers often rely on lead-salt lasers, which need cryogenic cooling and cover the mid infrared (MIR) spectral range from 3µm to beyond 10µm, where many gases can be detected with highest sensitivity. Recently developed Quantum Cascade Lasers (QCL) have their emission in the same range without the need of extreme cooling.

Introduction

Infrared spectroscopy is a well established method for the detection of gases for many applications. Traditionally a thermal source is used to generate the infrared radiation, which is then transmitted through the gas sample to be examined. The transmitted radiation is then analyzed using filtered detectors or a spectrometer. From the absorption characteristics the type and concentration of the gas can be derived. As these traditional instruments use a relative broad wavelength range they are vulnerable to interference from other gases which can give wrong indications of the measured gas concentration.

Moving to lasers as light sources with extreme small bandwidth nearly eliminates the interference problems and brings some other advantages as high spectral intensity and simpler beam collimation, which eases the optical design of a gas sensor significantly.

Most of the infrared active gases have their fundamental vibrational-rotational state transitions in a frequency range which corresponds to absorption lines in the 3µm to

12µm wavelength range. Higher harmonics of these frequencies usually exists and can be found as absorption lines at shorter wavelength's in the NIR where semiconductor lasers are commercially available, which have originally been developed for fiber optical communication around the wavelengths of 0,85µm, 1,31µm and 1,55µm.

The molecular absorption at near NIR wavelengths is much weaker than at the fundamental frequencies. For example CO_2 exhibits a more than 58.000 times [1] stronger absorption at 4,235µm than at the strongest absorption line in the NIR at 1,432µm.

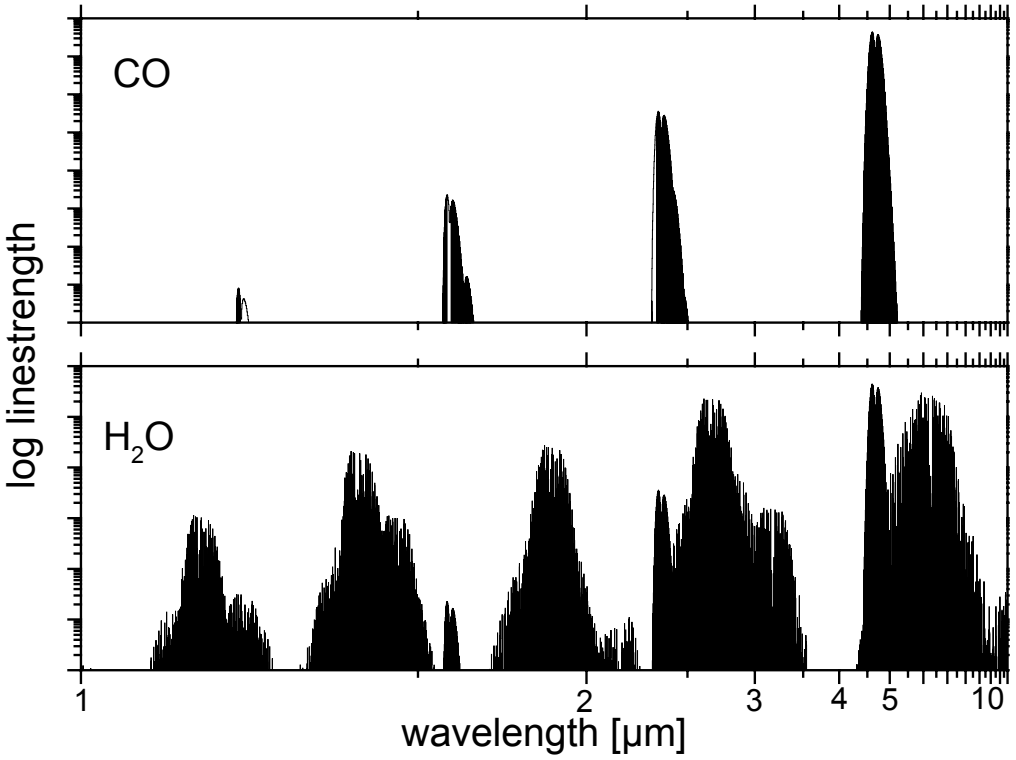

Figure 1: Example of absorption cross sections for Carbon Monoxide (CO, upper graph) showing the fundamental absorption band around 5µm and the weaker overtone and combination bands at shorter wavelengths. The lower graph shows the corresponding data for water (H_2O) which is the source for the strongest interference's under atmospheric conditions [1].

Measuring Principle

The diode laser as the core component of the gas analyzer is wavelength tunable due to temperature and drive current. Usually the temperature is set to a fixed value to select the central wavelength and the drive current is modulated with a triangular or sawtooth waveform to perform the wavelength scanning across the spectroscopic feature of the gas to be analyzed.

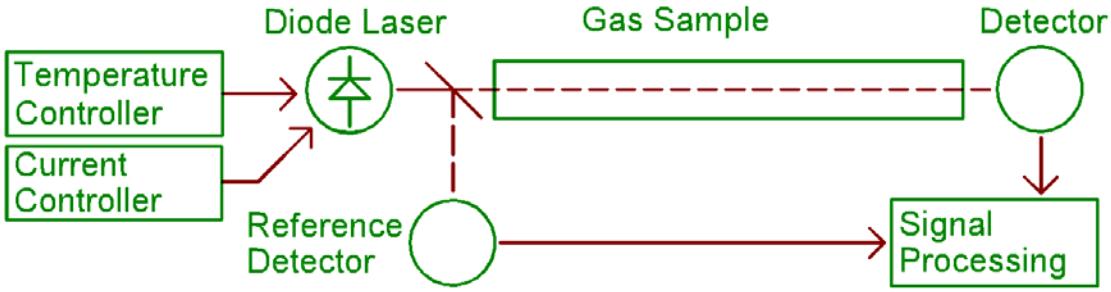

Figure 2: Basic diode laser gas sensor scheme (simplified)

To improve the signal to noise ratio of the signal and herewith the detection limit modulation techniques are often used. For applications needing high absolute accuracy and stability wavelength and gas sample references are frequently included in the analyzing system.

Under ideal conditions the absorption of monochromatic laser radiation of wavelength λ through a sample of gas of length L is described by Beer's law

$$I(\lambda) = I_0(\lambda)\, e^{-\alpha(\lambda)Ln}$$

where I_0 is the transmitted intensity without the absorbing gas, $\alpha(\lambda)$ the absorption coefficient and n the gas concentration.

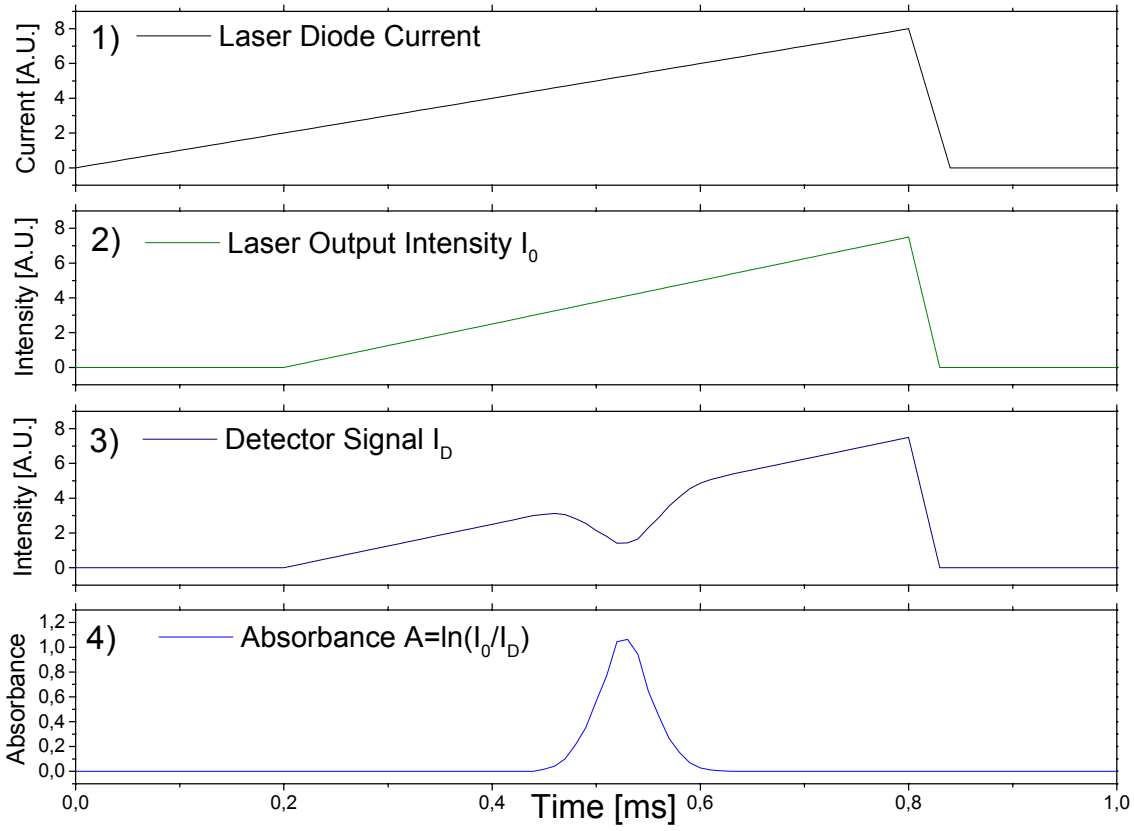

Figure 3: Principle of gas detection using continuous wave (cw) diode lasers. 1) shows the ramp modulating the driving current of the laser diode. 2) is the resulting laser output intensity I_0 measured by the reference detector and 3) the intensity signal I_D on the optical detector after the laser radiation is transmitted through the gas sample to be measured. In 4) the absorbance, calculated as $\ln(I_0/I_D)$ is shown. This is proportional to the concentration of the absorbing gas at given path length.

Lasers for gas detection

This chapter gives an overview of laser types actually used for gas sensing applications. The use of other types as gas, solid state or dye lasers is usually limited to special applications as they are often bulky and require frequent maintenance.

Near infrared lasers

The commercially attractive field of laser sources for fiber optical data communication has initiated the development of various types of lasers for the NIR spectral region. All laser types presented here operate at room temperature and above. For spectroscopic

applications they are usually temperature stabilized using thermoelectric (Peltier) elements.

As the absorption strength of fire related gases in the NIR is rather weak usually a relative long optical path in the order of several meters [2] has to be used for the detection of fire related gases like CO or CO_2 [3]. Multi-path optical cells provide long path lengths in a small volume, but they are adding complexity and cost to the gas sensor, so that a preferred configuration for a fire detector could be an open space linear arrangement over longer distances, e.g. with a retro-reflector.

The wavelength in the NIR is comparable to the size of fire particles and aerosols [4], therefore the particles cause a considerable scattering of the NIR radiation, thus damping the detector signal. For a well laid out laser gas detector a certain amount of damping through smoke, dust, fog or other small particles in the measured gas volume can be detected and the ability for quantitative gas analysis is only limited at very high damping conditions.

Fabry Perot Lasers

These lasers are the basic diode lasers, whose emission wavelengths are mainly controlled by the substrate material system. As their resonator size is sufficient for more than one mode, they usually show multimode emission and mode-hopping i.e. discontinuous change of wavelength and intensity with changes of temperature and drive current. This behavior limits their applications in the field of gas sensing.

Distributed feedback (DFB) and distributed Bragg reflector (DBR) lasers

These lasers types feature an integrated wavelength selective element such as a grating to suppress undesired laser modes and are readily available commercial devices from various vendors in the wavelength ranges used for fiber optic communication and can be fabricated from semiconductor materials with wavelengths ranging from 630nm to more than 2000nm. They exhibit a relative high optical power in the range of 20mW and more and their wavelength changes continuously with temperature at a rate of ~0.1nm/°C. So with a temperature tuning range of 40°C a wavelength tuning over typical some 4nm can be achieved. With a current tuning rate of 0,003nm/mA to

0,005nm/mA and a usable current range of typical 30mA to 100mA the wavelength tuning due to current modulation typically is limited to 0,1nm to 0,5nm.
Despite their high power, simplicity, and manufacturability, their narrow current tunable range limit their applications in the field of gas sensing.

External Cavity Lasers.

This laser type is wavelength tuned due to a external wavelength selective element usually consisting of a diffraction grating and a movable mirror. They can have relative high power (1mW to10mW) and continuous tuning over a >40nm range. Because of their relative complex optical setup especially due to the movable parts this is usually not a preferred laser type for gas sensing.

Vertical Cavity Surface Emitting Laser VCSELs.

These lasers are relatively new in the field of fiber communication. As they emit perpendicular to the wafer surface they are grown on, they can be tested and selected on waferscale as well as easily fabricated in arrays. These features provide a significant cost advantage over all other laser types, at least if mass production is envisioned.
They feature moderate power (0,1..1mW) and sufficient tuning range with temperature and current (typical some 4nm). Additionally they are operated at low current and therefore have low power consumption.
This attributes may lead to a significant market share for laser gas sensors [5].
Furthermore VCSELs can be integrated into a micro electromechanical system (MEMS) that provides a electrically adjustable variable cavity to extend the tuning range to 20nm to 30nm or more.

Mid infrared diode lasers

The applications for this radiation sources are mainly gas spectroscopic methods or ranging. Therefore the demand for these laser types is much lower than for near-infrared devices. For this reason, advancements in this field are usually much slower and up to now there is no real mass production. As soon as devices with higher power in the atmospheric transparent windows from 3µm to 5µm and 8µm to 12µm will become

available the development may be driven by the market of free space optical data communication systems e.g. for the “last mile” in metropolitan networks

In the MIR wavelength range fire related gases usually have an absorption strength that is 2 to 5 orders of magnitude higher than in the NIR. Therefore a gas sensor using these wavelength can be much smaller than a NIR instrument. On the other hand smoke and other particles with typical sizes of around 1µm show very little scattering in the MIR wavelength range [6], so a simultaneous smoke detection without additional effort is barely feasible especially when measuring with very short optical path lengths. This is an advantage, especially if accurate measurement also under thick smoke or fog conditions is required.

Lead salt lasers

These lasers are based on the lead salts PbSnTe, PbEuSeTe, PbSSe or PbSnSe and operate only at cryogenic temperatures. Newer devices operate up to 200K allowing liquid Nitrogen or Stirling cooling. This cooling requirement is prohibitive for most of the industrial applications thus mainly limiting the use of these lasers to laboratory instruments. However first laboratory-samples have shown pulsed operation at room temperature.

Devices are available in the 3µm to 16µm range. Although DFB-lead-salt lasers with single mode characteristics have been demonstrated, commercially available devices usually feature the simpler Fabry-Perot structure to exhibit a wider tuning range. For an actual application a laser is selected from a suitable production wafer to have no mode hopping in the spectral range of interest.

These laser show mode-hop free tuning ranges in the order of magnitude of 20nm at optical output powers of typical 0,2mW

Quantum cascade lasers (QCL)

QC lasers were invented at Bell Labs in 1994 [7] based on a concept proposed already in 1971 [8]. Their operation is unlike that of all other lasers. They operate like an electronic waterfall: When an electric current flows through a QC laser, electrons cascade down an energy staircase; every time they hit a step, they emit an infrared photon. At each step, the electrons perform a quantum jump between well defined

energy levels. The emitted photons are reflected back and forth between built-in mirrors, stimulating other electrons to perform quantum jumps to emit photons. This amplification process enables high output power. Actual devices feature up to 75 steps of the electronic staircase resulting in up to 75 photons per electron passing trough the diode laser. Traditional diode lasers have a theoretical maximum of one photon per electron.

Pulse operated QCL can have a very high peak power (100mW to 500mW or more) while the average power or the cw power respectively is in the range of 10 to 30mW. The tuning range can be up to one hundred nanometers or even more.

In addition devices can be designed to simultaneously emit at two dedicated wavelengths, which can be used to simplify gas analyzers for multiple gases.

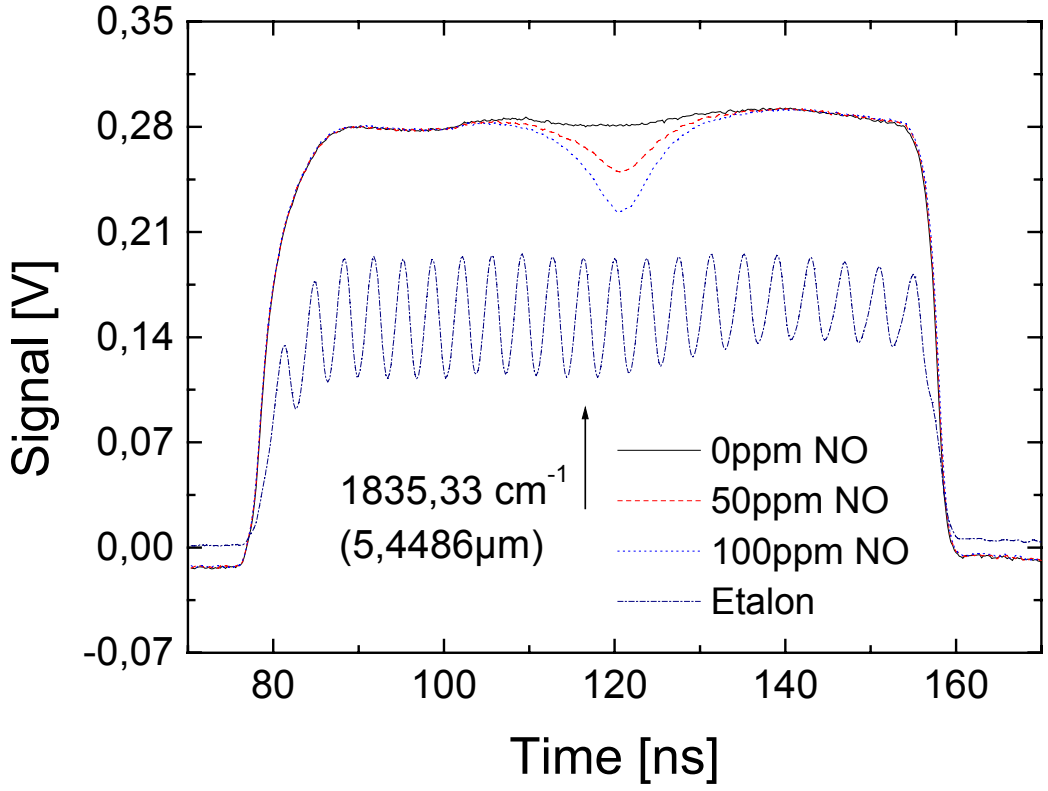

Figure 4: Experimental data of spectra of different NO concentrations taken with a pulsed QC-laser. The laser is driven with a rectangular current pulse. The wavelength shifts due to the diode laser self heating over time which is shown with the Etalon signal that is used as a relative wavelength reference. (data courtesy of m.u.t GmbH)

Due to the properties of the devices the market for open space optical data communication may soon drive the demand for such diode lasers as soon as high power, room temperature, high reliable lasers in the atmospheric windows are available and ready for mass production. This would also lead to more affordable laser sources appropriate for gas detection and could support the fast expansion of their use in industrial gas detectors and maybe in fire detectors.

Application of laser gas sensors as fire detectors

Nearly all fires produce gases like Carbon Dioxide (CO_2) Carbon Monoxide (CO), Hydrocarbons (C_xH_y), Ammonia (NH_3), Hydrogen Cyanide (HCN) Hydrogen Chloride (HCL) and many other more depending on the burning conditions and mixture of materials. In ambient air these gases are usually present in very low concentrations. The presence or a rapid increase can give a very early indication of fire.

NIR laser gas sensors in a linear arrangement for fire detection may replace linear smoke detectors or even capture new applications where nuisance source like dust are frequently present. The additional gas sensing capabilities enable the discrimination of these sources. This can be e.g. conveyor belts, tunnels or large open air or roofed industrial facilities.

MIR laser gas detectors for fire detection are much further down the road because the laser devices don't have other real mass applications and the cost sensitive market for fire detection is not willing to pay the actual prices. Despite of this, infrared transmissive optics are also more specialty products up to now. But the development of QC laser may soon reach a stage where these devices will become available from mass production and may also be used for compact, reliable and reasonable priced gas detectors that can be incorporated into fire detection systems.

Conclusions

The most promising candidates of diode lasers for gas detection which may soon find their way into fire detection systems are VCSELs in the NIR and QCLs in the MIR. NIR systems will mainly be used in open path arrangements and include the functionality of linear smoke detectors, while MIR sensors might be small enough to be incorporated into point style fire detectors.

As NIR laser gas analyzers are already used in a couple of industrial applications like process and emission control in incinerators (up to now mainly using Fabry-Perot or DFB lasers) these types will probably be the first candidates for fire detector applications.

A mayor hurdle for the widespread use of MIR lasers is the missing of an initial application, that requires large quantities of these devices that would push the development towards mass producible and reasonable priced diode lasers.

References

[1] L. S. Rothman et al, The HITRAN Molecular Spectroscopic Database: Edition of 2000 Including Updates through 2001, JQSRT 82, 5-44 (2003).

[2] D. S. Bomse, D. C. Hovde, S.-J- Chen and J. A. Silver, Early fire sensing using near-IR diode laser spectroscopy, Diode Lasers and Applications in Atmospheric Sensing, Proc. SPIE **4817**, 73-81 (2002).

[3] W. L. Grosshandler, Towards the development of a universal Fire Emulator / Detector Evaluator, 10th Int. Conf. on Automatic Fire Detection, AUBE `95, , 368-380 (1995).

[4] D. W. Weinert, T. G. Cleary, G. W. Mulholland and P. F. Beever, Light Scattering Characteristics and Size Distribution of Smoke and Nuisance Aerosols, Proc. of 7th Symp. of the Intl. Ass. for Fire Safety Science, 209-220 (2003).

[5] M. Lackner, F. Winter, G. Totschnig, M. Ortsiefer, J. Rosskopf, M.-C. Amann and R. Shau, Spectroscopic Application of Long-Wavelength (<2µm) VCSEL Diode Lasers, tm – Technisches Messen 70 6 (2003).

[6] S. Dunkelmann, I. Bebermeier, C. Oldorf and V. Leisten, Comparison of NIR, MIR and LWIR cameras for video based detection of fire, accepted for 13th Int. Conf. on Automatic Fire Detection, AUBE `04 (2004).

[7] J. Faist, F. Capasso, D. L. Sivco, C. Sirtori, A. L. Hutchinson, and A. Y. Cho, Quantum cascade laser, Science 264, 553-556 (1994).

[8] R. F. Kazarinov und R. A. Suris, Fiz. Tekh. Poluprov. **5**, 797 (1971) Sov. Phys. Semicond. **5**, 707 (1971).

Dieter Kohl, Andreas Eberheim, Institute of Applied Physics, University of Giessen, Heinrich-Buff-Ring 16, D-35392 Giessen and
Peter Schieberle, Institute for Food Chemistry, Technical University of Munich, Lichtenbergstr. 7, D-85748 Garching

Selective Recognition of Smoke from Spruce and Beech Wood by Gas Sensors

Abstract

Smouldering fires of wood were made in ambient atmosphere. Smoke was sampled on different kinds of substrates. It was shown that the reaction of an SnO_2 sensor to beech wood smoke is primarily due to 2-methoxyphenol and 2,6-dimethoxyphenol derivatives with para-substituted alkyl and alkenyl groups, which originate in hardwood lignia. Both types of compounds occur in relatively high concentrations during smouldering and both are sensitively detected by SnO_2 sensors. In spruce wood smoke only reactions to 2- methoxyphenol derivatives occur. Differences between beech wood and spruce wood smoke are due to structural differences in the composition of hardwood and softwood lignin. Reaction schemes are discussed.

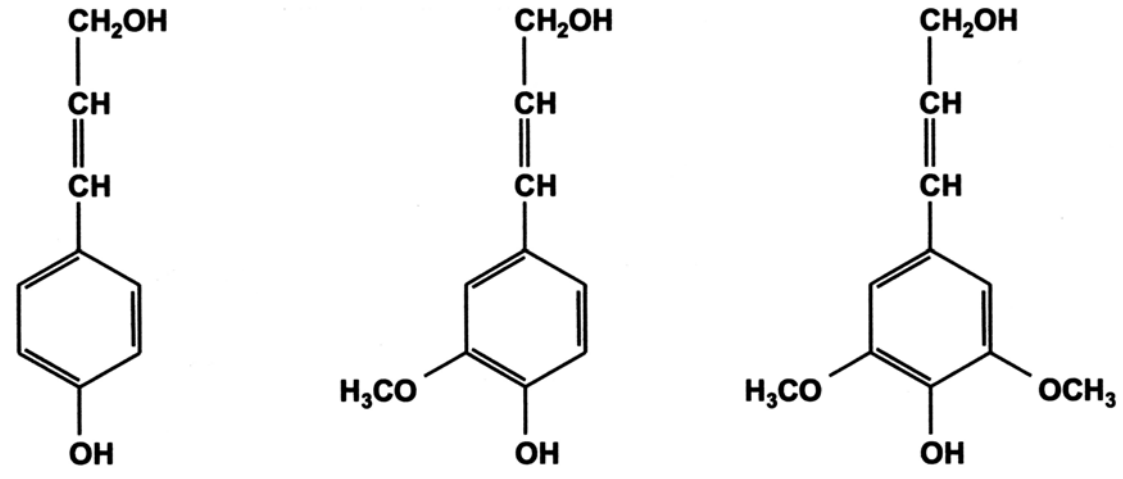

Fig. 1. Precursors of lignia formation:
left side: p-coumaryl alcohol (phenolic structure without a methoxy group)
middle: coniferyl alcohol (phenolic structure with one methoxy group)
right side phenolic structure with two methoxy groups

Introduction

Within the past years the detection of complex mixtures by gas sensors gained growing interest and made substantial progress. An important application field is fire detection. For sensor evaluation the HRGC/SOMMSA (High resolution gas chromatography / selective odorant measurement by multisensor array) approach has been established [1, 2]. An essential part of this method is the use of a gaschromatographic column ending in a split with the sensors working in parallel to a reference detector [1].

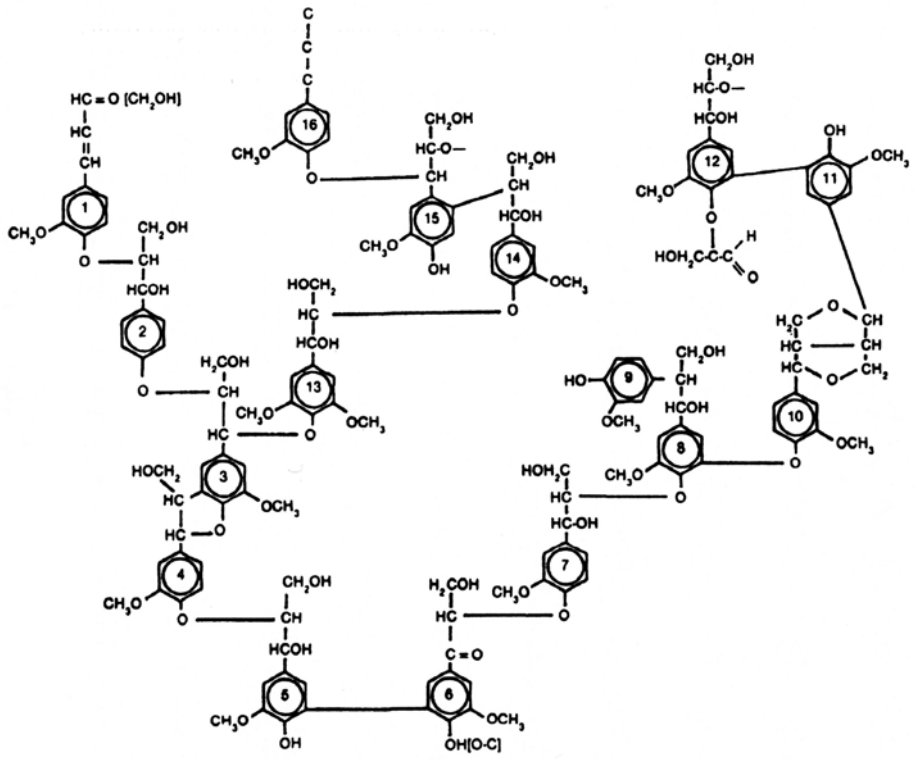

Fig. 2. 2D lignia structure of spruce wood containing nearly no phenolic structures with two methoxy groups

In an earlier study we presented results of sensor evaluation for the detection of specific organic smoke compounds by using the HRGC/SOMMSA approach [3, 4]. There smouldering fires of wood were made in ambient atmosphere. In beech wood smoke the ratio of CO to CO_2 concentration was 7 : 15. Smoke was sampled by different kinds of sample preparation. Settings were identical to settings in this study. It was shown that the reaction of an SnO_2 sensor to beech wood smoke is primarily due to 2-methoxyphenol and 2,6-dimethoxyphenol derivatives with para-substituted alkyl and

alkenyl groups, which originate by decomposition of hardwood lignia. Lignia is a polymer, some of its precursors are shown in Fig 1. They are arranged in a 2D structure, Fig. 2 gives an example. 2-methoxyphenoles and 2,6-dimethoxyphenoles occur in relatively high concentrations during smouldering and both are sensitively detected by SnO_2 sensors. In spruce wood smoke nearly only reactions to 2-methoxyphenol derivatives occur. Differences between beech wood and spruce wood smoke are due to structural differences in the composition of hardwood and softwood lignia. Softwood lignia is dominated by phenolic structures with one methoxy group (guaiacyl units), while hardwood lignia consists of phenolic structures with two methoxy groups (syringyl units), too [5]. For beech wood 2-Methoxyphenol (guaiacol) and 2,6-dimethoxyphenol (syringol) derivatives can be regarded as monomers of the corresponding lignia. Both are important for smoke flavour [6] and curing processes of meat [6, 7]. 2-methoxyphenol (guaiacol) is a tracer compound for the detection of forest fires by potato beetles [8] and a pheromone of gut bacteria in locusts [9].

From the other organic components in wood smoke (more than one hundred) only benzenediols and some individual components like hydroxyaceton and furfuryl alcohol cause significant sensor signals. A hydroxy group was found to be part of any compound evoking a signal of the sensor. In all of these compounds the hydroxy group acts as functional group and is not part of a carboxy group. About 20 of these compounds were found in the emissions of smouldering beech wood. Signals of organic compounds with hydroxy groups dominate in the investigated sensor temperature range between 165 °C and 330 °C. The highest sensitivities occur at 270 °C to 330 °C.

Experimental Details

Thick film sensors were prepared by applying a suspension (Merck, SnO_2 99 %) on an alumina substrate with interdigital platinum electrodes. Details are described in reference [1]. Sensors were sintered for 7 h, during which the surface temperature was increased steadily up to 550 °C, in synthetic air (50 % R. H.). The sensor element was pretreated sequentially in 100 ppm NO_2, 40 ppm diehtylamine and 100 ppm CO for 5 s at a temperature of 270 °C. Standard solutions used for calibration are listed in Table 1. 1 µl (equivalent to 10 ng) of each standard solution was injected splitless into a GC/MS system (Varian Saturn 2000) with an adapted sensor chamber. System and settings are

described in [3, 4]. Helium was used as carrier gas at a flow rate of 5 ml/min. The effluent flow was split between an ion trap mass spectrometer and a sensor box in proportion of 1 to 4. The sensor chamber (inner volume 2 ml) was maintained at 150 °C and had an additional inlet for humidified synthetic air (66 % R. H., 15 ml/min). Changes in sensor conductance were measured at a constant voltage of 0.5 V. Details have been described in [3, 4].

Test Substances	(ΔG/G)	Test Substances	(ΔG/G)
4-Methyl-2-methoxy-phenol	++	Furfuryl alcohol	++
4(2-Propenyl)-2-methoxyphenol	++	4-Acetyl-2-methoxyphenol	+
4-Methyl-2,6-dimethoxyphenol	++	1,3-Benzenediol	+
1,2-Benzenediol	++	1,3-Benzenediol	+
1,4-Benzenediol	++	Hydroxyacetone	+
Furfuryl alcohol	++	Toluene, Furfural, Acetone	x

Table 1 Standard solutions of tested compounds and relative conductance change (ΔG/G) of the SnO_2 sensor. 10 ng of a substance were dissolved in 100 ml methanol. Signal intensity is classified as ++ strong, + medium, x not significant. Conductance response of strong and medium signals differ by one order of magnitude.

Results

A comparison of chromatograms (column starting temperature 40°C) of spruce wood and beech wood smoke is shown in Fig. 3. The time range corresponds to a column temperature increase from 126 to 186°C. The sample was taken in a room-temperature glass vessel, and enriched by Solid Phase Micro Extraction, SPME, (PDMS PolyDiMethylSiloxane fibre 100 µm, adsorption at 80°C, desorption at 250°C).

In introductary investigations the sensor response to 4-methyl-2,6-dimethoxyphenol was measured at different operation temperatures (165 °C, 220 °C, 270 °C and 330 °C). Highest sensitivity occurs at 270 °C and at 330 °C. This result is in agreement with the results of chromatographic separated wood smoke samples. In wood smoke samples organic compounds with hydroxy groups dominate the sensor signals at these operation temperatures [3, 4]. 270 °C is used for further investigations, as previous studies show higher selectivities to specific groups of compounds at lower operation temperatures [2, 22]. Various metal oxides show at 270 °C higher selectvities than at 430 °C [2, 22],

because of less complete oxidation of the adsorbed species [2]. The SnO_2 sensor operated at 270 °C reacts to compounds with one or two hydroxy groups, while compounds without a hydroxy group do not affect the conductivity (Table 1).

The highest signal values appeared on exposure to molecules with phenolic structures. Methoxylated phenols with para-substituted alkyl and alkenyl groups are more reactive than 4-acetyl-2-methoxyphenol. Benzenediols with hydroxy groups in ortho and para position cause higher signals than the benzenediol with hydroxy groups in meta position.

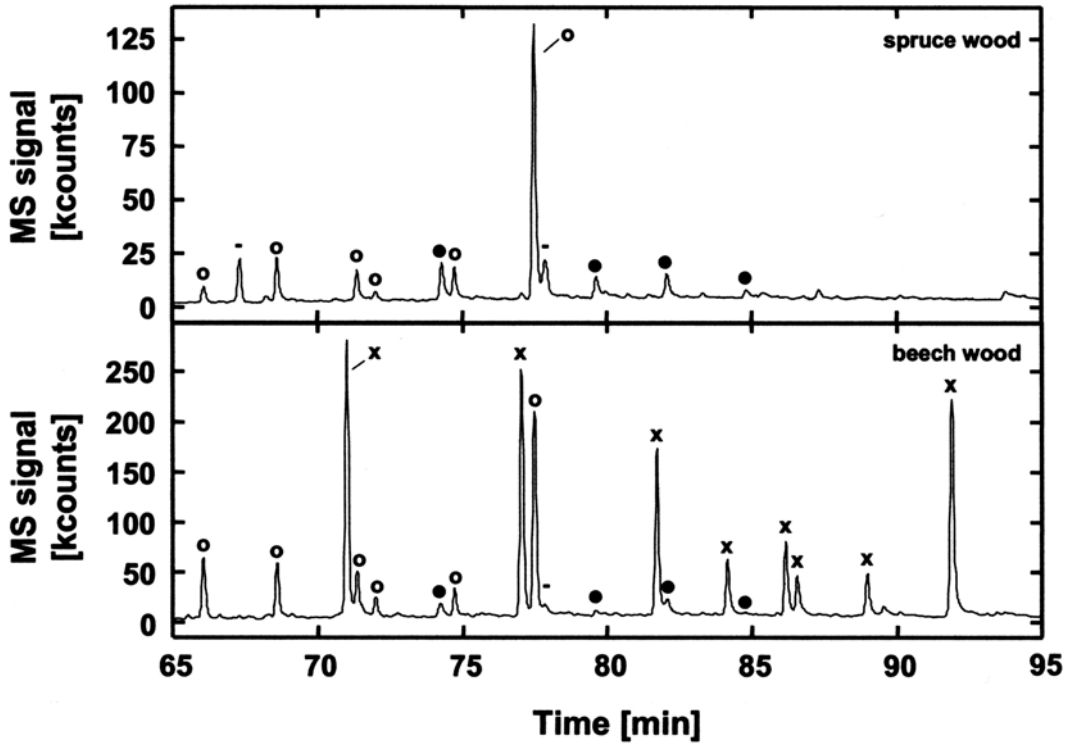

Fig. 3. Comparison of chromatograms of spruce wood and beech wood smoke, in the time range from 65 to 95 minutes corresponding to 126 to 186°C. The sample was taken in a room-temperature glass vessel, SPME enrichment (PDMS fiber, 100 µm, enrichment temperature 80°C). (x) dimethoxyphenols, (o) methoxyphenols (open and filled circles).

A chromatogram of beech wood smoke with parallel detection of sensor and mass spectrometer is shown in Fig. 4. The smoke was sampled by silica gel and extracted by methanol.Compounds to which the SnO_2 sensor react are signed. For spruce wood a chromatogram taken under the same conditions is reproduced in Fig. 5.

Discussion of Reaction Mechanics

Surface reactions of the hydroxy group of ethanol on tin oxide are extensively investigated [10, 11]. Thermal desorption spectroscopy was used to investigate mechanisms under ultra high vacuum conditions [10]. These investigations show a dissociative adsorption of ethanol to an ethoxy group and hydrogen (dehydrogenation) [10]. Adsorbed hydrogen reacts with lattice oxygen to water. In a further dehydrogenation step of the ethoxy group acetaldehyde and adsorbed hydrogen are formed. In effect ethanol is partially oxidized to acetaldehyde. Further oxidation / decomposition steps occur, too. A competing mechanism is the reaction of ethanol to ethene and water (dehydration). The dehydration is not connected with a redox process. Therefore no significant conductance changes are expected. These vacuum investigations involve only lattice oxygen. In air adsorbed oxygen is also present. Therefore additional reaction pathways are likely. Since adsorbed oxygen can be replaced much faster than lattice oxygen the sensor response is presumably due to the adsorption of reducing surface species and to the consumption of lattice oxygen. The created oxygen vacancies (colour centers) act as electron donors.

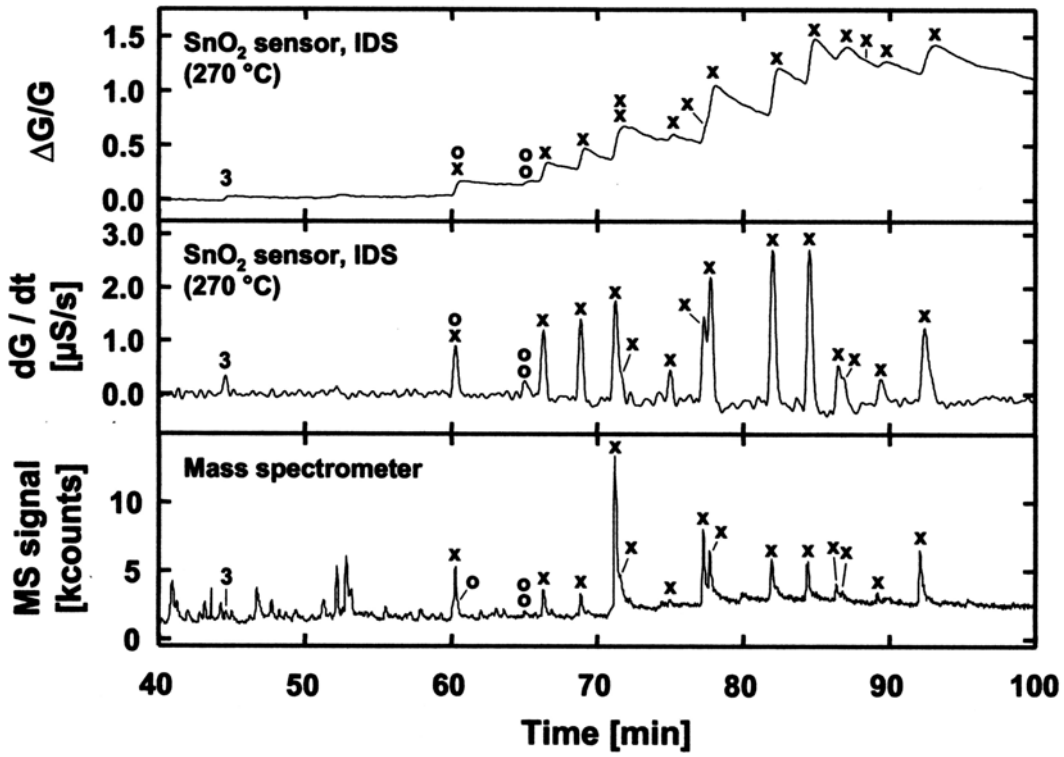

Fig. 4. Beech wood smoke: chromatogram (column start temperature 40°C), sampled by silica gel and extracted by methanol. IDS interdigital strucure. G conductance. MS total ion count of mass spectrometer. Compounds to which the SnO_2 sensor react are signed: (x) methoxyphenols and dimethoxyphenols, (o) dihydroxy benzol, (3) 4-hydroxy-5,6-dihydro-(2H)-Pyran-2-one.

The reaction of ethanol on metal oxide surfaces in air was investigated in reference [11]. There the surfaces of tin oxide sensors were modified by exchange of the metal atom in the uppermost surface layer. The resulting sensitivities to ethanol were correlated with the electronegativity of the exchanged metal atom or with the acid-base-properties of the modified surface. It was shown that metal oxides with a high basicity after an exchange treatment with a low electronegativity metal atom enhance sensitivity by up to an order of magnitude; a high electronegativity metal atom decreases sensitivity by up to an order of magnitude. The sensor response was ascribed to the dehydrogenation mechanism of ethanol, which is favoured on basic metal oxides, while dehydration prevails on acid metal oxides. The high sensitivity of the tin oxide sensor to substances with hydroxy groups indicates that their surface has a sufficiently high basicity for a prevailing dehydrogenation.

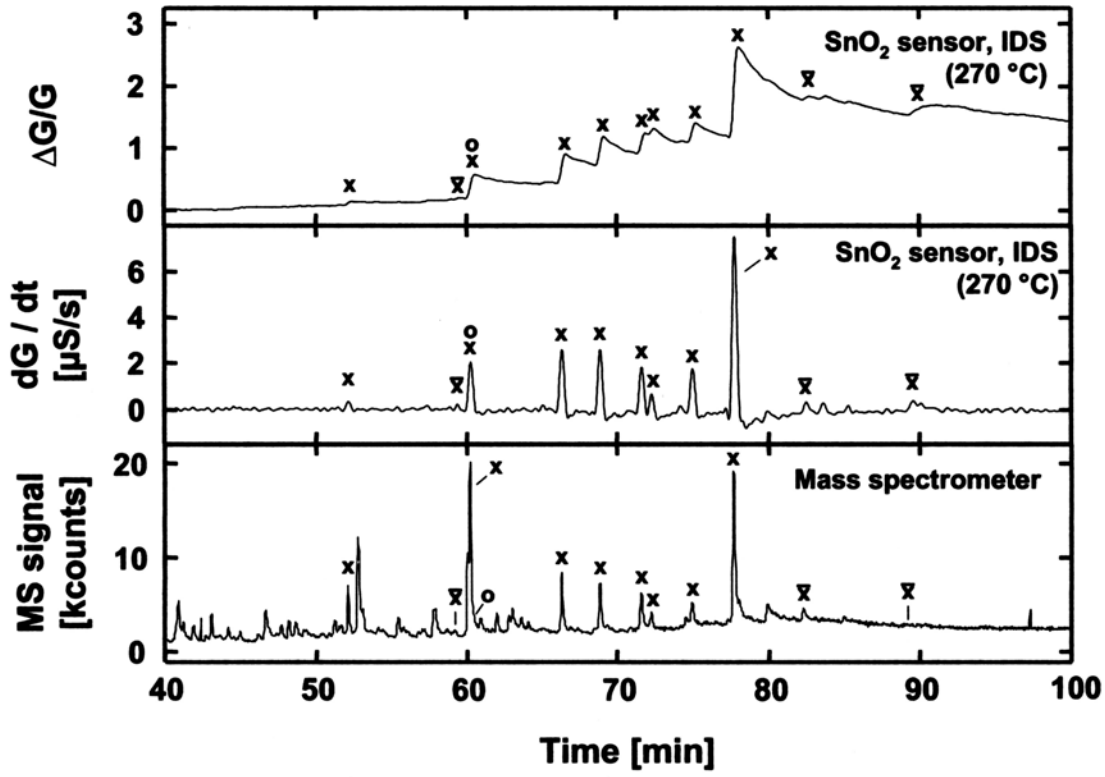

Fig. 5. Spruce wood smoke: chromatogram (column start temperature 40°C), sampled by silica gel and extracted by methanol. Compounds to which the SnO_2 sensor react are signed: (x) methoxyphenols and dimethoxyphenols with hydrocarbon group or other groups. The latter are indicated by a bar on top of the x. (o) dihydroxy benzol.

For basic oxides, a low electronegativity and a low electrophilic character is ascribed to oxygen in the literature [12]. Electronegativity of lattice oxygen is important for surface reactions in which an adsorbed molecule is oxidized by oxygen addition. This occurs, when electrophilic oxygen with high electronegativity attacks the double bond of olefins [10, 12], aldehydes [10] or ketones [10]. On metal oxides with low electronegativity of lattice oxygen these reactions are inhibited [12]. Complete oxidation of organic substances to carbon oxides is less common [12]. This can explain why furfural, acetone and toluene, which are usually oxidized by oxygen addition, do not cause changes in sensor conductivity.

In the literature reactions of tin oxide sensors to toluene [13] and acetone [14] are described. This can be due to a higher operation temperature, which offers more thermal energy for oxidation, or doping with catalytic active metals. In reference [13] it is

reported that sensitivity to toluene could be increased by doping with platinum and palladium.

In reference [15] zinc oxide sensors were modified by exchange of the metal atom in the uppermost surface layer. Sensitivity to acetone and capronaldehyde (n-hexanal) was investigated. Metal oxides with a high basicity produced by an exchange treatment with a low electronegativity metal atom show low sensitivity to acetone. However, oxides with enhanced acidity produced by incorporation of high electronegativity metal atoms into the surface are one order of magnitude more sensititive. For this reaction higher operation temperatures up to 500 °C improve sensitivity. Sensitivities could be correlated with catalytic activity for acetone oxidation.

For surface reactions of phenolic substances on tin oxide a dehydrogenation step is expected as observed for exposure to ethanol. This reaction is guessed as the first step in catalytic decomposition of phenolic species on metal oxides [16, 17]. In some catalytic pathways partial oxidation of 1,2-benzenediol to ortho-quinone or 1,4-benzenediol to para-quinone [17] is involved.

Hydroxy groups are electron-donating substituents on a phenyl ring [18, 19] and increase electron density of the delocalized π-electron system. This is ascribed to a high negative value of the electrophilic substituent constant. Electron-donating substituents are correlated with a high ability to be oxidized.

Easily oxidizable species need a less high activition energy for corresponding surface reactions. For low and intermediate sensor operation temperatures a higher sensor sensitivity to such species is frequently observed. Such effects were shown for Pt-doped ZnO sensors, which are more sensitive to 2-acetyl-pyrrol than to the oxidized species 2-acetyl-1-pyrroline, which needs higher activation energy for further oxidation [20]. So the high sensitivity of the tin oxide sensors to 1,2-benzenediol and 1,4-benzenediols, which are strongly reducing agents, can be explained. For 1,3-benzenediol no corresponding meta-quinone species exist. It is oxidized by decomposition of the ring system. This affords a higher oxidation energy, which may be the reason for the observed lower sensor signal.

Methoxy groups are electron-donating substituents, too. 2-Methoxyphenol derivatives are partially oxidized to corresponding ortho-quinone derivatives. Alkyl-substituents in para-position further increase electron density, while acetyl-substituents decrease it. These facts could explain the high sensor sensitivity to methoxylated phenols with alkyl-substituent and the lower sensitivity to methoxylated phenols with acetyl-substituent. Another explanation for the lower sensitivity to the species with acetyl group could be a different surface reaction with an adsorption by forming a carbonate group. Oxidation reactions of adsorbed carbonate groups are also posssible, but afford higher activation energies [10]. This would explain a lower sensor signal, too.

Conclusion

Sensitivity and selectivity of tin oxide sensors to organic compounds with hydroxy groups are in accordance with a sufficently strong basicity of the sensor surface. Surface modification by addition of metal oxides with stronger basicity is likely to improve selectivity. A corresponding promoting effect of e. g. La_2O_3, CaO and SrO in the uppermost layer of the surface of SnO_2 sensors for ethanol detection was described by Yamazoe et. al. [11]. Corresponding WO_3 and MoO_3 treatment of zinc oxide sensors reduce basicity / enhance acidity and promote sensitivity to acetone [15]. Further improvements in selectivity can presumably be made by varying the base oxide type or by using cycling of the operating temperature [21].

For fire detection the effects of anorganic smoke compounds, which are not separated by the gaschromatographic column used, have to be investigated. Especially for CO and H_2O emissions an increase in sensor conductance is expected, too. First results show that the sensitivity to a corresponding CO concentration is of the same order of magnitude as the sensitivity to the organic compounds with hydroxy groups presented in this study.

For eliminating the effect of CO a system with preconcentrator tubes (adsorption tubes) and a thermal desorption unit makes sense, as CO does not adsorb on common sorbents. Such an instrument has been designed and fabricated by Grate et. al. for the detection of

toxic organophosphorus and organosulfur vapours [23]. This instrument is able to eliminate effects of water vapour [23].

Recently even the identification of various cigarette brands by thick film sensors (Cyranose 320 featuring organic compounds with dispersed carbon and an Airsense EDU preconcentrator containing Tenax TA adsorbent) has been shown. So it seems possible to distinguish between the smoke of smouldering furniture and glowing cigarettes [24].

References

1 T. Hofmann, P. Schieberle, C. Krummel, A. Freiling, J. Bock, L. Heinert and D. Kohl, *Sens. Actuators, B,* 1997, **41**, 81-87.

2 P. Schieberle, T. Hofmann, D. Kohl, C. Krummel, L. Heinert, J. Bock and M. Traxler, in *Flavor Analysis. Development in Isolation and Characterization*, eds. C. J. Mussinan and M. J. Morello, American Chemical Society, Washington DC, 1998, p. 359-374.

3 A. Eberheim, D. Kohl, T. Hofmann and P. Schieberle, in *Proceedings of the 11. ITG/GMA-Fachtagung Sensoren und Mess-Systeme 2002*, Ludwigsburg, Germany, March 11-12, 2002, p. 305-308.

4 A. Eberheim, D. Kohl, T. Hofmann and P. Schieberle, in *Proceedings of the Sensor 2003*, Nuremberg, Germany, May 13-15, 2003, p. 145-150.

5 R. C. Petterson, in *Chemistry of Solid Wood*, ed. R. M. Rowell, American Chemical Society, Washington DC, 1984, p. 57-126.

6 M. D. Guillen and M. L. Ibargoitia, *J. Agric. Food Chem.*, 1996, **44**, 1302-1307.

7 J. Kjällstrand and G. Petersson, *Sci. Total Environ.*, 2001, **227**, 69-75.

8 S. Schütz, B. Weißbecker, U. T. Koch and H. E. Hummel, *Biosens. Bioelectron..*, 1999, **14**, 221-228.

9 R. J. Dillon, C. T. Vennard and A. K. Charnley, *Nature*, 2000, **403**, 851.

10 D. Kohl, Sens. Actuators, 1989, 18, 71-113.

11 N. Yamazoe and N. Miura, in Gas Sensors, ed. G. Sberveglieri, Kluwer Academic Publishers, Dordrecht, 1992, p. 1-42.

12 Y. Moro-oka, Catal. Today, 1998, 45, 3-12.

13 M. C. Horillo, J. Getino, J. Gutierrez, L. Ares, J. I. Robla, C. Garcia and I. Sayago, Sens. Actuators, B, 1997, 43, 193-199.

14 H. Gong, Y. J. Wang, S. C. Teo and L. Huang, Sens. Actuators, B, 1999, 54, 232-235.

15 Y. Anno, T. Maekawa, J. Tamaki, Y. Asano, K. Hayashi, N. Miura and N. Yamazoe, Sens. Actuators, B, 1995, 24-25, 623-627.

16 E. Iglesia, D. G. Barton, J. A. Biscardi, M. J. L. Gines and S. L. Soled, Catal. Today, 1997, 38, 339-360.

17 J. Levec and A. Pintar, Catal. Today, 1995, 24, 51-58.

18 J. Lind, X. Shen, T. E. Eriksen and G. Merenyi, J. Am. Chem. Soc., 1990, 112, 479-482.
19 T. Kajiyama and Y. Ohkatsu, Polym. Degrad. Stab., 2001, 71, 445 452.
20 D. Kohl, L. Heinert, J. Bock, T. Hofmann and P. Schieberle, Thin Solid Films, 2001, 391, 303-307.
21 T. Hofmann, J. Bock, L. Heinert, C.-D. Kohl and P. Schieberle, in Heteratomic Aroma Compounds, eds. G. A. Reineccius, T. A. Reineccius, Oxford University Press, Oxford, 2002, p. 328 344.
22 D. Kohl, L. Heinert, J. Bock, T. Hofmann, P. Schieberle, Sens. Actuators, B, 2000, 70, 43-50.
23 J. W. Grate, S. L. Rose-Pehrsson, M. Klusty, H. Wohltjen, in Proceedings of the symposium on chemical Sensors II (Proceedings (Electrochemical Society), V. 93-7., eds. M. Butler, A. Ricco, N. Yamazoe, Electrochemical Society Inc., 1993, p. 597-608.
24 D. Luo, H. G. Hosseini, J. R. Stewart, Sens. Actuators, 2004, B99, 253-257.

A. Walte, W. Münchmeyer
Airsense Analytics, Schwerin, Germany
R. Vater, T. Dudeck
WIS Engineering, Wismar, Germany

as Sensor Arrays for Detection of ases and Smoldering Fires

Abstract

Gas sensor arrays, also known as electronic noses, are instruments used to recognize complex mixtures of organic vapors or to detect variations in the mixtures. Special versions of the sensor arrays can be used to detect smoldering fires in order to provide an alarm before the fire starts spreading. This paper describes results of different test fires from different materials, measured over a period of 2 years. The materials and conditions were selected in order to meet the most probable conditions found in passenger cabins of cruise ships. Sensor arrays based on metal oxides can be used as detectors for hazardous situations in passenger cabins. Compared to classical fire detectors the systems react much faster and offer the capability to distinguish between different hazardous situations.

Introduction

Especially in cruise ships there is a demand for fast and reliable detection of hazardous situations such as smoldering fires. The effective detection of a hazardous situation at an early stage reduces the risk for a major harm or even fatal situations. The company WIS Engineering GmbH (WIS), as a manufacturer of ship cabins and supplier for shipbuilders, started a research project together with wma Airsense Analysentechnik GmbH (Airsense) and the Institut für Sicherheitstechnik/Schiffssicherheit e.V. (ISV) in order to develop a system for the detection of hazardous situations. A ship cabin was manufactured by WIS and installed in the fire test laboratory of ISV. The sensor array system developed by Airsense was tested over a period of 2 years and was finally installed in a cruise ship for a further evaluation.

Methods

Classical fire detectors measure the attenuation of light, the attenuation of radiation or the increase of temperature. The most common “low cost” detectors measure the attenuation of light, which is scattered due to the smoke particles in air. Some detectors use the combination of different effects, e.g. scattering and temperature increase, in order to improve their performance. The drawback of the classical detectors is that they detect the fire when it is already existing, which means that it is then normally too late.

An array of gas sensors, also know as electronic nose, can detect the gases released during overheating of materials (e.g. cables, textiles, etc.) before the fire starts. The sensor array can also detect hazardous situations due to high concentrations of flammable gases or liquids. The critical or non-normal situation can be detected much earlier.

An electronic nose usually consist of an array of simple sensors such as metal oxide semiconductors (MOS), combined with the required electronics and chemometrical software.

A first evaluation period was conducted over a period of 12 months using a sensor array system consisting of 10 different metal oxide sensors positioned into a small chamber (vol=1.8ml). The sensing system was based on the commercially available PEN-2 from Airsense (www.airsense.com). It has individual heater circuits for each sensor and a microprocessor unit for control and communication. An active sampling device is integrated in the system.

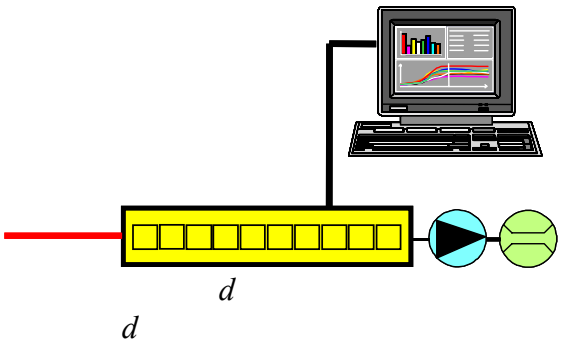

Fig 1 shows the gas flow diagram of the small sensor array system. A picture of the system is displayed in **Fig** .

With an internal pump the gaseous compounds are sucked through the sensor array. The flow is kept constant by using a gas flow sensor and adjusting the voltage of the pump. This sensor array was used to select the most suitable metal oxide sensors and to develop the method for the analysis of the cabin air. After the first testing period a smaller dedicated sensor array system was constructed and tested with the same procedures described later. **Fig** shows the "low cost" system developed during the project. The new sensor array has an array of 5 sensors and does not use an internal pump for sampling.

Fig shows the test cabin where most of the experiments took place. A smoke generator was used for visualization of the gas flow in the cabin. The cabin was constructed according to the actual dimensions installed at cruise ships. It consists of a living room with a surface of ca. 9m and a bathroom of ca. 1,7m . The cabin air was exchanged with a ventilation system designed to meet the actual condition found in ocean cruisers.

d *d*
d

Material from real cabins was set on fire and also all kind of probable gas emission sources were used for testing. The fires were burned as open fires and as smoldering fires. The tests were carried out with and without ventilation. Every test was repeated at least for three times. During the investigation also classical optical smoke detectors with passive and active sampling were used parallel to the gas sensor array system. After the first testing periods at the fire laboratory of ISV, the alarming system was also installed in an ocean cruiser for evaluation purposes. A lounge with a bar used exclusively by crew

members was used for the evaluation period. In order to correlate the sensor signals with the events also the video signals from a small web-cam were coupled to the data acquisition system.

Results

Different materials were heated until starting of fire at the fire test laboratory of ISV. Details of the facilities and the setup of the fire test laboratory can be found in an other publication presented at this conference (R. Rothe, "Detection reliability of different fire detector principles- results from investigations of the fire hazards under real conditions in cabins aboard seagoing vessels").

All relevant materials found in passenger cabins of cruisers were used. Among the burnt materials were textiles, carpets, wood, plastics and paper. Possible disturbances due to sprays, perfumes, solvents and cigarette smoke were also measured. **Table 1** shows the list of compounds used for the experiments.

d

Burnt Material	Disturbing Compounds
flooring, carpet	detergents
dust bin filled with paper	water vapor
furniture (wood based)	deodorant spray/ hair spray
curtains and wallpaper	cigarette- / cigar- / pipe-smoke
textiles for furniture	
electrical cable	
electrical installation material	
fire accelerant	

Every material used as solid fuel was heated with heating surfaces in order to measure the released compounds. In some cases an open fire started. Only the electrical cable was heated directly using a high power supply used for welding. In a next experiment the materials were also exposed to a smoldering cigarette. The materials were also inflamed by using fire accelerants. Each experiment was repeated three times and all relevant data was recorded.

During the first series of experiments the measurements were done in a ventilated and a non-ventilated cabin. **Fig** shows the sensor signals during the starting period of a

smoldering fire. **Fig** shows the sensor signals under the same conditions, but without the cabin ventilation. It can be seen, that the dynamic signal of the sensors strongly depends on the ventilation of the cabin.

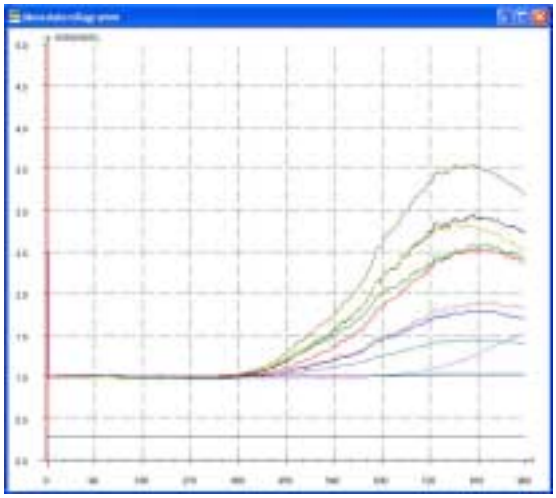

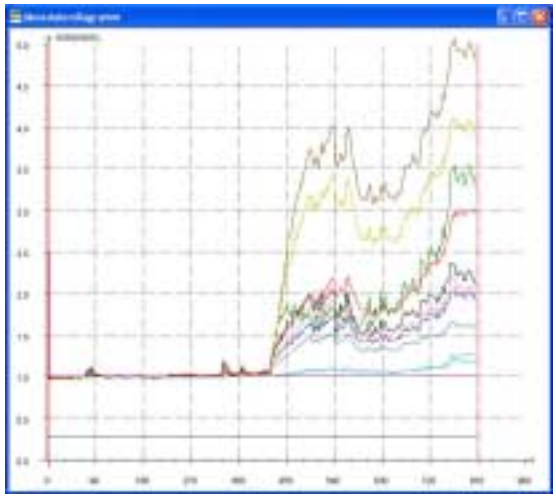

d

d

d

d

d

The data of the sensor signals was used in order to identify characteristic signals and the corresponding sensors. Data reduction techniques, such as principal component analysis (PCA) can be used to visualize the differences between the data sets. The data reduction extracts the most important information from the database, reducing the ten dimensional information (10 sensors) into two dimensions. The result can be displayed in a two dimensional view (see **Fig**).

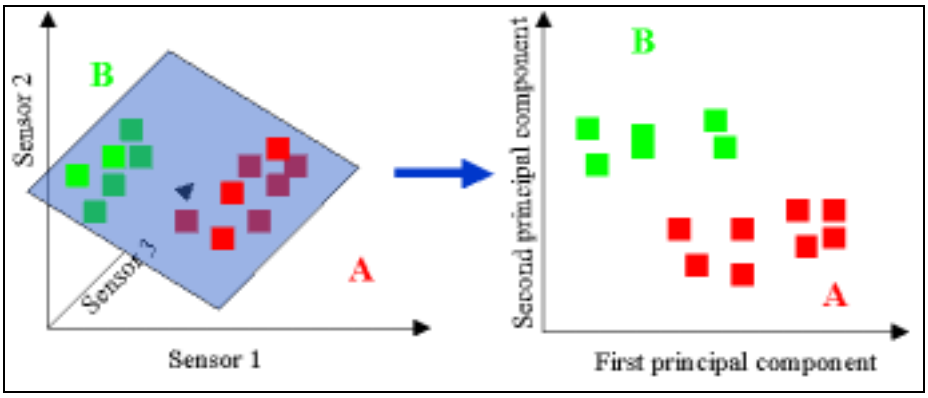

d *d*

If there is no significant difference between similar samples the transformed results will be located close to each other after transformation. Hence, the graphical output can be used for determining the difference between groups and comparing this difference to the distribution of pattern within one group.

The PCA always searches for the view of maximum distribution of all trained data points. It does not care about the relation of a data points to the specified classes. Training points of the same class are usually displayed in the same color.

The legends for the x- and y- axes contain the value of the variance achieved by the PCA transformation. A high value means that in the direction of that axis a major part of possible distribution has been found. There is no relevant information in the scaling of the x- or y-axes calculated by the PCA analysis. A result of a PCA transformation has no units.

Fig shows the PCA of all the measurements taken after a defined threshold value of the sensors. It can be seen that a smoldering fire situation (smoldering fire of carpet, furniture, textiles, paper, wood) can be differentiated from a non fire situation (ethanol, hair spray, deodorant spray). The clean spirit stove fire (fire accelerant) was not classified as a smoldering fire, possible due to the intensive vapor concentration of the spirit in the air.

The composition of the gases released during a smoldering cable is different than the gases from smoldering wood or paper. The pattern of the smoldering cable is located at the border of the “smoldering fire” group, because the furniture and some textiles had also plastic material inside. An actual problem is the smoldering tobacco pattern, which is displayed in the smoldering fire group. All the gaseous compounds in the air are considered to belong to a non standard situation (see normal air pattern).

When filtering the raw sensor data and omitting erroneous sensor peaks a better classification is possible. **Fig** shows the PCA of the same data after data filtering.

It is also interesting that the system is also capable to distinguish between the smoldering fire and the open fire situation. **Fig 10** shows the sensor signals from the transition of a smoldering fire into an open fire. **Fig 11** displays the corresponding PCA analysis with the open fire situation included in the pattern.

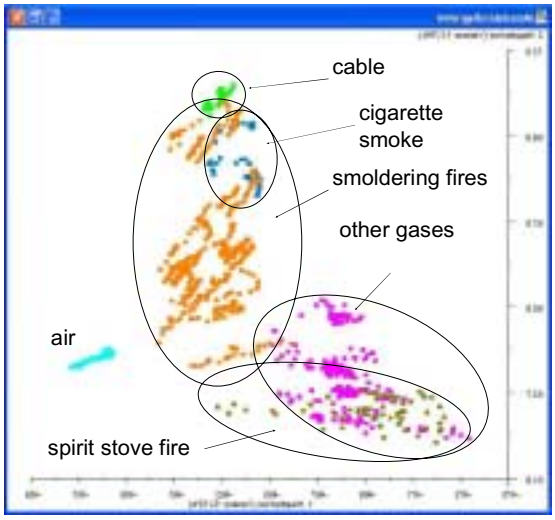

d

d

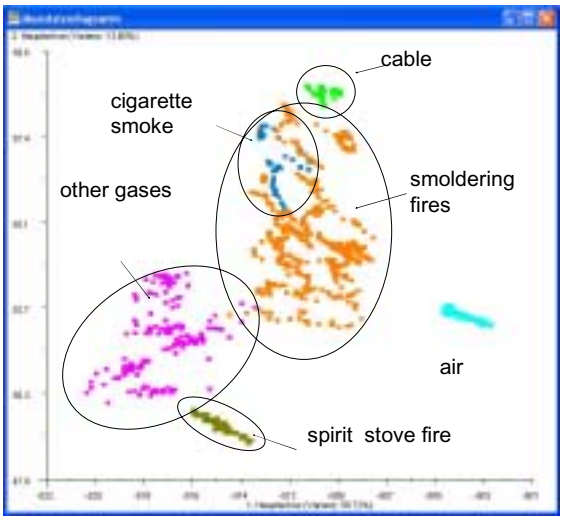

d

d *d*

d *d* *d*

With the data it was possible to reduce the numbers of sensors from 10 to 5. At the same time the optimal position of the gas sensor array was determined. Due to the fact that the cabins are ventilated and that a supervision of all the regions of the cabins is needed, the sensor array was positioned in the air outlet duct which is located in the bathroom. **Fig 1** displays the results obtained with the new sensor array.

The resolution of the new sensor array system is nearly the same as the standard sensor array. The intensity of the sensor signals is less due to the fact that the gases released during the smoldering fire are more diluted. Also the response of the sensors is delayed by 30 to 60 seconds because the gases have to be transported from the “living room” of the cabin, where the test fires took place, into the bathroom. Water vapor from the shower does not lead to a false alarm with the gas sensor array based on metal oxide sensors.

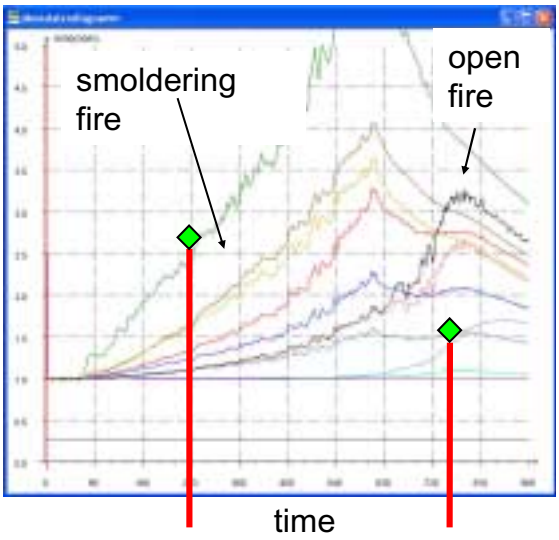
smoldering
fire
open
fire
time

d

d

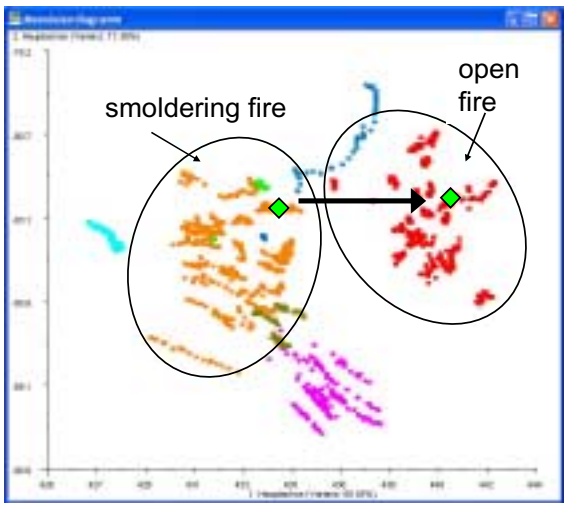
smoldering fire
open
fire

d

d

d

d

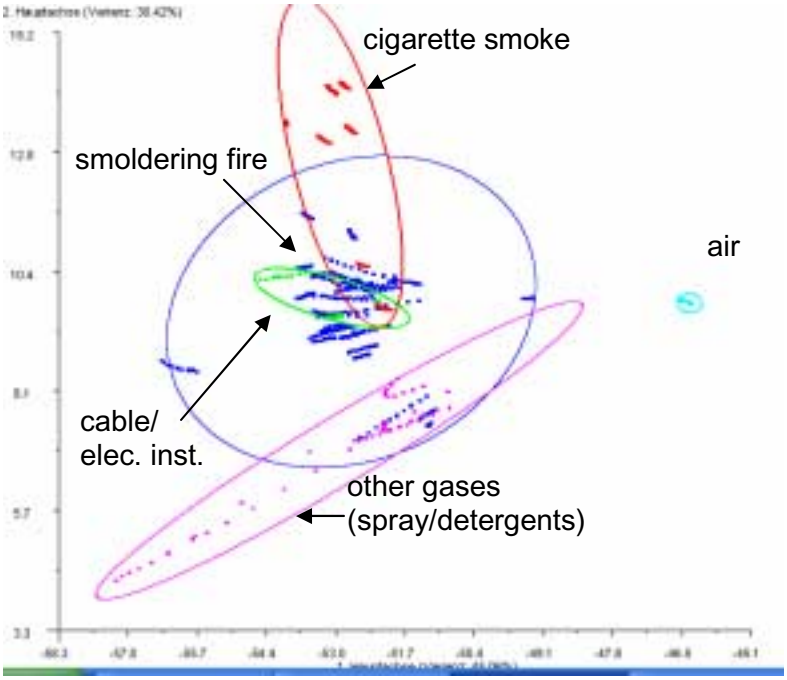
cigarette smoke
smoldering fire
air
cable/
elec. inst.
other gases
(spray/detergents)

d

Fig.12 shows the pattern “smoldering fire”, consisting of all smoldering fires, also the fires started with a fire accelerant. The group “cigarette smoke” consists of the pattern from cigarette, cigar and pipe smoke. The group “other gases” consists of the results obtained form measurements with solvents, detergents, sprays and gasoline. The pattern in fig.12 shows that there is an overlap between the cigarette smoke and the smoldering fire. This is because the composition of the gases released during smoking is very similar to the smoldering fires of paper and furniture (wood). There is also an overlap of some compounds of the group “other gases” with the “smoldering fire area”. The reason is that some of the fires were started with a fire accelerant (solvent). During the start the measurement file starts in the region “other gases”, because the gases consists mainly of the solvent vapors, and then moves into the region “smoldering fires”.

d

The response of the developed sensor array was compared to the response of the newest generation of “classical” fire detectors. The response time of all sensors was in the time range of 2,5 to 25 min. Open fires were detected with all detectors much faster than smoldering fires. The sensor arrays reacted much faster than the classical fire detectors, especially in the case of slowly developing smoldering fires. The sensor array system always reacted to hazardous situations and was capable to distinguish between smoldering fires, open fires and other gases. A reliable differentiation of smoldering fires and tobacco smoke was not possible with the actual sensor array configuration. The detection system was installed for “real situation” evaluation purposes in a lounge with a bar used exclusively by crew members from an ocean cruiser (AIDA, see **Fig 1**). In a period of two months over 5000 data files were generated. An alarm with an identification of a smoldering fire / tobacco smoke was generated in 12 occasions.

Conclusions

Gas sensor arrays based on metal oxide sensors can be used to detect hazardous situations in passenger cabins of cruisers. The reaction time of the developed sensor

array was much shorter than the reaction time of the classical fire detectors, especially for slowly developing smoldering fires. A false alarm due to water vapor was not observed with the sensor array, but false alarms due to tobacco smoke were observed. The gas sensor arrays also offer the possibility to identify the source of the hazardous situation. A combination of a detector for hazardous situations, based on metal oxide sensors, with a “classical” optical fire detector should be an ideal combination for improving safety in ocean vessels.

J. Goschnick [+], U. Stahl [*], D. Brein [°], P. Basmer [°]

[+] IFIA, Forschungszentrum Karlsruhe, Karlsruhe, Germany
[*] MMTWD, Bruchsal, Germany
[°] FFB, Universität Karlsruhe (TH), Karlsruhe, Germany

Fire Gas Characterization with the Electronic Nose KAMINA

Abstract

Measurements of the model gases acrolein, benzene, ammonia and CO were carried out to determine the analytical performance of the KAMINA chip (KAMINA = Karlsruher Micronose). The unique KAMINA gradient microarray exhibited detection limits at or below 1 ppm for 250 – 300 °C as min. and max. temperature of the temperature gradient. Data from model fires were recorded in order to develop a fire classification with a soot filter applied to protect the microarray from particles and aerosols. Materials like wood, cloth or polymers were burned. A multi-step signal pattern analysis was developed to allow a detailed classification of the burning material. The results of this study show that the KAMINA employed as a mobile fire gas screening device is capable of characterizing the burning material on site and detecting the spreading of the fire gases. Hence, although the complexity of the fire gas ensemble can not be broken down into individual gases by the KAMINA system, the signal patterns provide a fingerprint of the fire gas ensemble which allows to characterize the burning material, assess the progression state of the fire and quantify the concentration of the fire gas as an entity.

Introduction

In order to adapt fire-fighting strategies and security measures for protecting firemen as well as inhabitants in the vicinity which might be exposed to fire effluents, quick information on the fire itself and the released gas ensemble are essential. In a feasibility study the application potential of the Karlsruhe Electronic Nose (KAMINA) with its unique gradient microarray was examined for fast characterization of fire gases.

An electronic nose detects a gas ensemble (a mixture of different gases) as an entity with an integral concentration. However, similar to the human odor perception the integral can be quantitatively divided into a few components which themselves may be

complex mixtures. Due to the measuring principle [1] all fire gases except CO_2 can be sensitively detected in the atmosphere. Therefore the "odor" determined by the electronic nose should be understood as the fire gas ensemble no matter whether the human nose can smell the components or not.

The KAMINA is an electronic nose system originally developed for gas analytical applications in consumer products, for instance ventilation flap control in automobiles or surveillance of cooking and baking or indoor air monitoring. Concept and technical outfit of the KAMINA do not only take analytical demands into account but also aim at low costs, minimum spatial requirements, low power consumption and low weight which are mandatory for the equipment of mass products [2]. This also makes the KAMINA an attractive tool for real-time monitoring tasks.

Detection principle

The principle of detecting gaseous atmospheric components using conductivity measurements at n-semi-conducting metal oxides layers has been well-known for some decades now [1]. If a metal oxide surface at an elevated temperature of some hundred degrees Celsius is exposed to gas components other than the main components of the atmosphere, adsorption and maybe even catalytic reactions take place with higly reactive oxygen-species on the surface of the metal oxide (Fig 1.). As a result the density of mobile electrons is changed, directly affecting the conductivity of the semiconducting metal-oxide layer: oxygen consuming reactions with e.g. hydrocarbons increase, adsorption, NO_2 or ozone decrease conductivity. This change of conductivity is related to the concentration of the reacting gas species by a power law. If the metal oxide is exposed to clean air again after such a gas exposure, the conductivity of the layer is recovered to the typical value for unpolluted air. Thus, the metal oxide surface reacts reversibly. Surface reaction or only adsorption mechanisms allow nearly all gases to be detected, except rare gases and other inert gases, such as nitrogen. However, the sensor elements of the KAMINA carry a gas permeable coating on top of the metal oxide which makes the gas access to the sensitive layer dependent on the size and chemistry of the gas molecules.

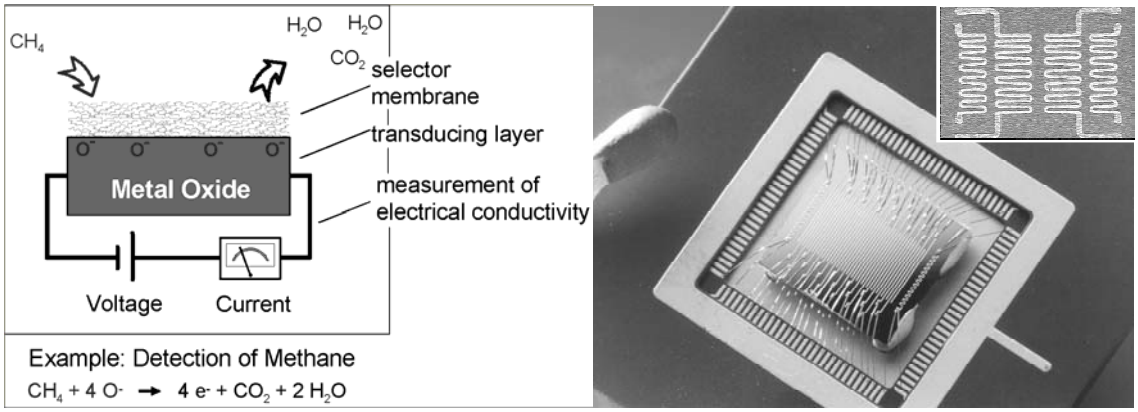

Fig.1.: *Gas detection principle of metal oxide conductivity sensors (left). The KAMINA sensor segments consist of a metal oxide layer of about 100 nm thickness which is buried underneath a gas-permeable SiO_2 or Al_2O_3 coating of a few µm. The detection of methane is shown as an example. On the right a 38 segment KAMINA chip is shown.*

Gas Sensor Microarray

To detect a single gas component out of a gas ensemble, a single-sensor system has to be extremely sensitive to this specific gas component only. However, such ideally selective sensors are not found in real life. Another approach using metal-oxide based sensors is to build an array of sensors with different selectivities to create gas characteristic signal patterns which can be used to distinguish between gas ensembles or single gases the sensor array is exposed to. Contrary to conventional macroarrays built of several individual sensors, the microarray developed at the Forschungszentrum Karlsruhe consists of a single monolithic metal oxide film. This film is divided into 38 sensor segments by parallel electrode strips to measure the electrical conductivity of the individual segments (see fig.1). Heating of the microarray is realized by four heating meanders at the reverse side of the chip. The difference in selectivity of the single elements is achieved by a gradient technique. Applying a temperature gradient as well as a permeable SiO_2-membrane coating of varying thickness yields sensor segments with different sensitivity spectra. Therefore, the sensor segments deliver conductivity patterns. The latter depend on type and quantity of ambient gases and allow gas discrimination and quantification.

Due to its uncomplicated and inexpensive microfabrication, this gradient microarray can be applied to realize a small and low cost electronic nose.

Experimental

In the first stage of the study, a SnO_2-based microarray chip was exposed to different target gases, chosen as model fire gas components - namely benzene, acrolein, NH_3 and CO in synthetic air at 60% r.h. with concentrations in the range of 1 – 300 ppm to examine the analytical properties of a typical KAMINA gas sensor microarray. To determine the best operating conditions, the pulse exposures with the test gases were performed in three different adjacent temperature ranges with a temperature difference of 50 °C across the array.

The concentrations were set by a computer-controlled gas mixing system, producing defined pulses of test gases alternating with clean air at 60% r.h.

The ability for gas discrimination was tested using pattern recognition algorithms such as Primary Component Analysis (PCA) and Linear Discrimination Analysis (LDA) [3]. The LDA plots are optimal 2-dim. Projections of the signal patterns originally being data points in a space of 39 dimensions corresponding to the 38 sensor elements of the microarray.

Prior to studies of the microarray chip in practical tests, a filter was developed to protect the microarray against smoke particles (s. Fig. 2).

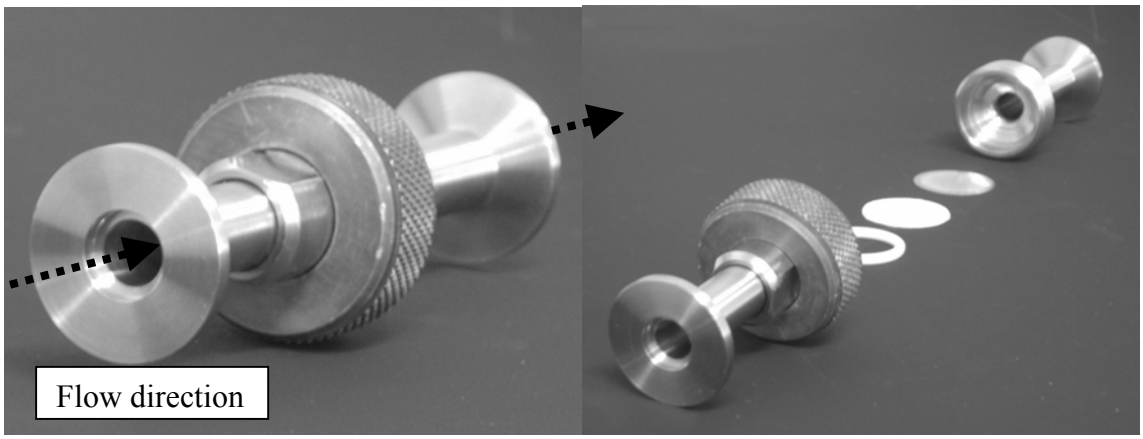

Fig 2.: *Photograph of the particle filter. Left: assembled filter. Right: disassembled filter showing parts (gasket, filter disc, sustaining grating).*

For optimal retention results a filter module using filter discs (Munktell, Type 227, 75g/m²) was found to protect the KAMINA without affecting the detection of fire gases. For practical tests several materials such as polymers, wood and cloth, etc. were burnt or pyrolysed in a furnace and the released gas ensembles was examined using the KAMINA and conventional analytical methods (e.g. FTIR, GC-MS) for comparison. The resulting data were investigated with LDA to evaluate the gas discrimination power of the microarray.

Results and Discussion

In Fig. 3 the target gas detection limits are shown with three different temperature ranges applied. As depicted, detection limits of 1ppm or below can readily be achieved. Furthermore, when applying a temperature difference of 250 to 300 °C across the array, the best detection limits are obtained. Measurements of acrolein revealed a detection limit of even below 10 ppb.

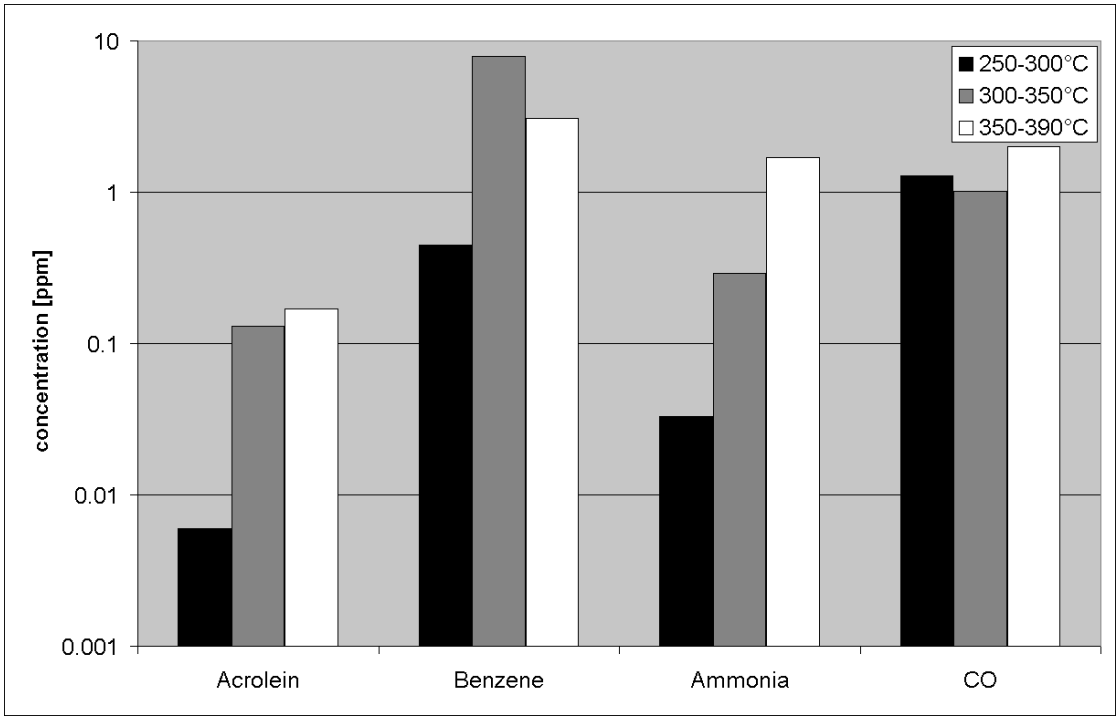

Fig. 3: *Detection limits of measured target gases for different temperature ranges applied to the microarray.*

The signal patterns obtained were analyzed by LDA to be able to distinguish all of the selected model gases (s. Fig. 4).

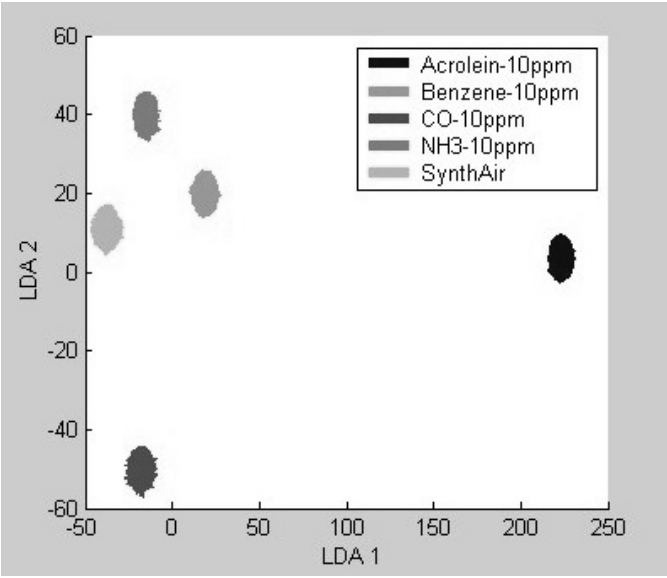

Fig. 4: *LDA-plot of signal patterns of the selected model gases at a concentration of 10 ppm. All selected gases can be safely distinguished from each other and from synthetic air used for purging.*

Practical tests

In order to examine application alternatives for an electronic nose of the KAMINA type practical tests with real fires and with pyrolytic processes were made in continuation of earlier experiments [4]. The ability to distinguish the quality of different fire gas ensembles, as well as to detect a specific gas in the mixture of fire gases were investigated. To evaluate the discriminative power of the microarray, different burning materials were used. Regarding the pyrolytic szenarios, attention was preferably paid to the heating phase of different materials used in households in order to test how far a determination of emitted characteristic gases is possible before the material starts to burn [5].

As reference analysis, online IR-spectrometry and GC-MS (offline, using sorption-devices) were used. Unfortunately, in many cases the IR-Spectrometer was found to be too insensitive to verify the low concentration gases to which the more sensitive KAMINA reacts.

In Fig. 5, a two step LDA of the pyrolytic experiments is depicted showing the analytical potential of the KAMINA microarray. At the first stage of signal pattern

analysis, a rough classification is made of the type of burning materials, which is specified in more detail in the second stage of the signal pattern analysis.

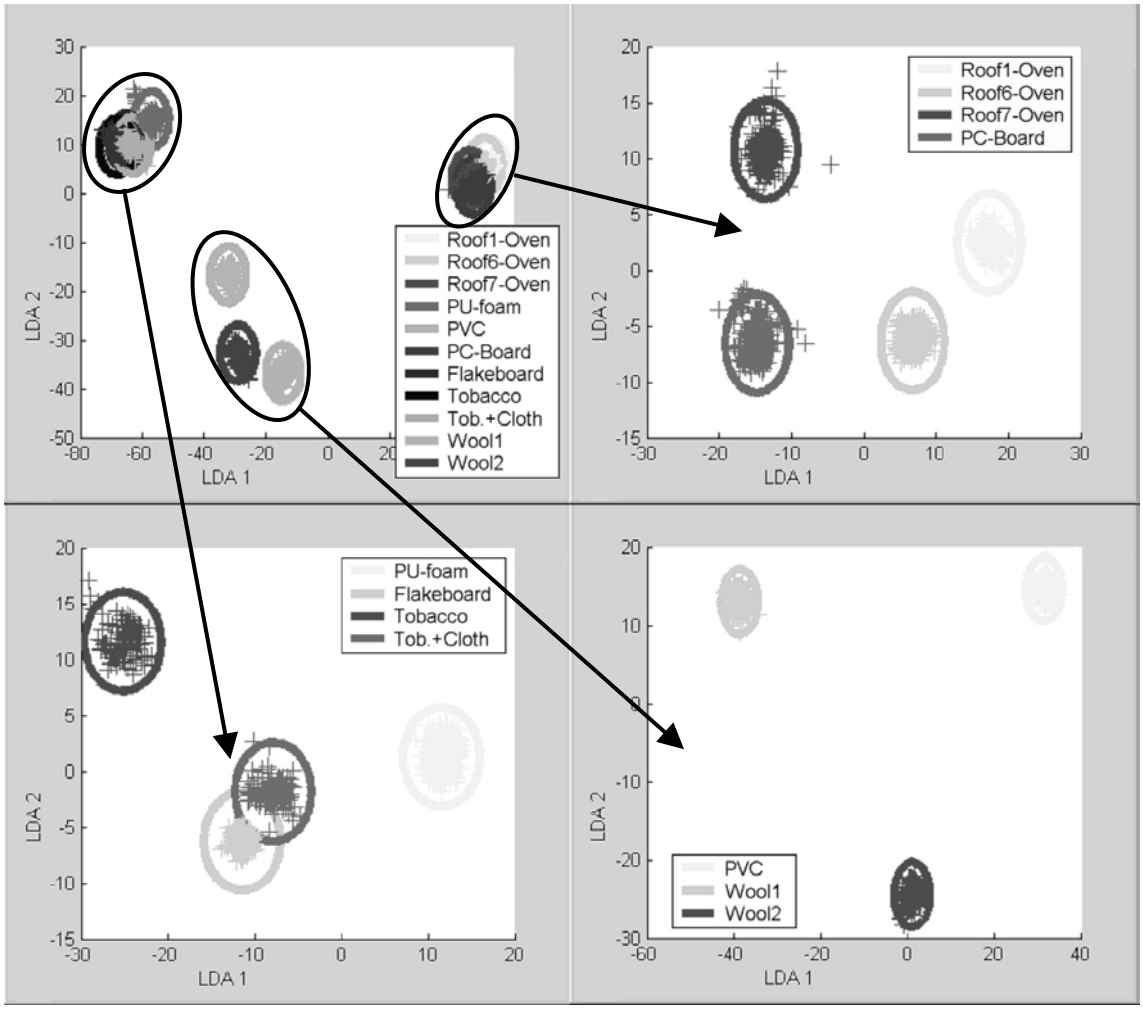

Fig. 5: *Illustration of the classification steps of pyrolising materials by a 2 step LDA. At first all possible burning materials are grouped to classes (upper left plot). Some of the classes show very similar signal patterns and therefore 3 main classes are formed (marked by ellipses) which exhibit high distinctiveness. The second step specifies the burning materials in a sub-class assignment process shown in 3 other LDA plots.*

The upper left LDA shows all classes of examined materials: bituminous roofing felt, wool, tobacco, polyurethane, PVC and wood (flake board). It can be clearly seen, that some of the classes are near by each other and seem to be grouped. Therefore, three main classes can be defined, which are marked by ellipses in the overall LDA. So in case of a fire analysis, the measured signal pattern will be assigned to one of the three

main classes if it fits in one of the ellipses. If not it will be classified as one of the unknown type. If an assignment to one of the main classes can be made, a second LDA is employed to further distinguish the burning material. Thus, in a second step LDA works as a sort of “magnification glass” to reinforce the recognition process of the KAMINA and improve the classification of the burning material of the first step analysis.

Another interesting question was the progression of the gas composition due to the deterioration of the burning materials in time. For that purpose polyurethane-foam was set on fire and the emitted gas ensemble was analysed over time.

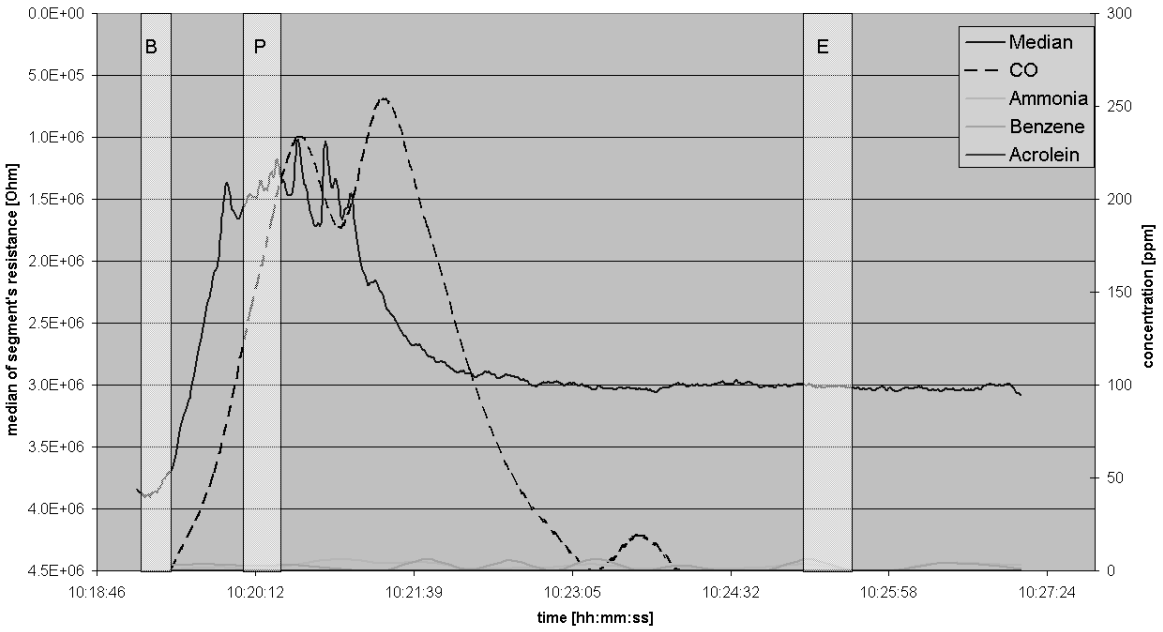

Fig. 6: *Combined diagram of the FT-IR analysis and the median of the KAMINA during the burning of polyurethane foam. CO is the major component released. Both concentration changes can be correlated to each other: a rise in the CO concentration of the FT-IR results in a fall of the microarray’s median resistance.*

As shown in a combined diagram of key gas concentrations determined by FT-IR and via the resistance median of the KAMINA microarray in Fig. 6., the changes in the gas concentration measured with the FT-IR were sensitively reflected in corresponding changes of the KAMINA signal medians. As a major compound CO was detected by the FT-IR. At the beginning of the experiment the concentration slowly rises, having an increasing effect on the median signal of the microarray. The peak and the falling

concentration of CO are also found when looking at the median signal of the KAMINA. The delay of the FT-IR signal may be due to differences of the fluidic setup of the two analytical techniques.

A LDA diagram of the microarray signal patterns versus time shows the possibility of visualizing the progress of material changes and gas emission during PU-foam burning (s. Fig.7). The variation of the composition of emitted gases in time is reflected in corresponding changes of the microarray signal patterns.

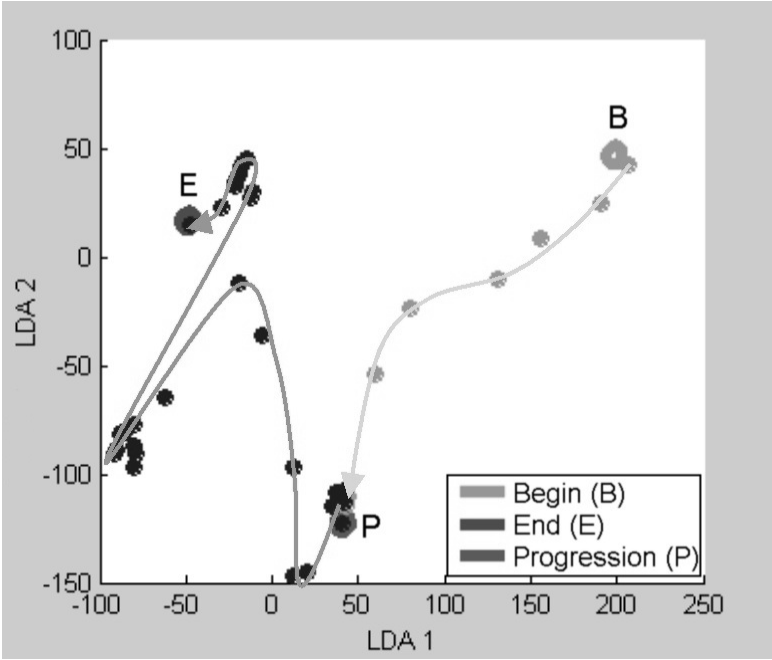

Fig. 7: *LDA diagram showing the changes of the signal patterns of the microarry during spreading of the fire. Three classes B, P, E and their transitions are shown. The arrows indicate the time response.*

These changes are shown in a LDA diagram which was defined using 3 classes B, P and E. B stands for “beginning” and represents the signal pattern measured before the outbreak of the fire. Class E comprises signal patterns obtained at the end of the burning process where the residual material only slightly glows. P is a class of signal patterns that belong to an intermediate burning state. For clarity, only a few data points between the classes are shown. The LDA diagram shows that in addition to the material specificity, the obtained signal patterns contain the information on the progression state of the burning material.

Dissemination of fire gases:

The release of fire gases similar to those of real urban fires was simulated by setting a fire with a pile of wood underneath a roof construction. The roof acting as a thermal barrier could be examined in this kind of experiment. To measure the vertical spreading of fire gases, both the KAMINA and a FT-IR instrument were continuously used at different heights during the model fire - using a remote-controlled crane to analyse gas components and determine some concentrations in the fire gas ensemble on-line. The variation of the sampling height was performed stepwise, not in a continuously uprising or declining, but in a statistical order (s. Fig.8).

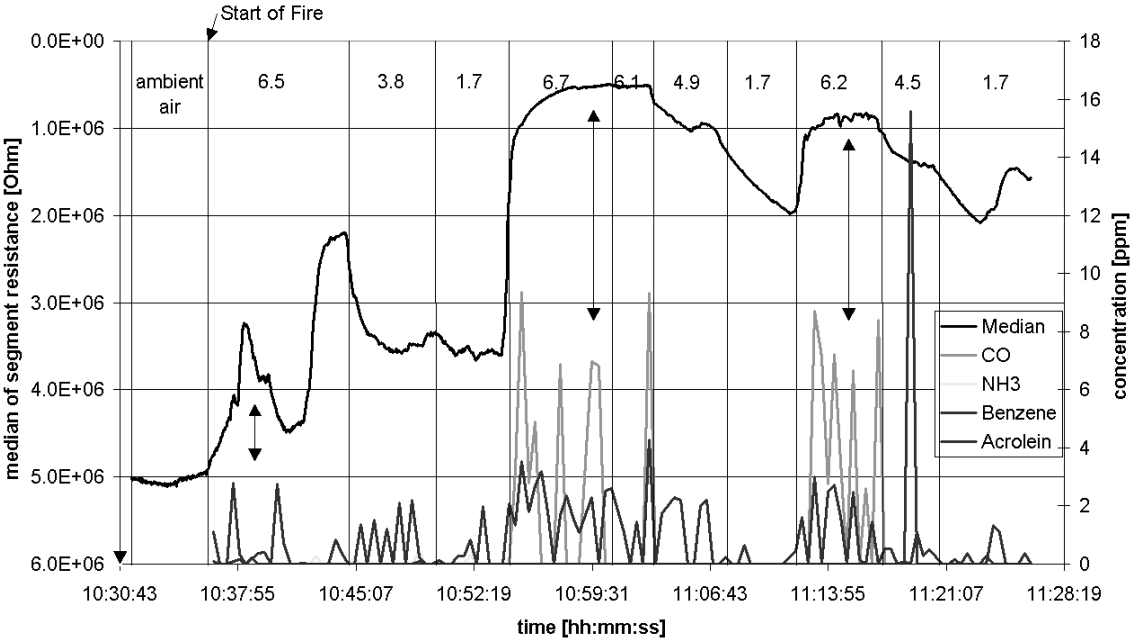

Fig. 8: *Combined diagram of FT-IR (right scale) and KAMINA (left scale) data showing fire gas concentrations in varying altitudes during the controlled fire experiment. The sampling distance from the ground and the changes in sampling altitude are given in meters at the upper edge of the diagram.*

First of all, the results show that while the FT-IR instrument was working at its detection limits, the KAMINA still offered strong gas response to clearly show differences between the signal patterns´ medians. The major component of the fire gas, CO, was well detected by both analytical instruments. Starting by sampling at a high altitude of 6.5 m, no CO and minimal concentrations of benzene is detected by the FT-

IR instrument, while the KAMINA obviously reacts to other released gas components of the fire gas ensemble. When lowering the sampling altitude, the microarray´s median resistance of the sensor segments rises (the air at 3.5 m height is cleaner), whereas it decreases again when sampling is carried out on the initial level. The data obtained at different altitudes of sampling reflect the rising concentrations of the fire gases and smoke compounds especially at elevated heights in the test hall. Indeed the testing facility was filled with smog during the experiment beginning at the roof successively comprising more and more lower air layers and finally reaching the ground.
Due to its broad detectability of gases, the high gas sensitivity and quick response times, the KAMINA microarray can be considered a powerful screening tool for quickly determining the spreading of hazardous fire gases or a valuable aid to find smouldering nests after the open fire has already extinguished.

References

[1] Madou, M. J. and Morrison, S. R., Chemical sensing with solid state devices. Academic Press, Inc. (London) Ltd., 1989

[2] J. Goschnick; An Electronic Nose for Intelligent Consumer Products Based on a Gas Analytical Gradient Microarray, Microelectronic Engineering, 57-58, 2001, pp. 693-704

[3] P.C.Jurs, G.A Bakken and H.E.McClelland; Computational Methods for the Analysis of Chemical Sensor Array Data from Volatile Analytes, Chem. Rev. 2000, 100, 2649-2678

[4] M. Harms, J. Goschnick , R. C. Young; Early Detection and Distinction of Fire Gases with a Gas Sensor Microarray, AUBE '01 : 12th Internat.Conf.on Automatic Fire Detection, Gaithersburg, Md., March 25-28, 2001, Proc. pp. 416-31

[5] R. C. Young, B. R. Linnell, W. J. Buttner, B. Mersqhelte; Evaluation of Electronic Nose for Space Program Applications, Presented at JANNAF Conference, Charlottesville, VA, United States, 25-27 March 2003.

Wang wenqing, Li jian, Yu guangzhi

Shenyang Fire Research Institute of Ministry of Public Security, Shenyang, P.R. China

Li dong

Shenzhen Fuan Security Systems Co. Ltd, Shenzhen, P.R. China

The design and analysis of optimizing model of dual bands IR beam gas detection system

Abstract

It is necessary for a high sensitivity combustible gas detection system, which is used in a open atmosphere circumstance, to eliminate all of the influence caused by random fluctuation of weather and component condition of air. The basic principle and the calibration method of the system are discussed in AUBE'99. In this paper, three principles of how to select the two IR bands and the design guidance policy for realizing the system are presented. Furthermore, a model and its modulating method are put forward, mathematics model of data processing is proposed as well. This system model can guarantee not only the flexible characteristic, but also the stability for system application.

1. Introduction

For the general conditions in which the dual bands IR beam gas detection systems are applied under open atmospheric environment, it is shown as the following figure:

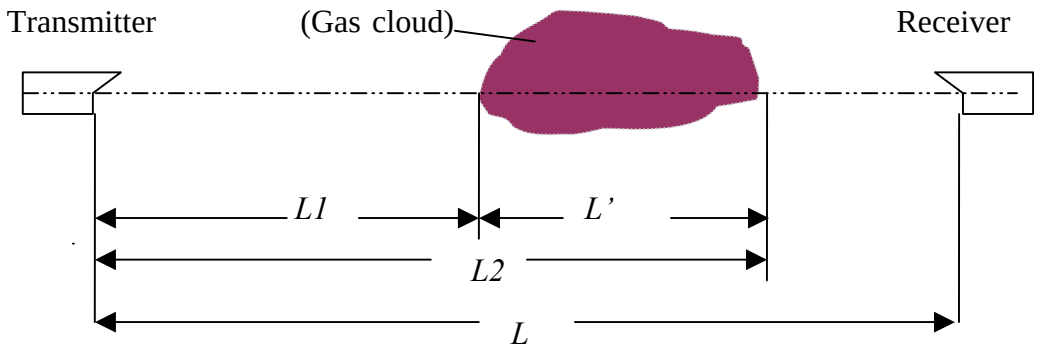

Fig.1 Illustration of Detection

Where L is the detection range of optical path and L' is the length of the path through gas cloud. On the basis of Lambert-Beer's law, the light-intensity of the detection band λ_1 is reduced following the function as below:

$$I_{\lambda 1} = I_{0\lambda 1} \exp\{-\int_0^L [\alpha(\lambda_1, x) + \beta(\lambda_1, x)]dx - \int_{L1}^{L2} [\alpha'(\lambda_1, x) + \beta'(\lambda_1, x)]dx\} \quad (1)$$

Where

$I_{0\lambda 1}$ is light-intensity at the transmitter;

$I_{\lambda 1}$ is the value at the receiver;

α, β are respectively specific absorption and scatter of atmosphere to band λ_1;

α', β' are respectively specific absorption and scatter of gas to band λ_1, which are related to the concentration of the gas under measurement.

Take non-intrinsic absorption band λ_2 of gas as a reference and comparison band and its atmospheric transmission law is as below:

$$I_{\lambda 2} = I_{0\lambda 2} \exp\{-\int_0^L [\alpha(\lambda_2, x) + \beta(\lambda_2, x)]dx - \int_{L1}^{L2} \beta'(\lambda_2, x)]dx\} \quad (2)$$

And meet as flows:

$$\alpha(\lambda_1, x) = \alpha(\lambda_2, x);$$

$$\beta(\lambda_1, x) = \beta(\lambda_2, x);$$

$$\beta'(\lambda_1, x) = \beta'(\lambda_2, x).$$

Divide both sides of equation (1) and (2) and again take logarithm, then result in:

$$\int_{L1}^{L2} \alpha'(\lambda_1, x)dx = \ln \frac{I_{0\lambda 1}}{I_{0\lambda 2}} - \ln \frac{I_{\lambda 1}}{I_{\lambda 2}} \quad (3)$$

according to Beer's law: specific absorption is related to gas concentration $\rho(x)$ when sample concentration become thin, and the following equation can be written:

$$\alpha'(\lambda_1 x) = k(\lambda_1)\rho(x) \quad (4)$$

where, $k(\lambda_1)$ is a constant for the specific absorption of unit concentration of gas;

Substitute equation (4) into equation (3) and so result in:

$$\int_{L1}^{L2} \rho(x)\,dx = \frac{1}{K(\lambda_1)}[\ln \frac{I_{0\lambda 1}}{I_{0\lambda 2}} - \ln \frac{I_{\lambda 1}}{I_{\lambda 2}}]..... \quad ..... \quad ....(5)$$

As seen from the above equation, the left side of the equation is concentration versus distance integral and its dimension is a product of concentration dimension and distance dimension (*LELm*).

$$Y(LELm) = \frac{1}{K(\lambda_1)}[\ln \frac{I_{0\lambda 1}}{I_{0\lambda 2}} - \ln \frac{I_{\lambda 1}}{I_{\lambda 2}}]..... \quad ..... \quad ..... \quad (6)$$

2. Dual bands design analysis

For a determined variety of a gas, its intrinsic absorption band λ_1 is determined. The key to the selection of dual band lies in the selection of the reference band λ_2 matchable to the λ_1 after it has been determined.

Under conditions of atmospheric transmission, it is not avoidable that the system might be influenced by random change in climatic conditions such as rain, snow, fog, smoke and dust, and concentration fluctuations as in vapor with component highly changed in the lower atmosphere layer and etc. Besides the strong absorption of component gases to their intrinsic absorption spectral band, light attenuation by atmospheric aerosols demonstrates steady and slow changing characteristic that it depends on the relative relationship between particles size (geometric dimensions) and the light wavelengths. Therefore, the selection of dual band shall comply with the following principles:

a) λ_1 is the intrinsic absorption band of the gas which to be detected, and λ_1 is the non-intrinsic absorption band of it.

b) λ_1 and λ_2 selected shall be near enough so as to enable beam only to demonstrate intrinsic absorption difference of the gases in its transmission process, but to do consistency to other light-attenuation causing factors in atmospheric environment.

c) λ_1 and λ_2 selected shall avoid the absorption band of vapor, and be in the same atmospheric window.

The essence of the dual band design thinking is to design and introduce a reference signal, and make use of its strong correlation with interfering signal, effectively reject the interfering signal within the original signals through proper signal processing technology so as to realize effective collection of the useful signal if the useful signal and the interfering signal are piled together in the original signals. Therefore, the technical design for strong correlation of the reference signal and interfering signal is the key to solve such kind of problems. For this system the design thinking shall be not only applied in the dual band selection, but also carried through in each link such as the system's optical path design, circuit design, data processing and so on, which is the fundamental guidance policy for realizing the dual bands IR beam gas detection system designs.

3. Model of a detection system

3.1 Optical transmission path

A problem with influence of atmospheric turbulence on optical path must be also considered in optical design. Atmospheric turbulence is a random movement of atmospheric molecular lumps in three dimensions. The main factors of causing turbulence are nonuniformity in air temperature, humidity, pressure and density. Since index of atmospheric refraction is a function of those factors, so random fluctuation in index of refraction caused by turbulence leads beam intensity, frequency, phase, polarization and direction to produce random shake phenomenon. The following several aspects can bring about more strong influence to this system (intensity measuring system):

a) Beat in facular location: several Hz to dozens of Hz for beat frequency;
b) Slow change occurred in beam direction: changing period longer to several minutes;
c) Beam fission, spread and deformation;
d) Flicker in beam intensity.

According to the strong correlation between the reference signal and interfering signal

required by the dual band design thinking, light from two bands must be ensured to pass through a complete same atmospheric transmission route, so as to enable the interference of atmospheric transmission to the dual bands signal to maintain common mode character. Therefore the optical model of the system is of transmitting and receiving dual bands with single beam, and wave division of the dual bands signals shall be achieved by the optical subsystem of the receiver.

3.2 Circuit model of receiver

In order to ensure strict transition from optical subsystem to the circuit portion in the dual band design thinking, time sharing response to the dual band signal using a single photoelectric detector and unified linear amplifier channel are adopted in the design of the circuit model, its design and adjustment ensure that the photoelectric detector and amplifier channel are working at linear range, so avoiding generation of nonlinear abnormal and distortion. The model is of great significance for ensuring strong correlation requirements between the reference signal and interfering signal of detection band:

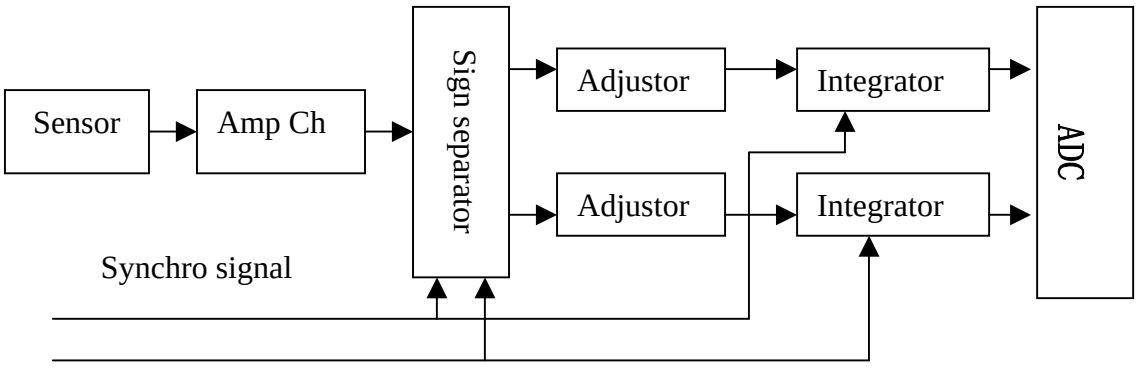

Fig.2 Circuit model of receiver

a) Avoid separation for characteristic parameters of two photoelectric detectors, especially dynamic separation of the parameters, such as difference in measuring

response to two-band signals, caused by slow time change due to temperature variety, component aging and etc.

b) Avoid separation of electric parameters of bias circuit and preamplifier, especially separation in measuring response to two-band signals, caused by nonuniformity in dynamic drift.

c) Simplify optical subsystem of the receiver and circuit design, component matching and selection, circuit adjustment as well.

4. Method of system adjustment and mathematic model of data processing

According to equation(6), $k(\lambda_1)$ is a constant, $I_{0\lambda 1}$ and $I_{0\lambda 2}$ are light-intensity of the two-band at the transmitter, and both are all constant under situations of ensuring steady spectral radiation from the transmitter, especially due to the principles of dual-band selection, $I_{0\lambda 1} / I_{0\lambda 2}$ is enabled to be more steady. Therefore, equation (6) can be rewritten to the following mode:

$$Y(LELm) = A - B \ln \frac{I_{\lambda 1}}{I_{\lambda 2}} \quad \text{.....(7)}$$

Where A and B are all a constant.

Shown from Fig.3 circuit model of the receiver, the front channel of the receiver is a linear one, so there exist:

$$V_1 = R_1 G T_1 I_{\lambda 1}$$

$$V_2 = R_2 G T_2 I_{\lambda 2}$$

Where V_1 is level output of channel λ_1;

V_2 is level output of channel $\lambda 2$;

R_1 and R_2 are response gain of the photoelectric detectors to $I_{\lambda 1}$ and $I_{\lambda 2}$, which are determined by the photoelectric detector characteristics. R_1 is approximately equal to R_2 when band selection is in compliance with the principle;

G is common gain of amplifier channel, which can be adjusted along with the different application requirements of the systems;

T_1 and T_2 are respectively balance adjusted gain of channels, which cannot be adjusted again after the detectors are calibrated.

$$\frac{V_2}{V_1} = \frac{R_2 T_2 I_{\lambda 2}}{R_1 T_1 I_{\lambda 1}} \text{.....(8)}$$

Substitute equation (8) into equation (7) and obtain:

$$Y(LELm) = A - B \ln \frac{R_2 T_2}{R_1 T_1} - B \ln \frac{V_1}{V_2} \text{.....(9)}$$

Under the conditions of ensuring the system circuit being at linearly operational state and no combustible gas cloud in optical path $Y(LELm)$=0, adjust balance adjusted gain of both channels and make output signal levels equal V_1=V_2, that is all. Afterwards balance adjustment of the system is not conducted again during its operation unless a great change has occurred in radiation spectrum of the transmitter.

After the system adjusted, there have an equation of V_1=V_2 and $Y(LELm)$=0, it is known from equation (9):

$$0 = A - B \ln \frac{R_2 T_2}{R_1 T_1} \text{.....(10)}$$

Through balance adjustment mentioned as the above, the equation (9) can be rewritten into the following one:

$$Y(LELm) = B \ln \frac{V_2}{V_1} \text{.....(11)}$$

Then, measure output values of V_1 and V_2 by using calibrated gas sample of 1(*LELm*) as proportion in the composition, and determine the parameter B from the equation (11). Then, by using the equation (11), $Y(LELm)$ can be directly calculated according to the measured level values of both channels. The equation (11) is just the mathematic model for the system data processing.

5 Analysis of the data processing model suitability

5.1 Guarantee condition for data processing mathematic model

The following conditions are only needed for guarantee validity of the system data processing mathematic model:

a) Comply with the several principles put forward in this paper for the realization of the system design;

b) Any practical use of the detection system shall ensure that receiver circuit is operating at linear state (the circuit is adjusted through common gain G);

c) The system shall be adjusted according to the system adjustment put forward in this paper).

5.2 Analysis of the system's response performance

Under situations of no combustible gas dispersion in the optical path, ratio of dual bands light-intensity received by the receiver for the detection at optional distance L:

$$\frac{I_{\lambda 1}}{I_{\lambda 2}}(L) = \frac{I_{0\lambda 1}}{I_{0\lambda 2}} \text{..... .....(12)}$$

the ratio is a constant determined by spectral power density of the transmitter, based on linearly operational state of the detector circuit, there exist the following relation at optional detection distance L of the system:

$$\frac{V_2}{V_1} = \frac{R_2 T_2 I_{\lambda 2}}{R_1 T_1 I_{\lambda 1}}$$

Under a certain condition (detection distance assumed as l when adjusted), adjust the system according to the method of the system adjustment, so as to enable V_1 equal V_2, at this time, there have the following relation:

$$\frac{R_1 T_1}{R_2 T_2} = \frac{I_{\lambda 2}}{I_{\lambda 1}}(l)$$

Known from the equation (12), under situation of no combustible gas dispersion in the optical path, ratio of the two bands light-intensity at optional distance is as following:

$$\frac{I_{\lambda 2}}{I_{\lambda 1}}(L) = \frac{R_1 T_1}{R_2 T_2} \text{..... .....(13)}$$

And the ratio of output level from the two channels shall meet the following relation:

$$\frac{V_2}{V_1}(L) = \frac{R_2 T_2 I_{\lambda 2}}{R_1 T_1 I_{\lambda 1}}(L) = 1$$

Substitute this relation into the equation (11) and result in the following relation:

$$Y(LELm) = B \ln \frac{V_2}{V_1}(L) = 0 \text{.....(14)}$$

This shown that zero response operating point of the system will no present a drift change alone with change in the system's detection distance.

For the situation of having combustible gases *Y(LELm)* in the detection path, response operation point is measured at optional detection distance *L* of the system according to Beer's law as follows:

$$\frac{V_2}{V_1'}(L) = \frac{R_2 T_2 I_{\lambda 2}}{R_1 T_1 I_{\lambda 1}'}(L) = \frac{R_2 T_2 I_{\lambda 2}}{R_1 T_1 I_{\lambda 1} e^{-\xi}} = \left(e^{\xi}\right) \text{.....(15)}$$

Where ξ is the factor for combustible gas intrinsic absorption of *Y(LELm)*. This shown that there is no relationship between the system's measuring response characteristics to the gas and its circuit parameters or its detection distance *L*, it only depends on intrinsic absorption of gas which will be detected, a physical effect itself.

6. Conclusions

Characteristics of the system's zero point not changing along with the detection distance, and combustible gas response measuring having no relationship with detection system circuit parameters and detection distance, enable the system model to have the most universal suitability, thereby enable the detection system to have both the most flexible application and the most stable detection performance. In fact, dual-band design adopted in the system can restrain any interference which have common mode character against dual band signals, so that the system model has been made to become the most optimizing system model of the dual bands IR combustible gas detection system.

References

[01] Zhang Xilin, Li Jian; IR beam gas detection system; AUBE’99 PROCEEDINGS P.114 – P.121

J.-T. Meyer*, A. Georgiadis**, J. Specht**, M. Witthaus**,
K.C. Persaud***, A.M. Pisanelli***, and E. Scorsone***

* Ing.Büro Dr. J-T. Meyer, Katlenburg-Lindau, Germany
** Fachhochschule Nordostniedersachsen, Lüneburg, Germany
*** University of Manchester, Institute for Technology, UK

Detection of significant tracer gases by means of polymer gas sensors

Abstract

Polymer gas sensors offer a cost efficient approach in the fire detection field. Besides the low costs of these sensors the "cold" surface with temperatures near room temperature are a major advantage for fire detection. The sensitivity of polymer gas sensor arrays have been tested in a number of alarm (according to EN54) and nuisance alarm situations.

The measurements have been performed in an EN54 test room and in the 1 m^3 – DFTC (Desktop Fire Test Cabinet). The alarm situations have been investigated by means of FT-IR measurements accompanied by GC/MS measurements. Conventional CO and CO_2 gas sensors have been used in parallel to the polymer gas sensor array. Furthermore an aspirating smoke detection system has been used for the control of the alarm and nuisance alarm situations.

The presented test results for various EN54 test fires and nuisance alarm situations using the prototype of the polymer gas sensor array with eight sensors show very promising results related to the possibility for the recognition of various fires. The work at this stage was focused on the identification of significant tracer gases by means of GC/MS and FT-IR measurements in order to train and to improve the polymer sensors.

1. Introduction

The aim of the reported measurements was to identify false alarm sources by means of an advanced conduction polymer sensor array. This device originates from air quality measurements and has been trained for the usage in fire situations.

Currently fire brigades deplore too many false alarms. For example, in Germany 9 alarms out of 10 fire alarms are false alarms. This is equivalent to a false alarm rate of 90 %, the false alarm rate being defined as percentage of alarms without fire. In some applications, such as in aircraft cargo compartments, false alarm rates as high as 99 % are encountered, resulting in over 150 unscheduled landings in the last four years in the USA.

There are two main groups of false alarm sources:

- Detector related false alarms: False alarms result from nuisance sources due to unforeseen processes undertaken in the protected area, e.g. steam generation, smoking, welding, working with solvents.
- Installation related false alarms: False alarms caused by planning and commissioning errors. For example, the planner chooses an unsuitable detector type for the application, the service engineer forgets to isolate equipment during maintenance .

To build up a reliable database in the short time available for the measurement campaign a small fire test room has been developed, the so-called Desktop Fire Test Cabinet, DFTC. This small and highly flexible fire test room allows a rate of eight test fires per day as a result of the easy purification of the walls after each test fire, which is an requirement for the setting of controlled gas sensor conditions.

The defined test fires from EN54 have been tested in the measurement campaign. A special focus was on the definition of nuisance alarm situations. Five false alarm situations have been defined for the measurement of a detector related false alarm situation. A strong focus of the analysed false alarm situations was on cigarette smoke.

2. The Desktop-Fire-Test-Cabinet – DFTC

The DFTC has been developed to assist the DIN EN 54 burning room. The advantage of the DFTC is the ability of:

- performing a lot more test fires in the same period of time (DFTC: 8 test fires a day, DIN EN 54 fire test room: 1 test fire in two days.
- easy cleaning => good background conditions.
- using different settings to control the fire.

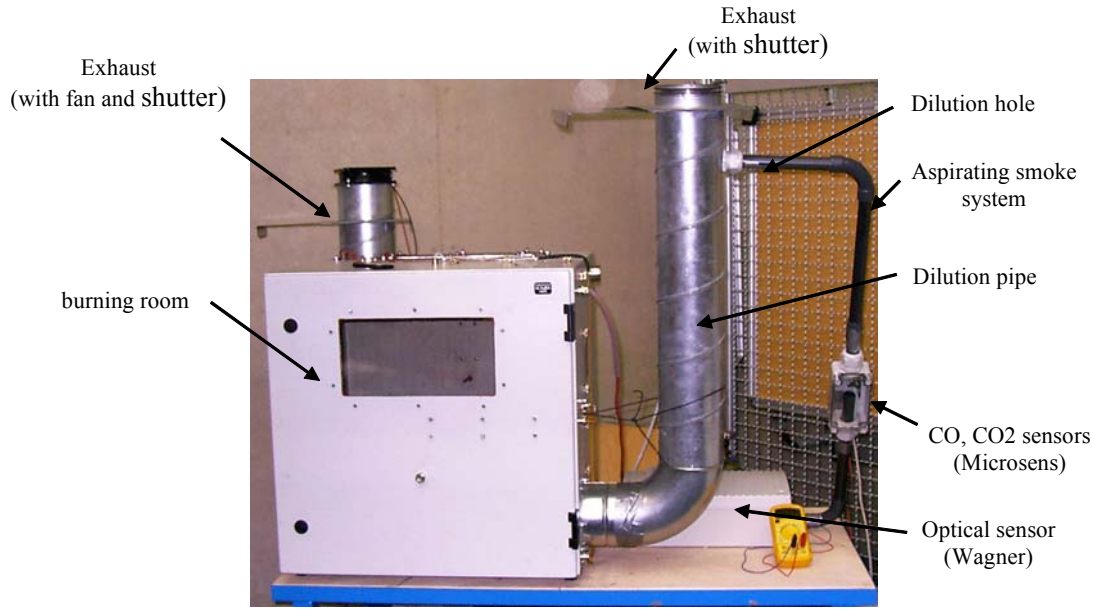

Fig. 1 Desktop Test Fire Cabinet

Function: The DFTC (size: 60cm x 57cm x 60cm) is constructed in a way to adapt the conditions of the DIN EN 54 burning room. Therefore the size of the test fires are chosen a lot smaller and a few control mechanisms are also included in the DFTC.
The test fire will be ignited inside the burning room. The smoke expands into the dilution pipe (through the through hole, standard Ø19mm). The suction point of the aspirating smoke system is at the top of the dilution pipe. The dilution pipe in combination with the through hole slows the velocity of propagation down. This can be

varied by using different through hole diameters. In addition to that the density of the smoke inside the burning room can be controlled by the fan and the shutter.

Reference Equipment: The fire condition is observed with 8 temperature sensors, two humidity and two air pressure sensors (inside and outside) and at the end of the aspirating smoke system an optical sensor. The compounds of the smoke are analysed with a **F**ourier **T**ransformed **I**nf**r**ared Gas Analyzer (FTIR). Depending on the test, the FTIR sampling point is inside the burning room, inside the dilution pipe or inside the aspirating smoke system. Additional sensors can be included to fulfil the task.

The temperature sensors are PT 100, 1/3 DIN b from Heraeus, Germany
The humidity sensors are FOM 8 /1 from Galltec, Germany
The air pressure sensors are MPX 4100 A from Motorola, Japan
The FTIR gas analyser is the GASMET DX-4000 from TEMET Oy, Finland.

3. Results and analysis of test fires

Test series 1

The first test series has been conducted in order to analyse the components of different fire and nuisance alarm situations and to build up a database with these data. Afterwards this database supports the differentiation between fire and nuisance alarm situations. The DIN EN 54 test fires have been used as the basic for the fire situations. The chosen nuisance alarm situations are: Cigarette smoke, Disco fog, MAG welding, Car exhaust and Kitchen oil.

Results

In order to point out small concentrations the FTIR takes the sample inside the burning room. Compared to the aspirating smoke system this leads to an approx. 50 times higher concentration. Each different test fire has been conducted 14 times.

Test Fire 1: Burning wood

6 stick beech wood (0,5x0,5x5)cm^3
0,5ml spirit for ignition

maximum concentration of the measured Components [ppm]:

CO_2	25.000
CO	550
H_2O	16
NO	17
Methan	31
Acetylen	5
Ethen	11
Ethan	4
Styrol	6
Chlorbenzol	4
Ethanol	84

Test Fire 2: Smouldering wood

one stick beech wood (1x1x2)cm^3

CO_2	1.900
CO	580
H_2O	3
NO	5
HCL	18
Methan	50
Ethan	37
o-Xylol	21
Chlorbenzol	7
Formaldehyd	18

Test Fire 3: Cotton wick

one piece of brained cotton wick
18cm long (0,17g)

CO_2	880
CO	110
H_2O	5
NO	4
Methan	4
Acetylen	4
Benzol	4
Formaldehyd	5
Ethanol	5
Acetaldehyd	4

Test Fire 4: Flaming polyurethane

CO_2	13.300
CO	70
H_2O	14
NO	140
NO_2	25
N_2O	6
HCN	9
Ethen	4
Styrol	4
Aceton	4

Soft polyurethane foam without flame retardant additives.
Size: 4x2 x40cm^3, (20kg m^{-3})

Test Fire 5: n-Heptane

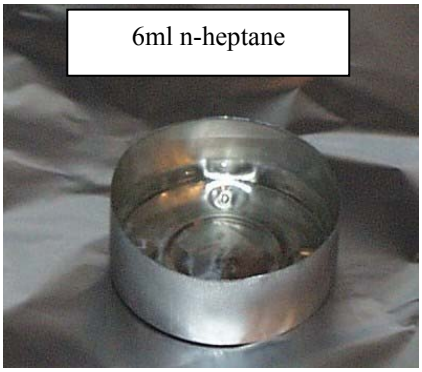

CO_2	49.000
CO	100
H_2O	16
NO	16
NO_2	6
Ethen	12
Ethan	7
Styrol	4
Chlorbenzol	4
Ethanol	4
HExan	42
Oktan-n	41

Test Fire 6: Flaming ethanol

CO_2	81.500
CO	120
H_2O	13
NO	27
Ethan	30
Styrol	15
Ethanol	1.700

Nuisance Alarm 1: Cigarette smoke

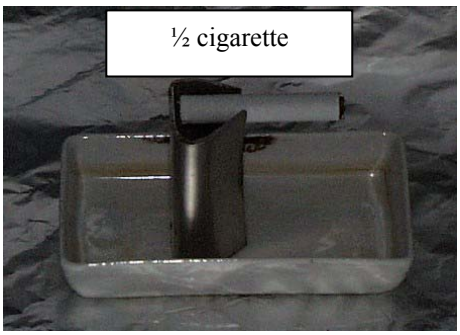

CO_2	1.100
CO	110
H_2O	5
NO	6
NH_3	15
Methan	14
Acetylen	4
Ethen	7
Styrol	5
Chlorbenzol	11
Ethanol	6
Essigsäure	5
Acetaldehyd	5

Nuisance Alarm 2: Disco fog

3 sec disco fog (ca. 1,5ml fluid)

CO_2	660

H_2O	7
Ethen	4
Chlorbenzol	4
Acetaldehyd	4

Nuisance Alarm 3: MAG welding

Active gas: Ar 82%, CO_2 18%
Welding wire: ELETRA BECKUM, 0.8 mm Ø /SG 2

CO_2	32.900
CO	190
H_2O	8
NO	23
Ethen	6
Ethanol	4

Nuisance Alarm 4: Car exhaust

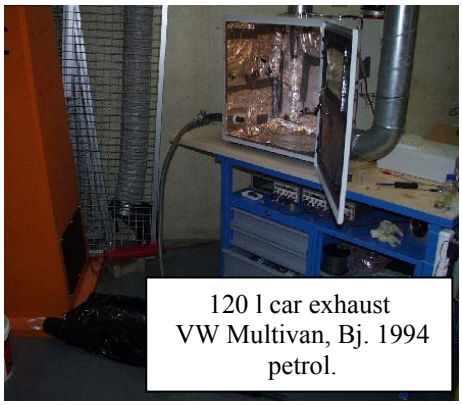

CO_2	133.000
CO	1.200
H_2O	16
NO	26
Methan	18
Acetylen	14
Ethen	36
m-Xylol	8
Ethylbenzol	8
Chlorbenzol	8
Ethanol	9
Hexan	13

Nuisance Alarm 5: Kitchen oil

CO_2	550
CO	4
H_2O	4
NO	6
p-Xylol	5
Chlorbenzol	4
Hexan	12
Acetaldehyd	12

The reproducibility of all fires is good. The ratio of the rise of CO_2 and CO gives a clue to the fire type. Open fire such as burning wood, polyurethane, n-heptane, ethanol,

MAG welding or car exhaust are showing a high ratio of 40 to 500. Smouldering fires such as smouldering wood, cotton wick and cigarette are showing a low ratio of 2 to 4. Non fire situations such as disco fog and kitchen oil show a very low increase of CO and CO_2. Unfortunately no significant tracer gases were found to identify the nuisance alarm situations which are caused by combustion. Only cigarette is showing with the ammonia concentration a significant tracer gas.

Test Series 2

The University of Manchester is developing a conduction polymer sensor (CP) with the focus to smoke components. The second test series was conducted at Manchester in order to test their first 8-CP sensor array prototype and to use their possibilities and their knowledge of GC/MS. The test results will be used to develop the next generation of an 8-CP sensors array with a focus to cigarette smoke and they will be used to expand the database of smoke components.

Two fires of smouldering wood, cotton wick, smouldering paper, flaming polyurethane and cigarette smoke are conducted at Manchester. The samples are taken from the aspirating smoke system, which worked with without dilution.

Results: GS/MS

Following compounds have been identified by the GS/MS as specific tracer gases:

Test fire 2: Smouldering wood	Hexanoic acid, Guaiacol and Heptanoic acid
Test fire 3: Cotton wick	Furfural, 2-(3H) Furanone
Test fire 7: Smouldering paper	Acetohydroxamic acid
Test fire 4: Flaming polyuretane	Benzonitrile
Nuisance alarm 1: Cigarette smoke	Toluene, Pyridine, Limonene, Nicotine, Isoprene

Results: first 8-CP sensor array prototyp

The first 8-CP sensor array prototype presented sufficient reactions to the different test fires. however, at this phase of the development it was not possible to discriminate

between those fires, but with the help of the first test results and the identified tracer gases the next generation of an 8-CP sensor array has been developed.

Test Series 3

The second 8-CP sensor array prototype is tested during the test series 3. Fires of flaming wood, smouldering wood, cotton wick, flaming polyurethane and cigarette smoke have been conducted. The first results are very promising. One of each different fire has been conducted until now. Fig. 2 shows the results of the sensors 1000s after the ignition. The resistance of the sensor 3 increases only during the cigarette test fire. This would be a good feature to discriminate between cigarette smoke and the other fires. To validate these results more test fires have to be done.

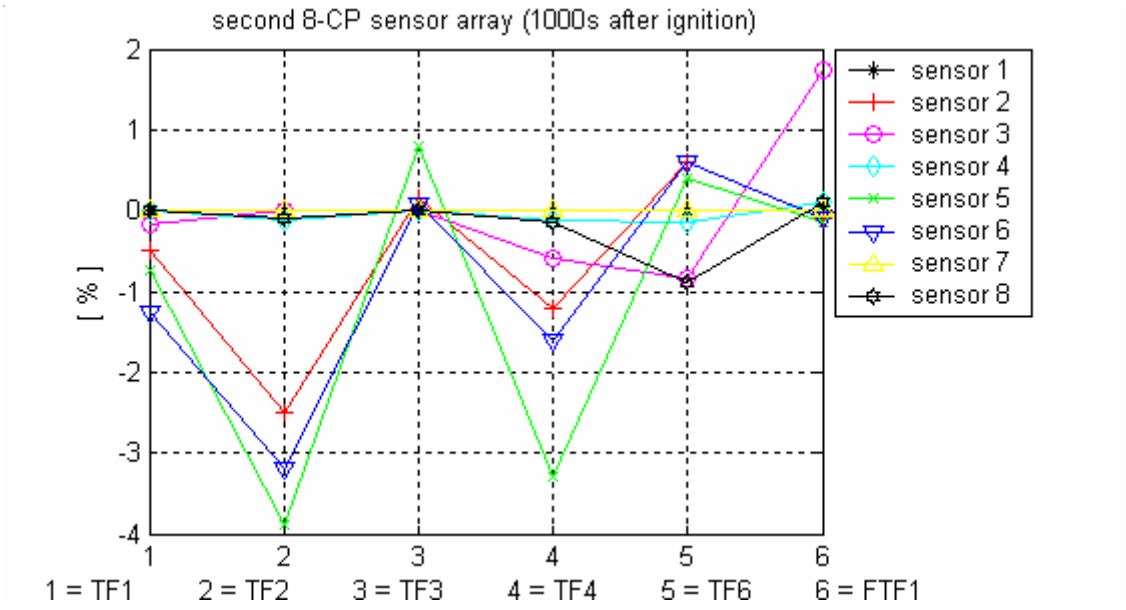

Fig. 2 Conducting Polymer sensor array test fire results of test series 3

The results of the principal components analysis are displayed in Fig. 3. The PCA shows a significant identification of TF 3 (cotton). For burning wood the measured value is time dependent as a result of the changing decomposition of the material during the fire. A very promising result has been developed for cigarette smoke (Nuisance Alarm 1). From Fig. 2 it is visible, that the polymer sensor 3 reacts to cigarette smoke only.

From the FT-IR measurements it is found that cigarette smoke is the only fire under consideration with a NH_3 fraction. The cohesion with sensor 3 is under investigation currently.

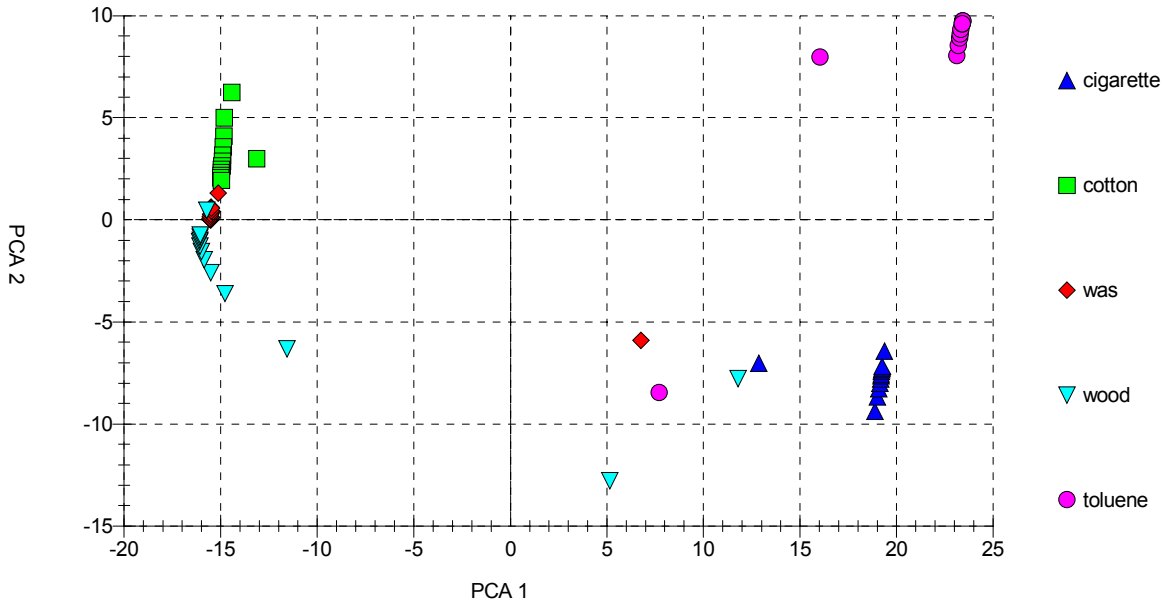

Fig. 3 Principle Components Analysis

4. Discussion and conclusions

The performed measurements in the DFTC show reliable and reproducible results. The identified material portions and the control mechanisms fulfil the requirements on the time dependent progression of the fire in order to mimic the EN54 test conditions. The results from the conducting polymer array show a possible identification of cigarette smoke as the main nuisance alarm source. From the measurements a correlation to the sensor 3 of the array seem to be significant. This has to be investigated further with additional nuisance alarm and test fire situations.Future investigations will focus on further DFTC measurements with CP arrays to develop the array composition and sensitivity for fire detection measurements.

The reported work is funded by the IST program of the Commission of the European Communities under the 5th framework.